Fermentation Microbiology and Biotechnology

Edited by

E.M.T. El-Mansi • C.F.A. Bryce • B. Dahhou
S. Sanchez • A.L. Demain • A.R. Allman

CRC Press
Taylor & Francis Group

Fermentation Microbiology and Biotechnology

Third Edition

This page intentionally left blank

Fermentation Microbiology and Biotechnology

Third Edition

Edited by

E.M.T. El-Mansi • C.F.A. Bryce • B. Dahhou
S. Sanchez • A.L. Demain • A.R. Allman

CRC Press
Taylor & Francis Group
Boca Raton London New York

CRC Press is an imprint of the
Taylor & Francis Group, an **informa** business

CRC Press
Taylor & Francis Group
6000 Broken Sound Parkway NW, Suite 300
Boca Raton, FL 33487-2742

Version Date: 20111007

International Standard Book Number-13: 978-1-4398-5581-2 (eBook - PDF)

A man lives not only his personal life as an individual, but also, consciously or unconsciously, the life of his epoch and his contemporaries.

Thomas Mann

Professor Dr. Mahmoud Ismael Taha,
A chemist of exactitude and graceful humility (1924–1981)

This edition is dedicated with affection and gratitude to the memory of the late Professor Dr. Mahmoud Ismael Taha, who ignited in me a lifelong passion for biochemistry; he often reminded me that Louis Pasteur was a chemist.

E.M.T. El-Mansi
(Editor-in-Chief)

This page intentionally left blank

Contents

Preface

I beseech you to take interest in these sacred domains, so expressively called laboratories. Ask that, there be more and that they be adorned for these are the temples of the future, wealth and well being.

Louis Pasteur

Microorganisms, free-living and immobilized, are widely used industrially as catalysts in the biotransformation of many chemical reactions, especially in the production of stereospecific isomers. The high specificity, versatility, and the diverse array of microbial enzymes (proteomes) are currently being exploited for the production of important primary metabolites including amino acids, nucleotides, vitamins, solvents, and organic acids, as well as secondary metabolites such as antibiotics, hypercholesterolemia agents, enzyme inhibitors, immunosuppressants, and antitumor therapeutics.

Recent innovations in functional genomics, proteomics, metabolomics, bioinformatics, biosensor technology, nanobiotechnology, cell and enzyme immobilization, and synthetic biology and *in silico* research are currently being exploited in drug development programs to combat disease and hospital-acquired infections as well as in the formulation of a new generation of therapeutics.

The third edition builds upon the fine pedigree of its earlier predecessors and extends the spectrum of the book to reflect the multidisciplinary and buoyant nature of this subject area. To that end, four new chapters have been commissioned:

- Functional Genomics
- Solid-State Fermentations
- Applications of Metabolomics to Microbial Cell Factories
- Current Trends in Culturing Complex Plant Tissues for the Production of Metabolites and Elite Genotypes

More exciting advances and discoveries are yet to be unraveled, and the best is yet to come as we enter a new era in which the exploitations of microorganisms continue to astonish the world community, especially the use of renewable resources and the generation of new therapeutics to combat disease are recognized as an urgent need. To that end, Professor Brian S. Hartley predicts the emergence of a new era in which "biorefineries" play a central role in climate control and the balance of geochemical cycles in our ecosystem.

To aid learning and to make the text more lively and interactive, boxes highlighting the definitions of new and central concepts are shown in the margin, a feature that is now synonymous with our book.

We very much hope that the third edition will be assimilated and appreciated by those actively engaged in the pursuit of advancing our field, and to that end, the editor-in-chief wishes to stress his readiness to receive your feedback, including suggestions by authors who wish to add or extend the knowledge base of our book, which is becoming increasingly global with every edition.

In future editions, our endeavor to keep our readers abreast with recent innovations in this exciting and buoyant field will continue unabatedly.

The Editorial Team

Acknowledgments

The third edition builds on the seminal work presented in earlier editions and owes much to the original and innovative work of our peers and colleagues worldwide. I wish to thank my editorial team and our distinguished authors for their sound contributions and for being very responsive throughout; in particular, I wish to thank Brian S. Hartley, whose encouragement and stimulating discussions across the Internet have been inspirational. It is also befitting to thank my two sons Adam and Sammy, for their love and the happiness, which they continue to bring to my life.

On behalf of the editorial team and authors, I wish to thank Barbra Norwitz (executive editor) and Albert Ebinesh (project manager) and their respective teams at CRC Taylor and Francis for transforming our manuscripts, into a high quality book, which I hope meets with your expectations as a reader.

The editorial team are only too conscious of mistakes and omissions, which may have crept in unnoticed; the credit of producing this book is only partly hours, it is the blame that rests totally with us.

Have a good read.

E.M.T. El-Mansi
Editor-in-Chief

This page intentionally left blank

Editors

Dr. Mansi El-Mansi is a graduate of the University of Assiut, El-Minya, Egypt (BSc, First Hons and MSc Microbiology). He was intrigued and fascinated by the versatility of microorganisms and soon realized that understanding their physiology demanded a clear understanding of their biochemistry. He made the conscious decision of undertaking his PhD in the field of microbial biochemistry and was fortunate enough to carry it out at UCW, Aberystwyth, United Kingdom, under the supervision of David J. Hopper, whose meticulous approach to experimental design was a towering influence. During the course of his PhD studies, he became familiar with the work of Stanley Dagley, the father of microbial biochemistry as we know it, and this in turn galvanized his resolve to further his understanding of microorganisms at the molecular level.

Immediately after the completion of his PhD, Dr. El-Mansi joined Harry Holms at the Department of Biochemistry, University of Glasgow, Scotland, and such a happy and stimulating association continued for the best part of a decade, during which their group was the first to clone and show that the structural gene encoding the bifunctional regulatory enzyme ICDH kinase/phosphatase is indeed a member of the glyoxylate bypass operon. Soon thereafter, Dr. El-Mansi became acquainted with flux control analysis and its immense potential in the fermentation and pharmaceutical industries. His interest in the application of flux control analysis was further stimulated by collaboration with Henrik Kacser, the founder of metabolic control analysis (MCA) theory, at the University of Edinburgh.

During the course of his employment in Edinburgh, Dr. El-Mansi was the first to postulate and unravel the role of HS-CoA in the partition of carbon flux among enzymes of central metabolism during growth of *Escherichia coli* on acetate. He was also the first to provide evidence supporting Dan Kosahland's theory of "ultrasensitivity". His research activities, which span the best part of 30 years, yielded an extensive list of publications of which four are single-author publications in peer-reviewed journals.

After 27 years of intensive research and teaching in Scotland, Dr. El-Mansi felt that the time was right to share his experience with others and to enrich him culturally. He is currently a professor of biotechnology at Sharda University, Greater Noida, India.

Dr. Charlie Bryce has held posts as Head of the School of Life Sciences and Dean of the Faculty of Sciences for over 20 years at Edinburgh Napier University. For the last three years he focused on International Development for the Faculty of Health, Life and Social Sciences and, more recently, he extended this to work with the Vice Chancellor on developing international research and technology transfer links for all areas of the university. He now acts as an independent, international consultant for program development, learning support material development including e-learning, continuing professional development, and quality assessment and audit at the departmental and institutional level.

In the last 30 years, he has published 100 refereed research publications and designed and produced approximately 30 teaching packages in a wide variety of media formats. He has undertaken an international survey of the biochemistry curriculum for science and medical students and a pan-European survey of curriculum content for programs in biotechnology and is currently developing programs in biomedical science for a partner in Singapore. Dr. Bryce has served on national and international committees including U.K. Deans of Science

(chairman), U.K. Interest Group on Education in Biotechnology (chairman), Education Group of the Biochemical Society (chairman), vice president of the European Federation of Biotechnology (EFB), EFB Task Group on Education and Mobility (chairman), EFB Task Group on Innovation (chairman), secretary general of the Association for Higher Education in Biotechnology (HEduBT, the body that oversees the operation of the Eurodoctorate in Biotechnology), specialist adviser to several British Council and COSTED Projects, member of the Editorial Board of New Biotechnology, and former executive editor of the journal *Bioinformatics*. He has acted as an auditor and a subject reviewer for the Quality Assurance Agency (QAA) and for the Scottish Funding Council (SFC) and has also undertaken audit/assessment work in Bangladesh and in Hong Kong. He currently chairs accreditation panels for the Forensic Science Society and has also undertaken research project evaluation for the Commission of the European Communities (CEC).

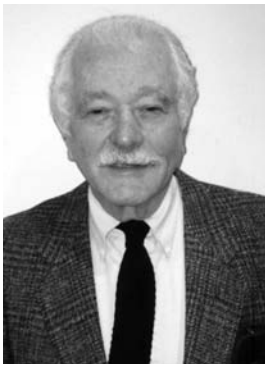

Dr. Arnold Demain, research fellow in microbial biochemistry at the Charles A. Dana Research Institute for Scientists Emeriti of Drew University in Madison, NJ, is an icon synonymous with excellence in the fields of industrial microbiology and biotechnology. Born in Brooklyn, New York City, in 1927, he was educated in the New York public school system and received his BS and MS in bacteriology from Michigan State University in 1949 and 1950, respectively. He obtained his PhD on pectic enzymes in 1954 from the University of California, having divided his time between the Berkeley and Davis campuses. In 1956, he joined Merck Research Laboratories at Rahway, NJ, where he worked on fermentation microbiology, β-lactam antibiotics, flavor nucleotides, and microbial nutrition. In 1965, he founded the Fermentation Microbiology Department at Merck and directed research and development on processes for monosodium glutamate, vitamin B_{12}, streptomycin, riboflavin, cephamycin, fosfomycin, and interferon inducers. In 1969, he joined MIT, where he set up the Fermentation Microbiology Laboratory. Since then, he has published extensively on enzyme fermentations, mutational biosynthesis, bioconversions, and metabolic regulation of primary and secondary metabolism. His success is evident in a long list of publications (over 530), 14 books of which he is co-editor or co-author, and 21 U.S. patents. His ability to "hybridize" basic studies and industrial applications was recognized by his election to the presidency of the Society for Industrial Microbiology in 1990, membership in the National Academy of Sciences in 1994, the Mexican Academy of Sciences in 1997, and in the Hungarian Academy of Science in 2002. In recognition of his outstanding contribution to our current understanding in fermentation microbiology and biotechnology, he has been awarded honorary doctorates from the University of Leon (Spain), Ghent University (Belgium), Technion University (Israel), Michigan State University (United States), Muenster University (Germany), and Drew University (United States).

Dr. Anthony (Tony) R. Allman, a graduate of the University of Liverpool (BSc, PhD), has been a member of the Institute of Biology and the Society of General Microbiology for more than 25 years. He began his career at Glaxo, where he spent six years carrying out research into the development of subunit bacterial vaccines. During that time, he became acquainted with fermentors and their applications. Subsequently, he acted as a specialist in this area for the U.K. agent of a major European fermentor manufacturer. When Infors U.K. was established in 1987, Tony joined the new company as Product Manager (later Technical Director) and in 2002, he became Fermentation Product Manager for the Swiss parent company, Infors AG. His work involves providing technical support, training, and application expertise in-house and throughout the world.

Dr. Allman is well known among research and industrial communities for having a passion for making fermentation accessible to the wider public. His "extracurricular activities" of devising practical workshops and giving lectures on fermentation technology speak volumes about the active pursuit of this aim.

Dr. Sergio Sanchez, born in Mexico City, Mexico, received his MD in 1970 and his PhD in 1973, both from the National University of Mexico. After two postdoctoral research fellowships at the U.S. Department of Agriculture in Peoria, IL, and then at the MIT, Cambridge, MA, Dr. Sanchez began his career as a researcher at the Institute of Biomedical Research, National University of Mexico and in 1984 he co-founded the first Biotechnology Department at the same University. He has served several times as a head of that department and more recently as technical secretary of the same institute.

As a professor of industrial microbiology, Dr. Sanchez published extensively and his work is characterized by a sustained level of important discoveries in several areas of industrial microbiology, including research on the interrelation between the role of glutathione and the amino acid transport systems and the production of penicillin in *Penicillium chrysogenum*. He also explored the regulatory relationships between primary and secondary metabolism in *Streptomyces peucetius* var. caesius; he was the first to show that in addition to *Glk*, an adjacent gene (*sco2127*) participates in the process of carbon catabolite repression in this organism.

He was elected as the first president to the Mexican Society for Biotechnology and Bioengineering (MSBB), and in recognition of his contributions, the MSBB has established the Sergio Sanchez award to recognize the best thesis research project for pre- and postgraduate students in biotechnology and bioengineering in Mexico. In 1986, he co-founded the Postgraduate Biotechnology Programme at the National University of Mexico, being its first coordinator.

Currently, he is an editor on the editorial board of *Applied Microbiology and Biotechnology* and the Editor-in-Chief of *BioTecnología*, an international journal published by the Mexican Society for Biotechnology and Bioengineering.

Dr. Boutaib Dahhou, a graduate of (PhD 1980) of Paul Sabatier University–Toulouse III, France, has been addressing various issues of supervision, control, and modeling of linear and nonlinear systems. In his studies, Dr. Dahhou adopted a new strategy consisting of adding a road base or a block of supervision in which one can exploit all of the available information. He further developed this process by modifying the layer immediately above than the adaptive loop, which is the layer of supervision of the control; at that level, the signals evolved from adaptation and feedback loops are used as signal identifiers to recognize specific physiological situations and to act on the parameters of the algorithms of control and estimation.

He recognized that, in a given system, significant signals have to be identified to test its validity on the basis of certain preset criteria. Violation of these criteria triggers the start of a second task by the supervisor. For example, in biotechnological processes, these anomalies can be related to specific biological reaction or ascribed to the operation of actuators or sensors.

Currently, the detection and isolation of faults in the dynamic of nonlinear systems is of particular interest. Addressing this aspect, Dr. Dahhou developed new algorithms on the basis of the adaptive observers that made possible the instantaneous detection of any fault. On the other hand,

the isolation of these faults demanded much time because of the procedure of parameter adaptation. To resolve this problem, he is currently developing a new approach of isolation that is based on the parameter intervals.

Dr. Dahhou has successfully supervised 18 PhD students and published more than 72 articles in international journals and 130 communications in international congresses.

Contributors

César Arturo Aceves-Lara
Université de Toulouse; UPS, INSA, INP, LISBP; Toulouse, France and INRA
UMR792, Ingénierie des Systèmes Biologiques et des Procédés
Toulouse, France

Anthony R. Allman
Infors U.K., Ltd.
Rigate, England, United Kingdom

Aristos A. Aristidou
Bioprocess Development
Centennial, Colorado

Namdar Baghaei-Yazdi
Biocaldol, Ltd., The London Bioscience Innovation Centre
London, England, United Kingdom

George N. Bennett
Department of Biochemistry and Cell Biology
Rice University
Houston, Texas

Charlie F.A. Bryce
Edinburgh Napier University
Edinburgh, Scotland, United Kingdom

Ross P. Carlson
Department of Chemical and Biological Engineering
Center for Biofilm Engineering
Montana State University
Bozeman, Montna

Surendra K. Chikara
Xcelrislabs, Ltd.
Ahmedabad, India

Arun P. Chopra
Department of Biotechnology
Hindustan College of Science and Technology
Farha, Mathura, India

Boutaib Dahhou
Centre National de la Recherche Scientifique
Laboratoire d'Analyse et d'Architecture des Systèmes
Université de Toulouse
Toulouse, France

Lalitha Devi Gottumukkala
Biotechnology Division
National Institute for Interdisciplinary Science and Technology
Council of Scientific and Industrial Research
Trivandrum, India

Arnold L. Demain
Research Institute for Scientists Emeriti
Drew University
Madison, New Jersey

E.M.T. El-Mansi
Department of Biotechnology, School of Medical Sciences and Research
Sharda University
Greater Noida, Uttar Pradesh, India

Chris E. French
Institute of Cell Biology
University of Edinburgh
Edinburgh, Scotland, United Kingdom

Craig J.L. Gershater
Institute of Continuing Education
University of Cambridge
Cambridge, England, United Kingdom

Chris Gwenin
School of Chemistry
Bangor University
Wales, United Kingdom

Brian S. Hartley
Grove Cottage
Cambridge, England, United Kingdom

Iain S. Hunter
Department of Pharmaceutical Sciences
University of Strathclyde
Glasgow, Scotland, United Kingdom

Muhammad Javed
Biocaldol, Ltd.
The London Bioscience Innovation Centre
London, England, United Kingdom

Toral Joshi
Xcelrislabs, Ltd.
Ahmedabad, India

Zetao Li
Electrical Engineering College
Guizhou University
Guiyang, Guizhou, People's Republic of China

Brian McNeil
Institute of Pharmacy and Biomedical Sciences
Royal College
Strathclyde University
Glasgow, Scotland, United Kingdom

David M. Mousdale
beòcarta Ltd.
Royal College Building
Glasgow, Scotland, United Kingdom

Jens Nielsen
Chalmers University of Technology
Department of Chemical and Biological Engineering
Gothenburg, Sweden

Ashok Pandey
Biotechnology Division
National Institute for Interdisciplinary Science and Technology, Council of Scientific and Industrial Research
Trivandrum, India

Kuniparambil Rajasree
Biotechnology Division
National Institute for Interdisciplinary Science and Technology, Council of Scientific and Industrial Research
Trivandrum, India

Gilles Roux
Centre National de la Recherche Scientifique
Laboratoire d'Analyse et d'Architecture des Systèmes
Université de Toulouse
Toulouse, France

Ka-Yiu San
Department of Bioengineering
Rice University
Houston, Texas

Sergio Sanchez
Departamento de Biología Molecular y Biotecnología, Instituto de Investigaciones Biomédicas, Universidad Nacional Autónoma de México
México City, México

Gregory Stephanopoulos
Department of Chemical Engineering
Massachusetts Institute of Technology
Cambridge, Massachusetts

Reeta Rani Singhania
Laboratoire de Genie Chimique et Biochimique
Universite Blaise Pascal
Clermont Ferrand, France

Carlos Ricardo Soccol
Biotechnology Division
Federal University of Parana
Curitiba, Brazil

Raymond Tham
Flinders Centre for Marine Bioprocessing and Bioproducts, School of Medicine
Flinders University
Adelaide, Australia

Melissa J. Towler
Department of Biology and Biotechnology
Worcester Polytechnic Institute
Worcester, Massachusetts

F. Bruce Ward
Institute of Cell Biology
University of Edinburgh, Darwin Building
Edinburgh, Scotland, United Kingdom

Pamela J. Weathers
Department of Biology and Biotechnology
Worcester Polytechnic Institute
Worcester, Massachusetts

Ronnie G. Willaert
Department of Structural Biology,
Flanders Institute for Biotechnology
Vrije Universiteit Brussel
Brussels, Belgium

Barbara E. Wyslouzil
William G. Lowrie Department of Chemical
and Biomolecular Engineering
Ohio State University
Columbus, Ohio

Wei Zhang
Flinders Centre for Marine Bioprocessing and
Bioproducts, School of Medicine
Flinders University
Adelaide, Australia

This page intentionally left blank

1 Fermentation Microbiology and Biotechnology: An Historical Perspective

E.M.T. El-Mansi, Charlie F.A. Bryce, Brian S. Hartley, and Arnold L. Demain

CONTENTS

"Dans le champ de l'observation, le hasard ne favorise que les esprits préparés."

Louis Pasteur, 1854

1.1 FERMENTATION: AN ANCIENT TRADITION

Fermentation has been known and practiced by humankind since prehistoric times, long before the underlying scientific principles were understood. That such a useful technology should arise by accident will come as no surprise to those people who live in tropical and subtropical regions, where, as Marjory Stephenson put it, "every sandstorm is followed by a spate of fermentation in the cooking pot" (Stephenson 1949). For example, the productions of bread, beer, vinegar, yogurt, cheese, and wine were well-established technologies in ancient Egypt (Figures 1.1 and 1.2). It is an interesting fact that archaeological studies have revealed that bread and beer, in that order, were the two most abundant components in the diet of ancient Egyptians. Everyone, from the pharaoh to the peasant, drank beer for social as well as ritual reasons. Archaeological evidence has also revealed that ancient Egyptians were fully aware not only of the need to malt the barley or the emmer wheat but also of the need for starter cultures, which at the time may have contained lactic acid bacteria in addition to yeast.

1.2 THE RISE OF FERMENTATION MICROBIOLOGY

With the advent of the science of microbiology, and in particular fermentation microbiology, we can now shed light on these ancient and traditional activities. Consider, for example, the age-old

FIGURE 1.1 Bread making as depicted on the wall of an ancient Egyptian tomb dated c. 1400 BC. (Reprinted with the kind permission of the Fitzwilliam Museum, Cambridge, England.)

FIGURE 1.2 Grape treading and wine making as depicted on the walls of Nakhte's tomb, Thebes, c. 1400 BC. (Reprinted with the kind permission of AKG, London, England/Erich Lessing.)

technology of wine making, which relies upon crushing grapes (Figure 1.2) and letting nature take its course (i.e., fermentation). Many microorganisms can grow on grape sugars more readily and efficiently than yeasts, but few can withstand the osmotic pressure arising from the high sugar concentrations. Also, as sugar is fermented, the alcohol concentration rises to a level at which only osmotolerant, alcohol-tolerant cells can survive. Hence inhabitants of ancient civilizations did not need to be skilled microbiologists in order to enjoy the fruits of this popular branch of fermentation microbiology.

In fact, the scientific understanding of fermentation microbiology and, in turn, biotechnology only began in the 1850s, after Louis Pasteur had succeeded in isolating two different forms of amyl alcohol, of which one was optically active (L, or *laevorotatory*) while the other was not. Rather unexpectedly, the optically inactive form resisted all of Pasteur's attempts to resolve it into its two main isomers, the laevorotatory (L) and the *dextrorotatory* (D) forms. It was this

observation that led Pasteur into the study of fermentation, in the hope of unraveling the underlying reasons behind his observation, which was contrary to stereochemistry and crystallography understandings at the time.

In 1857, Pasteur published the results of his studies and concluded that fermentation is associated with the life and structural integrity of the yeast cells rather than with their death and decay. He reiterated the view that the yeast cell is a living organism and that the fermentation process is essential for the reproduction and survival of the cell. In his paper, the words *cell* and *ferment* are used interchangeably (i.e., the yeast cell is the ferment). The publication of this classic paper marks the birth of fermentation microbiology and biotechnology as a new scientific discipline. Guided by his critical and unbiased approach to experimental design, Pasteur was able to confidently challenge and reject Liebig's perception that fermentation occurs as a result of contact with decaying matter. He also ignored the well-documented view that fermentation occurs as a result of "contact catalysis," although it is possible that this concept was not suspect in his view. The term "contact catalysis" probably implied that fermentation is brought about by a chain of enzyme-catalyzed reactions. In 1878, Wilhelm Kühne (1837–1900) was the first to use the term *enzyme*, which is derived from the Greek word ενζυμον ("in leaven") to describe this process. The word *enzyme* was used later to refer to nonliving substances such as pepsin, and the word *ferment* used to refer to chemical activity produced by living organisms.

Although Pasteur's interpretations were essentially physiological rather than biochemical, they were pragmatically correct. During the course of his further studies, Pasteur was also able to establish not only that alcohol was produced by yeast through fermentation but also that souring was a consequence of contamination with bacteria that were capable of converting alcohol to acetic acid. Souring could be avoided by heat treatment at a certain temperature for a given length of time. This eliminated the bacteria without adversely affecting the organoleptic qualities of beer or wine, a process we now know as *pasteurization*.

A second stage in the development of fermentation microbiology and biotechnology began in 1877, when Moritz Traube proposed the theory that fermentation and other chemical reactions are catalyzed by protein-like substances and that, in his view, these substances remain unchanged at the end of the reactions. Furthermore, he described fermentation as a sequence of events in which oxygen is transferred from one part of the sugar molecule to another, culminating in the formation of a highly oxidized product (i.e., CO_2) and a highly reduced product (i.e., alcohol). Considering the limited knowledge of biochemistry in general and enzymology in particular at the time, Traube's remarkable vision was to prove 50 years ahead of its time.

In 1897 Eduard Buchner, two years after Pasteur died, discovered that sucrose could be fermented to alcohol by yeast cell-free extracts and coined the term "zymase" to describe the enzyme that catalyses this conversion. The term "zymase" Is derived from the Greek word "zymosis", which means fermentation. In 1907, he received the Nobel Prize in Chemistry for his biochemical research and his discovery of cell-free fermentation. In the early 1900s, the views of Pasteur were modified and extended to stress the idea that fermentation is a function of a living, but not necessarily multiplying, cell and that fermentation is not a single step but rather a chain of events, each of which is probably catalyzed by a different enzyme.

1.3 DEVELOPMENTS IN METABOLIC AND BIOCHEMICAL ENGINEERING

The outbreak of the First World War provided an impetus and a challenge to produce certain chemicals that, for one reason or another, could not be manufactured by conventional means. For example, there was a need for glycerol, an essential component in the manufacture of ammunition, because no vegetable oils could be imported due to the naval blockade. German biochemists and engineers were able to adapt yeast fermentation, turning sugars into glycerol rather than alcohol. Although

this process enabled the Germans to produce in excess of 100 tons of glycerol per month, it was abandoned as soon as the war was over because glycerol could be made very cheaply as a by-product of the soap industry. There was also, of course, a dramatic drop in the level of manufacture of explosives and, in turn, the need for glycerol.

The diversion of carbon flow from alcohol production to glycerol formation was achieved by adding sodium bisulfite, which reacts with acetaldehyde to give an adduct that cannot be converted to alcohol (Figure 1.3). Consequently, NADH accumulates intracellularly, thus perturbing the steady-state redox balance (NAD^+:NADH ratio) of the cell. The drop in the intracellular level of NAD^+ is accompanied by a sharp drop in the flux through glyceraldehyde-3-phosphate dehydrogenase, which in turn allows the accumulation of the two isomeric forms of triose phosphate (i.e., glyceraldehyde-3-phosphate and dihydroxyacetone-3-phosphate). Accumulations of the latter together with high intracellular levels of NADH trigger the expression of glycerol-3-phosphate dehydrogenase, which in turn leads to the diversion of carbon flux from ethanol production to glycerol formation, thus restoring the redox balance within the cells by regenerating NAD^+ (Figure 1.3). Although this explanation is with the hindsight of modern biochemistry, the process can be viewed as an early example of metabolic engineering.

Following the First World War, research into yeast fermentation was largely influenced by the work of Carl Neuberg and his proposed scheme (biochemical pathway) for the conversion of sugars to alcohol (alcohol fermentation). Although Neuberg's scheme was far from perfect and proved erroneous in many ways, it provided the impetus and framework for many scientists at the Delft Institute, who vigorously pursued research into oxidation/reduction mechanisms and the kinetics of product formation in a wide range of enzyme-catalyzed reactions. Such studies were to prove important in the development of modern biochemistry as well as fermentation biotechnology.

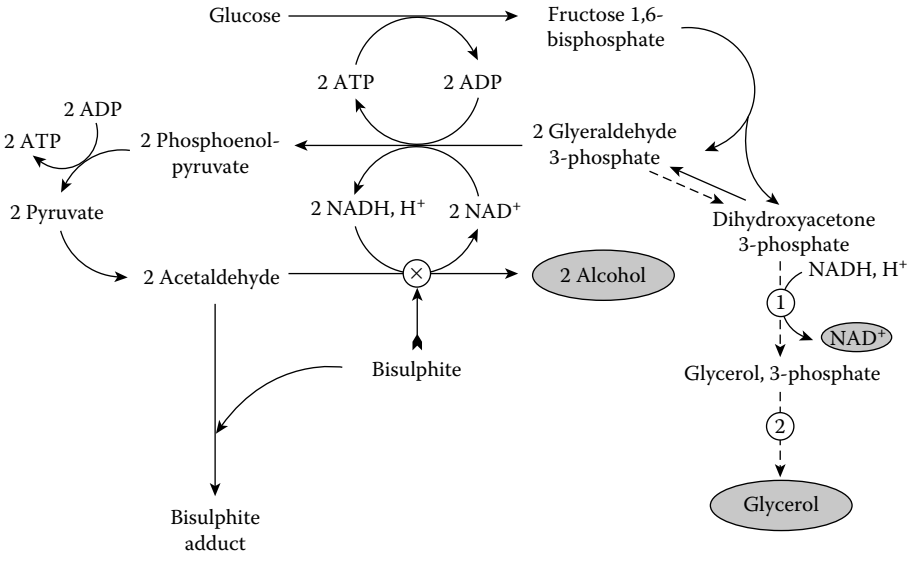

FIGURE 1.3 Diversion of carbon flux from alcohol production to glycerol formation in the yeast *Saccharomyces cerevisiae*. Note that the functional role of bisulfite is to arrest acetaldehyde molecules, thus preventing the regeneration of NAD^+ as a consequence of making alcohol dehydrogenase redundant. To redress the redox balance (i.e., the NAD^+:NADH ratio), *S. cerevisiae* diverts carbon flow (dashed route) toward the reduction of dihydroxyacetone-3-phosphate to glycerol-3-phosphate, thus regenerating the much-needed NAD^+. The glycerol-3-phosphate thus generated is then dephosphorylated to glycerol.

BOX 1.1 "FILL AND SPILL"

This pattern of fermentation is essentially a "batch fermentation" or "fed-batch fermentation" process in which the organism is allowed to grow, and once product formation has reached the maximum level, the fermentation pot is harvested, leaving some 10% of the total volume as an inoculum for the next batch. This process is repeated until the level of contamination becomes unacceptably high.

While glycerol fermentation was abandoned immediately after the First World War, the acetone-butanol fermentation process, catalyzed by *Clostridium acetobutylicum*, flourished. Production lines were modified to accommodate the new approach of "Fill and Spill" (see Box 1.1), which permitted substantial savings in fuels without adversely affecting the output of solvent production during the course of the Second World War. However, as soon as the production of organic solvents as a by-product of the petrochemical industry became economically viable, the acetone-butanol fermentation process was discontinued.

1.4 DISCOVERY OF ANTIBIOTICS AND GENETIC ENGINEERING

The discoveries of penicillin in the late 1920s and its antibacterial properties in the early 1940s represent a landmark in the development of modern fermentation biotechnology. This discovery, to a country at war, was both sensational and invaluable. However, *Penicillium notatum*, the producing organism, was found to be susceptible to contamination by other organisms, and therefore aseptic conditions were called for. Such a need led to the introduction of so-called stirred tank bioreactors, which minimize contamination with unwanted organisms. The demand for penicillin prompted a worldwide screen for alternative penicillin-producing strains, leading to the isolation of *Penicillium chrysogenum*, which produced more penicillin than the original isolate *P. notatum*. *P. chrysogenum* was then subjected to a very intensive program of random mutagenesis and screening. Mutants that showed high levels of penicillin production were selected and subjected to further rounds of mutagenesis, and so on. This approach was successful, as indicated by the massive increase in production from less than 1 g l^{-1} to slightly more than 20 g l^{-1} of culture.

Once the antibacterial spectrum of penicillin was determined and found to be far from universal, pharmaceutical companies began the search for other substances with antibacterial activity. These screening programs led to the discovery of many antibacterial agents produced by various members of the actinomycetes. Although the search for new antibiotics is never over, intensive research programs involving the use of genetic and metabolic engineering were initiated with the aim of increasing the productivity and potency of current antibiotics. For example, the use of genetic and metabolic engineering has increased the yield of penicillin manyfold.

1.5 THE RISE AND FALL OF SINGLE-CELL PROTEIN

The latter part of the 1960s saw the rise and fall of single-cell protein (SCP) production from petroleum or natural gas. A large market for SCP was forecast, as the population in the third world, the so-called underdeveloped countries, continued to increase despite a considerable shortfall in food supply. However, the development of SCP died in its infancy, largely due to the sharp rise in the price of oil, which made it economically nonviable. Furthermore, improvements in the quality and yields of traditional crops decreased demand for SCP production.

1.6 FERMENTATION BIOTECHNOLOGY AND THE PRODUCTION OF AMINO ACIDS

The next stage in the development of fermentation biotechnology was dominated by success in the use of regulatory control mechanisms for the production of amino acids. The first breakthrough was the discovery of glutamic acid overproduction by *Corynebacterium glutamicum* in the late 1950s and early 1960s, when a number of Japanese researchers discovered that regulatory mutants, isolated by virtue of their ability to resist amino acid analogs, were capable of overproducing amino acids. The exploitation of such a discovery, however, was hampered by the induction of degradative enzymes once the extracellular concentration of the amino acid increased beyond a certain level; for example, accumulation of tryptophan induced the production of tryptophanase, thus initiating the breakdown of the amino acid. This problem was resolved by the use of penicillin, which, with tryptophan as the sole source of carbon in the medium, eliminated the growing cells (i.e., those capable of metabolizing tryptophan, but not those that were quiescent). Following the addition of penicillin, the mutants that had survived the treatment (3×10^{-4}) were further tested. Enzymic analysis revealed that one mutant was totally devoid of tryptophanase activity. This approach was soon extended to cover the production of other amino acids, particularly those not found in sufficient quantities in plant proteins. The successful use of regulatory mutants stimulated interest in the use of auxotrophic mutants for the production of other chemicals. The rationale is that auxotrophic mutants will negate feedback inhibition mechanisms and in turn allow the accumulation of the desired end product. For example, an arginine-auxotroph was successfully used in the production of ornithine, while a homoserine-auxotroph was used for the production of lysine.

1.7 BIOFUELS AND THE "EVOLUTION" OF BIOREFINERIES

In the last decade, fermentation biotechnology has taken a leap forward in consequence of the rising price of oil and international concern about global warming. Brazil was a pioneer since the 1970s in developing bioethanol production from its huge sugarcane industry and alongside it an expanding industry for production of ethanol-utilizing cars; as a result, today about 80% of Brazilian vehicles are fueled by > 20% bioethanol–gasoline mixtures.

The United States, the largest consumer of gasoline, has expanded its program and increased its bioethanol production from corn by some sixfold over the last decade, thus superseding Brazil's production from sugarcane. However, this is still only a fraction of U.S. gasoline consumption. Ethanol production from corn is much less efficient than from sugarcane, so subsidies are required to market it as a 15% ethanol–gasoline blend, which can be used in conventional car engines without modification. Nevertheless, the rocketing price of oil is close to making unsubsidized corn bioethanol competitive with gasoline. Corn prices are also rising, but the increasing animal feed value of the fermentation residues (distillers' dried grains, or DDGs) almost compensates.

There is therefore a worldwide trend to increase conventional bioethanol production, even if subsidies or tariffs are required and although the carbon footprint of the fuel is only marginally better than that of gasoline. The production of bioethanol or the capacity to make it appears to have a buffering capacity against further increases in oil prices. There are many situations in which bioethanol production represents a logical alternative to farming subsidies, such as wheat production in the European Union. There is, however, valid opposition to "first-generation" bioethanol as a sustainable biofuel on grounds of minimal reduction of global warming and competition with food supply. Fortunately, fermentation biotechnology has an answer. We harvest at best 20% of what farmers grow and eat only a fraction of that. Agricultural residues such as corn stover, cereal straws, and palm oil wastes are lignocellulosic biomass that could dwarf current bioethanol production. Harvested factory residues, such as sugarcane bagasse, corn cobs, wheat bran, palm oilcake, and so on represent an immediate opportunity. Lignocellulosic residues alone could yield sufficient bioethanol to fuel all the cars in the world.

As we will be discussing in Chapter 9, these residues are composed mostly of bundles of long cellulose fibers (40–50% dry weight) waterproofed by a coat of lignin (15–25%) and embedded in a loose matrix of hemicelluloses (25–35%). Most R&D has been directed to cellulose utilization since it can be hydrolyzed to glucose and fermented by yeasts. However, this is a slow and/or energy-intensive process, so cellulosic ethanol is not competitive with corn or wheat bioethanol, let alone cane bioethanol. In contrast, hemicelluloses are easily hydrolyzed to a mixture of C5 and C6 sugars, most of which cannot be fermented by yeasts. Many microorganisms can ferment these sugars, but produce lactic acid rather than ethanol. Therefore, much effort has gone into genetic manipulation to divert carbon flux from lactate production to bioethanol formation.

Notable among such microorganisms are thermophilic *Geobacilli* found naturally in compost heaps and/or silage. They can be engineered to produce ethanol from hemicellulosic sugars with yields equivalent to those from yeast fermentations of starch sugars. They have the additional advantages of extremely rapid continuous fermentations at high temperatures in which ethanol vapor can be removed continuously from the broth. Hence, although such fermentations have not yet been commercialized, calculations indicate that the production cost will be well below that of cane bioethanol or gasoline, so the scene is set for the evolution of biorefineries.

By analogy with the emergence of petrochemicals from processing the by-products of oil refineries, new biochemicals will emerge from the processing of biomass in biorefineries. Sugarcane, for example, could yield sugar or ethanol from the juice, ethanol from the hemicellulosic pith, waxes from the external rind, plus heat and electricity from efficient combustion of the lignocellulosic fibers (KTC-Tilby 2011). Alternatively, the fibers could be used directly for packaging or building board or for paper production after ethanol extraction of the lignin. The lignin extract could make an efficient biodiesel or give rise to a new range of bioaromatics to compete with those currently derived from oil. The residual stillage from ethanol distillation has high animal feed value.

Another advantage of such biorefineries is that they would be self-contained units built close to existing food-processing plants, such as sugar refineries, flour mills, or oil-processing plants. Since rape seed or palm oils are already used for biodiesel production, an intriguing proposal to use the by-product glycerol together with hemicellulosic sugars for high-yield bioethanol production would produce biorefineries to rival oil refineries in producing both fuels from a single raw material. The scene is therefore set for the evolution of biorefineries.

1.8 IMPACT OF FUNCTIONAL GENOMICS, PROTEOMICS, METABOLOMICS, AND BIO-INFORMATICS ON THE SCOPE AND FUTURE PROSPECTS OF FERMENTATION MICROBIOLOGY AND BIOTECHNOLOGY

Modern biotechnology, a consequence of innovations in molecular cloning and overexpression in the early 1970s, has started in earnest in the early 1980s after the manufacture of insulin, with the first wave of products hitting the market in the early 1990s. During this early period, the biotechnology companies focused their efforts on specific genes/proteins (natural proteins) that were of well-known therapeutic value and typically produced in very small quantities in normal tissues. Later, monoclonal antibodies became the main products of the biopharmaceutical industry.

In the mid-1980s, Thomas Roderick coined the term *genomics* to describe the discipline of mapping, sequencing, and analyzing genomic DNA with the view to answering biological, medical, or industrial questions (Jones 2000). Recent advances in functional genomics, stimulated by the Human Genome Project and computer software technology, led many biotechnologists to venture from the traditional *in vivo* and *in vitro* research into the *in silico*

Functional genomics is a discipline of biotechnology that attempts to exploit the vast wealth of data produced by genome-sequencing projects. A key feature of functional genomics is their genome-wide approach, which invariably involves the use of a high-throughput approach.

approach, thus establishing a new science in the shape of bio-informatics. In this approach, microbiologists employ computers to store, retrieve, analyze, and compare a given sequence of DNA or protein with those stored in data banks from other organisms. Microbial biotechnologists were quick to realize that the key to successful commercialization of a given sequence relied on the development of an innovative methodology (bio-informatics) that facilitates the transformation of a given sequence into a diagnostic tool and/or a therapeutic drug, thus bridging the gap between academic research and commercialization.

Proteomics is a new discipline that focuses on the study and exploitation of proteomes. A **proteome** is the complete set of proteins expressed by a given organism under certain conditions.

The new innovations in functional genomics—proteomics, metabolomics, and bio-informatics—will certainly play a major role in transforming our world in an unparalleled way, despite political and ethical controversies.

Metabolomics is a new discipline that focuses on the study and exploitation of metabolomes. A **metabolome** refers to the complete set of primary and secondary metabolites as well as activators, inhibitors, and hormones that are produced by a given organism under certain conditions. It is noteworthy, however, that it is not currently possible to analyze the entire range of metabolites by a single analytical method.

In this book, we have addressed the multidisciplinary nature of this subject and highlighted its many fascinating aspects in the hope that we are providing a stepping stone in its progress. As we enter a new era in which the use of renewable resources for the production of desirable end products is recognized as an urgent need, fermentation microbiology and biotechnology have a central role to play.

REFERENCES

Jones, P.B.C. 2000. The commercialisation of bioinformatics. *EJB Electronic Journal of Biotechnology* 3(2): 33–34.

KTC-Tilby. 2011. Sweet sorghum and sugar cane separation technology. www.youtube.com/watch?v=YbQT7Yfmn7s

Stephenson, M. 1949. *Bacterial Metabolism*. London: Longmans, Green.

2 Microbiology of Industrial Fermentation: Central and Modern Concepts

E.M.T. El-Mansi, F. Bruce Ward, and Arun P. Chopra

CONTENTS

"..et le rêve de toute cellule: devenir deux cellules".

Jacques Monod, 1970

2.1 INTRODUCTION

Microorganisms play a central role in the production of a wide range of primary and secondary metabolites, industrial chemicals, enzymes, and antibiotics. The diversity of fermentation processes may be attributed to many factors, including the high surface-to-volume ratio and the ability to utilize a wide spectrum of carbon and nitrogen sources. The high surface-to-volume ratio supports a very high rate of metabolic turnover: for example, the yeast *Saccharomyces cerevisiae* has been reported to be able to synthesize protein by several orders of magnitudes faster than plants. On the other hand, the ability of microorganisms to adapt to different metabolic environments makes them capable of utilizing inexpensive renewable resources such as wastes and by-products of the farming and petrochemical industries as the primary carbon source. Industrially important microorganisms include bacteria, yeasts, molds, and actinomycetes.

While the metabolic route through which glucose is converted to pyruvate, glycolysis, is universally conserved among all organisms, microorganisms differ from eukaryotes in their ability to process pyruvate through a diverse array of routes (Figure 2.1), giving rise to a multitude of

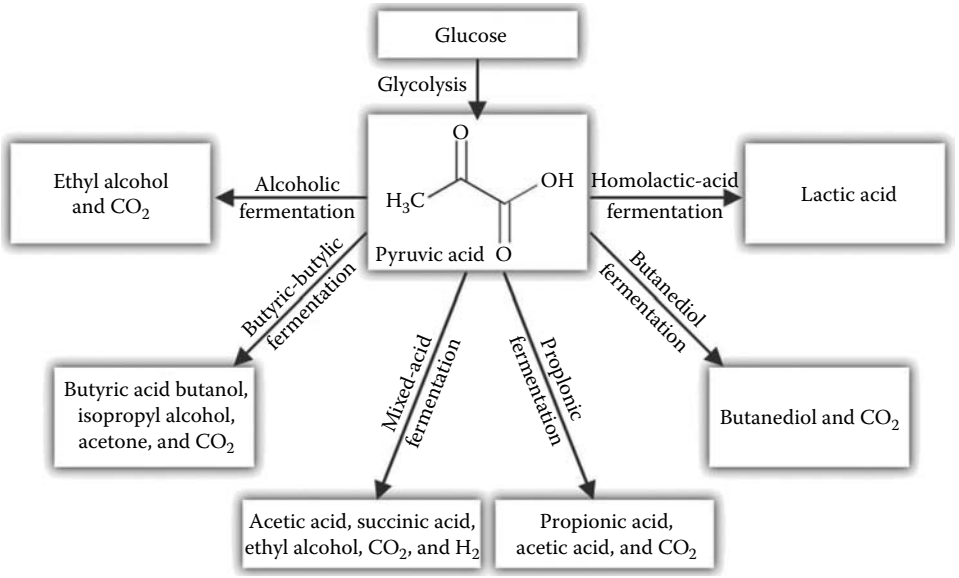

FIGURE 2.1 Diversity of fermentation pathways among microorganisms.

different end products. Such diversity has been fully exploited by fermentation technologists for the production of fine chemicals, organic solvents, and dairy products.

Prokaryotic organisms differ from yeast and fungi as well as other eukaryotes in a number of ways, including cell structure and growth cycle. For example, while DNA is compartmentalized within the nucleus in eukaryotes, it is neatly folded within the cytoplasm in prokaryotes. The site of oxidative phosphorylation represents yet another example; while oxidative phosphorylation is associated with mitochondria in eukaryotic organisms, oxidative phosphorylation in prokaryotes is associated with cytoplasmic membranes. Furthermore, the newly synthesized DNA molecules in prokaryotes need no special assembly to form a chromosome, as the DNA is already attached to the bacterial membrane, thus ensuring its successful segregations into two daughter cells. Any treatment that dislodges the DNA or compromises the attachment of DNA to the cytoplasmic membrane may lead to failure in segregation of DNA. This was the scientific bases on which sodium dodecyle sulphate (SDS) was used to cure large endogenous plasmids from *Klebsiella pneumoniae* and *Pseudomonas putida* (El-Mansi et al. 2001).

2.2 CHEMICAL SYNTHESIS OF BACTERIAL PROTOPLASM OR BIOMASS

In addition to carbon, nitrogen, phosphate, potassium, sulfur, irons, and magnesium, the chemical input required for growth also include trace elements. The necessity for such a multitude of inputs is paramount as it is required for enzymic activities. The contribution of each additive to biomass and product formation can be assessed quantitatively.

While central metabolism (glycolysis, the pentose phosphate pathway, and the Krebs cycle) is concerned with the breakdown of growth substrates and their conversion to the 12 biosynthetic precursors, ATP, and reducing powers, intermediary metabolism focuses on the conversion of those biosynthetic precursors to monomers and their subsequent polymerization and assembly into polymers.

2.2.1 Central and Intermediary Metabolism

Throughout Section 2.2, we will be addressing the function of enzymes of central and intermediary metabolism (Figure 2.2) with respect to their role in bacterial growth, and as such it would be helpful if we were to appreciate the functional role of each.

During growth on a glucose minimal medium under aerobic conditions, *Escherichia coli* catabolizes glucose through glycolysis and the Krebs cycle (Figure 2.2) to bring about its transformation to biosynthetic precursors; there are 12 in total, over half of which are phosphorylated adenosine-5'-triphosphate (ATP) and reducing powers in the shape of NADH, NADPH, and $FADH_2$ as well as esterified CoA derivatives (e.g., succinyl CoA and malonyl CoA). In this process a whole host of different reactions, the fueling reactions (Figure 2.3) are coordinated in a precise manner to ensure successful adaptation and survival of the organism. Once the biosynthetic precursors, ATP, and reducing powers are generated, the organism employs anabolic enzymes to convert those biosynthetic precursors into monomers (building blocks) in the shape of various sugars, amino acids, and nucleotides. The monomers are then polymerized into polymers (macromolecules), which, in turn, are assembled into different structures or organelles and thence to biomass (Figure 2.3). The central metabolic pathways (glycolysis, the pentose phosphate pathway, and the Krebs cycle) fulfill both catabolic (from *cata*, a Greek word for breakdown) and anabolic (from *ana*, a Greek word for buildup) functions and as such may be referred to as *amphibolic pathways.*

Although the central metabolic pathways are highly conserved in all organisms, microorganisms display a great deal of diversity even within a single species such as *E. coli* in response to growth conditions. As can be seen from Figure 2.2, microorganisms are capable of utilizing a wide range of substrates and afford a different entry point for each into central metabolism. As the point of entry into the central metabolic pathways of the Krebs cycle vary from one substrate to another, the makeup of the enzymic machinery necessary for metabolism changes accordingly (Guest and Russell 1992). For example, during growth on acetate or fatty acids, *E. coli* expresses uniquely the anaplerotic sequence of glyoxylate bypass (Cozzone 1998).

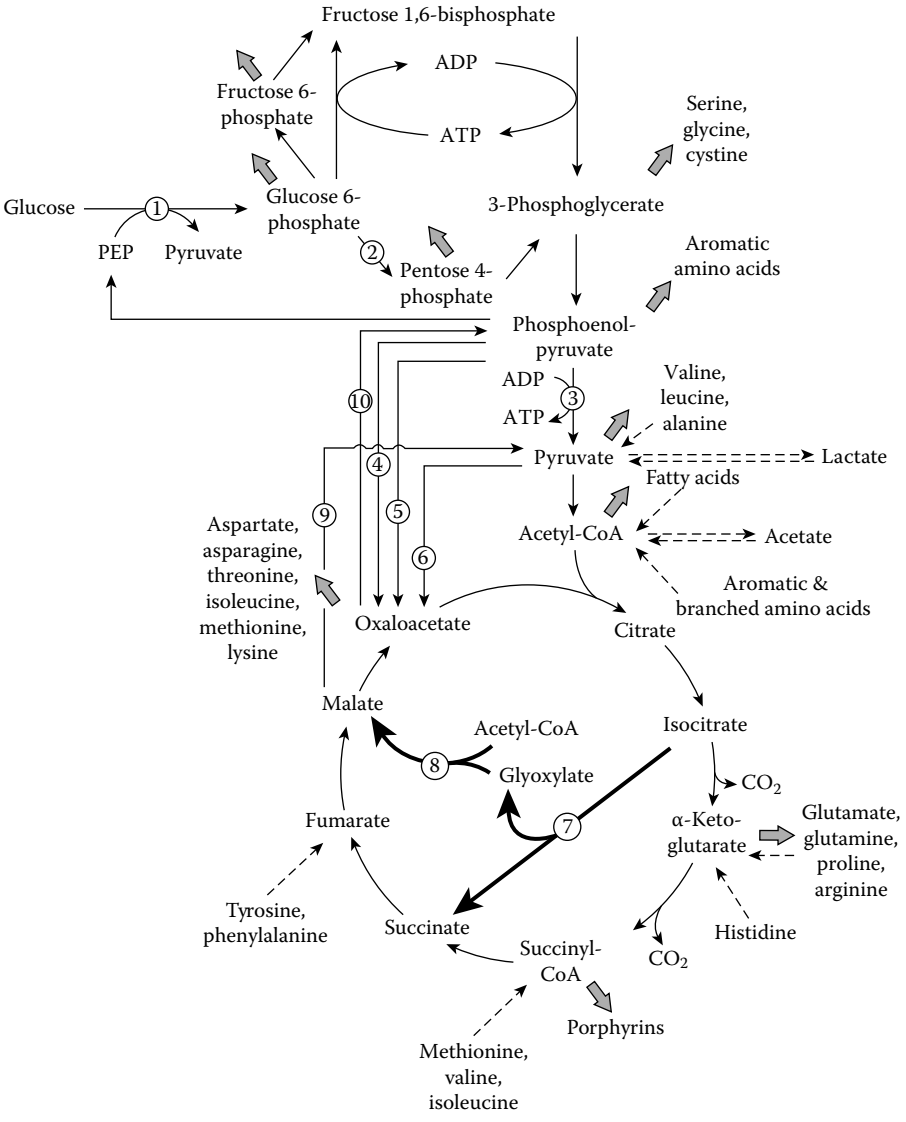

FIGURE 2.2 An overview of the metabolic pathways of central and intermediary metabolism employed by *E. coli* for the conversion of glucose and other substrates to biosynthetic precursors; indicated by heavy-dotted arrows, ATP, and reducing powers. Entry of substrates other than glucose into central metabolism is indicated by dashed arrows. Key enzymes are as follows: 1, glucose–phosphoenolpyruvate (PEP) phosphotransferase system; 2, the pentose phosphate pathway; 3, pyruvate kinase; 4, PEP carboxylase; 5, PEP carboxytransphosphorylase; 6, pyruvate carboxylase; 7, isocitrate lyase; 8, malate synthase; 9, malic enzyme; and 10, PEP carboxykinase.

2.2.2 Anaplerotic Pathways

During growth on glucose or other acetogenic substrates (i.e., those that support flux to acetate excretion), metabolites of the Krebs cycle, namely, α-ketoglutarate, succinyl CoA, and oxaloacetate (Figure 2.2), are constantly being withdrawn for biosynthesis. It follows, therefore, that such intermediates must be replenished; otherwise, the cycle will grind to a halt. The reactions that fulfill such a function are known as *anaplerotic*, a Greek word for replenishing, pathways. The makeup

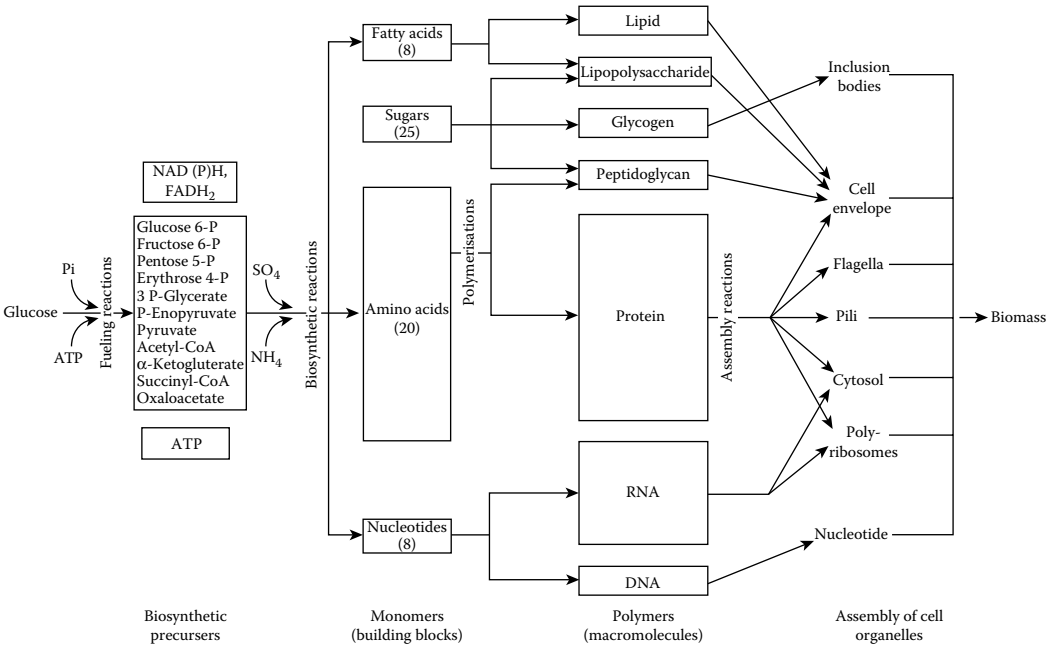

FIGURE 2.3 A diagrammatic representation of the reactions involved in the conversion of glucose and simple salts to biomass of *E. coli*. (This figure is a slight modification of Ingraham, J.L., Neidhardt, F.C., and Schaechter, M., *A Molecular Approach*, Sinauer Associates, Inc., Sunderland, MA, 1990, reproduced with the kind permission of Sinauer Associates, Inc., Sunderland, MA, 1990.)

of the anaplerotic enzymes differs from one phenotype to another, in other words, it is substrate dependent. For example, during growth on glucose, phosphoenolpyruvate carboxylase, pyruvate carboxylase, and phosphoenolpyruvate carboxytransphosphorylase (Figure 2.2) represent the full complement of anaplerotic enzymes that may be used in full or in part depending on the organism under investigation. During growth on acetate, however, *E. coli* employs the glyoxylate bypass operon enzymes, namely, isocitrate lyase and malate synthase, as an anaplerotic sequence. Interestingly, however, while the enzymes of the glyoxylate bypass in *E. coli* form an operon and include the bifunctional regulatory enzyme isocitrate dehydrogenase kinase/phosphatase, these enzymes are not organized in the same way in *Corynebacterium glutamicum*.

2.2.3 Polymerization and Assembly

Following transcription through the activity of RNA polymerase, mRNA is translated into protein by ribosomes. In this process, ribosomes attach to mRNA together with co-factors, enzymes, and complementary tRNA, thus forming a polysome and, in turn, initiating the synthesis of polypeptides. Polysomes are one of the most abundant organelles in growing cells; each polysome contains approximately 20 subunits of ribosomal RNA (Ingraham et al. 1983).

2.2.4 Biomass Formations

The rate of product formation in a given industrial process, a significant parameter, is directly related to the rate of biomass formation, which, in turn, is influenced directly or indirectly by a whole host of different environmental factors (e.g., oxygen supply, pH, temperature, and accumulation of inhibitory intermediates). It is, therefore, important that we are able to describe growth and production in quantitative terms. The study of growth kinetics and growth dynamics involves the formulation and

use of differential equations (for more details, see Chapter 3). While the mathematical derivation of these equations is beyond the scope of this chapter, it is important that we understand how such equations can be used to further our understanding of microbial growth in general and its impact on product formation (yield) in particular.

In microbiology we generally deal with very large numbers, and for convenience we express these numbers as multiples of 10 raised to an appropriate power; for example, 1 million (1,000,000) is written as 1×10^6.

2.2.5 Logarithms

Logarithms, otherwise known as *logs*, are very useful mathematical functions in both microbiology and biochemistry, especially in measuring important parameters such as growth, death, and enzyme kinetics.

The logarithm of a number is the exponent to which we must raise a base to obtain that number. The exponent is also known as the *index* or the *power*. For example, consider the number 1000 and the base 10; the number 10 is raised to the power 3 to obtain 1000; it follows that the logarithm to the base 10 of 1000 is 3. The base of a logarithm is conventionally written as a subscript. For example, the logarithm to the base 10 is written as $\log_{10}$ and the logarithm to the base e is written as $\log_e$. If a log is given without a subscript, it denotes a logarithm to the base 10. Logarithms to the base e ($\log_e$) are also called *natural logarithms*, which may also be written as In.

2.2.5.1 Use of Semilogarithmic Graph Paper

A *semilogarithmic* (semilog) graph paper is a graph paper that has an arithmetic scale on one axis and a logarithmic scale on the other. Although, it may appear very strange, it is user friendly and is very useful as it allows you to plot your data directly without having to calculate logs. On the logarithmic scale, there are a number of cycles. Each cycle represents a change in data of an order of magnitude, a factor of 10; any set of factors of 10 can be used, but remember that there is no zero on the log scale.

In plotting your data on semilog paper, the independent variable is plotted on the x-axis (abscissa), while the dependent variable is plotted on the y-axis (ordinate) of the graph. For example, in determining the mean generation time (T) of a given organism under certain conditions, time is the independent variable and is plotted on the x-axis, while the number of cells, which increases exponentially during the course of the logarithmic phase of growth, is plotted on the y-axis. However, it is noteworthy to remember that in determining the minimum inhibitory concentration (MIC) of antibiotics, the drug dosage increases in an exponential fashion and as such the log scale here becomes the x-axis.

2.3 GROWTH CYCLE

Now let us consider the basic equation used to describe microbial growth:

$$\frac{dx}{dt} = \frac{ax}{b} \tag{2.1}$$

While growth kinetics focuses on the measurement of growth rates during the course of fermentation, growth dynamics relates the changes in population (biomass) to changes in growth rate and other parameters (e.g., pH and temperature). To unravel such intricate interrelationships, the description of growth kinetics and growth dynamics relies on the use of differential equations.

Equation 2.1 implies that the rate of biomass (x) formation changes as a function of time (t) and that the rate of change is directly proportional to the concentration of a particular factor (a) such as growth substrate or temperature but is inversely proportional to the concentration of another factor (b) such as inhibitors. In Equation 2.1, both a and b are independent of time t, and

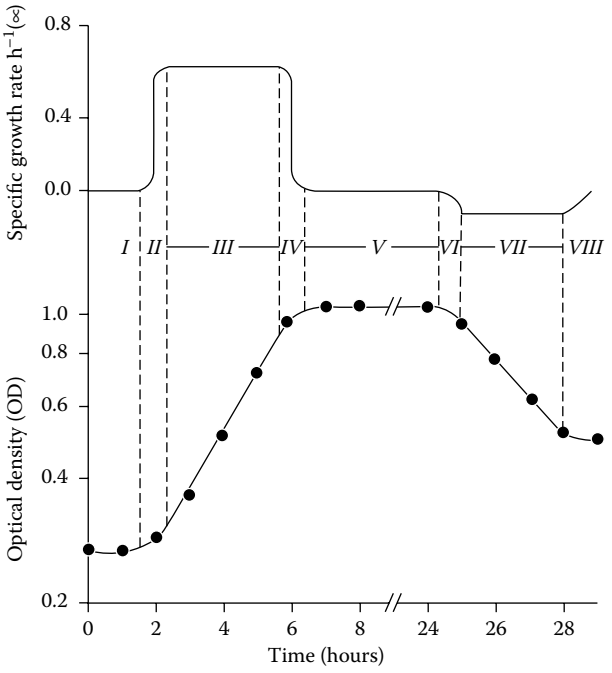

FIGURE 2.4 Typical pattern of growth cycle during the growth of microorganisms in batch cultures; the vertical dotted lines and the roman numerals indicate the changes in specific growth rate (μ) throughout the cycle.

the proportionality factor in Equation 2.1 can in effect be ignored. In the early stages of any fermentation process, the increase in biomass is unrestricted, and, as such, the pattern of growth follows an autocatalytic first-order reaction (autocatalytic growth) up to a point where either side of Equation 2.1 becomes negative, resulting in autocatalytic death.

The term *autocatalytic growth* is generally used to indicate that the rate of increase in biomass formation in a given fermentation is proportional to the original number of cells present at the beginning of the process, thus reflecting the positive nature of growth.

During batch fermentation, a typical pattern of growth curve, otherwise known as the *growth cycle*, is observed (Figure 2.4). Clearly, a number of different phases of the growth cycle can be differentiated. These are

The term *growth cycle* is used to describe the overall pattern displayed by microorganisms during growth in batch cultures. It is noteworthy that such a cycle is by no means a fundamental property of the bacterial cell, but rather a consequence of the progressive decrease in food supply or accumulation of inhibitory intermediates in a closed system to which no further additions or removals are made.

1. Lag phase
2. Acceleration phase
3. Exponential (logarithmic) phase
4. Deceleration phase
5. Stationary phase
6. Accelerated death phase
7. Exponential death phase
8. Death or survival phase

The changes in the specific growth rate (μ) as the organism progresses through the growth cycle can also be seen in Figure 2.4.

We shall now describe the metabolic events and their implications in as far as growth, survival, and productivity are concerned. Naturally, the scenario begins with the first phase of the growth cycle.

2.3.1 Lag Phase

In this phase, the organism is simply faced with the challenge of adapting to the new environment. While adaptation to glucose as a sole source of carbon appears to be relatively simple, competition with other carbon sources, although complex, is resolved in favor of glucose through the operation of two different mechanisms, namely, catabolite inhibition and catabolite repression.

Adaptation to other carbon sources, however, may require the induction of a particular set of enzymes that are specifically required to catalyze transport and hydrolysis of the substrate (e.g., adaptation to lactose) or to fulfill anaplerotic as well as regulatory functions, as is the case in adaptation to acetate as the sole source of carbon and energy. Irrespective of the mechanisms employed for adaptation, the net outcome at the end of the lag phase is a cell that is biochemically vibrant (i.e., capable of transforming chemicals to biomass).

Entering a lag phase during the course of industrial fermentation is not desirable as it is very costly and as such should be avoided. The question of whether a particular organism has entered a lag phase in a given fermentation process can be determined graphically by simply plotting log n (biomass) as a function of time, as shown in Figure 2.5.

Note that the transition from the lag phase to the exponential phase involves another phase: the acceleration phase, as described in Figure 2.4. This difficulty can be easily overcome by extrapolating the lag phase sideways and the exponential phase downward as shown, with the point of interception (L) taken as the time at which the lag phase ended. What is also interesting about the graph

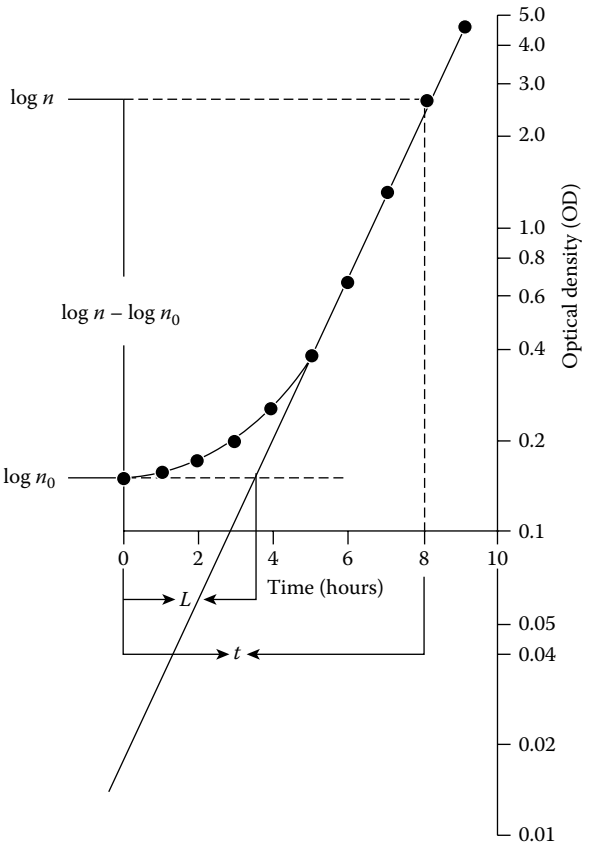

FIGURE 2.5 Graphical determination of the lag phase and the number of viable cells at the onset of batch fermentation; as the exponential phase is extrapolated downward, it intercepts the extrapolated line of the lag phase and the ordinate, respectively (see text for details).

in Figure 2.5 is that if one continues to extrapolate the exponential phase downward, then the point at which the ordinate is intersected gives the number of cells that were viable and metabolically active at the point of inoculation.

The question of whether a lag (L) has occurred during the course of the fermentation process and for how long can be easily determined by

$$\frac{\log n - \log n_0}{t - L} = \frac{\log 2}{T} \tag{2.2}$$

where n is the total number of cells after a given time (t) since the start of fermentation, n_0 is the number of cells at the beginning of fermentation, and T is the organism's mean generation time (doubling time). Equation 2.2 describes the exponential growth, taking into consideration a lag phase in the process. In Section 2.3.2, we shall describe the exponential phase in general and the derivation of Equation 2.2 in particular.

2.3.2 Exponential Phase

In this phase, each cell increases in size, and providing that conditions are favorable, it divides into two, which, in turn, grow and divide; and the cycle continues. During this phase, the cells are capable of transforming the primary carbon source into biosynthetic precursors, reducing power and energy, which is generally trapped in the form of ATP, phosphoenolpyruvate (PEP), and proton gradients. The biosynthetic precursors thus generated are then channeled through various biosynthetic pathways for the biosynthesis of various monomers (amino acids, nucleotides, fatty acids, and sugars) that, in turn, are polymerized to give the required polymers (proteins, nucleic acids, ribonucleic acids, and lipids). Finally, these polymers are assembled in a precise way, and the cell divides to give the new biomass characteristic of each organism (Figure 2.3). The time span of each cycle (cell division) is known as generation time or doubling time, but because we generally deal with many millions of cells in bacterial cultures, the term *mean generation time* (T) is more widely used to reflect the average generation times of all cells in the culture. Such a rate, providing conditions are favorable, is fairly constant.

Doubling time or mean generation time (T) is the time required for a given population (N_0) to double in number ($2N_0$).

If a given number of cells (n_0) is inoculated into a suitable medium and the organism was allowed to grow exponentially, then the number of cells after one generation is $2n_0$; at the end of two generations, the number of cells becomes $4n_0$ (or 2^2n_0). It follows, therefore, that at the end of a certain number of generations (Z), the total number of cells equals $2^Z n_0$. If the total number of cells, or its log value, at the end of Z generations is known, then

$$n = n_0 2^Z \tag{2.3}$$

$$\log n = \log n_0 + Z \log 2 \tag{2.4}$$

To determine the number of cell divisions, that is, the number of generations (Z) that have taken place during fermentation, Equation 2.4 can be modified to give

$$Z = \frac{\log n - \log n_0}{\log 2} \tag{2.5}$$

If T is the mean generation time required for the cells to double in number and t is the time span over which the population has increased exponentially from n_0 to n, then

$$Z = \frac{t}{T} = \frac{\log n - \log n_0}{\log 2} \tag{2.6}$$

If during the course of a particular fermentation, a lag time has been demonstrated, Equation 2.6 can be modified to take account of this observation. The modified equation is

$$Z = \frac{t - L}{T} = \frac{\log n - \log n_0}{\log 2} \tag{2.7}$$

Equations 2.6 and 2.7 can be rearranged to give the familiar equations governing the determination of T as follows:

$$\frac{\log n - \log n_0}{t} = \frac{\log 2}{T} \tag{2.8}$$

$$\frac{\log n - \log n_0}{t - L} = \frac{\log 2}{T} \tag{2.9}$$

While Equation 2.8 describes the exponential phase of growth in pure terms, Equation 2.9, however, takes into consideration the existence of a lag phase in the process.

The exponential scale (i.e., 2, 4, 8, 16, and so on) demonstrated in Figure 2.6 obeys Equations 2.8 for logarithmic growth. Note the different position of log n_0 to that cited in Figure 2.5.

Although the use of log to the base 2 has the added advantage of being able to determine the number of generations relatively easily, because an increase of one unit in log $2n$ corresponds to one generation, the majority of researchers continue to use log to the base 10. In this case, the slope of the line (Figure 2.6) equals $\mu/2.303$. The relationship between T and the specific growth rate (μ) can be described mathematically by

$$\ln 2 = \mu T \tag{2.10}$$

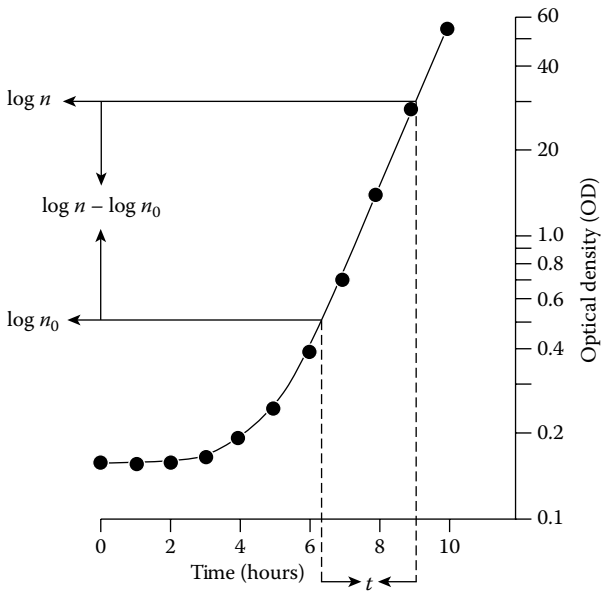

FIGURE 2.6 Graphical determination of the mean generation time (T) during batch fermentation; note the different position of log n_0 with respect to that in Figure 2.2.

or

$$\mu = \ln 2/T \tag{2.11}$$

Because ln 2 = 0.693, either Equation 2.10 or Equation 2.11 can be rearranged to give

$$T = \frac{0.693}{\mu} \tag{2.12}$$

During the course of exponential growth, the culture reaches a steady state. As such, the intracellular concentrations of all enzymes, cofactors, and substrates are considered to be constant. During this phase, one can therefore safely assume that all bacterial cells are identical and that the doubling time is constant with no loss in cell numbers due to cell death. The rate of growth of a given population (N) represents, therefore, the rate of growth of each individual cell in the population multiplied by the total number of cells. Such a rate can be described mathematically by this differential equation:

$$\frac{dN}{dt} = \mu N \tag{2.13}$$

This equation implies that the rate of new biomass formation is directly proportional to the specific growth rate (μ) of the organism under investigation and the number of cells (N). This pattern of growth may be referred to as *autocatalytic*, a term described in this chapter. If Equation 2.13 describes the exponential phase correctly, then a straight line should be obtained when ln N is plotted as a function of time (t). During the exponential phase, it is generally assumed that all cells are identical, and as such the specific growth rate (μ) of individual cells equals that of the whole population. Equation 2.13 can therefore be rearranged to take account of the fact that dN/dt is proportional to the number of cells (N) and that the specific growth rate (μ) is a proportionality factor to give

$$\mu = \frac{1}{N}\frac{dN}{dt} \tag{2.14}$$

The specific growth rate (μ) is usually expressed in terms of units per hour (h^{-1}).

Although Equations 2.9 and 2.10 describe the exponential phase satisfactorily, in some fermentations, as is the case during growth of *E. coli* on sodium acetate (El-Mansi unpublished results), the organism fails to maintain a steady state for any length of time and so μ falls progressively with time until the organism reaches the stationary phase. Such a drop in growth rate (μ) can be accounted for by a whole host of different factors, including nutrient limitations, accumulation of inhibitors, and/or the crowding factor (i.e., as the population increases in number, μ decreases).

2.3.2.1 Metabolic Interrelationship between Nutrient Limitations and Specific Growth Rate (μ)

To account for the effect of nutrient limitations on growth rate (μ), Monod modified Equation 2.14 so that the effect of substrate concentration (limitations) on μ could be assessed quantitatively. Monod's equation is

$$\mu = \frac{\mu_m S}{K_S + S} \tag{2.15}$$

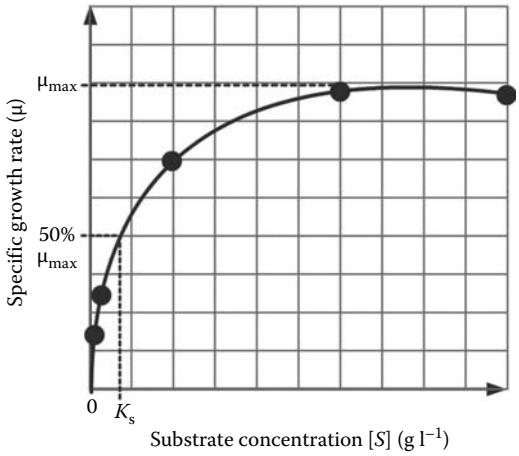

FIGURE 2.7 Graphical determination of specific growth rate (μ) and saturation constant (K_S) during batch fermentations; note that this graph was constructed without taking maintenance energy into consideration. With maintenance in mind, the curve should slide sideways to the right in direct proportion to the fraction of carbon diverted toward maintenance.

where S is the concentration of the limiting substrate, μ_m is the maximum specific growth rate, and K_S is the saturation constant (i.e., when $S = K_S$, then $\mu = \mu_m/2$), as illustrated in Figure 2.7.

During growth in a steady state, Equations 2.16 and 2.17 may be used to describe growth using biomass (X) rather than the number of cells (N) as a measure of growth:

$$\frac{dX}{dt} = \mu X \tag{2.16}$$

$$\frac{dS}{dt} = -\mu \frac{X}{Y} \tag{2.17}$$

where X is the biomass concentration and Y is the growth yield (e.g., biomass generated per gram of substrate utilized). It is noteworthy, however, that during steady-state growth (i.e., in a chemostat or a turbidostat), the terms used to describe the bacterial numbers (N) and biomass (X) in Equations 2.16 and 2.17 are identical. This is not necessarily the case in batch cultures because the size and shape of bacterial cells vary from one stage of growth to another.

While Equation 2.16 addresses the relative change in biomass (the first variable) with respect to time, Equation 2.17 addresses the relative change in substrate concentration (the second variable) as a function of time. Note that following the exhaustion of substrate, $dX/dt = dS/dt = 0$. While Equations 2.16 and 2.17 can surely predict the deceleration and stationary phases of growth, respectively, it should be remembered that nutrient limitation is not the only reason for the deceleration of growth and subsequent entry into the stationary phase. In addition to environmental factors, crowding is reported to have an adverse effect on growth rate (μ), that is, growth rate diminishes as the size of the population increases. Although the equation describing the effect of crowding on growth rate (the Verhulst–Pearl logistic equation) predicts a sigmoidal pattern of growth and fits rather well with the growth curve for populations of higher organisms, yeasts, and bacteria, it will not be further discussed in this chapter as it overlooks the effect of other environmental factors on growth.

2.3.3 Stationary Phase and Cell Death

As the exponential phase draws to an end, the organism enters the stationary phase and thence the death phase. If we assume that the kinetics of death are similar to that of growth, then the specific rate of cell death (λ) can be described mathematically by

$$\frac{dN}{dt} = (\mu - \lambda)N \tag{2.18}$$

Equation 2.18 clearly indicates that if μ is greater than λ, then the organism will grow at a rate equal to μ − λ. If, on the other hand, μ is less than λ, then the population dies at a rate equal to λ − μ. Under conditions where μ equals λ, neither growth nor death is observed, a situation thought to prevail throughout the course of the stationary phase. As the energy supply continues to fall, the equilibrium between λ and μ will finally shift in favor of λ, and consequently cell death begins.

Microorganisms respond differently to nutrient limitations during the stationary phase. For example, while *Bacillus subtilis* and other Gram-positive, spore-forming organisms respond by sporulation, *E. coli* and other Gram-negative, non-spore-forming bacteria cannot respond in the same way, and as such other mechanisms must have evolved. Although a fraction of the bacterial population dies during this phase of growth, a relatively large number remain viable for a long time despite starvation. The ability of cells to remain viable despite prolonged periods of starvation is advantageous, as most microorganisms in nature are subject to nutrient limitations in one form or another. Our understanding of the molecular mechanisms employed by microorganisms for survival during this phase of growth is rather limited. However, contrary to the notion that microorganisms enter a logarithmic death phase soon after the onset of the stationary phase, some microorganisms such as *S. cerevisiae* and *E. coli* adapt well to starvation, presumably through mutations and induction mechanisms, and do not readily enter a logarithmic phase of death.

The ability of some cells to survive prolonged starvation inspired some researchers to pursue the question of whether such cells are biochemically distinguishable from their predecessors, which were actively growing or had just entered the stationary phase. In the case of *S. cerevisiae*, analysis of mRNAs, which are specifically expressed following the onset of the stationary phase, revealed the presence of a new family of genes. This family is referred to as SNZ (short for *snooze*); sequence analysis revealed that they are highly conserved. The functional role of each member of this family, however, remains to be determined. It is interesting that some researchers use the term *viable but nonculturable* (VBNC) to describe cells in the stationary phase. However, as colony-forming ability is our only means of assessing whether a particular cell is alive or not, other microbiologists argue the case for reversibility, that is, the cell's ability to transform from being dormant to being metabolically active. Recent investigations have revealed that resuscitation of stationary phase cells may be aided by the excretion of pheromones as has been demonstrated in *Micrococcus luteus.*

In the case of *E. coli*, an attempt was made to identify the genes that are uniquely turned on in the stationary phase in response to starvation, that is, not expressed during the exponential phase, with the aid of random transposon mutagenesis. A number of mutants unable to survive in the stationary phase were isolated and subsequently designated as survival negative mutants (Sur^-). As such, the genes involved were designated as *sur* genes. While some genes, such as *surA*, are required for survival during "famine" (starvation), others such as *surB* enable the organism to exit the stationary phase as conditions change from "famine" to "feast." Recent studies have also revealed that starvation induces the production of a stationary phase-specific transcriptional activator (sigma factor) that is essential for the transcription of *sur* genes by RNA polymerase. The physiological function of the *sur* gene products is to downshift the metabolic demands made on central and intermediary metabolism for maintenance of energy.

2.3.4 Maintenance and Survival

Maintenance can be defined as the minimal rate of energy supply required to maintain the viability of a particular organism without contributing to biosynthesis. The fraction of carbon oxidized in this way is, therefore, expected to end up in the form of carbon dioxide (CO_2). The need for maintenance energy is obvious as the "living state" of any organism, including ourselves, is remote from equilibrium and as such demands energy expenditure. Moreover, in addition to the carbon processed for maintenance, another fraction of the carbon source may be wasted through excretion (e.g., acetate, α-ketoglutarate, succinate, or lactate). In this context, excretion of metabolites ought to be seen as an accidental consequence of central metabolism rather than by design to fulfill certain metabolic functions. The fraction of carbon required for maintenance differs from one organism to another and from one substrate to another. For example, maintenance requirements for the lactose phenotype of *E. coli* are greater than those observed for the glucose phenotype as the *lac*-permease is much more difficult to maintain than the uptake system employed for the transport of glucose, that is, the phosphotransferase system (PTS).

The metabolic interrelationship between maintenance and growth was first described by Pirt (1965). In his theoretical treatment of this aspect, he formulated a maintenance coefficient (m) based on the earlier work of Monod and defined the coefficient as the amount of substrate consumed per unit mass of organism per unit time (e.g., g substrate per g biomass per h). If s represents the energy source (substrate), then the rate of substrate consumption for maintenance is governed by

$$-\left(\frac{ds}{dt}\right)_{\mathrm{M}} = mX \tag{2.19}$$

where m is the maintenance coefficient. The yield can therefore be related to maintenance by

$$Y = \frac{\mathrm{D}x}{(\mathrm{D}s)_{\mathrm{G}}(\mathrm{D}s)_{\mathrm{M}}} \tag{2.20}$$

where Y is the growth yield, Δx is the amount of biomass generated, $(\Delta s)_{\mathrm{G}}$ is the amount of substrate consumed in biosynthesis, and $(\Delta s)_{\mathrm{M}}$ is the amount of substrate consumed for maintenance of cell viability.

If maintenance energy $(\Delta s)_{\mathrm{M}}$ was determined and found to be zero, then Equation 2.20 reduces to

$$Y_{\mathrm{G}} = \frac{\mathrm{D}x}{(\mathrm{D}s)_{\mathrm{G}}} \tag{2.21}$$

Equation 2.21 clearly means that growth yield (Y) is a direct function of the amount of substrate utilized. The growth yield (Y, gram dry weight per gram substrate) obtained in this case may be referred to as the *true growth yield* to distinguish it from the Y_{G} where maintenance $(\Delta s)_{\mathrm{M}}$ is involved. However, if a specific fraction of carbon is diverted toward maintenance energy or survival, then one might conclude that the slower the growth rate (μ), the higher the percentage of carbon that is diverted toward maintenance, and the less the growth yield.

On the other hand, during unrestricted growth (i.e., no substrate limitation), the interrelationship between substrate concentration and maintenance can be determined by (Pirt 1965)

$$ds/dt = (ds/dt)_{\mathrm{M}} + (ds/dt)_{\mathrm{G}} \tag{2.22}$$

In this case, Equation 2.22 implies that the overall rate of substrate utilization equals the rates of substrate utilization for both maintenance and growth. With growth rate expressed in the usual way ($dx/dt = \mu x$), and assuming that Y equals Y_G, Equations 2.16 and 2.18 can be rearranged to give

$$1/Y = m/\mu\ 1/Y_G \tag{2.23}$$

According to Equation 2.23, if m and Y_G are constants, then the plot of $1/Y$ against $1/\mu$ should give a straight line, the slope of which is maintenance (m) and the point at which the ordinate is intercepted is equal to $1/Y_G$, as illustrated in Figure 2.8. Further analysis of the data shown in Figure 2.8 (El-Mansi unpublished results) revealed that *E. coli* is capable of shifting down its maintenance requirements during growth on acetate from 5.8 mmoles per gram biomass per hour during exponential growth in batch culture and turbidostat to 0.55 mmoles per gram biomass per hour during growth in a chemostat at a low growth rate.

During the course of fermentation, the minimum rate of energy supply may fall below maintenance requirements due to a shortfall in the supply of phosphorylated intermediates, ATP, and/or reducing powers (NADH, NADPH, $FADH_2$, etc.). Although such a drop in energy supply may not be fatal, it is likely to have an adverse effect on the fitness of the organism; the cells become less capable of taking advantage of favorable changes in the environment, and consequently cells resume growth after a lag period. On the other hand, if the cells were able to grow immediately following inoculation or transfer into another medium (i.e., without lag), then the cells must have been left in optimal conditions. However, if the cells were to enter the lag phase prior to growth, then it is fair to suggest that the organism was left in a suboptimal state, that is, the organism must have suffered a drop in energy supply below its maintenance requirements.

Ribosome particles, which consist of protein and RNA, are the target to which mRNA and amino acyl-tRNA must bind in preparation for translation (the conversion of mRNA to a polypeptide chain).

It follows, therefore, that the physiological state of the cell at the time when energy supply falls below maintenance is very important and that the deeper the shortfall in energy supply, the longer the lag period. A lag period due to the lack of energy sources is surely different to that observed when the cells are faced with the challenge of changing phenotype, as is the case when glucose phenotype of *E. coli* is forced to change to lactose phenotype. Individual cells in a given population may respond differently when a given drop of energy supply is exerted. The ability of a given population to respond successfully to a "shift-up" or to survive a "shift-down" in nutrients appears to be directly related to the intracellular concentration of ribosomes. For example, in comparison with cells grown in rich medium, restricted growth of *Salmonella typhimurium* was accompanied by a 35-fold drop in the concentration of ribosomes. In the yeast *S. cerevisiae*, a drop in growth rate from 0.40 h^{-1} to 0.10 h^{-1} was accompanied by a drop in the cellular concentrations of

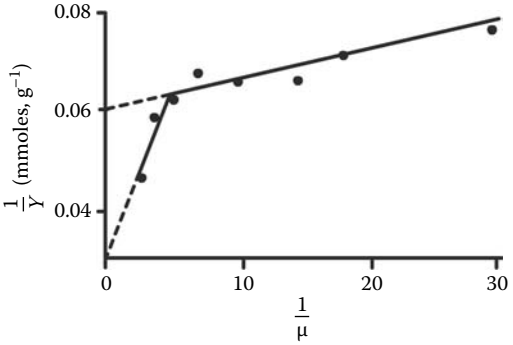

FIGURE 2.8 Graphical determination of maintenance (m) energy.

RNA, DNA, and proteins from 12.1%, 0.6%, and 60.1% to 6.3%, 0.4%, and 45%, respectively (Nissen et al. 1997). Furthermore, it was also demonstrated that the cells of *S. cerevisiae* were capable of "scaling up" or "scaling down" the intracellular level of ribosomes in response to the shift-up or the shift-down in nutrients, respectively.

Autogenous regulation: a regulatory control mechanism that is exerted at the level of translation; the conversion of mRNA to protein, rather than transcription.

Recent investigations revealed that such ability to modulate the cellular content of ribosomes is achieved through a mechanism of autogenous (posttranscriptional) regulation.

To account for such a phenomenon, Nomura et al. (1984) proposed a new hypothesis, translational couplings, which simply implies that binding to and initiation of translation at the first ribosome-binding site of the operon are essential in exposing the ribosome-binding sites of all other cistrons and that inhibition or prevention of translation at the first binding site means that all other sites within the polycistronic message will remain unexposed and as such will not be translated.

The argument over the question of whether smaller cells are less able to cope with environmental changes (i.e., nutrient limitations and the drop in energy supply below maintenance) because they contain less ribosomes can now be answered to the satisfaction of everyone as recent research revealed that it is not the number of ribosomes that matter but rather their concentration inside the cell. Furthermore, the need for the cell size to be relatively large during growth under no limitations is not a reflection of high concentration of ribosomes but rather the need to attain a certain mass before replication of the chromosome can be initiated (Donachie 1968). The essence of Donachie's discovery is that if initiation of replication is triggered in response to a certain volume of cell mass, then the faster the cell divides, the faster the growth rate, and the larger the size of the cell.

In addition to induction and autoregulatory control mechanisms, successful transition from one phase of growth to another might also involve proteolysis, a mechanism that is particularly significant when the cells have to remove certain proteins at a rate that is significantly higher than their specific growth rate (μ), such as key regulatory proteins that fluctuate from one phase of growth to another (Grunenfelder et al. 2001) and those that are specific to a particular phase of growth and might be detrimental to the organism as it switches to another phase (Weichart et al. 2003).

2.4 DIAUXIC GROWTH

Catabolite inhibition is a mechanism that, in the presence of glucose, prevents the uptake of lactose, thus allowing preferential utilization of glucose.

Catabolite repression is a glucose-induced mechanism, which switches off the synthesis of the *lac*-operon enzymes at the level of transcription, thus facilitating preferential utilization of glucose.

The ability of microorganisms to display biphasic (diauxic) growth patterns is well documented. For example, *E. coli* displays such a pattern when faced with glucose and lactose (Figure 2.9). Similarly, *Aerobacter aerogenes* displays the same pattern when grown in the presence of glucose and citrate. Both organisms preferentially utilize glucose to either of the competing substrates, due to catabolite inhibition and catabolite repression mechanisms elicited by the presence of glucose.

2.5 GROWTH YIELD IN RELATION TO CARBON AND ENERGY CONTENTS OF GROWTH SUBSTRATES

Unlike growth on sugars and polyhydrated alcohols, where a constant yield of 1.1 g dry weight biomass per gram substrate carbon was observed, growth yield on carboxylic acids gives a much inferior yield. An attempt to resolve this paradox was made (Linton and Stephenson 1978) by relating the maximum specific growth yield observed on any given carbon source to its carbon and energy content; the latter is defined by the heat combustion (kcal/g substrate carbon). Although the authors recognized the need for using chemostats to achieve steady-state growth and to account for maintenance energy requirements, their analysis of various data in the literature revealed that

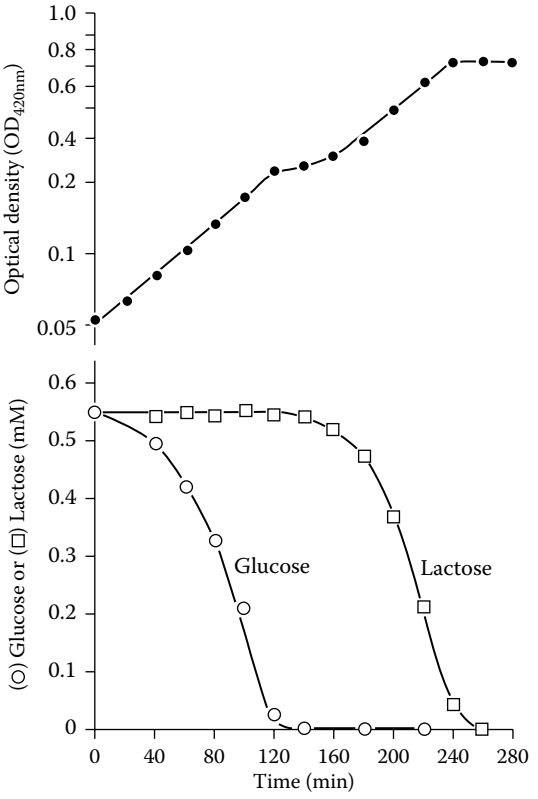

FIGURE 2.9 Diauxic pattern of growth and the pattern of sugar utilization during growth of *E. coli* ML30 on equimolar concentrations (0.55 mM) of glucose and lactose.

the growth yield was directly proportional to the heats of combustion up to 11.00 kcal/g substrate carbon and that beyond this level no increase in yield was observed, suggesting the involvement of another mechanism. It is possible, therefore, to argue that during growth on substrates with a heat of combustion value of less than 11.00 kcal/g substrate, the energy generated is insufficient to convert all the available carbon to biomass, and as such growth may be described as energy limited. Further analysis revealed that maximum growth yield is inherently set by the ratio between the biologically available energy and the carbon contents of the substrate. Assuming a bacterial carbon content of 48%, the maximum yield of 1.43 g bacterial dry weight per gram substrate carbon, representing a maximum carbon (substrate) to carbon (biomass) conversion of 68%, was observed. This treatment enables the prediction of growth yield with a good degree of accuracy and provides a rational basis for growth limitations; for example, while glycerol- and mannitol-limited growth of *A. aerogenes* may be described as carbon limited, gluconate-limited growth may be viewed as energy limited.

The relative contribution of each substrate to total biomass formation can also be assessed with a good deal of precision providing that growth limitation is a consequence of diminishing carbon supply in a chemostat rather than the accumulation of toxic end products or adverse changes in pH. The relationship between total biomass formation and the concentration of any given substance can therefore be determined from the plot of log n (biomass) as a function of substrate concentration, and providing that all other components are in excess, the organism will enter the stationary phase upon depletion of the substrate or the substance in question. This experiment should obviously be done over a wide range of substrate concentrations, and from the slope obtained, the yield constant or yield coefficient per unit of the substance in question can be determined. If the unit is, say, one

mole of a substrate, then the yield coefficient obtained is referred to as the molar growth yield coefficient. This method is used widely as a biological assay for the determination of vitamins, amino acids, purines, and pyridines.

2.6 FERMENTATION BALANCES

2.6.1 Carbon Balance

Apart from the fraction of carbon used for biomass formation, the remainder is partitioned between products and by-products, including carbon dioxide. The ratio of recovered carbon to that present at the onset of fermentation is referred to as the *Carbon Balance* or *Carbon Recovery Index*. Such a balance or an index is a measure of efficiency: the higher the index, the higher the carbon recovery, and the more efficient the fermentation process. The carbon balance is generally calculated by working out the number of moles (or millimoles) produced of a given product per 100 moles (or millimoles) of substrate utilized. The values obtained can then be multiplied by the number of carbon atoms in each respective molecule. The resulting values for the products in question can then be totaled and compared with that of the substrate. If the values are equal (i.e., a 1:1 ratio), then a complete recovery of carbon into product formation has been achieved. Although this is theoretically possible, our experience indicates otherwise, as part of this carbon is used for maintenance and assimilation to support growth, however slow. A complete carbon balance can, therefore, be calculated for any given fermentation if the fraction of carbon diverted toward biosynthesis and maintenance is determined. In addition to the carbon balance, some fermentations demand calculation of the redox balance.

2.6.2 Redox Balance

Fermentations of sugars and other primary carbon sources give rise to a whole host of different intermediates; some of these are phosphorylated (energy-rich), while others are not. While biosynthetic intermediates are utilized for the biosynthesis of monomers, other intermediates are produced in excess and this is balanced by their excretion into the medium. The stoichiometry of product and by-product formations of any given fermentation process can be ascertained by carefully analyzing the culture filtrates at different stages. From a physiological standpoint and in order for fermentation to go to completion, the redox balance must be maintained.

2.7 EFFICIENCY OF CENTRAL METABOLISM

2.7.1 Impact of Futile Cycling on the Efficiency of Central Metabolism

The efficiency of carbon conversion to biomass and desirable end products is influenced by many different factors (see Chapters 3, 6, and 7 for more details) of which futile cycling is a major contributor. For example, any transient increase in the intracellular concentration of pyruvate in *E. coli* may trigger a futile cycle in the central metabolic pathways at the junction of PEP. Futile cycling at the junction of PEP (Figure 2.10) involves, in addition to pyruvate dehydrogenase and malic enzyme, PEP carboxykinase and pyruvate kinase (ATP-generating reactions) on one hand and PEP-synthetase and PEP-carboxylase (ATP-utilizing reactions) on the other. The operation of this futile cycle may, in addition to wasting ATP, adversely affect the adenylate energy charge within the cell. Transient increase in the intracellular level of pyruvate may also trigger futile cycling in other organisms. For example, *K. aerogenes* triggers a futile cycle involving two enzymes: the first is the NAD^+-dependent pyruvate reductase, which catalyzes the transformation of pyruvate to D-lactate, and the second is the FAD-dependent D-lactate dehydrogenase, which completes the cycle (Figure 2.11). Flux of carbon through these two enzymes provides a futile cycle in which NADH is oxidized at the expense of reducing FAD^+, thus bypassing the first phosphorylation site

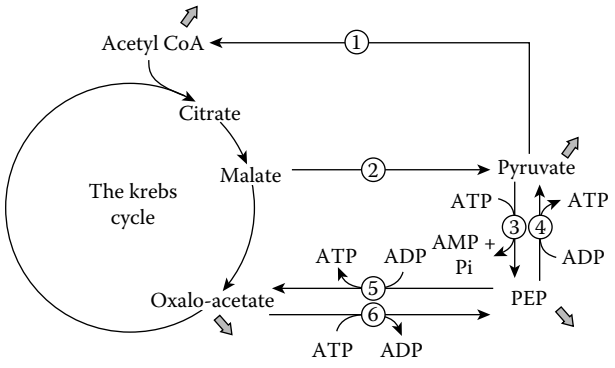

FIGURE 2.10 Futile cycle at the level of phosphoenolpyruvate (PEP) in central metabolism and its role in energy dissipation.

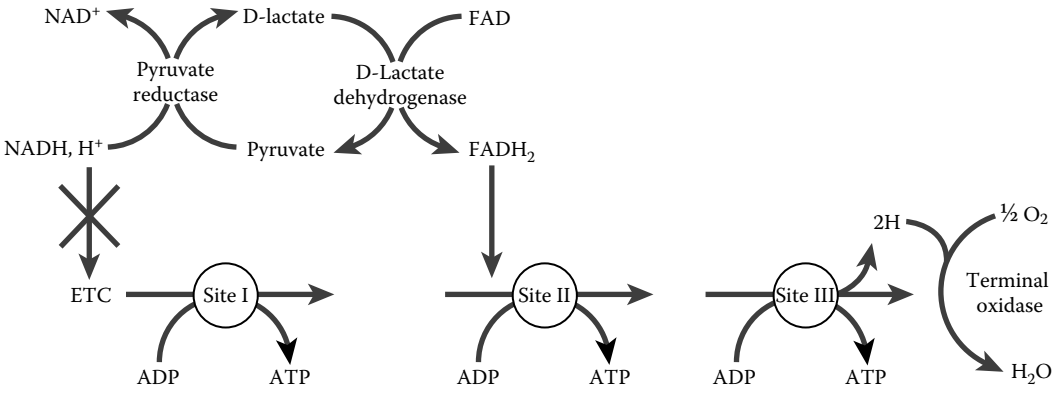

FIGURE 2.11 The role of pyruvate reductase and D-lactate dehydrogenase in bypassing the first phosphorylation site of the electron transport chain (ETC) in the oxidation of NADH, H^+.

in the electron transport chain (Figure 2.11). It follows, therefore, that any changes leading to transient increase in the intracellular level of pyruvate may lead to the operation of this futile cycle and, in turn, energy dissipation. The presence and function of glutamine synthetase and glutamines in ammonia-limited cultures represent yet another possible futile cycle (Figure 2.12) in which the synthetase generates glutamate while the other affects its hydrolysis with a net loss of one molecule of ATP per turn (Tempest 1978).

2.7.2 Impact of Metabolite Excretion on the Efficiency of Central Metabolism

Excretions of metabolites in general and acetate in particular diminish flux to product formation, which, in turn, adversely affects the efficiency of carbon conversion to desirable end products (El-Mansi 2004). Acetate, particularly in its undissociated form, is a potent uncoupler of oxidative phosphorylation. As such, conditions that promote flux to acetate excretion will, in turn, diminish flux to product formation, as a large fraction of the carbon source has to be diverted toward maintenance requirements (El-Mansi unpublished observations). While such a role is fully appreciated, it should be remembered that flux to acetate excretion is physiologically significant as it allows faster growth rate and facilitates high cell density growth

Chemostat: a continuous culture in which growth rate is limited by the rate of nutrients supply.

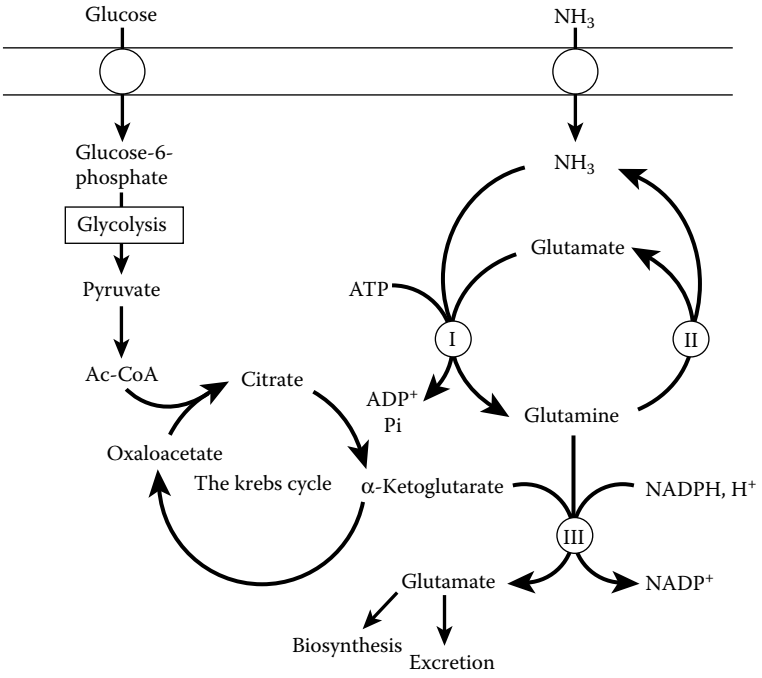

FIGURE 2.12 The role of glutamine synthetase and glutaminase in energy dissipation through the formation of a futile cycle.

(El-Mansi 2004). Flux to acetate excretion is also important as flux through phosphotransacetylase replenishes central and intermediary metabolism with free-CoA, thus fulfilling an anaplerotic function (El-Mansi 2005) that is central for the smooth operation of carbon flux through enzymes of central and intermediary metabolism. Interestingly, flux through pyruvate oxidase to acetate excretion, which may appear to be wasteful, has recently been shown to be equated with higher efficacy of growth and energy generation (Guest et al. 2004).

2.8 CONTINUOUS CULTIVATION OF MICROORGANISMS

Turbidostat: a continuous culture in which the organism grows at its maximum specific growth rate (μ_{max}), thus reaching a steady state of fixed turbidity.

The use of continuous cultures in the fermentation industry is, in some cases, preferred to batch cultures for the following reasons:

- It outperforms batch cultures economically by eliminating the inherent downtime that is lost for cleaning, sterilization, and the reestablishing of biomass within the bioreactor.
- Unlike batch cultures where the rate of product formation is at its peak for only a limited period of time, continuous cultures sustain such a period over a much longer span of time.
- The interpretation of data obtained from continuous cultures is much simpler than from batch cultures because continuous cultures afford a steady-state growth in which input and output are in perfect balance, unlike batch cultures where variations in the concentrations of primary carbon and nitrogen sources, product formation, pH, and the redox balance within the cells vary during the course of growth.
- Unlike batch cultures, continuous cultures can be manipulated to create certain environmental conditions to facilitate overexpression of recombinant proteins.

The earliest continuous fermentation process on record is the production of vinegar by *Acetobacter* sp. In this process, a sugar solution is trickled down a bioreactor containing cells of *Acetobacter* sp. adhered to wood shavings, the earliest recorded example of cell immobilization. The acetic acid produced renders the conditions inhospitable for other organisms, thus minimizing the risk of contaminations.

It is noteworthy, however, that the use of continuous cultures in the fermentation industry is much less common than batch processes primarily because quality control regulation stipulates the need for a "batch number." Furthermore, continuous cultivations are much more susceptible to contamination, which is rather risky especially in the production of bioactive pharmaceuticals.

2.8.1 Types of Continuous Cultures

There are three main types of continuous cultures: **chemostat, turbidostat**, and **auxostat**; the latter reflects the set parameter (e.g., pH-stat).

In an auxostat, the feeding rate is adjusted to match the rate of cellular metabolism. In that sense, a turbidostat is also an auxostat because the turbidity created as a consequence of bacterial growth is maintained at a set point by adjusting the rate of supply of fresh medium. The most popular auxostat, however, is the pH auxostat (pH-stat), a continuous culture in which pH is maintained at a set point by the addition of NaOH to counterbalance the excreted acetate and other acidic by-products.

Auxostat, nutristat, and *pH-stat* are synonymous names for a continuous culture in which the dilution rate changes to maintain a certain factor constant.

2.8.2 Principles and Theory of Continuous Cultures

Although the calculations of different growth parameters during growth in continuous cultures cultivation of microorganisms are based on the growth kinetics of exponentially growing unicellular organisms, such calculations can be equally applied to multicellular organisms (e.g., filamentous fungi).

A good continuous culture maximizes the number of biochemically active cells in the population while keeping the number of biologically inactive cells to a minimum.

2.8.2.1 Microbial Growth Kinetics in Continuous Cultures

The theories underlying growth kinetics can be represented by a number of equations, shown here.

***Specific growth rate* (μ)**: This parameter (Figure 2.13) can be calculated using

$$\frac{dx}{dt} = \mu(h^{-1}) \tag{2.24}$$

where dx is the change in biomass (Δ biomass), dt is the duration of time during which the measured increase in biomass has taken place (Δ time), and μ is the specific growth rate h^{-1}.

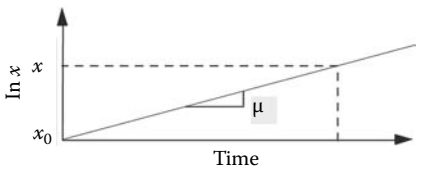

FIGURE 2.13 Graphical determination of specific growth rate (μ).

Doubling time **(T_d)** ***or mean generation time*** **(T)**: This parameter can be calculated using

$$T_d = \ln 2 / \mu \tag{2.25}$$

where ln 2 is the natural log of 2, which is 0.693, and μ is the specific growth rate.

Dilution rate **(D)**: This parameter can be measured using

$$D = F / V \tag{2.26}$$

where F is the flow rate (ml/min) and V is the volume (ml) of culture in the fermentation vessel.

During growth in continuous culture, the rate of change in the organism's concentration equals the organism's growth rate minus the rate of removal of the organism from the culture vessel. The rate of change in the concentration of biomass can therefore be calculated by

$$dx / dt = \mu - D \tag{2.27}$$

The Monod constant:

The Monod constant (Figure 2.7) can be calculated using Equation 2.28:

$$\mu = \mu_{max} S / S + K_S \tag{2.28}$$

where μ_{max} is the maximum specific growth rate, S is the substrate concentration, and K_S is the substrate concentration at which μ equals ½ μ_{max}.

2.8.2.2 Interrelationship between Growth Rate (μ) and Dilution Rate (D)

During steady-state growth in a chemostat (Equation 2.27), the rate of change in the concentration of both biomass ($dx / dt = 0$) and the limiting substrate ($ds / dt = 0$) equals zero. It follows, therefore, that during growth in a chemostat, where growth is limited by a given nutrient, D equals μ.

During growth in continuous cultures, however, the dilution rate (D) might exceed (μ), and the point at which D becomes larger than μ (Figure 2.14) is known as the critical dilution rate (D_c).

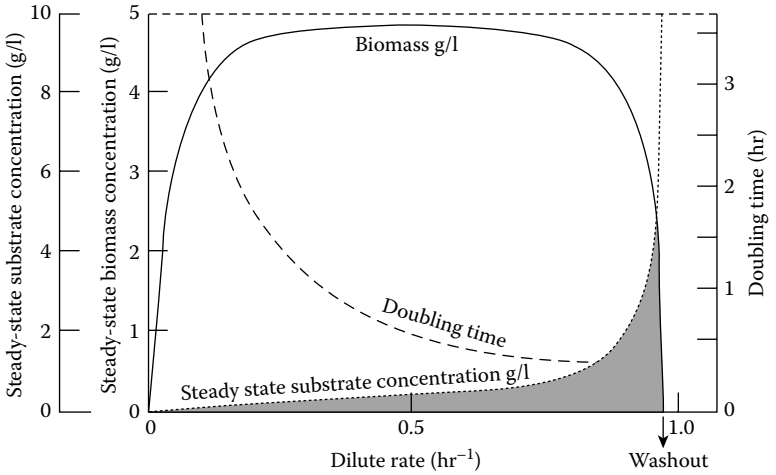

FIGURE 2.14 Impact of dilution rate (D) on doubling time (T), substrate concentration (S), and biomass formation (X) during continuous cultivation of microorganisms.

Whenever D > μ, a washout of biomass occurs. It follows that one can determine the maximum specific growth rate, μ_{max}, by increasing the flow rate past the critical dilution rate (D_c) and follow the decrease in biomass concentration over a period of time. The μ_{max} can then be determined using Equation 2.29:

$$\mu_{max} = [\ln X - \ln X_0 / t] + D \tag{2.29}$$

This impact of dilution rate (D) on biomass formation, the rate of change in biomass formation, the doubling time, and the concentration of substrate illustrated in Figure 2.14 can be described by Equation 2.30:

$$ds / dt = D (S_R - S) - \mu x / Y \tag{2.30}$$

where S_R is the concentration of the limiting substrate in the reservoir and Y is the biomass yield on that particular substrate.

Since $dx / dt = 0$ and $(ds / dt = 0)$ during steady-state growth in a chemostat, the steady-state values of biomass (X') and substrate (S') can be calculated using Equation 2.31:

$$X' = Y (S_R - K_S D) / (\mu_{max} - D) \tag{2.31}$$

where K_S is the limiting-substrate constant (the Monod constant).

2.8.2.3 Efficiency and Productivity of Fermentation Processes

The productivity of a given bioprocess is a significant factor and often plays a central role in deciding which fermentation process (batch, fed batch, or continuous) should be employed. Such a parameter can be assessed by (Pirt 1975)

$$\text{Productivity index} = \ln X_m / X_0 + 0.693 t_L / t_d \tag{2.32}$$

where X_0 and X_m are the initial and maximum biomass concentrations, respectively; t_L is the total shutdown time of a batch process; and t_d is the doubling time.

2.9 CURRENT TRENDS IN THE FERMENTATION AND PHARMACEUTICAL INDUSTRY

Although mammalian cell and other eukaryotic cell cultures like the yeast *Pichia* represent an attractive alternative to bacteria for the expression and production of recombinant proteins, especially those requiring posttranslational modification such as glycosylation, recombinant protein expression in bacteria remains the most cost-effective, and as such, from an industrial perspective, it is the most desirable option particularly since the development of tightly regulated promoters such as the T7 polymerase-specific promoter. In this case, effective control through repression ensures that expression and, in turn, production are turned off until significant biomass is formed, which is significant if the product was toxic in nature. Ingenious and effective approaches have recently been developed in bacterial expression systems including modification of ribosome-binding sites to increase yield, and expression at low temperature on its own and in combination with the expression of molecular chaperones, which reduce misfolding and precipitation of proteins, to aid correct folding of recombinant proteins.

2.9.1 "Quiescent Cell Factory": A Novel Approach

A nongrowing bacterial culture in which the primary nutrients are directly and quantitatively converted to products represents the ideal scenario for biotechnology. However, this is very difficult to achieve, and an alternative approach is to render transcription and translation processes to be gene specific. Although this approach may seem insurmountable, specific expression of certain proteins in eukaryotic organisms is a well-established phenomenon. Attempts to develop a bacterial system that mimics eukaryotic organisms in that direction led to the discovery of the *E. coli* "Quiescent Cell Protein Expression System," otherwise referred to as the Q-cells (Summer 2002).

Overexpression of Rcd in the mutant strain bns205, which apart from being defective in *bns* is capable of producing an N-terminal fragment of H-NS, led to a complete cessation of growth within 2–3 hours and the cells entered a quiescent (nongrowing) state (Summer 2002). Fortuitously, the Q-cells appear to preferentially express the plasmid encoded rather than the chromosomally encoded genes. The reason for this odd but useful feature was unraveled by the same author following DAPI–DNA staining and examination of Q-cells using fluorescence microscopy, which revealed that the bacterial nucleoid was highly condensed; this was a consequence of Rcd/H-NS complex formation, thus preventing its expression in a manner reminiscent of that observed for heterochromatin formation in eukaryotes, which results in global repression of transcription. The Q-cell system has now been shown to function well at the pilot scale and was not unduly sensitive to media composition or culture density. The Q-cell system is currently employed for the production of recombinant proteins. Further developments are currently underway for its adoption in other systems (Summer 2002).

Nucleoid: a structure within the bacterial cytoplasm representing the chromosome together with associated proteins.

2.9.2 Applications of Batch-Fed Two-Stage Fermentation in the Production of Biopharmaceuticals: A Robust Approach

The need to develop new methodologies and innovations for the production of biopharmaceuticals is considered an urgent need, so that we can effectively increase their production without compromising their affordability or safety. The prevalence of diabetes is expected to scale new heights; no less than 366 million people are projected to be diabetics by the year 2030. An increase in the production of insulin must therefore be planned to meet the projected rise in demand.

To that end, Gurramkonda et al. (2010) developed a two-stage cultivation process in which a recombinant strain of *Pichia pastoris* (strain X-33) carrying a synthetic insulin-precursor encoding gene fused in frame with the alpha-factor secretory signal peptide of *S. cerevisiae*.

The X-33 strain was first grown to high cell density in batch cultures on a low-salt and high-glycerol minimal medium. Following batch culture growth, the expression of the insulin precursor-fusion gene was achieved by growing the organism in a fed-batch culture on methanol (2 g l^{-1}); the concentration of methanol was kept constant throughout the production phase. This robust-batch and fed-batch two-stage strategy led to the secretion of nearly 4 g of insulin precursor per liter of culture supernatant. With the aid of immobilized metal ion affinity chromatography (IMAC), a novel approach in protein purification, 95% of the secreted product was recovered. The purified insulin precursor was trypsin digested and further purified, leading to approximately 1.5 g of 99% pure recombinant human insulin per liter of culture broth. Compared with the highest previously reported value, this approach resulted in an increase in the efficiency of insulin production by a factor of nearly 200%, thus significantly increasing the efficiency of insulin manufacture.

2.10 MICROBIAL FERMENTATIONS AND THE PRODUCTION OF BIOPHARMACEUTICALS

Throughout this chapter, we have outlined the principles underlying microbial fermentation in general. The case study given in Section 2.10.1, however, illustrates the applications of microbial fermentation for the commercial production of useful products.

2.10.1 Production of Insulin: A Case Study

2.10.1.1 History and Background

In addition to maintaining glucose concentration in blood within a certain range, thus avoiding hyperglycemia, insulin also stimulates lipogenesis, activates amino acids uptake, and diminishes lipolysis.

The biologically active insulin is a monomer consisting of two polypeptide chains A and B, 21 and 30 amino acid residues in length, respectively, that are interlinked through two disulfide bridges. However, insulin is first synthesized, in the β-cells of the islets of Langerhans in the pancreas, as a single polypeptide that is nonbiologically active, otherwise known as *preproinsulin* (Figure 2.15). The preproinsulin is then translocated into the cisternae of the endoplasmic reticulum, where its signal peptide is removed by a specific protease to give proinsulin, which in turn folds into its correct native tertiary structure through the formation of two disulfide bridges (Figure 2.15). Once this is achieved, the proinsulin is packaged into secretory vesicles in the Golgi apparatus. Finally, a specific protease cleaves off the C chain, leaving the amino terminal B-peptide disulfide bonded to the carboxy terminal A-chain (Figure 2.15). Failure to secret insulin causes diabetes, which if not treated leads to hyperglycemia. The number of diabetics in the world is increasing alarmingly, and as such all possible measures must be taken in order that we satisfy the demands for the provision of insulin. The quantities of exogenous insulin extracted from pig and beef pancreas could never satisfy market needs; a new approach was therefore called for, which was finally realized, after many years of intensive research, through fermentation microbiology and recombinant DNA technology.

2.10.1.2 Cloning and Commercial Production of Insulin

Based on the amino acid sequence of human insulin, Crea et al. (1978) successfully synthesized two oligodeoxyribonucleotides, 77 and 104 base pairs long, encoding the A and B chains, respectively.

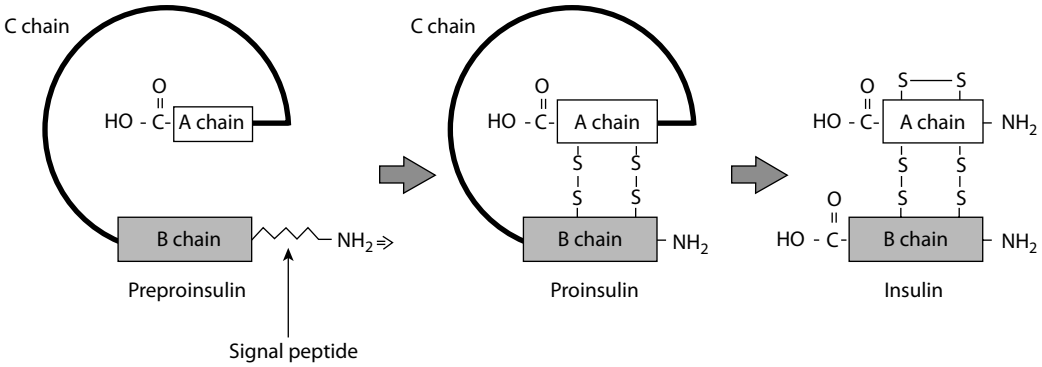

FIGURE 2.15 Posttranslational modifications of preproinsulin to proinsulin and thence to biologically active insulin molecule.

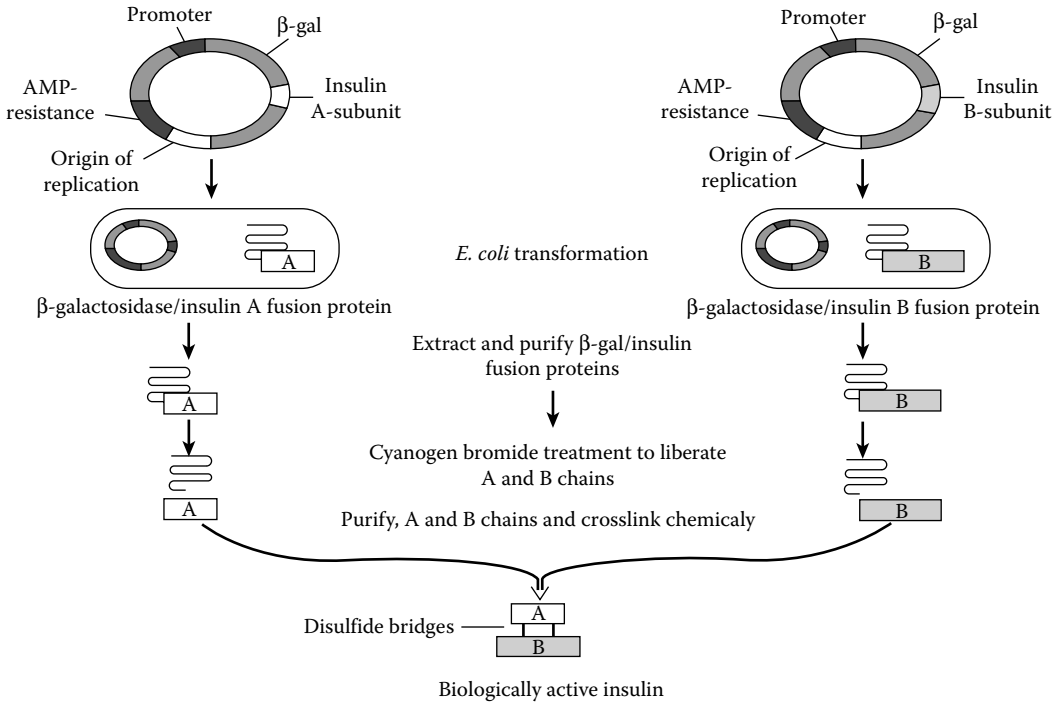

FIGURE 2.16 Applications of fermentation biotechnology and recombinant DNA technology in the commercial production of insulin. As can be seen in the diagram, an oligonucleotide expressing the A-chain and another expressing the B-chain are cloned independently, overexpressed, harvested, purified, and chemically cross-linked to give biologically active insulin.

Each oligo bears single-stranded cohesive termini for *Eco*RI and *Bam*HI to facilitate direct cloning into the pBR322 plasmid vector.

The two oligos encoding the A and B chains were fused into β-galactosidase gene on pBR322, and the resulting recombinant plasmids were used to transform competent cells of *E. coli* as illustrated in Figure 2.16. Expression of the chimeric plasmid in *E. coli* gave rise to hybrid polypeptides, including the sequence of amino acids corresponding to human insulin A and B chains.

The A and B polypeptide chains were cleaved off from the precursor (the hybrid polypeptide) by the action of cyanogens bromide. After separation and purification of the A and B chains, active human insulin was generated (Figure 2.16) by *in vitro* formation of the correct disulfide bridges between A and B chains.

2.10.2 Protein Engineering of Insulin

2.10.2.1 Fast-Acting Insulin Analogs

Fast-acting insulin is therapeutically desirable, and as such protein engineering of insulin to produce analogs with low association constant is of great commercial interest. Attempts to produce such analogs have been successful; examples include insulin *ispro* and insulin *aspart* (Owens 2002).

2.10.2.2 Long-Acting Insulin Analogs

The presence of a constant but low (basal) level of insulin in plasma during the fasting state is essential to maintain overall control of glycemia. Engineering insulin to produce long-acting insulin analogs is therefore of therapeutic and commercial interest. Such objective has now been achieved, and

products include insulin glargine, long-acting insulin, by virtue of introducing two extra arginine residues at the end of the B chain (Arg B31 and Arg B32). After subcutaneous injection of glargine, insulin level rises slowly to a plateau within 6–8 hours and remains essentially unchanged for up to 24 hours (Owens 2002).

SUMMARY

The diverse array of metabolic networks, together with a very high rate of metabolic turnover, makes microorganisms an ideal tool for the conversion of renewable resources into products of primary and secondary metabolism.

The conversion of a given carbon source to biomass involves a sophisticated net of biochemical reactions. These reactions can be classified according to their function into fueling reactions, biosynthetic (anabolic) reactions, anaplerotic reactions, polymerization, and assembly reactions.

Microorganisms change in size as the growth rate changes, which is consistent with the view that initiation of replication is dependent on cell mass.

Microorganisms' composition changes as a function of growth rate; for example, while the relative concentrations of protein, DNA, and RNA in *S. cerevisiae* increase (in ascending order) with growth rate, the intracellular concentrations of glycogen, trehalose, and carbohydrates decrease.

The drop in energy supply below maintenance requirement is not necessarily fatal, but the severity of such a drop is directly proportional to its magnitude and the relative concentration of ribosomes within the cell.

The question of whether a particular organism has lagged following inoculation, together with the number of viable cells at the onset of fermentation, can be ascertained graphically.

The interrelationships among various growth parameters during unrestricted and restricted growth have been described.

Microorganisms adopt different tactics to survive starvation. While Gram-positive organisms resort to sporulation, *S. cerevisiae* and *E. coli* express specific proteins, the primary function of which is scaling down the maintenance requirement on one hand and exiting the stationary phase on the other.

Microorganisms can be grown in batch, fed-batch, or continuous cultures. The latter provides a controlled environment in which a given microorganism can be grown at its maximum specific growth rate in a turbidostat, at constant pH in a pH-stat, or under the limitation of certain nutrients in a chemostat. Continuous culture is, therefore, an indispensible tool in the study of growth kinetics and fermentation processes.

The use of microorganisms for the production of recombinant proteins and bioactive pharmaceuticals has been enhanced significantly by the advent of genetic and protein engineering as evidenced by the production of fast-acting and long-acting recombinant insulin molecules.

REFERENCES

Cozzone, A. J. 1998. Regulation of acetate metabolism by protein phosphorylation in enteric bacteria. *Ann. Rev. Microbiol*. 52:127–64.

Crea, R., A. Kraszewski, T. Hirose, and K. Itakura. 1978. Chemical synthesis of genes for human insulin. *Proc. Natl. Acad. Sci. USA* 75(12): 5765–9.

Donachie, W. D. 1968. Relationship between cell size and time of initiation of DNA replication. *Nature* 219:1077–83.

El-Mansi, E. M. T. 2004. Flux to acetate and lactate excretions in industrial fermentations: Physiological and biochemical implications. *J. Ind. Microbiol. Biotechnol*. 31:295–300.

El-Mansi, E. M. T. 2005. Free-CoA mediated regulation of intermediary and central metabolism: A hypothesis which accounts for the excretion of α-ketoglutarate during aerobic growth on acetate. *Res. Microbiol*. 156:874–9.

El-Mansi, E. M. T., K. J. Anderson, C. A. Inche, L. K. Knowles, and D. J. Platt. 2001. Isolation and curing of the *Klebsiella pneumoniae* large indigenous plasmid using Sodium Dodecyle Sulphate. *Res. Microbiol.* 151:201–9.

Grunenfelder, B., G. Rummel, J. Vohradsky, D. Roder, H. Langen, and U. Jenal 2001. Proteomic analysis of the bacterial cell cycle. *Proc. Natl. Acad. Sci. USA* 98:4681–6.

Guest, J. R., and G. C. Russell 1992. Complexes and complexities of the citric acid cycle in *Escherichia coli*. *Curr. Top. Cell. Regul*. 33:231–47.

Guest J. R., A. M. Abdel-Hamid, G. A. Auger, L. Cunningham, R. A. Henderson, R. S. Machado, and M. M. Attwood 2004. Physiological effects of replacing the PDH complex of *E. coli* by genetically engineered variants or by pyruvate oxidase. In F. Gordon and M. S. Patel, eds., *Thiamine: Catalytic mechanisms and role in normal and disease states*, pp. 389–407. New York: Marcel Dekker Inc.

Gurramkonda, C., S. Polez, N. Skoko, N. Admabn, T. Gabel, D. Chugh, S. Swaminathan, N. Khanna, S. Tisminetzky, and U. Rinas. 2010. Applications of simple fed-batch to high level secretory production of insulin precursor using *Pichia pastoris*. *Microb. Cell Fact.* 12:9–31.

Ingraham, J. L., O. Maaloe, and F. C. Neidhardt 1983. *Growth of the bacterial cell*. Sunderland, MA: Sinauer.

Ingraham, J. L., F. C. Neidhardt, and M. Schaechter. 1990. Physiology of the bacterial cell. *A Molecular Approach*. Sinauer Associates, Inc., Sunderland, MA.

Linton, J. D., and R. J. Stephenson. 1978. A preliminary study of growth yields in relation to the carbon and energy content of various organic growth substrates. *FEMS Microbiol. Lett*. 3:95–8.

Nissen, L. N., U. Schulze, J. Nielsen, and J. Villadsen 1997. Flux distribution in anaerobic, glucose-limited continuous cultures of *Saccharomyces cerevisiae*, *Microbiology* 143:203–18.

Nomura, M., R. Gourse, and G. Baughman. 1984. Regulation of synthesis of ribosomes and ribosomal components. *Ann. Rev. Biochem*. 53:75–89.

Owens, D. R. 2002. New horizons: Alternative routes for insulin therapy. *Nat. Rev. Drug Discov*. 1:529–40.

Pirt, S. J. 1965. The maintenance energy of bacteria in growing culture. *Proc. R. Soc. London, Ser. B* 163:224–31.

Pirt, S. J. 1975. Principles of microbes and cell cultivation. Oxford: Blackwell Scientific.

Summer, D. 2002. A quiet revolution in the bacterial cell factory. *Microbiol. Today* 29:76–8.

Tempest, D. W. 1978. The biochemical significance of microbial growth yields: A reassessment. *Trends in Biochemical Sciences*. 3:180–184.

Weichart, D., N. Querfurth, M. Dreger, and R. Hengge-Aronis. 2003. Global role for ClpP-containing proteases in stationary phase adaptation of *Escherichia coli*. J. Bacteriol 185:115–25.

3 Fermentation Kinetics: Central and Modern Concepts

Jens Nielsen

CONTENTS

3.1 INTRODUCTION

Growth of microbial cells is the result of many chemical reactions, including fueling reactions, biosynthetic reactions, and assembly reactions (see Figure 2.3). In preparation for cell division, the cells increase in size (or extend their hyphae, in the case of filamentous microorganisms) as the macromolecules are assembled *en route* to biomass formation. Biomass formation can be quantified by measuring the increase in dry weight (see Box 3.1), RNA, DNA, and/or proteins. *In situ* measurements of biomass formation during the course of fermentation can also be monitored by following the increase in turbidity at a given wavelength, as illustrated by Olsson and Nielsen (1997).

Growth of microbial cells is often illustrated with a batch-wise growth of a unicellular organism (either a bacterium or yeast). Here the growth occurs in a constant volume of medium with one growth-limiting substrate component that is used by the cells. Cell growth is generally quantified by the so-called *specific growth rate* μ (h^{-1}), which for such a culture is given by

$$\mu = \frac{1}{x}\frac{dx}{dt} \tag{3.1}$$

BOX 3.1 STANDARD OPERATING PROCEDURE (SOP) FOR DRY WEIGHT DETERMINATION

Biomass is most frequently determined by dry weight measurements. This can be done either using an oven or a microwave oven, with the latter being the fastest procedure. An important prerequisite for the measurement is that the sample is dried completely, and it is therefore important to apply a consistent procedure. A suggested protocol is as follows:

1. Dry the filter (pore size 0.45 μm for yeast or fungi, 0.20 μm for bacteria) on a glass dish in the microwave oven on 150 W for 10 min. Place a tissue paper between the glass and the filter so that the filter does not stick to the glass.
2. Place the filter in a desiccator and allow to cool for 10–15 min. Weigh the filter.
3. Filter the cell suspension through the filter and wash the cells with demineralized water.
4. Place the filter on the glass dish again and dry in the microwave oven for 15 min at 150 W.
5. Put the filter in a desiccator and allow to cool for 10–15 min. Weigh the filter.
6. If more than 30 mg dry weight is present on the filter, the time in the microwave oven may have to be longer.

where x is the biomass concentration (or cell number). The specific growth rate is related to the *doubling time* t_d(h) of the biomass through

$$t_d = \frac{\ln 2}{\mu} \tag{3.2}$$

The doubling time t_d is equal to the generation time for a cell (i.e., the length of a cell cycle for unicellular organisms), which is frequently used by life scientists to quantify the rate of cell growth.

The design and optimization of a given fermentation process require a quantitative description of the process, which, considering the nature of microbial growth, is generally a complex task. Furthermore, often the product is not the cells themselves but a compound synthesized by the cells, and depending on the type of product the kinetics of its formation may vary from one phase of growth to another. Thus, while primary metabolites (see Chapter 4 for more details) are typically formed in conjunction with cellular growth, an inverse relationship between product formation and cell growth is often found in the case of secondary metabolites (see Chapter 5 for more details), and here flux to product formation may be greatest in the stationary phase.

With these differences in mind, it is clear that quantification of product formation kinetics may be a difficult task. However, with the rapid progress in biological sciences, our understanding of cellular function has increased dramatically, and this may form the basis for far more advanced modeling of cellular growth kinetics than seen earlier. Thus, in the literature one may find mathematical models describing events like gene expression, kinetics of individual reactions in central pathways, together with macroscopic models that describe cellular growth and product formation with relatively simple mathematical expressions. These models cannot be compared directly because they serve completely different purposes, and it is therefore important to consider the aim of the modeling exercise in a discussion of mathematical models.

In this chapter, the applications of kinetic modeling to fermentation and cellular processes will be discussed.

3.2 FRAMEWORK FOR KINETIC MODELS

The net result of the many biochemical reactions within a single cell is the conversion of substrates to biomass and metabolic end products (see Figures 2.3 and 3.1). Clearly the number of reactions involved in the conversion of, say, glucose into biomass and desirable end products is very large, and it is therefore convenient to adopt the structure proposed by Neidhardt et al. (1990) for describing cellular metabolism, which can be summarized as follows:

Assembly reactions carry out chemical modifications of macromolecules, their transport to prespecified locations in the cell, and, finally, their assembly to form cellular structures such as cell walls, membranes, the nucleus, and so on.

Polymerization reactions represent directed, sequential linkage of activated molecules into long (branched or unbranched) polymeric chains. These reactions lead to the formation of macromolecules from a set of building blocks such as amino acids, nucleotides, and fatty acids.

Biosynthetic reactions produce the building blocks used in the polymerization reactions. They also produce coenzymes and related metabolic factors, including signal molecules. Furthermore, a large number of biosynthetic reactions occur in functional units called *biosynthetic pathways*, each of which consists of sequential reactions leading to the synthesis of one or more building blocks. Pathways are easily recognized and are often controlled *en bloc*. In some cases their reactions are catalyzed by enzymes made from a polycistronic message of messenger RNA (mRNA) transcribed from a set of 12 genes forming an operon. All biosynthetic pathways begin with one of only 12 precursor metabolites from which all building blocks can be synthesized. Some pathways begin directly with such a precursor metabolite, others indirectly by branching from an intermediate or an end product of a related pathway.

Fueling reactions produce the 12 precursor metabolites needed for biosynthesis. Additionally, they generate Gibbs free energy in the form of adenosine-5'-triphosphate (ATP), which is used for biosynthesis, polymerization, and assembling reactions. Finally, the fueling reactions produce the reducing power needed for biosynthesis. The fueling reactions include all biochemical pathways referred to as *catabolic pathways* (degrading and oxidizing substrates).

Thus, the conversion of glucose into cellular protein, for example, proceeds *via* precursor metabolites formed in the fueling reactions, further *via* building blocks (in this case amino acids) formed in the biosynthetic reactions, and finally through polymerization of the building blocks (or amino acids). In the fueling reactions there are many more intermediates than the precursor metabolites, and similarly a large number of intermediates are also involved in the conversion of precursor

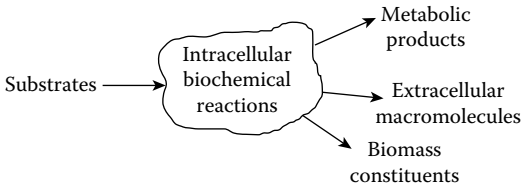

FIGURE 3.1 An overview of the intracellular biochemical reactions in micro-organisms; in addition to the formation of biomass constituents, for example, cellular protein, lipids, RNA, DNA, and carbohydrates, substrates are converted into primary metabolites, for example, ethanol, acetate, lactate; secondary metabolites, for example, penicillin; and/or extracellular macromolecules, for example, enzymes, heterologous proteins, polysaccharides.

TABLE 3.1
Overall Composition of an Average Cell of *Escherichia Coli*

Macromolecule	% of Total Dry Weight	Different Kinds of Molecules
Protein	55.0	1050
RNA	20.5	
rRNA	16.7	3
tRNA	3.0	60
mRNA	0.8	400
DNA	3.1	1
Lipid	9.1	4
Lippolysaccharide	3.4	1
Peptidoglycan	2.5	1
Glycogen	2.5	1
Metabolite pool	3.9	

Source: Data are taken from Ingraham, J.L., Maaloe, O., and Neidhardt, F.C., *Growth of the Bacterial Cell*. Sunderland, MA: Sinauer Associates, 1983.

metabolites into building blocks. The number of cellular metabolites is therefore very large, but still they only account for a small fraction of the total biomass (Table 3.1). The reason for this is the *en bloc* control of the individual reaction rates in the biosynthetic pathways mentioned above. Furthermore, the high affinity of enzymes for the reactants ensures that each metabolite can be maintained at a very low concentration even at a high flux through the pathway (see Box 3.2).

This control of the individual reactions in long pathways is very important for cell function, but it also means that in a quantitative description of cell growth it is not necessary to consider the kinetics of all the individual reactions, and this obviously leads to a significant reduction in the degree of complexity. Consideration of the kinetics of individual enzymes or reactions is therefore necessary only when the aim of the study is to quantify the relative importance of a particular reaction in a pathway.

3.2.1 Stoichiometry

The first step in a quantitative description of cellular growth is to specify the stoichiometry for those reactions to be considered for analysis. For this purpose it is important to distinguish between substrates, metabolic products, intracellular metabolites, and biomass constituents (Stephanopoulos et al. 1998):

A **substrate** is a compound present in the sterile medium, which can be further metabolized or directly incorporated into the cell.
A **metabolic product** is a compound produced by the cells and excreted to the extracellular medium.
Biomass constituents are pools of macromolecules that make up the biomass (e.g., RNA, DNA, protein, lipids, and carbohydrates), but also macromolecular products accumulating inside the cell (e.g., a polysaccharide or a nonsecreted heterologous protein).
Intracellular metabolites are all other compounds within the cell (i.e., glycolytic intermediates, precursor metabolites, and building blocks).

Note that this list distinguishes between biomass constituents and intracellular metabolites, because the timescales of their turnover in cellular reactions are very different: intracellular

BOX 3.2 CONTROL OF METABOLITE LEVELS IN BIOCHEMICAL PATHWAYS

The level of intracellular metabolites is normally very low. This is due to tight regulation of the enzyme levels and to the high affinity most enzymes have towards the reactants. To illustrate this consider two reactions of a pathway – one forming the metabolite X_i and the other consuming this metabolite:

$$....X_{i-1} \overset{v_i}{\rightarrow} X_i \overset{v_{i+1}}{\rightarrow} X_{i+1}....$$

Assuming that there is no allosteric regulation of the two enzyme-catalyzed reactions the kinetics can be described with reversible Michaelis–Menten kinetics:

$$v_i = \frac{v_{i,\max}\left(\frac{c_{i-1}}{K_{i-1}} - \frac{c_i}{K_i}\right)}{1 + \frac{c_{i-1}}{K_{i-1}} + \frac{c_i}{K_i}}$$

where c_i is the metabolite concentration and $v_{i,\max}$ expresses the enzyme activity. If the rate of the first reaction increases drastically, for example, due to an increase in the concentration of the metabolite X_{i-1}, the metabolite X_i will accumulate. This will lead to an increase in the second reaction rate and a decrease in the first reaction rate. Consequently the concentration of metabolite X_i will decrease again. The parameters K_i and K_{i-1} quantify the affinity of the enzyme for the reactant and the product in each reaction, and generally these are in the order of a few μM. Thus, even for low metabolite concentrations (in the order of 10 times K_i) the enzyme will be saturated and the reaction rate will be close to $v_{i,\max}$, but typically the metabolite concentration is of the order of K_i because hereby the enzyme can respond rapidly to changes in the metabolite level, and metabolite accumulations can be avoided.

metabolites have a very fast turnover (typically in the range of seconds) compared with that of macromolecules (typically in the range of hours). This means that on the timescale of growth, the intracellular metabolite pools can be assumed to be in pseudo-steady state.

With the goal of specifying a general stoichiometry for biochemical reactions, we consider a system where N substrates are converted to M metabolic products and Q biomass constituents. The conversions are carried out in J reactions in which K intracellular metabolites participate as pathway intermediates. The substrates are termed S_i, the metabolic products are termed P_i, the biomass constituents are termed $X_{\text{macro,i}}$, and the intracellular metabolites are termed $X_{\text{met,i}}$. With these definitions, the general stoichiometry for the j^{th} reaction can be specified as

$$\sum_{i=1}^{N} \alpha_{ji} S_i + \sum_{i=1}^{M} \beta_{ji} P_i + \sum_{i=1}^{Q} \gamma_{ji} X_{\text{macro,i}} + \sum_{i=1}^{K} g_{ji} X_{\text{met,i}} = 0;\ j = 1,..,J \tag{3.3}$$

Here, α_{ji} is a stoichiometric coefficient for the i^{th} substrate, β_{ji} is a stoichiometric coefficient for the i^{th} metabolic product, γ_{ji} is a stoichiometric coefficient for the i^{th} macromolecular pool, and g_{ji} is a stoichiometric coefficient for the i^{th} intracellular metabolite. All the stoichiometric coefficients are with sign. Thus, all compounds consumed in the j^{th} reaction have negative stoichiometric coefficients, whereas all compounds that are produced have positive stoichiometric coefficients.

Furthermore, compounds that do not participate in the j^{th} reaction have a stoichiometric coefficient of zero.

If there are many cellular reactions (i.e., J is large), it is convenient to write the stoichiometry for all the J cellular reactions in a compact form using matrix notation:

$$\mathbf{AS} + \mathbf{BP} + \mathrm{G}\mathbf{X}_{\mathrm{macro}} + \mathbf{GX}_{\mathrm{met}} = 0 \tag{3.4}$$

where the matrices **A**, **B**, G, and **G** are stoichiometric matrices containing stoichiometric coefficients in the J reactions for the substrates, metabolic products, biomass constituents, and pathway intermediates, respectively. In these matrices, rows represent reactions and columns metabolites, that is, the element in the j^{th} row and the i^{th} column of **A** specifies the stoichiometric coefficient for the i^{th} substrate in the j^{th} reaction. Formulation of the stoichiometry in matrix form may seem rather complex; however, if the model is simple (i.e., only a few reactions, a few substrates, and a few metabolic products are considered), it is generally more convenient to use the simpler stoichiometric representation in Equation 3.3.

3.2.2 Reaction Rates

The stoichiometry of the individual reaction is the basis of any quantitative analysis. However, of equal importance is specification of the rate of the individual reactions. Normally the rate of a chemical reaction is given as the *forward rate*, which, if termed v_i, specifies that a compound that has a stoichiometric coefficient β in the i^{th} reaction is formed with the rate βv_i. Normally the stoichiometric coefficient for one of the compounds is arbitrarily set to 1, whereby the forward reaction rate becomes equal to the consumption or production of this compound in this particular reaction. For this reason the forward reaction rate is normally specified with the unit moles (or g) h^{-1}, or if the total amount of biomass is taken as reference (so-called specific rates) with the unit moles (or g) (g DW h^{-1}).

For calculation of the overall production or consumption rate, we have to sum the contributions from the different reactions, that is, the total specific consumption rate of the i^{th} substrate equals the sum of substrate consumptions in all the J reactions:

$$r_{s,i} = -\sum_{j=1}^{J} \alpha_{ji} v_j \tag{3.5}$$

The stoichiometric coefficients for substrates are generally negative, that is, the specific formation rate of the i^{th} substrate in the j^{th} reaction given by $\alpha_{ji} v_j$ is negative, but the specific substrate uptake rate is normally considered as positive, and a minus sign is therefore introduced in Equation 3.5. For the specific formation rate of the i^{th} metabolic product, similarly we have

$$r_{p,i} = \sum_{j=1}^{J} \beta_{ji} v_j \tag{3.6}$$

Equations 3.5 and 3.6 specify some very important relations between what can be directly measured: the specific substrate uptake rates and the specific product formation rates, and the rates of the reactions in the metabolic model. If a compound is consumed or formed in only one reaction, it is quite clear that we can get a direct measurement of this reaction rate. For the biomass constituents

and the intracellular metabolites, we can specify similar expressions for the net formation rate in all the J reactions:

$$r_{\text{macro,i}} = \sum_{j=1}^{J} \gamma_{ji} v_j \tag{3.7}$$

$$r_{\text{met,i}} = \sum_{j=1}^{J} g_{ji} v_j \tag{3.8}$$

These rates are net specific formation rates, because a compound may be formed in one reaction and consumed in another, and the rates specify the net results of consumption and formation in all the J cellular reactions. Thus, if $r_{\text{met,i}}$ is positive there is a net formation of the i^{th} intracellular metabolite, and if it is negative there is a net consumption of this metabolite. Finally, if $r_{\text{met,i}}$ is zero, the rates of formation of the i^{th} metabolite exactly balance its consumption.

If the forward reaction rates for the J cellular reactions are collected in the rate vector **v,** the summations in Equations 3.5 through 3.8 can be formulated in matrix notation as

$$\mathbf{r}_{\text{s}} = -\mathbf{A}^{\text{T}}\mathbf{v} \tag{3.9}$$

$$\mathbf{r}_{\text{p}} = \mathbf{B}^{\text{T}}\mathbf{v} \tag{3.10}$$

$$\mathbf{r}_{\text{macro}} = \mathrm{G}^{\text{T}}\mathbf{v} \tag{3.11}$$

$$\mathbf{r}_{\text{met}} = \mathbf{G}^{\text{T}}\mathbf{v} \tag{3.12}$$

Here $\mathbf{r}_{\text{s}}$ is a rate vector containing the specific uptake rates of the N substrates, $\mathbf{r}_{\text{p}}$ a vector containing the specific formation rates of the M metabolic products, $\mathbf{r}_{\text{macro}}$ a vector containing the net specific formation rate of the Q biomass constituents, and $\mathbf{r}_{\text{met}}$ a vector containing the net specific formation rate of the K intracellular metabolites. Notice that what appears in the matrix equations are the transposed stoichiometric matrices, which are formed from the stoichiometric matrices by converting columns into rows and vice versa (see Example 3a, this chapter). Equations 3.7 and 3.11 give the net specific formation rate of biomass constituents, and because the intracellular metabolites only represent a small fraction of the total biomass, the specific growth rate μ of the total biomass is given as the sum of formation rates for all the macromolecular constituents:

$$\mu = \sum_{i=1}^{Q} r_{\text{macro,i}} = \mathbf{1}_Q^{\text{T}}\mathbf{r}_{\text{macro}} = \mathbf{1}_Q^{\text{T}}\Gamma^{\text{T}}\boldsymbol{v} \tag{3.13}$$

where $\mathbf{1}_Q$ is a Q-dimensional row vector with all elements being 1. Equation 3.13 is very fundamental because it links the information supplied by a detailed metabolic model with the macroscopic (and measurable) parameter μ. It clearly specifies that the formation rate of biomass is represented by a sum of formation of many different biomass constituents (or macromolecular pools), a point that will be discussed further in Section 3.4.3.

3.2.3 Yield Coefficients and Linear Rate Equations

The overall yield (e.g., how much carbon in the glucose ends up in the metabolite of interest) is a very important design parameter in many fermentation processes. This overall yield is normally

represented in the form of *yield coefficients*, which can be considered as relative rates (or fluxes) toward the product of interest with a certain compound as reference, often the carbon source or the biomass. These yield coefficients therefore have the units mass per unit mass of the reference (e.g., moles of penicillin formed per mole of glucose consumed or g protein formed per g biomass formed). An often used yield coefficient in the design and operation of aerobic fermentations is the respiratory quotient (RQ), which specifies the moles of carbon dioxide formed per mole of oxygen consumed (see also Example 3a). Several different formulations of the yield coefficients can be found in the literature. Here we will use the formulation of Nielsen et al. (2003), where the yield coefficient is stated with a double subscript Y_{ij}, which states that a mass of j is formed or consumed per mass of i formed or consumed. With the i^{th} substrate as the reference compound, the yield coefficients are given by

$$Y_{s_i s_j} = \frac{r_{s,j}}{r_{s,i}} \tag{3.14}$$

$$Y_{s_i p_j} = \frac{r_{p,j}}{r_{s,i}} \tag{3.15}$$

$$Y_{s_i x} = \frac{\mu}{r_{s,i}} \tag{3.16}$$

In the classical description of cellular growth introduced by Monod (1942) (see Section 3.4.2), the yield coefficient Y_{sx} was taken to be constant, and all the cellular reactions were lumped into a single overall growth reaction where substrate is converted to biomass. However, in the late 1950s it was shown (Herbert 1959) that the yield of biomass with respect to substrate is not constant. In order to describe this, Herbert introduced the concept of *endogenous metabolism* and specified substrate consumption for this process in addition to that for biomass synthesis. At the same time, Luedeking and Piret (1959) found that lactic acid bacteria produce lactic acid at nongrowth conditions, which was consistent with an endogenous metabolism of the cells. Their results indicated a linear correlation between the specific lactic acid production rate and the specific growth rate:

$$r_p = a\mu + b \tag{3.17}$$

In the mid-1960s, Pirt (1965) introduced a similar linear correlation between the specific rate of substrate uptake and the specific growth rate, and suggested the term *maintenance*, which is currently a widely used concept in endogenous metabolism. The linear correlation of Pirt takes the form of

$$r_s = Y_{xs}^{\text{true}}\,\mu + m_s \tag{3.18}$$

where Y_{xs}^{true} is referred to as the true yield coefficient and m_s as the maintenance coefficient. With the introduction of the linear correlations, the yield coefficients can obviously not be constants. Thus, for the biomass yield on the substrate:

$$Y_{sx} = \frac{\mu}{Y_{xs}^{\text{true}}\,\mu + m_s} \tag{3.19}$$

TABLE 3.2
True Yield and Maintenance Coefficients for Different Microbial Species and Growth on Glucose *or Glycerol*

Organism	Substrate	Y_{xs}^{true} [g (g DW)$^{-1}$]	m_s [g (g DW h)$^{-1}$]
Aspergillus nidulans		1.67	0.020
Candida utilis		2.00	0.031
Escherichia coli		2.27	0.057
Klebsiella aerogenes		2.27	0.063
Penicillium chrysogenum		2.17	0.021
Saccharomyces cerevisiae		1.85	0.015
Aerobacter aerogenes	Glycerol	1.79	0.089
Bacillus megatarium		1.67	–
Klebsiella aerogenes		2.13	0.074

Source: Data are taken from Nielsen, J. and Villadsen, J., *Bioreaction Engineering Principles*. New York: Plenum Press, 1994.

which shows that Y_{sx} decreases at low specific growth rates where an increasing fraction of the substrate is used to meet the maintenance requirements of the cell. When the specific growth rate becomes large, the yield coefficient approaches the reciprocal of Y_{xs}^{true}. A compilation of true yield and maintenance coefficients for various microbial species is given in Table 3.2.

The empirically derived linear correlations are very useful for correlating growth data, especially in steady-state continuous cultures where linear correlations similar to Equation 3.18 were found for most of the important specific rates. The remarkable robustness and general validity of the linear correlations indicate that they have a fundamental basis, and this basis is the continuous supply and consumption of ATP, which are tightly coupled in all cells. Thus the role of the energy-producing substrate is to provide ATP to drive biosynthesis and polymerization reactions as well as cell maintenance processes according to the linear relationship:

$$r_{ATP} = Y_{xATP}\mu + m_{ATP} \tag{3.20}$$

which is a formal analog to the linear correlation of Pirt. Equation 3.20 states that ATP produced balances the consumption for growth and for maintenance, and if the ATP yield on the energy-producing substrate is constant (i.e., r_{ATP} is proportional to r_s), it is quite obvious that Equation 3.20 can be used to derive the linear correlation in Equation 3.18, as illustrated in Example 3a. Notice that Y_{xATP} in Equation 3.20 is a true yield coefficient, but it is normally specified without the superscript "true."

The concept of balancing ATP production and consumption can be extended to other cofactors (e.g., NADH and NADPH), and as such it is possible to derive linear rate equations for three different cases (Nielsen and Villadsen 1994):

Anaerobic growth where ATP is supplied by substrate-level phosphorylation
Aerobic growth without metabolite formation
Aerobic growth with metabolite formation

For aerobic growth with metabolite formation, the specific substrate uptake rate takes the form of

$$r_s = Y_{xs}^{true}\mu + Y_{ps}^{true}r_p + m_s \tag{3.21}$$

This linear rate equation can be interpreted as a metabolic model with three reactions:

Conversion of substrate to biomass with a stoichiometric coefficient for the substrate and a forward reaction rate equal to the specific growth rate
Conversion of substrate to the metabolic product with a stoichiometric coefficient for the substrate and a forward reaction rate equal to the specific product formation rate
Metabolism of substrate to meet the maintenance requirements (normally, the substrate is oxidized to carbon dioxide) with the rate m_s

Consequently, the stoichiometry for these three reactions can be specified as

$$-Y_{xs}^{\text{true}} S + X = 0;\ \mu \tag{3.22}$$

$$-Y_{ps}^{\text{true}} S + P = 0;\ r_p \tag{3.23}$$

$$-S = 0;\ m_s \tag{3.24}$$

With this stoichiometry, the linear rate Equation 3.21 can easily be derived using Equation 3.5, that is, the overall specific substrate consumption rate is the sum of substrate consumption for growth, metabolite formation, and maintenance.

Thus, it is important to distinguish between true yield coefficients (which are rather stoichiometric coefficients) and overall yield coefficients, which can be taken to be stoichiometric coefficients in *one lumped reaction* (often referred to as the *black box model*; see Section 3.2.4), which represents all the cellular processes:

$$-Y_{xs} S + Y_{xp} P + X = 0;\ \mu \tag{3.25}$$

Despite the subscript "true," the true yield coefficients are only parameters for a given cellular system as they simply represent overall stoichiometric coefficients in lumped reactions; for example, reaction (3.22) is the sum of all reactions involved in the conversion of substrate into biomass. If, for example, the environmental conditions change, a different set of metabolic routes may be activated, and this may result in a change in the overall recovery of carbon in each of the three processes mentioned above (i.e., the values of the true yield coefficients change). Even the more fundamental Y_{xATP} cannot be taken to be constant, as illustrated in a detailed analysis of lactic acid bacteria (Benthin et al. 1994).

Example 3a: Metabolic Model for Aerobic Growth of *Saccharomyces cerevisiae*

To illustrate the derivation of the linear rate equations for an aerobic process with metabolite formation, we consider a simple metabolic model for the yeast *S. cerevisiae*. For this purpose we set up a stoichiometric model that summarizes the overall cellular metabolism, and based on assumptions of pseudo-steady state for ATP, NADH, and NADPH, linear rate equations can be derived where the specific uptake rates for glucose and oxygen and the specific carbon dioxide formation rate are given as functions of the specific growth rate. Furthermore, by evaluating the parameters in these linear rate equations, which can be done from a comparison with experimental data, information on key energetic parameters may be extracted.

TABLE 3.3
Macromolecular Composition of *Saccharomyces cerevisiae*

Macromolecule	Content [g (g DW)$^{-1}$]
Protein	0.39
Polysaccharides + trehalose	0.39
DNA + RNA	0.11
Phospholipids	0.05
Triacylglycerols	0.02
Sterols	0.01
Ash	0.03

From an analysis of all the biosynthetic reactions, the overall stoichiometry for synthesis of the constituents of a *S. cerevisiae* cell can be specified (Oura 1983) as

$$CH_{1.62}O_{0.53}N_{0.15} + 0.12\ CO_2 + 0.397\ NADH - 1.12\ CH_2O - 0.15\ NH_3 - Y_{xATP}ATP - 0.212\ NADPH = 0 \quad (3a1)$$

The stoichiometry (3a1) holds for a cell with the composition specified in Table 3.3; the substrate is glucose, and inorganic salts (i.e., ammonia) are the nitrogen source. The stoichiometry is given on a C-mole basis (i.e., glucose is specified as CH_2O), and the elemental composition of the biomass was calculated from the macromolecular composition to be $CH_{1.62}O_{0.53}N_{0.15}$ (see Table 3.3). The ATP and NADPH required for biomass synthesis are supplied by the catabolic pathways, and excess NADH formed in the biosynthetic reactions is, together with NADH formed in the catabolic pathways, reoxidized by transfer of electrons to oxygen via the electron transport chain. Reactions (3a2) through (3a5) specify the overall stoichiometry for the catabolic pathways. Reaction (3a2) specifies NADPH formation by the PP pathway, where glucose is completely oxidized to CO_2; reaction (3a3) is the overall stoichiometry for the combined EMP pathway and the TCA cycle; reaction (3a4) is the fermentative glucose metabolism, where glucose is converted to ethanol (this reaction only runs at high glucose uptake rates); and, finally, reaction (3a5) is the overall stoichiometry for the oxidative phosphorylation, where the P/O ratio is the overall (or operational) P/O ratio for the oxidative phosphorylation:

$$CO_2 + 2\ NADPH - CH_2O = 0 \quad (3a2)$$

$$CO_2 + 2\ NADH + 0.667\ ATP - CH_2O = 0 \quad (3a3)$$

$$CH_3O_{0.5} + 0.5\ CO_2 + 0.5\ ATP - 1.5\ CH_2O = 0 \quad (3a4)$$

$$P/O\ ATP - 0.5\ O_2 - NADH = 0 \quad (3a5)$$

Finally, consumption of ATP for maintenance is included simply as a reaction where ATP is used:

$$-ATP = 0 \quad (3a6)$$

Note that with the stoichiometry given on a C-mole basis, the stoichiometric coefficients extracted from the biochemistry (e.g., the formation of 2 moles ATP per mole glucose in the EMP pathway) are divided by six, because glucose contains 6 C moles per mole.

Above, the stoichiometry is written as in Equation 3.3, but we can easily convert it to the more compact matrix notation of Equation 3.4:

$$\begin{pmatrix} -1.120 & 0 \\ -1 & 0 \\ -1 & 0 \\ -1.5 & 0 \\ 0 & -0.5 \\ 0 & 0 \end{pmatrix} \begin{pmatrix} S_{glc} \\ S_{o_2} \end{pmatrix} + \begin{pmatrix} 0 & 0.120 \\ 0 & 1 \\ 0 & 1 \\ 1 & 0.5 \\ 0 & 0 \\ 0 & 0 \end{pmatrix} \begin{pmatrix} P_{eth} \\ P_{CO_2} \end{pmatrix} + \begin{pmatrix} 1 \\ 0 \\ 0 \\ 0 \\ 0 \\ 0 \end{pmatrix} X + \begin{pmatrix} -Y_{xATP} & 0.397 & -0.212 \\ 0 & 0 & 2 \\ 0.667 & 2 & 0 \\ 0.5 & 0 & 0 \\ P/O & -1 & 0 \\ -1 & 0 & 0 \end{pmatrix} \begin{pmatrix} X_{ATP} \\ X_{NADH} \\ X_{NADPH} \end{pmatrix} = \begin{pmatrix} 0 \\ 0 \\ 0 \\ 0 \\ 0 \\ 0 \end{pmatrix} \tag{3a7}$$

where X represents the biomass.

We now collect the forward reaction rates for the six reactions in the rate vector **v** given by

$$\boldsymbol{v} = \begin{pmatrix} \mu \\ v_{PP} \\ v_{EMP} \\ r_{eth} \\ v_{OP} \\ m_{ATP} \end{pmatrix}$$

In analogy with Equation 3.18, we balance the production and consumption of the three cofactors ATP, NADH, and NADPH. This gives the three equations:

$$-Y_{xATP}\mu + 0.667v_{EMP} + 0.5r_{eth} + P/Ov_{OP} - m_{ATP} = 0 \tag{3a8}$$

$$0.397\mu + 2v_{EMP} - v_{OP} = 0 \tag{3a9}$$

$$-0.212\mu + 2v_{PP} = 0 \tag{3a10}$$

Notice that these balances correspond to zero net specific formation rates for the three cofactors, and the three balances can therefore also be derived using Equation 3.12:

$$r_{met} = G^T v = \begin{pmatrix} -Y_{xATP} & 0 & 0.667 & 0.5 & P/O & -1 \\ 0.397 & 0 & 2 & 0 & -1 & 0 \\ -0.212 & 2 & 0 & 0 & 0 & 0 \end{pmatrix} \begin{pmatrix} \mu \\ v_{PP} \\ v_{EMP} \\ r_{eth} \\ v_{OP} \\ m_{ATP} \end{pmatrix} = \begin{pmatrix} 0 \\ 0 \\ 0 \end{pmatrix} \tag{3a11}$$

In addition to the three balances (3a8) through (3a10), we have the relationships between the reaction rates and the specific substrate uptake rates and the specific product formation rate given by Equations 3a5 and 3a6, or, using the matrix notation of Equations 3a9 and 3a10:

$$\begin{pmatrix} r_{glc} \\ r_{O_2} \end{pmatrix} = -\begin{pmatrix} -1.120 & -1 & -1 & -1.5 & 0 & 0 \\ 0 & 0 & 0 & 0 & -0.5 & 0 \end{pmatrix} \begin{pmatrix} \mu \\ v_{PP} \\ v_{EMP} \\ r_{eth} \\ v_{OP} \\ m_{ATP} \end{pmatrix} \tag{3a12}$$

$$= \begin{pmatrix} 1.120\mu + v_{PP} + v_{EMP} + 1.5r_{eth} \\ 0.5v_{OP} \end{pmatrix}$$

$$\begin{pmatrix} r_{eth} \\ r_{CO_2} \end{pmatrix} = \begin{pmatrix} 0 & 0 & 0 & 1 & 0 & 0 \\ 0.120 & 1 & 1 & 0.5 & 0 & 0 \end{pmatrix} \begin{pmatrix} \mu \\ v_{PP} \\ v_{EMP} \\ r_{eth} \\ v_{OP} \\ m_{ATP} \end{pmatrix} \tag{3a13}$$

$$= \begin{pmatrix} r_{eth} \\ 0.120\mu + v_{PP} + v_{EMP} + 0.5r_{eth} \end{pmatrix}$$

Clearly, the specific ethanol production rate is equal to the rate of reaction (3a5) because the stoichiometric coefficient for ethanol in this reaction is 1, and it is the only reaction where ethanol is involved. Using the combined set of Equations 3a11 through 3a13, the four reaction rates v_{EMP}, v_{PP}, v_{OP}, and m_{ATP} can be eliminated and the linear rate equations 3a14 through 3a16 can be derived:

$$r_{glc} = (a + 1.226)\mu + (1.5 - b)r_{eth} + c = Y_{xs}^{true}\mu + Y_{ps}^{true}r_{eth} + m_s \tag{3a14}$$

$$r_{CO_2} = (a + 0.226)\mu + (0.5 - b)r_{eth} + c = Y_{xc}^{true}\mu + Y_{pc}^{true}r_{eth} + m_c \tag{3a15}$$

$$r_{O_2} = (a + 0.229)\mu - br_{eth} + c = Y_{xo}^{true}\mu + Y_{po}^{true}r_{eth} + m_o \tag{3a16}$$

The three common parameters *a*, *b,* and *c* are functions of the energetic parameters Y_{xATP}, m_{ATP}, and the P/O ratio according to Equations 3a17 through 3a19:

$$a = \frac{Y_{xATP} - 0.458\text{P/O}}{0.667 + 2\text{P/O}} \tag{3a17}$$

$$b = \frac{0.5}{0.667 + 2P/O} \tag{3a18}$$

$$c = \frac{m_{ATP}}{0.667 + 2\text{P/O}} \tag{3a19}$$

If there is no ethanol formation, which is the case at low specific glucose uptake rates, Equation 3a14 reduces to the linear rate Equation 3.18, but the parameters of the correlation are determined by basic energetic parameters of the cells. It is seen that the parameters in the linear correlations are coupled via the balances for ATP, NADH, and NADPH, and the three true yield coefficients cannot take any value. Furthermore, the maintenance coefficients are the same. This is due to the use of the units C-moles per C-mole biomass per hour for the specific rates. If other units are used

for the specific rates, the maintenance coefficients will not take the same values but will remain proportional. This coupling of the parameters shows that there are only three degrees of freedom in the system, and one actually only has to determine two yield coefficients and one maintenance coefficient—the other parameters can be calculated using Equations 3a14 through 3a16.

The derived linear rate equations are certainly useful for correlating experimental data, but they also allow evaluation of the key energetic parameters Y_{xATP}, m_{ATP}, and the operational P/O ratio. Thus, if the true yield coefficients and the maintenance coefficients of Equations 3a14 through 3a16 are estimated, the values of *a*, *b,* and *c* can be found, and these three parameters relate the three energetic parameters through Equations 3a17 through 3a19. Thus, from one of the ethanol yield coefficients, *b* can be found, and, thereafter, the P/O ratio can be determined. Then m_{ATP} can be found from one of the maintenance coefficients, and finally Y_{xATP} can be found from one of the biomass yield coefficients. In practice, however, it is difficult to extract sufficiently precise values of the true yield coefficients from experimental data to estimate the energetic parameters—especially since the three parameters *a*, *b,* and *c* are closely correlated (especially *b* and *c*). However, if either the P/O ratio or Y_{xATP} is known, Equations 3a14 through 3a16 allow an estimation of the two remaining unknown energetic parameters. Consider the situation where there is no ethanol formation; here the true yield coefficient for biomass is 1.48 C-moles glucose (C-mole biomass)$^{-1}$ and the maintenance coefficient (equal to *b*) is 0.012 C-moles glucose (C-mole biomass h)$^{-1}$ (both values taken from Table 3.2). Thus, *a* is equal to 0.254 moles ATP (C-mole^{-1} biomass). If the operational P/O ratio is about 1.5 (which is a reasonable value for *S. cerevisiae*), we find that Y_{xATP} is 1.62 moles ATP (C-mole^{-1} biomass) or about 67 mmoles ATP (g DW^{-1}). Similarly, we find m_{ATP} to be about 2 mmoles (g DW h^{-1}).

In connection with baker's yeast production, it is important to maximize the yield of biomass on glucose:

$$Y_{sx} = \frac{\mu}{(a+1.226)\mu + (1.5-b)r_{eth} + c} \tag{3a20}$$

Clearly, this can best be done if ethanol production is avoided. Thus, the glucose uptake rate is to be controlled below a level where there is respiro-fermentative metabolism. A very good indication of whether there is respiro-fermentative metabolism is the RQ:

$$RQ = \frac{(a+0.226)\mu + (0.5-b)r_{eth} + c}{(a+0.229)\mu - br_{eth} + c} \tag{3a21}$$

If there is no ethanol production, RQ will be close to 1 (independent of the specific growth rate), whereas if there is ethanol production, RQ will be above 1 and will increase with r_{eth} (*b* is always less than 0.5). From measurements of carbon dioxide and oxygen in the exhaust gas, the RQ can be evaluated. If it is above 1, there is respiro-fermentative metabolism resulting in ethanol formation and hence a low yield of biomass on sugar. This is caused by so-called glucose repression of respiration, where a high sugar concentration causes decreased activity of the respiration resulting in ethanol production due to overflow metabolism. Thus, if RQ is larger than 1 it means that the sugar concentration in the reactor must be reduced, and this can be done by reducing the feed rate to the reactor (typically baker's yeast production is operated as a fed-batch process; see Section 3.4).

3.2.4 Black Box Model

In the black box model of cellular growth, all the cellular reactions are lumped into a single reaction. In this overall reaction, the stoichiometric coefficients are identical to the yield coefficients [see also Equation 3.25], and it can therefore be presented as

$$X + \sum_{i=1}^{M} Y_{xp_i} P_i - \sum_{i=1}^{N} Y_{xs_i} S_i = 0 \tag{3.26}$$

Because the stoichiometric coefficient for biomass is 1, the forward reaction rate is given by the specific growth rate of the biomass, which together with the yield coefficients completely specifies the system. As discussed in Section 3.2.3, the yield coefficients are not constants, and the black box model can therefore not be applied to correlate, for instance, the specific substrate uptake rate with the specific growth rate. However, it is very useful for validation of experimental data because it can form the basis for setting up elemental balances. Thus, in the black box model there are $(M + N + 1)$ parameters: M yield coefficients for the metabolic products, N yield coefficients for the substrates, and the forward reaction rate μ. Because mass is conserved in the overall conversion of substrates to metabolic products and biomass, the $(M + N + 1)$ parameters of the black box model are not completely independent but must satisfy several constraints. Thus, the elements flowing into the system must balance the elements flowing out of the system (e.g., the carbon entering the system via the substrates has to be recovered in the metabolic products and biomass). Each element considered in the black box obviously yields one constraint. Thus, a carbon balance gives

$$1 + \sum_{i=1}^{M} f_{\mathrm{p,i}} Y_{xp_i} - \sum_{i=1}^{N} f_{\mathrm{s,i}} Y_{xs_i} = 0 \tag{3.27}$$

where $f_{\mathrm{s,i}}$ and $f_{\mathrm{p,i}}$ represent the carbon content (C-moles mole^{-1}) in the i^{th} substrate and the i^{th} metabolic product, respectively. In the above equation, the elemental composition of biomass is normalized with respect to carbon (i.e., it is represented by the form $CH_aO_bN_c$; see also Example 3a). The elemental composition of biomass depends on its macromolecular content and, therefore, on the growth conditions and the specific growth rate (e.g., the nitrogen content is much lower under nitrogen-limited conditions than under carbon-limited conditions; see Table 3.4). However, except for extreme situations, it is reasonable to use the general composition formula $CH_{1.8}O_{0.5}N_{0.2}$ whenever the biomass composition is not exactly known. Often the elemental composition of substrates and metabolic products is normalized with respect to their carbon content, for example glucose is specified as CH_2O (see also Example 3a). Equation 3.27 is then written on a per C-mole basis as

$$1 + \sum_{i=1}^{M} Y_{xp_i} - \sum_{i=1}^{N} Y_{xs_i} = 0 \tag{3.28}$$

In Equation 3.28, the yield coefficients have units of C-moles per C-mole biomass. Conversion to this unit from other units is illustrated in Box 3.3. Equation 3.28 is very useful for checking the consistency of experimental data. Thus, if the sum of carbon in the biomass and the metabolic products does not equal the sum of carbon in the substrates, there is an inconsistency in the experimental data.

Similar to Equation 3.27, balances can be written for all other elements participating in the conversion (3.26). Thus, the hydrogen balance will read

$$a_x + \sum_{i=1}^{M} a_{\mathrm{p,i}} Y_{xp_i} - \sum_{i=1}^{N} a_{\mathrm{s,i}} Y_{xs_i} = 0 \tag{3.29}$$

where $a_{\mathrm{s,i}}$, $a_{\mathrm{p,i}}$, and a_x represent the hydrogen content (moles C-mole^{-1} if a C-mole basis is used) in the i^{th} substrate, the i^{th} metabolic product, and the biomass, respectively. Similarly, we have for the oxygen and nitrogen balances

$$b_x + \sum_{i=1}^{M} b_{\mathrm{p,i}} Y_{xp_i} - \sum_{i=1}^{N} b_{\mathrm{s,i}} Y_{xs_i} = 0 \tag{3.30}$$

TABLE 3.4
Elemental Composition of Biomass for *Several Microorganisms*

Microorganism	Elemental Composition	Ash Content (w/w %)	Growth Conditions
Candida utilis	$CH_{1.83}O_{0.46}N_{0.19}$	7.0	Glucose limited, $D = 0.05\ h^{-1}$
	$CH_{1.87}O_{0.56}N_{0.20}$	7.0	Glucose limited, $D = 0.45\ h^{-1}$
	$CH_{1.83}O_{0.54}N_{0.10}$	7.0	Ammonia limited, $D = 0.05\ h^{-1}$
	$CH_{1.87}O_{0.56}N_{0.20}$	7.0	Ammonia limited, $D = 0.45\ h^{-1}$
Klebsiella aerogenes	$CH_{1.75}O_{0.43}N_{0.22}$	3.6	Glycerol limited, $D = 0.10\ h^{-1}$
	$CH_{1.73}O_{0.43}N_{0.24}$	3.6	Glycerol limited, $D = 0.85\ h^{-1}$
	$CH_{1.75}O_{0.47}N_{0.17}$	3.6	Ammonia limited, $D = 0.10\ h^{-1}$
	$CH_{1.73}O_{0.43}N_{0.24}$	3.6	Ammonia limited, $D = 0.80\ h^{-1}$
Saccharomyces cerevisiae	$CH_{1.82}O_{0.58}N_{0.16}$	7.3	Glucose limited, $D = 0.080\ h^{-1}$
	$CH_{1.78}O_{0.60}N_{0.19}$	9.7	Glucose limited, $D = 0.255\ h^{-1}$
	$CH_{1.94}O_{0.52}N_{0.25}$	5.5	Unlimited growth
Escherichia coli	$CH_{1.77}O_{0.49}N_{0.24}$	5.5	Unlimited growth
	$CH_{1.83}O_{0.50}N_{0.22}$	5.5	Unlimited growth
	$CH_{1.96}O_{0.55}N_{0.25}$	5.5	Unlimited growth
	$CH_{1.93}O_{0.55}N_{0.25}$	5.5	Unlimited growth
Pseudomonas fluorescens	$CH_{1.83}O_{0.55}N_{0.26}$	5.5	Unlimited growth
Aerobacter aerogenes	$CH_{1.64}O_{0.52}N_{0.16}$	7.9	Unlimited growth
Penicillium chrysogenum	$CH_{1.70}O_{0.58}N_{0.15}$		Glucose limited, $D = 0.038\ h^{-1}$
	$CH_{1.68}O_{0.53}N_{0.17}$		Glucose limited, $D = 0.098\ h^{-1}$
Aspergillus niger	$CH_{1.72}O_{0.55}N_{0.17}$	7.5	Unlimited growth
Average	$CH_{1.81}O_{0.52}N_{0.21}$	6.0	

Source: Compositions for *P. chrysogenum* are taken from Christensen, L.H., et al., *J. Biotechnol*. 42:95–107, 1995; other data are taken *from* Roels, J.A., *Energetics and Kinetics in Biotechnology*. Amsterdam: Elsevier Biomedical Press, 1983.

BOX 3.3 CALCULATION OF YIELDS WITH RESPECT TO C-MOLE BASIS

Yield coefficients are typically described as moles (g DW)$^{-1}$ or g (g DW)$^{-1}$. To convert the yield coefficients to a C-mole basis, information on the elemental composition and the ash content of biomass is needed. To illustrate the conversion, we calculate the yield of 0.5 g DW biomass (g glucose)$^{-1}$ on a C-mole basis. First, we convert the g DW biomass to an ash-free basis, that is determine the amount of biomass that is made up of carbon, nitrogen, oxygen and hydrogen (and, in some cases, also phosphorus and sulfur). With an ash content of 8% we have 0.92 g ash-free biomass (g DW biomass)$^{-1}$, which gives a yield of 0.46 g ash-free biomass (g glucose)$^{-1}$. This yield can now be directly converted to a C-mole basis using the molecular weights in g C-mole^{-1} for ash-free biomass and glucose. With the standard elemental composition for biomass of $CH_{1.8}O_{0.5}N_{0.2}$ we have a molecular weight of 24.6 g ash-free biomass C-mole^{-1}, and therefore find a yield of 0.46/24.6 = 0.0187 C-moles biomass (g glucose)$^{-1}$. Finally, by multiplication with the molecular weight of glucose on a C-mole basis (30 g C-mole^{-1}), a yield of 0.56 C-moles biomass (C-mole glucose)$^{-1}$ is found.

$$c_x + \sum_{i=1}^{M} c_{\mathrm{p,i}} Y_{xp_i} - \sum_{i=1}^{N} c_{\mathrm{s,i}} Y_{xs_i} = 0 \tag{3.31}$$

where $b_{\mathrm{s,i}}$, $b_{\mathrm{p,i}}$, and b_{x} represent the oxygen content (moles C-mole^{-1}) in the i^{th} substrate, the i^{th} metabolic product, and the biomass, respectively; and $c_{\mathrm{s,i}}$, $c_{\mathrm{p,i}}$, and c_{x} represent the nitrogen content (moles C-mole^{-1}) in the i^{th} substrate, the i^{th} metabolic product, and the biomass, respectively. Normally, only these four balances are considered; balances for phosphate and sulfate may also be set up, but generally these elements are of minor importance. The four elemental balances (3.28) through (3.31) can be conveniently written by collecting the elemental composition of biomass, substrates, and metabolic products in the columns of a matrix **E**, where the first column contains the elemental composition of biomass, columns 2 through $M + 1$ contain the elemental composition of the M metabolic products, and columns $M + 2$ to $M + N + 1$ contain the elemental composition of the N substrates. With the introduction of this matrix, the four elemental balances can be expressed as

$$\mathbf{E\,Y = 0} \tag{3.32}$$

where **Y** is a vector containing the yield coefficients (the substrate yield coefficients are given with a minus sign). With $N + M + 1$ variables, $N + M$ yield coefficients and the forward rate of reaction (3.26) and four constraints, the degree of freedom is $F = M + N + 1 - 4$. If exactly F variables are measured, it may be possible to calculate the other rates by using the four algebraic equations given by (3.32), but, in this case, there are no redundancies left to check the consistency of the data. For this reason, it is advisable to strive for more measurements than the degrees of freedom of the system.

Example 3b: Elemental Balances in a Simple Black Box Model

Consider the aerobic cultivation of the yeast *S. cerevisiae* on a defined, minimal medium (i.e., glucose is the carbon and energy source and ammonia is the nitrogen source). During aerobic growth, the yeast oxidizes glucose completely to carbon dioxide. However, as mentioned in Example 3a, high glucose concentrations cause repression of the respiratory system, resulting in ethanol formation. Thus, at these conditions both ethanol and carbon dioxide should be considered as metabolic products. Finally, water is formed in the cellular pathways. This is also included as a product in the overall reaction. Thus, the black box model for this system is

$$X + Y_{\mathrm{xe}}\ \mathrm{ethanol} + Y_{xc}\ CO_2 + Y_{xw}\ H_2O - Y_{\mathrm{xs}}\ \mathrm{glucose} - Y_{xo}\ O_2 - Y_{xN}\ NH_3 = 0 \tag{3b1}$$

which can be represented with the yield coefficient vector

$$\mathbf{Y} = (1\ Y_{xe}\ Y_{xc}\ Y_{xw} - Y_{xs} - Y_{xo} - Y_{xN})\mathrm{T} \tag{3b2}$$

We now rewrite the conversion using the elemental composition of the substrates and metabolic products. For biomass we use the elemental composition of $CH_{1.83}O_{0.56}N_{0.17}$, and therefore we have

$$CH_{1.83}O_{0.56}N_{0.17} + Y_{xe}\ CH_3O_{0.5} + Y_{xc}\ CO_2 + Y_{xw}\ H_2O - Y_{xs}\ CH_2O - Y_{xo}\ O_2 - Y_{xN}\ NH_3 = 0 \tag{3b3}$$

Some may find it difficult to identify $CH_3O_{0.5}$ as ethanol, but the advantage of using the C-mole basis becomes apparent immediately when we look at the carbon balance:

$$1 + Y_{xe} + Y_{xc} - Y_{xs} = 0 \tag{3b4}$$

This simple equation is very useful for checking the consistency of experimental data. Thus, using the classical data of von Meyenburg (1969), we find $Y_{xe} = 0.713$, $Y_{xc} = 1.313$, and $Y_{xs} = 3.636$ at a dilution rate of $D = 0.3$ h^{-1} in a glucose-limited continuous culture. Obviously the data are not consistent as the carbon balance is not closed. A more elaborate data analysis (Nielsen and Villadsen 1994) suggests that the missing carbon may be accounted for by ethanol evaporation or stripping due to intensive aeration of the bioreactor.

Similarly, using Equation 3.31, we find that a nitrogen balance gives

$$Y_{xN} = 0.17 \tag{3b5}$$

If the yield coefficients for ammonia uptake and biomass formation do not conform to Equation 3b5, an inconsistency is identified in one of these two measurements, or the nitrogen content of the biomass is different from that specified.

We now write all four elemental balances in terms of the matrix equation 3.32:

$$\mathbf{E} = \begin{pmatrix} 1 & 1 & 1 & 0 & 1 & 0 & 0 \\ 1.83 & 3 & 0 & 2 & 2 & 0 & 3 \\ 0.56 & 0.5 & 2 & 1 & 1 & 2 & 0 \\ 0.17 & 0 & 0 & 0 & 0 & 0 & 1 \end{pmatrix} \begin{matrix} \leftarrow \text{carbon} \\ \leftarrow \text{hydrogen} \\ \leftarrow \text{oxygen} \\ \leftarrow \text{nitrogen} \end{matrix} \tag{3b6}$$

where the rows indicate, respectively, the content of carbon, hydrogen, oxygen, and nitrogen and the columns give the elemental composition of biomass, ethanol, carbon dioxide, water, glucose, oxygen, and ammonia, respectively. Using Equation 3.32, we find

$$\begin{pmatrix} 1 & 1 & 1 & 0 & 1 & 0 & 0 \\ 1.83 & 3 & 0 & 2 & 2 & 0 & 3 \\ 0.56 & 0.5 & 2 & 1 & 1 & 2 & 0 \\ 0.17 & 0 & 0 & 0 & 0 & 0 & 1 \end{pmatrix} \begin{pmatrix} 1 \\ Y_{xe} \\ Y_{xc} \\ Y_{xw} \\ -Y_{xs} \\ -Y_{xo} \\ -Y_{xN} \end{pmatrix} = \begin{pmatrix} 1 + Y_{xe} + Y_{xc} - Y_{xs} \\ 1.83 + 3Y_{xe} + 2Y_{xw} - 2Y_{xs} - 3Y_{xN} \\ 0.56 + 0.5Y_{xe} + 2Y_{xc} + Y_{xw} - Y_{xs} - 2Y_{xo} \\ 0.17 - Y_{xN} \end{pmatrix} = \begin{pmatrix} 0 \\ 0 \\ 0 \\ 0 \end{pmatrix} \tag{3b7}$$

The first and last rows are identical to the balances derived in Equations 3b4 and 3b5 for carbon and nitrogen, respectively. The balances for hydrogen and oxygen introduce two additional constraints. However, because the rate of water formation is impossible to measure, one of these equations must be used to calculate this rate (or yield). This leaves only one additional constraint from these two balances.

3.3 MASS BALANCES FOR BIOREACTORS

In Section 3.2, we derived equations that relate the rates of the intracellular reaction with the rates of substrate uptake, metabolic product formation, and biomass formation. These rates are the key elements in the dynamic mass balances for the substrates, the metabolic products, and the biomass, which describe the change in time of the concentration of these state variables in a bioreactor. The bioreactor may be any type of device, ranging from a shake flask to a well-instrumented bioreactor. Figure 3.2 is a general representation of a bioreactor. It has a volume V (unit: L), and it is fed with a stream of fresh, sterile medium with a flow rate F (unit: L h^{-1}). Spent medium is removed with a flow rate of F_{out} (unit: L h^{-1}). The medium in the bioreactor is assumed to be completely (or ideally) mixed, that is, there is no spatial variation in the concentration of the different medium compounds. For small-volume bioreactors (<1 L) (including shake flasks), this can generally be achieved through

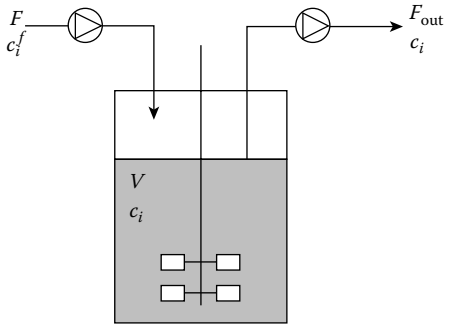

FIGURE 3.2 Bioreactor with addition of fresh, sterile medium and removal of spent medium where c^f_i is the concentration of the i^{th} compound in the feed and c_i is the concentration of the i^{th} compound in the spent medium. The bioreactor is assumed to be very well mixed (or ideal), so that the concentration of each compound in the spent medium becomes identical to its concentration in the bioreactor.

aeration and some agitation, whereas for laboratory stirred-tank bioreactors (1–10 L) special designs may have to be introduced in order to ensure a homogeneous medium (Sonnleitner and Fiechter 1988; Nielsen and Villadsen 1993). The bioreactor may be operated in many different modes of which we will only consider the three most common:

Batch, where $F = F_{out} = 0$ (i.e., the volume is constant)
Continuous, where $F = F_{out}$ 0 (i.e., the volume is constant)
Fed-batch (or semibatch), where F 0 and $F_{out} = 0$ (i.e., the volume increases)

These three different modes of reactor operation are discussed in this section, but first we derive general dynamic mass balances for the substrates, metabolic products, biomass constituents, and biomass.

3.3.1 Dynamic Mass Balances

The basis for derivation of the general dynamic mass balances is the mass balance equation

$$\text{Accumulated} = \text{Net formation rate} + \text{In} - \text{Out} \tag{3.33}$$

where the first term on the RHS is given by Equations 3.5 through 3.8 for substrate, metabolic product, biomass constituents, and intracellular metabolites, respectively. The term "In" represents the flow of the compound into the bioreactor, and the term "Out" the flow of the compound out from the bioreactor. In the following we consider substrates, metabolic products, biomass constituents, intracellular metabolites, and the total biomass separately.

We consider the i^{th} substrate, which is added to the bioreactor via the feed and is consumed by the cells present in the bioreactor. The mass balance for this compound is

$$\frac{d(c_{s,i}\mathrm{V})}{dt} = -r_{s,i}x\mathrm{V} + Fc^f_{s,i} - F_{out}c_{s,i} \tag{3.34}$$

where r_i is the specific consumption rate of the compound (unit: moles (g DW h^{-1}); $c_{s,i}$ is the concentration in the bioreactor, which is assumed to be the same as the concentration in the outlet (unit: moles L^{-1}), $c^f_{s,i}$ (i) is the concentration in the feed (unit: moles L^{-1}); and x is the biomass concentration in the bioreactor (unit: g DW L^{-1}). The first term in Equation 3.34 is the accumulation

term, the second term is the consumption (or reaction) term, the third term is accounting for the inlet, and the last term is accounting for the outlet. Rearrangement of this equation gives

$$\frac{dc_{s,i}}{dt} = -r_{s,i}x + \frac{F}{V}c_{s,i}^{f} - \left(\frac{F_{out}}{V} + \frac{1}{V}\frac{dV}{dt}\right)c_{s,i} \tag{3.35}$$

For a fed-batch reactor,

$$F = \frac{dV}{dt} \tag{3.36}$$

and $F_{out} = 0$. So the term within the parentheses becomes equal to the so-called **dilution rate** given by

$$D = \frac{F}{V} \tag{3.37}$$

For a continuous and a batch reactor, the volume is constant (i.e., $dV/dt = 0$, and $F = F_{out}$), and so for these bioreactor modes also the term within the parentheses becomes equal to the dilution rate. Equation 3.35 therefore reduces to the mass balance (3.38) for any type of operation:

$$\frac{dc_{s,i}}{dt} = -r_{s,i}x + D(c_{s,i}^{f} - c_{s,i}) \tag{3.38}$$

The first term on the right-hand side of Equation 3.38 is the volumetric rate of substrate consumption, which is given as the product of the specific rate of substrate consumption and the biomass concentration. The second term accounts for the addition and removal of substrate from the bioreactor. The term on the left-hand side of Equation 3.38 is the accumulation term, which accounts for the change in time of the substrate, which in a batch reactor (where $D = 0$) equals the volumetric rate of substrate consumption.

Dynamic mass balances for the metabolic products are derived in analogy with those for the substrates and take the form

$$\frac{dc_{p,i}}{dt} = r_{p,i}x + D(c_{p,i}^{f} - c_{p,i}) \tag{3.39}$$

where the first term on the right-hand side is the volumetric formation rate of the i^{th} metabolic product. Normally, the metabolic products are not present in the sterile feed to the bioreactor, and $c_{p,i}^{f}$ is therefore often zero. In these cases the volumetric rate of product formation in a steady-state continuous reactor is equal to the dilution rate multiplied by the concentration of the metabolic product in the bioreactor (equal to that in the outlet).

With sterile feed, the mass balance for the total biomass is derived directly:

$$\frac{dx}{dt} = (\mu - D)x \tag{3.40}$$

where μ (unit: h^{-1}) is the specific growth rate of the biomass given by Equation 3.13.

For the biomass constituents, we normally use the biomass as the reference (i.e., their concentrations are given with the biomass as the basis). In this case, the mass balance for the i^{th} biomass constituent is derived from (sterile feed is assumed)

$$\frac{d(X_{\text{macro,i}}x\text{V})}{dt} = r_{\text{macro,i}}x\text{V} - F_{\text{out}}X_{\text{macro,i}}x \tag{3.41}$$

where $X_{\text{macro,i}}x$ is the concentration of the i^{th} biomass component in the bioreactor (unit: g L^{-1}) and $r_{\text{macro,i}}$ is the specific net rate of formation of the i^{th} biomass constituent. Rearrangement of Equation 3.41 gives

$$\frac{dX_{\text{macro,i}}}{dt} = r_{\text{macro,i}} - \left(\frac{F_{\text{out}}}{\text{V}} + \frac{1}{x}\frac{dx}{dt} + \frac{1}{\text{V}}\frac{d\text{V}}{dt}\right)X_{\text{macro,i}} \tag{3.42}$$

Again, we have that for any mode of bioreactor operation:

$$D = \frac{F_{\text{out}}}{\text{V}} + \frac{1}{\text{V}}\frac{d\text{V}}{dt} \tag{3.43}$$

which, together with the mass balance (3.40) for the total biomass concentration, gives the mass balance:

$$\frac{dX_{\text{macro,i}}}{dt} = r_{\text{macro,i}} - \mu X_{\text{macro,i}} \tag{3.44}$$

where $X_{\text{macro,i}}$ is the concentration of the i^{th} biomass constituent within the biomass. Different units may be applied for the concentrations of the biomass constituents, but they are normally given as g (g DW)$^{-1}$, because then the sum of all the concentrations equals 1, that is,

$$\sum_{i=1}^{Q} X_{\text{macro,i}} = 1 \tag{3.45}$$

Furthermore, this unit corresponds with the experimentally determined macromolecular composition of cells, where weight fractions are generally used. In Equation 3.44, it is observed that the mass balance for the biomass constituents is completely independent of the mode of operation of the bioreactor (i.e., the dilution rate does not appear in the mass balance). However, there is indirectly a coupling via the last term, which accounts for dilution of the biomass constituents when the biomass expands due to growth. Thus, if there is no net synthesis of a macromolecular pool, but the biomass still grows, the intracellular level decreases.

For intracellular metabolites it is not convenient to use the same unit for their concentrations as for the biomass constituents. These metabolites are dissolved in the matrix of the cell; therefore, it is more appropriate to use the unit moles per liquid cell volume for the concentrations. The intracellular concentration can then be compared directly with the affinities of enzymes, typically quantified by their *K*m values, which are normally given with the unit moles per liter. If the concentration is known in one unit, it is, however, easily converted to another unit if the density of the biomass (in the range of 1 g cell per mL cell) and the water content (in the range of 0.67 ml water per ml cell) is

known. Even though a different unit is applied, the biomass is still the basis, and the mass balance for the intracellular metabolites therefore takes the same form:

$$\frac{dX_{\text{met,i}}}{dt} = r_{\text{met,i}} - \mu X_{\text{met,i}} \tag{3.46}$$

where $\boldsymbol{X}_{\text{met}}$,i is the concentration of the i^{th} intracellular metabolite. It is important to distinguish between concentrations of intracellular metabolites given in moles per liquid reactor volume and in moles per liquid cell volume. If concentrations are given in the former unit, the mass balance will be completely different.

3.3.2 Batch Reactor

This is the classical operation of the bioreactor, and many life scientists use it because it can be carried out in a relatively simple experimental setup. Batch experiments have the advantage of being easy to perform, and by using shake flasks a large number of parallel experiments can be carried out. The disadvantage is that the experimental data are difficult to interpret because there are dynamic conditions throughout the experiment (i.e., the environmental conditions experienced by the cells vary with time). However, by using well-instrumented bioreactors, at least some variables (e.g., pH and dissolved oxygen tension) may be kept constant.

As mentioned in the previous section, the dilution rate is zero for a batch reactor, and the mass balances for the biomass and the limiting substrate therefore take the form

$$\frac{dx}{dt} = \mu x \quad x(t=0) = x_0 \tag{3.47}$$

$$\frac{dc_s}{dt} = -r_s x \quad c_s(t=0) = c_{s,0} \tag{3.48}$$

where x_0 indicates the initial biomass concentration, which is obtained immediately after inoculation, and c_s,0 is the initial substrate concentration. According to the mass balance, the biomass concentration will increase as indicated in Figure 3.3 and the substrate concentration will decrease until its concentration reaches zero and growth stops. Because the substrate concentration is zero at the end of the cultivation, the overall yield of biomass on the substrate can be found from

$$Y_{sx}^{\text{overall}} = \frac{x_{\text{final}} - x_0}{c_{s,0}} \tag{3.49}$$

where x final is the biomass concentration at the end of the cultivation. Normally $X_0 \ll x_{\text{final}}$, and the overall yield coefficient can therefore be estimated from the final biomass concentration and the initial substrate concentration alone. Notice that the yield coefficient determined from the batch experiment is the overall yield coefficient and not Y_{sx} or $(Y_{xs}^{\text{true}})^{-1}$. The yield coefficient Y_{sx} may well be time dependent as it is the ratio between the specific growth rate and the substrate uptake rate; see Equation 3.16. However, if there is little variation in these rates during the batch culture (e.g., if there is a long exponential growth phase and only a very short declining growth phase), the overall yield coefficient may be very similar to the yield coefficient. The true yield coefficient, on the other hand, is difficult to determine from batch cultivation because it requires information about the maintenance coefficients, which can hardly be determined from a batch experiment. However, in batch cultivation the specific growth rate is close to its maximum throughout most of the growth

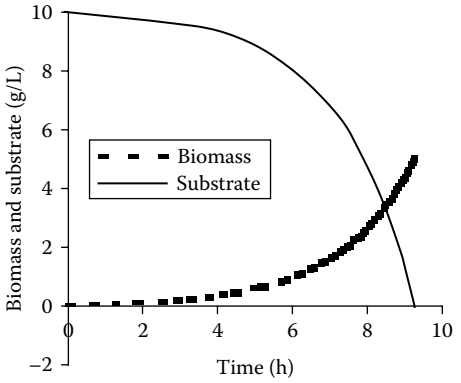

FIGURE 3.3 Batch fermentation described with Monod kinetics. The biomass concentration is found using Equation (c2) and the corresponding substrate concentration is found from Equation (c1). μ_{max} is 0.5 h^{-1}, K_s is 50 mg l^{-1} (a quite high value), and Y_{sx} is 0.5 g g^{-1}. The initial substrate concentration c_s, 0 is 10 g l^{-1}. The substrate concentration decreases from 0.5 g l^{-1} to 0 in less than 5 min, and this is the interesting substrate concentration range for estimation of K_s.

phase, and the substrate consumption due to maintenance is therefore negligible. According to Equation 3.17, the true yield coefficient is close to the observed yield coefficient determined from the final biomass concentration.

3.3.3 Chemostat

A typical operation of the continuous bioreactor is the so-called *chemostat*, where the added medium is designed such that there is a *single limiting substrate*. This allows for controlled variation in the specific growth rate of the biomass. The advantage of the continuous bioreactor is that a steady state can be achieved, which allows for precise experimental determination of specific rates. Furthermore, by varying the feed flow rate to the bioreactor the environmental conditions can be varied, and valuable information concerning the influence of the environmental conditions on the cellular physiology can be obtained. The continuous bioreactor is attractive for industrial applications because the productivity can be high. However, often the titer (i.e., the product concentration) is lower than can be obtained in the fed-batch reactor, and it is therefore a trade-off between productivity and titer. Furthermore, it is rarely used in industrial processes because it is sensitive to contamination (e.g., via the feed stream) and to the appearance of spontaneously formed mutants that may outcompete the production strain. Other examples of continuous operation besides the chemostat are the *pH-stat*, where the feed flow is adjusted to maintain the pH constant in the bioreactor, and the *turbidostat*, where the feed flow is adjusted to maintain the biomass concentration at a constant level.

From the biomass mass balance (3.40), it can easily be seen that in a steady-state continuous reactor, the specific growth rate equals the dilution rate:

$$m = D \tag{3.50}$$

Thus, by varying the dilution rate (or the feed-flow rate) in a continuous culture, different specific growth rates can be obtained. This allows detailed physiological studies of the cells when they are grown at a predetermined specific growth rate (corresponding to a certain environment experienced by the cells). At steady state, the substrate mass balance (3.38) gives

$$0 = -r_s x + D\left(c_s^f - c_s\right) \tag{3.51}$$

which, upon combination with Equation 3.50 and the definition of the yield coefficient, directly gives

$$x = Y_{sx}\left(c_s^f - c_s\right) \tag{3.52}$$

Thus, the yield coefficient can be determined from measurement of the biomass and the substrate concentrations in the bioreactor (the substrate concentration in the feed flow should generally be known as it is determined in the setup of the experiment).

Besides the advantage for obtaining steady-state measurements, the chemostat is well suited to study dynamic conditions because it is possible to perform well-controlled transients. Thus, it is possible to study the cellular response to a sudden increase in the substrate concentration by adding a pulse of the limiting substrate to the reactor or to a sudden change in the dilution rate. These experiments both start and end with a steady state, so the initial and end conditions are well characterized, and this facilitates the interpretation of the cellular response. One type of transient experiment is especially suited to determining an important kinetic parameter, namely, the maximum specific growth rate. By increasing the dilution rate to a value above μ_{max}, the cells will wash out from the bioreactor and the substrate concentration will increase (and eventually reach the same value as in the feed). After adaptation of the cells to the new conditions, they will attain their maximum specific growth rate and the dynamic mass balance for the biomass becomes

$$\frac{dx}{dt} = (\mu_{max} - D)x \tag{3.53}$$

or

$$\frac{x(t-t_0)}{x(t_0)} = \exp((\mu_{max} - D)(t-t_0)) \tag{3.54}$$

where t_0 is the time at which the cells have become adapted to the new conditions and grow at their maximum specific growth rate. Thus, the maximum specific growth rate is easily determined from a plot of the biomass concentration versus time on a semilog plot.

3.3.4 Fed-Batch Reactor

This operation is probably the most common in industrial processes, because it allows for control of the environmental conditions, for example maintaining the glucose concentration at a certain level, as well as enabling the formation of very high titers (up to several hundred grams per liters of some metabolites), which is important for subsequent downstream processing. For a fed-batch reactor, the mass balances for biomass and substrate are given by Equations 3.38 and 3.40. Normally, the feed concentration is very high (i.e., the feed is a very concentrated solution) and the feed flow is low, giving a low dilution rate.

For the fed-batch reactor, the dilution rate is given by

$$D = \frac{1}{V}\frac{dV}{dt} \tag{3.55}$$

To keep D constant, there needs to be an exponentially increasing feed flow to the bioreactor, which is normally practically impossible as it may lead to oxygen limitations. The feed flow is therefore adjusted or increased until limitations in the oxygen supply set in, at which point the feed flow is kept constant. This will give a decreasing specific growth rate. However, because the biomass

concentration usually increases, the volumetric uptake rate of substrates (including oxygen) may be kept approximately constant. From the above it is quite clear that there may be many different feeding strategies in a fed-batch process, and optimization of the operation is a complex problem that is difficult to solve empirically. Even when a very good process model is available, calculation of the optimal feeding strategy is a complex optimization problem. In an empirical search for the optimal feeding policy, the two most obvious criteria are

Keep the concentration of the limiting substrate constant.
Keep the volumetric growth rate of the biomass (or uptake of a given substrate) constant.

A constant concentration of the limiting substrate is often applied if the substrate inhibits product formation, and the chosen concentration is therefore dependent on the degree of inhibition and the desire to maintain a certain growth of the cells. A constant volumetric growth rate (or uptake of a given substrate) is applied if there are limitations in the supply of oxygen or in heat removal.

Fed-batch cultures were used in the production of baker's yeast as early as 1915. The method was introduced by Dansk Gæringsindustri and is therefore sometimes referred to as the Danish method. It was recognized that an excess of malt in the medium would lead to a higher growth rate, resulting in an oxygen demand in excess of what could be met in the fermentors. This resulted in the development of respiratory catabolism of the yeast, leading to ethanol formation at the expense of biomass production. The yeast was allowed to grow in an initially weak medium to which additional medium was added at a rate less than the maximum rate at which the organism could use it. In modern fed-batch processes for yeast production, the feed of molasses is under strict control, based on the automatic measurement of traces of ethanol in the exhaust gas of the bioreactor. Although such systems may result in low specific growth rates, the biomass yield is generally close to the maximum obtainable, and this is especially important in the production of baker's yeast, where there is much focus on the yield. Apart from the production of baker's yeast, the fed-batch process is used today for the production of secondary metabolites (where penicillin is a prominent group), industrial enzymes, and many other products derived from cultivation processes.

3.4 KINETIC MODELS

Kinetic modeling expresses the verbally or mathematically expressed correlation between rates and reactant or product concentrations that, when inserted into the mass balances derived in Section 3.3, permit a prediction of the degree of conversion of substrates and the yield of individual products at other operating conditions. If the rate expressions are correctly set up, it may be possible to express the course of an entire fermentation experiment based on initial values for the components of the state vector (e.g., concentration of substrates). This leads to simulations, which may finally result in an optimal design of the equipment or an optimal mode of operation for a given system. The basis of kinetic modeling is to express functional relationships between the forward reaction rates **v** of the reactions considered in the model and the concentrations of the substrates, metabolic products, biomass constituents, intracellular metabolites, and/or biomass:

$$v_i = f_i(c_s, c_p, X_{macro}, X_{met}, x) \tag{3.56}$$

If, during the cultivation, the biomass composition remains constant, then the rates of the internal reactions must necessarily be proportional. This is referred to as **balanced growth**. In this case the growth process can be described in terms of a single variable that defines the state of the biomass. This variable is quite naturally chosen as the biomass concentration x (g DW l^{-1}). This is the basis of the so-called **unstructured models** that have proved adequate during 50 years of practical application to design cultivation processes (especially steady-state or batch cultivations), to install suitable

control devices, and to estimate which process conditions are likely to give the best return on the investment in process equipment. However, these unstructured models generally have poor predictive strength and as such are of little value in fundamental studies of cellular function.

3.4.1 Degree of Model Complexity

A typical discussion on the complexity of mathematical modeling of biochemical systems may be initiated by asking the question of whether a mechanistic model or an empirical model should be applied instead. To illustrate this, consider the fractional saturation y of a protein at a ligand concentration c_l. This may be described by the Hill equation (Hill 1910):

$$y = \frac{c_l^{\mathrm{h}}}{c_l^{\mathrm{h}} + K} \tag{3.57}$$

where h and K are empirical parameters. Alternatively, the fractional saturation may be described by the equation of Monod et al. (1965):

$$y = \frac{\left(La\left(1 + \frac{ac_l}{K_\mathrm{R}}\right)^3 + \left(1 + \frac{c_l}{K_\mathrm{R}}\right)^3 \right)\frac{c_l}{K_\mathrm{R}}}{L\left(1 + \frac{ac_l}{K_\mathrm{R}}\right)^4 + \left(1 + \frac{c_l}{K_\mathrm{R}}\right)^4} \tag{3.58}$$

where L, a, and K_R are parameters. Both equations address the same experimental problem, but whereas Equation 3.57 is completely empirical with h and K as fitted parameters, Equation 3.58 is derived from a hypothesis for the mechanism; the parameters therefore have a direct physical interpretation. If the aim of the modeling is to understand the underlying mechanism of the process, Equation 3.57 can obviously not be applied because the kinetic parameters are completely empirical and give no (or little) information about the ligand binding to the protein. In this case, Equation 3.58 should be applied, because by estimating the kinetic parameter the investigator is supplied with valuable information about the system and the parameters can be directly interpreted.

If, on the other hand, the aim of the modeling is to simulate the ligand binding to the protein, Equation 3.57 may be as good as Equation 3.58—and this equation may even be preferable because it is simpler in structure, has fewer parameters, and actually often gives a better fit to experimental data than Equation 3.57. Thus, the answer to which model is preferred depends on the aim of the modeling exercise. The same can be said about the unstructured growth models (Section 3.4.2), which are completely empirical but are valuable for extracting key kinetic parameters for growth. Furthermore, they are well suited to simple design problems and for teaching.

If the aim is to simulate dynamic growth conditions, one may turn to simple structured models (Section 4.4.3), for example the compartment models, which are also useful for an illustration of structured modeling in the classroom. However, if the aim is to analyze a given system in further detail, it is necessary to include far more structure in the model. In this case one often describes only individual processes within the cell, such as a certain pathway or gene transcription from a certain promoter. Similarly, if the aim is to investigate the interaction between different cellular processes (e.g., the influence of a plasmid copy number on chromosomal DNA replication), a single-cell model (Section 3.4.4) has to be applied.

Finally, if the aim is to look into population distributions, which in some cases may have an influence on growth or production kinetics, either a segregated or a morphologically structured model has to be applied (Section 3.5).

3.4.2 Unstructured Models

Even when there are many substrates, one of these substrates is usually limiting (i.e., the rate of biomass production depends exclusively on the concentration of this substrate). At low concentrations c_s of this substrate μ is proportional to c_s, but for increasing values of c_s an upper value μ_{max} for the specific growth rate is gradually reached. This is the verbal formulation of the Monod (1942) model:

$$\mu = \mu_{max} \frac{c_s}{c_s + K_s} \tag{3.59}$$

which has been shown to correlate fermentation data for many different microorganisms. In the Monod model, K_s is that value of the limiting substrate concentration at which the specific growth rate is half its maximum value. Roughly speaking, it divides the μ versus c_s plot into a low substrate concentration range where the specific growth rate is strongly (almost linearly) dependent on c_s, and a high substrate concentration range where μ is independent of c_s.

When glucose is the limiting substrate, the value of K_s is normally in the micromolar range (corresponding to the mg l^{-1} range), and it is therefore experimentally difficult to determine. Some of the K_s values reported in the literature are compiled in Table 3.5. It should be stressed that the K_s value in the Monod model does not represent the saturation constant for substrate uptake but an overall saturation constant for the entire growth process.

Some of the most characteristic features of microbial growth are represented quite well by the Monod model:

The constant specific growth rate at high substrate concentration
The first-order dependence of the specific growth rate on substrate concentration at low substrate concentrations

In fact, one may argue that the two features that make the Monod model work so well in fitting experimental data are deeply rooted in any naturally occurring conversion process: the size of the machinery that converts substrate must have an upper value, and all chemical reactions

TABLE 3.5
Compilation of K_s values *for Sugars*

Species	Substrate	K_s (mg l^{-1})
Aerobacter aerogenes	Glucose	8
Escherichia coli	Glucose	4
Klebsiella aerogenes	Glucose	9
	Glycerol	9
Klebsiella oxytoca	Glucose	10
	Arabinose	50
	Fructose	10
Lactococcus cremoris	Glucose	2
	Lactose	10
	Fructose	3

Source: Values are taken from Nielsen, J. and Villadsen, J., *Bioreaction Engineering Principles*. New York: Plenum Press, 1994.

will end up as first-order processes when the reactant concentration tends to zero. The satisfactory fit of the Monod model to many experimental data should never be misconstrued to mean that Equation 3.59 is a mechanism of fermentation processes. The Langmuir rate expression of heterogeneous catalysis and the Michaelis–Menten rate expression in enzymatic catalysis are formally identical to Equation 3.59, but the denominator constant has a direct physical interpretation in both cases (the equilibrium constant for dissociation of a catalytic site–reactant complex) whereas K_s in Equation 3.59 is no more than an empirical parameter used to fit the average substrate influence on all cellular reactions pooled into the single reaction by which substrate is converted to biomass.

In the Monod model, it is assumed that the yield of biomass from the limiting substrate is constant; in other words, there is proportionality between the specific growth rate and the specific substrate uptake rate. The Monod model is, however, normally used together with a maintenance consumption of substrate, that is, the specific substrate uptake is described by the linear relation; see Equation 3.18. The Monod model including maintenance is probably the most widely accepted model for microbial growth, and it is well suited for analysis of steady-state data from a chemostat (see Example 3c). Often the model is combined with the Luedeking and Piret (1959) model for metabolite production in which the specific rate of product formation is given by Equation 3.17. The Luedeking and Piret model was derived on the basis of an analysis of lactic acid fermentation and is in principle only valid for metabolic products formed as a direct consequence of the growth process (i.e., metabolites of primary metabolism). However, the model may in some cases be applied to other products (e.g., secondary metabolites), but this should not be done automatically.

Example 3c: The Monod Model

Despite its simplicity, the Monod model is very useful for extracting key growth parameters, and it generally fits simple batch fermentations with one exponential growth phase and steady-state chemostat cultures (but rarely with the same parameters). We first consider a batch process, where substrate consumption due to maintenance can usually be neglected. In this case, there is an analytical solution to the mass balances for the concentrations of substrate and the limiting substrate (Nielsen and Villadsen 1994):

$$c_s = c_{s,0} - Y_{xs}\left(x - x_0\right) \tag{3c1}$$

$$\mu_{max} t = \left(1 + \frac{K_s}{c_{s,0} + Y_{xs} x_0}\right) \ln\left(\frac{x}{x_0}\right) - \frac{K_s}{c_{s,0} + Y_{xs} x_0} \ln\left(1 + \frac{Y_{sx}\left(x_0 - x\right)}{c_{s,0}}\right) \tag{3c2}$$

Using this analytical solution, it is in principle possible to estimate the two kinetic parameters in the Monod model, but since K_s generally is very low it is in practice not possible to estimate this parameter from a batch cultivation (see Figure 3.3).

For a steady-state, continuous culture, the mass balance for the biomass, together with the Monod model, gives

$$D = \mu_{max} \frac{c_s}{c_s + K_s} \tag{3c3}$$

or

$$c_s = \frac{D K_s}{\mu_{max} - D} \tag{3c4}$$

Thus, the concentration of the limiting substrate increases with the dilution rate. When substrate concentration becomes equal to the substrate concentration in the feed, the dilution rate attains its maximum value, which is often called the *critical dilution rate*:

$$D_{crit} = \mu_{max} \frac{c_s^f}{c_s^f + K_s} \tag{3c5}$$

When the dilution rate becomes equal to or larger than this value, the biomass is washed out of the bioreactor. Equation 3b4 clearly shows that the steady-state chemostat is well suited to studying the influence of the substrate concentration on the cellular function (e.g., product formation), because by changing the dilution rate it is possible to change the substrate concentration as the only variable. Furthermore, it is possible to study the influence of different limiting substrates on the cellular physiology (e.g., glucose and ammonia).

Besides quantification of the Monod parameters, the chemostat is well suited to determine the maintenance coefficient. Because the dilution rate equals the specific growth rate, the yield coefficient is given by

$$Y_{sx} = \frac{D}{Y_{xs}^{true} D + m_s} \tag{3c6}$$

or, if we use Equation 3.52,

$$x = \frac{D}{Y_{xs}^{true} D + m_s}\left(c_s^f - c_s\right) \approx \frac{D}{Y_{xs}^{true} D + m_s} c_s^f \tag{3c7}$$

because $c_s^f >> c_s$ except for dilution rates close to the critical dilution rate. Equation 3c7 shows that the biomass concentration decreases at low specific growth rates, where the substrate consumption for maintenance is significant compared with that for growth. At high specific growth rates (high dilution rates), maintenance is negligible and the yield coefficient becomes equal to the true yield coefficient (Figure 3.4). By rearrangement of Equation 3c7, a linear relationship between the specific substrate uptake rate and the dilution rate is found, and when using this, the true yield coefficient and the maintenance coefficient can easily be estimated using linear regression.

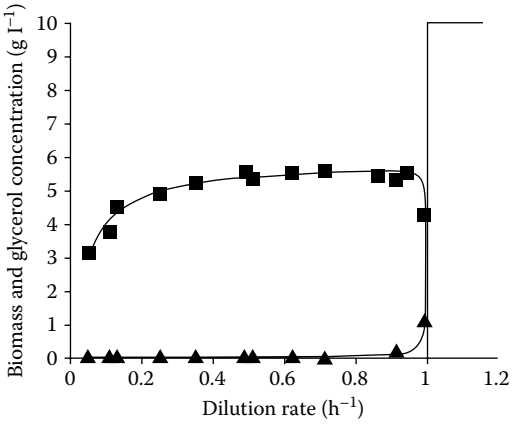

FIGURE 3.4 Growth of *Aerobacter aerogenes* in a chemostat with glycerol as the limiting substrate where the biomass concentration (■) decreases for increasing dilution rate due to the maintenance metabolism, and when the dilution rate approaches the critical value the biomass concentration decreases rapidly. The glycerol concentration (▲) increases slowly at low dilution rates, but when the dilution rate approaches the critical value it increases rapidly. The lines are model simulations using the Monod model with maintenance, and with the parameter values: $c_s^f = 10$ g L^{-1}; $\mu_{max} = 1.0$ h^{-1}; $K_S = 0.01$ g L^{-1}; $ms = 0.08$ g (g DW h)$^{-1}$; $Y_{xs}^{true} = 1.70$ g (g DW)$^{-1}$.

It is unlikely that the Monod model can be used to fit all kinds of fermentation data. Many authors have tried to improve on the Monod model, but generally these empirical models are of little value. However, in some cases growth is limited either by substrate concentration or by the presence of a metabolic product, which acts as an inhibitor. In order to account for this, the Monod model is often extended with additional terms. Thus, for inhibition by high concentrations of the limiting substrate

$$\mu = \mu_{max} \frac{c_s}{c_s^2/K_i + c_s + K_s} \tag{3.60}$$

and for inhibition by a metabolic product

$$\mu = \mu_{max} \frac{c_s}{c_s + K_s} \frac{1}{1 + p/K_i} \tag{3.61}$$

Equations 3.60 and 3.61 may be a useful way of including product or substrate inhibition in a simple model, and often these expressions are also applied in connection with structured models. Extension of the Monod model with additional terms or factors should, however, be carried out with some restraint because the result may be a model with a large number of parameters but of little value outside the range in which the experiments were made.

3.4.3 Compartment Models

Simple structured models are in one sense improvements to the unstructured models, because some basic mechanisms of the cellular behavior are at least qualitatively incorporated. Thus, the structured models may have some predictive strength, that is, they may describe the growth process at different operating conditions with the same set of parameters. But one should bear in mind that "true" mechanisms of the metabolic processes are of course not considered in simple structured models even if the number of parameters is quite large.

In structured models all the biomass components are lumped into a few key variables (i.e., the vectors $\mathbf{X}_{macro}$ and $\mathbf{X}_{met}$), which are hopefully representative of the state of the cell. The microbial activity thus becomes a function of not only the biotic variables, which may change with very small time constants, but also the cellular composition, and consequently the "history" of the cells (i.e., the environmental conditions the cells have experienced in the past).

The biomass can be structured in a number of ways. For example, in simple structured models only a few cellular components are considered, whereas in highly structured models up to 20 intracellular components are considered (Nielsen and Villadsen 1992). As discussed in Section 3.4.1, the choice of a particular structure depends on the aim of the modeling exercise, but often one starts with a simple structured model onto which more and more structures are added as new experiments are added to the database. Even in highly structured models many of the cellular components included in the model represent "pools" of different enzymes, metabolites, or other cellular components. The cellular reactions considered in structured models are therefore empirical in nature because they do not represent the conversion between "true" components. Consequently, it is permissible to write the kinetics for the individual reactions in terms of reasonable empirical expressions, with a form judged to fit the experimental data with a small number of parameters. Thus, Monod-type expressions are often used because they summarize some fundamental features of most cellular reactions (i.e., being first order at low substrate concentration and zero order at high substrate concentration). Despite their empirical nature, structured models are normally based on some well-known cell mechanisms, and they therefore have the ability to simulate certain features of experiments quite well.

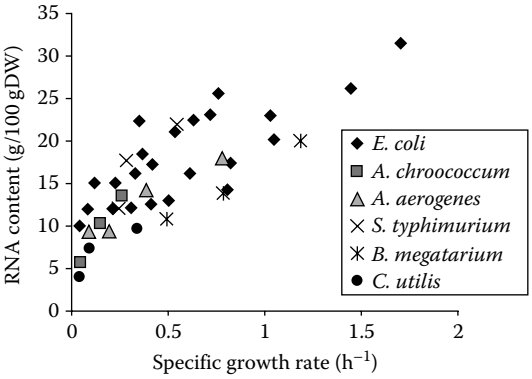

FIGURE 3.5 The level of stable RNA as a function of specific growth rate for different micro-organisms. (Data are taken from Nielsen, J. and J. Villadsen., *Bioreaction Engineering Principles*, New York: Plenum Press, 1994.)

The first structured models appeared in the late 1960s from the group of Fredrickson and Tsuchiya at the University of Minnesota (Ramkrishna et al. 1966, 1967; Williams 1967), who also were the first to formulate microbial models within a general mathematical framework similar to that used to describe reaction networks in classical catalytic processes (Tsuchiya et al. 1966; Fredrickson et al. 1967; Fredrickson 1976). Since this pioneering work, many other simple structured models have been presented (Harder and Roels 1982; Nielsen and Villadsen 1992).

In these simple structured models, the biomass is divided into a few compartments. These compartments must be chosen with care, and cell components with similar functions should be placed in the same compartment, for example, all membrane material and otherwise rather inactive components in one compartment, and all active material in another compartment. With the central role of the protein-synthesizing system (PSS) in cellular metabolism, this is often a key component in compartment models. Besides a few enzymes, the PSS consists of ribosomes, which contain approximately 60% ribosomal RNA (rRNA) and 40% ribosomal protein. Because rRNA makes up more than 80% of the total stable RNA in the cell, the level of the ribosomes is easily identified through measurements of the RNA concentration in the biomass. As seen in Figure 3.5, the RNA content of many different microorganisms increases linearly with the specific growth rate. Thus, the level of the PSS is well correlated with the specific growth rate. It is therefore a good representative of the activity of the cell, and this is the basis of most simple structured models (see Example 3d).

Example 3d: Two-Compartment Model

Nielsen *et al.* (1991a, 1991b) presented a two-compartment model for the lactic acid bacterium *Lactococcus cremoris*. The model is a direct descendant of the model created by Williams (1967) with similar definitions for the following two compartments:

The active (A) compartment contains the PSS and small building blocks.
The structural and genetic (G) compartment contains the rest of the cell material.

The model considers both glucose and a complex nitrogen source (peptone and yeast extract), but in the following presentation we discuss the model with only one limiting substrate (glucose). The model considers two reactions for which the stoichiometry is

$$\gamma_{11} X_A - s = 0 \tag{3d1}$$

$$\gamma_{22} X_G - X_A = 0 \tag{3d2}$$

In the first reaction, glucose is converted into small building blocks in the A compartment, and these are further converted into ribosomes. The stoichiometric coefficient γ_{11} can be considered as a yield coefficient because metabolic products (lactic acid, carbon dioxide, etc.) are not included in the stoichiometry. In the second reaction, building blocks present in the A compartment are converted into macromolecular components of the G compartment. In this process, some by-products may be formed and the stoichiometric coefficient γ_{22} is therefore slightly less than 1. The kinetics of the two reactions have the same form:

$$v_i = k_i \frac{c_s}{c_s + K_{s,i}} X_A; \quad i = 1,2 \tag{3d3}$$

From Equation 3.13, the specific growth rate for the biomass is found to be

$$\mu = \begin{pmatrix} 1 & 1 \end{pmatrix} \begin{pmatrix} \gamma_{11} & -1 \\ 0 & \gamma_{22} \end{pmatrix} \begin{pmatrix} v_1 \\ v_2 \end{pmatrix} = \gamma_{11} v_1 - (1 - \gamma_{22}) v_2 \tag{3d4}$$

or, with the kinetic expression for v_1 and v_2 inserted,

$$\mu = \left(\gamma_{11} k_1 \frac{c_s}{c_s + K_{s,1}} - (1 - \gamma_{22}) k_2 \frac{c_s}{c_s + K_{s,2}} \right) X_A \tag{3d5}$$

Thus, the specific growth rate is proportional to the size of the active compartment. The substrate concentration c_s influences the specific growth rate both directly and indirectly by determining the size of the active compartment. The influence of the substrate concentration on the synthesis of the active compartment can be evaluated through the ratio r_1/r_2:

$$\frac{r_1}{r_2} = \frac{k_1}{k_2} \frac{c_s + K_{s,2}}{c_s + K_{s,1}} \tag{3d6}$$

If $K_{s,1}$ is larger than $K_{s,2}$, the formation of X_A is favored at high substrate concentration, and it is thus possible to explain the increase in the active compartment with the specific growth rate. Consequently, when the substrate concentration increases rapidly, there are two effects on the specific growth rate:

First a rapid increase in the specific growth rate, which is a result of mobilization of excess capacity in the cellular synthesis machinery.
Thereafter, there is a slow increase in the specific growth rate, which is a result of a slow buildup of the active part of the cell (i.e., additional cellular synthesis machinery has to be formed in order for the cells to grow faster).

This is illustrated in Figure 3.6, which shows the biomass concentration in two independent wash-out experiments. In both cases the dilution rate was shifted to a value (0.99 h^{-1}) above the critical dilution rate (0.55 h^{-1}), but in one experiment the dilution rate before the shift was low (0.1 h^{-1}) and in the other experiment it was high (0.5 h^{-1}). The wash-out profile is seen to be very different, with a much faster wash-out when there was a shift from a low dilution rate. When the dilution rate is shifted to 0.99 h^{-1}, the glucose concentration increases rapidly to a value much higher than $K_{s,1}$ and $K_{s,2}$, and this allows growth at the maximum rate. However, when the cells come from a low dilution rate, the size of the active compartment is not sufficiently large to allow rapid growth, and XA therefore has to be built up before the maximum specific growth rate is attained. On the other hand, if the cells come from a high dilution rate, XA is already high and the cells immediately attain their maximum specific growth rate. It is observed that the model is

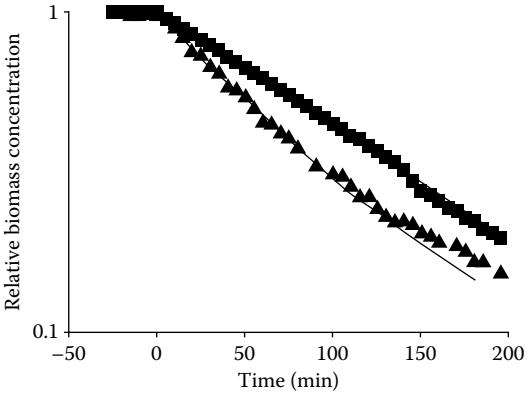

FIGURE 3.6 Measurement of biomass concentration, two transient experiments, of *L. cremoris* growing in glucose-limited chemostat; the dilution rate was shifted from an initial value of 0.10 h^{-1} (▲) or 0.50 h^{-1} (■) to 0.99 h^{-1}, respectively. The biomass concentration is normalized by the steady-state biomass concentration before the step change, which was made at time zero. The lines are model simulations. (The data are taken from Nielsen, J., Nikolajsen, K., and Villadsen, J., *Biotechnol. Bioeng.*, 38:11–23, 1991b.)

able to correctly describe the two experiments (all parameters were estimated from steady-state experiments), and the model correctly incorporates information about the previous history of the cells.

The model also includes the formation of lactic acid; the kinetics was described using a rate equation similar to Equation 3d3. Thus, the lactic acid formation increases when the activity of the cells increases, and so it is ensured that there is a close coupling between the formation of this primary metabolite and the growth of the cells.

It is interesting to note that even though the model does not include a specific maintenance reaction, it can actually describe a decrease in the yield coefficient of biomass on glucose at low specific growth rates. The yield coefficient is given by

$$Y_{sx} = \gamma_{21}\left(1-(1-\gamma_{22})\frac{k_2}{k_1}\frac{c_s+K_{s,1}}{c_s+K_{s,2}}\right) \tag{3d7}$$

Because $K_{s,1}$ is larger than $K_{s,2}$, the last term within the parentheses decreases for increasing specific growth rates, and the yield coefficient will therefore also increase for increasing substrate concentration.

3.4.4 Single-Cell Models

Single-cell models are in principle an extension of the compartment models, but with the description of many different cellular functions. Furthermore, these models depart from the description of a population and focus on the description of single cells. This allows consideration of characteristic features of the cell, and it is therefore possible to study different aspects of cell function:

- Cell geometry can be accounted for explicitly, and so it is possible to examine its potential effects on nutrient transport.
- Temporal events during the cell cycle can be included in the model, and the effect of these events on the overall cell growth can be studied.
- Spatial arrangements of intracellular events can be considered, even though this would lead to significant model complexity.

To set up single-cell models, it is necessary to have a detailed knowledge of the cell, and single-cell models have therefore only been described for well-studied cellular systems such as *Escherichia coli*, *S. cerevisiae*, *Bacillus subtilis*, and human erythrocytes. The most comprehensive single-cell model is the so-called Cornell model set up by Shuler and coworkers (Shuler et al. 1979), which contains 20 intracellular components. This model predicts a number of observations made with *E. coli,* and it has formed the basis for setting up several other models (Nielsen and Villadsen 1992). Thus, Peretti and Bailey (1987) extended the model to describe plasmid replication and gene expression from a plasmid inserted into a host cell. This allowed study of host–plasmid interactions, especially the effects of copy number, promoter strength, and ribosome binding site strength on the metabolic activity of the host cell and on the plasmid gene expression.

3.4.5 Molecular Mechanistic Models

Despite the level of detail, the single-cell models are normally based on an empirical description of different cellular events (e.g., gene transcription and translation). This is a necessity because the complexity of the model would become very high if all these individual events were to be described with detailed models that include mechanistic information. In many cases, however, it is interesting to study these events separately, and for models where mechanistic information is included, they have to be used. These models are normally set up at the molecular level, and they can therefore be referred to as *molecular mechanistic models.* Many different models of this type can be found in the literature, but most fall in one of two categories:

Gene transcription models
Pathway models

Gene transcription models aim at quantifying gene transcription based on knowledge of the promoter function. The *lac*-promoter of *E. coli* is one of the best studied promoter systems of all, and so this system has been modeled most extensively. Furthermore, this promoter (or its derivatives) is often used in connection with the production of heterologous proteins by this bacterium, because it is an inducible promoter. In a series of papers, Lee and Bailey (1984a, 1984b, 1984c, 1984d) presented an elegant piece of modeling of this system, and through combination with a model for plasmid replication they could investigate, for example, the role of point mutations in the promoter on gene transcription. This promoter system is quite complex, with both activator and repressor proteins, and empirical investigation can therefore be laborious; the detailed mathematical model is a valuable tool to guide the experimental work.

In pathway models the individual enzymatic reactions of a given pathway are described with enzyme kinetic models, and it is therefore possible to simulate the metabolite pool levels and the fluxes through different branches of the pathway. These models have mainly concentrated on glycolysis in *S. cerevisiae* (Galazzo and Bailey 1990; Rizzi et al. 1997), because much information about enzyme regulation is available for this pathway. However, complete models are also available for other pathways, such as the penicillin biosynthetic pathway (Pissarra et al. 1996). These pathway models are experimentally verified by comparing modeling simulations with measurements of intracellular metabolite pool levels – something that has only been possible with sufficient precision in the last couple of years, because it requires rapid quenching of the cellular activity and sensitive measurement techniques.

Pathway models are very useful in studies of metabolic fluxes, because they allow quantification of the control of flux by the individual enzymes in the pathway. This can be done by calculation of sensitivity coefficients (or the so-called *flux control coefficients*; see Box 3.4), which quantify the relative importance of the individual enzymes in the control of flux through the pathway (Stephanopoulos et al. 1998).

BOX 3.4 QUANTIFICATION OF FLUX CONTROL

In a study of flux control in a biochemical pathway the concept of metabolic control analysis is very useful (Stephanopoulos et al., 1998). Here the flux control of the individual enzymatic reactions on the steady state flux J through the pathway is quantified by the so-called flux control coefficients (FCC):

$$C_i^J = \frac{v_i}{J}\frac{dJ}{dv_i}$$

where v_i is the rate of the i^{th} reaction. If the enzyme concentration of the i^{th} enzyme is increased its rate will normally increase, and a higher flux through the pathway may be the result. However, it is likely that due to allosteric regulation (or other regulation phenomena) there may be a very small effect of increasing the enzyme concentration. This is exactly what is quantified by the FCC, that is the relative increase in the steady state flux upon a relative increase in the enzyme activity. Clearly a step with a high FCC has a large control of the flux through the pathway. If a kinetic model is available for the pathway the flux control coefficients for each step can easily be calculated using model simulations. The FCCs can also be determined experimentally by changing the enzyme concentration (or activity) genetically, by titration with the individual enzymes, or by adding specific enzyme inhibitors (Stephanopoulos et al. 1998).

A general criticism of the application of kinetic models for complete pathways is that despite the level of detail included, they cannot possibly include all possible interactions in the system and therefore only represent one model of the system. The robustness of the model is extremely important especially if the kinetic model is to be used for predictions, and unfortunately most biochemical models, even very detailed models, are only valid at operating conditions close to those where the parameters have been estimated (i.e., the predictive strength is limited). For analysis of complex systems it is, however, not necessary that the model gives a quantitatively correct description of all the variables, because even models that give a qualitatively correct description of the most important interactions in the system may be valuable in studies of flux control.

3.5 POPULATION MODELS

Normally it is assumed that the population of cells is homogeneous (i.e., all cells behave identically). Although this assumption is certainly crude if a small number of cells is considered, it gives a very good picture of certain properties of the cell population because there are billions of cells per ml medium (see Box 3.5).

Furthermore, the kinetics is often linear in the cellular properties (e.g., in the concentration of a certain enzyme), and the overall population kinetics can therefore be described as a function of the average property of the cells (Nielsen et al. 2003). There are, however, situations where cell property distributions influence the overall culture performance, and here it is necessary to consider the cellular property distribution, and this is done in the so-called *segregated models*. In the following we will discuss two approaches to segregated modeling.

3.5.1 Morphologically Structured Models

The simplest approach to model distribution in the cellular property is by the so-called *morphologically structured models* (Nielsen and Villadsen 1992; Nielsen 1993). Here the cells are divided into a finite number Q of cell states Z (or morphological forms), and conversion between the different

BOX 3.5 DETERMINISTIC VERSUS STOCHASTIC MODELING

In a description of cellular kinetics macroscopic balances are normally used, that is the rates of the cellular reactions are functions of average concentrations of the intracellular components. However, living cells are extremely small systems with only a few molecules of certain key components, and it does not really make sense to talk about 'the DNA concentration in the cell' for example, because the number of macromolecules in a cell is always small compared with Avogadro's number. Many cellular processes are therefore stochastic in nature and the deterministic description often applied is in principle not correct. However, the application of a macroscopic (or deterministic) description is convenient and it represents a typical engineering approximation for describing the kinetics in an average cell in a population of cells. This approximation is reasonable for large populations because the standard deviation from the average 'behavior' in a population with elements is related to the standard deviation for an individual cell through

$$\sigma_{pop} = \frac{\sigma}{\sqrt{e}}$$

Thus with a population of 10^9 cells mL^{-1}, which is a typical cell concentration during a cultivation process, it can be seen that the standard deviation for the population is very small. There are, however, systems where small populations occur, for example at dilution rates close to the maximum in a chemostat, and here one may have to apply a stochastic model.

cell states is described by a sequence of empirical metamorphosis reactions. Ideally these metamorphosis reactions can be described as a set of intracellular reactions, but the mechanisms behind most morphological conversions are largely unknown. Thus, it is not known why filamentous fungi differentiate to cells with a completely different morphology from that of their origin. It is therefore not possible to set up detailed mechanistic models describing these changes in morphology; empirical metamorphosis reactions are therefore introduced. The stoichiometry of the metamorphosis reactions is given by analogy with Equation 3.4:

$$\Delta \mathbf{Z} = \mathbf{0} \tag{3.62}$$

where Δ is a stoichiometric matrix. Z_q represents both the q^{th} morphological form and the fractional concentration (g q^{th}, morphological form (g DW^{-1}). With the metamorphosis reactions, one morphological form is spontaneously converted to other forms. This is of course an extreme simplification because the conversion between morphological forms is the sum of many small changes in the intracellular composition of the cell. With the stoichiometry in Equation 3.62, it is assumed that the metamorphosis reactions do not involve any change in the total mass, and the sum of all stoichiometric coefficients in each reaction is therefore taken to be zero. The forward reaction rates of the metamorphosis reactions are collected in the vector **u**. Each morphological form may convert substrates to biomass components and metabolic products. These reactions may be described by an intracellularly structured model, but in order to reduce the model complexity a simple unstructured model is used for description of the growth and product formation of each cell type (e.g., the specific growth rate of the q^{th} morphological form is described by the Monod model). The specific growth rate of the total biomass is given as a weighted sum of the specific growth rates of the different morphological forms:

$$\mu = \sum_{i=1}^{Q} \mu_i Z_i \tag{3.63}$$

The rate of formation of each morphological form is determined both by the metamorphosis reactions and by the growth-associated reactions for each form (for derivation of mass balances for the morphological forms, see Nielsen and Villadsen 1994). The concept of morphologically structured models is well suited to describing the growth and differentiation of filamentous microorganisms (Nielsen 1993), but it may also be used to describe other microbial systems where a cellular differentiation has an impact on the overall culture performance.

3.5.2 Population Balance Equations

The first example of a heterogeneous description of cellular populations was presented in 1963 by Fredrickson and Tsuchiya. In their model, single-cell growth kinetics was combined with a set of stochastic functions describing cell division and cell death. The model represents the first application of a completely segregated description of a cell population. In the model, the cell population is described by a number density function $f(X,t)$, where $f(X,t)\mathrm{d}X$ is the number of cells with property X being in the interval X to $X + \mathrm{d}X$. The dynamic balance for $f(X,t)$ is given by

$$\frac{\partial f(X,t)}{\partial t} + \frac{\partial}{\partial X}(f(X,t)v(X,t)) = 2\int_X^\infty b(X^*,t)\,p(X^*,X,t)\,f(X^*,t)\,dX^* - b(X,t)f(X,t) - Df(X,t) \tag{3.64}$$

where v is the net rate of formation of the cell property, X. $b(X,t)$ is the breakage function (i.e., the rate of cell division for cells with property X), and $p(X^*,X,t)$ is the partitioning function (i.e., the probability that a cell with property X is formed upon division of a cell with property X^*). Through the functions p and b, a stochastic element can be introduced into the model, but these functions can also be completely descriptive. The balance equation 3.64 was applied in the original work of Fredrickson and Tsuchiya, but in a later paper a general framework for segregated population models was presented (Fredrickson *et al.* 1967). Segregated models represent the complete description of a cell population, and they take into account that all cells in a population are not identical. However, complete cellular segregation is rarely applied in cell culture models for two main reasons:

- For large populations, the average properties will normally represent the overall population kinetics quite well.
- The mathematical complexity of Equation 3.64 is quite substantial, especially if more than a single-cell property is considered (i.e., the number density function becomes multidimensional).

If the kinetics for product formation is not zero or first order in a given cell property, application of an average property model will, however, not give the same result as a segregated description. This is the case for production of a heterologous protein in plasmid-containing cells of *E. coli*, where the product formation kinetics is not first order in the plasmid copy number. A segregated model therefore has to be applied to give a good description of the product formation kinetics (Seo and Bailey 1985). The simplest segregated models are when the cellular property is described by a single variable (e.g., cell age), and in Example 3e, the age distribution of an exponentially growing culture is derived from the general balance (Equation 3.64).

Example 3e: Age Distribution Model

The simplest segregated population models are those where the cellular property is taken to be described solely by the cell age a. In this case, the rate of increase in the cellular property $v(a,t)$ is

equal to 1. Furthermore, if it is assumed that cell division occurs only at a certain cell age $a = t_d$, the two first terms on the right-hand side of Equation 3.64 become equal to zero. At steady state, the balance therefore becomes

$$\frac{d\phi(a)}{da} = -D\phi(a) \tag{3e1}$$

where ϕ is a normalized distribution function:

$$\phi(a) = \frac{f(a)}{n} \tag{3e2}$$

with n being the total cell number, given as the zero moment of the number density function $f(a)$. The solution to Equation 3e1 is

$$\phi(a) = \phi(0)e^{-Da} \tag{3e3}$$

Due to the normalization, the 0th moment of $f(a)$ is 1, that is,

$$\int_o^{t_d} \phi(a)da = 1 \tag{3e4}$$

which leads to

$$\phi(a) = \frac{D}{1-e^{-Dt_d}}e^{-Da} \tag{3e5}$$

The cell balance relating to cell division (the so-called renewal equation) is given by

$$\phi(0) = 2\phi(t_d) \tag{3e6}$$

which, together with Equation 3e3, directly gives Equation 3.2. Furthermore, when Equation 3.2 is inserted in Equation 3e5, we have the simpler expression

$$\phi(a) = 2De^{-Da} \tag{3e7}$$

Thus, the fraction of cells with a given age decreases exponentially with age, and the decrease is determined by the specific growth rate of the culture (equal to the dilution rate at steady state). The average cell age is given as the first moment of $f(a)$:

$$\langle a \rangle = \int_0^{t_d} a\phi(a)da = \frac{1-\ln 2}{D} \tag{3e8}$$

Consequently, the average age of the cells decreases for increasing specific growth rates.

SUMMARY

Understanding microbial growth kinetics is an essential requirement for the design and successful operation of industrial fermentation processes and for obtaining quantitative information about the function of microbial cells.

The primary objective of this chapter is to introduce the reader to the basic principles of the wide-ranging aspects of microbial growth kinetics and dynamics, from the basic principles to the more advanced concept of modeling.

Based on the information given in this chapter, the reader should be able to design fermentation processes for the production of biomass and microbially derived products.

Furthermore, the reader should be able to set up simple mathematical models describing microbial growth as well as evaluate more complex mathematical models.

REFERENCES

Benthin, S., U. Schulze, J. Nielsen, and J. Villadsen. 1994. Growth energetics of *Lactococcus cremoris* FDI during energy, carbon and nitrogen limitation in steady state and transient cultures. *Chem. Eng. Sci*. 49:589–609.

Christensen, L.H., C.M. Henriksen, J. Nielsen, J. Villadsen, and M. Egel-Mitani. 1995. Continuous cultivation of *P. chrysogenum*: Growth on glucose and penicillin production. *J. Biotechnol*. 42:95–107.

Fredrickson, A.G. 1976. Formulation of structured growth models. *Biotechnol. Bioeng*. 18:1481–6.

Fredrickson, A.G., D. Ramkrishna, and H.M. Tsuchiya. 1967. Statistics and dynamics of procaryotic cell populations. *Math. Biosci*. 1:327–74.

Fredrickson, A.G. and H.M. Tsuchiya. 1963. Continuous propagation of micro-organisms. *AIChE J*. 9:459–68.

Galazzo, J.L. and J.E. Bailey. 1990. Fermentation pathway kinetics and metabolic ßux control in suspended and immobilized *Saccharomyces cerevisiae*. *Enzym. Microb. Technol*. 12: 162–72.

Harder, A. and J.A. Roels. 1982. Application of simple structured models in bioengineering. *Adv. Biochem. Eng*. 21:55–107.

Herbert, D. 1959. Some principles of continuous culture. *Recent Prog. Microbiol.* 7:381–96.

Hill, A.V. 1910. The possible effects of the aggregation of the molecules of haemoglobin on its dissociation curves. *J. Physiol. Lond*. 40:4–7.

Ingraham, J.L., O. Maaloe, and F.C. Neidhardt. 1983. *Growth of the Bacterial Cell*. Sunderland, MA: Sinauer Associates.

Lee, S.B. and J.E. Bailey. 1994a. A mathematical model for λdv plasmid replication: analysis of wild-type plasmid. *Gene* 11:151–65.

Lee, S.B. and J.E. Bailey. 1994b. A mathematical model for λdv plasmid replication: Analysis of copy number mutants. *Gene* 11:166–77.

Lee, S.B. and J.E. Bailey. 1994c. Genetically structured models for *lac* promoter-operator function in the *Escherichia coli* chromosome and in multicopy plasmids: *lac* operator function. *Biotechnol. Bioeng*. 26:1372–82.

Lee, S.B. and J.E. Bailey. 1994d. Genetically structured models for *lac* promoter-operator function in the *Escherichia coli* chromosome and in multicopy plasmids: *lac* promoter function. *Biotechnol. Bioeng*. 26:1383–9.

Luedeking, R. and E.L. Piret. 1959. A kinetic study of the lactic acid fermentation: Batch process at controlled pH. *J. Biochem, Microbiol. Technol. Eng*. 1:393–412.

Meyenburg, K. von. 1969. Katabolit-Repression und der Sprossungszyklus von *Saccharomyces cerevisiae*. PhD dissertation, ETH, Zürich.

Monod, J. 1942. *Recherches sur la Croissance des Cultures Bacteriennes*. Paris: Hermann and Cie.

Monod, J., J. Wyman, and J-P. Changeux. 1965. On the nature of allosteric transitions: A plausible model. *J. Molec. Biol*. 12:88–118.

Neidhardt, F.C., J.L. Ingraham, and M. Schaechter. 1990. *Physiology of the Bacterial Cell: A Molecular Approach*. Sunderland, MA: Sinauer Associates.

Nielsen, J. 1993. A simple morphologically structured model describing the growth of Þlamentous microorganisms. *Biotechnol, Bioeng*. 41:715–27.

Nielsen, J., K. Nikolajsen, and J. Villadsen. 1991a. Structured modeling of a microbial system 1: A theoretical study of the lactic acid fermentation. *Biotechnol. Bioeng*. 38:1–10.

Nielsen, J., K. Nikolajsen, and J. Villadsen. 1991b. Structured modelling of a microbial system 2: Verification of a structured lactic acid fermentation model. *Biotechnol. Bioeng*. 38:11–23.

Nielsen, J. and J. Villadsen. 1992. Modeling of microbial kinetics. *Chem. Eng. Sci*. 47:4225–70.

Nielsen, J. and J. Villadsen. 1993. Bioreactors: Description and modelling. In Rehm, H.J., and Reed, G., eds., *Biotechnology*, vol. 3, 2nd ed., pp. 77–104. Weinheim: VCR Verlag.

Nielsen, J. and J. Villadsen. 1994. *Bioreaction Engineering Principles*. New York: Plenum Press.

Nielsen, J. J. Villadsen, and G. Lidén. 2003. *Bioreaction Engineering Principles*, 2nd ed. New York: Kluwer Academic/Plenum.

Olsson, L. and J. Nielsen. 1997. On-line and in situ monitoring of biomass in submerged cultivations. *TIBTECH* 15:517–22.

Oura, E. 1983. Biomass from carbohydrates. In Rehm, H-J., and Reed, G., eds., *Biotechnology*, vol. 3, 2nd ed., pp. 3–42. Weinheim: VCR Verlag.

Peretti, S.W. and J.E. Bailey. 1987. Simulations of host–plasmid interactions in *Escherichia coli*: Copy number, promoter strength, and ribosome binding site strength effects on metabolic activity and plasmid gene expression. *Biotechnol. Bioeng*. 29:316–28.

Pirt, S.J. 1965. The maintenance energy of bacteria in growing cultures. *Proc. Roy. Soc. London*, *Ser. B*. 163:224–31.

Pissarra, P.N., J. Nielsen, and M.J. Bazin. 1996. Pathway kinetics and metabolic control analysis of a high-yielding strain of *Penicillium chrysogenum* during fed-batch cultivations. *Biotechnol. Bioeng*. 51:168–76.

Ramkrishna, D., A.G. Fredrickson, and H.M. Tsuchiya. 1966. Dynamics of microbial propagation: Models considering endogenous metabolism. *J. Gen. Appl. Microbiol*. 12:311–27.

Ramkrishna, D., A.G. Fredrickson, and H.M. Tsuchiya. 1967. Dynamics of microbial propagation: Models considering inhibitors and variable cell composition. *Biotechnol. Bioeng*. 9:129–70.

Rizzi, M., M. Baltes, U. Theobald, and M. Reuss. 1997. In vivo analysis of metabolic dynamics in *Saccharomyces cerevisiae*: II. Mathematical model. *Biotechnol. Bioeng*. 55:592–608.

Roels, J.A. 1983. *Energetics and Kinetics in Biotechnology*. Amsterdam: Elsevier Biomedical Press.

Seo, J.H. and J.E. Bailey. 1985. A segregated model for plasmid content and product synthesis in unstable binary fission recombinant organisms. *Biotechnol. Bioeng*. 27:156–65.

Shuler, M.L., S.K. Leung, and C.C. Dick. 1979. A mathematical model for the growth of a single bacterial cell. *Ann. NY Acad. Sci*. 326:35–55.

Sonnleitner, B. and A. Fiechter. 1988. High performance bioreactors: A new generation. *Anal. Chim. Acta* 213:199–205.

Stephanopoulos, G., J. Nielsen, and A. Aristodou. 1998. *Metabolic Engineering.* San Diego, CA: Academic Press.

Tsuchiya, H.M., A.G. Fredrickson, and R. Aris. 1966. Dynamics of microbial cell populations. *Adv. Chem. Eng*. 6:125–206.

Williams, F.M. 1967. Av model of cell growth dynamics. *J. Theor. Biol*. 15:190–207.

4 Microbial Synthesis of Primary Metabolites: Current Trends and Future Prospects

Arnold L. Demain and Sergio Sanchez

CONTENTS

4.1 INTRODUCTION

Primary metabolites are microbial products made during the exponential phase of growth whose synthesis is an integral part of the normal growth process. They include intermediates and end products of anabolic pathways leading to the formation of monomers, which are used by the cell as building blocks (e.g., amino acids and nucleotides) for the biosynthesis of polymers (e.g., protein and DNA) and coenzymes (e.g., vitamins). On the other hand, primary metabolites of catabolic pathways (e.g., citric acid, acetic acid, and ethanol) are not biosynthetic precursors but are essential for growth as they are related to energy generation, redox balance, and substrate utilizations. Industrially, the most important primary metabolites are amino acids, nucleotides, vitamins, solvents, and organic acids. These are made by a wide range of bacteria and fungi and have numerous applications in the food, chemical, pharmaceutical, and nutraceutical industries. Many of these metabolites are manufactured by microbial fermentation rather than chemical synthesis because the fermentations are economically competitive and produce biologically active isomers. Several other industrially important chemicals could be manufactured via microbial fermentations (e.g., glycerol and other polyhydroxy alcohols) but are presently synthesized cheaply as petroleum by-products. However, a renewed interest in the microbial production of ethanol, organic acids, and solvents has been triggered as a consequence of successive rises in the price of crude oils.

4.2 CONTROL OF PRIMARY METABOLISM

Microbial metabolism is a conservative process that usually does not expend energy or nutrients to make compounds already available in the environment and does not overproduce components of intermediary metabolism. Coordination of metabolic functions ensures that, at any given moment, only the necessary enzymes, and the correct amounts of each, are made. Once a sufficient quantity of a given metabolite or precursor is made, either the synthesis of the enzymes concerned is turned "off" at the level of transcription (repression) or their activities are turned down (inhibition) through a number of specific regulatory control mechanisms such as feedback inhibition and covalent modifications.

4.2.1 INDUCTION

While the majority of anabolic enzymes are subject to repression, most catabolic enzymes are subject to induction. The latter is a control mechanism by which a substrate (or a compound structurally similar to the substrate) "turns on" the synthesis of the enzymes required for its uptake and initiation of metabolism. Enzymes that are synthesized as a result of genes being turned "on" in response to signal molecules (substrates) are called *inducible enzymes*, with the substance that activates gene transcription being referred to as the *inducer.* Inducible enzymes are produced only in response to the presence of their substrate or substrate analogs, in other words, they are produced only when needed. The inducer molecule renders the repressor molecule unable to bind to the operator region, thus facilitating the binding of RNA polymerase to the promoter region and in turn initiation of transcription and translation into protein. Although most inducers are substrates of catabolic enzymes, products can sometimes function as inducers. For example, fatty acids induce lipase, whereas galacturonic acid induces polygalacturonase. In some cases, however, the synthesis

of a particular enzyme may be induced by substrate analogs that are not attacked by the enzyme (e.g., IPTG in the case of β-galactosidase); such analogs are referred to as *gratuitous inducers.*

4.2.2 Catabolite Repression

Catabolite repression is a mechanism, which allows microorganisms to preferentially utilize one substrate in preference to another, thus conserving energy and biosynthetic precursors. For example, in the presence of lactose and glucose, *Escherichia coli* preferentially utilizes glucose by preventing the uptake of lactose and switching off transcription of the lac operon. This mechanism is also known as *carbon catabolite repression*, which ensures that the cell produces enzymes to metabolize the assimilated carbon source but represses the synthesis of the enzymes required for the assimilation of the other substrate until the primary carbon substrate is exhausted.

4.2.3 Nitrogen Source Regulation (NSR)

Nitrogen can be assimilated from inorganic or organic sources. Its assimilation from inorganic sources requires reduction to ammonia, followed by incorporation into intracellular metabolites. The appropriate distribution of nitrogen among various pathways usually involves specific or local regulatory mechanisms, such as end product inhibition or end product-mediated transcriptional control. In addition, some global regulators control the expression of genes from several pathways and thereby coordinate metabolism. The ability to assimilate particular inorganic or organic nitrogen sources depends on the particular organism. Organic nitrogen sources are usually the monomeric units of macromolecules (e.g., amino acids or nucleic acids) or compounds derived from them (e.g., agmatine or putrescine). Ammonia usually supports the fastest growth rate and is therefore considered the preferred nitrogen source for *E. coli*. The biochemical basis of this "ammonium preference" is explained by the repression of enzymes acting on the alternative nitrogenous substrates present in the culture medium. NSR is known by many other names such as *nitrogen metabolite repression*, *nitrogen catabolite repression*, and *ammonia repression*. Enzymes typically under such control are proteases, amidases, and ureases, not to mention those involved in the degradation of amino acids.

4.2.4 Phosphorus Source Regulation

In natural environments, inorganic phosphorus is commonly a major growth-limiting nutrient. It is hardly surprising therefore to see that microorganisms have evolved specific regulatory control mechanisms to respond to "feast and famine" concentrations of phosphate in their immediate environment. In *E. coli*, the phosphate regulon (*pho* regulon) is composed of over 30 genes that are transcriptionally activated by phosphorylated PhoB as the level of phosphate in the medium becomes growth limiting. PhoR and PhoB comprise a two-component signal transduction system in which PhoR catalyzes the reversible phosphorylation and activation of PhoB in response to low and high levels of phosphate, respectively. PhoR autophosphorylates and transfers the phosphate to PhoB. The environmental concentration of phosphate is monitored by the periplasmic phosphate-binding protein PstS, which transmits the signal for excess phosphate across the cytoplasmic membrane via PstC, PstA, PstB, and PhoU to PhoR. Phosphorylated PhoB binds to the promoters of 31 genes containing *pho* boxes and interacts with RNA polymerase, allowing the initiation of mRNA synthesis.

In fungi, nucleases and phosphatases are usually repressed when the supply of phosphate is plentiful. Similarly, in *Neurospora*, phosphate represses proteases, isocitrate lyase, aldolase, NADP-specific isocitrate dehydrogenase, and malate dehydrogenase. Phosphate also suppresses the production of riboflavin by *Eremothecium ashbyii*. Phosphate-derepressed mutants can be selected by growth with a phosphate ester (e.g., β-glycerol phosphate) as the sole source of carbon, with

phosphate in excess of demands. Of great interest is inorganic polyphosphate (poly P), a linear polymer that carries numerous orthophosphate (P_i) residues linked by high-energy phosphoanhydride bonds. Poly P is found in the cells of all bacteria, archaea, fungi, protozoa, plants, and animals. It is produced by polyphosphate kinase (PPK), which catalyzes the reversible transfer of the terminal phosphate of ATP to form a long-chain polyphosphate. The *E. coli* gene (*ppk*) encoding PPK has been cloned, sequenced, and overexpressed (about 100-fold). The poly P plays a significant role in metabolism, including acting as a substitute for ATP as an energy source, reservoir for inorganic phosphate, chelator of metal ions, and regulator for stress and survival.

4.2.5 Sulfur Source Regulation

In common with other nutrients, the uptake of sulfur and its subsequent assimilation are controlled at the transcriptional level. However, in this case the control is achieved through the activity of pleiotropic regulatory proteins. Thus, in *E. coli*, sulfur metabolism is controlled by the CysB transcriptional activator. The cysteine regulon includes most of the genes required for the synthesis of cysteine and genes for uptake of sulfur sources such as L-cystine, sulfate, thiosulfate, and taurine. Transcriptional activation of these genes requires CysB protein, *N*-acetyl-L-serine as an inducer, and sulfur limitation. CysB's activity is regulated by an efflux pump specific for cysteine and related metabolites. CysB is also an autorepressor (i.e., capable of repressing its own expression at the transcriptional level). Similarly, carbohydrate metabolism and fermentations were found to be adversely affected by CysB. Cysteine inhibits inducer synthesis, resulting in maximal mutations in *cysB* genes. The aforementioned effects are exerted at the transcriptional level and are only partially reversible by exogenous cAMP or sulfur-containing substrates (e.g., cysteine or djenkolate), while growth under sulfur limitation or with poor sulfur sources, such as glutathione, turns "on" (derepresses) the expression of the sulfur regulon.

In *Neurospora crassa*, sulfate uptake is an important point of the regulation of sulfur metabolism as it is subject to sulfur (metabolite) repression in which excess sulfate turns "off" the expression of the sulfate permease-encoding genes. Also, structural genes encoding aryl sulfatase, choline sulfatase, sulfate permeases I and II, a high-affinity methionine permease, and an extracellular protease are turned "on" when sulfur becomes limiting.

4.2.6 Feedback Regulation

This category of regulation is predominantly used for the regulation of anabolic enzymes involved in the biosynthesis of amino acids, nucleotides, and vitamins. It exerts its function at two levels: enzyme action (feedback inhibition) and enzyme synthesis (feedback repression and attenuation).

In feedback inhibition, the final metabolite of a pathway, when present in sufficient quantities, inhibits the action of the first enzyme of the pathway, thus preventing the synthesis of unwanted intermediates on the one hand and the wasting of energy on the other. Feedback repression involves the turning "off" of enzyme synthesis when the amount of the product has been made in sufficient quantities to satisfy the biosynthetic demands. The end product of the pathway acts as a co-repressor. The apo-repressor specified by the regulator gene is inactive in the absence of its co-repressor and as such is unable to bind to the operator region. However, in the presence of a co-repressor, the inactive apo-repressor is converted to an active repressor that binds to the operator region, thus preventing the binding of RNA polymerase to the promoter region, which in turn brings enzyme biosynthesis to a halt.

4.2.7 Additional Types of Regulation

Other types of regulation include stringent control and regulatory inactivation. The effector of stringent control is the alarmone guanosine 5′-diphosphate 3′-diphosphate (ppGpp). *Regulatory*

inactivation refers to the selective inactivation of enzymes by two different mechanisms, namely, modification inactivation and degradative inactivation. In *modification inactivation*, the enzyme remains intact but its physical state is changed or is covalently modified. Covalent modifications include phosphorylation of a specific serine or threonine residue, nucleotidylation of a specific tyrosine residue, ADP-ribosylation of an arginine residue, methylation of a glutamate or aspartate carboxyl group, acetylation of an ε-amino group of a lysine residue, or tyrosinolation of a protein's terminal carboxyl group. In *degradative inactivation*, at least one peptide bond is broken, which may represent the first step in protein turnover. It is carried out by proteases, which are restricted from nonselective action by confinement in vacuoles or by protease inhibitors. Regulatory inactivation usually occurs after the exponential phase of growth, especially after exhaustion of a source of carbon or nitrogen. This inactivation serves to prevent futile cycles of metabolism, to destroy enzymes no longer needed, and to divert carbon flow at branch points from one branch to another.

4.3 APPROACHES TO STRAIN IMPROVEMENTS

Organisms used today for industrial production of primary metabolites have been developed by programs of intensive random mutagenesis followed by screening and selection of overproducers. Such efforts often start with organisms that have some capacity to make the desired product but that require multiple mutations leading to deregulation in a particular biosynthetic pathway before high productivity can be obtained. Auxotrophic mutants are often very useful (Figures 4.1 and 4.2). The sequential mutations ensure that nutrients are channeled efficiently to the appropriate products without significant deviation to other pathways. These mutations involve not only release of feedback controls but also enhancement of the formation of pathway precursors and intermediates. This approach to strain improvement has been remarkably successful in producing organisms that make industrially significant concentrations of primary metabolites. However, some of the problems with this "brute force" approach include (1) the necessity of screening large numbers of mutants for the rare combination of traits sequentially obtained that lead to overproduction, and (2) the possibility that the vigor of the producing strain may be substantially weakened following several rounds of mutagenesis.

More recent approaches employ recombinant DNA technology to develop strains that are capable of overproducing primary metabolites. This rationale for strain construction relies largely on the same principles of regulation discussed in the previous sections, but aims at assembling the appropriate characteristics by means of *in vitro* recombinant DNA techniques. This is particularly valuable in organisms with complex regulatory systems, where deregulation would involve many genetic alterations.

Production of a particular primary metabolite by deregulated organisms may inevitably be limited by the inherent capacity of the particular organism to make the appropriate biosynthetic enzymes, that is, even in the absence of repressive mechanisms, there may not be enough of the enzyme made

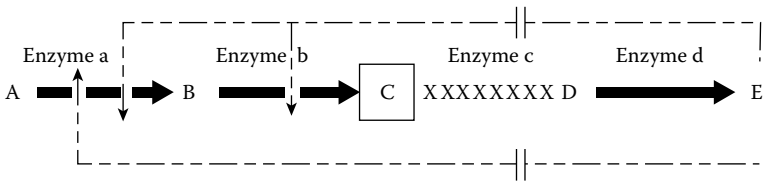

FIGURE 4.1 Overproduction of an intermediate of a linear primary metabolic pathway. Feedback inhibition by the end product inhibits the activity of enzyme a and feedback repression represses the formation of enzymes a and b. By making a genetic block (mutation) at enzyme c, an auxotrophic mutant is made, which cannot grow unless the metabolite E is added to the medium. As long as the amount of E present is not excessive, there will be no feedback effects and the metabolite C will be overproduced.

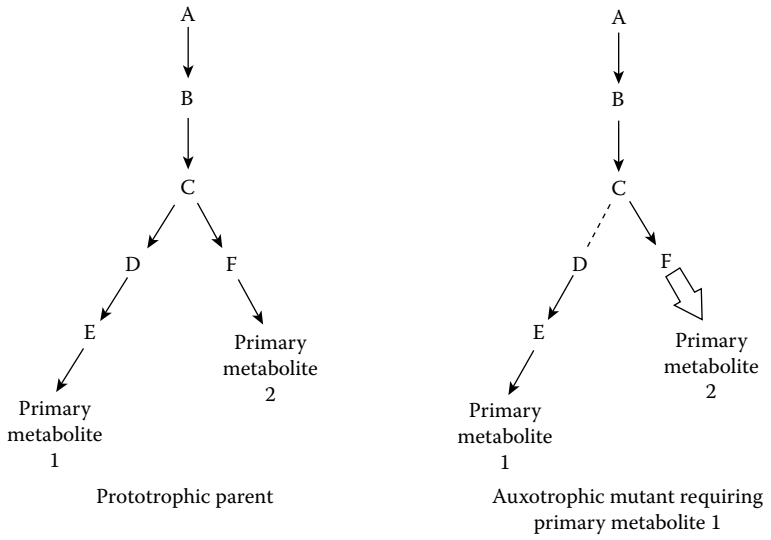

FIGURE 4.2 Use of auxotrophic mutation in a branched pathway. The auxotrophic mutant will require primary metabolite 1 for growth. When the concentration of metabolite 1 is not excessive to biosynthetic demands, primary metabolite 2 will be overproduced.

to obtain high productivity. One way to overcome this is to increase the number of copies of structural genes coding for these enzymes by genetic engineering. Another way often used in combination with this strategy is to increase the frequency of transcription, which is related to the frequency of binding of RNA polymerase to the promoter region. The former can be achieved by cloning the biosynthetic genes *in vitro* into a plasmid that, when introduced into the cell through transformation, will replicate into multiple copies. Increasing the frequency of transcription involves the construction of a recombinant plasmid *in vitro* that contains the structural genes of the biosynthetic enzymes but lacks the regulatory sequences (promoter and operator) normally associated with them. Instead, the structural genes are cloned downstream of an efficient promoter, thus facilitating a higher level of expression. The ideal plasmid for metabolite synthesis would contain a regulatory region with a constitutive phenotype, preferably not subject to nutritional repression. Novel genetic technologies such as *genome-based strain reconstruction* achieve the construction of a superior strain that contains only mutations crucial to hyperproduction, but not other unknown mutations that accumulate by brute-force mutagenesis and screening. This approach has successfully been used to improve lysine production (see Section 5.4.1.2). The directed improvement of product formation or cellular properties via modification of specific biochemical reactions or introduction of new ones with the use of recombinant DNA technology is known as *metabolic engineering*. Analytical methods are combined with molecular biological techniques to quantify fluxes and implement suggested genetic modifications. Different means of analyzing metabolic fluxes are (1) kinetic-based models, (2) control theories, (3) tracer experiment, (4) magnetization transfer, (5) metabolite balancing, (6) enzyme analysis, and (7) genetic analysis. The overall flux through a metabolic pathway depends on several steps, not just a single rate-limiting reaction.

A genome-wide transcript expression analysis called *massive parallel signature sequencing* has been successfully used to discover new targets for further improvement of riboflavin production by the fungus *Ashbya gossypii* (see Section 4.4.3.2). The development and combined application of the above technologies will help to develop "inverse metabolic engineering," which in turn will be used to construct certain phenotypes that are ideal for commercial purposes.

Molecular breeding techniques such as DNA shuffling come closer to mimicking natural recombination by allowing *in vitro* homologous recombination. These techniques not only recombine

DNA fragments but also introduce point mutations at a very low but controlled rate. Unlike site-directed mutagenesis, this method of pooling and recombining parts of similar genes from different species or strains has yielded remarkable improvements in the catalytic activities of enzymes within a relatively short space of time. *Whole-genome shuffling* is a novel technique for strain improvement combining the advantage of multiparental crossing allowed by DNA shuffling with the recombination of entire genomes.

4.4 PRODUCTION OF PRIMARY METABOLITES

4.4.1 Amino Acids Production

The amino acid market is more than US$6 billion and has been growing at 5–10% per year. Production of amino acids amounted to 3 million tons in 2002. Produced by fermentation are 1.5 million tons of l-glutamate, 850,000 tons of l-lysine-HCL, 70,000 tons of l-threonine, 13,000 tons of L-phenylalanine (including that made by chemical synthesis), 1,300 tons of L-glutamine, 1,200 tons of L-arginine, 3,000 tons of L-tryptophan (including enzymatic method), 500 tons of L-valine, 500 tons of L-leucine (including extraction), 400 tons of L-isoleucine (including extraction), 400 tons of L-histidine, 350 tons of L-proline, 300 tons of L-serine, and 170 tons of L-tyrosine. Ten thousand tons of L-aspartic acid and 500 tons of L-alanine are made enzymically. Dl-methionine is made chemically at 500,000 tons per year. In 2004, the amino acid market was about 4.5 billion dollars and is projected to grow at 6.8% annually through 2013.

Top fermentation titers reported in the literature are as follows: 88 g l^{-1} glutamic acid, 170 g l^{-1} L-lysine-HCL, 100 g l^{-1} L-threonine, 51 g l^{-1} L-phenylalanine, 96 g l^{-1} L-arginine, 58 g l^{-1} L-tryptophan, 99 g l^{-1} L-valine, 34 g l^{-1} L-leucine, 40 g l^{-1} L-isoleucine, 42 g l^{-1} L-histidine, 108 g l^{-1} L-proline, 65 g l^{-1} L-serine, 75 g l^{-1} L-alanine, 50 g l^{-1} L-tyrosine, and 25 g l^{-1} L-methionine. Genetic and metabolic engineering have made an impact by use of the following strategies: (1) amplification of the rate-limiting (controlling) enzyme of the pathway, (2) amplification of the first enzyme after a branch point, (3) cloning of a gene encoding an enzyme with more or less feedback regulation, (4) introduction of a gene encoding an enzyme with a functional or energetic advantage as replacement for the normal enzyme, and (5) amplification of the first enzyme leading from the central metabolism to increase carbon flow into the pathway followed by sequential removal of bottlenecks caused by the accumulation of intermediates. Transport mutations are also useful (i.e., mutations decreasing amino acid uptake often allow for improved excretion and lower intracellular feedback control). In cases where excretion is carrier mediated, increase in activity of these carrier enzymes increases production of the amino acid.

Amino acids produced by microbial process are the L-forms. Such stereospecificity makes the process advantageous as compared to synthetic processes. Microbial strains employed for amino acid production are divided into four classes: wild-type strains, auxotrophic mutants, regulatory mutants, and auxotrophic regulatory mutants. Using bacterial mutants, all the essential amino acids except L-methionine can be produced by "direct fermentation" from cheap carbon sources such as carbohydrate materials or acetic acid.

Plasmid vector systems for cloning in *Corynebacterium glutamicum* have been established, and amino acid production by *C. glutamicum* and related strains has been improved by gene cloning. Extensive research has been done on sequencing the genome of *C. glutamicum* and to investigate its genetic repertoire. The genome has been sequenced by several groups.

4.4.1.1 Production of L-Glutamic Acid

Monosodium glutamate (MSG) is a potent flavor enhancer, which was first made by fermentation in Japan in the late 1950s. Many organisms belonging to a wide range of taxonomically related genera, including *Micrococcus*, *Corynebacterium*, *Brevibacterium*, and *Microbacterium*, are capable of overproducing glutamate. *Brevibacterium lactofermentum* and *Brevibacterium flavum* are now

reclassified as subspecies of *C. glutamicum*. These organisms were shown to possess the Embden-Meyerhof Parnas glycolytic pathway (EMP), the hexose monophosphate pathway (HMP), the tricarboxylic acid (TCA) cycle, and the glyoxylate bypass (Figure 4.3). The TCA cycle, also widely known as the *Krebs cycle*, requires a continuous replenishment of oxaloacetate in order to replace the intermediates withdrawn for the synthesis of biomass and other amino acids. During growth on glucose and other glycolytic intermediates, the anaplerotic function is fulfilled by phosphoenolpyruvate carboxylase and pyruvate carboxylase.

Normally, glutamic acid overproduction would not be expected to occur due to feedback regulation. Glutamate feedback controls include repression of PEP carboxylase, citrate synthase, and NADP-glutamate dehydrogenase; the last-named enzyme is also inhibited by glutamate. However, by decreasing the effectiveness of the barrier to outward passage, glutamate can be pumped out of the cell, thus allowing its biosynthesis to proceed unabated. The excretion of glutamate frees the glutamate pathway from feedback control until a very high level is accumulated; commercial L-glutamate titer is in excess of 88 g l^{-1}.

Glutamate excretion is intentionally influenced by manipulations of growth conditions, biotin limitation was the first means discovered to bring about glutamate overproduction in *C. glutamicum*,

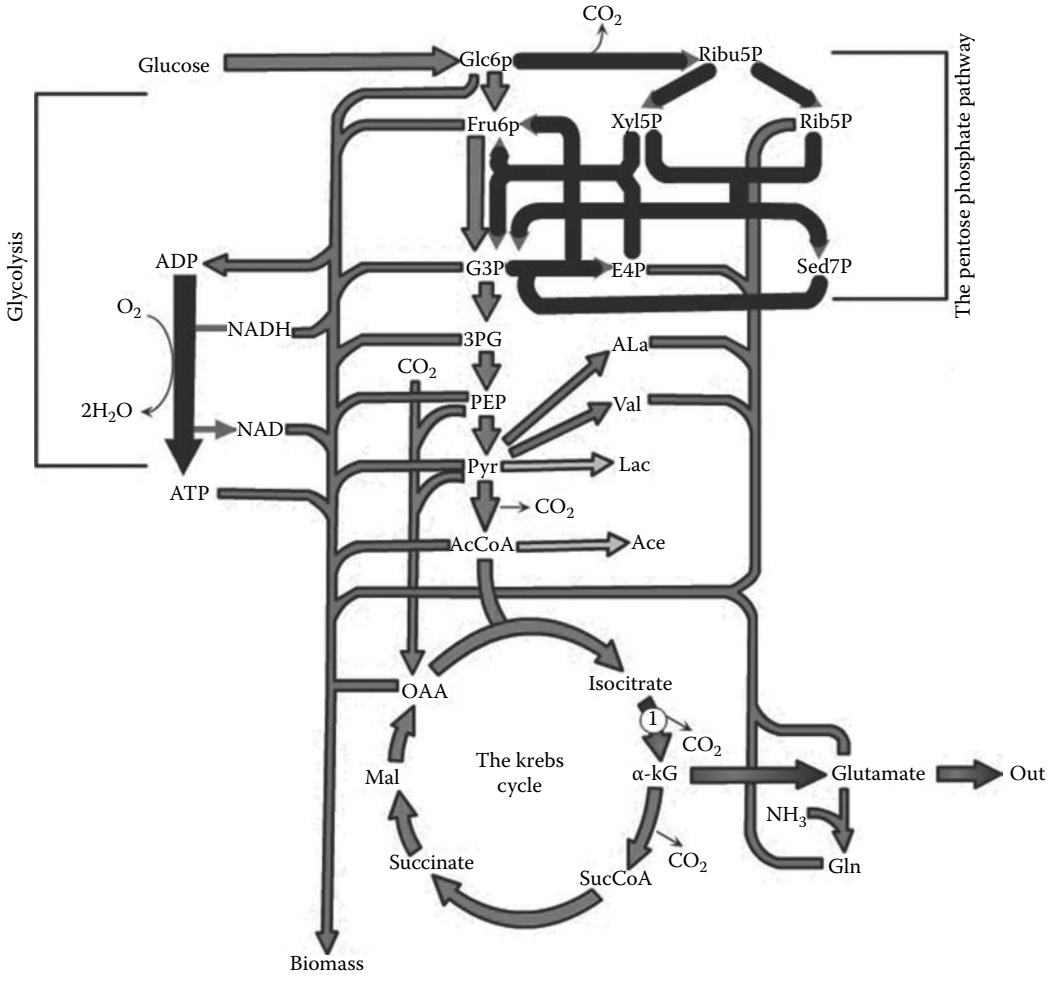

FIGURE 4.3 Microbial biosynthesis of glutamic acid from glucose. (Modified from Varela, C., et al. *Appl. Microbiol. Biotechnol.* 60, 547–55, 2003.)

and all glutamate overproducers are natural biotin auxotrophs (Figure 4.4). The finding that the addition of penicillin to cells grown in high biotin resulted in excretion of glutamic acid (Figure 4.5) led workers to postulate (1) that growth of the glutamate-overproducing bacterium in the presence of nonlimiting levels of biotin results in a cell membrane permeability barrier that restricts the excretion of glutamate, and (2) that inhibition of cell wall biosynthesis by penicillin alters the permeability

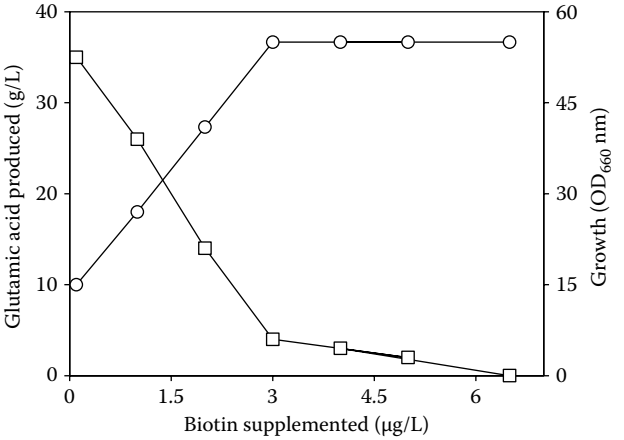

FIGURE 4.4 Effect of biotin concentration on the production of glutamate by *Corynebacterium glutamicum* strains, which are natural biotin auxotrophs.

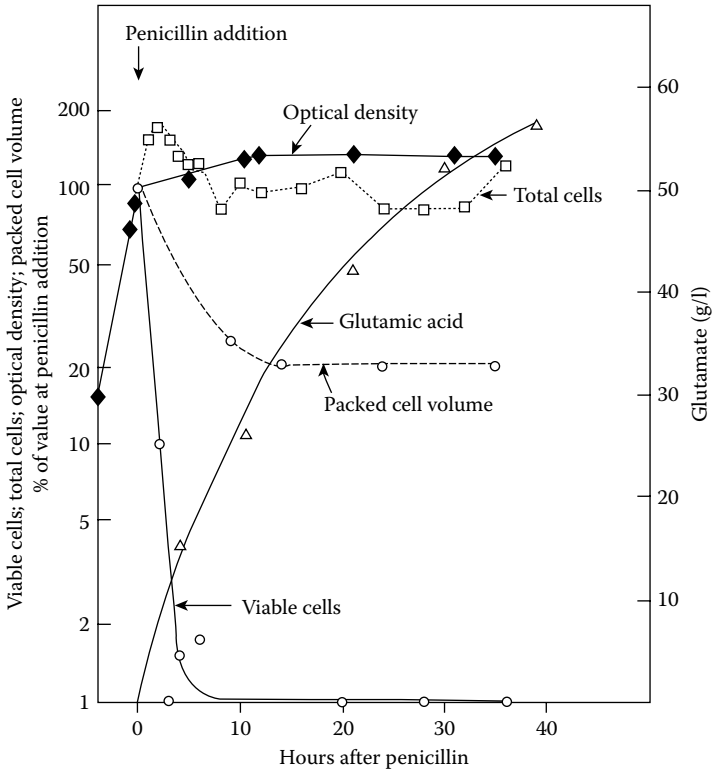

FIGURE 4.5 Effect of penicillin on the overproduction of glutamic acid during the growth of *Corynebacterium glutamicum* in the presence of excess biotin.

properties of the cell membrane and allows glutamate to flow out easily. The commonality in the various manipulations that were found to bring about high-level production of L-glutamic acid (i.e., the limitation of biotin, or addition of penicillin or fatty acid surfactants [e.g., tween 60], to exponentially growing cultures) was recognized. Apparently, all of these manipulations result in a phospholipid-deficient cytoplasmic membrane, which favors active excretion of glutamate from the cell. This view was further substantiated by the discoveries that oleate limitation of an oleate auxotroph and glycerol limitation of a glycerol auxotroph also bring about glutamate excretion. Furthermore, glutamate-excreting cells were later found to have a very low level of cell lipids, especially phospholipids. In addition, it was found that the various manipulations leading to glutamate overproduction cause increased permeability of the mycolic acid layer of the cell wall. The glutamate-overproducing bacteria are characterized by a special cell envelope containing mycolic acids that surrounds the entire cell as a structured layer and is thought to be involved in the permeation of solutes. The mycolic acids esterified with arabinogalactan and the noncovalently bound mycolic acid derivatives form a second lipid layer of the cell, with the cytoplasmic membrane being the first. Overexpression or inactivation of enzymes that are involved in lipid synthesis alters the chemical and physical properties of the cytoplasmic membrane and changes glutamate efflux dramatically.

4.4.1.2 Production of L-Lysine

The bulk of the cereals consumed in the world are deficient in the amino acid L-lysine. This is an essential ingredient for the growth of animals and is an important part of a billion-dollar animal feed industry. Lysine supplementation converts cereals into balanced food or feed for animals including poultry, swine, and other livestock. In addition to animal feed, lysine is used in pharmaceuticals, dietary supplements, and cosmetics.

Lysine is a member of the aspartate family of amino acids (Figure 4.6). It is made in bacteria by a branched pathway that also produces methionine, threonine, and isoleucine. This pathway is

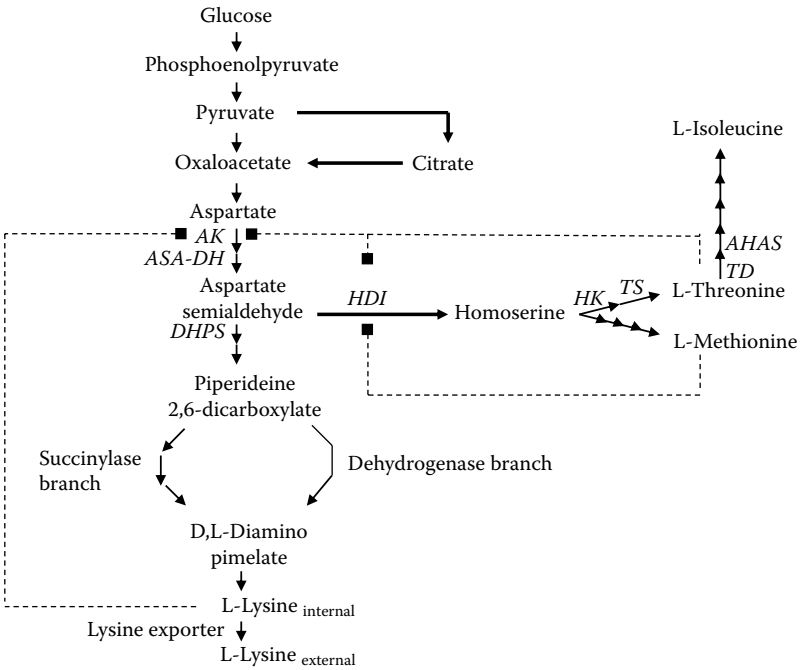

FIGURE 4.6 Biosynthetic pathway to L-lysine, L-threonine, and L-isoleucine productions. Abbreviations for key enzymes are given in the text.

controlled very tightly in organisms such as *E. coli*, which contains three aspartate kinases (AKs), each of which is regulated by a different end product. In addition, after each branch point, the initial enzymes are inhibited by their respective end product(s) and no overproduction usually occurs. However, *C. glutamicum*, the organism used for the commercial production of *L-lysine*, contains a single AK that is regulated via concerted feedback inhibition by threonine plus lysine. The relative contribution of carbon flux through the pentose phosphate pathway varies depending on the amino acid being produced; for example, while it contributes only 20% of the total flux in the case of glutamate formation, it contributes 60–70% in the case of lysine production. This is evidently due to the high level of NADPH required for lysine formation. Use of rDNA technology has shown that the factors that significantly limit the overproduction of lysine are (1) the feedback inhibition of AK by lysine plus threonine, (2) the low level of dihydrodipicolinate synthase (DHPS), (3) the low level of PEP carboxylase, and (4) the low level of aspartase. Much work has been done on auxotrophic and regulatory mutants of the glutamate-overproducing strains for the production of lysine. By genetic removal of homoserine dehydrogenase (HDI), a glutamate-producing wild-type *Corynebacterium* strain was converted into a lysine-overproducing mutant that cannot grow unless methionine and threonine are added to the medium. As long as the threonine supplement is kept low, the intracellular concentration of threonine is limiting and feedback inhibition of AK is bypassed, leading to excretion of over 70 g l^{-1} of lysine in culture fluids. In some strains, addition of methionine and isoleucine to the medium led to the increase of lysine overproduction. Selection for S-2-aminoethylcysteine (AEC, or thialysine) resistance blocks feedback inhibition of AK. Other antimetabolites useful for the deregulation of AK include a mixture of α-ketobutyrate and aspartate hydroxamate. Leucine auxotrophy can also increase lysine production. L-lysine titers are known to be as high as 170 g l^{-1}.

Excretion of lysine by *C. glutamicum* is by active transport reaching a concentration of several hundred millimolar in the external medium. Lysine, a cation, must be excreted against the membrane potential gradient (outside is positive), and the excretion is carrier mediated. The system is dependent on electron motive force, not ATP. Genome-based strain reconstruction has been used to improve the lysine production rate of *C. glutamicum* by comparing a high-producing strain (production rate slightly less than 2 g l^{-1} h^{-1}) and a wild-type strain. Comparison of 16 genes from the production strain, encoding enzymes of the pathway from glucose to lysine, revealed mutations in five of the genes. Introduction of three of these mutations (*hom*, *lysC*, and *pyc* encoding HDI, AK, and pyruvate carboxylase, respectively) into the wild type created a new strain that produced 80 g l^{-1} in 27 hours, at a rate of 3 g l^{-1} h^{-1}, the highest rate ever reported for a lysine fermentation. An additional increase (15%) in L-lysine production was observed by introducing a mutation in the 6-phosphogluconate dehydrogenase gene (*gnd*). Enzymatic analysis revealed that the mutant enzyme was less sensitive than the wild-type enzyme to allosteric inhibition by intracellular metabolites. Isotope-based metabolic flux analysis demonstrated that the *gnd* mutation resulted in an 8% increase in carbon flux through the pentose phosphate pathway during L-lysine production.

4.4.1.3 Production of L-Threonine

This amino acid is the second major amino acid used for feeding pigs and poultry. The pathway of threonine biosynthesis is similar in all microorganisms (Figure 4.6). Starting from L-aspartate, the pathway involves five steps catalyzed by five enzymes: AK, aspartate-semialdehyde dehydrogenase (ASA-DH), HDI, homoserine kinase (HK), and threonine synthetase (TS).

Production of L-threonine has been achieved with the use of several microorganisms. In *Serratia marcescens*, construction of a high threonine producer was done by transductional crosses that combined several feedback control mutations into one organism. Three classes of mutants were obtained from the parental strain as the source of genetic material for transduction: (1) one strain in which both the threonine-regulated AK and HD were resistant to feedback inhibition by threonine (it was selected on the basis of β-hydroxynorvaline resistance); (2) a second strain, also selected for β-hydroxynorvaline resistance, in which HDI was resistant to both inhibition and repression and the threonine-regulated AK was constitutively synthesized; and (3) a third strain that was resistant

to thialysine, in which the lysine-regulated AK was resistant to feedback inhibition and repression. Since at least one of the three key enzymes in threonine synthesis was still subject to regulation in these strains, each produced only modest amounts of threonine (4.1 to 8.7 g l^{-1}). Recombination of the three mutations by transduction yielded a strain that produced higher levels of threonine (25 g l^{-1}), had AK and HDI activities that were resistant to feedback regulation by threonine and lysine, and was also a methionine bradytroph (leaky auxotroph). Another six regulatory mutations derived by resistance to amino acid analogs were combined into a single strain of *S. marcescens* by transduction. These mutations led to desensitization and derepression of AKs I, II, and III and HDIs I and II. The resulting transductant produced 40 g l^{-1} of threonine, which was further improved to 63 g l^{-1} through overexpression of PEP carboxylase.

In *E. coli*, threonine production was increased to 76 g l^{-1} by conventional mutagenesis and by selection and screening techniques. Of major importance were mutations to decrease both regulation of the pathway and degradation of the amino acid. An *E. coli* fed-batch process with methionine and phosphate feeding yielded 98 g l^{-1} L-threonine at 60 hours. Another *E. coli* strain was developed via mutation and genetic engineering and optimized by inactivation of threonine dehydratase (TD), resulting in a process yielding 100 g l^{-1} in 36 hours of fermentation.

Threonine excretion by *C. glutamicum* is mainly (>90%) effected by a carrier-mediated export mechanism dependent on membrane potential. Cloning in extra copies of threonine export genes into an *E. coli* strain producing threonine led to increased production. Also increased was resistance to toxic antimetabolites of threonine. Another means of increasing threonine production was reduction in the activity of serine hydroxytransferase, which breaks down threonine to glycine. In *C. glutamicum* ssp. *lactofermentum*, threonine production reached 58 g l^{-1} when a strain producing both threonine and lysine (isoleucine auxotroph resistant to thialysine, α-amino-β-hydroxyvaleric acid, and S-methylcysteine sulfoxide) was transformed with a recombinant plasmid carrying its own *hom* (encoding HDI), *thrB* (encoding HK), and *thrC* (encoding TS) genes.

4.4.1.4 Production of L-Isoleucine

Isoleucine is of commercial interest as a food and feed additive and for parenteral nutrition infusions. This branched-chain amino acid is currently produced both by extraction of protein hydrolysates and by fermentation with classically derived mutants of *C. glutamicum*. The biosynthesis of isoleucine by *C. glutamicum* involves 11 reaction steps, of which at least five are controlled with respect to activity or expression (Figure 4.6). L-isoleucine synthesis shares reactions with the lysine and methionine pathways. In addition, threonine is an intermediate in isoleucine formation, and the last four enzymes also carry out reactions involved in valine, leucine, and pantothenate biosynthesis. Therefore, it is not surprising that multiple regulatory steps identified in *C. glutamicum*, as in other bacteria, are required to ensure the balanced synthesis of all these metabolites for cellular demands. In *C. glutamicum*, flux control is exerted by repression of the *homthrB* and *ilvBNC* operons. The activities of AK, HDI, TD, and acetohydroxy acid synthase (AHAS) are controlled by allosteric transitions of the proteins to provide feedback control loops, and HK is inhibited in a competitive manner. Isoleucine increases the Michaelis-Menten Kinetics (Km) of TD from 21 to 78 mM, whereas valine reduces it to 12 mM. The AHAS is 50% feedback inhibited by isoleucine plus valine plus leucine.

Isoleucine processes have been devised in various bacteria such as *S. marcescens*, *C. glutamicum* ssp. *flavum*, and *C. glutamicum*. In *S. marcescens*, resistance to isoleucine hydroxamate and α-aminobutyric acid led to derepressed TD and AHAS and production of 12 g l^{-1} of isoleucine. Further work involving transductional crosses into a threonine overproducer yielded isoleucine at 25 g l^{-1}. The *C. glutamicum* ssp. *flavum* work employed resistance to α-amino-β-hydroxyvaleric acid, and the resultant mutant produced 11 g l^{-1}. Mutation to D-ethionine resistance yielded a mutant producing 33.5 g l^{-1} isoleucine in a fermentation continuously fed with acetic acid. A threonine-overproducing strain of *C. glutamicum* was sequentially mutated to resistance to thiaisoleucine, azaleucine, and α-aminobutyric acid; it produced 10 g l^{-1} of isoleucine. An improved strain was

obtained by cloning multiple copies of *hom* (encoding HDI) and wild-type *ilvA* (encoding TD) into a lysine overproducer, and by increasing HK (encoded by *thrB*); 15 g l^{-1} isoleucine was produced. Independently, cloning of three copies of the feedback-resistant HDI gene (*hom*) and multiple copies of the deregulated TD gene (*ilvA*) in a deregulated lysine producer of *C. glutamicum* yielded an isoleucine producer (13 g l^{-1}) with no threonine production and reduced lysine production. Application of a closed-loop control fed-batch strategy raised production to 18 g l^{-1}, which was further amplified using metabolic engineering strategies to 40 g l^{-1} of isoleucine.

4.4.1.5 Production of Aromatic Amino Acids

In *C. glutamicum* ssp. *flavum*, 3-deoxy-D-arabino-heptulosonate 7-phosphate synthase (DAHPS) is feedback inhibited concertedly by phenylalanine plus tyrosine and weakly repressed by tyrosine. Other enzymes of the common pathway (Figure 4.7) are not inhibited by phenylalanine, tyrosine, and tryptophan, but the following are repressed: shikimate dehydrogenase (SD), shikimate kinase (SK), and 5-enolpyruvylshikimate-3-phosphate synthase. Elimination of the uptake system for aromatic amino acids in *C. glutamicum* results in increased production of aromatic amino acids in deregulated strains.

A tryptophan process was improved from 8 to 10 g l^{-1} by mutating the *C. glutamicum* ssp. *flavum* producer to azaserine resistance. Azaserine is an analog of glutamine, the substrate of anthranilate synthase (AS). Such a mutant showed a 2–3-fold increase in the activities of DAHPS, dehydroquinate synthase (DQS), SD, SK, and chorismate synthase (CS). Another mutant, selected for its ability to resist sulfaguanidine, showed additional increases in DAHPS and DQS and tryptophan production. The reason that sulfaguanidine was chosen as the selective agent involves the next limiting step after derepression of DAHPS (i.e., conversion of the intermediate chorismate to anthranilate by AS). Chorismate can also be undesirably converted to *p*-aminobenzoic acid (PABA), and sulfonamides are PABA analogs. A sulfaguanidine-resistant mutant was obtained with *C. glutamicum* ssp. *Flavum*, and production increased from 10 g l^{-1} tryptophan to 19 g l^{-1}. The sulfaguanidine-resistant

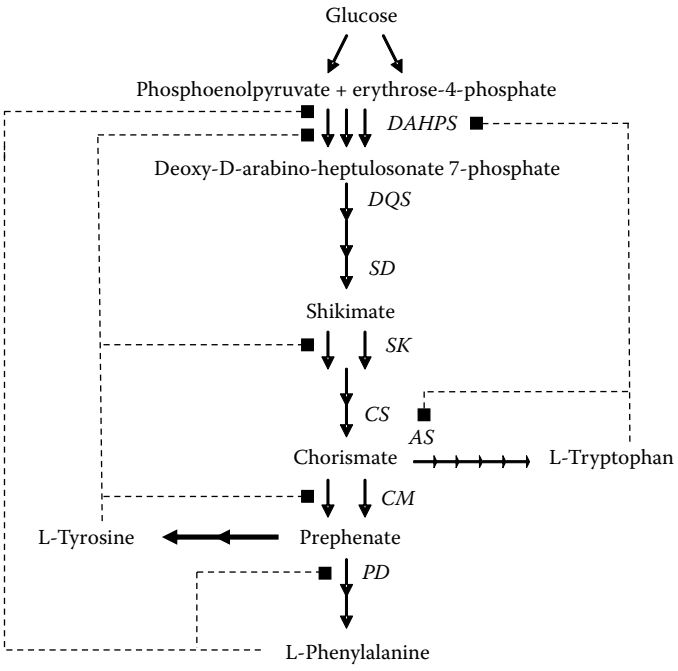

FIGURE 4.7 Biosynthetic pathways for L-tryptophan, L-phenylalanine, and L-tyrosine productions. Abbreviations for key enzymes are given in the text.

mutant was still repressed by tyrosine but showed higher enzyme levels at any particular level of tyrosine. Gene cloning of the tryptophan branch and mutation to resistance to feedback inhibition yielded a *C. glutamicum* strain producing 43 g l^{-1} L-tryptophan. The genes cloned were those that encoded AS, anthranilate phosphoribosyl transferase, a deregulated DAHPS, and other genes of tryptophan biosynthesis. However, sugar utilization decreased at the late stage of the fermentation, and plasmid stabilization required antibiotic addition. Sugar utilization stopped due to killing by accumulated indole. By cloning in the 3-phosphoglycerate dehydrogenase gene (to increase the production of serine, which combines with indole to form more tryptophan) and by mutating the host cells to deficiency in this enzyme, both problems were solved. The new strain produced 50 g l^{-1} tryptophan with a productivity of 0.63 g l^{-1} h^{-1} and a yield from sucrose of 20%. Further genetic engineering to increase the activity of the pentose phosphate pathway increased production to 58 g l^{-1}. A deregulated strain of *E. coli* in which feedback inhibition and repression controls were removed made 11 g l^{-1} phenylalanine in a fed-batch culture. Production was increased to 28.5 g l^{-1} when a plasmid was cloned into *E. coli* containing a feedback inhibition-resistant version of the CM-prephenate dehydratase (PD) gene, a feedback inhibition-resistant DAHPS, and the O_RP_R and O_LO_L operator-promoter system of lambda phage. Further process development of genetically engineered *E. coli* strains brought phenylalanine titers up to 46 g l^{-1}. Independently, genetic engineering based on cloning *aroF* and feedback-resistant *pheA* genes created an *E. coli* strain producing 51 g l^{-1}. A *C. glutamicum* ssp. *lactofermentum* culture, obtained by selection with *m*-fluorophenylalanine, produced 5 g l^{-1} phenylalanine, 7 g l^{-1} tyrosine, and 0.3 g l^{-1} anthranilate and contained desensitized DAHPS and PD. DAHPS in the wild type was inhibited cumulatively by phenylalanine and tyrosine, whereas PD was inhibited by phenylalanine. Cloning of the gene encoding PD from a desensitized mutant and the gene encoding desensitized DAHPS increased the enzyme activities and yielded a strain producing 18 g l^{-1} phenylalanine, 1 g l^{-1} tyrosine, and no anthranilate. Further cloning of a recombinant plasmid expressing desensitized DAHPS increased production to 26 g l^{-1} phenylalanine. Similarly, *C. glutamicum* strains have been developed, producing up to 28 g l^{-1} phenylalanine. When SK was cloned into a tyrosine-producing *C. glutamicum* ssp. *lactofermentum* strain, tyrosine production increased from 17 to 22 g l^{-1}. Cloning of desensitized genes encoding DAHPS and CM from a deregulated phenylalanine-producing *C. glutamicum* strain into the deregulated tryptophan producer, *C. glutamicum* KY 10865 (CM-deficient strain, phenylalanine, and tyrosine double auxotroph with a desensitized AS), shifted production from 18 g l^{-1} tryptophan to 26 g l^{-1} tyrosine. The use of *E. coli* for tyrosine overproduction was achieved by replacing the *pheLA* genes of a phenylalanine-producing strain with a multigene cassette comprising the *tyrA* gene under the control of the constitutive *trc* promotor and a kanamycin resistance gene. Surprisingly, deletion of the *lacI* repressor led to an increase in *tyrA* expression and a fivefold increase in tyrosine production to more than 50 g l^{-1} at a 200:l scale.

4.4.2 Production Processes for Purines and Pyrimidines and their Nucleosides and Nucleotides

Commercial interest in nucleotide fermentations is due to the activity of two purine ribonucleoside 5′-monophosphates, namely, guanylic acid (guanosine 5′-monophosphate, or GMP) and inosinic acid (inosine 5′-monophosphate, or IMP) as flavor enhancers. It is quite impressive that a 1:1 mixture of MSG with IMP or GMP gives flavor intensity 30 times stronger than that of MSG alone. Approximately 5,000 tons of GMP and IMP are produced annually in Japan alone, with a world market of US$360 million per year.

The purine residue of IMP is built up on a ribose ring in 10 enzymatic reactions after ribose phosphate pyrophosphokinase (PRPP synthetase) catalyzes the conversion of α-D-ribose-5-phosphate (R5P) and ATP to 5-phosphoribosyl-α-pyrophosphate (PRPP) (Figure 4.8). Adenosine-5′-monophosphate (AMP) and GMP are synthesized from IMP. AMP formation involves participation of two enzymes, adenylosuccinate synthetase and adenylosuccinate. GMP synthesis requires the participation of IMP dehydrogenase and GPM synthetase. PRPP synthetase is feedback inhibited by

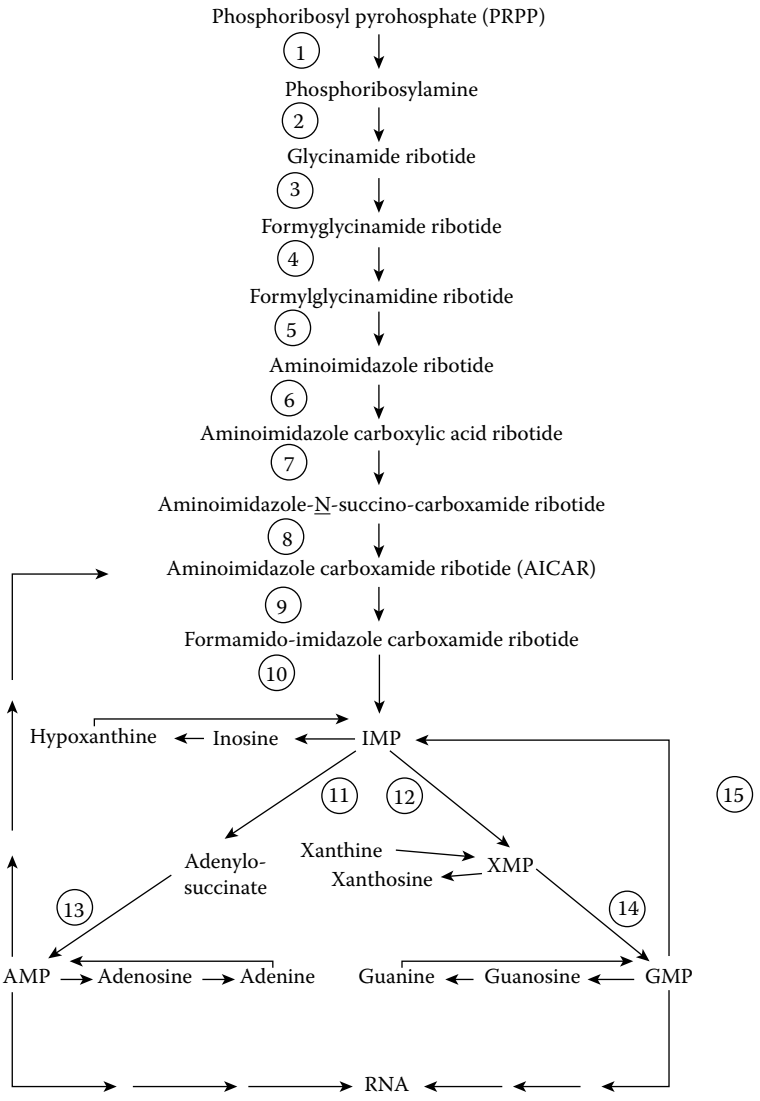

FIGURE 4.8 Biosynthesis of purine nucleotides. Key enzymes are as follows: Enzyme 1 is PRPP amidotransferase, Enzyme 11 is adenylosuccinate synthetase, Enzyme 12 is IMP dehydrogenase, Enzyme 13 is adenylsuccinase, and Enzyme 14 is XMP aminase.

AMP, GMP, and IMP; adenylosuccinate synthetase is inhibited by AMP; and IMP dehydrogenase is inhibited by xanthosine-5′-monphosphate (XMP) and GMP.

The genes encoding the enzymes of IMP biosynthesis in *Bacillus subtilis* constitute the *pur* operon, whereas the genes encoding the GMP biosynthetic enzymes, *guaA* (GMP synthetase) and *guaB* (IMP dehydrogenase), and the *purA* gene encoding adenylosuccinate synthetase all occur as single units. The *purB* gene encodes an enzyme involved in both IMP and AMP biosynthesis and is located in the *pur* operon. The levels of purine biosynthetic enzymes (except for GMP synthetase) are repressed in cells grown in the presence of purine compounds. Transcription of the *pur* operon is regulated negatively by adenine and guanine compounds including ATP, hypoxanthine, and guanine, which are corepressors. Feedback repression of purine nucleotide biosynthesis in *E. coli* is exerted by binding of the corepressor to the product of the *purR* gene. Hypoxanthine and guanine act cooperatively to change the conformation of *PurR*, thus enhancing its binding to DNA.

Techniques similar to those described above for amino acid fermentations have yielded IMP titers of 30 g l^{-1}. Since only low levels of GMP have been produced by direct fermentation, it is usually made by bioconversion of XMP, reaching GMP titers of about 30 g l^{-1}. Genetic modification of *Corynebacterium ammoniagenes* involving transketolase (an enzyme of the nonoxidative branch of the pentose phosphate pathway) resulted in the accumulation of 39 g l^{-1} of XMP. This work demonstrates the need for high levels of pentose (ribose) for nucleotide and nucleoside biosynthesis and overproduction.

The key to effective accumulation of purines and their derivatives is the limitation of intracellular AMP and GMP. This limitation is best achieved by restricting purine supply during growth of the purine auxotrophs. Thus, adenine-requiring mutants lacking adenylosuccinate synthetase accumulate hypoxanthine or inosine that results from the breakdown of intracellularly accumulated IMP. Certain adenine-auxotrophs of *B. subtilis* excrete over 10 g l^{-1} of inosine. These strains are still subject to GMP repression of enzymes of the common path. To minimize the severity of this regulation, the adenine auxotrophs are further mutated to eliminate IMP dehydrogenase. These adenine-xanthine double auxotrophs show a twofold increase in the specific activity of some common-path enzymes and accumulate inosine up to 15 g l^{-1} under conditions of limiting adenine and xanthine (or guanosine). Further deregulation is achieved by the selection of mutants resistant to purine analogs. Thus, mutants resistant to azaguanine with requirements for adenine and xanthine produce over 20 g l^{-1} inosine. Insertional inactivation of the IMP dehydrogenase gene in a *B. subtilis* strain yielded a culture producing inosine at 35 g l^{-1}. Cloning of IMP dehydrogenase has been used to improve guanosine production in *B. subtilis*. The donor strain produced a low level of purine nucleosides, but the distribution was in favor of guanosine (1 g l^{-1} of inosine vs. 9 g l^{-1} guanosine). The recipient strain was auxotrophic for adenine, lacked GMP reductase and purine nucleoside phosphorylase, and was resistant to 8-azaguanine, adenine, and adenosine; it produced 19 g l^{-1} inosine and 7 g l^{-1} guanosine. Cloning of IMP dehydrogenase from the first strain into the second strain yielded a recombinant that produced 5 g l^{-1} inosine and 20 g l^{-1} guanosine. Other *B. subtilis* mutants produce as much as 23 g l^{-1} of guanosine. Nucleosides such as inosine and guanosine are then converted to their active nucleotide derivatives chemically, microbiologically, or enzymically.

The de novo pyrimidine biosynthetic pathway involves five enzymes and results in uridine-5′-monophosphate (UMP) production. Aspartate transcarbamoylase, the first pathway enzyme committed to pyrimidine biosynthesis, catalyzes the conversion of aspartate and carbamoylphosphate to carbamoylaspartate. The subsequent biosynthetic pathway enzymes are dihydroorotase, dihydroorotate dehydrogenase, orotate phosphoribosyltransferase, and orotidine-5′-monophosphate (OMP) decarboxylase. Uridine triphosphate (UTP) is produced from UMP by the sequential actions of two nucleoside kinases. Cytidine triphosphate (CTP) is formed by the amination of UTP by CTP synthetase. The pyrimidine biosynthetic pathway is usually regulated at the level of gene expression. UMP kinases from *E. coli* and *B. subtilis* are activated by GTP and inhibited by UTP. The selection for antimetabolite resistance has proven to be successful in the development of pyrimidine nucleotide and nucleoside fermentations. Cytidine production by a *B. subtilis* cytidine deaminase-deficient mutant with resistance to fluorocytidine amounted to 10 g l^{-1}. Further mutation to 3-deazauracil resistance increased production to 14 g l^{-1}. By introducing a gene encoding a feedback-resistant carbamyl phosphate synthase, cytidine production was raised to 18 g 1^{-1}. Homoserine dehydrogenase (HSD) deficiency in *B. subtilis* increased cytidine production in a deregulated mutant from 9 to 23 g l^{-1}. Increasing the glucose concentration raised production to 30 g l^{-1}. Uridine production by mutants of *B. subtilis* resistant to pyrimidine antimetabolites has reached 55 g 1^{-1}.

4.4.3 Production Processes for Vitamins

Vitamins are one of the main products for the international markets of feed, medicine, and health care products. More than half of the vitamins produced commercially are fed to domestic animals. The vitamin market is a multibillion-dollar industry. According to Euromonitor estimates, in 2008

the global vitamin B consumer market generated annual sales in excess of 2.6 billion euros, or approximately US$3.4 billion. In the vitamin family, the total annual sales for vitamin C, vitamin E and vitamin A are about US$2 billion. Microbes produce five vitamins commercially: vitamin B_{12} (cyanocobalamin), ascorbic acid (vitamin C), riboflavin (vitamin B_2), pantothenic acid (vitamin B_5), and biotin.

4.4.3.1 Production of Vitamin B_{12}

Vitamin B_{12} is produced commercially at about 10 tons per year. Fermentations have to be run under complete or partial anaerobiosis when using species of *Pseudomonas* or *Propionibacterium*. The major industrial organisms are *Pseudomonas denitrificans and Propionibacterium shermanii*. Conventional strain improvement has yielded *P. denitrificans* strains producing 150 mg l^{-1}. *Propionibacterium freudenreichii* can produce 206 mg l^{-1}.

Increasing the activity of S-adenosyl-L-methionine uroporphyrinogen III methyltransferase (SUMT) by cloning in a DNA fragment containing this gene (*cobA*) in *P. denitrificans* increased vitamin B_{12} production by 100%. SUMT is at the branch point of the heme and B_{12} biosynthetic pathways. Cloning of the gene *cob1* increased S-adenosyl-L-methioninеprecorrin-2-methyltransferase (SP_2MT) and B_{12} production by 30%. SP_2MT is at the branch point of the siroheme and B_{12} pathways.

4.4.3.2 Production of Riboflavin

Annual production of riboflavin is over 6,000 tons/year by fermentation. Riboflavin overproducers include two yeast-like molds, *E. ashbyii* and *A. gossypii*, which synthesize riboflavin in concentrations greater than 20 g l^{-1}.

With *A. gossypii*, riboflavin production was found to be stimulated 3–4-fold by the addition of the precursors glycine and hypoxanthine. The level of production, which occurs after a growth rate declines, is determined by the activity of the promoter of gene *RIB3*. This gene encodes 3, 4-dihydroxy-2-butanone-4-phosphate (DHBP) synthase, the first enzyme of the pathway. Mutation of *A. gossypii* to resistance to aminomethylphosphonic acid (a glycine antimetabolite) yielded improved producers. Isocitrate lyase (ICL) is important for the use of fatty acids for riboflavin production. Itaconate, an inhibitor of ICL, eliminated the yellow color of *A. gossypii* colonies. A mutant strain, which was yellow on itaconate-containing agar, produced 15% more enzyme and 25-fold more riboflavin.

Processes using recombinant *B. subtilis* strains that produce at least 30 g l^{-1} riboflavin have been developed. In this species, riboflavin formation is regulated by feedback repression, not inhibition. An aporepressor encoded by *ribC*, whose effectors are riboflavin, FMN, and FAD, is responsible for this effect. Mutations of *ribC* lead to riboflavin overproduction. Sequential selection for resistance to 8-azaguanine, decoyinine, methionine sulfoxide, and roseoflavin plus cloning of multiple copies of the *riboflavin biosynthetic rib* operon yielded overproducing mutants. Further improvement was achieved when an extra copy of the *ribA* gene was introduced into the culture. This gene encodes both GTP cyclohydrolase II and 3, 4-dihydroxy-2-butanone 4-phosphate synthase, both of which act to commit precursors GTP and ribulose-5-phosphate to riboflavin biosynthesis.

A *Candida famata* (*Candida flareri*) strain produced 20 g l^{-1} in 200 hours. It was obtained by mutation and selection for resistance to 2-deoxyglucose (DOG), iron, tubercidin (a purine analog), and depleted medium, plus protoplast fusion. The process depends on the addition of glycine and hypoxanthine. Selection for resistance to the adenine antimetabolite 4-aminopyrazolo (3, 4-d) pyrimidine improved production. Threonine showed a ninefold stimulation in a strain with a cloned threonine aldolase, which converts threonine to glycine.

4.4.3.3 Production of Vitamin C

Vitamin C has a global production of 110,000 tons/year. It is used for nutrition of humans and animals and as a food antioxidant. The otherwise chemical Reichstein process utilizes one bioconversion reaction, the oxidation of D-sorbitol to L-sorbose by *Gluconobacter oxydans*, as the first

step in ascorbic acid production. The biotransformation proceeds at the theoretical maximum (i.e., 200 g l^{-1} of D-sorbitol can be converted to 200 g l^{-1} of L-sorbose) when using a mutant of *G. oxydans* selected for resistance to a high sorbitol concentration. The bioconversion is used rather than a chemical reaction since the latter produces unwanted D-sorbose along with L-sorbose. An excellent fed-batch bioconversion process uses a starting concentration of 100 g l^{-1} of D-sorbitol and achieves production of 280 g l^{-1} of L-sorbose in 16 hours with a productivity of 17.6 g l^{-1} h^{-1}. The Reichstein process converts glucose to 2-keto-L-gulonic acid (2-KLGA) in five steps with a yield of 50%. Then, 2-KLGA is chemically converted to L-ascorbic acid in two more steps.

Fermentation processes are competing with the Reichstein method. A mixed culture of *G. oxydans* (which converts L-sorbose to 2-KLGA) and *Gluconobacter suboxydans* (which converts D-sorbitol to L-sorbose) was able to convert 138 g l^{-1} of D-sorbitol to 112 g l^{-1} of 2-KLGA, with a molecular conversion yield of 75% in two days. A recombinant strain of *G. oxydans* containing genes encoding L-sorbose dehydrogenase and L-sorbosone dehydrogenase from *G. oxydans* was able to produce 2-KLGA effectively from D-sorbitol. Mutation to suppress the L-idonate pathway and improvement of the promoter led to production of 130 g l^{-1} 2-KLGA from 150 g l^{-1} D-sorbitol.

4.4.3.4 Production of Other Vitamins

Recombinant *E. coli*, transformed with genes encoding pantothenic acid (vitamin B_5) biosynthesis and resistant to salicylic and/or other acids, produce 65 g l^{-1} of D-pantothenic acid from glucose using β-alanine as a precursor. Seven thousand tons per year are made chemically and microbiologically. Thiamine (vitamin B_1) is produced synthetically at 4,000 tons per year. Pyridoxine (vitamin B_6) is made chemically at 2,500 tons per year. The vitamin F (polyunsaturated fatty acids) processes of *Mortierella isabellina* or *Mucor circinelloides* yield 5 g l^{-1} of γ-linolenic acid.

4.4.4 Production Processes for Organic Acids

Acetic, citric, gluconic, and lactic acids are the main primary metabolic organic acids with commercial application as chemicals, at least some of which are produced industrially by fermentation. Others include pyruvic, fumaric, succinic, glyceric, shikimic, propionic, and itaconic acids. Production has been improved by classical mutation, by screening and selection techniques, as well as by metabolic engineering. The world market for organic acids has reached US$1.5 billion.

4.4.4.1 Production of Acetic Acid

More than 7 million tons of acetic acid are made worldwide per year, over half of which is produced through microbial fermentations. Vinegar has been produced microbiologically as far back as 4000 BC Vinegar fermentation is best carried out with species of *Gluconacetobacter* and *Acetobacter.* A solution of ethanol is converted to acetic acid during which 90–98% of the ethanol is attacked, yielding a solution of vinegar containing 12–17% acetic acid. Titers of acetic acid have reached 53 g l^{-1} with genetically engineered *E. coli*, 83 g l^{-1} by a *Clostridium thermoaceticum* mutant, and 97 g l^{-1} by an engineered strain of *Acetobacter aceti* ssp. *xylinium*.

4.4.4.2 Production of Citric Acid

Production of citric acid by *Aspergillus niger* and yeasts amounts to 1.75 million tons per year with a major market of US$1.7 billion. The best strains of *A. niger* make over 200 g l^{-1} of citric acid. Keys to the fermentation are excess carbon source, low levels of pH and dissolved oxygen, and limited concentrations of certain trace metals and phosphate.

Glucose is converted, through the activities of the enzymes of the Embden-Meyerhof-Parnas (EMP) pathway, to pyruvate, which in turn is converted to acetyl coenzyme A through the activity of pyruvate dehydrogenase. Acetyl CoA is then condensed with oxaloacetate, the first committed step in the Krebs cycle to give citric acid through the activity of citrate synthase. Citric acid production by *A. niger* is stimulated by growing the organism in a glucose-rich (10–20%) medium. High

concentration of sucrose triggers the accumulation of fructose 2, 6-bisphosphate intracellularly, which in turn activates glycolysis. Another key to successful citric acid fermentation by this fungus is a deficiency of Mn^{2+} ions (cofactor of isocitrate dehydrogenase) as it is necessary for restricting carbon flux through this enzyme, while maintaining an active citrate synthase. Since the equilibrium of the reaction catalyzed by aconitase, which converts citric acid to isocitrate, is markedly in favor of citrate formation, citric acid accumulates. Two isocitrate dehydrogenases, mitochondrial and $NADP^+$ specific, are inhibited by citrate. Since the cofactor of this enzyme is Mg^{2+} or Mn^{2+}, citrate's ability to chelate these bivalent ions restricts the enzymic activity of isocitrate dehydrogenase, which in turn allows citrate to accumulate.

In addition to the Mn^{2+} ion, the metal deficiencies necessary for efficient citric acid production by different strains of *A. niger* include Fe^{2+} and Zn^{2+}. However, it is Mn^{2+} limitation that is paramount for the production of a high titer of citrate. The principal regulatory control site in the reactions from glucose to citrate is phosphofructokinase. This enzyme is inhibited by citrate, an event that would not be favorable for the overproduction of citric acid. However, Mn^{2+} deficiency slows down growth, leading to degradation of intracellular nitrogenous macromolecules and a fivefold increase in the concentration of NH_4^+ in mycelia. The high ammonium concentration reverses citrate inhibition of phosphofructokinase, thus ensuring the continued conversion of glucose to citrate. Mutants whose phosphofructokinase I is partially desensitized to citrate inhibition are less dependent on low Mn^{2+} for high citric acid production. Citrate inhibition of phosphofructokinase is reversed by fructose 2, 6-diphosphate and AMP. The optimum pH for citric acid production by *A. niger* is 1.7–2.0. At pH values higher than 3.0, oxalic and gluconic acids are produced instead. Low pH inactivates glucose oxidase and prevents gluconate production. Mutants of *A. niger* with greater resistance to low pH are improved citric acid producers. Other selective tools include resistance to high concentrations of citrate and sugars.

Species of the yeast genus *Candida* also excrete large amounts of citric acid and isocitric acid. The key event of the yeast citrate process appears to be a sharp drop in intracellular AMP following nitrogen depletion, inhibiting the AMP-requiring isocitrate dehydrogenase. *Candida guilliermondii* excretes large quantities of citric acid without the undesirable isocitric acid when cultured in the presence of metabolic inhibitors (e.g., sodium fluoroacetate, *n*-hexadecylcitric acid, and *trans*-aconitic acid). These inhibitors block the TCA cycle at the aconitase step. Mutation of *Candida lipolytica* to aconitase deficiency is also effective. The optimum pH for the yeast citrate process is above 5.0. Lower pH values lead to production of polyhydroxy compounds such as erythritol and arabitol. The yeast process utilizes hydrocarbons as substrate and citric acid yields as high as 225 g l^{-1} at a rate of 1.4 g l^{-1} h^{-1}.

High concentrations of citric acid are also produced by *Candida oleophila* from glucose. In chemostats, 200 g l^{-1} can be made, and more than 230 g l^{-1} can be made in continuous repeated fed-batch fermentations. This compares to 150 to 180 g l^{-1} by *A. niger* in industrial-batch or fed-batch fermentation in 6–10 days. The key to the yeast fermentation is nitrogen limitation coupled with an excess of glucose. The citric acid is secreted by a specific energy-dependent transport system induced by intracellular nitrogen limitation. The transport system is selective for citrate over isocitrate. *Yarrowia lipolytica* produces up to 198 g l^{-1} citric acid in fed-batch fermentations on sunflower oil with a very low production of isocitric acid.

4.4.4.3 Production of Lactic Acid

The global market for lactic acid is about 350,000 tons per year. *Rhizopus oryzae* is favored for production since it makes stereochemically pure L (+)-lactic acid, whereas lactobacilli produce mixed isomers; furthermore, lactobacilli require yeast extract. However, a mutant strain of *Lactobacillus lactis* has been developed that produces 195 g l^{-1} of L-lactic acid from 200 g l^{-1} of glucose. *R. oryzae* normally converts 60–80% of added glucose to lactate, with the remainder going to ethanol. By increasing lactic dehydrogenase levels via cloning, more lactate and less ethanol are produced. Mutation of wild-type *R. oryzae* led to L (+)-lactic acid production of 131–136 g l^{-1}, a yield from

glucose of 86–90% and a productivity of 3.6 g l^{-1} h^{-1}. This was a 75% improvement over the wild-type strain. The final strain was the result of a six-step mutation sequence. DL-lactic acid can be made at 129 g l^{-1} by *Lactobacillus* sp. and D-lactic acid at 120 g l^{-1}. A recombinant *E. coli* strain has been constructed that produces optically active pure D-lactic acid from glucose at virtually the theoretical maximum yield (e.g., two molecules from one molecule of glucose). The organism was engineered by eliminating genes of competing pathways encoding fumarate reductase, alcohol/aldehyde dehydrogenase, and pyruvate formate lyase, and by a mutation in the acetate kinase gene. Whole-genome shuffling has been used to improve the acid tolerance of a commercial lactic acid-producing *Lactobacillus* sp.

Products in development are nonchlorinated solvent, ethyl lactate, and bioplastic polylactide. Polylactide is made by converting corn starch to dextrose, fermenting dextrose to lactic acid, condensing lactic acid to lactide, and polymerizing lactide.

4.4.4.4 Production of Pyruvic Acid

A recombinant strain of *E. coli* that is a lipoic acid auxotroph and defective in F_1ATPase produces 31 g l^{-1} of pyruvic acid from 50 g l^{-1} glucose. The lowering of the energy level in the cell by the F_1ATPase deletion increases the glucose uptake and glycolysis rate, thereby leading to an increase in pyruvate production. An improved fermentation was developed using *Torulopsis glabrata* yielding a pyruvic acid concentration of 77 g l^{-1}, a conversion of 0.80 g g^{-1} glucose, and a productivity of 0.91 g l^{-1} h^{-1} in 85 hours. By directed evolution in a chemostat, a mutant *Saccharomyces cerevisiae* strain was obtained that produces from glucose 135 g l^{-1} pyruvic acid at a rate of 6 to 7 mmol per gram biomass per hour during exponential growth with a yield of 0.54 g^{-1}.

4.4.4.5 Production of Other Organic Acids

From 120 g l^{-1} of glucose, *Rhizopus arrhizus* produces 97 g l^{-1} fumaric acid. The molar yield from glucose is 145% and involves CO_2 fixation from pyruvate to oxaloacetate and the reductive reactions of the TCA cycle. Succinic acid is made chemically at 16,000 tons per year for commercial use as (1) a surfactant, detergent extender, or foaming agent; (2) an ion chelator in electroplating to prevent metal corrosion and pitting; (3) an acidulant, pH modifier, flavoring agent, or antimicrobial agent for food; and (4) a chemical in the production of pharmaceuticals. The market size is US$400 million per year. Production by fermentation with *Actinobacillus succinogenes* amounts to 106 g l^{-1}. Bioconversion from fumarate yields 85 g l^{-1} succinate after 24 hours. Metabolic engineering of *E. coli* yields a shikimic acid overproducer making 84 g l^{-1} with a 0.33 molar yield from glucose. Production of gluconic acid amounted to 150 g l^{-1} from 150 g l^{-1} glucose plus corn steep liquor in 55 hours by *A. niger*. Production level is about 50,000 tons per year. Cloning of fumarase in *S. cerevisiae* remarkably improved the malic acid bioconversion from fumaric acid from 2 g l^{-1} to 125 g l^{-1}; conversion yield was nearly 90%. Glyceric acid production amounts to 136 g l^{-1} by *Gluconobacter frateurii* from glycerol, and that of propionic acid is 106 g l^{-1} from the same carbon source by an acetate-negative mutant of *Propionibacterium acidipropionici*.

4.4.5 Production of Ethanol and Related Compounds

4.4.5.1 Production of Ethanol

Ethanol is a primary metabolite produced by fermentation of sugar, or of a polysaccharide that can be depolymerized to a fermentable sugar. *S. cerevisiae* is used for the fermentation of hexoses, whereas the *Kluyveromyces fragilis* or *Candida* species can be used if lactose or a pentose, respectively, is the substrate. Under optimum conditions, approximately 10–12% ethanol by volume is obtained within five days. At present, all beverage alcohol is made by fermentation. Industrial ethanol is mainly manufactured by fermentation, but some is still produced from ethylene by the petrochemical industry. Bacteria such as *Clostridia* and *Zymomonas* are being reexamined for

ethanol production after years of neglect. *Clostridium thermocellum*, an anaerobic thermophile, can convert waste cellulose and crystalline cellulose directly to ethanol (see Chapter 9 on renewable resources conversion to fine chemicals). The available cellulosic feedstock in the United States could supply 20 billion gallons of ethanol in comparison to the 3 billion gallons currently made from corn. This would be enough to add 10% ethanol to all gasoline used in the United States. Other *Clostridia* produce acetate, lactate, acetone, and butanol and will be used to produce these chemicals when the global petroleum supplies begin to become depleted.

Ethyl alcohol is produced in Brazil from cane sugar at over 4 billion gallons per year and is used either as a 25% blend or as a pure fuel. Most new cars in Brazil use pure ethanol, whereas the remainder utilizes a blend of 20–25% ethanol in gasoline. In the United States, over 3.4 billion gallons of ethanol were made from starchy crops (mainly corn) in 2004. It is chiefly added to gasoline to reduce CO_2 emissions by improving the overall oxidation and performance of gasoline.

Fuel ethanol produced from biomass would provide relief from air pollution caused by the use of gasoline and would not contribute to the greenhouse effect. *E. coli* has been converted into an excellent ethanol producer (43% yield, v/v) by cloning and expressing the alcohol dehydrogenase and pyruvate decarboxylase genes from *Zymomonas mobilis* and *Klebsiella oxytoca*. The recombinant strain was able to convert crystalline cellulose to ethanol in high yield when fungal cellulase was added. Other genetically engineered strains of *E. coli* can produce as much as 60 g l^{-1} of ethanol. An ethanol-resistant mutant of *S. cerevisiae* makes 96 g g l^{-1}.

4.4.5.2 Production of Glycerol

Glycerol is widely used in the manufacture of drugs, food, cosmetics, paint, and many other commodities. Some 600,000 tons of glycerol are produced annually primarily through extraction of materials from the fat and oil industries, or by chemical synthesis from propylene. However, yeast fermentations using *S. cerevisiae* can produce up to 230 g l^{-1}, while osmotolerant *Candida glycerinogenes* can produce 137 g l^{-1} with yields of 63–65% and a productivity of 32 g l^{-1} h^{-1}. Furthermore, *Candida magnoliae* produces 170 g l^{-1} in fed-batch fermentation, and in a similar type of process, *Pichia farinosa* can produce up to 300 g l^{-1}.

4.4.5.3 Production of 1, 3-Propanediol

A strain of *Clostridium butyricum* converts glycerol to 1, 3-propanediol (PDO) at a yield of 0.55 g per gram of glycerol consumed. In a two-stage continuous fermentation, a titer of 41–46 g l^{-1} was achieved with a maximum productivity of 3.4 g l^{-1} h^{-1}. At lower dilution rates, butyrate was produced, and at higher dilution rates, acetate was made. Recent metabolic engineering triumphs have included an *E. coli* culture that grows on glucose and produces PDO at 135 g l^{-1}, with a yield of 51% and a rate of 3.5 g l^{-1} h^{-1}. To do this, eight new genes were introduced to convert dihydroxyacetone phosphate (DHAP) into PDO. These included yeast genes converting dihydroxyacetone to glycerol and *Klebsiella pneumoniae* genes converting glycerol to PDO. Production in the recombinant was improved by modifying 18 *E. coli* genes, including regulatory genes. PDO is the monomer used to chemically synthesize polyurethanes and the polyester fiber Sorono™ by DuPont. This new bioplastic, polytrimethylene terephthalate (3GT polyester), is made by reacting terephthalic acid with PDO. PDO is also used as a polyglycol-like lubricant and as a solvent.

4.4.5.4 Production of Erythritol

The noncariogenic, noncaloric, and diabetic-safe sweetener erythritol is made by fermentation. It has 70–80% the sweetness of sucrose. Osmotic pressure increase was found to raise volumetric and specific production, but to decrease growth. By growing cells first at a low glucose level (i.e., 100 g l^{-1}) and then adding 200 g l^{-1} glucose at 2.5 days, erythritol titer was increased to 45 g l^{-1} as compared to single-stage fermentation with 300 g l^{-1} glucose, which yielded only 24 g l^{-1}. Production of erythritol by a *C. magnoliae* osmophilic mutant yielded a titer of 187 g l^{-1}, a rate of 2.8 g l^{-1} h^{-1}, and 41% conversion from glucose. Other processes have been carried out with

Aureobasidium sp. (165 g l^{-1} from glucose with a 48% yield), and the osmophile *Trichosporon* sp. (188 g l^{-1} with a productivity of 1.18 g l^{-1} h^{-1} and 47% conversion). Erythritol can also be produced from sucrose by *Torula* sp. at 200 g l^{-1} in 120 h with a yield of 50% and a productivity of 1.67 g l^{-1} h^{-1}. Recent studies have developed a *Pseudozyma tsukubaensis* process yielding 245 g l^{-1} of erythritol from glucose.

4.4.5.5 Production of other Compounds

Dihydroxyacetone is used as a cosmetic tanning agent and surfactants. It is produced from glycerol by *Gluconobacter* species with a conversion rate of up to 90%. D-mannitol is used in the food, chemical, and pharmaceutical industries. It is only poorly metabolized by humans, is about half as sweet as sucrose, and is considered a low-calorie sweetener. It is produced mainly by catalytic hydrogenation of glucose–fructose mixtures, but 75% of the product is sorbitol, not mannitol. For this reason, fermentation processes are being considered. Recombinant *E. coli* produces up to 91 g l^{-1} mannitol, and *Leuconostoc* sp. up to 98 g l^{-1}. Mannitol production reached 213 g l^{-1} from 250 g l^{-1} fructose after 110 hours by *C. magnoliae*. Sorbitol, also called D-glucitol, is 60% as sweet as sucrose and has use in the food, pharmaceutical, and other industries. Its worldwide production is 500,000 tons per year, and it is made chemically by catalytic hydrogenation of D-glucose. Toluenized (permeabilized) cells of *Z. mobilis* produce 290 g l^{-1} of sorbitol and 283 g l^{-1} of gluconic acid from a glucose and fructose mixture in 16 hours with yields near 95% for both products. Xylitol is a naturally occurring sweetener with anticariogenic properties used in some diabetes patients. It can be produced chemically by chemical reduction of D-xylose. A mutant of *Candida tropicalis* produces 40 g l^{-1} l from D-xylose in a yield of over 90%.

Early in the nineteenth century, the acetone–butanol fermentation process was a commercial operation but was later replaced by chemical synthesis from petroleum because of economic factors. These included the low concentration of butanol in the broth (1%) and the high cost of butanol recovery. *Clostridium beijerinckii* and *Clostridium acetobutylicum* are the organisms of choice for fermentation. Research on this aspect of fermentation continued over many years, dealing with process engineering, mutation, and metabolic engineering. Butanol-resistant mutants were isolated for their ability to overproduce butanol and acetone. Further research involving biochemical engineering modifications increased the production of acetone, butanol, and ethanol (ABE) to 69 g l^{-1}. A mutant in the presence of added acetate produced 21 g l^{-1} butanol and 10 g l^{-1} of acetone from glucose. Acetate both stimulates production and helps stabilize the culture, which is known to be highly unstable. 2,3-butanediol can be made from glucose at a titer of 130 g l^{-1} by a genetically engineered strain of *K. oxytoca* that no longer produces ethanol and has a lowered level of acetoin formation. The compound has a very high octane rating, making it a potential aviation fuel.

SUMMARY

The microbial production of primary metabolites, through fermentation, contributes significantly to the quality of life that we enjoy today. Microorganisms are capable of converting inexpensive carbon and nitrogen sources into voluble metabolites such as amino acids, nucleotides, organic acids, and vitamins, which can be added to food as a flavor enhancer and/or to increase its nutritional value. Also, many primary metabolites are proving invaluable as biosynthetic precursors for the manufacture of therapeutics.

Overproduction of microbial metabolites is related to developmental phases of microorganisms. Inducers, effectors, inhibitors, and various signal molecules play roles in different types of overproduction. Biosynthesis of enzymes catalyzing metabolic reactions in microbial cells is controlled by well-known positive and negative mechanisms (e.g., induction, nutritional regulation, and feedback regulation).

In the early years of fermentation processes, strain developments depended entirely on classical strain breeding involving intensive rounds of random mutagenesis, followed by an equally strenuous program of screening and selection. However, recent innovations in molecular biology, on one hand, and the development of new tools in functional genomics, transcriptomics, metabolomics, and proteomics, on the other, enabled more rational approaches for strain improvement.

The roles of primary metabolites and, in turn, microbial fermentations stand to grow in stature especially as we enter a new era in which the use of renewable resources is recognized as an urgent need.

REFERENCE

Varela, C., E. Agosin, M. Baez, M. Klapa, and G. Stephanopoulos. 2003. Metabolic flux distribution in *Corynebacterium glutamicum* in response to osmotic stress. *Appl. Microbiol. Biotechnol.* 60:547–55.

FURTHER READING

Abe, H., Y. Fujita, Y. Takaoka, E. Kurita, S. Yano, N. Tanaka, and K-I. Nakayama. 2009. Ethanol tolerant *Saccharomyces cerevisiae* strains isolated under selective conditions by over-expression of a proofreading DNA polymerase. *J. Biosci. Bioeng.* 108:199–204.

Da Silva, G. P., M. Mack, and J. Contiero. 2009. Glycerol: A promising and abundant carbon source for industrial microbiology. *Biotechnol. Adv.* 27:30–9.

Demain, A. L. 2000. Small bugs, big business: The economic power of the microbe. *Biotechnol. Adv.* 18:499–514.

Demain, A. L., M. Newcomb, and J. H. D. Wu. 2005. Cellulase, clostridia, and ethanol, *Microbiol. Mol. Biol. Rev*. 69:124–54.

Eggeling, L., and H. Sahm. 1999. L-glutamate and L-lysine: Traditional products with impetuous developments. *Appl. Microbiol. Biotechnol*. 52:146–53.

Eggeling, L., and H. Sahm. 2001. The cell wall barrier in *Corynebacterium glutamicum* and amino acid efflux. *J. Biosci. Bioeng.* 92:201–13.

El-Mansi, M. 2004. Flux to acetate and lactate excretions in industrial fermentations: Physiological and biochemical implications, *J. Indust. Microbiol. Biotechnol.* 31:295–300.

Eseji, T., C. Milne, N. D. Price, and H. P. Blaschek. 2010. Achievements and perspectives to overcome the poor solvent resistance in acetone and butanol-producing microorganisms. *Appl. Microbiol. Biotechnol.* 85:1697–712.

Han, L., and S. Parekh. 2004. Development of improved strains and optimization of fermentation processes. In Barredo, J. L., ed., *Microbial Processes and Products*, pp. 1–23. Totowa, NJ: Humana.

Ikushima, S., T. Fujii, O. Kobayashi, S. Yoshida, and A. Yoshida. 2009. Genetic engineering of *Candida utilis* yeast for efficient production of L-lactic acid. *Biosci. Biotechnol. Biochem.* 73:1818–24.

Jaya, M., K-M. Lee, M. K. Tiwari, J-S. Kim, P. Gunasekaran, S-Y. Kim, I-W. Kim, and J-K. Lee. 2009. Isolation of a novel high erythritol-producing *Pseudomonas tsukubaensis* and scale-up of erythritol fermentation to industrial level. *Appl. Microbiol. Biotechnol.* 83:225–31.

Jetten, M. S. M., and A. J. Sinskey. 1995. Recent advances in the physiology and genetics of amino acid-producing bacteria. *Crit. Rev. Biotechnol*. 15:73–103.

John, R. P., G. S. Anisha, M. Nampoothirti, and A. Pandey. 2009. Direct lactic acid fermentation: Focus on simultaneous saccharification and lactic acid production. *Biotechnol. Adv.* 27:145–52.

Kinoshita, S. 1987. Thom award address: Amino acid and nucleotide fermentations from their genesis to the current state. *Devel. Indust. Microbiol*. 28(Suppl. 2): 1–12.

Kraemer, R. 2004. Production of amino acids: Physiological and genetic approaches. *Food Biotech.* 18(2): 1–46.

Magnuson, J. K., and L. L. Lasure. 2004. Organic acid production by filamentous fungi. In Tkacz, J. and L. Lange, eds., *Advances in Fungal Biotechnology for Industry, Agriculture, and Medicine*, pp. 307–340. New York: Kluwer Academic/Plenum.

Nielsen, J. 2001. Metabolic engineering. *Appl. Microbiol. Biotechnol*. 55:263–83.

Ohnishi, J., S. Mitsuhashi, M. Hayashi, S. Ando, H. Yokoi, K. Ochiai, and M. Ikeda. 2002. A novel methodology employing *Corynebacterium glutamicum* genome information to generate a new L-lysine-producing mutant. *Appl. Microbiol. Biotechnol*. 58:217–23.

Sahm, H., L. Eggeling, and A. A. de Graaf. 2000. Pathway analysis and metabolic engineering in *Corynebacterium glutamicum*. *Biol. Chem*. 381:899–910.

Sanchez, S., and A. L. Demain. 2002. Metabolic regulation of fermentation processes. *Enzyme Microb. Technol*. 31:895–906.

Vinci, V. A., and G. Byng. 1999. Strain improvement by nonrecombinant methods. In Demain, A. L., and J. Davies, eds., *Manual of Industrial Microbiology and Biotechnology*, 2nd ed., pp. 103–13. Washington, DC: ASM Press.

5 Microbial and Plant Cell Synthesis of Secondary Metabolites and Strain Improvement

Wei Zhang, Iain S. Hunter, and Raymond Tham

CONTENTS

5.1 INTRODUCTION

Secondary metabolites from microorganisms and plants are typically low-molecular-weight natural products that are generally not essential for survival and growth of the producing organisms, but are involved in the interactions of microorganisms and plants with their environment as a result of secondary metabolism regulation. It is generally accepted that secondary metabolites are derived from primary metabolites, often having distinct and versatile physiological functions either induced or regulated by environmental and nutritional factors such as in plants (first proposed by Albrecht Kossel in 1891; Chapman 2000). As such, a large number of secondary metabolites have been found of both microbial and plant origin, which have been commercially applied for human health products, industrial biochemicals, agricultural chemicals, food, and nutritional additives. They include antibiotics, antiviral and antitumor agents, cholesterol-regulating drugs, pigments, flavors, fragrances, toxins, effectors of ecological competition and symbiosis, pheromones, enzyme inhibitors, immunomodulating agents, receptor antagonists and agonists, pesticides, and growth promoters of animals and plants (Ruiz et al. 2010). They have unusual chemical structures that are often synthesized and modified in complex multistep metabolic pathways of both biosynthetic steps and postbiosynthetic events. The level of production of these secondary metabolites can be influenced by factors or combination of factors such as the growth phase, the growth rate, nutrients, signal molecules (e.g., hormones and elicitors), feedback control, cultivation conditions (e.g., temperature, pH, light, and dissolved oxygen), and physical microenvironments (e.g., shear stress or mixing).

Though a huge variety of secondary metabolites have been identified in microorganisms and plants, the understanding and knowledge of their metabolic pathways and regulation are to a great extent still very poor. Commonly, the majority of these products are produced at a very low level in the original producing strains, as it is "secondary" to the living processes of microorganisms and plants. Such a level of production is far lower than the requirement for commercial production, thus creating a challenge for commercial translation of discoveries. This technological challenge is particularly true in the case of production of secondary metabolites using plant cell and tissue culture technologies. This has resulted in very limited successes in commercial production with only a handful of products having reached the market such as the anticancer drug taxol. In contrast, microbial fermentation technology has been well established with many successful commercial products for a variety of applications in the pharmaceutical industry (e.g., antibiotics, and antitumor and antiviral agents), food industry (e.g., amino acids, organic acids, vitamins, and flavoring compounds), agricultural industry (e.g., pesticides, insecticides, and antibacterial agents), chemical and biofuels industry (e.g., ethanol, butanol, methane, and biodiesels), and environmental industry (e.g., bioremediation compounds). However, these commercially successful microbial products still represent only a small fraction of the enormous diversity of secondary metabolites biosynthesized by microorganisms of both terrestrial and aquatic environments.

To develop a successful industrial production process of any useful products by microbial fermentation and plant cell culture, it is imperative to develop an elite strain or cell line, and efficient processing strategies that can achieve the following:

1. High and stable product yield and productivity under low-cost process conditions
2. High conversion rate of the cheapest available substrates
3. High product selectivity and specificity, facilitating downstream purification

With these targets in mind, this chapter focuses on two main themes:

1. The key process and strain improvement strategies of both classical and genetic approaches for microbial synthesis of secondary metabolites, drawing examples from the antibiotics industry and new therapeutics of extremely high value to humankind
2. The key process and cell line improvement strategies for plant cell synthesis of secondary metabolites, using the production of anthocyanins as a case study

5.2 MICROBIAL SYNTHESIS OF SECONDARY METABOLITES AND STRAIN IMPROVEMENT

Although the use of microorganisms in the production of commercially useful products is well established, the general public has yet to fully appreciate the microbial origin of some well-known commodities. For example, citric acid, an organic acid that chemists found very difficult if not impossible to synthesize with the correct stereo-specificity, is now widely produced through fermentation by either *Aspergillus niger* or the yeast *Yarrowia lipolytica*. It was the expertise gained with such fermentations that allowed the rapid development of the antibiotics industry in the early 1940s, with a consequential leap in quality of health care.

In our contemporary lifestyle, the microbial origins of many products are not well recognized. For example, xanthan gum, a product made by *Xanthomonas campestris*, is widely used in the manufacture of ice cream as it prevents the foams from collapsing with time. In a slightly modified form, xanthan gum gives paints their unique property of sticking to the brush without dripping but spreading smoothly and evenly from the brush to the surface.

In addition to natural products such as the chemicals mentioned above, recombinant strains of *Escherichia coli*, constructed by genetic engineering, are now used for the production of "non-natural products" to the organism such as human insulin. Another example is biological washing powders, which contain enzymes drawn from different species, particularly those belonging to the genus *Bacillus*. Microbial products thus have a significant impact on our everyday lives.

Significantly, the "new biotechnology" industry is critically dependent on microbial fermentations for the production of extremely high-value recombinant therapeutic products (e.g., human insulin and human growth hormone) as well as low-value recombinant products (e.g., prochymosin, which provides an ethically acceptable alternative to rennin [chymosin] in the manufacture of cheese).

In this section, both classical strain improvement strategies and modern recombinant (cloning) strategies will be discussed in regard to how to achieve industrially desired properties for the production of microbial secondary metabolites.

5.2.1 Economics and Scale of Microbial Product Fermentations

The type of fermentation used, as well as its size, duration, and nutrient profile, will depend critically on the nature of the microbial product. For "low-value, high-volume" products, such as citric acid and xanthan gum, high-capacity fermentors (often up to 800 m^3 in volume) are generally used. However, the duration of the fermentation process and the costs of nutrients and "utilities" (heating, cooling, and air) are the critical factors in the overall profitability of this business.

"Medium-value, medium-volume" products, such as antibiotics, are typically made in fermentors that are considerably smaller (100–200 m^3), and again the duration and the utility and nutrient costs are significant factors.

"High-value, low-volume" products, such as recombinant therapeutic proteins, are made in small (approximately 400 L, i.e., 0.4 m^3) fermentors for which the cost of the nutrients and utilities is a minor factor in the overall feasibility and profitability.

For all but the high-value products, nutrient costs (especially of the primary carbon source) are critical. Depending on the vagaries of world commodity markets, complicated further by artificially imposed trade tariffs, the availability and, in turn, cost of nutrients can fluctuate at alarming rates. Flexibility in the choice of nutrients is therefore of paramount importance, and strain improvement programs must take this factor into consideration.

By contrast, for the high-value (recombinant) products, the emphasis of the strain improvement program focuses on the following aspects:

The stability of the strain
The level of expression
The overall quality of the product, rather than the cost of the fermentation process per se

A fermentation process constitutes a business that aims to sell the product at an overall profit. This issue positions strain improvement programs at the interface between science and the commercial world, and requires a different set of criteria to judge whether a task is worthwhile or not. Strain improvement programs are positioned, and must first be vetted, to establish the cost of the research and development (R&D) that will be necessary to achieve the stated goal, and to set the expected cost against the annual savings likely to ensue should that piece of work deliver the expected gains in productivity. It often comes as a shock to researchers new to this field that projects that are highly innovative, but to which some risk of failure is attached, are not funded because the return on such an investment (set against the risk) is not high enough. For example, a strain improvement program for a "mature product" would be difficult to justify if the annual R&D cost could not be recouped in around three years through the projected increase in productivity. The annual cost of strain improvement programs must, therefore, be no more than three times the projected annual cost savings. Acclimatization to such rigorous reviews of research plans and draconian decision making constitutes a sharp learning curve for newly recruited research staff.

5.2.2 Different Products Need Different Fermentation Processes

At the "low-value" end of the microbial products business, the margins on profitability are extremely tight. For citric acid, the titer must be greater than 100 g L^{-1}, with carbon conversion efficiency (the amount of substrate converted to product on a per gram basis) close to 100% for the process to become economic. Citric acid is produced concurrently with microbial growth, but a fine balance has to be struck between the amount of cells that are made in the fermentation (which consumes some of the carbon source that otherwise could be used to make the product) and the fact that a doubling of the cell mass may result in twice the volumetric rate of citric acid production (as each cell acts as its own "cell factory"), but may hinder the eventual purification of the product. Growth can be arrested by, typically, limiting the amount of nitrogen available to the culture, in which case citric acid is still produced for some time by the cells in the stationary phase. Cheap carbon sources (e.g., unrefined molasses), fast production runs with minimal turnaround time, and a cheap and rapid means of extracting the product are most important, and the strain improvement program of this mature product will be focused on substrate flexibility and rapid production.

Medium-value products, such as antibiotics, are produced by microbes, which, when first isolated from the soil, usually make detectable, but vanishingly small, quantities (a few micrograms) of the bioactive substance. Most commercial fermentation processes will become economically viable only if the strain is eventually capable of making more than 15–20 g L^{-1} of the bioactive product using comparatively cheap carbon sources, such as rapeseed oil, and low-grade sources of protein, such as soya bean or fish meal. Antibiotic production usually occurs following the onset of the stationary phase (i.e., after growth has been arrested), but many antibiotics contain nitrogen as well as carbon, so growth is generally limited by the supply of phosphate. A steady supply of nutrients containing carbon and nitrogen, but not phosphate, is fed to the fermentation during the phase of antibiotic production.

Once a new microbial metabolite has been discovered, a campaign of "empirical strain improvement" is undertaken to boost the level of production to a titer at which the process becomes economically viable.

For "high-value" products, such as recombinant therapeutic proteins, the cost of the fermentation broth is not a major issue. To ensure consistency of the final product, expensive well-defined media (either Analar mineral medium or high-specification tryptone hydrolysates) are used along with a high-purity carbon source (usually glucose). Following the onset of the stationary phase, the production of high-value products is triggered, generally in response to an external signal such as temperature shift or the addition of an exogenous gratuitous inducer. The levels of production may be relatively modest (less than 1 g L^{-1}) to meet commercial targets, but higher levels are always

sought. This is because the products are often formulated into injectable medicines, in which there is a fear of raising an immune response if the recombinant protein is not 100% pure or not folded into the correct tertiary structure. A major objective of strain improvement programs, therefore, is to address this important regulatory issue rather than the cost of media and utilities.

5.2.3 Fed-Batch Culture: The Paradigm for Many Efficient Microbial Processes

Simple batch culture is a fairly inefficient way to synthesize a microbial product, as a substantial proportion of the nutrients present in the fermentation is used to make the biomass and the opportunity then to use the biomass as a cell factory to make the product is limited to the time of the growth period. Although very high levels of productivity can often be achieved in continuous culture, this technique has the disadvantages that large volumes of medium (often expensive medium) are required, and the product is made in a dilute stream that has to be concentrated before final isolation can take place. Fed-batch culture is a "halfway" approach. The cells are grown up in batch culture and then the resident biomass, which is no longer growing, is dedicated to product formation by feeding nutrients, except for that chosen to limit growth. This type of culture technique was developed by the antibiotics industry.

To understand the nature of antibiotic fermentations, it is important to take account of the life cycle of the producing microorganisms within the natural ecosystem. This example is from *Streptomyces*, the filamentous bacteria that make the majority (>60%) of natural antibiotics, including streptomycin, the tetracyclines, and erythromycin. The life cycles of the filamentous eukaryotic organisms, which produce the natural penicillins, are broadly similar. The cycle begins with the spore, which may lie dormant in the soil for many years; when nutrients and water become available, the spore germinates, thus leading to the formation of mycelium (Figure 5.1). These organisms are said to be "mycelial" in nature, as they colonize soil particles (or agar medium in Petri dishes, if they are in the laboratory) by extending outward in all directions (radial growth) in a fixed branched pattern, often called *vegetative mycelium*. Inevitably, at some point, nutrients or water become in

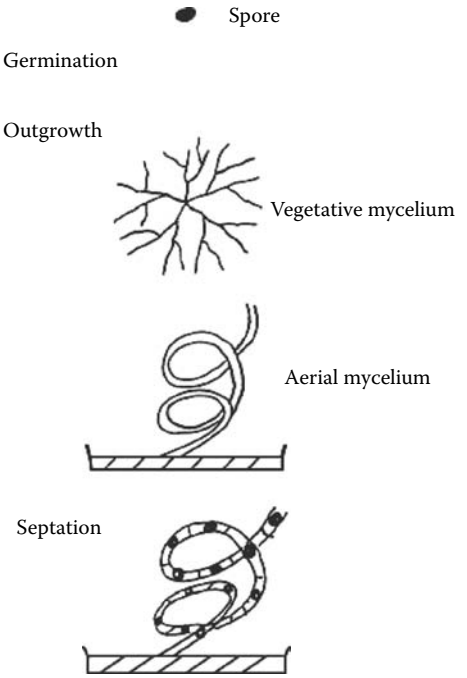

FIGURE 5.1 Diagram of the life cycle of *Streptomyces*.

short supply and it is at this point that they differentiate, ultimately to form spores again. Initially, the differentiation process involves the formation of aerial mycelium in which the biomass no longer extends out radially, but rises up and away from the plane of the radial growth and forms elaborate coiled structures that then septate after a while and the spores are formed again, thus completing the life cycle.

These enzymes digest the vegetative mycelium, in part, and the cellular building blocks that are released are used to construct the aerial mycelium. In this way, part of the vegetative mycelium is "sacrificed" to allow the aerial mycelium to be formed en route to sporulation. This process can be viewed as a survival strategy because, when the spores have formed, the organism's DNA is held in an inert state so that the life cycle can begin again when water and nutrients are plentiful. It has been suggested that the reason that these actinomycetes make antibiotics exactly at the same time as the differentiation step is to sterilize the micro-environment around the vegetative mycelia, so that other microbial predators cannot take advantage of the available nutrients released following mycelial lyses (a view that is not held by all scientists in the field).

5.2.4 Nutrient Limitation and the Onset of Secondary Metabolite Formation

Interestingly, antibiotics are made at the time of differentiation between the stage of vegetative mycelia and the aerial mycelial stage (Figures 5.1 and 5.2). This may seem a paradox, as the signal to undertake this differentiation step is lack of nutrients or water, which in turn begs the question of how a microorganism, starved of nutrients, elaborates such a complex structure as the aerial mycelium on one hand and the triggering of antibiotic production on the other. The answer to this apparent paradox lies in the ability of the organism to coordinate the production and release of extracellular lytic enzymes (proteolytic, lipolytic, and hydrolytic) and the turning on of the differentiation switch.

5.2.4.1 Role of RelA in Initiating Transcription of Antibiotic Synthesis Genes under Nitrogen Limitation

Much attention has recently been focused on the role of RelA, the ribosome associated ppGpp synthetase, in initiating secondary metabolism in actinomycetes under nitrogen limitation, but not phosphate. RelA is apparently central to antibiotic production under conditions of nitrogen limitations in *Streptomyces coelicolor* A3 (Chakraburtty and Bibb 1997; Bentley et al. 2002) and *Streptomyces clavuligerus* (Jin et al. 2004a, 2004b). The question of whether antibiotic production is triggered as a direct consequence of RelA or indirectly as a consequence of slow growth rate through inhibition of rRNA synthesis by ppGpp binding remains to be established (Bibb 2005). Evidence supporting the direct participation of ppGpp in activating the transcription of genes involved in the biosynthesis of

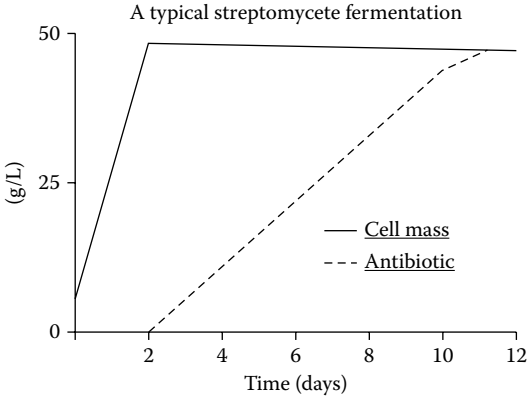

FIGURE 5.2 The time course of a typical *Streptomyces* fermentation for an antibiotic.

secondary metabolites (e.g., *act*II-orf4 genes involved in the biosynthesis of the antibiotic actinorhodin in *S. coelicolor*) has been given (Hesketh et al. 2001). However, the mechanism through which this is achieved has yet to be unraveled (Bibb 2005).

5.2.4.2 Role of Phosphate in Repressing Transcription of Antibiotic Synthesis Genes

Unlike conditions of nitrogen limitation, the signal that triggers the synthesis of secondary metabolism under phosphate limitation is RelA (ppGpp) independent (Chakraburtty and Bibb 1997). Under these conditions (i.e., nitrogen limitation), the polyphosphate reserve is hydrolyzed to inorganic phosphate, which in turn represses biosynthetic enzymes, to satisfy growth requirements. The negative role portrayed for polyphosphate kinase (PPK), the enzyme responsible for the biosynthesis of polyphosphate polymer, was ascertained as loss of enzymic activity and accompanied by increased level of antibiotic formation in *S. lividans* (Chouayekh and Virolle 2002). The following is generally accepted:

Conditions leading to elevated levels of inorganic phosphate lead to repression of enzymes of secondary metabolism and in turn diminish flux to antibiotic formation.
Conditions leading to inorganic phosphate depravation stimulate secondary metabolism and in turn increase flux to antibiotic formation.

However, the question of how elevated levels of inorganic phosphate might interfere with the onset of secondary metabolism and morphological differentiation of actinomycetes awaits further investigations.

5.2.4.3 Role of Quorum Sensing and Extracellular Signals in the Initiation of Secondary Metabolism and Morphological Differentiation in Actinomycetes

It is generally agreed that γ-butyrolactones are produced and, in turn, implicated specifically in the production of secondary metabolites as well as morphological differentiation in several species of *Streptomyces* (Mochizuki et al. 2003), for example the production of streptomycin by *Streptomyces griseus* and the production of tylosin in *S. fradiae*.

In sharp contrast to γ-butyrolactones-binding proteins, which downregulate the transcription of secondary metabolite gene clusters, another molecule, SpbR, has been shown to stimulate the biosynthesis of pristinamycin (Folcher et al. 2001). Deletion of SpbR not only was accompanied by the abolition of antibiotic formation but also severely impaired growth on agar media, thus lending further support to the positive role of SpbR in antibiotic production and the cellular growth and differentiation in actinomycetes (Bibb 2005).

Another factor, PI (2, 3-diamino-2, 3-bis (hydroxymethyl)-1, 4-butanediol), has recently been shown to be able to elicit the biosynthesis of pimaricin in *S. natalensis* (Recio et al. 2004), and its positive role was further substantiated when its addition to P1-defective mutants was accompanied by restoring the organism's ability to produce pimaricin.

5.2.4.4 Positive Activators of Antibiotic Expression

In antibiotic fermentations, temporal expression of antibiotic biosynthesis is regulated tightly as part of the cellular differentiation pathway (Figure 5.2). Production of antibiotics is costly to the cell in terms of carbon and energy. Therefore, it is hardly surprising that tight control of expression has evolved. The genes for antibiotic biosynthesis are invariably clustered together, irrespective of whether the microbe is a prokaryote or eukaryote. In *Streptomyces*, regulation of expression of such gene clusters is controlled by a positive activator—a master gene that, when switched on, makes a protein that targets itself to the various promoters of the gene cluster and switches them on in concert (Figure 5.7).

In this way, the cell ensures that the full complement of enzymes necessary to make the antibiotic is produced at the same time and at the correct levels.

The great majority of antibiotic pathways are regulated in this way. For example, the *tyl*R system that controls tylosin biosynthesis has been characterized (Stratigopoulos et al. 2004) as a newly discovered regulator for actinorhodin biosynthesis in the model organism *S. coelicolor* (Uguru et al. 2005). Sometimes, the expression of the activator gene is integrated tightly with the developmental pathway, such as the *bld*A-dependent regulation of ActIIOrf4 in *S. coelicolor* and *bld*G-dependent regulation of *cca*R in *S. clavuligerus* (Bignell et al. 2005), in which CcaR upregulates the biosynthesis of both cephamycin C and clavulanic acid (Perez-Llarena et al. 1997).

Other factors that may act in a pleiotropic manner (e.g., AfsR of *S. coelicolor*) play a key role in integrating multiple signals that are transduced through phosphorylation cascades (Horinouchi 2003). Another effector is AfsK, which on sensing appropriate signals autophosphorylates itself. Autophosphorylated (activated) AfsK phosphorylates the cytoplasmic AfsR, which, in turn, through its DNA-binding activity, activates the transcription of *dfsS*, the product of which is apparently capable of stimulating the biosynthesis of a number of different antibiotics (Bibb 2005).

5.2.5 Tactical Issues for Strain Improvement Programs

In attempting to harness the vast natural potential of the *Streptomyces* and related actinomycetes for the making of antibiotics on a large scale, the organisms have to be grown in large volumes of liquid cultures. Care has to be taken so that the essential features of the biology of the antibiotic production process are not lost following the transfer (inoculation) of the organism from a solid medium to liquid medium in the fermentor. In a liquid medium, it is very unusual for aerial mycelia to be made, and sporulation is observed even less frequently. Despite this, it is possible to induce the cultures to make an antibiotic in a liquid culture.

The physiology of the fermentation process has to be adapted to suit the biology of the microbe. As one of the triggers for differentiation in the natural ecosystem is deprivation of nutrients, then the same strategy may also be applied to the fermentation process. All antibiotics are composed of carbon atoms and many contain nitrogen atoms. Therefore, it would be a poor tactic to attempt to trigger the onset of antibiotic production by limiting the cells' supply of either of these elements, because after antibiotic production had commenced, the cells would be starved of one of the most important chemical elements needed to biosynthesize the antibiotic structures. Fortunately, very few antibiotics contain phosphorus in their elemental composition, so the cells are most often limited by the supply of phosphate to trigger antibiotic production. If all other nutrients are supplied in sufficient quantities (but not in vast excess), then antibiotic production will continue for many days (often 8–10 days) at a rate that is linear with time (Figure 5.2). Eventually, this rate starts to tail off. It makes economic sense to terminate the fermentation at this point, recover the maximal amount of product in the shortest possible time, and then prepare the vessel for another round of fermentation.

Fermentations for high-value recombinant therapeutic proteins are best undertaken by fed-batch cultures, which maximize the use of the biomass factory and deliver the product in the most concentrated form. However, the duration of the production phase for these high-value fermentations is considerably shorter than for the antibiotic fermentations, typically around 8 hours or less.

In practice, the order in which the experimental strategies for improving strains are used depends on the nature of the desired end product and of the fermentation. In the initial stages of developing an antibiotic-producing strain from a "soil isolate," random mutagenesis of a population of the producer microorganism is undertaken and the progeny of the mutagenic treatment are screened for higher levels of the antibiotic. Subsequently, more directed screens are used to further enhance the titer of the antibiotic.

By contrast, improvement of strains making recombinant therapeutic proteins starts with a very directed strategy and finishes with a more random, empirical approach. This is because, in the initial stages of strain improvement, there is a well-defined template of experimental improvements that can be followed. Subsequently, the performance of the strain can be improved further by the empirical approach.

5.2.6 Strain Improvement: The Random, Empirical Approach

In this approach a population of microorganisms is subjected to a mutagenic treatment (Figure 5.3), typically with the chemical carcinogen nitrosoguanidine (NTG), but other mutagenic agents such as ultraviolet (UV) light or caffeine may be used. The treatment is tailored so that each cell, on average, has a single mutation induced. The mutagenized population is plated on agar, which will support the growth of the normal (wild-type) strain. Some mutations will be very deleterious to the growth of the organism; cells containing these will not grow up to become colonies. The mutant strains (colonies, each of which is derived from a single cell) that show little or no growth impairment are then tested randomly for their ability to overproduce antibiotics. Classically, this was achieved by overlaying the agar plate containing the surviving colonies after mutagenesis with soft agar containing another microorganism that is sensitive to the antibiotic in question. Colonies producing more biologically active antibiotic will be surrounded with a larger clear zone of inhibition of the culture overlay. However, this technique does not take into account the fact that some colonies may be larger (i.e., have a greater diameter) than others. To circumvent this problem, a cylinder of the colony and the agar underneath is cut out (usually with a cork borer) and the "agar plug" placed on a fresh lawn of sensitive bacteria spread on a new agar plate. The cylinders are uniform and contain comparable amounts of cell material. This modification takes account of differences in sizes of different mutagenized colonies. The whole procedure is tedious but has to be undertaken in a painstaking manner. In recent times, the pharmaceutical industry has used robots to perform the tasks required in random screening. There has been a tendency to move away from screening for how much antibiotic is made by colonies on a plate, to liquid media-based cultures that reflect the situation in fermentors more accurately. It is not unusual for a screening robot to evaluate the performance of over a million mutants in a year—such "high-throughput screening" is orders of magnitude more efficient than using people for these tasks, leaving the human input focused on the design and efficiency of the overall screening program.

Most of the progeny will make lower levels (Figure 5.4) of the microbial product, and only a few will have larger titers, often showing 10% (or less) improvement. The reason for this is that most mutations are deleterious to production and only a few mutations will result in slightly elevated levels of production. It is very unusual to isolate mutants that have large (>20%) increases in titer.

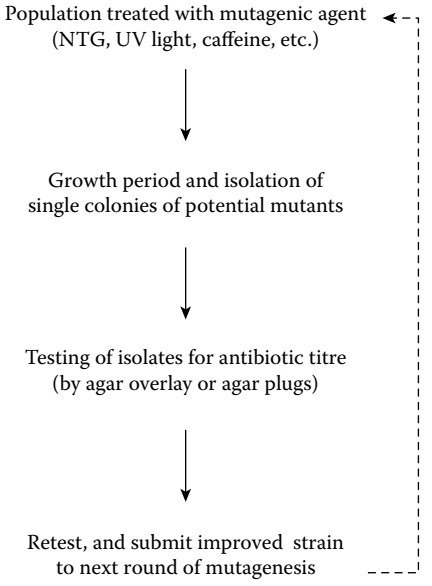

FIGURE 5.3 Random mutagenesis and the empirical approach to strain improvement.

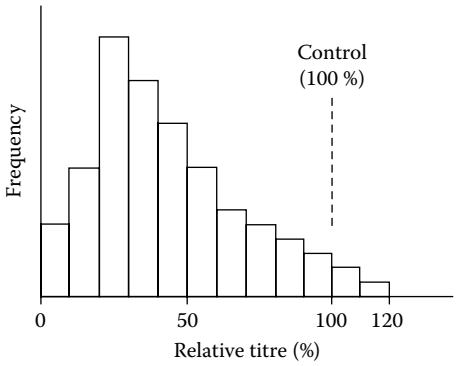

FIGURE 5.4 Antibiotic titers of individual survivors after random mutagenesis. The histogram shows the frequency distribution of titers of survivors after random mutagenesis, for a strain whose lineage has been developed for around 2 years. Notice that only a few isolates perform better than the control (some of this may be due to error in determining the titer) and that most survivors perform much worse than the control, as the mode is about 25%.

These individual isolates are then tested in small-scale fermentations to confirm that they really are improved mutants. Most turn out not to have improved titers and are discarded. Mutants that do show some promise will then be tested intensively at the laboratory and pilot plant levels.

Different companies have different strategies at this stage. Some may carry out extensive laboratory trials at around the 10 L level and scale up the mutants directly to the large production fermentors in one step. Other companies may adopt a more conservative posture and scale up the volume of fermentation in stages. For a process that is undertaken at a production scale of 100,000 L, the stages in scale-up would typically be from 10 to 500 L, then onward to 5,000 L and finally to the large fermentors. The doctrine is that the operation of these large fermentors is expensive—both in the cost of fermentation broth and in lost opportunity, as that large fermentor might otherwise have been used to make another valuable product. The view of those fermentation technologists who scale up in one step is that time is wasted solving problems associated with the intermediate stages and that a production fermentation that is modeled well at the bench scale should, by definition, predicate immediate translation of the new mutant and its process details to the production fermentor hall.

It is often overlooked that the initial improvement in titer, which is achieved with a new mutant at the production scale, can often be improved still further by process optimization through adjustments to the media and fermentation conditions that better suit the physiology of the new mutant. Process optimization invariably makes an equal, if not greater, contribution to overall increase in titer than the stepwise increase in fermentation performance achieved when the new mutant is adopted initially at the production scale.

5.2.7 Strain Improvement: The Power of Recombination in "Strain Construction"

In the early stages of undertaking a random mutagenesis program for a new product (i.e., starting from a new soil isolate that makes a small amount of product), there are likely to be rapid, concurrent advances in the performances of several strains. These strains, separately, will have individual desirable properties. For example, in an antibiotic program, one strain may give a higher titer, while another may use less carbon source to make a level of antibiotic equivalent to that of the parent (and so be more economical). Yet another strain may show no better performance in terms of titer of product or the amount of nutrients consumed to make it, but may carry out the fermentation at a lower viscosity, which will make it easier for the product to be extracted from the fermentation broth and purified. Different "lineages" of the strain are developed very rapidly in these early days in the

desire to improve the fermentation considerably. However, it soon becomes desirable to construct strains with a combination of several of the desirable properties already present in the individual lineages. To achieve this, desirable traits from each lineage must be "recombined" genetically into a single strain that possesses all of the desirable properties, or "traits."

Most microbial species are able to exchange genetic information with other members of their species by recombination. Construction of the genetic maps that appear in many textbooks is based on exploitation of these natural recombination processes. For *E. coli* and other enteric Gram-negative bacteria, protocols to undertake genetic recombination are well documented and depend on plasmid-based mobilization of the bacterial chromosome. However, the producers of many microbial metabolites, including the *Streptomyces*, have a life cycle that involves a sporulation stage. With these species, the most effective method of constructing recombinants that have combinations of several desirable traits is to undertake "spore mating": to mix spores of the parents with the individual traits, germinate them together, allow them to go through an entire life cycle (Figure 5.1), and (from the spores formed at the end of this life cycle) select those that have exchanged some genetic information (i.e., select those that show that they have undertaken some degree of recombination) and then screen them to identify the individuals that have received the desired combination of traits (Figure 5.5).

This screening process is usually conducted empirically, in the same way as screening of strains after random mutagenesis. Unfortunately, a major drawback with this procedure can often arise: as strains with further improved titers are selected and the strain lineage becomes longer, the ability

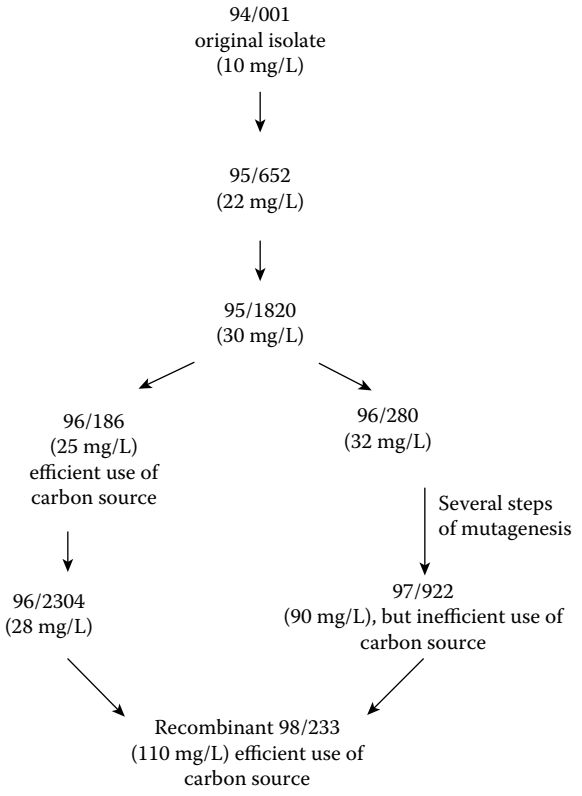

FIGURE 5.5 Strain construction by recombination. In this example, two lineages have been derived from the first soil isolate. One lineage shows a steady improvement in titer with each new strain, but this is accompanied by wasteful utilization of carbon source. The other lineage makes very little antibiotic, but does so in a very efficient way. By genetic recombination of these traits, the attributes of both strands of the culture lineage can be combined together in a single strain.

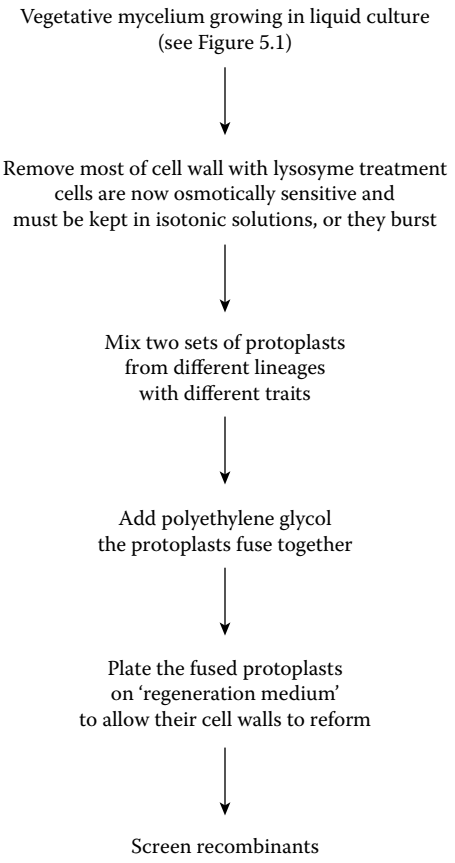

FIGURE 5.6 Schematic diagram of protoplast fusion.

to sporulate is often lost. Although sporulation is associated with the differentiation process, antibiotic production can often become decoupled from sporulation in the advanced high-titer strains. The strains become asporogenous, which makes such a spore-mating strategy impossible. For some strains, the problem can be circumvented by undertaking strain construction by recombination between the vegetative mycelia of different parents. However, not all strains are amenable to this approach. For them, a more involved strategy called *protoplast fusion* (Figure 5.6) has to be enacted. The most common pitfall with protoplast fusion is the time taken to develop the media conditions and culture techniques that allow the protoplasts to regenerate satisfactorily back into fully competent mycelia (see Figure 5.6). Often an extensive series of empirical range-finding experiments has to be undertaken to optimize the conditions for regeneration, and occasionally it proves impossible to develop a protocol for a particular species.

Recently, the power of recombination has been used to great advantage in combination with high-throughput screening in a "genome-shuffling" strategy that leads to a rapid increase in tylosin titer in the industrially relevant *S. fradiae* (Zhang, Perry, et al. 2002). Only two rounds of genome shuffling were needed to achieve results that had previously required at least 20 rounds of classical mutation and screening.

5.2.8 Directed Screening for Mutants with Altered Metabolism

Although the random mutagenesis and recombination approaches are fruitful in acquiring mutants, which give initial improvements in titers, in due course as the level of microbial product produced increases, it becomes more difficult (in parallel) to isolate further improved strains using the

empirical, random approach. For example, in the development of an antibiotic fermentation process, by this time the titer of product will have reached a few grams per liter and considerable background data will have been gathered on the physiology and biochemistry of the fermentation process.

These data can be analyzed to diagnose whether wasteful metabolites are being made during the fermentation process (see Chapters 3, 6, and 7 for further details). For example, many Streptomycete fermentations often consume copious quantities of glucose and excrete pyruvate and α-ketoglutarate, giving low conversion yields of glucose into product. If the overutilization of glucose can be prevented by careful process control (e.g., limiting the supply of glucose), then the economics of the process will improve substantially. However, the same objective can be achieved by generating mutants that will use the glucose less quickly. Such a strategy is amenable to a "directed screening" approach.

In the case of uncontrolled uptake and wasteful metabolism of glucose, it is known that mutants resistant to 6-deoxyglucose (a toxic analog of glucose) have reduced or impaired glucose uptake and subsequent metabolism. In this strategy, a mutagenic treatment is performed on a population of cells or spores, in the same way as described in Figure 5.3. However, instead of plating all of the survivors under nonselective conditions, the survivors are plated directly onto a nutrient agar to which the desired selective pressure can be applied. In this case, the survivors would be plated on media containing 6-deoxyglucose at a level that, under normal conditions, just prevents the growth of the microorganism. The media would also contain a second carbon source (usually glycerol) on which the cultures can normally grow quite vigorously. Out of the millions of survivors of the initial mutagenic treatment, only those which are altered in some aspect of their metabolism of 6-deoxyglucose will survive and grow on such a selective medium. These isolates can then be screened conventionally to identify the individuals among the population that may have the potential in the fermentor to display a reduced level of glucose uptake and consequently a more balanced metabolism of the sugar, which does not involve the wasteful production of pyruvate and the α-oxo-organic acids.

Many survivors that have become resistant to 6-deoxyglucose will have mutated to confer complete exclusion of the toxic analog from the cell, but in addition, they will no longer be able to utilize glucose at all and will have to be discarded. Strains that are totally incapable of glucose utilization are of no use to the fermentation industry, which is substantially based on cheap, glucose-rich carbon sources.

However, the minor class of analog-resistant survivors, which have impaired but still significant glucose uptake, are the sought-after prizes in this "directed screen." The term *directed* is appropriate because the researcher defines the exact conditions under which such mutants should survive—to generate new culture isolates with improved fermentation performance through less wasteful metabolism of glucose.

Directed screening is an extremely important tactic that may be employed to great advantage after the basic details of the fermentation have been worked out and understood. The value of directed screening is the reduction in numbers of mutants to be screened (typically by around 10,000-fold) before an isolate with the desired characteristics is identified. Such a reduction in workload allows time to establish the metabolite production profile of each survivor and to evaluate the data in greater depth. Such is the power of the directed screen that rare spontaneous mutants may be isolated, rather than those generated by mutagenic agents. If 106–108 cells are plated on a single plate containing a toxic analog, a few spontaneous mutants will always be isolated.

In addition to carbon utilization, the flux of nitrogen (fixation and metabolism of ammonia) and phosphorus (phosphate metabolism) can be altered by specific mutations, for which directed screens can be devised to select for potentially improved mutants. Fixation of ammonia takes place via the enzyme glutamine synthetase in virtually all microbes. The flux through this step is often altered in mutants that are resistant to bialaphos, a toxic compound that specifically inhibits glutamine synthetase. Mutants with altered phosphate metabolism may be obtained by directed screening for resistance to toxic analogs, such as arsenite or dimethyl arsenite.

Fluoroacetate is a classic metabolic inhibitor that poisons the tricarboxylic acid (TCA) cycle by being converted to fluorocitrate, a toxic analog of citric acid. Mutants more resistant (or sometimes those more sensitive) to fluoroacetate often have a TCA cycle with altered properties. As the TCA cycle is a fundamental component of cellular aerobic metabolism (conditions under which most fermentations are conducted), then these mutants can have important properties and be fruitful sources of improved strains.

The building blocks for all microbial products, including the antibiotics, are common metabolic precursors used in other biosynthetic processes of the cell. For example, the three components of penicillin are two amino acids, cysteine and valine, together with adipic acid, which is a precursor of lysine. Thus, penicillin can be viewed biosynthetically as a simple but modified tripeptide (Figure 5.8) of three common amino acids. During microbial growth, cellular metabolism is painstakingly controlled to ensure that supplies of all 20 amino acids needed for growth are available in a balanced fashion.

In a batch-fed culture, such as an antibiotic fermentation, tightly regulated metabolism during the growth phase is followed by the production phase (Figure 5.2), during which the commercial aim is to produce a single product quickly and at high levels—to the exclusion of others. As this microbial product will probably be made from a few key metabolic intermediates (e.g., during production of penicillin, only a supply of the three amino acids will be in high demand), then metabolism must be altered to satisfy this increased demand while minimizing the side reactions of wasteful metabolism. Directed screens can be devised that decouple the usual control strategies of the biosynthetic pathways (such as feedback inhibition and cross-pathway regulation), which normally keep the supply of all precursors just balanced to the needs of the growing cell.

By way of example, consider the supply of adipic acid (part of the lysine pathway) for the biosynthesis of penicillin (Figure 5.8). Normally, the lysine pathway is subject to end-product feedback inhibition. The toxic analog of lysine, δ-(2-amino-ethyl)-l-cysteine, also inhibits the first step of lysine biosynthesis. Mutants resistant to this toxic analog are no longer subject to end-product

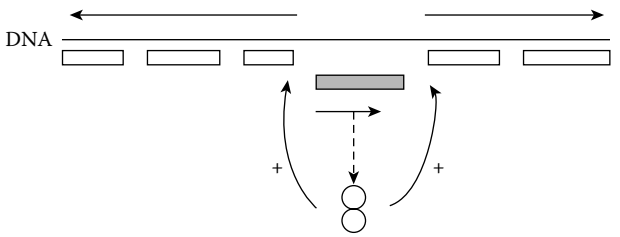

FIGURE 5.7 Schematic diagram to illustrate how antibiotic gene clusters are controlled. The DNA encodes a number of genes clustered together on the chromosome. The genes (rectangles) are usually transcribed as polycistronic mRNAs (shown by the unbroken straight arrows). Transcription of the production genes (unshaded rectangles) must be dependent on transcription of the positive activator (the master gene, shown by the shaded rectangle and the protein by the two circles) that migrates and binds to the DNA (curved arrows) to allow transcription of the production genes to take place. Without the activator protein, there is no expression of production genes.

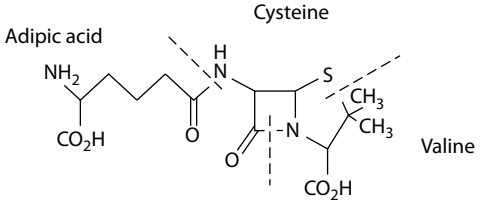

FIGURE 5.8 Diagram of the biosynthetic origin of isopenicillin N. This has three component amino acids, condensed together with peptide bonds. The origins of the amino acids are shown between the dotted lines.

feedback inhibition of the early part of the biosynthetic pathway. They have an enhanced flux of precursor supply to adipic acid and often produce higher titers of penicillin.

Almost every metabolic pathway that supplies the precursors of microbial products is amenable to this type of directed screening strategy. Thus, the rate of "fuel supply" for biosynthesis of microbial products can be enhanced.

The last example of directed screening relates to the selection of mutants that produce elevated levels of the enzymes responsible for catalysis of the precursor building blocks for the biosynthesis of the backbone structures of antibiotics, such as the tetracyclines and erythromycin. They are polymers of acetyl-CoA and methylmalonyl-CoA, respectively, and both are made by a process that is essentially the same as that for fatty acid biosynthesis. The antibiotic cerulenin targets the enzyme complexes responsible for fatty acid biosynthesis and acts to starve the growing cell of the fatty acids necessary for insertion into the membrane. Mutants resistant to toxic levels of cerulenin have circumvented this problem by making elevated levels of the fatty acid biosynthetic enzymes to "titrate out" the effect of the antibiotic. The close similarity between the enzymes of fatty acid biosynthesis and those that make the backbones of erythromycin and tetracycline allows cerulenin to inhibit the biosynthesis of these antibiotics. Mutants that can still make the antibiotic in the presence of cerulenin have elevated levels of the biosynthetic enzyme complexes. When cerulenin is removed, they retain the high level of biosynthetic capability, which, if supplied with enough of the metabolic precursor "fuel," results in higher titers of the antibiotic. The utility of the directed screening approach is that the survivors of the mutagenic treatment are invariably altered in some aspect of fatty acid or antibiotic biosynthesis.

Individual mutants made by directed screening approaches can be recombined together using genetic recombination, spore mating, or protoplast fusion to combine several desired traits.

5.2.9 Recombinant DNA Approaches to Strain Improvement for Low- and Medium-Value Products

The advent of recombinant DNA techniques, first devised for *E. coli* in the 1970s, has meant that new strategies can be applied to strain improvement for low- and medium-value microbial products. It has taken some time for recombinant techniques to be developed and applied to the commercial strains, such as the filamentous bacteria and filamentous fungi, which are the mainstay of this sector of the fermentation industry.

In addition, regulatory hurdles have to be crossed to gain approval to undertake fermentations at the production scale with these "genetically engineered microorganisms." Gaining such approval is time-consuming and costly. Thus, there have to be good long-term economic reasons for adopting a recombinant DNA strategy for strain improvement.

By cloning this master gene regulator (see Section 5.4.4) and then expressing it at unnaturally high levels, the cellular complement of the entire biosynthetic machinery for production of an antibiotic may be enhanced. Of course, there has to be sufficient fuel (metabolic precursors and energy) to realize the full potential available from this boosted level of biosynthetic machinery. The roles of metabolic flux analysis and process optimization (see Chapters 6 and 7 for more details) in assuring this advantage are very important.

It is also possible to force expression of the master gene during the growth phase and so to produce antibiotics during growth. In some instances, this may be to the advantage of the overall process, but often it is better to mimic the situation in nature: first to focus the design of the process on maximizing the acquisition of biomass, and then to turn that biomass to best advantage by using the cells as a factory (with the maximal level of installed biosynthetic capability) to make the product at a fast rate and to achieve a high titer. Therefore, controlled expression of the master gene so that it is switched on decisively at the end of growth is often preferred.

Molecular genetic analysis has also shown that some of the strains from improvement programs, isolated over the years by random mutagenesis and selection, have increased dosages of the

biosynthetic genes. Thus, some of the best strains for penicillin production have multiple copies of the critical part of the biosynthetic gene cluster arranged in tandem arrays. This effect can also be achieved by gene-cloning strategies.

The biochemical pathways for antibiotic biosynthesis are long linear series of enzyme reactions. The flux through the entire pathway is governed by the pace of the slowest catalytic step. If the flow of metabolic intermediates through that step can be improved, then there is a good chance that the productivity of the overall process will be improved. Thus, for the antibiotic tylosin, produced by *Streptomyces fradiae*, it was established that the rate of the last step in the pathway, conversion of macrocin to tylosin by macrocin-*O*-methyltransferase (encoded by the gene *tyl*F), limited the overall productivity. As the strain improvement program had developed with time and the production strain lineage was reviewed, it was apparent that mutants with higher titers of tylosin also displayed extremely high levels of macrocin, which was excreted as a shunt metabolite (Figure 5.9) because conversion of macrocin was limiting. Strains that had the methyltransferase gene cloned and expressed at high levels showed improved titers of tylosin.

Often, process analysis shows that some metabolites on the main biosynthetic pathway are being diverted to other shunt products (Figure 5.10). This not only represents a waste of valuable carbon source, but also presents a problem for the ultimate purification of the desired product, as the second metabolite has to be purified away. Genetic manipulation can be used to specifically inactivate the gene for the enzyme that diverts the metabolite to the shunt metabolite. This precise "genetic surgery" enhances the flow through the pathway to the desired product.

One last important contribution that genetic manipulation makes is in providing flexibility of utilization of a carbon source. If, for example, there is a plentiful supply of cheap lactose available (from the milk whey industry) but the strain does not use lactose naturally, then lactose utilization genes can be cloned from another species and introduced into it.

At times, the world marketplace has a glut of hydrolyzed sucrose. This cheap carbon source is problematic for fermentation because one of the hydrolysis products (glucose) is capable of inhibiting the utilization of the other (fructose). It is possible to overcome this problem by the cloning of the fructose utilization genes, which, in turn, ensures that the two monomeric carbon sources are

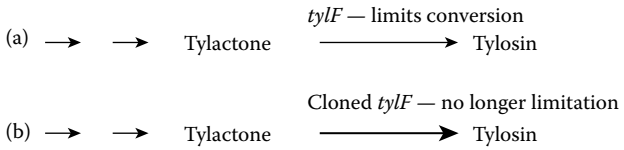

FIGURE 5.9 Schematic diagram highlighting (a) the limitation of tylosin biosynthesis by *Streptomyces fradiae* and (b) the elevation of such limitation by the use of a recombinant strain.

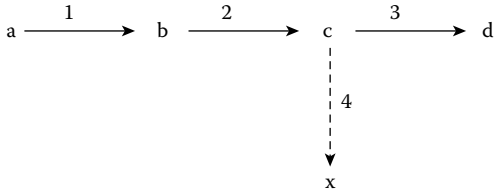

FIGURE 5.10 Schematic diagram highlighting the problem of shunt products and how this can be prevented. The metabolic pathway (from substrate a to product d) is composed of three enzymes (1, 2, 3) with intermediates b and c. Because the carbon flow through steps 1 and 2 is greater than through step 3 (shown by the width of the arrows), the shunt metabolite, X, is formed through the action of enzyme 4. The presence of shunt metabolite, X, may complicate the recovery and purification of the desired product, d. By making a mutant devoid of enzyme 4, this is prevented.

used concurrently. The overall economics of such a process benefits from being able to use a cheap and plentiful carbon source in an efficient manner, without excess fructose carbon being left in the broth at the end of the fermentation.

5.2.10 Strain Improvement for High-Value Recombinant Products

Strain improvement programs for products derived from cloned genes follow a completely different strategy from those undertaken for their lower value counterparts. The techniques used to clone a gene (or cDNA) usually place it precisely in a vector (most often, a plasmid) in a context that allows continuous high-level expression, or, more advisedly, expression of the gene is controlled and induced at a high level only after growth has ceased—in the same way as antibiotic fermentations are performed (Figure 5.2). A countless number of possibilities arise to tailor the gene within the vector, but this aspect involves only molecular biology and falls outside the remit of this chapter. The biology of the host strain is an equally critical factor in the overall performance of a fermentation process for a recombinant product, and strain improvement programs can have a significant impact on the economics of such a process.

In the early days of the "new biotechnology" industry, considerable difficulty was experienced in "scaling up" recombinant processes from the laboratory to the pilot plant (i.e., from a scale of around 100 ml to 400 L). This was because, at the larger volume, a greater proportion of cells had lost the recombinant plasmid from the cells. Plasmid-deficient cells do not make the recombinant protein, and this reduces the overall productivity. The root cause of the problem is the number of cell generations needed to attain significant growth of the culture at the larger volume, coupled to the inherent instability of engineered plasmids in cells. The growth rate of a cell carrying a plasmid is invariably slower than its counterpart that has shed its plasmid load. Therefore, plasmid-deficient cells will outgrow the plasmid-containing cells in a population, a phenomenon that becomes more significant as the number of generations in a culture increases: the larger the volume of the fully grown culture, the greater the proportion of plasmid-deficient cells in its population.

Resistance to an antibiotic, encoded by a plasmid-borne gene, is the usual selection strategy for the presence of a plasmid in a recombinant culture. The most commonly used selection is resistance to ampicillin, encoded by β-lactamase. Ampicillin-resistant cells survive because they are protected by β-lactamase, which breaks down the chemical backbone of the antibiotic. Eventually, all of the ampicillin in the fermentation broth is broken down and the selective pressure is lost—the longer the fermentation (i.e., the more generations that take place), the more likely it will be that the antibiotic will become inactivated and that plasmid-deficient cells will form.

The frequency at which plasmid-deficient cells are formed, in the absence of an antibiotic, is biased because of their natural tendency to form oligomers within the cell. Consider a theoretical situation in which a cell has a plasmid copy number of four. This may be conceptualized as four separate plasmids, two of which segregate into each daughter cell at division (Figure 5.11a). However, because of oligomerization, an equally common situation is that there will be a single tetramer of plasmids within the parent cell (i.e., the copy number will still be four); when the daughter cells are formed, one will receive the plasmid, which consists of four monomers, and the other will not (Figure 5.11b). In the absence of selective pressure (i.e., after all of the antibiotic has been exhausted), both will survive, and the plasmid-deficient daughter will outgrow its plasmid-containing sibling because of the advantage in growth rate.

Engineered plasmids undergo such oligomerization events at alarming rates. However, natural plasmids do not undergo such "segregational instability," because they have a natural tendency to break back down from oligomers to monomers again (Balding et al. 2006). This ability has been lost during the process of conversion of natural plasmids into genetically engineered vectors. It was discovered that a small piece of DNA, called *cer*, was the missing factor in the engineered vectors. When cer was reintroduced into vectors from the natural plasmids, the segregational stability of the plasmid construct containing the cloned gene to be expressed was improved. However, operation of

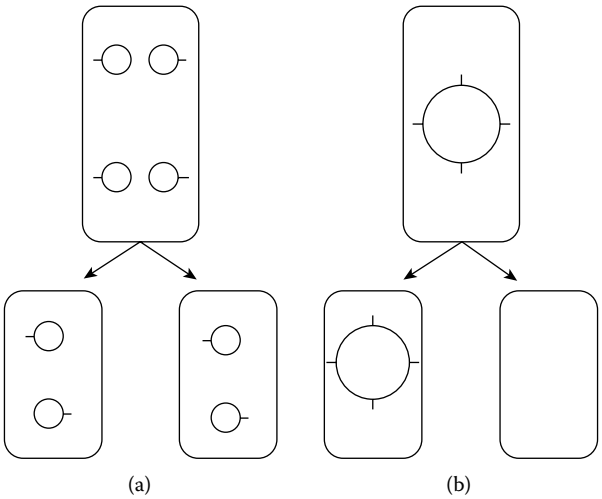

FIGURE 5.11 Plasmid segregation—the complication of plasmid oligomers. In case (a), the plasmids are present as four monomers, and two segregate (on average) into each of the daughter cells. By contrast, in case (b), the plasmids are present as a tetramer. During growth, one daughter cell receives the tetramer, whereas the other does not and, in turn, becomes plasmid deficient.

cer is dependent on the strain; this aspect of the biology of plasmid instability can be addressed by strain improvement programs. The cellular machinery that allows cer to operate is rather complex and involves at least three different genetic loci. If any of the three is defective or missing, the result is that plasmids (even those containing a fully competent *cer*) are unstable. Strain improvement of such cell lineages is best achieved using a targeted genetic approach, in other words, to use the power of genetic recombination to introduce the relevant machinery back into the chromosome of the strain, an extremely focused and targeted task.

Recombinant cultures are very prone to infection with bacterial viruses called *bacteriophages*. At a scale of fermentation above a liter, in a production environment, the recombinant cultures are at risk. There are two strain improvement strategies that can be brought into play. First, it is possible to mutate the strain to become resistant to viral infection. This approach works for known viruses, but there is always the risk that infection from a new source will take place. A second, more secure strategy is to introduce a restriction and modification system into the cell line. The modification enzyme will alter the host's DNA so that it is no longer a target for the resident restriction system. However, viral DNA that enters the cell will be recognized by the restriction system and degraded, thus preventing the infection. The strategy can be enhanced further by the introduction of a second restriction and modification system as a "backup," should some of the viral DNA escape restriction by the first enzyme system. Again, this is a much targeted approach to strain improvement.

Hosts for foreign gene expression often recognize the foreign protein as "not natural" and selectively degrade it, thus reducing the overall productivity. The enzyme system that undertakes this function, the lon protease, works in a similar way in ordinary cells, selectively degrading ordinary cellular proteins that have been made defectively with altered amino acids. By knocking out the *lon* protease gene, degradation of the foreign protein is prevented, albeit to the detriment of the host cell, which now has a slight growth rate disadvantage. Methods that generate *lon*-deficient cell lines are well established and extremely targeted.

In each of the examples in this section, there has been no need to use random mutagenesis and screening, as the blueprint to derive the improved strain is direct and straightforward. Subsequent to this phase, strain improvement programs use the random approach to fine-tune the genetic content

of the production recombinant strain to gain further advantages in productivity. Thus, the order of events is the reverse of that for the lower value counterparts.

5.3 PLANT CELL SYNTHESIS OF SECONDARY METABOLITES AND CELL LINE IMPROVEMENT

The plant kingdom is probably the best source of valuable secondary metabolites that are medicinally, agronomically, and commercially important. It is estimated that the total number of plant secondary metabolites exceeds 500,000, with less than a quarter discovered thus far (Verpoorte et al. 1999). While in many cases the desired products can be extracted from whole field-grown plant parts, there is a historical and increasing interest in the use of plant cell and tissue culture to overcome limitations encountered in traditional field production (Dornenburg and Knorr 1996; Verpoorte et al. 1999; Yeoman and Yeoman 1996). These limitations include low yield, insufficient supply of rare and endangered species, long growth cycles, supply and quality variations due to geographical, and seasonal and environmental factors (Rao and Ravishankar 2002). On the other hand, plant cell and tissue culture that uses the biosynthetic pathways of plant cells and tissues can produce valuable metabolites at high yield on demand under defined factory conditions. Despite these significant advantages and worldwide effort over 50 years, very few plant metabolites are currently commercially produced by plant cell and tissue cultures. The lack of commercial impact of this technology has been attributed to low yield, low productivity, production instability, and difficulties with scale-up (Endress 1994; Zhang and Furusaki 1999).

In the second part of this chapter, important strategies including cell line selection and screening, process integration and intensification, and metabolic engineering of both biosynthetic and postbiosynthetic pathways, will be discussed. The goal is to establish the technical framework for rational molecular plant cell bioprocessing to translate the "potential" of plant cell culture into "commercial success."

5.3.1 Economics and Scale of Plant Cell and Tissue Cultures

The technical feasibility of large-scale plant cell culture has long been demonstrated as an alternative production technology of valuable plant secondary metabolites. Despite many advances in plant cell culture technology, successful commercial applications of plant cell cultures are scarce, due to the lack of economic viability, stemming from technical difficulties with culture systems. Examples of commercially produced plant secondary metabolites include shikonin (*Lithospermum erythrorhizon*), ginsenoside (*Panax ginseng*), berberine (*Coptis japonica*), rosmarinic acid (*Coleus blumei*), and, more recently, paclitaxel (*Taxus spp.*) (Tabata 2004). The scales of production systems reported start from a few hundred liters up to 75,000 L, with examples shown in Table 5.1. Large-scale plant cell culture systems have generally been impeded by low product yield, low and variable productivity during long-term culture, and challenges in bioprocess scale-up (Choi et al. 2001).

The most widely accepted criteria for large-scale commercial plant cell culture have been based on the high-value and low-volume product, with high and stable yield, high productivity, and a strong market demand, as the production cost has been estimated at US$1,500/kg (Verpoorte et al. 1998). This cost analysis was based on a facility designed for the production of 3,000 kg ajmalicine (an antihypertensive drug used in therapy of high blood pressure) at a yield of 0.3 g/L per 2 weeks by *Catharanthus roseus* cell suspension culture. This yield was achieved in a two-stage process consisting of a biomass growth stage of one week in a growth-promoting medium achieving a high cell density of 40 g-dry weight/L, and an ajmalicine production stage of one week in a production medium. This production would require six huge bioreactors of 145 m^3. For such huge bioreactors, the depreciation cost is very high at about 65%, with significant operational costs such as media and energy. However the production unit cost can be significantly reduced to US$430/kg if the yield could be increased 10-fold to 3 g/L. With a market value of US$37,000/

TABLE 5.1
Selected Large-Scale Plant Cell Cultures from 100 L to 75,000 L

Product	Bioreactor Volume	Plant Species
Sepentine	100 L airlift	*C. roseus*
Rosmarinic acid	300 L airlift	*C. blumei*
Shikonin	750 L agitated	*L. erythrorhizon*
Biomass	1,500 L bubble column	*N. tabacum*
Biomass	20,000 L agitated	*N. tabacum*
Saponins	20,000 L agitated	*P. ginseng*
Biomass	750–75,000 L agitated	*P. ginseng*
Biomass	750–75,000 L agitated	*E. purpurea*
Biomass	750–75,000 L agitated	*R. serpentina*

kg, the production of ajmalicine by plant cell culture seems commercially viable. In another study, a preliminary economic evaluation of anthocyanin production by *Vitis vinifera* cell suspension culture is based on technical data from cultures performed in shake flasks and a 17 L bioreactor (Cormier et al. 1996). The authors assume that an optimized two-stage process could yield a biomass concentration of 300 g-fresh cell weight/L after 12 days of culture under cell proliferation conditions; and an anthocyanin concentration of 5 mg/g-fresh cell weight after 12 days of culture under anthocyanin-promoting conditions would be achieved. At a production scale of 5,800 kg/year of 100% purity anthocyanins, it was estimated that the cost for the production was approximately US$931/kg, with an estimated error of 30% based on the value of U.S. dollars in 1993. This cost estimation falls well in the range of the first study. Based on this criterion, a selected group of highly valued plant secondary metabolites could potentially be produced on a commercial scale, including paclitaxel (US$200,000/kg) and vincristine (US$2,000,000/kg), as shown in Table 5.2 (Rao and Ravishankar 2002). However, most of these expensive products are still produced at a very low yield (<0.01%), therefore the production cost would be much higher and further scale-up would be impractical.

5.3.2 General Strategies to Improve Plant Cell Synthesis of Secondary Metabolites

To improve the yield and productivity of plant-derived secondary metabolites, there are many strategies developed for plant cell culture, as shown in Table 5.3. These strategies can be generally grouped into five categories:

1. Strain improvement
2. Medium optimization
3. Culture environment optimization
4. Process optimization
5. Metabolic engineering

Typically, any improvement program starts with the selection and screening of high-growth and high-yield cell lines first in callus culture and then in suspension cell culture. Once the suspension cell culture is established, medium optimization is routinely applied to improve the production of every product, as the medium components can have significant impact on cell growth and synthesis of secondary metabolites. The effects of medium components cannot be generalized, and are very often product specific, especially in the case of the addition of precursors and antimetabolites.

TABLE 5.2
Selected Plant Secondary Metabolites with a Market Value Higher Enough for Commercial Production by Large-Scale Plant Cell Culture (based on a production cost at US$1,500/kg)

Product	Application	Plant Species	Cost (US$/Kg)
Ajmalicine	Antihypertensive	*Catharanthus roseus*	37,000
Anthocyanin	Food colorant	*Vitis* sp./*Daucus carota*	2,083
Berberine	Intestinal ailment	*Coptis Japonica*	3,250
Camptothecin	Antitumor	*Camptotheca acuminata*	432,000
Codeine	Sedative	*Papaver somniferum*	17,000
Colchicine	Antitumor	*Colchium autumnale*	35,000
Digoxin	Heart stimulant	*Digitalis lanata*	3,000
Ellipticine	Antitumor	*Orchrosia elliptica*	240,000
Morphine	Sedative	*Papaver somniferum*	340,000
Sanguinarine	Antiplaque	*Sanguinaria Canadensis P somniferum*	4,800
Shikonin	Antibacterial	*Lithospermum erythrorhizon*	4,500
Taxol	Anticancer	*Taxus brevifolia*	600,000
Vincristine	Antileukemic	*Catharanthus roseus*	2,000,000
Vinblastine	Antileukemic	*Catharanthus roseus*	1,000,000

TABLE 5.3
Strategies to Improve the Yield and Productivity of Plant Secondary Metabolites Produced by Plant Cell Culture

Strain Improvement	Medium Optimization	Culture Environments Optimization	Process Optimization	Metabolic Engineering
	Nutrients (e.g., sugar, nitrogen, and phosphate)	Inoculum size	Nutrient feeding	Metabolic manipulation of biosynthetic pathways
Screening	Phytohormones	pH	Elicitation	Metabolic manipulation of post-biosynthetic pathways
Differentiated cells	Precursors	Temperature	Immobilization	
Mutation	Antimetabolites	Light	Permeabilization	
Genetic engineering		Agitation	Two-phase systems	
		Aeration	Two-stage systems	
		Gas composition	*In situ* product removal (extraction and adsorption)	
			Cyclodextrin complexation	

Therefore, it is necessary to carry out an optimization of media for any new cell line established to improve the biosynthesis of target products. Following medium optimization, the culture environments, including inoculum size, pH, temperature, light, agitation, aeration, and gas composition in the media, will also have to be optimized for further improvement of product yield. These environmental factors have long been demonstrated to have significant influences on cell growth and metabolite synthesis. Of particular interest are agitation and aeration as they are not only important for improving product yield but also crucial for the viability of process scale-up. The fact that plant

cells are very sensitive to shear stress poses a dilemma between oxygen supply and shear stress. Sufficient oxygen supply to satisfy cell growth and product synthesis would require high agitation and aeration; however, this generates high shear stress and may lead to loss in cell viability and even cell death. The management of this dilemma has been regarded as a very challenging task in many studies concerning bioreactor design. With regard to gas composition, it is important to note that several gases such as ethylene and carbon dioxide are critical for plant cell physiology, and for primary and secondary metabolism. For examples, it has been reported that increasing carbon dioxide in the gas phase stimulated the synthesis of monoterpenes by muscat grape cell culture, and induced linalool synthesis (Ambid and Fallot 1981). Similarly, the use of 2% carbon dioxide can prevent cell browning and sustain berberine production in suspension cultures of *Thalictrum minus* in bubble column bioreactors (Kobayashi et al. 1991).

Following culture environment optimization, many process strategies can be developed to improve secondary metabolite production, and overcome different process limitations. Nutrient feeding is applied when one or more of the nutrient components become limited for growth and/or secondary metabolism. Feeding these limited nutrients as required will improve cell viability, cell growth, and substrates that are essential for the sustained high production of secondary products of interest. Elicitation is an efficient strategy as elicitors are signals triggering the formation of secondary metabolites by activating many enzymes of metabolic pathways that are otherwise not expressed or are expressed at very low levels. Immobilization aims to increase the cell density and reuse of the cell biomass for improved biosynthesis of secondary metabolites. However this strategy can only be applied for products secreted into media. When the products are stored in cell vacuoles and not secreted into the medium, permeabilization can be applied to penetrate two membrane barriers—the plasma membrane and the tonoplast of plant cells—enabling the release of these products out of the cells, and the uptake of essential substrates into the cells. The permeabilizing methods include chemical agents such as organic solvents and polysaccharides, and physical methods such as ultrasonication, electroporation, ionophoretic release (Brodelius 1988), high electric field pulses, and ultrahigh pressure (Dornenburg and Knorr 1993). Two-phase systems (i.e., extraction) and *in situ* product removal (i.e., adsorption) are very efficient process strategies when the products are toxic or inhibitive to cell metabolism or subject to degradation in the medium. The introduction of a second liquid and solid phase into the aqueous medium can improve productivity by removal and transfer of the products into the second phase. In a similar concept, cyclodextrin is introduced as a complexation agent to form inclusion complexes with target products when higher water solubility and a less toxic second phase rather than organic phases are required. While a two-phase system creates a spatial compartment for the products, the two-stage system is different in that the cultures grow in two temporally different stages: one Is cell growth, and the other is product biosynthesis. As the biosynthesis of many secondary metabolites is not growth associated or negatively associated, this strategy is efficient to improve yield and productivity by maximizing cell growth and product biosynthesis through their respective optimal conditions.

Metabolic engineering of biosynthetic pathways leading to desired products promises to create exciting opportunities for the improvement of the production of plant secondary metabolites in plant cell cultures. While there have been successes in determining the rate-limiting steps and in engineering these critical genes in the biosynthetic pathway of many important plant secondary metabolites, the improvements in yield and productivity required for commercially viable production have not been forthcoming.

If one considers the cell as a factory, postbiosynthetic steps such as transport, storage, catabolism and degradation, and secretion can also be rate-limiting steps that are not often considered in metabolic pathway engineering. Recent proposals of postbiosynthetic pathway engineering and integrated manipulation of both biosynthetic and postbiosynthetic pathways have opened new avenues to significantly improve the commercial viability of many plant cell culture-derived products, with some examples discussed later in this chapter.

5.3.3 Plant Cell Line Improvement: Selection and Screening

The objective of a plant cell line improvement program is to establish cell lines that have high growth rate, high product yield, high biosynthetic stability, and dark-producing capacity adapting to various cultivation scales (Zhang and Furusaki 1999). There are several strategies that have been applied in developing improved producing cell lines, as described in Table 5.4.

The most common strategy is to establish high-producing cell lines from high-producing parental plants or explants. Although this strategy has been proven to be successful in some cases, it is not based on a scientific principle but rather a statistical assumption (Deus and Zenk 1982). In Vitis sp., the source plant has a high anthocyanin yield of ca. 10% dry weight, which generates a cell line with an anthocyanin yield of 16% dry weight (Do and Cormier 1991), whereas a cell line of *Euphorbia millii* with lower anthocyanin yield (4% dry weight) was induced from a lower yield plant (0.3% dry weight) (Yamamoto et al. 1982). Selection of appropriate tissue for explants is also important, as shown by Mori et al. (1993), where calli originating from the petiole of strawberry produced lower anthocyanin levels than calli from the apical meristem or leaf. In contrast, the source plant of *Perilla frutescens* has a very low anthocyanin yield of 1.5% dry weight, but the cell line has a very high yield of 24% dry weight (Zhong 1992).

The second strategy is to select high-producing clones based on somaclonal variation. Examples of techniques include small aggregate selection (Krisa et al. 1999) and the generation of cell lines from individual protoplasts (Zubko et al. 1993). The process of establishing plant cell suspension culture via *in vitro* callus induction from explants always produces a heterogeneous cell population of different clones with a vastly variable level of target metabolites. The clonal selection is a progressive process of selecting improved cell lines during the course of repeated subculture cycles. The selection can be further enhanced by screening visible markers such as pigmented products, autofluorescent products, and products able to be stained by fluorescents. Up to a 20-fold increase in shikonin production has been achieved by repeated clonal selection and screening of *L. erythrorhizon* cell cultures (Fujita et al. 1984). During a course of 32 growth cycles of clonal selection, a suspension culture of *V. vinifera* improved anthocyanin content from 0.26 mg/g fresh weight to 1.02 ± 0.31 mg/g fresh weight (Cormier et al. 1994). Cell staining with fluorescein isothiocyanate (FITC) has been successfully used for the selection of a high anthocyanin-producing cell line of *Aralia cordata* (Sakamoto et al. 1994). The green fluorescence of FITC from the nonproducing cells was clearly observed by the naked eye. On the other hand, the fluorescence of the anthocyanin-producing cells was completely missing, as a result from compensation of the green fluorescence ($\lambda max = 525$ nm) of FITC and the green light absorption ($\lambda max = 530$ nm) of anthocyanin. Using this technique, a highly productive cell line of 7.7 ± 0.6 anthocyanin %/g dry weight was selected, which is comparable to that (7.3 ± 0.5 anthocyanin %/g dry weight) of the high anthocyanin-producing cell line selected by small-cell aggregate selection in the dark. However,

TABLE 5.4
Strategies for Plant Cell Line Improvement

Strain Improvement Strategies
Selection of high-producing parent plants or explants for callus induction
Clonal selection based on "somaclonal variation": small aggregate selection and generation of cell lines from Individual protoplasts
Visible marker screening by fluorescence stain, autofluorescence, and pigments
Repeated selection of stable-producing cell lines
Selection of dark-producing cell lines
Mutation by selective agents and environmental stress
Genetic manipulation

selection of *Aralia cordata* cell lines sorted by this method shortened the timeframe required to generate a cell line with enhanced anthocyanin levels.

A problem regularly encountered with plant cell culture is the variability over repeated batch culture in terms of secondary metabolite production (Hirasuna et al. 1991; Ketchum et al. 1999). Repeated or continual selection of the desired phenotype is typically required in order to maintain adequate productivity. The importance of this process is clearly illustrated by the example in Figure 5.12, where alkaloid biosynthesis in *Catharanthus roseus* was significantly enhanced immediately following periods of clonal selection (Deus-Neumann and Zenk 1984). Clearly, large variations in productivity such as this example are not amenable to commercial production.

Repeated selection of a stable producing cell line is therefore an essential strategy for the successful industrial application of a plant cell-based bioprocess. The biosynthetic instability of secondary metabolites is widely reported in plant cell cultures, namely, the instability in both yield and composition of metabolites of interest. The yield instability has been well addressed (Hirasuna et al. 1991; Ketchum et al. 1999), where subculture over long periods of time leads to a gradual repression of metabolic output, but little attention has been paid to the compositional stability. Consistent metabolic profiles are crucial for the design and development of downstream purification processes as complex metabolites are produced in addition to the metabolite of interest. Repeated phases of clonal selection were necessary to arrest a gradual loss of alkaloid production capacity in cultures of *Catharanthus roseus* (Deus-Neumann and Zenk 1984). Despite the importance of cell-line stability in bioprocess optimization, there have been few detailed studies examining metabolic instability or variability. There is a need to address this knowledge gap as metabolic instability influences and undermines yield and compositional stability, thus the ability to control metabolic stability can prove to be a cornerstone of commercial biosynthesis through plant cell culture.

In investigating what contributes to stability, it is recognized that the biosynthesis instability in plant cells is caused by their inherent genetic and epigenetic variability (Dornenburg and Knorr 1995). This variability that has been the theoretical basis for strain improvement, however, could be a problem for commercialization. Variability induces instability of biosynthesis that often leads to reduction in productivity and change in chemical composition in high-producing cell lines during

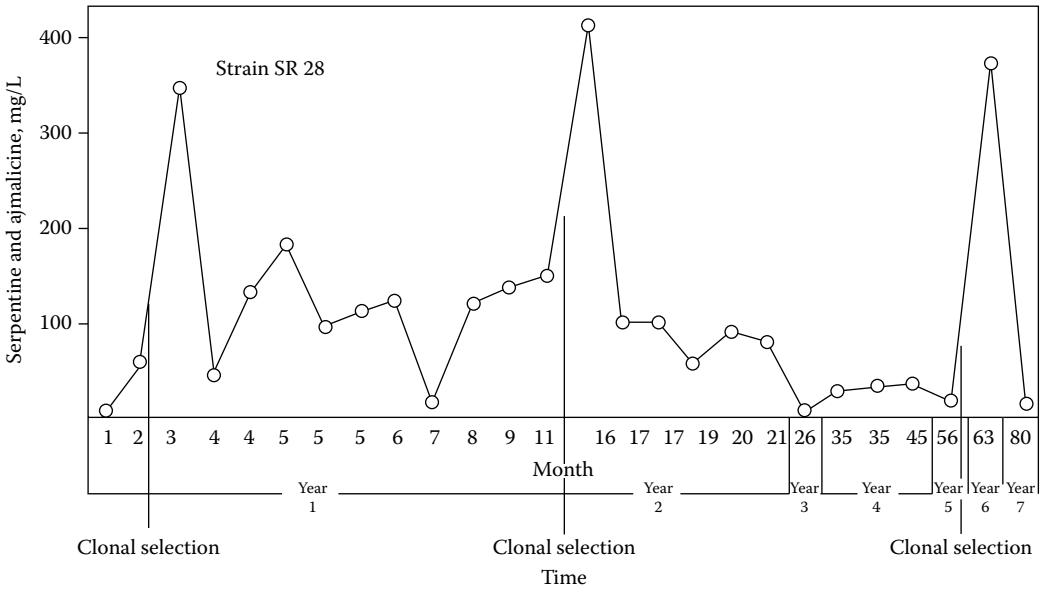

FIGURE 5.12 Impact of clonal selection on yields of the alkaloids serpentine and ajmalicine in suspension cultures of *Catharanthus roseus.* (Deus-Neumann, B. and Zenk, M. H., *Plant Med,* 50, 427–431, 1984. With permission.)

extended cultures. The reduction in productivity can be reversed by changes in the culture environment as well as by screening for a desired cell population from heterogeneous population typically present in plant cell cultures (Doodeman et al. 1985) In some cases, this problem may also be resolved by repetitive selection until stable productivity was reached (Yamamoto et al. 1982); however, this is a time-consuming and laborious process not amenable to commercialization.

Light is important for photosynthesis and many metabolic processes of plants; however, it could be very costly on an industrial scale. A critical characteristic for any plant cell line aimed at commercial production is the capability to produce products in the dark, due to the substantial ongoing costs involved with running photobioreactors and difficulties with the scale-up of such systems. Spontaneous mutation of light-grown *Fragaria ananassa* cells enabled the isolation of a cell line that produced anthocyanin under dark conditions (Nakamura et al. 1999), while dark-producing cell lines have also been established for *Aralia cordata* (Sakamoto et al. 1993) and *V. vinifera* (Cormier et al. 1996). Nevertheless, this "trial and error" selection method that mostly requires years of screening tends to be inefficient and costly, and carries a high risk of producing no positive outcome. It is therefore important to understand the light and dark regulation mechanisms of plant secondary metabolite biosynthesis for the development of rational and efficient selection technologies of dark-producing cell lines.

Mutation strategies involve the application of selective agents and environmental stresses as selection pressures for the selection of high-producing cell lines. The cell population that can survive under these selection pressures would be selected through repeated cycles of subculture. Examples of these selective agents include p-fluorophenylalanine (PFP), an analog of phenylalanine used for selecting high phenolics producing cell lines (Berlin 1980); 5-methyltryptophan; and glyphosate (Amrhein et al. 1983; Widholm 1974).

5.3.4 Process Integration and Intensification

The ability and capacity of biosynthesis of plant secondary metabolites in plant cell cultures are primarily determined by the inherent properties of cell lines; however, the actual yield and productivity achieved are functions of culture environmental conditions and process strategies. In a cell line screening program, low production yield may be a result of specific culture conditions employed for that cell line selection. To determine if a cell line is suitable for further studies and commercial development, it is critical to understand the production potential of secondary metabolites in a range of different culture conditions and process strategies for specific cell lines selected, even if the initial yield is low. The culture conditions that are commonly manipulated for improved production include medium nutrients (e.g., sugar, nitrate, phosphate, micronutrients, metal ions, and conditioned medium), environmental factors (e.g., pH, temperature, light, dissolved oxygen, and mixing), stress factors (e.g., osmotic stress and shear stress), growth hormones (e.g., auxin, cytokinin, and their ratios), and precursors. The optimization of these culture conditions is routinely carried out in any plant cell culture process development, and this method usually guarantees moderate to significant yield improvement (Rao and Ravishankar 2002; Zhang and Furusaki 1999; Zhong 2001).

Process manipulation is a very efficient method to improve metabolite yield and productivity in plant cell cultures, with common strategies shown in Table 5.3. These strategies can become more efficient with additive and/or synergistic improvements achieved when they are integrated and intensified (Table 5.5). The purpose of process integration and intensification is to provide additive and/or synergistic effect in improving productivity, product yield (product vs. substrate) and product content (product/cell weight) for intracellular metabolites or product levels (product/culture volume) for extracellular metabolites. Elicitation is a ubiquitous strategy that can be integrated with many other process strategies because the biotic and abiotic elicitors function as inducers of biosynthetic gene expression of secondary metabolites, therefore alleviating the limiting enzymatic steps. Elicitors are molecules that are capable of stimulating a plant's defense system by activating enzymes in metabolic pathways of phytoalexins (Radman et al. 2003). This may include compounds of biological

TABLE 5.5
Efficient Process Intensification Strategies to Improve the Yield and Productivity of Plant Secondary Metabolites Produced by Plant Cell Culture

Process Integration and Intensification	Effect and Mechanism	Improvements
Elicitation with multiple elicitors	Induce multiple pathways synergistically	High productivity and yield
Nutrient/precursor feeding and elicitation	Induce biosynthetic genes expression and supply limiting nutrients and substrates.	High productivity, yield, and product content for intracellular metabolites
Permeabilization, immobilization, and elicitation	Enable release of intracellular metabolites and high cell density and cell reuse, and induce biosynthetic gene expression.	Release of intracellular products; high productivity and yield
Elicitation and two-phase system	Induce biosynthetic gene expression and in situ removal of inhibiting or hydrophobic products, and maintain high cell viability by using aqueous two-phase systems.	High productivity and yield
Elicitation and cyclodextrin complexation	Induce biosynthetic gene expression, improve solubility of water-insoluble precursors, and maintain high cell viability.	High productivity and yield
Elicitation and two-stage systems	Induce biosynthetic gene expression and maximize the production yield by separating the growth and production in two different stages of respective optimal condition.	High productivity, yield, and product content for intracellular metabolites
Elicitation and In situ product removal (extraction and adsorption)	Induce biosynthetic gene expression and removal of feedback inhibition by metabolites or protection of products degradation in medium by using a second liquid or solid phase.	High productivity and yield
Immobilization and in situ product removal (extraction and adsorption)	High cell density and cell reuse and removal of feedback inhibition by metabolites or protection of products degradation in medium by using a second liquid or solid phase.	High productivity and yield

origin (biotic), such as pathogen-derived cell wall extracts, and compounds of nonbiological origin (abiotic), such as metal ions and physical stresses like wounding and UV light irradiation. Elicitors can induce different pathways and activate different gens and enzymes; therefore, intensification by multiple elicitors has also been applied, with examples shown in Table 5.6 (Fang et al. 1999).

The intensification of in situ product removal (by either extraction or adsorption) with elicitation has proven to be the most successful strategy in increasing the production of plant secondary metabolites (Choi et al. 1995; Komaraiah et al. 2003; Sajc et al. 1995). The fact that most plants' secondary metabolites are usually hydrophobic and toxic to the cell (Choi et al. 2001) leads to the use of in situ removal of secondary products so as to reduce end-product inhibition and to protect the products from being degraded. In addition, *in situ* product removal has also been shown to enhance the secretion of the product (Kurata et al. 1994). The extractive phase added to plant cell cultures, whether solid or liquid, usually consists of inert hydrophobic chemicals with a high absorption capacity for the hydrophobic plant products (Choi et al. 2001). It was reported that the productivity and yield of benzophenanthridine alkaloids in *E. californica* culture have been synergistically improved by the integration of elicitation and in situ extraction using silicon fluids (Byun and Pedersen 1994). The process integration achieved a yield of 48.7 mg/L, and a productivity of 2.3 mg/L/day. This result is more than additive when compared with 16.1 mg/L and 0.8 mg/L/day using elicitation only, and 21.0 mg/L and 1.0 mg/L/day using in situ extraction only. *In situ* product removal has also been integrated with

TABLE 5.6
Examples of Elicitation by Multiple Elicitors for Improved Anthocyanin Production in Plant Cell Cultures

Elicitor	Plant Species	Effective Level of Elicitors	Enhancement in Anthocyanin Level over the Control (%)	Reference
β-glucan	*Vaccinium pahalae* (Ohelo)	100 mg/l	190	Fang et al. (1999)
Methyl jasmonate (MeJ)		0.5 μM	200–300	
MeJ and ibuprofen			Highest	
β-glucanand ibuprofen			Highest	

immobilization in the production of anthraquinones by *Frangula alnus* Mill. Where immobilization by calcium alginate and silicon oil extraction alone increased productivity up to fivefold, a 10–30-fold increase was achieved by integrating these methods (Sajc et al. 1995).

The intensification of more than two process strategies is feasible, and one commonly cited example is the integration of immobilization, permeabilization, and elicitation in the production of gossypol by *Gossypium arboreum culture* (Choi et al. 1995). The integration of immobilization in a spirally wound cotton cloth matrix, permeabilization with dimethyl sulfoxide (DMSO), and elicitation with *Verticillium dahliae* has synergistically achieved a 23-fold increase in gossypol production, while the highest increase of eightfold was achieved by elicitation, amongst these strategies when applied alone.

It should be noted that the process integration and intensification strategies given in Table 5.5 are not comprehensive, but are examples of the most commonly used methods. Therefore, more innovative strategies can be developed and can be expected to open new avenues that significantly improve both process performance and commercial viability of plant cell culture bioprocesses.

5.3.5 Development of Transgenic Cell Lines: Metabolic Manipulation of Plant Biosynthetic Pathways

Commercial application of plant cell culture for the production of valuable secondary metabolites has limited success due to the following problems:

1. Yields and productivity are too low and unpredictable to be economical so as to justify commercial production.
2. The capacity of cultured cells for product accumulation is limited.
3. Many products are exclusively intracellular and difficult to export into an external medium for harvesting and purification.
4. Products of interest may not be expressed using conventional cell line selection and process manipulation.

Metabolic engineering has been proposed over the last 20 years as a powerful strategy to overcome these problems by fundamentally understanding the metabolic pathways and their regulation, and the potential rate-limiting steps in biosynthesis. As a result, metabolic manipulation of biosynthetic pathways using genetic engineering tools can be achieved either for overexpressing regulatory genes responsible for rate-limiting steps or for the transformation of foreign genes for the production of novel metabolites. The ultimate goal is to develop fast-growing transgenic cell lines with the ability to produce metabolites with stability of high yield and productivity and with desirable properties for commercial application.

As a first step for any genetic manipulation, it is essential to identify the biosynthetic genes, enzymes, and pathways for a specific secondary metabolite, and their associated metabolites (complimentary or competing). Although such identification has been a great challenge in earlier years, recent revolutionary advances in genome sequencing and discovery resulting in greater speed and lower cost have made large-scale functional analysis of secondary metabolism in plant more accessible than ever. With less technical and economical limitations, it is anticipated that the elucidation and understanding of plant secondary metabolisms will grow rapidly as a revived hot field of research in the coming decades. The availability of an enormous resource of genes encoding secondary metabolism will likely lead to a comprehensive construction of biosynthetic pathways of specific classes of secondary metabolites.

The second step is to identify pathway regulatory machineries and rate-limiting steps. It is without doubt that these analyses will benefit from the accumulated information in empirical studies of plant cell bioprocesses. Specific approaches that can be particularly useful for these studies include the analysis of cell lines with different biosynthetic capabilities, analysis of cells under different process conditions with either enhanced (e.g., elicitation) or inhibited metabolite production, and analysis of transgenic cell lines with specific genes. As part of the identification of rate-limiting steps, it is essential to analyze the interactions from a dynamic and global level among the primary metabolism, the biosynthetic pathways for secondary metabolism, and the postbiosynthetic events of specific metabolites. The elucidation of these interactions will provide important knowledge on the dynamic changes to rate-limiting steps, as a result of the complex metabolic network interactions. In other words, rate-limiting steps in plant cell bioprocesses are not fixed, but change dynamically.

The third step is to transform specific target genes into the metabolic pathways of plant cells, with appropriate gene integration sites, gene expression at high level with the desired pattern for optimal performance of de-bottlenecking metabolic pathways. The success in introducing and expressing either native or foreign genes in plant cells can fulfill the purpose of metabolic manipulation for improved production of secondary metabolites. The selection of transformation systems, design of recombinant transgenes, and delivery of transgenes in plant cells are now routine tasks in many laboratories. Common transformation methods include *Agrobacterium*-mediated transformation, and electroporation particle bombardment. In general, these methods have been successfully and extensively applied to obtain high levels of transient gene expression in plants and plant cells (Lessard et al. 2002). However, it is still a daunting task to develop a stably transformed cell line for commercial application. Several major challenges that must be resolved include tissue specificity, dynamic and complex regulation, subcellular localization of transgenes, and unpredictable modulation by numerous transcriptional and posttranscriptional processes. These challenges will make the metabolic manipulation of biosynthetic pathways in plant cell culture an exciting field of R&D. As a result, powerful toolkits and knowledge developed will empower plant cell bioprocess engineers with greater capability to stretch the limits of natural biosynthetic pathways of plant cells, by mobilizing genes of interest into transgenic plant cells so as to perform valuable functions for industry, medicine, and the environment.

5.3.6 Metabolic Manipulation of Postbiosynthetic Pathways

Metabolic engineering has been generally defined as the design of biochemical reaction networks by genetic manipulation to achieve specific objectives such as improved metabolite production in plant cell culture. The central notion of this approach is to consider cellular metabolism as a network and the participating biochemical reactions as a whole. Metabolic manipulation efforts have been devoted largely to the optimization of biosynthetic pathways by both process- and genetic-engineering approaches for the improvement of the production of secondary metabolites in plant cell cultures. If one considers each plant cell as a factory, secondary metabolism would include the synthesis, metabolism, and catabolism of secondary metabolites by specialized proteins as processes within that factory. Therefore, the entire metabolic pathway could be extended from the notion of

a biochemical reaction network (often called *biosynthetic pathways*) to include many important postbiosynthetic events after the core metabolite structures have been produced (Figure 5.13). These postbiosynthetic events include chemical and enzymatic modifications, transport, storage, catabolism and degradation, and extracellular secretion and release, which have been largely unexplored for metabolic engineering (Zhang, Curtin, et al. 2002). These postbiosynthetic steps can become rate limiting, simply due to the fact that the yield and productivity in plant cell culture to be achieved for commercialization are far higher than the natural capacity of plant cells. Therefore, ignorance of postbiosynthetic events for any metabolic engineering program would likely result in failure of that program. The concept of rate-limiting postbiosynthetic steps in plant metabolic engineering probably explains why little success has been achieved in increasing metabolite production to commercially viable levels by manipulation of biosynthetic pathway only (DellaPenna 2001).

As such, it has been proposed that research on postbiosynthetic processes may lead to new avenues for significant advances in commercial plant cell cultures. A good example is that of resveratrol production: up to 3,259 mg/L has been achieved in *V. vinifera* suspension cell culture when artificial storage sites were provided by adding up to 200 g/L of hydrophilic adsorbents, XAD-7 and HP2MG, in combination with elicitation (Takama 2004; Thu 2003). The factor of improvement in resveratrol yield is over 1,000-fold when compared with several milligrams per liter in untreated control culture, and is among the highest achieved for any plant cell cultures. Thu (2003) further demonstrated the importance of the optimization of postbiosynthetic events of resveratrol by increasing secretion with β-glucan, and storing and protecting resveratrol with adsorbents after enhancing biosynthesis of resveratrol with jasmonic acid (JA). This elevated yield warrants further development of commercial large-scale production of resveratrol by plant cell culture.

While the metabolic manipulation of postbiosynthetic pathways presents great promises and new opportunities for advancing plant cell culture bioprocesses, fundamental knowledge is still limited on postbiosynthetic pathways of almost all plant secondary metabolites (Zhang, Curtin, et al. 2002). Such manipulation is therefore still not a straightforward excise, before one can successfully characterize postbiosynthetic events for specific metabolites of interest. To tackle this challenge, one will need to design specific strategies for specific metabolites, depending on the knowledge available for their metabolism, and particularly the localization of either intracellular compartments or extracellular release. One case study to illustrate such strategy design is shown in Figure 5.14. Both anthocyanins and stilbenes are synthesized in the cytoplasm of plant cells, sharing common

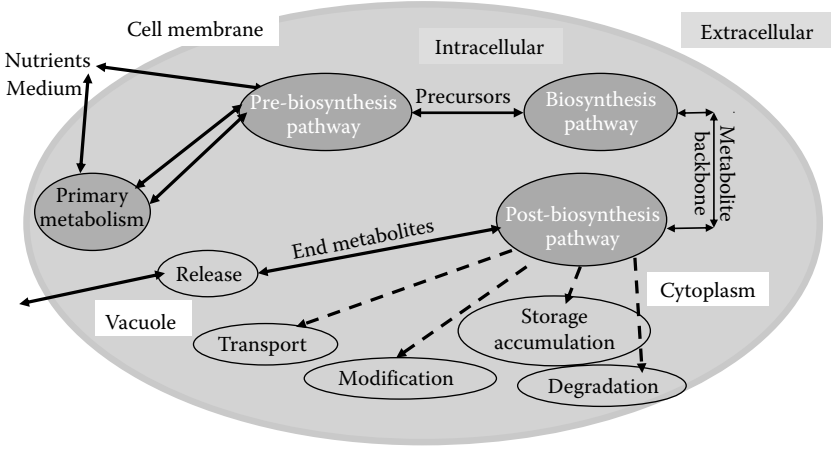

FIGURE 5.13 Illustration of pathway events involved in biosynthesis of a metabolite in plant cells: primary metabolism and secondary metabolism (prebiosynthetic, biosynthetic, and postbiosynthetic pathways). The postbiosynthetic pathway includes postbiosynthetic modification, transport, storage, catabolism and degradation, and extracellular release (secretion).

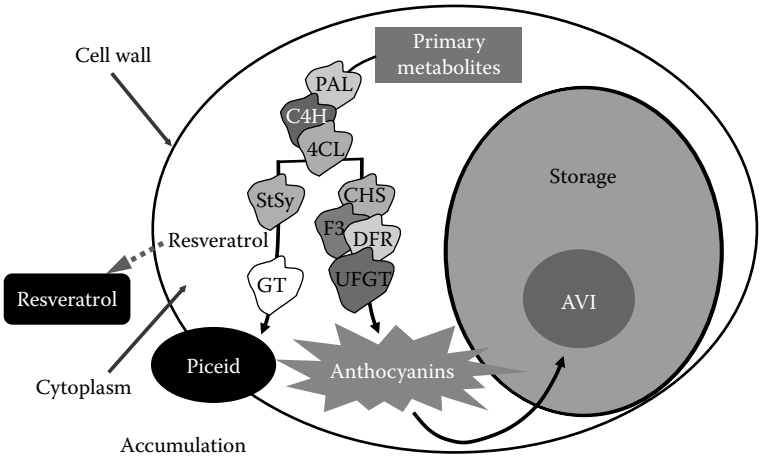

FIGURE 5.14 Illustration of the biosynthetic and postbiosynthetic pathways of anthocyanin and stilbenes (piceid and resveratrol) in plant cell cultures.

precursor pathways of phenylpropanoid and acetate to produce p-Coumaroyl-CoA and Malonyl-CoA, respectively. With three moles of Malonyl-CoA and one mole of p-Coumaroyl-CoA, two key enzymes, chalcone synthase and stilbene synthase, compete with the same substrates to direct the metabolic flux either into a series of multiple enzymatic steps for anthocyanin production to be transported and stored in the vacuole, or into the production of resveratrol to be released extracellularly and further glycosylated to form piceid to be stored in the cell wall. For extracellularly released resveratrol, the strategy to delineate its postbiosynthetic pathways starts with the test of its degradation, toxicity and feedback inhibition of cell growth and biosynthesis, as well as potential storage limitations (Thu 2003). These tests are easy to carry out in most laboratories, therefore providing valuable information for targeted manipulation. The next step would then be to investigate the transport and secretion machineries and measure the rate of transport and secretion, which are more challenging tasks. For the intracellular metabolites of piceid and anthocyanins, it is envisaged that the storage capacity would likely become limiting to the high level of product yield to be achieved for commercial production. Therefore, the strategy should start with the elucidation of storage sites and capacity, then transport pathways and rates, and finally catabolism and degradation.

In the case of anthocyanins, immunohistochemistry and cell-fractionation experiments were performed to determine the subcellular localization of the biosynthetic enzymes, showing anthocyanins compartmentalized within the cytoplasm and stored in the vacuole (Markham et al. 2000, 2001). Using *Vitis vinifera* cell culture, the studies in the authors' laboratory have characterized anthocyanin storage (Conn et al. 2010). Anthocyanin vaculor inclusions (AVIs) were documented in 45 of the highest anthocyanin-accumulating suspension cell cultures; however, none of them demonstrated detailed AVI characterization and understanding of their anthocyanin storage capacity. In our study, AVIs in grape cell cultures were found to be highly dense, membrane-delimited bodies containing a complex mix of anthocyanins, long-chain tannins, and other unidentified organic compounds. Furthermore, while the proportion of individual anthocyanin species were maintained between whole-cell and AVI extracts, the AVIs were found to selectively bind a subset of highly stable acylated (p-coumaroylated) anthocyanins. Strategies to enhance anthocyanin accumulation in grape suspension cultures lead to a proportionate increase in the abundance of AVIs. It is likely from this evidence that AVIs represent a by-product of ER-derived vesicular transport of anthocyanins, and therefore not a target for rational enhancement of anthocyanin production.

Further characterization of anthocyanin transport has however been very valuable, with potential rate-limiting targets identified. With the hypothesis that glutathione S-transferases (GSTs) may be involved in anthocyanin transport, we have affinity purified five GSTs from pigmented

grape suspension cells, characterized by nano-LC MS/MS and Edman sequencing, with the coding sequences identified and cloned (Conn et al. 2008). Bombardment of anthocyanin transport-deficient maize kernels with *V. vinifera* L. GST sequences indicated the potential involvement of two GSTs, GST1 and GST4, in anthocyanin transport. Gene expression analyses by q-PCR indicated a strong correlation of these two GSTs with anthocyanin accumulation. GST4 was enhanced 60-fold with veráison in shiraz berry skins, while GST1 and to a lesser extent GST4 were induced in *V. vinifera* suspension cells under elicitation with sucrose, jasmonic acid, and light irradiation (S/JA/L) to enhance anthocyanin synthesis. Purified GSTs quantified by reverse-phase HPLC from control and S/JA/L-treated suspension cells supported the gene expression data. Sequence alignments of these genes with known anthocyanin-transporting GSTs have shown conserved putative anthocyanin-binding regions. Furthermore, analysis of short upstream regions identified anthocyanin transcription factor (R/C1)–binding regions in the promoter of GST1. Increasing the expression of these GSTs provides an avenue to enhance anthocyanin production by more rapid removal of anthocyanins from biosynthetic complexes, potentially increasing biosynthetic flux.

Anthocyanin catabolism and degradation can be attributed to any modification that exposes the unstable aglyconated nucleus, such as alkaline pH, thermal treatment, and eznymes (e.g., glycosidases, oxidases, and hydroxylases) (Piffaut et al. 1994; Romero and Bakker 2000). These enzymes are all cytosolic and are therefore thought to have no effect on anthocyanin accumulation in viable cells with intact vacuoles.

As illustrated in the above examples, manipulation of postbiosynthetic pathways can start with empirical knowledge, and move up with targeted rational manipulation when a holistic fundamental understanding is available for given metabolites.

5.3.7 Toward Molecular Plant Cell Bioprocessing

Despite the large number of publications aimed at the optimization of plant cell culture-based bioprocesses, information on biosynthetic and postbiosynthetic pathway manipulation in a bioprocess context is limited. A recent literature survey revealed that empirical approaches were still employed predominantly for the development and optimization of plant cell based bioprocesses, despite we are at molecular era. Generally, researchers measure only the output (cell growth, nutrient uptake, etc.) in regard to the input (cell line, medium, culture parameters, bioreactor, etc.) in a plant culture system. What happens at the cellular and molecular levels remains largely obscure, akin to a "black box" (Figure 5.15). Empirical studies may allow further improvement by incorporation of other effectors, although interactions of positive effectors in plant cell culture do not always

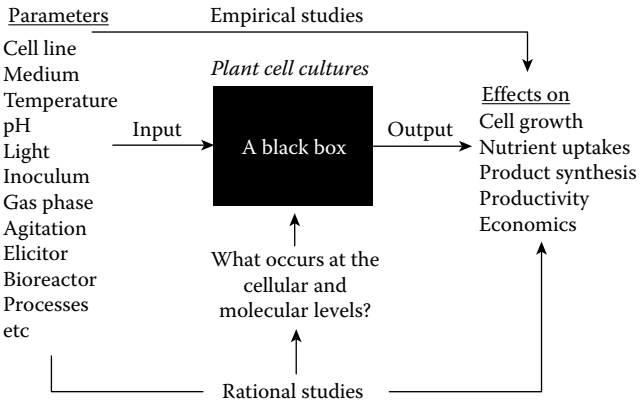

FIGURE 5.15 Moving from empirical approaches to rational approaches for molecular plant cell-based bioprocess optimization (Redrawn from Zhang, Y. et al., *Nature* 415, 644–647, 2002.).

lead to expected yield improvements. Specific pathway responses to yield improving conditions are unknown for this system and are needed to identify rational channels for further yield improvements.

Molecular bioprocessing is therefore a conceptual framework proposed to utilize pathway knowledge (Zhang, Curtin, et al. 2002; Zhang et al. 2004; Zhang and Franco 2005) in the rational optimization and redesign of plant cell culture bioprocesses for secondary metabolite production. With rapid developments in the "omic" sciences (genomics, transcriptomics, proteomics, and metabolomics), rapid and low-cost sequencing capacity has enabled large-scale functional analysis of plant secondary metabolism. Rational approaches employing the integrated analysis of gene expression, protein expression, and metabolite profiling can facilitate a comprehensive understanding of the dynamic interactions between primary and secondary metabolism, and the postbiosynthetic events of specific metabolites.

Comprehensive knowledge obtained from these mechanistic studies of plant cell culture systems, combined with an elite cell line, will provide a solid foundation for a rational and holistic manipulation and optimization of plant cell-based bioprocesses for many industrial applications. Challenges and opportunities would always come together in this endeavor, but with this approach, future decades can witness the realization of great commercial success of bioproduction using plant cell culture systems.

SUMMARY

- A wide range of secondary metabolites (e.g., antibiotics and anticancer therapeutics) are currently being produced on a large scale using microorganisms and plant cell lines.
- An impressive array of new techniques and methodologies have emerged and proved useful in strain improvement of both microorganisms and plant cells, and in increasing metabolic flux to product formation.
- Successful industrial production processes of desirable end products by microbial fermentation and/or plant cell culture rely on the development of a clear and sustainable strategy that ensures the reproducibility of high and stable yield using the cheapest possible feedstock available.
- The successful development of any industrial process for the production of secondary metabolites by plant cell culture demands the development of an elite cell line, and successful metabolic manipulation of both biosynthetic and postbiosynthetic pathways.
- In the production of new secondary metabolites, it is imperative that we carefully select a strategy that facilitates both production and efficient downstream purification processes.
- The commercial development of new and existing secondary metabolites by microbial fermentation and plant cell culture has a very bright future as we enter a new era in which new innovations in techniques and methodology stand to transform our understanding and capabilities.

REFERENCES

Ambid, C., and Fallot, J. (1981). Role of the gaseous environment on volatile compound production by fruit cell suspension cultured in vitro. In: Schreier P., editor. Flavour' 81. *Berlin: de Gruyter,* pp. 529–538.

Amrhein, N., Johanning, D., Schab, J., and Schulz, A. (1983). Biochemical basis for glyphosate-tolerance in a bacterium and a plant tissue culture. *FEBS Lett* 157(1), 191–195.

Balding, C., Blaby, I., and Summers, D. (2006). A mutational analysis of the ColE1-encoded cell cycle regulator Rcd confirms its role in plasmid stability. *Plasmid* 56, 68–73.

Bentley, S. D., Chater, K. F. et al. (2002). Complete genome sequence of the model actinomycetes *Streptomyces coelicolor* A3. *Nature* 417, 141–147.

Berlin, J. (1980). Para-fluorophenyalanine resistant cell lines of tabacco. *Zeit-fur pflan Physiol* 97, 317–324.

Bibb, M. J. (2005). Regulation of secondary metabolism in *Streptomycetes. Curr Opin Microbiol* 8, 208–215.

Bignell, D. R. G., Tahlan, K., Colvin, K. R., Jensen, S. E., and Leskiw., B. K. (2005). Expression of *ccaR*, Encoding the positive activator of Cephamycin C and Clavulanic acid production in *Streptomyces clavuligerus* is dependent on *bldG. Antimic. Agents. Chemotherapy* 49, 1529–1541.

Brodelius, P. (1988). Permeabilization of plant cells for release of intracellularly stored products: viability studies. *Appl Microbio Biotechnol* 27(5–6), 561–566.

Byun, S. Y., and Pedersen, H. (1994). Two-phase airlift fermentor operation with elicitation for the enhanced production of enzophenanthridine alkaloids in cell suspensions of *Escherichia californica. Biotechnol Bioeng* 44(1), 14–20.

Chakraburtty, R., and Bibb., M. J. (1997). The ppGpp synthetase gene (relA) of *Streptomyces coelicolor* A3 plays a conditional role in antibiotic production and morphological differentiation. *J Bacteriol* 179, 5854–5861.

Chapman, R.F. (2000). Entomology in the twentieth Century. *Annual Rev Entomology* 45, 261–285.

Choi, J-W., Cho, G. H., Byun, S. Y., and Kim, D-I. (2001). Integrated bioprocessing for plant cell cultures. *Adv Biochem Eng Biotechnol* 72, 63–102.

Choi, H. J., Tao, B. Y., and Okos, M. R. (1995). Enhancement of secondary metabolite production by immobilized *Gossypium arboreum* cells. *Biotechnol Prog* 11, 306–311.

Chouayekh, H., and M. J. Virolle. (2002). The polyphosphate kinase plays a negative role in the control of antibiotic production in *Streptomyces lividans. Mol Microbiol* 43, 919–930.

Conn, S., Curtin, C., Bezier, A., Franco, C., and Zhang, W. (2008). Purification, molecular cloning, and characterization of glutathione S-transferases (GSTs) from pigmented *Vitis vinifera* L. cell suspension cultures as putative anthocyanin transport proteins. *J Exp Botany* 59(13), 3621–3634.

Conn, S., Franco, C., and Zhang, W. (2010). Characterization of anthocyanic vacuolar inclusons in *Vitis Vinifera* L. cell suspension cultures. *Planta* 231, 1343–1360.

Cormier, F., Brion, C., Do, C. B., and Moresoli, C. (1996). Development of process strategies for anthocyanin-based food colorant using *Vitis vinifera* cell cultures. In: DiCosmo, F., and Misawa, M. (Eds.), *Plant cell cultures secondary metabolism*: toward industrial application. New York: CRC Press, pp. 167–185.

Cormier, F., Do, C. B., and Nicolas, Y. (1994). Anthocyanin production in selected cell lines of grape (*Vitis vinifera* L.). *In Vitro Cell Dev Biol* 30(3), 171–173.

DellaPenna, D. (2001). Plant metabolic engineering. *Plant Physiol* 125, 160–163.

Deus, B., and Zenk, M. H. (1982). Exploitation of plant cells for the production of natural products. *Biotechnol Bioeng* 24, 1965–1974.

Deus-Neumann, B., and Zenk, M. H. (1984). Instability of indole alkaloid productionin Catharanthus roseus cell suspension cultures. *Plant Med* 50, 427–431.

Do, C. B., and Cormier, F. (1991). Effects of low nitrate and high sugar concentrations on anthocyanin content and composition of grape (*Vitis vinifera* L.) cell suspension. *Plant Cell Rep* 9, 500–504.

Doodeman, M., Bino, R. J., Uytewaal, B., and Bianchi, F. (1985). Genetic analysis of instability in *Petunia hybrida*. 4. The effect of environmental factors on the reversion rate of unstable alleles. *Theor Appl Genet* 69(5–6), 489–495.

Dornenburg, H., and Knorr, D. (1993). Cellular permeabilization of cultured tissues by high electric field pulses or ultra high pressure for the recovery of secondary metabolites. *Food Biotechnol* 7, 35–48.

Dornenburg, H., and Knorr, D. (1995). Strategies for the improvement of secondary metabolite production in plant cell cultures. *Enzyme Microb Technol* 17, 674–684.

Dornenburg, H., and Knorr, D. (1996). Production of the phenolic flavour compounds with cultured cells and tissues of *Vanilla planifolia* species. *Food Biotechnol* 10, 75–92.

Endress, R. (1994). Plant cells as producers of secondary compounds. In: Plant cell biotechnology. Berlin: Springer-Verlag, 1994. pp. 121–242.

Fang, Y., Smith, M. A. L., and Pepin, M. F. (1999). Effects of exogenous methyl jasmonate in elicited anthocyanin-producing cell cultures of ohelo (*Vaccinium pahalae*). *In Vitro Cell Dev Biol Plant* 35 (1), 106–113.

Folcher, M., H. Gaillard, L. T. Nguyen, K. T. Nguyen, P. Lacroix, N. Bamas-Jacques, M., Rinkel, and C. J. Thompson. (2001). Pleiotropic functions of a *Streptomyces pristinaespiralis* autoregulator receptor in development, antibiotic biosynthesis, and expression of a superoxide dismutase. *J Biol Chem* 276, 44297–44306.

Fujita, Y., Takahashi, S., and Yamada, Y. (1984). Selection of cell lines with high productivity of shikonin derivatives through protoplasts of Lithospermum erythrorhizon. *Proc 3rd Euro Congr Biotechnol* 1,161–166

Hesketh, A., Sun, J., and Bibb., M. J. (2001). Induction of ppGpp synthesis in *Streptomyces coelicolor* A3 grown under conditions of nutritional sufficiency elicits actII-ORF4 transcription and actinorhodin biosynthesis. *Mol Microbiol* 39, 136–144.

Hirasuna, T. J., Shuler, M. L., Lackney, V. K., and Spanswick, R. M. (1991). Enhanced anthocyanin production in grape cell cultures. *Plant Sci* 78, 107–120.

Horinouchi, S. (2003). AfsR as an integrator of signals that are sensed by multiple serine/threonine kinases in *Streptomyces coelicolor* A3. *J Ind Microbiol Biotechnol* 30, 462–467.

Jin, W., Kim, H. K., Kim, J. Y., Kang, S. G., Lee, S. H., and Lee, K. J. (2004a). Cephamycin C production is regulated by *relA* and *rsh* genes in *Streptomyces clavuligerus* ATCC27064. *J Biotechnol* 114, 81–87.

Jin, W., Ryu, Y. G., Kang, S. G., Kim, S. K., Saito, N., Ochi, K., Lee, S. H., and Lee, K. J. (2004b). Two relA/spoT homologous genes are involved in the morphological and physiological differentiation of *Streptomyces clavuligerus. Microbiology* 150, 1485–1493.

Ketchum, R. E. B., Gibson, D. M., Croteau, R. B., and Shuler, M. L. (1999). The kinetics of taxoid accumulation in cell suspension cultures of *Taxus* following elicitation with methyl jasmonate. *Biotechnol Bioeng* 62, 94–105.

Kobayashi, Y., Fukui, H., and Tabata, M. (1991). Effect of carbon dioxide and ethylene on berberine production and cell browning in *Thalictrum minus* cell cultures. *Plant Cell Rep* 9, 496–499.

Komaraiah, P., Ramakrishna, S. V., Reddanna, P., and Kavi Kishor, P. B. (2003). Enhanced production of plumbagin in immobilized cells of *Plumbago rosea* by elicitation and in situ adsorption. *J Biotechnol* 101, 181–187.

Krisa, S., Teguo, P. W., Decendit, A., Deffieux, G., Vercauteren, J., and Merillon, J. M. (1999). Production of superior ^{13}C-labelled anthocyanins by *Vitis vinifera* cell suspension cultures. *Phytochemistry* 51 (5), 651–656.

Kurata, H., Kawai, A., Seki, M., and Furusaki, S. (1994). Increased alkaloid production in a suspension culture of *Coffea Arabica* cells using an adsorption column for product removal. *J Ferment Bioeng* 78 (1), 117–119.

Lessard, P. A., Kulaveerasingam, H., York, G. M., Strong, A., and Sinskey, A. J. (2002). Manipulating gene expression for the metabolic engineering of plants. *Metabolic Eng* 4, 67–79.

Markham, K. R., Gould, K. S., Winefield C. S., Mitchell, K. A., Bloor S. J. and Boase, M. R. (2000). Anthocyanic vacuolar inclusions: Their nature and significance in flower colouration. *Phytochemistry* 55, 327–336.

Markham, K., Gould, K., and Ryan, K. (2001). Cytoplasmic accumulation of flavonoids in flower petals and its relevance to yellow flower colouration. *Phytochmeistry* 58, 403–413.

Mochizuki, S., Hiratsu, K., Suwa, M., Ishii, T., Sugino, F., Yamada, K., and Kinashi, H. (2003). The large linear plasmid pSLA2-L of *Streptomyces rochei* has an unusually condensed gene organization for secondary metabolism. *Mol Microbiol* 48, 1501–1510.

Mori, T., Sakurai, M., Shigeta, J. I., Yoshida, K., and Kondo, T. (1993). Formation of anthocyanins from cells cultured from different parts of strawberry plants. *J Food Sci* 58, 788–792.

Nakamura, M., Takeuchi, Y., Miyanaga, K., Seki, M., and Furusaki, S. (1999). High anthocyanin accumulation in the dark by strawberry (*Fragaria ananassa*) callus. *Biotechnol Lett* 21, 695–699.

Perez-Llarena, F. J., Liras, P., Rodriguez-Garcia, A., and Martin, J. F. (1997). A regulatory gene (ccaR) required for cephamycin and clavulanic acid production in *Streptomyces clavuligerus*: amplification results in overproduction of both beta-lactam compounds. *J Bacteriol* 179, 2053–2059.

Piffaut, B., Kader, F., Girardin, M., and Metche, M. (1994). Comparative degradation pathways of malvidin 3,5-diglucoside after enzymatic and thermal treatments. *Food Chem* 50(2), 115–120.

Radman, R., Saez, T., Bucke, C., and Keshavarz, T. (2003). Elicitation of plants and microbial cell systems. *Biotechnol Appl Biochem* 37(1), 91–102.

Rao, S. R., and Ravishankar, G. A. (2002). Plant cell cultures: Chemical factories of secondary metabolites. *Biotechnol Adv* 20, 101–153.

Recio, E., Colinas, A., Rumbero, A., Aparicio, J. F., and Martin, J. F. (2004). PI actor, a novel type quorum-sensing inducer elicits pimaricin production in *Streptomyces natalensis. J Biol Chem* 279, 41586–41593.

Romero, C., and Bakker, J. (2000). Effect of storage temperature and pyruvate on kinetics of anthocyanin degradation, vitisin A derivative formation, and color characteristics of model solutions. *J Agric Food Chem* 48, 2135–2141.

Ruiz, B., Chávez, A., Forero, A., García-Huante, Y., Romero, A., Sánchez, M., Rocha, D., Sánchez, B., Rodríguez-Sanoja, R., Sánchez, S., and Langley, E. (2010). Production of microbial secondary metabolites: Regulation by the carbon source. *Crit Rev Microbiol* 36(2), 146–167.

Sajc, L., Vunjak-Novakovic, G., Grubisic, D., Kovacevic, N., Vukovic, D., and Bugarski, B. (1995). Production of anthraquinones by immobilized Frangula alnus Mill. plant cells in a four-phase air-lift bioreactor. *Appl Microbiol Biotechnol* 43, 416–423.

Sakamoto, K., Iida, K., Koyano, T., Asada, Y., and Furuya, T. (1994). Method for selecting anthocyanin-producing cells by a cell sorter. *Planta Medica* 60(3), 253–259.

Sakamoto, K., Iida, K., Sawamura, K., Hajiro, K., Asada, Y., Yoshikawa, T., and Furuya, T. (1993). Effects of nutrients on anthocyanin production in cultured cells of *Aralia cordata. Phytochemistry* 33, 357–360.

Stratigopoulos, G., Bate, N. and Cundliffe, E. (2004). Positive control of tylosin biosynthesis: Pivotal role of TylR. *Molec Microbiol* 54, 1326–1324.

Tabata, H. (2004). Paclitaxel production by plant-cell-culture technology. *Adv Biochem Eng Biotechnol* 87, 1–23.

Takama, K. (2004). Enhanced resveratrol production by elicitation and *in-situ* product removal in *Vitis vinifera* suspension culture. Master Thesis, Department of Medical Biotechnology, Flinders University, Adelaide, Australia.

Thu, V. V. (2003). Optimization of the production of resveratrol in *Vitis vinifera* cell suspension culture. Master Thesis, Department of Medical Biotechnology, Flinders University, Adelaide, Australia.

Uguru, G. C., Stephens, K. E., Stead, J. E., Towle, J. E., Baumberg, S., and McDowall, K. J. (2005). Transcriptional activation of the pathway-specific regulator of the actinorhodin biosynthetic genes in *Streptomyces coelicolor. Molec Microbiol* 58, 131–150.

Verpoorte, R., van der Heijden, R., and Memelink, J. (1998). Plant Biotechnology and the production of alkaloids. Prospects of metabolic engineering. In: Cordell, G. A. (Ed.), *The Alkaloids*. San Diego: Academic Press, pp. 50, 453–508.

Verpoorte, R., van der Heijden, R., ten Hoopen, H. J. G., and Memelink, J. (1999). Metabolic engineering of plant secondary metabolite pathways for the production of fine chemicals. *Biotechnol Lett* 21, 467–479.

Widholm, J. M. (1974). Evidence for compartmentation of tryptophan in cultured plant tissues. Free tryptophan levels and inhibition of anthranilate synthetase. *Physiol Plant* 30, 323–326.

Yamamoto, Y., Mizuguchi, R., and Yamada, Y. (1982). Selection of a high and stable pigment-producing strain in cultured *Euphorbia millii* cells. *Thero Appl Genet* 61(2), 113–116.

Yeoman, M. M., and Yeoman, C. L. (1996). Manipulating secondary metabolism in cultured plant cells. *New Phytologist* 134, 553–569.

Zhang, W., Curtin, C., and Franco, C. (2002). Toward manipulation of post-biosynthetic events in secondary metabolism of plant cell cultures. *Enzyme Microbial Technol* 30, 688–696.

Zhang, W., and Furusaki, S. (1999). Production of anthocyanins by plant cell cultures. *Biotechnol Bioprocess* Eng 4, 231–252.

Zhang, Y., Perry, K., Vinci, V. A., K. Powell, K., Stemmer, W. P. C., and del Cardayre, S. P. (2002). Genome shuffling leads to rapid phenotypic improvement in bacteria. *Nature* 415, 644–647.

Zhang, W., Franco, C. M. M., Curtin, C., Conn, S. (2004). To stretch the boundary of secondary metabolite production in plant cell-based bioprocessing: anthocyanin as a case study. *J Biomedicine Biotechnol* 5, 264–271.

Zhang, W., Franco, C. M. M. (2005). Molecular bioprocessing: A new paradigm of bioprocess engineering. *BIOforum Europe* 1, 1–3.

Zhong, J. J. (1992). Bioprocess engineering studies on suspended cultures of *Perilla frutescens* in bioreactors for anthocyanin production. PhD Thesis, Osaka University, Japan.

Zhong, J. J. (2001). Biochemical engineering of the production of plant-specific secondary metabolites by cell suspension cultures. *Adv Biochem Eng Biotechnol* 72, 1–26.

Zubko, M. K., Schmeer, K., Glaessgen, W. E., Bayer, E., and Seitz, H. U. (1993). Selection of anthocyanin-accumulating potato (*Solanum tuberosum* L.) cell from calli derived from seedlings produced by gamma-irradiated seeds. *Plant Cell Rep* 12, 555–558.

This page intentionally left blank

6 Applications of Metabolomics to Microbial "Cell Factories" for Biomanufacturing: Current Trends and Future Prospects

David M. Mousdale and Brian McNeil

CONTENTS

6.1 RISE AND APPLICATION OF METABOLOMICS TO INDUSTRIAL FERMENTATIONS

6.1.1 Rise of Metabolomics

The rise of metabolomics to international scientific stature was underlined in 2004, when the Metabolomics Technology Development Initiative emerged from the National Institutes of Health (NIH) in the United States as a roadmap to understanding biological pathways and networks. As stated in the initiative,

> A general aim of metabolomics is to identify, measure and interpret the complex time-related concentration, activity and flux of endogenous metabolites in cells, tissues, and other biosamples… (Castle 2008)

Metabolomics is a recent addition to the current trend of "omics" and investigates metabolite analysis and its applications. As a discipline, it is distinguishable from genomics (genome sequences), transcriptomics (DNA microarrays and the transcriptome), proteomics (protein analysis and the proteome), and fluxomics (metabolism and flux analysis). All the various "omics" can be seen as channeling into fluxomics (Tang et al. 2009a). The number of review articles that had been published by 2008 certainly show that metabolomics (900) lagged behind genomics (22,500), proteomics (92,000), and transcriptomics (6,500) but did clearly "outrank" fluxomics (400).

In this chapter, we will explore examples where metabolomics have been or can be applied to biomanufacturing, with the view to improving yield, reproducibility, and process management. The premier research portal, *Metabolomics*, has since its inception in 2005 published very few articles directly related to fermentations of commercial significance, and, when fermentation science is included, the focus has been on yeast and ethanol (Ding et al. 2010). Nevertheless, the application of metabolomics is widely considered to have changed metabolic and genetic engineering strategies away from the narrow and local pathway level to the "whole system" level (Zhang et al. 2010). The Metabolomics Conference held in Amsterdam (27 June–1 July 2010) provided a snapshot of progress in applying metabolomics to a range of research areas within life sciences. Of the 125 talks given, 41% were on methods development, while animal and plant biological topics each accounted for 26%. For fewer, the microbial studies were a distinct minority (7%). This picture was also replicated in poster presentations: 11% microbial (including human pathogens), 15% methods development, 27% plants, and 47% animals (including humans).

The rapid take-up by plant biologists is not surprising given that many commercial uses of plants depend on optimizing or changing the metabolic and chemical features of fruits, vegetables, cereal grains, and so on. Phytochemistry easily elides with plant metabolomics, and there is an established and wide-ranging interest in trace analysis of plant materials for flavor chemicals, plant hormones, alkaloids, and many other secondary metabolites.

For microbial fermentations, in contrast, a major restriction on the application of metabolomics is the apparent lack of appropriate technologies. The Metabolomics Society's Fifth International Conference (Edmonton, Canada, 30 August–2 September 2009) commenced with workshops emphasizing *techniques*: nuclear magnetic resonance (NMR), mass spectroscopy (MS) and its "hyphenated" variants with gas–liquid (GL-MS), and modern liquid chromatography (LC-MS), data processing, and sampling. Sample preparation remains a major area of research: how can the multifaceted metabolic activity of any cell type (human, animal, plant, yeast, fungal, or bacterial) be "frozen" in an instant of time to provide a true and validated sample for detailed analysis? In bacterial cells, intracellular metabolites concentrations ("pools") vary in response to changes in nutritional environment by more than twofold on a timescale of 20 seconds or less (Oldiges et al. 2004).

Continued research demonstrates that different cell types require differently optimized sampling approaches even in the case of relatively well-understood microorganisms, such as the yeast

Saccharomyces cerevisiae and the bacterium *Escherichia coli* (Oldiges et al. 2007). Even worse is the realization that variable amounts of the metabolome may be reliably contained within a bacterial cell. The ideal method would be to capture the intracellular metabolites in a single pool; rapid quenching in cold organic solvents or solvent–water mixtures were considered to be the method of choice, but more careful examination of the procedure revealed a major flaw (Winder et al. 2008). Once treated with the quenching agent, the mixture was then separated by centrifugation at low temperature into cell and supernatant fractions; when analyzed, the supernatants contained considerably more metabolites than found in "footprint" samples—rapid filtrates of the cell culture to provide a control for leakage of material and metabolites from the intracellular compartment. With a commitment to rapid sampling and sample processing, however, and the use of state-of-the-art analytical and computational tools, at least some important metabolic details in quantitative and time-based frameworks can be defined for microbes growing in fed-batch cultures (Nöh et al. 2007).

The successful application of such advanced methodologies is nevertheless severely limited in applied and industrial use, as commercial manufacturing utilizes large fermentors (100–750 m^3), markedly different from laboratory-scale fermentors. Research and development (R&D) programs have yielded small- to microscale fermentation devices capable of supporting very high cell densities and higher productivities than in conventional bioreactors (Panula-Perälä et al. 2008). But, while these laboratory systems are certainly amenable to the application of state-of-the-art metabolomics, little is known about the detailed metabolic physiology of producer organisms during growth in large industrial vessels. For commercial purposes, attention is almost invariably focused on *scaling up* functionality to translate (insofar as possible) productivity to full biomanufacturing status. This heavily relies on engineering capabilities to supply air and nutrients (in massive quantities), stirring (or, more rarely, airlift) technologies to mix the fermentation broth and on control parameters that can be regulated on a real-time basis (Allman 2007).

There is also a *biological* dimension to be considered. In addition to *S. cerevisiae* and *E. coli*, commercial biomanufacturing uses a wide spectrum of microorganisms, not all of which have a fully annotated genome (or, at least, not in a published form). Before the advent of genetic engineering, it was the practice to scale up microbial fermentations with fragmentary knowledge of their physiology and biochemistry. There are hundreds of microbial producers, by now highly evolved by decades of classical strain improvement programs. While nonconventional species have been largely ignored in the fuel ethanol industry (despite claims for significantly higher productivities than the widely used *S. cerevisiae* and other yeasts), they have proved to be widely welcomed for the fermentative production of secondary metabolites such as antibiotics.

6.1.2 Analytical Techniques Employed in Metabolomics

Understandably, many analytical techniques have evolved to meet the challenging demands of metabolomics. The current armory of analytical techniques includes

- Continuous measurements by mass spectrometric methods of gas exchange, CO_2, and O_2 (Allman 2007)
- Online sampling interfaced with spectrophotometry, polarimetry, and ion-sensitive electrodes for glucose, phosphate, and ammonia (Schmidt et al. 1984)
- Online sampling interfaced with LC analysis for medium components, fermentation products, and their precursors and metabolites (Möller et al. 1986)
- Nondestructive and continuous analysis of medium components and fermentation analytes using near-infrared spectroscopy (NIR; Scarff et al. 2006)
- Online measurements of live cell concentrations using radiofrequency impedance (November and Van Impre 2006)

6.1.3 Central Issues of Metabolomics

Ultimately, the key to understanding a fermentation process is to pose meaningful questions, that is, what information and data are required to

- Upscale the productive potential of an organism?
- Maximize productivity in an environment imposing multiple physical and biological stresses?
- Understand the implications of making a rational change in gene dosage, gene expression, or gene deletion?
- Predict how changes in nutrient supply may be sidelined by the operation of competing biochemical pathways?
- Guide the search for novel metabolites of importance to the yield of the process for the final purity of its product(s)?

In commercial practice, these questions intersect on managing a complex but established biological process (i.e., the fermentation itself). In addition to introducing novel strains, a clearer and deeper understanding of metabolic networks is also required for successful fermentation. However, efforts directed toward the latter objectives are hampered by the lack of adequate resources. Thus, the "roadmap" to understanding bioprocess metabolomics has to be based on a clear strategy to maximize the value added by further R&D.

6.2 PHYSICAL (OPERATING) AND METABOLIC PARAMETERS

Industrial fermentations evolved by the combined efforts of microbiologists, biotechnologists, and chemical engineers. For many microbial fermentations, complex media are used that include sources of carbon such as starch hydrolysates or sugarcane molasses and nitrogen inputs that could be yeast extracts, corn steep liquors, soybean, and other vegetable proteins (intact or after protease degradation). Such inputs are often assumed to supply sufficient inorganic nutrients (cations and anions), but additional salts can be added to the medium in the form of inorganic phosphates or (more rarely) trace element mixes.

Similarly, continued operation of a commercial fermentation narrows down the range of operating parameters, so that ideally (in chemical engineers' eyes) a near-automated process can be evolved with restricted variation in the changes of key parameters.

Ideally, the same highly and deliberately repetitive practice is applied to the one- or two-step generation of the biological input to the fermentation (i.e., the seed inoculum). The reality, however, is that the biological system has a considerable built-in variability. Six Sigma programs using commercial management strategy derived from minimizing variability in manufacturing are employed (Taylor 2008). Such modern variants of *good management and laboratory practice* might encounter severe limitations, but it is instructive to consider the inevitable causes of variation in large-scale bioprocesses.

6.2.1 Medium Design and Composition

Medium design and composition are key to successful fermentation or animal cell culture. In the laboratory, the proper selection and handling of medium constituents can be achieved, and chemically defined media might be appropriate (Harvey and McNeil 2008). With complex media operated on the 100 m^3 scales, however, and despite rigorous quality control checks, seasonal variations in the exact chemical compositions of vegetable oils and complex peptidic nitrogen sources (corn steep liquors, soya peptones, and yeast extracts) as well as sugarcane molasses are inevitable as the raw materials are sourced from different geographical locations. Table 6.1 shows a data set obtained after routine analysis of protein from soya beans prepared for use in fermentation.

TABLE 6.1
Typical Contents of Soy Flour

Test	Result (% or % of Total Fatty Acids)
Amino acids:	
Aspartic	6.5
Glutamic	9.8
Glycine	2.4
Serine	2.5
Threonine	2.1
Lysine	3.6
Arginine	4.2
Methionine	0.8
Valine	2.8
Leucine	4.4
Isoleucine	2.7
Phenylalanine	2.9
Tryoptophan	0.8
Proline	2.7
Cysteine	0.8
Tyrosine	2.0
Histidine	1.5
Moisture and oil contents:	
Moisture	6.8
Oil	0.7
Sugars:	
Glucose	trace
Sucrose	7.8
Fructose	trace
Maltose	trace
Raffinose	1.4
Stachyose	6.5
Fatty acids:	
Linoleic	60.2
Palmitic	19.6
Oleic	9.5
Linolenic	9.2
Stearic	4.7

With different starting points, variation in the utilization patterns of major and minor fermentation inputs is to be expected with obvious consequences for growth rates and maximal densities of producing cells (Mousdale et al. 1999). With highly structured control systems for fermentations employing computer-controlled airflow and agitation rates, timing of the onset of feeds, and temperature ramps (both upward and downward), slight differences in initial growth can then cascade into major "excursions" from predicted and expected behavior. The design, measure, analyze, improve and control (DMAIC) approach of Six Sigma practice often fails because the analysis may be restricted to the symptom and not the underlying cause; if, for example, variation in vegetable protein or other nitrogen input content is suspected, there may be no remedy because all suppliers are subject to climatic and field conditions in a growing season.

The question then becomes, what to analyze in the fermentation? The answer may lie deep in the metabolome or in the chain of biochemical events that link nutrient uptake.

6.2.2 Variability in Secondary Metabolite Fermentations

Consider a typical microbial bioprocess that exemplifies problems in variability. Secondary product processes are usually based on complex media, one or more major nutrient feeds, and regulated in response to factors such as pH. In this "model" process, the main fermentation tank is filled to very precise gravimetric standards with, for example, soybean meal, soya oil, various salts, and a local supply of water; after a tightly controlled sterilization and subsequent cooling, a seed inoculum is introduced that may or may not be the result of an equally tightly timed fermentation (or from a final seed vessel that is the end product sequentially produced from shake flasks and small fermentors)—secondary product processes often require in excess of 240 hours for completion and exact timing of seed and main tank availability, and synchronization is very difficult to achieve on industrial sites.

Early metabolism might be subject to a definable "lag" phase in which airflow is maintained at a low rate while foaming might occur—with catastrophic loss of fermentor contents and blockage of outlet ports and airstream routes. A plausible sequence of events thereafter is as follows:

- Slow growth might begin within 1–2 hours as the cells utilize mono- and disaccharides released following heat sterilization of the medium and hydrolysis of di-, tri-, and tetrasaccharides (Table 6.1).
- Carbon dioxide is evolved, carboxylic acids may be generated as metabolic overspill products, and the pH decreases—this would be augmented by the uptake of free ammonium ion in the medium and its incorporation into organic nitrogen compounds.
- With the onset of growth, inorganic phosphate is taken up to support nucleic acid synthesis and other cellular demands for this precursor; this causes the pH to stabilize and then rise, which may trigger the beginning of a carbon feed.
- Once foaming has decreased, the airflow and agitation rates are increased; faster growth requires free amino acids and peptides to be catabolized as carbon and nitrogen sources, but an excess of nitrogen may be present and appears as an ammonium ion in the medium, accelerating the pH rise. The growth rate increases.
- Proteases are secreted by the growing cells, and soluble protein is degraded mostly to peptides that can be transported into the cells or hydrolyzed to smaller peptides and free amino acids in the extracellular phase by peptidases. The major carbon source in the medium (for example, soya oil) begins to be broken down to glycerol and fatty acids by lipases also secreted by the biomass. The pH decreases again due to the accumulation of low concentrations of fatty acids and the increased production of CO_2 that partly dissolves in the liquid phase.
- The pH will stabilize, or a control strategy will impose a pH set point by adding a strong mineral acid or base on demand. Airflow and agitation rates may be increased—within foaming control limits. Peak growth rates are reached, as evidenced by maxima in CO_2 evolution rate (CER) and O_2 uptake rate (OUR), both of these parameters being measured by off-gas analysis and calculated by computational programs (Figure 6.1).
- Carbon feed rate is increased, but a growth rate limitation is encountered: OUR, phosphate depletion, and exhaustion of readily utilizable nitrogen (ammonia, free amino acids, and small peptides). Another crucial parameter is the dissolved O_2 concentration (DO), which has fallen rapidly for several hours and which might require adjustment if it reaches a critical minimum (Figure 6.1); in that event, other control factors can increase airflow and agitation rates further (if this is possible in engineering terms), decreasing the carbon feed rate or (as a last resort) decreasing the operating temperature of the fermentor.

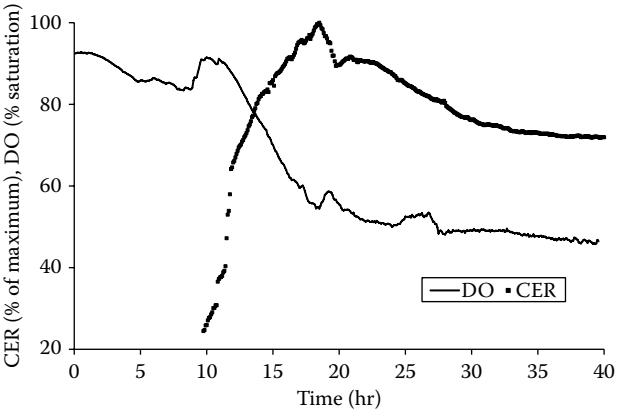

FIGURE 6.1 Online data collection in a microbial fermentation.

- Once growth has slowed below a critical point, secondary product formation commences, although this may not be routinely assayed for a further 24 hours or longer (based on accumulated past experience).
- The various physical parameters (including pH) are controlled to varying degrees of accuracy for the remaining 200-plus hours of the fermentation to ensure maximal product accumulation rate but with due note of space–time volume considerations and process economics (Mousdale et al. 1999).

This outline of a realistic industrial bioprocess—typical of those run around the world for the biomanufacture of antibiotics, enzyme inhibitors, vitamins, animal feed ingredients, antifungal agents and other bioactives, primary metabolites such as amino acids and carboxylic acids, and enzymes—has very different practical features from the ideal laboratory processes operated in replicated small fermentors with "clean" chemically defined media, sophisticated control mechanisms, and (sometimes) the means for rapid sample removal and processing. For a process with *E. coli*, the events will be compacted into a short timeframe (40–48 hours); for a Streptomycete, events unfold over 100–150 hours. Whatever the producer organism, however, the yield and productivity may be determined by undetermined metabolic features and responses in the opening 1–5 or 1–12 hours; a time course of production rate change is then set up, which is not "rescue-able" in any meaningful way by later changes in feed rates and operating conditions (Figure 6.2).

The extensive data sets represented by accumulated operational information from any commercial fermentation are themselves a valuable source of insights into metabolic networks. When process changes are compared, immediate targets for understanding metabolism usually present themselves. The key methodological step is to relate observations with the analytical data obtained. In the case of DO trends (Figure 6.1), growth measurements are essential to interpret apparent growth rates deduced from DO (or CER or OUR) profiles; robust methodologies certainly exist for nucleic acid measurements in complex-media bioprocesses, as do analytical techniques for inorganic phosphate, ammonium and other cations, carbohydrates, amino acids, and accumulated primary metabolites (Mousdale 1996). Chemical sampling methods can "fix" ex-fermentor samples so that postmortem changes are minimized when enzyme activities are abolished; once stabilized, extensive analysis can be undertaken—and it is often of great importance to be wide ranging in the selection analyses because both primary and secondary metabolite fermentations can harbor "surprises" of overlooked or undiscovered metabolic pathways. A recent exemplar is *Aspergillus terreus*, an organism that is commercially used for the production of the carboxylic acid itaconic acid at low pH and the secondary product lovastatin at higher pH (Bizukojc and Ledakowicz 2009). When used as a carbon source, glucose can be diverted to the production of gluconic acid, a product well known in

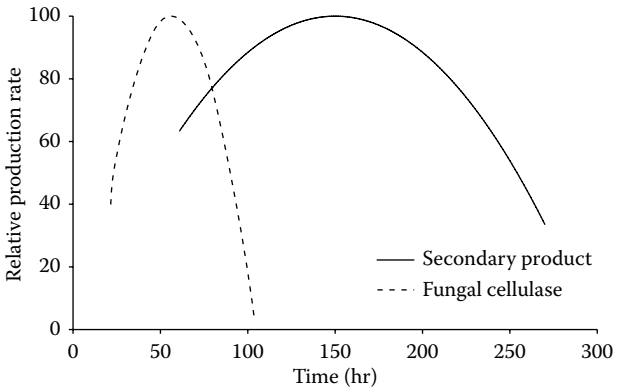

FIGURE 6.2 Time courses of productivity (product formed per hour) in microbial fermentations.

industrial fermentations using *A. niger*; this unexpected metabolite was only recognized when large amounts of base (NaOH) were observed to be required for the maintenance of a set pH when no metabolic demand for pH control was predicted (Dowdells et al. 2010).

Indeed, few of the largest-scale industrial fermentations can be reliably stated to have progressed beyond the "black box" stage of comprehension (Legiša and Mattey 2007). A reasonable optimism in understanding the majority of the metabolome can be adduced in fermentations using *E. coli* and *S. cerevisiae* (Almaas et al. 2004). Beyond those "islands" of detailed knowledge lies a wide number and diversity of producing organisms with sometimes little known beyond their basic use of defined carbon sources before upscaling to commercial production occurs.

For the foreseeable future, therefore, the most useful question is, what to analyze? Operating data provide many clues; detailed metabolic analysis fills in major gaps, while intuitive exploration can find the unexpected, for example:

- Unrecognized metabolites (Dowdells et al. 2010)
- Intermediates or side products of long biosynthetic pathways that can be accumulated in parallel or in rivalry to the desired product (Nakano et al. 2000)
- Unexpected effects of the overexpression of primary anabolic and catabolic pathways (Kern et al. 2007a, 2007b)

6.3 PRODUCTS OF SECONDARY METABOLISM

6.3.1 Clavulanic Acid

Although itself only a weak antibiotic, clavulanic acid is a potent inhibitor of β-lactamases that degrade β-lactam antibiotics and is mixed with semisynthetic penicillins to increase their potency (Baggaley et al. 1997; Saudagar et al. 2008). Clavulanic acid is one of a family of secondary metabolites produced by *Streptomyces clavuligerus*; cross-regulation of at least three different biosynthetic pathways in this one species has been recognized (Romero et al. 1984; de la Fuente et al. 2002). A network of regulatory mechanisms controls the formation of different metabolites by pathway-specific regulators or pleiotropic regulators (Liras et al. 2008).

Metabolic analysis was important in elucidating the unusual β-lactam biosynthetic pathway of the clavams, in particular in defining arginine as the precursor (Baggaley et al. 1997). A partial metabolic model was explored in chemostat cultures under varying nutritional limitations (Kirk et al. 2000). This model omits the production of urea as an obligatory pathway side product in the proclavaminate amidino hydrolase step (Elkins et al. 2002; Figures 6.3 and 6.4). The discovery of

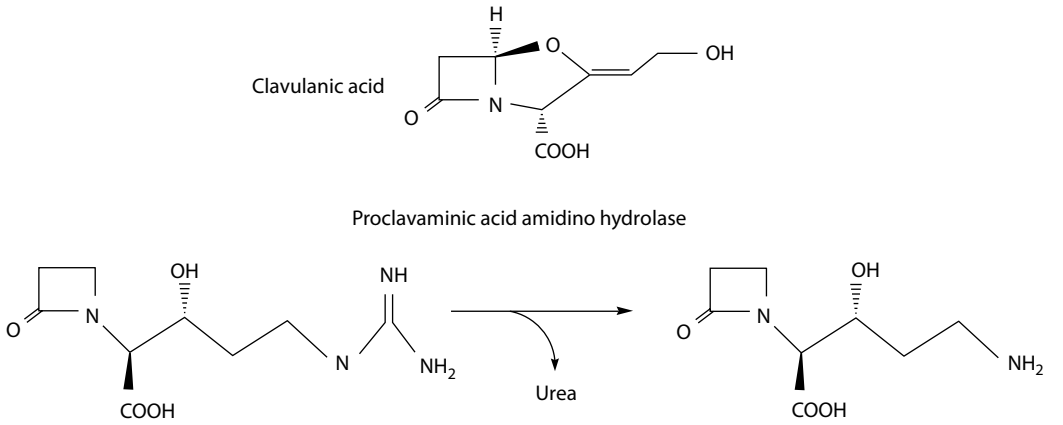

FIGURE 6.3 Clavulanic acid and proclavaminate amidino hydrolase in *Streptomyces clavuligerus*.

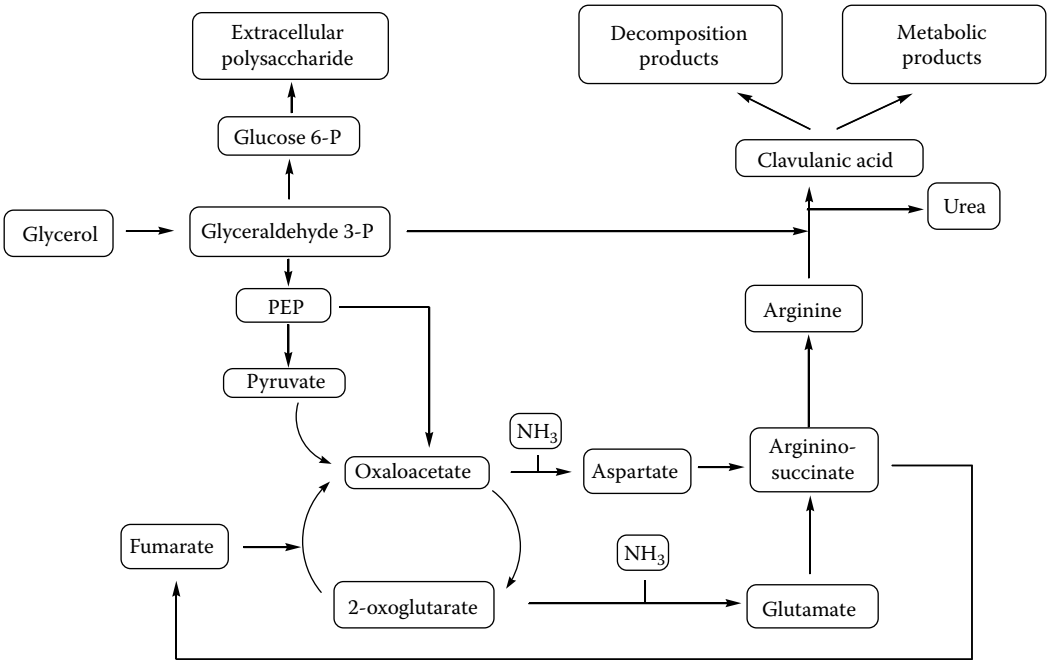

FIGURE 6.4 Metabolic analysis of the clavulanic acid fermentation.

urea as a fermentation product (in the absence of urease activity) was an unexpected outcome of investigations of the total nitrogen balance in the process (Valentine et al. 1995).

The degradation of clavulanic acid in fermentations with *S. clavuligerus* has a strong influence on product titers and productivity (Roubos et al. 2002). Moreover, cell-associated decomposition of clavulanic acid accompanies its chemical instability (Mayer and Deckwer 1996). This product loss might explain catastrophic failures to maintain clavulanic acid production noted with industrial-scale fermentations (Neves et al. 2001). Moreover, effects on OUR and glycerol consumption have been observed after the deliberate addition of clavulanic acid degradation products to fermentations; degradation products also promote the decomposition of their parent compound (Brethauer et al. 2008a, 2008b).

A logical conclusion is, therefore, that urea (if urease activities are suppressed by high ammonia concentrations) will accumulate in the fermentation independent of clavulanic acid losses

(chemical and/or biological). The time courses of urea and clavulanic acid production—at any level of productivity—would be a guide to the balance of biosynthesis and degradation rates.

A method of near real-time monitoring of key analytes, including ammonium and biomass, in a bioprocess for clavulanic acid using a complex medium has been described using attenuated total-reflectance mid-infrared spectroscopy (Roychoudhury et al. 2006).

6.3.2 Tetracyclines

In 2000, some 50 years after its discovery, researchers in Japan reported that the polyketide biosynthetic pathway for the 6-methyl family of tetracyclines produced the precursor for melanoid pigments—in fact, the melanin-like pigments (rather than the antibiotic) were the major products of the fermentation (Nakano et al. 2000). Evidence from both microbial physiology and genetic mutants showed that the branch point occurs before the chlorination step in the lengthy polyketide pathway (Figure 6.5). Surprisingly, the enzyme responsible for a late step in the pathway, anhydrotetracycline (ATC) oxygenase, could use an earlier intermediate as a substrate and, in effect, redirect metabolism toward pigment formation. Industrially, tetracyclines may have been manufactured for decades as "minor" fermentation products, with more of the fluxes being used to elaborate pigments as "shunt" metabolites. This suggests that rational enzyme reengineering or the use of gene-shuffling technologies could radically improve productivity in tetracycline producers.

Industrial practice, however, has frequently chosen a very different path. Many secondary producers are pigmented; albino mutants tend to be of low or negligible productivity. A spectacular example of multiple genes for pigment production in an industrially relevant microorganism arose from the complete genome sequencing of *Streptomyces avermitilis* (Omura et al. 2001). This large genome sequence contained 25 secondary metabolite gene clusters; four are concerned with the biosyntheses of melanin pigments, and two encode an ochronotic pigment and another polyketide-derived melanin.

Chlortetracycline and oxytetracycline producers also generate massive amounts of pigment (even wild-types produce some pigment, see Figure 6.6). The ability to quantitatively shift the balance of antibiotic and pigment would be of immense practical significance for the metabolic efficiencies

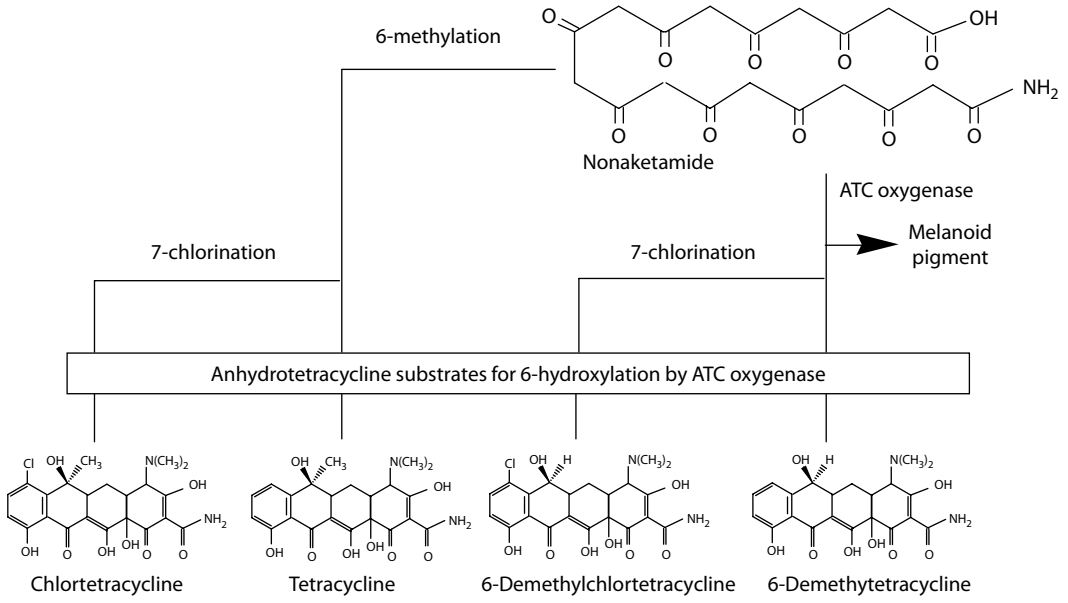

FIGURE 6.5 Biosynthesis of tetracyclines and pigments in *Streptomyces* spp.

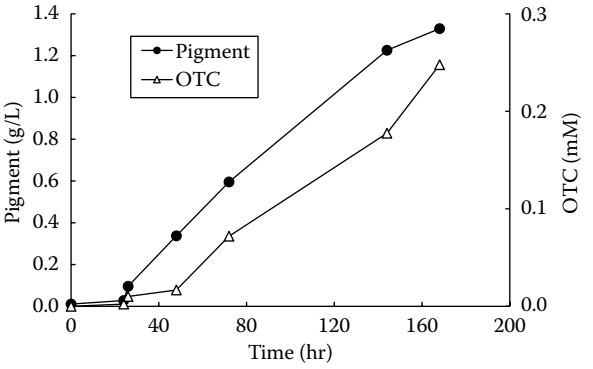

FIGURE 6.6 Accumulation of oxytetracycline and pigment in a wild-type *Streptomyces rimosus* stirred-tank fermentation.

of carbon and nitrogen use in commercial processes. In a genome like that of *S. avermitilis*, the progressive knocking out of pigment genes—and the detailed analysis of effects on the metabolome under fermentation conditions—would be an attractive route toward isolating a "designer" microbial producer with minimized waste of fermentation inputs in the form of pigmented material discarded in downstream processing.

6.3.3 Metabolomic Machinery of a Typical Streptomycete

Streptomyces coelicolor is a widely quoted model for industrially relevant Streptomycetes; the metabolic network of biochemistry inside this microbe includes 971 metabolic reactions (819 biochemical conversion and 152 transport events) and 500 metabolites (Borodina et al. 2005). Only 13% of the characterized genes in the genome are functional during metabolism. While the genome probably encodes over 7,800 genes encoding known proteins and enzymes, 2,300 of these require being assigned definite cellular functions.

Analysis of the genetic makeup of *S. coelicolor* suggests that only 30% of the metabolic network genes are always expressed, while 27% are often required, but 29% are required for growth on a restricted group of substrates (carbohydrates, organic acids, amino acids, nucleotides, or nitrates). A defined but small group (2%) is active when antibiotics are being biosynthesized, and a curious group of 12% appears to be required only under metabolic conditions that are presently unknown or difficult to simulate.

6.4 MICROBIAL PRODUCTION OF INDUSTRIAL ENZYMES

6.4.1 Proteases

Alkaline endopeptidases have been widely commercialized from *Bacillus* spp. for use in industries as diverse as food, brewing, detergent ("bio" washing powder) manufacture, meat processing, and others. For household detergents, alkaline proteases (optimally active at high pH and stable at high temperature) are widely used; genes encoding such alkaline proteases are widely distributed in microorganisms and have been cloned and sequenced. Spore-forming bacteria have an array of regulatory systems, some of which act to suppress protease formation until the appropriate developmental stage is reached, often at the end of rapid or exponential growth (Pero and Sloma 1993). This evolutionarily acquired feature acts to repress the metabolically expensive formation of exoenzymes if the nutritional conditions (in particular, the availability of low-molecular-weight carbon and nitrogen sources) make their formation superfluous—an example of how microorganisms avoid metabolic "burdens."

In chemostat experiments, the regulation of protease formation is clearly seen in the dependence of specific protease production rate on specific growth rate (Figure 6.7). Maximal rates of protease formation are, therefore, confined to a narrow range of moderate growth rates; process optimization, therefore, centers on how growth rates can be best managed to maximize the time during which optimal growth rates are sustained while supplying the required precursors for protein synthesis.

Within this framework of growth kinetics, the use of preformed amino acids is only fully apparent if analyses of total and peptidic amino acids are combined with measurements of protease activity, specific activity, and an exact knowledge of the primary amino acid sequence of the protease. For each individual amino acid—or, at least, those that survive acid hydrolysis of proteins and peptides—the sequence of release, solubilization, anabolic use (polymerization into cellular proteins and exoenzymes), and the catabolism of excess (as carbon and/or nitrogen sources) can be quantified (Figure 6.8). Such analysis can account for only some of the total amino acid use in the fermentation since tryptophan is entirely lost during acid hydrolysis, while chemical protecting agents are required for cysteine, cystine, and methionine measurements; asparagine and glutamine are quantitatively converted to aspartate and glutamate, respectively. Some amino acids can be used "excessively" (i.e., over and above the requirements for growth and exoprotein production); amino acid and peptide uptake mechanisms are regulated independently of those for glucose and ammonia, and amino acids and peptides can be utilized as both carbon and nitrogen sources, depending on the metabolic requirements of the cell population. As a consequence, successive phases of the fermentation can exhibit competition between the demands of growth and exoprotein synthesis for

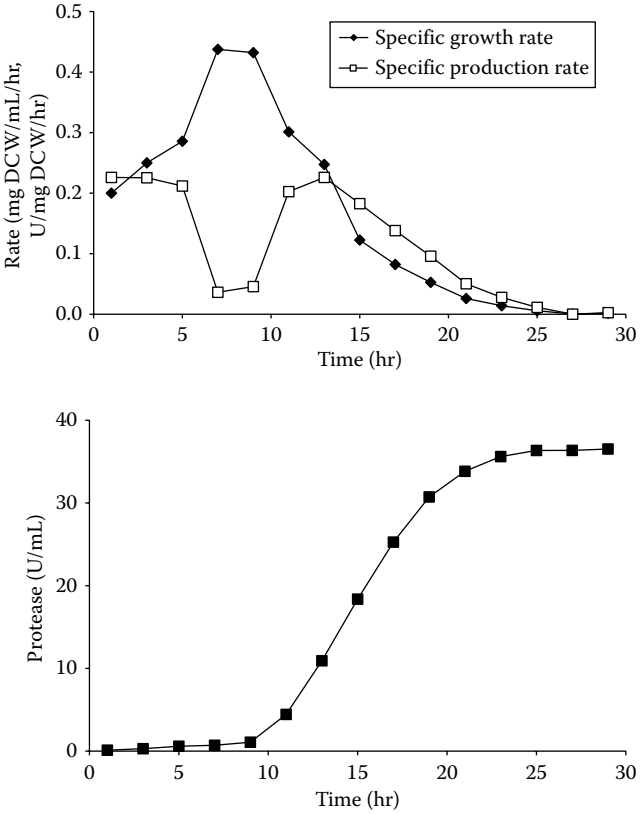

FIGURE 6.7 Growth and production rates in protease fermentation. (Data redrawn from Frankena, J., van Verseveld, H. W., and Stouthamer, A. H., *Appl. Microbiol. Biotechnol.* 22:169–76, 1985.)

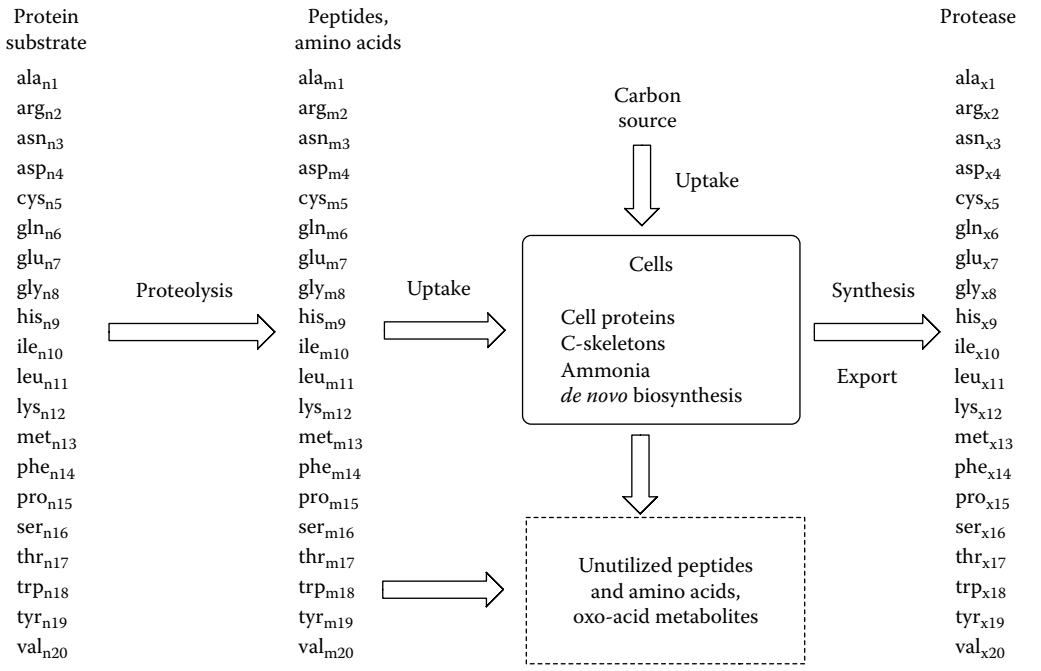

FIGURE 6.8 Processing of proteins inputs in protease fermentation.

amino acids and the partial catabolism of amino acids to yield oxo-acids and other degradation products that can be highly malodorous (for example, short-chain fatty acids from branched-chain amino acids).

To some extent, a protease fermentation operated commercially can be seen as a biotransformation: inexpensive protein inputs (vegetable proteins) are used as substrates to synthesize high-value-added enzymes. An idiosyncratic feature of a protease process, however, is that the protease is required to rapidly transform input proteins into its own biomass. A complete nitrogen-balancing approach to one such protease fermentation found that approximately 30% of the nitrogen remained unused (or perhaps unusable) in a pool of soluble peptides (Dowdells and Mousdale unpublished; and see Figure 6.9). The survival of minor exopeptidases in the presence of phenomenally high activities of the commercially protease is a crucial parameter in this bioprocess.

6.4.2 Cellulases

Over 10,000 species of fungi and bacteria are known to produce and secrete *cellulases*, a portmanteau term for the combination of four distinct enzymic activities (exo- and endo-β-glucanases, cellobiose hydrolase, and β-glucosidase). While the biochemistry and molecular biology of cellulases has been extensively studied, the biotechnology of cellulase fermentations is in its infancy (Lynd et al. 2002).

Cellulases are of low catalytic activity in comparison with other glycosidases (Klyosov 1988). This inconvenient fact—especially for a future biobased economy with "green" processing of plant biomass feedstock—has prompted Novozymes Biotech and Genencor to initiate intensive research programs to find or create thermostable cellulases (Mousdale 2010). A typical cellulase-producing organism might, therefore, be forced to divert large amounts of amino acids toward exoprotein secretion—the classic "metabolic burden"; much of the known regulation of cellulase production in microbes is consistent with molecular mechanism seeking to tightly regulate cellulase production.

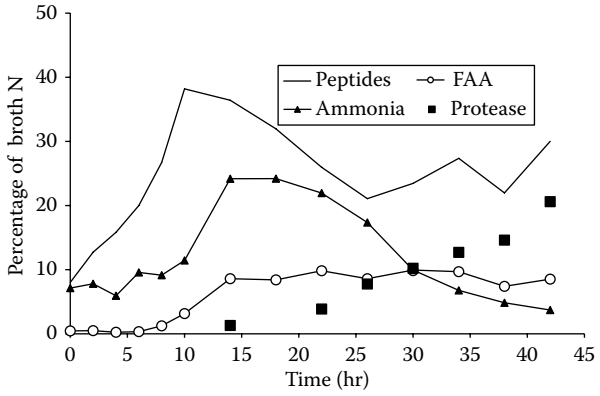

FIGURE 6.9 Dynamics of nitrogen use in protease fermentation.

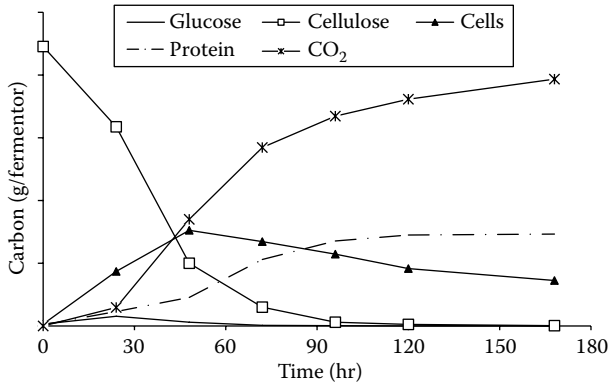

FIGURE 6.10 Carbon use in a fungal cellulase fermentation. (Redrawn from data Sáez, J. C. et al., *Biotechnol. Prog.*, 18, 1400–07, 2002.)

The principal industrial producer for cellulase is *Trichoderma reesei* (now often renamed *Hypocrea jecorina*). Examination of the genome sequence of this fungus yielded some startling results (Martinez et al. 2008), including:

- Although over 9,000 genes are potentially coded, the genome encodes fewer cellulases than rival fungal cellulase producers.
- Genomic analysis provided little mechanistic clues as to the organism's capacity for protein secretion.
- Numerous genes encoding biosynthetic pathways for secondary metabolites were identified.

Much of the metabolome may be irrelevant for cellulase production; a useful focus could be on the types of carbohydrate generated in situ during the course of the fermentation, in particular glucose, cellobiose, and disaccharides that may inhibit or stimulate cellulase production. In addition, cellulose substrate use can be sufficiently fast so that a carbon starvation occurred in batch fermentations (Sáez et al. 2002). Carbon use by the cellulase-hyperproducing strain was found to be inefficient with more than 75% of the output carbon accounted for as CO_2 (Figure 6.10). As with protease fermentations, attention must equally be paid to nitrogen inputs for cellulase synthesis, and most of the caveats expressed earlier for proteases apply equally well to cells producing and

secreting large amounts of cellulase. Sufficient dimensions of the metabolome must be included in the analysis to coalesce insights into operating guidelines. With an industrial medium containing multiple nitrogen sources—corn steep liquor, soya flour, wheat bran, ammonium sulfate, and yeast extract—the inclusion of protein, peptide, amino acid, and ammonia analysis is mandatory.

6.4.3 Recombinant Protein Production by Yeasts

Yeasts can perform posttranscriptional modifications directed by foreign genes, and several different species have been used for the production of recombinant proteins. *Pichia pastoris* has the added advantage of being able to grow to high cell densities and produce heterologous proteins using simple carbon sources (glycerol and methanol) with ammonia as the primary nitrogen source (usually added as ammonium hydroxide solution for pH control) in defined media free from animal-derived ingredients. The alcohol oxidase (*aox-1*) promoter from *P. pastoris* can be incorporated into methanol-inducible expression vectors for foreign genes; over 100 different proteins have been produced in this system with correct protein folding and secretion into the medium. The lack of endotoxins in *P. pastoris* makes any produced protein eminently suitable for therapeutic use, and *P. pastoris* (unlike some other yeasts) does not hyperglycosylate proteins, has no highly immunogenic cell wall oligosaccharides, and can accumulate the protein product to a high degree (80% of the total secreted protein), thus making downstream processing relatively straightforward.

An attempt to model fermentations with *P. pastoris* incorporated features of the known biochemistry of methanol use (Figure 6.11). Alcohol oxidase catalyzes the oxidation of methanol to formaldehyde, which then can be either catabolized (via formic acid) to CO_2 or condensed with xylulose 5-phosphate (a dihydroxyacetone synthase-catalyzed reaction) to give glyceraldehyde 3-phosphate.

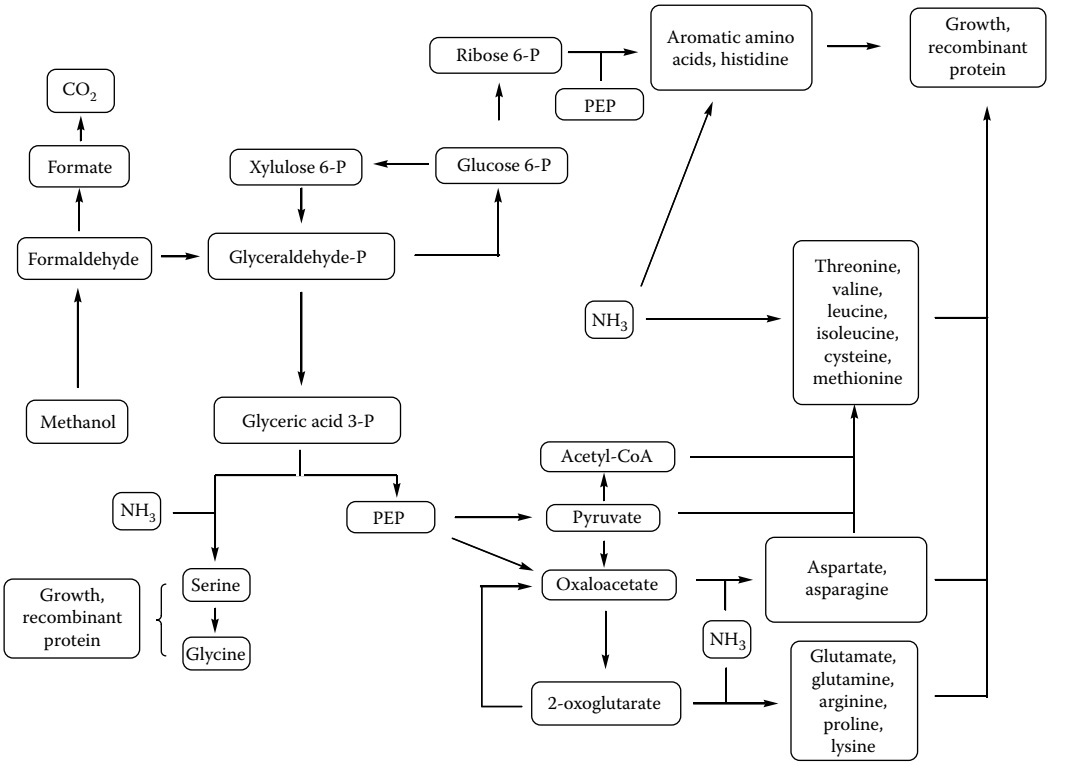

FIGURE 6.11 Metabolic analysis of methanol feeding to Pichia *pastoris* fermentation. (Based on the metabolic scheme of Ren, H. T., Yuan, J. Q., and Bellgardt, K. H., *J. Biotech*., 106, 53–68, 2003.)

The biochemical model, combined with feed rates, measured concentrations and estimates for specific rates, and so on, accounted for recombinant protein production in fed-batch mode but failed to predict the behavior in a methanol-overfed experiment, where, contradicting the belief that methanol in excess is toxic to *P. pastoris*, the growth rate increased greatly, the recombinant protein was degraded, and the accumulated methanol rapidly was utilized. An important area for future investigation is in understanding the metabolic responses of protein-secreting *P. pastoris* cells to excessive methanol supply.

One explanation for this unexpected breakdown of the *P. pastoris* fermentation could be the known ability of the cells to secrete proteases capable of degrading the secreted protein. This is worse in high-density fermentations and has only been partially remedied by adding amino acids, changing the pH, or using protease-deficient strains (Goodrick et al. 2001). Metabolomics techniques could provide a more complete account of proteases and the expression of protease genes in a recombinant protein process; a quite separate area of metabolism has, however, been identified in *P. pastoris*, namely, the great potential for diverting its primary biochemistry toward the production of 2,3-butanediol and other potential "biorefinery" outputs (Chung et al. 2010).

Microbial production of proteins differs from animal cell culture systems in that microbes (yeast or bacteria) are assumed to be entirely prototrophic for amino acids. Animal cell models can incorporate multiple rates of uptake, polymerization, and interconversion; some amino acids in the medium can be used as carbon sources via deamination (Mousdale 2007). The "traditional" means of medium and process optimization has relied on lavish resources for online and offline analyses (Gorfien et al. 2003). Increasingly, as animal cell biopharmaceuticals enter into biogeneric product competition, costs of media and feeds will become commercial issues, and the actual rates and extents of the use of medium components may come under intense scrutiny (Mousdale 2008). The metabolomics approach has been successful for optimization of growth conditions in serum-free and serum-reduced systems and in optimizing cell cultures for antibody production (Čuperlović-Culf et al. 2010). Studies with industrial-scale mammalian cell cultures suggest a future for metabolomics as a high-resolution molecular analysis tool in cell culture engineering (Chrysanthopoulos et al. 2010).

6.4.4 Metabolomic Machinery of a Yeast Cell

The metabolic network of biochemistry inside a yeast (*S. cerevisiae*) cell has been modeled as 1,175 metabolic reactions and 584 metabolites (Förster et al. 2003). Of the reactions, 1,035 could be assigned to enzymes encoded by known genes in the yeast genome, while another 140 could be assigned from knowledge of biochemistry and cell physiology. Only 16% of the known and characterized genes in the yeast genome were involved in this computational exercise—the genome probably encodes over 6,000 genes for proteins and enzymes, but 2,000 have unknown or speculative functions.

6.5 BIOTECHNOLOGY OF PRODUCTS FROM HIGHER FUNGI

The exploitation of this group of organisms has somewhat been neglected, primarily due to the complex nature of their life cycles (Lin et al. 2005). When discussing a group of microorganisms as metabolically and biochemically diverse as the higher fungi, which occupy a vast range of habitats from terrestrial forests to marine environments, it is important to begin by defining what is meant by *higher fungi*. Different meanings of this term can be found (Carlile et al. 2001), and at present, fungal taxonomy is in flux due to the impact of new DNA-based classification methods (Hibbett 2007); but, in this context, the definition of Fazenda et al. (2008), which follows that of Worgan (1968), is probably the simplest. These authors defined the higher fungi as those filamentous fungi having a distinct macroscopic sporing structure or body. This immediately differentiates the higher fungi from the fungi the biotechnology industry is more familiar with, for example, lower fungi

such as *Penicillium*, *Aspergillus*, and *Rhizopus*, which do not produce such conspicuous macrosporing structures. The two major divisions of the Eumycota (true fungi), which contain members of the higher fungi, are the Basidiomycota and the Ascomycota.

Members of the higher fungi may metabolize lignocellulosic or algal fibrous materials (Lin et al. 2005), and thus make a tremendous contribution to the carbon cycle; may be pathogenic to plants, insects, and animals; or may be symbiotic with plants (e.g., ectomycorrizhal fungi). Many of their conspicuous sporing bodies have traditionally been consumed by humankind as foods, such as *Lentinula edodes*, the shiitake mushroom, and *Grifola frondosa*, or the maitake mushroom; or, if nonedible, as medicines (e.g., *Ganoderma lucidum*, *Schizophyllum commune*, and *Trametes versicolor*; Sullivan et al. 2006). Traditionally, these valuable products (mushrooms) have been produced by solid substrate fermentation (SSF), using materials rich in carbon sources but low in nitrogen. This usually takes from several weeks to months before the product, the sporing body, is harvested. The production process is slow, subject to the vagaries of climate and raw materials, and generally poorly controlled.

In Eastern traditional medicine, there is considerable evidence for the impact of consumption of higher fungi or their extracts upon disease processes, such as tumor formation, cancers, and infections. This was often associated with the synthesis of complex exopolysaccharides related to the spore structures. In turn, this led to an interest in obtaining "purified" compounds from these fungi, which could be evaluated in Western-style drug trials. Given the limitations of the traditional SSF approach described in the previous paragraph, this contributed to the development and investigation of the culture of the vegetative (hyphal) forms of these fungi in submerged liquid fermentation (SLF) systems. Here, the production environment could be defined and controlled, allowing a link between processing factors and product quality (or pharmacological potency).

Before going further, it is relevant to all that follows to keep in mind the very complex life cycles of the higher fungi. Both the Ascomycota and the Basidiomycota are characterized by the formation of a dikaryotic stage in their life cycle. In the Basidiomycetes this dikaryotic stage, where each compartment in the fungi contains two haploid nuclei, is long lasting, and the dikaryotic stage may be dominant; in Ascomycetes, this stage is usually of far shorter duration. However, the genetic complexity and sophistication of these fungi imply a considerable synthetic burden, which fundamentally affects such process-related factors as specific growth rates, nutrient uptake rates, and metabolite synthesis rates. Since the rates of replication of these fungi in fermentors and their associated metabolism are usually significantly lower than the simpler industry fungal workhorses listed earlier (Fazenda et al. 2008, 2010), there must be pressing reasons for culturing higher fungi in fermentation systems in order to make the process worthwhile.

Despite the vast metabolic potential of the higher fungi, relatively little is known about their process physiology, which might be simply defined as how they interact with the environment within bioreactor vessels. Many fermentation studies into the production of higher fungal biomass or metabolites lack the level of detail normally seen in more familiar industrial fermentation reports. In many instances, not much is known about the genetic makeup of these organisms, although modern molecular techniques are contributing to rapid change here. There is a pressing need for systematic and detailed investigations into the bioprocessing challenges occurring within higher fungal cultures in fermentor systems, including analysis of carbon flux to growth, product, and by-product formation. The aim of the cultivation process or the nature of the product itself can be used to group higher fungal culture processes in order to illustrate the nature of the challenges in the bioprocessing of higher fungi.

6.5.1 Higher Fungal Biomass

The first recorded culture of the vegetative stages of a higher fungus took place more than 60 years ago and was intended to rapidly generate the mycelia biomass of *Agaricus campestris* (edible mushroom) for use as a food ingredient in processed foods. This was considered as a cheaper, purer route to mushroom flavoring in foodstuffs.

Fungal biomass ranges from 40% to 60% by weight as protein, so potentially this is a very valuable source of protein of good quality (Finn et al. 2006). Traditionally, the sporing structures have been eaten for this reason, especially where other protein sources are scarce within a diet, but cultivation of the vegetative cells in fermentors significantly increases the rate of protein production.

Vegetative cultures of ectomycorrizhal fungi have been grown in fermentors for use as plant growth symbionts (Harvey 1991). The presence of the fungal symbiont increases plant growth rate and disease resistance by increasing the available area for nutrient absorption in the root zone. The primary aim of these cultures is the maximization of biomass, but almost equally important is the generation of fungal cells with clamp connections, as the presence of these seems essential to the fungus "infecting" the plant partner (Fazenda et al. 2010). Cultivation of *Laccaria* as a potential ectomycorrizhal inoculant for commercial forestry plants is carried out in stirred tank vessels at low stirrer speed (Fazenda et al. 2010).

Generally such processes are batch in nature, running at 20–36°C, often without pH control, and with very modest agitation rates (100 to 200 rpm); lower fungal processes require a stirring speed between 300 to 800 rpm. Aeration rates tend also to be much lower, suggesting shear-sensitive microorganisms, with comparatively low growth rates. Batch processing times are substantially longer than lower fungal processes; cultures last usually 5–7 days as opposed to 2–3 days.

6.5.2 Exopolysaccharides from the Higher Fungi

Bioactive exopolysaccharides (EPS) have been purified from medicinal mushrooms and from cultures of the vegetative forms of these microorganisms. Although structurally diverse, most of these are water-soluble β-D glucans, sometimes with heterosaccharide side chains or proteoglucan complexes (Sullivan et al. 2006). There is substantial evidence for the immunostimulatory role of these (often) high-molecular-weight EPS compounds. Battle et al. (1998) reported that the immunomodulatory effects of fungal glucans may be mediated by binding to a membrane complement receptor Type 3 on macrophages. The evidence of efficacy in cancer therapy is sufficiently convincing for some of these compounds, such as lentinan (e.g., from *L. edodes*), to have undergone clinical trials. Scleroglucan has a unit repeated structure with a trio of β-1,3-linked glucose residues and a β-1,6-glucosyl side chain (Figure 6.12). This natural polymer dissolves in water to give solutions that have stable viscosities even at high temperatures and over a remarkable range of pH values; scleroglucan has found applications in the oil industry and in adhesives, watercolors, and printing inks.

Fermentation processes have been developed for the manufacture of pure EPS from vegetative cultures of a range of higher fungi, including *L. edodes*, *G. frondosa*, *Sclerotium rolfsii*,

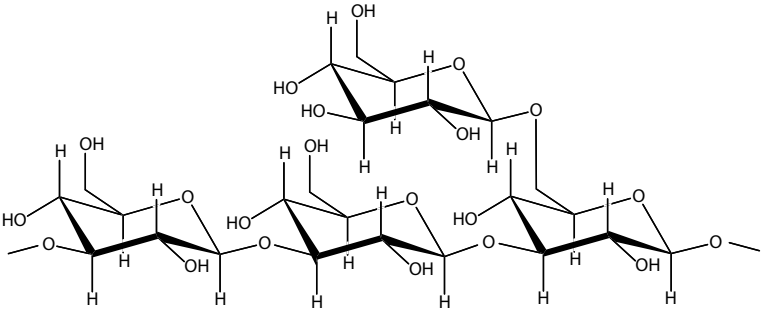

FIGURE 6.12 Chemical structure of the exopolysaccharide scleroglucan produced by the higher fungus *Sclerotium glucanicum*.

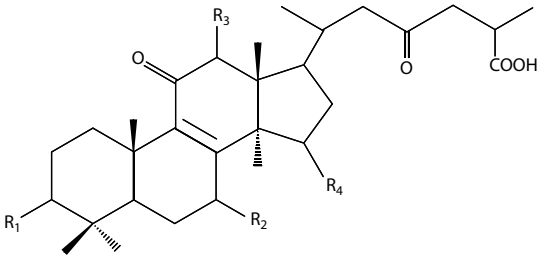

FIGURE 6.13 Chemical structure of ganoderic acids produced by the higher fungus *Ganoderma lucidum*.

S. glucanicum, and *G. lucidum*. Although involving different microorganisms, such processes share many characteristics, and focusing on two examples for which there is a relative abundance of published material will illustrate the general approach: *S. glucanicum* (scleroglucan) and *G. lucidum*, which produces ganoderic acids (Figure 6.13) as well as EPS.

The recent realization that fungal β-glucans are potent bioactive molecules has led to a large number of studies into their production, usually in simple shake-flask batch culture systems. However, there are far fewer studies in stirred-tank reactor (STR) and other fermentor systems (Seviour et al. 2010a, 2010b). Most fermentor studies into scleroglucan production have involved STR fermentors usually fitted with Ruston turbines (often described as "high shear," although no mention is made of impeller speeds!). Typical yields of scleroglucan in STR batches range from around 10g/L (Wang and McNeil 1995a) up to 15g/L and over in fed-batch systems (Wang and McNeil 1994). Control of dissolved oxygen tension is especially important as high DO favors biomass formation at the expense of scleroglucan (Wang and McNeil 1994). Rau (1992) reported that low dissolved oxygen tension (DOT) specifically stimulates scleroglucan formation. Hsieh et al. (2006) also noted this effect in relation to grifolan formation from *G. frondosa*.

In a study into temperature effects on scleroglucan synthesis, Wang and McNeil (1995b) showed that the temperature optima for scleroglucan production and growth were distinct (28°C and 32°C, respectively). More significantly, they showed that oxalate production rose significantly as process temperature fell from 28°C, such that at lower temperatures close to ambient (e.g., 20°C) most carbon flux went to oxalate formation, not to EPS. Additionally, they reported that at 20°C only 50% of the total organic acids present was oxalate, and the remainder were malic and fumaric acids. These findings clearly indicate a relatively poor understanding of the metabolomes in higher fungi, and it is possible, therefore, that we could be missing out on a great deal of potentially exploitable metabolic diversity.

Reports into the morphological form of the fungus associated with EPS production generally indicate a pelleted form, although there are contradictory reports of a more dispersed mycelial form being optimal; these are summarized in Wang and McNeil (1996). Although most studies have been carried out in conventional STRs, some research into airlift fermentors (Kang et al. 2001) indicates that scleroglucan formation in nonmechanically agitated fermentors may produce equivalent or higher final concentrations of the EPS at lower costs and slightly faster than in the STR. This seems understandable given the DOT effects previously reported. Further discussion on the bioprocessing aspects of scleroglucan can be found in Giavasis et al. (2005).

G. lucidum has been used in traditional Chinese medicine for at least four millennia (Sullivan et al. 2006). It has widely asserted antitumor, cholesterol- and blood pressure-lowering, and anti-infection properties linked to the presence of glucan-type polymers in the spore body. Numerous studies have examined production of both cell mass and EPS using vegetative mycelial cultures of *G. lucidum* in a range of fermentor systems, from shake flasks up to STR and airlift reactors (Chen and Seviour

2007). Often there is little actual structural characterization of the biopolymer produced in these studies, with simple alcohol precipitation being used to quantify total EPS. This approach to product quality assessment in all probability hides much structural variation in the EPS and obscures much of the relationship between important factors, such as EPS molecular weight distribution and composition and reactor operational features (Seviour et al. 2010a, 2010b).

A recent study by Fazenda et al. (2010) showed the effect of oxygen supply to cultures of *G. lucidum* in an STR at 300 rpm and 30°C on growth and EPS production. Two fed-batch protocols were followed: one where oxygen was set at a minimum value of 30% saturation, and another in which culture DOT was allowed to fall naturally to zero with culture growth. Under oxygen-controlled conditions, biomass reached a maximum of 27 g/L within seven days, and the culture was largely in a dispersed highly branched form by process end, consistent with more rapid growth. By contrast, the oxygen-limited culture was largely clumped or pelleted, and produced very high levels of EPS (around 4.55 g/L). As noted earlier, oxygen limitation has been widely reported to increase the production of a range of β-glucans. This study reported an unusually high level of EPS in the oxygen-limited cultures, whereas Seviour et al. (2010a, 2010 b) commented on the normally very low levels of EPS in *Ganoderma* cultures. Tang et al. (2009b), using an optimized fed-batch with bi-staged pH and DOT control, achieved maximal levels of EPS (assayed using the phenol sulfuric acid method) of around only 1.38 g/L in a STR vessel. They contrasted this with a previous study (Lee et al. 1999) where EPS of around 13.6 g/L was reported using gravimetric analysis following precipitation. According to Tang et al. (2009b), the analytical method used by Lee and colleagues could overestimate EPS by a factor of 10. This gives a significant insight into the real difficulties in comparing many studies involving higher fungi in fermentors. Differing assay techniques lead to differences in "product" levels, and product is not always clearly structurally defined in all of these studies.

Clearly, fermentor cultivation has the potential to generate much increased quantities of EPS from pure cultures of higher fungi in defined media, but considerably more attention needs to be paid to characterization of the range of products arising from these cultures using benchmarked analytical techniques before certainty about the validity of this approach can be achieved.

6.5.3 Higher Fungal Enzymes

Like all fungi, the higher fungi are absorptive in nature, and this requires them to secrete into the extracellular environment "digestive" enzymes to degrade macromolecules into simpler sugars and small nitrogenous molecules, which can then be absorbed. Many higher fungi can degrade lignocellulose, and the white rot fungi are specialists in this activity (Fazenda et al. 2008). In order to degrade a highly recalcitrant molecule such as lignocellulose the fungi secrete a coordinated battery of enzymes, including lignin peroxidase, manganese peroxidase, and phenol oxidase (laccase; Baldrian 2006). Although many studies into the overproduction of these enzymes by selected white rot fungi in submerged liquid culture have reported high yields and activities, there has been far less research into the development of an effective large-scale lignocellulose degradation system.

Given the current drive toward fuels from renewable resources, and since lignocellulosics represent the largest renewable source, it would be surprising if the higher fungi did not have a future role to play. It may be that their metabolic potential may be exploited by introducing fungal genes encoding lignin-degrading enzymes into more industrially tractable hosts.

6.5.4 Bioremediation by Higher Fungi

White rot fungi (and derived enzymes) are capable of degrading a wide range of xenobiotics, from polychlorinated biphenyls to polyhydroxyalkanoates and plastics. They have been examined for

bleaching of dyes and pigments (Couto and Herrera 2006). This area has received relatively little research attention so far, and once again the higher fungi may well be regarded in these days of movable genes as a rich source of useful metabolic activities that, through metabolic engineering, could find their way into other species, with more desirable growth rates and better suitability to industrial biotechnology.

6.5.5 Metabolomics of Higher Fungi

Given the practical difficulties posed by higher fungi (and their lifestyles), how feasible is the task of pursuing knowledge of their metabolism for biotechnology? Given a sufficiently high-value product with medicinal or nutraceutical impact, metabolomics—because of the broad scope of its investigational approach—would be a promising route for unraveling the apparent complexities of growth kinetics and cell development and the massive reordering of metabolism that is required during the transition from growth (the trophophase of classical industrial microbiology) to rapid and extensive product formation (idiophase).

Indeed, a published investigation of EPS production by *G. resinaceum* illustrated an apparent conflict between EPS formation (maximal in the early stages of the fermentation) and rapid growth with a later onset (Figure 6.14). Fermentation practice copes best with distinct tropho- and idiophases; the occurrence of product (EPS) formation that could compete with growth implies that investigation of the full metabolome would offer the breadth of data and insights necessary to define optimized process management strategies. Minimal information on cell compositional analysis for higher fungi is available (Gottlieb and Van Etten 1966). Yeast cell models may, however, provide testable computational tools for initial process modeling (Förster et al. 2003).

Cyclic depsipeptides synthesized by isolates of *Rosellinia* fungus prove to be biologically active against nematodes of veterinary and agricultural importance (Yanai et al. 2004; Jeschke et al. 2005). The PF1022A depsipeptide anthelmintics typify the biochemical complexity of many secondary products; the precursors N-methyl-L-leucine, D-lactic acid, and D-phenyllactic acid derive from pools of amino acid (leucine), aromatics (L-phenyllactic acid), and glycolytic (L-lactic acid) intermediates and act as substrates for a nonribosomal peptide synthetase (Figure 6.15). The integration and harmonization of different aspects of primary metabolism and its use to drive secondary metabolism in this organism comprise a persuasive example of where wide-ranging metabolic studies would be advantageous for process design and management.

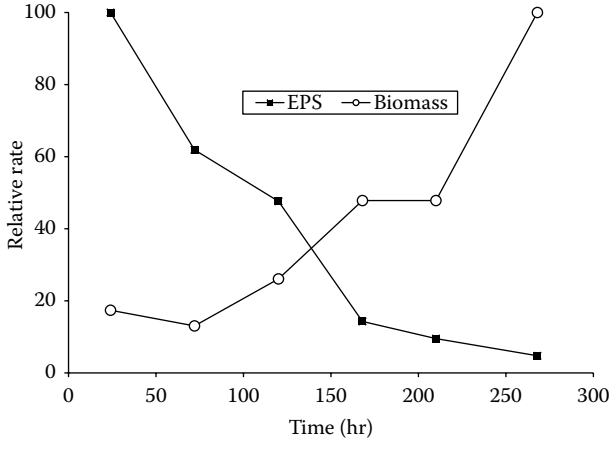

FIGURE 6.14 Exopolysaccharide production and growth in *Ganoderma resinaceum* fermentations. (Redrawn from data Kim, H. M. et al., *J. Microbiol.*, 44:233–42, 2006.)

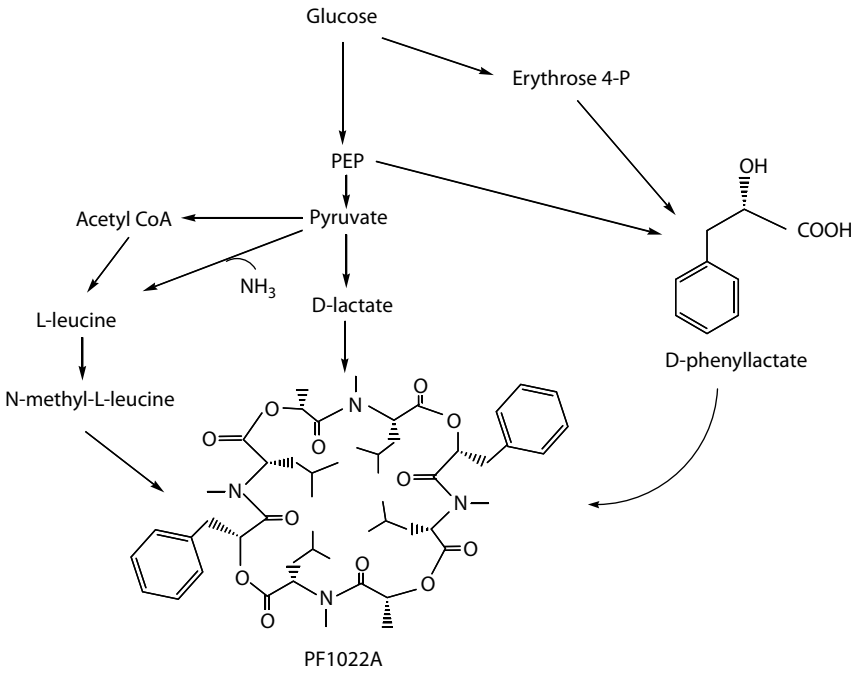

FIGURE 6.15 Metabolic "routing" of precursors to PF1022A anthelmintic formation by *Rosellinia* fungus.

6.6 HOW LARGE IS THE METABOLOME AND HOW MUCH IS RELEVANT TO INDUSTRIAL AND COMMERCIAL BIOMANUFACTURING?

Neither question is trivial. Limiting the metabolome to the metabolic intermediates of known enzymes seriously underestimates its potential size because so many genes have no defined functions. Present databases may not be capable of comprehensively retrieving all known metabolites (Kind et al. 2009). There is a definite need to increase coverage on small molecules in databases for all taxonomic species (microbial, plant, and animal) by, for example, interrogating multiple chemical databases. With the rice plant, for example, different databases gave "hits" in a very wide range (from under 50 to nearly 10,000), and there remain serious concerns about confusions with bacterial and fungal compounds, pesticide metabolites, and so on and about obstacles to compiling peer-reviewed public databases with a knowledge base of metabolites.

For the industrial biotechnologist, the successful application of metabolomics depends on the features of an individual fermentation process: the desired targets of improvement, the guidelines presented by experience and operating data, the availability of analytical data sets, the relevance (or otherwise) of results from published sources, and—ultimately—budgetary considerations. Examples have been given of where limitations on product formation and yield, such as clavulanic acid (a secondary metabolite, the net formation of which is heavily constrained by degradation) and protease fermentations (a near-biotransformation with severe potential nutrient bottlenecks), can be given high-resolution study with a small subset of the total metabolome. In contrast, novel processes with higher fungi would benefit enormously from understanding the metabolic networks that compose the metabolome.

Curiosity-led research and experimentation would naturally tend to whole-metabolome studies. In the case of the higher fungi, this may be the optimal approach for understanding complex interactions between growth and production kinetics. Elsewhere, the case for metabolomics supplanting metabolic and combinatorial engineering is weak (Vaidyanathan 2005). For secondary metabolites,

manipulating natural regulatory networks' pathway-specific regulators has emerged as a powerful technique (Chen et al. 2010). Given that 30% of known open reading frames in microbes lack any functional annotation, the metabolome is—within present definitions—woefully incomplete (Saqi et al. 2009).

The pragmatic solution is that metabolomics needs focused *questions* for microbial biotechnology. Since much of the primary metabolism in many bacteria and yeasts is understood, detailed chemical and biochemical analysis can generate working models of metabolism. If, however, these models fail to account for all encountered symptoms in fermentations, this should not be taken as failure but as the starting point for further refinement, integrating information from all available sources and approaches to discover novel metabolic properties of cells. In other words, successive approximation rather than global understanding is likely to remain the viable route toward fermentation optimization.

This would change if *real-time metabolomics* were to be realized. The term real-time metabolomics has appeared in strategic scenarios for clinical research (Lauer and Skarlatos 2010). Further development of infrared spectroscopy techniques for the noninvasive monitoring of fermentations, and subsequent inferring of enzyme activities in computational models, would be an advance toward this desirable goal (Roychoudhury et al. 2007). A recently announced Biotechnology and Biological Sciences Research Council (BBSRC) funded project in the United Kingdom has this objective as its strategic goal (http://oasis.bbsrc.ac.uk/netans-bin/gate.exe?f=doc&state=9np68u.1.1); the planned research aims to investigate the feasibility of measuring flux in chemostat cultures of *P. pastoris* in real time via a combination of in situ near-infrared and mid-infrared spectroscopies, off-gas analysis, novel error minimization strategies, and referencing to offline metabolome analysis. This rather appropriately returns us to the question posed earlier in this chapter, "How much of the metabolome do we need to measure?" Real-time metabolome research in the field of bioprocessing should help us answer that question.

SUMMARY

Metabolomics is one of the emerging "omics" that can potentially provide a detailed account of the metabolic routes and local and global regulatory mechanisms under steady-state conditions. Metabolomics studies also depict species' dynamic responses to genetic, biotic, and abiotic changes in their environment.

Metabolomics approaches can be applied to microbiological systems, in particular industrial bioprocesses. Since major fermentation outputs are secreted products, the "system" for microbial biotechnology is the fermentor or bioreactor viewed as a totality of fluxes, metabolites, enzymes, and transport and export mechanisms.

The understanding of microbial physiology is a clearly desirable aim for knowledge generation. Because many genes in sequenced microbial genomes are of undefined function, and because novel metabolites have constantly been identified in both poorly explored and well-understood prokaryotic and eukaryotic species, an important place will remain for curiosity-led research and the necessity to accept "surprises" in microbial metabolism.

The continued development of adequate sampling methods and modern analytical techniques for metabolomics research will enable in-depth knowledge of microbial production of metabolites and macromolecules (proteins, enzymes, extracellular polysaccharides, etc.). Accurately focused questions will, however, need to be framed to reap the maximum benefit of metabolomics. Extending methodologies to encompass real-time metabolomics with noninvasive analysis to monitor events inside fermentors and bioreactors is a key area for conceptual advances.

The higher fungi represent a poorly exploited group of organisms that exhibits great biodiversity and a treasure trove of novel products and genetic capabilities. Their complex life cycles and little-understood bioprocess behaviors provide fertile ground for metabolomics approaches and research to provide the knowledge base for their wider introduction to modern biotechnology.

REFERENCES

Allman, A. A. 2007. Fermentors: Design, operation, and applications. In El-Mansi, E. M. T., Bryce, C. F. A., Demain, A. L., Allman, A. R., (eds.) *Fermentation Microbiology and Biotechnology*, 2nd edition, pp. 451–92. Boca Raton, FL: CRC/Taylor and Francis.

Almaas, E., B. Kovács, T. Vicsek, Z. N. Oltvai, A. L. Barabási. 2004. Global organization of metabolic fluxes in the bacterium *Escherichia coli*, *Nature* 427:839–43.

Baggaley, K. H., A. G. Brown, C. J. Schofield. 1997. Chemistry and biochemistry of clavulanic acid and other clavams, *Nat. Prod. Rep*. 140:309–33.

Baldrian, P. 2006. Fungal laccases—occurrence and properties. *FEMS Microbiol. Rev*. 30:215–42.

Battle, J., T. Ha, C. Li, V. D. Della Beffa, et al. 1998. Ligand binding to (1→3)-β-D-glucan receptor stimulates NFκB activation, but not apoptosis in U937 cells. *Biochem. Biophys. Res. Comm.* 249, 499–504.

Bizukojc, M., S. Ledakowicz. 2009. Physiological, morphological and kinetic aspects of lovastatin biosynthesis by *Aspergillus terreus*, *Biotechnol. J*. 4:647–64.

Borodina, I., P. Krabben, J. Nielsen. 2005. Genome-scale analysis of *Streptomyces coelicolor* A3(2) metabolism, *Genome Res*. 15:820–9.

Brethauer, S., M. Held, S. Panke. 2008a. High concentrations of clavulanic acid but not of its degradation products decrease glycerol consumption and oxygen uptake rates in cultures of *Streptomyces clavuligerus*, *Biotechnol. Bioeng*. 100:439–47.

Brethauer, S., M. Held, S. Panke. 2008b. Clavulanic acid decomposition is catalyzed by the compound itself and by its decomposition products, *J. Pharm. Sci.* 97:3451–5.

Carlile, M. J., S. C. Watkinson, G. W. Gooday. 2001. *The Fungi*. London: Academic Press.

Castle, A. 2008. The NIH roadmap to understanding biological pathways and networks with metabolomics. http://www.metabolomicssociety.org/images/tutorials/Metabolomics_2008_Castle.pdf.

Chen, J., R. Seviour. 2007. Medical importance of fungal β-(1→3),(1→6) glucans, *Mycol. Res*. 111:635–52.

Chen, Y., M. J. Smanski, B. Shen. 2010. Improvement of secondary metabolite production in Streptomyces by manipulating pathway regulation, *Appl. Microbiol. Biotechnol*. 86:19–25.

Chrysanthopoulos, P. K., C. T. Goudarb, M. I. Klapa. 2010. Metabolomics for high-resolution monitoring of the cellular physiological state in cell culture engineering, *Met. Eng*. 12:212–22.

Chung, B. S., S. Selvarasu , A. Camattari , J. Ryu , H. Lee, J. Ahn , H. Lee, D-Y. Lee. 2010. Genome-scale metabolic reconstruction and in silico analysis of methylotrophic yeast *Pichia pastoris* for strain improvement, *Microb. Cell Fact*. 9:50.

Couto, S. R., J. L. Toca Herrera. 2006. Industrial and biotechnological applications of laccases, *Biotechnol. Adv*. 24:500–13.

Čuperlović-Culf, M., D. A. Barnett, A. S. Culf, I. Chute. 2010. Cell culture metabolomics: applications and future directions*, Drug Discovery Today* 15:610–21.

de la Fuente, A., L. M. Lorenzana, J. F. Martín, P. Liras. 2002. Mutants of *Streptomyces clavuligerus* with disruptions in different genes for clavulanic acid biosynthesis produce large amounts of holomycin: Possible cross-regulation of two unrelated secondary metabolic pathways, *J. Bacteriol*. 184:6559–65.

Ding, M-Z., W.-H. Xiao, Y.-J. Yuan. 2010. Metabolome profiling reveals adaptive evolution of *Saccharomyces cerevisiae* during repeated vacuum fermentations, *Metabolomics J.* 6:42–55.

Dowdells, C., R. L. Jones, M. Mattey, M. Benčina, M. Legiša, D. M. Mousdale. 2010. Gluconic acid production by *Aspergillus terreus*, *Lett. Appl. Microbiol*. 51:252–7.

Elkins, J. M., I. J. Clifton, H. Hernández, L. X. Doan, C. V. Robinson, C. J. Schofield, K. S. Hewitson. 2002. Oligomeric structure of proclavaminic acid amidino hydrolase: evolution of a hydrolytic enzyme in clavulanic acid biosynthesis, *Biochem. J*. 366:423–34.

Fazenda, M. L., L. H. Harvey, B. McNeil. 2010. Effects of dissolved oxygen on fungal morphology and process rheology during fed-batch processing of *Ganoderma lucidum*, *J. Microbiol. Biotechnol*. 20:844–51.

Fazenda, M. L., R. Seviour, B. McNeil, L. M. Harvey. 2008. Submerged culture fermentation of "higher fungi": the macrofungi, *Adv. Appl. Microbiol*. 63:33–109.

Finn, B., L. H. Harvey, B. McNeil. 2006. Near infrared spectroscopic monitoring biomass, glucose, ethanol and protein content in a high cell density baker's yeast fed-batch culture, *Yeast* 23:507–17.

Förster, J., I. Famili, P. Fu, B. Ø. Palsson, J. Nielsen. 2003. Genome-scale reconstruction of the *Saccharomyces cerevisiae* metabolic network, *Genome Res*. 13:244–53.

Frankena, J., H. W. van Verseveld, A. H. Stouthamer. 1985. A continuous culture study of the bioenergetic aspects of growth and production of exocellular protease in *Bacillus licheniformis*, *Appl. Microbiol. Biotechnol*. 22:169–76.

Giavasis, I., L. M. Harvey, B. McNeil. 2005. Scleroglucan. In Steinbuchl, A., Doi, Y. (eds.) *Biotechnology of Biopolymers*, pp. 679–702. Weinheim: Wiley-VCH.

Goodrick, J. C., M. Xu, R. Finnegan, B. M. Schilling, S. Schiavi, H. Hoppe, N. C. Wan. 2001. High-level expression and stabilization of recombinant human chitinase produced in a continuous constitutive *Pichia pastoris* expression system, *Biotechnol. Bioeng*. 74:492–7.

Gorfien, S. F., W. Paul, D. Judd, L. Tescione, D. W. Jayme. 2003. Optimized nutrient additives for fed-batch cultures, *BioPharm International* 16(4): 34–40.

Gottlieb, D., J. L. Van Etten. 1966. Changes in fungi with age. 1. Chemical composition of *Rhizoctonia solani* and *Sclerotium bataticola*, *J. Bacteriol*. 91:161–8.

Harvey, L. M. 1991. Cultivation techniques for the production of ectomycorrhizal fungi, *Biotechnol. Adv*. 9:13–29.

Hayward, A. 2008. On-line, in-situ, measurements within fermenters. In McNeil, B., Harvey, L. M. (eds.) *Practical Fermentation Technology*, pp. 271–88. Chichester, UK: John Wiley.

Hibbett, D. S., M. Binder, J. F. Bischoff, M. Blackwell, P. F. Cannon, O. E. Eriksson, S. Huhndorf. 2007. A higher-level phylogenetic classification of the fungi, *Mycol. Res*. 111:509–47.

Hsieh, C., C. J Liu, M.H. Tseng, C. T. Lo, Y. C. Yang. 2006. Effect of olive oil on the production of mycelial biomass and polysaccharides of *Grifola frondosa* under high oxygen concentration aeration, *Enz. Microb. Technol*. 39:434–9.

Jeschke R, K. Iinum, A. Harder, M. Schindler, T. Murakami. 2005. Influence of the cyclooctadepsipeptides PF1022A and PF1022E as natural products on the design of semi-synthetic anthelmintics such as emodepside, *Parasitol. Res*. 97(Suppl. 1): S11–16.

Kang, X., H. Wang, Y. Wang, L. M. Harvey, B. McNeil. 2001. Hydrodynamic characteristics and mixing behaviour of *Sclerotium glucanicum* culture fluids in an airlift reactor with an internal recirculation loop used for scleroglucan production, *J. Ind. Microbiol. Biotechnol*. 27:208–14.

Kern, A., F. S. Hartner, M. Freigassner, J. Spielhofer, C. Rumpf, L. Leitner, K. U. Fröhlich, A. and Glieder. 2007a. *Pichia pastoris* "just in time" alternative respiration, *Microbiology* 153:1250–60.

Kern, A., E. Tilley, I. S. Hunter, M. Legiša, A. Glieder. 2007b. Engineering primary metabolic pathways of industrial micro-organisms, *J. Biotechnol*. 129:6–29.

Kim, H. M., S.-Y. Paik, K.S. Ra, K. B. Koo, J. W. Yun, J. W. Choi. 2006. Enhanced production of exopolysaccharides by fed-batch culture of *Ganoderma resinaceum* DG-6556. *J. Microbiol*. 44:233–42.

Kind T, M. Scholz, O. Fiehn. 2009. How large is the metabolome? A critical analysis of data exchange practices in chemistry. *PLoS ONE* 4(5): e5440. doi:10.1371/journal.pone.0005440

Kirk, S., C. A. Avignone-Rossa, M. E. Bushell. 2000. Growth limiting substrate affects antibiotic production and associated metabolic fluxes in *Streptomyces clavuligerus*. *Biotechnol. Lett*. 22:1803–9.

Klyosov, A.A., 1988. Cellulases of the third generation, in Aubert, J.-P., Beguin, P., Millet, J.(eds.) *Biochemistry and Genetics of Cellulose Degradation*, London: Academic Press, pp. 87–99.

Lauer, M. S. and S. Skarlatos. 2010. Translational research for cardiovascular diseases at the national heart, lung, and blood institute, *Circulation* 121, 929–33.

Lee, K. M., S. Y. Lee, H. Y. Lee. 1999. Bistage control of pH for improving exopolysaccharide production from mycelia of *Ganoderma lucidum* in an airlift fermentor, *J. Biosci. Bioeng*. 88, 646–50.

Legiša, M., M. Mattey. 2007. Changes in primary metabolism leading to citric acid overflow in *Aspergillus niger*, *Biotechnol. Lett*. 29, 181–90.

Lin, X., Y. Huang, M, Fang, J. Wang, Z. Zheng, W. Su. 2005. Cytotoxic and antimicrobial metabolites from marine lignicolous fungi, *Diaporthe* sp., *FEMS Microbiol. Lett*. 251, 53–8.

Liras. P., J. P. Gomez-Escribano, I. Santamarta. 2008. Regulatory mechanisms controlling antibiotic production in *Streptomyces clavuligerus*, *J. Ind. Microbiol. Biotechnol*. 35, 667–76.

Lynd, L. R., P. J. Weimer, W. H. van Zyl, I. S. Pretorius. 2002. Microbial cellulose utilization: fundamentals and biotechnology, *Micro. Mol. Biol. Rev*. 66, 506–77.

Martinez, D., R. M. Berka, B. Henrissat, M. Saloheimo and 44 other authors. 2008. Genome sequencing and analysis of the biomass-degrading fungus *Trichoderma reesei* (syn. *Hypocrea jecorina*), *Nature Biotechnology* 26, 553–60

Mayer, A. F., W. D. Deckwer. 1996. Simultaneous production and decomposition of clavulanic acid during *Streptomyces clavuligerus* cultivations, *Appl. Microbiol. Biotechnol*. 45, 41–6.

Möller, J., R. Hiddessen, J. Niehoff, K. Schügerl. 1986. On-line high-performance liquid chromatography for monitoring fermentation processes for penicillin production, *Anal. Chim. Acta*, 190, 195–203.

Mousdale, D. M. 1996. The analytical chemistry of microbial cultures. In Rhodes, P. M., Stanbury, P. F. (eds.) *Applied Microbial Physiology: A Practical Approach*, Oxford: IRL Press (Oxford University Press), pp. 165–92.

Mousdale, D. M. 2007. Metabolic analysis and optimization of microbial and animal cell bioprocesses. In El-Mansi, E. M. T., Bryce, C. F. A., Demain, A. L., Allman, A. R. (eds.) *Fermentation Microbiology and Biotechnology*, 2nd edition, Boca Raton: CRC/Taylor and Francis, pp. 159–86.

Mousdale, D. M. 2008. Bioprocess Expression and Production Technologies in India. In Langer, E. S. (ed.) *Advances in Biopharmaceutical Technology in India*, American Society for Microbiology/BioPlan Associates, Inc., pp. 519–54.

Mousdale, D. M. 2010. *Introduction to Biofuels*, Boca Raton: CRC/Taylor and Francis, pp. 61–75.

Mousdale, D. M., Melville, J. C., Fischer, M. 1999. Optimization of fermentation bioprocesses by quantitative analysis: from analytical chemistry to chemical engineering. In El-Mansi, E. M. T., Bryce, C. F. A. (eds.) *Fermentation Microbiology and Biotechnology*, 1st edition, London: Taylor and Francis Ltd., pp. 147–78.

Nakano, T., K. Miyake, M. Ikeda, T. Mizukami, R. Katsumata. 2000. Mechanism of the incidental production of a melanin-like pigment during 6-demethylchlortetracycline production in *Streptomyces aureofaciens*, *Appl. Environ. Microbiol*. 66, 1400–04.

Neves, A. A., L. M. Vieira, J. C. Menezes. 2001. Effects of preculture on clavulanic acid fermentation, *Biotechnol. Bioeng*. 72, 628–33.

Nöh, K., K. Grönke, B. Luo, R. Takors, M. Oldiges, W. Wiechert. 2007. Metabolic flux analysis at ultra short time scale: isotopically non-stationary ^{13}C labeling experiments, *J Biotechnol*. 129, 249–67.

November, E. J., J. F. Van Impre. 2000. Evaluation of on-line viable biomass measurements during fermentations of *Candida utilis*, *Bioproc. Biosys. Eng*. 23, 473–7.

Oldiges, M., M. Kunze, D. Degenring, G. A. Sprenger, R. Takors. 2004. Stimulation, monitoring and analysis of pathway dynamics by metabolic profiling in the aromatic amino acid pathway, *Biotechnol. Prog*. 20, 1623–33.

Oldiges, M., S. Lütz, S. Pflug, K. Schroer, N. Stein, C. Wiendahl. 2007. Metabolomics: current state and evolving methodologies and tools, *Appl Microbiol Biotechnol*. 76, 495–511.

Omura, S., H. Ikeda, J. Ishikawa, A. Hanamoto, C. Takahashi, M. Shinose, Y. Takahashi, H. Horikawa, H. Nakazawa, T. Osonoe, H. Kikuchi, T. Shiba, Y. Sakaki, M. Hattori. 2001. Genome sequence of an industrial micro-organism *Streptomyces avermitilis*: deducing the ability of producing secondary metabolites, *Proc. Natl. Acad. Sci. USA* 98, 12215–20.

Panula-Perälä, J., J. Šiurkus, A. Vasala, R. Wilmanowski, M. G. Casteleijn, P. Neubauer. 2008. Enzyme controlled glucose auto-delivery for high cell density cultivations in microplates and shake flasks, *Microb. Cell Fact*. 7, 31–43.

Pero, J., A. Sloma. 1993. Proteases. In Sonensheim, A. L., Hoch J. A., Losick, R. (eds.) Bacillus subtilis *and Other Gram-Positive Bacteria: Biochemistry, Physiology, and Molecular Genetics*, Washington, DC: ASM Press, pp. 939–52.

Rau, U., R. J. Muller, E. Olszewsli, F. Wagner. 1992. Enhanced glucan formation of filamentous fungi by effective mixing, oxygen limitation and fed-batch processing, *J. Ind. Microbiol*. 9, 19–25.

Ren, H. T., J. Q. Yuan, K. H. Bellgardt. 2003. Macrokinetic model for methylotropic *Pichia pastoris* based on stoichiometric balance, *J. Biotech*. 106, 53–68.

Romero, J., P. Liras, J. F. Martín. 1984. Dissociation of cephamycin and clavulanic acid biosynthesis in *Streptomyces clavuligerus*, *Appl. Microbiol. Biotechnol*. 20, 318–25.

Roubos, J. A., P. Krabben, W. T. A. M. de Laat, R. Babuška, J. J. Heijnen. 2002. Clavulanic acid degradation in *Streptomyces clavuligerus* fed-batch cultivations, *Biotechnol. Prog*. 18, 451–7.

Roychoudhury, P., L. M. Harvey, B. McNeil. 2006. At-line monitoring of ammonium, glucose, methyl oleate and biomass in a complex antibiotic fermentation process using attenuated total reflectance-mid-infrared (ATR-MIR) spectroscopy, *Anal. Chim. Acta* 561, 218–24.

Roychoudhury, P., B. McNeil, L. M. Harvey. 2007. Simultaneous determination of glycerol and clavulanic acid in an antibiotic bioprocess using attenuated total reflectance mid infrared spectroscopy, *Anal. Chim. Acta* 585, 246–52.

Sáez, J. C., D. J. Schell, A. Tholodur, J. Farmer, J. Hamilton, J. A. Colucci, J. D. McMillan. 2002. Carbon mass balance evaluation of cellulase production on soluble and insoluble substrates, *Biotechnol. Prog*. 18, 1400–07.

Saqi, M., R. J. B. Dobson, P. Kraben, D. A. Hodgson, D. L. Wild. 2009. An approach to pathway reconstruction using whole genome metabolic models and sensitive sequence searching, *J. Integrative Bioinform*. 6, 107–21.

Saudagar, P. S., S. A. Survase, R. S. Singhal. 2008. Clavulanic acid: a review, *Biotechnol. Adv*. 26, 335–51.

Scarff, M., S. A. Arnold, L .M. Harvey, B. McNeil. 2006. Near infrared spectroscopy for bioprocess monitoring and control: current status and future trends, *Crit. Rev. Biotechnol*. 26, 17–39.

Schmidt, W.J., H.-D. Meyer, K. Schügerl, W. Kuhlmann, K.-H. Bellgardt. 1984. On-line analysis of fermentation media, *Anal. Chim. Acta*, 163, 101–09.

Seviour, R., B. McNeil, M. Fazenda, L. M. Harvey. 2010a. Operating bioreactors for microbial exopolysaccharide production, *Crit. Rev. Biotechnol*. (in press).

Seviour, R., F. Schmid,. B.C. Campbell. 2010b. Polysaccharides in Popa, V. (ed.) Medicinal and pharmaceutical applications, Shrewsbury (UK): Smithers Rapra (in press).

Sullivan, R., J. E. Smith, N. J. Rowan. 2006. Medicinal mushrooms and cancer therapy, *Perspectives Biol. Med*. 49, 159–70.

Tang, Y. J., H. G. Martin, S. Myers, S. Rodriguez, E. E. K. Baidoo, J. D. Keasling. 2009a. Advances in analysis of microbial metabolic fluxes via ^{13}C isotopic labeling, *Mass Spec. Rev*. 28, 362–75.

Tang, Y. J, W. Zhang, J. J. Zhong. 2009b. Performance analyses of a pH-shift and DOT-shift integrated fed-batch fermentation process for the production of ganoderic acid and *Ganoderma* polysaccharides by medicinal mushroom *Ganoderma lucidum*, *Biores Technol*. 100, 1852–9.

Taylor, G. 2008. *Lean Six Sigma Service Excellence: A Guide to Green Belt Certification and Bottom Line Improvement*. New York: J. Ross Publishing, pp. 177–87.

Vaidyanathan, S. 2005. Profiling microbial metabolomes: what do we stand to gain? *Metabolomics* 1, 17–28.

Valentine, B. P., P. A. Jeffkins, W. H. Holms, D. M. Mousdale, International Patent Publication No. WO96/18743: "Process methods for the fermentative preparation of clavam derivatives whereby the levels of ammonia and urea are kept low." 7 December 1995.

Wang, Y., B. McNeil. 1994. Scleroglucan and oxalic acid formation by *Sclerotium glucanicum* in sucrose supplemented fermentation, *Biotechnol. Letts*. 16, 605–10.

Wang, Y., B. McNeil. 1995a. pH effects on exopolysaccharide and oxalic acid production in cultures of *Sclerotium glucanicum*, *Enz. Microb. Technol*. 17, 124–30.

Wang, Y., B. McNeil. 1995b. The effect of temperature on scleroglucan synthesis and organic acid production by *Sclerotium glucanicum*, *Enz. Microb. Technol*. 17, 566–70.

Wang, Y., B. McNeil. 1996. Scleroglucan, *Crit. Rev. Biotechnol*. 16, 185–215.

Winder, C. L., W. B. Dunn, S. Schuler, D. Broadhurst, R. Jarvis, G. M. Stephens, R. Goodacre. 2008. Global metabolic profiling of *Escherichia coli* cultures: an evaluation of methods for quenching and extraction of intracellular metabolites, *Anal Chem.* 80, 2939–48.

Worgan, J. T. 1968. Culture of the higher fungi, *Prog. Ind. Microbiol*. 8, 74–139.

Yanai, K., N. Sumida, K. Okakura, T. Moriya, M. Watanabe, T. Murakami. 2004. *Para*-position derivatives of fungal anthelmintic cyclodepsipeptides engineered with *Streptomyces venezuelae* antibiotic resistance genes, *Nature Biotechnol.* 22, 848–55.

Zhang, W., F. Li, L. Nie. 2010. Integrating multiple 'omics' analysis for microbial biology: application and methodologies, *Microbiology* 156, 287–301.

This page intentionally left blank

7 Flux Control Analysis and Stoichiometric Network Modeling: Basic Principles and Industrial Applications

E.M.T. El-Mansi, Gregory Stephanopoulos, and Ross P. Carlson

CONTENTS

> "When you can measure what you are speaking about and express it in numbers, you know something about it, and when you cannot measure it, when you cannot express it in numbers, your knowledge is of a meager and unsatisfactory kind.
>
> **Lord Kelvin**

7.1 INTRODUCTION: TRADITIONAL VERSUS MODERN CONCEPTS

The rate-limiting step was defined as the slowest step in a given pathway. Such a definition resulted from the observation made in the mid-1960s that the reaction rate of a sequence of unsaturated enzymes (i.e., where the concentration of substrates is below the K_m value for each of the enzymes involved) depended nonlinearly on the kinetic parameters of all the enzymes involved. However, no theoretical basis was given to validate or substantiate the existence of such a concept.

Industrial biotechnologists are generally, but not entirely, of the view that flux through a given pathway is usually limited by one step. Such a step is termed the rate-limiting step or the bottleneck with the enzyme catalyzing such a step being referred to as the "pacemaker." However, the question of how such a step can be identified and quantified in a given pathway remained unanswered, largely because of the lack of an experimental procedure that describes how such a rate-limiting step can be identified and quantified.

Clearly, if a rate-limiting step exists in a given pathway, then increasing the activity of the enzyme catalyzing such a step will increase the overall flux through the pathway and, by the same token, varying the activity of any other enzyme will have no effect whatsoever on the overall flux of the pathway in question. Although several studies have been published in support of the concept of the rate-limiting step, by and large such a concept does not appear to be a tenable proposition because it does not adequately explain why flux and, in turn, yield could not be improved after the overexpression of enzymes that are considered to be rate limiting. For example, a 3.5-fold (350%) increase in the activity of phosphofructokinase, the enzyme widely regarded as the "rate-limiting step" in glycolysis, had no appreciable effect on carbon flux through the glycolysis in *Saccharomyces cerevisiae*. Furthermore, the erroneous nature of the concept of the rate-limiting step has also been emphasized in the elegant example given on tryptophan biosynthesis in the yeast *S. cerevisiae* (Cornish-Bowden 1995; Cornish-Bowden et al. 1995). Biosynthesis of tryptophan in this organism involves the conversion of chorismate to anthranilate through the activity of anthranilate synthase (E1). The latter intermediate is then converted to tryptophan through the activities of four different enzymes: anthranilate phosphoribosyl transferase (E2), phosphoribosyl anthranilate isomerase (E3), indolglycerol phosphate synthase (E4), and tryptophan synthase (E5). In this study the aforementioned authors revealed that singularly increasing the enzymic activity of any of the five enzymes involved by a factor of up to 50-fold had no significant effect on the flux to tryptophan. However, increasing the concentration of all five enzymes by a factor of 20-fold was accompanied by a significant increase in flux to tryptophan formation.

Several techniques have been devised to assess the relative contribution of each enzyme to the overall flux in a given pathway, and although *in vitro* measurement of the maximal velocity (V_{max}) of a given enzyme is useful, the value obtained does not necessarily reflect the rate of catalysis *in vivo* because of a lack of hard data regarding the intracellular concentrations of substrates and effectors, primarily because of rapid "turnover" of metabolic pools, which in turn renders such measurements difficult if not impossible. Therefore, a new quantitative approach was called for, not only to explain the many outstanding observations relating to flux control in industrial fermentations but also to provide a rational basis for the exploitation of the diverse array of metabolic pathways in microorganisms.

Although several approaches have been used as an alternative to the rate-limiting step, it is Kacser's theory of metabolic control analysis (MCA) that has grown in stature since its inception in 1973 and proved, without undermining the intellectual capacity of other approaches, to be the ultimate

approach. The controversy over the question of whether a given method can be used successfully to predict or determine the relative contribution of each enzyme to the overall flux in a given pathway was finally resolved when Kacser and Burns (1973) and Heinrich and Rapaport (1974) independently proposed the theory of MCA. The fundamental difference between the rate-limiting step as a concept and that of the theory of MCA is that whereas the former is a qualitative parameter, the latter examines biological systems in a quantitative way that excludes bias, expectations, or preconceived ideas.

7.2 FLUX CONTROL ANALYSIS: BASIC PRINCIPLES

Kacser's MCA theory facilitates the assessment of not only how perturbation of a particular enzymic activity affects metabolic flux, but also by how much. The response to changes in the concentration of a particular enzyme on flux varies over a wide range. For example, the response could be immediate, with a strong correlation between the increase in flux and the increase in enzymic activity, as is the case for adenylate kinase en route to ATP synthesis. In this case, one might justifiably describe such an enzyme as rate limiting or a pacemaker. However, most enzymes do not enjoy such a high profile and as such an increase in flux may or may not be brought about by increasing the activity of a single enzyme.

Furthermore, the degree of control exerted by a particular enzyme on the overall flux of a given pathway is not purely dependent on the numerical value of its intracellular concentration but rather on whether the enzyme has the capacity for higher throughput, which can only be ascertained from the value of the enzyme's "flux control coefficient," the first pillar of the theory of MCA.

7.2.1 Flux Control Coefficient

The flux control coefficient is a parameter that describes in quantitative terms the relative contribution of a particular enzyme to flux control in a given pathway. It is not an intrinsic property of the enzyme per se but rather a system property and so is subject to change as the environment changes. It is generally expressed as the fractional change in flux in response to a fractional change in the concentration of the enzyme in question, and its value ranges between 0 and 1.0.

The measurement of the flux control coefficient of a particular enzyme allows an accurate prediction of how flux through a given pathway might fluctuate in response to a specific change in the enzyme's catalytic activity or concentration. Although a change in the concentration can be brought about by cloning and subsequent overexpression of the structural gene encoding the enzyme in question, changes in the catalytic activity of the enzyme without changing its concentration can be brought about through site-directed mutagenesis and protein engineering techniques. For example, consider pyruvate dehydrogenase (PDH) with the view of assessing its effect or influence on flux to acetate excretion in *Escherichia coli* (Figure 7.1). The influence of PDH in that direction can be assessed from the enzyme's flux control coefficient, which can be calculated from the tangent to the curve of a log-log plot of flux (J) as a function of enzymic activity or concentration (E). Assuming that a small increase in the concentration of PDH (dEpdh) was accompanied by a small increase in the steady-state flux (J) of the enzyme acetate kinase (dJak), it follows that if we were to change the concentration of PDH very slightly, then the ratio dJak/dEpdh becomes equal to the slope of the tangent to the curve of Jak against Epdh as depicted in Figure 7.2. However, analyzing the data in this way is somewhat imperfect because the numerical value of enzyme concentration and units of enzymic activity will be different from one enzyme to another. This problem could be overcome if we were to relate the fractional changes in flux through acetate kinase to the fractional increase in the concentration of PDH (i.e., dJak/Jak and dEpdh/Epdh), and as such the flux control coefficient will assume a value between 0 and 1.0, which can then be expressed in terms of a percentage.

However, it is possible for an enzyme to have a flux control coefficient with a negative value, as is the case at branch points where one metabolite has to be partitioned between two enzymes. In such a case the increase in flux through one branch is generally at the expense of the other, as exemplified

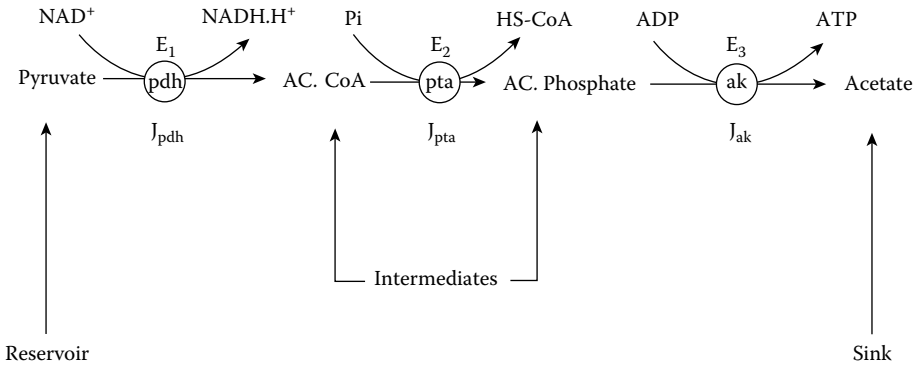

Key: pdh (E_1), pyruvate dehydrogenase
pta (E_2), phosphotransacetylase
ak (E_3), acetate kinase

FIGURE 7.1 The enzymes and metabolites en route to acetate excretion.

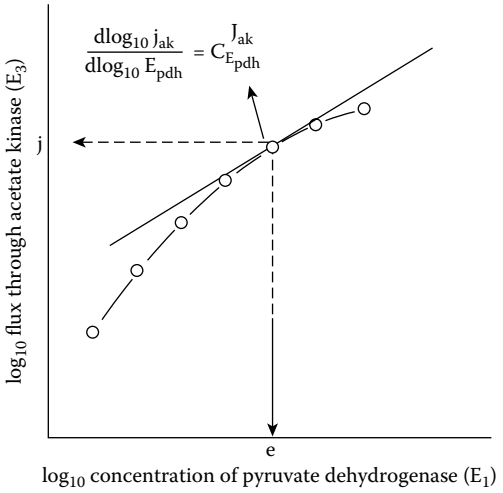

FIGURE 7.2 Graphical determination of PDH flux control coefficient with respect to acetate excretion. The graph depicts a typical pattern of variation in flux to acetate; measured as acetate kinase (Jak), in response to changes in the concentration of pyruvate dehydrogenase (Epdh).

in the case study for the partition of carbon flux at the junction of isocitrate (see Section 7.3). At this junction, any increase in the concentration of isocitrate dehydrogenase (ICDH) is concomitant with a decrease in flux through the competing enzyme, namely isocitrate lyase (ICL). It is possible, therefore, to describe ICDH as having a negative flux control coefficient on flux through ICL. Although any increase in the concentration of ICDH is accompanied by a decrease in flux through ICL, the opposite is not true for reasons that will become apparent later on; for further details, see El-Mansi et al. (1994).

7.2.2 Summation Theorem

The summation theorem, the second pillar of the MCA theory, states that the total sum of flux control coefficients of all enzymes in a given pathway adds up to 1.0. The summation theorem also shows that the flux control coefficient of an enzyme is a system property because any increase in

the concentration of a particular enzyme is accompanied by a decrease in its flux control coefficient. According to the summation theorem, such a decrease will have to be balanced by increasing the flux control coefficient of another enzyme—or more than one enzyme—within the same pathway so that the sum of all flux control coefficients remains constant (i.e., 1.0). For example, in a linear pathway consisting of enzymes with usual kinetic properties (i.e., where substrates stimulate and products inhibit reaction rate), the flux control coefficients for every enzyme must be 0 or higher with a total sum of 1.0. If an enzyme were to show a flux control coefficient of 1.0 with all other enzymes showing flux control coefficients of 0, such an enzyme could justifiably be described as rate limiting. The summation theorem also shows that this is not necessarily the case because it is also possible for some or all of the enzymes to have values greater than 0 providing that the total does not exceed 1.0. In practice, we would expect a pathway flux to be influenced mainly by enzymes in that pathway, and to a much lesser extent by closely related pathways, and that distantly connected enzymes would have negligible influence or none at all. In other words, the flux control coefficients of hundreds or even thousands of enzymes that are not directly related or connected to the pathway in question will be zero although flux control is shared among all enzymes.

Another consequence of the highly branched and intricate nature of cellular metabolism is that the central pathways provide biosynthetic precursors and energy for other pathways. So, as biosynthetic precursors are made, some are fed directly into the biosynthetic routes, which in turn diminish flux through the central metabolic pathways. Therefore, It follows that biosynthetic enzymes are likely to have negative flux control coefficients with respect to flux through the central metabolic pathways. According to the summation theorem, if one or more enzymes possess a negative value of flux control coefficient, then it is possible to see some other enzymes displaying a flux control coefficient higher than the numerical value of 1.0. This is because if there are negative flux control coefficients, one or more flux control coefficients would have to be greater than 1.0 so that the total sum adds up to 1.0. This shows that the flux control coefficient is not an intrinsic property of the enzyme itself but rather a property of the whole system.

7.2.3 Elasticity Coefficient

The flux control coefficient of an enzyme is influenced by the enzyme's ability to respond to changes in the concentration of its immediate substrate, as well as its ability to influence the concentrations of other metabolites in the pathway, a linkage that was first demonstrated by Heinrich and Rapaport (1974). The elasticity coefficient, the third pillar of the MCA theory, was therefore introduced to describe how flux is influenced by changes in the concentration of a given metabolite. In other words, elasticity is a parameter that describes, in quantitative terms, the sensitivity and responsiveness of an enzyme to a metabolite.

Unlike the flux control coefficient, elasticity is a property of individual enzymes and not of the pathway. The elasticity of an enzyme to a metabolite is defined by the slope of the curve of enzyme units (reaction rate) plotted as a function of metabolite concentrations, with the measurements taken at the metabolite concentration found *in vivo*. By analogy with the flux control coefficient (Figure 7.2), the value of the elasticity coefficient, which can be calculated from the slope, will depend upon the units used for the measurement of enzymic activities, which may vary from one enzyme to another. This can be avoided, as described earlier for the flux control coefficient, by directly calculating the elasticity coefficient from a log-log plot of catalytic activity versus metabolite concentration to give the fractional change in enzymic activity as a function of the fractional change in the concentration of the substrate. As highlighted in the case study presented in Section 7.3, elasticities have positive values for metabolites that stimulate enzymic activity (substrates, activators) and negative values for those that decrease reaction rate, such as products and inhibitors. Therefore, elasticity is a parameter that describes, in quantitative terms, the sensitivity and responsiveness of an enzyme to a particular metabolite that could be a substrate, a product, or an effector.

7.2.4 Connectivity Theorem

This theorem, the fourth pillar of the MCA theory, addresses the question of how the flux control coefficient of a given enzyme can be related to its kinetic properties. Such an inter-relationship is governed by the connectivity theorem, which states that the sum of all connectivity values in a given pathway is zero. The connectivity value for any given enzyme can be calculated by multiplying its flux control coefficient by its elasticity with respect to the metabolite in question. Enzymes not affected by the metabolite in question will naturally have an elasticity of zero and as such will make no contribution toward the final sum obtained. Further analysis of connectivity values has revealed that large elasticities are associated with small flux control coefficients and vice versa. The mathematical equations relating the connectivity theorem to linear pathways, branch points, and cycles have been extensively described and dealt with elsewhere (Fell 1997).

7.2.5 Response Coefficients

Induction and repression of enzyme synthesis in response to internal or external environmental stimuli are widely distributed in nature and are very effective in "turning on" and "switching off" transcription. Covalent modification through reversible phosphorylation is another mechanism that regulates the activity of existing enzymes by rendering them active or inactive, as is the case for ICDH in *E. coli* during adaptation to acetate (Koshland 1987; Cozzone 1988). In addition to degradation of mRNA and proteins, enzymes may also be the subject of allosteric control mechanisms, which change the enzyme's affinity toward its substrate and/or cofactor(s).

The response coefficient, the fifth pillar of the MCA theory, reflects the effectiveness of a particular effector on flux through a given pathway and is dependent on two factors: the flux control coefficient of the target enzyme and the strength of the effector, which Is given by its elasticity coefficient. For an effector to have a significant effect on flux, each of the above parameters with respect to the target enzyme clearly has to be of a value higher than zero.

Under circumstances in which a particular effector may activate or inactivate more than one enzyme in a given pathway, the total response will be the sum of the individual responses from each enzyme affected. However, this is only true when the changes in the concentration of the effector are very small because of the nonlinear relationship of the kinetics in metabolic systems (Hofmeyr and Cornish-Bowden 1991).

Now, let us consider how carbon flux is partitioned at the junction of isocitrate during growth of *E. coli* on acetate.

7.3 CONTROL OF CARBON FLUX AT THE JUNCTION OF ISOCITRATE IN CENTRAL METABOLISM DURING AEROBIC GROWTH OF *E. COLI* ON ACETATE: A CASE STUDY

During aerobic growth on acetate as a sole source of carbon and energy, *E. coli* requires the operation of the anaplerotic sequence of the glyoxylate bypass for the provision of biosynthetic precursors (Kornberg 1966). Under these conditions a new junction is created at the level of isocitrate (Figure 7.3), where ICL of the glyoxylate bypass is in direct competition with the Krebs cycle enzyme ICDH. Although ICDH has a much higher affinity for isocitrate, flux through ICL and thence the anaplerotic enzyme malate synthase (MS) is assured by virtue of high intracellular levels of isocitrate and the inactivation of a large fraction (75%) of ICDH (El-Mansi et al. 1985; Cozzone and El-Mansi 2005). Although the *in vivo* signal that triggers the "acetate-switch" and, in turn, the expression of the glyoxylate bypass operon has yet to be unraveled, acetate *per se* can be safely ruled out as a possible signal (El-Mansi 1998). With the aid of radiolabeled isotopes and NMR spectroscopy, Walsh and Koshland (1984) reported that during steady-state growth of *E. coli* on

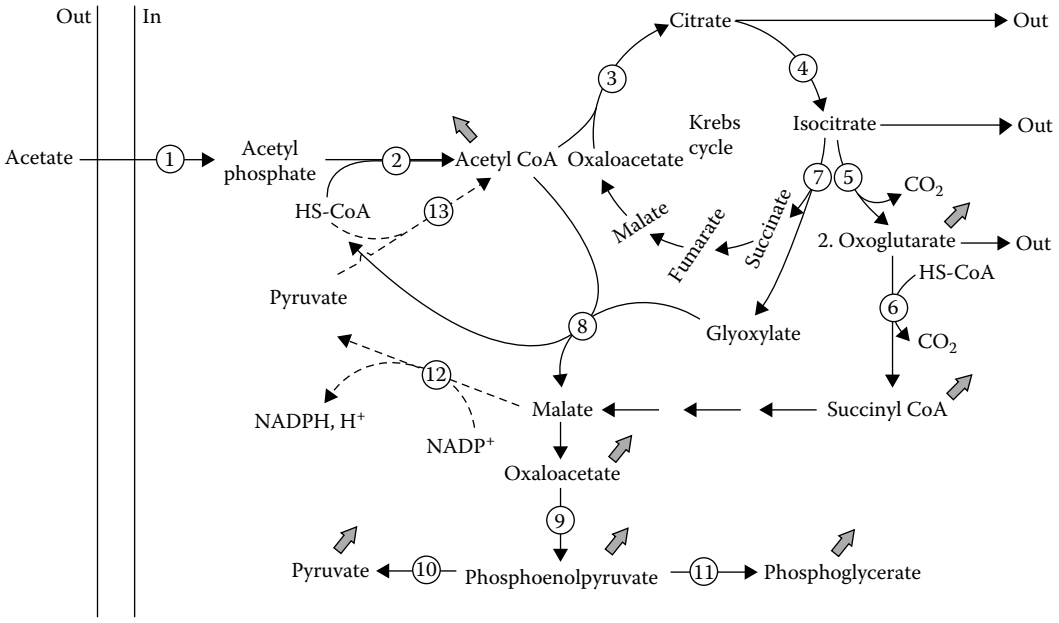

FIGURE 7.3 The metabolic route used by *E. coli* for the assimilation of acetate highlighting the direct competition between the Krebs cycle enzyme ICDH (5) and the glyoxylate bypass enzyme ICL (7). This diagrammatic representation also highlights flux to citrate and isocitrate excretion as well as the biosynthetic role assumed by ICDH under these circumstances for the provision of α-ketoglutarate and succinyl CoA; both are biosynthetic precursors. This metabolic network also accounts for the long-standing observation that expression of malic enzyme (12) and PDH (13) are not essential for growth on acetate. Key enzymes are as follows: 1, acetate kinase; 2, phosphotransacetylase; 3, citrate synthase; 4, aconitase; 5, isocitrate dehydrogenase; 6, α-ketoglutarate dehydrogenase; 7, isocitrate lyase; 8, malate synthase; 9, PEP carboxykinase; 10, pyruvate kinase; 11, enolase; 12, malic enzyme; 13, pyruvate dehydrogenase. (Reproduced from Cozzone and El-Mansi, 2005. With kind permission of Karger AG, Basel).

acetate under aerobic conditions, flux through ICL is 31.0 mmol of isocitrate per minute, which in turn represents 33% of the total carbon processed at this junction.

To assess the relative contribution of each of the above enzymes to the overall distribution of carbon flux among various enzymes of central metabolism, the computer software package Gepasi (Mendes 1993) was used to calculate the steady-state fluxes and the concentration of various metabolites during growth of *E. coli* on acetate. This computer package also enabled us to formulate the matrices of the elasticity coefficients as well as the control and response coefficients under different steady states. In the next section, we will discuss the data in the light of Kacser's MCA theory as well as the traditional concept of the rate-limiting step.

7.3.1 The Model

To explore the consequences of controlled adjustment of ICL and ICDH enzymic activities on the partition of carbon flux at the junction of isocitrate on one hand and among various enzymes of central metabolism on the other, the complex metabolic pathways of central metabolism used by Walsh and Koshland (1984) was reduced to a skeleton model (Figure 7.4).

It is noteworthy that the model depicted previously for the Krebs cycle and the glyoxylate bypass (Figure 7.4) does not constitute a moiety-conserved cycle (Hofmeyr et al. 1986) because there are reversible sinks to the cycle as well as branching from within the cycles, thus giving rise to metabolite pools that are involved in three different reactions.

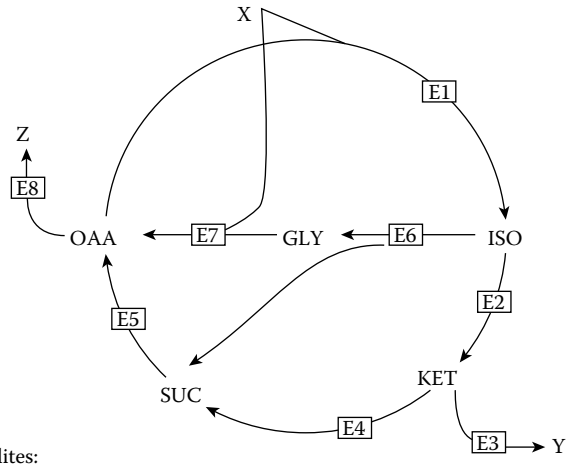

Metabolites:
X = acetyl-CoA
ISO = isocitrate
KET = α-ketoglutarate (reservoir excluding flux to fatty acids)
SUC = succinate
OAA = oxaloacetate
GLY = glyoxylate
Y = glutamate (sink for cell constituents)
Z = gluconeogenesis and biosynthesis (sink for cell constituents)

Enzymes:
E1 = citrate synthase/aconitase
E2 = isocitrate dehydrogenase
E3 = glutamate dehydrogenase
E4 = α-ketoglutarate dehydrogenase/succinate thiokinase
E5 = succinate dehydrogenase/fumarase/malate dehydrogenase
E6 = isocitrate lyase
E7 = malate synthase
E8 = PEP carboxykinase

FIGURE 7.4 A skeleton model describing the central metabolic pathways used by *E. coli* during growth on acetate as a sole source of carbon and energy. Key to metabolites and enzymes are given below.

According to the summation theorem, flux through ICDH can be affected by other enzymes of central metabolism, with the sum of the flux control coefficients of all enzymes on J_{ICDH} being 1.0. Whereas the flux control coefficient is a measure of the relative change in flux through a particular enzyme in a given pathway in response to a small change in its concentration, the elasticity coefficient of a given enzyme is a measure of the relative change in flux in response to a small change in the concentration of its substrate or cofactor.

It is noteworthy that other metabolic modeling programs are also available and can be obtained free of charge, although some are no longer maintained by their respective authors for one reason or another, including MMT (Metabolic Modeling Tool), which unlike other programs uniquely contains a tool that provides a pathway overview and identifies parameter algorithms (Hurlebaus 2001; http://www.bioinfo.de/isb/gcb01/poster/hurlebaus.html).

7.3.2 Modeling of Carbon Flux at the Junction of Isocitrate in Central Metabolism

To gain some insight into the consequences of changing the concentration of ICHD and ICL on flux through the enzymes themselves as well as the intracellular concentrations of associated metabolites, Gepasi, version 3.30, a Windows-based application that is user-friendly, was used. The entry of

reaction equations and rate laws (kinetics) is straightforward and easily achieved. Several predefined rate laws are available, and it is possible to create user-defined rate laws. The reaction rates and rate laws are first entered followed by the starting concentrations of fixed and variable metabolites.

Once this basic configuration is achieved, the MCA steady-state values can be calculated. Interestingly, the data obtained on the effect of ICL (E6) and ICDH (E2) on the partition of carbon flux at the junction of isocitrate as well as isocitrate concentrations using Gepasi have the added advantage of plotting multifunction analysis as shown in Figures 7.5 and 7.6, respectively. Although the output in the two figures appears to be significantly different with respect to isocitrate concentration and flux through ICDH and ICL, the reaction equation input only differs in the sign used in the denominator; whereas addition (+) was used in Figure 7.5, multiplication (×) was used in Figure 7.6. Although the question of whether which sign is correct is arguable, the *in vivo* analysis of isocitrate concentration is in good agreement with using addition rather than multiplication in the denominator of formula template.

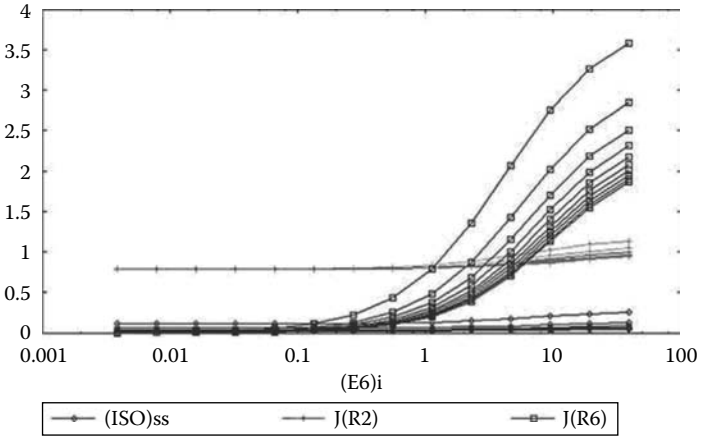

FIGURE 7.5 Effect of ICL (E6) concentrations on flux through the enzyme itself (J6), flux through ICDH (J2), and isocitrate concentration as calculated by Gepasi. Note that the data presented in this graph are composed of a combined scan of E6 (14 values) and E2 (10 values), thus giving rise to 140 separate steady-state data points. The variations of E6 are shown along the abscissa, whereas the variations in E2 are shown as multiple contours of J6, J2, and isocitrate concentrations

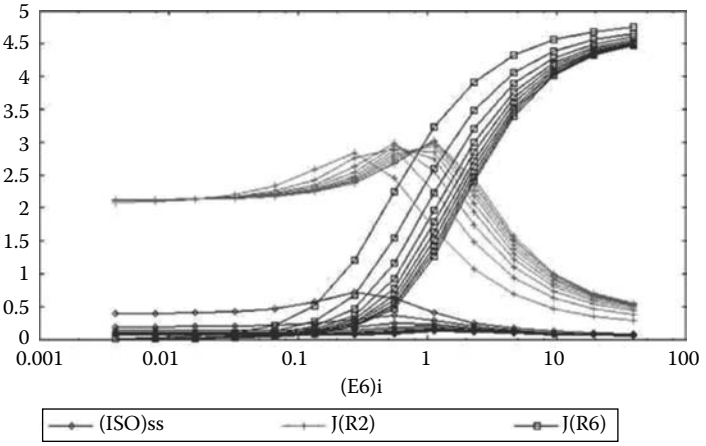

FIGURE 7.6 Effect of ICL (E6) concentrations on flux through the enzyme itself (J6), flux through ICDH (J2), and isocitrate concentration as calculated by Gepasi.

7.4 STRATEGIES FOR MANIPULATING CARBON FLUXES EN ROUTE TO PRODUCT FORMATION IN INTERMEDIARY METABOLISM

7.4.1 Validity of the Concept of the Rate-Limiting Step As an Approach to Increasing Flux to Product Formation

Industrialists, driven by a strong faith in genetic engineering, often argue that if one can identify the enzyme catalyzing the rate-limiting step in a given pathway, then the rest is simple. However, this approach has proved to be, by and large, erroneous, and examples illustrating this notion are given in the introductory section of this chapter. Alternative approaches, which may be beneficiary to the industrialists, include Kacser's theory of MCA. MCA argues that the rate-limiting step is an oversimplification of metabolism and as such should be abandoned; instead, the control of metabolic flux in a given pathway is shared among all of the enzymes involved, albeit to a varying degree of extent as described earlier in this chapter. Although MCA overlooks peculiarities in the metabolic network and ignores regulatory enzymes, "the victim of MCA," as Kacser used to say, it is nevertheless a very powerful tool for examining the general properties of metabolic networks.

7.4.2 Modulation of Carbon Flux En Route to Product Formation

7.4.2.1 The Model

In the model pathway (Figure 7.7), the biosynthesis of two end products, S_{4a} and S_{4b}, from a biosynthetic precursor, X_0, via a branch-point metabolite, S_2, is highlighted. Also note that the precursor metabolite X_0 is external to the system; that is, its concentration is fixed and, unlike all other metabolites within the pathway, does not depend on the properties of the eight enzymes involved in the skeleton model (Figure 7.7) (Cornish-Bowden et al. 1995). Although the numerical values assumed by the aforementioned authors for the eight kinetic equations are arbitrary, the essential features of the model are not and correspond to a typical case of sequential feedback inhibition in which each of the two end products (S_{4a} and S_{4b}) inhibits the enzymes (E_{3a} and E_{3b}) catalyzing the first committed step of their formation, respectively, with the branch-point metabolite S_2 inhibiting E_1, the enzyme catalyzing the first step in the whole pathway (Figure 7.7). All simulations were carried out using the latest available version of MetaModel, which was first conceived by Cornish-Bowden and Hofmeyr (1991).

7.4.2.2 Strategies for Manipulating Metabolic Fluxes

Several different strategies (i.e., opposition, oblivion, evasion, suppression, and subversion) have been used in an attempt to increase carbon flux to product formation; in this case S_{4a} and S_{4b} (Cornish-Bowden et al. 1995). The terms coined for the aforementioned strategies reflect the possible effect of each on cellular regulation (Cornish-Bowden 1995). Opposition as a strategy is widely used. In opposition, industrialists attempt to increase flux in a given pathway by increasing the relative concentration of the enzyme considered to be rate limiting, often the enzyme that is subject to feedback inhibition (e.g., E_1 and/or E_{3a} in the model system portrayed above) (Figure 7.7). Whereas oblivion strategy utilizes mathematical modeling of certain matrices to determine the degree of change needed to achieve certain increase in flux, evasion utilizes fluxes to calculate the changes needed in enzymic activity to achieve the desired increase in the concentration of end product without adversely affecting the concentrations of intracellular metabolites. Suppression as a strategy makes full use of the primary regulatory function of feedback inhibition [i.e., to transfer control from the biosynthetic reactions (supply) to polymerization and assembly (demand) (Figure 7.7)] and as such seeks to increase flux to product formation through increasing the demand made on central and intermediary metabolism. Suppression relies on the elimination

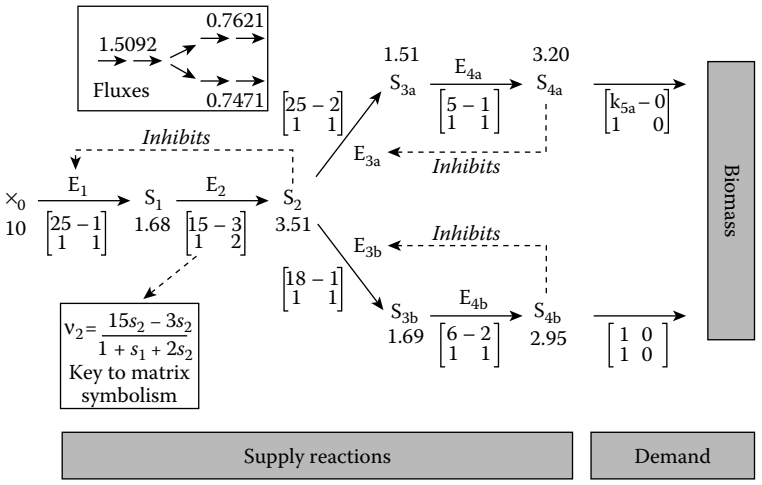

FIGURE 7.7 A model representing a branched biosynthetic pathway that is used for the production of two final end products (i.e., S_{4a} and S_{4b}). Note that the whole pathway can be divided into two main sections (i.e., supply and demand). Although the supply involves enzymes E_1–E_4, the demand section only involves E_5. Also note that each end product S_{4a} and S_{4b} inhibits the enzymic activities of E_{3a} and E_{3b}, respectively, and that the metabolite (S_2) inhibits the enzymic activity of E_1. It was assumed that the reactions obeyed the Michaelis–Menten equation, and that the pool concentration of X_o was held constant at 10 with the steady-state concentrations of various metabolites; shown underneath each metabolite are calculated values of 1 for K_{5a} as described by (Cornish-Bowden, A., Hofmeyr, J.-H.S., and Cardenas, M. L., *Bioorganic Chem.,* 23:439–49, 1995). The steady-state fluxes through the common pathway and the two branches are highlighted by shading (i.e., 1.5092 for the common pathway and 0.7621 and 0.7471 for the fluxes through branches a and b, respectively). This steady state was used as the starting point for examining the effect of different strategies on flux to S_{4a}. (This diagram is a modification of the original model of Cornish-Bowden, A., Hofmeyr, J.-H.S., and Cardenas, M. L., *Bioorganic Chem.,* 23:439–49, 1995, reproduced with the kind permission of Elsevier.)

of feedback loops whereas subversion relies on increasing the demands made on the biosynthetic enzymes.

With the exception of oblivion strategy, all other strategies have been examined *in silico,* and their effect on flux to product formation has been assessed (Table 7.1). Suppression is an "all-or-none" strategy because feedback loops are present or absent and had only a very modest effect on flux. Elimination of the feedback loop to E_{3a} gave a 30% increase in flux, which was accompanied by 17-fold increase in the concentrations of the metabolites in branch a (Figure 7.7). On the other hand, elimination of the feedback loop E_1 yielded a 17% increase in flux with some 50–fold increase in the concentrations of metabolites in the common part of the pathway (Figure 7.7). It is noteworthy to indicate that a large increase in the concentrations of metabolites *in vivo* might adversely affect cell viability and flux to desired end product. In all other strategies, the manipulations were performed with the view of achieving a 5-fold increase in flux through branch a (Figure 7.7). Simulation analysis revealed that opposition as a strategy is largely ineffective because changes in the concentration of one or two enzymes alone was accompanied by a very limited increase in flux to product formation. On the other hand, evasion produced the desired increase in flux (i.e., 5-fold) without adversely affecting the intracellular concentrations of metabolites (Table 7.1). Furthermore, although evasion is more effective than subversion as a strategy for increasing fluxes (Table 7.1), it is important. that we recognize that the latter strategy achieved an appreciable increase in flux as a result of manipulating only one enzymic activity rather than all enzymes and that the changes in the intracellular concentrations of metabolites associated with it are modest and as such may be favorable to the organism *in vivo.*

TABLE 7.1
Impact of Various Strategies on Metabolites Concentrations and Flux Through Branch a in the Model Shown in Figure 7.7

	Relative Activity of Each Enzyme									Relative Metabolite Concentrations			
Strategy	E_1	E_2	E_{3a}	E_{4a}	E_{5a}	E_{3b}	E_{4b}	E_{5b}	**Relative J_{5a}**	S_1	S_2	S_{3a}	S_{4a}
Wild-type	1	1	1	1	1	1	1	1	1.00	1.00	1.00	1.00	1.00
Opposition[b]	5	1	1	1	1	1	1	1	1.02	1.50	1.51	1.11	1.11
Opposition[b]	1	1	5	1	1	1	1	1	1.08	1.02	0.99	1.49	1.47
Opposition[b]	5	1	5	1	1	1	1	1	1.10	1.52	1.49	1.66	1.63
Evasion#	3.02	3.02	5	5	5	1	1	1	5.00	1.00	1.00	1.00	1.00
Suppression	*	1	1	1	1	1	1	1	1.17	49.5	47.7	2.64	2.56
Suppression	1	1	*	1	1	1	1	1	1.29	1.06	0.96	17.8	16.9
Suppression	*	1	*	1	1	1	1	1	1.31	47.4	42.7	795	780
Subversion	1	1	1	1	5	1	1	1	4.13	1.74	0.76	3.66	0.53

Source: This table is reproduced from Cornish-Bowden, A., Hofmeyr, J.-H.S., and Cardenas, M. L., *Bioorganic Chem.,* 23:439–49, 1995. With the kind permission of Elsevier.

Note: The factors of 5 and 1 for the enzymes reflect the desired increases in flux. In the common part of the pathway (see Figure 7.10), the factor 3.02 was calculated from the fluxes in the starting steady-state as follows: $(5J_{3a} + J_{3b})/(J_{3a} + J_{3b}) = (5 \times 0.7621 + 0.7471)/(0.7621 + 0.7471) = 3.02$.

[a] In cases marked by asterisk (*), the activities of the enzymes were not changed except for omitting the feedback inhibition terms from the denominators of the rate equations.

[b] The three cases of opposition were also examined with much larger changes in activity, 100- instead of 5-fold in each case. Effects on the flux were only trivially different from those shown, but the effects on concentrations were much larger.

7.5 CONVERSION OF FEEDSTOCK TO BIOMASS AND DESIRABLE END PRODUCTS

The conversion of a given feedstock to desirable end product by microorganisms involves a wide range of metabolic activities depending on the nature of the feedstock and the identity of the desired end product. Unlike products of primary metabolism (see Chapter 4), synthesis of secondary metabolites (see Chapter 5) is usually sequential to cessation of growth, at which point more feedstock (input) is added intermittently (fed-batch culture) or continuously (continuous cultures, e.g., turbidostat, auxostat, pH-stat) to sustain the metabolic fluxes required for the biosynthesis of desired end product (output) and maintenance of cell viability. During the productive stage, the primary feedstock (input) is generally channeled through specific metabolic routes, and provided that such routes are known, careful measurements of all inputs and outputs in a given fermentation process provide the data from which the fluxes through all of the pathways involved can be calculated (Holms 1996). A metabolic chart for central and intermediary metabolism can then be constructed that relates input to biosynthesis of desired end product. Flux analysis invariably shows that the efficiency with which a given feedstock is converted to biomass is far from optimal because of excretion of intermediates; usually those upstream of bottlenecks, those that result from the accumulation of intracellular polymers, or both. Analysis of culture filtrates allows for the identification of undesired fluxes, which become targets for metabolic intervention by metabolic engineers (El-Mansi and Holms 1989; El-Mansi 2004). Therefore, flux analysis highlights wasteful fluxes, thus enabling the metabolic engineer to develop a rationale for the diversion of wasted fluxes to product formation, a primary target for the discerning biotechnologist.

7.5.1 Kacser's Universal Method for Increasing Flux to Product Formation without Perturbing Steady-State Concentrations of Metabolites

In this method, Kacser and Acerenza (1993) provide a sound theoretical framework for increasing *in vivo* flux to product formation by a certain percentage without perturbing steady-state concentrations of metabolites.

7.5.1.1 The Model

In their analysis, Kacser and Acerenza viewed the cell as a "transparent box" (Figure 7.8) connected to external inputs "N" (carbon, oxygen, nitrogen, phosphate, etc.,) and exports outputs "P", which could be a primary or secondary metabolite. Kacser stressed the following understandings:

- In a nongrowing but metabolically active culture, fluxes through central metabolism are essentially dedicated to satisfy maintenance requirements, and as such fluxes to biosynthesis of macromolecules such as DNA, protein, lipids, etc., are negligible; assumed to be zero.

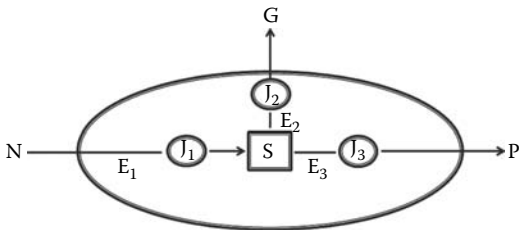

FIGURE 7.8 Kacser's universal model. N, all input; P, desired product; G, flux to biomass and metabolite excretion; S, intracellular concentrations of all metabolites of central and intermediary metabolism.

- However, during the course of exponential growth, fluxes to biosynthesis of macromolecules are large. However, once a steady state is achieved in either case (i.e., nongrowing but metabolically active or exponentially growing cells) a "time-invariant" concentration of all metabolites and fluxes within the cell and out to product formation is realized, thus achieving perfect balance between input and output fluxes.

Kacser used a very simple model (Figure 7.8) to describe his theory. He represented all inputs by "N", desired product by "P", and gathered all other outputs to "G", with "S" representing the intracellular concentrations of all metabolites.

7.5.1.1.1 Assumptions and Scenario

In describing his method, Kacser made the following assumptions:

- That the sequence of reactions involved in the conversion of "N" to "S", "S" to "G", and "S" to "P" are unique to each pathway.
- That the metabolic pathways involved in the conversion of "S" to "G" are complex but will in a steady state reach time invariant with respect to all components, the concentration of which is represented by "S".
- That P and G are excreted into a very large volume of medium, thus rendering their concentrations negligible; that is, zero.

The challenge facing Kacser at the time was how to increase flux to product formation (J_3) without perturbing the steady-state concentration of metabolites or fluxes to metabolite excretions (J_2); Figure 7.8.

To validate his theory, Kacser had to set a target of a certainfold increase in flux through J_3. Therefore, the steady-state fluxes through the scheme shown above (Figure 7.8) are constrained by Equation (7.1), with J^o denoting fluxes in the original state (i.e., wild-type strain):

$$J_1 = J_2 + J_3 \tag{7.1}$$

Similarly, following genetic modifications using recombinant DNA technology, a new set of fluxes are obtained. Again, these fluxes are constrained by Equation 7.1, with "r" replacing "o" as a superscript.

The increase in flux Δj can be calculated by the following equation:

$$\Delta J_1 = \Delta J_2 + \Delta J_3 \tag{7.2}$$

However, because no change in the J_2 flux is desired (i.e., $\Delta J_2 = 0$), then

$$\Delta J_1 = \Delta J_3 \tag{7.3}$$

In his mathematical treatment, Kacser stressed that ΔJ is the absolute change in flux, which will be same for J_1 and J_3. By adding ΔJ *to the synthesis of S and its conversion to product, the original value* S^0 *will* remain constant because $\Delta J_2 = 0$. Kacser went on to stress that this is true no matter what the original fluxes J_1 and J_3 are. He also stressed that the ratio of the original fluxes (j_3^0/j_1^0) will be different from (j_3^r/j_1^r) in the recombinant strain. This is the central device that allows for the identification of which enzyme to overexpress.

7.5.1.1.2 Application of the Universal Method: Increasing Flux to Tryptophan Formation in the Yeast S. cerevisiae

In this example, Kacser used the metabolic pathways depicted in Figure 7.9, which are the generally accepted pathway for the production of tryptophan by the yeast S. cerevisiae (Niederberger et al.

1992). The aforementioned authors have also experimentally determined fluxes through j_1^0 and j_2^0 as well as j_3^0 and found them to be 3, 2.5, and 0.5 respectively.

Using the above information, the universal method can be used to calculate the multiplication factor by which the expression of the enzymes constituting "E1" and "E3" (Figure 7.9) must be increased by to achieve the desired level of increase in flux to product formation by applying the following equations:

$$r_1 = 1 + \Delta J/J_1^0 \tag{7.4}$$

$$r_3 = 1 + \Delta J/J_3^0 \tag{7.5}$$

Calculating ΔJ in the wild-type strain can be achieved as follows:

$$\Delta J = J_1^0 - J_3^0 \tag{7.6}$$

$$\Delta J = 3 - 0.5 = 2.5$$

The impact of increasing ΔJ from 2.5(wild type) to 12 in the recombinant strain on flux to product formation can be calculated using the following calculation:

$$r_3 = 1 + \Delta J/J_3 = 1 + 12/0.5 = 1 + 24 = 25\text{-fold}$$

As can be seen from the above calculation, an increase in ΔJ from *2.5*(wild type) to 12 in the recombinant strain was accompanied by a 25-fold increase in flux to product formation. To achieve this increase in flux without perturbing the concentrations of central and intermediary metabolites, a 5-fold increase in the expression of all enzymes involved in the conversion of primary carbon source "N" to "CA" (chorismate) is required as evidenced by the following calculation:

$$r_1 = 1 + \Delta J/J_1 = 1 + 12/3 = 1 + 4 = 5\text{-fold}$$

Now, remember that flux through J_0^r remains constant because $\Delta J_2 = 0$. It therefore follows that a 5-fold increase in the enzymic activities leading to the formation of chorismate (CA) and a 25-fold increase in the activities of the enzymes leading from CA to tryptophan (Figure 7.9) would yield some 25-fold increase in flux to tryptophan without perturbing the intracellular concentration of CA or J_2 fluxes.

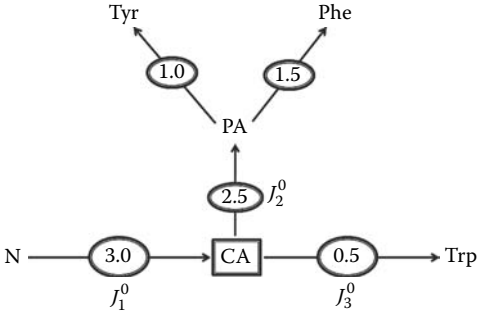

FIGURE 7.9 The metabolic pathways used by the yeast *S. cerevisiae* for the production of tryptophan. N, primary carbon source; CA, chorismate acid; Trp, tryptophan; PA, protocatechuate; Phe, phenylalanine; Tyr, tyrosine.

However, the question that remains is if we can achieve such a level of overexpression of the entire shikamate pathway (E1) through genetic manipulation? The answer to this is of course we can, and several strategies exist for doing so, including cloning the entire shikamate pathway on a plasmid that has five copies per chromosome and/or cloning downstream of a titratable promoter or indeed using the technique of promoter swapping (McCleary 2009).

7.6 STOICHIOMETRIC ANALYSIS OF METABOLIC NETWORKS

Stoichiometry-based modeling of metabolic pathways is of practical importance because it extracts systemic information such as phenotypes from molecular-level network structure. Stoichiometric analysis requires knowledge of the system's enzymatic reactions and the stoichiometries of their associated substrates and products. Mass conservation is a powerful constraint that restricts how the enzymatic reactions can be integrated to create a functioning steady-state metabolism. Results are specific to metabolic network structure and therefore typically vary from one organism to another. Stoichiometric modeling can utilize various *"omics"*, or datasets to build and verify models. Stoichiometry-based methods are in contrast to kinetic modeling methods, which often require large condition-sensitive parameter sets (e.g., v_{max} and K_m for each enzyme). Such parameters are very difficult, if not impossible, to reliably determine *in vivo*, and literature values often vary over an order of magnitude, thus limiting the usefulness of kinetic modeling.

7.6.1 Applications of Stoichiometric Analysis

To illustrate the usefulness of stoichiometric analysis in biochemical and metabolic engineering studies, let us consider the classical example of phenylalanine production. This example will highlight central concepts of stoichiometric analysis using a relatively simple system that permits manual analysis.

7.6.1.1 Optimization of Phenylalanine Production: A Case Study

In *E. coli*, biosynthesis of phenylalanine and other aromatic amino acids is initiated by the condensation of phosphoenolpyruvate (PEP) and erythrose 4-phosphate (E-4P) to give 3-deoxy-D-arabino-heptulosonate 7-phosphate (DAHP), This condensation reaction is catalyzed through the activities of three different DAHP synthases, the products of *aroF, aroG,* and *aroH*, which are subject to feedback inhibition by tyrosine, phenylalanine, and tryptophan, respectively. The metabolic routes to phenylalanine are well established, and assuming that no unknown byproducts are being formed, the theoretical yield coefficient for the production of phenylalanine—or any given product—can be calculated (Foberg et al. 1988).

The overall reaction for the formation of phenylalanine can be expressed by

$$\begin{aligned} &2\text{PEP} + \text{E4-P} + 2\text{NADPH} + \text{ATP} + \text{Glutamate} \rightarrow \\ &\text{Phenylalanine} + \text{CO}_2 + \text{2-Oxoglutarate} + 2\text{NADP}^+ + \text{ADP} + 4\text{Pi} \end{aligned} \tag{7.7}$$

Assuming that E4-P is generated through the activities of transketolase and transaldolase of the pentose phosphate pathway (PPP) and that PEP, which is generated through glycolysis, is required for the uptake of glucose and its activation to glucose 6-phosphate, the overall reaction of phenylalanine production can be described as follows:

$$\text{X-Glucose} \rightarrow 2\ \text{PEP} + \text{E4-P} + \text{X-Pyruvate} \rightarrow \text{Phenylalanine} \tag{7.8}$$

Taking the number of carbon atoms in each of the above molecules into consideration, the carbon balance of Equation 7.8 can be resolved as follows:

$$\text{X (6)} \rightarrow 2\ (3) + 1\ (4) + \text{X (3)}$$

This, in turn, can be solved as follows:

$$X\,(6) \rightarrow 6 + 4 + X\,(3)$$

$$X\,(6) - X\,(3) = 6 + 4$$

$$X\,3 = 10;\ \text{it follows}$$

$$X = 10/3 = 3 \text{ and } 1/3^{rd} \text{ moles of glucose.}$$

According to the above stoichiometry, 3.33 moles of glucose (MW 180) are required for the production of 1 mole of phenylalanine (MW 165.2), thus giving a maximum theoretical yield coefficient of 0.275 g of phenylalanine per gram of glucose.

Taking into consideration that the biosynthesis of phenylalanine (Equation 7.7) requires 2 moles of NADPH, which is generated as a consequence of pyruvate oxidation In the Krebs cycle at the level of ICDH, the overall reaction can be rewritten as follows:

$$X \text{ Glucose} \rightarrow 2 \text{ PEP} + \text{E4-P} + 2 \text{ Pyruvate} \rightarrow \text{Phenylalanine} \tag{7.9}$$

Solving Equation 7.9 in the same way as for Equation 7.8, the carbon balance under these circumstances is that 2.67 moles of glucose are required for the production of 1 mole phenylalanine and as such the overall stoichiometry will therefore be as follows:

$$2.67 \text{ moles of glucose} \rightarrow 1 \text{ mole of phenylalanine} + 7 \text{ moles of } CO_2 \tag{7.10}$$

Further consideration of the stoichiometry balance for the above equation reveals a shortfall of PEP supply by a factor of 0.67 mole. Similarly, on close examination, one can see that 0.66 mole of pyruvate is wasted in the form of CO_2 (Figure 7.10). Diversion of pyruvate to PEP formation rather than CO_2 production therefore becomes a suitable target for metabolic intervention through the expression of PEP synthetase (Figure 7.10). Because this enzyme is subject to catabolite repression by glucose in *E. coli*, the use of recombinant DNA technology to construct a mutant strain that is insensitive to

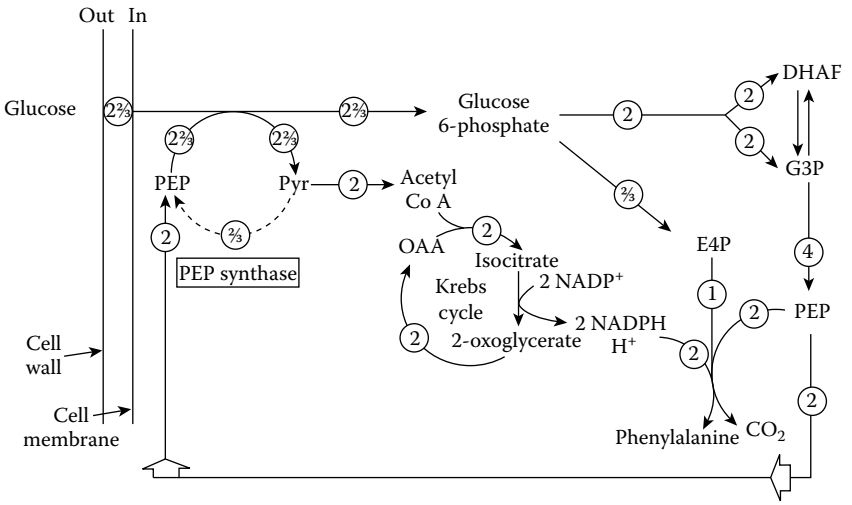

FIGURE 7.10 Diagrammatic representation of the metabolic network used by *E. coli* for the production of phenylalanine. Note the role of PEP synthase on the recycling of pyruvate to PEP and its consequences on the efficiency of carbon conversion to phenylalanine.

catabolite repression or a recombinant strain that is capable of expressing PEP synthetase constitutively affords a good example in which metabolic and genetic engineering work in concert.

Interestingly, an appreciable increase in flux to DAHP and, in turn, phenylalanine as a result of overexpression of PEP synthetase has been reported in the literature (e.g., Stephanopoulos et al. 1998), thus lending further support to the analysis portrayed above. The effect of overexpression of PEP synthetase on the efficiency of carbon conversion to DAHP and, in turn, phenylalanine production can be assessed quantitatively as illustrated in the stoichiometric diagram shown in Figure 7.10. From Figure 7.10, it can be seen that constitutive expression of PEP synthetase resulted in the formation of a PEP regenerating cycle that, under these circumstances, proved to be advantageous—rather than futile—as evidenced by a 100% increase in flux to DAHP; the biosynthetic precursor for phenylalanine, to give 0.787 g of DAHP per gram of glucose utilized. Therefore, the production of phenylalanine is a classic example in which stoichiometric flux analysis and metabolic and genetic engineering were integrated successfully.

7.6.1.2 *In Silico* Analysis of Stoichiometric Models

The phenylalanine example from the preceding section was evaluated manually using reaction stoichiometry and carbon balances. Biochemical networks are typically highly branched, and fluxes must simultaneously satisfy multiple conservation criteria (e.g., balances of carbon, nitrogen, and reducing equivalents). These systems are often too complex to solve manually. Computational stoichiometric modeling methods are readily scalable and can analyze systems with hundreds or thousands of reactions. These methods can be broadly divided into three major approaches:

1. Metabolic flux analysis (MFA)
2. Constraint-based linear programming including flux balance analysis (FBA)
3. Metabolic pathway analysis including elementary flux mode analysis (EFMA)

All three approaches define a system-specific solution space based on metabolic network structure and conservation relationships; this solution space contains all possible, biologically relevant flux distributions. The three approaches differ in how they select distinct metabolic flux distributions from the solution space; details of these approaches have been reported elsewhere (e.g., Stephanopoulos et al. 1998; Schilling et al. 1999; Schuster et al. 2000; Reed and Palsson 2003; Trinh et al. 2009).

This section further develops the phenylalanine synthesis case study by constructing a more detailed network model and analyzing it using *in silico* stoichiometric analysis. Phenylalanine synthesis is made possible by a metabolic network that integrates the required carbon, nitrogen, and reducing equivalent fluxes. This network can be defined using a series of conservation relationships linking each reaction's substrates and products. A graphical representation of the current case study network is shown in Figure 7.11a. The conservation equations for each reaction are listed in Figure 7.11b. The presented model balances each reaction for carbon, nitrogen, and reducing equivalents; hydrogen, oxygen, and inorganic phosphate are assumed to be balanced on the basis of implicit cellular maintenance processes. Notable network differences from the case study in Section 7.6.1.1 include consideration of glutamate dehydrogenase in the assimilation of ammonia, the oxidative branch of the pentose phosphate pathway that generates carbon dioxide (CO_2) and NADPH, oxygenic respiration that produces ATP and regenerates NAD^+, anaplerotic reactions, excretion of acetate, and the consumption of ATP for cellular maintenance processes (MainE, reaction R20). To simplify the case study, nonbranching enzyme series have been combined into single model reactions that account for the overall transformation. For instance, reaction R2 accounts for the coupled activities of enzymes *Pgi, Pfk,* and *Fba*.

Stoichiometric modeling approaches consider steady-state metabolic scenarios. This treatment necessitates the classification of metabolites as balanced or unbalanced (sometimes referred to as internal and external metabolites, respectively). A balanced metabolite is constrained by the steady-state assumption and is not allowed to accumulate while an unbalanced metabolite serves

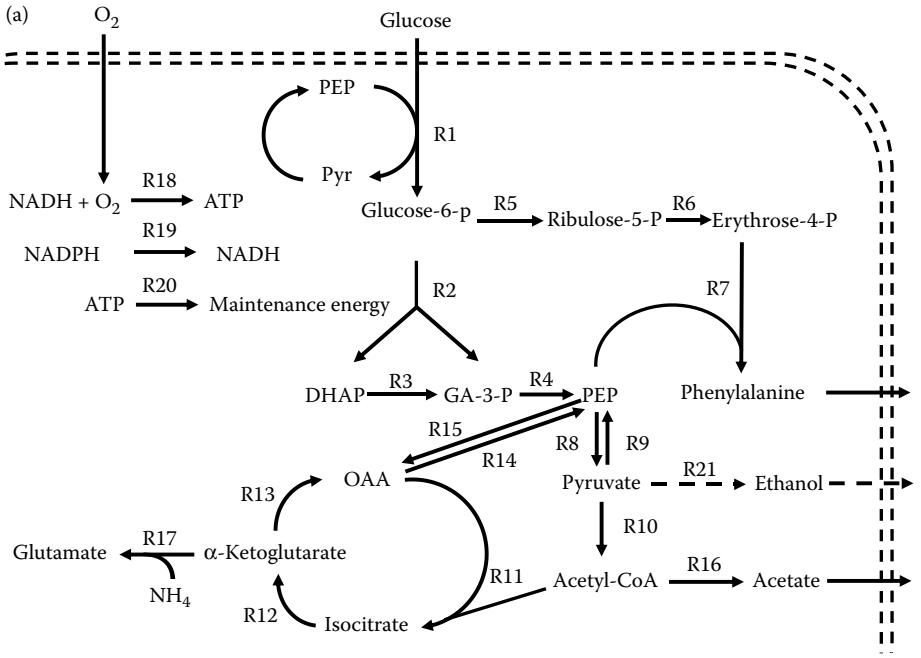

Key: PEP = Phosphoenolpyruvate
Pyr = Pyruvate
DHAP = Dihydroxyacetone phosphate
OAA = Oxaloacetate
GA-3-P = Glyceraldehyde-3-phosphate

(b)

R1 : Glucose + PEP = Glucose-6-P + Pyruvate.
R2 : Glucose-6-P + ATP = DHAP + Glyceralhyde-3-P + ADP.
R3 : DHAP = Glyceraldhyde-3-P.
R4 : Glyceraldhyde-3-P + NAD + ADP = PEP + ATP + NADH.
R5 : Glucose-6-P + 2 NADP = 1 Ribulose-5-P + 2 NADPH + CO_2.
R6 : 2 Ribulose-5-P = Erythrose-4-P + Glucose-6-P.
R7 : 2 PEP + Erythrose-4-P + NADPH + ATP + Glutamate = NADP + ADP + Phenylalanine + α-Ketoglutarate + CO_2.
R8 : PEP + ADP = Pyruvate + ATP.
R9 : Pyruvate + 2 ATP = PEP + 2 ADP.
R10 : Pyruvate + CoASH + NAD = Acetyl-CoA + NADH + CO_2.
R11 : Acetyl-CoA + Oxaloacetate = Isocitrate + CoASH.
R12 : Isocitrate + NADP = α-Ketoglutarate + NADPH + CO_2.
R13 : α-Ketoglutarate + 2 NAD = Oxaloacetate + 2 NADH + CO_2.
R14 : Oxaloacetate + ATP = PEP + CO_2 + ADP.
R15 : PEP + CO_2 = Oxaloacetate.
R16 : Acetyl-CoA + ADP = ATP + CoASH + Acetate.
R17 : α-Ketoglutarate + NADPH + NH_4 = Glutamate + NADP.
R18 : 2 NADH + O_2 + 4 ADP = 4 ATP + 2 NAD.
R19 : NADPH + NAD = NADH + NADP.
R20 : ATP = MaintE + ADP.

FIGURE 7.11 (a) Graphical representation of case study *E. coli* metabolic network producing phenylalanine from glucose. (b) Stoichiometries for each network reaction. Every reaction is considered irreversible and glucose, O_2, NH_4, CO_2, acetate, phenylalanine, and maintenance energy (MainE) are considered as unbalanced system inputs and outputs.

as a system input or output and is permitted to accumulate. Definitions of balanced and unbalanced metabolites have significant effects on analysis and must be selected carefully. There are seven unbalanced metabolites in this model; that is, system inputs of glucose, ammonium (NH_4) and oxygen (O_2) as well as system outputs of CO_2, phenylalanine, acetate, and maintenance energy.

Conservation equations defining the metabolic reaction network can be written in a matrix format that concisely organizes the reaction information:

$$\mathbf{S} \bullet \mathbf{r} = \mathbf{C} \tag{7.11}$$

where **S** is a *m x n* matrix containing the substrate and product stoichiometric coefficients for each reaction, **r** is an *n* element column vector containing the rate (flux) through each network reaction (moles/L/h), and **C** is an *m* element column vector detailing accumulation (time-dependent change in concentration) of each network metabolite (moles/L/h). Reactions from Figure 7.11b are presented as a stoichiometric matrix **S** in Table 7.2; note each column corresponds to a reaction (R1–R20) and each row corresponds to a metabolite. Metabolites consumed in a reaction have a negative coefficient, metabolites produced in a reaction have positive coefficient, and metabolites that do not participate in a reaction have a zero coefficient. Unbalanced network metabolites (system inputs and outputs) are highlighted in gray rows.

To prevent accumulation under steady-state functioning, production of balanced metabolites must equal consumption. The system written in Equation 7.11 can be rewritten in terms of just balanced metabolites:

$$\mathbf{S'} \bullet \mathbf{r'} = \mathbf{0} \tag{7.12}$$

where **S'** and **r'** are identical to **S** and **r** except the unbalanced metabolites have been removed (gray rows in Table 7.2). The right side of Equation 7.12 is a column vector comprised of zeroes; the balanced metabolite concentrations are not a function of time. All elements of **S'** are known from the reaction stoichiometries. The elements of the rate vector **r'** are unknown, and identifying their magnitudes is the typical aim of Equation 7.12. As presented, **r'** has 20 unknown rates whereas **S'** is comprised of 19 balanced metabolite conservation relationships. The rank of **S'** is 15, indicating that there are only 15 linearly independent relationships that can be used to identify the 20 unknown elements of **r'**. Most biological metabolic networks, because of their high connectivity, have more unknowns (elements in vector **r'**) than linearly independent relationships (rank of **S'**). This class of linear algebra problem is termed "underdetermined" and more than one solution exists. A solution would represent a metabolic flux distribution (denoted in vector **r'**) that balances system inputs with outputs. There are two widely used approaches for identifying solutions to this problem: constraint-based linear programming such as FBA (Reed and Palsson 2003) and metabolic pathway analysis such as EFMA (Schuster et al. 2000); EFMA will be presented here.

EFMA deconstructs all possible, biologically significant solutions to Equation 7.12 into a minimal set of nondecomposable network reaction fluxes. These reaction combinations are called elementary flux modes (EFMs) and can be viewed as mathematically defined biochemical pathways. Each EFM is genetically independent because each uses a unique combination of genes/reactions (Schuster et al. 2000). EFMs represent the simplest balanced flux unit for a biochemical network operating at steady state and therefore are ideal starting points for understanding metabolic organization and phenotypes. EFMs are fundamental biochemical building blocks that can define any steady state. EFMA can be performed using publically available software (Kamp and Schuster 2006; Klamt et al. 2007; Terzer and Stelling 2008). The work presented here used Metatool version 5.0 (http://pinguin.biologie.uni-jena.de/bioinformatik/networks/index.html).

The model described here possesses 13 unique EFMs that balance the system inputs with outputs. The 13 EFMs (EFM1–EFM13) are listed as rows in Table 7.3a. Each column entry is a relative flux through the corresponding network reaction. As mentioned earlier, each EFM is genetically independent and uses a unique combination of reactions. There are seven distinct EFMs that produce

TABLE 7.2
Stoichiometry Matrix (S) for the Case Study Reaction Network. Network Reactions (R1–R20) are Listed as Columns and Network Metabolites are Listed as Rows. Unbalanced Network Metabolites are Highlighted in Gray Rows. G3P, Glyceraldehydes 3-phosphate; CoASH, Coenzyme A; E-4P, erythrose-4-phosphate; Ribulose-5-P, Ribulose-5-phosphate

	R1	R2	R3	R4	R5	R6	R7	R8	R9	R10	R11	R12	R13	R14	R15	R16	R17	R18	R19	R20
PEP	–1	0	0	1	0	0	–2	–1	1	0	0	0	0	1	–1	0	0	0	0	0
Glucose-6-P	1	–1	0	0	–1	1	0	0	0	0	0	0	0	0	0	0	0	0	0	0
ATP	0	–1	0	1	0	0	–1	1	–2	0	0	0	0	–1	0	1	0	4	0	–1
ADP	0	1	0	–1	0	0	1	–1	2	0	0	0	0	1	0	–1	0	–4	0	1
Pyruvate	1	0	0	0	0	0	0	1	–1	–1	0	0	0	0	0	0	0	0	0	0
Glyceraldehyde-3-P	0	1	1	–1	0	0	0	0	0	0	0	0	0	0	0	0	0	0	0	0
DHAP	0	1	–1	0	0	0	0	0	0	0	0	0	0	0	0	0	0	0	0	0
NADH	0	0	0	1	0	0	0	0	0	1	0	0	2	0	0	0	0	–2	1	0
NAD	0	0	0	–1	0	0	0	0	0	–1	0	0	–2	0	0	0	0	2	–1	0
NADPH	0	0	0	0	2	0	–2	0	0	0	0	1	0	0	0	0	–1	0	–1	0
NADP	0	0	0	0	–2	0	2	0	0	0	0	–1	0	0	0	0	1	0	1	0
Acetyl-CoA	0	0	0	0	0	0	0	0	0	1	–1	0	0	0	0	–1	0	0	0	0
CoASH	0	0	0	0	0	0	0	0	0	–1	1	0	0	0	0	1	0	0	0	0
Isocitrate	0	0	0	0	0	0	0	0	0	0	1	–1	0	0	0	0	0	0	0	0
Oxaloacetate	0	0	0	0	0	0	0	0	0	0	–1	0	1	–1	1	0	0	0	0	0
α-Ketoglutarate	0	0	0	0	0	0	1	0	0	0	0	1	–1	0	0	0	–1	0	0	0
Erythrose-4-P	0	0	0	0	0	1	–1	0	0	0	0	0	0	0	0	0	0	0	0	0
Ribulose-5-P	0	0	0	0	1	–2	0	0	0	0	0	0	0	0	0	0	0	0	0	0
Glutamate	0	0	0	0	0	0	–1	0	0	0	0	0	0	0	0	0	1	0	0	0
Glucose	–1	0	0	0	0	0	0	0	0	0	0	0	0	0	0	0	0	0	0	0
O_2	0	0	0	0	0	0	0	0	0	0	0	0	0	0	0	0	0	–1	0	0
NH_4	0	0	0	0	0	0	0	0	0	0	0	0	0	0	0	0	–1	0	0	0
CO_2	0	0	0	0	1	0	1	0	0	1	0	1	1	1	–1	0	0	0	0	0
Phenylalanine	0	0	0	0	0	0	1	0	0	0	0	0	0	0	0	0	0	0	0	0
Acetate	0	0	0	0	0	0	0	0	0	0	0	0	0	0	0	1	0	0	0	0
Maintenance ATP	0	0	0	0	0	0	0	0	0	0	0	0	0	0	0	0	0	0	0	1

TABLE 7.3

(a) EFMA Results for Case Study Network. The 13 EFMs are Listed as Rows; Network Reactions are Listed as Columns with each entry Representing the Relative Flux through the Reaction. Yp/g, Phenylalanine Yield on Glucose (mol/mol); Yp/O_2, is the Phenylalanine Yield on O_2 (mol/mol). (b) Overall Transformation of each EFM written in Terms of Unbalanced System Inputs and Outputs. MainE, Maintenance Energy

a.

Reaction	R1	R2	R3	R4	R5	R6	R7	R8	R9	R10	R11	R12	R13	R14	R15	R16	R17	R18	R19	R20	Yp/g	Yp/O_2
EFM1	2	1	1	2	2	1	1	0	2	0	0	0	0	4	4	0	1	2	2	0	0.50	0.50
EFM2	2	1	1	2	2	1	1	0	2	0	0	0	0	0	0	0	1	2	2	4	0.50	0.50
EFM3	2	1	1	2	2	1	1	4	6	0	0	0	0	0	0	0	1	2	2	0	0.50	0.50
EFM4	1	1	1	2	0	0	0	1	0	2	0	0	0	12	12	2	0	2	0	0	0.00	0.00
EFM5	1	1	1	2	0	0	0	1	0	2	2	2	2	22	22	0	0	5	2	0	0.00	0.00
EFM6	1	1	1	2	0	0	0	1	0	2	0	0	0	0	0	2	0	2	0	12	0.00	0.00
EFM7	1	1	1	2	0	0	0	1	0	2	2	2	2	0	0	0	0	5	2	22	0.00	0.00
EFM8	1	1	1	2	0	0	0	13	12	2	0	0	0	0	0	2	0	2	0	0	0.00	0.00
EFM9	1	1	1	2	0	0	0	23	22	2	2	2	2	0	0	0	0	5	2	0	0.00	0.00
EFM10	4	3	3	6	2	1	1	0	0	4	0	0	0	30	30	4	1	6	2	0	0.25	0.17
EFM11	4	3	3	6	2	1	1	0	0	4	4	4	4	50	50	0	1	12	6	0	0.25	0.08
EFM12	4	3	3	6	2	1	1	0	0	4	0	0	0	0	0	4	1	6	2	30	0.25	0.17
EFM13	4	3	3	6	2	1	1	0	0	4	4	4	4	0	0	0	1	12	6	50	0.25	0.08

b.

Overall Transformation	
EFM1	2 Glucose + 2 O_2 + NH_4 = 3 CO_2 + Phenylalanine
EFM2	2 Glucose + 2 O_2 + NH_4 = 4 MaintE + 3 CO_2 + Phenylalanine
EFM3	2 Glucose + 2 O_2 + NH_4 = 3 CO_2 + Phenylalanine
EFM4	Glucose + 2 O_2 = 2 CO_2 + 2 Acetate
EFM5	Glucose + 5 O_2 = 6 CO_2
EFM6	Glucose + 2 O_2 = 12 MaintE + 2 CO_2 + 2 Acetate
EFM7	Glucose + 5 O_2 = 22 MaintE + 6 CO_2
EFM8	Glucose + 2 O_2 = 2 CO_2 + 2 Acetate
EFM9	Glucose + 5 O_2 = 6 CO_2
EFM10	4 Glucose + 6 O_2 + NH_4 = 7 CO_2 + Phenylalanine + 4 Acetate
EFM11	4 Glucose + 12 O_2 + NH_4 = 15 CO_2 + Phenylalanine
EFM12	4 Glucose + 6 O_2 + NH_4 = 30 MaintE + 7 CO_2 + Phenylalanine + 4 Acetate
EFM13	4 Glucose + 12 O_2 + NH_4 = 50 MaintE + 15 CO_2 + Phenylalanine

phenylalanine (reaction R7). The efficiency of each EFM to produce phenylalanine can be determined from yields. Because each column in Table 7.3a represents a relative reaction flux, calculating yields only requires calculating flux ratios between phenylalanine production and either glucose consumption or O_2 consumption. The phenylalanine glucose yield ranges from 0.25 to 0.5 moles phenylalanine synthesized per mole glucose consumed and from 0.08 to 0.5 moles phenylalanine synthesized per mole O_2 consumed. Six EFMs do not produce phenylalanine but instead represent other metabolic functioning. Table 7.3b lists the overall transformation for each EFM written in terms of the unbalanced system metabolites (inputs and outputs).

All EFMs satisfy the network steady-state relationship in Equation 7.12 as do any nonnegative linear combination of EFMs. For instance, 2*EFM1 + 3*EFM5 + 1*EFM8 is a solution to Equation 7.12. This flux distribution would produce phenylalanine with a glucose yield of 0.25 moles phenylalanine per mole of glucose.

7.6.1.3 *In Silico* Design of Recombinant Systems

EFMA identifies a set of nondivisible biochemical pathways that define a network's steady-state metabolic capabilities. The output explicitly lists which reactions are necessary and unnecessary for each EFM. This information provides metabolic engineering targets for increasing or forcing flux toward a desired product. For instance, using the phenylalanine case study (Table 7.3) it is possible to identify a single gene deletion (*pyk*, reaction R8) that would force the network to produce phenylalanine. Reaction R8 is used by all EFMs that do not make phenylalanine, although it would also prevent functioning of EFM3, which makes phenylalanine. The deletion would alter network structure so that only phenylalanine-producing fluxes would be possible under steady-state conditions. It should be noted that EFM1 and EFM2 would require expression of PEP synthetase (reaction R9); as mentioned in Section 7.6.1.1, this enzyme is typically associated with gluconeogenesis and activity is repressed by glucose.

EFMA is a useful tool for analyzing potential fluxes through recombinant metabolic pathways (Liao et al. 1996; Carlson et al. 2002, 2005; Wlaschin et al. 2006). EFMA identifies how recombinant fluxes can integrate into a host's native metabolic structure; the approach can also identify gene deletion strategies for diverting *in vivo* fluxes through the recombinant pathway; for example, the case study network can be modified to consider recombinant expression of the pyruvate decarboxylase and alcohol dehydrogenase of *Zymomonas mobilis*. This experimental *E. coli* system has been built and used to produce significant amounts of ethanol (Ingram et al. 1987; Ohta et al. 1991). To model expression of this pathway, the following reaction can be added to the model listed in Figure 7.11b:

$$\text{R21} : \text{Pyr} + \text{NADH} = \text{Ethanol} + \text{CO}_2 + \text{NAD}. \tag{7.13}$$

This reaction represents the combined activity of both *Z. mobilis* enzymes. Ethanol is treated as an unbalanced system output. Analyzing this modified model results in 18 unique EFMs. Five EFMs produce ethanol (Table 7.4) and the remaining 13 are identical to the results from the original simulation (Table 7.3). The output explicitly lists which reactions are required and not required for ethanol production. For instance, removing genes associated with R9 and R10 (*ppsA* and *aceE*, respectively) would force the network to produce ethanol under steady-state conditions.

The *E. coli* central metabolism is a highly robust system capable of many unique metabolic fluxes, and multiple gene deletions are often required to construct a desired strain. Models containing millions of EFMs and examples of strain construction through targeted gene deletions have been reported (Trinh et al. 2006; Wlaschin et al. 2006; Carlson 2007).

7.6.1.4 Modeling Cellular Growth

Bioprocess synthesis of desired chemicals is often linked to cellular growth. Growth requires a combination of maintenance energy and biomass macromolecule synthesis. The case study

TABLE 7.4
(a) EFMA Results for Recombinant, Ethanologenic Network. The five EFMs that Produce Ethanol are Listed as Rows; Network Reactions are Listed as Columns with Each Entry Representing the Relative Flux Through the Reaction. The five Listed EFMs are in Addition to the 13 EFMs Identified for the Base Model. (b) Overall Transformation of each EFM Written in Terms of Unbalanced System Inputs and Outputs. MainE, Maintenance Energy

a.

Reaction	R1	R2	R3	R4	R5	R6	R7	R8	R9	R10	R11	R12	R13	R14	R15	R16	R17	R18	R19	R20	R21
EFM14	1	1	1	2	0	0	0	1	0	0	0	0	0	2	2	0	0	0	0	0	2
EFM15	1	1	1	2	0	0	0	1	0	0	0	0	0	0	0	0	0	0	0	2	2
EFM16	1	1	1	2	0	0	0	3	2	0	0	0	0	0	0	0	0	0	0	0	2
EFM17	4	3	3	6	2	1	1	0	0	0	0	0	0	10	10	0	1	2	2	0	4
EFM18	4	3	3	6	2	1	1	0	0	0	0	0	0	0	0	0	1	2	2	10	4

b.

EFM14	Glucose = 2 CO_2 + 2 Ethanol
EFM15	Glucose = 2 MaintE + 2 CO_2 + 2 Ethanol
EFM16	Glucose = 2 CO_2 + 2 Ethanol
EFM17	4 Glucose + 2 O_2 + NH_4 = 7 CO_2 + Phenylalanine + 4 Ethanol
EFM18	4 Glucose + 2 O_2 + NH_4 = 10 MaintE + 7 CO_2 + Phenylalanine + 4 Ethanol

considers maintenance energy (MainE, reaction R20) but not biomass synthesis. Metabolic network models are often used to analyze metabolite fluxes associated with cellular growth. There are two widely utilized strategies for predicting fluxes associated with growth. The first approach is based on the observations of Neidhardt and colleagues who deduced that all major biomass macromolecules (protein, RNA, DNA, lipids, polysaccharides) are derived from a few biosynthetic precursors drawn from central metabolism (Neidhardt et al. 1990). Using this information, it is possible to consider biomass synthesis by accounting for the metabolic draw of these biosynthetic precursors. These fluxes unravel the effect of growth rate on the macromolecular composition of biomass (Pramanik and Keasling 1997; Carlson and Srienc 2004a). Table 7.5 lists the *E. coli* growth-rate-dependent macromolecular composition and appropriate growth-rate-dependent stoichiometries for synthesizing the corresponding biomass using a dozen intermediates drawn from central metabolism. The ATP consumption requirements listed in Table 7.5 are solely for biosynthetic purposes, including polymerization of monomers into polymers (amino acids to proteins, nucleotides into DNA, etc.); maintenance energy requirements in the form of ATP are not included. An integrated analysis of biomass synthesis and maintenance-energy-associated fluxes can be found in Carlson and Srienc (2004b). For convenience, each overall biomass synthesis reaction is normalized to four glucose-6-phosphate molecules and therefore represents a different physical mass of cells; the cellular mass is listed as C-moles (carbon moles) in Table 7.5 and is further illustrated in Section 7.6.1.5.

The second approach for modeling biomass synthesis considers the explicit metabolic reactions and metabolites necessary to construct each biomass constituent, including macromolecules, vitamins, cofactors, and other minor constituents. This approach, depending on the level of detail considered, can require hundreds or thousands of reactions and metabolites (Feist et al. 2007). The detailed treatment of biomass is an excellent means of analyzing microbial growth medium requirements and anabolic pathways, but it requires significant a priori information, including accurate gene annotation and detailed biomass composition measurements. Subject to the focus of the research, it is often reasonable to use the simpler biomass treatment. Although the central metabolism is highly robust, most biosynthetic pathways are linear series of enzyme-catalyzed reactions without alternative routes. In addition, constituents such as vitamins and cofactors represent a minor fraction of total cellular biomass, typically within the error of experimental biomass measurements.

7.6.1.5 *In Silico* Analysis of Compartmentalized Systems: From Eukaryotes to Microbial Consortia

Eukaryotes such as yeast and fungi are widely used by industrial microbiologists for the production of a wide range of chemicals, including primary and secondary metabolites. In addition, in the natural habitat, microbial populations exist as a well balanced and interacting consortium and there is growing interest in exploiting microbial consortia as a platform in bioprocess technology (Kleerebezem and van Loosdrecht 2007). EFMA can be used to consider metabolite transformation and fluxes in systems with complex physical architectures, including eukaryotes with multiple subcellular compartments and interactions in microbial consortia. Modeling these systems requires the assignment of reactions and metabolites to distinct physical compartments. For instance, Figure 7.12 illustrates an interacting microbial consortium with respect to CO_2 exchange between the organisms on one hand and the environment on the other. The extracellular environment is treated in two manners, including a balanced "pool" compartment constrained by steady-state, no accumulation constraints and as an external, unbalanced compartment that permits CO_2 to enter or leave the system. Transport reactions (TR1–TR3) permit transfer of CO_2 from one compartment to another. It should be noted that model reactions do not necessarily have to be enzyme-catalyzed reactions. CO_2, a small uncharged molecule, readily diffuses across cellular membranes.

TABLE 7.5
***E. coli* Biomass Macromolecular Composition Listed as Mass Fraction Dry Weight (Gray Columns) and Stoichiometric Coefficients for Biomass Generating Reactions as a Function of Culture Doubling Time. The "other" Category includes Lipopolysaccarides, Peptidoglycan, Polysaccharides, and Lipids. Cmole Biomass Refers to the Mass of Cells Produced by the Reaction Stoichiometry. See Carlson and Srienc (2004a) for References. glc-6-p, glucose-6-P; rib-5-p, ribulose-5-P; ery-4-p, erythrose-4-P; pep, Phosphoenolpyruvate; pyr, Pyruvate; Ace-coa, Acetyl-CoA; Akg, Alpha-Ketoglutarate (Oxo-glutarate); Oxalo, Oxaloacetate**

Doubling	Mass Fraction																Cmole
Time (min)	Protein	DNA	RNA	Other	glc-6-p	rib-5-p	ery-4-p	pep	pyr	ace-coa	akg	Oxalo	NADH	NH_4	CO_2	ATP	Biomass
30	52	2	20	26	4	13	5	32	38	41	14	24	178	139	–2	547	565
40	55	3	18	25	4	13	5	34	41	42	16	26	192	148	–3	584	599
50	58	3	17	22	4	14	6	39	50	43	19	31	218	171	–4	678	686
60	61	3	16	20	4	16	7	45	58	44	22	36	249	198	–6	786	777
80	66.5	4.5	15	14	4	22	11	64	87	49	32	53	347	291	–10	1153	1091
100	70.5	5.5	14	10	4	32	17	91	129	55	47	78	487	424	–15	1674	1554
200	78	6	10	6	4	46	31	156	237	72	86	139	856	731	–35	2921	2652

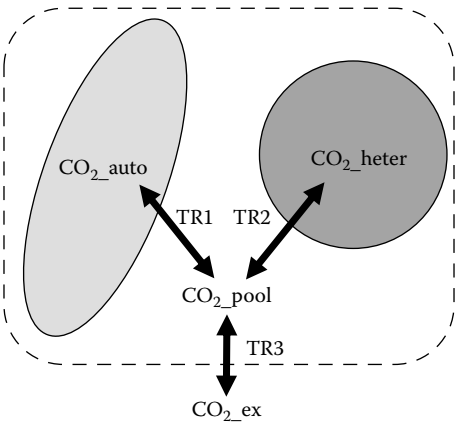

FIGURE 7.12 Diagram illustrating the partitioning of CO_2 between four distinct physical compartments indicated by suffixes: "auto" refers to an autotrophic bacterium, "heter" refers to a heterotroph bacterium, "pool" refers to a balanced extracellular compartment, and "ex" refers to an unbalanced external compartment.

Stoichiometric modeling can analyze fundamental metabolic interactions in microbial populations (Stoylar et al. 2007; Taffs et al. 2009). An example model based on interactions between a *photoautotroph* and a *heterotroph* is shown in Figure 7.13 with explicit reactions listed in Table 7.6. The consortium model is comprised of four distinct compartments analogous to Figure 7.12. Metabolites associated with each compartment have a suffix designating their location. Metabolites and therefore reactions associated with the photoautotroph have the suffix "auto" whereas metabolites associated with the heterotrophs have the suffix "heter", metabolites in a balanced extracellular compartment are labeled with the suffix "pool", and unbalanced, external metabolites that serve as system inputs and outputs have the suffix "ex". Metabolites such as glycolate or oxygen can be transferred from the photoautotroph to the heterotroph by first transiting the balanced pool compartment, or they can leave the system passing from the pool compartment to the external compartment.

The photoautotroph uses energy from sunlight to extract electrons from water, releasing O_2 as a byproduct in a biological process known as *oxygenic photosynthesis* (reaction A1). The electrons can be used to fix CO_2 into organic carbon compounds (reaction A15). Some of this organic carbon (e.g., glycolate) can be secreted, which feeds associated heterotrophic organisms (reactions A14 and H1, respectively). The consortium model system considers growth of both microbes. The biomass-synthesizing reactions (reactions A28, H29) use the 200-min doubling time biomass composition from Table 7.5. Although these organisms are not *E. coli*, basic macromolecular composition for many bacteria is similar and biosynthetic pathways are highly conserved. For modeling purposes only, photosynthetically available *photons* are considered (hv_ex). These photons would be collected by the appropriate photoantennae. The presented ecological template of primary productivity (photoautotrophy) and associated heterotrophy is globally widespread and is relevant to many proposed CO_2 remediation strategies and to proposed cyanobacterial bioprocess platforms (Burja et al. 2001).

EFMA of the consortium model identifies 720 unique EFMs with 560 EFMs synthesizing photoautotroph or heterotroph biomass. Every EFM utilizes energy absorbed from the photoautotroph's photosynthetic apparatus to fuel the consortium. All heterotrophic growth is based on oxidation of glycolate secreted by the photoautotroph. Plotting the results from EFMA quickly visualizes trends in system behavior. For instance, Figure 7.14 examines photoefficiency (C-mole biomass/photons absorbed) of the 560 biomass-synthesizing EFMs as a function of O_2 and CO_2 flux at the RuBisCO enzyme (reactions A15 and A13, respectively). RuBisCO (ribulose-1,5-bisphosphate carboxylase

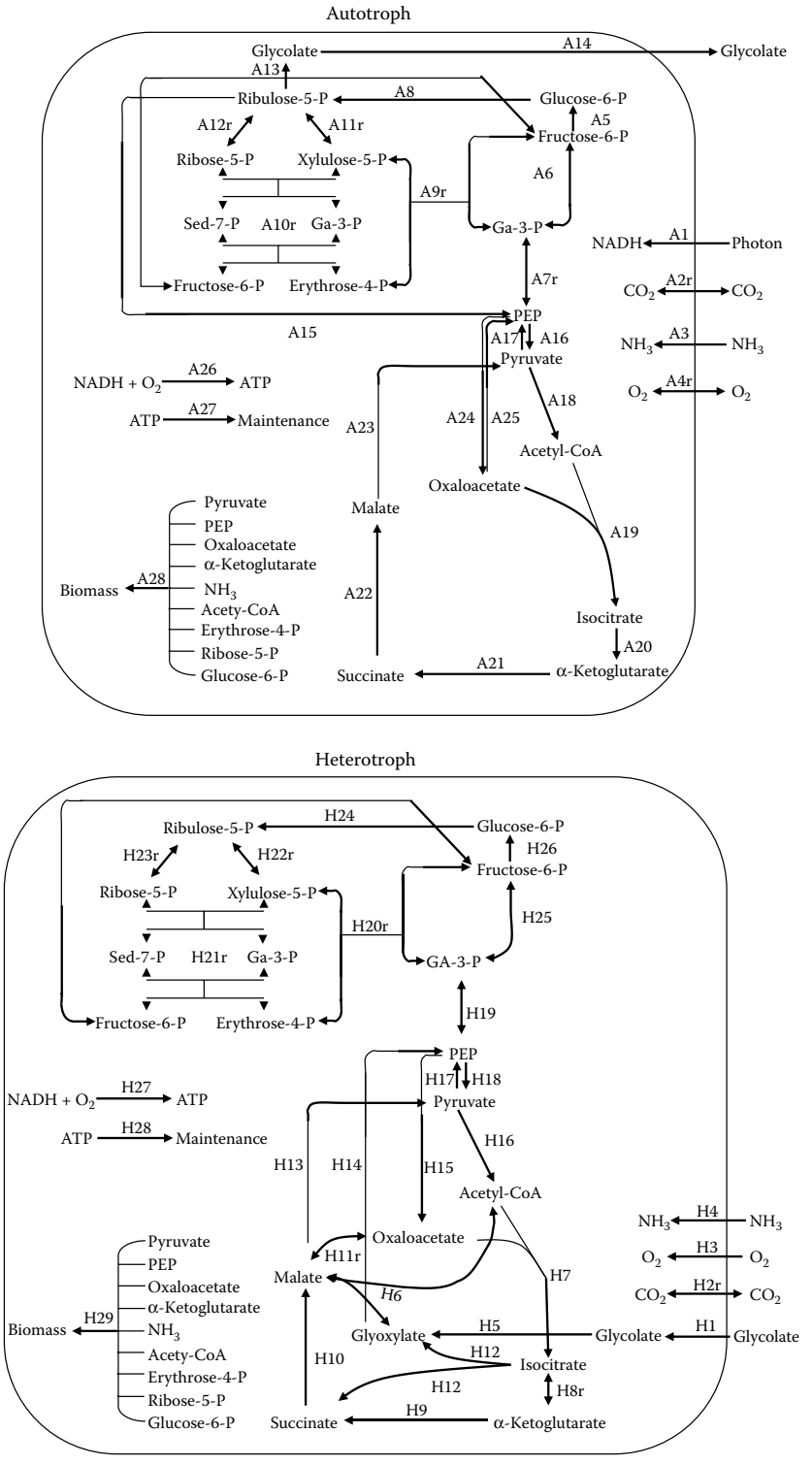

FIGURE 7.13 Graphical illustrations of photoautotroph and heterotroph metabolic networks from an interacting microbial consortium. The photoautotroph secretes glycolate, which is the sole reduced carbon and energy source for the heterotroph. Reaction designations are defined in Table 7.6.

TABLE 7.6
Reaction Network Model for Interacting Microbial Consortium

A1: 8 hv_ex + 3 ADP_auto + 2 NAD_auto = 3 ATP_auto + 2 NADH_auto + O_2_auto.
A2r: CO_2_auto = CO_2_pool.
A3: NH_3_pool = NH_3_auto.
A4r: O_2_auto = O_2_pool.
A5: fru6p_auto = glc6p_auto.
A6r: ATP_auto + fru6p_auto = 2 ga3p_auto + ADP_auto.
A7r: ga3p_auto + ADP_auto + NAD_auto = ATP_auto + NADH_auto + PEP_auto.
A8: glc6p_auto + 2 NAD_auto = CO_2_auto + 2 NADH_auto + rbl5p_auto.
A9r: ery4p_auto + xll5p_auto = fru6p_auto + ga3p_auto.
A10r: rbo5p_auto + xll5p_auto = ery4p_auto + fru6p_auto.
A11r: rbl5p_auto = xll5p_auto.
A12r: rbl5p_auto = rbo5p_auto.
A13: ATP_auto + rbl5p_auto + O_2_auto = PEP_auto + glyc_auto + ADP_auto.
A14: glyc_auto = glyc_pool.
A15: ATP_auto + CO_2_auto + rbl5p_auto = 2 PEP_auto + ADP_auto.
A16: PEP_auto + ADP_auto = ATP_auto + pyr_auto.
A17: 2 ATP_auto + pyr_auto = PEP_auto + 2 ADP_auto.
A18: pyr_auto + CoASH_auto + NAD_auto = ac_CoA_auto + CO_2_auto + NADH_auto.
A19: ac_CoA_auto + oaa_auto = icit_auto + CoASH_auto.
A20: icit_auto + NAD_auto = akg_auto + CO_2_auto + NADH_auto.
A21: akg_auto + ADP_auto + NAD_auto = ATP_auto + CO_2_auto + NADH_auto + succ_auto.
A22: O_2_auto + 2 succ_auto + 2.5 ADP_auto = 2.5 ATP_auto + 2 mal_auto.
A23: mal_auto + NAD_auto = CO_2_auto + NADH_auto + pyr_auto.
A24: CO_2_auto + PEP_auto = oaa_auto.
A25: ATP_auto + oaa_auto = CO_2_auto + PEP_auto + ADP_auto.
A26: 2 NADH_auto + O_2_auto + 5 ADP_auto = 5 ATP_auto + 2 NAD_auto.
A27: ATP_auto = MainE_auto_ex + ADP_auto.
A28: 4 glc6p_auto + 46 rbo5p_auto + 31 ery4p_auto + 156 PEP_auto + 237 pyr_auto + 72 ac_CoA_auto + 86 akg_auto + 139 oaa_auto + 731 NH3_auto + 856 NADH_auto + 2921 ATP_auto = bm_auto_ex + 35 CO_2_auto + 72 CoASH_auto + 2921 ADP_auto + 856 NAD_auto.
T1r: CO_2_pool = CO_2_ex.
T2: glyc_pool = glyc_ex.
T3r: O_2_pool = O_2_ex.
T4: NH_3_ex = NH_3_pool.
H1: glyc_pool = glyc_heter.
H2r: CO_2_heter = CO_2_pool.
H3: O_2_pool = O_2_heter.
H4: NH_3_pool = NH_3_heter.
H5: glyc_heter + NAD_heter = glyox_heter + NADH_heter.
H6r: ac_CoA_heter + glyox_heter = mal_heter + CoASH_heter.
H7: ac_CoA_heter + oaa_heter = icit_heter + CoASH_heter.
H8r: icit_heter + NAD_heter = akg_heter + CO_2_heter + NADH_heter.
H9: akg_heter + ADP_heter + NAD_heter = ATP_heter + CO_2_heter + NADH_heter + succ_heter.
H10: succ_heter + 0.5 O_2_heter + 1.25 ADP_heter = 1.25 ATP_heter + mal_heter.
H11r: mal_heter + NAD_heter = NADH_heter + oaa_heter.
H12: icit_heter = glyox_heter + succ_heter.
H13: mal_heter + NAD_heter = CO_2_heter + NADH_heter + pyr_heter.

(*Continued*)

TABLE 7.6 (CONTINUED)
Reaction Network Model for Interacting Microbial Consortium

H14: ATP_heter + 2 glyox_heter + NADH_heter = CO_2_heter + PEP_heter + NAD_heter + ADP_heter.

H15: CO_2_heter + PEP_heter = oaa_heter.

H16: pyr_heter + CoASH_heter + NAD_heter = ac_CoA_heter + CO_2_heter + NADH_heter.

H17: 2 ATP_heter + pyr_heter = PEP_heter + 2 ADP_heter.

H18: PEP_heter + ADP_heter = ATP_heter + pyr_heter.

H19r: ATP_heter + NADH_heter + PEP_heter = ga3p_heter + ADP_heter + NAD_heter.

H20r: ery4p_heter + xll5p_heter = fru6p_heter + ga3p_heter.

H21r: rbo5p_heter + xll5p_heter = ery4p_heter + fru6p_heter.

H22r: rbl5p_heter = xll5p_heter.

H23r: rbl5p_heter = rbo5p_heter.

H24: glc6p_heter + 2 NAD_heter = CO_2_heter + 2 NADH_heter + rbl5p_heter.

H25r: ATP_heter + fru6p_heter = 2 ga3p_heter + ADP_heter.

H26: fru6p_heter = glc6p_heter.

H27: 2 NADH_heter + O_2_heter + 5 ADP_heter = 5 ATP_heter + 2 NAD_heter.

H28: ATP_heter = MainE_heter_ex + ADP_heter.

H29: 4 glc6p_heter + 46 rbo5p_heter + 31 ery4p_heter + 156 PEP_heter + 237 pyr_heter + 72 ac_CoA_heter + 86 akg_heter + 139 oaa_heter + 731 NH3_heter + 856 NADH_heter + 2921 ATP_heter = bm_heter_ex + 35 CO_2_heter + 72 CoASH_heter + 2921 ADP_heter + 856 NAD_heter.

Note: Reactions labeled with "A" are associated with the photoautotroph whereas reactions labeled with "H" are associated with the heterotroph. reactions labeled with a "T" are transport reactions moving metabolites between the balanced "pool" and unbalanced "external" extracellular spaces. Reactions with a lower-case "r" were considered reversible for metatool simulations. Unbalanced system input and outputs were hv_ex (photon), CO_2_ex, NH_3_ex, bm_auto_ex (photoautotroph biomass), bm_heter_ex (heterotroph biomass), O_2_ex, MainE_auto_ex (photoautotroph maintenance energy), MainE_heter_ex (heterotroph maintenance energy), and glyc_ex (glycolate). All other metabolites were treated as balanced and constrained by the no-accumulation assumption.

oxygenase) is a major CO_2-fixing enzyme that transfers reducing equivalents produced during photosynthetic water-splitting to CO_2, fixing an additional carbon mole (C-mole). O_2, a byproduct of photosynthetic water-splitting, can compete with CO_2 for the RuBisCO active site. When O_2 binds, the oxidized organic metabolite glycolate is formed instead of an additional fixed C-mole. Glycolate is typically secreted by the photoautotroph as an undesirable byproduct. Glycolate can be used as a reduced carbon and energy source by heterotrophs.

Figure 7.14 demonstrates that increased RuBisCO O_2 competition reduces photoautotroph biomass synthesis efficiency by diverting reduced carbon toward glycolate biosynthesis, thus favoring heterotrophic growth. Overall consortium functioning can be modeled as linear combinations of distinct EFMs. The line on Figure 7.14 demonstrates the most efficient photoautotroph biomass synthesis (left end point) and the most efficient heterotroph biomass synthesis (right end point). The figure also shows the effect of varying levels of O_2 competition at the RuBisCO active site on biomass formation in the consortium. A more detailed account of a similar ecological scenario can be found in Taffs et al. (2009).

The metabolite partitioning approach presented for an interacting microbial consortium has already been used to model metabolic interactions between eukaryotic organelles and the cytosol (Fell and Small 1986; Carlson et al. 2002; Forster et al. 2003). Enzymes and metabolites must be

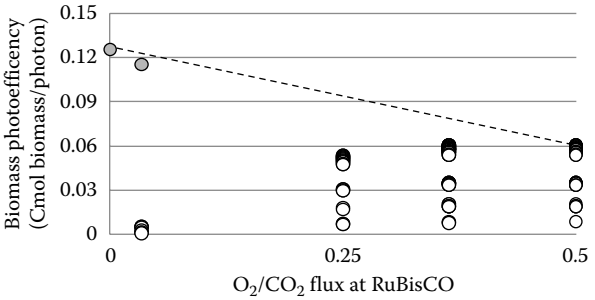

FIGURE 7.14 Consortium biomass photoefficiency as a function of O_2 competition at the RuBisCO active site. Each circle represents one distinct EFM, which produces biomass (gray circle, photoautotroph biomass; white circle, heterotroph biomass). Overall consortium functioning can be described by nonnegative linear combinations of distinct EFMs. The dotted line represents strategies defined by combinations of the highest yielding photoautotroph biomass strategy and the highest yielding heterotroph strategy. Community functioning, as defined by position along this line, is determined by the O_2 competition at the RuBisCO active site (ratio of O_2 to CO_2 fluxes).

assigned to different physical subcellular compartments. The use of convenient suffixes such as "ex", "cyt", or "mit" would facilitate editing of modeling files and analysis of results.

7.7 RECENT PRODUCT FORMATION INNOVATIONS

Xu et al. (2003) developed a new process for the production of phenylalanine using two different strains of *E. coli*. In their system, the coupling of transaminase activity from strain EP8-10, with that of aspartase from strain EA-1 led to rapid and efficient production of phenylalanine. This method also has the added advantage of being economical because aspartate could be replaced by ammonium fumarate, a relatively cheaper substrate than aspartate. This process is currently in operation on a pilot scale with an annual yield of 10 tons. Recombinant ethanologenic *E. coli* strains, analogous to the system explored in Section 7.6.1.3, have been licensed for cellulosic ethanol production. The petroleum giant BP acquired this cellulosic biofuel technology and a production facility from Verenium in 2010.

SUMMARY

- It is proposed that qualitative terms used to describe an enzyme as "rate-limiting", "bottleneck", or "pacemaker" should be abandoned and replaced by the term "rate-controlling" and further qualified by the flux control coefficient to describe, in quantitative terms, the capacity of the enzyme in question with respect to flux control within a given pathway.
- The flux control coefficient of a particular enzyme is a system property (i.e., its value is not entirely independent of other enzymes in the pathway). The inter-relationship between the flux control coefficients in a given pathway is governed by the summation theorem, which dictates that the total sum of all flux control coefficients adds up to 1.
- In a steady state, the influence of a particular metabolite on flux through a given enzyme on the one hand and the whole pathway on the other can be determined from the enzyme's elasticity coefficient, a quantitative term that is directly related to the kinetic properties of the enzyme involved.

The metabolic inter-relationship between the flux control coefficient and the elasticity coefficient is described by the connectivity theorem, which takes into account the kinetic properties of each of the enzymes involved.

The action of external effectors on metabolic flux can be assessed by measuring the response coefficient, which, to a large extent, is dependent on the flux control coefficient and the elasticity coefficient of the enzyme with respect to the effector. For an effector to be able to influence the flux through a certain enzyme, the values of the aforementioned coefficients must be relatively high.

Activating or increasing the catalytic activity of a single enzyme is not usually accompanied by a significant increase in flux (productivity), even with enzymes possessing a relatively large flux control coefficient. This is simply because the flux control shifts to other enzymes as the target enzyme is activated. This, in turn, implies that amplification of single enzymic activity is not a viable option for increasing productivity. However, this limitation does not apply to the reduction of catalytic activity because reduction or inactivation is generally accompanied by a considerable drop in flux.

A universal method has been developed to calculate the exact degree of overexpression required for increasing flux to product formation by a certain factor without perturbing the steady-state fluxes in other enzymes.

Increasing the concentration of an effector that activates all enzymes in the pathway will be accompanied by an appreciable increase in flux and, in turn, yield. Furthermore, an effector that stimulates the activity of more than one enzyme in a given pathway may lead to increase in flux (productivity), particularly if those enzymes share a relatively high flux control coefficient.

The case study presented in this chapter on the partition of carbon flux between ICDH and ICL revealed that during growth on acetate as sole source of carbon and energy, ICDH is not rate-controlling and that flux through isocitrate ICL is essential not only to replenish central metabolism with biosynthetic precursors but also to sustain a high intracellular level of isocitrate. Furthermore, above a certain threshold concentration of ICL, the Krebs cycle and the glyoxylate bypass can work in concert without the need for the inactivation of ICDH.

Among the five different strategies reported for the manipulation of carbon flux *in silico*, evasion and subversion are the most suitable strategies for increasing fluxes to product formation without adversely affecting the intracellular concentrations of metabolites; although evasion has the added advantage of being applicable to all metabolic pathways because it does not make any assumption about the regulatory control systems used *in vivo*.

However, subversion affords a practical strategy because it only involves the manipulation of one enzymic activity and as such may prove more of an attractive proposition for industrialists. Subverting feedback inhibition by the desired end product can simply be achieved by generating a mutant that leaks the end product into the medium. Such a system is highly desirable because the recovery and downstream processing become more effective and less expensive.

Flux models, in association with the universal method of Kacser, allow for the development of a rationale for strain improvement.

Stoichiometric modeling approaches do not require extensive kinetic parameters and can be broadly subdivided into three main categories: MFA, FBA, and EFMA.

EFMA dissects complex and highly sophisticated metabolic networks into their simplest, nondivisible flux units known as EFMs. EFMs can be viewed as mathematically defined biochemical pathways and represent a practical starting point for analyzing metabolic network structure and function.

EFMA is a convenient tool for metabolic engineering. EFMA identifies which network reactions are and are not necessary for desired cellular function highlighting targets for gene deletions and overexpression. EFMA can also be used to analyze expression of recombinant metabolic pathways and for identifying genetic manipulations to divert flux through the pathway.

The conversion of 12 biosynthetic precursors, drawn from central metabolism, into biomass can be used to model cellular growth. By varying the ratios of these intermediates, it is possible to consider different growth-rate-dependent biomass macromolecular compositions.

Flux through systems with complex physical architectures including microbial communities and eukaryotes can be modeled by assigning metabolites and reactions to distinct compartments.

ACKNOWLEDGMENT

The authors wish to thank Gordon Lang, for skilled assistance in the compilation of flux matrices.

REFERENCES

Burja, A.M., B. Banaigs, E. Abou-Mansour, J.G. Burgess, and P.C. Wright. 2001. Marine cyanobacteria: A prolific source of natural products. *Tetrahedron* 57:9347–77.

Carlson, R.P. 2007. Metabolic systems cost-benefit analysis for interpreting network structure and regulation. *Bioinformatics* 23:1258–64.

Carlson, R., D.A. Fell, and F. Srienc. 2002. Metabolic pathway analysis of a recombinant yeast for rational strain development. *Biotechnol Bioeng* 79:121–34.

Carlson, R., and F. Srienc. 2004a. Fundamental *Escherichia coli* biochemical pathways for biomass and energy production: Identification of reactions. *Biotechnol Bioeng* 85:1–19.

Carlson, R., and F. Srienc. 2004b. Fundamental *Escherichia coli* biochemical pathways for biomass and energy production: Creation of overall flux states. *Biotechnol Bioeng* 86:149–62.

Carlson, R., A. P. Wlaschin, and F. Srienc. 2005. Kinetic studies and biochemical pathway analysis of anaerobic poly-(R)-3-hydroxybutyric acid synthesis in *Escherichia coli. Appl Environ Microbiol* 71:713–20.

Cornish-Bowden, A. 1995. In H.-J. Rehm and G. Read, eds., *Biotechnology: A comprehensive treatise*, 2nd ed., Vol. 9, pp. 121–36. Weinheim, Germany: Springer-Verlag.

Cornish-Bowden, A., J.-H.S. Hofmeyr, and M.L. Cardenas. 1995. Strategies for manipulating metabolic fluxes in biotechnology. *Bioorganic Chem* 23:439–49.

Cornish-Bowden, A., and J.-H.S. Hofmeyr. 1991. MetaModel: A program for modelling and control analysis of metabolic pathways on the IBM PC and compatibles. *Comput. Applic. Biosci.* 7:89–93.

Cozzone, A.J. 1988. Protein phosphorylation in prokaryotes. *Ann Rev Microbiol* 42:97–125.

Cozzone, A.J., and E.M.T. El-Mansi. 2005. Control of Isocitrate Dehydrogenase Catalytic Activity by Protein Phosphorylation in *Escherichia coli. J Mol Microbiol Biotechnol* 9:132–46.

El-Mansi, E.M.T. 1998. Control of metabolic interconversion of isocitrate dehydrogenase between the catalytically active and inactive forms in *Escherichia coli*. *FEMS Microbiol. Lett* 166:333–9.

El-Mansi, E.M.T., and W.H. Holms. 1989. Control of carbon flux to acetate excretion during growth of *Escherichia coli* in batch and continuous cultures. *J Gen Microbiol* 135:2875–83.

El-Mansi, E.M.T., G.C. Dawson, and C.F.A. Bryce. 1994. Steady-state modelling of metabolic flux between the tricarboxylic acid cycle and the glyoxylate bypass in *Escherichia coli*. *Comp Appl Biosci* 10:295–9.

El-Mansi, E.M.T., H.G. Nimmo, and W.H. Holms. 1985. The role of isocitrate in control of the phosphorylation of isocitrate dehydrogenase in *Escherichia coli*. *FEBS Lett* 183:251–5.

Feist, A.M., C.S. Henry, J.L. Reed, M. Krummenacker, A.R. Joyce, P.D. Karp, L.J. Broadbelt, V. Hatzimanikatis, and B.O. Palsson. 2007. A genome-scale metabolic reconstruction of *Escherichia coli* K-12 MG1655 that accounts for 1260 ORFs and thermodynamic information. *Mol Sys Biol* 3:e121.

Fell, D. 1997. *Understanding the control of metabolism*. London: Portland Press.

Fell, D.A., and J.R. Small. 1986. Fat synthesis in adipose tissue: An examination of stoichiometric constraints. *Biochem J* 238:781–6.

Foberg, C., T. Eliaeson, and L. Haggstrom. 1988. Correlation of theoretical and experimental yields of phenylalanine from non-growing cells of a recombinant *Escherichia coli* strain. *J Biotechnol* 7:319–31.

Forster, J., I. Famili, P. Fu, B.O. Palsson, and J. Nielsen. 2003. Genome-scale reconstruction of the *Saccharomyces cerevisiae* metabolic network. *Genome Res* 13: 244–53.

Heinrich, R., and T. Rapaport. 1974. A linear steady-state treatment of enzymatic chains. *Eur J Biochem* 42:89–95.

Hofmeyr, J.H.S., and A. Cornish-Bowden. 1991. Quantitative assessment of regulation in metabolic systems. *Eur J Biochem* 200:223–36.

Hofmeyr, J.-H.S., H. Kacser, and K.J. Merwe. 1986. Metabolic control analysis of moiety-conserved cycles. *Eur J Biochem* 155:631–41.

Holms, W.H. 1996. Flux analysis and control of the central metabolic pathways in *Escherichia coli*. *FEMS Microbiol Rev* 19:85–116.

Hurlebaus, J. 2001. A pathway modeling tool for metabolic engineering. PhD thesis, University of Bonn, 2001.

Ingram, L.O., T. Conway, D.P. Clark, G.W. Sewell, and J.F. Preston. 1987. Genetic engineering of ethanol production in *Escherichia coli*. *Appl Environ Microbiol* 53:2420–5.

Kacser, H., and L. Acerenza. 1993. A universal method for achieving increases in metabolite production. *Eur J Biochem* 216:361–367.

Kacser, H., and J. Burns. 1973. The control of flux. *Symp Soc Exp Biol* 27:65–104. (Reprinted in *Biochem Soc Trans* 23: 341–66, 1995)

Kamp, A., and S. Schuster. 2006. Metatool 5.0: Fast and flexible elementary modes analysis. *Bioinformatics* 22:1930–1.

Klamt, S., J. Saez-Rodriguez, and E.D. Gilles. 2007. Structural and functional analysis of cellular networks with CellNetAnalyzer. *BMC Systems Biol* 1:e2.

Kleerebezem, R., and M.C.M. van Loosdrecht. 2007. Mixed culture biotechnology for bioenergy production. *Curr Opin Biotechnol* 18:207–12.

Kornberg, H.L. 1966. The role and control of the glyoxylate cycle in *Escherichia coli*. *Biochem J* 99:1–11.

Koshland, D.E., Jr. 1987. Switches, thresholds and ultrasensitivity. *Trends Biochem Sci* 12: 225–9.

Liao, J.C., S.Y. Hou, and Y.P. Chao. 1996. Pathway analysis, engineering and physiological considerations for redirecting central metabolism. *Biotechnol Bioeng* 52:129–40.

McCleary, W.R., 2009. Applications of promoter swapping techniques to control of expression of chromosomal genes. *Appl Microbiol Biotechnol* 84:641–8.

Mendes, P. 1993. GEPASI: A software package for modelling the dynamics, steady states and control of biochemical and other systems. *Comput Appl Biosci* 9:563–71.

Niederberger, P., R. Prasad, G. Miozzari, and H. Kacser. 1992. A strategy for increasing an in vivo flux by genetic manipulations: The tryptophan system of yeast. *Biochem. J.* 287:473–80.

Neidhardt, F. C., J. Ingraham, and M. Schaechter. 1990. *Physiology of the bacterial cell: A molecular approach*, pp. 1–29. Sunderland, MA: Sinauer Associates.

Ohta, K., D.S. Beall, J.P. Mejia, K.T. Shanmugan, and L.O. Ingram. 1991. Genetic improvements of *E. coli* for ethanol production: Chromosomal integration of *Zymomonas mobilis* gene encoding pyruvate decarboxylase and alcohol dehydrogenase II. *Appl Environ Microbiol* 57:893–900.

Pramanik, J., and J.D. Keasling. 1997. Effect of *Escherichia coli* biomass composition on central metabolic fluxes predicted by a stoichiometric model. *Biotechnol Bioeng* 60:230–8.

Reed, J, and B.O. Palsson. 2003. Thirteen years of building constraint-based in silico models of *Escherichia coli*. *J Bacteriol* 185:2692–9.

Schilling, C.H., S. Schuster, B.O. Palsson, and R. Heinrich. 1999. Metabolic pathway analysis: Basic concepts and scientific applications in the post-genomic era. *Biotechnol Prog* 15:296–303.

Schuster, S., D.A. Fell, and T. Dandekar. 2000. A general definition of metabolic pathways useful for systematic organization and analysis of complex metabolic networks. *Nat Biotechnol* 18:326–32.

Stephanopoulos G.N., A.A. Aristidou, and J. Nielsen. 1998. *Metabolic engineering. Principles and methodologies*, New York: Academic Press, 1998.

Stoylar, S., S. Van Dien, K.L. Hillesland, N. Pinel, T.J. Leigh, and D.A. Stahl. 2007. Metabolic modeling of a mutualistic microbial community. *Mol Syst Biol* 3:e92.

Taffs, R., J.E. Aston, K. Brileya, Z. Jay, C.G. Klatt, S. McGlynn, N. Mallette, S. Montross, R. Gerlach, W.P. Inskeep, D.M. Ward, and R.P. Carlson. 2009. *In silico* approaches to study mass and energy flows In microbial consortia: A syntrophic case study. *BMC Sys Biol* 3:e114.

Terzer, M., and J. Stelling. 2008. Large-scale computation of elementary flux modes with bit pattern trees. *Bioinformatics* 24:2229–35.

Trinh, C.T., R. Carlson, A. Wlaschin, and F. Srienc. 2006. Design, construction and performance of the most efficient biomass producing *E. coli* bacterium. *Metab Eng* 8:628–38.

Trinh, C.T., A. Wlaschin, and F. Srienc. 2009. Elementary mode analysis: A useful metabolic pathway analysis tool for characterizing cellular metabolism. *Appl Microbiol Biotechnol* 81:813–26.

Walsh, K., and D. E. Koshland. 1984. Determination of flux through the branch point of two metabolic cycles: The tricarboxylic acid cycle and the glyoxylate shunt. *J Biol Chem* 259:9646–54.

Wlaschin, A.P., C.T. Trinh, R. Carlson, and F. Srienc. 2006. The fraction contributions of elementary modes to the metabolism of *Escherichia coli* and their estimation from reaction entropies. *Metab Eng* 8:338–52.

Xu, H., P. Wei, H. Zhou, F. Fan, and P. Ouyang. 2003. Efficient production of L-phenylalanine catalyzed by a coupled enzymatic system of transaminase and aspartase. *Enz Microb Technol* 33:537–43.

This page intentionally left blank

8 Enzyme and Cofactor Engineering: Current Trends and Future Prospects in the Pharmaceutical and Fermentation Industries

George N. Bennett and Ka-Yiu San

CONTENTS

8.1 INTRODUCTION

The effect of molecular genetics and recombinant DNA technology on industrial biotechnology is well documented. In this chapter, we will address some general themes and use a few examples to illustrate the concepts involved in enzyme and cofactor engineering.

In considering a biological process for metabolic and enzyme engineering purposes, two main points must be addressed to identify the right enzyme for metabolic intervention. In addition to the flux control coefficient (see Chapter 7 for more details), there are two other main approaches to identifying target enzymes. Whereas the first makes use of the diversity in the properties of enzymes, the other relies on the enzymes' unique structural properties. By making deliberate structural alterations through rational design or random mutagenesis, a desired enzyme variant can be obtained.

8.2 TYPES OF MAJOR INDUSTRIAL ENZYMES AND DESIRED MODIFICATIONS

8.2.1 Desired Targets for Enzyme Engineering

In identifying targets for enzyme engineering, several factors need to be considered. These include

- The projected long-term market value of the product(s) and the inherent economic advantages that follow,
- The applicability of the engineered enzyme to other industrial processes,
- The availability and validity of suitable strategies for engineering, screening, and detection of the desired variant.

One general area in which enzymes with engineered properties may become more important is the production of optically active amines as precursors for bioactive pharmaceuticals. Particular additional classes include esterases, racemases, and redox enzymes (oxidoreductases) including peroxidases and cytochrome P450. The use of enzymatic procedures that are stereospecific can enhance the overall synthetic process. Specific processes in which the chemical reaction yields a mixture of isomers that are hard to separate are attractive candidates for enzyme engineering.

8.2.1.1 Hydrolytic Enzymes

Most enzymes used in large quantity are hydrolytic enzymes. Proteases are widely used as additives to remove protein-rich stains or blood stains from laundry. The *Bacillus* alkaline serine protease subtilisin is the most common enzyme used for this application. Desirable properties for such enzymes include stability and activity at high temperature and high pH associated with typical laundry conditions. Stability in the face of other harsh substances and chelating agents is also desirable property. Amylases represent another class of hydrolytic enzymes that are widely used in starch liquefaction and the removal of starchy foods from clothing in laundries. Alpha-amylases are derived from *Bacillus* species whereas the major beta-amylases are derived from *Bacillus* and plants. The ability to act on crude substrates under harsh conditions or extreme environments is also desirable property.

The production of high-fructose corn syrup represents a classic example in which glucose isomerase is used to convert glucose into fructose, thus considerably enhancing the level of sweetness. Under industrial conditions, the glucose isomerase reaction requires high temperature and low pH to avoid side reactions. Various enzymes from *Bacillus coagulans*, *Streptomyces rubiginusus,* and other bacterial species have been used for this purpose. With the increased interest in degrading plant biomass to soluble sugars that can be used as a feedstock for biofuels and chemical production, a good deal of attention has been diverted toward enhancing the properties and the efficacy of cellulases (Blumer-Schuette et al. 2008; Doi 2008; Dowe 2009; Maki et al. 2009) and xylanases (Khandeparker and Numan 2008), which breakdown the cellulose and hemicelluloses in plant cell wall into sugars.

Cheese-making is yet another example in which proteases play a central role not only in the formation of the curd, which is catalyzed by the enzyme chymosin (Rennin), but also for ripening and maturation. Although chymosin used to be made from the gastric juice of the fourth stomach chamber of weaning calves or fungi, it is now recombinant chymosin that enjoys center stage, especially at the industrial level.

Lipases are another group of hydrolytic enzymes used in various ways, including removing grease stains and clogs; hydrolysis of fats in the food industry is a major concern. Lipases can also be used under conditions of low water content in an organic solvent to modify oils and fats for food use by transesterification of the acyl chains to generate a product with a desirable pattern (e.g., level of saturation or chain length).

Another widely used hydrolytic enzyme is penicillin acylase. In the production of various β-lactam antibiotics, penicillinase or cephalosporin acylase has been successful in the production of useful derivatives (Sio et al. 2004). It is also noteworthy that the hydration of certain molecules in a specific fashion is desirable industrially. For example, nitrile hydratase (Chen et al. 2009) from *Pseudomonas chlororaphis* B23 has been used to convert nitrile into acrylamide on a large scale; such a useful reaction has environmental and economic advantages.

8.2.1.2 Specialty Enzymes for Pharmaceuticals

In the pharmaceutical industry, much interest has been focused on the formation of compounds with specific chiral structure for the synthesis of stereospecific biopharmaceuticals The ability to interconvert one stereoisomer into another is of special interest because only one of the two forms has the desired pharmaceutical properties and is very difficult to separate from the other isomer. Different **enantiomers** may also have different metabolic and pharmacokinetic properties and side effects. Therefore, efforts to selectively form the functional chiral product have intensified. The use of enzymatic steps can also improve yields and reduce the use of hazardous chemicals to provide a more "green chemistry" process (Tao and Xu 2009). In addition to the specific synthetic pharmaceuticals, the nutritional area of natural amino acids and vitamins involves many processes that require chiral production systems. Therefore, enzymes that can catalyze stereospecific reactions on complex molecules, particularly those such as **sterols**, alkaloids, etc., are used in many synthetic processes. Another use of enzymes exhibiting stereospecific catalytic activity is in the separation or isomerization of a racemic mixture after chiral chemical synthesis; for example, the separation of (*R,S*)-Naproxen 2,2,2-trifluoroethyl thioester to produce the desired (*S*)-Naproxen, an anti-inflammatory drug (Ng and Tsai 2005). The general aspects of formation of chiral products and specificity have been discussed (Turner 2003; Jaeger and Eggert 2004).

Enantiomers: Enantiomers of a chemical compound are equivalent in composition and bonding pattern of the atoms but differ in the relative positioning of a group on one of the atoms. The two forms are mirror images like right and left hands. This difference allows each to interact differently with other molecules.

Sterols: Sterols are a wide group of lipid molecules with the same basic four-fused ring system of steroids but encompass a wider class, including plant and fungal sterols as well as the animal sterols and steroids.

A large family of proteins that has received much attention in recent times is the cytochrome P450 family. Redox-active enzymes that are central in detoxifications of radicals and aromatics in the body and as such testing lead compounds against the activities of these enzymes has become an important parameter in drug discovery programs (Purnapatre et al. 2008).

8.3 ALTERATION OF PHYSICAL PROPERTIES OF ENZYMES FOR PROCESS APPLICATIONS

Thermostability of enzymes is a prerequisite for successful applications in most industrial processes. Recent studies revealed that thermostability is due to the dense hydrophobic core of amino acids along with an increased density of intramolecular hydrogen bonds and ionic interactions

(Matsui and Harata 2007). Examples of widely used thermostable enzymes include glucoisomerases (Asboth and Naray-Szabo 2000; Hartley et al. 2000) and glucoamylases (Sauer et al. 2000). The engineering of thermostable subtilisin using molecular biology tools has been described (Zhao and Arnold 1999). Similarly, psychrophilic (cold-loving) enzymes are useful, especially if the enzyme is to be inactivated after the completion of the reaction. Successful adaptations to cold temperatures are linked to increased flexibility around the active site of the enzymes (Feller 2003; Georlette et al. 2004). Examples of enzymes that are active at cold temperature have been cited (Georlette et al. 2004; Siddiqui and Cavicchioli 2006; Joseph et al. 2008), and protein engineering of cold-adapted subtilisin has been described (Taguchi et al. 2000).

Compatibility of enzymic activity with conditions of high salt or organic solvents is also a challenge, and the isolation and engineering of enzymes that operate effectively under these conditions has been described (Luetz et al. 2008; Gupta and Khare 2009).

8.4 TOOLS AND METHODOLOGIES OF ENZYME ENGINEERING

8.4.1 Site-Specific Mutagenesis

Site-specific mutagenesis has been developed and practiced by many researchers. In this method, a primer incorporating the desired nucleotide change is constructed and, in turn, annealed to a circular single-stranded template vector containing the gene to be mutated; the primer is then extended by the action of DNA polymerase in the presence of deoxynucleoside triphosphates. After extension of the primer by DNA polymerase, the double-stranded molecule is introduced into a host cell (e.g., *Escherichia coli*). The strand made by extending the primer is preferentially replicated, and the dU-containing template strand is preferentially degraded by host enzymes, yielding a high proportion of the progeny vector with the desired mutation (Kunkel et al. 1991). This method has been adapted in various ways for use with other plasmids (Jung et al. 1992).

Recently, new methods based on PCR incorporation of designed primer sequences carrying the desired mutation and standard kits have become commercially available. In these methods, a specific codon change is introduced into the sequence of the designed primers, and this, in turn, ensures the desired change in the DNA sequence of the cloned gene. Replication of the modified strand can be enhanced through selective digestion of the parent strand by enzymes, or through using a special set of primers that facilitate selection on selective medium. The commercial kits allow for rapid site-specific mutagenesis and generate a relatively high proportion of recombinant colonies bearing the desired mutation (Figure 8.1). These methods, coupled with the greater availability of low-cost synthesized oligonucleotides and sequencing services, have made site-specific mutagenesis a routine technique in many laboratories.

8.4.2 Cassette Mutagenesis

To simultaneously introduce several nearby mutations, the technique of cassette mutagenesis has been devised (Wells et al. 1985; Kegler-Ebo et al. 1996). This method allows for a short segment of the gene to be cut out and replaced by a specifically designed oligonucleotide segment carrying different nucleotides at a given position. After substitution and replication of the target codon, several mutants carrying different amino acids can be isolated. In this way, several different amino acid residues at a particular position in the protein could be made and individually tested for their effect on enzyme properties. The use of segments with more extensively changed nucleotide sequences could allow for the formation of protein variants with several amino acid changes within the section replaced, giving a localized patch on the protein where there are many alterations.

As the technology for oligonucleotide synthesis improves, the opportunity of synthesizing entire genes, or even genomes, becomes possible. With this approach, the gene encoding the desired protein could be designed in such a way that it contains several unique restriction sites

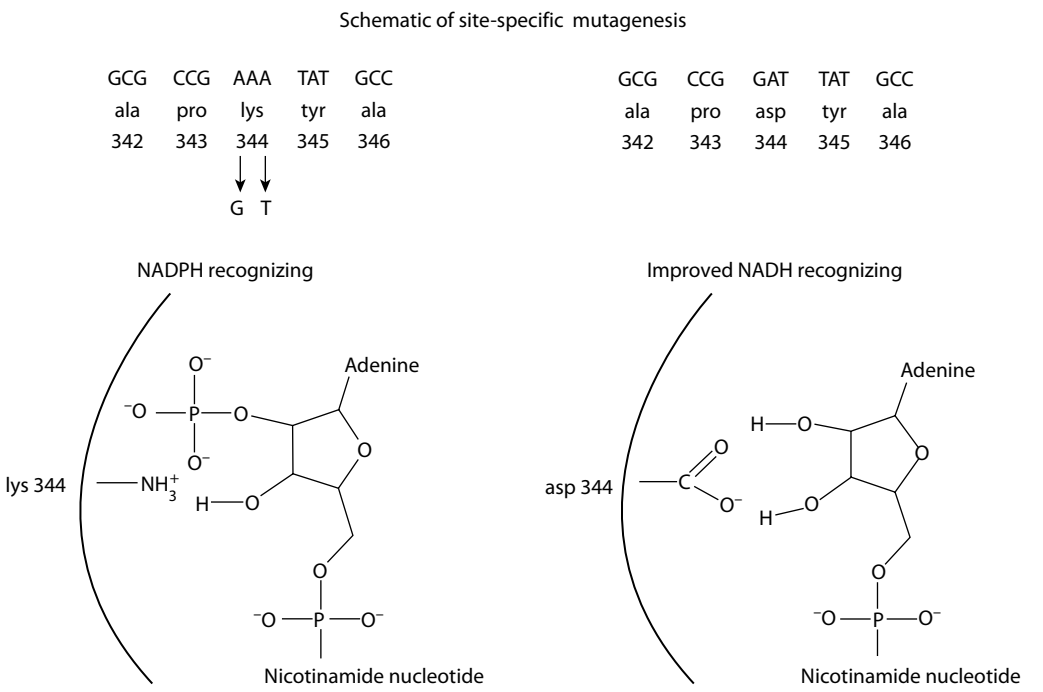

FIGURE 8.1 In the example, the cofactor specificity of ICDH has been changed from NADPH to NADH by (Hurley et al. 1996). The lys-344 is central to NADPH binding because lysine is a positively charged residue and as such can interact with the negatively charged phosphate group of NADPH. When the codon encoding lys-344 was changed to GAT (the codon specifying aspartic acid, which is a negatively charged amino acid residue) the enzyme could no longer bind NADPH. Under these conditions, another kind of interaction occurs with the hydroxyl groups of the nonphosphorylated ribose to form hydrogen bonds with the carboxylic group of aspartic acid. Such an interaction would favor binding of NADH rather than NADPH at the active site. As with most enzymes there are several amino acids that contribute to specificity at the active site. More details are given in (Chen et al. 1995; Hurley et al. 1996; Yaoi et al. 1996), and other alterations affecting substrate specificity are described in a crystallographic study (Doyle et al. 2001).

for replacement of different segments of the protein by cassette mutagenesis, which is illustrated in Figure 8.2.

8.4.3 Gene Synthesis (Synthetic Biology)

As synthesis of oligonucleotides becomes more affordable and as the technology for their assembly becomes more accessible, it is possible to create and engineer new genes for specific purposes. Such advent has led to the creation of a new branch in science otherwise termed "synthetic biology" (Keasling 2008; Xiong et al. 2008; Tian et al. 2009). For example, if a change in the kinetic property or specificity of a given protein is desired, several genes from various organisms can be synthesized and placed into the desired expression system for *in vivo* testing of performance. The choice of genes for synthesis and testing would be made based on data from the sequence databases from organisms likely to have a robust activity for that reaction and the *in vitro* activity and characteristics of enzymes provided by databases such as the Brenda enzyme database http://www.brenda-enzymes.org/. During the synthesis of the gene, several variants at specific positions can be introduced and the mixture can be cloned and examined for performance. The use of this synthetic biology approach has been reviewed, and wider implications of designer circuits for appropriate expression within a host are discussed (Keasling 2008; Carothers et al. 2009; Landrain et al. 2009).

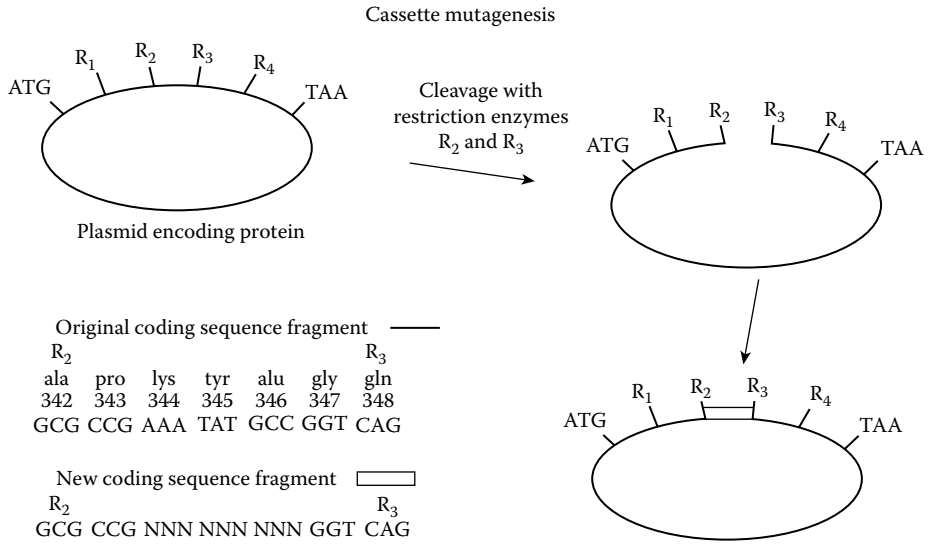

FIGURE 8.2 In the initial plasmid, the ATG indicates the codon encoding the first amino acid of the protein (N-terminus), whereas the TAA indicates the stop codon, which terminates synthesis at the C-terminus of the protein. The sites R_1, R_2, R_3, and R_4 denote the positions of cleavage of the plasmid at a unique place by the restriction enzymes R_1, R_2, R_3, and R_4, respectively. Cleavage by R_2 and R_3 then removes a defined segment, and this segment can be replaced by a synthetic segment having a mixture of nucleotides (N for a mixture of A, T, G, C) at a particular position within the segment. In the example shown, the nine positions specifying amino acids 344, 345, and 346 are mixed and could then encode any amino acid at these positions. Replacement of the R_2–R_3 segment in the plasmid would generate various plasmid molecules with different possibilities for codons at positions 344, 345, and 346 in this protein. After transformation and replication of individual molecules of the plasmid and plating to generate individual colonies, the protein from each colony could be isolated and examined and the nucleotide sequence of the specific R_2–R_3 segment determined.

8.4.4 Tertiary Structure and Specific Mutations

If one wishes to enhance a particular property of an enzyme through site-specific mutagenesis, the three-dimensional 3D structures of the enzyme before and after binding to substrate analogue must be examined to gain an understanding of the positioning of the substrate in the active site and to identify the amino acid residues needed for catalysis (Benkovic and Hammes-Schiffer 2003). Computational approaches to analyzing mechanistic aspects of enzyme action have been developed and are widely used in protein engineering (van der Kamp and Mulholland 2008). An example of a change in substrate specificity of the protease subtilisin illustrates this approach. When the binding cavity of subtilisin is reduced in size by substituting glycine 127 (a small amino acid) with a larger amino acid, the enzyme exhibits a distinct preference for smaller substrates (Takagi et al. 1996). In general, expanding the size of the substrate binding site can lead to a broadening of the specificity of the enzyme because a wider range of substrates may be able to fit within the active site. However, the affinity of the enzyme for the substrate may decrease (i.e., requiring a higher concentration of the substrate for effective catalysis) (Zhang et al. 2008).

Another important specificity is cofactor requirement. The pools of NADH and NADPH in the cell influence the redox potential within the cell on one hand and product formation on the other. Generally speaking, NADH is the preferred cofactor for *in vitro* oxidation/reduction reactions because of its greater stability. The conversion of the NADPH-specific 2,5-diketo-D-gluconic acid reductase A, an enzyme used in the synthesis of vitamin C, into an NADH-specific enzyme has been reported (Banta et al. 2002b). Similarly, the NADPH-dependent carbonyl reductase that is used for the synthesis of optically active alcohols has also been modified to become NADH-specific (Morikawa et al. 2005). However, in

some cases it may be preferable to have NADPH specificity to avoid interference with other reducing enzymes, and examples of the conversion of NADH specificity to that of NADPH have been reported for xylitol dehydrogenase (Watanabe et al. 2005) and lactate dehydrogenase (Holmberg et al. 1999).

8.4.5 Directed Evolution and DNA Shuffling

The ability to make and screen many random mutations within a localized region is referred to as "directed evolution." This approach can be used without knowledge of the three-dimensional structure of the enzyme and can be applied to a wider range of sequences and structures to find the desired protein sequence. Successful application of directed evolution, which makes use of error-prone PCR and DNA shuffling techniques, has recently been reviewed (Labrou 2010). However, it must be born in mind that such an approach demands an efficient screening and selection program (Jestin and Kaminski 2004; Boersma et al. 2007).

The effect of PCR and DNA shuffling techniques on biomolecular engineering has been reported, and reviews that specifically focus on directed evolution of industrially important organisms have been published (Cherry and Fidantsef 2003; Hult and Berglund 2003). As the use of this approach continues to grow, many enzymes are likely to be modified in one way or another to improve their performance in industrial fermentations.

Error-prone PCR (Figure 8.3) takes advantage of the misincorporation of nucleotides into DNA during polymerization to yield a newly synthesized strand with random changes. The level of

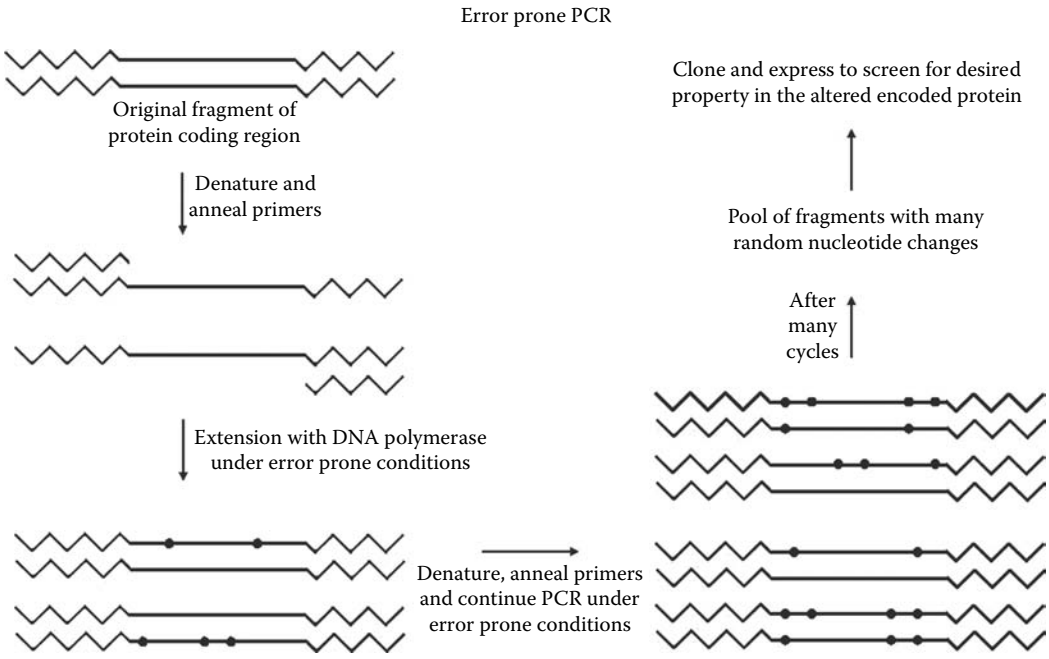

FIGURE 8.3 In error-prone PCR, the template is annealed with primers that allow for extension (by DNA polymerase) and incorporation of the dNTPs, deoxynucleotide triphosphates, in the incubation mixture. The condition of the extension and the enzyme used will define how frequently a mistake or misincorporation (e.g., A for G) is made. Denaturation of the strand at high temperature followed by reannealing of the primers can then allow the strands with mistakes to be copied, and the original strands and further errors by misincorporation are introduced, giving a product that may have many variations within the product molecules. Conditions can be used that will give an appropriate level of altered molecules (e.g., 1 mutation per 100 or 1000 residues on average). Because the molecules can be cloned and replicated independently within a plasmid, individual colonies with separate variants can again be isolated and screened for enzyme properties (e.g., high-temperature activity) and the specific DNA sequence of interesting variants can be analyzed.

misincorporation can be manipulated by the use of different polymerases, inclusion of different metal ions, or addition of allosteric substrates that affect the structure of the polymerase or its ability to discriminate base pairing (Cirino et al. 2002). Theoretical models relating the error rate to the overall distribution of base changes in the final population of molecules have been reported (Bessler et al. 2003).

DNA shuffling technique utilizes fragments from closely related genes in a PCR misincorporation process to generate a high diversity of full-length genes (Figure 8.4). This technique allows for a wider expanse of diverse sequences to be created than the original error-prone PCR technique because of the presence of a greater variety of genes. However, because many variants are generated, developing a suitable protocol for screening and selection is a significant consideration. The applicability of this technique to pharmaceutical and vaccine production (Patten et al. 1997; Locher et al. 2005) and improvement of industrial enzymes (Powell et al. 2001) has been reviewed.

Where possible, it is useful to couple molecular evolution with an effective screening strategy for optimized enzyme activity. In the case of growth coupling, the adapted strain may display significant improvement in performance. The changes in genotypes that are associated with enhanced performance can be unraveled by genome sequencing of high-performing variants. This technique has successfully been applied to kanamycin (Yanai et al. 2006) and lysine (Ohnishi et al. 2002)

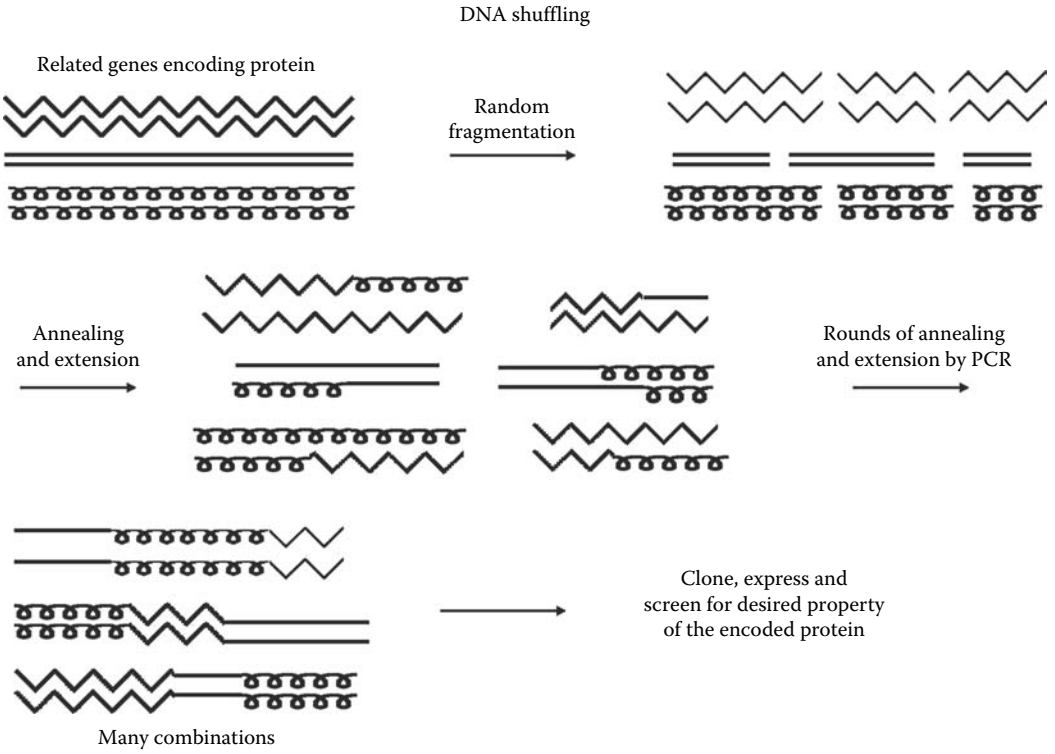

FIGURE 8.4 In the DNA shuffling procedure, several gene fragments encoding similar proteins are used. The segments must have a high enough sequence similarity to anneal well in heterologous combinations so that the polymerase can extend the various duplexes formed. The repeated denaturation and reannealing give a chance for different sequences to be represented. The combination of various sections and the individual base-pair mutations introduced during the repeated process generates a great variety of altered sequences. These DNA fragments can be cloned, the individual variant genes encoding protein are expressed in individual colonies, and screening schemes or selections impressed on individual colonies are used to identify variants with desired properties. The DNA encoding the variant gene can be isolated and sequenced to identify the changes producing the effect.

production. This approach has also been applied to improving the ability of *E. coli* to grow on glycerol as a sole source of carbon and energy (Fong et al. 2005; Herring et al. 2006).

Although details of screening systems are not addressed here, the usual practice is to make use of a substrate or a coupled reaction that yields a chromogenic compound that serves as an indicator of the desired genotype. The conditions of assay and detection can be modified to include the desired physical parameters such as pH, temperature, or the presence of organic solvents or other inhibitors. The use of high-throughput detection systems in combination with a multiwell plate format allows for identification of modified proteins with enhanced activity. In some cases the use of fluorescence-activated cell sorting (FACS) or microdroplet screening processes can allow cells to be screened rapidly for improved variants (Kwon et al. 2004).

A recent development is the direct use of oligonucleotides in mutagenesis of the chromosome of bacteria (Grogan and Stengel 2008; Weiss 2008) or yeast (Storici et al. 2001). This approach can either be used to alter a specific nucleotide in the chromosome in a manner similar to that of site-specific mutagenesis or a multiple of nucleotides. In either case, a screening process follows to identify colonies with desired phenotypes. This combinatorial approach has been used to generate *E. coli* strains able to form a high level of lycopene (Wang et al. 2009).

8.5 MODIFICATION OF PHARMACEUTICAL PROPERTIES OF PROTEIN AGENTS

In the case of therapeutic proteins, protein engineering is used to produce a form with reduced immunogenicity, improved stability of therapeutic action, and increased half-life in circulation (Shanafelt 2005). Such modifications can also alter the solubility, cofactor specificity, and susceptibility to degradation by proteases. Modifications such as **pegylation** (i.e., addition of polyethylene glycol) or **glycosylation** (i.e., addition of carbohydrate moiety) to a protein often improves its pharmacological properties such as absorption, circulation lifetime, and reduced clearance rate (Sola and Griebenow 2010) and may be especially useful in conjunction with delivery through microcapsules or bioimplants (Pai et al. 2009; Zilberman et al. 2010). Site-specific modifications that allow pegylation or glycosylation to occur on the protein is one important avenue that can be explored to enhance the pharmaceutical properties of proteins (Graddis et al. 2002). The effect of pegylation on the properties of drugs has recently been reviewed (Veronese and Mero 2008; Bailon and Won 2009). The addition of the soluble polymer prevents clearance from the bloodstream by the kidney, reduces enzymatic degradation, and reduces immunogenic problems. Specific proteins where this has been advantageous include interferon alpha-2a. The enhanced pharmacokinetic properties of the modified protein can allow for more convenient and appropriate dosing schedules for patients.

Certain drugs can be better agents if they are modified to enhance uptake or pharmacokinetic properties. For example, the **acylation** of one of the two hydroxyl groups of the drug lobucavir improved its antiviral potency.

Pegylation: Pegylation refers to the attachment of polyethyleneglycol (PEG) to a protein or small molecule, typically to improve its lifetime for pharmaceutical purposes. PEG can be specifically attached to a protein through binding with amino or sulfhydryl groups on the surface of the protein.

Glycosylation: Glycosylation is an abundant form of post-translational modification that covalently attaches an oligosaccharide chain containing 4–15 sugars through the activity of oligosaccharyl transferase. It plays a significant role in ***cell-cell recognition*** and affords a "***steric***" protection against digestion by proteases. In this mechanism a carbohydrate moiety is attached to a protein, typically through linkage to exposed asparagine (N-link) or serine and threonine (O-link) residues on the protein.

Acylation: The binding of an acyl group to a protein or other molecule, typically forming an amide link with the side-chain amino group of a surface lysine residue or with a hydroxyl group of a small molecule.

8.6 MODIFICATION OF ENZYMES FOR *IN VIVO* BIOSYNTHETIC PROCESSES

The application of enzyme engineering to biomolecules, whole-cell biocatalysts, or immobilized enzymes in the manufacture of pharmaceuticals has been an area of expansion in recent years; examples include β-lactam acylases, which have been modified and in turn used to carry out reactions beyond their usual hydrolytic specificities on penicillin G and cephalosporin C.

Goals in this area include enhancing performance of immobilized enzymes and creating suitable specialized reaction conditions that are compatible with downstream processing. Because the chiral nature of products is central in many cases, the resolution of racemic mixtures into its component parts is of great importance. Selective hydrolysis of acyl groups has been used to facilitate the separation of isomers. In this case, the racemic mixture is typically treated with an enzyme that can only hydrolyze one stereoisomer, and after the reaction is completed, the acylated form is easily separated from the unacylated form using biochemical techniques.

Another group of antibiotics is the polyketides, and there has been considerable work on altering the complex enzymes involved in the biosynthesis of these compounds (e.g., Khosla et al. 2007; Khosla 2009; Khosla et al. 2009, Zhan 2009). In these articles, the modularity of the biosynthetic pathways together with the formation of large multifunctional proteins and multiprotein complexes were discussed in great depth. The modification of the individual functional domains and switching of these modules among the gene clusters specifying the biosynthesis of different antibiotics have given rise to a considerable industry that uses advanced genetic techniques for the synthesis of novel polyketide-based pharmaceuticals.

Sterols are an important group of compounds with many uses as pharmaceuticals. Yeast has been engineered to make pregnenolone and progesterone (Duport et al. 1998), hydrocortisone (Szczebara et al. 2003; Brocard-Masson and Dumas 2006), and triterpenes (Kirby et al. 2008), and metabolic flux through the pathways involved has been analyzed (Maczek et al. 2006) and subsequently manipulated (Paradise et al. 2008). Cytochrome P450's reactions on **steroids** as a substrate is of medical importance, and the broad potential for engineering yeast for sterol modifications has been reviewed (Veen and Lang 2004). Plants have also been engineered for improved production of phytosterols and related compounds (Seo et al. 2005). Furthermore, synthesis and applications of such biotransformation have been reviewed (Malaviya and Gomes 2008). Several other organisms are used to make specific chiral modifications of the basic sterol structure and are used for chemical conversions or assays (MacLachlan et al. 2000). Protein engineering of specific amino acids at key positions in particular enzymes has altered the activities of steroid dehydrogenases involved in steroid hormone metabolism; in particular, the role of oxygenated sterols has been discussed with regard to various medical and biotechnological applications (Brown and Jessup 2009; Lordan et al. 2009; Pasqualini 2009; Pollegioni et al. 2009).

Steroids: Steroids are lipid molecules with four interconnected ring systems—three fused six-member rings and one five-member ring—that are commonly found in membranes and hormones.

Carotenoids represent a group of compounds containing several conjugated double bonds and are of interest for their color, nutritional, and pharmaceutical values. They are made by various microorganisms, and the genes encoding the enzymes of the biosynthetic pathways are known. Recent work has involved the expression of biosynthetic enzymes in different hosts and in unique combinations. The possibility of evolving novel pathways for the formation of a new family of carotenoids is being explored using combinatorial approach (Tanaka and Ohmiya 2008; Chemier et al. 2009; Harada and Misawa 2009; Liu et al. 2009; Muntendam et al. 2009; Nishihara and Nakatsuka 2010).

The biosynthetic pathways involved in the formation of carotenoids and flavonoids require reducing power in the form of NADPH or reduced CoA by way of cofactors. Cofactor engineering is therefore directly relevant to pathway engineering.

8.7 WHOLE-CELL BIOCATALYSTS

Whole-cell biocatalysts that incorporate genes producing specific enzymes for catalysis of an entire biosynthetic pathway have become more widely used. In designing and implementing such metabolic engineering schemes, a two-stage strategy involving the removal and/or deregulation of competing metabolic pathways as well as the introduction of novel pathways into the organism of choice is often used. In the first stage, gene "knockouts" are constructed to eliminate activity of the competing pathway using recombination methods routinely used in *E. coli* or yeast genetics (Datsenko and Wanner

2000). In the second stage, a novel pathway is introduced, or alternatively tandem copies of the gene of interest (Tyo et al. 2009), cloned downstream of a powerful promoter, are used to transform the organism under investigation (Yuan et al. 2006; McCleary 2009). Expression of genes brought in from other organisms can be done in the same fashion as those from the native host, but additional problems may be encountered related to the codon preference of the host versus the heterologous donor, mRNA stability and structure, protein stability or aggregation, and location or interaction with other proteins or cell constituents. In these complex engineering endeavors, it is important to not only account for the flow of carbon through the network but also to consider the flow and stoichiometry of oxidation/reduction equivalents to redox balance. Strains constructed using this approach are currently used for the production of biofuel, specialty chemicals, and biopharmaceuticals.

There are also applications for carrying out an individual redox process in which regeneration of the cofactor is an important consideration, and these have become useful industrial processes. Some of these features have been reviewed and discussed recently (Carballeira et al. 2009). Such processes use an active cofactor-regenerating system to ensure the regeneration of the desired cofactor. In this system, a specific precursor molecule is processed by the engineered cells to ensure the continuation of the regenerating cycle without supporting growth.

8.8 COFACTOR ENGINEERING

The term "cofactor engineering" was coined in the early 1990s in a general article (Duine 1991) that drew attention to the essential role of cofactors in different reactions. It had long been known that the level of biotin could greatly affect the production of glutamate by *Corynebacterium glutamicum* (Kimura 2003). A related experience was noted in the early production of citric acid with respect to iron, which is normally a constituent of certain enzymes or hemes.

Specific oxidation reactions and their bioprocess considerations have been reviewed (Buhler and Schmid 2004), and the limitation of cofactor regeneration has been considered (Schroer et al. 2009). The cofactor most studied is the reductant used in many reactions (i.e., NADH or NADPH). Although reductions are very important and the chiral nature of the product is often crucial, there is less industrial usage of specific oxido-reduction pathways because of the lack of cofactor regenerating systems *in vivo*. However, *in vitro*, the cofactor can be regenerated by another enzyme that can form the reduced cofactor by oxidation of a readily available substrate that will not interfere with the desired reaction. An enzyme often used in the *in vitro* systems to form NADH is formate dehydrogenase. This enzyme can use formate to produce the reduced form of the cofactor NADH and carbon dioxide (CO_2). The CO_2 is easily removed and does not generally interfere with redox reactions (Wandrey 2004). This and other cofactor regenerating systems have been reviewed (Wichmann and Vasic-Racki 2005; Weckbecker et al. 2010). For NADPH regeneration, glucose dehydrogenase has been used, and with the use of permeabilized cells efficient coupled processes have been developed (Zhang et al. 2009). In some cases a large amount of an alcohol can be supplied and a rather nonspecific alcohol dehydrogenase can perform the desired reduction and the regeneration of cofactor if the enzyme parameters and appropriate concentrations are used (Hollrigl et al. 2008; Schroer et al. 2009). Because NADH is more stable and generally available in higher quantities, it is preferred to NADPH. Thus, for *in vitro* processes, it is often considered useful to convert an NADPH-dependent enzyme to an NADH-utilizing enzyme (see above example in Figure 8.1). This is also true for some *in vivo* processes in which reaction rates are dependent on the availability of NADPH on one hand and/or the NADH-NADPH ratio. A specific example of this is the formation of xylitol as a byproduct in the fermentation of **xylose** to ethanol by engineered yeasts, where the xylose is first converted to **xylulose** so

Xylose: A five-carbon sugar, the d form of which commonly found in hemicellulose is shown. Xylose exists in two different forms: linear or cyclic.

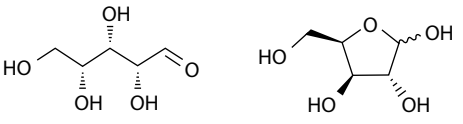

Xylulose: Xylulose is a five-carbon sugar but is a ketose rather than aldose, as is the case with xylose.

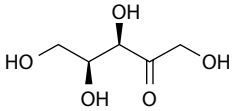

it can be metabolized by the yeast. However, the activity of the NAD^+-dependent xylitol dehydrogenase forms **xylitol** and lowers the yield of ethanol. This imbalance has been redressed by altering the specificity of the xylitol reductase (Petschacher and Nidetzky 2008), and this, in turn, allows for better utilization of mixed substrates and yields a low level of xylitol formation (Krahulec et al. 2010)

Xylitol: All of xylitol's oxygen is in the hydroxyl form.

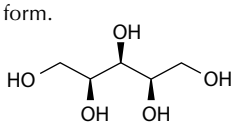

8.8.1 NADH versus NADPH Specificity of Enzymes

Isocitrate dehydrogenase (ICDH), an NADPH-dependent enzyme from *E. coli*, has been engineered, on the basis of the basis of data derived from its three-dimensional structure, by the introduction of seven mutations that change the specificity from favoring NADPH by 7000-fold to an enzyme that prefers NADH by 200-fold (Hurley et al. 1996). In general, a major difference between the $NADP^+$ and NAD^+ utilizing enzymes is the presence of a carboxylate side chain that chelates the diol group at the ribose near the adenine of NAD^+, whereas in enzymes that utilize $NADP^+$, there is frequently a highly positively charged arginine side chain oriented toward the adenine that interacts with the negatively charged ribose 3′-phosphomonoester (Carugo and Argos 1997). See the example of mutagenesis illustrated in Figure 8.1 and the associated literature (Chen et al. 1995; Hurley et al. 1996; Yaoi et al. 1996).

In the important group of cytochrome P450 enzymes, the NADPH specificity of an enzyme was altered so the enzyme could use NADH for recycling (Dohr et al. 2001). *Corynebacterium's* 2,5-diketo-D-gluconic acid (2,5-DKG) reductase, an enzyme used in the synthesis of vitamin C, has been mutated at four different sites giving rise to the F22Y/K232G/R238H/A272G quadruple mutant that is capable of utilizing NADH and NADPH (Banta et al. 2002c). The consequences of such alterations on vitamin C production have been modeled and were claimed to be economically beneficial through cost savings (Banta et al. 2002a).

Although *in vitro* regeneration of NADH has been addressed for some time (Wichmann and Vasic-Racki 2005), alteration of *in vivo* metabolism by use of cofactor manipulation is a recent development (Schroer et al. 2009; Weckbecker et al. 2010). An illustration of the importance of redox cofactor balance was illustrated in the engineering of an escape valve for excess NADPH accumulation in phosphoglucose-isomerase-deficient yeast. This mutant yeast cannot grow on glucose in absence of an NADPH oxidizing system. Accumulation of NADPH was prevented through cofactor engineering by altering the organism's own butanediol dehydrogenase specificity from NADH to NADPH (Ehsani et al. 2009).

Enzymatic reactions involved in the formation of flavor components vanillin, gamma-decalactone, carboxylic acids, C6 aldehydes and alcohols ("green notes"), esters, and 2-phenylethanol, including the need for cofactors and efficient recycling, have been discussed (Schrader et al. 2004).

8.8.2 Manipulation of NADH and NADPH *in vivo*

Expression of NADH oxidase *in vivo* was used to change the pattern of metabolic products formed by *Lactococcus lactis* (Lopez de Felipe et al. 1998). In such a strain, preference was for the production of more oxidized final products because of restricted supply in NADH, which is essential for the reduction of oxidized intermediates. Several cofactor engineering alterations have been reported in the literature (San et al. 2002), including a system for using formate dehydrogenase (FDH) to recycle NADH *in vivo* as well as the manipulation of CoA levels in the formation of products derived from acetyl-CoA. The *in vivo* use of the *Candida boidinii* FDH system (Allen and Holbrook 1995; Sakai et al. 1997) was further investigated. The coupling of FDH to L-amino acid dehydrogenases could produce optically active amino acids from α-keto acids in the presence of ammonium formate and a whole-cell biocatalyst (Galkin et al. 1997). Enhancement of ethanol production during growth on glucose was found in cells expressing *C. boidinii* FDH grown under anaerobic conditions. In fact, some ethanol could be formed under aerobic conditions when formate

was added to an FDH-expressing strain (Berrios-Rivera et al. 2002a, 2002b). The increased availability of NADH in an organism could provide potential for reducing other molecules present in the cell or added to the media (Figure 8.5). The coupling of FDH with a transhydrogenase to increase the intracellular level of NADPH for chiral alcohol production has been reported (Weckbecker and Hummel 2004). Engineering of the enzyme by mutagenesis to aid stabilization of the enzyme to oxidation and other improved characteristics of FDH have been reported (Slusarczyk et al. 2000; Tishkov and Popov 2006) and the temperature stability of a this enzyme from *Pseudomonas sp. 101* has been improved (Rojkova et al. 1999). Several FDHs from other species have been recently cloned, characterized, and altered (Karaguler et al. 2007). A comparison between FDH and glucose dehydrogenase (GDH) revealed that the latter enzyme was more effective in the regeneration of NADH required for the reduction of 4-chloroacetoacetate to form (*S*)-4-chloro-3-hydroxybutanoate, an important pharmaceutical intermediate (Yamamoto et al. 2004). The use of GDH to supply reduced cofactor for reactions *in vivo* such as the production of chiral alcohols has also been reported (Kataoka et al. 2003).

Mannitol can be produced by the enzymatic reduction of fructose (Liu et al. 2005), with NADH being generated through the coupling of mannitol dehydrogenase with FDH (Kaup et al. 2003). The extension of the system to the formation of other chiral compounds such as conversion of methyl acetoacetate to chiral hydroxy acid derivatives [methyl (*R*)-3-hydroxy butanoate] was developed by using the *fdh* gene from *Mycobacterium vaccae* N10. The gene encoding the NAD^+-dependent FDH was co-expressed in *E. coli* with an alcohol dehydrogenase from *Lactobacillus brevis* that is able to catalyze a highly regioselective and enantioselective reduction (Ernst et al. 2005).

Cofactor regeneration has also been used to increase the intracellular levels of NADPH and NADH, through the expression of a soluble transhydrogenase, for the production of hydromorphone (Boonstra et al. 2000). In the utilization of xylose by *Saccharomyces cerevisiae* for

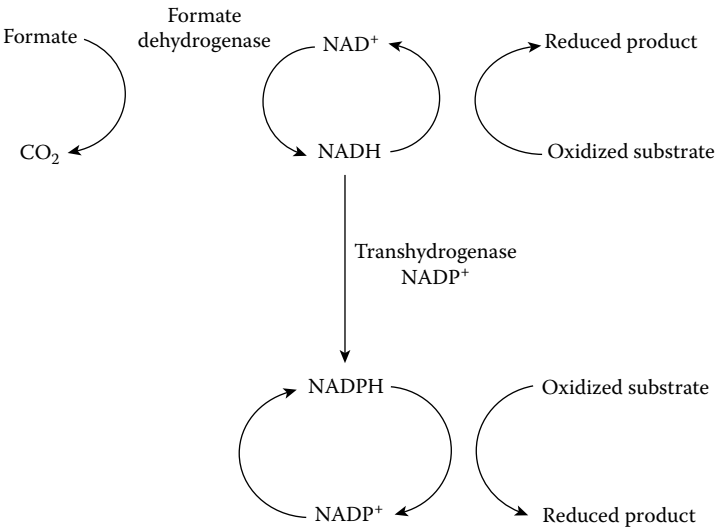

FIGURE 8.5 Coupling of *in vivo* activity of FDH to other redox reactions. Through internally produced or externally added formate, the reducing power of formate is used to produce NADH by the action of FDH. The NADH formed can be used by another enzyme in the cell, either an existing enzyme such as alcohol dehydrogenase or a heterologous enzyme from another organism capable of reducing a desired substrate. Various oxidoreductases can be produced in a host organism by introduction of appropriate genes by recombinant DNA techniques. The reduced product formed can be derived from a substrate normally produced by the growing cell from metabolism of a carbon source or it could be an added substrate molecule that is not otherwise metabolized by the organism. For reduced products, which require the participation of NADPH-dependent enzymes, an NADPH regenerating system can be constructed with the aid of transhydrogenase.

ethanol production, an imbalance of NADPH was observed. Such imbalance can be redressed through changing the cofactor specificity of the enzyme as illustrated earlier (Petschacher and Nidetzky 2008).

In the ammonia pathway, conversion of the NADPH-dependent glutamate dehydrogenase to an NADH-dependent (GDH2), and its subsequent expression, was accompanied by increase in flux to ethanol formation, while reducing flux to xylitol formation. This approach seems promising for improving batch culture performance. However, overexpression of the GS-GOGAT complex modestly improved ethanol yield only under special continuous culture conditions. An improvement of ethanol production was found when GDP1, which codes for a fungal $NADP^+$-dependent D-glyceraldehyde-3-phosphate dehydrogenase (NADP-GAPDH), was used to reduce the cofactor imbalance (Verho et al. 2003).

In some examples of the practical application of redox cofactors in pharmaceutical production, the conversion of ketoisophorone (2,6,6-trimethyl-2-cyclohexen-1,4-dione) to (6R)-levodione (2,2,6-trimethylcyclohexane-1,4-dione) was stimulated by the overexpression of old yellow enzyme (Oye) from *Candida macedoniensis in E. coli*. This enzyme is a well-characterized oxidoreductase. It was reported that the use of *E. coli* BL21 (DE3) cells co-expressing *oye* and *gdh* as a whole-cell catalyst was advantageous for the practical synthesis of (6R)-levodione (Kataoka et al. 2004).

8.8.3 CoA Compounds and S-Adenosyl Methionine

8.8.3.1 Acetyl-CoA Levels

The key intermediate acetyl-CoA is involved in the formation of many products of interest from isoprene compounds, carotenoids, flavanones, and polyketides to fatty acids and biofuel-related molecules. Manipulation of the acetyl-CoA levels for improved formation of esters derived from condensation of an alcohol with the acetyl-CoA has been reported (Vadali et al. 2004a, 2004b, 2004c). The high levels of CoA were produced by overexpression of a pantothenate kinase, and increased acetyl-CoA was achieved by overexpression of pyruvate dehydrogenase. In the experiments described, the acetyl-CoA was condensed with an alcohol by an acetyl-CoA-alcohol transferase to form an ester. This reaction could serve as a useful reporter of available acetyl-CoA without disrupting other areas of metabolism. The recycling and balance of CoA-utilizing pathways can serve as a possible means to influence the flux to other sinks for this intermediate and affect the overall pattern of metabolites (Figure 8.6). Although feedback systems generally control these CoA levels, they can be manipulated to some extent, which can contribute to enhanced production of acetyl-CoA-derived compounds. Alteration of the acetyl-CoA levels could have wide application because many pathways for production of larger molecules rely on the sequential addition of acyl-CoA groups. Because the mevalonate pathway compounds synthesize the intermediate isopentanyl pyrophosphate and many valuable compounds including terpenes and sterols are derived for this precursor, this pathway has been effectively introduced into *E. coli* (Yoon et al. 2009). Efforts to engineer the acetyl-CoA carboxylase-catalyzed carboxylation of acetyl-CoA to malonyl-CoA have been studied (Zha et al. 2009), and the effect of engineering this component on the production of flavanones showed a strong effect on the levels of flavanones obtained in engineered *E. coli* (Fowler et al. 2009).

One area where the level of acyl-CoA compounds is important is in the production of polyhydroxybutyrate and its various derivatives. In this process, hydroxyacyl-CoA compounds are polymerized into a large polymer. Different physical properties within the polymer are obtained depending on the composition of monomers incorporated. Therefore, copolymerization of hydroxybutyryl-CoA with other acyl-CoA compounds has been investigated extensively (Steinbuchel and Schlegel 1991; Liu and Chen 2007; Chung et al. 2009; Elbahloul and Steinbuchel 2009; Jian et al. 2010). To obtain high levels of the nonstandard acyl-CoA substrates, the mechanisms of uptake and activation of the corresponding acids, including the use of the *prpE* gene, were targeted (Valentin et al. 2000; Aldor and Keasling 2001) Expression of a combination of a butyrate kinase and

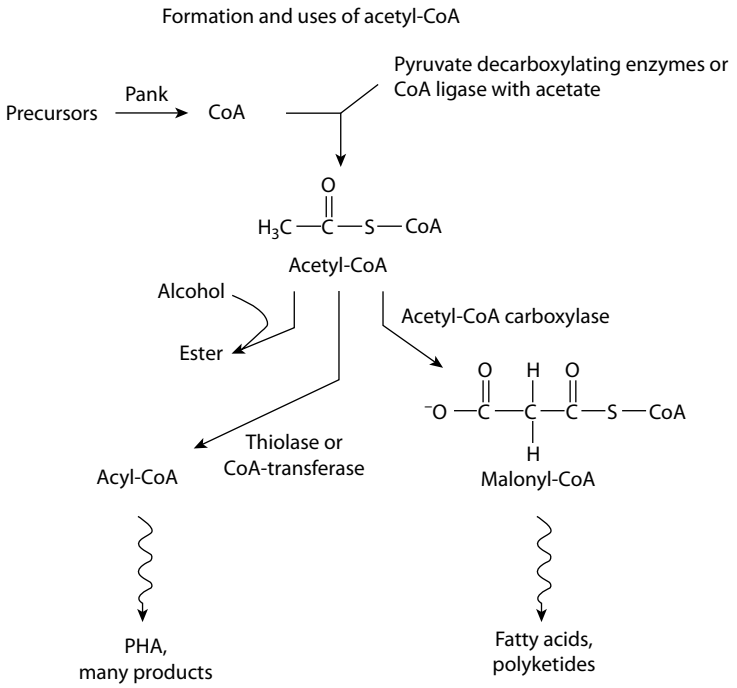

FIGURE 8.6 The CoA level can be raised by overexpression of a key enzyme in the biosynthetic pathway of CoA from pantothenate. The CoA can then be more effectively converted to acetyl-CoA or other acyl-CoA by pyruvate dehydrogenases or CoA ligases; the acetyl-CoA is then more available for conversion to esters.

phosphotransbutyrylase (Liu et al. 2003) and development of a means to take advantage of the connection in formation of acyl-CoA compounds between the pathways of fatty acid degradation and those acyl-CoA compounds needed for desired product formation have also been investigated (Liu and Chen 2007; Jian et al. 2010; Chung et al. 2009). For example, the use of CoA transferases to bring other acids into the polymerization process has also been reported with 4-hydroxybutyrate-containing polymers (Song et al. 2005). The use of glycerol as a feedstock for the formation of poly(3-hydroxypropionate) in engineered *E. coli* (Andreessen et al. 2010) and the engineering/evolution of polyhydroxyalkanoate synthase have generated enzymes with higher activity and altered specificity (Amara et al. 2002) and even allowed for the formation of polylactate in *E. coli* (Jung et al. 2010; Matsumoto and Taguchi 2010; Yang et al. 2010). The introduction of acyltransferases that can transfer the long-chain fatty acid moiety from acyl-CoA compounds to alcohols has allowed for the formation of long-chain esters relevant to biofuels "microdiesel" (Stoveken and Steinbuchel 2008; Elbahloul and Steinbuchel 2010).

A large group of compounds built from acyl-CoA precursors are the polyketides, a group of bioactive structures [e.g., avermectin (Ikeda et al. 2001)]. In these reactions, malonyl-CoA is a major precursor. Malonyl-CoA is formed from acetyl-CoA by addition of a carboxyl group and is a precursor for fatty acid synthesis. In the case of polyketide synthesis, the group is transferred to an acyl carrier protein for incorporation into the chain as the longer chain polyketide is synthesized (Khosla 2009). The acyl carrier proteins require activation by addition of a 4'-phosphopantotheinyl group from CoA by specific enzymes, PPTases (Mofid et al. 2004). The analysis and overexpression of acetyl-CoA carboxylase from various sources have led to increased levels of malonyl-CoA (Davis et al. 2000; Gande et al. 2004). Manipulation of the acyl-CoA pools or use of selective acyl-transferases can lead to alterations of the polyketide product (Liou and Khosla 2003). Providing enzymes such as CoA ligases for forming methylmalonyl-CoA or propionyl-CoA has increased the pool of the

corresponding acyl-CoAs and improved synthesis of the erythromycin precursor, 6-deoxyerythronolide B (Murli et al. 2003). Furthermore, the use of CoA ligases with broad specificities has also been exploited for the precursors pools (Pohl et al. 2001; Arora et al. 2005).

8.8.3.2 S-Adenosyl Methionine Levels

The modification by addition of a methyl group to generate methoxy side chains is a widely used event in many secondary metabolites. This and the volatility of biologically important methylate compounds generated a good deal of interest in exploiting methylation reactions using *S*-adenosyl methionine (SAM) as the methyl donor. In a biotechnological context, methyl transfer strategy has been used to generate methyl halides in engineered strains of *E. coli* and yeast (Bayer et al. 2009). The engineering of methionine adenosyltransferase by DNA shuffling of *E. coli*, *S. cerevisiae*, and *Streptomyces spectabilis* MAT genes resulted in a more active enzyme and allowed for a high level SAM productivity during the course of large-scale fermentation (Hu et al. 2009).

SUMMARY

Recent innovations in functional genomics, proteomics, transcriptomics, metabolomics, and bioinformatics have revolutionized the scope of enzyme engineering and its role in the production of biopharmaceuticals. Many enzymes have been targeted individually and in combinations with the view of improving industrial processes. In addition to random mutagenesis coupled with high-throughput screening, other techniques including site-directed mutagenesis, molecular breeding, and synthetic biology are currently being exploited to improve the physical and pharmokinetic properties of key industrial enzymes.

The ability to manipulate the intracellular levels of cofactors to favor the formation of desired products further extends and expands the repertoire of tools available for enzyme and metabolic engineering.

The coupling of these experimental methods with better understanding of global cellular metabolism via advanced analytical techniques and mathematical treatments bodes well for further developments in the applications of enzymes and microbial biocatalysts in industrial and pharmaceutical bioprocesses.

REFERENCES

Aldor, I., and J.D. Keasling. 2001. Metabolic engineering of poly(3-hydroxybutyrate-co-3-hydroxyvalerate) composition in recombinant *Salmonella enterica* serovar typhimurium. *Biotechnol Bioeng* 76:108–14.

Allen, S.J., and J.J. Holbrook. 1995. Isolation, sequence and overexpression of the gene encoding NAD-dependent formate dehydrogenase from the methylotrophic yeast *Candida methylica*. *Gene* 162:99–104.

Amara, A.A., A. Steinbuchel, and B.H. Rehm. 2002. In vivo evolution of the Aeromonas punctata polyhydroxyalkanoate (PHA) synthase: Isolation and characterization of modified PHA synthases with enhanced activity. *Appl Microbiol Biotechnol* 59:477–82.

Andreessen, B., A.B. Lange, H. Robenek, and A. Steinbuchel. 2010. Conversion of glycerol to poly(3-hydroxypropionate) in recombinant *Escherichia coli*. *Appl Environ Microbiol* 76:622–6.

Arora, P., A. Vats, P. Saxena, D. Mohanty, and R.S. Gokhale. 2005. Promiscuous fatty acyl CoA ligases produce acyl-CoA and acyl-SNAC precursors for polyketide biosynthesis. *J Am Chem Soc* 127:9388–9.

Asboth, B., and G. Naray-Szabo. 2000. Mechanism of action of D-xylose isomerase. *Curr Protein Pept Sci* 1:237–54.

Bailon, P., and C.Y. Won. 2009. PEG-modified biopharmaceuticals. *Expert Opin Drug Deliv* 6:1–16.

Banta, S., M. Boston, A. Jarnagin, and S. Anderson. 2002a. Mathematical modeling of in vitro enzymatic production of 2-keto-L-gulonic acid using NAD(H) or NADP(H) as cofactors. *Metab Eng* 4:273–84.

Banta, S., B.A. Swanson, S. Wu, A. Jarnagin, and S. Anderson. 2002b. Alteration of the specificity of the cofactor-binding pocket of Corynebacterium 2,5-diketo-D-gluconic acid reductase A. *Protein Eng* 15:131–40.

Banta, S., B.A. Swanson, S. Wu, A. Jarnagin, and S. Anderson. 2002c. Optimizing an artificial metabolic pathway: Engineering the cofactor specificity of Corynebacterium 2,5-diketo-D-gluconic acid reductase for use in vitamin C biosynthesis. *Biochemistry* 41:6226–36.

Bayer, T.S., D.M. Widmaier, K. Temme, E.A. Mirsky, D.V. Santi, and C.A. Voigt. 2009. Synthesis of methyl halides from biomass using engineered microbes. *J Am Chem Soc* 131:6508–15.

Benkovic, S.J., and S. Hammes-Schiffer. 2003. A perspective on enzyme catalysis. *Science* 301:1196–202.

Berrios-Rivera, S.J., G.N. Bennett, and K.Y. San. 2002a. Metabolic engineering of *Escherichia coli*: Increase of NADH availability by overexpressing an NAD(+)-dependent formate dehydrogenase. *Metab Eng* 4:217–29.

Berrios-Rivera, S.J., G.N. Bennett, and K.Y. San. 2002b. The effect of increasing NADH availability on the redistribution of metabolic fluxes in *Escherichia coli* chemostat cultures. *Metab Eng* 4:230–7.

Bessler, C., J. Schmitt, K.H. Maurer, and R.D. Schmid. 2003. Directed evolution of a bacterial alpha-amylase: toward enhanced pH-performance and higher specific activity. *Protein Sci* 12:2141–9.

Blumer-Schuette S.E., I. Kataeva, J. Westpheling, M.W. Adams, and R.M. Kelly. 2008. Extremely thermophilic microorganisms for biomass conversion: Status and prospects. *Curr Opin Biotechnol* 19:210–7.

Boersma, Y.L., M.J. Droge, and W.J. Quax. 2007. Selection strategies for improved biocatalysts. *FEBS J* 274:2181–95.

Boonstra, B., D.A. Rathbone, C.E. French, E.H. Walker, and N.C. Bruce. 2000. Cofactor regeneration by a soluble pyridine nucleotide transhydrogenase for biological production of hydromorphone. *Appl Environ Microbiol* 66:5161–6.

Brocard-Masson, C., and B. Dumas. 2006. The fascinating world of steroids: *S. cerevisiae* as a model organism for the study of hydrocortisone biosynthesis. *Biotechnol Genet Eng Rev* 22:213–52.

Brown, A.J., and W. Jessup. 2009. Oxysterols: Sources, cellular storage and metabolism, and new insights into their roles in cholesterol homeostasis. *Mol Aspects Med* 30:111–22.

Buhler, B., and A. Schmid. 2004. Process implementation aspects for biocatalytic hydrocarbon oxyfunctionalization. *J Biotechnol* 113:183–210.

Carballeira J. D., M.A. Quezada, P. Hoyos, Y. Simeo, M.J. Hernaiz, A.R. Alcantara, and J.V. Sinisterra. 2009. Microbial cells as catalysts for stereoselective red-ox reactions. *Biotechnol Adv* 27:686–714.

Carothers, J. M., J.A. Goler, and J.D. Keasling. 2009. Chemical synthesis using synthetic biology. *Curr Opin Biotechnol* 20:498–503.

Carugo, O., and P. Argos. 1997. NADP-dependent enzymes. I: Conserved stereochemistry of cofactor binding. *Proteins* 28:10–28.

Chemier, J.A., Z.L. Fowler, M.A. Koffas, and E. Leonard. 2009. Trends in microbial synthesis of natural products and biofuels. *Adv Enzymol Relat Areas Mol Biol* 76:151–217.

Chen, J., R.C. Zheng, Y.G. Zheng, and Y.C. Shen. 2009. Microbial transformation of nitriles to high-value acids or amides. *Adv Biochem Eng Biotechnol* 113:33–77.

Chen, R., A. Greer, and A.M. Dean. 1995. A highly active decarboxylating dehydrogenase with rationally inverted coenzyme specificity. *Proc Natl Acad Sci U S A* 92:11666–70.

Cherry, J.R., and A.L. Fidantsef. 2003. Directed evolution of industrial enzymes: An update. *Curr Opin Biotechnol* 14:438–43.

Chung, A., Q. Liu, S.P. Ouyang, Q. Wu, and G.Q. Chen. 2009. Microbial production of 3-hydroxydodecanoic acid by pha operon and fadBA knockout mutant of *Pseudomonas putida* KT2442 harboring tesB gene. *Appl Microbiol Biotechnol* 83:513–9.

Cirino, P.C., and F.H. Arnold. 2002. Protein engineering of oxygenases for biocatalysis. *Curr Opin Chem Biol* 6:130–5.

Cirino, P.C., K.M. Mayer, and D. Umeno. 2003. Generating mutant libraries using error-prone PCR. *Methods Mol Biol* 231:3–9.

Datsenko, K.A., and B.L. Wanner. 2000. One-step inactivation of chromosomal genes in *Escherichia coli* K-12 using PCR products. *Proc Natl Acad Sci USA* 97:6640–5.

Davis, M.S., J. Solbiati, and J.E. Cronan, Jr. 2000. Overproduction of acetyl-CoA carboxylase activity increases the rate of fatty acid biosynthesis in *Escherichia coli*. *J Biol Chem* 275:28593–8.

Dohr, O., M.J. Paine, T. Friedberg, G.C. Roberts, and C.R. Wolf. 2001. Engineering of a functional human NADH-dependent cytochrome P450 system. *Proc Natl Acad Sci USA* 98:81–6.

Doi, R.H. 2008. Cellulases of mesophilic microorganisms: cellulosome and noncellulosome producers. *Ann N Y Acad Sci* 1125:267–79.

Dowe, N. 2009. Assessing cellulase performance on pretreated lignocellulosic biomass using saccharification and fermentation-based protocols. *Methods Mol Biol* 581:233–45.

Doyle, S.A., P.T. Beernink, and D.E. Koshland, Jr. 2001. Structural basis for a change in substrate specificity: Crystal structure of S113E isocitrate dehydrogenase in a complex with isopropylmalate, Mg^{2+}, and NADP. *Biochemistry* 40, 4234–41.

Duine, J.A. 1991. Cofactor engineering. *Trends Biotechnol* 9:343–6.

Duport, C., R. Spagnoli, E. Degryse, and D. Pompon. 1998. Self-sufficient biosynthesis of pregnenolone and progesterone in engineered yeast. *Nat Biotechnol* 16:186–9.

Ehsani, M., M.R. Fernandez, J.A. Biosca, and S. Dequin. 2009. Reversal of coenzyme specificity of 2,3-butanediol dehydrogenase from *Saccharomyces cerevisae* and in vivo functional analysis. *Biotechnol Bioeng* 104:381–9.

Elbahloul, Y., and A. Steinbuchel. 2009. Large-scale production of poly(3-hydroxyoctanoic acid) by *Pseudomonas putida* GPo1 and a simplified downstream process. *Appl Environ Microbiol* 75:643–51.

Elbahloul, Y., and A. Steinbuchel. 2010. Pilot-scale production of fatty acid ethyl esters by an engineered *Escherichia coli* strain harboring the p(Microdiesel) plasmid. *Appl Environ Microbiol* 76:4560–5.

Ernst, M., B. Kaup, M. Muller, S. Bringer-Meyer, and H. Sahm. 2005. Enantioselective reduction of carbonyl compounds by whole-cell biotransformation, combining a formate dehydrogenase and a (R)-specific alcohol dehydrogenase. *Appl Microbiol Biotechnol* 66:629–34.

Feller, G. 2003. Molecular adaptations to cold in psychrophilic enzymes. *Cell Mol Life Sci* 60:648–62.

Fong, S.S., A.R. Joyce, and B.O. Palsson. 2005. Parallel adaptive evolution cultures of *Escherichia coli* lead to convergent growth phenotypes with different gene expression states. *Genome Res* 15:1365–72.

Fowler, Z.L., W.W. Gikandi, and M.A. Koffas. 2009. Increased malonyl coenzyme A biosynthesis by tuning the *Escherichia coli* metabolic network and its application to flavanone production. *Appl Environ Microbiol* 75:5831–9.

Galkin, A., L. Kulakova, T. Yoshimura, K. Soda, and N. Esaki. 1997. Synthesis of optically active amino acids from alpha-keto acids with *Escherichia coli cells* expressing heterologous genes. *Appl Environ Microbiol* 63:4651–6.

Gande, R., K.J. Gibson, A.K. Brown, K. Krumbach, L.G. Dover, H. Sahm, S. Shioyama, T. Oikawa, G.S. Besra, and L. Eggeling. 2004. Acyl-CoA carboxylases (accD2 and accD3), together with a unique polyketide synthase (Cg-pks), are key to mycolic acid biosynthesis in Corynebacterianeae such as *Corynebacterium glutamicum* and *Mycobacterium tuberculosis*. *J Biol Chem* 279:44847–57.

Georlette, D., V. Blaise, T. Collins, S. D'Amico, E. Gratia, A. Hoyoux, J.C. Marx, G. Sonan, G. Feller, and C. Gerday. 2004. Some like it cold: Biocatalysis at low temperatures. *FEMS Microbiol Rev* 28:25–42.

Graddis, T.J., R.L. Remmele, Jr. and J.T. McGrew. 2002. Designing proteins that work using recombinant technologies. *Curr Pharm Biotechnol* 3:285–97.

Grogan, D.W., and K.R. Stengel. 2008. Recombination of synthetic oligonucleotides with prokaryotic chromosomes: Substrate requirements of the *Escherichia coli*/lambda Red and Sulfolobus acidocaldarius recombination systems. *Mol Microbiol* 69:1255–65.

Gupta, A., and S.K. Khare. 2009. Enzymes from solvent-tolerant microbes: Useful biocatalysts for non-aqueous enzymology. *Crit Rev Biotechnol* 29:44–54.

Harada, H., and N. Misawa. 2009. Novel approaches and achievements in biosynthesis of functional isoprenoids in *Escherichia coli*. *Appl Microbiol Biotechnol* 84:1021–31.

Hartley, B.S., N. Hanlon, R.J. Jackson, and M. Rangarajan. 2000. Glucose isomerase: Insights into protein engineering for increased thermostability. *Biochim Biophys Acta* 1543:294–335.

Herring, C.D., A. Raghunathan, C. Honisch, T. Patel, M.K. Applebee, A.R. Joyce, T.J. Albert, F.R. Blattner, D. van den Boom, C.R. Cantor, and B.O. Palsson. 2006. Comparative genome sequencing of *Escherichia coli* allows observation of bacterial evolution on a laboratory timescale. *Nat Genet* 38:1406–12.

Hollrigl, V., F. Hollmann, A.C. Kleeb, K. Buehler, and A. Schmid. 2008. TADH, the thermostable alcohol dehydrogenase from Thermus sp. ATN1: A versatile new biocatalyst for organic synthesis. *Appl Microbiol Biotechnol* 81:263–73.

Holmberg, N., U. Ryde, and L. Bulow. 1999. Redesign of the coenzyme specificity in L-lactate dehydrogenase from bacillus stearothermophilus using site-directed mutagenesis and media engineering. *Protein Eng* 12:851–6.

Hu, H., J. Qian, J. Chu, Y. Wang, Y. Zhuang, and S. Zhang. 2009. DNA shuffling of methionine adenosyltransferase gene leads to improved S-adenosyl-L-methionine production in *Pichia pastoris*. *J Biotechnol* 141:97–103.

Hult, K., and P. Berglund 2003. Engineered enzymes for improved organic synthesis. *Curr Opin Biotechnol* 14:395–400.

Hurley, J.H., R. Chen, and A.M. Dean. 1996. Determinants of cofactor specificity in isocitrate dehydrogenase: Structure of an engineered $NADP^+ \rightarrow NAD^+$ specificity-reversal mutant. *Biochemistry* 35:5670–8.

Ikeda, H., T. Nonomiya, and S. Omura. 2001. Organization of biosynthetic gene cluster for avermectin in *Streptomyces avermitilis*: Analysis of enzymatic domains in four polyketide synthases. *J Ind Microbiol Biotechnol* 27:170–6.

Jaeger, K.E., and T. Eggert. 2004. Enantioselective biocatalysis optimized by directed evolution. *Curr Opin Biotechnol* 15:305–13.

Jestin, J.L., and P.A. Kaminski. 2004. Directed enzyme evolution and selections for catalysis based on product formation. *J Biotechnol* 113:85–103.

Jian, J., Z.J. Li, H.M. Ye, M.Q. Yuan, and G.Q. Chen. 2010. Metabolic engineering for microbial production of polyhydroxyalkanoates consisting of high 3-hydroxyhexanoate content by recombinant *Aeromonas hydrophila*. *Bioresour Technol* 101:6096–102.

Joseph, B., P.W. Ramteke, and G. Thomas. 2008. Cold active microbial lipases: Some hot issues and recent developments. *Biotechnol Adv* 26:457–70.

Jung, R., M.P. Scott, L.O. Oliveira, and N.C. Nielsen. 1992. A simple and efficient method for the oligodeoxyribonucleotide-directed mutagenesis of double-stranded plasmid DNA. *Gene* 121:17–24.

Jung, Y. K., T.Y. Kim, S.J. Park, and S.Y. Lee. 2010. Metabolic engineering of *Escherichia coli* for the production of polylactic acid and its copolymers. *Biotechnol Bioeng* 105:161–71.

Karaguler, N.G., R.B. Sessions, B. Binay, E.B. Ordu, and A.R. Clarke. 2007. Protein engineering applications of industrially exploitable enzymes: *Geobacillus stearothermophilus* LDH and Candida methylica FDH. *Biochem Soc Trans* 35:1610–5.

Kataoka, M., K. Kita, M. Wada, Y. Yasohara, J. Hasegawa, and S. Shimizu. 2003. Novel bioreduction system for the production of chiral alcohols. *Appl Microbiol Biotechnol* 62:437–45.

Kataoka, M., A. Kotaka, R. Thiwthong, M. Wada, S. Nakamori, and S. Shimizu. 2004. Cloning and overexpression of the old yellow enzyme gene of Candida macedoniensis, and its application to the production of a chiral compound. *J Biotechnol* 114:1–9.

Kaup, B., S. Bringer-Meyer, and H. Sahm. 2003. Metabolic engineering of *Escherichia coli*: Construction of an efficient biocatalyst for D-mannitol formation in a whole-cell biotransformation. *Commun Agric Appl Biol Sci* 68:235–40.

Kaup, B., S. Bringer-Meyer, and H. Sahm. 2004. Metabolic engineering of *Escherichia coli*: Construction of an efficient biocatalyst for D-mannitol formation in a whole-cell biotransformation. *Appl Microbiol Biotechnol* 64:333–9.

Keasling, J.D. 2008. Synthetic biology for synthetic chemistry. *ACS Chem Biol* 3:64–76.

Kegler-Ebo, D.M., G.W. Polack, and D. DiMaio. 1996. Use of codon cassette mutagenesis for saturation mutagenesis. *Methods Mol Biol* 57:297–310.

Khandeparker, R., and M.T. Numan. 2008. Bifunctional xylanases and their potential use in biotechnology. *J Ind Microbiol Biotechnol* 35:635–44.

Khosla, C. 2009. Structures and mechanisms of polyketide synthases. *J Org Chem* 74:6416–20.

Khosla, C., S. Kapur, and D.E. Cane. 2009. Revisiting the modularity of modular polyketide synthases. *Curr Opin Chem Biol* 13:135–43.

Khosla, C., Y. Tang, A.Y. Chen, N.A. Schnarr, and D.E. Cane. 2007. Structure and mechanism of the 6-deoxyerythronolide B synthase. *Annu Rev Biochem* 76:195–221.

Kimura, E. 2003. Metabolic engineering of glutamate production. *Adv Biochem Eng Biotechnol* 79:37–57.

Kirby, J., D.W. Romanini, E.M. Paradise, and J.D. Keasling. 2008. Engineering triterpene production in *Saccharomyces cerevisiae*-beta-amyrin synthase from Artemisia annua. *FEBS J* 275:1852–9.

Krahulec, S., B. Petschacher, M. Wallner, K. Longus, M. Klimacek, and B. Nidetzky. 2010. Fermentation of mixed glucose-xylose substrates by engineered strains of *Saccharomyces cerevisiae*: Role of the coenzyme specificity of xylose reductase, and effect of glucose on xylose utilization. *Microb Cell Fact* 9:16.

Kunkel, T.A., K. Bebenek, and J. McClary. 1991. Efficient site-directed mutagenesis using uracil-containing DNA. *Methods Enzymol* 204:125–39.

Kwon, S.J., R. Petri, A.L. DeBoer, and C. Schmidt-Dannert. 2004. A high-throughput screen for porphyrin metal chelatases: Application to the directed evolution of ferrochelatases for metalloporphyrin biosynthesis. *Chembiochem* 5:1069–74.

Labrou, N.E. 2010. Random mutagenesis methods for in vitro directed enzyme evolution. *Curr Protein Pept Sci* 11:91–100.

Landrain, T. E., J. Carrera, B. Kirov, G. Rodrigo, and A. Jaramillo. 2009. Modular model-based design for heterologous bioproduction in bacteria. *Curr Opin Biotechnol* 20:272–9.

Liou, G.F., and C. Khosla. 2003. Building-block selectivity of polyketide synthases. *Curr Opin Chem Biol* 7:279–84.

Liu, G.N., Y.H. Zhu, and J.G. Jiang. 2009. The metabolomics of carotenoids in engineered cell factory. *Appl Microbiol Biotechnol* 83:989–99.

Liu, S., B. Saha, and M. Cotta. 2005. Cloning, expression, purification, and analysis of mannitol dehydrogenase gene mtlK from Lactobacillus brevis. *Appl Biochem Biotechnol* 121–124:391–401.

Liu, S.J., T. Lutke-Eversloh, and A. Steinbuchel. 2003. Biosynthesis of poly (3-mercaptopropionate) and poly (3-mercaptopropionate-co-3-hydroxybutyrate) with recombinant *Escherichia coli*. *Sheng Wu Gong Cheng Xue Bao* 19:195–9.

Liu, W., and G.Q. Chen. 2007. Production and characterization of medium-chain-length polyhydroxyalkanoate with high 3-hydroxytetradecanoate monomer content by fadB and fadA knockout mutant of *Pseudomonas putida* KT2442. *Appl Microbiol Biotechnol* 76:1153–9.

Locher, C.P., M. Paidhungat, R.G. Whalen, and J. Punnonen. 2005. DNA shuffling and screening strategies for improving vaccine efficacy. *DNA Cell Biol* 24:256–63.

Lopez de Felipe, F., M. Kleerebezem, W.M. de Vos, and J. Hugenholtz. 1998. Cofactor engineering: A novel approach to metabolic engineering in *Lactococcus lactis* by controlled expression of NADH oxidase. *J Bacteriol* 180:3804–8.

Lordan, S., J.J. Mackrill, and N.M. O'Brien. 2009. Oxysterols and mechanisms of apoptotic signaling: Implications in the pathology of degenerative diseases. *J Nutr Biochem* 20:321–36.

Luetz, S., L. Giver, and J. Lalonde. 2008. Engineered enzymes for chemical production. *Biotechnol Bioeng* 101:647–53.

MacLachlan, J., A.T. Wotherspoon, R.O. Ansell, and C.J. Brooks. 2000. Cholesterol oxidase: Sources, physical properties and analytical applications. *J Steroid Biochem Mol Biol* 72:169–95.

Maczek, J., S. Junne, P. Nowak, and P. Goetz. 2006. Metabolic flux analysis of the sterol pathway in the yeast *Saccharomyces cerevisiae*. *Bioprocess Biosyst Eng* 29:241–52.

Maki, M., K.T. Leung, and W. Qin. 2009. The prospects of cellulase-producing bacteria for the bioconversion of lignocellulosic biomass. *Int J Biol Sci* 5:500–16.

Malaviya, A., and J. Gomes. 2008. Androstenedione production by biotransformation of phytosterols. *Bioresour Technol* 99:6725–37.

Matsui, I., and K. Harata. 2007. Implication for buried polar contacts and ion pairs in hyperthermostable enzymes. *FEBS J* 274:4012–22.

Matsumoto, K., and S. Taguchi. 2010. Enzymatic and whole-cell synthesis of lactate-containing polyesters: Toward the complete biological production of polylactate. *Appl Microbiol Biotechnol* 85:921–32.

McCleary, W.R. 2009. Application of promoter swapping techniques to control expression of chromosomal genes. *Appl Microbiol Biotechnol* 84:641–8.

Mofid, M.R., R. Finking, L.O. Essen, and M.A. Marahiel. 2004. Structure-based mutational analysis of the 4'-phosphopantetheinyl transferases Sfp from *Bacillus subtilis*: Carrier protein recognition and reaction mechanism. *Biochemistry* 43:4128–36.

Morikawa, S., T. Nakai, Y. Yasohara, H. Nanba, N. Kizaki, and J. Hasegawa. 2005. Highly active mutants of carbonyl reductase S1 with inverted coenzyme specificity and production of optically active alcohols. *Biosci Biotechnol Biochem* 69:544–52.

Muntendam, R., E. Melillo, A. Ryden, and O. Kayser. 2009. Perspectives and limits of engineering the isoprenoid metabolism in heterologous hosts. *Appl Microbiol Biotechnol* 84:1003–19.

Murli, S., J. Kennedy, L.C. Dayem, J.R. Carney, and J.T. Kealey. 2003. Metabolic engineering of *Escherichia coli* for improved 6-deoxyerythronolide B production. *J Ind Microbiol Biotechnol* 30:500–9.

Ng, I.S., and S.W. Tsai. 2005. Hydrolytic resolution of (R,S)-naproxen 2,2,2-trifluoroethyl thioester by *Carica papaya* lipase in water-saturated organic solvents. *Biotechnol Bioeng* 89:88–95.

Nishihara, M., and T. Nakatsuka. 2010. Genetic engineering of novel flower colors in floricultural plants: Recent advances via transgenic approaches. *Methods Mol Biol* 589:325–47.

Ohnishi, J., S. Mitsuhashi, M. Hayashi, S. Ando, H. Yokoi, K. Ochiai, and M. Ikeda. 2002. A novel methodology employing *Corynebacterium glutamicum* genome information to generate a new L-lysine-producing mutant. *Appl Microbiol Biotechnol* 58:217–23.

Pai, S.S., R.D. Tilton, and T.M. Przybycien. 2009. Poly(ethylene glycol)-modified proteins: Implications for poly(lactide-co-glycolide)-based microsphere delivery. *AAPS J* 11:88–98.

Paradise, E.M., J. Kirby, R. Chan, and J.D. Keasling. 2008. Redirection of flux through the FPP branch-point in *Saccharomyces cerevisiae* by down-regulating squalene synthase. *Biotechnol Bioeng* 100:371–8.

Pasqualini, J.R. 2009. Breast cancer and steroid metabolizing enzymes: The role of progestogens. *Maturitas* 65(Suppl 1):S17–21.

Patten, P.A., R.J. Howard, and W.P. Stemmer. 1997. Applications of DNA shuffling to pharmaceuticals and vaccines. *Curr Opin Biotechnol* 8:724–33.

Petschacher, B., and B. Nidetzky. 2008. Altering the coenzyme preference of xylose reductase to favor utilization of NADH enhances ethanol yield from xylose in a metabolically engineered strain of *Saccharomyces cerevisiae*. *Microb Cell Fact* 7:9.

Pohl, N.L., M. Hans, H.Y. Lee, Y.S. Kim, D.E. Cane, and C. Khosla. 2001. Remarkably broad substrate tolerance of malonyl-CoA synthetase, an enzyme capable of intracellular synthesis of polyketide precursors. *J Am Chem Soc* 123:5822–3.

Pollegioni, L., L. Piubelli, and G. Molla. 2009. Cholesterol oxidase: Biotechnological applications. *FEBS J* 276:6857–70.

Powell, K.A., S.W. Ramer, S.B. Del Cardayre, W.P. Stemmer, M.B. Tobin, P.F. Longchamp, and G.W. Huisman. 2001. Directed evolution and biocatalysis. *Angew Chem Int Ed Engl* 40:3948–3959.

Purnapatre, K., S.K. Khattar, and K.S. Saini. 2008. Cytochrome P450s in the development of target-based anticancer drugs. *Cancer Lett* 259:1–15.

Rojkova, A.M., A.G. Galkin, L.B. Kulakova, A.E. Serov, P.A. Savitsky, V.V. Fedorchuk, and V.I. Tishkov. 1999. Bacterial formate dehydrogenase. Increasing the enzyme thermal stability by hydrophobization of alpha-helices. *FEBS Lett* 445:183–8.

Sakai, Y., A.P. Murdanoto, T. Konishi, A. Iwamatsu, and N. Kato. 1997. Regulation of the formate dehydrogenase gene, FDH1, in the methylotrophic yeast *Candida boidinii* and growth characteristics of an FDH1-disrupted strain on methanol, methylamine, and choline. *J Bacteriol* 179:4480–5.

San, K.Y., G.N. Bennett, S.J. Berrios-Rivera, R.V. Vadali, Y.T. Yang, E. Horton, F.B. Rudolph, B. Sariyar, and K. Blackwood. 2002. Metabolic engineering through cofactor manipulation and its effects on metabolic flux redistribution in *Escherichia coli*. *Metab Eng* 4:182–92.

Sauer, J., B.W. Sigurskjold, U. Christensen, T.P. Frandsen, E. Mirgorodskaya, M. Harrison, P. Roepstorff, and B. Svensson. 2000. Glucoamylase: Structure/function relationships, and protein engineering. *Biochim Biophys Acta* 154:275–93.

Schrader, J., M.M. Etschmann, D. Sell, J.M. Hilmer, and J. Rabenhorst. 2004. Applied biocatalysis for the synthesis of natural flavour compounds—Current industrial processes and future prospects. *Biotechnol Lett* 26:463–72.

Schroer, K., B. Zelic, M. Oldiges, and S. Lutz. 2009. Metabolomics for biotransformations: Intracellular redox cofactor analysis and enzyme kinetics offer insight into whole cell processes. *Biotechnol Bioeng* 104:251–60.

Seo, J.W., J.H. Jeong, C.G. Shin, S.C. Lo, S.S. Han, K.W. Yu, E. Harada, J.Y. Han, and Y.E. Choi. 2005. Overexpression of squalene synthase in *Eleutherococcus senticosus* increases phytosterol and triterpene accumulation. *Phytochemistry* 66:869–77.

Shanafelt, A.B. 2005. Medicinally useful proteins—Enhancing the probability of technical success in the clinic. *Expert Opin Biol Ther* 5:149–51.

Siddiqui, K.S., and R. Cavicchioli. 2006. Cold-adapted enzymes. *Annu Rev Biochem* 75:403–33.

Sio, C.F., and W.J. Quax. 2004. Improved beta-lactam acylases and their use as industrial biocatalysts. *Curr Opin Biotechnol* 15:349–55.

Slusarczyk, H., S. Felber, M.R. Kula, and M. Pohl. 2000. Stabilization of NAD-dependent formate dehydrogenase from *Candida boidinii* by site-directed mutagenesis of cysteine residues. *Eur J Biochem* 267:1280–9.

Sola, R.J., and K. Griebenow. 2010. Glycosylation of therapeutic proteins: An effective strategy to optimize efficacy. *BioDrugs* 24:9–21.

Song, S.S., H. Ma, Z.X. Gao, Z.H. Jia, and X. Zhang. 2005. Construction of recombinant *Escherichia coli* strains producing poly (4-hydroxybutyric acid) homopolyester from glucose. *Wei Sheng Wu Xue Bao* 45:382–6.

Steinbuchel, A., and H.G. Schlegel. 1991. Physiology and molecular genetics of poly(beta-hydroxy-alkanoic acid) synthesis in *Alcaligenes eutrophus*. *Mol Microbiol* 5:535–42.

Storici, F., L.K. Lewisand, and M.A. Resnick. 2001. In vivo site-directed mutagenesis using oligonucleotides. *Nat Biotechnol* 19:773–6.

Stoveken, T., and A. Steinbuchel. 2008. Bacterial acyltransferases as an alternative for lipase-catalyzed acylation for the production of oleochemicals and fuels. *Angew Chem Int Ed Engl* 47:3688–94.

Szczebara, F.M., C. Chandelier, C. Villeret, A. Masurel, S. Bourot, C. Duport, S. Blanchard, A. Groisillier, E. Testet, P. Costaglioli, G. Cauet, E. Degryse, D. Balbuena, J. Winter, T. Achstetter, R. Spagnoli, D. Pompon, and B. Dumas. 2003. Total biosynthesis of hydrocortisone from a simple carbon source in yeast. *Nat Biotechnol* 21:143–9.

Taguchi, S., S. Komada, and H. Momose. 2000. The complete amino acid substitutions at position 131 that are positively involved in cold adaptation of subtilisin BPN'. *Appl Environ Microbiol* 66:1410–5.

Takagi, H., T. Maeda, I. Ohtsu., Y.C. Tsai, and S. Nakamori. 1996. Restriction of substrate specificity of subtilisin E by introduction of a side chain into a conserved glycine residue. *FEBS Lett* 395:127–32.

Tanaka, Y., and A. Ohmiya. 2008. Seeing is believing: Engineering anthocyanin and carotenoid biosynthetic pathways. *Curr Opin Biotechnol* 19:190–7.

Tao, J., and J.H. Xu. 2009. Biocatalysis in development of green pharmaceutical processes. *Curr Opin Chem Biol* 13:43–50.

Tian, J., K. Ma, and I. Saaem. 2009. Advancing high-throughput gene synthesis technology. *Mol Biosyst* 5:714–22.

Tishkov, V.I. and V.O. Popov. 2006. Protein engineering of formate dehydrogenase. *Biomol Eng* 23:89–110.

Turner, N.J. 2003. Controlling chirality. *Curr Opin Biotechnol* 14:401–6.

Tyo, K.E., P.K. Ajikumar, and G. Stephanopoulos. 2009. Stabilized gene duplication enables long-term selection-free heterologous pathway expression. *Nat Biotechnol* 27:760–5.

Vadali, R.V., G.N. Bennett, and K.Y. San. 2004a. Applicability of CoA/acetyl-CoA manipulation system to enhance isoamyl acetate production in *Escherichia coli*. *Metab Eng* 6:294–9.

Vadali, R.V., G.N. Bennett, and K.Y. San. 2004b. Cofactor engineering of intracellular CoA/acetyl-CoA and its effect on metabolic flux redistribution in *Escherichia coli*. *Metab Eng* 6:133–9.

Vadali, R.V., G.N. Bennett, and K.Y. San. 2004c. Enhanced isoamyl acetate production upon manipulation of the acetyl-CoA node in *Escherichia coli*. *Biotechnol Prog* 20:692–7.

Valentin, H.E.,T.A. Mitsky, D.A. Mahadeo, M. Tran, and K.J. Gruys. 2000. Application of a propionyl coenzyme A synthetase for poly(3-hydroxypropionate-co-3-hydroxybutyrate) accumulation in recombinant *Escherichia coli*. *Appl Environ Microbiol* 66:5253–8.

van der Kamp, M.W., and A.J. Mulholland. 2008. Computational enzymology: Insight into biological catalysts from modelling. *Nat Prod Rep* 25:1001–14.

Veen, M., and C. Lang. 2004. Production of lipid compounds in the yeast *Saccharomyces cerevisiae*. *Appl Microbiol Biotechnol* 63(6):635–46.

Verho, R., J. Londesborough, M. Penttila, and P. Richard. 2003. Engineering redox cofactor regeneration for improved pentose fermentation in *Saccharomyces cerevisiae*. *Appl Environ Microbiol* 69:5892–7.

Veronese, F.M., and A. Mero. 2008. The impact of PEGylation on biological therapies. *BioDrugs* 22:315–29.

Wandrey, C. 2004. Biochemical reaction engineering for redox reactions. *Chem Rec* 4:254–65.

Wang, H.H., F.J. Isaacs, P.A. Carr, Z.Z. Sun, G. Xu, C.R. Forest. and G.M. Church. 2009. Programming cells by multiplex genome engineering and accelerated evolution. *Nature* 460:894–8.

Watanabe, S., T. Kodaki, and K. Makino. 2005. Complete reversal of coenzyme specificity of xylitol dehydrogenase and increase of thermostability by the introduction of structural zinc. *J Biol Chem* 280:10340–9.

Weckbecker, A., H. Groger, and W. Hummel. 2010. Regeneration of nicotinamide coenzymes: Principles and applications for the synthesis of chiral compounds. *Adv Biochem Eng Biotechnol* 120:195–242.

Weckbecker, A., and W. Hummel. 2004. Improved synthesis of chiral alcohols with *Escherichia coli* cells co-expressing pyridine nucleotide transhydrogenase, $NADP^+$-dependent alcohol dehydrogenase and NAD^+-dependent formate dehydrogenase. *Biotechnol Lett* 26:1739–44.

Weiss, B. 2008 Removal of deoxyinosine from the *Escherichia coli* chromosome as studied by oligonucleotide transformation. *DNA Repair (Amst)* 7:205–12.

Wells, J.A., M. Vasser, and D.B. Powers. 1985. Cassette mutagenesis: An efficient method for generation of multiple mutations at defined sites. *Gene* 34:315–23.

Wichmann, R., and D. Vasic-Racki. 2005. Cofactor regeneration at the lab scale. *Adv Biochem Eng Biotechnol* 92:225–60.

Xiong, A.S., R.H. Peng, J. Zhuang, F. Gao, Y. Li, Z.M. Cheng, and Q.H. Yao. 2008. Chemical gene synthesis: Strategies, softwares, error corrections, and applications. *FEMS Microbiol Rev* 32:522–40.

Yamamoto, H., K. Mitsuhashi, N. Kimoto, A. Matsuyama, N. Esaki, and Y. Kobayashi. 2004. A novel NADH-dependent carbonyl reductase from *Kluyveromyces aestuarii* and comparison of NADH-regeneration system for the synthesis of ethyl (S)-4-chloro-3-hydroxybutanoate. *Biosci Biotechnol Biochem* 68:638–49.

Yanai, K., T. Murakami, and M. Bibb. 2006. Amplification of the entire kanamycin biosynthetic gene cluster during empirical strain improvement of *Streptomyces kanamyceticus*. *Proc Natl Acad Sci U S A* 103:9661–6.

Yang, T.H., T.W. Kim, H.O. Kang, S.H. Lee, E.J. Lee, S.C. Lim, S.O. Oh, A.J. Song, S.J. Park, and S.Y. Lee. 2010. Biosynthesis of polylactic acid and its copolymers using evolved propionate CoA transferase and PHA synthase. *Biotechnol Bioeng* 105:150–60.

Yaoi, T., K. Miyazaki, T. Oshima, Y. Komukai, and M. Go. 1996. Conversion of the coenzyme specificity of isocitrate dehydrogenase by module replacement. *J Biochem (Tokyo)* 119:1014–8.

Yoon, S.H., S.H. Lee, A. Das, H.K. Ryu, H.J. Jang, J.Y. Kim, D.K. Oh, J.D. Keasling, and S.W. Kim. 2009. Combinatorial expression of bacterial whole mevalonate pathway for the production of beta-carotene in E. coli. *J Biotechnol* 140:218–26.

Yuan, L.Z., P.E. Rouviere, R.A. Larossa, and W. Suh. 2006. Chromosomal promoter replacement of the isoprenoid pathway for enhancing carotenoid production in *E. coli*. *Metab Eng* 8:79–90.

Zha, W., S.B. Rubin-Pitel, Z. Shao, and H. Zhao. 2009. Improving cellular malonyl-CoA level in *Escherichia coli* via metabolic engineering. *Metab Eng* 11:192–8.

Zhan, J. 2009. Biosynthesis of bacterial aromatic polyketides. *Curr Top Med Chem* 9:1958–610.

Zhang, K., M.R. Sawaya, D.S. Eisenberg, and J.C. Liao. 2008. Expanding metabolism for biosynthesis of nonnatural alcohols. *Proc Natl Acad Sci USA* 105:20653–8.

Zhang, W., K. O'Connor, D.I. Wang, and Z. Li. 2009. Bioreduction with efficient recycling of NADPH by coupled permeabilized microorganisms. *Appl Environ Microbiol* 75:687–94.

Zhao, H., and F.H. Arnold. 1999. Directed evolution converts subtilisin E into a functional equivalent of thermitase. *Protein Eng* 12:47–53.

Zilberman, M., A. Kraitzer, O. Grinberg, and J.J. Elsner. 2010. Drug-eluting medical implants. *Handb Exp Pharmacol* 197:299–341.

This page intentionally left blank

9 Conversion of Renewable Resources to Biofuels and Fine Chemicals: Current Trends and Future Prospects

Aristos A. Aristidou, Namdar Baghaei-Yazdi, Muhammad Javed, and Brian S. Hartley

CONTENTS

"There's enough alcohol in one year's yield of an acre of potatoes to drive the machinery necessary to cultivate the fields for one hundred years."

Henry Ford

9.1 INTRODUCTION

Fermentation microbiology and industrial biotechnology are poised to revolutionize the way we produce our energy and the chemicals needed by other industries. It affords a great opportunity to substitute fossilized organic matter, such as petroleum, with annually renewable organic biomass. This new technology allows the chemical industries to use plant biomass to produce fuels such as biodiesel or bioethanol; polymers such as polylactic acid (PLA); or fine or bulk chemicals such as organic acids, polyols, or esters. The abundance of available plant biomass makes it the only foreseeable sustainable source of organic fuels. Success in this area will have major implications on human society by reducing the world's dependence on oil, thus minimizing carbon dioxide (CO_2) emissions and the climatic changes associated with it.

Bioethanol production (Table 9.1) currently relies predominantly on the utilization of dextrose derived from corn starch (United States) or sucrose from sugar cane (Brazil). However, the relatively high value and increasing demand of these feedstocks for food production is a major manufacturing cost that renders current bioethanol production uncompetitive with gasoline. Consequently, several economic studies have shown that successful fermentation of sugars derived from lignocellulosic wastes is crucial for achieving commercial success.

Lignocellulose represents approximately 80% of what farmers already grow, but it has not yet been used for production of biofuels. Many different biomass feedstocks can be used for the production of fuels and chemicals (Figure 9.1). The chemical composition of agricultural waste varies among species, but biomass consists of approximately 25% lignin and 75% carbohydrate polymers,

TABLE 9.1
World Ethanol Production, 2004

Country	Million Gallons	Country	Million Gallons
Brazil	3,989	Australia	33
United States	3,535	Japan	31
China	964	Pakistan	26
India	462	Sweden	26
France	219	Philippines	22
Russia	198	South Korea	22
South Africa	110	Guatemala	17
United Kingdom	106	Cuba	16
Saudi Arabia	79	Ecuador	12
Spain	79	Mexico	9
Thailand	74	Nicaragua	8
Germany	71	Mauritius	6
Ukraine	66	Zimbabwe	6
Canada	61	Kenya	3
Poland	53	Swaziland	3
Indonesia	44	Others	338
Argentina	42		
Italy	40	**Total**	**10,770**

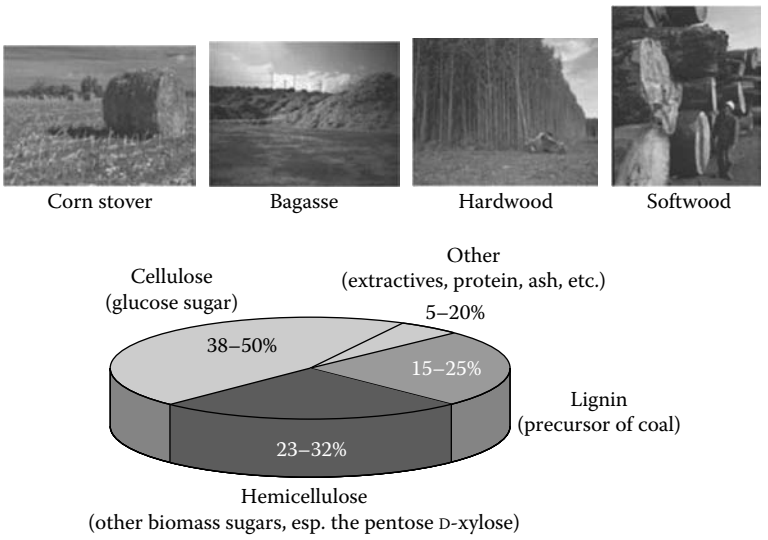

FIGURE 9.1 Examples of lignocellulosic biomass and relative macromolecular composition.

mainly cellulose and hemicellulose (Lerouge et al. 1998). Cellulose is a high-molecular-weight linear glucose polysaccharide, with a degree of polymerization (DP) in the range of 200–2000 kDa (4000–8000 glucose molecules connected with β–1,4 glycosidic bonds). Cellulose is very strong, and its links are broken by common cellulases (Figure 9.2). The cellulases can be divided into two classes: endoglucanases (EG) and cellobiohydrolases (CBH) (Teeri et al. 1998). CBHs hydrolyze the cellulose chain from one end, whereas an EG hydrolyzes randomly along the cellulose chain. On the other hand, hemicellulose (Figure 9.2) is a rather low-molecular-weight heteropolysaccharide (DP < 200, α–1,3 glycosidic links) with a wide variation in structure and composition. In contrast to cellulose, which is crystalline, strong, and resistant to hydrolysis, hemicellulose has a random, amorphous structure that is easily hydrolyzable enzymically or by dilute acid or base (Kuhad et al. 1997). The cellulose fraction of biomass is typically high (25–60%), whereas the hemicellulose fraction is typically low (10–35%). The monomeric composition of lignocellulosic material varies depending on the biomass source (Table 9.2). In general, the carbohydrate fraction is made up primarily of glucose, with small amounts of galactose and pentose moieties. However, the pentoses fraction is rather significant: xylose 5–20% and arabinose 1–5%. Xylose is second only to glucose in natural abundance and it is the most copious sugar in the hemicellulose of hardwoods and crop residues.

The conversion of cellulose and hemicellulose for production of fuel ethanol is being studied extensively with a view to develop a technically and economically viable bioprocess. Ethanol's high octane and high heat of vaporization values make it more efficient than gasoline. Furthermore, ethanol is low in toxicity, volatility, and photochemical reactivity, resulting in reduced ozone emission and smog formation compared with conventional fuels. Researchers at the National Renewable Energy Laboratory (NREL) estimate that the United States potentially could convert 2.45 billion ton of biomass to 270 billion gal of ethanol each year, which is approximately twice the current annual gasoline consumption in the United States. Bioethanol, also used as a hydrogen fuel source for fuel cells, could become a vital part of the long-term solution to climate change.

The important key technologies required for the successful biological conversion of lignocellulosic biomass to ethanol have been extensively reviewed (Lee 1997; Chandrakant and Bisaria 1998; Gong et al. 1999). Microbial conversion of the sugar residues present in wastepaper and yard trash from U.S. landfills alone could provide more than 400 billion: of ethanol (Lynd et al.

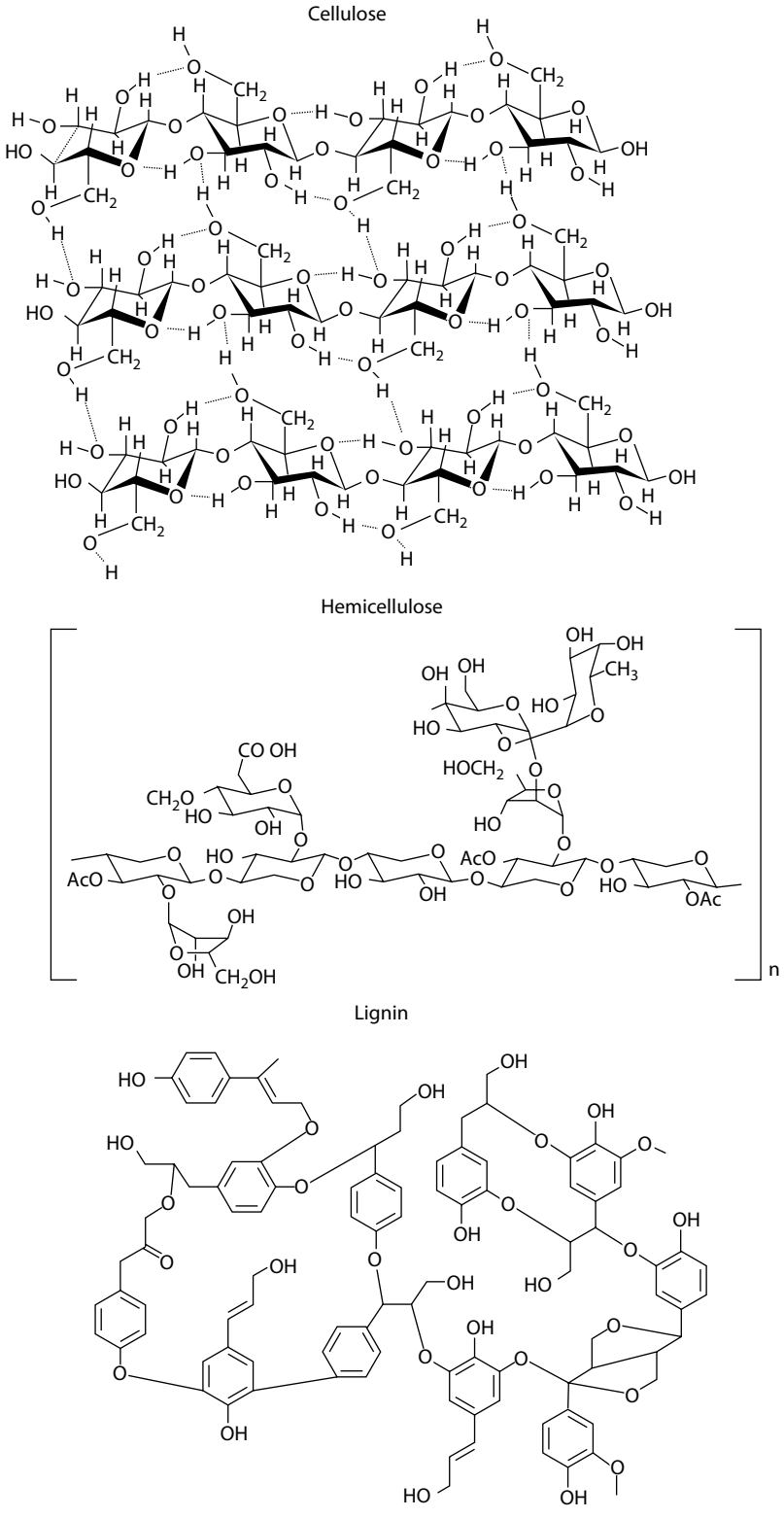

FIGURE 9.2 Lignocellulose structures and utilization.

TABLE 9.2
Composition of Various Biomass Raw Materials

	Corn Stover	Wheat Straw	Rice Straw	Rice Hulls	Baggase Fiber	Newsprint	Cotton Gin Trash	Douglas Fir
Carbohydrate								
Glucose (C6)	39.0	36.6	41.0	36.1	38.1	64.4	20.0	50.0
Mannose (C6)	0.3	0.8	1.8	3.0	—	16.6	2.1	12.0
Galactose (C6)	0.8	2.4	0.4	0.1	1.1	—	0.1	1.3
Xylose (C5)	14.8	19.2	14.8	14.0	23.3	4.6	4.6	3.4
Arabinose (C5)	3.2	2.4	4.5	2.6	2.5	0.5	2.3	1.1
Total C6	40.1	39.8	43.2	39.2	39.2	81	22.2	63.3
Total C5	18	21.6	19.3	16.6	25.8	5.1	6.9	4.5
Noncarbohydrate								
Lignin	15.1	14.5	9.9	19.4	18.4	21.0	17.6	28.3
Ash	4.3	9.6	12.4	20.1	2.8	0.4	14.8	0.2
Protein	4.0	3.0	—	—	3.0	—	3.0	—

Source: Lee, J., *J Biotechnol.,* 56:1–24, 1997. With Permisson

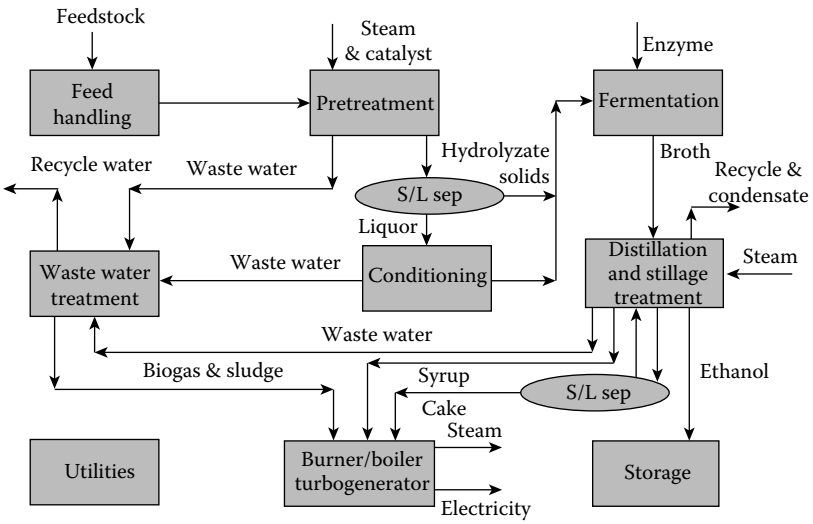

FIGURE 9.3 Conversion of lignocellulose to ethanol. Crystalline cellulose, the largest (50%) and most difficult fraction, is hydrolyzed by a combination of acid and enzymatic processes. After hydrolysis, 95–98% of the xylose and glucose are recovered and, in turn, fermented to alcohol by appropriate microorganisms.

1999), 10 times the corn-derived ethanol burned annually as a 10% blend with gasoline (Keim and Venkatasubramanian 1989).

The biological conversion of lignocellulose to ethanol (Figure 9.3) requires the following steps:

1. Delignification to liberate cellulose and hemicellulose from their complex with lignin,
2. Depolymerization of the carbohydrate polymers (cellulose and hemicellulose) to produce free sugars, and
3. Fermentation of mixed hexose and pentose sugars to produce ethanol.

The development of a delignification process should be possible if lignin-degrading microorganisms, their ecophysiological requirements, and optimal bioreactor design are established. Some thermophilic anaerobes and recently developed recombinant bacteria have advantageous features for direct microbial conversion of cellulose to ethanol. Bioconversion of xylose, the main pentose sugar obtained on hydrolysis of hemicellulose, is essential for the economical production of ethanol; the average cost of biomass amounts is approximately $0.06/kg of sugar.

Applied research in the area of biomass conversion to ethanol in the last 20 years has answered most of the major challenges on the road to commercialization, but, as with any new technology, there is still room for improvement. Over the past decade, the total cost of ethanol has dropped significantly whereas the cost of gasoline has increased substantially to the level that these two are now very comparable (Figure 9.4). Further cost reductions in ethanol production can be accomplished through the use of lignocellulosic raw material, although several technical challenges remain unsolved. As several studies have indicated, efficient utilization of the hemicellulose component of lignocellulosic feedstocks offers an opportunity to reduce the cost of producing fuel ethanol by more than 25% (Hamelinck et al. 2005). The fact that no naturally occurring organism possesses the enzymic machinery required for the fermentation of pentoses and hexoses dictates the need to develop recombinant strains that are capable of fermenting both types of sugars. Two such examples include the introduction of ethanol genes in the bacterium *Escherichia coli* as well as the engineering of pentose-metabolizing pathways in natural ethanol producers such as the yeast *Saccharomyces cerevisiae* or the Gram-positive bacterium *Zymomonas mobilis*. *E. coli* offers several desirable attributes, such as its ability to effectively utilize C6 and C5 carbon sources, fast growth on salt media, and established genetic tools. *S. cerevisiae* and *Z. mobilis*, albeit unable to utilize C5 sugars, are considered to be good ethanol-producing microbes, with the former being one of the primary industrial organisms for ethanol production from C6 sugars.

Genetic improvements in the cultures have been made to enlarge the range of substrate utilization or to specifically channel metabolic intermediates toward ethanol or other desirable products (e.g., organic acids). These contributions represent real significant advancements in the field and have been adequately dealt with from the point of view of their effect on utilization of cellulose and hemicellulose sugars to ethanol. The bioconversion of lignocellulosics to ethanol could be successfully developed and optimized by aggressively applying recent innovations in system biology to solve the key problems in xylose fermentation. The efficient fermentation of xylose and other hemicellulose constituents may prove essential for the development of an economically viable process to produce fuels and chemicals from biomass.

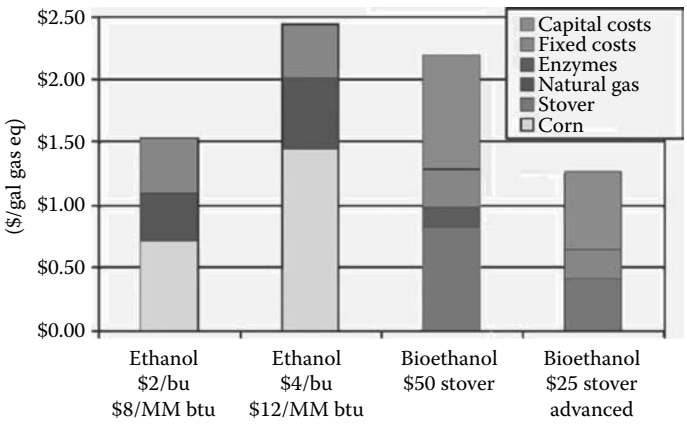

FIGURE 9.4 Comparison of production cost of gasoline versus ethanol derived from lignocellulose.

9.2 PENTOSE FERMENTATION

The ideal organism should be able to ferment all monosaccharides present and withstand potential inhibitors in the hydrolysate. Pentose-fermenting microorganisms are found among bacteria, yeasts, and fungi, with the yeasts *Pichia stipitis*, *Candida shehatae*, and *Pachysolen tannophilus* being the most promising naturally occurring microorganisms. Yeasts produce ethanol efficiently from hexoses by the pyruvate decarboxylase–alcohol dehydrogenase (PDC-ADH) system. However, during xylose fermentation the byproduct xylitol accumulates, thereby reducing the yield of ethanol. Furthermore, yeasts are reported to ferment L-arabinose only very weakly. Only a handful of bacterial species are known that do possess the important PDC-ADH pathway to ethanol. Among these, *Z. mobilis* has the most active PDC-ADH system; however, it is incapable of dissimilating pentose sugars.

In general, microorganisms metabolize xylose to xylulose through two separate routes (Figure 9.5). The one-step pathway catalyzed by xylose isomerase (XI, EC 5.3.1.5) is typical in bacteria, whereas the two-step reaction involving xylose reductase (XR) and xylitol dehydrogenase (XDH) is usually found in yeast. Xylulose is subsequently phosphorylated with xylulokinase (XK) to xylulose-5-phosphate that can be further catabolized via the pentose phosphate pathway and the Embden-Meyerhof-Parnas (EMP) pathway or the Entner–Doudoroff (ED) pathway in organisms such as *Z. mobilis*.

Empowered with the modern tools of genetic engineering and high throughput screening, several groups have been pursuing the construction of yeast or bacterial organisms that can efficiently convert most of the sugars present in biomass derived hydrolysates to useful products. The approaches can be divided in two groups:

1. Engineering organisms with an expanded substrate spectrum
2. Engineering organisms with enhanced abilities of converting key intermediates of central carbon metabolism (e.g., pyruvate) to useful compounds such as ethanol, lactate, or succinate

The first approach has focused on good ethanologenic organisms, such as *S. cerevisiae* or *Z. mobilis*, with the aim of introducing the pathways for xylose or arabinose metabolism. The second approach starts with organisms that have a wide sugar substrate range (C6 and C5), such as *E. coli*, and introduce pathways for converting these sugars to various fermentation products, including ethanol, lactate, acetate, pyruvate, or succinate.

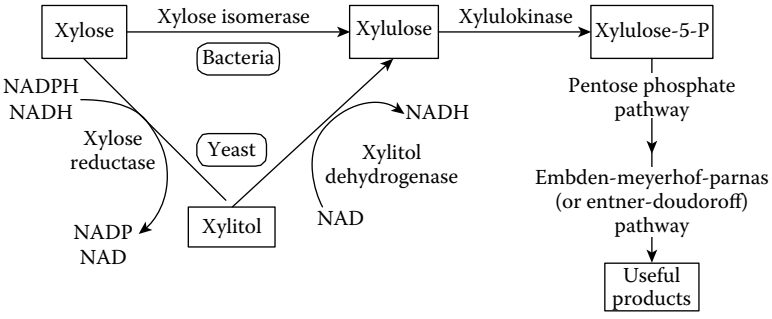

FIGURE 9.5 Xylose utilizing pathways in bacteria and yeast.

9.3 GENETICALLY ENGINEERED BACTERIA

Initial studies were only partially successful in redirecting fermentative metabolism in *Erwinia chrysanthemi* (Tolan and Finn 1987a), *Klebsiella planticola* (Tolan and Finn 1987b), and *E. coli* (Yomano et al. 1998; Ingram et al. 1999a). The first generation of recombinant organisms depended on the overexpression of pyruvate decarboxylase (PDC) activity and the endogenous levels of alcohol dehydrogenase (ADH) activity to couple the further reduction of acetaldehyde to the oxidation of NADH (Figure 9.6). Because ethanol is just one of several fermentation products normally produced by these enteric bacteria, a deficiency in ADH activity together with NADH accumulation contributed to the formation of various unwanted byproducts.

9.3.1 *E. Coli*

Most recent bacteria work in this area has focused on *E. coli*. This is an attractive host organism for the conversion of renewable resources to ethanol and other useful products for several reasons:

- It can grow efficiently on a wide range of carbon substrates that includes five-carbon sugars (has the ability to ferment—in addition to glucose—all other sugar constituents of lignocellulosic material: xylose, mannose, arabinose, and galactose).
- It can sustain high glycolytic fluxes (both aerobically and anaerobically).
- It has a reasonable ethanol tolerance (at least up to 50 g/L).

This was accomplished by assembling the *Z. mobilis* genes coding for PDC and ADH (*pdc* and *adhB*) into an artificial operon to produce a portable genetic element for ethanol production (the so-called PET operon). In the recombinant *E. coli*, overexpression of both enzymes (PDC and ADH) required to divert pyruvate metabolism to ethanol (Figure 9.6) were overexpressed to high levels. The combined effect of high PDC level and high affinity for pyruvate, as judged by its K_m value (Table 9.3), effectively diverts carbon flow to ethanol at the expense of flux through native lactate dehydrogenase (Figure 9.6). When the recombinant strain was grown on a mixture of sugars typically present in hemicellulose hydrolysates, the organism sequentially utilized the sugars in a

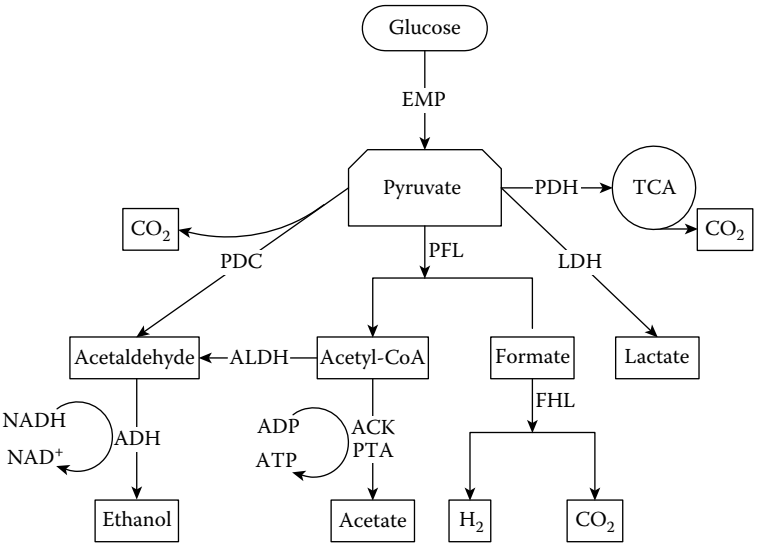

FIGURE 9.6 Competing pathways at the branch point of pyruvate. ACK/PTA, phosphotransacetylase and acetate kinase; FHL, formate hydrogen lyase.

TABLE 9.3
Comparison of Apparent K_m Values for Pyruvate for Selected *E. Coli* and *Z. Mobilis* Pyruvate Acting Enzymes

		K_m	
Organism	**Enzyme**	**Pyruvate**	**NADH**
E. coli	PDH	0.4 mM	0.18 mM
	LDH	7.2 mM	> 0.5 mM
	PFL	2.0 mM	—
	ALDH	—	50 μM
	NADH-OX	—	50 μM
Z. mobilis	PDC	0.4 mM	
	ADH II		12 μM

Note: ALDH, aldehyde dehydrogenase; NADH-OX, NADH oxidase; ADH II, alcohol dehydrogenase II.

strict order—glucose was followed by arabinose and xylose was the last to be utilized—to produce near-maximum theoretical yields of ethanol (Takahashi et al. 1994).

Depending on the prevailing environmental conditions, wild-type *E. coli* metabolizes pyruvate through PDH and pyruvate formate lyase (PFL) ($K_m = 0.4$ and 2.0 mM, respectively; Table 9.3), with main products CO_2 and acetate, the latter formed by the hydrolysis of excess acetyl-CoA. The apparent K_m for the *Z. mobilis* PDC is similar to that of PDH and lower than those of PFL and lactate dehydrogenase (LDH), thereby facilitating acetaldehyde production. NAD^+ regeneration under aerobic conditions primarily results from bisynthesis and from the NADH oxidase coupled to the electron transport system. Again, because the apparent K_m for *Z. mobilis* ADH II is over 4-fold lower than that for *E. coli* NADH oxidase, the heterologous ADH II effectively competes for endogenous pools of NADH, allowing the reduction of acetaldehyde to ethanol. Under anaerobic conditions, wild-type *E. coli* metabolize pyruvate primarily via LDH and PFL. As indicated again in Table 9.3, the apparent K_m values for these two enzymes are 18- and 5-fold higher, respectively, than that for *Z. mobilis* PDC. Furthermore, the apparent K_m values for primary native enzymes involved in NAD^+ regeneration are also considerably higher in *E. coli* than those of *Z. mobilis* ADH. Thus, overexpressed ethanologenic *Z. mobilis* enzymes in *E. coli* can favorably compete with the native enzymes for pyruvate and redox co-substrates channeling pyruvate carbon to ethanol.

The University of Florida was awarded U.S. Patent No. 5,000,000 for the ingenious microbe created at its Institute of Food and Agricultural Sciences. This recombinant strain of *E. coli* was capable of producing significant amounts of ethanol by virtue of harboring the newly constructed PET operon, under both aerobic and anaerobic conditions (Table 9.4). Typical final ethanol concentrations are in excess of 50 g/L, with product yields on sugar approaching a theoretical maximum [i.e. 0.5 g of ethanol/g of sugar (sugar → 2ethanol + $2CO_2$)] (Ohta et al. 1991). Published volumetric and specific ethanol productivities with xylose in simple batch fermentations are 0.6 g of ethanol per liter per hour and 1.3 g of ethanol per gram cell dry weight per hour, respectively. Current sugar conversion to ethanol yields are in the 90–95% range. Elimination of pathways competing for pyruvate (e.g., phosphotransacetylase and acetate kinase or PFL) was one approach to maximize yields. Inactivation of native *E. coli* alcohol-aldehyde dehydrogenase (*adhE*), which uses acetyl-CoA as an electron acceptor, had no beneficial effect on growth, which was consistent with a minor role for this enzyme during ethanol production (Underwood et al. 2002). Further improvements have resulted in volumetric productivities exceeding 2 g of ethanol/L h. It is estimated that this organism can produce ethanol from biomass at a cost of approximately $1.30/gal (Luli and Ingram 2005).

TABLE 9.4
Comparison of Fermentation Products During Aerobic and Anaerobic Growth of Wild-Type and Recombinant *E. Coli*

		Fermentation product (mM)			
Growth	**Plasmid**	**Ethanol**	**Lactate**	**Acetate**	**Succinate**
Aerobic	None	0	0.6	55	0.2
	PLO1308-10 (PET)	337	1.1	17	4.9
Anaerobic	None	0.4	22	7	0.9
	PLO1308-10 (PET)	482	10	1.2	5.0

Source: Ingram, L.O. and Conway. T. *Appl Environ Microbiol*., 54:397–404, 1988. With permission; Lerouge, P. et al. *Plant Molec Biol.,* 38:31–48, 1998.

BC International in Alachua, FL, planned to build a 30-million-gal biomass-to-ethanol plant in Jennings, LA, in 2006, presumably using the genetically engineered *E. coli* as a production organism. BC International holds exclusive rights to use and license the engineering organism. According to the BC International website, they have successfully tested several cellulosic feedstocks (e.g., sugarcane, rice straw, rice hulls, softwood forest thinning, and pulp mill sludge), and waste from the sugarcane industry is believed to be the main plant feedstock for bioethanol production.

It is worth noting that there are various groups working on engineering *E. coli* for the production of fermentation products other than ethanol from biomass. For example, the same group from the University of Florida has engineered *E. coli* for the stereospecific production of D- or L-lactic acid.

The microbial production of L-(+)-lactic acid is rapidly expanding to allow increased production of PLA, a renewable, biodegradable plastic. *E. coli* W3110 has been engineered as a homofermentative producer of L-lactic acid, an alternative to homolactic acid bacteria. Unlike lactic acid bacteria, *E. coli* has the ability to grow and ferment sugars on minimal media, which is a big advantage. This can potentially eliminate the need for complex media components, such as oligopeptides and amino acids that are required by most lactic acid bacteria, hence reducing media and downstream costs. This engineered strain contains five chromosomal deletions (*focA-pflB*, *frdBC*, *adhE*, *ackA*, *ldhA*) and was constructed from a D-(–)-lactic-acid-producing strain, SZ63 (*focA-pflB*, *frdBC*, *adhE*, *ackA*), by replacing part of the chromosomal *ldhA* coding region with *Pediococcus acidilactici ldhL* encoding for L-LDH. The resulting strain produced L-lactic acid in M9 mineral salts medium containing glucose or xylose with a yield of 93–95%, a purity of 98%, and an optical purity greater than 99% (Zhou et al. 2003a).

Along similar lines, a corresponding D-lactic acid *E. coli* strain has also been constructed. D- and L-lactic acid can potentially be combined to generate PLA stereocomplexes with unique and desirable physical properties. These strains (SZ40, SZ58, and SZ63) require only mineral salts as nutrients and lack all plasmids and antibiotic resistance genes used during construction. Competing pathways were eliminated by chromosomal inactivation of genes encoding fumarate reductase (*frdABCD*), alcohol/aldehyde dehydrogenase (*adhE*), and PFL (*pflB*). D-Lactic acid production yield by these new strains approached the theoretical maximum of 2 moles/mole glucose. As above, the chemical purity of this D-lactic acid was close to 98% with respect to soluble organic compounds, and the optical purity exceeded 99%. Deleting the acetate kinase gene (*ackA*) further improved the cell yield and lactate productivity (Zhou et al. 2003a).

E. coli TC44, a derivative of W3110, was engineered for the production of pyruvate from glucose by combining the genetic changes Δ*atpFH,* Δ*adhE,* Δ*sucA*, which were aimed at minimizing ATP yield, cell growth, and respiration. This was combined with gene deletions to eliminate acetate production—*poxB::FRT* Δ*ackA*—and other byproducts—Δ*focA-pflB,* Δ*frdBC,* Δ*ldhA,* Δ*adhE*. In mineral salts glucose medium, strain TC44 converted glucose to pyruvate with a yield of 0.75 g of

pyruvate per gram of glucose (77.9% of theoretical yield) at a rate of 1.2 g of pyruvate/L per hour, and a maximum pyruvate titer of approximately 0.75 M. According to the authors, the efficiency of pyruvate production by strain TC44 is equal to or better than previously reported figures for other biocatalysts including yeast or bacteria (Causey et al. 2004).

Early attempts to engineer a succinate-overproducing *E. coli* involved the deletion of PFL and LDH. Such an organism can accumulate high amounts of succinate under anaerobic conditions (Vemuri et al. 2002). Recently, new genetic engineering approaches have been applied with an aim of generating strains that can produce succinate under aerobic conditions. Aerobic production offers the advantages over anaerobic fermentation in terms of faster biomass generation, carbon throughput, and product formation, albeit it introduces a significant capital and operating cost. Genetic manipulations were performed on two aerobic succinate-producing systems to increase their succinate yield and productivity. One of the aerobic succinate production systems includes five gene deletions—Δ*sdhAB,* Δ*icd,* Δ*iclR,* Δ*poxB*, and Δ *(ackA-pta)*—resulting in a strain with a highly active glyoxylate cycle. A second variation of the above includes four of the five above mutations—Δ*sdhAB,* Δ*iclR,* Δ*poxB*, and Δ *(ackA-pta)*—having two routes for succinate production. One is the glyoxylate cycle and the other is the oxidative branch of the TCA cycle. Furthermore, inactivation of *ptsG* and overexpression of a mutant sorghum *pepc* in these two production systems resulted in strains having succinate yield of 1.0 mol/mol glucose (close to maximum theoretical). Furthermore, the two-route production system with *ptsG* inactivation and *pepc* overexpression demonstrated substantially higher succinate productivity than the previous system (Lin et al. 2005).

9.3.2 *Klebsiella Oxytoca*

In the early 1990s, the control of expression of the *pdc* and *adh* genes in *Z. mobilis* and *Klebsiella oxytoca* was investigated (Ohta et al. 1991). The wild-type organism has the capability to transport and metabolize cellobiose, thus minimizing the need for extracellular additions of cellobiase. In *Klebsiella* strains, two additional fermentation pathways are present compared with *E. coli* that convert pyruvate to succinate and butanediol. As in the case of *E. coli*, it was possible to divert more than 90% of the carbon flow from sugar catabolism away from the native fermentative pathways and toward ethanol (strain P2). Overexpression of recombinant PDC alone produced only about twice the ethanol level of the parental strain. However, when PDC and ADH were elevated in *K. oxytoca* M5A1, ethanol production was very rapid and efficient: volumetric productivities more than 2.0 g/L per hour, yields 0.5 g of ethanol per gram of sugar, and final ethanol of 45 g/L for glucose and xylose carbon sources were obtained.

The development of methods to reduce costs associated with the solubilization of cellulose is essential for the utilization of lignocellulose as a renewable feedstock for fuels and chemicals. One promising approach is the genetic engineering of ethanol-producing microorganisms that also produce cellulase enzymes during fermentation. Recent efforts with this organism focused on enabling cellulose conversion to ethanol without addition of expensive cellulase enzymes. A derivative of *K. oxytoca* M5A1-containing chromosomally integrated genes for ethanol production from *Z.mobilis* (*pdc*, *adhB*) and EG genes from *E. chrysanthemi* (*celY*, *celZ*) produced over 20,000 U EG l-1 activity during fermentation. Because this organism has the native ability to metabolize cellobiose and cellotriose, this strain was able to ferment amorphous cellulose to ethanol without externally added cellulases with an efficiency of 58–76% of the theoretical yield (Zhou and Ingram 2001).

9.3.3 *Z. Mobilis*

Xylose also could be a useful carbon source for the ethanol producer *Z. mobilis*. This is a bacterium that has been used as a natural fermentative agent in alcoholic beverage production and has been shown to have ethanol productivity superior to that of yeast. Overall, it demonstrates many of the desirable traits sought in an ideal biocatalyst for ethanol, such as high ethanol yield, selectivity and

specific productivity, as well as low pH and high ethanol tolerance. In glucose medium, *Z. mobilis* can achieve ethanol levels of at least 12% (w/v) at yields of up to 97% of the theoretical value. When compared with yeast, *Z. mobilis* exhibits 5–10% higher yields and up to 5-fold greater volumetric productivities. The notably high yield of this microbe is attributed to reduced biomass formation during fermentation, apparently limited by ATP availability.

As a matter of fact, *Zymomonas* is the only genus identified to date that exclusively utilizes the ED pathway anaerobically. The stoichiometry of ethanol production in this recombinant organism can be summarized as follows [neglecting the NAD(P)H balances]:

$$3\ \text{Xylose} + 3\ \text{ADP} + 3\ \text{P}_\text{i} \rightarrow 5\ \text{Ethanol} + 5\ \text{CO}_2 + 3\ \text{ATP} + 3\ \text{H}_2\text{O} \tag{9.1}$$

Thus, the theoretical yield on ethanol is 0.51 g of ethanol/g of xylose (1.67 mol mol^{-1}). It is important to note that the metabolically engineered pathway yields only 1 mol of ATP from 1 mol of xylose, compared with the 5/3 moles typically produced through a combination of the pentose phosphate and EMP pathways. When converting glucose to ethanol, this organism produces only 1 mol of ATP per mole of glucose through the ED pathway compared with 2 moles produced via the more common EMP pathway. The energy limitation is expected to result in a lower biomass formation, and thus a more efficient conversion of substrate to product.

Furthermore, glucose can readily cross the cell membrane of this organism by facilitated diffusion, efficiently be converted to ethanol by an overactive PDC-ADH system, and is a generally recognized as a safe (GRAS) organism for use as an animal feed. As discussed earlier, the main drawback of this microorganism is that it can only utilize glucose, fructose, and sucrose and thus is unable to ferment the widely available pentose sugars.

This led Zhang and his coworkers. to attempt to introduce a pathway for pentose metabolism into *Z. mobilis* (Zhang et al. 1995). Early attempts by other groups using the xylose isomerase (*xylA*) and XK (*xylB*) genes (Figure 9.7) from either *Klebsiella* or *Xanthomonas* were met with limited success, despite the functional expression of these genes in *Z. mobilis*. It soon became evident that such failures were due to the absence of detectable transketolase and transaldolase activities in *Z. mobilis*, which are necessary to complete a functional pentose metabolic pathway (Figure 9.8). After the transketolase *E. coli* gene was cloned and introduced in *Z. mobilis*, a small conversion of xylose to CO_2 and ethanol occurred (Feldmann et al. 1992). The next step was to introduce the transaldolase reaction because this strain intracellularly accumulated significant amounts of sedoheptulose-7-phosphate. Therefore, sophisticated cloning techniques were applied for the construction of a chimeric shuttle vector (pZB5) that carries two independent operons: the first encoding the *E. coli xylA* and *xylB* genes and the second expressing transketolase (*tktA*) and transaldolase (*tal*) again from *E. coli*. The two operons that included the four xylose assimilation and nonoxidative pentose phosphate pathway genes were expressed successfully in *Z. mobilis* CP4. The recombinant strain was capable of fast growth on xylose as the sole carbon source, and moreover it efficiently converted glucose and xylose to ethanol with 86 and 94% of the theoretical yield from xylose and glucose, respectively.

In a subsequent article, the same laboratory reported the construction of a *Z. mobilis* strain with a yet expanded substrate fermentation range to include the pentose sugar, L-arabinose, which is commonly found in agricultural residues and other lignocellulosic biomass (Deanda et al. 1996). Five genes encoding L-arabinose isomerase (*araA*), L-ribulokinase (*araB*), L-ribulose-5-phosphate-4-epimerase (*araD*), transaldolase (*talB*), and transketolase (*tktA*) were isolated from *E. coli* and introduced into *Z. mobilis* under the control of constitutive promoters. The engineered strain grew on and produced ethanol from L-arabinose as a sole carbon source at 98% of the maximum theoretical ethanol yield, indicating that arabinose was metabolized almost exclusively to ethanol as the sole fermentation product. The authors indicate that this microorganism may be useful, along with the previously developed xylose-fermenting *Z. mobilis* (Zhang et al. 1995), in a mixed culture for efficient fermentation of the predominant hexose and pentose sugars in agricultural residues and other lignocellulosic feedstocks to ethanol.

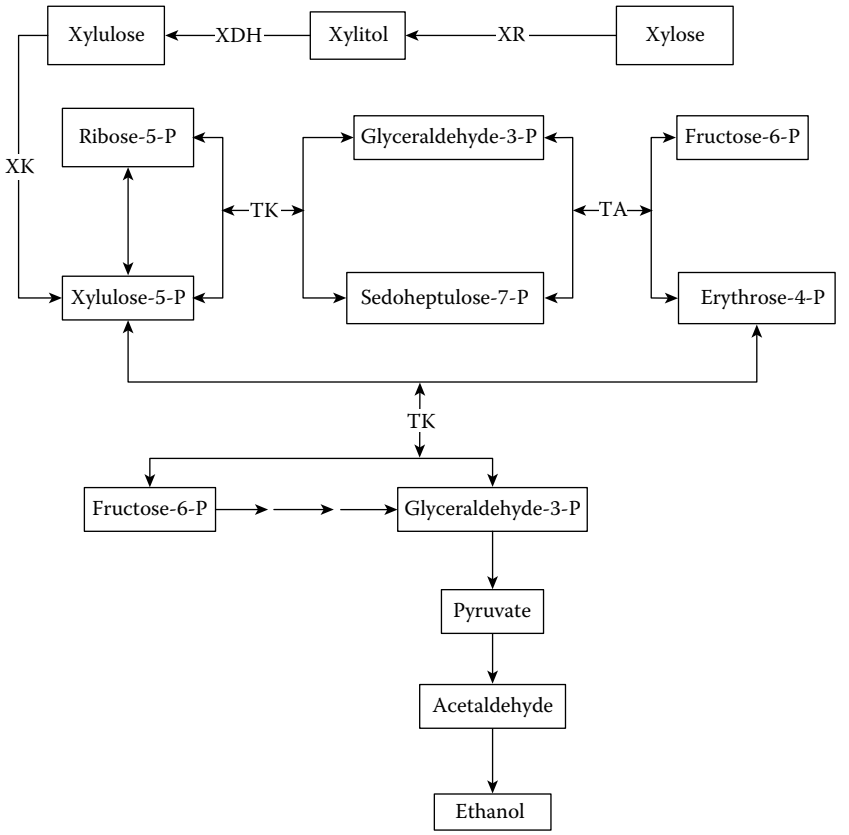

FIGURE 9.7 Ethanol production from pentose sugars in metabolically engineered *Z. mobilis.* TK, transketolase; TA, transaldolase.

Iogen Corporation of Ottawa, Canada, has recently built a 50 t/day biomass-to-ethanol production plant adjacent to its enzyme production facility. Iogen, in collaboration with the University of Toronto, has recently tested the C6/C5 cofermentation performance characteristics of the NREL's metabolically engineered *Z. mobilis* using Iogen's biomass hydrolysates (Lawford et al. 2001). In this study, the biomass feedstock was an agricultural waste, namely oat hulls, which was hydrolyzed in a proprietary two-stage process involving pretreatment with dilute sulfuric acid at 200–250°C, followed by cellulase hydrolysis. The oat hull hydrolysate (OHH) contained glucose, xylose, and arabinose in a mass ratio of approximately 8:3:0.5. This work examined the growth and fermentation performance of xylose-utilizing recombinant *Z. mobilis* cultures CP4:pZB5, and a hardwood prehydrolysate-adapted variant of 39676:pZB4L. In pH-stat batch fermentations with unconditioned 6% (w/v) glucose, 3% xylose, and 0.75% acetic acid, ZM4:pZB5 gave the best performance with a fermentation time of 30 h with a volumetric productivity of 1.4 g/L h. On the basis of the available glucose and xylose, the process ethanol yield for both strains was 0.47 g/g (92% maximum theoretical). Acetic acid tolerance appeared to be a major determining factor in successful cofermentation.

9.4 GENETICALLY ENGINEERED YEAST

Yeasts produce ethanol efficiently from hexoses by the PDC-ADH system. The most commonly used ethanol producer, *S. cerevisiae*, has the intrinsic limitation of not being able to ferment pentoses such as xylose or arabinose. Although certain types of yeast such as *P. tannophilus*, *P. stipitis,* or

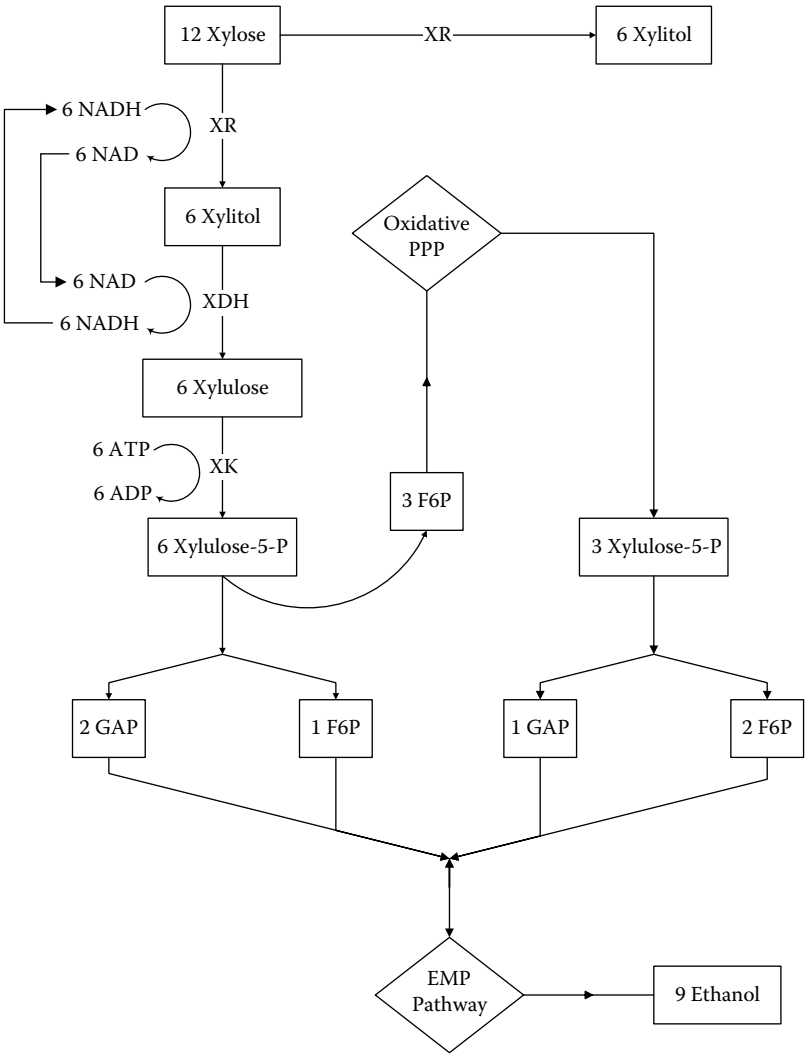

FIGURE 9.8 Anaerobic xylose utilization and cofactor regeneration in recombinant *S. cerevisiae*. ppp, pentose.

C. shehatae are xylose-fermenting yeasts, they have poor ethanol yields on pentoses (Bruinenberg et al. 1984) and low ethanol tolerance compared with the common glucose-fermenting yeasts such as *S. cerevisiae*.

9.4.1 *S. Cerevisiae*

Saccharomyces spp. are the safest and most effective microorganisms for fermenting sugars to ethanol and traditionally have been used in industry to ferment glucose (or hexose sugar)-based agricultural products to ethanol. Cellulosic biomass, which includes agriculture residues, paper wastes, wood chips, etc., is an ideal inexpensive, renewable, abundantly available source of sugars for fermentation to ethanol, particularly ethanol used as a liquid fuel for transportation. However, *Saccharomyces* spp. are not suitable for fermenting sugars derived from cellulosic biomass because *Saccharomyces* spp., including *S. cerevisiae*, are not able to ferment xylose to ethanol or to use this pentose sugar for aerobic growth. Although *Saccharomyces* spp. are not able to metabolize xylose aerobically and anaerobically, there are other yeasts, such as *P. stipitis* and *C. shehatae*, that are

able to ferment xylose to ethanol and to use xylose for aerobic growth. However, these naturally occurring xylose-fermenting yeasts are not effective fermentative microorganisms, and they have a relatively low ethanol tolerance.

Many attempts to introduce the one-step pathway by cloning the gene coding for xylose isomerase from *E. coli* or *Bacillus subtilis* in *S. cerevisiae* were unsuccessful because of the inactivity of the heterologous protein in the recombinant host cell (Sarthy et al. 1987). Subsequently, the *Thermus thermophilus xylA* gene encoding xylose (or glucose) isomerase was cloned and expressed in *S. cerevisiae* under the control of the yeast *PGK1* promoter (Walfridsson et al. 1996). The recombinant xylose isomerase showed the highest activity at 85°C with a specific activity of 1.0 U/mg protein. This study also demonstrated a new functional, yet low-throughput, metabolic pathway in *S. cerevisiae* with ethanol formation during oxygen-limited xylose fermentation.

In most yeasts and fungi, XR and XDH are dependent on NADPH and NAD, respectively (Figure 9.8). However, examples of yeast XRs exist that have dual coenzyme specificity (i.e., NADPH and NADH), such as those from *P. stipitis* and *C. shehatae*. Such a type of enzyme has the advantage of preventing imbalances of the NAD/NADH redox system, especially under oxygen-limiting conditions (Granstrom et al. 2000).

The first step in yeast xylose metabolism is carried out by xylose (aldose) reductase. The gene coding for this enzyme has been given the designation *XYL1*. In most yeasts and fungi, this enzyme has cofactor specificity for NADPH, but in *P. stipitis*, the enzyme shows 70% as much activity with NADH as with NADPH (Verduyn et al. 1985). The *P. stipitis XYL1* gene has been cloned independently by at least three groups (Amore et al. 1991; Hallborn et al. 1991; Takuma et al. 1991). Several XR genes from various organisms have since been cloned, including those from *Kluyveromyces lactis* (Billard et al. 1995), *P. tannophilus* (Bolen et al. 1996), and even *S. cerevisiae* (Toivari et al. 2004). However, the relative affinity of various XRs for NADH and NADPH vary widely. For the most part, this enzyme has a preference for NADPH. One notable exception is the XR enzyme from *Candida boidinii* that was reported to have a higher activity with NADH than with NADPH (Vandeska et al. 1995).

The second step in xylose metabolism is coded for by XDH (*XYL2*), which, unlike XR, is almost always specific for NAD. Attempts have been made to modify the XR cofactor specificity (Metzger and Hollenberg 1995; Leitgeb et al. 2005). The mutation D207→G and the double mutation D207→G and D210→G within the binding domain (GXGXXG) increased the apparent K_m for NAD 9-fold and decreased the XDH activity to 47 and 35%, respectively, as compared with the unaltered enzyme. The introduction of the potential NADP-recognition sequence (GSRPVC) of the ADH from *Thermoanaerobium brockii* into the XDH allowed the mutant enzyme to use NAD and NADP as a cofactor with equal apparent K_m values. The mutagenized *XYL2* gene could still mediate growth of *S. cerevisiae* transformants on xylose minimal-medium plates when expressed together with the *XYL1*. More recently, the gene coding for a *S. cerevisiae* XDH enzyme was also discovered (Aristidou et al. 2000; Toivari et al. 2004).

Several laboratories have attempted to engineer a xylose-fermenting *S. cerevisiae* through the expression of *XYL1* or both *XYL1* and *XYL2*. Expression of *XYL1* alone has not proven sufficient to enable *S. cerevisiae* to ferment or even to grow on xylose, but in the presence of glucose, *S.cerevisiae* strains expressing *XYL1* will produce primarily xylitol from xylose (Hallborn et al. 1991; Meinander et al. 1994). Production of xylitol appears to be a consequence of redox imbalance in the cell and is affected by glycerol production (Meinander et al. 1996).

Expression of *XYL1* and *XYL2* has proven to be more successful, enabling *S. cerevisiae* to grow aerobically on xylose and accumulate low levels of ethanol. Kotter and Ciriacy studied the xylose fermentation in *S. cerevisiae* more extensively and compared the fermentative activities to *P.stipitis* (Amore et al. 1991). In the absence of respiration, *S. cerevisiae* transformed with *XYL1* and *XYL2* converts approximately half of the xylose present in the medium into xylitol and ethanol in roughly equimolar amounts. By comparison, *P. stipitis* produces only ethanol. They proposed, as had Hahn-Hägerdal et al., that in *S. cerevisiae*, ethanol production is limited by cofactor imbalance.

Additional limitations of xylose utilization in *S. cerevisiae* were also attributed to the inefficient capacity of the nonoxidative pentose phosphate pathway, as indicated by the accumulation of sedoheptulose-7-phosphate (Senac and Hahn-Hägerdal 1989; Senac and Hahn-Hägerdal 1991).

Tantirungkij et al. (1993) took the approach one step further by subcloning *Pichia stipitis XYL1* into *Saccharomyces cerevisiae* under the control of the enolase promoter on a multicopy vector. This achieved 2–3 times the level of *XYL1* expression as was observed in *P. stipitis*. *XYL2* was also cloned and co-expressed in *S. cerevisiae* at approximately twice the level achieved in induced *P. stipitis*. Despite these higher levels of expression, only low levels of ethanol (~5 g/L) were observed under optimal conditions after 100 h. These researchers also selected mutants of *S. cerevisiae* carrying *XYL1* and *XYL2* that exhibited rapid growth on xylose medium (Tantirungkij et al. 1994). The fastest growing strain showed a lower activity of XR but a higher ratio of XDH to XR activity. Southern hybridization showed that the vector carrying the two genes had integrated into the genome resulting in increased stability of the cloned genes. The yield and production rate of ethanol increased 1.6- and 2.7-fold, respectively, but the maximum concentration of ethanol reported was only 7 g/L after 144 hour.

The effect of the relative levels of expression of the *XYL1* and *XYL2* genes from *P. stipitis* in *Saccharomyces cerevisiae* has also been investigated (Walfridsson et al. 1997). These two genes were placed in different directions under the control of the ADH I (*ADHI*) and phosphoglycerate kinase (*PGK*) promoters and inserted into the *E. coli*–yeast shuttle plasmid YEp24. Different recombinant *S. cerevisiae* strains were constructed with different specific activities of XR and XDH. The highest XR or XDH activities were obtained when the expressed gene was controlled by the *PGK* promoter and located downstream after the *ADHI* promoter gene-terminator sequence. The XR/XDH ratio (i.e., the ratio of specific enzyme activities of XR and XDH) in these recombinant *S. cerevisiae* strains varied from 0.06 to 17.5. To enhance xylose utilization, in the *XYL1*- and *XYL2*-containing *S. cerevisiae* strains, the native *TKL1* gene encoding transketolase and the *TALI* gene encoding transaldolase were also overexpressed, which showed considerably good growth on the xylose plate. Fermentation of the recombinant *S. cerevisiae* strains containing *XYL1*, *XYL2*, *TKL1*, and *TAL1* were studied with mixtures of glucose and xylose. A strain with an XR:XDH ratio of 17.5 formed 0.82 g xylitol/g consumed xylose, whereas a strain with an XR:XDH ratio of 5.0 formed 0.58 g xylitol/g xylose. On the other hand, the strain with an XR:XDH ratio of 0.06 formed no xylitol and less glycerol and acetic acid compared with strains with the higher XR:XDH ratios. In addition, the strain with an XR:XDH ratio of 0.06 produced more ethanol than the other strains.

Ho and Chang (1989) have reported the construction of a recombinant *Saccharomyces* strain expressing the genes for the three xylose metabolizing enzymes: the XR and XDH genes from *P. stipitis* and XK from *S. cerevisiae*. Cloning of the *XYL3* gene from *P. tannophilus was* first reported in 1987 (Stevis et al. 1987). Cloning of *S. cerevisiae XYL3* by complementation of a XK-deficient mutant of *E. coli* was first reported in 1988 (Rodriguez-Peña et al. 1998), and its role in xylose utilization by *S. cerevisiae* was established soon thereafter (Ho et al. 1998). Ho's group developed recombinant plasmids that can transform *Saccharomyces* spp. into xylose-fermenting yeasts. These plasmids, designated pLNH31, –32, –33, and –34, are 2-μm-based high-copy-number yeast-*E. coli* shuttle plasmids. In addition to the geneticin resistance and ampicillin resistance genes that serve as dominant selectable markers, these plasmids also contain three xylose-metabolizing genes: the *P. stipitis* genes for XR (*PsXYL1*) and XDH (*PsXYL2*) and the *S. cerevisiae* gene for XK (*XYL3*). The parental yeast strain *Saccharomyces* 1400 is a fusion product of *Saccharomyces diastaticus* and *Saccharomyces uvarum*. It exhibits high ethanol and temperature tolerance and a high fermentation rate. Overexpression of *XYL3* in the *Saccharomyces* 1400 fusant along with *XYL1* and *XYL2* results in production of approximately 47 g/L of ethanol in 84% of theoretical yield from a 1:1 glucose/xylose mixture (Ho et al. 1998).

Researchers at the Finnish Technical Research Institute (VTT) have addressed the redox imbalance of the XR and XDH reactions by introducing artificial transhydrogenase cycles in

xylose-utilizing *S. cerevisiae* (Aristidou et al. 1999). This work was based on the simultaneous expression of dehydrogenase enzymes having different cofactor specificities (e.g., the yeast glutamate dehydrogenase 1 and 2—*GDH1*, *GDH2*) and in combination with enzymes that can be driven by ATP (e.g., the malic enzyme), thus overcoming intrinsic limitations due to the physiological redox cofactor concentrations. Results from such genetically engineered organisms so far have been encouraging in terms of improving xylose utilization rates and ethanol productivities.

9.4.2 *P. Stipitis*

This organism has also received significant attention in the past few years in terms of developing and applying genetic engineering techniques to address metabolic imperfections, such as the oxygen requirements for efficient xylose utilization. Respiratory and fermentative pathways coexist to support growth and product formation in *P. stipitis*. This yeast grows rapidly without ethanol production under fully aerobic conditions, and it ferments glucose or xylose under oxygen-limited conditions, but it stops growing within one generation under anaerobic conditions.

Expression of *S. cerevisiae URA1* (*ScURA1*) in *P. stipitis* enabled rapid anaerobic growth in minimal defined medium containing glucose when essential lipids were present. *ScURA1* encodes a dehydrogenase that utilizes fumarate as an alternative electron acceptor to confer anaerobic growth. Initial *P. stipitis* transformants grew and produced 32 g/L ethanol from 78 g/L glucose. Cells produced even more ethanol faster after two anaerobic serial subcultures. Control strains without *ScURA1* were incapable of growing anaerobically and showed only limited fermentation. *P. stipitis* cells bearing *ScURA1* were viable in anaerobic xylose medium for long periods, and supplemental glucose allowed cell growth, but xylose alone could not support anaerobic growth even after serial anaerobic subculturing. These data imply that *P.stipitis* can grow anaerobically using metabolic energy generated through fermentation, but that it exhibits fundamental differences in cofactor selection and electron transport with glucose and xylose metabolism. This is the first report of genetic engineering to enable anaerobic growth of a eukaryote.

The *P. stipitis* XR gene (*XYL1*) was inserted into an autonomous plasmid that *P. stipitis* maintains in multicopy (Dahn et al. 1996). The plasmid pXOR with the *XYL1* insert or a control plasmid pJM6 without *XYL1* was introduced into *P. stipitis*. When grown on xylose under aerobic conditions, the strain with pXOR had up to 1.8-fold higher xylose reductase (XR) activity than the control strain. Oxygen limitation led to higher XOR activity in experimental and control strains grown on xylose. However, the XOR activities of the two strains grown on xylose were similar under oxygen limitation. When grown on glucose under aerobic or oxygen-limited conditions, the experimental strain had XOR activity up to 10 times higher than that of the control strain. Ethanol production was not improved, but rather it decreased with the introduction of pXOR compared with the control, and this was attributed to nonspecific effects of the plasmid.

Jeffries's group also studied the expression of the genes encoding group I ADHs (*PsADH1* and *PsADH2*) in the xylose-fermenting yeast *P. stipitis* CBS 6054. The cells expressed PsADH1 approximately 10 times higher under oxygen-limited conditions than under fully aerobic conditions when cultivated on xylose. Transcripts of PsADH2 were not detectable under either aeration condition. The *PsADH1::lacZ* fusion was used to monitor *PsADH1* expression and it was found that expression increased as oxygen decreased. The level of *PsADH1* transcript was repressed approximately 10-fold in cells grown in the presence of heme under oxygen-limited conditions. Concomitantly with the induction of PsADH1, PsCYC1 expression was repressed. These results indicate that oxygen availability regulates *PsADH1* expression and that regulation may be mediated by heme. The regulation of *PsADH2* expression was also examined in other genetic backgrounds. Disruption of *PsADH1* dramatically increased *PsADH2* expression on nonfermentable carbon sources under fully aerobic conditions, indicating that the expression of *PsADH2* is subject to feedback regulation under these conditions.

9.4.3 *Pichia Pastoris*

A XR gene (*xyl1*) of *Candida guilliermondii* ATCC 20118 was cloned and characterized. The derived amino acid sequence of *C. guilliermondii* XR was 70.4% homologous to that of *P. stipitis*. The gene was placed under the control of an alcohol oxidase promoter (*AOX1*) and integrated into the genome of the methylotrophic yeast *Pichia pastoris*. Methanol induced the expression of the XR and the expressed enzyme preferentially utilized NADPH as a cofactor. The authors speculated that the different cofactor specificity between *P. pastoris* and *C. guilliermondii* XRs might be due to the difference in the numbers of histidine residues and their locations between the two proteins. The recombinant was able to ferment xylose, and the maximum xylitol accumulation (7.8 g/L) was observed when the organism was grown under aerobic conditions.

9.4.4 Fungal Xylose Isomerase in Yeast

Recently, a significant breakthrough in xylose conversion to ethanol or other fermentation products by yeast came about as a result of completely independent and parallel efforts at NatureWorks LLC (Minneapolis, MN) and Delft Technical University in the Netherlands. All previous efforts to overexpress xylose isomerase (XI) in yeast focused on bacterial XI genes, and their success was limited. However, none of these bacterial XIs resulted in ethanol titers, rates, or yields that could be considered as commercially relevant. The most notable of these attempts was the overexpression of the original or mutated XI gene from *T. thermophilus* (Walfridsson et al. 1996).

This breakthrough came about as a result of identifying the first fungal XI gene, which was isolated from the anaerobic fungus *Piromyces sp.* strain E2 (Xarhangi et al. 2003). This organism metabolizes xylose via XI and D-XK as was shown by enzymatic and molecular analyses; this resembles the situation in bacteria. An early attempt to introduce the *Piromyces sp.* E2 XI gene into *S. cerevisiae* resulted in good XI activity. However, slow growth on xylose did not result in reported ethanol production (Kuyper et al. 2003). It was subsequently reported that expression of this particular gene in yeast, including *S. cerevisiae* (Kuyper et al. 2004, 2005a, 2005b) and nonconventional yeast such as *Kluyveromyces sp.* or *Candida sp.* (Rajgarhia et al. 2004), in conjunction with other targeted-or-not genetic changes of the xylose pathway resulted in engineered yeast able to convert xylose to ethanol at high rates and yields. Since the isolation of the *Piromyces* XI gene, additional homologous genes have also been isolated from other anaerobic fungi (e.g., *Cyllamyces aberensis*) and successfully expressed in yeast (Rajgarhia et al. 2004). Interestingly, XI isolated from such anaerobic yeasts turned out to be very homologous to the XI gene of the anaerobic Gram-positive bacterium *Bacteroides thetaiotaomicron*, which is a dominant member of human distal intestinal microbiota.

On the basis of public literature, a Saccharomyces strain expressing the *Piromyces* XI together with some additional genetic modifications of the xylose pathway was reported to have good anaerobic growth and fermentation on xylose. In addition to XI, the overexpressed enzymes were XK, ribulose 5-phosphate isomerase, ribulose 5-phosphate epimerase, transketolase, and transaldolase. Furthermore, the GRE3 gene encoding aldose reductase was deleted to further minimize xylitol production. During growth on xylose, xylulose formation was absent and xylitol production was negligible. The specific xylose consumption rate in anaerobic xylose cultures was 1.1 g xylose per gram biomass per hour (Kuyper et al. 2005a). Further improvements were achieved through evolutionary engineering in xylose-limited chemostats followed by selection in anaerobic cultivation in automated sequencing-batch reactors on glucose-xylose mixtures. A final single-strain isolate, RWB 218, rapidly consumed glucose-xylose mixtures anaerobically, in synthetic medium, with a specific rate of xylose consumption exceeding 0.9 g/g h and a corresponding ethanol specific productivity of approximately 0.5 g/g h. When the kinetics of zero trans-influx of glucose and xylose of RWB 218 were compared with that of the initial strain, a 2-fold higher capacity (V_{max}) and an improved K_m for xylose was apparent in the selected strain (Kuyper et al. 2005b).

When put in perspective, the above is quite an accomplishment given that up until 2003 the maximum corresponding ethanol rate in other xylose-engineered yeast had been less than 0.1–0.15 g/g h. This could potentially be the breakthrough necessary for the effective conversion of biomass sugars, in sugar hydrolysates, to useful products such as ethanol or organic acids. Nevertheless, a tremendous amount of further technological development will be necessary before having a technology that can be industrially implemented, and this includes aspects such as enhancing tolerance to hydrolysate inhibitors, genetic stability (especially in continuous processes), and ability to utilize all sugars present in hydrolysates that includes not only glucose and xylose, but also mannose, galactose, and arabinose.

9.5 MICROBES PRODUCING ETHANOL FROM LIGNOCELLULOSE

It would be desirable if microbes producing ethanol from lignocellulose also had means to depolymerize cellulose, hemicellulose, and associated carbohydrates. Many plant pathogenic bacteria (soft-rot bacteria), such as *Erwinia carotovora* and *E. chrysanthemi*, have evolved sophisticated systems of hydrolases and lyases that aid the solubilization of lignocellulose and allow them to break up and penetrate plant tissue (Brencic and Winans 2005). Genetic engineering of these bacteria for ethanol production represents an attractive alternative to the solubilization of lignocellulosic biomass by chemical or enzymatic means. *E. carotovora* SR38 and *E. chrysanthemi* EC16 were genetically engineered with the PET operon and shown to produce ethanol and CO_2 efficiently as primary fermentation products from cellobiose and glucose (Beall and Ingram 1993). Both ethanologenic *Erwinia* strains produced approximately 50 g/L ethanol from 100 g/L cellobiose in less than 48 h with a maximum volumetric productivity of 1.5 g/L of ethanol per hour. This rate is over twice that reported for the cellobiose-utilizing yeast, *Brettanomyces custersii,* in batch culture.

Along similar lines, the incorporation of saccharifying traits into ethanol-producing microorganisms was also attempted. The gene encoding for the xylanase enzyme (*xynZ*) from the thermophilic bacterium *Clostridium thermocellum* was expressed at high cytoplasmic levels in ethanologenic strains of *E. coli* KO11 and *Klebsiella oxytoca* M5A1(pLOI555) (Ohta et al. 1991). This is a temperature-stable enzyme that de-polymerizes xylan to its primary monomer (99%) xylose. To increase the amount of xylanase in the medium and facilitate xylan hydrolysis, a two-stage cyclical process was used for the fermentation of polymeric feedstocks to ethanol by a single, genetically engineered microorganism. Cells containing xylanase were harvested and added to a xylan solution at 60°C, thereby lysing and releasing xylanase for saccharification. After cooling to 30°C, the hydrolysate was fermented to ethanol while replenishing the supply of xylanase for the subsequent saccharification. *K. oxytoca* was found to be a superior strain for such an application because, in addition to xylose (metabolizable by *E. coli*), it can also consume xylobiose and xylotriose. Although the maximum theoretical yield of M5A1(pLOI555) is in excess of 48 g/L ethanol from 100 g/L xylose, approximately one third of that was achieved in this process because xylotetrose and longer oligomers remained unmetabolized by this strain. The yield appeared to be limited by the digestibility of commercial xylan rather than by the lack of sufficient xylanase activity or by ethanol toxicity.

9.6 PRODUCTION OF ETHANOL FROM CELLULOSE: AN INDUSTRIAL PERSPECTIVE

The development of commercial processes for the conversion of lignocellulosic biomass to bioethanol was constrained by the realization that "first-generation" bioethanol (made from sugar cane, maize, or wheat) was in direct competition with food production and supplies on one hand and carbon footprint on the other (Inderwildi and King 2009). In contrast, bioethanol from agricultural and food processing wastes, which represent approximately 80% of the dry weight of crops, is free from such constraints.

Almost all of such research and development was funded by the U.S. Department of Energy (DOE) and has been focused on cellulose as a substrate, which forms 38–50% of agricultural wastes (Figure 9.3). The aims and achievements of this program have been admirably summarized in a 2006 U.S. DOE report, "Breaking the Biological Barriers to Cellulosic Ethanol" (DOE/SC-0095 www.doegenomestolife.org/biofuels/). The title itself recognizes the major problem:

> The core barrier is cellulosic-biomass recalcitrance to processing to ethanol. Biomass is composed of nature's most ready energy source, sugars, but they are locked in a complex polymer exquisitely evolved to resist biological and chemical degradation.

To overcome such a barrier, the steps described in the following sections are necessary.

9.6.1 Removal of the Lignin That Waterproofs the Cellulosic Fibers

In itself this is already a mature technology because it is the basis of the paper-pulping industry, which is designed to produce delignified cellulose fibers from wood chips. However paper pulping is an energy-intensive process, as illustrated by the Kraft pulping process in which strong alkali is used to wash away the lignin and hemicelluloses as a "black liquor", which is then burned at high temperature to recover the alkali. This is the most costly step in the process and has a huge carbon footprintbecause 50–60% of the wood is converted to atmospheric CO_2, so Kraft pulping is not feasible for green bioethanol production. Use of waste paper might be a cheap route to cellulosic bioethanol production, but it would directly compete with paper recycling.

The Alcell paper-pulping process (Pye and Lora 1991) is potentially less polluting because it uses hot ethanol to extract the lignin, leaving behind cellulose and hemicellulose. However it has not been commercialized because of the associated fire risks. Although additional energy is required to redistill the ethanol, the residual lignin might be used to fuel that step.

9.6.2 Conversion of the Cellulose Fibers to Glucose

Cellulose fibers consist mostly of parallel $\tilde{\beta}$–1:4-linked glucose polymers that are linear and rigid because they are extensively crosslinked by hydrogen bonds and thereby arranged in a crystalline array that is impervious to water. Cellulose is therefore resistant to hydrolysis by mild acids or alkalis; thus, strong acids and/or high temperatures are required to convert it into fermentable glucose. Such processes have not found favor because strong acids must be recovered, and dilute acids at high temperature cause "browning" reactions and the release of inhibitors, which reduce the glucose yield and can inhibit subsequent ethanol fermentations. Consequently, enzyme hydrolysis by a mixture of cellulases and cellobiases has been the preferred strategy.

However, cellulases can attack only the loose ends (exo-$\tilde{\beta}$–1:4 glucanases) or intermittent flexible regions of amorphous cellulose at the surface of the fibers (endo-$\tilde{\beta}$–1:4 glucanases). Both classes of enzyme produce cellobiose, which yeasts cannot ferment, so addition of cellobiases is needed to convert this disaccharide into glucose. The overall hydrolysis rate is slow and dictated by the nature of the preceding delignification step because harsh treatments will increase the number of amorphous sites or loose ends available for cellulase attack. The "rate-limiting" step is the adsorption of the enzymes to the limited number of target sites, so one cannot increase the hydrolysis rate by adding more enzyme as in conventional enzyme reactions. Hence, cellulose hydrolysis is still very slow and many large reactors are required. Nevertheless a compensating advantage is that hydrolysis and fermentation can be carried out together in the fermentation broth in a simultaneous saccharification fermentation (SSF) process. This also eliminates the product inhibition of cellulases by glucose, thus making SSF the preferred strategy of hydrolysis. However cost-effective delignification remains a major problem in cellulosic bioethanol production.

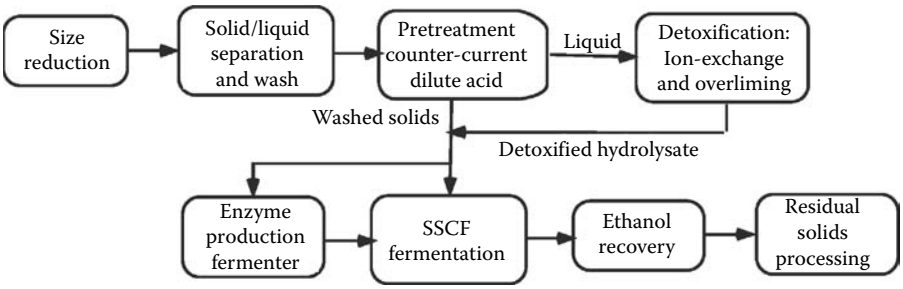

FIGURE 9.9 Flow diagram for the 1999 NREL model process.

For this reason a steam-explosion treatment of wood chips was explored by the Iotech Corporation, Ltd., of Canada, which caused a 10-fold increase in the susceptibility of the chips to cellulase hydrolysis (Jurasek 1978). The chips are permeated for a brief period with high-pressure steam in a sealed container, which causes an explosive decompression in the fibers when the pressure is released. This solubilizes and partly degrades the hemicellulose matrix and causes extensive depolymerization of the lignin, thus making it more readily extractable by dilute alkalis or by ethanol as in the Alcell process described in Section 9.6.1.

A sophisticated cost analysis of a hypothetical SSF process that is based on available evidence was reported by NREL in 1999 (Wooley et al. 1999). The steps in the model process are shown in Figure 9.9. The total cost was calculated on the basis of the following assumptions:

- *Feedstocks:* Yellow aspen sawdust or corn stover at an assumed cost of $27.5/dry t.
- *Plant size:* 2000 t feedstock/day (2 weeks/year downtime). Annual bioethanol production is approximately 200 million L.
- *Products:* Ethanol and electricity generated from combustion of the lignin-rich residues. As we shall see, these neglect the animal feed value of dried distillers grains (DDGS) from the fermentation residues, which could be considerable.
- *Pretreatment:* After size reduction, the feedstock is pretreated with dilute acid at high temperature in a countercurrent reactor similar to pulp digesters. This separates the soluble hemicellulose hydrolysate and inhibitors such as acetic acid from the lignocellulosic solid phase, which is thereby rendered more amenable to cellulase hydrolysis. The acid and inhibitors are removed by "overliming" and ion exchange, and the hemicellulosic sugars are utilized for enzyme production.
- *SSCF fermentation:* The enzymes are combined with the pretreated lignocellulose for SSF fermentations with a genetically engineered *Zymomonas* strain that gives 92% theoretical yield of ethanol from glucose and 85% from xylose but produces relatively low concentrations of ethanol. The lignin-rich residues are dewatered and burned to produce steam for the plant.
- *Distillation:* The broth ethanol concentration is less than 2% w/v, so considerable energy is required to distill it to 95% ethanol in a traditional two-stage system. A vapor-phase molecular sieve is used to remove the remaining water.
- *Capital costs:* The total project investment (1997) is approximately $240 million.
- *Ethanol production cost:* $1.44/U.S. gal. ($0.37/L)

This production cost compares unfavorably with the $1.20 price of 1997 U.S. corn-derived ethanol, but the authors predict future process improvements that might reduce the cellulosic ethanol cost to a similar level and also speculate future NREL-funded research that might drop the cost even further. But even then it is difficult to see how cellulosic ethanol could ever compete with the

price of Brazilian bioethanol from sugar cane ($0.83/U.S. gal in 2006), let alone current tax-free prices of gasoline.

Nevertheless political and environmental considerations may still justify production of cellulosic bioethanol, particularly when low-cost or polluting feedstocks can be used. For example, a Danish company (Nielsen et al. 2002) has developed an integrated biomass utilization system (IBUS) that features new technology for continuous pretreatment and liquefaction of lignocellulosic biomass in which the biomass is converted using only steam and enzymes. High pressure steam pretreatment solubilizes most of the hemicelluloses and converts the lignin into a high-quality particulate solid biofuel. The residual cellulose fibers are then readily hydrolyzed to glucose by commercial cellulases. Enzyme hydrolysis and yeast fermentation are combined in a SSF step that gives high ethanol yields from the cellulose consumed, albeit slowly. The process is energy efficient because of very high dry matter content in all process steps and by integration with a lignin-fueled power plant that provides all of the process energy plus a surplus of heat and power. The soluble hemicellulose is currently used as feed molasses but could be used in the future for additional ethanol production. However, plant capital costs are high and the production price is still above the world market price for first-generation bioethanol fuel. A more plausible solution would be to hydrolyze and ferment the hemicelluloses and burn the residual lignocellulose to produce heat or electricity.

9.7 ETHANOL FROM HEMICELLULOSIC WASTES

An alternative way to process agricultural wastes is to make ethanol only from the hemicelluloses, which form 23–32% of the dry weight (Figure 9.1) and use the lignocellulosic fibers as boiler fuel, animal feed, or for packaging. Hemicelluloses are a family of various $\tilde{\alpha}$-linked pentose and hexose sugars, some acetylated. They form a hydrophilic matrix that surrounds the lignin-coated cellulose fibers and allows transport of nutrients throughout the plant. Because the loose matrix is not stabilized by rigid hydrogen bonds, they are readily hydrolyzed to fermentable mono- and disaccharides by cheap and abundant microbial hemicellulases or by a short treatment with dilute acids at relatively low temperatures. For example, 83% of the xylans in sugar-cane bagasse are hydrolyzed to xylose after treatment with 0.1% w/w sulfuric acid at 140°C for 20 min. (Pessoa et al. 1997). Such treatment increases the dry weight of the residual lignocellulosic fibers, which therefore have enhanced fuel value. (Brazilian cane-juice bioethanol plants are already fueled by bagasse, in which most of the hemicelluloses have been destroyed by natural microbial attack during long storage).

Although hemicelluloses are abundant in all agricultural and food-processing wastes (e.g., brewers or distillers spent grains), they have little or no use except as a low-value component of animal feed. They could in principle be converted easily to feedstocks for production of cheap bioethanol, but yeasts cannot ferment the C5 sugars that are their major component. Many soil microorganisms can hydrolyze and utilize all of the hemicelluloses but produce lactic acid as the main anaerobic product (as in silage). Early attempts to select or engineer such microorganisms to produce high yields of ethanol from mixtures of C5 and C6 sugars are discussed in Sections 9.2–9.4, but none have yet provided a commercial fermentation process that competes with current yeast bioethanol fermentations. Although the feedstock costs are greatly reduced, the process costs are much higher because

- Low ethanol yield is the most important factor. With conventional sugars, yeasts or *Zymomonas* strains can achieve 0.44–0.47 g ethanol per gram of sugars, which approaches the maximum theoretical yield of 0.51 g per gram of sugars. Some xylose-utilizing yeasts strains can produce over 0.4 g ethanol per gram of xylose, but none can use the full range of hemicellulosic sugars.
- Volumetric productivity is the next biggest factor that directly affects plant capital and labor costs. Yeast fermentations are carried out on 12–20% g/L sugars in large-batch fermentors

at 20–32°C over 1–3 days to produce 6–12% v/v ethanol. Hence, average volumetric productivity is approximately 0.16 L ethanol per liter of broth. All previously described xylose-utilizing strains fail this test.

- *Energy costs:* In current yeast fermentations the 6–10% v/v ethanol is concentrated in distillation columns to 95% v/v. The required distillation energy is inversely proportional to the ethanol concentration but rises exponentially below 4% w/v; few novel strains reach this minimum requirement.

9.8 ETHANOL PRODUCTION BY THERMOPHILIC *BACILLI*

When fresh wet grass is put on compost heaps, there can be a very rapid rise in temperature of up to 70°C. This is caused by a class of thermophilic *Bacilli*, now classified as *Geobacilli*, which are capable of very rapid fermentation of all of the hemicellulosic sugars to produce mainly L-lactate with only minor amounts of acetate, formate, and ethanol. However a group at Imperial College in London has made genetic engineering modifications that divert anaerobic sugar metabolism from lactate to ethanol production.

A remarkable and unique feature of these thermophilic *Bacilli* is that sugar uptake and glycolysis do not appear to be regulated. Sugar uptake continues until all of the transport permeases are saturated. The resulting flood of sugars through glycolysis therefore produces huge amounts of intracellular pyruvate, NADH, and ATP. Excess NADH and ATP must be cycled by the cell to maintain the redox balance and the adenylate energy charge, respectively.

Like most microorganisms, these thermophiles grow aerobically by the pyruvate dehydrogenase (PDH) pathway. PDH is an enzyme complex that converts pyruvate and NAD^+ to acetyl-CoA (used for cell growth) and NADH, which is then reoxidized to NAD^+ by the membrane-bound electron transport chain (ETC) to produce the large amount of ATP required for cell growth. However, as the temperature rises the oxygen solubility in the sap drops and anaerobic fermentation is observed.

As illustrated in Figure 9.10, their anaerobic growth is via glycolysis and the PFL pathway, which converts pyruvate to acetyl-CoA and formate, which is excreted. Half of the acetyl-CoA is converted by phosphotransacetylase to acetyl-phosphate to recycle CoA and then by acetate kinase to acetate, which is excreted. This final step produces the ATP required for cell growth. To maintain redox balance, the other half of the acetyl-CoA is reduced to acetaldehyde and then to ethanol by the NADH generated by glycolysis.

In the wild-type strain, as sugar input and glycolytic flux increase, the PFL pathway becomes saturated and the excess NADH and pyruvate are recycled via L-LDH to NAD^+ and lactate, which is

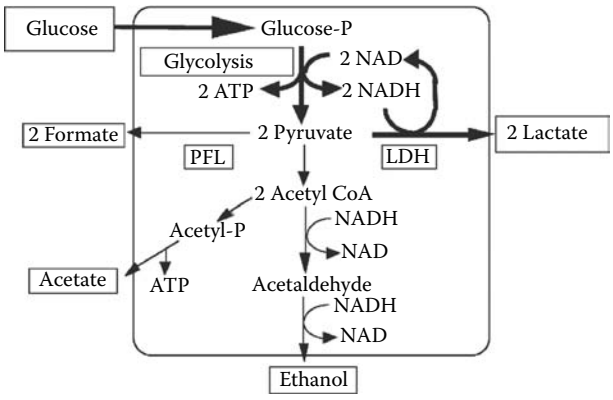

FIGURE 9.10 Anaerobic sugar metabolism in thermophilic *Bacilli*. The PFL growth pathway is on the left and the LDH overflow pathway is on the right.

excreted. This major anaerobic "overflow" pathway cannot provide growth but produces excess ATP that is far beyond that required for cell growth, so the excess is hydrolyzed to ADP. In the native environment of these microorganisms, such as compost heaps, the excess energy produces heat, which rapidly raises the sap temperature above 60°C, where competing hemophilic microorganisms cannot grow, so thereafter the thermophiles form a monoculture. After the sap sugars are exhausted, they secrete enzymes into the plant cell wall that hydrolyze the hemicellulose and amorphous cellulose to provide a further supply of C5 and C6 sugars. When the temperature eventually drops, the thermophiles sporulate and slower-growing mesophiles take over until a new load of fresh biomass arrives. The thermophile spores then quickly germinate and once again take over. This vignette of life in a compost heap is useful to help to understand the challenges that have been encountered in trying to develop commercial ethanol fermentations with strains such as LLD-15 that lack LDH.

Figure. 9.11 (Hartley and Shama 1987) shows that batch fermentations of the lactate-deficient strain LLD-15 on sucrose yielded much more ethanol than was expected from the PFL pathway alone. Up to that time, it was assumed that PDH was inactive anaerobically, but these results showed that is not the case. In such strains, an anaerobic PDH pathway appears to act as an alternative to the LDH overflow pathway to convert the excess pyruvate to ethanol and CO_2. The PFL flux and PDH flux are approximately equal at pH 7.0, but at pH 6.2 it can be seen that the PFL flux and growth rate have declined considerably, so the PDH overflow flux predominates, giving ethanol yields commensurate with those from yeast fermentations.

Figure 9.12 shows the pathways for anaerobic sugar metabolism in mutants such as LLD-15 that lack LDH. As postulated, the cells continue to very rapidly take up a wide range of disaccharides, including all of the C5 and C6 sugars in hemicellulose hydrolysates. These are then rapidly converted to glucose-6-phosphate by the Emden-Meyerhof and/or ED pathways (see Figure 9.2) and thereafter to pyruvate by the glycolytic pathway. As expected, the PFL growth pathway converts this pyruvate to formate and acetyl-CoA, half of which is converted to acetyl phosphate to

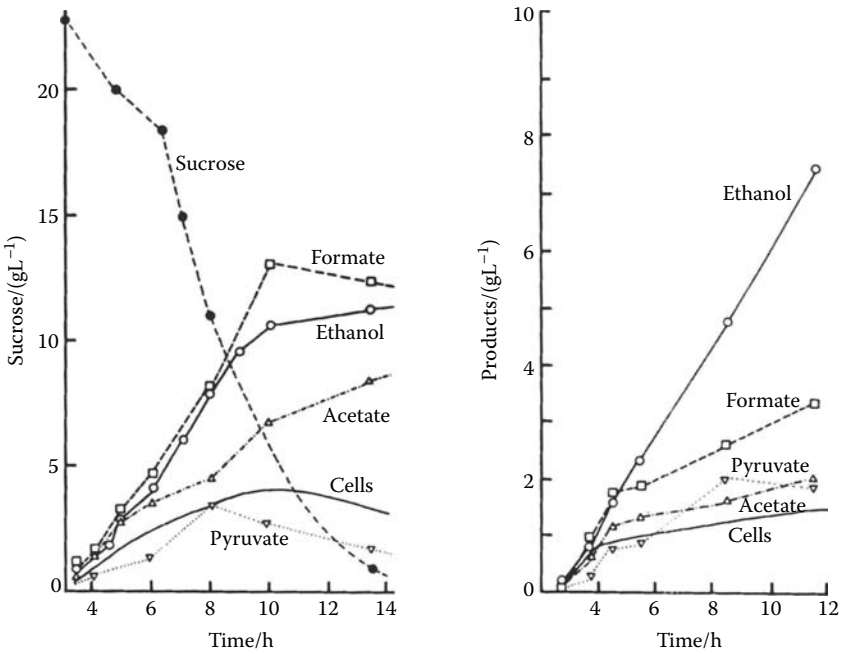

FIGURE 9.11 Anaerobic batch fermentations by strain LLD-15 on sucrose (2.35 g/L), tryptone (2.0 g/L), and yeast extract (1.0 g/L) at 60°C, pH 7.0 (left) or pH 6.2 (right).

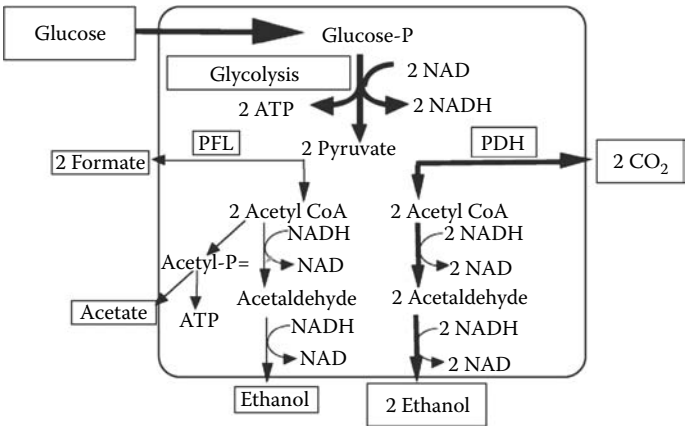

FIGURE 9.12 Anaerobic sugar metabolism in strain LLD-15. The PFL growth pathway is on the left and the anaerobic PDH overflow pathway is on the right.

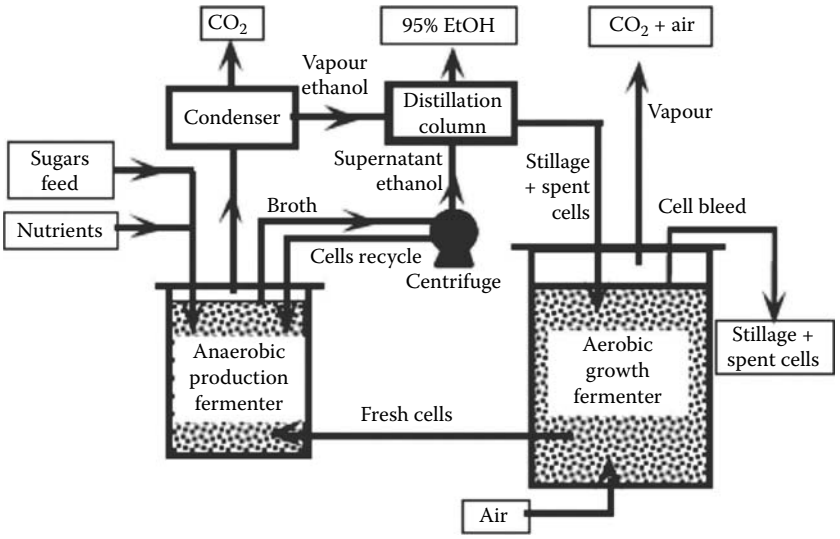

FIGURE 9.13 The model closed system for thermophilic ethanol production. (Hartley, B.S., *International Patent Application* PCT/GB88/004, 1988.)

recycle the CoA and then excreted as acetate to generate ATP. The products are therefore 1 mol of acetate +1 mol of ethanol +2 mol of formate per mole of glucose consumed.

In strains lacking LDH, the rest of the pyruvate is converted to acetyl-CoA and CO_2 by the anaerobic PDH pathway, which substitutes as an overflow pathway to recycle the excess NADH arising from unregulated sugar uptake. The acetyl-CoA is reduced by NADH to acetaldehyde via acetaldehyde dehydrogenase and then by a second NADH to ethanol via ADH, thereby regenerating the 2 NAD^+ required to maintain the glycolytic flux. The products are therefore 2 mol of ethanol +2 mol of CO_2 per mole of glucose equivalent consumed, as in conventional yeast fermentations.

It is obvious from Figure 9.12 that maximum ethanol yields are given by slow or nongrowing cells, so Hartley (1988) conceived a continuous "closed system" fermentation to achieve this, as illustrated in Figure 9.13. The anaerobic production fermentor (F1) is operated at 65°C and pH 6.2, at which the growth by the PFL pathway is minimal, so this is fed continuously by fresh cells from an aerobic growth fermentor (F2). After stripping off the ethanol under mild vacuum, the spent

cells are centrifuged and recycled to F1 to maintain high volumetric productivity and partly to the aerobic growth module, F2. The stillage consisting of cell debris, residual sugars, acetate, formate, residual sugars, and nutrients is fed to the aerobic growth fermentor (F2), which is operated with vigorous aeration at 65°C and pH 7. This converts most of the stillage into fresh cells, most of which are recycled to the production fermentor to maintain cell viability.

The residual F2 broth containing residual cells and stillage is bled off for use as animal feed. The sugar feed rate and the F2 bleed rate essentially control the productivity of the whole system.

In 1993 a start-up company, Agrol, Ltd., was formed to develop and exploit this model process, but the final objective could not be achieved for two reasons. The first is that the spontaneous gene mutation in strain LLD-15 proved to be unstable and reverted to wild type at high frequency. This mutation was found to arise from the insertion of an indigenous transposon into a "hot spot" within the *lld* gene that encodes L-LDH. The transposon can also jump out from the hot spot at high frequency, causing reversion to wild-type cells that can grow quickly in the production fermentor and displace the slow-growing mutant cells so as to cause production of lactic acid instead of ethanol. This phenomenon is illustrated in the studies of continuous cultures of strain LLD-15 fed with 2% w/v sucrose at pH 7.0 sucrose in a defined minimal medium (San Martin et al. 1993). As can be seen in Figure 9.14, the PFL and PDH fluxes are approximately equal at this pH and continuous cultures can be maintained almost indefinitely at dilution rates below 0.2 h^{-1}. However at higher dilution rates, pyruvate secretion and reversion to lactate production is seen as soon as the sugar uptake rate exceeds 4.2 g sucrose per gram of cells per hour.

An obvious way to prevent reversion was to delete the *lld* gene, but conventional genetic engineering techniques developed for mesophiles such as *E. coli* are not readily applicable to thermophiles that grow very slowly below 60°C. However, suitable techniques were eventually developed (Baghaei-Yazdi et al 2006) and a stable *lld*-deleted strain was constructed. The obvious conclusion was that the PDH-overflow pathway becomes saturated above a critical point and cell death results.

The second reason that the final objective was not achieved was that although this new strain performed well in the closed system at the low sugar concentrations used in previous experiments, it died rapidly at the high concentrations of sugar required for commercial production of bioethanol.

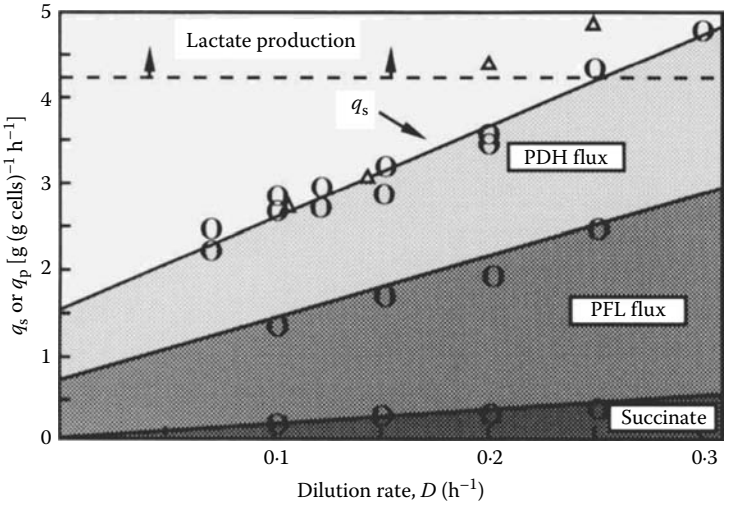

FIGURE 9.14 Specific sucrose consumption rate at 70 "C, pH 7.0. (qs = g. sucrose per g. cells per hour) for strain LLD-15 at 10 g. (O) and 15 g, (Δ) input sucrose per l. The hatched areas under the q_s line (arrowed) represent the proportion of the total pyruvate flux which goes via the PDH pathway, PFL pathway or to succinate. When q_s exceeds about 4.2 g sucrose (g cells)-' h-', LLD-R revertants take over the cultures.

Agrol, Ltd. attempted to solve this problem by introducing the PDC (*pdc*) gene from *Z. mobilis* (Green et al. 2001). The *Zymomonas* enzyme was predictably inactive at the high temperatures necessary for thermophile growth. Agrol ran out of funds and was wound up in 2003.

However, the former Agrol management team succeeded in raising new capital to form TMO Biotec, Ltd. (now TMO Renewables) to pursue the project. To try to avoid the Agrol patents, they selected an alternative thermophilic *Geobacillus* similar to the Agrol LLD-R strain but more convenient for genetic manipulation. They again deleted the LDH gene and again explored the PDC approach to try to find more thermostable strains. However, TMO Renewables later abandoned this approach but also inactivated the *pfl* (PFL) gene to eliminate acetate production so that the microorganism can only grow aerobically. They currently use their modified thermophile in a continuous process analogous to that described by Hartley (1988) that they intend to exploit in association with a U.S. company, Fiberight, to produce bioethanol from the cellulosic fraction of municipal solid waste (MSW). The economics of this approach look promising because the costs of cellulose hydrolysis are offset by the fees for waste disposal and energy production from incineration of the plastic fraction of the MSW.

The three founding Agrol scientists were not involved in TMO but were able in 2005 to raise modest funds to set up a small company, Bioconversion Technologies, Ltd. (now Biocaldol, Ltd.), to explore alternative solutions to the sudden "redox death" problems encountered by Agrol, Ltd. The explanation for this phenomenon can be seen in the structure and mechanism of the PDH complex (Berman et al. 1981) illustrated in Figure 9.15. It consists of three types of subunits that catalyze consecutive steps in the reaction sequence. The E2 component forms the internal core of the complex and comprises 24 polypeptide chains arranged with octahedral symmetry. The 24 E1 components and 12 E3 components lie above this core and catalyze other steps in the reaction sequence, as schematically illustrated in Figure 9.15a. Each E2 chain contains two lipoyl-lysine residues that lie at the surface of the cluster and act as "swinging arms" that convey the reaction intermediates from one active site to another. This is normally the rate-limiting step in PDH activity.

However as sugar feed rates increase, glycolysis and pyruvate production rates increase in parallel. They eventually exceed the maximum PDH flux rate, which is dictated by the rate-limiting E2 acetyl migration step. Thereafter, intracellular pyruvate accumulates and is in part excreted. However, unfettered glycolysis continues to consume most of the available NAD^+ until its concentration falls below the NAD^+ binding constant for the E3 lipoate dehydrogenase. At this critical point, the whole PDH flux begins to decrease dramatically. The decrease in NAD^+ levels then accelerates and the cells suffer catastrophic redox imbalance, which leads to a shortage of ATP insufficient to maintain the cell membrane potential, and instant redox death results.

By analyzing the reasons for this phenomenon, Biocaldol found several avenues to avoid the redox death problem that are capable of commercialization.

1. The first approach uses an *lld*-deleted derivative of the original Imperial College strain LLD-R in fed-batch fermentations that are feedback controlled to maintain residual sugar levels below the critical point that leads to redox death. These have been shown to produce ethanol in high yield from mixed C5 and C6 sugars at acid pH but are relatively slow in absence of a vigorous PFL growth pathway. To help to solve this problem, Biocaldol has recently developed improved strains that can be used in a novel continuous process that is approaching commercialization.
2. The second Biocaldol solution avoids redox death by creating an entirely novel pathway for ethanol production. A synthetic gene encoding a formate dehydrogenase (FDH) is introduced into the thermophile in place of the LDH gene. As illustrated in Figure 9.16, this creates an artificial PFL-FDH pathway, not found in nature that produces only ethanol and CO_2. The PDH overflow pathway also produces only ethanol and CO_2, so ethanol yields exceeding those in yeast fermentations are expected. Another important advantage is that ethanol production will be optimal when the cells are growing most vigorously at neutral

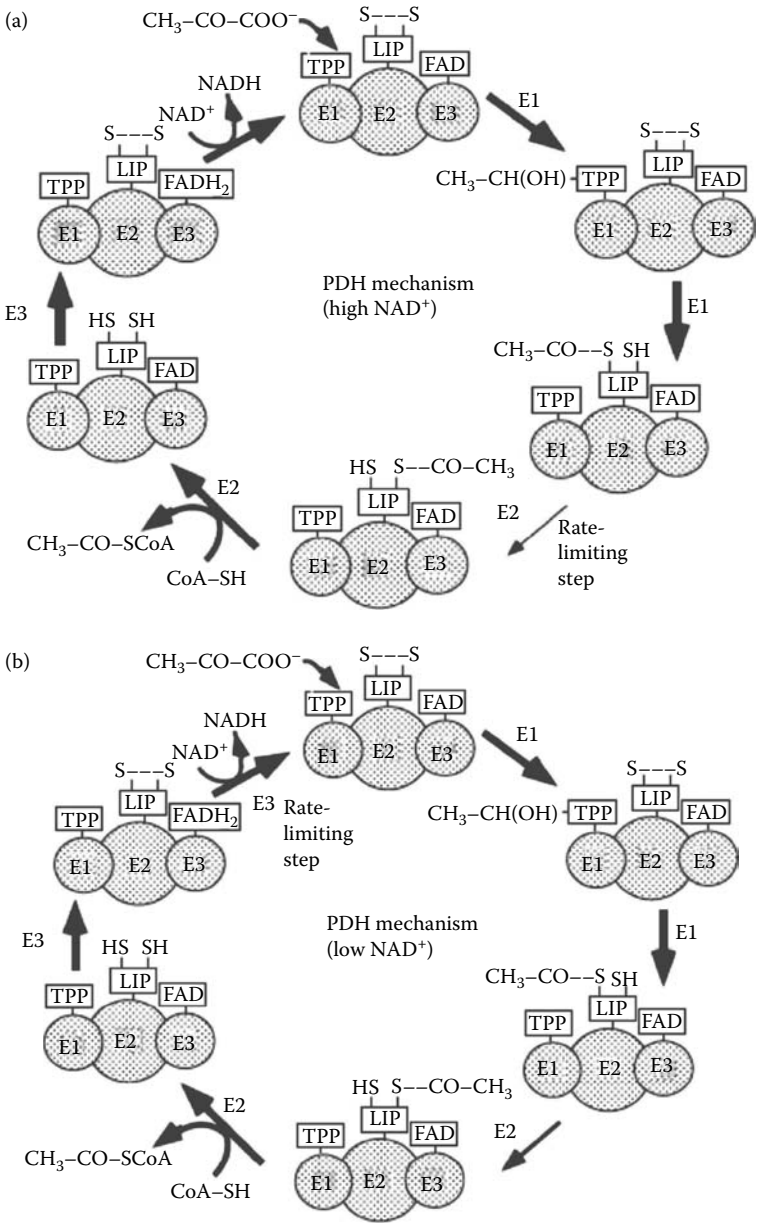

FIGURE 9.15 Mechanism of pyruvate dehydrogenase highlighting the change in the "rate-controlling" step as the metabolic environment changes from (a) NADH-rich to (b) NADH-lacking.

pH, so yields will be close to theoretical in any type of fermentation system. However, the artificial FDH is active only below 60°C, whereas the desired growth temperature is 70°C, so Biocaldol is using protein engineering to construct a more thermostable enzyme.

3. An alternative solution to the redox death problem is to supplement the sugar feedstock with a co-substrate that provides additional intracellular reducing power. Glycerol is such a co-feedstock and is currently cheap and available on an increasingly large scale as a byproduct of biodiesel production. Figure 9.16 shows that the extra NADH arising from anaerobic glycerol metabolism can be used to reduce the excess acetyl-CoA arising from the PFL growth pathway, so again ethanol and CO_2 are the only products (Baghaei-Yazdi et al. 2009).

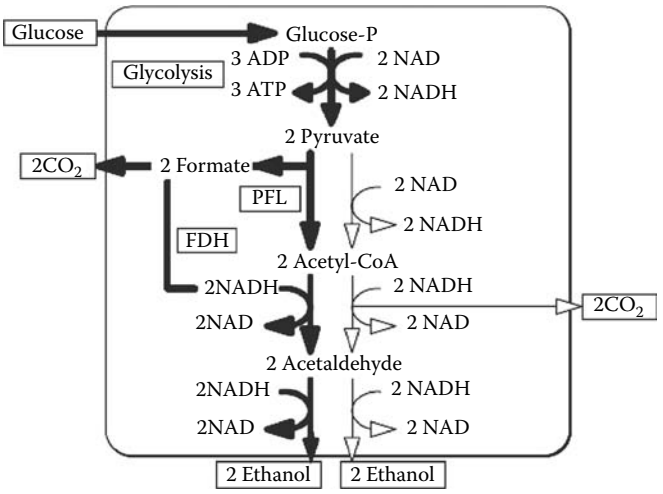

FIGURE 9.16 Anaerobic pathways for combined glycerol and sugar utilization. The glycerol pathway involves GK and glycerol phosphate dehydrogenase (GPD) followed by glycolytic enzymes.

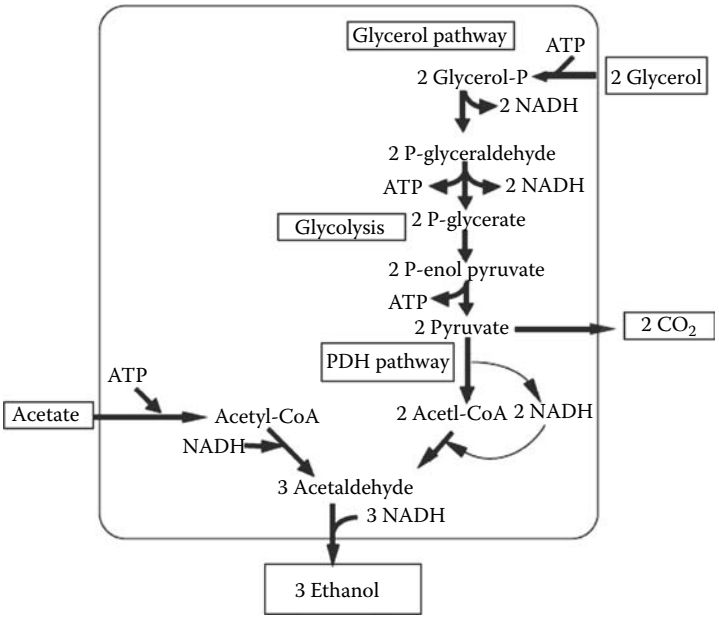

FIGURE 9.17 Metabolic routs for (a) acetate and (b) glycerol metabolism.

Acetate is a major undesirable component in acid hydrolysates of biomass because at acidic pH the acetic acid is toxic to the cells because it acts as an "uncoupling agent" that destroys the cell membrane potential. Moreover Figure 9.17 shows that the same concept applies to a mixed fermentation of glycerol and acetate alone because imported acetate is converted to acetyl-CoA using the abundant ATP arising from the unregulated sugar glycolysis. The acetyl-CoA can then be reduced to ethanol using the excess NADH arising from glycerol metabolism. Hence, ethanol yields from crude hydrolysates of biomass are potentially much higher than from conventional yeast fermentations.

However another remaining problem is the regulation of glycerol metabolism in these thermophile strains. *E. coli* ferments glycerol aerobically and anaerobically by different pathways, as

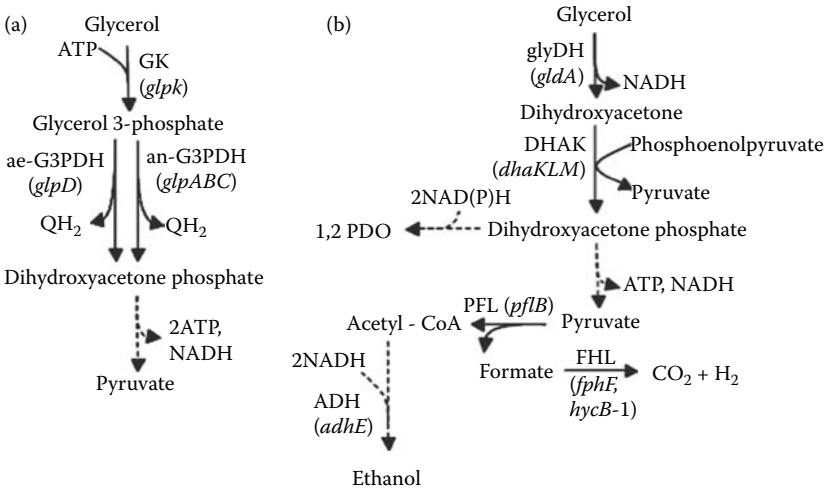

FIGURE 9.18 Anaerobic pathways for the co-utilization of glycerol and and its conversion to pyruvate (a) and alcohol (b) by microorganisms. The glycerol pathway involves glycerol kinase (GK) and glycerol phosphate dehydrogenase (GPD) followed by glycolytic enzymes. (Durnin, G., et al. *Biotechnology and Bioengineering*, 103, 143–161, 2009.)

illustrated in Figure 9.18 (Durnin et al. 2009). The aerobic pathway (a) involves phosphorylation by glycerol kinase (GK) encoded by the *glpK* gene followed by a membrane-bound flavoprotein, glycerophosphate dehydrogenase, which forms reduced ubiquinone that is reoxidized by the ETC to provide an adequate supply of ATP for growth. The resulting dihydroxyacetone phosphate is isomerized to phosphoglyceraldehyde and metabolized by glycolysis.

The anaerobic pathway (b) uses glycerol dehydrogenase (glyDH) encoded by gene *gldA* to form NADH and dihydroxyacetone, which is then phosphorylated by dihydroxyacetone kinase (DHAK) using phosphoenolpyruvate as a phosphate donor. The resulting dihydroxyacetone phosphate can then be isomerized to phosphoglyceraldehyde and metabolized by glycolysis. In some cases, this anaerobic pathway leads to the formation of 1,2-propanediol to maintain redox balance, but it is not a growth pathway and is not relevant to the ethanol process.

Nevertheless, Durwin et al. (2009) have shown that modest yields of ethanol can be obtained from glycerol by a microaerobic process in which growth and redox balance are maintained by a minimal flux through pathway a. The excess pyruvate is then guided into ethanol production. This process differs from that proposed by Baghaei-Yazdi et al. (2009) in Figure 9.18 that uses sugars metabolized by the anaerobic PFL pathway for growth and a combination of the PFL and glycerol pathways to maintain redox balance. Thereby all of the sugars and glycerol are converted to ethanol in yields greater than those provided by conventional yeast fermentations.

However, another problem is the regulation of glycerol uptake. In *E. coli*, a membrane-bound glycerol transport facilitator protein (permease) encoded by the *glpF* is required for rapid glycerol uptake by the aerobic pathway (Weissenborn et al. 1992). The *glpF* gene is in an operon followed by the *glpK* gene for GK, which is preceded by a *glpR* gene that encodes a 30-kDa tetrameric repressor protein that is induced by glycerol phosphate. The glycerophosphate dehydrogenase gene *glpD* is in a different operon that is also repressed by *glpR*. Biocaldol has identified sequences within the thermophile genome that are homologous to these *E. coli* genes and are in the process of deleting the putative *glpR* homologue to provide a strain that can constitutively metabolize sugars and glycerol.

It is therefore probable that a glycerol/sugar fermentation process will shortly be available that will produce ethanol profitably from hemicellulosic sugars and glycerol that are the major byproducts of existing bioethanol and biodiesel plants. It is therefore timely to consider the feedstocks that may become available from this and other thermophilic fermentation processes described above.

9.9 HEMICELLULOSIC FEEDSTOCKS FOR THERMOPHILIC ETHANOL FERMENTATION PROCESSES

Optimal feedstocks are lignocellulosic residues arising from processing of already harvested crops in which all agricultural and transport costs are borne by the primary product. Such residues are generally dried and burned as plant fuel or sold as low-grade animal feed, but they are sometimes composted and returned to the soil. Mild acid or enzyme hydrolysis releases most of the hemicellulosic sugars for bioethanol production and can actually add value to the insoluble lignocellulosic fibers by reducing drying costs and/or supplementing the animal feed with protein-rich spent thermophile cells, which resemble fishmeal in containing lysine and methionine and as such have similar animal feed value. Hence, the cost of the C5 and C6 sugar feedstock is essentially only the hydrolysis cost. Some examples are discussed in Sections 9.9.1–9.9.7.

9.9.1 Sugar Cane

World sugar cane production in 2007 was reported to be in excess of 1500 million t, with Brazil and India as the major producers. The cane is shredded, crushed, and washed to yield 10–15% v/v cane juice, which is evaporated and crystallized to yield granulated sugar and residual molasses (20–30% sucrose and 15–25% glucose and fructose), which are mostly fermented to rum. Alternatively the cane juice is fermented directly to ethanol, as described in Section 9.1.

Baggase is the residual crushed cane that contains mainly the lignocellulosic rind and significant amounts of hemicelluloses and residual cane sugars arising from the pith (Table 9.2). The bagasse is normally air-dried, which allows fermentation of the residual sugars by adventitious microorganisms, including thermophiles, to increase calorific value.

The Tilby process (www.canefibertech.com/tilby_tech.com) could greatly increase bioethanol yield from sugar cane. Instead of crushing the cane, it is chopped mechanically into 30-cm billets that are sliced down the middle to expose the central pith core. This is mechanically scraped out to leave the dry external rind that contains all of the lignocellulosic fibers (6% of the dry weight of cane). These fibers can yield various useful products such as building board, pulp, or paper, but they also have high calorific value sufficient to fuel the whole bioethanol plant. The pith contains the cane juice (~17% dry weight) sugars, and hemicellulosic fibers (~7% dry weight) that could be hydrolyzed by enzymes and/or mild acid to increase the total sugar concentration by approximately 40%. Thermophilic fermentations of the juice and the hemicellulosic sugars would slash the cost of cane bioethanol, already the lowest, to below that of gasoline.

9.9.2 Sugar Beet

Approximately 30% of world sugar production is derived from sugar beet, mainly in Europe. Yields per hectare are lower than for cane sugar, so this crop has not found wide favor as a source of first-generation bioethanol. However, the whole crop is rich in hemicelluloses and pectins that could potentially greatly lower the production cost as in the above example. Only the roots are currently harvested and the tops are used for fodder or ploughed in. These could be combined with the beet pulp and vinasse that are major byproducts of beet sugar production to produce yet more bioethanol from thermophilic fermentations. Because that bioethanol would be produced from agricultural wastes it would not carry a significant carbon footprint.

9.9.3 Brewers and Distillers Spent Grains

These are residues from conventional yeast fermentations of barley, wheat, or maize that are predominantly marketed as animal feed. Large breweries and conventional bioethanol plants produce a large volume of such residues that are rich in hemicelluloses. For example, wheat bran

contains 34% w/w of residual starch and fibers that contain 40% hemicelluloses, 13.5% crude protein, and only 5% lignin. Palmarois-Adrados et al. (2005) have shown that a combination of mild acid and enzymic hydrolysis can convert 80% of the total carbohydrate to sugars that could all be converted to ethanol by the thermophilic fermentation process. Moreover, as described above, the animal feed value of the fibrous residues remains similar to that of the original bran, so feedstock costs will be essentially only the hydrolysis costs.

9.9.4 Oilseed Rape

Oilseed rape is increasingly grown for biodiesel production, but the straw is left to rot uselessly in the field. Unlike cereal straws it is low in lignin, so the hemicelluloses are easily hydrolyzed to fermentable sugars by a combination of mild acid and steam. Fresh whole-crop oilseed rape can be harvested efficiently by a process devised by a Danish research group, and the seeds could be separated, dried, and crushed at the factory, saving combine harvesting costs. They would then be transesterified with ethanol to produce biodiesel, glycerol, and rapeseed meal as major byproducts. The latter is currently used as low-grade animal feed but could be combined with the fresh straw for acid/steam hydrolysis to produce C5 and C6 sugars suitable for the glycerol/sugar fermentation envisaged in the Biocaldol patent application described in Section 9.8.

There is already evidence that rape-straw can be used for cardboard or paper production (www.foe.co.uk/pubsinfo/briefings/html/19971215150023.html), so it is probable that the residual fibers from this process would be even more useful. Hence, the whole crop could be converted into biodiesel + bioethanol + renewable packaging + high-protein animal feed.

9.9.5 Palm-Oil Residues

Huge volumes are available in tropical countries and could be another major feedstock for bioethanol production. The main byproducts from oil extraction factories are lignocellulosic residues (~6 t per ton of palm oil) that include empty fruit bunches, palm kernels, and oil presscake that all have high hemicellulosic content. The oil and presscake are increasingly being exported for biodiesel and animal feed production, respectively, but this has engendered a "fuel versus food" debate. It would make economic and environmental sense to combine the oil extraction with biodiesel production on-site and to use the palm-oil residues and glycerol to produce bioethanol and animal feed by the Biocaldol process described in Section 9.8. A portion of the ethanol could be used to enhance oil extraction from the kernels and presscake and to recycle the extract for use in transesterification in the biodiesel process.

9.9.6 Paper-Pulping Residues

As discussed in previous sections, production of bioethanol from cellulose is not an attractive economic or environmental option, but bioethanol from paper-pulping residues could be both. Removal of xylans to produce top-grade paper pulps by enzyme or mild alkali treatment after mechanical paper pulping is already a commercial practice, but the solubilized pentose polymers are not commercially utilized. These could be a significant international target for thermophilic ethanol fermentations.

9.9.7 Straw Pretreatment

Cereal straws contain large amounts of potassium chloride that sublimes at high temperatures and attacks the stainless steel tubing in boilers that are used for efficient electricity production. Pretreatments to remove the potassium chloride can be combined with hydrolysis to solubilize hemicelluloses so as to increase the calorific value of the straw. As discussed in Section 9.6.2, steam

explosion followed by cellulase and cellobiase hydrolysis can give high yields of fermentable sugars (Galbe and Zacchi 2002). If hemicellulase and cellulase hydrolysis were used instead, the lignin content and calorific value of the residues would increase, and over half of the straw could be converted to ethanol in thermophilic fermentations.

SUMMARY

The major component cellulose can be converted to glucose, which is easily fermented to ethanol by yeasts, but this requires expensive and energy-intensive pretreatment to separate the cellulose fibers from their lignin coat. In contrast, hemicelluloses can easily be hydrolyzed to a mixture of glucose, xylose, and arabinose, but yeasts cannot efficiently ferment the latter.

The initial enthusiasm for biofuels as a sustainable alternative to gasoline and an answer to global warming has died down with the realization that first-generation biofuels compete for limited land and water resources with the food production required by an expanding world population. However, that criticism does not apply to "second-generation" bioethanol derived from the relatively useless lignocellulosic residues that are 80% of what farmers grow, because the food production already carries the agronomic carbon footprint.

Lignocellulosic materials (cellulose, hemicellulose, and lignin) are the most abundant renewable organic resource on earth, so the development of new processes for their conversion to useful products has been recognized as an urgent need.

Until recently, cellulose pretreatment, hydrolysis, and fermentation have been the major focus for research and development, but the resulting bioethanol is still not competitive with gasoline.

Unfortunately, the emphasis on cellulose utilization has also cast a cloud over second-generation biofuels because the energy inputs required to break down the lignocellulose scarcely match the energy output of the resulting bioethanol. Wood is already a sustainable biofuel for much of the world's population, so efficient use of lignocellulosic residues for heat and electricity production remains a sensible target. But none of these criticisms apply to the production of bioethanol from hemicelluloses, as illustrated in this chapter.

A good deal of attention has therefore been focused on the developments of genetically modified strains that are capable of efficiently utilizing all of the hemicellulose sugars. Because powerful genetic engineering tools have been developed for enteric bacteria such as *E. coli*, it is natural that these were first choice for developing strains to ferment hemicellulosic sugars such as xylose. However, they are far from ideal production hosts because they grow naturally at 37°C° in a semiaerobic environment on various feedstocks produced by the action of intestinal enzymes.

Pentoses are not among these, so foreign genes must be introduced to import and metabolize them. Also, sugar uptake is regulated in these microorganisms, so utilization of mixed sugars will be relatively slow and stepwise. Unlike yeasts, they are not ethanol tolerant, so they can produce only low ethanol concentrations, *Zymomonas* species are an exception to some of these criticisms, but they require considerable genetic manipulation for pentose fermentations.

In our opinion, the future lies in ethanol fermentations by thermophilic Bacilli such as *Geobacillus*. As described above, they are naturally selected to ferment a wide range of C5 and C6 sugars extremely rapidly by relying on unregulated sugar uptake. In consequence, they squander energy to raise the ambient temperature to 70–75°C and thereby take over competing mesophiles.

Because oxygen solubility is very low at these temperatures, they are well adapted to anaerobic or microaerobic environments. Moreover ethanol solubility is low at these temperatures, so excess ethanol is easily removed by gas sparging or mild vacuum to keep the broth ethanol

concentration safely below 3% v/v. No such fermentation system is yet commercialized, but the powerful tools now available from a combination of protein engineering, genetic engineering, and metabolic engineering combined with novel fermentation systems that make it almost certain that commercialization is close.

The inherent advantages of such thermophilic fermentations guarantee that they will then slash the costs of bioethanol for the following reasons:

- Reduced feedstock costs from cheaper processing of agricultural and municipal wastes.
- Reduced capital costs from rapid continuous fermentations with high volumetric productivity.
- Reduced energy costs from elimination of cooling water.
- Reduced distillation costs from continuous ethanol removal as a 20–30% w/v vapor.
- The only byproduct is spent cells with high animal feed value.

Given such commercial profitability and abundant waste resources, hemicellulosic bioethanol will make a major contribution to replacement of gasoline as a transport fuel and to reduction of global warming.

The application of metabolic engineering also offers the potential to revolutionize the chemical industry. It is estimated that in less than 10 years, integrated biorefineries will play a role comparable to today's petrochemical manufacturers.

Biorefineries will use row crops, energy crops, and agricultural waste as inputs to extract oil and starch for food, protein for feed, lignin for combustion or chemical conversion, cellulose for conversion into fermentable sugars, and other byproducts.

One can conclude that the future of integrated biorefineries is bright, and that the role of metabolic engineering is only limited by our imagination.

REFERENCES

Amore, R., P. Kotter, C. Kuster, M. Ciriacy, and C. P. Hollenberg. 1991. Cloning and expression in *Saccharomyces cerevisiae* of the NAD(P)H-dependent xylose reductase-encoding gene (*XYL1*) from the xylose- assimilating yeast *Pichia stipitis*. *Gene* 109:89–107.

Aristidou, A., J. Londesborough, M. Penttilä, P. Richard, L. Ruohonen, H. Soderlund, A. Teleman, and M. Toivari. 1999. Transformed micro-organisms with improved properties. Patent Application PCT/FI99/00185, WO 99/46363.

Aristidou, A., P. Richard, L. Ruohonen, M. Toivari, J. Londesborough, and M. Penttilä. 2000. Redox balance in fermenting yeast. *Monograph European Brewing Convention* 28:161–70.

Baghaei-Yazdi, N., F. Cusdin, E.M. Green, and M. Javed. 2006. Modification of bacteria, *Intn'l Patent Application* 664076.

Baghaei-Yazdi, N.B., M. Javed, and B.S. Hartley. 2009. Enhancement of ethonal production. *International Patent Application*. WO 2009/10145 A1.

Beall, D.S., L.O. Ingram. 1993. Genetic engineering of soft-rot bacteria for ethanol production from lignocellulose. *J Ind Microbiol* 11:151–5.

Berman, J.N., G.X. Chen, G. Hale, and R.N. Perham. 1981. Lipoic acid residues in a take-over mechanism for the pyruvate dehydrogenase multienzyme complex of *Escherichia coli*. *Biochem J* 199:513–20.

Billard, P., S. Ménart, R. Fleer, and M. Bolotin-Fukuhara. 1995. Isolation and characterization of the gene encoding xylose reductase from *Kluyveromyces lactis*. *Gene* 162:93–7.

Bolen, P.L., G.T. Hayman, and H.S. Shepherd. 1996. Sequence and analysis of an aldose (xylose) reductase gene from the xylose-fermenting yeast *Pachysolen tannophilus*. *Yeast* 12:1367–75.

Brencic, A., and S.C. Winans. 2005. Detection of and response to signals involved in host-microbe interactions by plant-associated bacteria. *Microbiol Molec Biol Rev* 69:155–94.

Bruinenberg, P.M., P.H.M. De Bot, J.P. Van Dijken, and W.A. Scheffers. 1984. NADH-linked aldose reductase: The key to anaerobic alcoholic fermentation of xylose by yeasts. *Appl Microbiol Biotechnol* 19:256–60.

Causey, T.B., K.T. Shanmugam, L.P. Yomano, and L.O. Ingram. 2004. Engineering *Escherichia coli* for efficient conversion of glucose to pyruvate. *Proc Natl Acad Sci USA* 101:2235–40.

Chandrakant, P., and V.S. Bisaria. 1998. Simultaneous bioconversion of cellulose and hemicellulose to ethanol. *Crit Rev Biotechnol* 18:295–331.

Dahn, K., B. Davis, P. Pittman, W. Kenealy, and T. Jeffries. 1996. Increased xylose reductase activity in the xylose-fermenting yeast *Pichia stipitis* by overexpression of *XYL1*. *Appl Biochem Biotechnol* 57–58:267–76.

Deanda, K., M. Zhang, C. Eddy, and S. Picataggio. 1996. Development of an arabinose-fermenting *Zymomonas mobilis* strain by metabolic pathway engineering. *Appl Environ Microbiol* 62:4465–70.

Durnin, G, J. Clomburg, Z. Yeates, J.J. Pedro, P.J.J Alvarez, K. Zygourakis, P. Campbell, and R. Gonzalez. 2009. Understanding and harnessing the microaerobic metabolism of glycerol in Escherichia coli. *Biotechnology and Bioengineering* 103(1).

Feldmann, S., H. Sahm, and G.A. Sprenger. 1992. Pentose metabolism in *Zymomonas mobilis* wild type and recombinant strains. *Appl Microbiol Biotechnol* 38:354–61.

Galbe, M., and G. Zacchi. 2002. A review of the production of ethanol from softwood. *Appl Microbiol Biotechnol* 6:618–28.

Gong, C.S., N.J. Cao, J. Du, and G.T. Tsao. 1999. Ethanol production from renewable resources. *Adv Biochem Eng Biotechnol* 65:207–41.

Granstrom, T.B., A.A. Aristidou, J. Jokela, and M. Leisola. 2000. Growth characteristics and metabolic flux analysis of *Candida milleri*. *Biotechnol Bioeng* 70:197–207.

Green, E.M., N. Baghaei-Yazd, and M. Javed. 2001. Fermentative production of ethanol by heterologous expression of a pyruvate decarboxylase gene in Bacillus species. *Intn'l Patent Appl.* WO01049865.

Hallborn, J., M. Walfridsson, U. Airaksinen, H. Ojamo, B. Hahn-Hagerdal, M. Penttilä, and S. Keranen. 1991. Xylitol production by recombinant *Saccharomyces cerevisiae*. *Biotechnology* 9:1090–5.

Hamelinck, C.N., G.V. Hooijdonk, and A.P.C. Faaij. 2005. Ethanol from lignocellulosic biomass: Techno-economic performance in short-, middle- and long-term. *Biomass Bioenergy* 28:384–410.

Hartley, B.S., and G. Shama. 1987. Novel ethanol fermentations from sugar cane and straw. *Phil Trans Roy Soc Lond* A321:555–68.

Hartley, B.S. 1988. Thermophilic ethanol production. *International Patent Application* PCT/GB88/004.

Ho, N.W., Z. Chen, and A.P. Brainard. 1998. Genetically engineered *Saccharomyces* yeast capable of effective cofermentation of glucose and xylose. *Appl Environ Microbiol* 64: 1852–9.

Ho, N.W.Y., and S.F. Chang. 1989. Cloning of yeast xylulokinase gene by complementation of *E. coli* and yeast mutations. *Enzyme Microbiology and Technology* 11:417–21.

Inderwildi, OR., and King, DA., 2009. 'Quo Vadis Biofuels', *Energy & Environmental Science* 2, 343–346.

Ingram, L.O., H.C. Aldrich, A.C.C. Borges, T.B. Causey, A. Martinez, F. Morales, A. Saleh, S.A. Underwood, L.P. Yomano, S.W. York, J. Zaldivar, and S. Zhou. 1999. Enteric bacterial catalysts for fuel ethanol production. *Biotechnol Prog* 15:855–66.

Keim, C.R., and K. Venkatasubramanian. 1989. Economics of current biotechnological methods of producing ethanol. *Trends Biotechnol* 7:22–9.

Kuhad, R.C., A. Singh, and K.E. Eriksson. 1997. Micro-organisms and enzymes involved in the degradation of plant fiber cell walls. *Adv Biochem Eng Biotechnol* 57:45–125.

Kuyper, M., H.R. Harhangi, A.K. Stave, A.A. Winkler, M.S.M. Jetten, W.T.A.M. De Laat, J.J.J. Den Ridder, H.J.M. Op den Camp, J.P. Van Dijken, and J.T. Pronk. 2003. High-level functional expression of a fungal xylose isomerase: The key to efficient ethanolic fermentation of xylose by *Saccharomyces cerevisiae*? *FEMS Yeast Res* 4:69–78.

Kuyper, M., M.M.P. Hartog, M.J. Toirkens, M.J.H. Almering, A.A. Winkler, J.P. van Dijken, J.T. Pronk. 2005a. Metabolic engineering of a xylose-isomerase-expressing *Saccharomyces cerevisiae* strain for rapid anaerobic xylose fermentation. *FEMS Yeast Res* 5:399–409.

Kuyper, M., M.J. Toirkens, J.A. Diderich, A.A. Winkler, J.P. van Dijken, and J.T. Pronk. 2005b. Evolutionary engineering of mixed-sugar utilization by a xylose-fermenting *Saccharomyces cerevisiae* strain. *FEMS Yeast Res* 5:925–34.

Kuyper, M., A.A. Winkler, J.P. van Dijken, and J.T. Pronk. 2004. Minimal metabolic engineering of *Saccharomyces cerevisiae* for efficient anaerobic xylose fermentation: A proof of principle. *FEMS Yeast Res* 4:655–64.

Lawford, H.G., J.D. Rousseau, and J.S. Tolan. 2001. Comparative ethanol productivities of different *Zymomonas* recombinants fermenting oat hull hydrolysate. *Appl Biochem Biotechnol* 91–93:133–46.

Lee, J. 1997. Biological conversion of lignocellulosic biomass to ethanol. *J Biotechnol* 56:1–24.

Leitgeb, S., B. Petschacher, D.K. Wilson, and B. Nidetzky. 2005. Fine tuning of coenzyme specificity in family 2 aldo-keto reductases revealed by crystal structures of the Lys-274toArg mutant of *Candida tenuis* xylose reductase (*AKR2B5*) bound to NAD^+ and $NADP^+$. *FEBS Lett* 579:763–7.

Lerouge, P., M. Cabanes-Macheteau, C. Rayon, A.C. Fischette-Lainé, V. Gomord, and L. Faye. 1998. N-glycoprotein biosynthesis in plants: Recent developments and future trends. *Plant Molec Biol* 38:31–48.

Lin, H., G. N. Bennett, and K.-Y. San. 2005. Metabolic engineering of aerobic succinate production systems in *Escherichia coli* to improve process productivity and achieve the maximum theoretical succinate yield. *Metabolic Eng* 7:116–27.

Luli, G., and L. Ingram. 2005. UF/IFAS researcher's biomass-to-ethanol technology could help replace half of auto fuel in U.S. *University of Florida News*.

Lynd, L.R., C.E. Wyman, and T.U. Gerngross. 1999. Biocommodity engineering. *Biotechnol Prog* 15:777–93.

Meinander, N., B. Hahn-Haegerdal, M. Linko, P. Linko, and H. Ojamo. 1994. Fed-batch xylitol production with recombinant *XYL1* expressing *Saccharomyces cerevisiae* using ethanol as a co-substrate. *Appl Microbiol Biotechnol* 42:334–9.

Meinander, N., G. Zacchi, and B. Hahn-Hagerdal. 1996. A heterologous reductase affects the redox balance of recombinant *Saccharomyces cerevisiae*. *Microbiology* 142:165–72.

Metzger, M.H., and C.P. Hollenberg. 1995. Amino acid substitutions in the yeast *Pichia stipitis* xylitol dehydrogenase coenzyme-binding domain affect the coenzyme specificity. *Eur J Biochem* 228:50–4.

Nielsen, C., J. Larsen, F. Iversen, C. Morgen, and B.H. Christensen. 2002. Integrated Biomass Utlisation System (IBUS) for co-production of electricity and bioethanol. *EU Contract Report* ENK6-CT-2002-00650.

Ohta, K., D.S. Beall, J.P. Mejia, K.T. Shanmugam, and L.O. Ingram. 1991. Metabolic engineering of *Klebsiella oxytoca* M5A1 for ethanol production from xylose and glucose. *Appl Environ Microbiol* 57:2810–5.

Palmarois-Adrados, B., P. Choteborska, M. Gelbe, and G. Zacchi. 2005. Ethanol production from non-starch carbohydrates of wheat bran. *Bioresource Technol* 96:843–50.

Pessoa, A., I.M. Mancilha, and S. Sato. 1997. Acid Hydrolysis of Hemicellulose from. Sugarcane Bagasse. *Brazilian Journal of Chemical Engineering* 14(3).

Pye, E.K., and Lora, J.H., (1991). The Alcell process, a proven alternative to kraft pulping. *Tappi J.* 74:113–118.

Rajgarhia, V., K. Koivuranta, M. Penttilä, M. Ilmen, P. Suominen, A. Aristidou, C. Miller, S. Olson, and L. Ruohonen. 2004. Genetically modified yeast species and fermentation processes using genetically modified yeast. Patent Application WO 2004099381.

Rodriguez-Peña, J.M., V.J. Id, J. Arroyo, and C. Nombela. 1998. The *YGR194c* (*XKS1*) gene encodes the xylulokinase from the budding yeast *Saccharomyces cerevisiae*. *FEMS Microbiol Lett* 162:155–60.

San Martin, R., D. Busshell, D. Leak, and B.S. Hartley. 1993. Ethanolic fermentation of lignocellulose hydrolysates. *J Gen Microbiol* 139:1033–40.

Sarthy, A.V., B.L. McConaughy, Z. Lobo, J.A. Sundstrom, C.E. Furlong, and B.D. Hall. 1987. Expression of the *Escherichia coli* xylose isomerase gene in *Saccharomyces cerevisiae*. *Appl Environ Microbiol* 53:1996–2000.

Senac, T., and B. Hahn-Hägerdal. 1989. Intermediary metabolite concentrations in xylulose- and glucose-fermenting *Saccharomyces cerevisiae* cells. *Appl Environ Microbiol* 56:120–6.

Senac, T., and B. Hahn-Hägerdal. 1991. Effects of increased transaldolase activity on D-xylulose and D-glucose metabolism in *Saccharomyces cerevisiae* cell extracts. *Appl Environ Microbiol* 57:1701–6.

Stevis, P.A., J.J. Hang, and N.W.Y. Ho. 1987. Cloning of the *Pachysolen tannophilus* xylulokinase gene by complementation in *Escherichia coli*. *Appl Environ Microbiol* 53: 2975–7.

Takahashi, D.F., M.L. Carvalhal, and F. Alterhum. 1994. Ethanol production from pentoses and hexoses by recombinant *Escherichia coli*. *Biotechnol Lett* 16:747–50.

Takuma, S., N. Nakashima, M. Tantirungkij, S. Kinoshita, H. Okada, T. Seki, and T. Yoshida. 1991. Isolation of xylose reductase gene of *Pichia stipitis* and its expression in *Saccharomyces cerevisiae*. *Appl Biochem Biotechnol* 28–29:327–40.

Tantirungkij, M., T. Izuishi, T. Seki, and T. Yoshida. 1994. Fed-batch fermentation of xylose by a fast growing mutant of xylose-assimilating recombinant *Saccharomyces cerevisiae*. *Appl Microbiol Biotechnol* 41:8–12.

Tantirungkij, M., N. Nakashima, T. Seki, and T. Yoshida. 1993. Construction of xylose-assimilating *Saccharomyces cerevisiae*. *J Ferment Bioeng* 75:83–6.

Teeri, T.T., A. Koivula, M. Linder, G. Wohlfahrt, C. Divne, and T.A. Jones. 1998. *Trichoderma reesei* cellobiohydrolases: Why so efficient on crystalline cellulose. *Biochem Soc Trans* 26:173–8.

Toivari, M.H., L. Salusjärvi, L. Ruohonen, and M. Penttilä. 2004. Endogenous xylose pathway in *Saccharomyces cerevisiae*. *Appl Environ Microbiol* 70:3681–6.

Tolan, J.S., and R.K. Finn. 1987a. Fermentation of D-xylose and L-arabinose to ethanol by *Erwinia chrysanthemi*. *Appl Environ Microbiol* 53:2033–8.

Tolan, J.S., and R.K. Finn. 1987b. Fermentation of D-xylose to ethanol by genetically modified *Klebsiella planticola*. *Appl Environ Microbiol* 53:2039–44.

Underwood, S.A., S. Zhou, T.B. Causey, L.P. Yomano, K.T. Shanmugam, and L.O. Ingram. 2002. Genetic changes to optimize carbon partitioning between ethanol and biosynthesis in ethanologenic *Escherichia coli*. *Appl Environ Microbiol* 68:6263–72.

Vandeska, E., S. Kuzmanova, and T. W. Jeffries. 1995. Xylitol formation and key enzyme activities in *Candida boidinii* under different oxygen transfer rates. *J Ferment Bioeng* 80:513–6.

Vemuri, G.N., M.A. Eiteman, and E. Altman. 2002. Succinate production in dual-phase *Escherichia coli* fermentations depends on the time of transition from aerobic to anaerobic conditions. *J Indust Microbiol Biotechnol* 28:325–32.

Verduyn, C., R. Van Kleef, J. Frank, H. Schreuder, J.P. Van Dijken, and W.A. Scheffers. 1985. Properties of the NAD(P)H-dependent xylose reductase from the xylose-fermenting yeast *Pichia stipitis*. *Biochem J* 226:669–77.

Walfridsson, M., M. Anderlund, X. Bao, and B. Hahn-Hagerdal. 1997. Expression of different levels of enzymes from the *Pichia stipitis XYL1* and *XYL2* genes in *Saccharomyces cerevisiae* and its effects on product formation during xylose utilisation. *Appl Microbiol Biotechnol* 48:218–24.

Walfridsson, M., X. Bao, M. Anderlund, G. Lilius, L. Bulow, and B. Hahn-Hägerdal. 1996. Ethanolic fermentation of xylose with *Saccharomyces cerevisiae* harboring the *Thermus thermophilus xylA* gene, which expresses an active xylose (glucose) isomerase. *Appl Environ Microbiol* 62:4648–51.

Weissenborn, D.L., N. Wittekindt, and T.J. Larson. 1992. Structure and regulation of the glpFK operon encoding glycerol diffusion facilitator and glycerol kinase of Escherichia coli K-12. *J Biol Chem* 267:6162–31.

Wooley, R., M. Ruth, J. Sheehan, K. Ibsen, H. Majdeski, and A. Galvez. 1999. Lignocellulosic biomass to ethanol process design and economics. *NREL Technical Report* TP-580-26157.

Xarhangi, H.R., A.S. Akhmanova, R. Emmens, C. van der Drift, W.T.A.M. de Laat, J.P. van Dijken, M.S.M. Jetten, J.T. Pronk, H.J.M. Op den Camp. 2003. Xylose metabolism in the anaerobic fungus *Piromyces* sp. strain E2 follows the bacterial pathway. *Arch Microbiol* 180:134–41.

Yomano, L.P., S.W. York, and L.O. Ingram. 1998. Isolation and characterization of ethanol-tolerant mutants of *Escherichia coli* KO11 for fuel ethanol production. *J Ind Microbiol Biotechnol* 20:132–8.

Zhang, M., C. Eddy, K. Deanda, M. Finkelstein, S. Picataggio. 1995. Metabolic engineering of a pentose metabolism pathway in ethanologenic *Zymomonas mobilis*. *Science* 267:240–3.

Zhou, S., T. B. Causey, A. Hasona, K.T. Shanmugam, and L.O. Ingram. 2003a. Production of optically pure D-lactic acid in mineral salts medium by metabolically engineered *Escherichia coli* W3110. *Appl Environ Microbiol* 69:399–407.

Zhou, S., and L.O. Ingram. 2001. Simultaneous saccharification and fermentation of amorphous cellulose to ethanol by recombinant *Klebsiella oxytoca* SZ21 without supplemental cellulase. *Biotechnol Lett* 23:1455–62.

Zhou, S., K.T. Shanmugam, and L.O. Ingram. 2003b. Functional replacement of the *Escherichia coli* D-(–)-lactate dehydrogenase gene (*ldhA*) with the L-(+)-lactate dehydrogenase gene (*ldhL*) from *Pediococcus acidilactici*. *Appl Environ Microbiol* 69:2237–44.

This page intentionally left blank

10 Functional Genomics: Current Trends, Tools, and Future Prospects in the Fermentation and Pharmaceutical Industries

Surendra K. Chikara and Toral Joshi

CONTENTS

10.1 INTRODUCTION

Functional genomics is a discipline and enterprise that exploits the vast wealth of data produced by genome sequencing projects. A key feature of functional genomics is their genome-wide approach, which invariably utilizes high-throughput technologies and relies on sophisticated analytical tools.

Understanding the genome sequence and its relevance for various applications is therefore central to the development and production of new biopharmaceuticals. Current advances in bioinformatics and high-throughput technologies such as microarray analysis have revolutionalized our perception and understanding of the molecular mechanisms underlying normal and abnormal (dysfunctional) biological functions. Microarray studies and other genomic techniques are also inspiring the discovery of new targets for disease treatment and control, thus aiding drug development immunotherapeutics, and gene therapy (Zhao et al. 2011). Current trends and challenges in the field include

- Exploitation of new innovations in nanotechnology and microfluidics for the development of low-cost technologies for sequencing and genotyping as well as for the identification and confirmation of functional elements that do not encode protein (e.g., introns, promoters, **telomeres** and regulatory and structural features);
- *In vivo,* real-time monitoring of gene expression and functional modification of gene products in all relevant cell types using large-scale mutagenesis, small-molecule inhibitors, and knockdown approaches;
- Identifying genes and pathways that have thus far proved difficult to study biochemically and deciphering cellular phenomena related to the networking of metabolic pathways;
- Monitoring of membrane proteins, modified proteins, and regulatory proteins of low concentrations; and
- Correlation of genetic variation to human health and disease using haplotype and comprehensive variation information to provide large databases that are amenable to statistical methods.

Telomere: A telomere is a region of repetitive DNA located at the end of chromosomes to protect them from degradation.

The challenges faced in the human genome project and the need for high-throughput capacity have led to the development of next-generation sequencing technology (NGST), which has dramatically accelerated biological and biomedical research because it renders the comprehensive analysis of genomes, transcriptomes, and interactomes inexpensive, which should be helpful toward

achieving the goal of personalized medicine and designer crops (Horner et al. 2010). Of pharmaceutical relevance is sequencing of multiple strains of pathogens to monitor drug resistance and pathogenicity. Resequencing of selected regions to search for human variation in population and for tumor profiling to guide cancer therapies is also of great interest. In this chapter, we review current trends and methodologies in functional genomics and assess their relevance, strengths, and weaknesses.

Completion of the human genome project signalled a new beginning for modern biology, one in which most biological and biomedical research will be conducted in a sequence-based fashion. It is now possible to deconstruct the genomic sequences of multiple organisms with the view to unravel the interrelationship between the physiology or the pathogenicity of a given organism and its genome constituent parts (genes) (Cook Degan 1991; Evans 2010; Greenhalgh 2005; Johnson 1992). The deconstruction of the genome to assign biological functions to genes, groups of genes, and particular gene-gene or gene-protein interactions is well underway and documented in MEDLINE (Patterson and Gabriel 2009). These functions may be directly or indirectly the result of a gene's transcription (Mamanova et al. 2010). A computationally intensive branch of functional genomics has emerged as a result of the practical implementation of technologies to assess gene expression of thousands of genes at a time. The ability to comprehensively measure gene expression affords an excellent opportunity to further expand a target-oriented approach as opposed to the conventional hypothetical-based approach.

The need to generate, analyze, and integrate large and complex sets of molecular data has led to the development of whole-genome approaches, such as microarray technology, to expedite the process of translating molecular data into biologically meaningful information (Miyake and Matsumoto 2005). The comparison of the strengths and weakness of next-generation sequencing and microarray techniques is illustrated in Table 10.1 (Asmann et al. 2008).

The paradigm shift from traditional single-molecule studies to whole-genome approaches requires standard statistical modelling and algorithms as well as high-level hybrid computational/statistical automated learning systems for improving the understanding of complex traits. Microarray experiments provide unprecedented quantities of genome-wide data on gene expression patterns. The implementation of a successful uniform program of expression analysis requires the development of various laboratory protocols and the development of database and software tools for efficient data handling and mining (Teng and Xiao 2009). The computational tools necessary to analyze the data are rapidly evolving. The effect of microarray measurements on biology and bioinformatics has been astonishing.

TABLE 10.1
The Strength and Weaknesses of NGS and Microarray Techniques

Microarray Analysis		Massively Parallel, or NGS	
Pros	**Cons**	**Pros**	**Cons**
Relatively inexpensive	High background, low sensitivity	Low background, very sensitive	Expensive
Easy sample preparation	Limited dynamic range	Large dynamic range	Complex sample preparation
Mature informatics and statistics	Not quantitative	Quantitative	Limited bioinformatics
Competitive hybridization		Massive information technology infrastructure required	
Annotation of the probes			

Source: Information from Asmann, Y.W., Wallace, M.B., and Thompson, E.A., *Gastroenterology*, 135:1466–8, 2008 and reproduced with the kind permission of Elsevier, New York.

10.2 MICROARRAYS: ROLE IN FUNCTIONAL GENOMICS

Complementary DNA microarrays, oligonucleotide microarrays, or serial analysis of gene expression (SAGE) are widely used microarray tools (Antipova et al. 2002). In this section, we will focus on microarrays, which are artificially constructed grids of DNA such that each holds a DNA sequence that is a reverse complement to the target RNA sequence. Although there are many protocols, the basic technique involves the incorporation of fluorescent nucleotides or a tag, which is later stained with fluorescence, into the extracted RNA. The labelled RNA is then hybridized to a microarray for a period of time, after which the excess is washed off and the microarray is scanned under laser light. All probes are designed to be hypothetically similar with regard to hybridization temperature and binding affinity for oligonucleotide microarrays (Brennan et al. 2004), and for which each microarray measures the level of each RNA molecule in each sample, although this absolute measurement might not correlate exactly with RNA concentration in terms of micrograms per unit volume (Steibel and Rosa 2005). With cDNA microarrays (Rogers et al. 2005), in which each probe has its own hybridization characteristic, each microarray measures two samples and provides a relative measurement level for each RNA molecule. Because a complete experiment involves hundreds of microarrays, the resultant RNA expression data sets can vary greatly in size. As the cost of microarrays continues to drop, it is clear that microarrays are becoming more integral to the drug discovery programs (Wu et al. 2005). In addition to the obvious use of functional genomics in basic research and target discovery, there are many other specific uses (e.g., biomarker determination) to find genes that correlate with and presage disease progression, and in toxicogenomics, to find gene expression patterns in tissues or organisms exposed in response to a given drug to develop early warning diagnostic predictors for the onset of disease (Wu et al. 2005). Many free and commercial software packages are available to analyze microarray data, although it is still difficult to find a single off-the-shelf software package that answers all functional genomics questions (Aburatani 2005).

The two basic applications of DNA microarrays are studying genome structure and gene expression analysis.

10.2.1 Applications of Microarray to the Study of Genome Structure

Microarray methods used for the study of genome structure include

- *Comparative genomic hybridisation (CGH) arrays*: This method has been widely used for the detection of large changes in the genome (e.g., deletions, insertions, and copy number variation) (Miyake and Matsumoto 2005).
- *Single-nucleotide polymorphism (SNP) arrays*: This method is useful in genotyping, designed at present to identify SNPs, other than that it also identifies loss of heterozygosity (LOH), copy number variation (CNV), allelic imbalance (AI), and uniparental dispute (UPD).
- *Tiling arrays*: This method is used in the study and analysis of DNA-protein interactions, methyl-DNA immunoprecipitation (MeDIP-chip, epigenetic studies), chromatin hypersensitive sites localization (DNase-chip), gene annotation, and mapping.

10.2.2 Applications of Microarray to the Study of Gene Expression and Profiling

Gene expression profiles are precise, and the methods of microarrays used and their applications are as follows:

- *cDNA arrays*: In this method, the probes and cDNA clones are spotted onto a glass slide using printing robots.
- *Tiling arrays*: Play a major role in discovering new transcriptionally active regions and splice variants.

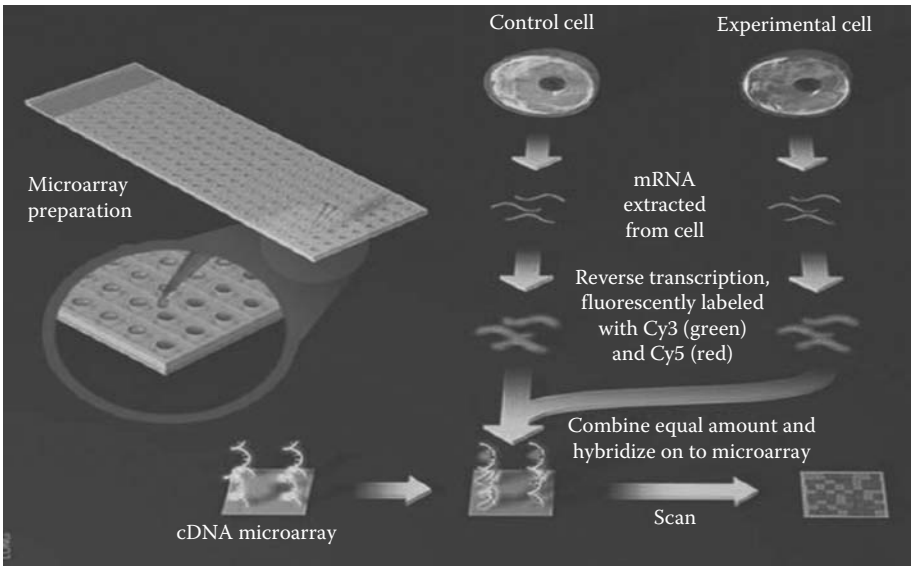

FIGURE 10.1 Microarray technology. The picture depicts extraction of mRNA from two types of cells (e.g., tumor cells and control cells) and then labels the samples with different fluorescent dyes. When washed over the microarray, these colored transcripts bind to their complementary probes, leaving a trail of informative spots: red for genes turned on in cancer cells, green for genes turned on in normal cells, yellow for genes turned on in both types of cells—with more intense color indicating higher gene activity. (Courtesy of the *Science Creative Quarterly*, Jiang Long, artist.)

- *Exon arrays*: Utilizes separate probes designed to detect individual exons and is useful in the detection of splicing isoforms.
- *CSH array*: This method is specially designed for the organisms for which the genome is not sequenced and also helps to identify the gene expression for the same.

A few microarray platforms have been developed to accomplish this task, and the basic idea for each is simple: A glass slide or membrane is spotted or "arrayed" with DNA fragments or an oligonucleotide that represents specific gene coding regions. After that, purified RNA is fluorescently or radioactively labeled and hybridized to the slide or membrane. In some cases, hybridization is done simultaneously with reference RNA to facilitate comparison of data across multiple experiments. Subsequent to thorough washing, the raw data are obtained by laser scanning or autoradiographic imaging (Figure 10.1).

10.3 MICROARRAY QUALITY CONTROL

Microarray quality control (MAQC) compares performance of different microarray platforms with respect to their sensitivity, specificity, dynamic range, precision, and accuracy (Hardiman 2004). The study included microarrays from five major vendors—Affymetrix, Agilent, Applied BioSystems, Nimblegen, and Illumina—and is published online in *Nature Biotechnology* 2006 http://www.nature.com/nature/journal/v442/n7106/full/4421067a.html. One of the major limitations of expanding the use of microarray technology is that the values of expression generated on different platforms cannot be directly compared because of the unique labelling methods and probe sequences used. However, the results of the MAQC consortium demonstrated that most major commercial platforms can be selected with confidence (Hester et al. 2009).

10.3.1 Affymetrix

Affymetrix microarray technology is based on the hybridization of small, high-density arrays containing tens of thousands of synthetic oligonucleotides (Elo et al. 2005). The arrays are designed based on sequence information alone and are synthesized in situ using a combination of photolithography and oligonucleotide chemistry. RNAs present at a frequency of 1:300,000 are readily detected and quantified; the method is readily scalable to the simultaneous monitoring of tens of thousands of genes. The Affymetrix integrated GeneChip arrays include up to 500,000 unique probes corresponding to tens of thousands of gene expression measurements (Della et al. 2008).

Affymetrix manufactures arrays that monitor the global activities of genes in yeast, *Arabidopsis*, *Drosophila*, mice, rats, and humans. Apart from that, custom expression arrays can be designed for other model organisms, proprietary sequences, or specific subsets of known genes. For the starting point, the clusters are used, and sequences are further subdivided into subclusters representing distinct transcripts. This categorization process involves alignment to the genome, which reveals splicing and polyadenylation variants. The newest product for Affymetrix is Axiom for genome-wide association studies (GWAS), replication studies, and candidate gene association studies. It includes predesigned and personalized array plates with validated genomic content from the Axiom genomic database. This solution also includes complete reagent kits, data analysis tools, and a fully automated workflow.

10.3.2 NimbleGen MS 200 Microarray and Scanner

Roche NimbleGen, Inc., distinctively produces high-density arrays of long oligonucleotide probes that provide better information content and higher data quality necessary for studying the full diversity of genomic and epigenomic variation. Roche NimbleGen ensures high-definition genomics by providing scientists with cost-effective, high-throughput tools for extracting and integrating complex data on important forms of genomic and epigenomic variation not previously accessible on a genome-wide scale. This enhanced feature is made possible by Roche NimbleGen's proprietary Maskless Array Synthesis (MAS) technology, which utilizes digital light processing, and rapid, high-yield photochemistry to synthesize long oligonucleotide, high-density DNA microarrays with extreme flexibility, thus facilitating a clearer understanding of epigenomics. Roche NimbleGen offers a complete catalog of gene expression arrays for whole-genome expression profiling. With the unique combination of long oligonucleotide probes, flexible array content, and high probe density (up to 385,000 probes per array), NimbleGen gene expression arrays enable analysis of eukaryotic and prokaryotic genomes. Built on the ultrahigh-density HD2 platform, the 12- by 135-K array format combines a multiplex option with high probe density for high-throughput projects (Figure 10.2). It allows for running of replicates within the same array that validate analysis within the same experiment. Also, conducting the array hybridization is relatively straightforward, and analysis of the results is user-friendly and does not require highly specialized informatics skills (Mueckstein et al. 2010).

NimbleGen microarrays enable precise, sensitive, and specific interrogation of genome-wide expression for any prokaryotic or eukaryotic sequenced and annotated genome.

10.3.3 Agilent DNA Microarray and Scanner

Agilent Technologies manufactures probes using a proprietary DNA synthesis method based on inkjet printing technology for microarrays. The method, in which layers of DNA nucleotides are "printed" onto desired microarray feature locations to synthesize probes, circumvents many of the limitations of light-based synthesis methods and is capable of producing oligonucleotide probes of unprecedented quality and length. Light-based DNA chemistry is another common method

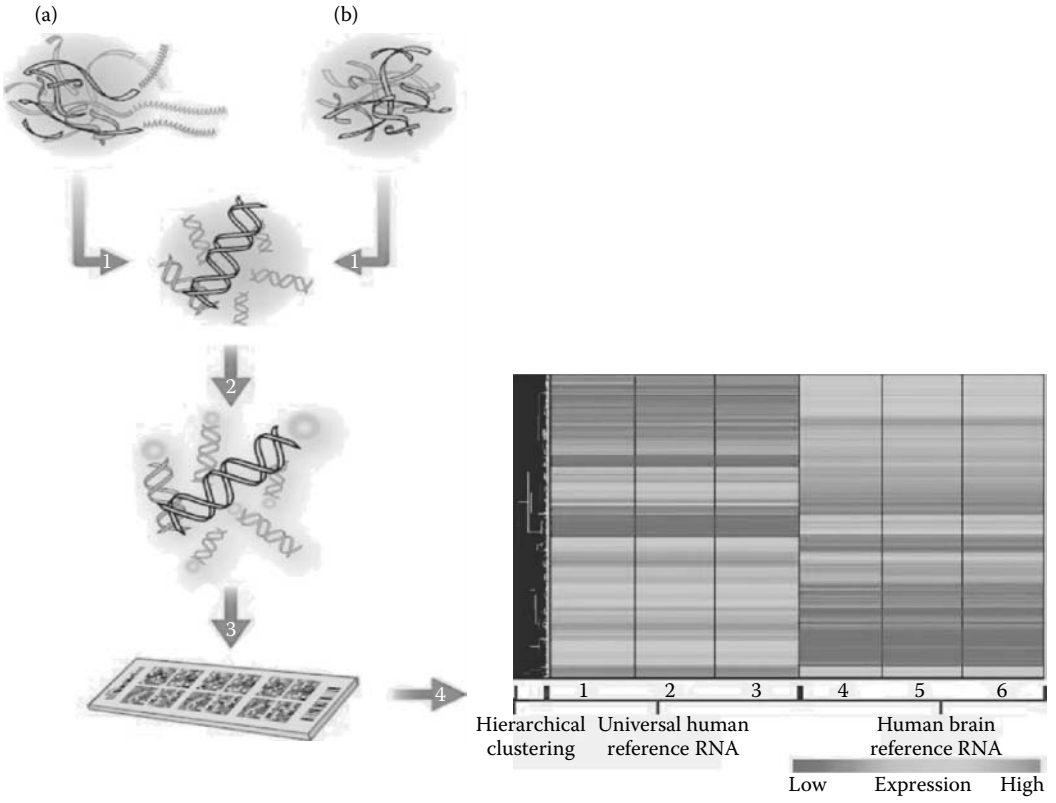

FIGURE 10.2 (1) cDNA synthesis: eukaryotic (a) or prokaryotic mRNA (b) is converted via oligo-dT or random priming, respectively, to double-stranded cDNA. (2) cDNA labeling: The cDNA is labeled with Cy3 dye. (3) Hybridization: labeled cDNA is hybridized to a NimbleGen gene expression array. (4) Data analysis: Data are extracted using NimbleScan software and analyzed for differentially expressed genes.

implemented for synthesizing oligonucleotide probes for microarrays (Zahurak et al. 2007). Agilent has combined some of the best features of both of these approaches and has gained widespread acceptance as a result.

Agilent combines two-sample hybridization with use of long (60-mer) oligonucleotides. These arrays are hybridized with two different fluorescent samples and measurements of differential expression obtained from the relative abundance of hybridized mRNA. Agilent's methodology achieves an extraordinary 99.5% stepwise DNA synthesis yield and produces probes with very high sequence fidelity. This platform can produce accurate relative quantization of gene expression levels over a range of more than 5 orders of magnitude, far exceeding the capabilities of other systems.

Agilent's Feature Extraction algorithms were developed aiming to reduce systematic errors that arise from labeling bias, irregular feature morphologies, and mismatched sample concentrations and crosshybridization. They quantify feature signals and their background, perform background subtraction and dye normalization, and calculate feature log ratios and error estimates (Lopez-Romero et al. 2010). The error estimates, which are based on an extensive error model and pixel-level statistics calculated from the feature and background for each spot, are used to generate a *P* value for each log ratio. The file produced by Agilent's extraction software also contains raw pixel intensity data. These intensities, whether they are mean or median values, can easily be exported to other software, such as R.

10.4 MICROARRAY APPLICATIONS

10.4.1 Gene Expression Profiling

Gene expression profiling is the measurement of the activity (the expression) of thousands of genes at once to create a global picture of cellular function (Velculescu et al. 1995). These profiles can distinguish between cells that are actively dividing or show how the cells react to a particular treatment. Many experiments of this sort simultaneously measure an entire genome; that is, every gene present in a particular cell (Shiu and Borevitz 2008).

In an mRNA or gene expression profiling experiment, the expression levels of thousands of genes are simultaneously monitored to study the effects of certain treatments, diseases, and developmental stages on gene expression. Gene expression profiling may become an important diagnostic test. Expression profiling provides new information about what genes do under various conditions. Overall, microarray technology produces reliable expression profiles. Apart from this the other applications are in the field of comparative genomic hybridization using oligonucleotide microarray (Barrett et al. 2004).

10.4.2 CGH

CGH provides an alternative means of genome-wide screening for CNVs (Pinkel and Albertson 2005). First developed to detect copy number changes in solid tumors, CGH uses two genomes—a test and a control—that are differentially labeled and competitively hybridized to metaphase chromosomes. The fluorescent signal intensity of the labeled test DNA relative to that of the reference DNA can then be linearly plotted across each chromosome, allowing for the identification of copy number changes.

Unlike traditional techniques used to detect copy number gains and losses, which rely on the examination of a single target and prior knowledge of the region under investigation, CGH can be used to quickly scan an entire genome for imbalances (Hester et al. 2009). In addition, CGH does not require cells that are undergoing division. However, as with earlier cytogenetic methods, the resolution of CGH has been limited to alterations of approximately 5–10 Mb for most clinical applications.

10.4.3 Detection of SNP

An SNP array is a useful tool to study the whole genome. The most important application of SNP array is in determining disease susceptibility and, consequently, in pharmacogenomics by measuring the efficacy of drug therapies specifically for the individual. Because each individual has many SNPs that together create a unique DNA sequence, SNP-based genetic linkage analysis could be performed to map disease loci and hence determine disease susceptibility genes for an individual (Rauch et al. 2004). The combination of SNP maps and high-density SNP array allows for the efficient use of SNPs as the markers for Mendelian diseases with complex traits. A SNP array can also be used to generate a virtual **karyotype** using specialized software to determine the copy number of each SNP on the array and then align the SNPs in chromosomal order. In addition, SNP array can be used for studying the LOH. LOH is a form of AI that can result from the complete loss of an allele or from an increase in copy number of one allele relative to the other (Leykin et al. 2005; Kamath et al. 2009). SNP array is also capable of detecting extra chromosomes due to UPD.

Karyotype [kar-ee-uh-tahyp]: A systematized arrangement of chromosomes displayed in pairs and arranged in descending order of size.

10.4.4 Chromatin Immunoprecipitation

ChIP-on-chip is a technique that combines chromatin immunoprecipitation with microarray technology. ChIP-on-chip is used to investigate *in vivo* interactions between proteins and DNA. It allows for the identification of the cistrome, which is the set of DNA binding sites of a *trans*-acting factor

on a genome-wide basis. Whole-genome analysis can be performed to determine the locations of binding sites for almost any protein of interest. The aim is to localize protein binding sites that may help identify functional elements in the genome. For example, in the case of a transcription factor as a protein of interest, one can determine its transcription factor binding sites throughout the genome. Other proteins allow for the identification of promoter regions, enhancers, repressors and silencing elements, insulators, boundary elements, and sequences that control DNA replication. One of the long-term goals of ChIP-on-chip is to establish a catalogue of organisms that lists all protein-DNA interactions under various physiological conditions (Von 2008). This knowledge would ultimately help in the understanding of the machinery behind gene regulation, cell proliferation, and disease progression. Hence, ChIP-on-chip offers not only huge potential to complement our knowledge about the orchestration of the genome on the nucleotide level, but also on higher levels of information and regulation as it is propagated by research on epigenetics (Gebauer 2004).

10.4.5 Transcriptome Analysis

Whole **transcriptome** analysis is one of the most general requirements to address many applied or basic biological questions. One of the most efficient tools to carry out such analyses relies on the use of microarrays coupled to specific labeling of cDNA populations generally reflecting two states of the transcriptome. Up until recently, DNA microarray was the procedure of choice for transcriptome analysis, but it has now been superseded by high-throughput sequencing technologies (RNA-Seq), which have become an additional alternative to microarrays.

Transcriptome: A transcriptome is the entire set of all RNA molecules, including mRNA, rRNA, and tRNA species that exist in a given organism under certain conditions. Because it includes all mRNA transcripts in the cell, the transcriptome reflects the genes that are actively expressed under certain conditions.

10.4.6 Application of DNA Microarray in the Pharmaceutical Industries

Natural product research is often based on ethnobotanical information, and many of the drugs used today were used in indigenous societies. The aim of ethnopharmaceutical research is better understanding of the pharmacological effects of different medicinal plants traditionally used in healthcare. Plants are regarded as a promising source of novel therapeutic agents because of their higher structural diversity as compared with standard synthetic chemistry. Plants have applications in the development of therapeutic agents as a source of bioactive compounds for possible use as drugs. There are three approaches to natural product-based drug discovery: screening of crude extracts, screening of prefractionated extracts, and screening of pure compounds. There are three main applications of DNA microarrays:

1. The pharmacodynamics for discovery of new diagnostic and prognostic indicators and biomarkers of therapeutic response; elucidation of molecular mechanism of action of an herb, its formulations, or its phytochemical components; and identification and validation of new molecular targets for herbal drug development (Crowther 2002).
2. Pharmacogenomics for prediction of potential side effects of the herbal drug during preclinical activity and safety studies, identification of genes involved in conferring drug sensitivity or resistance, and prediction of patients most likely to benefit from the drug and use in general pharmacogenomics studies.
3. Pharmacognosy for correct botanical identification and authentication of crude plant materials, which is done as part of standardization and quality control (Crowther 2002).

10.4.7 Microarray Future Prospects

At present, the major practical applicability of DNA microarrays remains in SNP mapping, genotyping, and pharmacogenetics. In recent years, array-based sequencing that combines target

hybridization with enzymatic primer extension reactions has emerged as a powerful means to scan for all possible DNA sequence variations. Although DNA microarrays have huge potential for pharmacodynamic and toxicogenomic applications, these are still in the exploratory stage and need validation by other biological experiments (Debouck and Goodfellow 1999). With the development of new, uniform, and more sophisticated experimental designs, data management system statistical tools, and algorithms for data analysis, DNA microarrays can be optimally used in herbal drug research. Despite the huge potential offered by microarray technology, the importance of *in vitro* biological assays, cell-line studies, and *in vivo* animal studies cannot be ignored. A comprehensive strategy integrating information from diverse scientific experiments and technologies will lead to molecular evidence-based herbal medicine.

Functional genomics: Functional genomics is a discipline of biotechnology that attempts to exploit the vast wealth of data produced by genome sequencing projects. A key feature of functional genomics is its genome-wide approach, which invariably involves the use of a high-throughput approach.

Microarrays play an important role in **functional genomics**, and the completion of many genome sequencing projects fuels more and more projects in the area (Jares 2006). Genomic differences such as SNPs can result in functional differences by changing particular entities (e.g., protein coding parts) or affecting gene regulation (regulatory SNPs). In short, genotypic differences need to be seen in a functional context and do not provide conclusive information on their own or in isolation.

A thorough downstream analysis of functional connections and consequences is mandatory to close the gap between mere data (sequence tags) and functional changes observed on a higher level paralleling the requirements already known from microarray analyses (Putonti 2007). The very first step on this path from data to knowledge is to put the raw sequence reads into the coordinate system of a reference genome via genome annotation establishing the physical context.

10.5 NEXT-GENERATION DNA SEQUENCING

Next-generation sequencing (NGS) is well suited to provide all of the primary data required (i.e., the sequences) for genomics, epigenetics, transcription factor binding, and transcriptomics in virtually unlimited detail. NGS also enables the cheapest and fastest method of *de novo* sequencing and resequencing. New sequencing technologies have emerged, including 454 life sciences (Roche), Genome Analyser (Illumina, Inc.), SOLiD (Applied BioSystems), HeliScope (Helicos BioSciences), Pacific Bio, VisiGen, and Ion torrent, and provide sequencing capability with much higher throughputs and at greatly reduced costs (Mardis 2008a). In Section 10.5.1, we shall highlight the strength and limitations of current and emerging techniques.

10.5.1 First-Generation Sequencers

10.5.1.1 Sanger's Sequencing Method

Sanger's method, also referred to as "dideoxy sequencing" or "chain termination", is based on the use of dideoxynucleotides (ddNTPs) in addition to the normal nucleotides (NTPs) found in DNA. ddNTPs differ from NTPs in that the hydroxyl group at the 3'-carbon atom is replaced by a hydrogen atom. Incorporation of a ddNTP will prevent the formation of a 3'-5' phosphodiester bond, which in turn brings chain extension to an end. Apart from nonspecific binding of the primer to the DNA, this method is time-consuming and excessively expensive.

10.5.2 Second-Generation Sequencers

The second-generation sequencers are those based on massive parallel analysis. "Second generation" is in reference to the various implementations of cyclic-array sequencing that has recently been realized in a commercial product. A detailed comparison of second-generation sequencers is given in Table 10.2.

TABLE 10.2
Comparison between Second-Generation Sequencers Depending on the Read Lengths Data per Run, Cost of the Machine, and Cost of the Base per Run

	ABI 3730 XL (First Released in 2005)	Roche GS FLX (First Released in October 2005)	GAIIx (First Released in June 2006)	5500, 5500XL, and SOLiD4 (First Released in October 2007)
Read length	600–900 bp	25, 100, 300, 400, and 500 bp	18, 26, 36, 50, 75, and 100 bp	10,25,35,50,75 bp
Data per run	1 mbps	350–450 Mb	30–100 Gb	40–300 Gb
Machine cost	$400,000	$700,000	$850,000	800,000$
Run cost per base	$1000/Mb	$27,000/Gb	$1200/Gb	1250$/Gb
Limitation	Expensive, low throughput, labor-intensive	High cost, repetitive region	Short read assembly mapping	Short read assembly mapping
Application of choice	De novo sequencing of complex genome	De novo genome, de novo transcript, metagenomics	Resequencing SNP transcriptome	Resequencing SNP, miRNA transcriptome

10.5.2.1 Roche GS FLX (Pyrosequencing)

In pyrosequencing, incorporation of each nucleotide by DNA polymerase results in the release of pyrophosphate, which initiates a series of cascading reactions that ultimately yield light by the firefly enzyme luciferase. The amount of light produced is proportional to the number of nucleotides incorporated. In the Roche/454 approach, the library fragments are mixed with a population of agarose beads for which the surfaces are coated with oligonucleotides complementary to the 454-specific adapter sequences on the fragment library so that each bead is associated with a single fragment (Mardis 2008a). Each of these fragment bead complexes is isolated into individual oil water micelles that also contain PCR reactants, and thermal cycling (emulsion PCR) of the micelles produces approximately 1 million copies of each DNA fragment on the surface of each bead. These amplified single molecules are then sequenced in mass. First, the beads are arrayed into a picotiter plate that holds a single bead in each of several hundred thousand single wells; this provides a fixed location at which each sequencing reaction can be monitored. Enzyme-containing beads that catalyze the downstream pyrosequencing reaction steps are then added to the Picotiter Plate (PTP), and the mixture is centrifuged to surround the agarose beads (Ansorge 2009). On the instrument, the PTP acts as a flow cell into which each pure nucleotide solution is introduced in a stepwise fashion with an imaging step after each nucleotide incorporation step. The PTP is seated opposite a CCD camera that records the light emitted at each bead. The first four nucleotides (TCGA) on the adapter fragment adjacent to the sequencing primer added in library construction correspond to the sequential flow of nucleotides into the flow cell. For more details, the reader is advised to consult http://www.454.com (Morozova and Marra 2008a).

The present Genome Sequencer FLX Instrument, powered by GS FLX Titanium series reagents, features a groundbreaking combination of long reads, exceptional accuracy, and high throughput. The breadth of applications includes *de novo* sequencing and resequencing of whole genomes, metagenomics, and RNA analysis (Shendure and Ji 2008).

10.5.2.2 Illumina Genome Analyzer

The Solexa sequencing platform was commercialized in 2006. The principle is based on sequencing-by-synthesis chemistry with novel reversible terminator nucleotides for the four bases, each labeled with a different fluorescent dye, and a special DNA polymerase enzyme able to incorporate

them. DNA fragments are ligated at both ends to adapters and, after denaturation, are immobilized at one end on a solid support. The surface of the support is coated densely with the adapters and the complementary adapters (Ansorge 2009). Each single-stranded fragment, immobilized at one end on the surface, creates a "bridge" structure by hybridizing with its free end to the complementary adapter on the surface of the support. In the mixture containing the PCR amplification reagents, the adapters on the surface act as primers for the following PCR amplification. Again, amplification is needed to obtain sufficient light signal intensity for reliable detection of the added bases. After several PCR cycles, random clusters of approximately 1000 copies of single-stranded DNA fragments (termed DNA "polonies", resembling cell colonies after polymerase amplification) are created on the surface. The reaction mixture for the sequencing reactions and DNA synthesis is supplied onto the surface and contains primers, four reversible terminator nucleotides each labeled with a different fluorescent dye, and the DNA polymerase. After incorporation into the DNA strand, the terminator nucleotide, as well as its position on the support surface, is detected and identified via its fluorescent dye by the CCD camera as shown in Figure 10.3 (Mardis 2008b). The terminator group at the 3'-end of the base and the fluorescent dye are then removed from the base and the synthesis cycle is repeated. The sequence read length achieved in the repetitive reactions is approximately 35 nucleotides. The sequence of at least 40 million polonies can be simultaneously determined in parallel, resulting in a very high sequence throughput on the order of gigabases per support. A base-calling algorithm assigns sequences and associated quality values to each read, and a quality-checking pipeline evaluates the Illumina data from each run, removing poor-quality sequences.

In 2008, Illumina introduced an upgrade, the Genome Analyser II, that triples output compared with the previous Genome Analyser instrument. Evidenced by a vast number of peer-reviewed publications in an ever-broadening range of applications, Illumina sequencing technology with the Genome Analyser is a proven platform for genomic discovery and validation.

10.5.2.3 Applied Biosystems SOLiD™ 4 System

The SOLiD platform uses an adapter-ligated fragment library and an emulsion PCR approach with small magnetic beads to amplify the fragments for sequencing. Unlike other platforms, SOLiD uses DNA ligase and a unique approach as illustrated in Figure 10.4.

In this technique, DNA fragments are ligated to adapters and then bound to beads. A water droplet in oil emulsion contains the amplification reagents and only one fragment bound per bead; the emulsion PCR amplifies DNA fragments on the beads. After DNA denaturation, the beads are deposited onto a glass support surface. Libraries may be constructed by any method that gives rise to a mixture of short, adaptor-flanked fragments, although much effort with this system has been put into protocols for mate-paired tag libraries with controllable and highly flexible distance distributions. Clonal sequencing features are generated by emulsion PCR, with amplicons captured to the surface of 1-μM paramagnetic beads. After breaking the emulsion, beads bearing amplification products are selectively recovered and then immobilized to a solid planar substrate to generate a dense, disordered array. Sequencing by synthesis is driven by a DNA ligase rather than a polymerase. A universal primer complementary to the adaptor sequence is hybridized to the array of amplicon-bearing beads (Ansorge 2009). Each cycle of sequencing involves the ligation of a degenerate population of fluorescently labeled octamers. The octamer mixture is structured in that the identity of specific position(s) within the octamer (e.g., base 5) correlate with the identity of the fluorescent label. After ligation, images are acquired in four channels that effectively collect data for the same base positions across all template-bearing beads. The octamer is then chemically cleaved between positions 5 and 6, removing the fluorescent label. Progressive rounds of octamer ligation enable sequencing of every fifth base (e.g., bases 5, 10, 15, and 20). Upon completing several such cycles, the extended primer is denatured to reset the system. Subsequent iterations of this process can be directed at a different set of positions (e.g., bases 4, 9, 14, and 19) by using a primer that is set back one or more bases from the adaptor-insert junction or by using different mixtures of octamers in which a different position (e.g., base 2) is correlated with the label. An additional feature of this

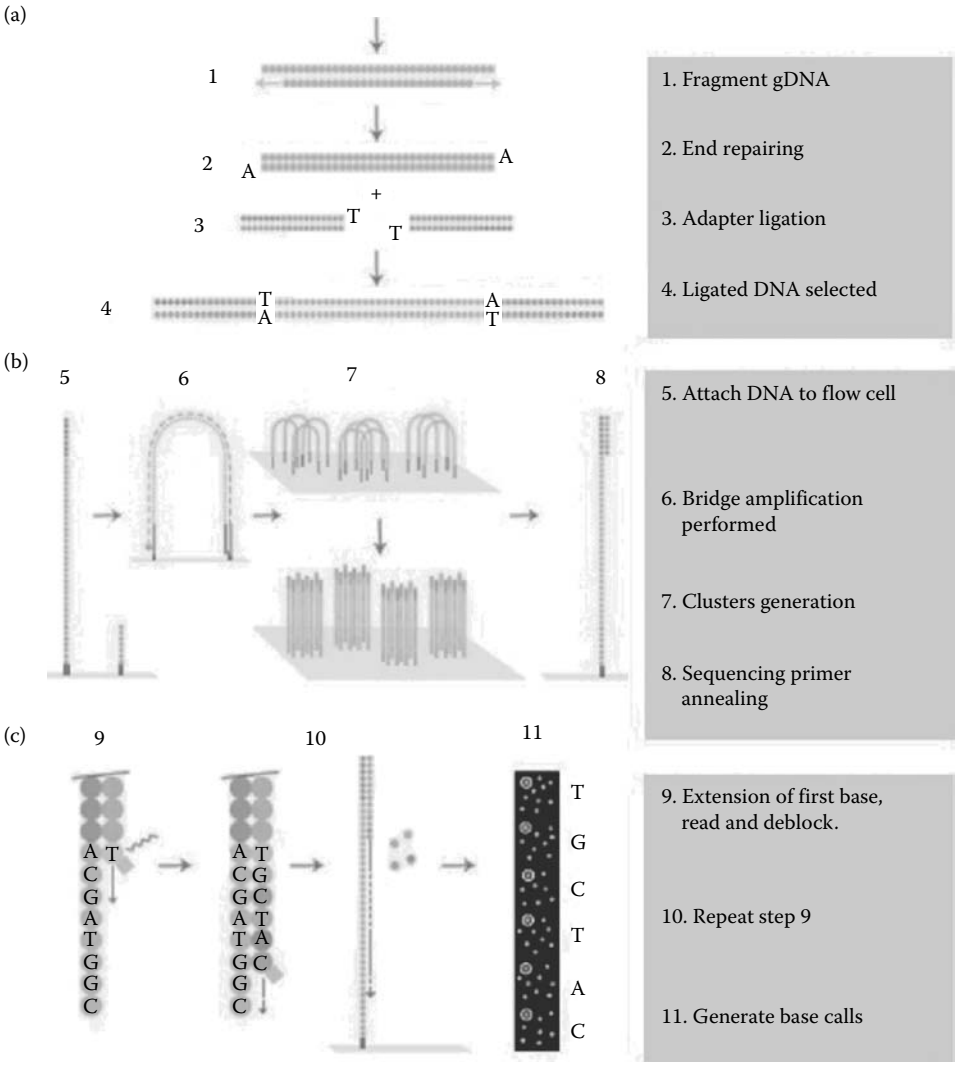

FIGURE 10.3 Outline of the Illumina Genome Analyser workflow. Similar fragmentation and adapter ligation steps take place (a), before applying the library onto the solid surface of a flow cell. Attached DNA fragments form "bridge" molecules that are subsequently amplified via an isothermal amplification process, leading to a cluster of identical fragments that are subsequently denatured for sequencing primer annealing (b). Amplified DNA fragments are subjected to sequencing-by-synthesis using 30 blocked labeled nucleotides (c).

platform involves the use of two-base encoding, which is an error-correction scheme in which two adjacent bases (Mardis 2008a), rather than a single base, are correlated with the label. Each base position is then queried twice such that miscalls can be more readily identified.

The Applied Biosystems SOLiD 4 system is a revolutionary genetic analysis platform (Figure 10.5) that enables parallel sequencing of clonally amplified DNA fragments linked to beads. The method has the following advantages over its counterparts:

- It enables researchers to obtain higher-quality genomes at lower cost without the purchase of a new instrument.
- *Scalable system:* The open-slide format and flexible bead densities enable increases in throughput with protocol and chemistry optimizations.

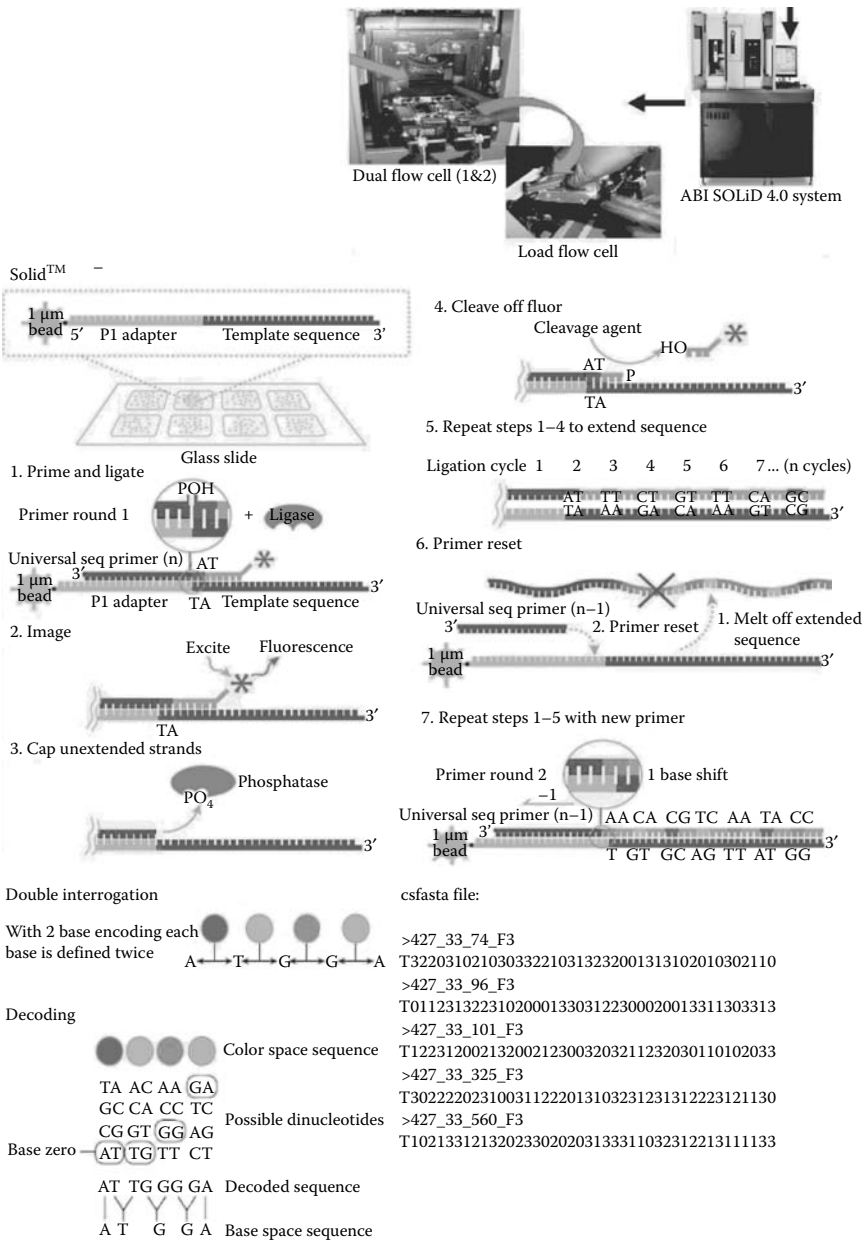

FIGURE 10.4 Sequencing-by-ligation using, the SOLiD DNA sequencing platform. Step 1–6 (a): Primers hybridize to the P1 adapter within the library template. A set of four fluorescence labeled di-base probes competes for ligation to the sequencing primer. These probes have a partly degenerated DNA sequence (indicated by n and z) and for simplicity only one probe is shown (labeling is denoted by asterisk). Specificity of the di-base probe is achieved by interrogating the first and second base in each ligation reaction (CA in this case for the complementary strand). Following ligation, the fluorescent label is enzymatically removed together with the three last bases of the octamer. Step–7 (b): Sequence determination by the SOLiD DNA sequencing platform is performed in multiple ligation cycles, using different primers, each one shorter from the previous one by a single base. The number of 5–15 ligation cycles determines the eventual read length, from primer (n) to primer (n _ 4), and double interrogation and decoding of csfasta format of the read data.

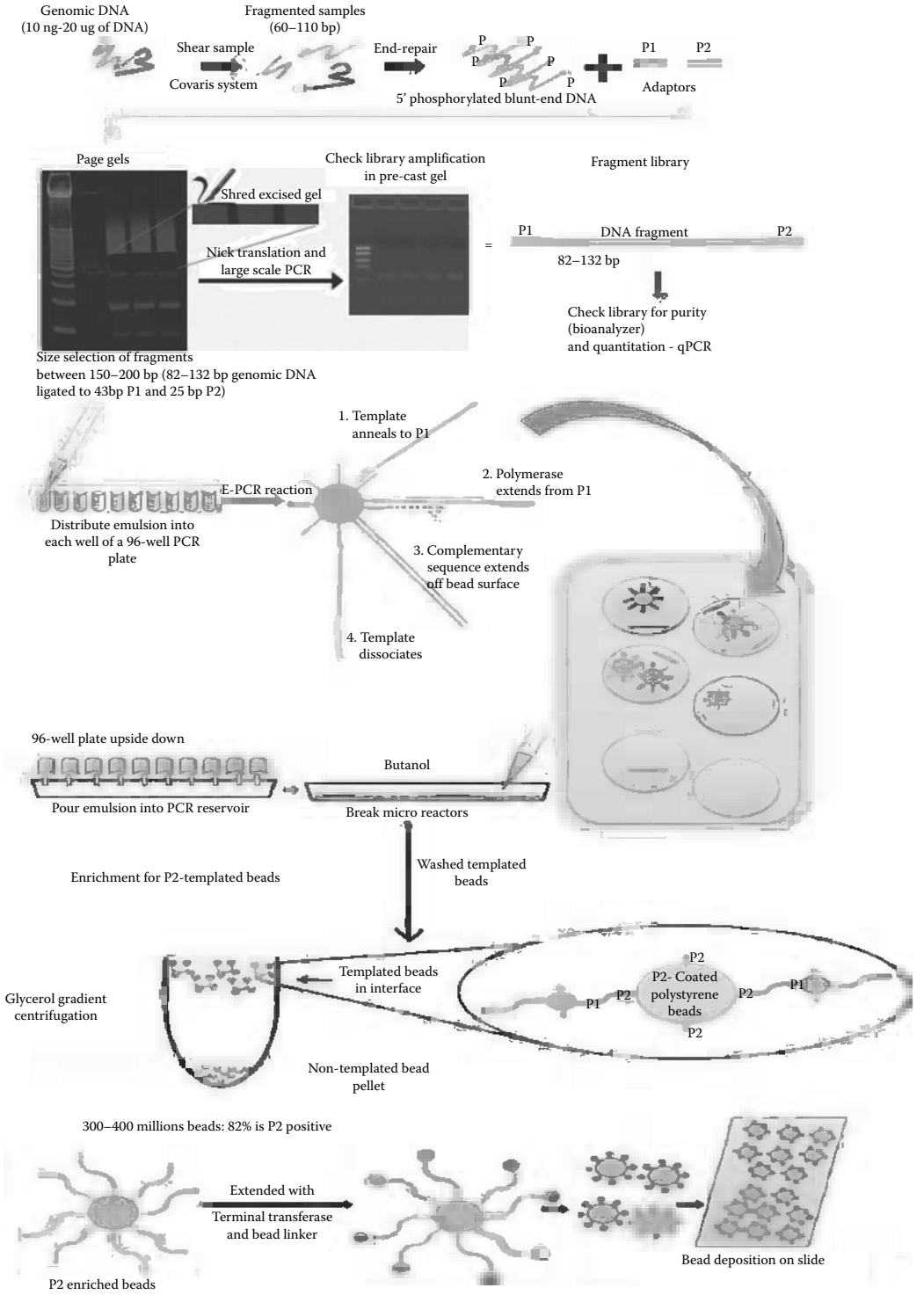

FIGURE 10.5 The process depicted fragment library construction from genomic DNA, preparation of the P2 templated beads using ePCR, and enrichment of the P2-positive beads using glycerol gradient centrifugation. The enriched beads modification and its deposition on treated glass slides for carrying out the sequencing on a SOLiD system.

- *Superior accuracy:* Accuracy greater than 99.94% because of two-base encoding.
- *Uniform coverage:* Coverage is consistent for the sequencing.
- *High throughput:* It generates over 100 gigabases and 1.4 billion tags per run.
- *Flexible:* The independent flow cell configuration of the SOLiD analyzer enables users to run two completely independent experiments in a single run—essentially providing two instruments in one.

10.5.2.4 Ion Personal Genome Machine Sequencer

Ion Torrent has developed the world's first semiconductor-based DNA sequencing technology that directly translates chemical information into digital data. DNA sequencing is performed with all natural nucleotides and Ion Torrent has developed a DNA sequencing system that directly translates chemical signals (A, C, G, T) into digital information (0, 1) on a semiconductor chip. The result is a sequencing system that is simpler, faster, and more cost-effective and scalable than any other technology available.

The Ion Torrent Personal Genome Machine (PGM™) sequencer is a bench-top system utilizing ground-breaking and disruptive semiconductor technology that enables rapid and scalable sequencing experiments. Ion Torrent technology uses a massive, parallel array of proprietary semiconductor sensors to perform direct real-time measurement of the hydrogen ions produced during DNA replication. A high-density array of wells on the Ion Torrent semiconductor chips provides millions of individual reactors, and integrated fluidics allow reagents to flow over the sensor array. This unique combination of fluidics, micromachining, and semiconductor technology enables the direct translation of genetic information (DNA) to digital information (DNA sequence), rapidly generating large quantities of high-quality data. The PGM along with Ion Torrent semiconductor sequencing chips, Ion Torrent reagent kits, and the Torrent Server/Torrent Suite software allow Ion Torrent to deliver a cutting-edge sequencing solution that is simple, stable, and fast.

The systems discussed above require the emulsion PCR amplification step of DNA fragments to make the light signal strong enough for reliable base detection by the CCD cameras (Mamanova et al. 2010). PCR amplification has revolutionized DNA analysis, but in some instances it may introduce base sequence errors into the copied DNA strands or favor certain sequences over others, thus changing the relative frequency and abundance of various DNA fragments that existed before amplification. Ultimate miniaturization into the nanoscale and the minimal use of biochemicals would be achieved if the sequence could be determined directly from a single DNA molecule without the need for PCR amplification and its potential for distortion of abundance levels. This requires a very sensitive light detection system and a physical arrangement capable of detecting and identifying light from a single dye molecule. Techniques for the detection and analysis of single molecules have been under intensive development over past decades, and several very sensitive systems for single-photon detection have been produced and tested. Therefore, the third generation was developed for which PCR emulsion is not needed (Reis-Filho 2009; Metzker 2010).

10.5.3 Third-Generation Sequencers

The desired characteristics and features for the third-generation sequencers are high throughput, low cost, and long and fast read through (Buehler et al. 2010). Measurements are directly linked to the nucleotide sequence rather than capturing images that require a conversion into quantitative data for base calling. Third-generation sequencers are those based on single-molecule sequencing in addition to massive parallel analysis.

10.5.3.1 Helicos

Helicos single-molecule sequencing provides a unique view of genome biology through direct sequencing of cellular nucleic acids in an unbiased manner, providing quantitative and accurate sequence information. The simple sample preparation involves no ligation or PCR amplification,

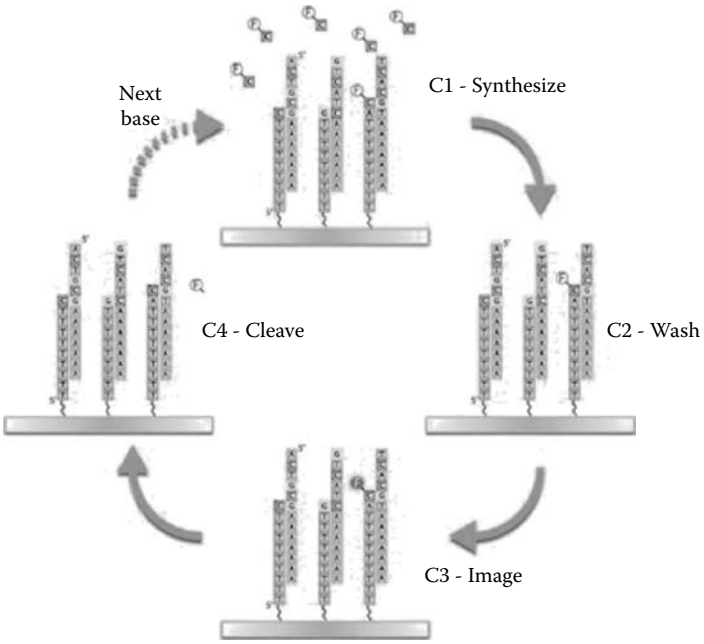

FIGURE 10.6 Helicos BioSciences' approach to single-molecule sequencing involves binding of targets to a flow cell followed by sequential rounds of nucleotide addition, imaging, and cleavage. (Courtesy of Helicos BioSciences, Cambridge, MA.)

allowing for direct sequencing of targeted DNA or RNA molecules. DNA and RNA can be directly hybridized to the flow cell, eliminating many intermediary steps that can introduce sample loss or bias. One of the first techniques for sequencing from a single DNA molecule was described by the team of S. Quake and licensed by Helicos BioSciences. Helicos introduced the first commercial single-molecule DNA sequencing system in 2007. The nucleic acid fragments are hybridized to primers covalently anchored in random positions on a glass coverslip in a flow cell. The primer, polymerase enzyme, and labeled nucleotides are added to the glass support. The next base incorporated into the synthesized strand is determined by analysis of the emitted light signal in the sequencing-by-synthesis technique (Figure 10.6). This system also simultaneously analyzes many millions of single DNA fragments, resulting in sequence throughput in the gigabase range (Milos 2008; Thompson and Steinmann 2010). Although still in the first years of operation, the system has been tested and validated in several applications with promising results. In the homopolar regions, multiple fluorophore incorporations could decrease emissions, sometimes below the level of detection; when errors did occur, most were deletions. Helicos announced that it has recently developed a new generation of "one-base-at-a-time" nucleotides that allows for more accurate homopolymer sequencing and lower overall error rates. The latest model of Helicos sequencer consists of the following (Metzker 2010):

- It utilizes an advanced fluidics and optics configuration, simultaneously performing strand synthesis and imaging to maximize run efficiency.
- It provides the simplicity and flexibility to balance numerous experimental factors associated with today's experiments, including those applications requiring high coverage, strand-counting, or both—all at a cost lower than other technologies.
- It currently outperforms any other genetic analysis technology, yet it is designed to accommodate future enhancements in accuracy and throughput without the need to upgrade the instrument.

10.5.3.2 Pacific Biosciences

Pacific Biosciences have developed a novel approach to study the synthesis and regulation of DNA, RNA, and protein. Combining recent advances in nanofabrication, biochemistry, molecular biology, surface chemistry, and optics, the powerful technology platform called "single molecule, real-time", or SMRT technology, was created. Pacific Biosciences have introduced a platform for SMRT observation of biological events named PacBio RS (Shendure and Ji 2008). This uses the proprietary SMRT technology and maintains many of the key attributes of currently available sequencing technologies while solving many of the inherent limitations of previous technologies. The PacBio RS consists of an instrument platform that uses our consumables including the proprietary SMRT cell. PacBio RS is a user-friendly instrument that conducts monitors and analyzes single-molecule biochemical reactions in real time. The PacBio RS uses a high numerical aperture objective lens and four single-photon-sensitive cameras to collect the light pulses emitted by fluorescence, allowing the observation of biological processes. An optimized set of algorithms is used to translate the information that is captured by the optics system. Using the recorded information, light pulses are converted into an A, C, G or T base call with associated quality metrics. Once sequencing is started, the real-time data are delivered to the system's primary analysis pipeline, which outputs base identity and quality values (QVs). To generate a consensus sequence from the data, an assembly process aligns the different fragments from each ZMW based on common sequences. The system provides long read lengths, flexibility in experimental design, fast time to result, and is easy to use (Metzker 2010).

10.5.3.3 VisiGen

VisiGen Biotechnologies is developing a breakthrough technology to sequence a human genome in less than a day for less than $1000. The ability to achieve $1000 human genome sequencing is directly related to the successful implementation of a single-molecule approach, and the ability to accomplish this feat in a day is directly related to the implementation of the approach on a massive parallel scale (Shendure and Ji 2008). VisiGen is distinguished from other leading developers of NGS technologies in that it exploits the natural process of DNA replication in a way that enhances accuracy and minimally affects efficiency. VisiGen has engineered polymerase, the enzyme that synthesizes DNA and nucleotides—the building blocks of a DNA strand, to act as direct molecular sensors of DNA base identity in real time, effectively creating nanosequencing machines that are capable of determining the sequences of any DNA strand (Figure 10.7). The technology platform detects sequential interactions between a single polymerase and each nucleotide that the polymerase inserts into the elongating DNA strand. Importantly, before initiating sequencing activity, the nanosequencers are immobilized on a surface so that the activity of each can be monitored in parallel.

VisiGen builds nanosequences by drawing on the disciplines of single-molecule direction, fluorescent molecule chemistry, computational biochemistry, and genetic engineering of biomolecules. VisiGen's strategy involves monitoring single-pair Forster resonance energy transfer between a donor fluorophore attached to or associated with a polymerase and a color-coded acceptor fluorophore attached to the γ-phosphate of a dNTP during nucleotide incorporation and pyrophosphate release. The purpose of the donor is to excite each acceptor to produce a fluorescent signal for which the emission wavelength and intensity provide a unique signature of base identity. Working at a single-molecule level makes sequencing signal maximization and background noise minimization critical; thus, the core of VisiGen's technology exploits aspects of physics that enhance signal detection to enable real-time, single-molecule sequencing.

10.5.3.4 BioNanomatrix

BioNanomatrix and Complete Genomics announced in 2007 the formation of a joint venture to develop technology to sequence a human genome in 8 h for less than $100. The proposed platform will use Complete Genomics' sequencing chemistry and BioNanomatrix's nanofluidic technology. They plan to adapt DNA sequencing chemistry with linearized nanoscale DNA imaging to create

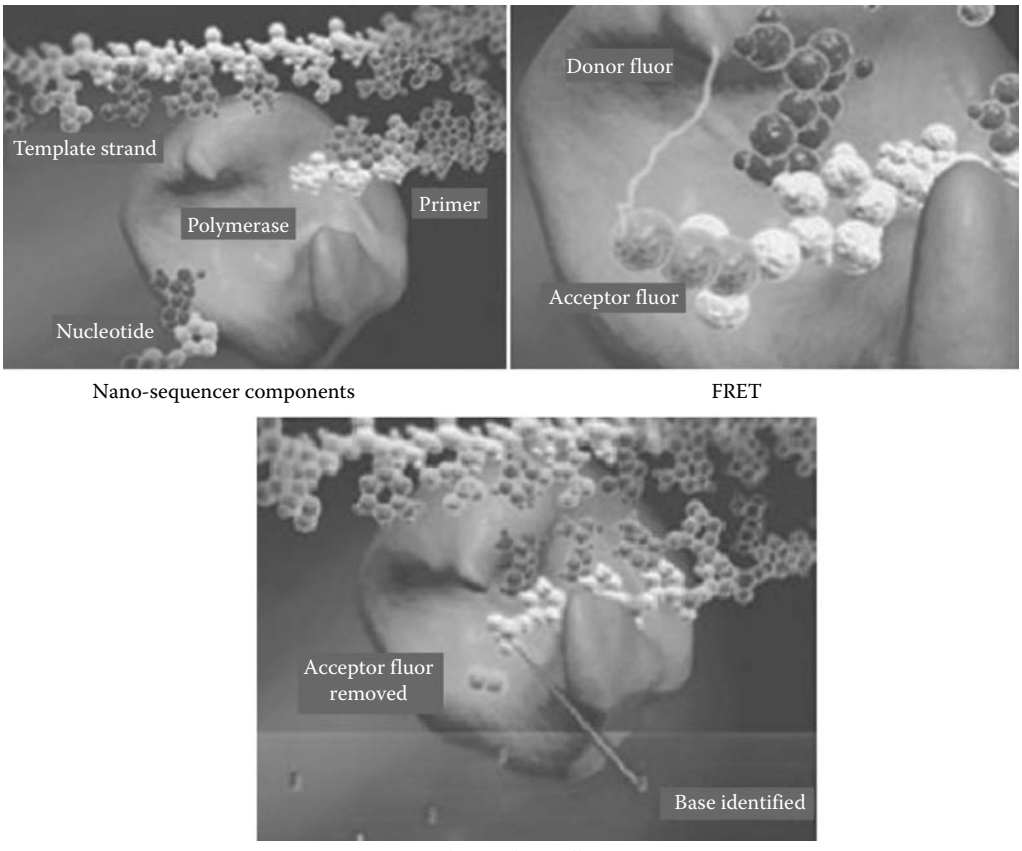

FIGURE 10.7 VisiGen Biotechnologies is developing a fluorescence resonance energy transfer (FRET)-based approach to single-molecule sequencing. VisiGen's technology is a third-generation technology that uses the nanosequencer components. It based on single-molecule changes.

a system that can read DNA sequences larger than 100,000 bases. With their design and price, they target the possible sequencing of many genomes. Complete Genomics recently presented a new method using rolling circle PCR amplification that resulted in DNA nanoballs and a modified ligation technique for fast and inexpensive sequencing of human genomes. A very different approach to single-molecule DNA sequencing using RNA polymerase (RNAP) has been presented recently (Metzker 2010).

In the planned method, RNAP is attached to one polystyrene bead whereas the distal end of a DNA fragment is attached to another bead. Each bead is placed in an optical trap, and the pair of optical traps levitates the beads. The RNAP interacts with the DNA fragment, and the transcriptional motion of RNAP along the template changes the length of the DNA between the two beads. This leads to displacement of the two beads that can be registered with precision in the Angstrom range, resulting in single-base resolution on a single DNA molecule. By aligning four displacement records, each with a lower concentration of one of the four nucleotides and in a role analogous to the primers used in Sanger sequencing, and using for calibration the known sequences flanking the unknown fragment to be sequenced, it is possible to deduce the sequence information. Thirty of the 32 bases were correctly identified in approximately 2 min. The technique demonstrates that the movement of a nucleic acid enzyme and the very sensitive optical trap method may allow for direct extraction of sequence information from a single DNA molecule (Ansorge 2009).

10.6 COMPARISON OF THE SEQUENCING TECHNIQUES

The sequencing techniques provided by various companies follow different techniques, which are listed above, and all of these techniques have various advantages and disadvantages. All of the characteristics are listed (Table 10.3). Other than the platform comparison, the analysis and annotation of the data generated by the sequencers are to be done. This analysis is easy to understand and interpret with the help of Bioinformatics (Morishita 2009; Sugano 2009). The strength of NGS lies in its diverse array of applications; listed in Table 10.4, and illustrated in Figure 10.8 (Marguerat et al. 2008).

10.7 DISCOVERY OF SNP

One of the central themes in genomics is to study genome differences or variations, including SNP. In the past, human SNP discovery relied on PCR amplification of targeted regions, followed by capillary sequencing and *in silico* sequence alignment. However, this approach was impractical for other species because it was rather laborious and costly. The NGS platforms, which produce millions of short reads significantly faster and cheaper, fit in perfectly and have started to change the processes for SNP discovery (Shen et al. 2010; Chan 2009).

10.8 TRANSCRIPTOME ANALYSIS

10.8.1 Gene Expression: Sequencing the Transcriptome

Historically, the mRNA expression has been gauged with microarray or quantitative PCR (qPCR)-based approaches; the latter is most efficient and cost-effective for a genome-wide survey of gene expression levels. However, even the exquisite sensitivity of qPCR is not absolute, nor is it straightforward or reliable to evaluate novel alternative splicing isoforms using either technology (Bateman and Quackenbush 2009). In the past, serial analysis of gene expression (SAGE) and its variants have provided a digital readout of gene expression levels using DNA sequencing. These powerful approaches have the ability to report the expression of genes at levels below the sensitivity of microarrays, but they have been limited in their application by the cost of DNA sequencing. In contrast, the rapid and inexpensive sequencing capacity offered by the NGS instruments meshes perfectly with SAGE tagging or conventional complementary DNA sequencing approaches (Morozova et al. 2009), as evidenced by several studies that used Roche/454 technology. Without doubt, the shorter read lengths offered by the Illumina and Applied Biosystems instruments will be utilized with these approaches in the future, offering the advantage of sequencing individual SAGE tags rather than requiring concatenation of the tags before sequencing. Indeed, combining the data obtained from isolating and sequencing ChiP-derived DNA bound by a transcription factor of interest to the corresponding co-isolated and sequenced mRNA population from the same cells might be imagined (Forrest and Carninci 2009).

10.8.2 Applications of Transcriptomics Analysis

Transcriptome analysis could be applied at several stages of clinical drug development (Morozova et al. 2009). A basic paradigm of clinical pharmacology is that a drug can be distinguished from a poison by its therapeutic index. As the dose of a drug increases, the pharmacologic effect increases, as do the toxicologic effects. Drugs have pharmacologic effects at doses lower than their toxicologic effects, whereas poisons have toxicologic effects at doses lower than their pharmacologic effects. When human testing commences, the pharmacokinetics is carefully studied, usually in healthy normal volunteers, and adverse effects are carefully monitored. When plasma levels are achieved that would be predicted to have appropriate pharmacologic activity, and that appear to be safe and

TABLE 10.3
Comparison of NGS Technologies

Platform	Library/ Template Preparation	Read Length (Bases)	Run Time (Days)	Gb Per Run	Pros	Cons	Biological Applications
Roche/454's GS FLX Titanium	Fragment, MP/ emPCR	330	0.35	0.45	Longer reads improve mapping in repetitive regions; fast run times	High reagent cost; high error rates in homopolymer repeats	Bacterial and insect genome de novo assemblies; medium scale (<3 Mb) exome capture; 16S in metagenomics
Illumina/ Solexa's GAII	Fragment, MP/ solid-phase	75 or 100	4–9	18, 35	Currently the most widely used platform in the field	Low multiplexing capability of samples	Variant discovery by whole-genome resequencing or whole-exome capture; gene discovery in metagenomics
Life/APG's SOLiD 3	Fragment, MP/ emPCR	50	7, 14	30–50	Two-base encoding provides inherent error correction	Long run times	Variant discovery by whole-genome resequencing or whole-exome capture; gene discovery in metagenomics
Polonator G.007	MP only/emPCR	26	5	12	Least-expensive platform; open source to adapt alternative NGS chemistries	Users are required to maintain and quality-control reagents; shortest NGS read lengths	Bacterial genome resequencing for variant discovery
Helicos BioSciences HeliScope	Frag, MP/single molecule	32	8	37	Non-biased Representation of templates for genome and sequence-based applications	High error rates compared with other reversible terminator chemistries	Sequence-based methods
Pacific Biosciences	Frag only/single molecule	964	N/A	N/A	Has the greatest potential for reads exceeding 1 kb	Highest error rates compared with other NGS chemistries	Full-length transcriptome sequencing; complements other resequencing efforts in discovering large structural variants and haplotype blocks

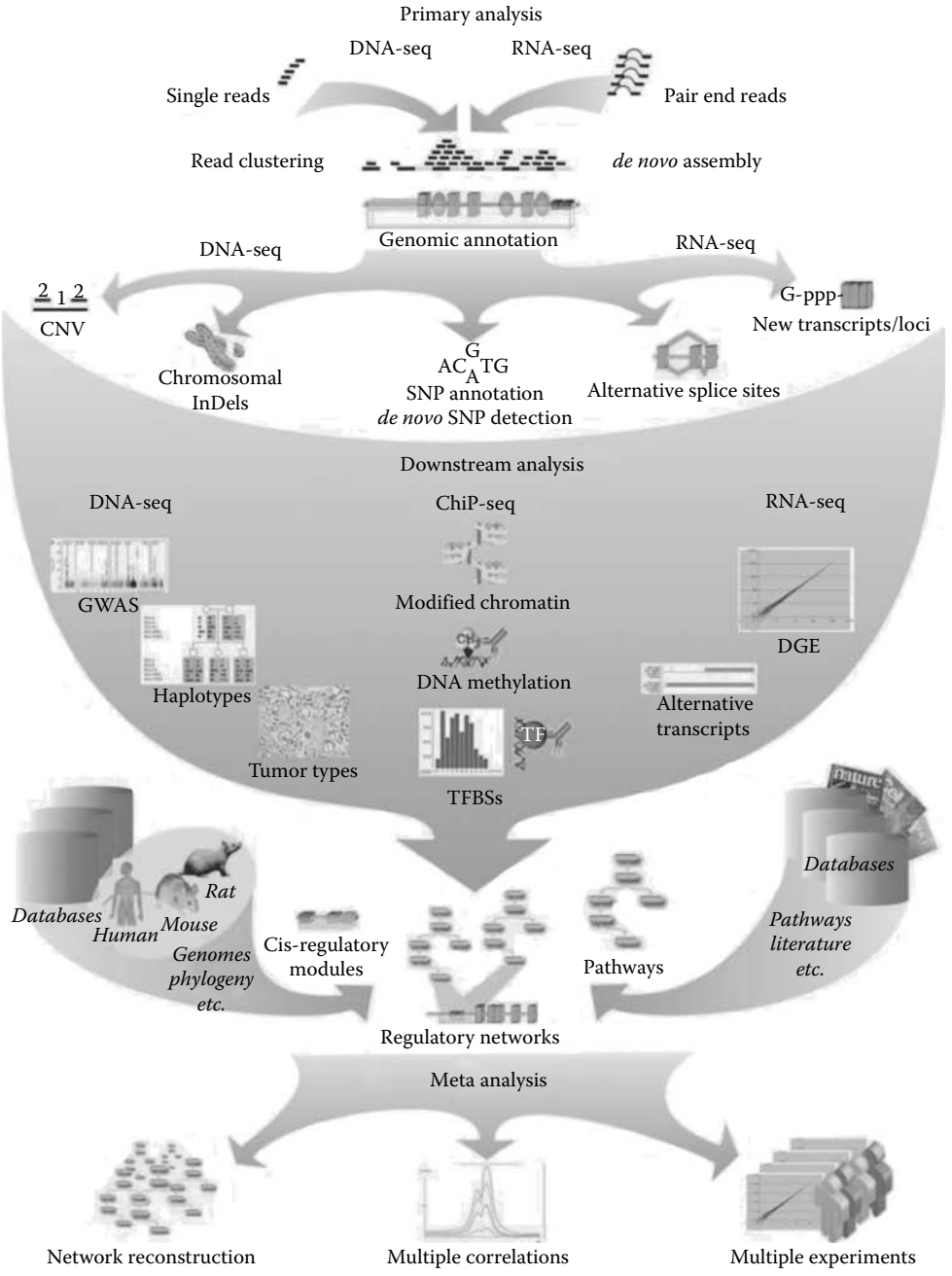

FIGURE 10.8 Overview of NGS-based analysis strategies. Primary analysis: This part describes analyses steps that are used directly on the reads: CNV, chromosomal Indels are insertions or deletions, SNP annotation, alternative splice sites can be detected and new transcripts/loci are derived by direct mapping of novel exons and splice overlaps. Downstream analysis: This part differs for the three major application areas: GWAS, the definition of haplotypes and tumor typing. ChIP-Seq determines genome-wide patterns of modified chromatin, usually DNA-dependent RNA polymerases or transcription factors leading to the definition of patterns such as transcription factor binding sites. RNA-Seq determines the unknown transcripts. Finally, meta-analysis allows merging of several fields via network reconstruction, multiple correlations of various lines of evidence, and the crossexamination of multiple experiments such as transcriptional profiles from several patients.

well tolerated, the drug proceeds to testing in patients with the target disease. If a biomarker or a surrogate marker for pharmacologic activity is available, it can be used to assess dose-responses in normal volunteers and in patients. Conversely, if a biomarker for a potential toxic effect is available, this will also be assessed in the normal volunteers and in patients. Such biomarkers are extremely important in early clinical development where their utilization enables more rapid and accurate definition the potential clinical dose range, detection of pharmacologic activity, and assessment of the risk of side effects (Tanaka 2000). Transcriptome analysis provides the opportunity to simultaneously measure many potential biomarkers. Such measurements could provide more comprehensive assessment of the pharmacologic and toxicologic effects of drugs early in clinical development. This is how transcriptome analysis has obtained its importance in the pharmaceutical sector.

10.8.3 Small RNA Analysis

Small RNA (**sRNA**) is a functional RNA molecule that is not translated into a protein. It is also called noncoding RNA (NC-RNA), nonprotein-coding RNA (npcRNA), nonmessenger RNA (nmRNA), or functional RNA (fRNA) Small NC-RNAs are typically only approximately 18–40 nucleotides in length; however, their effect on cellular processes is profound (Axtell et al. 2007). Small RNA has been shown to play critical roles in developmental timing, tumor progression, and neurogenesis.

sRNA (small RNA): sRNA refers to small bacterial NC-RNAs, with the DNA coding sequences being referred to as **RNA genes** or noncoding RNA genes.

- **MicroRNA (miRNA)**
- **Short interfering RNA (siRNA)**
- **Piwi-interacting RNA (piRNA)**
- **siRNA RNA (rasiRNA)**

miRNAs: MicroRNAs are post-transcriptional regulator molecules that are capable of binding to mRNA complementary sequences. This in turn brings about a repression of translation.

siRNA (small-interfering RNA, or **silencing RNA):** siRNA is a class of double-stranded RNA molecules that play various roles [e.g., repression of expression of enzymes of RNAi (RNA interference) pathway].

piRNA (**Piwi-interacting RNA):** Small RNA molecules that are capable of forming RNA-protein complexes through interactions with Piwi proteins. piRNA are slightly larger in size than miRNA.

rasiRNA (repeat-associated small-interfering RNA (rasiRNA): rasiRNA are a class of small RNA that associates with the Ago and Piwi proteins. rasiRNA is involved in establishing and maintaining heterochromatin structure, controlling transcripts that emerge from repeat sequences, and silencing transposons and retrotransposons

NC-RNA (noncoding RNA molecule): NC-RNA is also known as nonprotein-coding RNA (npcRNA), non-messenger RNA (nmRNA), small non-messenger RNA (snmRNA), and functional RNA (fRNA).

10.8.3.1 Techniques for the RNA Analysis

Deep sequencing RNA analysis pipeline (DSAP) is an automated multiple-task web service designed to provide a total solution to analyzing deep-sequencing small RNA data sets generated by NGS technology (Huang et al. 2010). DSAP uses a tab-delimited file as an input format that holds the unique sequence reads (tags) and their corresponding number of copies generated by the Solexa sequencing platform. The input data will go through four analysis steps in DSAP:

1. *Cleanup:* removal of adaptors and poly-A/T/C/G/N nucleotides
2. *Clustering:* grouping of cleaned sequence tags into unique sequence clusters
3. *NC-RNA matching:* Sequence homology mapping against a transcribed sequence library from the NC-RNA database Rfam
4. *Known miRNA matching:* detection of known miRNAs in miRBase based on sequence homology

The expression levels corresponding to matched NC-RNAs and miRNAs are summarized in multicolor clickable bar charts linked to external databases. DSAP is also capable of displaying miRNA expression levels from different jobs using a $\log_2$-scaled color matrix. Furthermore, a cross-species comparative function is also provided to show the distribution of identified miRNAs in different species as deposited in miRBase.

TABLE 10.4
Applications of NGS

Category	Examples of Applications
Complete genome resequencing	Comprehensive polymorphism and mutation discovery in individual human genomes
Reduced representation sequencing	Large-scale polymorphism discovery
Targeted genomic resequencing	Targeted polymorphism and mutation discovery
Paired end sequencing	Discovery of inherited and acquired structural variation
Metagenomic sequencing	Discovery of infectious and commensal flora
Transcriptome sequencing	Quantification of gene expression and alternative splicing; transcript annotation; discovery of transcribed SNPs or somatic mutation
Small RNA sequencing	MiRNA profiling 64 sequencing of bisulfite- treated DNA determining patterns of cytosine methylation in genomic DNA
Chromatin immunoprecipitation sequencing	Genomic-wide mapping of protein-DNA interactions
Nuclease fragmentation and sequencing	Nucleosome positioning
Molecular barcoding	Multiplex sequencing of samples from multiple individuals

10.8.3.2 Discovering NC-RNA

One of the most exciting areas of biological research in recent years has been the discovery and functional analysis of NC-RNA systems in different organisms. Perhaps the most profound impact of NGS technology has been on the discovery of novel NC-RNAs belonging to distinct classes in an extraordinarily diverse set of species. In fact, this approach has been responsible for the discovery of NC-RNA classes in organisms not previously known to possess them. These discoveries are being coupled with an ever-expanding comprehension of the functions embodied by these unique RNA species, including gene regulation by various mechanisms. In this regard, studying the roles of specific miRNAs in cancer is helping to uncover certain aspects of the disease. NC-RNA discovery is best accomplished by sequencing because the evolutionary diversity of NC-RNA gene sequences makes it difficult to predict their presence in a genome with high certainty by computational methods alone. The unique structures of the processed NC-RNAs pose difficulties for converting them into NGS libraries, but remarkable progress has already been made in characterizing these molecules. With these barriers dissolving, the high capacity and low cost of next-generation platforms ensure that discovery of NC-RNAs will continue at a rapid pace and that sequence variants with important functional impacts will also be determined. For example, because the readout from next-generation sequencers is quantitative, NC-RNA characterization will include detecting expression level changes that correlate with changes in environmental factors, with disease onset and progression, and perhaps with complex disease onset or severity. Importantly, the discovery and characterization of NC-RNAs will enhance the annotation of sequenced genomes such that, especially in model organisms and humans, the effect of mutations will become more broadly interpretable across the genome (Mardis 2008b).

10.9 EPIGENETICS

Epigenetics is the study of inherited changes in phenotype (appearance) or gene expression caused by mechanisms other than changes in the underlying DNA sequence. These changes may remain through cell divisions for the remainder of the cell's life and may also last for multiple generations. However, there is no change in the underlying DNA sequence of the organism; instead, nongenetic factors cause the organism's genes to behave (or "express themselves") differently.

The molecular basis of epigenetics is complex. It involves modifications of nucleotides in a given sequence, without changing the order or the sequence itself. Additionally, the chromatin proteins

associated with DNA may be activated or silenced (Bird 2007; Suzuki and Bird 2008). This accounts for the observation that differentiated cells in a multicellular organism express only the genes that are necessary for their own activity. Epigenetic changes are preserved when cells divide. Most epigenetic changes only occur within the course of one individual organism's lifetime; however, some epigenetic changes are inherited from one generation to another, which begs the question of whether or not epigenetic changes in an organism alter the basic structure of its DNA (Zhou et al. 2010).

Specific epigenetic processes include paramutation, bookmarking, imprinting, gene silencing, X chromosome inactivation, position effect, reprogramming, transvection, maternal effects, the progress of carcinogenesis, many effects of teratogens, regulation of histone modifications and heterochromatin, and technical limitations affecting parthenogenesis and cloning. Epigenetic research uses a wide range of molecular biologic techniques to further our understanding of epigenetic phenomena, including chromatin immunoprecipitation (together with its large-scale variants ChIP-on-chip and ChIP-seq), fluorescent in situ hybridization, methylation-sensitive restriction enzymes, DNA adenine methyl transferase identification, and bisulfite sequencing (Park 2008).

10.10 CHROMATIN IMMUNOPRECIPITATION, CHIP-SEQ TECHNIQUE

NGS technology allowed replacement of microarrays in the mapping step with high-throughput sequencing of DNA binding sites, and their direct mapping to a reference genome in the database. The sequence of the binding site is mapped with high resolution to regions shorter than 40 bases, a resolution not achievable by microarray mapping. Moreover, the ChiP-Seq technique is not biased and allows for the identification of unknown protein binding sites, which is not the case with the ChiP-on-chip approach, in which the sequence of the DNA fragments on the microarray is predetermined (e.g., in promoter arrays, exon arrays, etc.) (Nelson et al. 2006).

The association between DNA and proteins is a fundamental biological interaction that plays a key part in regulating gene expression and controlling the availability of DNA for transcription, replication, and other processes. These interactions can be studied in a focused manner using a technique called chromatin immunoprecipitation (ChIP). ChIP entails a series of steps:

1. DNA and associated proteins are chemically crosslinked.
2. Nuclei are isolated, lysed, and the DNA is fragmented.
3. An antibody specific for the DNA binding protein (transcription factor, histone, etc.) of interest is used to selectively immunoprecipitate the associated protein-DNA complexes.
4. The chemical crosslinks between DNA and protein are reversed, and the DNA is claimed for downstream analysis.

In early applications, typical analyses examined the specific gene of interest by quantitative PCR or Southern blotting to determine if corresponding sequences were contained in the captured fragment population. Recently, genome-wide ChIP-based studies of DNA-protein interactions became possible in sequenced genomes by using genomic DNA microarrays to assay the released fragments (Carey et al. 2009). Although utilized for several important studies, it has several drawbacks, including a low signal-to-noise ratio and a need for replicates to build statistical power to support putative binding sites.

10.11 METAGENOMICS

Cataloging the biodiversity found on Earth is of particular interest as we enter a critical stage in which our ecosystem is changing on an alarming scale. DNA- or RNA-based approaches for this purpose are becoming increasingly powerful as the growing number of sequenced genomes enables us to interpret partial sequences obtained by direct sampling of specific environmental niches (Mardis 2008a). Such investigations are referred to as metagenomics. Conventionally, metagenomics

are addressed by isolating DNA from an environmental sample, amplifying the collective of 16S ribosomal RNA (rRNA) genes with degenerate PCR primer sets, subcloning the PCR products that result, and classifying the taxa present according to a database of assigned 16S rRNA sequences. As an alternative, DNA (or RNA) is isolated, subcloned, and then sequenced to produce a fragment pool representative of the existing population. These sequences can then be translated *in silico* into protein fragments and compared with the existing database of annotated genome sequences to identify community members. In both approaches, deep sequencing of the population of subclones is necessary to obtain the full spectrum of taxa present and is limited by potential cloning bias that can result from the use of bacterial cloning. With aids of **metabolomics** and sampling RNA sequences from a metagenomic isolate, one can attempt to reconstruct metabolic pathways that are active in a given environment. By contrast, the rapid, inexpensive, and massive data production enabled by next-generation platforms has caused a recent explosion in metagenomic studies. These studies include previously sampled environments such as the ocean and an acid mine site, but soil and coral reefs also were studied by Roche/454 pyrosequencing (Tringe and Rubin 2005; Wommack et al. 2008).

Metabolomics: Metabolomics involves the rapid, high throughput characterization of the small molecule metabolites found in an organism. It is closely tied to the genotype of an organism, its physiology and its environment.

Metabolome: A metabolome refers to the complete set of primary and secondary metabolites as well as activators, inhibitors, and hormones that are produced by a given organism under certain conditions. However, it is noteworthy that it is not currently possible to analyze the entire range of metabolites by a single analytical method.

A new generation of non-Sanger-based sequencing technologies have delivered on their promise of sequencing DNA at unprecedented speed, thereby enabling impressive scientific achievements and novel biological applications (Gill et al. 2006). However, before stepping into the limelight, NGS had to overcome the inertia of a field that relied on Sanger-sequencing for 30 years. Each next-generation platform is optimized for specific sequencing applications. Next-generation DNA sequencing has the potential to dramatically accelerate biological and biomedical research by enabling the comprehensive analysis of genomes, **transcriptomes**, and **interactomes** to become inexpensive, routine, and widespread rather than requiring significant production-scale efforts (Wooley et al. 2010).

Transcriptome: The transcriptome is the set of all RNA molecules, including mRNA, rRNA, tRNA, and other non-coding RNA produced in one or a population of cells

Interactome: An interactome is the whole set of interactions that takes place between different molecules within the cell, both within a given family of molecules or between molecules belonging to different biochemical families. When discussed in terms of functional genomics, it refers to gene-gene interaction.

There are numerous applications of NGS because NGS plays a huge role in functional genomic and expressional analysis. The DNA sequencing process is followed by the assembly and the annotation of the genome. The annotation of the genome is a key step for identifying the functional genes and predicting the proteins. The genome analysis and the genome annotation are explained in Section 10.12.

10.12 GENOME ANALYSIS

10.12.1 Whole-Genome Sequencing

Most of the methods give rather short read lengths; they have mainly been used for resequencing. In this case, it is not necessary to do a complete, independent genome assembly, but the sequence reads can be aligned to a reference genome sequence (Sundquist et al. 2007). For example, the sequence reads from a single person can be aligned to the reference human genome. However, all of the methods have been modified to produce "paired reads" in which both ends of a DNA fragment of known length are sequenced (Bentley et al. 2009). This makes it possible to do de novo assemblies of genomes. In whole-genome sequencing the aim is to produce a complete, continuous sequence of high quality or a fragmented draft version of the genome. Although the draft version can be produced faster and at lower cost compared with the complete sequence, only the latter can be reliably used in different analyses; for example, because a gene that is not found in the sequence is truly missing. If a certain

region of the genome is of special interest it can be sequenced separately; for example, a gene known to be associated with this specific disease can be sequenced from several individuals with differing symptoms or disease outcomes to establish the connection between the genotype and phenotype.

Two major strategies—clone-by-clone and whole-genome shotgun approaches—have been used for whole-genome sequencing. The most suitable methods depend on the organism to be sequenced. For relatively small and nonrepetitive genomes the whole-genome shotgun methods is advantageous because mapping and construction of a large insert clone are avoided (Ng and Kirkness 2010). More complex genomes such as human genomes are difficult to sequence using this method. The high levels of repetitive sequences cause difficulties in the assembly of the genome. Combination of the two methods (i.e., hybrid strategies) might be more successful when sequencing complex genomes (Huang et al. 2009; Zhao and Grant 2010).

10.12.2 *De Novo* Assembly

Genome assembly refers to the process of taking many short DNA sequences, all of which were generated by a shotgun sequencing project, and putting them back together to create a representation of the original chromosomes from which the DNA originated. In a shotgun-sequencing project, the entire DNA from a source is first fractured into millions of small pieces (Pevzner et al. 2004). These pieces are then "read" by automated sequencing machines, which can read up to 900 nucleotides or bases at a time. A genome assembly algorithm works by taking all of the pieces and aligning them to one another and detecting all places where two of the short sequences, or reads, overlap. These overlapping reads can be merged together, and the process continues (Morozova 2008a).

The assembly of a genome is a very difficult computational problem, made more difficult because many genomes contain many identical sequences, known as repeats. These repeats can be thousands of nucleotides long, and some occur in thousands of different locations, especially in the large genomes of plants and animals. The resulting genome sequence is created by combining information from the sequenced contigs and using linking information for creating scaffolds. These scaffolds are positioned along the physical map of the chromosomes creating a "golden path". The efficiency of the *de novo* genome sequence assembly processes depends heavily on the length, fold-coverage, and per-base accuracy of the sequence data. Despite substantial improvements in the quality, speed, and cost of Sanger sequencing, generating a high-quality draft *de novo* genome sequence for a eukaryotic genome remains expensive. The newly available sequencing-by-synthesis systems from Roche (454), Illumina (Genome Analyser), and ABI (SOLiD) offer greatly reduced per-base sequencing costs. Although they are attractive for generating *de novo* sequence assemblies for eukaryotes, these technologies add several complicating factors: they generate short (typically 450 base pairs for Roche/454; 50–100 base pairs for Illumina and SOLiD) reads that cannot resolve low-complexity sequence regions or distributed repetitive elements, they have system-specific error models, and they can have higher base-calling error rates (Li et al. 2010). The whole process of *de novo* sequencing is illustrated in Figure 10.9.

De novo sequencing using next-generation technologies necessitates the development of new algorithms for assembling the short and more error-prone reads that they generate. Several de novo assembly algorithms based on de-Bruijn graphs (EULER-SR and Velvet), hash-extension (VCAKE), and overlap layout (EDENA) and for paired-end reads (ALLPATHS) have been recently developed. These algorithms are able to assemble millions of short reads from NGS technologies into thousands of contigs with varying degrees of efficiency (Paszkiewicz and Studholme 2010).

10.12.3 Annotation of Genome Assembly

Annotation of the genome is the process of attaching biological information to sequences. It consists of two main steps: Identifying the elements on the genome, a process called "gene finding", and attaching biological information to these elements (Srinivasan et al. 2005). Automatic annotation

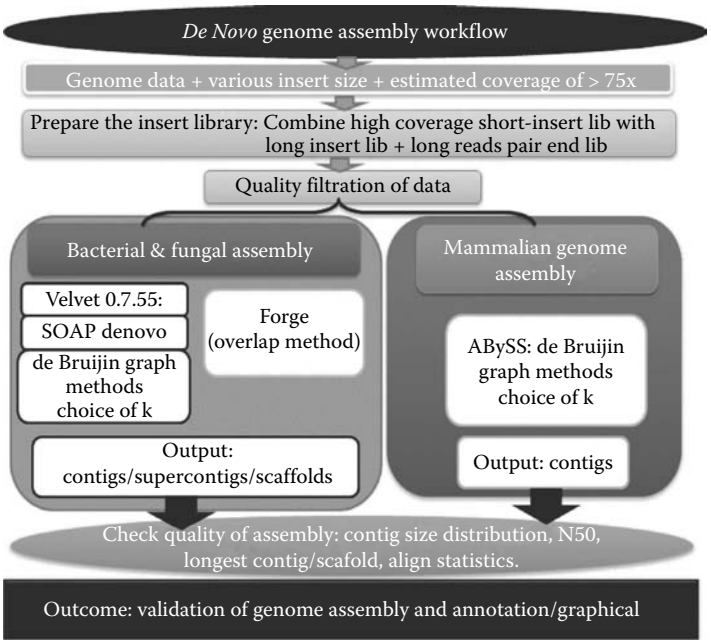

FIGURE 10.9 Schematic overview of the *de novo* genome assembly workflow for assembling the genome. (Zhao, Z. et al. *Physiol Genomics*, 43:325–45, 2011)

tools try to perform all of these with computational analysis, as opposed to manual annotation that involves human expertise. These approaches ideally co-exist and complement each other in the same annotation pipeline (Morozova 2008a).

The basic level of annotation is done using BLAST to find similarities and then annotating genomes on the basis of that. However, nowadays more and more information is added to the annotation platform. The additional information allows manual annotators to deconvolute discrepancies between genes that are given the same annotation. The genome annotations are of two types: structural annotation and functional annotation. Structural annotation consists of the identification of the genomic elements (1) open reading frames and their localization, (2) gene structure, (3) coding region, and (4) location of regulatory motifs. Functional annotation consists in attaching (1) biological information to genetic elements, (2) biochemical function, (3) regulatory elements, and (4) interaction expression. Genome annotation is an active area of investigation involving several different organizations in the life science community that publish the results of their efforts in publicly available biological databases accessible via the Web and other electronic means (Kawaji and Hayashizaki 2008). The NGS and the genome annotation procedures are inseparable.

10.12.4 Genome Mapping of Next Generation Sequencing Data

Assembling reads against an existing backbone sequence, building a sequence is called "genome mapping", which is similar but not necessarily identical to the backbone sequence. The NGS technologies pose new challenges to the sequencing community (Swidan et al. 2006). In addition to the enormous amount of data that they can produce through their high throughput, the read length of the sequence tags is also much shorter than the conventional sequencing methods. Whereas Sanger sequencing can produce read lengths over 700 base pairs, the GS FLX (Roche/454 life sciences) can read average lengths of up to 400 base pairs and the Genome Analyser (Illumina) and SOLiD (Applied Bio Systems) can read tags up to 35 or 50 base pairs, respectively. Mapping those short reads to the reference genomes can pose different challenges in determining the nature of

mismatches (Mychaleckyj 2007). A mismatch can occur because of sequencing error, differences between the query sequence and the reference sequence, or existence of repetitive regions. Although read lengths have constantly been improved by different technologies over the past few years after the release, there will remain a certain cutoff read length that is practical for bioinformatics use, economical, and affordable. The region for finding a balance here is that the cost of sequencing goes up through higher read lengths because of the use of more chemical reagents. In Section 10.12.5; the emphasis will be on alignment programs developed for the Genome Analyser and SOLiD because those two technologies produce ultrashort reads and are therefore more challenging to use with older alignment programs developed for Sanger sequencing. The drawbacks of the NGS methods are that they generate short read lengths and higher errors, which are not taken into account by sequence alignment programs that have been developed for conventional sequencing methods, such as BLAST (Shumway et al. 2010).

10.12.5 Targeting Resequencing

The process of targeted resequencing involves isolation of genomic regions of interest in a sample library for a focused genomic search. Leveraging superior data quality and high throughput, the Genome Analyser is the system of choice for the most flexible and efficient targeted resequencing solution (Marguerat et al. 2008). The isolating of genomic regions of interest through targeted resequencing of many samples enables systematic detection of common and rare variants for high-throughput sequencing at a lower cost per sample. The Genome Analyser offers a flexible and efficient solution for targeted resequencing applications, including

- Sequencing genes or regions in very large populations
- Following up on identified genomic regions of interest in GWAS
- Focusing on genes involved in certain pathways
- Identifying signatures associated with disease prevalence
- Discovering rare variants

Despite great efforts, the scientific community still faces tremendous challenges in understanding the genetics behind complex diseases such as cancer. Systematic detection of common and rare variants through targeted resequencing of many samples will likely hold the key to advancing our knowledge of the basis of disease and the development of treatments (Li et al. 2009).

Targeted resequencing experiments have been limited by the high costs of Sanger sequencing and lack of a scalable, efficient method for partitioning genomic regions of interest. The Genome Analyser is the most widely adopted and easiest to use NGS platform. Superior data quality and a wide range of read lengths have made it the system of choice for whole genome *de novo* sequencing and resequencing. In addition to these applications, the ever-increasing output of the Genome Analyser can be harnessed to analyze a select region of interest in the genome (Prabhu and Pe'er 2009).

REFERENCES

Aburatani, H. 2005. [Functional genomic analysis with microarray technology]. *Nippon Rinsho* 63(Suppl 12):171–5.

Ansorge, W.J. 2009. Next-generation DNA sequencing techniques. *N Biotechnol* 25:195–203.

Antipova, A.A., P. Tamayo, and T.R. Golub. 2002. A strategy for oligonucleotide microarray probe reduction. *Genome Biol* 3:RESEARCH0073.1–4.

Asmann, Y.W., M.B. Wallace, and E.A. Thompson. 2008. Transcriptome profiling using next-generation sequencing. *Gastroenterology* 135:1466–8.

Axtell, M.J., J.A. Snyder, and D.P. Bartel. 2007. Common functions for diverse small RNAs of land plants. *Plant Cell* 1:1750–69.

Barrett, M.T., A. Scheffer, A. Ben-Dor, N. Sampas, D. Lipson, R. Kincaid, P. Tsang, B. Curry, K. Baird, P.S. Meltzer, Z. Yakhini, L. Bruhn, and S. Laderman. 2004. Comparative genomic hybridization using oligonucleotide microarrays and total genomic DNA. *Proc Natl Acad Sci USA* 101:17765–70.

Bateman, A., and J. Quackenbush. 2009. Bioinformatics for next generation sequencing. *Bioinformatics* 25:429.

Bentley, G., R. Higuchi, B. Hoglund, D. Goodridge, D. Sayer, E.A. Trachtenberg, and H.A. Erlich. 2009. High-resolution, high-throughput HLA genotyping by next-generation sequencing. *Tissue Antigens* 74:393–403.

Bird, A. 2007. Perceptions of epigenetics. *Nature* 447:396–8.

Brennan, C., Y. Zhang, C. Leo, B. Feng, C. Cauwels, A.J. Aguirre, M. Kim, A. Protopopov, and L. Chin. 2004. High-resolution global profiling of genomic alterations with long oligonucleotide microarray. *Cancer Res* 64:4744–8.

Buehler, B., H.H. Hogrefe, G. Scott, H. Ravi, C. Pabon-Pena, S. O'Brien, R. Fermosa, and S. Happe. 2010. Rapid quantification of DNA libraries for next-generation sequencing. *Methods* 50:S15–8.

Carey, M.F., C.L. Peterson, and S.T. Smale. 2009. Chromatin immunoprecipitation (ChIP). *Cold Spring Harb Protoc* 2009:pdb.prot5279.

Chan, E.Y. 2009. Next-generation sequencing methods: Impact of sequencing accuracy on SNP discovery. *Methods Mol Biol* 578:95–111.

Cook-Deegan, R.M. 1991. The genesis of the Human Genome Project. *Mol Genet Med* 1:1–75.

Crowther, D.J. 2002. Applications of microarrays in the pharmaceutical industry. *Curr Opin Pharmacol* 2:551–4.

Debouck, C., and P.N. Goodfellow. 1999. DNA microarrays in drug discovery and development. *Nat Genet* 21:48–50.

Della, B.C., F. Cordero, and R.A. Calogero. 2008. Dissecting an alternative splicing analysis workflow for GeneChip Exon 1.0 ST Affymetrix arrays. *BMC Genomics* 9:571.

Elo, L.L., L. Lahti, H. Skottman, M. Kylaniemi, R. Lahesmaa, and T. Aittokallio. 2005. Integrating probe-level expression changes across generations of Affymetrix arrays. *Nucleic Acids Res* 33:e193.

Evans, J.P. 2010. The Human Genome Project at 10 years: A teachable moment. *Genet Med* 12:477.

Forrest, A.R., and P. Carninci. 2009. Whole genome transcriptome analysis. *RNA Biol* 6:107–12.

Gebauer, M. 2004. Microarray applications: Emerging technologies and perspectives. *Drug Discov Today* 9:915–7.

Gill, S.R., M. Pop, R.T. Deboy, P.B. Eckburg, P.J. Turnbaugh, B.S. Samuel, J.I. Gordon, D.A. Relman, C.M. Fraser-Liggett, and K.E. Nelson. 2006. Metagenomic analysis of the human distal gut microbiome. *Science* 312:1355–59.

Green, P. 1998. Human Genome Project: Data quality. *Science* 279:1115–6.

Greenhalgh, T. 2005. The Human Genome Project. *J Royal Soc Med* 98:545.

Hardiman, G. 2004. Microarray platforms—Comparisons and contrasts. *Pharmacogenomics* 5:487–502.

Hester, S.D., L. Reid, N. Nowak, W.D. Jones, J.S. Parker, K. Knudtson, K. 2009. Comparison of comparative genomic hybridization technologies across microarray platforms. *J Biomol Technol* 20:135–51.

Horner, D.S., G. Pavesi, T. Castrignano, P.D. De Meo, S. Liuni, M. Sammeth, E. Picardi, and G. Pesole. 2010. Bioinformatics approaches for genomics and post genomics applications of next-generation sequencing. *Brief Bioinform* 11:181–97.

Huang, P.J., Y.C. Liu, C.C. Lee, W.C. Lin, R.R. Gan, P.C. Lyu, and P. Tang. 2010. DSAP: Deep-sequencing small RNA analysis pipeline. *Nucleic Acids Res* 38:W385–91.

Huang, X., Q. Feng, Q. Qian, Q. Zhao, L. Wang, A. Wang, J. Guan, D. Fan, Q. Weng, T. Huang, G. Dong, T. Sang, and B. Han. 2009. High-throughput genotyping by whole-genome resequencing. *Genome Res* 19:1068–76.

Jares, P. 2006. DNA microarray applications in functional genomics. *Ultrastruct Pathol* 30:209–19.

Johnson, V.P. 1992. Human genome project. *S D J Med* 45:161–2.

Kamath, B.M., B.D. Thiel, X. Gai, L.K. Conlin, P.S. Munoz, J. Glessner, D. Clark, D.M. Warthen, T.H. Shaikh, E. Mihci, D.A. Piccoli, S.F. Grant, H. Hakonarson, I.D. Krantz, and N.B. Spinner. 2009. SNP array mapping of chromosome 20p deletions: Genotypes, phenotypes, and copy number variation. *Hum Mutat* 30:371–8.

Kawaji, H., and Y. Hayashizaki. 2008. Genome annotation. *Methods Mol Biol* 452:125–39.

Leykin, I., K. Hao, J. Cheng, N. Meyer, M.R. Pollak, R.J. Smith, W.H. Wong, C. Rosenow, and C. Li. 2005. Comparative linkage analysis and visualization of high-density oligonucleotide SNP array data. *BMC Genet* 6:7.

Li, R., Y. Li, X. Fang, H. Yang, J. Wang, K. Kristiansen, and J. Wang. 2009. SNP detection for massively parallel whole-genome resequencing. *Genome Res* 19:1124–32.

Li, R., H. Zhu, J. Ruan, W. Qian, X. Fang, Z. Shi, Y. Li, S. Li, G. Shan, K. Kristiansen, S. Li, H. Yang, J. Wang, and J. Wang. 2010. De novo assembly of human genomes with massively parallel short read sequencing. *Genome Res* 20:265–72.

Lopez-Romero, P., M.A. Gonzalez, S. Callejas, A. Dopazo, and R.A. Irizarry. 2010. Processing of Agilent microRNA array data. *BMC Res Notes* 3:18.

Mamanova, L., A.J. Coffey, C.E. Scott, I. Kozarewa, E.H. Turner, A. Kumar, E. Howard, J. Shendure, and D.J. Turner. 2010. Target-enrichment strategies for next-generation sequencing. *Nat Methods* 7:111–8.

Mardis, E.R. 2008a. Next-generation DNA sequencing methods. *Annu.Rev.Genomics Hum Genet* 9:387–402.

Mardis, E.R. 2008b. The impact of next-generation sequencing technology on genetics. *Trends Genet* 24:133–41.

Marguerat, S., B.T. Wilhelm, and J. Bahler. 2008. Next-generation sequencing: applications beyond genomes. *Biochem Soc Trans* 36:1091–6.

Metzker, M.L. 2010. Sequencing technologies—The next generation. *Nat Rev Genet* 11:31–46.

Milos, P. 2008. Helicos BioSciences. *Pharmacogenomics* 9:477–80.

Miyake, N., and N. Matsumoto. 2005. [Microarray CGH]. *Nippon Rinsho* 63(*Suppl* 12):167–70.

Morishita, S. 2009. [How can we combine next-generation DNA sequencing and bioinformatics to reveal novel findings?]. *Tanpakushitsu Kakusan Koso* 54:1239–47.

Morozova, O., M. Hirst, and M.A. Marra. 2009. Applications of new sequencing technologies for transcriptome analysis. *Annu Rev Genomics Hum Genet* 10:135–51.

Morozova, O., and M.A. Marra. 2008a. Applications of next-generation sequencing technologies in functional genomics. *Genomics* 92:255–64.

Morozova, O., and M.A. Marra. 2008b. From cytogenetics to next-generation sequencing technologies: Advances in the detection of genome rearrangements in tumors. *Biochem Cell Biol* 86:81–91.

Morrissy, A.S., R.D. Morin, A. Delaney, T. Zeng, H. McDonald, S. Jones,Y. Zhao, M. Hirst, and M.A. Marra. 2009. Next-generation tag sequencing for cancer gene expression profiling. *Genome Res* 19:1825–35.

Mueckstein, U., G.G. Leparc, A. Posekany, I. Hofacker, and D.P. Kreil. 2010. Hybridization thermodynamics of NimbleGen microarrays. *BMC Bioinformatics* 11:35.

Mychaleckyj, J.C. 2007. Genome mapping statistics and bioinformatics. *Methods Mol Biol* 404:461–88.

Nelson, J.D., O. Denisenko, and K. Bomsztyk. 2006. Protocol for the fast chromatin immunoprecipitation (ChIP) method. *Nat Protoc* 1:179–85.

Ng, P.C., and E.F. Kirkness. 2010. Whole genome sequencing. *Methods Mol Biol* 628:215–26.

Park, P.J. 2008. Epigenetics meets next-generation sequencing. *Epigenetics* 3:318–21.

Paszkiewicz, K., and D.J. Studholme. 2010. De novo assembly of short sequence reads. *Brief Bioinform* 11:457–72.

Patterson, N., and S. Gabriel. 2009. Combinatorics and next-generation sequencing. *Nat Biotechnol* 27:826–7.

Pevzner, P.A., H. Tang, and G. Tesler. 2004. De novo repeat classification and fragment assembly. *Genome Res* 14:1786–96.

Pinkel, D., and D.G. Albertson. 2005. Comparative genomic hybridization. *Annu Rev Genomics Hum Genet* 6:331–54.

Prabhu, S., and I. Pe'er. 2009. Overlapping pools for high-throughput targeted resequencing. *Genome Res* 19:1254–61.

Putonti, C. 2007. The diverse and informative future of microarray applications. *Pharmacogenomics* 8:137–40.

Rauch, A., F. Ruschendorf, J. Huang, U. Trautmann, C. Becker, C. Thiel, K.W. Jones, A. Reis, and P. Nurnberg. 2004. Molecular karyotyping using an SNP array for genomewide genotyping. *J Med Genet* 41:916–22.

Reis-Filho, J.S. 2009. Next-generation sequencing. *Breast Cancer Res* 11(Suppl 3):S12.

Rogers, S., M. Girolami, C. Campbell, and R. Breitling. 2005. The latent process decomposition of cDNA microarray data sets. *IEEE/ACM Trans Comput Biol Bioinform* 2:143–56.

Salser, W.A. 1974. DNA sequencing techniques. *Annu Rev Biochem* 43:923–65.

Shaffer, C. 2007. Next-generation sequencing outpaces expectations. *Nat Biotechnol* 25:149.

Shen, Y., Z. Wan, C. Coarfa, R. Drabek, L. Chen, E.A. Ostrowski, Y. Liu, G.M. Weinstock, D.A. Wheeler, R.A. Gibbs, and F. Yu. 2010. A SNP discovery method to assess variant allele probability from next-generation resequencing data. *Genome Res* 20:273–80.

Shendure, J., and H. Ji. 2008. Next-generation DNA sequencing. *Nat Biotechnol* 26:1135–45.

Shiu, S.H., and J.O. Borevitz. 2008. The next generation of microarray research: Applications in evolutionary and ecological genomics. *Heredity* 100:141–9.

Shumway, M., G. Cochrane, and H. Sugawara. 2010. Archiving next generation sequencing data. *Nucleic Acids Res* 38:D870–1.

Srinivasan, B.S., N.B. Caberoy, G. Suen, R.G. Taylor, R. Shah, F. Tengra, B.S. Goldman, A.G. Garza, and R.D. Welch. 2005. Functional genome annotation through phylogenomic mapping. *Nat Biotechnol* 23:691–8.

Steibel, J.P., and G.J. Rosa. 2005. On reference designs for microarray experiments. *Stat Appl Genet Mol Biol* 4:Article36.

Sugano, S. 2009. [Introduction: next-generation DNA sequencing and bioinformatics]. *Tanpakushitsu Kakusan Koso* 54:1233–7.

Sundquist, A., M. Ronaghi, H. Tang, P. Pevzner, and S. Batzoglou. 2007. Whole-genome sequencing and assembly with high-throughput, short-read technologies. *PLoS One* 2:e484.

Suzuki, M.M., and A. Bird. 2008. DNA methylation landscapes: Provocative insights from epigenomics. *Nat Rev Genet* 9:465–76.

Swidan, F., E.P. Rocha, M. Shmoish, and R.Y. Pinter. 2006. An integrative method for accurate comparative genome mapping. *PLoS Comput Biol* 2:e75.

Tanaka, T. 2000. [Transcriptome analysis and pharmacogenomics]. *Nippon Yakurigaku Zasshi* 116:241–6.

Teng, X., and H. Xiao. 2009. Perspectives of DNA microarray and next-generation DNA sequencing technologies. *Sci China C Life Sci* 52:7–16.

Thompson, J.F., and K.E. Steinmann. 2010. Single molecule sequencing with a HeliScope genetic analysis system. *Curr Protoc Mol Biol* Chapter 7:Unit7.10.

Tringe, S.G., and E.M. Rubin. 2005. Metagenomics: DNA sequencing of environmental samples. *Nat Rev Genet* 6:805–14.

Velculescu, V.E., L. Zhang, B. Vogelstein, and K.W. Kinzler. 1995. Serial analysis of gene expression. *Science* 270:484–7.

Von, B.A. 2008. Next-generation sequencing: The race is on. *Cell* 132:721–3.

Wommack, K.E., J. Bhavsar, and J. Ravel. 2008. Metagenomics: Read length matters. *Appl Environ Microbiol* 74:1453–63.

Wooley, J.C., A. Godzik, and I. Friedberg. 2010. A primer on metagenomics. *PLoS Comput Biol* 6:e1000667.

Wu, L., P.M. Williams, and W. Koch. 2005. Clinical applications of microarray-based diagnostic tests. *Biotechniques* 39:S577–82.

Zahurak, M., G. Parmigiani, W. Yu, R.B. Scharpf, D. Berman, E. Schaeffer, S. Shabbeer, L. Cope. 2007. Pre-processing Agilent microarray data. *BMC Bioinformatics* 8:142.

Zhao, J., and S.F. Grant. 2010. Advances in whole genome sequencing technology. *Curr Pharm Biotechnol* 12:293–305.

Zhao, Z., T. Miki, A. Van Oort-Jansen, T. Matsumoto, D.S. Loose, and C.C. Lee. 2011. Hepatic gene expression profiling of 5'-AMP induced hypometabolism in mice. *Physiol Genomics* 43:325–45.

Zhou, X., L. Ren, Q. Meng, Y. Li, Y. Yu, and J. Yu. 2010. The next-generation sequencing technology and application. *Protein Cell* 1:520–36.

11 Beyond Cells: Culturing Complex Plant Tissues for the Production of Metabolites and Elite Genotypes

Pamela J. Weathers, Melissa J. Towler, and Barbara E. Wyslouzil

CONTENTS

In memoriam: We dedicate this chapter to Alexander L.G. DiIorio who passed away too young at the age of 48 on July 9, 2010. He was a brilliant scientist and engineer who conducted the first studies using the mist bioreactor to culture hairy roots. The creativity and friendly demeanor of this wonderful student mentor will be sorely missed.

11.1 INTRODUCTION

The use of *in vitro* plant cultures for production of chemicals and elite genotypes that are tolerant to drought and pollution or have higher nutritional value has been the focus of much attention in recent years. This interest is mainly due to consumer demands for more plant-derived compounds rather

than synthetics. Furthermore, "natural" products often have fewer international trade restrictions. Such a high demand drives the need for developing rapid and inexpensive methods for producing new genotypes with enhanced features on a large scale.

Although plant cells have some peculiarities, they can generally be cultured using methods similar to those used for the cultivation of microorganisms. In addition to more than 400,000 species of higher plants, which are currently being exploited for the production of a vast array of natural products, most of which are small molecules, plants can also be genetically modified to produce vaccines, antibodies, and other therapeutic agents (Franconi et at. 2010). For example, plant cell suspensions are currently being used for the production of secondary metabolites including ginseng saponins, shikonin, berberine, and Taxol® (Zhao and Verpoorte 2007). Furthermore, Protalix's carrot cell recombinant glucocerebrosidase (www.protalix.com; Shaaltiel et al. 2007) is close to being approved by the U.S. Food and Drug Administration. However, commercial success mainly depends on high productivity (e.g., shikonin) or high market value (e.g., Taxol).

The production of millions of elite plant genotypes by micropropagation, or the production of useful chemicals by, for example, root cultures, requires quite different cultivation methods than those used for plant cells. Thus, the production plant or plant tissues provides new and interesting bioengineering challenges. Indeed, more novel production systems are emerging, including the use of the protonema stage of the moss, *Physcomitrella patens* (Decker and Reski 2007) and duckweed (*Lemna* and *Spirodela;* Rival et al. 2008) for production of engineered proteins. As new biology is harnessed, production technology must also keep pace. Although many issues that plagued plant-based production systems decades ago still exist today, significant progress has been made in addressing the low yields, biochemical or genetic instability, and scale-up challenges.

11.2 BIOREACTORS FOR PLANT CELLS, TISSUES, ORGANS, AND PLANTLETS

Liquid-phase and gas-phase reactors comprise the two main categories of bioreactors used to culture plants or their cells, tissues, and organs (Kim et al. 2002a). Because plant tissues are immersed in the medium in liquid-phase reactors, one of the biggest challenges is delivering oxygen to them. Because gases are very insoluble in liquids, gas-phase reactors were developed to enhance oxygen (O_2) delivery. Gas-phase reactors expose the biomass to air or a gas mixture, and nutrients are delivered as gas-infused droplets. In addition to presenting a general overview, this chapter focuses on the more novel aspects of recent work culturing complex plants and tissues, including micropropagation, hairy roots, co-cultures, disposable plant reactors, and scale-up.

11.3 MICROPROPAGATION

Globally, approximately 1 billion plants are produced per year using micropropagation. The typical micropropagation system uses small culture boxes with semi-solid medium. Repeated proliferation of microshoots in these boxes is achieved by manually cutting, separating, and transferring inocula to new boxes, a very labor- and cost-intensive process. In micropropagation, there are six stages labeled 0–5. In stage 0, the donor plant is selected and may be subjected to genetic testing and disease indexing. In stage 1, an explant is isolated and disinfected, and sterile culture is initiated on the appropriate nutrient medium to generate shoots. Multiplication of the explant shoots, stage 2, usually involves application of exogenous phytohormones to stimulate branching, and subcultures are performed as needed. In stage 3, the shoots are stimulated to produce roots by altering the phytohormone content of the medium. Rooting may instead be initiated during stage 4 (acclimatization) to prevent damage to the fragile young roots during transplant to soil. *In vitro* developed roots are often considered nonfunctional, but for some plants the presence of even those roots at the time of transplanting can have beneficial effects on the plant's water status. During stage 4, acclimatization,

the plant is transitioned to the nonsterile environment at lower relative humidity (RH) and increasing light intensity. *In vitro* cultures typically have a high RH that stalls mature structural development of the shoot's cuticle, wax deposits, stomata, and mesophyll cells, thus inhibiting photosynthesis. Acclimatization accounts for approximately 30% of the total production cost of micropropagation. The final stage, 5, involves verifying the status of the plant with respect to its original genetic integrity and to validate that it is disease-free.

Micropropagation environments typically have high RH (95–100%), low light intensity (30–75 $\mu mol\ m^{-2}s^{-1}$), and large variations in carbon dioxide (CO_2). When compared with field-grown plants, *in vitro* conditions can reduce photosynthetic ability and increase transpiration and hyperhydration (Ziv 2000). The presence of sucrose in the growth medium compensates for the decreased photosynthesis, but it also reduces CO_2 fixation. CO_2 deficiencies are further exacerbated by the sealed culture chamber, a necessity for maintaining sterility of the carbon-rich media. Consequently, there is poor gas exchange between the culture and the outside atmosphere.

The composition of the headspace gas in tissue culture vessels has a major influence on plant growth and development *in vitro* (Ziv 2000). This gas is composed mainly of nitrogen, O_2, and CO_2 and may contain ethylene (C_2H_4), acetaldehyde, ethanol, and other hydrocarbons (Ziv 2000). One of the main problems for plants growing in an *in vitro* environment is hyperhydration. Hyperhydration is caused by inadequate ventilation of the culture vessel headspace and results in poor plant development *in vitro* and, later, *ex vitro* (Ziv 2000). Hyperhydrated plants have poor cuticle development and dysfunctional stomata and thus often do not survive ex vitro (Ziv 2000).

Several different reactor types have been studied for micropropagation (Figure 11.1). These are again generally divided into liquid- and gas-phase bioreactors and are described in more detail as follows.

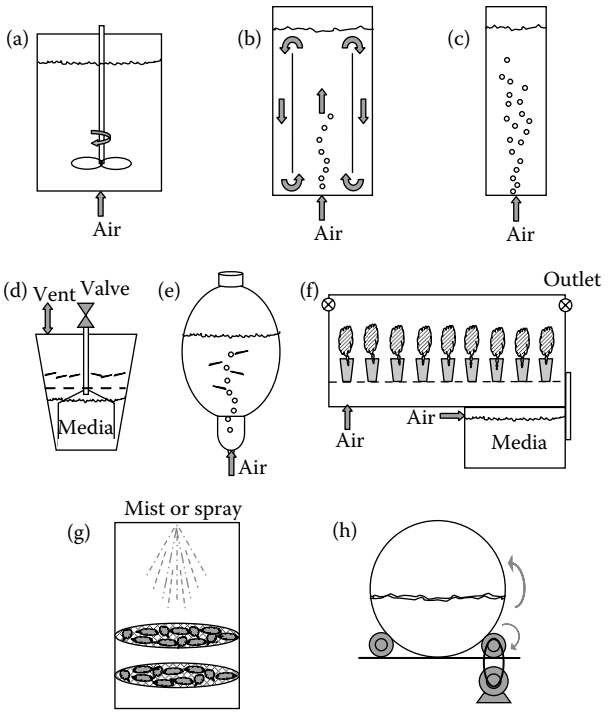

FIGURE 11.1 Schematics of typical bioreactors: (a) stirred tank; (b) airlift; (c) bubble column; (d) temporary immersion; (e) balloon-type bubble bioreactor; (f) ebb and flow; (g) mist reactor; and (h) rotating drum.

11.3.1 Liquid-Phase Reactors for Micropropagation

Because vitrification or hyperhydricity is a serious problem for micropropagated plantlets, reducing this problem is critical to the success of any bioreactor used to generate large quantities of plantlets. Plantlets, embryos, roots, etc., were initially cultured using reactors modeled after those used for microbes: stirred tank, airlift, and bubble column reactors (Figure 11.1 a, b, and c, respectively). However, the most successful liquid-based reactors also include a substantial exposure to a gas phase along with some degree of liquid immersion. Such reactors are generally termed temporary immersion bioreactors (TIBs) (Afreen 2006; Figure 11.1d). TIBs have different designs and ways to add and drain liquid. For example, the rocker box system provides nonsubmerged conditions by gently rocking the rectangular boxes containing the tissues back and forth in the liquid (Adelberg 2006). The balloon-type bubble bioreactor (Figure 11.1e), first used to culture cells and roots, can also be operated as an ebb-and-flow reactor and has proven useful for micropropagation. Ebb-and-flow operation involves flooding the culture chamber with media for a few minutes and then draining the liquid for a much longer time. The process is repeated until plantlets are fully developed (Figure 11.1f), and this approach minimizes the exposure of plantlets to excessive liquid, whereas insertion of a gas-permeable membrane in the wall of the culture box provides passive gas exchange. Considerable effort has been devoted to establishing optimized conditions for this reactor type. The temporary root-zone immersion bioreactor (TRI; Figure 11.1f) is a variant of the TIB in which only the roots are periodically submerged. The TRI has been shown to produce plantlets with better growth, normal physiology, and higher *ex vitro* growth and survival rates than those in GA-7 culture boxes or in conventional TIBs. For an excellent collection of discussions on this topic, see the book edited by Hvoslef-Eide and Preil (2005).

11.3.2 Gas-Phase Reactors for Micropropagation

The problems inherent in liquid propagation systems led to the development of gas-phase reactors. When used for micropropagation, gas-phase systems such as the nutrient mist bioreactor (mist reactor; Figure 11.1g), offer a significant advantage because the gas composition and RH surrounding the plants can be closely controlled, and these parameters can significantly affect multiplication rates, rooting, and acclimatization (Zobel 1987; Ziv 2000). However, there are significant engineering challenges in the design and development of an effective and inexpensive mist reactor for micropropagation. As summarized in Table 11.1, studies have shown that using the mist reactor in its various configurations promoted equivalent or better growth of plant inocula compared with traditional controls (Liu et al. 2002), increased shooting (Cheetham et al. 1992) as well as the formation of somatic embryos (Tisserat et al. 1993) and microtubers (Hao et al. 1998), and yielded generally higher rates of regeneration overall.

Light intensity, CO_2, and humidity (RH) all affect hyperhydration, and the latter two parameters can be readily varied and controlled in mist reactors (Correll and Weathers 2001a, 2001b). CO_2 enrichment promotes net photosynthesis and prepares plants for *ex vitro* acclimatization (Ziv 2000) and may significantly reduce the acclimatization time (see review by Pospisilova et al. 1999). Using a mist reactor, Correll et al. (2001) reduced hyperhydration in *Dianthus caryophyllus* plants by altering the mist feed rate and duty cycle. Increased CO_2 levels also decreased hyperhydration in *D. caryophyllus* plants grown in the mist reactor (Correll and Weathers 2001a) but only when used in conjunction with higher light intensity. These studies showed that hyperhydration can be reduced or eliminated using a mist reactor.

In a further development, Correll and Weathers (2001b) used a mist reactor to both grow and acclimatize carnation plants *in vitro*, thus avoiding expensive, time-consuming and labor-intensive (Fila et al. 1998) *ex vitro* acclimatization techniques. *Ex vitro* plant survival rates were higher for plants grown in the mist reactor (91% survival) compared with a conventional propagation system (GA-7 culture boxes) that only had a 50% survival rate (Correll and Weathers 2001b). This study was

TABLE 11.1
Examples of Micropropagation Mist Reactor Studies

Species	Type of Mist System	Inoculum	Results	References
Artemisia	Submerged ultrasonics	Shoots	Higher biomass and artemisinin than liquid reactors	Liu et al. 2002
Asparagus	Submerged ultrasonics	Shoots	Higher root and shoot initiation and elongation	Cheetham et al. 1992
Daucus	Submerged ultrasonics	Shootlets	Induction of asexual embryoids, not in liquid or agar	Tisserat et al. 1993
		Embryogenic callus	More somatic embryos than agar; none in liquid controls	
Dianthus	Acoustic window[a]	Node cuttings	Hyperhydration reduced by misting scheme	Correll et al. 2001
			Hyperhydration reduced by higher light and CO_2	Correll and Weathers 2001a
			Higher ex vitro survival than GA7 culture boxes	Correll and Weathers 2001b
Solanum	Submerged ultrasonics	Nodal explants	98% of inocula formed tubers	Hao et al. 1998

[a] Polypropylene.

important because it suggested that a mist reactor could eliminate the intermediate labor-intensive subculture steps and take tissues directly from inoculation to fully developed and acclimatized rooted plantlets ready for field planting.

Although contamination is another significant concern in long-running plant bioreactors, studies by Sharaf-Eldin and Weathers (2006) showed that areas of contamination that develop in the mist reactor growth chamber remained relatively isolated and spread more slowly than in liquid or semi-solid media. In addition, contamination could be controlled, even after inoculation, by using periodic sprays of disinfectants such as bleach or plant preservative mixture (PPM). The latter method was recently used by Sivakumar et al. (2010) during 1-L culture of *Artemisia annua* hairy roots in a mist reactor.

11.3.3 Challenges in Scaling up Micropropagation

Of the many challenges facing the micropropagation industry, the main one is the cost and time associated with labor. With increasing use of low-wage workers from underdeveloped countries, the success of the industry is challenged when economic or political instability arises in these countries. Most of the labor involves the manual tasks of cutting, transplanting, and acclimatizing plant tissues. These steps are slow and increase the rate of contamination, thus increasing loss of product and the overall costs. Automation of these steps could decrease production time and reduce contamination rates and labor costs if not cost-prohibitive. The development of bioreactors, such as the TIB and mist reactor, offers the potential for automating some of the stages in micropropagation. By combining shoot and root production with acclimatization, the mist reactor may offer some potential for further cost reduction (Correll and Weathers 2001a). The mist reactor is also currently being further developed to take plants from cells to fully acclimatized plantlets ready for field planting, and preliminary results are promising.

Because of concerns about contamination, most efforts to scale-up micropropagation have used a more modular approach. The most common type of reactor in this case is a variation on the TIB that uses rocker boxes or a fill-and-drain process. Using rocker boxes, Adelberg (2006) demonstrated high-quality production of plantlets of diverse species including many monocots (orchids,

Hosta, Zingiber, etc.). Using a more traditional impeller-type bioreactor, shoot primordia of *Stevia-rebaudiana* were grown at 500 L, and growth efficiency was almost the same as in a 10-L bioreactor or shake flasks (Takayama and Akita 2006). Furthermore, more than 90% of the shoots were successfully acclimatized in soil.

One bioreactor being scaled-up for plant tissue culture and micropropagation is the balloon-type bubble bioreactor (Paek et al. 2005), which, unlike the TIB, can be scaled to high volumes—up to 20,000 L (Choi et al. 2006)—a commercially useful scale. These reactors have been used to propagate Siberian ginseng somatic embryos at the 500-L scale (Paek et al. 2005). Unfortunately, there is no reasonable method for providing adequate light to large-volume cultures ($> \approx$ 5-L working volume) beyond the first few centimeters inside of the reactor wall, so for large-scale photosynthetic cultures, the balloon reactor may not be practical.

11.4 HAIRY ROOTS

Hairy roots are a plant root production system that is the result of genetic transformation of a specific plant species with the plant pathogen, *Agrobacterium rhizogenes,* containing the Ri plasmid, which can also contain "your favorite gene" (Guillon et al. 2006). After insertion of the Ri plasmid into a plant cell, the plasmid intercalates into the plant's genome resulting in a stably transformed cell that only yields a root phenotype. Each root that forms is considered a separate clone, and each can be isolated, screened for the product of interest, and then cultured indefinitely as roots. The often prolific root hairs present on these cultured roots led to the term "hairy roots". Hairy roots grow faster than untransformed roots, often produce novel chemicals, can produce secondary compounds at or greater than the parent plant, and are proving to be good producers of engineered proteins (Guillon et al. 2006; Liu et al. 2009).

11.4.1 Liquid-Phase Reactors for Hairy Roots

Hairy roots have been cultured in a wide variety of liquid-phase reactors including stirred tanks (Figure 11.1a) that are widely used for plant cells, as well as in bubble column (Figure 11.1c) and airlift (Figure 11.1b) reactors (see review by Srivastava and Srivastava 2007). Rotating drum bioreactors (Figure 11.1h), generally used in fermentations, have also been used for roots (Wu et al. 2007). The balloon-type bubble bioreactor in particular (Figure 11.1e) has shown commercial promise, and several Korean companies are using it for ginseng root culture (Choi et al. 2006). More recently, disposable reactors like the Wave reactor (see Figure 11.2d) have been successfully used to grow various plant cells and tissues in liquid including hairy roots; these are discussed in more depth in Section 11.6. Dense beds of roots have high O_2 demands, and although O_2 enriched air sparging has increased yields of roots (Ramakrishnan and Curtis 2004), this approach is costly, and thus large scale culture of dense root beds in reactors still remains somewhat challenging.

11.4.2 Gas-Phase Reactors for Hairy Roots: Using a Mist Deposition Model to Improve Nutrient Delivery

The high O_2 demand of rapidly growing hairy roots encouraged the development gas-phase reactors. At high biomass concentrations, improved mass transfer and O_2 availability make liquid-dispersed or gas-phase bioreactors (Figure 11.1g) more favorable for culture of, for example, hairy roots (Suresh et al. 2005), than liquid-phase bioreactors. Here we update a recent detailed review (Weathers et al. 2008) on mist reactors. A summary of hairy root mist reactor studies is given in Table 11.2.

Droplet and mist reactors are the two most commonly studied gas-phase reactors for hairy roots. The main difference between the reactors lies in the droplet size, with droplet sizes ranging from

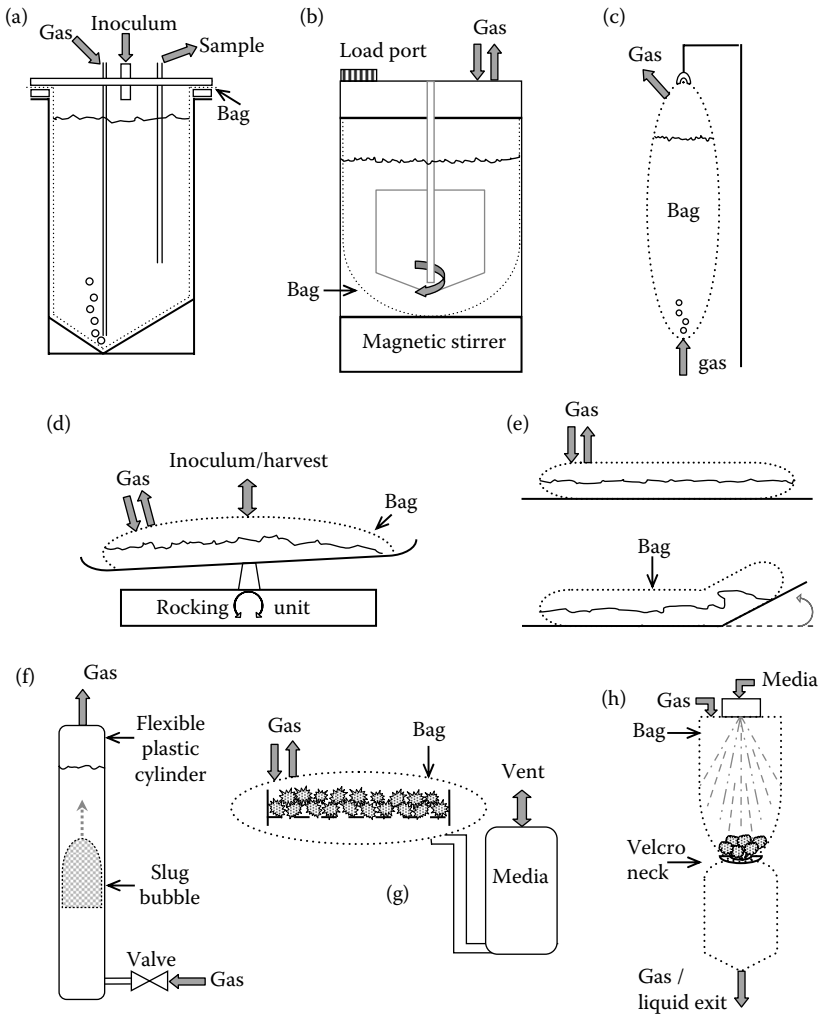

FIGURE 11.2 Schematics of disposable bioreactors: (a) bag liner in vessel; (b) MantaRay®; (c) hanging bag; (d) wave bioreactor; (e) wave and undertow; (f) slug bubble; (g) temporary immersion (Box-In-Bag); and (h) mist bag reactor.

approximately 0.01–10 μm for mists 1–100 μm for fogs, and 10–10^3 μm for sprays (Perry and Green 1997). In a gas-phase culture system, mass transfer limitations, especially of O_2, can be significantly reduced or eliminated (Weathers et al. 1999) relative to liquid-phase culture. Smaller droplets offer two main advantages over larger ones: (1) longer settling times that ease transport and distribution of the dispersed nutrient solution and enhance the ability of the small droplets to penetrate dense beds of tissues and more evenly distribute nutrients, and (2) large surface-to-volume ratios that ensure good mass transfer of gases between the gas and liquid phases, thereby enhancing gas transfer to the root tissue. However, if droplets are too small, inadequate medium will be supplied to the roots. If droplets are too large, they will impede adequate gas transfer into the roots. Although the optimum droplet size is not known and is not easily studied other than by measuring the size of droplets that exit dense beds of roots (Wyslouzil et al. 1997), Weathers and Zobel (1992) suggested that for roots the minimum acceptable droplet size is probably approximately 1 μm.

To understand how a mist reactor functions for growing roots, Wyslouzil et al. (1997) used empirical data to test a droplet deposition model in which root beds were treated as fibrous filters. For a

TABLE 11.2
Examples of Hairy Root Mist Reactor Studies

Species	System Used	Results	References
Artemisia	Acoustic window[a] mist reactor	No O_2 limitation, but 50% less biomass than liquid systems	Weathers et al. 1999
		Altered branching rate versus flasks	Wyslouzil et al. 2000
		3x higher artemisinin content than bubble column	Kim et al. 2001
		Growth comparable to bubble column	Kim et al. 2002a, 2003
	Mist reactor	Growth greater than shake flasks	Sivakumar et al. 2010
Carthamus	Submerged ultrasonics	Growth comparable to flasks; 15% faster than airlift reactor	DiIorio et al. 1992b
Cichorium	Acoustic window[b] mist reactor	Higher biomass and esculin content than bubble column	Bais et al. 2002
Datura	Hybrid submerged/ droplet reactor	Successful large-scale (500 L) culture	Wilson 1997
Fragaria	Mist reactor	Higher biomass yield than droplet bioreactor	Nuutila et al. 1997
Hypogaea	Mist reactor	Growth greater than shake flasks	Sivakumar et al. 2010
Nicotiana	Mist reactor	50% higher production of mouse interleukin-12 in mist vs. airlift reactor	Liu et al. 2009
Tagetes	Acoustic window[b] mist reactor	Thiophene content and growth comparable to shake flask; higher than bubble column and nutrient sprinkle	Suresh et al. 2005

[a] Teflon.
[b] Polycarbonate.

fixed droplet size D_p, the droplet capture efficiency (η_B) of the root bed is $\eta_B = 1 - \exp[(-4L\alpha\eta_C)/(D_R(1-\alpha))]$, where α is the packing fraction of the biomass, L is the length of the root bed, D_R is the diameter of the root, η_C is the combined capture efficiency due to impaction and interception ($\eta_{IMP+INT}$) and diffusion (η_D), and where these efficiencies are all functions of D_p (Crawford 1976; Friedlander 1977). The overall mass deposition efficiency (η_{OM}) of the root bed is the product of the root bed efficiency $\eta_B(D_{Pi})$ and the mass fraction $m(D_{Pi})$ of mist droplets of diameter D_{Pi} summed over the aerosol size distribution data: $\eta_{OM} = \sum_i \eta_B(D_{Pi}) \times m(D_{Pi})$. Finally, the medium captured by the roots (V_{dep}, mL d^{-1}) is expressed as: $V_{dep} = 24\omega \times Q_L \times \eta_{OM}$, where 24 converts from hours to days, ω is the duty cycle (min h^{-1}), and Q_L is the medium flow rate (mL min^{-1}) during the mist "on" cycle. The model is valid only when the flow rate is low and the Reynolds number (Re), based on D_R, is less than 10 (Wyslouzil et al. 1997).

In turn, the culture medium required to support the growth of roots (V_{req}, mL d^{-1}) depends on the root biomass growth rate μ (d^{-1}), the apparent biomass yield of the growth-limiting nutrient $Y_{X/S}$ [g dry weight (DW) biomass per gram nutrient consumed] and the concentration of the limiting nutrient in the medium C_S (g L^{-1}, usually taken as the carbon source). Kim et al. (2002b) suggested that at low packing fractions a lack of nutrients was likely limiting root growth in the mist bioreactor. Because V_{dep} is a strong nonlinear function of α, increasing α rapidly increases V_{dep} and supports a higher growth rate because roots can capture more nutrients. V_{req} also depends on α, but that relationship is linear. To maintain a desired growth rate, μ, V_{dep} must be greater than or equal to V_{req}.

The mist deposition model suggests several ways to increase root growth rates. These include increasing the initial biomass density (packing fraction, α) to increase the droplet capture efficiency of the roots to satisfy the biological demand and increasing the total carbon available to the roots, either by increasing the sugar concentration (C_S) of the medium or by increasing the mist duty cycle (ω). Towler et al. (2007) showed that α and C_S are the two most important factors to optimize to achieve high growth rates of hairy roots in mist reactors. In contrast, increasing the

mist duty cycle did not substantially enhance growth, an observation later confirmed by Sivakumar et al. (2010).

Other factors that have been observed to affect root growth in mist reactors include the direction of the mist flow, inoculum distribution, gas composition, medium "conditioning" factors (e.g., auxins), and medium preparation methods (autoclaving vs. filter sterilization) (DiIorio et al. 1992a; Wyslouzil et al. 2000; Kim et al. 2002b). Mist reactors fed from the top have the advantage of co-current downflow of the gas and liquid phases, and, together with gravity, this facilitates root bed drainage. If mist is provided at the bottom of the reactor and flows up through the root bed, then coalescence is greatest on the roots closest to the mist feed, less mist reaches tissues at the top of the growth chamber, and the lower regions become waterlogged, which can result in necrosis (Wyslouzil et al. 2000).

Hairy roots also respond to changes in gas composition in a manner similar to roots of whole plants, and responses vary with plant species. In addition to O_2, CO_2 and C_2H_4 can also alter root growth. For example, CO_2- enriched air decreases the lag time in some root cultures but not in others (Wyslouzil et al. 2000; Kim et al. 2002b), and an optimal concentration often exists at which growth rates are maximized (DiIorio et al. 1992a). C_2H_4 is a phytohormone that, among other effects, can alter root growth. In a mist reactor it is therefore important not to overaerate the root bed because this may purge these potentially beneficial gases from the reactor. The option to provide a controlled amount of CO_2- or C_2H_4-enriched air to root beds is one of the design benefits of using a mist reactor.

11.5 CO-CULTURES

One unusual approach to overproduction of secondary metabolites in particular has been to simultaneously grow two cultures within the same reactor. Examples of the co-culture approach, summarized in Table 11.3, include shoots and roots of a single or different species, two species of hairy roots, and microbes or insects and some plant cell/tissues or organs.

11.5.1 Shoot-Root

Subroto et al. (1996) were the first to describe co-culture of roots and shoots for the overproduction of scopolamine. Using shooty teratomas (produced via *Agrobacterium tumefaciens*) with hairy roots of *Atropa belladonna*, they observed that although neither monoculture produced scopolamine, co-cultures did, with the maximum scopolamine:hyoscyamine ratio reaching nearly 2:1 in the co-cultures. The root:shoot ratio appeared critical for the production, and increasing this ratio increased scopolamine yield up to 11-fold. The highest scopolamine production, 4.4 mg g^{-1} inoculum, was obtained in co-cultures grown in shake flasks, but production in 1- and 3-L [working volume (WV)] bioreactors also reached reasonable levels of 3.1 and 3.0 mg g^{-1} inoculum, respectively.

Sidwa-Gorycka et al. (2003) used a similar approach to successfully co-culture two species, *Ammi majus* hairy roots and *Ruta graveolens* shoots, for the overproduction of furanocoumarins (assayed as xanthotoxins). When cultures were grown in the light, the co-cultured *A. majus* hairy roots produced 2.6 times more xanthotoxin (38.1 mg g DW^{-1}) than the monoculture (14.9 mg g DW^{-1}).

In another example, Kuczkiewicz and Kokotkiewicz (2005) successfully co-cultured untransformed *Genistia tinctoria* shoots and their hairy roots to improve production of phytoestrogen 5-hydroxyisoflavones including genistin, diadzin, and diadzein. Without shoots, *G. tinctoria* hairy roots produced a large amount of a precursor, isoliquiritigenin (24.7 mg g DW^{-1}). Compared with shoot or root cultures alone, co-cultures produced significantly more diadzein and diadzin (3.3 vs. 0.04 mg g DW^{-1} and 16.5 vs. 0.86 mg g DW^{-1}, respectively). In contrast, co-cultures produced only slightly more genistin than shoot cultures (69.4 vs. 66.4 mg g DW^{-1}). Because these isoflavones increased in the shoots, the precursor isoliquiritigenin declined, suggesting a possible role for this compound in shoot isoflavone production.

TABLE 11.3
***In Vitro* Plant Co-Cultures and Their Products**

Species in Co-culture and Type	Product	Fold increase vs. Monoculture	References
Ammi majus hairy roots and *Ruta graveolens* shoots	Furanocoumarins	2.6	Sidwa-Gorycka et al. 2003
Adventitious roots of *Panax ginseng* + *Echinacea purpurea*	Ginsenosides	Less than single cultures	Wu et al. 2008
Taxus chinensis var. mairei + its endophytic fungi, *Fusarium mairei*	Paclitaxel	38	Li et al. 2009
Linum persicum + *L. austriacum* hairy roots	Podophyllotoxin	None	Mohagheghzadeh et al. 2008
L. flavum hairy roots + *Podophyllum hexandrum* cell suspension		2.4	Lin et al. 2003
L. album cells + arbuscular mycorrhiza-like fungi, *Piriformospora indica* and *Sebacina vermifera*		4	Baldi et al. 2008
Hairy roots + shoots of *Genistia tinctoria*	Phytoestrogen isoflavones	19–82[a]	Kuczkiewicz and Kokotkiewicz 2005
Hairy roots + shooty teratomas (via *A. tumefaciens*) of *Atropa belladonna*	Scopolamine	11	Subroto et al. 1996
	Nonchemical Products		
Eight aphid species on six hairy roots of six plant species	Aphids	NA	Wu et al. 1999
Meloidogyne incognita + *Cucumis melo*	Nematodes	NA	Adachi 1992
TMV (tobacco mosaic virus) + *Nicotiana benthamiana* hairy roots	Viruses	NA	Shadwick and Doran 2007

NA, not applicable.
[a] Depends on which isoflavone was measured.

11.5.2 Plant-Microbe or Plant-Animal

Other interesting and novel co-culture strategies include the production of paclitaxel by *Taxus chinensis* var. mairei co-cultured with its endophytic fungi, *Fusarium mairei* (Li et al. 2009), the production of plant viruses using host species hairy roots (Shadwick and Doran 2007), and the co-culture of insects (e.g., aphids or nematodes) on hairy roots to study interactions between the two organisms (Adachi 1992; Wu et al. 1999). In addition to the fundamental nature of these studies, co-cultures of insects with plant shoots or roots could eventually lead to the discovery of novel plant-produced compounds of therapeutic or agricultural use.

11.5.3 Podophyllotoxin

Podoyphyllotoxin production offers an interesting case study for co-culture. Using two separately cultured hairy root species of *Linum*, *Linum persicum* and *Linum austriacum*, Mohagheghzadeh et al. (2008) grew the former species inside of a 1-mm^2 mesh cotton bag inside of a shake flask whereas the latter species was grown outside of the bag in the same flask. Although podophyllotoxin did not increase compared with either of the single species, immobilization of *L. persicum* in the cloth bag significantly enhanced its monoculture productivity. Alternatively, Lin et al. (2003)

co-cultured two different genera, *Linum flavum* and *Podophyllum hexandrum*, which resulted in 240 and 72% increases in podophyllotoxin production in shake flasks and in 2-L reactors, respectively, compared with monocultures of *P. hexandrum*. This was likely a result of feeding phenyalanine to the co-cultures. *L. flavum* produces coniferin, a precursor of podophyllotoxin, which then in turn increased the podophyllotoxin concentration in the co-cultured *P. hexandrum* cells. In another instance, Baldi et al. (2008) used co-cultures of *Linum album* cells with arbuscular mycorrhiza-like fungi, *Piriformospora indica* and *Sebacina vermifera*, and obtained podophyllotoxin levels at 29 mg L^{-1}; however, the yield was less than the 77 mg L^{-1} obtained by Lin et al. (2003).

11.5.4 Challenges for Commercializing Co-Cultures

Co-culture systems are not simple. There is often an optimum ratio of the two species, and establishing controls to minimize competition between them is critical. For example, after elicitation, Wu et al. (2008) showed that ginsenosides and caffeic acid derivatives were produced in higher amounts when inoculum ratios of *Ginseng* to *Echinacea* were 4:1 and 3:2, respectively. Furthermore, as in most cultures, conditions must be adjusted to accommodate productivity of the desired compound(s) by one of the organisms, whereas media optimization must accommodate the growth of both. For example, *G. tinctoria* hairy roots grew best on SH media without growth regulators, but shoots required indole-3-butyric acid (IBA). Thus, when co-cultures included IBA, genistin production in the shoots was not altered (Kuczkiewicz and Kokotkiewicz 2005). The use of two morphologically diverse species may also require modification of reactor design. For example, in the study by Kuczkiewicz and Kokotkiewicz (2005), the two cultures were not mixed together but were inoculated into partially nested stainless steel baskets within the glass airlift reactor. The design allowed for roots to be fully immersed and shoots to be only partially immersed while simplifying the harvest and extraction of shoots. Considering these challenges, large-scale and/or long term co-culture of two or more species is far from being commercially practical.

11.6 DISPOSABLE SYSTEMS FOR CULTURING PLANT TISSUES

Recently, emphasis has been placed on culturing cell tissue and organs in disposable and scalable reactors, usually made from plastic bags (Ducos et al. 2008; Eibl et al. 2009). The main types of disposable reactors are shown schematically in Figure 11.2 and summarized in Table 11.4. Reasons for the move in this direction include the fact that disposable culture systems often have lower capital costs than stainless steel tanks. Furthermore, good manufacturing practice (GMP) requirements are stringent for therapeutic compounds and require dedicated vessels or costly cleaning operations between runs. These concerns can limit scale-up. Despite the limitation in the size of scaled-up disposable reactor systems, modularity is readily achieved. This is an advantage because losses due to contamination or other problems are minimized. Process line redundancy provides some product insurance while also allowing a manufacturer to remain better attuned to fluctuating market demands.

Hsiao et al. (1999) provided one of the earliest reports of a rather large-volume disposable reactor used for plant cultures. Vessels of different sizes up to 40 L (WV = 28.5 L) were lined with plastic bags and aerated to grow *Hyoscyamus muticus* cells (Figure 11.2a). A 6-mil plastic liner was sterilized and sandwiched between a glass cylindrical vessel and a head plate. At 40 L these reactors achieved a specific growth rate of 0.26 d^{-1}, a rate comparable to that in stirred tank reactors.

Other disposable reactor designs use plastic bags for culture vessels, but provide gas and agitation by other means than direct aeration (Table 11.4 and Figure 11.2). These are described briefly because the various design concepts have helped advance the overall area of disposable plant bioreactor technology. The MantaRay (Figure 11.2b) further developed the bag-in-a-vessel concept

TABLE 11.4
Disposable Bioreactors Available for Plant Cell and Tissue Culture (Figure 11.2 Correlating Letter a–h).

Culture Type	Reactor Type	Manufacturer	Maximum Volume (L)	Medium Form	References
Embryos, cells, hairy roots	Bag liner in a vessel (a)	None identified.	40 (28.5 WV)	Liquid	Hsiao et al. 1999
Embryos, cells	Mechanically driven membrane bioreactor - miniPerm®	Sartorius AG	0.015		Eibl et al. 2009
Embryos, cells, hairy roots, micropropagules	Pneumatically driven bag reactor	Osmotek[a]	5		
	LifeReactor® (c)				
	Ebb-and-flow bioreactor				
	Mechanically driven bag reactor	Wheaton	1		
		Science	10		
	MantaRay® (b)	Products	500		
		Metabios[a]	600		
	Optima and OrbiCell (d)	Wave Biotech AG	(300 WV)[b]		
	Wave bioreactor (d)				
Embryos, cells, micropropagules	Wave and undertow (e)	Nestlé	750 (250 WV)		Terrier et al. 2007
	Slug bubble (f)		90 (70 WV)		
Embryos	Temporary immersion (Box-In-Bag) (g)	None identified	10		Ducos et al. 2008
Hairy roots, micropropagules, one-step acclimatization	Mist bag bioreactor (h)	None identified	1–4 WV 20 WV	Gas-suspended droplets	Liu et al. 2009; Sivakumar et al. 2010
Hairy roots		Rootec[c]	NA		See footnote

NA, not available.

[a] Company appears to be out of business.

[b] Number 600 and WV taken from http://www.sartorius-stedim.com/fileadmin/sartorius_pdf/alle/biotech/Data_BIOSTAT CultiBagRM600_Optical_SBI2023-e.pdf

[c] Information gleaned from www.rootec.com

described by Hsiao et al. (1999), but maximum culture volume was limited to 1 L, mainly because the culture is mixed using a magnetic stirrer to achieve aeration. Greater volume and disposability was achieved by Osmotek using a simple culture bag (Figure 11.2c) without any supporting external wall structure to culture various cells or tissue types. However, a drawback of this system was that as it was scaled-up, and the weight of the liquid medium inside of the bag placed undue stress upon the walls, thereby limiting its functional volume. To counter the hanging weight of liquid in the Osmotek bag, Protalix more recently used an external open wire cage around the bag to produce therapeutic proteins [e.g., glucocerebrosidase (GCD)] using carrot cells (www.protalix.com; Shaaltiel et al. 2007). The wave reactor is a similar design, but here the plastic bag is laid on a platform that gently rocks to induce very slight wave action in the liquid inside of the bag (Figure 11.2d). A perfusion system or ports can be sealed into the bag wall to facilitate input and output of

gases or liquids. Although the wave reactor has been used to successfully culture many different plant cells and tissues, a drawback of this design is that it scales horizontally, thereby using precious, and expensive, floor space.

Newer designs have built upon these earlier bag systems and include the wave undertow (WU) reactor, the slug bubble (SB) reactor, and the "Box In Bag" (BIB) reactor (Table 11.4; Terrier et al. 2007; Ducos et al. 2008). The WU reactor altered the original wave reactor design by reducing the mechanical force involved by having the platform upon which the bag rests only move one section of the bag up and down (Figure 11.2e). At 10, 30, and 100 L in the WU, tobacco cells had specific growth rates of 0.31, 0.34, and 0.31 h^{-1}, respectively, values that are less than or equal to growth in 250-mL shake flasks and a 10-L stirred tank at 0.34 and 0.38, respectively. In contrast to the WU, the SB reactor (Figure 11.2f) functions very differently. A large gas bubble is formed at the base and moves up a cylinder of suspension cells, thereby providing aeration and mixing. Growth of tobacco cells in the SB reactor was similar to that in the WU reactor. The WU and SB reactors should also be amenable for culturing shoots, embryos, and hairy roots. The BIB reactor (Figure 11.2g; Ducos et al. 2008) has four rectangular walls that are connected by a stiff, fine-porosity screen a short distance above the base of the walls. This screened box is placed into a bag with a port in the bottom of the bag. Medium is pumped up through the port, flooding the tissues seated on the screen, and then allowed to drain via gravity, making the system in effect a TIB. The rigid walls of the box maintained a headspace above the screen where the developing embryos were seated. The BIB reactor was specially designed for somatic embryo development, and as many as 20,000 embryos per system have been successfully propagated using a BIB reactor (Ducos et al. 2008).

Recently the Weathers laboratory (Liu et al. 2009) reported on a disposable but scalable version of the mist reactor (MR) (Figure 11.2h). Using unoptimized tobacco hairy roots, growth and productivity of mIL-12 were compared in three culture systems: shake flasks, an airlift bioreactor, and the MR. As determined by a functional ELISA, roots in the mist reactor produced a yield of mIL-12 of up to 5.3 μg g FW^{-1}, with overall productivity of 22 μg L^{-1} d^{-1}. Although less than that in shake flasks (31 μg L^{-1} d^{-1}), it was approximately 50% more than in an airlift reactor. About 16% of the total mIL-12 produced by mist-grown roots was secreted into the medium, and levels declined once protease activity began to significantly increase. In addition, mist-grown roots had little to no visible necrosis compared with roots grown in the airlift reactor. The bag MR has also been used to culture *Artemisia annua* shoots and initiate rooting; root initiation from shoots occurred approximately 25–50% faster in the MR than in liquid shake flask cultures or in GA-7 boxes with semi-solid medium (unpublished data).

11.7 Scaling up

Different reactor types have been successfully scaled-up for the production of suspension cultures, micropropagules, and hairy roots. The benchmark for successful scale-up of most cultures is matching or exceeding the growth obtained in shake flasks (for liquid-based cultures such as hairy roots) or tissue culture boxes (for micropropagation). More recent successes in scale-up are detailed in the following paragraphs.

Several cell suspension cultures have been successfully scaled-up in SB, wave, and WU reactors with WVs as high as 100 L, with growth kinetics similar to those in shake flasks. Even Nalgene carboys have been scaled to 50 L with aeration provided by rotary shaking (Raval and Büchs 2008).

The most notable large-scale hairy root culture to date is probably the balloon reactor, which is reported to 20,000 L for ginseng root production (Choi et al. 2006). As this reactor was scaled from 4 to 1000 L, the growth yield decreased 20%, possibly because of inadequate gas mass transfer throughout the liquid phase of the reactor as the volume was increased. Similarly, when production of *Echinacea purpurea* roots was scaled-up from a 4-L balloon reactor to a 500-L balloon reactor

FIGURE 11.3 *A. hypogaea* hairy roots after harvest from a 20-L mist reactor. (Photo courtesy of G. Sivakumar.)

TABLE 11.5
Some Comparative Biomass Productivities of Root Cultures in Different Larger Scale Bioreactors

Plant species (g FW L^{-1})[a]	Culture Type	Bioreactor Type	WV (L)	Productivity[b] (g DW L^{-1} d^{-1})	References
Glycyrrhiza glabra (4)	Hairy roots	Bubble column	4	0.25[b]	Mehrota et al. 2008
Hyoscyamus muticus (2)[b]		Co-current gas/liquid spray	14	1.43[d]	Ramakrishnan and Curtis 2004
Stizolobium hassjoo (1.5)[b]		Countercurrent dual mist	9	0.05	Huang and Chou 2006
Atropa belladonna (1.8)		Co-current gas/liquid spray	4.5	0.44	Williams and Doran 2006
Salvia sclarea (2.15)		Sprinkle reactor	2.0	0.18	Kuźma et al. 2009
Artemisia annua (8)		Mist	1	0.25[e]	Sivakumar et al. 2010
Arachis hypogaea (6)			1	0.62[f]	
			4	0.49[f]	
			20	0.39[f]	
Panax ginseng (5)	Adventitious roots	Balloon	1,000	0.23[c]	Paek et al. 2009, and K.-Y Paek to P.J.W.[c]
			10,000	0.18[c]	
Echinacea purpurea (7)		Balloon	4	0.06[b]	Jeong et al. 2009
		Balloon	500	0.13[b]	Wu et al. 2008
		rotating drum	1,000	0.09[b]	

[a] Inoculum level.

[b] If only FW given, DW was estimated as 10% of FW and vice versa.

[c] In personal e-mail from Y.-K. Paek to P.J. Weathers (January 18, 2010), these cultures were indicated to have been optimized as follows: fed batch nutrient feed; stepped increase in aeration from 0.05 to 0.2 vvm; increase O_2 concentration in air to 40%.

[d] Optimized as follows: fed batch during trickle mode; nutrient delivery as liquid (0–12 d), trickle bed (12–25 d); increased aeration from 0.2 to 0.7 vvm partway through trickle-bed mode; O_2 enriched to 37% at 19 d.

[e] Maximum productivity from fed batch runs (see Figure 11.2).

[f] After 20 d in culture; growth not optimized.

or to a 1000-L rotating drum, growth declined approximately 30 and 50%, respectively (Wu et al. 2007). Unfortunately, this decline in productivity with scale-up is still all too common for plant cultures (Zhao and Verpoorte 2007).

To overcome gas transfer limitations inherent in liquid-based systems, gas-phase reactors were developed. However, only recently have these been successfully scaled-up beyond approximately 1 L. For example, the biomass yield of hairy roots of *Salvia sclarea* in a 10-L sprinkle bioreactor increased 40% compared with that in shake flasks. A 2.4-fold increase in diterpenoid concentration was observed in the 10-L reactor compared with shake flask cultures when both cultures were elicited with methyl jasmonate (Kuzma et al. 2009). When Ramakrishnan and Curtis (2004) used a 14-L hybrid reactor (trickle bed and liquid) along with O_2-enriched air in a fed-batch mode, they achieved a very high yield of roots (752 g FW L^{-1}). However, it is not clear if the hybrid reactor has been successfully scaled beyond 14 L. Recently, using *Arachis hypogaea* hairy roots, successful scale-up from 1 to 20 L of the mist bioreactor has been achieved with growth rates at 20 L nearly equal to those in shake flasks. There was a dense cluster of healthy roots with little or no necrosis in the interior of the root mass (Figure 11.3). Scaling mainly depended on increasing the medium flow rate delivered to the misting nozzle and the diameter of the culture vessel (Sivakumar et al. 2010). Comparative biomass productivities of roots in scaled-up mist reactors are summarized in Table 11.5.

11.8 CONCLUSIONS

With industry now involved in plant-produced pharmaceuticals, specifically the production of Taxol and Uplyso® (recombinant glucocerebrosidase), by Bristol Myers Squibb and Pfizer, respectively, *in vitro* phytopharms are finally being recognized as an important source of cost-effective therapeutics. Although there remain many challenges to developing commercially successful production systems for the more complex three-dimensional plant cultures, considerable success has been achieved, and new solutions will surely emerge.

SUMMARY

Plant cell culture as whole plants/organs has clear advantages and economic benefits over simple suspension culture of cells.

Several different methodologies can be used to mitigate some problems with culture in bioreactors (e.g., limited immersion providing better gas transfer).

The mist bioreactor design offers a scalable system with good yields and has great potential for research and manufacture of biologically active products.

REFERENCES

Adachi, H. 1992. Culture of *Meloidogyne incognita* on oriental-melon roots genetically transformed by *Agrobacterium rhizogenes*. *Jap J Appl Entomol Zool* 36:225–30.

Adelberg, J. 2006. Agitated, thin-films of liquid media for efficient micropropagation. In Gupta, S.D., and Y. Ibaraki, eds., *Plant Tissue Culture Engineering*, pp.101–17. Dordrecht, The Netherlands: Springer.

Afreen, F. 2006. Temporary immersion bioreactor. In Gupta, S.D., and Y. Ibaraki, eds., *Plant Tissue Culture Engineering*, pp. 187–201. Dordrecht, The Netherlands: Springer.

Bais, H.P., B. Suresh, K.S.M.S. Raghavarao, and G.A. Ravishankar. 2002. Performance of hairy root cultures of *Cichorium intybus* L. in bioreactors of different configurations. *In Vitro Cell Dev Biol Plant* 38:573–80.

Baldi, A., A. Jain, N. Gupta, A..K. Srivastava, and V.S. Bisaria. 2008. Co-culture of arbuscular mycorrhiza-like fungi (*Piriformospora indica* and *Sebacina vermifera*) with plant cells of *Linum album* for enhanced production of podophyllotoxins: A first report. *Biotechnol Lett* 30:1671–7.

Cheetham, R.D., C. Mikloiche, M. Glubiak, and P. Weathers. 1992. Micropropagation of a recalcitrant male asparagus clone (MD 22-8). *Plant Cell Tissue Org Cult* 31:15–9.

Choi, Y.E., Y.S. Kim, and K.Y. Paek. 2006. Types and designs of bioreactors for hairy root culture. In Gupta, S.D., and Y. Ibaraki, eds., *Plant Tissue Culture Engineering*, pp. 161–72. Dordrecht, The Netherlands: Springer.

Correll, M.J., Y. Wu, and P.J. Weathers. 2001. Controlling hyperhydration of carnations (*Dianthus caryophyllus* L.) grown in a mist reactor. *Biotechnol Bioeng* 71:307–14.

Correll, M.J., and P.J. Weathers. 2001a. Effects of light, CO_2 and humidity on carnation growth, hyperhydration and cuticular wax development in a mist reactor. *In Vitro Cell Dev Biol Plant* 37:405–13.

Correll, M.J., and P.J. Weathers. 2001b. One-step acclimatization of plantlets using a mist reactor. *Biotechnol Bioeng* 73:253–8.

Crawford, M. 1976. *Air Pollution Control Theory*, pp. 424–33. New York: McGraw-Hill.

Decker, E.L., and R. Reski. 2007. Moss bioreactors producing improved biopharmaceuticals. *Curr Opin Biotechnol* 18:393–8.

DiIorio, A.A., R.D. Cheetham, and P.J. Weathers. 1992a. Carbon dioxide improves the growth of hairy roots cultured on solid medium and in nutrient mists. *Appl Microbiol Biotechnol* 37:463–7.

DiIorio, A.A., R.D. Cheetham, and P.J. Weathers. 1992b. Growth of transformed roots in a nutrient mist bioreactor: Reactor performance and evaluation. *Appl Microbiol Biotechnol* 37:457–62.

Ducos, J.P., B. Terrier, D. Courtois, and V. Pétiard. 2008. Improvement of plastic-based disposable bioreactors for science needs. *Phytochem Rev* 7:607–13.

Eibl, R., S. Werner, and D. Eibl. 2009. Disposable bioreactors for plant liquid cultures at litre scale. *Eng Life Sci* 9:156–64.

Fila, G., J. Ghashghaie, J. Hoarau, and G. Cornic. 1998. Photosynthesis, leaf conductance, and water relations of in vitro cultured grapevine rootstock in relation to acclimatization. *Physiol Plant* 102:411–8.

Franconi, R., O.C. Demurtas, and S. Massa. 2010. Plant-derived vaccines and other therapeutics produced in contained systems. *Expert Rev Vaccines* 9:877–92.

Friedlander, S.K. 1977. *Smoke, Dust and Haze: Fundamentals of Aerosol Behavior*, p. 338. New York: Wiley.

Guillon, S., J. Trémouillaux-Guiller, P.K. Pati, M. Rideau, and P. Gantet. 2006. Harnessing the potential of hairy roots: Dawn of a new era. *Trends Biotechnol* 24:403–9.

Hao, Z., F. Ouyang, Y. Geng, X. Deng, Z. Hu, and Z. Chen. 1998. Propagation of potato tubers in a nutrient mist bioreactor. *Biotechnol Technol* 12:641–4.

Hsiao, T.Y., F.T. Bacani, E.B. Carvallo, and W.R. Curtis. 1999. Development of a low capital investment reactor system: Application for plant cell suspension culture. *Biotechnol Prog* 15:114–22.

Hvoslef-Eide, K.A., and W. Preil, eds. 2005. Liquid culture systems for in vitro plant propagation. Springer, Dordrecht, The Netherlands.

Jeong, J.A., C.H. Wu, H.N. Murthy, E.J. Hahn, and K.Y. Paek. 2009. Application of an airlift bioreactor system for the production of adventitious root biomass and caffeic acid derivatives of Echinacea purpurea. *Biotechnol Bioproc Eng* 14:91–8.

Kim, Y., B.E. Wyslouzil, and P.J. Weathers. 2001. A comparative study of mist and bubble column reactors in the in vitro production of artemisinin. *Plant Cell Rep* 20:451–5.

Kim, Y., B.E. Wyslouzil, and P.J. Weathers. 2002a. Secondary metabolism of hairy root cultures in bioreactors. *In Vitro Cell Dev Biol Plant* 38:1–10.

Kim, Y.J., P.J. Weathers, and B.E. Wyslouzil. 2002b. Growth of *Artemisia annua* hairy roots in liquid- and gas-phase reactors. *Biotechnol Bioeng* 80:454–64.

Kim, Y.J., P.J. Weathers, and B.E. Wyslouzil. 2003. Growth dynamics of *Artemisia annua* hairy roots in three culture systems. *Biotechnol Bioeng* 83:428–43.

Kuczkiewicz, M., and A. Kokotkiewicz. 2005. Co-cultures of shoots and hairy roots of *Genista tinctoria* L. for synthesis and biotransformation of large amounts of phytoestrogens. *Plant Sci* 169:862–71.

Kuzma, K., E. Bruchajzer, and H. Wysokinska. 2009. Methyl jasmonate effect on diterpenoid production accumulation in *Salvia sclarea* hairy root culture in shake flasks and sprinkle bioreactor. *Enz Microb Technol* 44:406–10.

Li, Y.C., W.Y. Tao, and L. Cheng. 2009. Paclitaxel production using co-culture of *Taxus* suspension cells and paclitaxel-producing endophytic fungi in a co-bioreactor. *Appl Microbiol Biotechnol* 83:233–9.

Lin, H.W., K.H. Kwok, and P.M. Doran. 2003. Production of podophyllotoxin using cross-species coculture of *Linum flavum* hairy roots and *Podophyllum hexandrum* cell suspensions. *Biotechnol Bioeng* 19:1417–26.

Liu, C.Z., C. Guo, Y.C. Wang, and F. Ouyang. 2002. Comparison of various bioreactors on growth and artemisinin biosynthesis of *Artemisia annua* L. shoot cultures. *Process Biochem* 39:45–9.

Liu, C.Z., M.J. Towler, G. Medrano, C.L. Cramer, and P.J. Weathers. 2009. Production of mouse interleukin-12 is greater in tobacco hairy roots grown in a mist reactor than in an airlift reactor. *Biotechnol Bioeng* 102:1074–86.

Mehrota, S., A.K. Kukreja, S.P.S. Khanuja, and B.N. Mishra. 2008. Genetic transformation studies and scale up of hairy root culture of Glycyrrhiza glabra in bioreactor. *Elec J Biotechnol* 11:1–7.

Mohagheghzadeh, A., A. Gholami, S. Hemmati, and S. Dehshahri. 2008. Bag culture: A method for root-root co-culture. *Zeitshrift fur Naturforschung* 63c:157–60.

Nuutila, A.M., A.S. Lindqvist, and V. Kauppinen. 1997. Growth of hairy root cultures of strawberry (*Fragaria* x *ananassa* Duch.) in three different types of bioreactors. *Biotechnol Technol* 11:363–66.

Paek, K.Y., D. Chakrabarty, and E.J. Hahn. 2005. Application of bioreactor systems for large scale production of horticultural and medicinal plants. In Hyoslef-Eide, A.K., and Preil, W., eds., *Liquid Culture Systems for In Vitro Plant Propagation*, pp. 95–116. Dordrecht, The Netherlands: Springer.

Paek, K.Y., H.N. Murthy, E.J. Hahn, and J.J. Zhong. 2009. Large scale culture of ginseng adventitious roots for production of ginsenosides. *Adv Biochem Engin/Biotechnol* 113:151–76.

Perry, R.H., and D.W. Green. 1997. *Perry's Chemical Engineer's Handbook*, 7th ed., pp. 14–82. New York: McGraw-Hill.

Pospisilova, J., I. Ticha, P. Kadlecek, D. Haisel, and S. Plzakova. 1999. Acclimatization of micropropagated plants to ex vitro conditions. *Biol Plant* 42:481–97.

Ramakrishnan, D., and W.R. Curtis. 2004. Trickle-bed root culture bioreactor design and scale up: Growth, fluid dynamics and oxygen mass transfer. *Biotechnol Bioeng* 88:248–60.

Raval, K., and J. Büchs. 2008. Extended method to evaluate power consumption in large disposable shaking bioreactors. *J Chem Engin Japan* 41:1075–82.

Rival, S., J.P. Wisniewski, A. Langlais, H. Kaplan, G. Freyssinet, G. Vancanneyt, R. Vunsh, A. Perl, and M. Edelman. 2008. *Spirodela* (duckweed) as an alternative production system for pharmaceuticals: A case study, aprotinin. *Transgenic Res* 17:503–13.

Shaaltiel, Y., D. Bartfeld, S. Hashmueli, G. Baum, E. Brill-Almon, G. Galili, O. Dym, S.A. Boldin-Adamsky, I. Silman, J.L. Sussman, A.H. Futerman, and D. Aviezer. 2007. Production of glucocerebrosidase with terminal mannose glycans for enzyme replacement therapy of Gaucher's disease using a plant cell system. *Plant Biotechnol J* Sep 5:579–90.

Shadwick, F.S., and P.M. Doran. 2007. Infection, propagation, distribution and stability of plant virus in hairy root cultures. *J Biotechnol* 131:318–29.

Sharaf-Eldin, M., and P.J. Weathers. 2006. Movement and containment of microbial contamination in the nutrient mist bioreactor. *In Vitro Cell Dev Biol Plant* 42:553–7.

Sidwa-Gorycka, M., A. Królicka, M. Kozyra, K. Głowniak, F. Bourgaud, and E. Kojkowska. 2003. Establishment of a co-culture of *Ammi majus* L. and *Ruta graveolens* L. for the synthesis of furanocoumarins. *Plant Sci* 165:1315–9.

Sivakumar, G., C.Z. Liu, M.J. Towler, and P.J. Weathers. 2010. Biomass production of hairy roots of *Artemisia annua* and *Arachis hypogaea* in a scaled-up mist bioreactor. *Biotechnol Bioeng* 107:802–13.

Srivastava, S., and A.K. Srivastava. 2007. Hairy root culture for mass production of high-value secondary metabolites. *Crit Rev Biotechnol* 27:29–43.

Subroto, M.A., K.H. Kwok, J.D. Hamill, and D.M. Doran. 1996. Coculture of genetically transformed roots and shoots for synthesis, translocation, and biotransformation of secondary metabolites. *Biotechnol Bioeng* 49:481–94.

Suresh, B., H.P. Bais, K.S.M.S. Raghavarao, G.A. Ravishankar, and N.P. Ghildyal. 2005. Comparative evaluation of bioreactor design using *Tagetes patula* L. hairy roots as a model system. *Proc Biochem* 40:1509–15.

Takayama, S., and M. Akita. 2006. Bioengineering aspects of bioreactor application in plant propagation. In Gupta, S.D., and Y. Ibaraki, eds., *Plant Tissue Culture Engineering*, pp. 83–100. Dordrecht, The Netherlands: Springer.

Terrier, B., D. Courtois, N. Hénault, A. Cuvier, M. Bastin, A. Akin, J. Dubreuil, and J. Pétiard. 2007. Two new disposable bioreactors for plant cell culture: The wave and undertow bioreactor and the slug bubble bioreactor. *Biotechnol Bioeng* 96:914–23.

Tisserat, B., D. Jones, and P.D. Galletta. 1993. Construction and use of an inexpensive in vitro ultrasonic misting system. *Hort Technol* 3:75–8.

Towler, M.J., B.E. Wyslouzil, and P.J. Weathers. 2007. Using an aerosol deposition model to increase hairy root growth in a mist reactor. *Biotechnol Bioeng* 96:881–91.

Weathers, P.J., and R.W. Zobel. 1992. Aeroponics for the cultures of organisms, tissues and cells. *Biotech Adv* 10:93–115.

Weathers, P.J., B.E. Wyslouzil, K.K. Wobbe, Y.J. Kim, and E. Yigit. 1999. Workshop on bioreactor technology. The biological response of hairy roots to O_2 levels in bioreactors. *In Vitro Cell Dev Biol Plant* 35:286–9.

Weathers, P.J., C.Z. Liu, M.J. Towler, and B.E. Wyslouzil. 2008. Mist reactors: Principles, comparison of various systems, case studies. *Elec J Integrative Biol* 3:29–37.

Wilson, D.G. 1997. The pilot-scale cultivation of transformed roots. In Doran, P.M., ed., *Hairy Roots: Culture and Applications*, pp. 179–90. Oxford, UK: Gordon and Breach/Harwood Academic.

Wu, C.H., H.N. Murthy, E.J. Hahn, and K.Y. Paek. 2007. Large-scale cultivation of adventitious roots of *Echinacea purpurea* in airlift bioreactors for the production of chichoric acid, chlorogenic acid and caftaric acid. *Biotechnol Lett* 29:1179–82.

Wu, T.S., J. Wittkamper, and H.E. Flores. 1999. Root herbivory in vitro: Interactions between roots and aphids grown in aseptic coculture. *In Vitro Cell Dev Biol Plant* 35:259–64.

Wu, C.H., H.N. Murthy, E.J. Hahn, and K.Y. Paek. 2008. Establishment of adventitious root co-culture of *Ginseng* and *Echinacea* for the production of secondary metabolites. *Acta Physiologiae Plantarum* 30:891–6.

Wyslouzil, B.E., R.G. Waterbury, and P.J. Weathers. 2000. The growth of single roots of *Artemisia annua* in nutrient mist bioreactors. *Biotechnol Bioeng* 70:143–50.

Wyslouzil, B.E., M. Whipple, C. Chatterjee, D.B. Walcerz, P.J. Weathers, and D.P. Hart. 1997. Mist deposition onto hairy root cultures: Aerosol modeling and experiments. *Biotechnol Prog* 13:185–94.

Zhao, J., and R. Verpoorte. 2007. Manipulating indole alkaloid production by *Catharanthus roseus* cell cultures in bioreactors: From biochemical processing to metabolic engineering. *Phytochem Rev* 6:435–57.

Ziv, M. 2000. Bioreactor technology for plant micropropagation. In, Janick, J., ed., *Horticultural Reviews*, pp. 1–30. New York: John Wiley and Sons.

12 Cell Immobilization and Its Applications in Biotechnology: Current Trends and Future Prospects

Ronnie G. Willaert

CONTENTS

"The great men of science are supreme artists."

Martin H. Fischer

12.1 INTRODUCTION

The immobilization of whole cells can be defined as "the physical confinement or localization of intact cells to a certain region of space; without loss of desired biological activity." When cells are encapsulated in an immobilized cell system, the term "bioencapsulation" or "microencapsulation" is used; the latter is used when cells are immobilized in microcapsules (i.e., micrometer-sized systems surrounded by a barrier membrane). Recently, nanoencapsulation of biological molecules such as proteins have also been successful.

Immobilizing individual enzymes, for simple reactions such as hydrolysis and isomerization, has been used to create biocatalysts for the production of various chemicals through simple and conjugated reactions. Many applications have also been developed for single and multicellular organisms.

The suitability of a given system of immobilization is dictated by the type of application and the physical and biochemical characteristics of the immobilizing matrix/agent. Accordingly, requirements will differ from one case to another; however, in any system, the following characteristics are generally desirable:

- High cell mass-loading capacity
- Affords easy access to nutrient media
- Is a simple and "nontoxic" immobilization procedure
- Affords high surface-to-volume ratio
- Facilitates optimum mass transfer
- Is sterilizable and reusable
- Facilitates easy separation of cells and carrier from media
- Is suitable for conventional reactor systems as well as cell suspension and anchorage-dependent cells
- Should be biocompatible for animal cells
- Contains immunoprotection barrier
- Should be economically viable.

12.2 IMMOBILIZED CELL SYSTEMS

On the bases of physical localization and the nature of microenvironment, immobilized cell systems can be classified into four categories (Figure 12.1).

12.2.1 Surface Attachment of Cells

Although this is not suitable where cell-free effluent is desired, immobilization of cells by adsorption to a support material can be achieved naturally or induced artificially by using linking agents (metal oxides or covalent bonding agents such as glutaraldehyde or aminosilane) (Figure 12.2). A

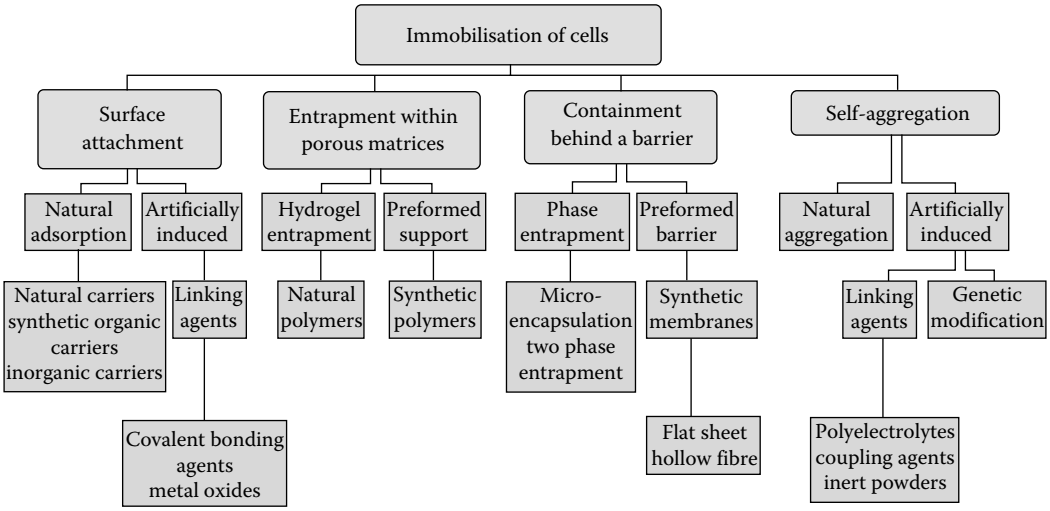

FIGURE 12.1 Classification of immobilized cell systems according to the physical localization and the nature of the microenvironment (Willaert, R.G. and Baron, G.V., *Rev Chem Eng.,* 12:1–205, 1996. With permission.).

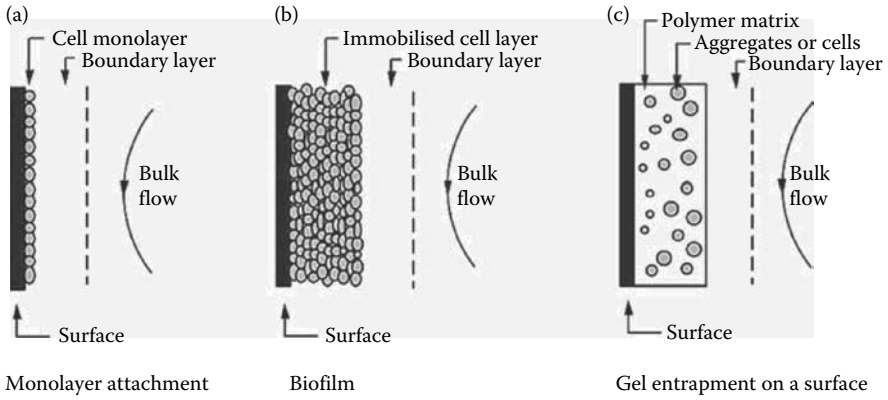

FIGURE 12.2 Cell-immobilization by adsorption/attachment to a surface: (a) adsorption of a monolayer, (b) adsorption of a biofilm, and (c) adsorption of an "artificial" biofilm (i.e., adsorption of a gel layer containing immobilized cells or cell aggregates).

suitable adsorbent for spontaneous attachment should possess a high affinity toward the biocatalyst and cause minimal denaturation. The adsorption of cells to an organic or inorganic support material is achieved *via* the Van der Waals forces and ionic interactions.

The adhesion behavior of viable cells is influenced by

- The physical and chemical properties of the adsorption matrix
- The identity and the biochemical characteristics of the immobilized organism (especially the outer surface of the cell wall)
- The composition and chemical and physical properties of the surrounding mobile phase

The effects of different environmental and/or physiological conditions on the adhesion mechanisms of different bacteria have been intensively studied (Mavituna 2004). Recent studies revealed that cells interact with their surrounding through specialized structures [e.g., pilus-associated adhesions, exopolymers (glycocalyx in the case of bacteria), and complex ligand interactions involving signaling molecules and quorum-sensing mechanisms]. Therefore, it follows that sensing a biotic or an abiotic surface may turn on genetic switches, and this in turn may lead to changes in the organism's phenotype (Loo et al. 2000).

Recently, the structural and developmental complexities of microbial biofilm formation investigated using new sophisticated techniques including proteomics revealed that biofilm formation by *Pseudomonas aeruginosa* proceeds as a regulated developmental sequence comprising five stages (Sauer et al. 2002; Stoodley et al. 2002). Stages I and II are generally identified by loose or transient association with the surface, followed by a robust adhesion. Stages III and IV involve the aggregation of cells into microcolonies and subsequent growth and maturation, whereas stage V is characterized by a return to transient motility in which biofilm cells are sloughed/shed off. Biofilm structures can be flat or mushroom-shaped depending on the nutrient source, which seems to influence the interactions between localized clonal growth and the subsequent rearrangement of cells through type IV pilus-mediated gliding motility (Klausen et al. 2003).

Most animal cells from solid tissue grow as adherent monolayers, unless transformed into anchorage-independent cells. However, anchorage-dependent cells are often diploid and exhibit **contact inhibition**. After tissue disaggregation or subculturing, they will need to attach and spread out on the substrate before proliferating.

Contact inhibition: Animal cells that exhibit contact inhibition stop growing when cell-cell contact takes place as the culture reaches confluence.

Whereas cell adhesion is mediated by specific cell-surface receptors, cell-substrate interactions are mediated primarily by integrins, receptors for matrix molecules such as fibronectin, entactin, laminin, and collagen, which bind them *via* a specific motif usually containing the arginine-glycine-aspartic acid (RDG) sequence (Yamada and Geiger 1997). Each integrin comprises one α and one β subunit, both of which are highly polymorphic, thus generating considerable diversity among integrins.

The first step of the cell-surface interaction of anchorage-dependent cells is attachment, in which the cells retain the round shape they possessed in suspension. The cells undergo conformational change, known as spreading, in which the cells increase their surface area before attachment to the surface. The kinetics of attachment and spreading have been determined by measuring the effective refractive index of the waveguide, the number of cells per unit area, and a parameter uniquely characterizing their shape, such as the area in contact with the surface. Examples of cell immobilization by attachment to the surface are given in Table 12.1.

12.2.2 Entrapment within Porous Matrices

Cell entrapment can be achieved through *in situ* immobilization in the presence of the porous matrix (i.e., gel entrapment) or by allowing the cells to move into a preformed porous matrix (Figure 12.3). Entrapped cells can reach high densities in the matrix and, compared with surface immobilization,

TABLE 12.1
Examples of Cell-Immobilization by Attachment to a Surface

Material	Cell Type	Application
	Bacteria	
Ion exchange resin	*Bacillus stearothermophilus*	Amylase production
Coke	*Zymomonas mobilis*	Ethanol production
Seashell pieces	*Bacillus* sp. + *Aeromonas* sp. + *Alcaligenes* sp.	Decolorization and degradation of triphenyl methane dyes
	Fungi	
Celite	*Penicillium chrysogenum*	Penicillin production
Stainless steel fiber cloth	*Saccharomyces cerevisiae*	Beer production
Sugarcane bagasse	*Candida guilliermondii*	Xylitol production
Straw	*Agaricus* sp.	Laccacase production
Structural fibrous network of papaya wood	*Aspergillus terreus*	Itaconic acid production
	Animal Cells	
Surface modified polyethylene film	Midbrain cells	Neural differentiation
Poly(lactide-co-glycolide), poly(D,L-lactide)	Chondrocyte	Growth on biodegradable scaffolds (tissue engineering)
Pyrex glass, polysterene, glass beads	*Trichoplusia ni*	Recombinant protein production

Source: Adapted from Willaert, R.G. and Baron, G.V., *Rev Chem Eng.,* 12:1–205, 1996; Willaert, R. *Fermentation Microbiology and Biotechnology*, 2nd ed., pp. 287–361, 2007b. Boca Raton, FL: CRC Press.

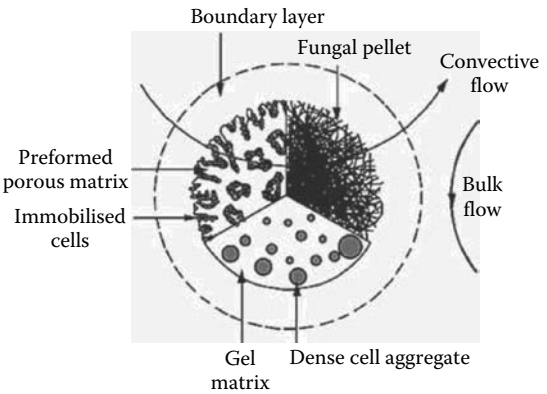

FIGURE 12.3 Spherical particle showing three immobilization methods: (1) cell immobilization in a preformed porous particle (upper left), (2) immobilization by self-aggregation (i.e., a fungal pellet), and (3) immobilization in a gel matrix (lower part).

cells are well protected from fluid shear. However, these dense cell packings may lead to mass transport limitations.

12.2.2.1 Hydrogel Entrapment

Most research in the domain of immobilized cells has used gel entrapment because of its simplicity and excellent cell containment.

TABLE 12.2
Gel Formation Mechanisms for Cell Entrapment

Principle of Gelation	Material
Ionotropic gelation	Alginate, chitosan
Thermal gelation	Agar, agarose, κ-carrageenan, collagen, gelatin, gellan gum, curdlan
Precipitation	Cellulose, cellulose triacetate
Polymerization with crosslinking reagent	Polyacrylamide, polymethacrylate, polyacrylamide-hydrazide
Polycondensation	Polyurethane, epoxy resin
Radical-mediated polymerization by irradiation with near-ultraviolet light	Photocrosslinkable resin prepolymers
Crosslinking through photodimerization by irradiation with visible or ultraviolet light	Photosensitive resin prepolymers
Radiation polymerization	Poly(2-hydroxyethyl methacrylate/acrylate), Poly(vinyl alcohol), poly(ethylene glycol) diacrylate/dimethacrylate
Gelation by iterative freezing and thawing or crosslinking with boric acid (and calcium alginate)	Polyvinyl alcohol

A wide variety of natural (polysaccharides and proteins) and synthetic polymers can be gelled into hydrophilic matrices under mild conditions to allow cell entrapment with minimal loss of viability. Gel formation mechanisms of frequently used gels are shown in Table 12.2. The polymer-cell mixture can be formed in different shapes and sizes. The most common forms are small beads approximately 1–5 mm in diameter. Although natural polymers dominate, synthetic polymers have recently been developed and applied for the immobilization of living cells. The synthetic polymers can be easily and artificially designed for adequate properties. The porosity of the gel as well as the ionic and hydrophobic or hydrophilic properties can be adjusted. Additionally, the mechanical strength and longevity of the gels formed from synthetic polymers are generally superior to those from natural polymers.

Gel entrapment has the disadvantage of limited mechanical stability. It has been frequently observed that the gel structure is easily destroyed by cell growth in the gel matrix and carbon dioxide production. However, the gel structure can usually be reinforced (e.g., alginate gel was made stronger by the reaction of alginate with other molecules such as polyethyleneimine, glutaraldehyde crosslinking, silica, genipin, poly(vinyl alcohol), or by partial drying of the gel). Another disadvantage of cell entrapment, compared with other immobilized cell systems, is oxygen limitations in the matrix. Examples of cell entrapment applications are given in Table 12.3.

12.2.2.1.1 Hydrogels from Natural Polymers

Various natural hydrogels have been used to immobilize living cells. The most important gel materials will be discussed in more detail.

12.2.2.1.1.1 Alginates Alginates constitute a family of unbranched copolymers of 1,4-linked β-D-mannuronic (M) and α-L-guluronic acid (G) of widely varying composition. The monomers are arranged in a pattern of blocks along the chain, with homopolymeric regions interspersed with regions of alternating structure (MG blocks). Divalent cation-induced gelling of alginates in solution reflects their specific ion binding capacity and the conformational change associated with it.

Entrapment of cells within spherical beads of calcium alginate has become one of the most widely used methods for immobilizing living cells. The success of this method is mainly due to the very mild conditions under which immobilization is performed, and it is a fast, simple, and cost-effective technique. The cell suspension is mixed with a sodium alginate solution, and the mixture is dripped into a solution containing calcium ions. The droplets instantaneously form gel spheres, entrapping the cells in a three-dimensional lattice of ionically crosslinked alginate. A major

TABLE 12.3
Some Applications of Cell Entrapment in Hydrogels

Hydrogel Material	Organism	Application
	Bacterial Cells	
Alginate	*Bifidobacterium longum*	Lactic acid production from whey
	Lactococcus lactis	Cell growth and release
	Streptococcus thermophilus	Inoculation of milk
Alginate-whey protein	*Lactococcus lactis*	Nisin production
Cellulose acetate phtalate	*Bifidobacterium pseudolongum*	Probiotics production
NPAE alginate	*Lactobacillus rhamnosus*	Probiotics production
PVA cryogel	*Bacillus agaradhaerens*	β-Cyclodextrin production
	Microalgae	
Calcium alginate	*Chlorella vulgaris*	Removal of the pollutants: nitrogen and phosphorus, heavy metals (Cd, Cr, Cu, Fe, Pb, Ni), biocides
κ-Carrageenan	*Scenedesmus acutus*	Removal of heavy metals: cadmium, chromium, zinc
Chitosan	*Scenedesmus bicellaris*	Removal of nitrogen and phosphorus
	Fungi	
Calcium alginate	*Saccharomyces cerevisiae*	Ethanol production
Polyethylene oxide	*Candida versatilis* and *Zygosaccharomyces rouxii*	Bioflavor of soy sauce
	Mammalian Cells	
Barium alginate	Engineered NIH/3T3 cells	Continuous release of interleukin 12 for cancer therapy
Calcium alginate	Engineered HEK 293 EBNA	Angiostatin release for cancer therapy
	Rat bone marrow cells	Cell proliferation in a 3D scaffold
Gelatin-HPA	MDCK and NIH/3T3 cells	Scaffold and carrier for tissue engineering
RGDS chitosan	Rat osteosarcoma cells	Regeneration of bone-like tissue

Source: Adapted from Willaert, R.G. and Baron, G.V., *Rev Chem Eng.,* 12:1–205, 1996; Willaert, R. *Fermentation Microbiology and Biotechnology*, 2nd ed., pp. 287–361, 2007b. Boca Raton, FL: CRC Press.

Note: PVA, polyvinyl alcohol; RGDS, Arg-Gly-Asp-Ser; NPAE, *N*-palmitoylaminoethyl; HPA, hydroxyphenylpropionic acid.

disadvantage of the use of calcium alginate beads is its sensitivity toward chelating agents such as phosphate, citrate, EDTA, and lactate, or antigelling cations such as Na^+ or Mg^{2+}. Various ways to overcome this limitation are to keep the beads in a medium containing a few millimolar free calcium ions and keep the Na^+/Ca^{2+} ratio low. Alginate beads can also be stabilized by replacing Ca^{2+} with other divalent (e.g., $Ba^{2+} > Sr^{2+} > Ca^{2+} >> Mg^{2+}$) or multivalent cations (e.g., Al^{3+} or Ti^{3+}). Other stabilization methods involve the use of **polyelectrolytes** [e.g., polyethyleneimine (PEI) and polypropyleneimine (PPI), glutaraldehyde, colloidal silica, propylene glycol ester of alginic acid with PEI, and potassium poly(vinyl alcohol) sulfate] and trimethylammonium glycol chitosan iodide.

Polyelectrolyte: A macromolecular substance that, on dissolving in water or another ionizing solvent, dissociates to give polyions (polycations or polyanions, i.e., multiply charged ions) and an equivalent amount of ions of small charge and opposite sign. Polyelectrolytes dissociating into polycations and polyanions with no ions of small charge are also conceivable. A polyelectrolyte can be a polyacid, a polybase, a polysalt, or a polyampholyte.

12.2.2.1.1.2 Carrageenans Carrageenans possess a backbone of alternating 1,3-linked β-D-galactose and 1,4-linked α-D-galactose. Differences in structure arise from the number and location of ester sulfate groups on these sugars and the extent to which the 1,4-linked residues exist as the

3,6-anhydro derivative. Gelation can be achieved by cooling or by contact with a solution containing gel-inducing reagents such as K^+, NH_4^+, Ca^{2+}, Cu^{2+}, Mg^{2+}, Fe^{3+}, amines, and water-miscible organic solvents. Both procedures are easy to perform and facilitate high viable cell content.

There are three main types of carrageenan [i.e., lambda (λ)-, kappa (κ)-, and iota (ι)], all of which are extracted from red seaweeds, with the κ form considered to be the most suitable for cell immobilization. κ-Carrageenan gel can easily be produced in different shapes (bead, cube, membrane) according to the particular application. Bead formation can be accomplished by the dripping technique. The resonance nozzle technique has also been used to produce beads of a more spherical and uniform shape and to scale up the process (Buitelaar et al. 1990).

12.2.2.1.1.3 Agar and Agarose Agar and agarose are polysaccharides isolated from marine red algae. Two kinds of agar can be distinguished by their gelling temperatures and their methoxyl content. Whereas the first type gels in the 40s (°C) and contains methyl ether groups, the second type gels in the low to mid-30s (°C) and is essentially devoid of methyl ether groups.

Agarose represents the basic gel-forming component of agar. Agarose is a linear polysaccharide composed of repeating agarobiose units consisting of alternating 1,3-linked β-D-galactopyranose and 1,4-linked 3,6-anhydro-α-L-galactopyranose (i.e., L-galactose anhydride). The other species present in agar include compounds derived from the β-D-galactose by substitution of anhydride in position 6 (e.g., the 6-methyl ether and 6-sulfate) and the compounds obtained by substitution of anhydride in position 2 (the 2-sulfate derivative). Pentagonal pores are the essential feature of agarose supports. The pores are large enough to be readily penetrated by a protein with a molecular mass of several millions. The stability of the pores is dependent on the hydrogen bond formation between the strands of the triple helix of agarose chains. Disruption of these bonds results in dissolving the soluble monomeric agarose. Urea, guanidine hydrochloride, chaotropic agents, and certain detergents may disrupt the hydrogen bonds. The strength of the bonds, and therefore the porosity and size of the beads, are altered by a change in ionic strength.

Agar or agarose (2–5% w/w) is dissolved in a suitable buffer/medium by heating followed by cooling to a temperature 5–10°C above the gelling temperature before mixing or adding the cells. The physical form can be cast as a sheet, bead, or cylinder. A mold can be used or a "gel-block" can be produced with subsequent mechanical disintegration into smaller particles. Spherical beads can also be produced by adding the molten preparation dropwise to ice-cold buffer via emulsification in vegetable oil (Nilsson et al. 1987) or using the resonance nozzle immobilization technique (Buitelaar et al. 1990).

12.2.2.1.1.4 Chitin and Chitosan Chitin is a fibrous glucan derivative, 1,4–linked 2-deoxy-β-D-glucan, that is partially acetylated, is water insoluble, and contains amino groups. Chitosan is artificially deacetylated chitin that is water soluble with nitrogen contents higher than 7% (w/w). Chitosan can be formed ionotropically in a manner similar to that described earlier for alginate: gel formation will occur using a chitosan solution with a pH value lower than 6 to protonate the amino (NH_2) groups and multivalent anion **counterions**.

Counterions: Ions of low relative molecular mass, with a charge opposite to that of the colloidal ion, are called counterions; if their charge has the same sign as that of the colloidal ion, they are called co-ions.

Crosslinking of chitosan with high-molecular-weight counterions results in capsules, whereas crosslinking with low-molecular-weight counterions results in globules in which the cells are entrapped. Low-molecular-weight ions (e.g., ferricyanide, ferrocyanide, and polyphosphates) and high-molecular-weight ions [e.g., poly(aldehydocarbonic acid), poly(1-hydroxy-1-sulfonate-2-propene), and alginate] can be used. With more hydrophobic counterions (e.g., octyl sulfate, lauryl sulfate, hexadecyl sulfate, and cetylstearyl sulfate) it is also possible to produce hydrophobic gels. Bead formation in a crosslinking solution can also occur at a pH above 7.5, but in this case it is merely a precipitation of chitosan. At pH values greater than 7.5, chitosan is totally deprotonated and becomes water insoluble.

Combining chitosan with other polymers led to the development of a wide range of tissues such as bone, liver, neural tissue, vascular grafts, cartilage, and skin (Brown and Hoffman 2002; Di Martino et al. 2005). Chitosan's ability to stabilize and deliver proteins has allowed for the incorporation of growth factors into many of these structures, thus promoting angiogenesis in tissue-engineered structures.

Chitosan ionotropic gel beads are, unlike calcium alginate and potassium carrageenan, stable in phosphate-buffered media, and their mechanical stability is comparable to that of calcium alginate beads.

12.2.2.1.1.5 Pectins, Pectates, and Pectinates Pectins are acidic, structural polysaccharides that are present in the cell wall of plant cells. Although pectins are branched in their native form, when extracted they are predominantly linear polymers that are based on a 1,4-linked α-D-galacturonate backbone that is randomly interrupted by 1,2-linked L-rhamnose. Like alginate, pectin is based on a diaxially linked backbone and forms gels with calcium ions. Gel formation studies indicate a very strong binding of these counterions. Because of the variability of the chemical structure of the commercially available pectins, gels can be formed in several ways. Polygalacturonic acid as the principal constituent is partly esterified with methoxyl groups. The free acid groups may be partly or fully neutralized with monovalent ions (i.e., Na^+, K^+, NH_4^+). The degree of methoxylation (DM) has an essential influence on the properties of pectin, especially on its solubility and its requirements for gelation, which are directly derived from the solubility. Pectins with a DM lower than 5% are called "pectic acids", whereas those with higher DM value are called "pectinic acids". Pectinic acids with a DM greater than 50% are called "high-methoxyl (HM) pectins", and those with lower DM value are called "low-methoxyl (LM) pectins".

The ionotropic gelation of pectate is simple, mild, and inexpensive. Dripping the polymer-cell solution into a crosslinking solution can easily produce beads with calcium or aluminum as counterions.

Calcium pectate and aluminum pectate beads are much less sensitive to small mono- and multivalent anions [i.e., citrate, phosphate, lactate, gluconate, and chloride, and Ca^{2+} (Al^{3+}) complexing agents], which diminish the stability of the beads. Stabilization and hardening of pectate beads can be performed using a treatment with polyethyleneimine followed by glutaraldehyde (Gemeiner et al. 1994).

12.2.2.1.1.6 Gellan Gum Gellan gum is a gel-forming polysaccharide secreted by the bacterium *Pseudomonas elodea* and is produced via aerobic fermentation. Gellan gum is a linear, anionic heteropolysaccharide with tetrasaccharide repeating units consisting of two β-D-glucose, one β-D-guluronic acid, and one α-L-rhamnose residue. The polymer contains approximately 1.5 acyl substituents per tetrasaccharide repeating unit. These substituents have been identified as an L-glyceric ester on C2 of the 3-linked D-glucose and an acetic ester on C6 of the same glucose residue. The presence of these substituents, in particular the bulky glycerate groups, hinders chain association and accounts for the change in gel texture brought about by de-esterification. The substituted form produces soft, elastic, and cohesive gels, whereas hard, firm, and brittle gels are obtained from the unsubstituted form. The rheological properties of unsubstituted gels are superior to those of other common polysaccharides such as agar, κ-carrageenan, and alginate at equimolar concentrations (Sanderson et al. 1989).

Gelation initially occurs by the formation of double helices followed by ion-induced association of these helices. Gel formation occurs when the fibrils associate in the presence of gel-promoting cations. Gelation depends upon the gum concentration, ionic strength, and the type of stabilizing cation (divalent are more effective than monovalent cations). A dispersion of gellan gum with a minimum amount of sequestrant and divalent cations will form a coherent, demoldable gel on cooling to ambient temperature. The gelation temperature increases from 35 to 55°C with increasing cation concentration.

Gellan gum is suitable for the immobilization of thermophilic bacteria because of its high setting temperature (>50°C), which can be decreased by the addition of sequestrants such as citrate, metaphosphate, and EDTA, thus rendering it suitable for the immobilization of mesophilic bacteria (Camelin et al. 1993).

12.2.2.1.1.7 Hyaluronic Acid Hyaluronic acid is the largest glycosaminoglycan (GAG) found in nature. It is well suited for tissue engineering because it shows a minimal inflammatory or foreign body reaction upon implantation (Gutowska et al. 2001).

12.2.2.1.1.8 Collagen Collagens are a family of highly characteristic fibrous proteins found in all multicellular animals. The central feature of all collagen molecules is their stiff, triple-stranded helical structure. Collagen chains are extremely rich in glycine and proline, both of which are important in the formation of the stable triple helix. Collagen is hydrophilic; it swells in the presence of water, is soluble at low pH, and is insoluble at high pH values.

The mechanism of cell immobilization in collagen involves the formation of multiple ionic interactions, hydrogen bonds, and van der Waals forces between the cells and collagen. Preparation of the collagen solution and mixing with cells has to be performed at low temperatures (4°C). Gelification is accomplished by raising the pH and ionic strength of the collagen solution and exposure to 37°C. Its natural ability to bind cells makes it a promising material for controlling cellular distribution within immunoisolated devices, and its enzymatic degradation can provide appropriate degradation kinetics for tissue regeneration in micro- and macroporous scaffolds (Riddle and Mooney 2004). Although collagen is widely used in cell immobilization, it is expensive to purify for use in tissue engineering.

12.2.2.1.1.9 Gelatine Gelatine is a hydrolytic derivative of collagen. Gelification is accomplished by cooling the gelatine solution below a temperature of 30–35°C. The sol-gel transformation is reversible. The gel structure can be stabilized by adding organic (e.g., glutaraldehyde or formaldehyde) or inorganic (e.g., acetate or sulfate chromium salts) compounds (Sungur and Akbulut 1994). The three-dimensional structure of gelatin is formed by secondary interactions between the polypeptide chains. These interactions are broken upon heating. The stabilization by aldehydes is based on covalent bond formations between the gelatine strands.

In a typical procedure, the cell suspension is mixed with an aqueous gelatin solution at 40°C, the suspension is cooled, and the gel is lyophilized. Subsequently, the dry preparation is disintegrated into small particles. The glutaraldehyde treatment can be performed before the cooling of the suspension or after the lyophylization process. Uniform beads can be formed by dripping the hot suspension in a hydrophobic liquid (e.g., butyl acetate).

12.2.2.1.2 Hydrogels from Synthetic Polymers

The application of synthetic polymers for the immobilization of living cells has some interesting benefits compared with the use of natural polymers because synthetic polymers of adequate properties can be easily and artificially designed. The porosity of the gel as well as the ionic and hydrophobic or hydrophilic properties can be easily adjusted. Additionally, the mechanical strength and longevity of the gels formed from synthetic polymers are generally superior to those from natural polymers.

12.2.2.1.2.1 Polyacrylamide The first synthetic gel used to entrap living microbial cells was polyacrylamide. Entrapment is performed by the polymerization of an aqueous solution of acrylamide monomers in which the cells are suspended. Polymerization of polyacrylamide is a free radical process in which linear chains of polyacrylamide are crosslinked by inclusion of a bifunctional reagent (e.g., *N,N′*-methylene-bisacrylamide). The crosslinking degree is a function of the relative amounts of acrylamide and bifunctional reagent and determines the porosity and fragility of the gel. Initiation of the free radical polymerization can be performed by a chemical or a photochemical

reaction. Persulfate and β-dimethylaminopropionitrile or *N,N,N′,N′*-tetramethylenediamine (TEMED) are chemical catalysts, whereas sodium hydrosulfite, riboflavin, and TEMED act as photochemical polymerization initiators.

It is an easy immobilization technique, but the polymerization of the acrylamide monomers in the presence of viable cells usually results in a reduction of the viability of the entrapped cells because of the toxicity of the monomers (e.g., acrylamide and bisacrylamide) and the heat evolved during polymerization. The level of the "immobilization shock" of polyacrylamide-entrapped cells depends to a large extent on the initial physiological state of the population.

12.2.2.1.2.2 Polyacrylamide Hydrazide To eliminate the unfavorable influences caused by the acrylamide monomer, techniques have been developed that use prepolymerized linear polyacrylamides, partially substituted with acylhydrazide groups, for the entrapment of living cells with good retention of viability. The prepolymerized material is crosslinked in the presence of viable cells by the addition of controlled amounts of dialdehydes [glyoxal, glutaraldehyde, periodate-oxidized poly(vinyl alcohol)]. The porosity of these gels is affected by the crosslinking agent. The best results were obtained using glyoxal. The concentration of polymeric backbone also affects gel porosity. The mechanical stability of this gel is superior to gels made with similar concentrations of polymeric backbone from acrylamide-bisacrylamide copolymerization. This polyacrylamide hydrazide (PAAH) gel is less brittle, is chemically stable, and does not undergo deformation as a result of changes in salinity or pH.

12.2.2.1.2.3 Methacrylates The preparation of methacrylate gels is analogous to that of polyacrylamide gels. Methacrylate monomers such as methylacrylamide, hydroxyethylmethacrylate, or methylmethacrylate are polymerized in the presence of a crosslinking agent (e.g., tetraethyleneglycol dimethacrylate) to form a porous gel.

Poly(ethylene glycol) dimethacrylate has also been used as a crosslinking agent for the entrapment of biocatalysts by radical polymerization of acrylic acid and *N,N*-dimethylaminoethyl methacrylate. Living cells can also be immobilized in methacrylate by γ-ray irradiation at low temperatures (Carenza and Veronese 1994).

12.2.2.1.2.4 Photocrosslinkable Resin Prepolymers Illumination with near-ultraviolet light of photo-crosslinkable resin prepolymers initiates radical polymerization of the prepolymers and completes gel formation within 3–5 min. Various types of prepolymers possessing photosensitive functional groups have been developed. Poly(ethylene glycol) dimethacrylate (PEGM) was synthesized from poly(ethylene glycol) (PEG) and methacrylate. Hydrophylic (ENT) and hydrophobic (ENTP) photocrosslinkable prepolymer resins were prepared from hydroxyethylacrylate, isophorone diisocyanate, and PEG or poly(propylene glycol), respectively. Each prepolymer has a linear skeleton of optional length at both terminals, to which are attached the photosensitive functional groups such as acryloyl or methacroyl. PEGM and ENT containing PEG as the main skeleton are water soluble and give hydrophilic gels, whereas ENTP with poly(propylene glycol) as the main skeleton is water insoluble and forms hydrophobic gels. Using PEG or poly(propylene glycol) of different molecular weight, prepolymers of different chain lengths can be prepared: from PEGM-1000 to PEGM-4000 (molecular weight of main chain from ~1000 to 4000, respectively), ENT-1000 to ENT-6000, and ENTP-1000 to ENTP-4000. The chain length of the prepolymers corresponds to the size of the network of gels formed from these prepolymers. Anionic and cationic prepolymers can also be prepared by introducing anionic and cationic functional group(s) to the main skeleton of the prepolymers.

The entrapment of cells can be achieved by illumination of a mixture consisting of a prepolymer, a photosensitizer (e.g., benzoin ethyl ether or benzoin isobutyl ether), and the cell suspension. A suitable buffer is used for the hydrophilic prepolymer and an adequate organic solvent for the

hydrophobic prepolymer. Suitable mixtures of these two types of prepolymers can also be used. In some cases, a detergent is used to mix a hydrophobic prepolymer with the suspension of biocatalysts.

Laser-induced photopolymerization of PEG diacrylates and multiacrylates has been used to entrap living mammalian cells. These molecules of various molecular weights were synthesized by reaction of PEG with acryloyl chloride using triethylamine as a proton acceptor. Tetrahydroxy-PEG was used for the multiacrylate synthesis. The advantages of this entrapment method are that the laser light is not absorbed by the cells in the absence of an exogenous, cell-binding chromophore; there is no significant heat of polymerization because of the nature, size, and dilution of the macromers used; the polymerization can proceed extremely rapidly in oxygen-containing aqueous environments at physiological pH; and gels with the proper formulation are capable of being immunoprotective and can be used for cell therapy purposes.

Synthetic resin prepolymers have the following advantages as gel-forming starting materials:

- Entrapment procedures are very simple under very mild conditions.
- Prepolymers do not contain monomers that have adverse effects on the biocatalysts to be entrapped.
- The network structure of gels can be controlled by using prepolymers of optional chain length.
- Optional physicochemical properties of gels (e.g., hydrophobicity-hydrophilicity balance and ionic nature) can be changed by selecting suitable prepolymers that were synthesized in advance in the absence of biocatalysts.

12.2.2.1.2.5 Polyurethane Urethane prepolymers have isocyanate groups at both terminals of the linear chain and are synthesized by heating for 1–2 h at 80°C from toluene diisocyanate and polyether diols composed of PEG and poly(propylene glycol) or PEG alone. Prepolymers with a different hydrophilic or hydrophobic character can be obtained by changing the ratio of PEG and poly(propylene glycol) in the polyether diol moiety of the prepolymers. The chain length and the content of isocyanate group can also be changed.

Cells can be entrapped by the "self-crosslinking" gel. The prepolymers are water miscible and when a liquid prepolymer is mixed with an aqueous cell suspension, the isocyanate functional groups at both terminals of the molecule react with each other only in the presence of water, forming urea linkages with liberation of carbon dioxide. Cells have also been entrapped in conventional polyurethanes, which were obtained by polycondensation of polyisocyanates. The polyurethane can be made in foam or in a gel structure depending on the type and concentration of the polycyanate used.

12.2.2.1.2.6 Poly(vinyl alcohol) Poly(vinyl alcohol) (PVA) is a raw material of vinylon and is a low-cost material. PVA is nontoxic to microorganisms and, consequently, can be used to entrap living cells. A PVA solution becomes gelatinous by freezing, and the gel strength increases during iterations of freezing and thawing. Using this technique, a rubber-like, elastic hydrogel can be obtained without using any chemical reagent. The gel strength increases with iteration number of freezing-thawing until seven iterations. A decrease of activity due to the freezing and thawing can be prevented by adding cryoprotectants such as glycerol and skim milk to the PVA-cell solution. PVA cryogels can be used up to a temperature of 65°C and have also been used to immobilize thermophilic microorganisms like *Clostridium thermocellum*, *Clostridium thermosaccharolyticum,* and *Clostridium thermoautotrophicum* to perform fermentations at 60°C (Varfolomeyev et al. 1990).

Elastic PVA gels with a high strength and durability can also be formed by crosslinking PVA with a boric acid solution to produce a monodiol-type PVA-boric acid gel lattice. This technique has two potential problems. First, the saturated boric acid solution used to crosslink the PVA is highly acidic and could cause difficulty in maintaining cell viability. Second, PVA is an extremely sticky material. As a result, PVA beads have a tendency to agglomerate, which can cause problems

in fluidized-bed reactors. This latter problem can be solved by using a combination of PVA-boric acid and a small amount of calcium alginate (0.02%) (Wu and Wisecarver 1992).

Chen and Lin (1994) developed a method based on the usage of phosphorylated PVA, in which PVA was first crosslinked with boric acid for a short time to form a spherical structure, which was followed by solidification of the gel beads by esterification of PVA with phosphate. The short contact time with boric acid prevented severe damage to the entrapped microorganisms.

Recently, PVA has been used to immobilize cells in Lentikats®, which are lens-shaped hydrogel particles (Wittlich et al. 2004). Because of their lenticular shape (diameter of 3–4 mm and a thickness of 200–400 μm), Lentikats have the advantage of improved mass transport compared with beads with the same diameter. They are prepared by mixing a sol solution with the biocatalyst solution, and small droplets are floored on a suitable surface where the gelation takes place. These particles have also been produced on an industrial scale (production output between 2 and 50 kg/h) using a conveyer-belt system.

12.2.2.1.2.7 Photosensitive Resin Prepolymers Photosensitive resin prepolymers are derivatives of PVA introduced by styrylpyridinium (SbQ) groups as photosensitive sites and are polymerized by photodimerization with irradiation of visible or ultraviolet light (PVA-SbQ gel). Hydrophilicity of the prepolymers can be controlled by changing the saponification degree of PVA.

12.2.2.1.2.8 Radiation Polymers Living cells can be entrapped by γ-irradiation of a wide variety of functional monomers or prepolymers at low temperature. Utilization of this method is limited because radiation equipment is required. Irradiation of cells at low temperatures is necessary to avoid the radiation damage. The rigidity of the polymer matrix can be increased and the porosity decreased by increasing the monomer concentration.

12.2.2.1.2.9 Stimuli-sensitive Hydrogels Stimuli-sensitive polymer hydrogels, which swell or shrink in response to changes in environmental conditions, have been extensively investigated and used as "smart" biomaterials and drug-delivery systems [e.g., copoly(*N*-isopropylacrylamide/acrylamide) (NIAAm/AAm)], which is a "lower critical solution temperature" (LCST) hydrogel (Hoffman 2004). This gel gradually shrinks as temperature is raised and then collapses when it is warmed through the LCST region. It expands and reswells as it is cooled below LCST. Cells containing gel beads have been prepared by inverse suspension polymerization. The conversion and activity of the immobilized cells may be enhanced by thermal cycling of the gel below its LCST because of the reduced mass transfer resistance as the gel bead "squeezes out" and "draws in" substrate when it shrinks and swells during the thermal cycling. Pore sizes and their interconnections will change significantly as the gel is shrunk or swelled. This can significantly affect the diffusion rates of substrate in and product out of the gel.

12.2.2.2 Preformed Support Materials

Cell immobilization in preformed carriers involves passive/natural immobilization usually *in situ* in the bioreactor or the culture environment (Baron and Willaert 2004; Mavituna 2004). Most of the carriers are porous with a wide range of pore sizes to suit immobilization of various organisms or tissues. For passive immobilization, cells, flocs, mycelia, cell aggregates, or spores are inoculated into the sterilized medium containing empty preformed carriers. Depending on the cell and the carrier type, immobilization then takes place in a combination of filtration, adsorption, growth, and colonization processes. Furthermore, surfaces of the carriers can be modified by various pretreatments to enhance immobilization efficiency.

The cells are entrapped in a matrix that protects them from the shear field outside of the particles. This is of particular importance for fragile cells such as mammalian cells. Unlike gel systems, porous supports can be inoculated directly from the bulk medium. As with the adsorption method, cells are not completely separated from the effluent in these systems. Mass transport of substrates

and products can be achieved by molecular diffusion and convection by proper particle design and organization of external flow. Consequently, mass transport limitations are less severe under optimal conditions. When the colonized porous matrix ideally retains some free space for flow, immobilization occurs partly by attachment to the internal surface, self-aggregation, and retention in dead-end pockets within the material. This is only possible when cell adhesion is not very strong and the application of high external flow rates reversibly removes cells from the matrix. When high cell densities are obtained, convection is no longer possible and the cell system behaves as dense cell agglomerates with strong diffusion limitations. Cell immobilization methods are simple, and a high degree of cell viability is retained upon entrapment. The preformed matrix is chemically inert, resistant to microbial attack, and is incompressible. Steam sterilization is often possible and the matrix can be reused. Usually, the matrix takes up a significant volume fraction resulting in a lower immobilized cell density compared with other immobilization methods.

Various porous matrices have been described for living cell immobilization as shown in Table 12.4. The choice will usually depend on the cell type used and the kind of application. For example, the immobilization of microbial cells for the production of biochemicals in large packed-bed bioreactors requires a matrix with excellent mechanical characteristics to withstand the high-pressure drop in the reactor; tissue engineering porous matrices need to be an excellent scaffold for cell attachment, and growth and must be characterized by excellent biocompatibility characteristics. Usually, guided by the following parameters, a choice has to be made from several suitable matrices.

- What matrix material is the cheapest?
- Which matrix is the most suitable for our purpose and is it not patented?
- Is it reusable?

In tissue engineering, some applications require porous biodegradable scaffolds. The repair of large cartilage defects requires the use of a three-dimensional scaffold to provide a structure for cell proliferation and control the shape of the regenerated tissue. For example, cartilage implants based on chondrocytes and three-dimensional fibrous polyglycolic acid scaffolds closely resembled normal cartilage histologically as well as with respect to cell density and tissue composition (Freed et al. 1994).

12.2.3 Containment behind a Barrier

When cell separation from the effluent is required or when some high-molecular-weight or specific product (permaselectivity) needs to be separated from the effluent, these systems are highly useful. The barrier can be preformed (hollow fiber systems and flat membrane reactors) or formed around the cells to be immobilized (microcapsules and two-phase entrapment). The synthetic membranes are usually polymeric microfiltration or ultrafiltration membranes, although other types of membranes have been used, such as ceramic, silicone rubber, or ion exchange membranes. Mass transfer through the membrane is not only dependent on the pore size and structure but also on the hydrophobicity/hydrophilicity and charge. Transport can be by diffusion and/or by flow induced by application of a pressure difference over the membrane. Various mild micro-encapsulation methods have been developed to entrap living cells, and some are combined with gel immobilization within the microcapsule. The barrier can be as simple as the liquid/liquid phase interface between two immiscible fluids.

Entrapment behind preformed membranes represents a gentle immobilization method because no chemical agents or harsh conditions are used. Cells are often immobilized by filtration of a cell suspension followed by some growth in the seeded reactor. Two-phase systems can be used in applications where substrates or products are partitioned separately (product inhibition, water-insoluble

TABLE 12.4
Some Examples of Cell Immobilization in Preformed Porous Support Materials

Material	Microorganism	Application/Product
	Natural Organic Polymers	
Bacteria		
Cotton towel	*Propionibacterium acidipropionici*	Propionic acid production
Microalgae		
Luffa sponge	Chlorella sorokiniana	Removal of heavy metals (Cd, Cr, Ni)
Fungi		
Cellulose carrier	*Rhizopus niveus*	Wax ester production
Luffa sponge	*Saccharomyces cerevisiae*	Ethanol production
	Synthetic Organic Polymers	
Bacteria		
Silicone carrier (ImmobSil®)	*Lactobacillus rhamnosus*	Exopolysaccharide production
Fungi		
Polystyrene foam	*Phanerochaete chrysosporium*	Peroxidase production
Polyurethane foam	*Agaricus* sp.	Laccacase production
	Aspergillus niger	Citric acid production
	Yarrowia lipolytica	Oil degradation
Mammalian cell		
Polyester fibrous matrix	Hybridoma cells	Monoclonal antibody production
Polyethylene terephthalate	Human trophoblast	Tissue engineering
	Anorganic Materials	
Bacteria		
Kiezelguhr (Celite)	*Xanthomonas campestris*	Xanthan gum production
Fungi		
Ceramics	*Saccharomyces cerevisiae*	Ethanol production
Kiezelguhr (Celite)	*Penicillium chrysogenum*	Penicillin production
Porous glass	*Saccharomyces cerevisiae*	Beer maturation
	Metallics	
Bacteria		
Alumina pellets	*Zymomonas mobilis*	Ethanol production
Stainless steel knitted mesh	*Zymomonas mobilis*	Levan and ethanol production
Fungi		
Stainless steel fiber cloth	*Saccharomyces cerevisiae*	Beer production
Stainless steel knitted mesh	*Phanerochaete chrysosporium*	Peroxidase production

Source: Adapted from Willaert, R.G. and Baron, G.V., *Rev Chem Eng.,* 12:1–205, 1996; Baron, G.V. and Willaert, R.G., *Fundamentals of Cell Immobilization Biotechnology*, pp. 229–44, 2004. Dordrecht, The Netherlands: Kluwer Academic Publishers; and Willaert, R. *Fermentation Microbiology and Biotechnology*, 2nd ed., pp. 287–361, 2007b. Boca Raton, FL: CRC Press.

substrates). These systems also allow for the recycling of the cell-containing phase, which is difficult with other immobilization methods. The small spheres involved in phase entrapment have a superior surface-to-volume ratio compared with flat sheets or hollow fibers and can be used in conventional bioreactors. Also, membranes have been used to contact aqueous and organic streams in bioprocesses. The high membrane surface area in hollow fiber reactors is especially advantageous for the culture of anchorage-dependent mammalian cells, without the drawbacks occurring with immobilized growing microorganisms (Sirkar and Kang 2004). The maintenance of high-density cultures of animal and plant cells in membrane reactors resulted in long-term production with reduced cell growth. Membrane entrapment may be particularly helpful if aggregation is an advantage, as suggested for plant cells. In the biomedical engineering field, microencapsulation or macroencapsulation lead to immunoprotection for artificial organs (Lysaght and Rein 2004). In most cases, nutrients are supplied to, and products are removed from, the cell mass by diffusion. Consequently, mass transfer limitations can reduce the efficiency of these systems. However, in the case of hollow fiber systems, mass transfer can be governed by convective mass transport, otherwise known as "**Starling flow**."

Starling flow: In a hollow fiber reactor, some fluid will flow from the lumen into the extracapillary space (ECS) in the entrance half of the reactor, along the fibers in the ECS, and return to the lumen in the exit half of the reactor because of the pressure gradient in the lumen (highest pressure at the entrance). This type of flow is called Starling (or toroidal) flow, in honor of the discoverer of this same fluid behavior in tissues surrounding blood capillaries.

In these systems, the cells are usually situated in the membrane porous support layer or the shell space and medium flows in the lumen. Alternatively, the cells can be contained in the lumen space in the case of macroencapsulation (also known as "diffusion chambers") for encapsulated cell therapy such as for diabetes, alleviation of chronic pain, treatment of neurodegenerative disorders, and delivery of neurotrophic factors. Here, the hollow fiber membrane allows for the diffusion of low-molecular-weight molecules (lower than the **molecular weight cutoff value**)—such as oxygen, glucose, nutrients, and waste product—but prevents the passage of larger molecules such as antibodies.

Molecular weight cutoff: The molecular weight cutoff (MWCO) of a membrane is defined as the molecular weight at which the membrane rejects 90% of solute.

12.2.3.1 Microencapsulation

A typical microencapsulation process involves the formation of a spherical gel mold containing cells on which is deposited a polymeric membrane. The internal gel matrix can also be liquefied and allowed to diffuse out of the capsule, leaving behind the membrane and the contained cells. The type and porosity of the membrane and size of the microcapsules can be varied to accommodate many reactant-product systems. Capsule diameters from 20 μm to 2 mm are possible. The porosity of the membrane can be varied over a range of several orders of magnitude; from glucose (180 Da) to IgG (155,000 Da) can be made to be freely permeable. The polymer membrane should offer minimal resistance to the mass transfer of essential molecules as well as the toxic end products of cell metabolism in order for the encapsulated mass to maintain normal physiological activity. For **immunoisolation** purposes, the capsule must be impermeable to host cells and soluble components of the immune system (Wilson and Chaikof 2008).

Immunoisolation: By using membranes, the free passage of immunoglobulins and complement proteins can be prevented from interacting with implanted "foreign" biological material.

The demand for specific properties of the capsules vary; for example, proliferating cells need a stronger capsule membrane than nonproliferating cells, but it is noteworthy that the former may tolerate a tougher encapsulation procedure because viable cells will grow and replace the dead cells in the capsules. This immobilization technique is of particular interest for the immobilization of animal cells. Large process intensification over conventional cell suspension culture with low density and low productivity can be achieved. Cell encapsulation and long-term continuous culture lead to significantly higher cell densities, which results in higher productivities. The high-culture densities provide a high degree of cell–cell contact and interaction, resulting in more favorable possible microenvironmental conditions. In addition, this

technique can provide protection from shear for the sensitive animal cells and other sudden changes in the culture medium. It also permits direct aeration by air bubbles without risk of damaging the cells. The produced toxic metabolites, such as lactic acid and ammonium, will diffuse out of the capsule because of the concentration gradient, resulting in higher growth and product formation rates. Microencapsulation can provide simultaneous product separation and cell cultivation, resulting in concentration of high-molecular-weight metabolic products (e.g., monoclonal antibodies) within the capsule.

Microencapsulation of human cells or tissues is a recent technology to overcome biomedical problems because the membrane may create an immunological barrier between the host and the transplanted cells. The immunoisolation of the encapsulated cells or tissue from the elements of the immune system prevents the rejection of the transplanted cells/tissue. Consequently, the necessity of immunosuppressive drugs in allo- and xenotransplantations can be avoided. The idea of using an ultrathin polymer membrane for the immunoprotection of transplanted cells, despite its apparent promise in preclinical trials, failed to live up to expectations and continues to elude the scientific community.

12.2.3.1.1 Microencapsulation Techniques

The techniques that are used to produce the semipermeable microcapsule membranes are classified as phase inversion, polyelectroyte coacervation, and interfacial precipitation (Hunkeler 1997). Phase inversion involves the induction of phase separation in a previously homogeneous polymer solution by a temperature change or by exposing the solution to a nonsolvent component in a bath (wet process) or in a saturated atmosphere (dry process). Polymer precipitation time, polymer-diluent compatibility, and diluent concentration all influence phase separation and membrane porosity. Examples of polymer materials are polyacrylate and poly(hydroxyethylmet-hacrylate-co-methyl methacrylate) (Feng and Sefton 2002).

In the polyelectrolyte coacervation process, a hydrogel membrane is formed by the complexation of oppositely charged polymers to yield an interpenetrating network. Mass transport characteristics can be modulated by osmotic conditions, diluents, and the molecular-weight distribution of the polyionic species (Chaikof 1999). To reduce membrane permeability and to improve biocompatibility as well as mechanical properties, one or more additional coating layers with oppositely charged polymer can be added.

The interfacial precipitation technique involves the coating of a hydrogel bead with a semipermeable membrane (Lacik 2004). A lot of research has been focused on the alginate-poly-L-lysine (PLL)-PEI microcapsule, originally developed by Lim and coworkers in the early 1980s (Lim and Sun 1980; Lim and Moss 1981). Immunoisolation of the islets of Langerhans (bioartificial pancreas) has been studied extensively and evaluated thoroughly (Teramura and Iwata 2010). Examples of applications of cell immobilization in microcapsules are listed in Table 12.5.

12.2.3.2 Cell Immobilization Using Membranes

The main advantage of membrane bioreactors is that they provide simultaneous bioconversion and product separation, which is especially attractive for the production of high-value biological molecules. As compared with conventional reactor types, the design of membrane reactors is relatively more complex and more expensive (mainly because of the high cost of the membrane material). However, because the attainment of highly concentrated products could eliminate the need for some steps of costly product purification, the utilization of these reactors can be favorable. For low-value biological products, conventional bioreactors are usually more appropriate. An exception is the case in which cofactors need to be co-entrapped to perform coenzyme-dependent bioconversion reactions.

Membrane reactors can be configured as flat-sheet or hollow-fiber modules. Hollow-fiber modules provide a higher surface-to-volume ratio without the need for membrane support. However, the geometry of flat-sheet modules is simpler, providing an accurate regulation of the distances between

TABLE 12.5
Cell Immobilization in Microcapsules: Some Examples

Material	Cell Type	Application
	Bacterial Cells	
Alginate-PLL-alginate	*Escherichia coli*	Urea and ammonia removal
Alginate-PLL-alginate	*Erwinia herbicola*	Tyrosine production
Alginate-PLL-alginate	Various bacteria	Therapeutic delivery of live bacteria
Alginate-alginate	*Lactococcus lactis*	Bacteriocin production
Cellulose acetate phthalate	*Lactobacillus acidophilus* + *Bifidobacterium lactis*	Probiotics
	Fungal Cells	
1,6-hexanediamine-poly-(allylamone)-dodecane-dioyl dichloride	*Saccharomyces cerevisiae*	Bioconversion in organic solvents
CS^c-PDMDAAC	*Yarrowia lipolytica*	Citrate production
	Animal Cells	
Alginate/agarose-PLL- alginate	BHK fibroblast, C_2C_{12} myoblast	Viability assessment
Alginate-PLL-alginate	Engineered mouse myoblast	Tumor suppression
Alginate-PLL-alginate	Engineered C_2C_{12} myoblast to secrete erythropoietin	*In vivo* erythropoietin delivery
Alginate-PLL-alginate	Engineered 293-EBNA	Endostatin production
	JN3 myeloma	Hepatocyte growth factor production
Alginate-PLL-alginate	Islets of Langerhans	Diabetes treatment
Alginate-PLL-alginate	Murine fibroblast	High throughput GMP encapsulation using JetCutter technology
Alginate/agarose/cellulose sulfate/pectin-PLL-alginate	GDNF secreting 3T3 fibroblast	Treatment central nervous system diseases
Alginate-poly-L-ornithine-alginate	HEK 293, HCT 116 and HEP G2 Cell Spheroids	Cell implantation
Alginate-CS-pDADMAC	Engineered CHO	Erytropoietine production
Alginate-PMCG	Islets of Langerhans	Diabetes treatment
Collagen-HEMA-MMA- MAA-MeOCPMA	Rat hepatocytes	Bioartificial liver

Source: Adapted from Willaert, R.G. and Baron, G.V., *Rev Chem Eng.,* 12:1–205, 1996; Willaert, R. *Fermentation Microbiology and Biotechnology*, 2nd ed., pp. 287–361, 2007b. Boca Raton, FL: CRC Press.

Note: GDNF, glial cell line-derived neurotrophic factor; CS, cellulose sulfate; pDADMAC, poly-diallyl-dimethyl-ammoniumchloride; HEMA-MMA-MAA-MeOCPMA, hydroxyethylmethacrylate-methacrylate-methacylic acid-4-(4-methoxycinnamoyl)phenyl methacrylate; PDMDAAC, poly(dimethyldiallylammonium chloride); PMCG, polymethyl- co-guanidine.

the membranes. Additionally, these modules can be easily disassembled, providing an easy access to module compartments and options for membrane cleaning and replacement.

Membranes can be used for three types of cell immobilization as illustrated in panels A, B, and C of Figure 12.4 (i.e., immobilization within the membrane, immobilization on the membrane where a biofilm is formed, and immobilization in a cell compartment, which is separated by a membrane).

12.2.3.2.1 Immobilization within the Membrane

Cell immobilization in a membrane can give very high cell densities. The permaselective membrane permits the transport of nutrients from the bulk medium to the cells and the removal of

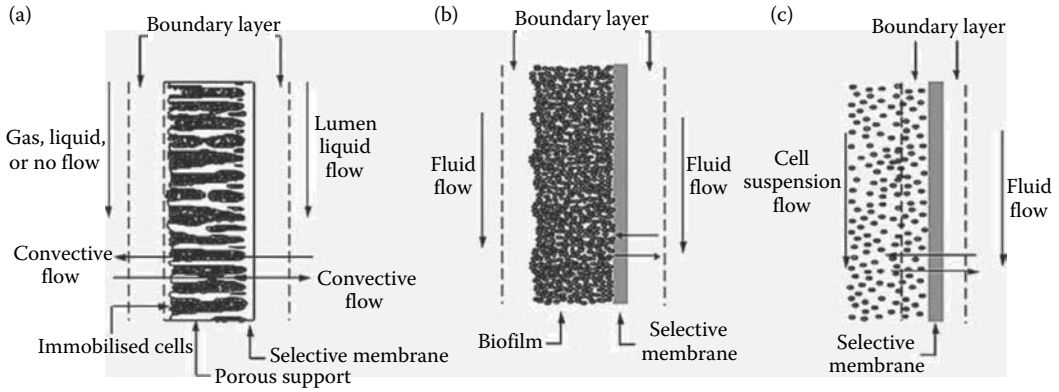

FIGURE 12.4 Synthetic membranes for cell immobilization: (a) immobilization in the porous structure of an asymmetric membrane, (b) attachment of a biofilm on a permeable membrane, and (c) a membrane to separate the cell compartment from a cell-free liquid compartment.

products, whereas the release of cells into the bulk liquid is prevented. Various setups can be used, and depending on the membrane type even convective transport through the membrane is possible. Preformed asymmetric polymetric membranes are usually used. A hollow fiber module consists of a bundle of porous hollow-fiber membranes potted at both ends in a cylindrical module. They were originally developed for separation processes.

12.2.3.2.2 Immobilization on the Membrane

Membranes can act as support for biofilm development with direct oxygen transfer through the membrane wall in one direction and nutrient diffusion from the bulk liquid phase into the biofilm in the other direction. This type of immobilization has successfully been used in aerobic cultivation of mammalian and microbial cells.

12.2.3.2.3 Immobilization in a Cell Compartment

In this case, a high suspended cell concentration is obtained by preventing the cells from escaping from the bioreactor. Membrane filters, which can be positioned internally (e.g., a spin filter for the continuous cultivation of mammalian cells) or externally, are used to keep the cells in the reactor. Alternatives for an external membrane filter are a centrifuge or a settling tank (Table 12.6).

Very high cell densities (and high productivities) have been reported for membrane-based cell recycle systems. These systems have also the advantage of being homogeneous. Although none of the intrinsic benefits of cell immobilization are obtained (e.g., shear protection), most other advantages such as high productivity, avoiding washout, and simpler product recovery are retained. Some of the drawbacks of immobilization, and especially the substrate transport limitation or product inhibition, can be avoided or reduced. Oxygen transport can be a major problem at high cell densities and limits the attainable cell densities.

12.2.4 Self-Aggregation of Cells

Cells that naturally aggregate, clump, form pellets, or flocculate can also be considered as immobilized (Figure 12.3). Many industrially important products (e.g., antibiotics) are produced during secondary metabolism by fungal pellets. Microbial aggregates can be encountered in wine-making and brewing, where yeast cells flocculate at the end of fermentation. The culturing of algae, plant cells, and animal cells can also result in aggregation phenomena. Simple serum-free medium appeared to be adequate to support the growth of anchorage-dependent animal aggregates of several commercially important cell types such as African Green Monkey Cells (Vero), Baby Hamster Kidney (BHK) cells , and Chinese Hamster Ovary (CHO) cells (Litwin 1992). During callus culture—in the

TABLE 12.6
Cell Immobilization Using a Membrane As a Barrier: Some Examples

Material	Cell Type	Application
	Immobilization within the Membrane	
Polypropylene	Bovine aortic endothelial cells	Artificial lung
Polysulfone	*Saccharomyces cerevisiae*	Ethanol production
Polyvinyl chloride/polyvinylidine chloride/ polyacrylonitrile	*Escherichia coli*	Production of β-lactamase
Silicon carbide	*Saccharomyces cerevisiae*	Beer production
	Immobilization on the Membrane	
Polypropylene	*Aspergillus niger*	Citric acid production
Polylysine-coated polysulfone	H1 fibroblast	Aerobic cell growth
	Immobilization in a Cell Compartment (Cell Recycle)	
Ceramic	*Bacillus stearothermophilus*	Lactic acid production
Polydimethylsiloxane layer on polysulfone	*Saccharomyces cerevisiae*	Ethanol production
Polyethersulfone	*Leuconostoc mesenteroides*	D-mannitol production
Polysulfone	*Halobacterium halobium*	Bacteriorhodopsin production
	Lactobacillus rhamnosus	Lactic acid production

Source: Adapted from Willaert, R.G. and Baron, G.V., *Rev Chem Eng.,* 12:1–205, 1996; Willaert, R. *Fermentation Microbiology and Biotechnology*, 2nd ed., pp. 287–361, 2007b. Boca Raton, FL: CRC Press.

absence of shear fields—aggregates may reach several centimeters across. Consequently, plant cell aggregates are very susceptible to the hydrodynamic conditions in the bioreactor.

The cell-wall region is directly and indirectly influenced by biological and environmental factors through metabolism. Biological factors that affect microbial aggregation are the cell wall, extracellular secretions, genetics, growth rate, nutrition, and physiological age. Environmental factors can be subdivided into physical (hydrodynamic properties, interfacial phenomena, ionic properties, and temperature), chemical (presence of chelating agents, carbon-to-nitrogen ratio, enzymes, ferrocyanide, nitrogenous substances, oils, sugars, and trace metals), and biological factors (inoculum size, presence of other organisms or strains). Artificial flocculating agents or crosslinkers may be added to enhance the aggregation process for cells that do not naturally flocculate. Polyelectrolytes (i.e., coupling agents by covalent bond formation) or inert powders can be used as linking agents.

An example of self-aggregation is the flocculation of yeast cells. Many fungi contain a family of cell wall glycoproteins (called "adhesines") that confer unique adhesion properties. These molecules are required for the interactions of fungal cells with each other (flocculation and filamentation) (Viyas et al. 2003), inert surfaces such as agar and plastic (Reynolds and Fink 2001), and mammalian tissues (Li and Palecek 2003); they are also crucial for the formation of fungal biofilms (Green et al. 2004).

In hazardous environmental conditions, *Saccharomyces cerevisiae* cells possess the remarkable property to adhere to other cells or to substrates such as agar or plastics. Adhesion to surfaces is a mechanism that may lead to biofilm formation. It is often used as a model to study biofilm formation of pathogenic yeasts, responsible for 41% of the mortality rate in hospitals (Wisplinghoff et al. 2004). The flocculation phenomenon is exploited in the brewery industry as an easy, convenient, and cost-effective way to separate the aggregated yeast cells from the beer at the end of the primary fermentation. The timing of flocculation is crucial for brewers because the quality of beer highly depends on it. When cells start to flocculate too early, the fermentation will be incomplete with

TABLE 12.7
Cell Immobilization by Self-Aggregation of Cells

Microorganism	Application	Bioreactor Type
	Bacteria	
Zymomonas mobilis	Ethanol production	Fluidized-bed reactor
	Fungi	
Aspergillus awamori	Enzyme production	Stirred tank reactor
Aspergillus oryzae	α-Amylase production	Stirred tank reactor
Penicillium chrysogenum	Penicillin production	Stirred tank reactor
Saccharomyces cerevisiae	Beer production	Cylindro-conical tank (batch)
Trichoderma reesei	Cellulolytic enzymes	Stirred tank reactor
	Mammalian Cells	
BHK cells	Recombinant protein	Stirred tank reactor
Neural stem cells	High-cell-density expansion	Stirred tank reactor
Vero cells	Recombinant protein	Stirred tank reactor
293 cells	Recombinant protein	Stirred tank reactor

Source: Adapted from Willaert, R.G. and Baron, G.V., *Rev Chem Eng.,* 12:1–205, 1996; Willaert, R. *Fermentation Microbiology and Biotechnology*, 2nd ed., pp. 287–361, 2007b. Boca Raton, FL: CRC Press.

undesirable aromas and too many residual sugars. On the other hand, when the flocculation is delayed, problems can arise during beer filtration (Willaert 2007a).

The *S. cerevisiae* adhesin protein family responsible for its flocculation in is encoded by *FLO1*, *FLO5*, *FLO9,* and *FLO10.* These proteins are called flocculins (Goossens and Willaert 2010) because these proteins promote cell–cell adhesion to form multicellular clumps that sediment out of solution. The flocculation mechanism is based on a lectin (the Flo protein)-carbohydrate interaction, but it is not yet fully understood, although the first model dates back to the 1950s. Table 12.7 lists some examples of cell immobilization by self-aggregation.

12.3 DESIGN OF IMMOBILIZED CELL REACTORS

12.3.1 Mass Transport Phenomena in Immobilized Cell Systems

The analysis of the influence of mass transfer on the reactor performance in immobilized-cell reactors can be quite useful because the performance of these reactors are often limited by the rate of transport of reactants to and products (external mass transfer limitation) and by the rate of transport inside of the immobilized cell system (internal mass transfer limitation) (Willaert 2009). External mass transfer limitations can be reduced or eliminated by a proper choice or design of the reactor and immobilized cell system. Internal mass transfer limitations are often more difficult to eliminate. An estimation of the significance of mass transport limitations is a prerequisite to optimize the performance of an immobilized-cell bioreactor.

12.3.1.1 Diffusion Coefficient

Mass transport by molecular diffusion is defined by Fick's law; that is the rate of transfer of the diffusing substance through a unit area is proportional to the concentration gradient measured normal to the section:

$$J = -D\frac{\partial C}{\partial x} \tag{12.1}$$

where J is the mass transfer rate per unit area of a section, C the concentration of diffusing substance (amount per total volume of the system), x the space coordinate, and D the diffusion coefficient. It is general practice to use an effective diffusion coefficient (D_e), which can be readily used in the expression for the Thiele modulus and for the determination of the efficiency factor of a porous biocatalyst. When D is replaced by D_e in Equation 12.1, the corresponding concentration (C_L) is expressed as the amount of solute per unit volume of the liquid void phase. Concentration C may be correlated with C_L by using the void fraction (ε), which is the accessible fraction of a porous particle to the diffusion solute as $C = \varepsilon C_L$. Hence, the relationship between the effective diffusion coefficient and the diffusion coefficient is

$$D_e = \varepsilon D \tag{12.2}$$

12.3.1.2 Diffusion in Immobilized Cell Systems

The effective diffusion coefficient through a porous support material (matrix) is lower than the corresponding diffusion coefficient in the aqueous phase (D_a) because of the exclusion and obstruction effect. By the presence of the support, a fraction of the total volume ($1 - \varepsilon$) is excluded for the diffusing solute. The impermeable support material obstructs the movement of the solute and results in a longer diffusional path length, which can be represented by a tortuosity factor (τ), which equals the square of the tortuosity (Epstein 1989). The influence of both effects on the effective diffusion coefficient can be represented by

$$D_e = \frac{\varepsilon}{\tau} D_a \tag{12.3}$$

This equation holds as long as there is no specific interaction of the diffusion species with the porous carrier. In the case of gel matrices, predictions using the polymer volume fractions are recommended by the Equation 12.4 because neither e nor t can be measured for a gel in a simple way:

$$D = \frac{(1-\phi_p)^2}{(1+\phi_p)^2} D_a \tag{12.4}$$

where ϕ_p is the polymer volume fraction. For low-molecular-weight solutes in cell-free gels, an approximate measure of ε can be given as

$$\varepsilon = 1 - \phi_p \tag{12.5}$$

D_e can also be expressed as a function ϕ_p by combining Equations 12.2 through 12.5 to give

$$D_e = \frac{(1-\phi_p)^3}{(1+\phi_p)^2} D_a \tag{12.6}$$

12.3.1.3 External Mass Transfer

In the case of permeable spheres, the effect of the external mass transfer resistance on the overall uptake and/or release rate by the beads may be quantitatively evaluated by calculating the time

constant for the external film (τ_e) and comparing it with the time constant for diffusion in the sphere (τ_i). The internal time constant can be calculated using Equation 12.7:

$$\tau_i = \frac{R^2}{15D_e} \tag{12.7}$$

where R is the radius of the bead. The Biot number (Bi) for beads is defined by Equation 12.8 as the ratio of the characteristic film transport rate to the characteristic intraparticle diffusion rate:

$$Bi = \frac{k_s R}{D_e} \tag{12.8}$$

An estimation of the external mass transfer coefficient (k_s) is required to calculate τ_e, Bi, or the film thickness. The value of k_s can be calculated by a procedure recommended by Harriot and coworkers in the mid-1970s (Sherwood et al. 1975). Merchant and coworkers (1987) determined Bi for a rotating sphere. Using the empirical correlation of Noordsij and Rotte (1967), k_s could be estimated using Equation 12.9:

$$Sh = \sqrt{4 + 1.21\left(Re_p Sc\right)^{0.67}} \tag{12.9}$$

where Sh is the Sherwood number, Re_r is the rotational Reynolds number, and Sc is the Schmidt number. In the case of diffusion through a membrane or thin disc, Bi can also be calculated. k_s can be determined for free-moving particles using the following correlations (van't Riet and Tramper 1991):

$$Sh = \sqrt{4 + 1.21\left(Re_p Sc\right)^{0.67}} \quad \text{for} \quad Re_p Sc > 10^4 \tag{12.10}$$

$$Sh = 2 + 0.6 Re_p^{0.5} Sc^{0.33} \quad \text{for} \quad Re_p < 10^3 \tag{12.11}$$

where Re_p is the (particle) Reynolds number, which can be estimated using the following correlations:

$$Re_p = Gr/18 \quad \text{for} \quad Gr < 36 \tag{12.12}$$

$$Re_p = 0.153 Gr^{0.71} \quad \text{for} \quad 36 < Gr < 8 \times 10^4 \tag{12.13}$$

$$Re_p = 1.74 Gr^{0.5} \quad \text{for} \quad 8 \times 10^4 < Gr < 3 \times 10^9 \tag{12.14}$$

where Gr is the Grashof number. Another correlation used to estimate k_s for gel beads in agitated reactors is (Kikuchi et al. 1988)

$$Sh = 2 + 0.52\left(e_s^{1/3} d_p^{4/3}/\nu\right)^{0.59} Sc^{1/3} \tag{12.15}$$

where d_p is the average diameter of the particle, n is the kinematic viscosity, e_s is the energy dissipation given as $e_s = N_p n_i^3 D_i^5/V$ for a stirred tank (where N_p is the power number, n_i is the impeller speed, D_i is the impeller diameter, and V is the volume of the reactor). The ranges of validity for this correlation are

$$10 < \left(e_s^{1/3} d_p^{4/3}/\nu\right) < 1500 \quad \text{and } 120 < Sc < 1450 \tag{12.16}$$

Also, a correlation has been recommended for agitated dispersions of small, low-density solids (Øyaas et al. 1995):

$$k_s = \frac{2D_{e0}}{d_p} + 0.31(Sc)^{-2/3}\left(\frac{\Delta\rho\upsilon g}{\rho_l}\right)^{1/3} \tag{12.17}$$

where $\Delta\rho$ is the particle/liquid density difference and ρ_l is the density of the bulk liquid. For spherical particles in a packed bed, k_s depends on the liquid velocity around the particles. For the range $10 < Re_p < 10^4$, the Sherwood number has been correlated by Equation 12.18 (Moo-Young and Blanch 1981):

$$Sh = 0.95 Re_p^{0.5} Sc^{0.33} \tag{12.18}$$

An estimation of k_s can be calculated if the stirred chambers have the shape of flat cylinders using the correlation in Equation 12.19 (Sherwood et al. 1975):

$$k_s = 0.62 D_a^{2/3} \nu^{-1/6} \omega^{1/2} \tag{12.19}$$

where ν is the kinematic viscosity and ω is the rotational speed of the stirrer (in rad/s). Other correlations can be adapted from heat transfer correlations (Axelsson and Westrin 1991).

The external mass transfer limitation can be experimentally investigated by observing the concentration-time profile at different mixing regimes in the bioreactor (e.g., rotation speeds of the stirrer) (Sun et al. 1989).

12.3.2 Reaction and Diffusion in Immobilized Cell Systems

In immobilized cell systems, cellular reactions can take place in the presence of significant concentration gradients. These reactions are also called "heterogeneous reactions." Reactions can only take place when the substrate molecules are transported to the reaction place (i.e., mass transport phenomena can have a profound effect on the overall conversion rate). The concentration in each internal position has to be known to determine the local rates. In most cases, these internal concentrations cannot be measured but can be estimated using a reaction-diffusion model.

12.3.2.1 Reaction-Diffusion Models

The major issues involved in modeling immobilized cell reactors are very similar to those in heterogeneous chemical reactors. This analogy has encouraged a rapid development in the model building for immobilized cell systems, even if the level of understanding of biocatalysts is lower than for chemical catalysis. The ability to predict the behavior of immobilized cell systems is required for the understanding, design, and optimization of an appropriate bioreactor. It is necessary to consider the bioreactor performance and microbial kinetics. Description of the bioreactor performance involves modeling of mass transfer effects and the flow pattern in gas and liquid phases whereas microbial kinetics deals with the kinetics on the individual cell level and on the level on the whole cell population. Single-cell kinetics can be described with an unstructured model (no intracellular components considered) or with a structured model (intracellular components considered). The population model may be either unstructured (all cells in the whole population assumed to be identical, i.e., only one morphological form) or morphologically structured (with an infinite number of morphological forms, the term "segregated population model" is often used). The models describing immobilized cell behavior are usually of the unstructured type.

Models that described immobilized cell kinetics were initially based on the steady-state models for immobilized enzymes. Steady-state models can give valuable information for design purposes, but they fail to describe transient phenomena (such as the start-up dynamics and response to changing conditions in the reactor) encountered in growing immobilized cell systems. Therefore, dynamic models have been developed to simulate the transient behavior of growing immobilized cells.

In general, gel-immobilized cell systems are considered as effective continua. However, it has been observed that when gel beads are inoculated with a low cell concentration, each growing cell will be the origin of a microcolony and growth results in the formation of expanding microcolonies (e.g., Willaert and Baron 1993; Picioreanu et al. 1998). A rigorous modeling approach of this microcolony system requires consideration of the microstructure of the immobilized cell system: diffusion in the gel phase and reaction and diffusion in the microcolony ("two-phase" system).

12.3.2.1.1 Intrinsic Kinetics

Intrinsic kinetics describes the growth and product formation rates of cells in the immobilized (or free) state as a function of the local concentrations. A typically simple unstructured model of microbial kinetics for growth on a single substrate can be described by Equations 12.20 through 12.22:

$$\text{Biomass growth: } \mu = f(C_S) \tag{12.20}$$

$$\text{Substrate consumption: } q_s = \frac{1}{Y_{X/S}}\mu + m_s \tag{12.21}$$

$$\text{Product formation: } q_p = \frac{1}{Y_{X/P}}\mu + m_p \tag{12.22}$$

where μ is the specific growth rate of the cells (gDW/gDW per hour), C_S is the substrate concentration, q_s is the specific substrate utilization rate (g substrate used/gDW per hour), q_p is the specific product formation rate (g product formed/gDW per hour), $Y_{X/S}$ (gDW/g substrate) and $Y_{X/P}$ (gDW/g product) are the yield coefficients, and m_s (g substrate/gDW per hour) and m_p (g product/gDW per hour) are the specific maintenance rates for substrate and product, respectively. In some cases, these maintenance coefficients may be omitted or combined with a "cell death coefficient" (e.g., Doran 1995). The specific growth rate is a function of the substrate concentration and is usually of the Monod kinetics form. The model can also be extended to include growth inhibition by the product (and biomass), and $f(C_S)$ becomes some function of substrate and product (and biomass). The Monod equation is bound by zero-order (at high substrate concentrations relative to the Monod constant K_S) and first-order (at vanishingly small substrate concentrations) kinetics. The solutions of reaction-diffusion problems with these two simple rate equations are valuable in that they can be applied as lower or upper bounds to the general problem without requiring detailed knowledge of the rate expressions and thus considerably facilitating the calculations.

In the interpretation of kinetic data for immobilized cells, it is important to assess the significance of mass transfer limitations. If negligible mass transfer limitation is present, the externally observed kinetics is the intrinsic cell kinetics. Any external or internal mass transfer limitation will lead to externally observed lower conversion rates. Mass transfer limitations may appear in the external film around the support matrix, or within the gel matrix, or in both.

Various claims have been made regarding changes in the intrinsic growth rate of immobilized cells, primarily regarding cells adhering to a surface. It has been asserted that the growth rate for immobilized cells is much higher than that for free-living cells. For gel-immobilized cell systems, it has been observed that the metabolic rates of gel-immobilized cells depend only on the local solution concentrations and are identical to those for free cells if diffusional limitations are absent, although some reports showed a decreased growth rate upon entrapment. Some researchers found

TABLE 12.8
Comparison of the Specific Growth Rates for Gel-Immobilized (μ_i) and Free (μ_f) Cells

Microorganism	Gel System	μ_i (h^{-1})	μ_f (h^{-1})
	Bacteria		
Escherichia coli	Carrageenan (2%)	2.04[a]	2.08
		1.69[b]	1.63
E. coli B/pTG201	Carrageenan (2%)	0.24[c]	0.30
		0.18[d]	
E. coli B/pTG201	Carrageenan (2%)	0.18	0.36
	Fungi		
Candida guilliermondii	Ba-alginate	0.021	0.029
Saccharomyces cerevisiae	Calcium alginate (2%)	0.30[e]	0.31
		0.27[f]	
S. cerevisiae	Gelatin (25–30%)	0.28	0.51
S. cerevisiae	Calcium alginate (1.5%)	0.115	0.126
	Carrageenan (2.5%)	0.100	
S. cerevisiae	Calcium alginate (2%)	0.25	0.41
S. cerevisiae	Calcium alginate (2%)	0.46	0.50
Thiosphaera pantotropha	Agarose (5%)	0.45[g]	0.45
		0.58[h]	

Source: Willaert, R., Nedovic, V., and Baron G.V., *Fundamentals of Cell Immobilization Biotechnology,* 2004. Dordrecht, The Netherlands: Kluwer Academic Publishers; Willaert, R. *Fermentation Microbiology and Biotechnology*, 2nd ed., pp. 287–361, 2007b. Boca Raton, FL: CRC Press.

[a] Supply of 21% oxygen.
[b] Supply of 100% oxygen.
[c] Growth in gel slabs.
[d] Growth in gel beads.
[e] Single immobilized cells;
[f] Cells in a microcolony.
[g] Growth in stirred-tank reactor.
[h] Growth in Kluyver flask.

no significant difference between the maximum specific growth rates for immobilized yeast and bacteria and those for free cells (Table 12.8). On the contrary, a significant decrease has been noted by other researchers for the same microorganisms. This change of metabolic activity upon immobilization may be due to diffusional limitations or to a change in cellular physiology.

12.3.2.1.2 Modeling

By the entrapment of cells in gel matrices, an additional barrier to mass transfer relative to free cells is introduced. This tends to lower the overall reaction rate and creating a specific microenvironment around the cells. Immobilized cells can grow in the gel matrix and the mass transfer limitations on substrate delivery and product removal lead to time-dependent spatial variations in growth rates and biomass densities, which may be accompanied by alterations in cellular physiology and biocatalytic activity. Because the local effective diffusion coefficient depends on the local biomass density, this nonhomogeneous growth will influence the local diffusive rates. The existence of chemical environmental gradients in immobilized cell systems has been verified experimentally with various microprobe techniques (Willaert et al. 2004).

12.3.2.1.2.1 Dynamic Modeling A general dynamic model that describes the growth of the immobilized cells and the resulting time-dependent spatial variation of substrate and product in the system can be constructed by writing the mass balances over the immobilization matrix (it is usually assumed that diffusion in the system is governed by Fick's law, the cells are initially distributed homogeneously over the carrier, and there is no deformation of the matrix due to cell growth or gas production):

$$\frac{\partial}{\partial t}(\varepsilon\beta C_{\mathrm{i}}) = z^{-n}\frac{\partial}{\partial z}\left(z^{n} D_{\mathrm{e,i}}\frac{\partial C_{\mathrm{i}}}{\partial z}\right) \pm \varepsilon\beta r_{\mathrm{i}} \tag{12.23}$$

where ε is the ratio of the volume of the pores of the matrix to the total volume; β is the ratio of the volume of the pores minus the volume of the cells to the volume of the pores in the matrix; C_{i} is the substrate ($i = S$) or product ($i = P$) concentration (expressed per volume available for substrate; n is a shape factor of value 0 for planar, 1 for cylindrical, or 2 for spherical geometry; and $D_{\mathrm{e,i}}$ is the effective diffusion coefficient for species i. The substrate consumption rate (r_{s}) and the product formation rate (r_{p}) are linked to the growth rate (r_{x}) by Equations 12.24 and 12.25:

$$\frac{\partial}{\partial t}(\varepsilon C_{\mathrm{X}}) = \varepsilon r_{\mathrm{x}} = \varepsilon\mu C_{\mathrm{X}} \tag{12.24}$$

$$r_{\mathrm{s}} = \frac{1}{Y_{\mathrm{X/S}}} r_{\mathrm{x}} \quad \text{and} \quad r_{\mathrm{p}} = \frac{1}{Y_{\mathrm{X/P}}} r_{\mathrm{x}} \tag{12.25}$$

where C_{X} is the biomass concentration expressed per volume available for the cells. Because ε is constant with time, the left-hand side of Equation 12.23 can be written as

$$\frac{\partial}{\partial t}(\varepsilon\beta C_{\mathrm{i}}) = \varepsilon\beta\frac{\partial C_{\mathrm{i}}}{\partial t} + \varepsilon C_{\mathrm{i}}\frac{\partial\beta}{\partial t} \tag{12.25}$$

If a dry weight cell density ρ_{c} is defined as the ratio of the cell dry mass per cell volume, β can be expressed as function of C_{X}:

$$\beta = 1 - \frac{C_{\mathrm{X}}}{\rho_{\mathrm{c}}} \tag{12.26}$$

Using the relationship $Y_{\mathrm{X/S}} = dC_{\mathrm{X}}/dC_{\mathrm{S}}$, the second term on the right side of Equation 12.25 is negligible when C_{S} is much smaller than $\beta\rho_{\mathrm{c}}/Y_{\mathrm{X/S}}$, and under those conditions substitution into Equation 12.23 gives

$$\varepsilon\beta\frac{\partial C_{\mathrm{i}}}{\partial t} = z^{-n}\frac{\partial}{\partial z}\left(z^{n} D_{\mathrm{e,i}}\frac{\partial C_{\mathrm{i}}}{\partial z}\right) \pm \varepsilon\beta r_{\mathrm{i}} \tag{12.27}$$

These equations can be integrated to yield the substrate and biomass profiles as a function of time (usually together with the reactor model) using the correct initial and boundary conditions. These equations are valid for a wide range of immobilized cell systems.

12.3.2.1.2.2 Pseudo-steady-state Modeling Under certain conditions, the full dynamic modeling to describe transient behavior can be simplified to "pseudo-steady-state" modeling. Therefore, the biomass growth and the substrate consumption rate and/or product formation rate are treated separately. This approach is valid as long as the time scale for growth is much larger than the time scale for consumption and product formation. Hence, a pseudo-steady-state substrate/product distribution is assumed at each instant. As a result, the system of partial differential equations is reduced to a system of ordinary differential equations that facilitates the numerical solution.

12.3.2.1.2.3 Steady-state Modeling If the cell mass does not vary rapidly, or is fairly uniform, the concentration profiles in a gel matrix with entrapped cells can be simulated using a steady-state model at any point in time. These models can give valuable information for design purposes or can be combined with experimental *in situ* measurements (e.g., microelectrodes). In this case, mathematical calculations can be very simple, and straightforward analytical solutions can be obtained for simple reaction kinetics (e.g., zero- or first-order kinetics).

12.3.2.1.2.4 Effectiveness Factor The effectiveness factor (η) can be calculated to obtain a numerical measure of the influence of mass transfer on the reaction rate. The effectiveness factor is defined as

$$\eta = \frac{\text{observed reaction rate}}{\begin{array}{c}\text{rate which would be obtained}\\ \text{without mass transfer resistance}\end{array}} \tag{12.28}$$

Effectiveness factor calculations can be based on steady-state or dynamic reaction-diffusion models with the assumption of a homogeneous distribution of cells over the carrier (e.g., Willaert and Baron 1994). The effectiveness factor for substrate consumption can mathematically be expressed as the volume-averaged reaction rate relative to the rate at bulk-phase concentration:

$$\eta = (n+1)\frac{\left(D_e \dfrac{dC'_S}{dz'}\right)_{z'=1}}{r_s(1)} \tag{12.29}$$

or

$$\eta = (n+1)\frac{\displaystyle\int_0^1 z'^{n'} r_s(C'_S)dz'}{r_s(1)} \tag{12.30}$$

where n is a shape factor (0 for planar, 1 for cylindrical, or 2 for spherical geometry) and z' is the dimensionless position coordinate; and r_s is the substrate reaction rate, which is a function of the dimensionless substrate concentration (C'_S; and also of the position in the case of transient effectiveness factor).

12.3.3 Bioreactor Design

A classification of immobilized cell reactors with their advantages and disadvantages is given in Table 12.9. Three categories can be distinguished: bioreactors filled with (1) mixed, suspended particles; (2) fixed particles or large surfaces; or (3) moving surfaces.

Most bioreactors (Figure 12.5) contain three phases: solid (the carrier or cell aggregate), bulk liquid, and gas (air/oxygen or gas feed, gaseous products).

TABLE 12.9
Classification of Immobilized Cell Reactors

Reactor Type	Advantages	Disadvantages
	Mixed, Suspended Particles	
Stirred-tank reactor	Flexible	High power consumption
	Variable mixing intensity	Shear damage to sensitive matrices
	Suitable for high viscosity	High cost
Gas/air lift reactor	No moving parts	Low local mixing intensity
Bubble column reactor	Simple	Only for low viscosities
	High solids fraction possible	Excessive foaming possible
	High gas transfer	
	Good heat transfer	
Fluidized bed reactor	No moving parts in reactor	Difficult matching of feed and fluidization rates
	Simple, low cost	Requirements on particle density (dense support)
	Very high solids contents	Good local mixing intensity
	Good heat transfer	Only for low viscosity
	Variable mixing characteristics for liquid and solid	
	Fixed Particles or Large Surfaces	
Packed-bed reactor	Simple, low cost	Plugging by solids at low flow rates
Monolith reactor	Plug flow characteristics possible	High pressure drop
	Large surface to volume ratio	Aeration only externally possible
		Channeling and maldistribution
		Gas build-up and formation of "dry" spots
		Low external mass transfer rate at low flow rates
Trickle-bed reactor	Simple, very low cost	Plugging by excessive growth (cleaning possible)
	Plug flow approached	Only large supports possible
	Large surface-to-volume ratio	Only for low viscosities
	High oxygen transfer rate	
	Suitable for gas cleaning (biofilter)	
Solid (surface) culture	Simple	High cost (often manual)
	Flexible	Only batch
	Low humidity (mould fermentation)	Difficult control over operation
	Low contamination risk (by bacteria or yeasts)	Usually limited to solid substrates
Membrane reactor	Very high cell densities	Sterilization problems
	Very high productivities	Microbial damage (membrane perforation)
	Perfusion operation possible	Low capacities only
	Simultaneous product separation possible	High cost
	Separate feed of gas and liquid possible	
	Low shear	
	Moving Surfaces	
Rotating surfaces (disc, cylinder, or packing)	Low shear on biofilm	Power consumption
	Batch or continuous	Maintenance
	Excellent aeration	
	High productivity	
	Suitable for high viscosity	

Source: Baron, G.V., Willaert, R.G., and De Backer, L., *Immobilized Living Cell Systems: Modeling and Experimental Methods*, pp. 67–95, 1996. Chichester, United Kingdom: John Wiley & Sons. With permission.

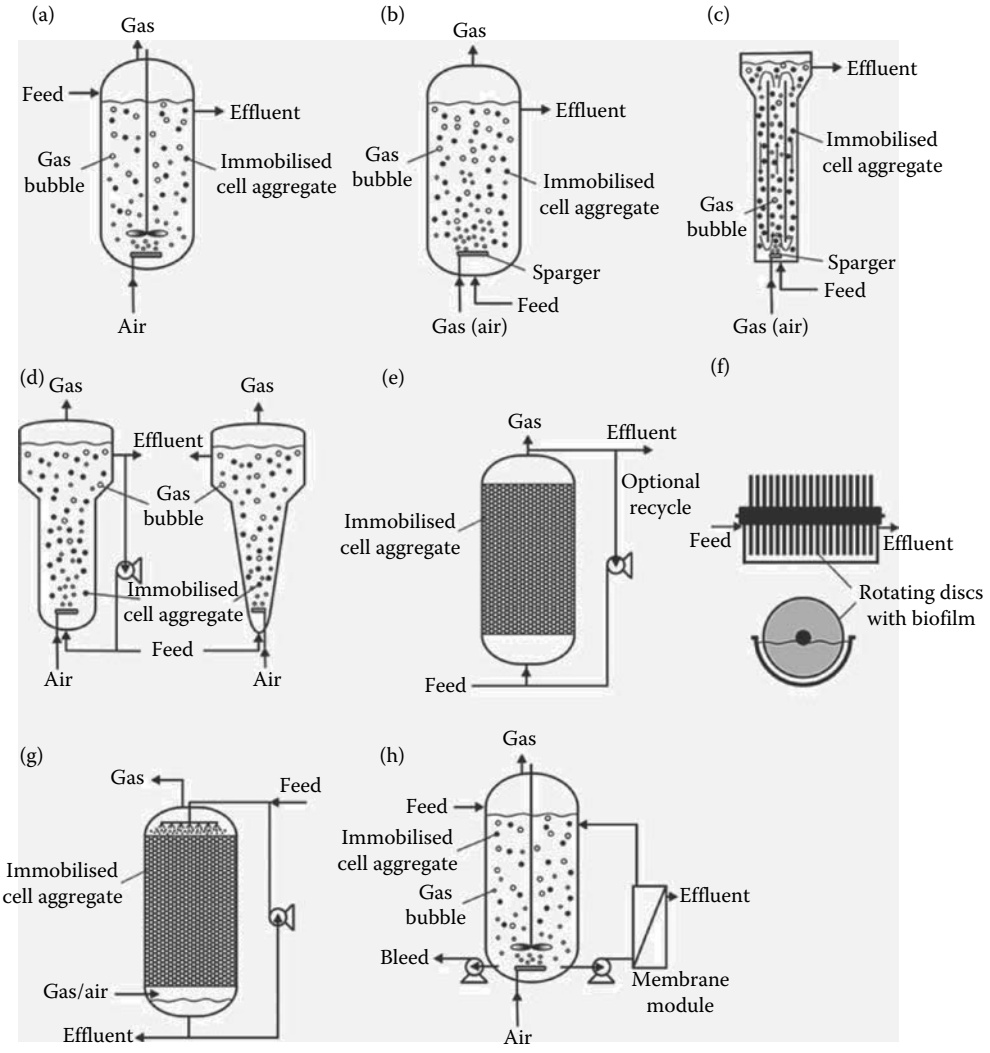

FIGURE 12.5 Immobilized cell bioreactors: (a) stirred-tank reactor; (b) bubble column reactor; (c) gas (air) lift reactor; (d) fluidized-bed reactor (left), tapered fluidized reactor (right); (e) packed-bed reactor with optional recycle loop; (f) rotating drum reactor; (g) trickle bed reactor; and (h) membrane cell-recycle reactor.

Criteria for the selection of an appropriate bioreactor for immobilized cells and reactor types satisfying certain criteria are summarized in Table 12.10. The cell aggregate can only be fully active if the external supply or removal rates match the internal transport, utilization, and production rates. The high cell densities in the reactors put higher demands on nutrient supply and transport rates.

In aerobic fermentations, oxygen is often the limiting substrate because the liquid film around the gas bubbles is a major resistance to oxygen transfer. Gas-liquid mass transport is characterized by the liquid-phase mass transfer coefficient k_L (usually expressed as $k_L a$, with a the area of the bubble per volume). Additionally, intraparticle resistance of oxygen in the cell aggregate can also become significant depending on the Thiele modulus. Consequently, the Thiele modulus and $k_L a$ are important parameters for the design and scale-up of immobilized cell bioreactors. The parameters, which are grouped in the Thiele modulus, are the size of the aggregate, cell kinetics (kinetic parameters), and the diffusion coefficient. Therefore, the particle size or biofilm thickness are major design variables. Because substrate concentration is often not a free parameter, only aggregate size and biomass loading are

TABLE 12.10
Criteria for the Selection of the Reactor Type

Criterion		Stirred Tank	Air Lift Bubble Column	Fluidized Bed	Packed Bed	Trickle Bed	Membrane Reactor	Rotating Biological Contactor
Matrix	Strong	x	x	x	x	x		
	Weak		x	x				
Biocatalyst	Biofilm				x	x		x
	Particles	x	x	x	x			
	Membrane						x	
Sterilizability	Good	x	x	x			x	
	Poor				x	x		x
High capacity		x	x	x	x	x		
High feed viscosity		x						x
Solids in feed		x	x	x				x
Flexibility required		x	x					
Equipment cost	High	x		x			x	x
	Low		x		x	x		
High oxygen (gas) requirement		x	x		x	x		
High cell growth rate		x	x	x				
High gas production		x	x	x		x		x
Cell free effluent								
Low shear rate	Low		X		X	x	x	

Source: Modified from Baron, G.V., Willaert, R.G., and De Backer, L., *Immobilized Living Cell Systems: Modeling and Experimental Methods*, pp. 67–95, 1996. Chichester, United Kingdom: John Wiley & Sons.

engineering parameters. Unless the substrate concentration is very low (e.g., degradation of pollutants), diffusion limitation for substrate only occurs for particles of more than several millimeters in diameter. In contrast, the penetration depth of oxygen in particles for aerobic processes is only 50–100 μm.

12.4 PHYSIOLOGY OF IMMOBILIZED MICROBIAL CELLS

The microenvironment of microbial cells is altered upon immobilization depending on the method of immobilization. The changed chemical composition and/or the physical interaction between the matrix material and the cell can have a profound effect on the physiology of the cells. Some examples of the effect of immobilization upon the cell's physiology are discussed for bacteria and fungi. An overview of observed effects (discussed in Section 12.4.1) upon immobilization of bacterial and fungal cells is summarized in Tables 12.11 and 12.12, respectively.

12.4.1 Bacterial cells

12.4.1.1 Plasmid Stability

Recombinant plasmid stability in host cells can be increased upon immobilization (Table 12.10), presumably because of the significant drop in the rate of cell division.

TABLE 12.11
Some Observed Effects of Bacterial Cell Immobilization on Its Physiology

Immobilization Effect	Microorganism	Immobilization System
	Increased Plasmid Stability	
	Escherichia coli	Calcium alginate, agarose, κ-carrageenan, cotton cloth, hollow fiber, polyacrylamide/hydrazide, PVA, silicone beads
	Lactococcus lactis	κ-Carrageenan/locust bean gum
	Myxococcus xanthus	κ-Carrageenan
	Protective Microenvironment	
Increased phenol degradation	*Pseudomonas putida*	Calcium alginate, polyacryl amide-hydrazide
	Trichosporium sp.	Calcium alginate
Increased antibiotics tolerance	*Pseudomonas aeruginosa*	Calcium alginate
Increased phenol tolerance	*Escherichia coli* *Stapylococcus aureus*	Calcium alginate
Increased benzene degradation	*Pseudomonas putida* and *Pseudomonas fluorescens*	Cotton terry cloth
Increased degradation of linear alkyl benzene sulfonate	*Pseudomonas aeruginosa*	Calcium alginate
Increased stress tolerance	*Bifidobacterium longum* and *Lactococcus lactis*	κ-Carrageenan/locust bean gum
Metabolic differences	*Marinobacter* sp.	Porous glass
Degradation of DMP at higher concentration	*Bacillus* sp.	Calcium alginate, polyurethane foam
Protection from bacteriophage attack	*Streptococcus lactis* *Streptococcus cremoris*	Calcium alginate
Different protein profile after cold shock	*Escherichia coli*	Agar
Increased survival rate at low pH	*Bifidobacterium longum*	Gellan-xanthan, Ca-alginate
	Influence of Mass Transport Limitation	
Decreased pH-dependent morphology change	*Lactobacillus helveticus*	κ-Carrageenan/locust bean gum
Changed citrate metabolism and lactate production	*Lactococcus lactis*	Ca-alginate
Loss of SDS metabolization	*Pseudomonas fluorescens*	Polyacrylamide
	Changed Productivity of Enzymes and Other Products	
Increased α-amylase production	*Bacillus* sp.	κ-Carrageenan
	Bacillus subtilis	Polyacrylamide
Reduced α-amylase production	*B. amyloliquefaciens*	Calcium alginate
Increased dextransucrase production	*Leuconostoc mesenteroides*	Calcium alginate
Increased α-galactosidase	*Streptomyces griseoloalbus*	Calcium alginate
Increased β-galactosidase	*Escherichia coli*	Calcium alginate
Increased proteinase production	*Humicola lutea*	Polyhydroxyethylmethacrylate
Increased protease production	*Myxococcus xanthus*	Calcium alginate
Increased alginate production	*Pseudomonas aeruginosa*	κ-Carrageenan
Increased gellan gum production	*Pseudomonas elodea*	κ-Carrageenan

TABLE 12.11 (CONTINUED)
Some Observed Effects of Bacterial Cell Immobilization on Its Physiology

Immobilization Effect	Microorganism	Immobilization System
	Changed Morphology	
	Escherichia coli	Agar
	Lactobacillus helveticus	κ-Carrageenan/locust bean gum
	Pseudomonas putida	Cotton terry cloth
	P. fluorescens	Cotton terry cloth

Source: Adapted from Willaert, R., Nedovic, V., and Baron G.V., *Fundamentals of Cell Immobilization Biotechnology,* 2004. Dordrecht, The Netherlands: Kluwer Academic Publishers; Willaert, R. *Fermentation Microbiology and Biotechnology*, 2nd ed., pp. 287–361, 2007b. Boca Raton, FL: CRC Press.

Note: DMP, dimethylphtalate; SDS, sodium dodecyl sulfate.

12.4.1.2 Protective Microenvironment

Immobilization can confer protection to cells exposed to toxic or inhibitory substrates or environments (Table 12.10). Gel immobilized *Trichosporium* sp. and *Pseudomonas putida* showed higher rates of phenol degradation and phenol tolerance. Alginate-entrapped *E. coli* cells grown entrapped in calcium alginate showed low lipid-to-protein ratios even without phenol in the growth medium. Immobilization of cells also markedly changed the protein pattern of the outer membrane. Calcium-alginate-immobilized cultures of *Streptococcus* cells were protected from bacteriophage attack because of the exclusion of phage particles from the gel matrix. These cultures were also functionally proteinase deficient when immobilized and grown in milk, which resulted in a lower acid production due in part to the inability of the immobilized cells to hydrolyze milk proteins and to diffusional limitations of substrate into the beads. A different protein profile was found after submitting agar-entrapped *E. coli* to a cold shock (Perrot et al. 2001). It was suggested that such induction of specific molecular mechanisms in immobilized bacteria might explain the high resistance of sessile-like organisms to stresses. The degradation rate of alkyl benzene sulfonate by calcium-alginate-entrapped *P. aeruginosa* was considerably increased compared with free cells and could be further increased using low-intensity ultrasonic irradiation (Lijun et al. 2005) because ultrasound can improve the osmosis of the cell membrane, cell growth, and enzyme activities. Recently, a new ultrasound-based cell immobilization technique was described that allows manipulation and positioning of cells/particles within various gel matrices before polymerization (Gherardini et al. 2005). Proteomic analysis of agar-entrapped *P. aeruginosa* showed that the immobilized bacteria were physiologically different from free cells (Vilain et al. 2004).

12.4.1.3 Effect of Mass Transport Limitation

Mass transport limitations can have an influence on the morphology of immobilized *Lactobacillus helveticus* because of the long response time of entrapped cells to random pH changes. The citrate metabolism (Cachon and Divies 1993) and lactate production (Klinkenberg et al. 2001) of *Lactococcus lactis* were altered because of the concentration and pH gradients in the gel beads. The germination time of *Bacillus subtilis* cells was significantly longer than for free cells; after a time lag due to encapsulation, the growth of the cells was uninhibited and no differences between entrapped and free cells were found.

12.4.1.4 Enhanced Productivity of Enzymes and Other Products

It has been observed that the production of several enzymes is increased upon immobilization (Table 12.11). In one case (α-amylase by alginate-entrapped *Bacillus amyloliquefaciens*), enzyme production was decreased (Argirakos et al. 1992). Protease production by alginate-entrapped *Myxococcus*

TABLE 12.12
Some Observed Effects of Fungal Cell Immobilization on Its Physiology

Immobilization Effect	Microorganism	Immobilization System
	Increased Plasmid Stability	
	Saccharomyces cerevisiae	Calcium alginate bead, cotton cloth sheet, gelatin
		beads, porous glass beads
	Protective Microenvironment	
Altered osmotic conditions in microenvironment	*Saccharomyces cerevisiae*	Calcium alginate
Decreased ethanol tolerance	*Pichia stipitis*	κ-Carrageenan
Increased ethanol tolerance	*Saccharomyces cerevisiae*	κ-Carrageenan
Increased organic solvent tolerance	*Saccharomyces cerevisiae*	Polyhydroxylated silane
Decreased inhibition of cell growth and metabolism by better carbon dioxide removal	*Saccharomyces cerevisiae*	Stainless steel fiber cloth
Increased tolerance for nitriles and amides	*Candida guilliermondii*	Barium alginate
More efficient treatment of dairy effluents	*Candida pseudotropicalis*	Calcium-alginate
More sensitive for sucrose	*Aspergillus niger*	Calcium alginate
Protection against inhibitory substances	*Saccharomyces cerevisiae*	Calcium alginate
Retention of high metabolic activity during long-term fermentation	*Saccharomyces cerevisiae*	Calcium alginate
	Influence of Mass Transport Limitation	
Less susceptible of enzyme to endogenous proteolysis	*Saccharomyces cerevisiae*	Gelatin
Lower specific productivity	*Kluyveromyces lactis*	Calcium alginate
	Changed Productivity	
Increased ethanol production	*Saccharomyces formosensis*	Calcium alginate and co-entrapped sand
	Saccharomyces bayanus	κ-Carrageenan
Increased laccacase production	*Agaricus* sp.	Polyurethane foam, straw, textile strips
Increased penicillin production	*Penicillium chrysogenum*	κ-Carrageenan
Shifted phosphate concentration optimum for alkaloid production	*Claviceps purpurea*	Calcium alginate
Changed secondary metabolite production	*Fusarium moniliforme*	Alginate, carrageenan, polyurethane
	Changed Morphology/Composition	
	Aspergillus niger	Calcium alginate
	Claviceps fusiformis	Calcium alginate
	Gibberella fujikuroi	Calcium alginate
	Saccharomyces cerevisiae	Calcium alginate, agar, gelatine
	Saccharomyces cerevisiae	Calcium alginate
	Enhanced Enzyme Stability	
Hydroxylase	*Mortierella isabellina*	Calcium alginate, polyurethane foam

Source: Adapted from Willaert, R., Nedovic, V., and Baron G.V., *Fundamentals of Cell Immobilization Biotechnology,* 2004. Dordrecht, The Netherlands: Kluwer Academic Publishers; Willaert, R. *Fermentation Microbiology and Biotechnology*, 2nd ed., pp. 287–361, 2007b. Boca Raton, FL: CRC Press.

xanthus cells was increased because of a reduced inhibition by peptone and gelatin as result of mass transfer limitation in the gel (Fortin and Vuillemard 1990).

12.4.2 Fungal Cells

12.4.2.1 Plasmid Stability

As in the case of recombinant bacteria, improved plasmid stability in immobilized *S. cerevisiae* has also been demonstrated.

12.4.2.2 Protective Microenvironment

Immobilization can create a protective microenvironment for the cells (Table 12.11). In the case of co-immobilization of *S. cerevisiae* cells with vegetable oils, cells could be protected against inhibitory substances because of a better solubility of the inhibitory compounds in the oil phase. An increased tolerance for ethanol by immobilized brewer's yeast (Norton et al. 1995) and a decreased inhibition of ethanol productivity in entrapped *Kluyveromyces marxianus* at high osmolality (Dale et al. 1994) have been observed. Immobilized *S. cerevisiae* contained significantly higher percentages of saturated fatty acids because of altered osmotic conditions in the microenvironment of the cells; other examples are shown in Table 12.11.

12.4.2.3 Influence of Mass Transport Limitation

A high invertase activity, which was exhibited by immobilized cells, was due to a maintained expression of the *SUC2* gene and a reduced susceptibility of the enzyme to endogenous proteolytic attack (de Alteriis et al. 1999). These results have been interpreted in terms of diffusional limitations and changes in the pattern of invertase glycosylation due to growth of yeast in an immobilized state.

12.4.2.4 Enhanced Productivity

The increase in ethanol productivity by gel-entrapped and co-entrapped cells of *S. cerevisiae* was attributed to stimulation in cell permeability by Si^{4+} whereas higher ethanol production by κ-carrageenan-entrapped *Saccharomyces bayanus* was attributed to a favorable media supplement in the aqueous phase of the matrix (Brito et al. 1990). However, the reduced yield of ethanol in calcium-alginate-entrapped *S. cerevisiae* was due to lower substrate concentrations toward the center of the bead because of mass transport limitations (Gilson and Thomas 1995).

12.4.2.5 Enhanced Enzyme Stability

A hydroxylase from entrapped *Mortierella isabellina* was found to retain its activity over a longer period compared with free mycelia. The effect of immobilization on the physiology of yeast cells and fungi is given in Table 12.12.

12.4.3 Stem Cells

A stem cell is an unspecialized cell that can self-renew (reproduce itself) and differentiate into functional phenotypes (Atala et al. 2008). Stem cells originate from embryonic, fetal, or adult tissue and are broadly categorized accordingly. The integration of stem cells and tissue-engineered scaffolds has the potential to revolutionize the field of regenerative medicine. It promises great things, including the ability to grow organs composed of multiple cell types and complex structures, therapies for the correction of congenital diseases, and the promise of readily obtainable immunocompatible tissues. Creating reserves of undifferentiated stem cells and subsequently driving their differentiation to a lineage of choice in an efficient and scalable manner is critical for the ultimate clinical success of cellular therapeutics (Dawson et al. 2008). In recent years, various biomaterials

have been incorporated in stem cell cultures, primarily to provide a conducive microenvironment for their growth and differentiation and to ultimately mimic the stem cell niche.

With the inherent plasticity and multilineage potential provided by stem cells comes an increased need for regulating cell differentiation, growth, and phenotypic expression (Guilak et al. 2009). Stem cells, like all cells, are influenced by their microenvironment, including chemical and physical cues. Until recently, chemical cues have been the primary means by which stem cells self-renew and their differentiation has been influenced. Soluble factors and substrate coating have been used in maintaining undifferentiated stem cells, as well as in promoting a particular differentiation pathway. Recent efforts have begun focusing on controlling the cellular microenvironment by engineering three-dimensional biomaterials and/or applying physical forces. Biomaterials are rapidly being developed to display and deliver stem-cell-regulatory signals in a precise and near-physiological fashion and serve as powerful artificial microenvironments in which to study and instruct stem-cell fate in culture and *in vivo* (Lutolf et al. 2009). Table 12.13 shows some examples of observed effects of immobilization materials on stem cell culture.

TABLE 12.13
Some Examples of Observed Effects of Immobilization Biomaterials on Stem Cell Culture

Biomaterial Effect	Stem Cell Type	Immobilization System
Natural Materials		
Maintaining pluripotency and undifferentiated state	hESC	Hyaluronic acid hydrogel
Differentiation into neural lineage cells	mESC	Fibrin gels
More efficient collagen II and proteoglycan synthesis of differentiated cells	MSC	Fibrin gels
Encouraging osteogenic differentiation	mESC	Hydroxyapatite
Promoted differentiation toward a hepatic lineage without the need for embryoid body formation	mESC	Alginate poly-L-lysine
Differentiation into endothelial cells	hBMC	Crosslinked pullulan/dextran/fucoidan
Assemble and reorganize of the pellet structure	hMSC	Type II collagen
Improve overall viability, longer maintenance of hematopoitic functions, ability to engraft into bone marrow	hUCBC	Collagen microbeads
Synthetic Materials		
Polymers		
Pore size and polymer composition influence differentiation into the hematopoietic	mESC	Poly(lactic-co-glycolic acid)/ poly(L-lactic acid) (50/50 blend)
Encouraging cell proliferation and cell–cell interaction	MSC, mESC	Nanofibrous poly(ε-caprolactone)
Upregulation of chondrogenic markers	EB from mESC	PEG hydrogel
Ceramics		
Continued osteoblastic phenotypic properties	MSC	Biphasic calcium phosphate
Metals		
Attachment , proliferation, enhanced osteogenic differentiation in bioreactor (shear stress)	MSC	Titanium scaffold (fiber meshes)
Induction of EB formation, significant differences in gene expression	mESC	Cytomatrix™ (tatalum-based scaffold)

Source: Dawson et al. 2008; Walker et al. 2009.

Note: hESC, human embryonic stem cell; mESC, mouse embryonic stem cell; MSC, mesenchymal stem cell; hBMC, human bone marrow cell; hMSC, human mesenchymal stem cell; hUCB, human umbilical cord blood cells; EB, embryonic body.

12.5 BEER PRODUCTION USING IMMOBILIZED CELL TECHNOLOGY: A CASE STUDY

12.5.1 Flavor Maturation of Green Beer

Green beer: During the beer fermentation, wort is fermented to beer. Wort is the carbohydrate extract from grinded barley malt. The fermentation proceeds in two stages. The first stage is called the "primary fermentation" and the second one is the "secondary fermentation" or "maturation". The obtained beer after the primary fermentation is called "green" beer.

One of the objectives of the maturation (or secondary fermentation) of **green beer** is the removal of unwanted aroma compounds. The removal of the vicinal diketones diacetyl and 2,3-pentanedione is especially important because these compounds have very low flavor thresholds. Diacetyl is quantitatively more important than 2,3-pentanedione and is therefore used as a marker compound. It has a taste threshold around 0.10–0.15 mg/ml in lager beer, approximately 10 times lower than that of pentanedione. These compounds impart a "buttery," "butterscotch" aroma to the beer. During the primary fermentation, these flavor-active compounds are produced as byproducts of the synthesis pathway of isoleucine, leucine, and valine (ILV pathway) and are linked to the amino acid metabolism and the synthesis of higher alcohols. The excreted α-acetohydroxy acids are overflow products of the ILV pathway and are nonenzymatically converted to the corresponding vicinal diketones (Figure 12.6). This nonenzymatic oxidative decarboxylation step is the rate-limiting step and proceeds faster at a high temperature and lower pH. The produced amount of α-acetolactate is very dependent on the used strain. The production also increases with increasing yeast growth. For classical lager fermentation, 0.6 ppm α-acetolactate is typically formed. At high aeration, this value can raise to 0.9 ppm and in cylindro-conical fermentation tanks even to 1.2–1.5 ppm. Yeast cells possess the necessary enzymes (reductases) to reduce diacetyl to acetoin and further to 2,3-butanediol and to reduce 2,3-pentanedione to 2,3-pentanediol. These reduced compounds have much higher taste thresholds and have no effect on the beer flavor. The reduction reactions are dependent on the yeast strain and occur during the course of maturation after fermentation. Sufficient yeast cells in suspension are necessary to obtain an efficient reduction. Yeast strains, which flocculate early during the main fermentation, need a long maturation time to reduce the vicinal diketones.

The traditional maturation process is characterized by a near-zero temperature, low pH, and low yeast concentration, resulting in a very long maturation period of 3–4 weeks. Nowadays, the

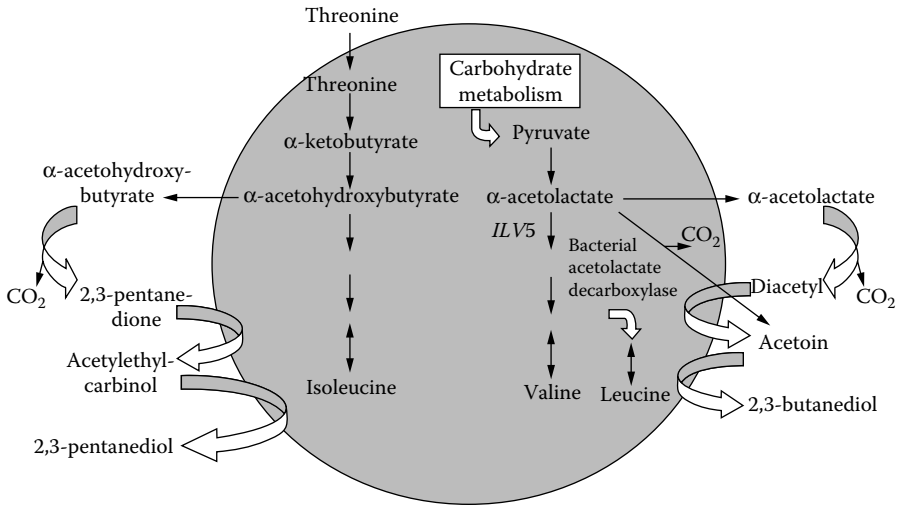

FIGURE 12.6 The synthesis and reduction of the vicinal diketones diacetyl and 2,3-pentanedione in *S. cerevisiae*.

TABLE 12.14
ICT for Beer Maturation

Immobilization Method	Immobilization Matrix	Reactor Type	Scale
Surface attachment	DEAE-cellulose beads	Packed bed	Industrial
Entrapment	Porous glass beads	Packed-bed	Industrial
Entrapment	Polyvinyl alcohol beads	Gas lift	Pilot
Entrapment	Calcium alginate beads	Fluidised-bed	Laboratory

Source: Adapted from Willaert, R., *Handbook of Food Products Manufacturing*, pp. 443–506, 2007a. Hoboken, NJ: John Wiley & Sons; Willaert, R., *Fermentation Microbiology and Biotechnology*, 2nd ed., pp. 287–361, 2007b. Boca Raton, FL: CRC Press.

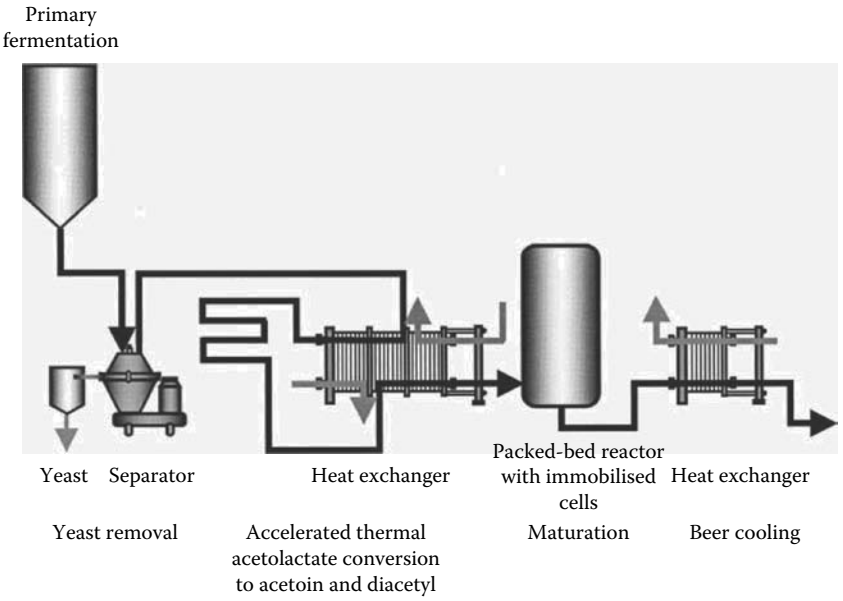

FIGURE 12.7 Process scheme for the maturation of beer using immobilized yeast cells (modified after Willaert, R., *Minerva Biotechnot*, 12:319–330, 2000).

maturation phase is considerably reduced to approximately one week because several strategies are used to accelerate the vicinal diketone removal. Using immobilized cell technology, this maturation period can be further reduced to a time range of a few hours. Examples of immobilized cell technology (ICT) maturation processes are illustrated in Table 12.14. An example of a process scheme is illustrated in Figure 12.7.

It should also be mentioned that accelerated beer maturation can also be performed by increasing the maturation temperature, which can be realized by integrating the secondary fermentation in the primary fermentation. In this way, the production of beer can be accomplished in less than two weeks in one cylindroconical vessel.

12.5.2 Production of Alcohol-Free or Low-Alcohol Beer

The technology to produce alcohol-free or low-alcohol beer is based on the suppression of alcohol formation by arrested (restricted) free-cell batch fermentation. However, the resulting beers are

TABLE 12.15
ICT for the Production of Alcohol-Free or Low-Alcohol Beer

Immobilization Method	Immobilization Matrix	Reactor Type	Scale
Surface attachment	DEAE-cellulose	Packed bed	Laboratory
Surface attachment	DEAE-cellulose	Packed bed	Industrial
Entrapment	Porous glass	Fluidized bed	Pilot
Entrapment	Silicon carbide rods	Cartridge loop reactor	Pilot
Entrapment	Calcium alginate	Gas lift	Laboratory
Entrapment	Calcium pectate	Packed bed	Laboratory

Source: Adapted from Willaert, R., *Handbook of Food Products Manufacturing*, pp. 443–506, 2007a. Hoboken, NJ: John Wiley & Sons; Willaert, R., *Fermentation Microbiology and Biotechnology*, 2nd ed., pp. 287–361, 2007b. Boca Raton, FL: CRC Press.

characterized by an undesirable wort aroma because the wort aldehydes have only been reduced to a limited degree. An alternative method of producing these beers is based on the removal of ethanol from stronger beers by using membrane, distillation, or vacuum evaporation processes. These methods have the disadvantage that the production cost is increased.

Controlled ethanol production for low-alcohol and alcohol-free beers have been successfully achieved by partial fermentation using immobilized yeast (Table 12.15). The reduction of the wort aldehydes can be quickly achieved by a short contact with the immobilized yeast cells. The process is performed at a low temperature to avoid undesirable cell growth and ethanol production. A disadvantage of this short-contact process is the production of only a small amount of desirable esters. Nuclear mutants of *S. cerevisiae,* which are defective in the synthesis of tricarboxylic acid cycle enzymes (i.e., fumarase or 2-oxoglutarate dehydrogenase) can be used for the production of nonalcohol beer because they produce minimal amounts of ethanol, but much lactic acid. These mutants have been used in a continuous immobilized-cell process (Navrátil et al. 2000).

12.5.3 Continuous Main Fermentation

Traditional beer fermentation technology uses freely suspended yeast cells to ferment wort in a nonstirred batch reactor. These fermentations are very time-consuming. The traditional primary fermentation for lager beer takes approximately seven days with a subsequent secondary fermentation (maturation) of several weeks. However, the resulting beer has a well-balanced flavor profile that is very well accepted and appreciated by the consumer. Nowadays, large breweries use an accelerated fermentation scheme that is based on using a higher fermentation temperature and specific yeast strains, thus facilitating the speedy production of beer—approximately 15 days.

Narziss and Hellich (1971) developed one of the first well-described ICT processes for beer production. Yeast cells were immobilized in kieselguhr (which is widely used in the brewing industry as a filter aid), and a kieselguhr filter was used as bioreactor (called the "bio-brew bioreactor"). This process was characterized by a very low residence time of 2.5 h, but required the addition of viable yeast and a 7-d maturation period to reduce the high concentration of vicinal diketones in the green beer. Although this result looked very good, the bio-brew bioreactor gave no satisfying result overall because it contained a high amount of α-acetolactate; this was later optimized (Dembowski et al. 1993). An aerobic reactor was installed in front of the bio-brew reactor, the beer flow though the filter was optimized, and a cooling plate was installed in the filter reactor to control the temperature, thus increasing cell viability and improving the organolyptic qualities of beer. However, the concentration of the low-molecular-weight nitrogenous substances in the beer remained too high.

TABLE 12.16
ICT for the Main Beer Fermentation

Immobilization Method	Immobilization Matrix	Reactor Type
Entrapment	Calcium alginate beads	Stirred tank[a] + 2 packed bed[b]
Entrapment	Ceramic beads	Stirred tank[a] + 2 packed bed[b]
Entrapment	Calcium alginate microbeads	Gas lift
Entrapment	Silicon carbide rods	Cartridge loop reactor[b] + stirred tank[a]
Entrapment	Porous organic or glass beads	Packed bed
Entrapment	κ-Carrageenan beads	Gas lift
Entrapment	Chitosan beads	Fluidized bed
Entrapment	Calcium pectate beads	Gas lift
Entrapment	PVA beads	Gas lift
Adsorption	Woodchips (aspen, beech)	Packed bed
Adsorption	DEAE-cellulose	Packed bed
Adsorption	Gluten pellets	Fluidized bed
Adsorption	Spent grains	Gas lift

Source: Adapted from Willaert, R., *Handbook of Food Products Manufacturing*, pp. 443–506, 2007a. Hoboken, NJ: John Wiley & Sons; Willaert, R., *Fermentation Microbiology and Biotechnology*, 2nd ed., pp. 287–361, 2007b. Boca Raton, FL: CRC Press.

[a] Free cells.

[b] Immobilized cells.

Baker and Kirsop (1973) were the first to use heat treatment of green beer to considerably accelerate the chemical conversion of α-acetolactate to diacetyl. They designed a two-step continuous process. The first reactor was a packed-bed reactor, also containing kieselguhr as immobilization matrix, to perform the primary fermentation. The green beer was heated using a heating coil to accelerate the α-acetolactate conversion. It was next cooled before it entered a smaller packed-bed reactor to perform the secondary fermentation. Problems associated with this process were a gradual blocking of the packed bed and a changed beer flavor.

The design and optimization of an ICT process for primary and secondary fermentations remain a challenging task, although encouraging results have been obtained recently albeit only on laboratory and pilot scales (Table 12.16). The reasons why these ICT processes have not yet been adopted in the brewing industry include complexity of operations compared with batch processes, flavor problems (because of a lack of understanding and controllability of the changed metabolism), yeast viability, and carrier price. The altered metabolism and the knowledge to tune the metabolism to the desired flavor especially await further investigation.

12.6 CELL IMMOBILIZATION NANOBIOTECHNOLOGY

12.6.1 Nanobiotechnology

Nanotechnology is the ability to work at the atomic, molecular, and supramolecular levels (on a scale of ~1–100 nm) to understand, create, and use material structures, devices, and systems with fundamentally new properties and functions resulting from their small structure (Roco et al. 2000). Nanobiotechnology is defined as a field that applies the nanoscale principles and techniques to understand and transform biosystems (living or nonliving) and that uses biological principles and materials to create new devices and systems integrated from the nanoscale (Roco 2003). The biological and physical sciences share a common interest in small structures (the definition of "small" depends on the application but can range from 1 nm to 1 mm) (Whitesides 2003). Biological structures are

relatively large compared with structures in electronics and in physical nanosciences. A microbial cell is approximately 1 μm, a fungal cell is 5 μm, and a mammalian cell is 10 μm when rounded and 50 μm when fully spread in attached culture. A vigorous trade across the borders of these areas of science is developing around new materials and tools (largely from the physical sciences) and new phenomena (largely from the biological sciences). The physical sciences offer tools for synthesis and fabrication of devices for measuring the characteristics of cells and sub-cellular components and of materials useful in cell and molecular biology. Biology offers a window into the most sophisticated collection of functional nanostructures that exist.

Nanobiotechnology offers new solutions for the transformation of biosystems and provides a broad technological platform for applications in several areas, including bioprocessing in industry, molecular medicine, investigating the health effects of nanostructures in the environment, improving food products (food conservation), and improving human performance (Roco 2003).

Cell immobilization applications are directed to the control of the interaction of cells with its microenvironment (cell-substrate and cell–cell interaction) by using nanofabrication technologies. Some examples of applications of nanotechnology that are linked to cell immobilization are listed in Table 12.17. These technologies are emerging as powerful tools for tissue engineering and regenerative medicine. Precise control of the cellular environment provides new opportunities for understanding biochemical and mechanical processes responsible for changes in cell behavior; for

TABLE 12.17
Some Examples of Cell Immobilization Applications of Nanotechnology

Application	Reference
Surfaces patterned with self-assembled monolayers (SAMs) to guide cell attachment and growth. SAMs terminating in methyl groups are hydrophobic and adsorb proteins from solution. SAMs terminating in oligo(ethylene glycol) moieties resist the adsorption of proteins from solution. When cells attach to a surface, they do not, in general, attach to the surface directly: they attach to proteins adsorbed on the surface. The combination of SAMs with "printing" using elastomeric stamps ("soft lithography") or dip-pen nano-lithography, allows the surface to be patterned into regions to which cells attach and regions to which they do not.	Whitesides et al. 2001; Spatz, 2004; Falconnet et al. 2006; Shin 2007; Salaita et al. 2007; Zhao and Zhang 2007
Self-assembling peptide-based biomaterials for use as three-dimensional scaffolds for cell cultures, tissue engineering and regenerative medicine.	Gelain et al. 2007; Wei and Ma, 2008; Semino 2008; Kyle et al. 2009
Nanostructured polymer scaffolds for tissue engineering and regenerative medicine.	Barnes et al. 2007; Madu-rantakam et al. 2009;
The structural features of scaffolds are engineered to support cell adhesion.	Smith et al. 2009; Ayres et al. 2010; Kim et al. 2010
Engineering substrate mechanics to change the behavior of cells. The mechanical environment surrounding the cell and the intracellular cytoskeletal mechanics play an important role in determining the magnitude of these forces and the resulting changes in cellular behavior.	Gray et al. 2003; Patrito et al., 2007; Tzvetkova-Chevolleau et al. 2008
Dynamically changing the adhesive environment during cell culture to locally regulate cell adhesion: – using thermally responsive materials – using electroactive substrates	Cheng et al. 2004; da Silva et al., 2007; Nagase et al. 2009 Jiang et al. 2005; Yeo and Mrksich,2006
Engineering stem cell microenvironment to control stem cell differentiation. Two- and three-dimensional materials can be designed to control stem-cell fate *in vitro* and *in vivo* (see also Section 12.4.3).	Sands and Mooney 2007; Bratt-Leal et al. 2009; Guilak et al. 2009; Clause et al. 2010; Reilly and Engler 2010

example, the effects of cell shape on the anchorage dependence of cell growth (Chen et al. 1997; Théry et al. 2005), engineering stem cell microenvironment to control stem-cell fate *in vitro* and *in vivo* (see Section 12.4.3), and the effect of surface patterning for spatially controlling cell attachment (Table 12.17).

Several techniques are currently being used to create nanoscale topographies for cell scaffolding (Norman and Desai 2006). These techniques fall into two main categories: techniques that create ordered topographies and those that create unordered topographies. Electron beam lithography and photolithography are two standard techniques for creating ordered features. Polymer demixing, phase separation, colloidal lithography, and chemical etching are most typically used for creating unordered surface patterns.

12.6.2 Microscale Technologies in Cell Immobilization

Because of the micromolar scale of cells, microscale technologies are also potential tools for addressing some of the challenges in cell immobilization biotechnology (Khademhosseini et al. 2006). In particular, they are potentially powerful tools for addressing some of the challenges in tissue engineering. MEMS (microelectromechanical systems), which are an extension of the semiconductor ad microelectronics industries, can be used to control features at length scales from less than 1 μm to more than 1 cm (Whitesides et al. 2001). These techniques are compatible with cells and are now being integrated with biomaterials to facilitate fabrication of cell-material composites that can be used for tissue engineering. In addition, microsystems create new opportunities for the spatial and temporal control of cell growth and stimuli by combining surfaces that mimic complex biochemistries and geometries of the extracellular matrix with microfluidic channels that regulate transport of fluids and soluble factors.

Microfluidics involves the manipulation of very small fluid volumes, enabling the creation and control of micro- to nanoliter volume reactors. Microfluidic devices can be fabricated using soft lithography and rapid prototyping techniques (McDonald et al. 2000). Soft lithography refers to a collection of techniques for creating microstructures and nanostructures that are based on printing, molding, and embossing (Weibel et al. 2007). The advantages of soft lithography to fabricate microfluidic devices include low cost of production, the ease and speed of fabrication, the reduction in the amount of reagents consumed, and compatibility with cells. In rapid prototyping, a computer-aided design program is used to create a design for channels, which are printed at high resolution onto transparency film. The transparency film then serves as the photomask. The master molds are generated by using the photomask in contact lithography to produce a positive relief of photoresist. In replica molding, poly(dimethylsiloxane) (PDMS) is poured over the master and heat-cured to generate a negative replica of the master. The PDMS is then removed from the mold and sealed against a glass coverslip to form the device features and channels.

Microsystems can be integrated with bioanalytic microsystems resulting in multifunctional platforms for basic biological insights into cells and tissues, as well as for cell-based sensors with biochemical, biomedical, and environmental functions. Highly integrated microdevices show great promise for basic biomedical and pharmaceutical research (El-Ali et al. 2006; Wlodkowic et al. 2009). Much cell-based microsystem research takes place under "lab-on-a-chip" or "micro-total-analysis-system" (μTAS) framework that seeks to create microsystems incorporating several steps of an assay into a single system (Dittrich and Manz 2006; Haeberle and Zengerle 2007; Le Gac and van den Berg 2010). Integrated microfluidic devices perform rapid and reproducible measurements on small sample volumes while eliminating the need for labor-intensive and potentially error-prone laboratory manipulations. Microscale technologies can miniaturize assays and facilitate high-throughput experimentation and therefore provide a tool for screening libraries. Robotic spotters capable of dispensing and immobilizing nanoliters of material have been used to fabricate cellular microarrays in which cells can be screened in a high-throughput manner (Hart et al. 2009). Recently, dip-pen nanolithography (DPN) has been used to immobilize motile bacterial

cells in a cellular microarray (Nyamjav et al. 2010). DPN is a scanning probe microscopy-based nanofabrication technique that uniquely combines direct-write soft-matter compatibility with the high resolution and registry of atomic force microscopy (AFM) (see Section 12.6.3), which makes it a powerful tool for depositing soft and hard materials in the form of stable and functional architectures on various surfaces (Salaita et al. 2007).

12.6.3 Microscopic Techniques for Nanoscale Imaging and Manipulation

We use microscopy to see objects in more detail. The best distance that one can resolve with optical instruments, disregarding all aberrations, is approximately 0.5 times the wavelength of light, or on the order of 250 nm with visible radiation. High-resolution microscopy techniques that are used for nanoimaging and nanoscale characterization have been developed. They can be divided into three categories: optical microscopes, scanning probe microscopes (SPMs), and electron microscopes. Recently developed microscopy-based technologies can also be used to control and manipulate objects at the nanoscale. The unique imaging and manipulation properties of AFMs have prompted the mergence of several probe-based nanolithographies (Wouters and Schubert 2004; Garcia et al. 2006). Scanning-probe-based patterning techniques, such as dip-pen lithography, local force-induced patterning, and local-probe oxidation-based techniques are highly promising because of their relative ease and widespread availability. The latter of these is especially interesting because of the possibility of producing nanopatterns for a broad range of chemical and physical modification and functionalization processes.

12.6.3.1 Electron Microscopy

Microscopes consist of an illumination source, a condenser lens to converge the beam on the sample, an objective lens to magnify the image, and a projector lens to project the image onto an image plane, which can be photographed or stored. In electron microscopes, the wave nature of the electron is used to obtain an image. There are two important forms of electron microscopy: scanning electron microscopy (SEM) and transmission electron microscopy (TEM). Both use electrons as the source for illuminating the sample. The lenses used in electron microscopes are electromagnetic lenses.

For high-resolution surface investigations, two commonly used techniques are atomic force microscopy and scanning electron microscopy SEM. The operation of the SEM consists of applying a voltage between a conductive sample and filament, resulting in electron emission from the filament to the sample. This occurs in a vacuum environment. The electrons are guided to the sample by a series of electromagnetic lenses in the electron column. The resolution and depth of field of the image are determined by the beam current and the final spot size. The electrons interact with the sample within a few nanometers to several microns of the surface, depending on the beam parameters and sample type.

Along with the secondary electron emission, which is used to form a morphological image of the surface in the SEM, several other signals are emitted as a result of the electron beam impinging on the surface. Each of these signals carries information about the sample that provides clues to its composition. Two of the most commonly used signals for investigating composition are x-rays and backscattered electrons. X-ray signals are commonly used to provide elemental analysis. The percentage of beam electrons that become backscattered electrons has been found to be dependent on the atomic number of the material, which makes it a useful signal for analyzing the material composition.

Electron microscopy is conducted in a vacuum environment. This is a disadvantage to study hydrated samples, like attached/immobilized cells and some immobilization materials (i.e., hydrogels). To image poorly conductive surfaces without sample charging may require conductive coatings or staining, which may alter or obscure the features of interest; or it may require low-voltage operation or an environmental chamber, which may sacrifice resolution. Recently, an electron microscopy technique was described for imaging whole cells in liquid that offers nanometer spatial resolution and a high imaging speed using a scanning transmission electron microscope (STEM) (de Jonge

et al. 2009; Peckys et al. 2009). The cells were placed in buffer solution in a microfluidic device with electron-transparent windows inside of the vacuum of the electron microscope.

In TEM, the transmitted electrons are used to create an image of the sample. Scattering occurs when the electron beam interacts with matter. Scattering can be elastic (no energy change) or inelastic (energy change). Elastic scattering can be coherent and incoherent (with and without phase relationship). TEMs with resolving powers in the vicinity of 1 Å are now common. A relative recent electron microscopy technique that can be used to study immobilized cells at the nanoscale is electron tomography.

Electron tomography (ET) is the most widely applicable method for obtaining three-dimensional information by electron microscopy (Baumeister et al. 1999; Downing et al. 2007; Stahlberg and Walz 2008). A tomogram is a three-dimensional volume computed from a series of projection images that are recorded as the object in question is tilted at different orientations. ET has the potential to fill the gap between global cellular localization and the detailed three-dimensional molecular structure because it can reveal the localization within the cellular context at true molecular resolution and the shapes and three-dimensional architecture of large molecular machines. It can also reveal the interaction of individual proteins and protein complexes with other cellular components, such as DNA and membranes. A recent development is cryo-electron tomography (cryo-ET), which allows the visualization of cellular structures under close-to-life conditions (Lucić et al. 2008). Rapid freezing followed by the investigation of the frozen-hydrated samples avoids artifacts notorious to chemical fixation and dehydration procedures. Furthermore, the biological material is observed directly, without heavy metal staining, avoiding problems in interpretation caused by unpredictable accumulation of staining material. Consequently, cryo-ET of whole cells has the advantage that the supramolecular architecture can be studied in unperturbed cellular environments.

12.6.3.2 Atomic Force Microscopy

Scanning probe microscopies are a family of instruments that are used to measure properties of surfaces, including AFMs and STMs. The main feature that all scanning probe microscopies have in common is that the measurements are performed with a sharp probe operating in the near field (i.e., scanning over the surface while maintaining a very close spacing to the surface). The STM, invented in the early 1980s by Binnig and Rohrer (1982), was the first to produce real space images of atomic arrangements on flat surfaces. The development of the STM arose from an interest in the study of the electrical properties of thin insulating layers. This led to an apparatus in which the probe-surface separation was monitored by measuring electron tunneling between a conducting surface and a conducting probe. A few years later, Binnig and colleagues (1986) announced the birth of the second member of the SPM family, the AFM (also known as the scanning probe microscopy, SPM). Numerous variations of these techniques have been developed later on.

Atomic force microscopy is extensively used for imaging surfaces ranging from micro- to nanometer scales, with the objective of visualizing and characterizing surface textures and shapes (Kada et al. 2008). It has evolved into an imaging method that yields structural details of biological samples such as proteins, nucleic acids, membranes, and cells in their native environment. AFM is a unique technique for providing subnanometer resolution at a reasonable signal-to-noise ratio under physiological conditions. It complements EM by allowing visualization of biological samples in buffers that preserve their native structure over extended time periods. Unlike EM, atomic force microscopy yields three-dimensional maps with an exceptionally good vertical resolution (<1 nm). Additionally, the measurement of mechanical forces at the molecular level provides detailed insights into the function and structure of biomolecular systems. Inter- and intramolecular interactions can be studied directly at the molecular level.

12.6.3.3 Light Microscopy

Since the earliest examination of cellular structures, biologists have been fascinated by observing cells using a light microscope. Being able to observe processes as they happen by light microscopy

adds a vital extra dimension to our understanding of cell behavior and function (Stephens and Allan 2003). Microscopy has evolved to provide not only quantitative images but also a significant capability to perturb structure-function relationships in cells. These advances have been especially useful in the study of cell adhesion and migration: molecular interactions and dynamics, local perturbation of actin-based structures, and the traction forces exerted by motile cells on substrates can be measured (Roy et al. 2002).

Recent advances in fluorescence microscopy allowed imaging of structures at extremely high resolutions (Gitai 2009). The past decade witnessed an explosion of fluorescence-microscopy-based approaches to image protein dynamics and interactions (Fricker et al. 2006), including fluorescence recovery after photobleaching (FRAP) or photoactivation using photoconvertible fluorescent proteins to assay protein mobility and maturation in cells (Lippincott-Schwartz et al. 2001) and Förster resonance energy transfer (FRET) to monitor physical intra- or intermolecular associations in space and time (Jares-Erijman and Jovin 2003; Roy et al. 2008).

Despite the advantages of standard fluorescence microscopy, ultrastructural imaging is not possible because of a resolution limit set by the diffraction of light. Therefore, the maximal spatial resolution of standard optical microscopy is approximately 200 nm, which is more than an order of magnitude higher than the length of cellular molecules. Several approaches have been used to break this diffraction limit (Table 12.18); for example, by exploiting the distribution of fluorescence intensity from a single molecule. When imaged, a fluorophore behaves as a point source with an Airy disc point spread function. The center of mass of the function, and therefore the position of the molecule, can be obtained by performing a least-squares fit of an appropriate function to the measured fluorescence intensity profile of the spot (Thompson et al. 2002). With a sufficient number of photons, these methods can provide a localization of 1–2 nm, allowing the measurement of distances on the scale of individual proteins. Single-molecule detection offers new possibilities for obtaining subdiffraction-limit spatial resolution (Sako 2006; Walter et al. 2008; Dehmelt and Bastiaens 2010).

12.6.3.4 Force Microscopy

The ability to apply force to or measure forces generated by multiple (cell adhesion) up to a single biopolymer opens up new avenues for single cell interaction (Helenius et al. 2008) and manipulating biomolecules and interrogating cellular processes (Walter et al. 2008). Three forms of force microscopy are commonly used to study single molecules: optical tweezers, magnetic tweezers, and atomic force microscopy. An important advantage of single-molecule techniques is that they do not suffer from problems associated with population averaging inherent in ensemble measurements. Rare or transient phenomena that would otherwise be obscured by averaging can be resolved provided that the measurement technique has the required resolution and that the events can be captured often enough to ensure that they are not artifactual (Neuman and Nagy 2008; Knight 2009).

Optical tweezers use light to levitate a transparent bead of distinct refractive index. The trapped bead is suspended at the waist of the focused (typically infrared) laser beam. The displacement of the bead from the focal center results in a proportional restoring force and can be measured by interferometry or back-focal plane detection. A single biopolymer can be suspended between two beads or a bead and a motorized platform. Magnetic tweezers use an external, controllable magnetic field to exert force and/or torque on a superparamagnetic bead that is tethered to a surface via a single molecule. Atomic force microscopy-based force spectroscopy exerts pulling forces on a single attached molecule by retraction of the tip in the z direction (perpendicular to the x-y scanning plane). Cantilever bending is detected by the deflection of a laser beam onto a position-sensitive detector such as a quadrant photodiode. A piezoelectric actuator stage is used to control the positioning of the sample relative to the tip. Atomic force microscopy-based force spectroscopy is also used to study single-cell interactions (cell-cell and cell-substrate adhesion).

TABLE 12.18
Super-Resolution Optical Microscopy Techniques

Technique	Description	Spatial Resolution	Time Scale	Reference
Fluorescence imaging with one-nanometer accuracy (FIONA)	Localizes and tracks single-molecule emitters by finding the center of their diffraction-limited point-spread function (PSF).	~1.5 nm	~0.3 ms	Yildiz et al. 2003
Single-molecule high-resolution colocalization (SHREC)	Two-color version of FIONA. Two fluorescent probes with different spectra are imaged separately and then localized and mapped onto the plane of the microscope.	< 10 nm	~1 s per frame	Churchman et al. 2005
Single-molecule high-resolution imaging with photobleaching (SHRImP)	Uses the strategy that upon photobleaching of two or more closely spaced identical fluoro-phores their position is sequentially determined by FIONA starting from the last bleached fluorophore.	~5 nm	~0.5 s per frame	Gordon et al. 2004
Nanometer-localized multiple single-molecules (NALMS)	Uses a similar principle as SHRImP to measure distances between identical fluo- rescent probes that overlap within a diffraction-limited spot.	~8 nm	~1 s per frame	Qu et al. 2004
Photoactivatable localization microscopy (PALM)	Serially photoactivates and photodeactivates many sparse subsets of photoactivatable fluoro-phores to produce a sequence of images that are combined into a super-resolution composite	~2 nm	~1 min	Betzig et al. 2006
PALM with independently running acquisition (PALMIRA)	Records nontriggered spontaneous off-on-off cycles of photoswitchable fluorophores without synchronizing the detector to reach faster acquisition.	~50 nm	~2.5 min	Egner et al. 2007
Single particle tracking PALM	Combines PALM with live-cell single fluorescent particle tracking.			Manley et al. 2008
Stimulated emission depletion (STED)	Reduces the excitation volume below that dictated by the diffraction limit, by coaligning one beam of light capable of fluorophore excitation with another that induces de-excitation by stimulated emission	~16 nm	~10 min	Hell and Wichmann, 1994
Stochastic optical reconstruction microscopy (STORM)	Small sub-populations of photoswitchable fluorophores are turned on and off using light of different colors, permitting the localization of single molecules. Repeated activation cycles produce a composite image of the entire sample.	< 0 nm	~ min	Rust et al. 2006

12.6.4 Case Study: Cell–Cell Adhesion Nanobiomechanics

Various immobilization technologies require cell-substrate and/or cell-cell adhesion. Cell adhesion in general is commonly defined as the binding of a cell to a substrate, which can be another cell, a surface, or an organic matrix. The adhesion of a biological cell involves complex couplings at the level of cellular biochemistry, structural mechanics, and/or surface bonding. The interactions are dynamic and act through association and dissociation of bonds between very large molecules at rates that change considerably under stress. Combining molecular cell biology with single-molecule force spectroscopy provides a powerful tool for exploring the complexity of cell adhesion; that is, how cell signaling processing strengthens adhesion bonds and how forces applied to cell-surface bonds act on intracellular sites to catalyze chemical processes or switch molecular interactions on and off.

Molecular and genetic approaches have identified various cell adhesion molecules (CAMs) with their ligand specificities and have determined the processes in which they are involved. However, the molecular mechanisms by which CAMs regulate different types of adhesion are open debates (Ludwig et al. 2008). To understand cell adhesion, the vast amount of qualitative data that is available must be augmented with quantitative data of the biophysics of adhesion. Historically, the strength of cell adhesion to a substrate has been studied using simple washing assays (Klebe 1974). Washing assays have proven to be versatile and useful in identifying CAMs, important extra-cellular matrix components, and other proteins that are involved in various forms of cell adhesion. To estimate the force to which cells are subjected, various assays that are based on the regulated flow of media have been implemented, including flow chamber methods (Kaplanski et al. 1993). However, these assays only give estimates of adhesion forces because the shear force that is exerted on the cells depends on parameters such as cell size, cell shape, and how the cell is attached to the substrate. Recently, single-cell and single-molecule techniques have been developed to obtain more controlled and quantitative measurements of adhesion strength.

Single-cell force spectroscopy assays on living cells have been applied to measure the strength of cell adhesion down to single-molecule levels (Helenius et al. 2008). A living cell can be attached to a tipless cantilever of an AFM and the interacting partner (molecule or cell) on a substrate-coated surface. Alternatively, the tip is functionalized with the interacting molecule and the interaction with the attached living cell on a surface is monitored. Atomic force microscopy-based force spectroscopy with a cantilever-bound cell can be used to investigate cell–cell and cell–matrix interactions. The approach and withdrawal of this cell to and from its surface can be precisely controlled by parameters such as applied force, contact time, and pulling speed by benefiting from the AFM's high-force sensitivity and spatial resolution. The data collected in these experiments include information on repulsive forces before contact, cell deformability, maximum unbinding forces, individual unbinding events, and the total work required to remove a cell from the surface. Force spectroscopy can identify cell subpopulations and characterize the regulation of cell adhesion events with single-molecule resolution (Taubenberger et al. 2007).

Examples of using atomic force microscopy-based force spectroscopy to study cell adhesion include single *S. cerevisiae* cells that have been attached to a tipless AFM cantilever and used as a living single-cell probe to perform single-cell force spectroscopy (Kang and Elimelech 2009). The contributions of several galectin family members in cell-substratum adhesion of Madin–Darby canine kidney cells have been studied using quantitative single cell atomic force microscopy-based force spectroscopy (Friedrichs et al. 2007). Optical tweezers have been used to orient uropathogenic *Escherichia coli* (which present a FimH lectin at the tip of their type 1 pilus) relative to a mannose-presenting surface, and thus limit the number of points of attachment (Liang et al. 2000). It was possible to quantify the forces required to break a single interaction between pilus and mannose groups.

Yeast cell flocculation is an example of self-aggregation of cells. The Flo proteins Flo1p, Lg-Flo1p, Flo5p, Flo9p, and Flo10p are lectins because they have an affinity toward specific sugar

moieties (Goossens and Willaert 2010). Recently, atomic force microscopy-based force spectroscopy has been used to directly measure the forces involved in single carbohydrate-lectin interactions (Touhami et al. 2003). Atomic force microscopy-based force spectroscopy has been used to determine the unbinding force of oligoglucose carbohydrates and Lg-Flo1p present on the cell wall of industrial brewer's yeast strains. Atomic force microscopy force probes functionalized with carboxymethyl-amylose were used to record force-distance curves on living cells. Flocculation cells showed adhesion forces of 121 ± 53 pN. Unbinding forces of other lectin-carbohydrate interactions range from 30 to 200 pN.

SUMMARY

Selections of immobilization matrix and method as well as bioreactor type and design are usually interrelated.

For optimization, knowledge of fluid dynamics and external/internal mass transfer is a good starting point.

The use of mathematical models to quantitatively describe and analyze the behavior of immobilized cells is an important component; steady-state, pseudo-steady state, and dynamic models are discussed.

The physiology of living cells upon immobilization can be changed because they are present in a different microenvironment compared with free living cells.

Different physiological effects due to the changed chemical composition and/or the physical interaction between the matrix material and immobilized bacterial, fungal, and stem cells are discussed.

The production of beer using immobilized cell technology has been described by way of a case study.

Cell immobilization has been implemented for the production of alcohol-free lager, flavor maturation of green beer, and continuous main stream fermentation.

The use of cell immobilization technology has been successful at the industrial level in the production of biological reagents from animal cell cultures and tissue engineering. On the other hand, the full potential of cell immobilization for the production of biopharmaceuticals using microbial cells has yet to be fully realized and exploited. A few reasons are that the biopharmaceutical (fermentation) industry is very conservative and reluctant to replace the existing robust systems using free cells with this new technology; an immobilized cell system is more complex and means a higher risk; and validation, regulatory, and health and safety issues are costly and time-consuming.

Successful industrial/commercial fermentation processes/products that are based on immobilized living cells have recently been introduced. Examples include the production of alcohol-free beer, stabilized probiotic products, protective bacterial cultures for meat products, and bioethanol as well as wastewater treatment.

For the production of low-added-value fermentation products, the added cost of immobilization techniques and in some cases higher complexity *versus* free cell culture will not be justified unless the volumetric productivity is strongly increased.

Future research will increase our understanding of these "complex" systems and will lower the barrier for exploitation on an industrial/commercial and medical scale. Nanobiotechnology techniques will be applied more and more to characterize these complex systems and used to create nanoscale topographies for cell immobilization.

REFERENCES

Argirakos, G., K. Thayanithy, and D.A. John Wase. 1992. Effect of immobilization on the production of α-amylase by an industrial strain of *Bacillus. J Chem Technol Biotechnol* 53:33–8.

Atala, A., R. Lanza, J. Thomson, and R. Nerem, eds. 2008. Principles of regenerative medicine. Academic Press, Burlington, MA.

Axelsson, A., and B. Westrin. 1991. Application of the diffusion cell for the measurement of diffusion in gels. *Chem Eng Sci* 46:913–915.

Ayres, C.E., B.S. Jha, S.A. Sell, G.L. Bowlin, and D.G. Simpson. 2010. Nanotechnology in the design of soft tissue scaffolds: Innovations in structure and function. *Wiley Interdiscip. Rev Nanomed Nanobiotechnol* 2:20–34.

Baker, D.A., and B.H. Kirsop. 1973. Rapid beer production and conditioning using a plug fermentor. *J Inst Brew* 79:487–94.

Barnes, C.P., S.A. Sell, E.D. Boland, D.G. Simpson, and G.L. Bowlin 2007. Nanofiber technology: Designing the next generation of tissue engineering scaffolds. *Adv Drug Deliv Rev* 59:1413–33.

Baron, G.V., and R.G. Willaert. 2004. Cell immobilization in pre-formed porous matrices. In Nedovic, V., and Willaert, R., eds., *Fundamentals of Cell Immobilization Biotechnology*, pp. 229–44. Dordrecht, The Netherlands: Kluwer Academic Publishers.

Baron, G.V., R.G. Willaert, and L. De Backer. 1996. Immobilized cell reactors. In Willaert, R.G., Baron, G.V., and De Backer, L. eds., *Immobilized Living Cell Systems: Modeling and Experimental Methods*, pp. 67–95. Chichester, United Kingdom: John Wiley & Sons.

Baumeister, W., R. Grimm, and J. Walz. 1999. Electron tomography of molecules and cells. *Trends Cell Biol* 9:81–5.

Betzig, E., G.H. Patterson, R. Sougrat, O.W. Lindwasser, S. Olenych, J.S. Bonifacino, M.W. Davidson, J. Lippincott-Schwartz, and H.F. Hess. 2006. Imaging intracellular fluorescent proteins at nanometer resolution. *Science* 313:1642–5.

Binnig, G., and H. Rohrer. 1982. Scanning tunneling microscopy. *Helv Phys Acta* 55:726–35.

Binnig, G., C.F. Quate, and C. Gerber. 1986. Atomic force microscope. *Phys Rev Lett* 56:930–3.

Bratt-Leal, A.M., R.L. Carpenedo, and T.C. McDevitt. 2009. Engineering the embryoid body microenvironment to direct embryonic stem cell differentiation. *Biotechnol Prog* 25:43–51.

Brito, L.C., A.M. Vieira, J.G. Leitão, I. Sá-Correia, J.M. Novais, and J.M.S. Cabral. 1990. Effect of the aqueous soluble components of the immobilization matrix on ethanol and microbial exopolysaccharides production. In de Bont J.A.M., Visser J., Mattiasson B., Tramper J. eds., *Physiology of Immobilized Cells,* pp. 399–404. Amsterdam, The Netherlands: Elsevier.

Brown, C.D., and A.S. Hoffman. 2002. Modification of natural polymers: chitosan. In Atala, A., and Lanza, R.P., ed., *Methods of Tissue Engineering,* pp. 565–74. San Diego: Academic Press.

Buitelaar, R.M., A.C. Hulst, and J. Tramper. 1990. Cell immobilization in thermogels: Activity retention after gelling in various organic solvents. In de Bont, J.A.M., Visser, J., Mattiasson, B., and Tramper, J. eds., *Physiology of Immobilized Cells*, pp. 205–8. Dordrecht, The Netherlands: Elsevier.

Cachon, R., and C. Divies. 1993. Localization of *Lactococcus lactis* ssp. *lactis* bv. *diacetylactis* in alginate gel beads affects biomass density and synthesis of several enzymes involved in lactose and citrate metabolism. *Biotechnol Technol* 7:453–6.

Camelin, I., C. Lacroix, C. Paquin, H. Prévost, R. Cachon, and C. Divies. 1993. Effect of chelatants on gellan gel rheological properties and setting temperature for immobilization of living bifidobacteria. *Biotechnol Prog* 9:291–7.

Carenza, M., and F.M. Veronese. 1994. Entrapment of biomolecules into hydrogels obtained by radiation-induced polymerization. *J Control Rel* 29:187–93.

Chaikof, E.L. 1999. Engineering and material considerations in islet cell transplantation. *Ann Rev Biomed Eng* 1:103–27.

Chen, K.C., and Y.F. Lin. 1994. Immobilization of microorganisms with phosphorylated polyvinyl alcohol (PVA) gel. *Enzyme Microb Technol* 16:79.

Chen, C.S., M. Mrksich, S. Huang, G.M. Whitesides, and D.E. Ingber. 1997. Geometric control of cell life and death. *Science* 276:1425–8.

Cheng, X., Y. Wang, Y. Hanein, K.F. Böhringer, and B.D. Ratner. 2004. Novel cell patterning using microheater-controlled thermoresponsive plasma films. *J Biomed Mater Res A* 70:159–68.

Churchman, L.S., Z. Okten, R.S. Rock, J.F. Dawson, and J.A. Spudich. 2005. Single molecule high-resolution colocalization of Cy3 and Cy5 attached to macromolecules measures intramolecular distances through time. *Proc Natl Acad Sci USA* 102:1419–23.

Clause, K.C., L.J. Liu, and K. Tobita. 2010. Directed stem cell differentiation: The role of physical forces. *Cell Commun Adhes* 17:48–54.

Dale, M.C., A. Eagger, and M.R. Okos. 1994. Osmotic inhibition of free and immobilized *K. marxianus* anaerobic growth and ethanol productivity in whey permeate concentrate. *Process Biochem* 29:535–44.

da Silva, R.M., J.F. Mano, and R.L. Reis. 2007. Smart thermoresponsive coatings and surfaces for tissue engineering: Switching cell-material boundaries. *Trends Biotechnol* 25:577–83.

Dawson, E., G. Mapili, K. Erickson, S. Taqvi, and K. Roy. 2008. Biomaterials for stem cell differentiation. *Adv Drug Deliv Rev* 60:215–28.

de Alteriis, E., P.M. Alepuz, F. Estruch, and P. Parascandola. 1999. Clues to the origin of high external invertase activity in immobilized growing yeast: Prolonged *SUC2* transcription and less susceptibility of the enzyme to endogenous proteolysis. *Can J Microbiol* 45:413–7.

Dehmelt, L., and P.I. Bastiaens. 2010. Spatial organization of intracellular communication: Insights from imaging. *Nat Rev Mol Cell Biol* 11:440–52.

de Jonge, N., D.B. Peckys, G.J. Kremers, and D.W. Piston. 2009. Electron microscopy of whole cells in liquid with nanometer resolution. *Proc Natl Acad Sci USA* 106:2159–64.

Dembowski, K., L. Narziss, and H. Miedaner. 1993. Technologisch optimierte Bierherstellung im Festbettfermentor bei sehr kurzer Produktionszeit. *Proceedings 24th European Brewery Convention Congress*, Oslo, Norway; pp. 299–306.

Di Martino, A., M. Sittinger, and M.V. Risbud. 2005. Chitosan: A versatile biopolymer for orthopedic tissue-engineering. *Biomaterials* 26:5983–90.

Dittrich, P.S., and A. Manz. 2006. Lab-on-a-chip: Microfluidics in drug discovery. *Nat Rev Drug Discov* 5:210–8.

Doran, P.M. 1995. *Bioprocess Engineering Principles*. London: Academic Press.

Downing, K.H., H. Sui, and M. Auer. 2007. Electron tomography: A 3D view of the subcellular world. *Anal Chem* 79:7949–57.

Egner, A., C. Geisler, C. von Middendorff, H. Bock, D. Wenzel, R. Medda, M. Andresen, A.C. Stiel, S. Jakobs, C. Eggeling, A. Schönle, and S.W. Hell. 2007. Fluorescence nanoscopy in whole cells by asynchronous localization of photoswitching emitters. *Biophys J* 93:3285–90.

El-Ali, J., P.K. Sorger, and K.F. Jensen. 2006. Cells on chips. *Nature* 442:403–11.

Epstein, N. 1989. On tortuosity and the tortuosity factor in flow and diffusion through porous media. *Chem Eng Sci* 44:777–9.

Falconnet, D., G. Csucs, H.M. Grandin, and M. Textor. 2006. Surface engineering approaches to micropattern surfaces for cell-based assays. *Biomaterials* 27:3044–63.

Feng, M., and M.V. Sefton. 2002. Microencapsulation methods: Polyacryaltes. In Atala, A., and Lanza, R.P. eds., *Methods of Tissue Engineering*, pp. 825–39. San Diego: Academic Press.

Fortin, C., and J.C. Vuillemard. 1990. Elucidation of the mechanism involved in the regulation of protease production by immobilized *Myxococcus xanthus* cells. *Biotechnol Lett* 12:913.

Freed, L.E., J.C. Marquis, G. Vunjak-Novakovic, J. Emmanual, and R. Langer. 1994. Composite of cell-polymer cartilage implants. *Biotechnol Bioeng* 43:605–14.

Fricker, M., J. Runions, and I. Moore. 2006. Quantitative fluorescence microscopy: From art to science. *Annu Rev Plant Biol* 57:79–107.

Friedrichs, J., J.M. Torkko, J. Helenius, T.P. Teräväinen, J. Füllekrug, D.J. Muller, K. Simons, and A. Manninen. 2007. Contributions of galectin-3 and -9 to epithelial cell adhesion analyzed by single cell force spectroscopy. *J Biol Chem* 282:29375–83.

Garcia, R., R.V. Martinez, and J. Martinez. 2006. Nano-chemistry and scanning probe nanolithographies. *Chem Soc Rev* 35:29–38.

Gelain, F., A. Horii, and S. Zhang. 2007. Designer self-assembling peptide scaffolds for 3-d tissue cell cultures and regenerative medicine. *Macromol Biosci* 7:544–51.

Gemeiner, P., L. Texova-Benkova, F. Svec, and O. Norrlöw. 1994. Natural and synthetic carriers suitable for immobilization of viable cells, active organelles, and molecules. In Veliky, I.A., and McLean, R.J.C., eds., *Immobilized Biosystems: Theory and Practical Applications,* pp. 1–128. Glasgow, United Kingdom: Blackie Academic & Professional.

Gherardini, L., C.M. Cousins, J.J. Hawkes, J. Spengler, S. Radel, H. Lawler, B. Devcic-Kuhar, M. Groschl, W.T. Coakley, and A.J. McLoughlin 2005. A new immobilization method to arrange particles in a gel matrix by ultrasound standing waves. *Ultrasound Med Biol* 31:261–72.

Gilson, C., and A. Thomas. 1995. Ethanol production by alginate immobilized yeast in a fluidised bed bioreactor. *J Chem Technol Biotechnol* 62:38–45.

Gitai, Z. 2009. New fluorescence microscopy methods for microbiology: Sharper, faster, and quantitative. *Curr Opin Microbiol* 12:341–6.

Goossens, K.V.Y., and R.G. Willaert. 2010. Flocculation protein structure and cell-cell adhesion mechanism in *Saccharomyces cerevisiae*. *Biotechnol Lett* 32:1571–85.

Gordon, M.P., T. Ha, and P.R. Selvin. 2004. Single-molecule high-resolution imaging with photobleaching. *Proc Natl Acad Sci USA* 101:6462–5.

Gray, D.S., J. Tien, and C.S. Chen. 2003. Repositioning of cells by mechanotaxis on surfaces with micropatterned Young's modulus. *J Biomed Mater Res A* 66:605–14.

Green, C.B., G. Cheng, J. Chandra, P. Mukherjee, M.A. Ghannoum, and L.L. Hoyer. 2004. T-PCR detection of *Candida albicans ALS* gene expression in the reconstituted human epithelium (RHE) model of oral candidiasis and in model biofilms. *Microbiol* 150:267–75.

Guilak, F., D.M. Cohen, B.T. Estes, J.M. Gimble, W. Liedtke, and C.S. Chen. 2009. Control of stem cell fate by physical interactions with the extracellular matrix. *Cell Stem Cell* 5:17–26.

Gutowska, A., B. Jeong, and M. Jasionowski. 2001. Injectable gels for tissue engineering. *Anat Rec* 263:342–349.

Haeberle, S., and R. Zengerle. 2007. Microfluidic platforms for lab-on-a-chip applications. *Lab Chip* 7:1094–1110.

Hart, T., A. Zhao, A. Garg, S. Bolusani, and E.M. Marcotte. 2009. Human cell chips: Adapting DNA microarray spotting technology to cell-based imaging assays. *PLoS One* 4:e7088.

Helenius, J., C.P. Heisenberg, H.E. Gaub, and D.J. Muller. 2008. Single-cell force spectroscopy. *J Cell Sci* 121:1785–91.

Hell, S.W., and J. Wichmann. 1994. Breaking the diffraction resolution limit by stimulated emission: Stimulated-emission-depletion fluorescence microscopy. *Opt Lett* 19:780–2.

Hoffman, A.S. 2004. Applications of "smart polymers" as biomaterials. In Ratner, B.D., Hoffman, A.S., Schoen, F.J., and Lemons, J.E. eds., *Biomaterials Science—An Introduction to Materials in Medicine*, pp. 107–15. London: Elsevier Academic Press.

Hunkeler, D. 1997. Polymers for bioartificial organs. *Trends Polymer Sci* 5:286–293.

Jares-Erijman, E.A., and T.M. Jovin. 2003. FRET imaging. *Nat Biotechnol* 21:1387–95.

Jiang, X., D.A. Bruzewicz, A.P. Wong, M. Piel, and G.M. Whitesides. 2005. Directing cell migration with asymmetric micropatterns. *Proc Natl Acad Sci USA* 102:975–8.

Kada, G., F. Kienberger, and P. Hinterdorfer. 2008. Atomic force microscopy in bionanotechnology. *NanoToday* 3:12–9.

Kang, S., and M. Elimelech. 2009. Bioinspired single bacterial cell force spectroscopy. *Langmuir* 25:9656–9.

Kaplanski, G., C. Farnarier, O. Tissot, A. Pierres, A.M. Benoliel, M.C. Alessi, S. Kaplanski, and P. Bongrand. 1993. Granulocyte-endothelium initial adhesion. Analysis of transient binding events mediated by E-selectin in a laminar shear flow. *Biophys J* 64:1922–33.

Khademhosseini, A., Langer, R.J. Borenstein, and J.P. Vacanti. 2006. Microscale technologies for tissue engineering and biology. *Proc Natl Acad Sci USA* 103:2480–2487.

Kikuchi, K.I., T. Sugarawa, and H. Ohashi. 1988. Correlation of liquid-side mass transfer coefficient based on the new concept of specific power group. *Chem Eng Sci* 43:2533–40.

Kim, M.H., M. Kino-oka, and M. Taya. 2010. Designing culture surfaces based on cell anchoring mechanisms to regulate cell morphologies and functions. *Biotechnol Adv* 28:7–16.

Klausen, M., A. Heydorn, P. Ragas, L. Lambertsen, A. Aaes-Jørgensen, S. Molin, and T. Tolker-Nielsen. 2003. Biofilm formation by *Psudomonas aeruginosa* wild type, flagella and type IV pili mutants. *Mol Microbiol* 48:1511–24.

Klebe, R.J. 1974. Isolation of a collagen-dependent cell attachment factor. *Nature* 250:248–51.

Klinkenberg, G., K.Q. Lystad, D.W. Levine, and N. Dyrset. 2001. pH-controlled cell release and biomass distribution of alginate-immobilized *Lactococcus lactis* subsp. *lactis*. *J Appl Microbiol* 91:705–14.

Knight, A.E., ed. 2009. *Single Molecule Biology*. San Diego: Academic Press.

Kyle, S., A. Aggeli, E. Ingham, and M.J. McPherson. 2009. Production of self-assembling biomaterials for tissue engineering.*Trends Biotechnol* 27:423–433.

Lacik, I. 2004. Polyelectrolyte complexes for microcapsule formation. In Nedovic, V., and Willaert, R. eds., *Fundamentals of Cell Immobilization Biotechnology*, pp. 103–20. Dordrecht, The Netherlands: Kluwer Academic Publishers.

Le Gac, S., and A. van den Berg. 2010. Single cells as experimentation units in lab-on-a-chip devices. *Trends Biotechnol* 28:55–62.

Liang, M.N., S.P. Smith, S.J. Metallo, I.S. Choi, M. Prentiss, and G.M. Whitesides. 2000. Measuring the forces involved in polyvalent adhesion of uropathogenic *Escherichia coli* to mannose-presenting surfaces. *Proc Natl Acad Sci USA* 97:13092–6.

Li, F., and S.P. Palecek 2003. *EAP1*, a *Candida albicans* gene involved in binding human epithelial cells. *Eukaryot Cell* 2:1266–73.

Lijun, X., W. Bochu, L. Zhimin, D. Chuanren, W. Qinghong, and L. Liu. 2005. Linear alkyl benzene sulphonate (LAS) degradation by immobilized *Pseudomonas aeruginosa* under low intensity ultrasound. *Colloids Surf B Biointerfaces* 40:25–29.

Lim, F., and R.D. Moss 1981. Microencapsulation of living cells and tissues. *J Pharm Sci* 70:351–4.

Lim, F., and A.M. Sun 1980. Microencapsulated islets as a bioartificial endocrine pancreas. *Science* 210:908–10.

Lippincott-Schwartz, J., E. Snapp, and A. Kenworthy. 2001. Studying protein dynamics in living cells. *Nat Rev Mol Cell Biol* 2:444–56.

Litwin, J. 1992. The growth of Vero cells in suspension as cell aggregates in serum-free medium. *Cytotechnol* 10:169–74.

Loo, C.Y., D.A. Corliss, and N. Ganeshkumar. 2000. *S. gordonii* biofilm formation: Identification of genes that code for biofilm phenotypes. *J Bacteriol* 182:1374–82.

Lucić, V., A. Leis, and W. Baumeister. 2008. Cryo-electron tomography of cells: Connecting structure and function. *Histochem Cell Biol* 130:185–96.

Ludwig, T., R. Kirmse, K. Poole, and U.S. Schwarz. 2008. Probing cellular microenvironments and tissue remodeling by atomic force microscopy. *Pflügers Arch Eur J Physiol* 456:29–49.

Lutolf, M.P. P.M. Gilbert, and H.M. Blau. 2009. Designing materials to direct stem-cell fate. *Nature* 462:433–41.

Lysaght, M.J. and D. Rein. 2004. Immunoisolation. In Ratner, B.D., Hoffman A.S., Schoen, F.J., and Lemons, J.E., eds., *Biomaterials Science—An Introduction to Materials in Medicine*, pp. 728–34. London: Elsevier Academic Press.

Madurantakam, P.A., C.P. Cost, D.G. Simpson, and G.L. Bowlin. 2009. Science of nanofibrous scaffold fabrication: Strategies for next generation tissue-engineering scaffolds. *Nanomedicine (Lond)* 4:193–206.

Manley, S., J.M. Gillette, G.H. Patterson, H. Shroff, H.F. Hess, E. Betzig, and J. Lippincott-Schwartz. 2008. High-density mapping of single-molecule trajectories with photoactivated localization microscopy. *Nat Methods* 5:155–7.

Mavituna, F. 2004. Pre-formed carriers for cell immobilization. In Nedovic, V., Willaert, R., eds., *Fundamentals of Cell Immobilization Biotechnology*, pp. 121–39. Dordrecht, The Netherlands: Kluwer Academic Publishers.

McDonald, J.C., D.C. Duffy, J.R. Anderson, D.T. Chiu, H. Wu, O.J. Schueller, and G.M. Whitesides. 2000. Fabrication of microfluidic systems in poly(dimethylsiloxane). *Electrophoresis* 21:27–40.

Merchant, F.J.A., A. Margaritis, and J.B. Wallace. 1987. A novel technique for measuring solute diffusivities in entrapment matrices used in immobilization. *Biotechnol Bioeng* 30:936–45.

Moo-Young, M., and H.W. Blanch. 1981. Design of biochemical reactors: Mass transfer criteria for simple and complex systems. *Adv Biochem Eng* 19:1–69.

Nagase, K., J. Kobayashi, and T. Okano. 2009. Temperature-responsive intelligent interfaces for biomolecular separation and cell sheet engineering. *J Roy Soc Interface* 6(Suppl 3):S293–309.

Narziss, L., and P. Hellich. 1971. Ein Beitrag zur wesentlichen Beschleunigung der Gärung und Reifung des Bieres. *Brauwelt* 111:1491–1500.

Navrátil, M., P. Gemeiner, E. Sturd'k, Z. Dömény, D. Smogrovicová, and Z. Antalova. 2000. Fermented beverages produced by yeast cells entrapped in ionotropic hydrogels of polysaccharide nature. *Minerva Biotec* 12:337–44.

Neuman, K.C., and A. Nagy. 2008. Single-molecule force spectroscopy: Optical tweezers, magnetic tweezers and atomic force microscopy. *Nat. Methods* 5:491–505.

Nilsson, K., P. Brodelius, and K. Mosbach. 1987. Entrapment of microbial and plant cells in beaded polymers. *Methods Enzymol* 135:222–30.

Noordsij, P., and J.W. Rotte. 1967. Mass transfer coefficients to a rotating and a vibrating sphere. *Chem Eng Sci* 22:1475–1481.

Norman, J.J., and T.A. Desai. 2006. Methods for fabrication of nanoscale topography for tissue engineering scaffolds. *Ann Biomed Eng* 34:89–101.

Norton, S., K. Watson, and T. D'Amore. 1995. Ethanol tolerance of immobilized brewers' yeast cells. *Appl Microbiol Biotechnol* 43:18–24.

Nyamjav, D., S. Rozhok, and R.C. Holz. 2010. Immobilization of motile bacterial cells via dip-pen nanolithography. *Nanotechnology* 21:235105.

Øyaas, J., I. Storrø, M. Lysberg, H. Svendsen, and D.W. Levine. 1995. Determination of effective diffusion coefficients and distribution constants in polysaccharide gels with non-steady-state measurements. *Biotechnol Bioeng* 47:501–7.

Patrito, N., C. McCague, P.R. Norton, and N.O. Petersen. 2007. Spatially controlled cell adhesion via micropatterned surface modification of poly(dimethylsiloxane). *Langmuir* 23:715–9.

Peckys, D.B., G.M. Veith, D.C. Joy, and N. de Jonge. 2009. Nanoscale imaging of whole cells using a liquid enclosure and a scanning transmission electron microscope. *PLoS One* 4:e8214.

Perrot, F., M. Hebraud, R. Charlionet, G.A. Junter, and T. Jouenne. 2001. Cell immobilization induces changes in the protein response of *Escherichia coli* K-12 to a cold shock. *Electrophoresis* 22:2110–9.

Picioreanu, C., M.C.M. van Loosdrecht, and J.J. Heijnen. 1998. A new combined differential-discrete cellular automaton approach for biofilm modeling: Application for growth in gel beads. *Biotechnol Bioeng* 57:718–31.

Qu, X., D. Wu, L. Mets, and N.F. Scherer. 2004. Nanometer-localized multiple single-molecule fluorescence microscopy. *Proc Natl Acad Sci USA* 101:11298–303.

Reilly, G.C., and A.J. Engler. 2010. Intrinsic extracellular matrix properties regulate stem cell differentiation. *J Biomech* 43:55–62.

Reynolds, T.B., and G.R. Fink. 2001. Baker's yeast, a model for fungal biofilm formation. *Science* 291:878–81.

Riddle, K.W., and D. Mooney. 2004. Biomaterials for cell immobilization: A look at carrier design. In Nedovic, V., and Willaert, R. eds., *Fundamentals of Cell Immobilization Biotechnology,* pp. 15–32. Dordrecht, The Netherlands: Kluwer Academic Publishers.

Roco, M.C. 2003. Nanotechnology: Convergence with modern biology and medicine. *Curr Opin Biotechnol* 14:337–46.

Roco, M.C., R.S. Williams, and P. Alivisatos, eds., 2000. *Biological, Medical and Health Applications: Nanotechnology Research Directions*, Chapter 8. Dordrecht, The Netherlands: Kluwer Academic Publishers.

Roy, R., S. Hohng, and T. Ha. 2008. A practical guide to single-molecule FRET. *Nat Methods* 5:507–16.

Roy, P., Z. Rajfur, P. Pomorski, and K. Jacobson. 2002. Microscope-based techniques to study cell adhesion and migration. *Nat Cell Biol* 4:E91–6.

Rust, M.J., M. Bates, and X. Zhuang. 2006. Sub-diffraction-limit imaging by stochastic optical reconstruction microscopy (STORM). *Nat Methods* 3:793–5.

Sako, Y. 2006. Imaging single molecules in living cells for systems biology. *Mol Syst Biol* 2:56.

Salaita, K., Y. Wang, and C.A. Mirkin. 2007. Applications of dip-pen nanolithography. *Nat Nanotechnol* 2:145–55.

Sanderson, G.R., V.L. Bell, and D.A. Ortega. 1989. A comparison of gellan gum, agar, κ-carrageenan and algin. *Cereal Foods World* 34:991–8.

Sands, R.W., and D.J. Mooney. 2007. Polymers to direct cell fate by controlling the microenvironment. *Curr Opin Biotechnol* 18:448–53.

Sauer, K., A.K. Camper, G.D. Ehrlich, J.W. Costerton, and D.G. Davies. 2002. *Pseudomonas aeruginosa* displays multiple phenotypes during development as a biofilm. *J Bacteriol* 184:1140–54.

Semino, C.E. 2008. Self-assembling peptides: From bio-inspired materials to bone regeneration. *J Dent Res* 87:606–16.

Sherwood, T.K.A., R.L. Pigford, and C.R. Wilke. 1975. *Mass Transfer*, London: McGraw-Hill.

Shin, H. 2007. Fabrication methods of an engineered microenvironment for analysis of cell-biomaterial interactions. *Biomaterials* 28:126–33.

Sirkar, K., and W. Kang. 2004. Whole cell immobilization in chopped hollow fibers. In Nedovic, V., and Willaert, R. eds., *Fundamentals of Cell Immobilization Biotechnology*, pp. 245–56. Dordrecht, The Netherlands: Kluwer Academic Publishers.

Smith, I.O., X.H. Liu, L.A. Smith, and P.X. Ma. 2009. Nanostructured polymer scaffolds for tissue engineering and regenerative medicine. *Wiley Interdiscip Rev Nanomed Nanobiotechnol* 1:226–36.

Spatz, J.P. 2004. Cell-nanostructure interactions. In Niemeyer, C., and Mirkin, C., eds., *Nanobiotechnology*, pp. 53–65. Weinheim, Germany: Wiley-VCH.

Stahlberg, H., and T. Walz. 2008. Molecular electron microscopy: State of the art and current challenges. *ACS Chem Biol* 3:268–81.

Stephens, D.J., and V.J. Allan. 2003. Light microscopy techniques for live cell imaging. *Science* 300:82–6.

Stoodley, P., K. Sauer, D.G. Davies, and J.W. Costerton. 2002. Biofilms as complex differentiated communities. *Ann Rev Microbiol* 56:187–209.

Sun, Y., S. Furusaki, A. Yamauchi, and K. Ichimura. 1989. Diffusivity of oxygen into carriers entrapping whole cells. *Biotechnol Bioeng* 34:55–8.

Sungur, S., and U. Akbulut. 1994. Immobilization of β-galactosidase onto gelatin by glutaraldehyde and chromium(III) acetate. *J Chem Technol Biotechnol* 59:303–6.

Taubenberger, A., D.A. Cisneros, J. Friedrichs, P.H. Puech, D.J. Muller, and C.M. Franz. 2007. Revealing early steps of alpha2beta1 integrin-mediated adhesion to collagen type I by using single-cell force spectroscopy. *Mol Biol Cell* 18:1634–44.

Teramura, Y., and H. Iwata. 2010. Bioartificial pancreas microencapsulation and conformal coating of islet of Langerhans. *Adv Drug Deliv Rev* 62:827–40.

Théry, M., V. Racine, A. Pépin, M. Piel, Y. Chen, J.B. Sibarita, and M. Bornens. 2005. The extracellular matrix guides the orientation of the cell division axis. *Nat Cell Biol* 7:947–53.

Thompson, R.E., D.R. Larson, and W.W. Webb. 2002. Precise nanometer localization analysis for individual fluorescent probes. *Biophys J* 82:2775–83.

Touhami, A., B. Hoffmann, A. Vasella, F.A. Denis, and Y.F. Dufrêne. 2003. Probing specific lectin-carbohydrate interactions using atomic force microscopy imaging and force measurements. *Langmuir* 19:1745–51.

Tzvetkova-Chevolleau, T., A. Stéphanou, D. Fuard, J. Ohayon, P. Schiavone, and P. Tracqui. 2008. The motility of normal and cancer cells in response to the combined influence of the substrate rigidity and anisotropic microstructure. *Biomaterials* 29:1541–51.

van 't Riet, K., and J. Tramper. 1991. *Basic Bioreactor Design*. New York: Marcel Dekker.

Varfolomeyev, SD., E.I. Rainina, V.I. Lozinsky, S.V. Kalyuzhny, A.P. Sinitsyn, T.A. Makhlis, G.P. Bachurina, I.G. Bokova, O.A. Sklyankina, and E.B. Agafonov. 1990. Application of polyvinyl alcohol cryogels for immobilization of mesophilic and thermophilic micro-organisms. In de Bont, J.A.M., Visser, J., Mattiasson, B., Tramper, J. eds., *Physiology of Immobilized Cells*, pp. 325–30. Dordrecht, The Netherlands: Elsevier.

Vilain, S., P. Cosette, M. Hubert, C. Lange, G.A. Junter, and T. Jouenne. 2004. Proteomic analysis of agar gel-entrapped *Pseudomonas aeruginosa*. *Proteomics* 4:1996–2004.

Viyas, V.K., S. Kuchin, C.D. Berkely, and M. Carlson. 2003. Snf1 kinases with different β-subunit isoforms play distinct roles in regulating haploid invasive growth. *Mol Biol Cell* 23:1341–8.

Walker, P.A., K.R. Aroom, F. Jimenez, S.K. Shah, M.T. Harting, B.S. Gill, and C.S. Cox, Jr. 2009. Advances in progenitor cell therapy using scaffolding constructs for central nervous system injury. *Stem Cell Rev* 5:283–300.

Walter, N.G., C.Y. Huang, A.J. Manzo, and M.A. Sobhy. 2008. Do-it-yourself guide: How to use the modern single-molecule toolkit. *Nat Methods* 5:475–89.

Wei, G., and P.X. Ma. 2008. Nanostructured biomaterials for regeneration. *Adv Funct Mater* 18:3566–82.

Weibel, D.B., W.R. DiLuzio, and G.M. Whitesides. 2007. Microfabrication meets microbiology. *Nature Rev Microbiol* 5:209–18.

Whitesides, G.M. 2003. The 'right' size in nanobiotechnology. *Nat Biotechnol* 21:1161–5.

Whitesides, G.M., E. Ostuni, S. Takayama, X. Jiang, and D.E. Ingber. 2001. Soft lithography in biology and biochemistry. *Annu Rev Biomed Eng* 3:335–73.

Willaert, R. 2000. Beer production using immobilised cell technology. *Minerva Biotechnol* 12:319–330.

Willaert, R. 2007a. The beer brewing process: Wort production and beer fermentation. In Hui, Y.N., ed., *Handbook of Food Products Manufacturing*, pp. 443–506. Hoboken, NJ: John Wiley & Sons.

Willaert, R. 2007b. Cell immobilization and its applications in biotechnology: Current trends and future prospects. In El-Mansi, E.M.T., Bryce, C.F.A., Demain, A.L., and Allman, A.R. eds., *Fermentation Microbiology and Biotechnology*, 2nd ed., pp. 287–361, Boca Raton, FL: CRC Press.

Willaert, R. 2009. Engineering aspects of cell immobilization. In *Encyclopedia of Industrial Biotechnology*, pp. 1385–1413. Hoboken, NJ: John Wiley & Sons.

Willaert, R.G., and G.V. Baron. 1994. Effectiveness factor calculations for immobilized growing cell systems. *Biotechnol Techn* 8:695–700.

Willaert, R.G., and G.V. Baron. 1996. Gel entrapment and micro-encapsulation: Methods, applications and engineering principles. *Rev Chem Eng* 12:1–205.

Willaert, R., and G.V. Baron. 1993. Growth kinetics of gel-immobilized yeast cells studied by on-line microscopy. *Appl Microbiol Biotechnol* 39:347–352.

Willaert, R., V. Nedovic, and G.V. Baron. 2004. Physiology of immobilized cells. In Nedovic V., and Willaert, R. eds., *Fundamentals of Cell Immobilization Biotechnology*. Dordrecht, The Netherlands: Kluwer Academic Publishers.

Wilson, J.T., and E.L. Chaikof. 2008. Challenges and emerging technologies in the immunoisolation of cells and tissues. *Adv Drug Deliv Rev* 60:124–45.

Wisplinghoff, H., T. Bischoff, S.M. Tallent, H. Seifert, R.P. Wenzel, and M.B. Edmond. 2004. Nosocomial bloodstream infections in US hospitals: Analysis of 24179 cases from a prospective nationwide surveillance study. *Clin Infect Dis* 39:309–317.

Wittlich, P., E. Capan, M. Schlieker, K.D. Vorlop, and U. Jahnz. 2004. Entrapment in Lentikats: Encapsulation of various biocatalysts—Bacteria, fungi, yeast or enzymes into polyvinyl alcohol based hydrogel particles. In Nedovic, V., Willaert, R. eds., *Fundamentals of Cell Immobilization Biotechnology*. pp. 53–63, Dordrecht, The Netherlands: Kluwer Academic Publishers.

Wlodkowic, D., S. Faley, J. Skommer, D. McGuinness, and J.M. Cooper. 2009. Biological implications of polymeric microdevices for live cell assays. *Anal Chem* 81:9828–33.

Wouters, D., and U.S. Schubert. 2004. Nanolithography and nanochemistry: Probe-related patterning techniques and chemical modification for nanometer-sized devices. *Angew Chem Int Ed Engl* 43:2480–95.

Wu, K.Y.A., and K.D. Wisecarver. 1992. Cell immobilization using PVA crosslinked with boric acid. *Biotechnol Bioeng* 39:447–449.

Yamada, K.M., and B. Geiger. 1997. Molecular interactions in cell adhesion complexes. *Curr Opin Cell Biol* 9:76–85.

Yeo, W.S., and M. Mrksich. 2006. Electroactive self-assembled monolayers that permit orthogonal control over the adhesion of cells to patterned substrates. *Langmuir* 22:10816–20.

Yildiz, A., J.N. Forkey, S.A. McKinney, T. Ha, Y.E. Goldman, and P.R. Selvin. 2003. Myosin V walks hand-over-hand: single fluorophore imaging with 1.5-nm localization. *Science* 300:2061–5.

Zhao, X., and S. Zhang. 2007. Designer self-assembling peptide materials. *Macromol Biosci* 7:13–22.

This page intentionally left blank

13 Biosensors in Bioprocess Monitoring and Control: Current Trends and Future Prospects

Chris E. French and Chris Gwenin

CONTENTS

13.1 INTRODUCTION

The application of sensors to bioprocess monitoring of fermentation parameters such as pH, temperature, and dissolved oxygen, once a major challenge, is now a standard procedure irrespective of the scale of fermentation because the enabling technologies are well established; for further details on control of fermentation processes, see chapter 16 and 17 in this volume. Offline monitoring of other parameters, such as substrate utilization and product formation, is also important and is achieved using enzymic assays and analytical techniques such as HPLC, GCMS, or ELISA, but this involves inevitable delays, with implications for process control and management. In this chapter, we examine the scientific basis underlying biosensor design and control and explore the potential benefits of their applications.

13.2 BIOSENSORS IN PROCESS MONITORING

Functionally speaking, a biosensor couples a biological element, which transmits a specific recognition signal of the target analyte, to a transducer, which in turn generates an electrical signal. The electrical signal can then be directed to a digital readout, logged, or sent as an input to a control system. The biological recognition element may be an enzyme, an antibody, another binding molecule, or a living cell. The transducer may detect a redox reaction, light emission, altered levels of an ion, a luminescent or fluorescent signal, or a change in mass associated with a surface. Whatever the nature of the initial response, it is converted into an electrical signal which, in turn, is used in monitoring and control of the process in question (Figure 13.1). The application of biosensor technology to fermentation processes allows rapid, highly specific, quantitative response, with minimal or no requirements for sample preprocessing.

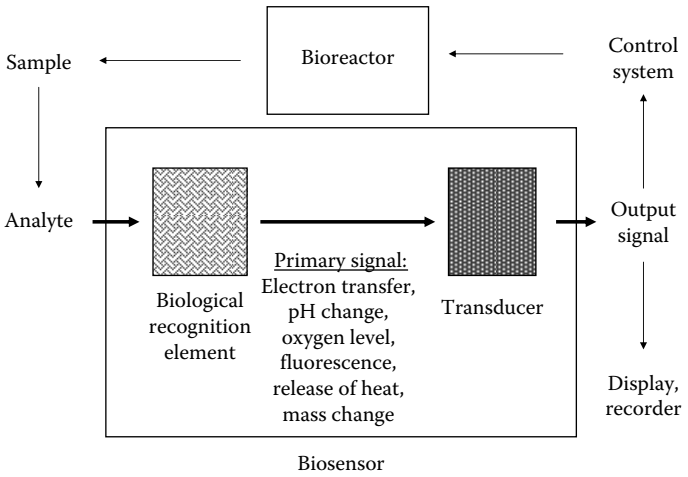

FIGURE 13.1 Schematic representation of a general biosensor.

Biosensors are superior to traditional analytical methods such as HPLC or ELISA, because they afford a much higher specificity within a very short time span. For example, HPLC utilizes relatively nonspecific detector systems such as ultraviolet absorption or refractive index, and identification of specific substances is based on retention time within a column. Thus, there is an intrinsic and unavoidable delay before the results are obtained. By contrast, a biosensor uses a specific biological detection element and ideally supplies a steady-state response in less than approximately 60 s. Techniques such as ELISA also use a biological detection element, but they require considerable sample processing over several steps, again leading to delays. The ideal of a biosensor (not always achieved!) is to apply such a biological detection element in a configuration that gives a rapid automatic output without such sample processing.

The biological element of the biosensor is critical in that it provides the specificity of response. This relies on the evolved ability of biological molecules (especially proteins) to recognize their interaction partners with extremely high affinity. The main types of recognition element used are enzymes and antibodies. In some cases nucleic acids or whole living cells, usually bacteria, can be used.

The use of a biological sensing element is the strength and weakness of biosensors. Biological sensing elements are relatively labile and do not tolerate high temperatures or other sterilizing agents. Therefore they cannot be directly inserted into the fermentation vessel unless they are separated from the fermentation broth by an semi-permeable membrane. The efficiency of biosensors diminishes with time and as such their performance must be monitored and they must be replaced on a regular basis. Expected lifetime of the biological element is an important parameter to bear in mind when considering the use of a biosensor.

From an historical perspective, the first medical application of biosensor technology was in the detection and measurement of glucose concentration in blood for the control of diabetes. Glucose-oxidase-based biosensors are widely used as a routine assay in hospitals as well as by members of the public; for a recent review consult Yoo and Lee (2010). Biosensors are also applied to the detection of many other analytes in clinical samples and to the detection of pollutants in the environment, monitoring of various components in the food industry, and monitoring of metabolites during fermentation processes. This chapter describes the scientific principles underlying biosensor design and operation and highlights recent developments in the field.

One of the many hurdles that has to be overcome in the application of biosensors to process monitoring and control is the lability of the detection element to sterilization, which in turn renders direct insertion of the biosensor probe into the fermentation vessel impossible, with some noteworthy recent exceptions; for example, the CITSens biosensors for glucose, glutamate, and lactate are designed to be inserted directly into disposable bioreactors.

Biosensors can be used for in situ measurements if coupled with a suitable device for separation from the cells, such as a tangential flow microfiltration unit. One of the most popular ways of using biosensors in bioprocess monitoring is flow injection analysis (FIA). In this system, the samples are withdrawn automatically and injected into a flow of a carrier liquid that is passed through the detection element, thus ensuring continuous monitoring (Schugerl 2001). The use of FIA and other flow-based techniques such as sequential injection analysis (SIA) with optical and electrochemical biosensors has been recently reviewed by Hartwell and Grudpan (2010).

Some types of biosensor, such as amperometric enzyme electrodes, are better suited to continuous monitoring; others, especially those based on antibodies, may require regeneration of the detection surface by removal of bound ligand, or even replacement of the detection surface, between measurements. Also, some types of biosensors, particularly those based on redox enzymes, may require the addition of small soluble cofactors or co-substrates along with the sample and are therefore not suitable for in situ use. Sensors that do not require such additions are referred to as "**reagent-less**". The reagent-less condition is more desirable, and a great deal of ingenuity has gone into the designing of reagent-less biosensors.

Reagent-less or reagent-free: Refers to a biosensor in which all components required for the generation and transduction of the signal are immobilized, so that addition of soluble molecules (e.g., enzyme cofactors, substrates, or mediators) is not required.

13.3 TRANSDUCTION METHODS: AN OVERVIEW

The transduction method to be used depends on the type of signal generated by the biological recognition element. The main types of transducer are electrical (potentiometric, amperometric, conductimetric, and capacitive), optical (based on absorbance, fluorescence, luminescence, or surface plasmon resonance), thermal (calorimetric), and mechanical (piezoelectric). The most commonly used techniques in biosensors currently suitable for process monitoring, or likely to become so in the next few years, include amperometric and potentiometric biosensors.

13.3.1 Amperometric

In an amperometric transducer, an electrode is held poised at a constant voltage relative to a reference electrode (usually Ag/AgCl) by the use of a circuit known as a **potentiostat**. Redox-active molecules can be oxidized or reduced at the electrode surface, generating a current that is measured. The potential at which the electrode is held is chosen so as to allow for oxidation or reduction of the target analyte while minimizing the oxidation or reduction of other substances that may be present. Interference by redox-active molecules such as ascorbic acid, which may be present in fermentation broths, must always be considered. Amperometric transduction is ideal when an enzyme reaction generates or consumes a redox-active substance such as oxygen (O_2), hydrogen peroxide (H_2O_2), NAD(P)H, or pyrroloquinoline quinone (PQQ). For recent reviews, see Grieshaber et al. (2008) and Ronkainen et al. (2008). Amperometric biosensors are the best developed systems for detection of small molecules such as glucose, glutamate, and lactate.

Potentiostat: A circuit that holds an electrode poised at a constant voltage relative to a reference electrode.

13.3.2 Potentiometric

The simplest type of potentiometric transducer utilizes an ion-selective electrode, and the build-up of the appropriate ion causes a change in potential (voltage) with very little current flow. The standard pH electrode is an example of an ion-selective electrode. Various other ion- or gas-selective electrodes are available, and these can easily be used as the basis for a biosensor if an enzyme is available that acts on the target analyte to generate or consume the appropriate ion or gas. Potentiometric transduction may be suitable when the reaction generates or consumes H^+, NH_4^+ (NH_3), or CO_3^{2-} (CO_2). Another type of potentiometric device is the enzyme field effect transistor (ENFET), a solid-state device consisting of an ion-selective field effect transistor (ISFET) with an immobilized enzyme layer over the gate electrode (Miao et al. 2003). A third type is the light-addressable potentiometric sensor (LAPS), in which the voltage change at the surface is measured by a change in the photocurrent when the surface is illuminated. LAPS devices can be used in the same way as other potentiometric sensors, but, with the use of a scanning laser as a light source, can also be used to detect spatially localized changes on the sensor surface.

13.3.3 Capacitance and Impedance

Binding of ligands to a surface alters the electrical properties of the surface layer, and this can be measured by electrochemical impedance spectroscopy (EIS). This involves applying an oscillating voltage and measuring current to generate a response related to the resistance and capacitance of the surface layer of the electrode (Grieshaber et al. 2008; Ronkainen et al. 2008). It is thus suited to the detection of binding events and can be used for reagent-less real-time detection of ligands binding to immobilized antibodies (Guan et al. 2004). These systems do not appear to be as well developed as amperometric or potentiometric sensors, but they have good potential for label-free detection of binding events, whereas potentiometric and amperometric sensors only detect enzymic reactions.

13.3.4 Thermal

Thermistor: A very sensitive solid-state temperature-measuring device in which electrical resistance is strongly affected by temperature.

In this case, an extremely sensitive temperature-sensing element (**thermistor**) is used to detect the increase in temperature due to heat released by an enzyme-catalyzed reaction. This technique is potentially more widely applicable than amperometric or potentiometric transduction in that it can potentially be used with any enzyme-catalyzed reaction, although obviously it is likely to be most sensitive when the reaction is highly exothermic. For a recent review of thermal biosensors, see Ramanathan and Danielsson (2001).

13.3.5 Optical Fiber Biosensors

Optical transduction in optical fiber biosensors is based on the transmission of light along an optical fiber to a detector. Light may be generated by fluorescent or luminescent reactions associated with enzymes immobilized at the tip of the fiber-optic bundle. Compared with electrical transduction, optical transduction has the advantage of not being affected by electrically noisy environments but the disadvantage that it may be affected by turbidity. Optical transduction is suitable when an enzyme consumes or generates a fluorescent cofactor such as NAD(P)H, or where a reaction product can be used to generate light in a chemiluminescent reaction, as in the peroxidase-catalyzed reaction of H_2O_2 with luminol. Another application is the bioluminescent detection of ATP that is based on the firefly luciferase reaction. Optical fibers can also be applied to indirect methods of antibody-based detection using fluorescently labeled competing ligands or second antibodies. For recent reviews, see Bosch et al. (2007) and Borisov and Wolfbeis (2008).

13.3.6 Surface Plasmon Resonance

Surface plasmon resonance (SPR) is an altogether different class of optical technique that is applied to the detection of small changes in mass due to ligand binding in a film of immobilized antibodies (or other binding molecules). A ligand (the analyte) essentially binds to a film of immobilized antibody, and the change in mass of the film due to ligand binding is detected based (usually) on a minute change in the incidence angle at which reflectance dips as photons are absorbed to generate surface plasmons. SPR is most suitable for direct detection of relatively large analytes such as proteins; for example, it may be useful in monitoring the production of recombinant proteins in a bioreactor. Small molecules can also be detected using indirect (competitive) assays. There are several related techniques , including resonant mirror biosensors, which have similar applications (see, for example, Hulme et al. 2002). A recent development is the use of gold nanoparticles rather than a continuous gold film. In this case, the effect is slightly different and is referred to as *localized SPR* (LPR or LSPR) because the surface plasmons are localized to single gold nanoparticles rather than being free to propagate along the gold film. In some cases, this has been reported to give enhanced sensitivity.

13.3.7 Piezoelectric

Like SPR, piezoelectric transduction is applied to the detection of small changes in mass due to ligand binding to a film of immobilized antibodies. In this case, the film is immobilized on the surface of a piezoelectric crystal such as quartz, and detection is based on changes in the mechanical properties of the surface film as its mass increases, measured by changes in its vibration properties when an electrical potential is applied. The most commonly used type are bulk acoustic wave devices, such as the quartz crystal microbalance (QCM); for a recent review, see Ferriera et al. (2009). An alternative configuration is known as the *surface acoustic wave* (SAW) biosensor, which has been recently reviewed by Länge et al. (2008) and Gronewald (2007).

13.3.8 Mechanical

Recent progress in the ability to generate microstructured silicon surfaces has resulted in the development of new classes of biosensor that directly detect binding events (e.g., binding of a ligand to an antibody) based on mechanical deflection of nanometer-scale structures. The most commonly described type seems to be the cantilever biosensor, which typically consists of an array of silicon cantilevers approximately 1 μm thick, and several hundred micrometers in other dimensions, coated with gold on one side. Binding of a ligand to a molecule immobilized on the gold surface (or alternatively, on the silicon surface) results in bending of the cantilevers that is detected by changes in the reflection of laser light from the cantilever tips. For recent reviews, see Fritz (2008) and Alvarez and Lechuga (2010). The use of these devices and their applications in large-scale commercial processes awaits further development.

Recent innovations in nanotechnology offer the potential to revolutionize biosensor design and significantly extend the range of biosensor applications (Fortina et al. 2005; Erickson 2008; Asefa et al. 2009). For example, metal oxide nanoparticles and carbon nanotubes have been used to make improved electrodes for electrochemical biosensors (Rahman et al. 2010; Sadik et al. 2010), and carbon nanotubes can be used in field-effect transistors (Hu et al. 2010). Gold and silver nanoparticles, nanorods, and nanowires are increasingly applied to optical techniques such as localized SPR, as well as spectroscopic techniques such as surface-enhanced Raman spectroscopy (SERS). The fact that nanoparticles have similar dimensions to many biological binding molecules will surely open up new possibilities for structured immobilization of recognition elements as well as novel transduction methods. With many resources being devoted to nanotechnology, we can expect rapid progress in this area.

13.4 CATALYTIC BIOSENSORS: ENZYMES AS BIOLOGICAL SENSING ELEMENTS

Enzymes catalyze specific reactions and in turn produce certain products; some are stereospecific. The appearance of the product or the disappearance of the substrate or a cofactor may elicit a signal, which in turn is transmitted to a transducer and hence to a controller.

When compared with antibodies and other related substrates, enzymes offer a second layer of recognition specificity; a nontarget compound with roughly similar shape to the target analyte may be able to bind to the enzyme's active site, but unless it can also undergo the same reaction, it will not be detected, so it will not give a false positive. The downside of this is that enzyme reactions are subject to competitive and noncompetitive inhibition. A competitive inhibitor is a compound similar in shape to the target analyte (the enzyme substrate) and as such may bind to the active site and reduce the number of active sites available for target analyte binding, thereby decreasing the signal level; a noncompetitive inhibitor is one that binds elsewhere on the enzyme, decreasing the reaction rate by other means. The possible presence of inhibitors in the sample must always be considered when using an enzyme in a biosensor or any other type of enzyme-based assay, and some sample pretreatment may be necessary to remove any inhibitors that may be present.

Any biosensor device must be calibrated to establish its sensitivity (the lowest concentration of analyte that can be detected) and the **dynamic range** of the response (the range of substrate concentrations at which the biosensor will give a response from which the substrate concentration can be estimated). Figure 13.2 shows a simplified enzyme reaction scheme and standard equations used to describe enzyme activity. One important parameter is the K_m value, otherwise known as the *Michaelis constant*, which is a measure of the affinity of the substrate for the enzyme. In the simplest case in which substrate binding and unbinding is much more rapid than reaction, it is equal to K_d, the dissociation constant; in more realistic cases, it also takes into account of the

Dynamic range: The range of substrate concentration over which the sensor will produce a response from which the substrate concentration can be determined, or the range of values of output signal that the sensor can produce.

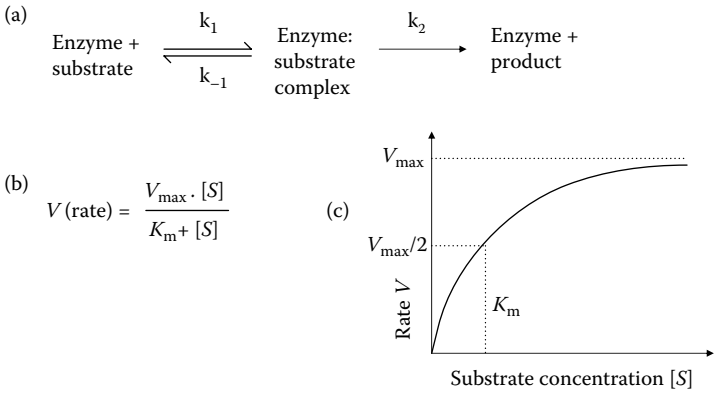

FIGURE 13.2 Enzyme kinetics. (a) Scheme for single-substrate enzyme reactions. The enzyme and substrate interact to form an enzyme-substrate complex, which reacts to form an enzyme-product complex, from which the product is released. The enzyme-substrate complex and enzyme-product complex are not distinguishable by steady-state kinetics. (b) The Michaelis–Menten equation for simple enzyme-catalyzed reactions. V = rate of reaction; V_{max} = maximum rate of reaction at saturating substrate concentrations; $[S]$ = substrate concentration; K_m = Michaelis constant, the substrate concentration at which V is half of V_{max}. This equation makes several assumptions, one of which is that the enzyme concentration is much smaller than the substrate concentration. (c) Graph showing the shape of the rate dependence on substrate concentration.

rate of reaction. In practical terms, K_m is the substrate concentration at which the rate of reaction, and therefore signal formation, is half of the maximal rate (V_{max}). At substrate concentrations below the K_m, the reaction rate and, in turn, signal formation, follow first-order kinetics (i.e., the signal produced is proportional to substrate concentration). However, at substrate concentrations much higher than the K_m (in practice, ≥ 3 times the K_m), the reaction rate, and in turn the signal, show zero-order kinetics and as such are no longer dependent on substrate concentration. This simplified analysis assumes that diffusion of substrates or products is not rate-limiting. In a biosensor context, in which the enzyme and perhaps cofactors are immobilized, kinetics may be controlled by the rate of diffusion of substrate to the sensor, which is proportional to the difference between the substrate concentration at the surface of the sensor and that of the medium in the bioreactor.

The use of an enzyme as a recognition element in a biosensor depends on its ability to generate a signal that can easily be detected and converted into an electrical response. In this regard, not all enzymes are equally convenient. For example, isomerases, which simply alter the configuration of their substrates, are unlikely to generate a useful signal. Generally, the most useful class of enzymes for biosensors are oxidoreductases, which oxidize or reduce substrates; by their very nature they are involved in the movement of electrons and lend themselves to amperometric detection methods. Hydrolytic and lyase enzymes split substrate molecules into smaller parts; they may be useful if they generate or consume a substance that can be detected potentiometrically. Thermal detection is based on the release of energy during an enzyme-catalyzed reaction as detected by an extremely sensitive thermistor. In principle, this type of device can be used for almost any type of enzyme-catalyzed reaction, although clearly it is likely to work better for highly exothermic reactions.

In some cases, enzyme-based systems require additional small soluble molecules (e.g., cofactors or co-substrates) to be added for enzyme activity. For example, many dehydrogenases require stoichiometric amounts of cofactors such as NAD^+ or PQQ. This necessity for the addition of reagents departs from the ideal concept of the biosensor, in which the sensor is simply exposed to the analyte solution and generates a rapid, specific response. Systems that do not require the addition of reagents are called *reagent-free* or *reagent-less* systems. Many ingenious concepts have been applied to convert reagent-requiring systems to reagent-less systems; some of these are discussed below.

Recent innovations in synthetic biology as well as enzyme and pathway engineering are currently being exploited for the design of enzymes with novel substrate and cofactor specificities; for further details see Chapter 8 in this volume. The ability to design enzymes with specific properties, rather than relying on naturally occurring enzymes, will offer many new possibilities for biosensor design. Among the many techniques that have evolved recently in enzyme and pathway engineering is "directed evolution" (Arnold and Volkov 1999). In this method, many randomly generated mutants within a given pathway are generated and screened for a desired change in substrate specificity; see Chapter 8 for a detailed description of this method.

13.5 AFFINITY BIOSENSORS: ANTIBODIES AND OTHER BINDING MOLECULES AS BIOLOGICAL DETECTION ELEMENTS

Compared with enzymes, antibodies and similar binding molecules have the advantage of much greater versatility. In principle, an antibody or other binding molecule can be generated for almost any target analyte. The disadvantage is that, unlike enzymic reactions, a binding event does not intrinsically generate a strong specific signal, thus making it harder to detect than an enzymic reaction. In the context of biosensors, binding events can be detected directly, as in SPR or piezoelectric systems, or indirectly, using competitive assays with labeled competing ligands, or sandwich assays with labeled second antibodies. Biosensors based on antibodies are sometimes called *immunosensors*. For a recent review, see Byrne et al. (2009).

Although antibodies are the most commonly used type of affinity element in biosensors, other possibilities exist; for example, nucleic acids can be used to detect complementary strands (Palchetti and Mascini 2008). Nucleic acids can also be generated to bind non-nucleic acid targets. Such binding molecules are called *aptamers*. Aptamers can be generated to bind any target molecule through a process of systematic evolution (Figure 13.3) (Han et al. 2010). Aptamers can easily be manufactured in large quantities by chemical methods and are more robust than antibodies, so they can have considerable advantages. Another option is the use of **molecular imprinting**. In this approach, a monomer is polymerized in the presence of the target ligand. Removal of the ligand leaves cavities that may be capable of specifically binding the same ligand (Andersson 2000). Molecularly imprinted polymers (MIPs) can be applied to electrochemical biosensors (Piletsky and Turner 2002)

Aptamers: Nucleic acid molecules designed or selected to bind to a target analyte.

Molecular imprinting: A process in which a monomer is polymerized in the presence of a target analyte, and the analyte is then removed, leaving cavities in the polymer that are capable of specifically binding the analyte.

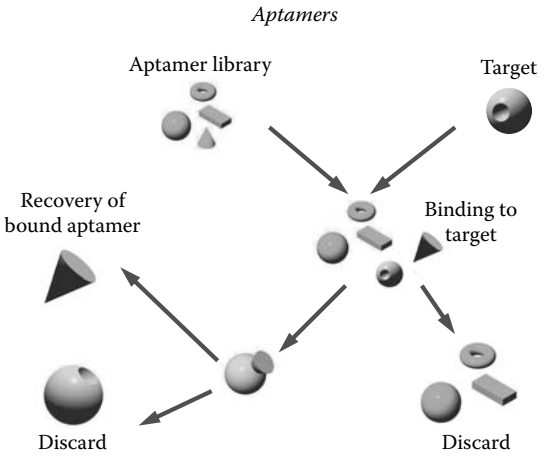

FIGURE 13.3 Pictorial representation of an aptamer selection process.

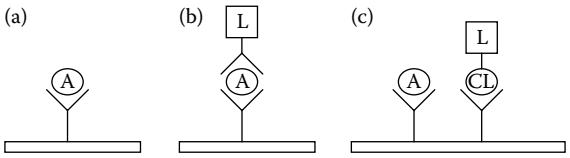

FIGURE 13.4 Affinity-based assays. (a) Direct assay. Binding of the analyte ligand (A) to the immobilized capture molecule is detected directly through some change in the properties of the immobilized film due to ligand binding. This is suited to SPR and piezoelectric transduction. (b) Sandwich assay. A second, labeled affinity molecule (e.g., antibody) binds to the captured analyte ligand. Detection is based on the quantity of label (L) at the capture surface. The label (L) may be a fluorophore or an enzyme; detection may be optical or electrical. (c) Competitive assay. There are several variants of this. In the version depicted here, the analyte ligand and a labeled competing ligand (CL) compete for binding sites on the film of immobilized capture molecules. Increased quantities of analyte in the sample mean that less label is detected at the capture surface.

and piezoelectric biosensors (Uludag et al. 2007). A third option is to use a protein, such as a receptor, which is known to specifically bind the target ligand. In some cases it may even be possible to use a small molecule that specifically binds the ligand of interest.

Indirect detection of antibody-binding events is based on the use of labeled molecules that are detectable optically or electrically. The two major types of label-based assay are sandwich assays and competitive assays (Figure 13.4). The label may be a fluorescent molecule, in which case detection is by fluorescence, or an enzyme, in which case various transduction methods are possible, including chemiluminescence (using peroxidase as the label and adding luminol as substrate) and amperometric detection. In sandwich assays, one antibody (the capture antibody) is bound to the surface, and a second, labeled antibody, which binds to another epitope on the same antigen, is present in solution. Ligand (analyte) binds to the immobilized antibody, and the labeled antibody then binds to this. Detection is based on the concentration of label bound at the film surface. Sandwich assays only work when the analyte ligand is large enough to simultaneously bind two antibody molecules. Competitive assays can be used for smaller analytes. Various configurations are possible, but they all rely on competition between the analyte and a labeled ligand for binding sites. In one common version, the capture antibody is immobilized, and a mixture of analyte ligand and a known concentration of competing labeled ligand are applied to the system. These compete for binding sites. As the amount of analyte ligand increases, the amount of labeled ligand that becomes bound decreases. Detection may be based on the amount of label that ends up bound at the surface (in which case a larger signal corresponds to a smaller amount of analyte ligand present in the assay) or on the amount of label that remains unbound (in which case a larger signal corresponds to a higher concentration of analyte). In an alternative configuration, the competing ligand is immobilized, and a labeled antibody is present in solution. The presence of the analyte (ligand) in solution reduces the amount of labeled antibody that binds at the surface.

Direct detection methods are sometimes referred to as *label-free* because they detect the binding event directly rather than via a labeled additive. Label-free systems are intrinsically preferable for online monitoring because they do not require addition of a reagent to the system. However, label-dependent systems can also be used for process monitoring if the necessary reagents are provided as needed.

Direct detection of binding by SPR or piezoelectric methods has the advantage of being intrinsically reagent-less, but is more demanding than detecting a label because the mass change will usually only be a small fractional change compared with the mass of antibody bound to the surface. Thus, these techniques are perhaps best suited to the quantitation of relatively large analytes such as proteins. A major problem with such techniques is nonspecific binding. In contrast to label-based methods, which detect only binding at the proper binding site, mass-based techniques will detect any binding to the surface whatsoever. Fermentation broths are often complex and contain many

large molecules, such as proteins, which are capable of binding nonspecifically to surfaces or to other proteins. Such potential interference must always be considered.

Binding of a ligand to a molecule, assuming a homogeneous preparation and that sufficient time is allowed for the system to reach equilibrium, is governed by the dissociation constant (K_d). Under conditions in which steady state is not achieved, the parameters which determine the binding of a ligand to a substrate are the association rate k_1, and the dissociation rate k_{-1}, which are related to K_d by the simple formula $K_d = k_{-1}/k_1$. This also assumes that diffusion of the ligand to the binding molecule is not rate-limiting. If the interactions between the ligand and binding molecule are relatively weak, then continuous monitoring of the ligand concentration may be possible by following the instantaneous level of bound ligand (Ohlson et al. 2000). When binding interactions are stronger, it is necessary to take a series of measurements, replacing or regenerating the detection film between measurements.

13.6 IMMOBILIZATION OF THE BIOLOGICAL RECOGNITION ELEMENT

Immobilization of the biological recognition element is essential for the retention of the recognition element within the biosensor. In most cases applicable to process monitoring and control, the recognition element is a protein—either an enzyme or an antibody. Immobilization of proteins may be achieved in several different ways; for a comprehensive account, see Chapter 12 in this volume.

13.6.1 Adsorption

In this case, the enzyme or antibody is simply exposed to the surface and attaches by adsorption. The advantage of this method is simplicity; the disadvantage is that attachment is relatively weak and reversible, leading to loss of the protein from the system over time. Adsorption may be useful for preliminary experiments, but it may not be ideal for production systems. Some systems are more suitable for adsorption than others; for example, nanostructured zinc oxide electrodes are reported to provide a good surface for adsorption of proteins with low isoelectric point (Zhao et al. 2010). Adsorption can achieve high loadings on common support materials such as anion exchange resin, metal oxide, cellulose, silica gel, and glass (Santano et al. 2002). Adsorption is the simplest, cheapest, and oldest of the immobilization methods and consists of adsorption of the enzyme to a nonreactive matrix/support by ionic bonds, hydrophobic interactions, hydrogen bonds, and or van der Waals forces. These weak interactions allow for easy desorption of the enzyme from the matrix via changes in ionic strength, pH, or temperature. Clearly, the enzyme could interact with the surface in several different ways depending on the orientation with which it approaches the surface. In an unperturbed solution this process and the reverse process are under mass transport control. If every molecule that encounters the surface is adsorbed, a concentration gradient rapidly develops at the surface and the rate of adsorption then becomes proportional to the rate of diffusion such that

$$\frac{dn}{dt} = C_o\sqrt{\frac{D}{\pi t}} \tag{13.1}$$

where n is the number of molecules, C_o is the bulk concentration of protein, and D is the diffusion coefficient (Cosnier 1999).

13.6.2 Covalent Attachment

Covalent immobilization is the most extensively used method whereby the enzyme is attached to a highly hydrophilic matrix by covalent bonds, resulting in a strong attachment between the enzyme

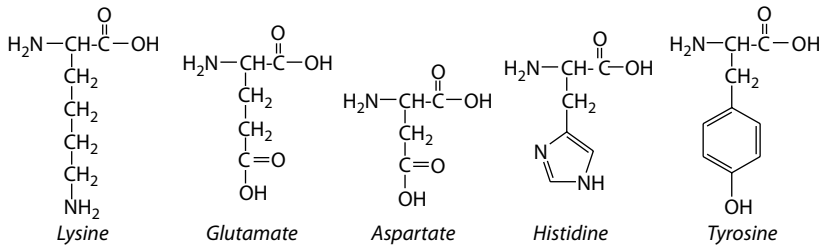

FIGURE 13.5 Chemical structure of lysine, glutamate, aspartate, histidine, and tyrosine.

and matrix; subsequently little enzyme is washed off during the process. Common amino acid side chains that are useful for coupling include lysine, glutamate, aspartate, histidine, and tyrosine (Figure 13.5). Because these are the most chemically reactive amino acids, they are also frequently found in the active site of an enzyme, thus the enzymes may attach to the support via these amino acids at the active site, resulting in major changes to the K_m and V_{max} values, or even inactivation; this can be minimized by immobilizing in the presence of analytes.

13.6.3 Protein Crosslinking

The protein is applied to the surface and then covalently crosslinked to form a macromolecular film using a bifunctional reagent such as glutaraldehyde. Sometimes a nonfunctional protein such as albumin is included to provide extra protein for binding. This may be combined with other methods of immobilization for enhanced permanence.

13.6.4 Entrapment

Enzymes can be trapped in the pores of gels, fibers, or a highly crosslinked polymer. This is very convenient if the enzyme acts on low-molecular-weight analytes because very high loadings can often be achieved, over 1 g protein/g matrix (Borole et al. 2002). Entrapment can be purely physical or involve covalent coupling. For example, it is possible to react surface lysine residues (Figure 13.5) with acryloyl chloride (CH_2=CH-CO-Cl) and co-polymerize it into a polyacrylamide gel; polyacrylamide (Gonzalez-Saiz and Pizarro 2001), alginate (Knezevic et al. 2002), gelatine (Munjal et al. 2002), agarose (Miranda et al. 2002), and silica gel (Doumeche et al. 2002) have all been used for entrapment immobilization. Unfortunately, entrapment can suffer from three major drawbacks: large diffusion barriers to the transport of analyte or product, loss of enzyme activity (because these materials generally do not have a narrow pore size distribution) and shrinkage and/or swelling of the polymer depending upon the ionic strength of the environment (Tal et al. 2001). Many recent reports have described the use of electrically conductive polymers, such as polypyrrole and polyaniline, which may be easily polymerized on an electrode surface by application of an appropriate potential, reviewed by Vidal et al. (2003) and Cosnier (2003). Nonconducting polymers may also be generated by electropolymerization at an electrode surface with the potential advantage that very thin films are generated because the film growth is self-limiting (Miao et al. 2004).

13.6.5 Attachment to a Gold Film via Thiol-Gold Interactions

When transduction is by SPR or piezoelectric methods, the relevant surface is usually a gold film on the surface of a crystal. A noble metal film can also be added to an electrode surface for amperometric transduction. Proteins may be attached to gold films via the interaction of thiol groups with gold atoms. In some cases, surface-exposed thiols on the protein may serve this purpose. In other

cases, one can use an "adapter", consisting of a molecule with a thiol at one end and a covalent or high-affinity protein-binding active group at the other. Usually a self-assembled monolayer (SAM) of a substituted alkanethiol is used (Chaki and Vijayamohanan 2002).

13.7 AMPEROMETRIC BIOSENSORS BASED ON REDOX ENZYMES

As described previously, amperometric biosensors measure the current generated between a test electrode and a reference electrode when the potential between them is maintained at a constant level by means of a potentiostat. The reference electrode most commonly used is Ag/AgCl. The test/working electrode is usually platinum or carbon, with a coating of a suitable immobilized enzyme. To generate a detectable current, the enzyme must catalyze a redox reaction specific to the target analyte. Zhang et al. (2000) provide a description of materials and techniques used in the construction of electrochemical biosensors. Electrochemical biosensors have been reviewed recently by Grieshaber et al. (2008) and Ronkainen et al. (2008).

The enzymes most commonly used in such biosensors are oxidases. "Oxidase" is a general term for an enzyme that reacts with a substrate and with molecular oxygen (O_2) to generate an oxidized substrate and H_2O_2. Oxidases generally contain a tightly bound flavin [flavin adenine dinucleotide (FAD)] as a prosthetic group. In a typical reaction cycle, the substrate XH_2 binds to the enzyme active site and interacts with the flavin, FAD, to generate the oxidized product X and the reduced flavin, $FADH_2$ (Figure 13.6). The oxidized product then dissociates. O_2 then binds to the active site and reacts with the reduced flavin, regenerating FAD and being reduced to H_2O_2. Oxidases are highly suitable for biosensors because they are simple single-component enzymes that do not require soluble cofactors, and they consume and generate redox-active substances suitable for amperometric transduction (H_2O_2 may also be detected optically by chemiluminescence, as described below).

Oxidase-based biosensors are widely used in the quantitation of glucose in blood and, in turn, the detection of diabetes (Yoo and Lee 2010). Glucose-oxidase based electrodes were the earliest enzyme-based biosensors to be manufactured. They were developed by Leland Clark and commercially pioneered by Yellow Springs Instruments (YSI). For a more detailed discussion of blood

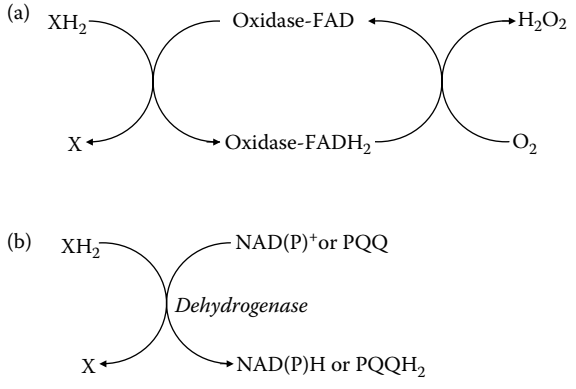

FIGURE 13.6 Enzyme-catalyzed redox reactions used in biosensors. (a) Oxidases. The reduced substrate, XH_2, reduces the bound flavin of the oxidase, FAD, to $FADH_2$. Oxygen then interacts with the reduced flavin, reoxidizing it to FAD and being reduced to H_2O_2. The flavin remains bound to the enzyme throughout the catalytic cycle. (b) Dehydrogenases. The reduced substrate XH_2 and an oxidized cofactor such as $NAD(P)^+$ or PQQ form a tertiary complex, and reducing equivalents are transferred to the cofactor, which generates the reduced form, such as NAD(P)H or $PQQH_2$, which then dissociates from the enzyme. In a living cell, the reduced cofactor would be reoxidized by a separate enzyme.

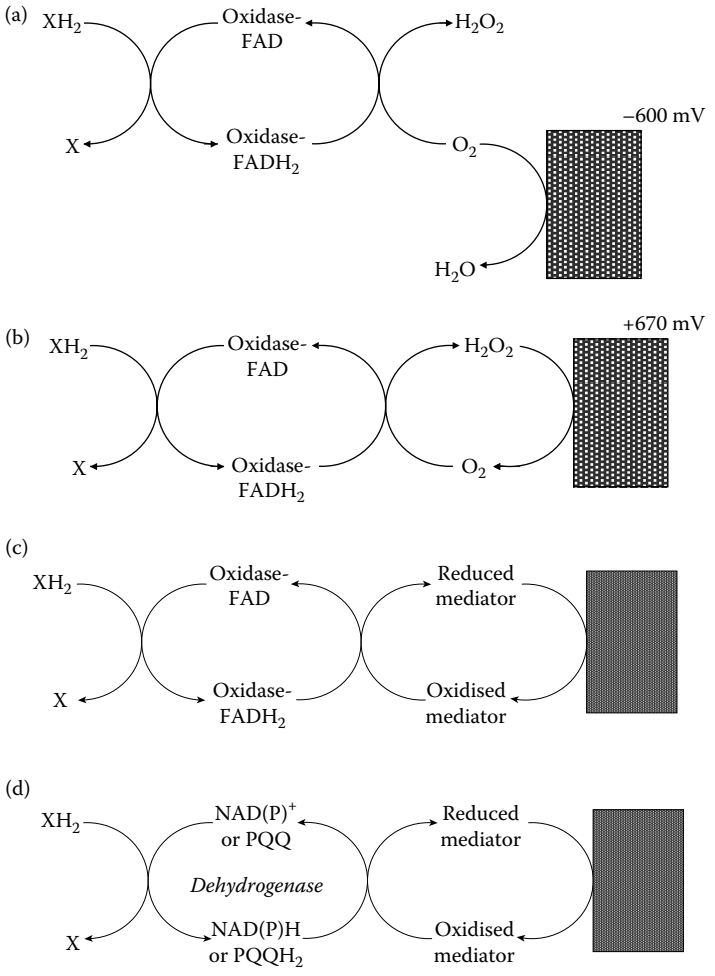

FIGURE 13.7 Use of redox enzymes in amperometric biosensors. (a) Oxidase with detection by an oxygen electrode. Presence of the substrate (analyte) leads to consumption of oxygen and a reduced signal from the oxygen electrode. This method was used in the earliest amperometric glucose sensors, but it is no longer widely used. (b) Oxidase with detection of H_2O_2. H_2O_2 is oxidized at the electrode. In an alternative version, H_2O_2 can be reduced to water at an electrode held at approximately –50 mV relative to Ag/AgCl; this reduces interference from redox-active substances in the sample. (c) Oxidase with mediator. This configuration eliminates the requirement for oxygen, which has low solubility in aqueous solutions. (d) Dehydrogenase with mediator. Some mediators can react directly with the cofactor; in other cases, another enzyme, known as a *diaphorase*, is used to facilitate reaction between the cofactor and the mediator.

glucose monitoring, see the case study in Section 13.14. Although glucose oxidase initiated biosensor development at the industrial level, many other oxidases suitable for biosensor use including glutamate oxidase, alcohol oxidase, and lactate oxidase are commercially available.

The oxidase reaction cycle lends itself to many variations on amperometric detection (Figure 13.7). The earliest oxidase-based biosensors simply used Clark oxygen electrodes with a layer of enzyme immobilized at the surface. The Clark oxygen electrode is simply a platinum electrode held at around –600 mV (relative to an Ag/AgCl counterelectrode); oxygen is reduced to water at the electrode surface, leading to a detectable current proportional to the oxygen concentration in the bulk fluid. When a layer of glucose oxidase is immobilized at the electrode surface, the glucose oxidase reaction reduces the oxygen concentration, leading to a reduced signal from the oxygen electrode. The

electrode is held at a potential such that the reaction is diffusion controlled so that the reduction in signal is related to the glucose concentration. This transduction method is no longer widely used in biosensors. Later generations of oxidase-based biosensors detected hydrogen peroxide produced in the reaction. In general, detection of a reaction product always allows for higher sensitivity than monitoring decreased concentration of a substrate because at low reaction rates, one is detecting a small positive signal against a low background, rather than a small negative signal against a high background. H_2O_2 itself is a redox-active molecule and may be detected at an electrode surface by oxidation to O_2 (at a potential of approximately +670 mV). However, the high oxidizing potential of the electrode can lead to interference from other redox-active molecules. In the context of glucose sensing in body fluids, the major problems are ascorbic and uric acids, but redox-active molecules may also be present in fermentation broths. Alternatively, the oxidase can be co-immobilized with horseradish peroxidase, a heme-containing enzyme that reduces H_2O_2 to water. The enzyme can then be reduced, either directly or via a suitable mediator, by an electrode at approximately 0 to –50 mV (see, for example, Dock et al. 2001).

All of these systems require oxygen as a reactant. Oxygen is poorly soluble in water, and its concentration is difficult to control. More recent generations of oxidase-based biosensor have removed oxygen from the equation altogether, transferring electrons directly from $FADH_2$ to the electrode surface. This may be accomplished in several ways. If the enzyme is immobilized sufficiently close to the electrode surface, simple proximity may allow direct electron transfer, but this is generally not efficient because the FAD is located some distance from the surface of the protein. More generally, a redox-active molecule known as a mediator is used to transfer electrons between the FAD and the electrode (Figure 13.7). Ferrocenes were the first class of mediator to be used in this way and are still widely used. A soluble mediator can carry electrons between the enzyme and electrode, but this is not altogether satisfactory because the mediator is not immobilized and may escape from the system. In this case, it is necessary to replenish the system with an ample supply of mediator. A better solution is to immobilize the mediator as well as the enzyme, giving a reagent-less system. Most recent reports describe systems in which the oxidase and mediator are co-immobilized by entrapment within a film of an electrically conductive polymer, which conducts electrons from the $FADH_2$ via the mediator to the electrode; the use of mediators in electrochemical biosensors has been discussed by Chaubey and Malhotra (2001).

Because oxidases all work in the same way and generate the same signal but recognize different substrates, arrays of oxidases may be used for simultaneous detection of multiple analytes. For example, Moser et al. (2002) described a microflow sensor using glucose oxidase, lactate oxidase, glutamate oxidase, and glutamate oxidase in conjunction with glutaminase for the simultaneous determination of glucose, lactate, glutamate, and glutamine, respectively.

The use of mediators in amperometric biosensors also allows for the use of other classes of redox enzymes (oxidoreductases), such as dehydrogenases. Dehydrogenases are enzymes that catalyze reaction of a substrate XH_2 with a (usually soluble) cofactor C as follows: $XH_2 + C \rightarrow X + CH_2$ (Figure 13.6). The reaction may be freely reversible or essentially irreversible depending on the relative reducing potentials of the substrate and cofactor. Among the most common cofactors are the pyridine nucleotides NAD (nicotinamide adenine dinucleotide) and NADP (nicotinamide adenine dinucleotide phosphate). The oxidized forms of these cofactors are written as NAD^+ and $NADP^+$, or collectively $NAD(P)^+$; the reduced forms as NADH and NADPH, or collectively, NAD(P)H (Figure 13.8). Pyridine nucleotide cofactors themselves do not readily react at electrodes, but inclusion of a suitable mediator in the system allows transfer of electrons from NAD(P)H to an electrode surface (Figure 13.7). Alternatively, the dehydrogenase can be co-immobilized with a diaphorase, a general term for a (usually) flavin-containing enzyme, in which the flavin is reduced by NAD(P)H and then re-oxidized by oxygen or some other electron acceptor. The diaphorase flavin can thus facilitate transfer of electrons between NAD(P)H and a mediator (see, for example, Takamizawa et al. 2000). The NAD(P) itself can also be immobilized by covalent attachment to a larger molecule; for example, Mak et al. (2003) reported the use of

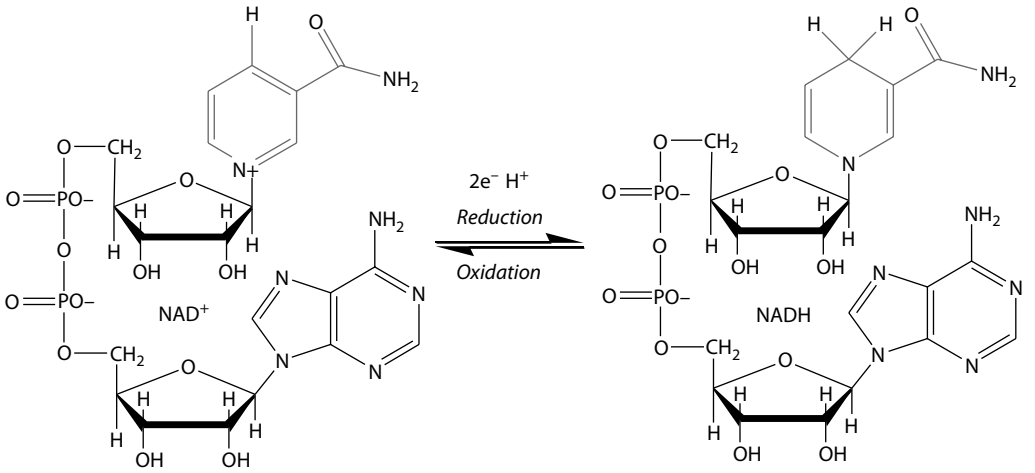

FIGURE 13.8 Chemical structures illustrating the reduction of NAD^+ and the oxidation of NADH.

NAD covalently linked to polyethylene glycol (PEG) in a formate biosensor based on formate dehydrogenase. If the cofactor is not immobilized, then it must be supplied to the system to replace losses.

Several recent reports describe biosensors based on NAD(P)-dependent dehydrogenases. For example, Nicelescu et al. (2003) described a glycerol biosensor suitable for the analysis of glycerol levels in wine, based on NAD-dependent glycerol dehydrogenase, co-immobilized with a mediator [phenazine methosulfate (PMS)] or embedded in a redox-active polymer film. Santos et al. (2003) described a biosensor for ethanol, based on NAD-dependent alcohol dehydrogenase, with a working lifetime exceeding three months. Zhao et al. (2002) described the generation and use of films of Prussian blue as immobilized mediators in amperometric biosensors using NAD-dependent formate dehydrogenase immobilized in a polypyrrole film. Maestre et al. (2001) reported a coupled sensor for sucrose determination using three enzymes: sucrose phosphorylase, phosphoglucomutase, and glucose-6-phosphate dehydrogenase (G6PDH). This sensor was used in a FIA system. Saidman et al. (2000) described a sorbitol biosensor based on sorbitol dehydrogenase, and Takamizawa et al. (2000) reported a sensor for xylitol.

Other dehydrogenases use PQQ as a cofactor rather than NAD(P). PQQ-dependent alcohol dehydrogenases and glucose dehydrogenases (derived from various bacteria) have been used in biosensors. For example, Malinauskas et al. (2004) reported the construction of a mediator-less glucose biosensor based on PQQ-dependent glucose dehydrogenase immobilized within a redox-active polymer on a carbon electrode. Razumiene et al. (2001) described the construction of enzyme electrodes based on PQQ-dependent alcohol dehydrogenase and glucose dehydrogenase immobilized on a carbon electrode with 4-ferrocenylphenol as a mediator, and Tkac et al. (2001) described a fructose sensor based on PQQ-dependent fructose dehydrogenase immobilized in a cellulose acetate film. Okuda et al. (2002) reported that co-immobilization of cytochrome c or cytochrome b562 with the PQQ-dependent glucose dehydrogenase greatly enhanced the signal.

Several recent reports have described the use of novel electrode materials based on metal oxide nanoparticles or carbon nanotubes (Rahman et al. 2010; Sadik et al. 2010). The high surface area of nanoparticles may lead to increased sensitivity and more rapid response. There may also be other advantages; for example, nanostructured zinc oxide electrodes adsorb acidic proteins well (Zhao et al. 2010).

Several manufacturers sell complete instruments suitable for monitoring of glucose and other molecules by amperometric methods. For example, Trace Analytics (www.trace.de) supplies the Process TRACE system, designed specifically for aseptic online monitoring of levels of glucose,

lactate, sucrose, ethanol, and methanol in laboratory and industrial cultures. The company that first introduced a commercial amperometric glucose biosensor in 1975, YSI (www.ysi.com), is still a market leader in the technology. For example, the YSI 2700 SELECT instrument is designed for process analysis in the food and bioprocess industries and can provide offline or online measurements of glucose, galactose, lactose, sucrose, lactate, glutamine, glutamate, and ethanol, among other analytes. An attachment is also available for automated aseptic sampling and control of a feed pump based on results. The typical working lifetime for the biological components is quoted as ranging from five days for alcohol oxidase to 21 days for glucose oxidase. Another example is the CITSens-Bio (www.c-cit.ch/public/englisch/ glucosesensor.htm), designed for online monitoring of glucose, glutamate, and lactate in mammalian cell cultures growing in disposable plastic bioreactors, which are becoming increasingly popular because they do not require cleaning or sterilization. The sensor is supplied in a sterile, γ-irradiated form and is mounted within the bioreactor to remove the requirement for sampling, which would open the possibility of contamination. Data are transmitted by radio to a receiver outside of the reactor. For those who wish to build their own electrochemical biosensor, see Zhang et al. (2000).

13.8 POTENTIOMETRIC BIOSENSORS AND ENFETS

Hydrolytic enzymes and lyases cleave a substrate bond, usually releasing a small molecule. In the former case, the cleavage is hydrolytic; in the latter case, a carbon-carbon double bond is generated. Such cleavage reactions do not intrinsically generate a strong signal suitable for transduction. However, in some cases, one of the products generated may be detectable by a second enzyme, usually an oxidoreductase, or may be detected potentiometrically. Potentiometric detection is based on the generation and detection of a voltage at an electrode surface. The best-known potentiometric sensor is the common laboratory pH electrode. Ion-selective electrodes are also available, consisting basically of pH electrodes surrounded by gas-permeable membranes that allow passage of, for example, ammonia (NH_3) or carbon dioxide (CO_2). Most potentiometric biosensors discussed in the recent literature are for the detection of urea in clinical contexts or pesticides in environmental contexts, but some devices suitable for bioprocess monitoring have also been described.

The simplest case is where the reaction alters the local pH sufficiently that the reaction can be detected using a pH electrode; however, the buffering capacity of the fermentation medium must be considered. For example, Park et al. (2004) described a potentiometric biosensor using penicillinase (β-lactamase) to quantify penicillin G and derivatives. The enzyme was immobilized on a cellulose nitrate membrane on a pH electrode; in a 2 mM phosphate buffer, pH 7.2, as little as 1 μM penicillin could be detected. Glucose can also be detected potentiometrically using glucose oxidase immobilized on a pH electrode because the glucose oxidase reaction generates gluconic acid, which decreases the local pH. For example, Tinkilic et al. (2002) described the construction of miniaturized glucose and urea biosensors based on glucose oxidase and urease immobilized on pH and ammonium electrodes, respectively, obtaining a linear response between 0.1 and 50 mM glucose.

In other cases, an ammonium or carbonate-responsive electrode can be used to detect a reaction product. For example, Kim and Kim (2003) described a potentiometric biosensor based on a carbonate electrode for the quantitation of isocitrate in foodstuffs. Similarly, ammonium-responsive electrodes have been used to make potentiometric biosensors for lysine using lysine oxidase (Garcia-Villar et al. 2003).

An ISFET is a solid-state version of an ion-selective electrode in which the potential at a gate electrode (with an ion-selective membrane and electrolyte solution with a reference electrode) determines the conductivity, and thus the current drawn, between source and drain connections held at different potentials. Changes in pH alter the potential at the gate electrode, changing the conductivity of the transistor and causing a measurable change in the drain current. Thus, an ISFET

can be used as a robust, solid-state pH-sensing device. An ENFET is an ISFET with a layer of enzyme immobilized at the gate electrode surface. Enzyme reactions altering the local pH can be detected, as described above for standard potentiometric biosensors. For example, Poghossian et al. (2001a) reported a penicillin-sensitive ENFET (dubbed a PenFET) based on immobilised β-lactamase. Glucose can also be detected by an ENFET with glucose oxidase (see, for example, Luo et al. 2004).

Interestingly, it has also been reported than ENFETs can be used to detect dehydrogenase-catalyzed redox reactions. In this case, an NAD-dependent dehydrogenase is immobilized at the gate surface along with PQQ, which acts as a mediator. The dehydrogenase reaction reduces NAD^+ to NADH, which reduces PQQ to $PQQH_2$. $PQQH_2$ can be reoxidized by O_2. Increased NADH levels change the steady-state ratio of $PQQH_2$ to PQQ at the gate, altering the local pH and the conductivity of the FET. Devices of this nature have been used to quantify lactate and ethanol using lactate dehydrogenase and alcohol dehydrogenase (Pogoroleva et al. 2003).

Another class of potentiometric devices is the LAPS, in which the surface potential is measured by changes in the photocurrent when the surface is illuminated. For a comparison of ENFETs, LAPS devices, and capacitive sensors, see Schöning and Poghossian (2006). LAPS devices can be used in much the same way as ENFETs. For example, Mourzina et al. (2004) described a LAPS with immobilized urease as a potentiometric urea sensor, and Poghossian et al. (2001b) prepared and compared LAPS, ENFET, and capacitive versions of the penicillinase-based penicillin biosensor. However, LAPS devices have a unique advantage when combined with a scanning laser [giving a laser-scanned semiconductor transducer (LSST)]: the interrogating laser beam can be scanned across the sensor surface to detect spatially localized changes in potential. This means that LAPS devices can be used to detect changes in single cells immobilized on the sensor surface (Schöning and Poghossian 2006). Several recent reports describe such devices and their uses, mainly in drug screening, but these are beyond the scope of this review.

13.9 THERMAL BIOSENSORS

Thermal biosensors are based on the use of a thermistor to detect the tiny amounts of heat released by an enzyme-catalyzed reaction. Almost all enzyme-catalyzed reactions release small amounts of heat detectable by a suitably sensitive thermal sensor such as a thermistor. Usually, the enzyme is immobilized on resin beads packed in a column that is attached to the thermistor. A control column lacking enzyme can be used to control for background temperature changes. The combination of thermistor and immobilized enzyme is sometimes referred to as an *enzyme thermistor.*

In principle, thermal detection of enzyme reactions is possible with any class of enzyme provided that the heat released by the reaction can be measured with sufficient sensitivity. For example, Rank et al. (1992) reported the use of a thermal biosensor for monitoring penicillin V production in a Novo-Nordisk production-scale fermentor (160 m^3). Energy release due to penicillin hydrolysis was measured in a column packed with immobilized β-lactamase or penicillin acylase. To correct for background temperature changes, a control column lacking active enzyme was used. Values were reported to correlate well with those obtained by HPLC. More recently, Lawung et al. (2001) described flow-injection analysis for the quantitation of penicillin- and cephalosporin-based antibiotics using two different β-lactamases immobilized on an affinity column. In another example, Navratil et al. (2001) used an online thermal biosensor with immobilized glycerokinase and galactose oxidase to monitor the bioconversion of glycerol to dihydroxyacetone by cells of *Gluconobacter oxydans* in an airlift fermentor. Finally, thermal biosensors provide yet another option for the quantitation of glucose with glucose oxidase. Ramanathan et al. (2001) described the use of immobilized glucose oxidase in an enzyme thermistor. To increase the amount of heat released per molecule of glucose oxidized, a second enzyme, catalase, was co-immobilized with the glucose oxidase to catalyze degradation of the hydrogen peroxide formed in the oxidase reaction.

13.10 OPTICAL BIOSENSORS BASED ON REDOX ENZYMES

Optical biosensors are based on the detection of colorimetric, fluorescent, or luminescent signals at the tip of a bundle of optical fibers. The fibers relay the light signal to a detector, which generates an appropriate electrical signal. A sensor based on optical fibers is sometimes referred to as an "**optode**" or "**optrode**". For some enzymes, a choice between optical and electrical transduction is possible. Optical transduction has the advantage that it is not affected by electrically noisy environments, and an optical fiber can be inserted, for example, directly into a bioreactor. However, optical transduction systems may be affected by turbidity. Optical biosensors have recently been reviewed by Bosch et al. (2007) and Borisov and Wolfbeis (2008).

Optode or optrode: A general term for a probe that generates an optical signal (by analogy with "electrode").

Although oxidases are ideally suited to amperometric detection, as described above, they are also suitable for use in optical fiber biosensors. H_2O_2 may be detected with great sensitivity by chemiluminescence on the basis of its peroxidase-catalyzed reaction with luminol, enhanced by *p*-iodophenol. Various optical biosensors that are based on this reaction have been reported. For example, Blankenstein et al. (1994) reported simultaneous online analysis of multiple analytes including glucose, lactate, and glutamate in animal cell culture using a multichannel oxidase-based FIA system. Another way of optically transducing oxidase reactions involves the ability of oxygen to quench the fluorescence of certain metal complexes. In the presence of the oxidase substrate, the local oxygen concentration at the optical fiber surface is reduced, leading to increased fluorescence.

The activity of NAD(P)-dependent dehydrogenases may also be detected by optical fiber biosensors. The signal in this case is based on the fact that the reduced form of the cofactor, NAD(P)H, absorbs light at approximately 340 nm and fluoresces at approximately 450 nm. Thus the presence of a dehydrogenase substrate leads to an increase in the NAD(P)H concentration and increased levels of light absorption and fluorescence. To cite a single example, Dominguez et al. (2010) described a sequential injection (SIA) sensor for measuring glycerol in the *Saccharomyces cerevisiae* fermentation process that is based on the enzyme glycerol dehydrogenase, which reduces NAD^+ to NADH.

Enzymes that cause a change in the local pH, such as β-lactamase, can also be transduced optically using indicator dyes that alter their fluorescence characteristics according to the local pH. This provides an alternative to potentiometric transduction.

13.11 INDIRECT AFFINITY SENSORS: OPTICAL AND ELECTRICAL BIOSENSORS BASED ON LABELED ANTIBODIES

Detection of binding events can be accomplished by displacement of a labeled competing ligand, as in indirect immunoassays, or by binding of a second labeled antibody as in a sandwich-type immunoassay. This can be detected optically. The label may be a fluorescent molecule, in which case optical transduction is possible, or an enzyme, which can be detected optically via a chemiluminescent reaction or electrically.

One configuration reported frequently in the literature is the use of antibodies labeled with horseradish peroxidase (HRP). Such antibodies are routinely used in laboratories for colorimetric or fluorimetric detection protocols and are based on the reaction of HRP with luminol or chromogenic substrates such as 4-aminophenazone. When used in a biosensor, horseradish peroxidase can be detected optically by chemiluminescence. For example, Jain et al. (2004) reported a generic competitive immunosensor using a flow analysis configuration in which analyte and a HRP-labeled analogue compete for antibody binding sites, with the amount of peroxidase being detected by enhanced chemiluminescence after the addition of luminol and *p*-iodophenol, which intensifies the

chemiluminescent reaction. Alternatively, as noted above, HRP in the presence of a suitable mediator, or in some cases even without a mediator, can transfer electrons between H_2O_2 and an electrode poised at approximately 0 to –50 mV with respect to a Ag/AgCl reference electrode. Thus, after its capture at an electrode surface, the HRP-labeled antibody, or analyte competitor, can be quantified amperometrically by the addition of H_2O_2 and a suitable mediator. For example, Lopez et al. (1998) reported an amperometric immunosensor for the detection of atrazine using a competitive configuration in which atrazine in the sample competed with peroxidase-labeled atrazine for binding sites on an antibody layer immobilized on an electrode. In an extension to this approach, Darain et al. (2003) reported an amperometric immunosensor device in which the electrode surface was modified with HRP and antibody, and the analyte was detected after competition with glucose oxidase-labeled analyte; H_2O_2 produced by the glucose oxidase reaction was reduced by the electrode at –350 mV via the peroxidase.

An interesting variation on this was reported by Ikebukuro et al. (2005), using aptamers (artificially-evolved ligand-binding nucleic acids) rather than antibodies, in a sandwich-type assay. The capture aptamer was immobilized on a gold electrode surface, and the detection aptamer was labeled with PQQ-dependent glucose dehydrogenase (described above). The amount of enzyme captured near the electrode surface was detected amperometrically after the addition of glucose.

Potentiometric biosensors can also be used to detect suitably labeled antibodies. For example, Campanella et al. (1999) compared the use of antibodies labeled with glucose oxidase (detected amperometrically) and urease (detected potentiometrically) for quantitation of human immunoglobulins. Such a system could potentially be adapted for detection of protein products in a biological process.

13.12 DIRECT AFFINITY DETECTION USING OPTICAL AND ELECTRICAL BIOSENSORS

In direct affinity detection systems, the binding of ligand (analyte) to immobilized capture molecule (e.g., antibody or aptamer) is detected directly by monitoring the amount of mass associated with the capture surface. Attachment of large ligands to the capture molecule increases the mass of the film to a detectable degree. The main methods used for such systems are SPR and piezoelectric transduction, mainly using the QCM. Such systems have the advantage of being intrinsically label-free and reagent-less but are prone to interference from nonspecific binding of nonanalyte molecules to the detection surface.

In the case of SPR, a beam of laser light is shone through a transparent medium coated with a thin film of gold, with a fluid layer on the other side of the gold film (Homola 2003). Above a certain angle of incidence, total reflectance from the surface will occur because of the difference in refractive index between the transparent medium and the fluid film. The reflected radiation intensity can be easily measured. During the process of reflectance, an evanescent wave, essentially an electrical field, is generated on the fluid side of the interface. At one particular narrow band of angles of incidence in this range, the phenomenon of SPR occurs as photons are absorbed and converted to surface plasmons, leading to a sharp reduction in the intensity of the reflected light. The angle of incidence at which this effect peaks is strongly affected by the mass of material, such as antibodies plus any bound ligands, which are bound at the surface. Thus, as more ligand binds to a layer of immobilized antibody in such a system, the angle at which resonance occurs changes fractionally, and this can be detected with very high sensitivity. The measurement is given in resonance units (RU), in which 1 RU corresponds to a change of 0.0001° in the angle of incidence at which the reflected radiation intensity minimum occurs.

As discussed above, the sensitivity of SPR detection depends on the fractional change in mass caused by binding of the ligand to the detection surface. Thus SPR is better suited for the detection of large molecules, such as proteins, than to small molecules. SPR may be suited to monitoring the

production of recombinant proteins. Ivansson et al. (2002) described the use of an SPR instrument for monitoring intracellular production of recombinant human superoxide dismutase in *Escherichia coli*. Initially samples of bacteria were withdrawn from the reactor and disrupted by sonication before analysis. A later paper (Tkac et al. 2004) reported disruption of cells by exposure to a non-ionic surfactant before SPR analysis, a technique more suited to automated sample processing. Hsieh et al. (1998) reported offline monitoring of the production of *Clostridium perfringens* β-toxin by applying fermentation broth directly to an SPR sensor chip. McCormick et al. (2004) developed an SPR assay for recombinant factor VIII, a blood-clotting factor, and suggested that their assay might be suitable for monitoring the recombinant production process.

SPR can also be applied to the detection of small molecules using sandwich or competition assays similar to those described above. Sandwich assays are essentially the same as those described above except that the second antibody need not be labeled; the increase in surface mass due to the mass of the second antibody is sufficient for detection. For competitive assays, instead of an enzyme or fluorescent label, a large protein is used to provide a sufficient mass change for detection. It has also been reported that recent SPR instruments are sufficiently sensitive for direct detection of the binding of small molecules to immobilized proteins (Rich and Myszka 2000).

Some reports have also described integration of multiple sensors of different types in a single chip. For example, Suzuki et al. (1999) reported the construction of an SPR immunosensor chip for human IgG also bearing integrated amperometric sensors for glucose and lactate; this was used for simultaneous online monitoring of glucose, lactate, and IgG in a cell culture bioreactor.

The first commercial SPR biosensor system was manufactured by Biacore (www.biacore.com) in 1990, and the technology has now matured to the point where it is suitable for routine monitoring purposes. Biacore supplies a range of SPR instruments, as well as sensor chips; for example, CM5, which is essentially a glass slide coated with a 50 nm layer of gold covered with a film of carboxymethylated dextran suitable for covalent attachment of antibodies or other binding molecules. Other types of sensor chips are also available (see the Biacore website or catalogue for further details). Another supplier of SPR instrumentation is Texas Instruments, which has recently introduced a small, relatively inexpensive SPR device known as *Spreeta*, which is discussed in Chinowsky et al. (2003). Other commercial suppliers of SPR instrumentation are listed by Rich and Myszka (2007).

A closely related type of sensor is based on LSPR. When SPR occurs on gold nanoparticles, smaller than the wavelength of the illuminating light, rather than on a continuous gold film, the resulting surface plasmons oscillate around the nanoparticles rather than propagating along the surface. These are known as *localized surface plasmons*, hence localized SPR (Willets and Van Duyne 2007). LSPR sensors are less sensitive than SPR sensors to changes in the bulk refractive index of the medium, but they are comparably sensitive to changes in the surface film, which is the important feature for affinity biosensors. To give a single example, Fujiwara et al. (2006) described an LSPR biosensor based on gold nanoparticles (~40 nm diameter) deposited on a glass surface modified with a self-assembled monolayer of amine-terminated silane. Bovine and human serum albumins were immobilized on the gold surfaces via a SAM of a thiol-bearing linker, and binding of antibodies to these was followed by LSPR. LSPR devices seem to have some way to go to catch up with conventional SPR systems, but rapid progress is being made; for example, Huang et al. (2009) recently described an LSPR device with integrated microfluidics for sample delivery and reported that results of an antibody-antigen binding assay were comparable to those of a Biacore SPR system.

In addition to SPR, there are several related techniques using instruments with similar configuration. Perhaps the most advanced of these is the resonant mirror biosensor. This is similar to SPR, but the configuration is such that incident light travels along the reflection surface for a period as an evanescent wave before reflection (Hulme et al. 2002). Huang et al. (2008) compared a resonant mirror (IAsys) biosensor with a quartz crystal microbalance for measuring binding of a traditional Chinese medicine component (propyl gallate) to the human protein endothelin-1 and ultimately concluded that the resonant mirror sensor showed superior performance in this application. Rich and Myszka (2007) surveyed 1219 published articles from the 2006 literature relating to commercial optical

biosensors. By far the majority of these used Biacore systems, with Affinity Sensors (IAsys) and Texas Instruments in second and third places.

An alternative which is receiving increased attention is the use of EIS to detect electrical changes at a sensor surface caused by ligand binding (Guan et al. 2004; Grieshaber et al. 2008; Ronkainen et al. 2008). Essentially, a sinusoidally varying voltage is applied at the electrode, and the resulting current is measured. The characteristics of the output current are affected by the capacitance and impedance of the surface layer. A range of different frequencies can be tested. Antibodies can be attached directly to gold electrodes or entrapped in conductive polypyrrole films at the electrode surface. Nucleic acid binding events can also be detected. Recent reports (summarized by Ronkainen et al. 2008) have described improved performance using gold nanoparticles or carbon nanotubes as the interface elements. Because of the desirability of simple, label-free affinity biosensors, this would seem to be a promising technology for further development.

13.13 DIRECT AFFINITY DETECTION USING ACOUSTIC AND MECHANICAL BIOSENSORS

Acoustic wave (piezoelectric) systems can also be used to measure mass changes due to ligand binding in a film of immobilized antibody. These devices are generally based on detection of changes in the nature of vibration of a piezoelectric material such as quartz when an electrical potential is applied. In this case, the antibody film is immobilized on the surface of a piezoelectric crystal. An applied voltage causes vibration of the crystal, and various characteristics of this vibration can be detected and used to infer the quantity of bound ligand. Various configurations are available. The most widely discussed type for biosensor use is the bulk acoustic wave (BAW) thickness shear mode (TSM) device, also known as a *QCM*. Biosensors of this type have been recently reviewed by Ferriera et al. (2009). The mechanical load on the crystal consists of a layer of adsorbed enzyme immersed in a comparatively deep buffer solution. The mechanical shear wave load impedance offered by this system can then be described in terms of the densities (ρ), shear wave velocities (v), and attenuations (α) of the enzyme layer of thickness (t) and phosphate buffer solution above it. The expected electrical impedance due to the mechanical load can then be deduced and compared with that found experimentally. Using a curve-fitting routine, the shear wave parameters are deduced with good accuracy. Any observed difference between the expected impedance and the measured impedance can be attributed to a change in the electrical impedance of the layer. Changes in electrical impedance are presented as changes in its two components, the resistance (r_e) and the capacitance (c_e).

An alternative configuration is known as the surface acoustic wave (SAW) biosensor; for recent reviews see Gronewald (2007) and Länge et al. (2008). The input transducer launches a high-frequency acoustic wave, which travels through the chemical film and is detected by the output transducer. The acoustic waves are sensitive to the viscoelasticity (plasticisation or stiffening) and the mass of the thin film, which allows for the identification of the contaminant. Additionally, the heating elements under the chemical film can be used to desorb chemicals from the device. SAW devices are in principle more sensitive but generally seem to be less suited for detection in aqueous environments than BAW devices because of greater damping of oscillations by the liquid medium, but several recent publications have reported their use for detecting antibody-protein, antibody-bacteria, and DNA-DNA interactions. However, for the moment, QCM devices seem to dominate the literature (Cooper and Singleton 2007).

Proteins are typically immobilized on the surface of piezoelectric devices via thiol-gold interactions, as with SPR (Chaki and Vijayamohanan 2002). The most obvious bioprocess monitoring application for QCM, as with SPR, is in the direct detection of relatively large molecules, such as recombinant proteins. To cite a single example, Saha et al. (2002) reported the use of a QCM-based sandwich assay for the quantitation of insulin. Reported applications of QCM from 2001 to 2005 were surveyed by Cooper and Singleton (2007).

Some interesting recent reports have discussed the use of binding molecules other than antibodies as capture molecules in piezoelectric biosensors. As discussed above, piezoelectric immunosensors, like SPR immunosensors, are only expected to show a strong response for relatively large ligands, where binding of the ligand causes a significant mass shift at the detection surface. However, in some cases even small ligands may provoke a large response. For example, Carmon et al. (2004) reported an unexpectedly strong signal from the binding of glucose to an *E. coli* glucose receptor protein immobilized on a QCM surface. They postulated that this was due to a conformational change on glucose binding leading to a change in the film structure from a viscous to a more rigid state. This it appears that piezoelectric sensors may sometimes be suitable for direct detection of small molecules, with an appropriate choice of capture molecule, when ligand binding is associated with a conformational change. Another interesting point in this report is that the glucose receptor protein was modified by site-directed mutagenesis to incorporate a surface-exposed thiol-bearing cystine residue, allowing for simple immobilization by direct binding of the thiol to the gold surface.

Another option for detection of small molecules is the use of a MIP as the capture molecule, rather than an antibody. This is a polymer that was polymerized in the presence of the analyte so that removal of the analyte leaves vacant spaces in the polymer of the correct size and conformation to bind the analyte specifically (Andersson 2000). For example, Feng et al. (2004) reported the use of an electropolymerized MIP for the detection of sorbitol. The use of MIPs in piezoelectric sensors has been reviewed by Uludag et al. (2007). Yet another possibility is an aptamer, a nucleic acid specifically evolved to bind the target ligand (Han et al. 2010). Aptamers may be more robust than antibodies; for example, Liss et al. (2002) compared the use of an aptamer and an antibody for the detection of human IgE and reported that the aptamer showed similar sensitivity and specificity to the antibody, along with improved dynamic range and a greater tolerance for the regeneration procedure. Finally, the capture molecule can be a small molecule with a specific affinity for the target analyte. For example, Yang and Chen (2002) reported the use of immobilized polymyxin B on a QCM for the quantitation of endotoxin (toxic lipopolysaccharide shed from the cell walls of Gram-negative bacteria, a great concern in the manufacture of injectable biological products).

Interestingly, piezoelectric sensors can also be used as a transduction system to detect oxidase activity. In this case the oxidase generates H_2O_2, which is used by a peroxidase to oxidize and polymerize a small molecule such as diaminobenzidine or *o*-dianisidine, forming a polymer that is deposited on the detection surface, leading to an increase in mass that is detected as described above. This has been described for the detection of cholesterol using cholesterol oxidase (Martin et al. 2003) and glucose using glucose oxidase (Reddy et al. 1998).

Commercial piezoelectric devices are available from several manufacturers, but relatively few seem to offer dedicated biosensor devices based on this principle. One example is Akubio, a spinoff from the University of Cambridge, United Kingdom, which supplies acoustic biosensors based on a principle the company refers to as "resonant acoustic profiling" (RAP) for real-time label-free detection of binding events. The Akubio RAPid 4™ instrument allows flow analysis and may have various applications. Another example is Attana Sensor Technologies (Stockholm, Sweden; www.attana.com), which sells devices based on QCM technology. Both systems seem to be designed for biomedical research, but they may also be applicable for monitoring protein levels in bioprocesses.

Another recent development is the cantilever biosensor, which can also be used for direct detection of binding events (Ziegler 2004; Fritz 2008; Alvarez and Lechuga 2010). These devices are based on arrays of tiny silicon cantilevers (beams with one attached end and one free end) approximately 1 μm thick and perhaps several hundred micrometers long. In one common configuration, each cantilever is coated with gold on one side. The biological recognition molecule can be attached to this gold surface as described above. Several detection methods are possible. The best characterized for detection of biomolecules in aqueous buffers seems to be static detection, or surface stress mode, in which bending caused by ligand binding on one side of the cantilever is detected, for example, by measuring reflection of laser light from the cantilever tips. Deflections of as little as 1 nm can be detected, making these devices very sensitive. An alternative, dynamic or resonant

detection, involves changes in the resonant frequency of vibration due to ligand binding, but this seems to be less effective in liquid environments because of viscous damping of the oscillations. Several reports describe sensitive detection of protein-antibody and nucleic acid binding events in laboratory or clinical applications. Interestingly, cantilever bending does not seem to reflect simple mass effects, but it is also sensitive to other changes in the local environment. For example, it has been reported that cantilevers coated with glucose oxidase show a highly specific bending effect in the presence of glucose, which could form the basis for novel glucose biosensors (Pei et al. 2004). On the basis of the current literature, cantilever biosensors do not seem to be quite ready for deployment in routine process monitoring applications, but they may be a promising future technology for process monitoring.

13.14 AMPEROMETRIC GLUCOSE BIOSENSORS FOR BLOOD GLUCOSE MONITORING: A CASE STUDY

As noted in Section 13.7, the most commonly used and convenient type of biosensor for the continuous monitoring of small molecule concentrations is the amperometric biosensor, in which electrons from an enzyme-catalyzed redox reaction are transferred to an electrode, and the current flow is used as a measure of the rate of enzyme reaction, from which the analyte concentration can be deduced. The abundant literature relating to biosensors certifies that this is an attractive field of research, at the junction of chemistry, biology, and physics (Willner and Katz 2000). Hence, there is immense interest in enzyme electrodes and in the development of various new strategies in which the electrons are transferred to and from redox enzymes, which are preferably coupled close to the electrode via the use of cofactors and modified electrodes (Scheller et al. 2002). In general, direct electron transfer between the electrode and the active site of the enzyme is difficult, especially when the enzyme does not contain a metal center, and a redox cofactor is needed in the catalytic cycle. The electrode monitors the concentration of one of the reactants or products in the natural enzyme reaction and thus, indirectly, the concentration of the enzyme analyte. The classic example of this approach is the innovative glucose sensor described by Clark and Lyons (1962), derivatives of which are now widely applied to blood glucose monitoring for the control of diabetes mellitus. In this device, glucose oxidase (GOx) was entrapped in front of an oxygen electrode. In the absence of glucose, the electrode responds to the ambient oxygen concentration. When glucose is added to the sample, oxygen is consumed by reaction with glucose, catalyzed by the enzyme, and consequently less oxygen reaches the oxygen electrode (Peteu et al. 1996). This, in turn, leads to a fall in the observed current. The magnitude of this change in current is related to the glucose concentration. The reaction catalyzed by GOx and similar oxidases is shown in Figure 13.6. Another alternative was to detect, at that same platinum electrode but at a different voltage, the production of H_2O_2 rather than the consumption of oxygen. This system turns out to be more reliable because the sensor is less sensitive to varying background oxygen concentrations in the sample. An inner membrane of cellulose acetate is directly placed on the electrode to exclude certain interferences, such as ascorbic acid, while still allowing the free passage, and thus detection of H_2O_2. Finally, an outer membrane protects the sensing layers from fouling by proteins in the blood.

Because of the enormous number of diabetes sufferers requiring frequent blood glucose measurements, the manufacture of blood glucose biosensors is a major industry, completely dominating the biosensor industry. In this case study, we will consider the development and current state of blood glucose monitoring systems.

13.14.1 Diabetes Mellitus

Diabetes mellitus is one of the most common chronic diseases in western and developing countries. This metabolic disorder is characterized by hyperglycemia and disturbances of carbohydrate, protein, and fat metabolism, secondary to an absolute or relative lack of the hormone insulin

(Alberti and Zimmet 1998). There are currently five major clinical categories of disordered glucose homeostasis:

- Type 1 diabetes, also known as *insulin-dependent diabetes*;
- Type 2 diabetes, also known as *non-insulin-dependent diabetes*;
- Impaired glucose tolerance/impaired fasting glucose;
- Gestational diabetes; and
- Other rare forms that include maturity-onset diabetes of the young (MODY) and pancreatic diseases.

Therefore, it follows that the measurements of glucose levels in blood is of immense importance to the control and treatment of diabetes (French and Cardosi 2007).

13.14.2 Glucose Meter

The main aim of treatment of diabetes is to achieve blood glucose and blood pressure levels as near to normal as possible. This, together with a healthy lifestyle, will help to improve well-being and protect against long-term damage to the eyes, kidneys, nerves, heart, and major arteries.

An important tool in the homeostatic control of diabetes is home blood glucose monitoring (HBGM). It can help to maintain day-to-day control, detect hypoglycemia, assess control during any illness, and help to provide information that can be used in the prevention of long-term complications. Blood glucose monitoring gives a direct measure of the glucose concentration at the time of the test and can detect hypoglycemia and hyperglycemia. The Diabetes Control and Complications Trial (DCCT) (Diabetes Control and Complications Trial Research Group 1993), a 10-year nationwide study of 1441 diabetics, conclusively demonstrated that improved control of blood sugar delayed or prevented many of the aforementioned complications at least 50% better than with poorly controlled subjects. Subsequent studies have corroborated this conclusion. This good control is enabled by frequent, consistent, and accurate self-testing of blood glucose to optimize therapy. Blood glucose monitors that utilize an enzyme electrode (biosensor) as the glucose sensing element are particularly suitable medical devices for HBGM. The advantages offered by biosensors in HBGM arise for the following reasons. Blood is a complex fluid, and glucose levels vary widely over time in a single patient. Many factors in addition to glucose vary in blood from healthy patients (**hematocrit**, oxygen levels, and metabolic by-products), therefore great specificity is a prime requirement. In addition, patients with diabetes may have a wide range of other medical problems creating even greater variation in their blood. Finally, biosensors can be used directly in the blood without requiring major modifications to the biological sample (increased temperature or pressure, dramatic pH changes, addition of highly reactive chemicals, etc.). Commercial examples of biosensors used for HBGM are shown in Figure 13.9.

Hematocrit: An index of the ratio of erythrocytes to plasma in the blood sample.

There are several essential elements in a medical device designed for patient self-monitoring. Because these systems are medical devices, used to make medical decisions or avoid potentially life-threatening incidents every day, they must be of very high quality, and the information displayed must be accurate. The sensors must be easily manipulated by sight-impaired users, and the system must be very user-friendly to encourage more frequent testing for better control. In the hospital or doctor's office there are additional quality requirements and the possibility of multiple sample types (e.g., capillary, arterial, venous, and neonatal blood). Many commercially available systems, meter plus sensing electrode (see Table 13.1), meet these needs by providing accurate and dependable glucose measurement using a tiny drop of blood, for many blood sample types over a wide range of hematocrit.

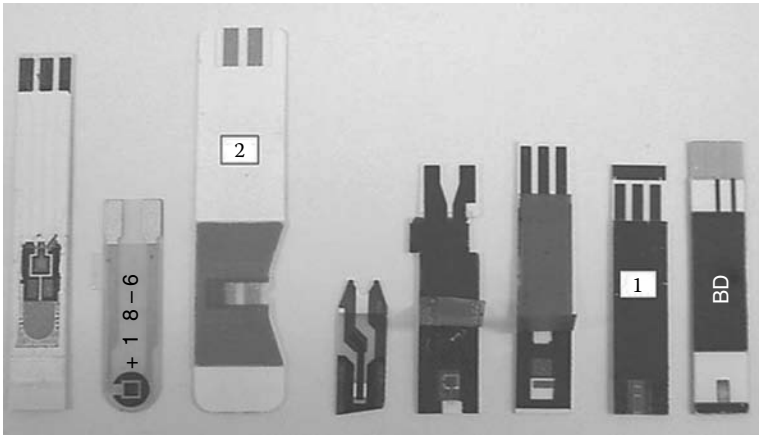

FIGURE 13.9 Commercial examples of biosensors available for HBGM. In some examples, the "top tape" has been removed to expose the underlying electrode configuration. Examples 1 and 2 are the One Touch Ultra and the Accu-Check Advantage strip, which are discussed in more detail in the text. Photograph kindly provided by Dr. Maria Teodorczyk, LifeScan, Milpitas, USA. (Reprinted from French, C.E. and Cardosi, M.F. *Fermentation Microbiology and Biotechnology*, 2nd ed., CRC Press: Boca Raton, FL, 2007. With permission)

TABLE 13.1
Examples of Commercially Available HBGM Test Kits

Company	Meter	Test Strip Required	Blood Range in mmol/L	Sample Volume in ml
Abbott Diabetes Care	Precision QID	MediSense G2 Sensor electrodes	1.1–33.3	3.5
Therasense	FreeStyle Classic	FreeStyle	1.1–27.8	0.3
	FreeStyle Mini	FreeStyle	1.1–27.8	0.3
Bayer Diagnostics	Ascensia Contour	Ascensia Microfill	0.6–33.3	0.6
	Ascensia Breeze	Ascensia Autodisc (10-test disc)	0.6–33.3	2.0–3.0
DiagnoSys Medical	Prestige Qx Smart System	Prestige Smart System	1.3–33.3	4
Hypoguard	Supreme Plus	Hypoguard Supreme	2.0–25.0	7
LifeScan	OneTouch Ultra	OneTouch Ultra	1.1–33.3	1
	OneTouch UltraSmart	OneTouch Ultra	1.1–33.3	1
Menarini Diagnostics	GlucoMen Glyco	GlucoMen Sensors	1.1–33.3	2
	GlucoMen PC	GlucoMen Sensors	1.1–33.3	2
Roche Diagnostics	Accu-Chek Compact	Accu-Chek Compact	0.55–33.3	1.5
	Accu-Chek Advantage	Accu-Chek	0.55–33.3	4
	Accu-Chek Active	Accu-Chek Active	0.55–33.3	2

Source: Data adapted from Diabetes UK website (http://www.diabetes.org.uk/products/index.html).

13.14.2.1 Enzymes Used in Glucose Biosensors

Traditionally, two glucose oxidizing enzymes have been used in the manufacture of glucose biosensors for HBGM. Although both enzymes oxidize the pyranose form of β-D-glucose (at the C1 position) to the corresponding lactone, they use different cofactors to carry out the redox process. One is the flavoprotein GOx, which has FAD as a cofactor and the other is the quino-protein-dependent glucose dehydrogenase (PQQ-GDH). Although both enzymes catalyze the oxidation of glucose,

their biological properties differ, so choice of enzyme is normally determined by the intended use of the sensor under specific clinical conditions.

GOx is a very specific enzyme (99.9% specific for β-D-glucose) that is commercially available in highly purified form and is therefore the enzyme of choice in most devices. However, it does suffer from the problem of crossreactivity with oxygen, which means that under situations of high oxygen partial pressure the reading obtained from the meter can be lower than expected. Recognition of this fact is of clinical importance because high blood oxygen tensions are frequently observed in the critically ill and in patients receiving oxygen therapy or undergoing surgery. Hence, changes in oxygen partial pressure ($_PO_2$) levels can falsely lower glucose meter measurements and may mislead medical decision-making. Mechanisms by which oxygen affects GOx-based amperometric test strips are suggested by the reactions in Table 13.2. Oxygen, a known natural electron acceptor, competes with electron mediators such as ferrocenium used with the Precision PCx and Precision QID (Table 13.2, Equation 13.5) and ferricyanide used with the Glucometer Elite (Table 13.2, Equation 13.13), for the reoxidation of GOx/$FADH_2$. At high $_PO_2$, oxygen outcompetes the electron mediator for the re-oxidation of GOx/$FADH_2$, which results in reduced chemical reaction between the electron mediator and GOx/$FADH_2$, leading to fewer electrons produced. As a result, low glucose measurements are obtained at high $_PO_2$ levels.

On the other hand, PQQ-GDH does not react with oxygen, so it is suitable for use as the biocatalyst in the clinical scenarios described above. However, the wild-type enzyme is not as specific as GOx, as illustrated by the kinetic data in Figures 13.10 and 13.11. Consequently, patients that have high levels of, for example, maltose in the blood (which could result as a side effect of peritoneal dialysis) or have an inbred genetic disorder resulting in impaired carbohydrate metabolism would obtain an inaccurate high reading when testing with glucose electrodes incorporating this enzyme. Because of the oxygen insensitivity of PQQ-GDH, there is much commercial interest in producing

TABLE 13.2
Examples of Commercially Available Glucose Test Strips and the Associated Chemical Reactions

Test and Chemical Reaction	Equation
Advantage H, Comfort Curve	
Glucose + GD/PQQ → gluconic acid + $GD/PQQH_2$	13.1
$GD/PQQH_2$ + ferricyanide → GD/PQQ + ferrocyanide	13.2
Ferrocyanide → ferricyanide + e^-	13.3
Precision PCx, Precision QID	
Glucose + GO/FAD → gluconic acid + $GO/FADH_2$	13.4
$GO/FADH_2$ + ferricinium → GO/FAD + ferrocene	13.5
Ferrocene → ferricinium + e^-	13.6
$GO/FADH_2 + O_2 \rightarrow GO/FAD + H_2O_2$	13.7
SureStep	
Glucose + GO/FAD → gluconic acid + $GO/FADH_2$	13.8
$GO/FADH_2 + O_2 \rightarrow GO/FAD + H_2O_2$	13.9
H_2O_2 + MBTH-R + HRP → $MBTH\text{-}R^+$	13.10
$MBTH\text{-}R^+ + ANS + ½O_2$ → blue-green dye	13.11
Glucometer Elite	
Glucose + GO/FAD → gluconic acid + $GO/FADH_2$	13.12
GO/FADH2 + ferricyanide → GO/FAD + ferrocyanide	13.13
Ferrocyanide → ferricyanide + e^-	13.14
$GO/FADH_2 + O_2 \rightarrow GO/FAD + H_2O_2$	13.15

Source: Tang, Z., et al. *Critical Care Medicine* 29(5):1062–1070, 2001.

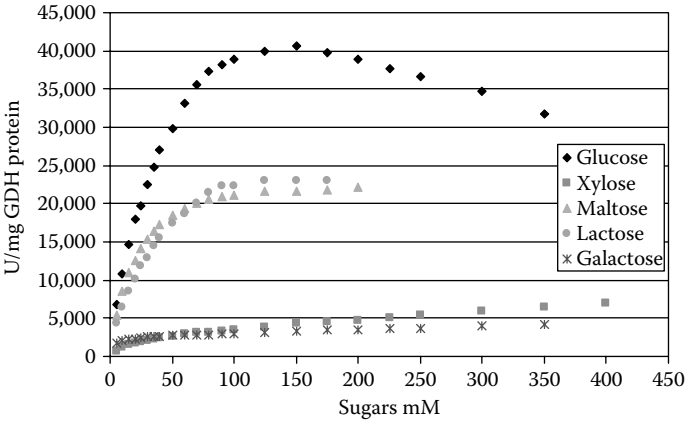

FIGURE 13.10 Kinetic plot for wild-type soluble PQQ-GDH showing the relative enzymic activity (Units/mg GDH protein) as a function of the concentration of glucose, xylose, maltose, lactose, and galactose in the assay. Data kindly provided by Dr. Patricia Byrd, LifeScan, Milpitas, USA. (Reprinted from French, C.E. and Cardosi, M.F. *Fermentation Microbiology and Biotechnology*, 2nd ed., CRC Press: Boca Raton, FL, 2007. With permission)

	K_m (mM)	V_{max} (U/mg, %)	V_{max}/K_m (%)
Glucose	25.0	4610 (100)	184 (100)
3-O-m-glucose	28.7	3596 (78)	123 (67)
Allose	35.5	2997 (65)	84.6 (46)
Maltose	26.0	2305 (50)	88.3 (48)
Lactose	18.9	1982 (43)	105 (57)
Galactose	5.3	277 (6)	52.3 (28)

FIGURE 13.11 Summary of the kinetics of sugar oxidation by wild-type soluble PQQ-GDH. (Reprinted from French, C.E. and Cardosi, M.F. *Fermentation Microbiology and Biotechnology*, 2nd ed., CRC Press: Boca Raton, FL, 2007. With permission)

a mutant form of the enzyme that retains its nonreactivity to oxygen but shows improved specificity with respect to β-D-glucose.

13.14.2.2 Mediated Electrochemistry

Although enzymes offer many advantages as the biocatalysts in glucose sensors, they rarely exchange electrons directly with electrodes. The same is true for many other biological molecules, such as glucose. An electrochemical measurement often requires a substance to facilitate (or mediate) this transfer and such reagents are termed "mediators"; a well-known mediator is potassium ferricyanide. The sequences of reactions are as follows:

1. Glucose first reacts with the enzyme (GOx or PQQ-GDH). Glucose is oxidized to gluconic acid, and the enzyme is temporarily reduced by two electrons transferred from glucose to the enzyme.
2. The reduced enzyme next reacts with the mediator, transferring a single electron to each of two mediator ions. The enzyme is returned to its original state, and the two oxidized mediator molecules are reduced.

3. Ferricyanide and ferrocyanide (the oxidized and reduced forms of the mediator, respectively) are capable of rapidly transferring electrons with an electrode. The electrons may thus be transferred between glucose and the electrode via enzyme and mediator.

We now have a chemical mechanism for transferring electrons from glucose to the electrode. The biosensor reagent is actually more complex, containing several other active ingredients (e.g., stabilizers, processing aids), but for simplicity we shall assume it is simple a deposited layer or enzyme and mediator.

13.14.2.3 Electrochemical Measurement

An extremely useful method is amperometry. This technique sets the electrode potential (a potential difference represents a difference in the average electron energy at two points) at a level where every molecule or ion reaching the electrode surface undergoes an electron transfer reaction. The current (rate of electron transfer) is thus limited by how rapidly the reactants arrive, a diffusion-controlled current, because diffusion is the primary transport mechanism. Because reactant is being converted (consumed) at the electrode surface, its average concentration will be decreasing in the vicinity of the electrode, so current should decrease with time. Under certain boundary conditions this behavior is described by the Cottrell equation,

$$i_t = \frac{nFAC_0D^{1/2}}{(\pi t)^{1/2}} \tag{13.2}$$

where i_t is the current (A), n is the number of electrons transferred in the reaction (for ferrocyanide, $n = 1$), F is the Faraday constant (the quantity of charge carried by 1 mol of electrons = 96,485 C/mol), A is the electrode area (cm^2), D is the diffusion coefficient (a measure of how rapidly reactant is transported; for ferrocyanide the diffusion coefficient is $\sim 7 \times 10^{-6}$ cm^2 /s at room temperature but varies with the medium), C_0 is the concentration of reactant (mol/cm^3; the model assumes uniform concentration before the potential difference is applied), and t is time (s).

13.14.2.4 Assay Protocol

The measurement protocol may be summarized as follows:

1. An enzyme (GOx or PQQ-GDH) rapidly transfers electrons from glucose to a mediator such as ferricyanide, which then transfers them to an electrode.
2. An electrode potential is imposed on the system. In any circuit, current must be identical at all points. If we put two electrodes in a circuit, electron flow rate out of one electrode (working electrode) has to equal the electron flow rate into the other (*counterelectrode*). Because ferrocyanide is oxidized at the working electrode, an equal quantity of material must be reduced at the counterelectrode. Because ferricyanide is normally present in large quantities, this species normally provides the counter-reaction. This is called *biamperometry*. In biamperometry, the counterelectrode and working electrode are normally made of the same material. For example, in the Accu-Check Advantage systems the electrodes are made of palladium metal. In the One Touch Ultra system, the electrodes are made of carbon.
3. The exact measurement sequence that is used for detecting glucose can vary from manufacturer to manufacturer. For example, in the Accu-Check Advantage system, inserting the glucose electrode automatically switches on the meter. When the sample is detected, an incubation period follows (under conditions of zero current flow) wherein glucose reacts

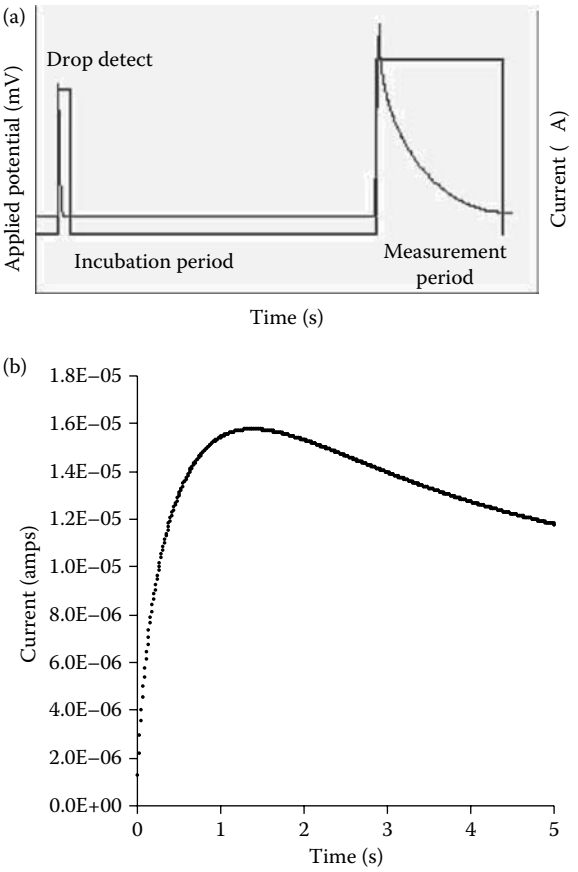

FIGURE 13.12 (a) Measurement sequence diagram for the Accu-Check Advantage meter. After sample detection, there is a defined incubation period during which ferrocyanide is allowed to accumulate. This is measured by amperometry, resulting in the current transient shown. (b) Current transient obtained with the One Touch Ultra biosensor. Unlike the Accu-Check Advantage, there is no incubation period. The potential is applied throughout the duration of the test. (Adapted from French, C.E. and Cardosi, M.F. *Fermentation Microbiology and Biotechnology*, 2nd ed., CRC Press: Boca Raton, FL, 2007. With permission).

with the enzyme (PQQ-GDH) to generate ferrocyanide. At the end of the incubation period, the meter applies a potential difference and the current is measured. Current data are analyzed and the result is recorded and displayed to the user. On the other hand, the One Touch Ultra system does not have an incubation period. After sample detection, the current flows throughout the 5-s sample test time. At the end of this period the current is analyzed and the level of glucose in the sample is calculated. Unlike the aforementioned system, there is no separate incubation period. These two protocols are summarized in Figure 13.12.

SUMMARY

Biosensors offer a method for automated monitoring of metabolites and reaction products during fermentation and can be used in control systems. The analyte of interest is recognized specifically by a biological molecule such as an enzyme or antibody, and an electrical signal is generated by a transducer. A very wide range of transduction methods have been reported in the literature, although relatively few seem to have been commercially adopted for process control as yet.

For small molecules such as sugars, alcohols, and hydroxy acids for which oxidase or dehydrogenase enzymes are available, the most obvious choice is an amperometric enzyme electrode. This is a well-established technology. Indeed, amperometric biosensors for the detection of common substrates and metabolites such as glucose and other sugars, ethanol, lactate, and glutamate, are commercially available in systems specifically designed for process monitoring and control.

For small molecules for which no redox enzyme is available but that can be acted upon by an enzyme (such as a hydrolase) yielding or consuming H^+, NH_4^+ (NH_3), or HCO_3^- (CO_2), a potentiometric enzyme electrode or ENFET would be a good choice.

For small molecules for which no enzyme is available, but against which an antibody could be raised, a competitive or sandwich immunoassay using optical or electrical transduction might be suitable. For larger molecules, such as recombinant proteins, a direct affinity sensor-based on SPR, piezoelectric, or mechanical transduction might offer a suitable detection system.

New technologies such as cantilever biosensors and nanostructured materials are leading to rapid advances in biosensor technology, bringing us closer to the ideal of a near-instant reagent-less response to any desired target analyte.

REFERENCES

Alberti, K.G., and P.Z. Zimmet. 1998. New diagnostic criteria and classification of diabetes – again? *Diabetic Medicine* 15:535–6.

Alvarez, M., and L.M. Lechuga. 2010. Microcantilever-based platforms as biosensing tools. *Analyst* 135:827–36.

Andersson, L.I. 2000. Molecular imprinting: Developments and applications in the analytical chemistry field. *J Chromatogr B Biomed Sci Appl* 745:3–13.

Arnold, F.H., and A.A. Volkov. 1999. Directed evolution of biocatalysts. *Curr Op Chem Biol* 3:54–9.

Asefa, T., C.T. Duncan, and K. Sharma. 2009. Recent advances in nanostructured chemosensors and biosensors. *Analyst* 134:1980–90.

Blankenstein, G., U. Spohn, F. Preuschoff, J. Thommes, and M.R. Kula. 1994. Multi-channel flow injection analysis biosensor system for on-line monitoring of glucose, lactate, glutamine, glutamate and ammonia in animal cell culture. *Biotechnol Appl Biochem* 20:291–307.

Borisov, S.M., and O.S. Wolfbeis. 2008. Optical biosensors. *Chem Rev* 108:423–61.

Borole, D.D., U.R. Kapadi, P.P. Kumbhar, and D.G. Hundiwale. 2002. Influence of inorganic and organic supporting electrolytes on the electrochemical synthesis of polyaniline, poly(*o*)-toluidine. and their copolymer thin films. *Mater Lett* 56:685–91.

Bosch, M.E., A.J.R. Sánchez, F.S. Rojas, and C.B. Ojeda, C.B. 2007. Recent development in optical fibre biosensors. *Sensors* 7:797–859.

Byrne, B., E. Stack, N. Gilmartin, and R. O'Kennedy. 2009. Antibody-based sensors: Principles, problems and potential for detection of pathogens and associated toxins. *Sensors* 9:4407–45.

Campanella, L., R. Attioli, C. Colapiccioni, and M. Tomassetti. 1999. New amperometric and potentiometric immunosensors for anti-human immunoglobulin G determination. *Sensors Actuators B Chem* 55:23–32.

Carmon, K.S., R.E. Baltus, and L.A. Luck. 2004. A piezoelectric quartz crystal biosensor: the use of two single cysteine mutants of the periplasmic *Escherichia coli* glucose/galactose receptor as target proteins for the detection of glucose. *Biochemistry* 43:14249–56.

Chaki, N.K., and K. Vijayamohanan. 2002. Self-assembled monolayers as a tunable platform for biosensor applications. *Biosens Bioelectron* 17:1–12.

Chaubey, A., and B.D. Malhotra. 2001. Mediated biosensors. *Biosens Bioelectron* 17:441–56.

Chinowsky, T.M., J.G. Quinn, D.U. Bartholemew, R. Kaiser, and J.L. Elkind. 2003. Performance of the Spreeta 2000 integrated surface plasmon resonance affinity sensor. *Sensors Actuators B Chem* 91:226–74.

Clark, L.C. and C. Lyons. 1962. Electrode systems for continuous monitoring in cardiovascular surgery. *Ann NY Acad Sci* 102:29–45.

Cooper, M.A., and V.T. Singleton. 2007. A survey of the 2001 to 2005 quartz crystal microbalance biosensor literature: Applications of acoustic physics to the analysis of biomolecular interactions. *J Molec Recog* 20:154–84.

Cosnier, S. 1999. Biomolecule immobilisation on electrode surfaces by entrapment or attachment to electrochemically polymerized films: A review. *Biosens Bioelectron* 14:443–56.

Cosnier, S. 2003. Biosensors based on electropolymerized films: New trends. *Anal Bioanal Chem* 377:507–20.

Darain, F., S.U. Park, and Y.B. Shim. 2003. Disposable amperometric immunosensor system for rabbit IgG using a conducting polymer modified screen-printed electrode. *Biosens Bioelectron* 18:773–80.

Diabetes Control and Complications Trial Research Group. 1993. The effect of intensive treatment of diabetes on the development and progression of long-term complications in insulin-dependent diabetes. *New Engl J Med* 329:977–93.

Dock, E., A. Lindgren, T. Ruzgas, and L. Gorton. 2001. Effect of interfering substances on current response of recombinant peroxidase and glucose oxidase—Recombinant peroxidase modified graphite electrodes. *Analyst* 126:1929–35.

Dominguez, K., I.V. Toth, M.R.S. Souto, F. Mendes, C.G. Maria, I. Vasconcelos, and A.O.S.S. Rangel. 2010. Sequential injection kinetic flow assay for monitoring glycerol in a sugar fermentation process by *Saccharomyces cerevisiae. Appl Microbiol Biotechnol* 160, 1664–73.

Doumeche, B., M. Heinemann, J. Buchs, W. Hartmeier, and M.B. Ansorge-Schumacher. 2002. Enzymatic catalysis in gel-stabilized two-phase systems: Improvement of the solvent phase. *J Mol Catal B Enzym* 18:19–27.

Erickson, D., S. Mandal, A.H.J. Yang, and B. Cordovez. 2008. Nanobiosensors: Optofluidic, electrical and mechanical approaches to biomolecular detection at the nanoscale. *Microfluid Nanofluidics* 4:33–52.

Feng, L., Y. Liu, Y. Tan, and J. Hu. 2004 Biosensor for the determination of sorbitol based on molecularly imprinted electrosynthesized polymers. *Biosens Bioelectron* 19:1513–19.

Ferreira, G.N.M., A.C. Da Silva, and B. Tome. 2009. Acoustic wave biosensors: Physical models and biological applications of quartz crystal microbalance. *Trends Biotechnol* 27:689–97.

Fortina, P., L.J. Kricka, S. Surrey, and P. Grodzinksi. 2005. Nanobiotechnology: The promise and reality of new approaches to molecular recognition. *Trends Biotechnol* 23:168–73.

French, C.E., and M.F. Cardosi. 2007. Biosensors in bioprocess monitoring and control: current trends and future prospects. In El-Mansi, E.M.T., Bryce, C.F.A., Demain, A.L., and Allman, A.R., eds., *Fermentation Microbiology and Biotechnology*, 2nd ed., CRC Press: Boca Raton, FL.

Fritz, J. 2008. Cantilever biosensors. *Analyst* 133:855–63.

Fujiwara, K., H. Watari, H. Itoh, E. Nakahama, and N. Ogawa. 2006. *Anal Bioanal Chem* 386:639–44.

Garcia-Villar, N., J. Saurina, and S. Hernandez-Cassou. 2003. Flow injection differential potentiomtric determination of lysine by using a lysine biosensor. *Anal Chim Acta*, 477:315–24.

Gonzalez-Saiz, J.M., and C. Pizarro. 2001. Polyacrylamide gels as support for enzyme immobilization by entrapment. Effect of polyelectrolyte carrier, pH and temperature on enzyme action and kinetics parameters. *Eur Polym J* 37:435–44.

Grieshaber, D., R. MacKenzie, J. Vörös, and E. Reimhut. 2008. Electrochemical biosensors—Sensor principles and architectures. *Sensors* 8:1400–58.

Gronewold, T.M.A. 2007. Surface acoustic wave sensors in the bioanalytical field: Recent trends and challenges. *Anal Chim Acta* 603:119–28.

Guan, J.-G., Y.-Q. Miao, and Q.-J. Zhang. 2004. Impedimetric biosensors. *J Biosci Bioeng* 97:219–26.

Rich, R.L., and D.G. Myszka. 2000. Advances in surface plasmon resonance biosensor analysis. *Curr Opin Biotechnol* 11:54-61.

Han, K., Z. Liang, and N. Zhou. 2010. Design strategies for aptamer-based biosensors. *Sensors* 10:4541–57.

Hartwell, A.K., and K. Grudpan. 2010. Flow based immono/bioassay and trends in micro-immuno/biosensors. *Microchim Acta* 169:201–20.

Homola, J. 2003. Present and future of surface plasmon resonance biosensors. *Anal Bioanal Chem* 377:528–39.

Hsieh, H.V., B. Stewart, P. Hauer, P. Haaland, and R. Campbell. 1998. Measurement of *Clostridium perfringens* β- toxin production by surface plasmon resonance immunoassay. *Vaccine* 16:997–1003.

Hu, P.A., J. Zhang, L. Li, Z. Wang, W. O'Neill, and P. Estrela. 2010. Carbon nanostructure-based field-effect transistors for label-free chemical/biological sensors. *Sensors* 10:5133–59.

Huang, C., K. Bonroy, G. Reekmans, W. Laureyn, K. Verhaegen, I. De Vlaminck, L. Lagae, and G. Borghs. 2009. Localized surface plasmon resonance biosensor integrated with microfluidic chip. *Biomed Microdevices* 11:893–901.

Huang, J.D., Q. Lin, J.H. Yu, S.G. Ge, J. Li, M. Yu, Z.X. Zhao, X.S. Wang, X.M. Zhang, X.R. He, L. Yuan, H.J. Yin, T. Osa, K. Chen, and Q. Chen. 2008. Comparison of a resonant mirror biosensor (IAsys) and a quartz crystal microbalance (QCM) for the study on interaction between Paeoniae Radix 801 and endothelin-1. *Sensors* 8:8275–90.

Hulme, J., C. Malins, K. Singh, P.R. Fielden, and N.J. Goddard. 2002. Internally-referenced resonant mirror for chemical and biochemical sensing. *Analyst* 127:1233–36.

Ikebukuro, K., C. Kiyohara, and K. Sode. 2005. Novel electrochemical system for protein using the aptamers in sandwich manner. *Biosens Bioelectron* 20:2168–72.

Ivansson, D., K. Bayer, and C.F. Mandenius. 2002. Quantitation of intracellular recombinant human superoxide dismutase using surface plasmon resonance. *Anal Chim Acta* 456:193–200.

Jain, S.R., E. Borowska, R. Davidsson, M. Tudorache, E. Ponten, and J. Emneus. 2004. A chemiluminescence flow immunosensor based on a porous monolithic methacrylate and polyethylene composite disc modified with Protein G. *Biosens Bioelectron* 19:795–803.

Kim, M., and M.J. Kim. 2003. Isocitrate analysis using a potentiometric biosensor with immobilised enzyme in a FIA system. *Food Res Int* 36:223–30.

Knezevic, Z., S. Bobic, A. Milutinovic, B. Obradovic, L. Mojovic, and B. Bugarski. 2002. Alginate-immobilized lipase by electrostatic extrusion for the purpose of palm oil hydrolysis in lecithin/isooctane system. *Process Biochem* 38:313–8.

Länge, K., B.E. Rapp, and M. Rapp. 2008. Surface acoustic wave biosensors: A review. *Anal Bioanal Chem* 391:1509–19.

Lawung, R., B. Danielsson, V. Prachayasittikul, and L. Bulow. 2001. Calorimetric analysis of cephalosporins using an immobilised TEM-1 β-lactamase on Ni^{2+} chelating sepharose fastflow. *Anal Biochem* 296:57–62.

Liss, M., B. Petersen, H. Wolf, and E. Prohaska. 2002. An aptamer-based quartz crystal biosensor. *Analyt Chem* 74:4488–95.

Lopez, M.A., F. Ortega, E. Dominguez, and I. Katakis 1998. Electrochemical immunosensor for the detection of atrazine. *J Molec Recog* 11:178–81.

Luo, X.L., J.J. Xu, W. Zhao, and H.-Y. Chen. 2004. Glucose biosensor based on ENFET doped with SiO_2 nanoparticles. *Sensors Actuators B Chem* 97:249–55.

Maestre, E., I. Katakis, and E. Dominguez. 2001. Amperometric flow-injection determination of sucrose with a mediated tri-enzyme electrode based on sucrose phosphorylase and electrocatalytic oxidation of NADH. *Biosens Bioelectron* 16:61–8.

Mak, K.K.W., U. Wollenberger, F.W. Scheller, and R. Renneberg. 2003. An amperometric bi-enzyme sensor for determination of formate using cofactor regeneration. *Biosens Bioelectron* 18:1095–100.

Malinauskas, A., J. Kuzmarskyte, R. Meskys, and A. Ramanavicius. 2004. Bioelectrochemical sensor based on PQQ-dependent glucose dehydrogenase. *Sensors Actuators B Chem* 100:387–94.

Martin, S.P., D.J. Lamb, J.M. Lynch, and S.M. Reddy. 2003. Enzyme-based determination of cholesterol using the quartz crystal acoustic wave sensor. *Analyt Chim Acta* 487:91–100.

McCormick, A.N., M.E. Leach, G. Savidge, and A. Alhaq. 2004. Validation of a quantitative SPR assay for recombinant FVIII. *Clin Lab Haematol* 26:57–64.

Miao, Y.-Q., J.-R. Chen, and X.-H. Wu. 2004. Using electropolymerised non-conducting polymers to develop enzyme amperometric biosensors. *Trends Biotechnol* 22:228–31.

Miao, Y.-Q., J.-G. Guan, and J.-R. Chen. 2003. Ion sensitive field effect based biosensors. *Biotechnol Adv* 21:527–34.

Miranda, M.V., M.L. Magri, A.A. Navarro del Canizo, and O. Cascone. 2002. Study of variables involved in horseradish and soybean peroxidase purification by affinity chromatography on concanavalin A-agarose. *Process Biochem* 38:537–43.

Moser, I., G. Jobst, and G.A. Urban. 2002. Biosensor arrays for simultaneous measurement of glucose, lactate, glutamate, and glutamine. *Biosens Bioelectron* 17:297–302.

Mourzina, I.G., T. Yoshinobu, Y.E. Ermolenko, Y.G. Vlasov, M.J. Schöning, and H. Iwasaki. 2004. Immobilization of urease and cholinesterase on the surface of semiconductor transducer for the development of light-addressable potentiometric sensors. *Microchim Acta* 144:41–50.

Munjal, N. and S.K. Sawhney. 2002. Stability and properties of mushroom tyrosinase entrapped in alginate, polyacrylamide and gelatin gels. *Enzyme Microb Technol* 30:613–619.

Navratil, M., J. Tkac, J. Svitel, B. Danielsson, and E. Sturdik. 2001. Monitoring of the bioconversion of glycerol to dihydroxyacetone with immobilized *Gluconobacter oxydans* cell using thermometric flow injection analysis. *Process Biochem* 36:1045–52.

Nicelescu, M., S. Sigina, and E. Csoregi. 2003. Glycerol dehydrogenase based amperometric biosensor for monitoring of glycerol in alcoholic beverages. *Analyt Lett* 36:1721–37.

Ohlson, S., C. Jungar, M. Strandh, and C.F. Mandenius. 2000. Continuous weak affinity immunosensing. *Trends Biotechnol* 18:49–52.

Okuda, J., J. Wakai, and K. Sode. 2002. The application of cytochromes as the interface molecule to facilitate the electron transfer for PQQ glucose dehydrogenase employing mediator type glucose sensor. *Analyt Lett* 35:1465–78.

Palchetti, I., and M. Mascini. 2008. Nucleic acid biosensors for environmental pollution monitoring. *Analyst* 133:846–54.

Park, I.S., D.K. Kim, and N. Kim. 2004. Characterization and food application of a potentiometric biosensor measuring β-lactam antibiotics. *J Microbiol Biotechnol* 14:698–706.

Pei, J., F. Tian, and T. Thundat. 2004. Glucose biosensor based on the microcantilever. *Analyt Chem* 76:292–7.

Peteu, S.F., D. Emerson, and R.M. Worden. 1996. A Clark-type oxidase enzyme-based amperometric microbiosensor for sensing glucose, galactose, or choline. *Biosens Bioelectron* 11:1059–71.

Piletsky, S.A., and A.P.F. Turner. 2002. Electrochemical sensors based on molecularly imprinted polymers. *Electroanalysis* 14:317–23.

Poghossian, A., M.J. Schoning, P. Schroth, A. Simonis, and H. Lüth. 2001a. An ISFET-based penicillin sensor with high sensitivity, low detection limit and long lifetime. *Sensors Actuators B Chem* 76:519–26.

Poghossian, A., T. Yoshinobu, A. Simonis, H. Ecken, H. Lüth, and M.J. Schöning. 2001b. Penicillin detection by means of field-effect based sensors: EnFET, capacitive EIS sensor or LAPS? *Sensors Actuators B Chem* 78:237–42.

Pogoroleva, S.P., M. Zayats, A.B. Kharitnov, E. Katz, and I. Willner. 2003. Analysis of $NAD(P)^+$ cofactors by redox-functionalized ISFET devices. *Sensors Actuators B Chem* 89:40–7.

Rahman, M.M., A.J.S. Ahammad, J.-H. Jin, A.J. Ahn, and J.J. Lee. 2010. A comprehensive review of glucose biosensors based on nanostructured metal-oxides. *Sensors* 10:4855–86.

Ramanathan, K., and B. Danielsson. 2001. Principles and applications of thermal biosensors. *Biosens Bioelectron* 16:417–23.

Ramanathan, K., B.R. Jonsson, and B. Danielsson. 2001. Sol-gel based thermal biosensor for glucose. *Analyt ChimActa*, 427:1–10.

Rank, M., B. Danielsson, and J. Gram. 1992. Implementation of a thermal biosensor in a process environment: On-line monitoring of penicillin V in production scale fermentations. *Biosens Bioelectron* 7:631–5.

Razumiene, J., V. Gureviciene, V. Laurinavicius, and J.V. Grazulevicius. 2001. Amperometric detection of glucose and ethanol in beverages using flow cell and immobilised on screen-printed carbon electrode PQQ-dependent glucose or alcohol dehydrogenases. *Sensors Actuators B Chem* 78:243–8.

Reddy, S.M., J.P. Jones, T.J. Lewis, and P.M. Vadgama. 1998. Development of an oxidase based glucose sensor using thickness-shear-mode quartz crystals. *Analyt Chim Acta* 363:203–13.

Rich, R.L., and D.G. Myszka. 2007. Survey of the year 2006 commercial optical biosensor literature. *J Molec Recog* 20:300–66.

Ronkainen, N.J., H.B. Halsall, and W.R. Heineman. 2008. Electrochemical biosensors. *Chem Soc Rev* 39:1747–63.

Sadik, O.A., S.K. Mwilu, and A. Aluoch. 2010. Smart electrochemical biosensors: From advanced materials to ultrasensitive devices. *Electrochim Acta* 55:4287–95.

Saha, S., M. Raje, and C.R. Suri. 2002. Sandwich microgravimetric immunoassay: sensitive and specific detection of low molecular weight analytes using piezoelectric quartz crystal. *Biotechnol Lett* 24:711–6.

Saidman, S.B., M.J. Lobo-Castanon, A.J. Miranda-Ordieres, and P. Tunon-Blanco. 2000. Amperometric detection of D-sorbitol with NAD^+-D-sorbitol dehydrogenase modified carbon paste electrode. *Analyt Chim Acta* 424:45–50.

Santano, E., M. del Carmen Pinto, and P. Macias. 2002. Xenobiotic oxidation by hydroperoxidase activity of lipoxygenase immobilized by adsorption on controlled pore glass. *Enzyme Microb Technol* 30:639–46.

Santos, A.S., R.S. Freire, and L.T. Kubota. 2003. Highly stable amperometric biosensor for ethanol based on Meldola's blue adsorbed on silica gel modified with niobium oxide. *J Electroanalytic Chem* 547:135–42.

Scheller F.W., U. Wollenberger, C. Lei, W. Jin, B. Ge, C. Lehmann, F. Lisdat, and V. Fridman. 2002. Bioelectrocatalysis by redox enzymes at modified electrodes. *Crit Rev Biotechnol* 82:411–24.

Schöning, M.J., and A. Poghossian. 2006. Bio-FEDs (Field-Effect Devices): State-of-the-art and new directions. *Electroanalysis* 18:1893–1900.

Schugerl, K. 2001. Progress in monitoring, modelling and control of bioprocesses during the last 20 years. *J Biotechnol* 85:149–73.

Suzuki, M., Y. Nakashima, and Y. Mori. 1999. SPR immunosensor integrated two miniature enzyme sensors. *Sensors Actuators B Chem* 54:176–81.

Takamizawa, K., S. Uchida, M. Hatsu, T. Suzuki, and K. Kawai. 2000. Development of a xylitol biosensor composed of xylitol dehydrogenase and diaphorase. *Can J Microbiol* 46:350–7.

Tal, Y., B. Schwartsburd, A. Nussinovitch, and J. van Rijn. 2001. Enumeration and factors influencing the relative abundance of a denitrifier, *Pseudomonas sp*. JR12, entrapped in alginate beads. *Environ Pollut* 112:99–106.

Tang, Z., Louie, R.F., Lee, J.H., Lee, D.M., Miller, E.E., and Kost, G.J. 2001. Oxygen effects on glucose meter measurements with glucose dehydrogenase- and oxidase-based test strips for point-of-care testing. *Critical Care Medicine* 29(5):1062–1070.

Tinkilic, N., O. Cubuk, and I. Isildak. 2002. Glucose and urea biosensors based on all solid-state PVC-NH_2 membrane electrodes. *Analyt Chim Acta* 452:29–34.

Tkac, J., I. Vostiar, and C.F. Mandenius. 2004. Evaluation of disruption methods for the release of intracellular recombinant protein from *Escherichia coli* for analytical purposes. *Biotechnol Appl Biochem* 40:83–8.

Tkac, J., I. Vostiar, E. Sturdik, P. Gemeiner, V. Mastihuba, and J. Annus. 2001. Fructose biosensor based on D-fructose dehydrogenase immobilised on a ferrocene-embedded cellulose acetate membrane. *Analyt Chim Acta* 439:39–46.

Uludag, Y., S.A. Piletsky, A.P.F. Turner, and M.A. Cooper. 2007. Piezoelectric sensors based on molecular imprinted polymers for detection of low mass analytes. *FEBS J* 274:5471–80.

Vidal, J.-C., E. Garcia-Ruiz, and J.-R. Castillo. 2003. Recent advances in electropolymerized conducting polymers in amperometric biosensors. *Microchim Acta* 143:93–111.

Willets, K.A., and R.P. Van Duyne. 2007. Localized surface plasmon resonance spectroscopy and sensing. *Ann Rev Phys Chem* 58:267–97.

Willner, I., and E. Katz. 2000. Integration of layered redox-proteins and conductive supports for bioelectronic applications. *Angew Chem Int Ed* 39:1180–218.

Yang, M.X., and J.R. Chen. 2002. Self assembled monolayer based quartz crystal biosensors for the detection of endotoxin. *Analytic Lett* 35:1775–84.

Yoo, E.-H., and S.-Y. Lee. 2010. Glucose biosensors: An overview of use in clinical practice. *Sensors* 10:4558–76.

Zhang, S., G. Wright, and Y. Yang. 2000. Materials and techniques for electrochemical biosensor design and construction. *Biosens Bioelectron* 15:273–82.

Zhao, Z., W. Lei, X. Zhang, B. Wang, and H. Jiang. 2010. ZnO-based amperometric enzyme biosensors. *Sensors* 10:1216–31.

Zhao, H., Y. Yuan, S. Adeljou, and G.G. Wallace. 2002. Study on the formation of the Prussian Blue films on the polypyrrole surface as a potential mediator system for biosensing applications. *Analyt Chim Acta* 472:113–21.

Ziegler, C. 2004. Cantilever-based biosensors. *Anal Bioanal Chem* 379:946–59.

Zimmet, P., K.G. Alberti, and J. Shaw. 2001. Global and societal implications of the diabetes epidemic. *Nature* 414:782–7.

14 Solid-State Fermentation: Current Trends and Future Prospects

Lalitha Devi Gottumukkala, Kuniparambil Rajasree, Reeta Rani Singhania, Carlos Ricardo Soccol, and Ashok Pandey

CONTENTS

14.1 INTRODUCTION

Solid-state fermentation (SSF) is defined as the fermentation process, which involves a solid matrix that contains enough moisture to support microbial activities; without adding water. The solid matrix could be the source of nutrients or simply a support matrix impregnated with all of the nutrients that are required for microbial growth (Pandey 1992, 1994; Singhania et al. 2009). SSF resembles the natural habitat of microorganisms and has proved to be a useful tool in the production of value-added products.

SSF processes [e.g., composting and ensiling (the preservation of green fodder in pits] recycle agricultural wastes and play a major role in the utilization renewable resources. In addition, SSF is considered to be one of the oldest fermentation processes known to have been practiced by mankind; it has been associated with the production of traditional fermented foods such as Indonesian "tempeh" and Indian "ragi". Furthermore, the use of *Aspergillus oryzae* in the making the "koji" and the use of *Penicillium roquefortii* in the manufacture of cheese in Europe, the manufacture of Soja sauce in Asia, and bread-making in Egypt are well-established technologies (Pandey 1992; also see Chapter 1 in this edition).

In the 1970s, SSF rose to prominence with the discovery of mycotoxins as a product of SSF fungal metabolism as well as the realization that SSF can be used effectively to produce protein-rich animal feed. In addition, SSF is being used for the production of high value-added products such as enzymes, organic acids, bio-pesticides, flavur enhancers, and biofuels (Table 14.1).

In the last few years, SSF has emerged as a viable technology for the bioremediation and biodegradation of hazardous compounds as well as the recycling of agriculture residues and biomass conservation. Moreover, it has been argued that SSF is the best method known method for the production of fungal spores (Pandey 1994; Ramachandran et al. 2007). However, one disadvantage is that the SSF process variables are not easily accessible or measurable.

14.2 SUITABILITY OF MICROORGANISMS FOR SSF PROCESSES

The ability of a given microorganism to grow on solid substrate depends on

- The capacity of the organism to adhere and penetrate the substrate
- The ability of the organism to assimilate complex substrates
- The level of water-activity requirement

Many bacteria and fungi are capable of growing on solid substrates (Table 14.2). However, filamentous fungi are better adapted to solid substrates because hyphal growth allows the fungi to penetrate the substrates. In addition, filamentous fungi possess a good tolerance to low water activity (A_w) and high osmotic pressure (Chundakkadu 2005).

However, bacteria and yeasts have also been used in traditional SSF processes (e.g., the production of enzymes, composting, ensiling, and food manufacturing). Yeasts have been mainly used for ethanol production and protein enrichment of agricultural residues. Measurement of the specific growth rate of a given microorganism is necessary for the understanding of fermentation kinetics; this aspect was dealt with in Chapter 2 and more extensively in Chapter 3 of this edition.

14.3 BIOMASS MEASUREMENT

Biomass is a fundamental parameter in the characterization of microbial growth. Direct measurement of biomass is not possible in SSF because microbial biomass cannot be separated from the substrate. The consumption of oxygen and the liberation of carbon dioxide (CO_2) are directly associated with cellular metabolism and as such can be used as indicators of microbial growth. Similarly,

TABLE 14.1
Applications of SSF in Different Sectors

Economical Sector	Application	Products and the Microorganism Involved
Agro-food industry	Traditional food fermentations	Koji, fermented cheese
	Mushroom production and spawn	*Agaricus, Pleurotus*
	Bioconversion byproducts	Sugar pulp bagasse, coffee pulp' silage composting, detoxication
	Food additives	Flavors dyestuffs, essential fat, and organic acids
Agriculture	Biocontrol, bioinsecticide	*Beauveria, Metarhizium, Trichoderma*
	Plant growth hormones	*Gibberellins, Rhizobium*
	mycorhization, wild mushroom	Plant inoctiation
Industrial fermentation	Enzymes production	Amylases, cellulases proteases, pectinases, xylanases
	Antibiotic production	Penicillin, feed, and probiotics
	Organic acid production	Citric acid, fumaric acid, gallic acid, lactic acid
	Ethanol production	*Saccharomyces* sp. starch malting and brewing
	Fungal metabolites	Hormones alkaloides

Source: Adapted from Raimbault, M., *Elect J Biotech*., 1:11–15, 1998. With permission.

the excretion of extracellular enzymes and the production of primary metabolites can also be used as indicators of microbial growth.

Because direct measurement of biomass is difficult; the following global stoichiometric equation is used:

$$\text{Carbon source} + \text{Oxygen} + \text{Water} + \text{Phosphorus} + \text{Nitrogen}$$

$$= \text{Biomass} + CO_2 + \text{Metabolites} + \text{Heat} \tag{14.1}$$

Measuring any one of the above component allows for determining the evolution of others if all of the coefficients are maintained constant.

14.3.1 Biomass Components

Specific components in biomass can be measured to estimate the growth of the biomass. It is necessary to determine the particular component of the cell or mycelium that is not present in the solid substrate.

14.3.2 Protein Content

Protein content of the biomass can be measured by determining the nitrogen content by the Kjeldahl method. Accurate measurement of biomass can be obtained by an amino-acid analyzer. The principal problem in determining protein content is which part of the protein present in the substrate is not consumed or transformed. This method of biomass measurement is reliable if the solid substrate has no protein or high protein content.

14.3.3 Glucosamine Content

Glucosamine is present as acetylglucosamine monomers in the chitinous cell wall of fungi. Chitin is an insoluble polymer present in the mycelium and it should be depolymerized first for glucosamine

TABLE 14.2
Examples of Products Produced by the SSF Process Highlighting the Primary Substrate and the Microorganism Used

Product	Substrate	Organism
Cellulase	Rice straw, wheat bran, wheat straw	*Aspergillus niger, Trichoderma reesei Humicola fasiolense, Penicillium* sp.
Xylanase	Rice straw, sorghum flour, rice bran	*Aspergillus niger Trichoderma harzianum Bacillus* sp. JB-99
Aroma	Cassava, soyabean, amaranth grain	*Rhizopus oryzae*
Neutral protease	Wheat bran	*Aspergillus oryzae* NRRL 1808
Pectinase	Grape pomace	*Aspergillus awamori*
α-Amylase	Wheat bran, coconut oil cake	*Aspergillus* sp. *Bacillus subtilis Aspergillus oryzae*
Lipase	Wheat bran + olive oil	*Aspergillus niger*
Phytase	Wheat bran + soy meal coconut oil cake	*Aspergillus niger Rhizopus oligosporous Mucor recemosus*
Chitinase	Wheat bran + chitin + yeast extract, wheat bran + chitin	*Trichoderma harzianum, P. chrysogenum*
Alkaline protease	Wheat bran + soy protein	*Pencillium* spp.
Lipase	Soy cake, sugarcane bagasse	*P. simplicissimum, Rhizopus homothallicus*
Alkaline protease	Green gram husk	*Bacillus* sp.
Pectinase	Wheat bran + polygalacturonic acid	*Bacillus* sp.
Aflatoxin	Cassava, rice, maize, pea nuts	*Aspergillus niger Aspergillus panasitus*
Antibiotic	Wheat, corn	*Alternaria brassicola*
Bacterial endotoxins	Coconut	*Bacillus thurungiensis*
Cephalosporin	Rice grains, barley	*Streptomyces clavuligerus*
Gibberlic acid	Wheat bran	*Fusarium moniliforme, Gibberlla fujikuroi*
Mycotoxins	Corn, wheat, oats	*Aspergillus flavus*
Penicillin	Bagasse	*Penicillium chrysogenum*
Surfactin	Soya	*Bacillis subtilis*
Tetracyclines	Sweet potato	*Aspergillus*
Zearalenone	Corn	*Fusarium moniliforme*
Citric acid	Pineapple waste	*Aspergillus niger* DS-1
γ-Linolenic acid	Rice bran and soya bean meal	*Mucor rouxii*
Mycophenolic acid	Pearl barley	*Penicillium brevicompactum*
Gluconic acid	Sugar cane molasses	*Aspergillus niger* ARNU-4
Lipopeptides + poly-γ-glutamic acid	Soybean and sweet potatoes	*Bacillus subtillus*
Cephalosporin	Rice grains, barley	*Streptomyces clavuligerus*
Gibberlic acid	Wheat bran	*Fusarium moniliforme, Gibberlla fujikuroi*
Penicillin	Bagasse	*Penicillium chrysogenum*
Surfactin	Soya	*Bacillis subtilis*
Tetracyclines	Sweet potato	*Aspergillus*
Zearalenone	Corn	*Fusarium moniliforme*
Citric acid	Pineapple waste	*Aspergillus niger* DS-1
Gamma-linolenic acid	Rice bran and soya bean meal	*Mucor rouxii*
Lactic acid	Cassava bagasse	*Lactobacillus delbrueckii*
Mycophenolic acid	Pearl barley	*Penicilliu brevicompactum*

determination. Glucosamine determination has a disadvantage of a lengthy procedure, which takes approximately 24 h. Interference with this method may occur when using complex agricultural substrates containing glucosamine in glucoproteins.

14.3.4 Nucleic Acid Determination

DNA content in the medium depends on the growth of the biomass. DNA contents increase during early growth and level off as the stationary phase is approached. Methods based on DNA and RNA determination are reliable only if the substrate has little nucleic acid and no interfering chemical present.

14.3.5 Ergosterol Measurement

Ergosterol is the predominant sterol in fungi. It is easy to determine ergosterol because it can be separated from other sterols endogenous to the solid substrate by using high-performance lipid chromatography (HPLC) and can be quantified simply by spectrophotometry. Ergosterol determination is an unreliable method to follow the growth of the microorganism as it varies with culture conditions, aeration, and substrate composition.

14.3.6 Physical Measurement of Biomass

Biomass can be measured physically by determining the electrical conductivity difference between biomass and the substrate. Pressure drop is another simple, indirect approach to measure biomass. It can be monitored online and is sensible to conidiation. Early condiophore stage makes the pressure to drop drastically and a breaking point can be easily observed.

14.4 FACTORS AFFECTING SSF

The SSF process (Figure 14.1) can be affected by various factors, and depending upon the nature of substrates and the microorganisms used they may vary from process to process. These factors can be broadly divided into biological, physicochemical, and environmental factors. Because the microorganism predominately used for SSF is a fungal species, the main focus of this discussion is also based on fungal species.

14.4.1 Inoculum Type

Mainly two types of inocula are currently used in SSF: spore inocula and mycelial inocula. There are several advantages of using spore inocula, including evenness, prolonged storability, ease of handling during inoculum preparation, etc. However, some organisms require vegetative inocula. Mycelial inocula yield a higher protein content in a fermentation system of wheat straw and *Chaetomium cellulolyticum* because of instant availability of the necessary enzymes (Abdullah et al. 1985). Another important factor is the density of the inoculum because higher density decreases the chances of contamination.

14.4.2 Moisture and Water Activity

Moisture and water content of the substrate have a critical role in the SSF process. An optimal moisture level is needed for microbial growth. Lower moisture content causes reduction in solubility of nutrients of the substrate whereas higher moisture levels can cause a reduction in enzyme yield by reduction in porosity (interparticle spaces) of the solid matrix, thus interfering with oxygen transfer. Evaporation and microbial growth reduces the water level of the substrate during fermentation and

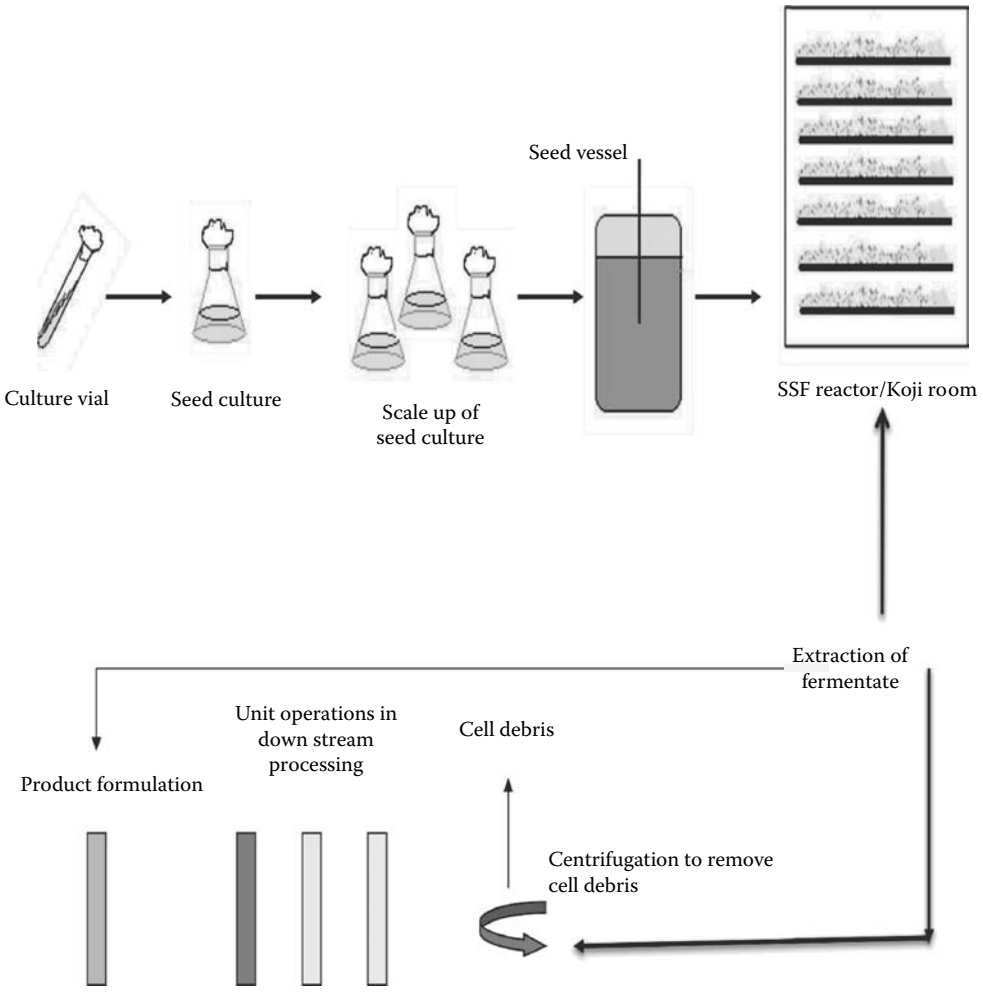

FIGURE 14.1 A schematic representation of the steps involved in a typical SSF process.

this leads to the loss of humidity. Water activity (A_w) is the accessible or available water for the growth of the microorganism. It gives the amount of unbounded water available in the immediate surroundings of the microorganism. It is closely related, but not equal to, the water content. The definition of the water activity is:

$$A_w = P_s/P_o \tag{14.2}$$

where P_s is the equilibrium vapor pressure of water within the solid substrate and P_o is the vapor pressure of pure water.

14.4.3 Temperature

Temperature is one of the most important factors affecting the SSF process. Growth of microorganisms, production of enzymes, secondary metabolite synthesis, etc., depend on temperature. Fungi can grow under a wide range of temperatures; however, the optimal temperature for growth and product formation varies greatly. When the growth and metabolic activity increase, the temperature also increases inside of the fermentor. If there is not a proper functioning system to remove the heat

generated, this will adversely affect the product formation and growth. Aeration and agitation are the two main conventional methods used to control the temperature of the substrate. In aeration, water-saturated air is used to control the temperature so that it can reduce the water activity of the substrate.

14.4.4 Hydrogen ion concentration (pH)

Because the substrate used in SSF itself having a buffering effect due to its complex chemical composition, though it is difficult to monitor the changes. Filamentous fungi and yeasts have a broad range of pH for growth that can be exploited to prevent bacterial contamination by using a low pH. To control the pH in SSF, ammonium salts have been used in combination with urea or nitrate salts to neutralize the effect of acidification and alkalization.

14.4.5 Substrates

Substrates that are meant for solid support in SSF have a common basic macromolecular structure such as cellulose, starch, pectin, lignocellulose, fibers, etc. Generally this matrix can also serve as a carbon and energy source. On the basis of the nature of the substrate, certain preparative and pretreatment steps are necessary to convert the raw substrate into a suitable form:

- Size reduction by grinding, rasping, or chopping;
- Physical, chemical, or enzymatic hydrolysis of polymers to increase substrate availability by the fungus;
- Supplementation with nutrients (phosphorus, nitrogen, salts) and setting the pH and moisture content with a mineral solution; and
- Cooking or vapor treatment for macromolecular structure predegradation and elimination of major contaminants.

Several factors influence the selection of substrates for SSF. Three crucial factors are cost, availability, and heterogeneity of the substrates. On the basis of the nature of substrates, two types of SSF systems exist. Most common among them is having natural substrates that can act as a carbon and energy source, whereas less common is inert material supplemented with a mineral medium, which can give only solid support. As already mentioned, agroindustrial residues are the best choice as a solid substrate for the growth of microorganisms and include sugar cane bagasse, wheat bran, rice bran, wheat and rice straw, coconut coir pith, tea and coffee waste, cassava waste, various pulps, etc. One of the major drawback of using these natural substrates as a solid support is that during the growth of microorganisms, physical and geometrical changes occur in the structure of the substrates that eventually lead to a reduction in the heat and mass transfer. This problem can be solved by using an inert support as a solid substrate so that it can maintain the physical structure throughout. This will give a proper control over heat and mass transfer.

14.4.5.1 Particle Size

Particle size is an important parameter for helping gaseous exchange as well as heat and mass transfer between particles. It affects the surface area-to-volume ratio of the particle that is initially accessible to the microorganism and the packing density within the surface mass. The size of the substrate determines the void space, which is occupied by air. Because the rate of oxygen transfer into the void space affects growth, the substrate should contain particles of suitable size to enhance mass transfer (Singhania et al. 2009). Smaller substrate particles would generally provide larger surface area for microbial action, but too small of particles may result in substrate agglomeration, which may interfere with microbial respiration/aeration and thus result in poor growth. Smaller particle size is also advantageous for heat transfer and exchange of oxygen and CO_2 between the

air and the solid surface. At the same time, larger particles also provide better respiration/aeration efficiency but provide limited surface for microbial action (Mithell et al. 1992).

14.4.5.2 Aeration and Agitation

Aeration and agitation play a significant role in the SSF process because they face two fundamental problems such as oxygen demand in the aerobic process and heat and mass transport phenomena in a heterogeneous system. Oxygen demand in SSF can be satisfied with relatively low aeration levels. Agitation may also promote or prevent aggregate formation of the fermenting mass depending on the nature of the solids (Lonsane et al. 1992). More is discussed in Section 14.5.3.

14.5 SCALE-UP

After standardization of unit operations on a laboratory scale, scale-up studies should be done for setting up a pilot plant. Scale-up is a crucial link in transferring laboratory-scale processes to a commercial production scale. For a process or a product to be commercialized, it has to undergo studies on four different levels: flask level (50–100 g), laboratory fermentor level (5–20 kg), pilot fermentor level (50–5000 kg), and production fermentor level (25–1000 t) (Lonsane et al. 1992). During scale-up several problems are encounted because of the size of fermentation and process productivity. Scale-up using any type of SSF bioreactor is a complicated process because of intense heat generation in the system and heterogeneity. A proper bioreactor should be selected or designed for efficient heat removal, moisture balance, aeration, agitation, etc., but because of the heterogeneity of the system, difficulties will be encountered in achieving proper mass transfer and diffusions with an increase in scale. There are several major and minor areas to be studied for a proper SSF scale-up. Important ones will be discussed in this chapter.

14.5.1 Large-Scale Inoculum Development

Generally in large-scale SSF, high inoculum density is used to reduce the risk of contamination and to produce the desired level of product in a shorter time. In large-scale production, inoculum generation itself becomes a distinct unit operation. If the inoculum has to be generated in liquid medium, large-scale fermentors should be used. In many cases, a spore inoculum is preferred over an inoculum generated in liquid medium because of ease of uniform mixing of spores with a moist solid substrate. Generating spore inocula, especially in fungal cultures, takes more time, and the chance of mutation is high because of the formation of spores in earlier inoculum development stages and their germination in the production stage (Reusser et al. 1961). To potentially reduce the chance of mutation, a minimal amount of subculturing should be done during inoculum development.

14.5.2 Medium Sterilization

Batch sterilization is preferred over continuous sterilization because there are difficulties due to the physical nature of moist solid medium in SSF systems. Solid substrates such as wheat bran are modified and more amenable to microbial growth during autoclaving. It is essential that each solid particle is heated to 121°C for 60 min in large-scale sterilization.

14.5.3 Aeration and Agitation

Aeration essentially has two functions: oxygen supply (most important) and removal of CO_2, heat, and volatile compounds. Oxygen uptake by the microorganisms present in the SSF system depends on different parameters such as porosity of the moist substrate, bed depth, perforations in the culture vessel, forced aeration, and mixing. Flow rate and air pressure matter if the aeration is forced into the culture vessel. Gaseous diffusion increases with an increase in pore size and decreases with a

reduction of diameter. The rate of aeration has to be determined by the growth requirements of the organism and heat evolution. In the case of a static fermentor, gaseous diffusion is difficult and the hyphae penetrating into the moist solid particles encounter problems in oxygen uptake. It is always good to combine aeration with agitation for efficient distribution of oxygen throughout the SSF system and proper mass transfer. Agitation also helps in efficient nutrient mixing, which is important for bacteria and yeast. Agitation may also prevent or promote aggregation of solid mass depending on the nature of the solid. Intermittent mixing and low agitation speed help to prevent damage to mycelia and reduce aggregation of solids. In certain conditions such as tray fermentation agitation is not possible and these are usually kept as static systems.

14.5.4 Heat removal and moisture balance

Heat generated is proportional to the metabolic activity in the system. Generally there is an increase in temperature in the center of the bed that is higher by 17–20ºC compared with the set value. It is very difficult to control the temperature of the system just by placing it in a temperature-controlled room or by passing cooling water through the jacket of the fermentor. Heat removal through conduction and convection is not effective because of a low or no rate of agitation and poor thermal conductivity of solid substrates. Evaporative cooling is beneficial but has the disadvantage of moisture loss (Narahara et al. 1984). Moisture of the substrate should also be maintained properly for better productivity. This can be achieved with a high initial moisture content of the medium and a humidified atmosphere in the fermentor (90–98%) (Ahmed et al. 1957).

14.5.5 pH control

In large-scale solid-state fermentation it is tough to have a continuous monitor of pH change and hence it is advised to use buffers in the medium (see Section 14.4.4 for more detail). In open systems such as tray fermentation, aseptic operation is not possible and therefore pH and moisture play a crucial role in reducing the risk of contamination.

14.5.6 Product Recovery

Recovery of product from solid substrates is a highly complex and labor-intensive process. Product should be leached out from the solid substrate using a proper solvent system. Efficiency of product recovery depends on temperature, pH, incubation time, agitation speed, type of solvent, miscibility of the product in the solvent, ratio of solids to solvent, etc. There are several types of leaching techniques, including percolation, multiple-contact countercurrent leaching, pulsed plug-flow extraction in column, hydraulic pressuring, and supercritical fluid extraction. A proper economically feasible leaching technique should be selected based on the fermentation product.

14.6 MODELING IN SSF

The concept of modeling in SSF is the search for mathematical expressions that represent the system under consideration. The objective of these expressions is to establish the relationships or functions between two different variables that characterize the system. This is to ascertain the validity of the system, to establish different parameters that characterize a particular process, and to find appropriate mechanisms for development and control of the process (Pandey et al. 2001). Modelling of bioreactors used in SSF processes can play a crucial role in the analysis, design, and development of bioprocesses based on phenomena that encompass various applications ranging from the production of enzymes to the treatment of agroindustrial residues. Existing models of SSF processes describe coupled substrate conversion and diffusion and the consequent microbial growth, neglecting many of the significant phenomena that are known to influence SSF. As a result, the available models fail

to explain the generation of numerous products that form during any SSF process and the outcome of the process in terms of the characteristics of the final product.

Information regarding modeling in SSF has been limited because of the unavailability of a suitable method for direct measurement of microorganism growth because of the difficulty in separating microorganisms from the substrate and determination of the rate of substrate utilization. Among the several approaches to tackle this problem, an important one has been to use a synthetic model substrate. It is well known that the fermentation kinetics are extremely sensitive to the variation in ambient and internal gas compositions. Therefore, the cellular growth of the microorganisms can be determined by measuring the change in gaseous compositions inside of the bioreactor.

The importance of models in SSF, as in any chemical or biochemical process, lies in the establishment of the parameter values that explain a particular process; the basis to evaluate the process, including the way in which a process could be economically scaled-up; and the design and control criteria. The developments of models in SSF focused on the representation of the microbial activity (kinetic patterns and thermodynamic concerns), studies of the problems of heat and mass transfer in the solid systems, the connection between the two above systems, and the selection of the best type of the fermentor.

14.7 TYPES OF SSF BIOREACTORS

SSF bioreactor design largely depends on the solid matrix. Some of the important criteria while designing a SSF include perfect control systems for temperature, airflow, and humidity; maintenance of aseptic conditions for preventing contamination; maintenance of homogenous water activity, temperature, and composition so that microbes can grow uniformly; and quick and efficient removal of harmful metabolites for labor saving and easy handling. SSF processes could be operated in batch, fed-batch, or continuous modes, although batch processes are the most common.

Two categories of bioreactors exist for SSF processes: (1) laboratory-scale bioreactors that use quantities of dry solid medium from a few grams up to few kilograms, and (2) pilot- and industrial-scale bioreactors where several kilograms up to several tons are used. In laboratory-scale bioreactors, Petri dishes, jars, wide-mouth Erlenmeyer flasks, Roux bottles, and roller bottles can be used as fermentors for SSF. In laboratory-scale bioreactors, maintenance of completely aseptic conditions is possible to a certain extent; however, aeration and agitation are not possible. Several industrial-level SSF bioreactors have been designed, but all of them invariably face the problem of heat generation and its removal along with handling difficulties.

14.7.1 Shallow-Tray Fermentor

This is one of the technologies used in China and other countries for SSF. The shallow tray can be made up of wood, bamboo, metal, or plastic. The bottom of the tray is made up of sieve plate or wire mesh to help airflow. The tray is 30–50 mm. A suitable space is left between two trays. The shallow-tray fermentor needs to be kept in a sterile environment to prevent contamination. Low investments and simplicity in construction are the two main advantages of using shallow-tray fermentors. Figure 14.2 shows the shallow-tray fermentor schematic representation. Air saturated with water vapor was blown into the bottom of a culture vessel, and the exhaust air was withdrawn at the top.

14.7.2 Column Fermentors

A column fermentor is a fixed-bed reactor. Solid medium is put into the column with entries at both ends for aeration. Figure 14.3 shows a column fermentor developed by Saucedo-Castaneda and colleagues (1990). Sterile air can be supplied by a radial or axial gradient method. The water activity is maintained by humidified air. The temperature for the solid fermentation is monitored

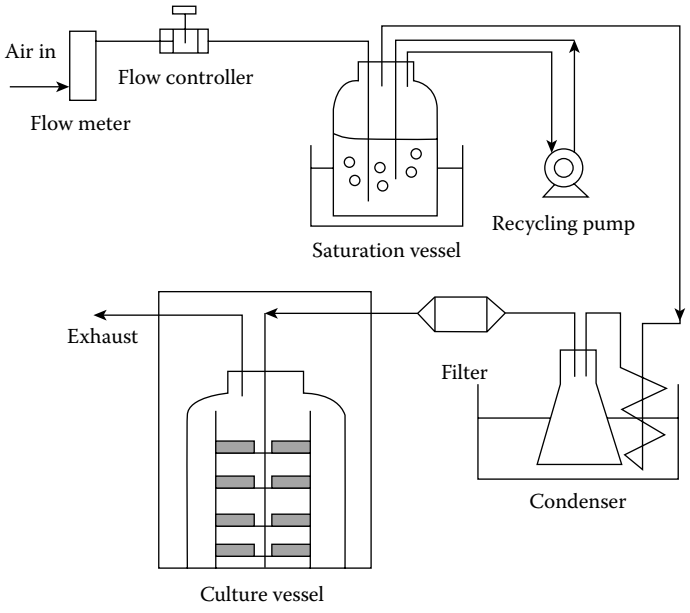

FIGURE 14.2 Shallow tray fermentor used for solid-state cultivation.

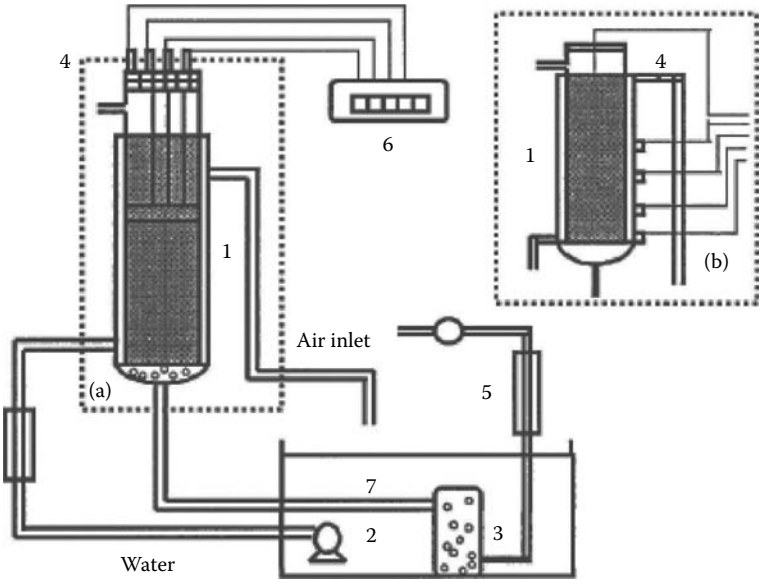

FIGURE 14.3 Column fermentor for SSF: (a) radial gradient and (b) axial gradient. Column fermentor (volume = 1 L, radius = 6 cm, length = 35 cm): 1, jacket fermentor; 2, water pump; 3, humidifier; 4, thermocouples; 5, pressure and airflow controls; 6, temperature display device; 7, water bath.

and controlled by recycling water in the jacket from an isothermal bath. In a fixed-bed column fermentor, the oxygen transfer and CO_2 dissipation are improved by forced convection. However, it is difficult to regulate the water activity and temperature in the fixed bed. In addition, handling the solid materials in a column fermentor is a huge problem, and scale-up to a column fermentor is troublesome.

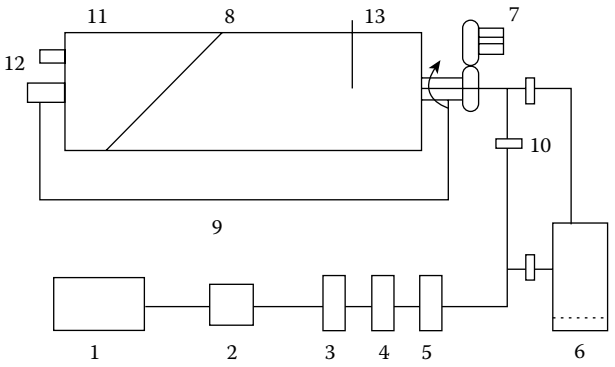

FIGURE 14.4 Rotation drum bioreactor: 1, air compressor; 2, pressure regulation valve; 3, oil separator; 4, air filter; 5, air heater; 6, atomizer; 7, rotating device; 8, rotary-drum fermentor; 9, fermentor stand; 10, gas valve; 11, fermentor cover, 12, air outlet; 13, thermister (Pandey, A., *Process Biochem*, 27:109–17, 1992).

14.7.3 Rotating Drum Bioreactors

Drum bioreactors are mainly of two types: continuously rotating and discontinuously rotating drums. Continuously rotating drum reactors are mainly used in laboratory-scale and prepilot-scale bioreactors. They consist of a rotating drum that is meant for proper mixing of the substrate particles. When the rotation rate of the drum is increased, it can affect the mycelium growth presumably because of shear effects (Fung et al. 1995). The largest bioreactor cited in the literature was a stainless steel rotating drum (Ø 56 and 90 cm long) that used 10 kg of steamed wheat bran as substrate (Stuart et al. 1998) for kinetic studies of *Rhizopus*. In the case of discontinuously rotating drum reactors, the operating principle is intermittent mixing and static conditions, which help to reduce the rotation rate. During the static period, the reactor is similar to tray reactors. In addition to the above, rocking drum bioreactors, gas solid fluidized bed reactors, continuously stirred aerated bed reactors, etc., are also available, having continuous mixing and forced aeration. It leads to overcome few limitations such as the oxygen mass transfer is enhanced and overheating is prevented. The heterogeneity of the system is also reduced to a large extent as compared with static trays or a packed-bed fermentor. Figure 14.4 shows a rotating drum bioreactor used by Tao et al. (1997) for cellulase production. However, during scale-up major limitations with all of the SSF bioreactors include the maintenance of a sterile environment, irregular growth, and heat removal, which necessitated further research toward engineering of SSF bioreactors.

14.8 CHALLENGES IN SSF

The SSF process has advantages such as higher fermentation productivity; higher end concentration of products; higher product stability; lower catabolic repression; cultivation of microorganisms specialized for water-insoluble substrates or mixed cultivation of various fungi; and last but not least, lower demand on sterility because of the low water activity used in SSF. But at the same time there are many known and hidden challenges associated with its operation. The most important challenge to be considered is downstream processing. Separation of product from the solids is a technically and economically challenging process, and although there is much advent in biochemical engineering, SSF is generally being used only for the production of less-purity-needed metabolites.

Another well-known and difficult challenge of SSF is bioreactor design for large-scale production. The design of bioreactor varies with substrate, organism, type of product, etc. With the present advanced technology, several bioreactors are designed with online facility monitoring of several parameters as well as heat and mass transfer. Monitoring biomass growth and its estimation is

necessary for kinetic studies of fermentation. However, in SSF, separation of biomass from solid mass is not possible, and accurate measurement of biomass is almost impractical. There are several indirect methods to measure biomass, and almost every method has its own drawback. In addition to these major drawbacks, there are several other minor drawbacks such as solid handling, waste management, etc. If fermented solid itself is not the final product, waste-treatment expenses add heavily to the product cost. Various management strategies such as recycling of the spent solid as animal feed or biogas generation could be beneficial.

SUMMARY

- SSF is widely used in the production of many products, including animal feed, biofuel, and industrial and pharmaceutical chemicals.
- More recently, SSF has proved to be a great success in the production of biologically active secondary metabolites.
- In some applications, SSF has emerged as an attractive alternative to submerged fermentation.
- SSF is currently being used for bioremediation, bioleaching, biopulping, and biobeneficiation.
- SSF stands to play a major role in the conversion of renewable resources in general and agricultural wastes in particular into useful products.
- Full exploitation of SSF in bioprocess technology awaits further investigation to overcome the various limitations and hurdles that have been discussed in this chapter.

REFERENCES

Abdullah, A.L., R.P. Tengerdy, and V.G. Murphy. 1985. Optimization of solid-state fermentation of wheat straw. *Biotechnol Bioeng* 27:20–27.

Ahmed, S.Y., B.K. Lonsane, N.P. Ghildyal, and S.V. Ramakrishna. 1957. Design of solid state fermentor for production of fungal metabolites on large-scale. *Biotechnol Techniques* 1:97–102.

Chundakkadu, K. 2005. Solid-state fermentation systems: An overview. *Crit Rev Biotechnol* 25:1–30.

Fung, C.J., and D.A. Mitchell. 1995. Baffles increase performance of solid state fermentation in rotating drums. *Biotechnol Tech* 9:295–8.

Lonsane, B.K., G. Saucedo-Castaneda, M. Raimbault, S. Roussos, G. Viniegra-Gonzalez, N.P. Ghildyal, M. Ramakrishna, and M.M. Krishnaiaha. 1992. Scale up strategies for solid state fermentation systems. *Process Biochem* 27:259–73.

Mitchell, D.A., Z. Targonski, J. Rogalski, and A. Leonowicz. 1992. Substrates for processes in solid substrate cultivation. *App Biotech* 29–52.

Narahara, H., Y. Koyama, T. Yoshidu, P. Atthaspunna, and H.J. Taguchi. 1984. Control of water content in a solid state culture of *Aspergillus oryzae. Ferment Tech* 62:453–9.

Pandey, A. 1992. Recent process developments in solid-state fermentation. *Process Biochem* 27:109–17.

Pandey, A. 1994. Solid-state fermentation: An overview. In Pandey, A. ed., *Solid State Fermentation*, pp. 3–10. New Delhi, India: Wiley.

Pandey, A., C.R. Soccol, J.A.R. Leo, and P. Nigam. 2001. *Solid-State Fermentation in Biotechnology*, p. 221. New Delhi, India: Asiatech Publishers.

Raimbault, M. 1998. General and microbiological aspects of solid substrate fermentation. *Elect J Biotech* 1:11–15.

Ramachandran, S., P. Fontanille, A. Pandey, and C. Larroche. 2007. Spores of *Aspergillus niger* as reservoir of glucose oxidase synthesized during solid-state fermentation and their use as catalyst in gluconic acid production. *Lett Appl Microbiol* 44:155–60.

Reusser, F., H.I. Koepseil, and G.M. Savage. 1961. Degeneration of *Streptomyces niveus* with repeated transfers. *Appl Microbiol* 9:342–5.

Saucedo-Castaneda, G., M. Guierrez Rojas, G. Bacquet, M. Raimbault, and G. Viniegra Gonzalez. 1990. Heat transfer simulation in solid substrate fermentation. *Biotechnol Bioengin* 35:802.

Singhania, R.R., A.K. Patel, C.R. Soccol, and A. Pandey. 2009. Recent advances in solid-state fermentation. *Biochem Eng J* 44:13–8.

Stuart, D.M., D.A. Mitchell, M.R. Johns, and J.D. Lister. 1998. Solid-state fermentation in rotating drum bioreactors: Operating variables affect performance through their effects on transport phenomena. *Biotechnol Bioeng* 63:383–91.

Tao, S., L. Beihui, and L. Zuohu. 1997. Enhanced cellulase production in fed-batch solid-state fermentation for *Trichoderna viride* SL-1. *J Chem Tech Biotechnol* 69:429–32.

15 Bioreactors: Design, Operation, and Applications

Anthony R. Allman

CONTENTS

15.1 BIOREACTORS: AN OVERVIEW

This chapter aims to provide an understanding of the factors governing bioreactor design, operation, and applications with special emphasis on the following aspects:

- Unraveling and describing the scientific principles underpinning bioreactor design, bioreactor instrumentation, and control
- Describing bioreactor assembly and operation
- Describing how a bioreactor can be adapted to a range of specific applications

15.2 COMPONENT PARTS OF BIOREACTORS

The main subdivisions of a standard stirred tank reactor (STR) are

- A base unit connected to pipe work components for control of temperature, stirring, gasing, and additions of reagents
- A culture-vessel with fittings and ports to aid gas transfer, liquid addition/removal, mixing, sampling, and fitting of sensors
- Peripheral equipment such as reagent containers, additional sensors, and special systems for sterilization, cooling, separation, and removal of culture constituents
- Instrumentation for measurement and/or control of key process parameters with links to supervisory software and remote control facility

The example used to illustrate this aspect is the smallest and simplest of all fermentation systems (i.e. a bench-top bioreactor). More specialized versions for the propagation of photosynthetic organisms and fermentation of solid substrates will also be described, albeit briefly.

A range of basic modifications are also illustrated to facilitate reconfiguration and adaptation of bioreactors for the applications discussed in the following sections.

15.3 COMPONENT PARTS OF A "TYPICAL" VESSEL

The vessel can be constructed as a single-walled cylinder of borosilicate glass or as a glass-jacketed system, which typically has a round bottom. The top plate is made from "316"L stainless steel and is compressed onto the vessel flange by nuts or a quick-release clamping system. A seal separates the vessel glass from the top plate. Port fittings of various sizes are provided for insertion of probes, inlet pipes, exit gas cooler, cold fingers, sample pipes, etc. These work by compressing the sides of the probe/pipe against an O-ring seal. A special inoculation port will have a membrane seal held in place with a collar. Culture can be withdrawn into a sampling device or a reservoir bottle via a sample pipe situated in the bulk of the bioreactor fluid. A gas sparger is also fixed into the top plate and this terminates in a special assembly that ensures that incoming air is dispersed efficiently within the culture by "Rushton-type" impellors fixed to the drive shaft (see Box 15.1). A drive motor provides stirring power to the drive shaft and is usually fitted directly to the drive hub on the vessel top plate. An exit gas cooler works as a condenser to remove as much moisture as possible from the gas leaving the bioreactor to prevent excessive liquid losses during the fermentation and wetting of the exit air filter.

A narrow platinum resistance **Pt-100 temperature sensor** completes the list of minimum essential fittings. Heating is achieved through direct heating using a heater pad or by circulating warm water around the vessel jacket. If direct heating is used, a cold finger is used to control temperature by cooling the vessel contents (more than one could be used, if need be).

Pt-100 temperature sensor: A platinum resistance electrode used to give an accurate indication of vessel temperature by relating changes in electrical resistance of the sensor to temperature.

The sensors are directly coupled through a thread on the body of the electrode, as is the case in the gel-filled type of pH electrode, or through a special fitting on the vessel top plate, which provides a clamping mechanism for long sensors. Another system involves the use of a simple compression fitting that holds the body of the electrode, as with the foam probe. In this case, the height is variable and the tip of the probe has to be adjusted so that it is above the surface of culture. Figure 15.1 illustrates all of the main components of a typical stirred tank bioreactor.

BOX 15.1 MIXING AND AERATION

Mixing is important for heat transfer, homogenous environment, and keeping solids in suspension. Rheology describes how a culture behaves when subjected to shear forces. There are two main types of mixing behavior:

1. *Newtonian:* The viscosity of the culture is independent of shear force.
2. *Non-Newtonian:* The viscosity varies with shear forces. These are usually fungal broths that can alter in apparent viscosity during fermentation. The increasing viscosity can affect bubble retention and, in turn, gas transfer, as described below.

AERATION

The key parameter is oxygen transfer rate (OTR), often expressed as a related parameter, kLa, as hr^{-1}. kLa is a combination of the film resistance between the gas and liquid phases in an aerated fermentor and the surface area in contact between the gas and the liquid. Essentially, the more and smaller gas bubbles you have, the better the gas will be dissolved and the better the kLa value achieved for a given vessel configuration. For maximum time for gas exchange with sparging, a tall vessel is better (hence the typical aspect ratio of 3:1). With the use of oxygen supplementation, a shorter vessel can be used. Similarly, a low aspect ratio 2:1 (or even 1:1) was used for a cell culture vessel for gas transfer via the headspace, but now sparging at a low gas flow rate has been almost universally adopted so a taller vessel is an advantage.

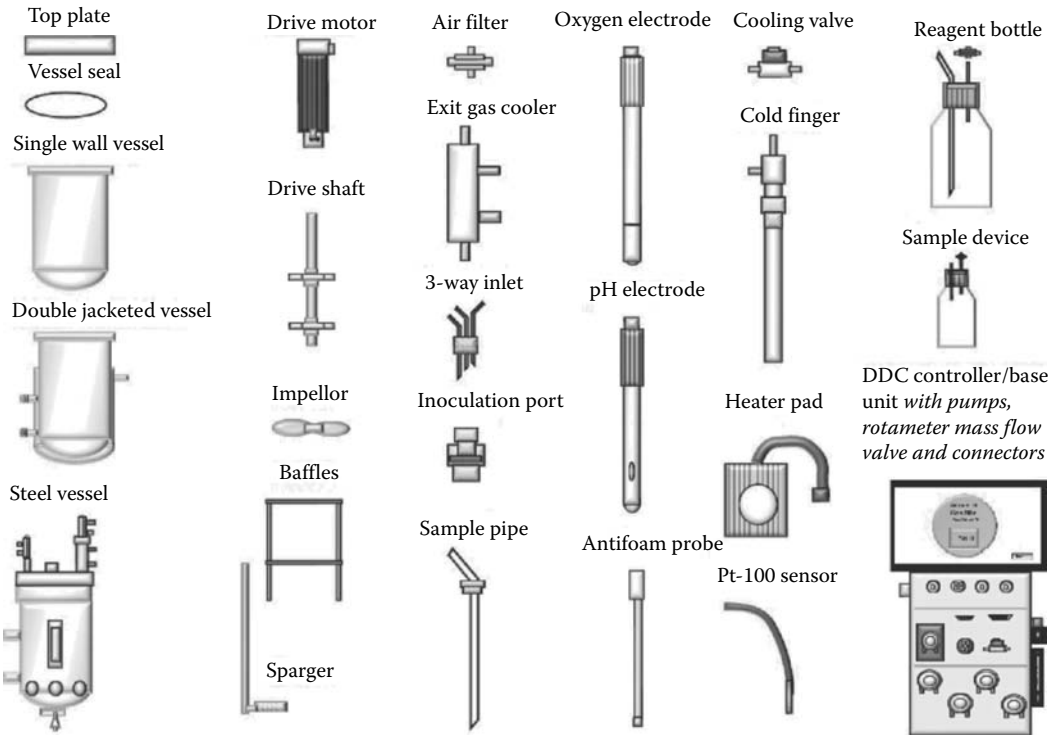

FIGURE 15.1 Major components of a bioreactor.

15.4 PERIPHERAL PARTS AND ACCESSORIES

15.4.1 Peristaltic Pumps

Peristaltic pumps are normally part of the instrumentation system for pH and antifoam control. The flow rate, which depends upon the bore size of the tubing used, is controlled through "shot and delay" feeding mechanism. The feed is delivered via peristaltic tubes, which link the reservoir bottles to the vessel multiway inlet and the tubing can be aseptically connected after autoclaving.

For accurate monitoring of additives into the culture vessel, the respective reservoir bottles can be placed on analytical balances, thus allowing accurate additions of reagents.

15.4.2 Medium Feed Pumps and Reservoir Bottles

Media feed pumps are often of variable speed to cover the desired possible range of flow rate. Pump speed can be set manually or computer controlled. The reservoir bottles are usually large (e.g., 5–20 L) but are prepared in the same way as normal reagent bottles. These bottles may have to be changed several times during the course of a fermentation experiment and as such tubing is fitted with aseptic coupling devices. A harvest pump is often used to remove culture fluid from the bioreactor vessel into a storage reservoir.

15.4.3 Rotameter/Gas Supply

The flow of gas supply, which is oil and dust free, is controlled by a flow meter (**rotameter**) fitted with a pressure regulator valve to ensure safety. A sterile filter (usually 0.22 μm) is fitted to ensure the removal of bacteria in the air delivered to the sparger and in turn the culture. Another filter is fitted onto the exit gas cooler (often 0.45 μm) prevents the releasing of microbes into the laboratory. In fermentation processes leading to the release of unpleasant odors or potentially dangerous gases, an extraction system should be fitted to ensure the safe disposal of the undesirable or harmful gases.

Rotameter: A variable area flow meter that indicates the rate of gas flow into a bioreactor. A manual valve is adjusted until an indicator ball rises up a tube of increasing width until the required flow rate value is reached on a calibrated scale marked on the glass wall of the tube. The bottom of the ball should rest on the calibration line.

15.4.4 Sampling Device

This allows culture fluid to be withdrawn for analysis aseptically; at intervals decided by the user.

15.5 ALTERNATIVE VESSEL DESIGNS

Alternatives to the conventional stirred tank bioreactor have been designed to overcome the configuration problem, which does not allow for adequate growth of certain organisms (e.g., animal cells are often disrupted by shear forces in bioreactors with turbine impellors). Also, large-scale fermentation necessitates different designs of bioreactor for effective and economical reasons (e.g., production of large quantities of single-cell protein is cheaper on a large scale if air lift bioreactors are used to eliminate energy costs associated with a drive system). Several of these special designs are available at the bench/pilot scale of operation to allow for small-scale research into the suitability of a particular method.

The use of lights surrounding a standard stirred tank bioreactor vessel is somewhat critical because it is essential in algal growth. Variable light intensity and the ability to simulate day/night cycles are common requirements. Special designs for commercial-scale production of photosynthetic organisms exist, but these tend to be simple tubes or tubs with external light sources. The high

yield of oil in some species of algae (up to 60% of biomass) makes them an ideal resource for biofuel generation; a domain that is currently enjoying a center stage in biotechnology.

15.5.1 Air Lift

Air-lift fermentors are generally tall and thin with a vessel **aspect ratio** of approximately 10:1 (height-to-base diameter). It does not contain stirring blades and sometimes may have a "conical" section at the top end of the vessel to facilitate effective gas exchange. Sensors are generally mounted on a steel base at the top end or base of the vessel. The culture fluid is aerated, and in turn mixed, by a stream of air that enters near the base of the vessel. A hollow pipe or draft tube in the center of the vessel provides a "riser" for the air (which is full of bubbles) to move upward to the top of the vessel. If a very large vessel is used, the hydrostatic head of the fluid provides a pressurizing effect to the lowest region of the culture where the air enters and so increases the dissolved oxygen concentration. The draft tube is usually double-walled to allow for heating and cooling using a thermocirculator system.

Aspect ratio: The ratio of the height of a fermentation vessel to its diameter. Typically, vessels for microbial work have an aspect ratio of 2.5 up to 3:1, whereas vessels for animal cell culture tend to have an aspect ratio closer to 1:1.

When the aerated culture fluid reaches the top of the draft tube, it "spills over" and begins to fall toward the bottom of the vessel via the space between the outer wall of the draft tube and the inner wall of the vessel. A large headspace above the top of the draft tube allows for easy gas transfer from the liquid to the gas phase, which in turn causes the density/specific gravity of the liquid to increase and so it descends down to the bottom of the vessel. The descending liquid returns to the base of the vessel where it is re-aerated and begins to rise again (see Figure 15.2).

A common use of airlift bioreactors is the growth of shear-sensitive cells such as plant and animal cell cultures. Also, the design has been used for the production of large amounts of biomass as single-cell protein.

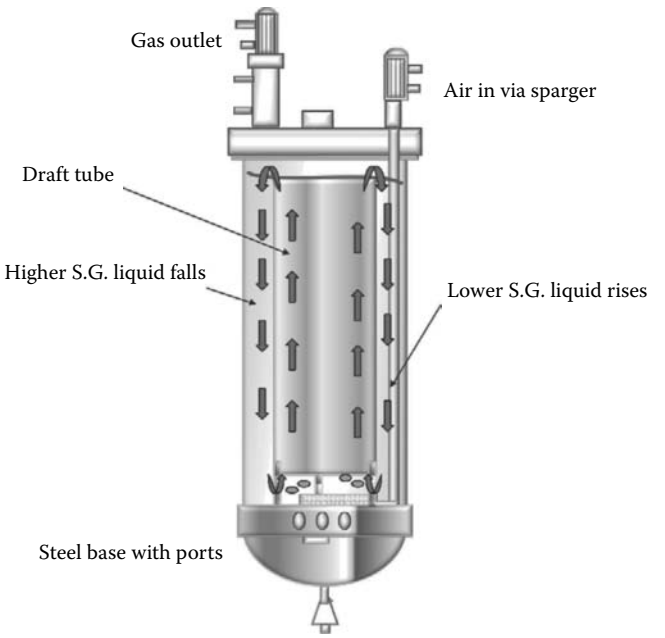

FIGURE 15.2 Air lift bioreactor.

15.5.2 Fluidized Bed, Immobilized, and Solid-State Systems

This important area of bioreactor design and application will only be mentioned in outline here because Chapter 14 is devoted to this aspect.

The microbes/cells are trapped in a physical medium (e.g., alginate beads) and held in the vessel by a mesh. The medium is fed and recirculated via a pump to give a continuous/semicontinuous flow to allow the entrapped cells to affect the desired biochemical reactions without the cells being washed out along with spent medium. This system is well suited to growth of animal cells on the smaller scale and has large-scale application in effluent/decontamination treatment plants.

Some animal cell lines benefit from being immobilized on polymer beads in a STR system because it provides a surface for attachment of anchorage-dependent cells and affords protection to the cells against damage by bubbles and shear forces. Bacteria and fungi can also be grown in immobilized systems, using entrapment, or on solid surface, membrane bioreactors.

Solid-state fermentation is a biological process in which solid or semi-solid substrates are used for growth. In some designs, the solids remain static on trays, whereas others require mixing to provide aeration and homogeneous distribution of added reagents. The substrate is rotated or mechanically mixed and temperature control is achieved by air and water circulation. It is possible to create *in situ* sterilizable versions of these systems using direct injection of steam into the vessel and rapid airflow to provide subsequent drying.

Commercial-scale bioremediation often involves the heating of solid-substrate containing mounds using heat blowers. Once heated to the correct temperature, the mound is mixed mechanically and the reagents fed via large-bore size tubing. For biofuel and biogas applications, the commercial process may involve passage of materials through different vessels and/or physical/chemical pretreatment to release fermentable products from nonbiodegradable materials. Applications include the bioremediation of soils to remove toxins or toxic wastes, which improves the efficiency of composting for fertilizer. Furthermore, the production of some enzymes using solid-state fermentation proved very advantageous; in this case, *in situ* sterilization is advantageous. As expected, conventional instrumentation is difficult when the whole vessel rotates; exit gas analysis is commonly used to follow the progress of a process (see Section 15.10.2).

15.5.3 Hollow Fiber

In this case, the cells are embedded in fibers contained in a cartridge bathed in circulating culture medium. This is often used for mammalian cell culture, where anchorage-dependent cell lines can perfuse in oxygenated medium. An extension of this method is to use cartridges containing two different bundles of fibers and allow dissolved gases and metabolites to be exchanged without cells crossing the barrier. A closely related application is microfiltration, in which medium is passed through an external cartridge to allow for the elution of small quantities of medium for biochemical analysis or the recovery of desired products (e.g., a protein).

15.5.4 *In Situ* Sterilizable Bioreactors

Sterilization of large bioreactor vessels (>10 L) is difficult and impractical. Such vessels are currently made of stainless steel (316 L) so that it can be sterilized *in situ* using an electrical heating element or steam generator, which may be built into the base unit of the bioreactor. The heating for the vessel is normally provided via a double jacket, which can be the full length of the vessel or cover just the bottom third. Internal coils within the vessel are sometimes used for heating and/or cooling where rapid changes in temperature are needed. Because the vessel body is steel, a sight window and a light have to be fitted to see the culture.

Most animal cell culture vessels are top-driven to minimize shear damage to the delicate cells. The vessel top plate has port fittings, which use a membrane seal and port closure.

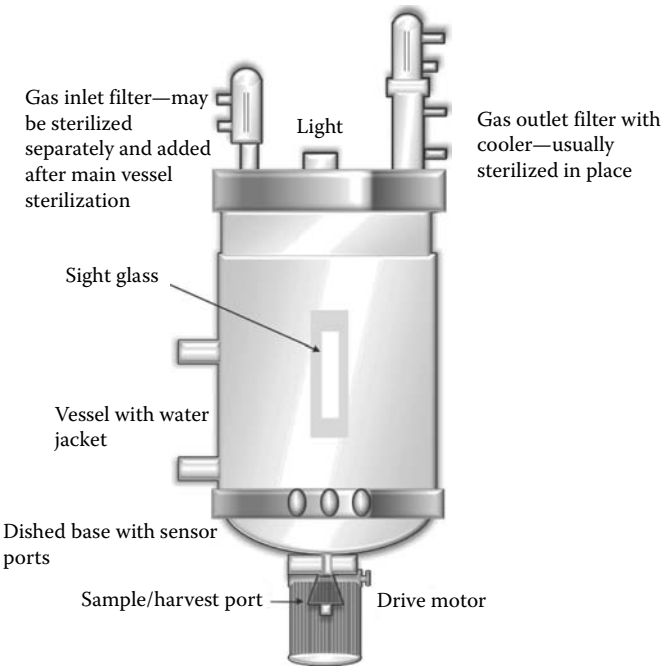

FIGURE 15.3 Major components of an ISS bioreactor vessel.

Options such as "push valves" and steam-sterilizable inlet lines (which create a "sterile cross" of valves and pipe work) are becoming used more commonly to remove the need for needle injection of transfer lines for medium, reagent, etc.

The medium in the vessel is heated to 151ºC or above and often supplies the steam for sterilization of the exit gas filter (see Figure 15.3). The steam for vessel sterilization can be relatively impure, but sterilization of air filters and valves has use clean steam (i.e., it must pass through a 5-μm filter).

Another increasingly common element in the configuration of larger in situ sterilizable (ISS) systems is the use of clean-in-place (CIP) systems. A CIP system may be integrated into the support frame or can be a freestanding unit, which can be transferred from one vessel to another as needed. Typically, a powerful centrifugal pump circulates liquid through the vessel using spray balls located near the top to clean the inner walls of the vessel. Several different cycles are used to ensure adequate level of cleanliness, including rinsing with deionized water and cleaning with a caustic solution followed by rinsing with pure water. Full cleanliness of the vessel is ensured by measuring the electrical conductivity of final effluent after cleaning and the water is used.

15.5.5 Containment of Pathogenic and/or Genetically Modified Organisms

An ISS bioreactor may have to be altered in certain ways if the organism to be cultured is pathogenic or genetically modified. The alterations are designed to contain any release of microbes into the environment by using features such as a double mechanical seal, magnetic coupling, additional air filters, extra foam control systems, and special sampling devices. More elaborate precautions include steam lines to all vessel fittings and direct discharge of any released liquid to a tank of disinfectant (a "kill tank"). Applications for this sort of technology are medical research and vaccine manufacturing.

15.6 BIOREACTOR INSTRUMENTATION

Modern instrumentation now almost exclusively uses digital controllers of one sort or another. These will be described in outline below. The trend is toward color touch screens with a graphical user interface, and this can accomplish several functions previously reserved for remote software (e.g., creation of synoptic displays and real-time trend graphs).

15.6.1 Digital Controllers—Embedded Microprocessor

The measurement sensors link directly to the single control module, and several parameters are displayed immediately on a single screen. Control is by direct action on heaters, valves, etc. (direct digital control, or DDC). The microprocessor is permanently embedded in the instrumentation and may even be a single chip. Operation is usually via a simple menu system or a link to a higher-level HMI (human machine interface) such as touch screen may be provided.

15.6.2 Digital Controllers—Process Controller

A complete process controller (usually from a production control environment) is added to a housing containing all of the signal processing and control actuators for the bioreactors. It exerts control in the same way as an embedded controller but is essentially a "plug-in" component. The controller is usually programmed using simple commands to input set-point values, etc. Again, links may be provided via common industrial communications protocols to a local or remote HMI providing additional functions.

Digital controller: A digital controller uses a processor to store information about control output characteristics as mathematical algorithms. Consequently, changing the characteristics of such a controller is achieved by reprogramming the processor.

15.6.3 Digital Controllers—Direct Computer Control

In this case, there is no external instrumentation or processor between the actuators and the computer. A printed circuit board with operational amplifiers for the probe input signals is the only electronic part that may be present in the bioreactor base unit. A special input/output (I/O) card is needed for the computer, which allows the input values to be accessed by the measurement and control software and sends signals out to operate relays (e.g., to turn a heater on or off). The processing power and speed of modern PCs make them more than capable of replacing separate Programmable Logic Controllers (PLCs) or embedded controllers.

The advantage with this system is that the computer display and control software is totally integrated with the bioreactor. Fewer components mean that these systems are usually less expensive. However, the bioreactor cannot be used without the computer and there is no backup for the control systems should the computer develop a fault and "hang". This system may be especially useful when multiple bioreactors are controlled as a single system.

15.7 COMMON MEASUREMENT AND CONTROL SYSTEMS

15.7.1 Speed Control

Speed control relies on the feedback from a **tachometer** located within the drive motor. Actual speed in revolutions per minute is displayed, as determined by the tachometer signal. A power meter is sometimes included and indicates how hard the motor has to work to maintain the set speed and, thereby, indirectly, the viscosity or "density" of the culture fluid. A DC, low-voltage (24–50 V) motor is often used for safety reasons. Speed range is typically from 50 to 1500 rpm for bacterial systems and 10–300 rpm for cell culture units. It is now

Tachometer: An electronic device usually integrated into a drive motor to provide feedback about rotational speed in the form of an analog signal.

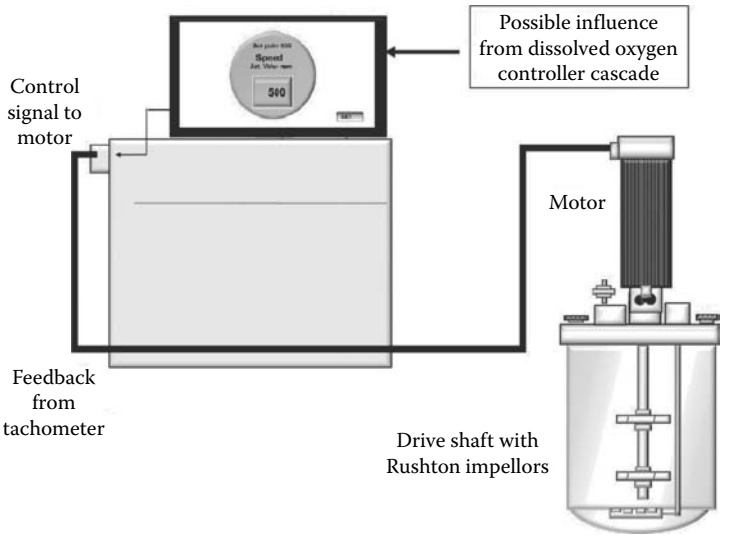

FIGURE 15.4 Speed control system.

possible to use "universal motors" that can cover the complete range of speeds for microbial and cell culture applications for bench-sale bioreactors.

Where speed is used to control the level of dissolved oxygen, an external signal from the oxygen controller can have an effect on stirrer speed. In this case, an absolute maximum and minimum value for speed can be set on the speed control module to limit the effects of the oxygen controller (which could set either too low a speed and impair mixing or too high a speed and cause excessive foaming; see Figure 15.4). More sophisticated examples of cascade control involve the use of gas flow, gas mixing, and even control of medium feed related to levels of dissolved oxygen in the culture.

15.7.2 Temperature Control

A thermocirculation system around a vessel jacket has been chosen as an example here because it is the most complex of all of the methods of temperature control. For simple direct systems such as a heater pad, it is simply a matter of fitting the heater, setting the desired temperature, and switching on. Cooling is normally via a **cold finger** and flow of cooling water is controlled via the action of a solenoid valve. The Pt-100 sensor provides the feedback signal, which causes the controller to take one of the following actions:

Cold finger: A closed pipe or coil that passes through the bioreactor top plate and allows cooling water to circulate to act as a heat exchanger with the culture.

- Heat at full power because the actual temperature is some way below the set point.
- Pulse the heater power because the actual temperature is close to set point.
- Turn on the cooling valve because the actual temperature is above set point.

There is usually some indication to show which action the controller is taking at any given moment. A circulation pump and pipe work are added to the system for water circulation, and any heating is indirect (i.e., on the water circulating in the vessel jacket and not direct heating of the culture). In this case, a connection to the cold water supply must be made (securely, using jubilee clips or cable ties). A drainpipe should also be provided from the overflow point to a sink with a clear fall to the drain (i.e., the sink must be the lowest point for the whole length of this pipe). The water

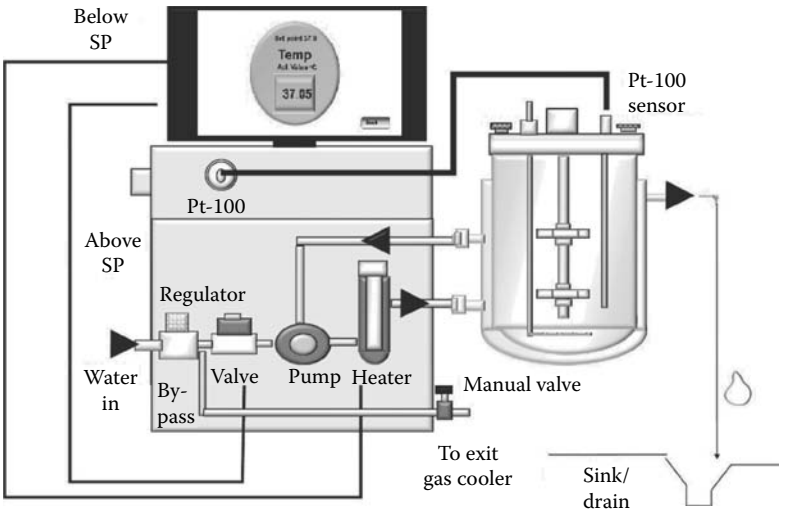

FIGURE 15.5 Temperature control system using water circulation.

should be delivered from the mains at a minimum pressure of 1.5–2 bar and a flow rate of greater than 5 L/min. The water hardness should be no more than 50 ppm suspended solids to protect the heating elements from "furring". The vessel must be connected to the circulation loop (normally by rapid coupling connectors and flexible pressure tubing). See Figure 15.5.

Use of chillers for cooling water circulation is becoming more common and this usually requires the addition of a bypass and pressure relief valve to accommodate the cooling water valve being closed at the bioreactor. Unless the cooling system has a large cooling capacity, it will be unsuitable for rapid cooling after vessel sterilization, so a supply of house water may still be needed. Larger vessels can use twin heat exchangers for heating (by steam) and cooling (by chilled water) with a closed-loop thermocirculator to transfer heat to and from the vessel contents. Water is first supplied by opening a manual valve until the jacket is filled. The heating and cooling is controlled in exactly the same way as a directly heated system, but only the water in the jacket is affected. The jacket provides a large surface area in contact with the vessel wall for heat exchange. Good temperature control can be achieved from approximately 5–8°C above the ambient temperature or above the temperature of the cooling water. Countercooling with water ensures stable temperature control when operating near ambient temperatures. Measured range is typically from 0 to 60°C (exceptionally up to 90°C).

A common alternative for bench-scale bioreactors is to use electrical heating using a silicone mat. This is wrapped around a single-walled vessel after autoclaving and secured in place. A coil or a cold finger dipping into the vessel provides cooling. A less common alternative is a heater block with an electrical element and a cooling coil. This, in turn, allows for easy handling and can be used on multiple, parallel bioreactors.

15.7.3 Control of Gas Supply

A compressed gas (normally oil-free air) is supplied to the bioreactor at a maximum of 0.5–0.75 bar. The rotameter controls the actual flow rate of air through the bioreactor. This should not exceed 1.5 vessel volumes per minute otherwise droplets of water may be carried out with the gas leaving the bioreactor, thus wetting the exit gas filter, which in turn causing it to block. A valve at the bottom of the rotameter is turned and the indicator ball in the rotameter tube rises or falls in proportion to the valve position. A scale on the tube gives flow rates in milliliters per minute or liters per hour.

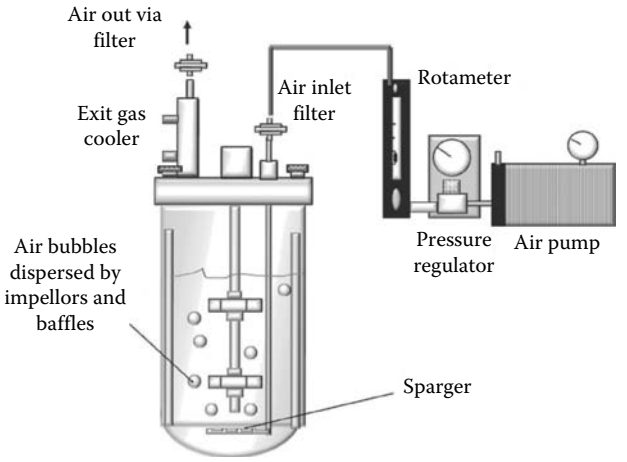

FIGURE 15.6 Gas supply system.

The air passes through the inlet air filter (Figure 15.6), which prevents any microbes from entering the vessel via this path. The end of the sparger is typically a ring with small holes through which the air is forced. The bubbles are immediately broken up and dispersed by the impellors on the drive shaft and the baffles, which can be fitted near the wall of the vessel. The use of several impellors ensures that all regions of the vessel receive good aeration. A "headspace" of approximately 20–30% is normally left between the culture level and the vessel top plate. Sometimes, gas can also be introduced into this region via a short pipe in the bioreactor top plate (e.g., CO_2). For certain types of fermentation (e.g., mammalian cell culture), a **gas mixing station** can be used to premix several gases before they are introduced into the bioreactor.

Gas mixing station: A device used for animal cell culture that allows a mixture of air, oxygen, nitrogen, and carbon dioxide gases to be blended into any desired combination before they are introduced into a bioreactor. This allows great flexibility in how dissolved oxygen concentration and pH are controlled within the culture.

15.7.4 Control of Ph

The hydrogen ion concentration (pH) is controlled by the addition of acid or alkali as the conditions change with growth. The controller uses a pH electrode (typically a gel type) to sense these pH changes and provide a feedback signal, which activates the supply of acid or alkali to bring the pH back to the set point. The pH meter is calibrated before the electrode is autoclaved. Steam-sterilizable electrodes have a limited life cycle (20–50 sterilizations cycles). The pumps supplying the acid and alkali are normally built into the instrumentation or base unit housing.

The reagent bottles are connected to the bioreactor via silicone tubing; the bore size of which determine the volume of acid or base that can be added when the pumps are turned on. Selecting the concentration of the acid or alkali will determine how much effect each dose has on the vessel contents. Normally, the concentration of acids and alkali are in the region of 0.5–2 M. The use of ammonium salt as an alkali has the added advantage of adding extra nitrogen for the growing culture. Care should be taken when using ammonia water because the ammonia can become gaseous in the tubing.

A set-point value as well as an upper and lower limit is fed into the controller to provide a "**dead band**" range in which the controller is inactive. This band is normally ±0.5 pH units of

Dead band: An area around a set-point value that can be set where no control action will take place even if the actual value deviates from the set point. This is used especially for a parameter such as pH, where small changes are often not critical and attempts to control them would lead to excessive controller action.

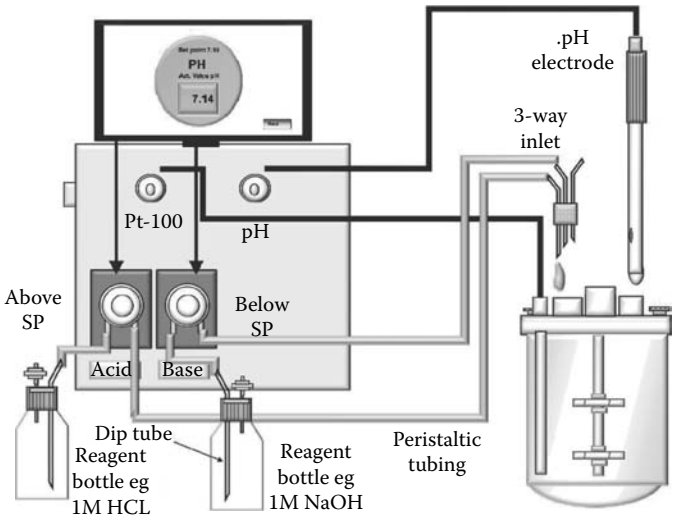

FIGURE 15.7 pH measurement and control.

the desired value. A proportional band adjustment may be present to widen or tighten the range of pH value over which the controller acts (see Figure 15.7).

15.7.5 Control of Dissolved Oxygen

Dissolved oxygen is one of the most difficult parameters to control. The electrodes used to measure dissolved oxygen are now almost exclusively of the polarographic type, which respond rapidly, robustly, and accurately to changes in the oxygen concentrations. The key point with this type of electrode is that it requires a voltage to polarize the anode and cathode of the detecting cell. This polarization can take between 2 and 6 h to complete. During this time, the electrode must be connected to its relevant module, which in turn must be switched on. To set the electrode to zero after autoclaving, first pass oxygen-free nitrogen through the culture vessel for a few minutes and once all oxygen is expelled, set the zero point.

The 100% value is a relative setting made after autoclaving and polarization of the electrode by turning on the airflow and stirrer speed to the maximum speed needed for a few minutes and then adjusting the controller to display 100%.

The membrane of the polarographic electrode needs to be replaced periodically and a special cartridge kit is available from the manufacturer to make this a simple task.

Control of dissolved oxygen can simply be achieved through influencing speed control, adjusting airflow, or by a combination of both. Increasing the speed of mixing and/or airflow may increase foaming to a level that becomes problematic. The most accurate form of flow control is to use a thermal mass flow control valve, which measures and controls airflow on the basis of the cooling effect the gas exerts when passed over a heated element.

An additional option for high density cultures (e.g., *Escherichia coli* or *Pichia pastoris*) is the use of a solenoid valve to supplement the airflow with pure oxygen in pulses (see Figure 15.8). For larger steel bioreactors, pressure control is also used to increase the amount of dissolved oxygen. Several control strategies are often used sequentially during fermentation as a cascade. This can include the option to control feeding to match the available dissolved oxygen if a limit has been reached. The range for control is typically 0–150%, but in some brewing applications, the range increases to 0–500% (addition of pure oxygen).

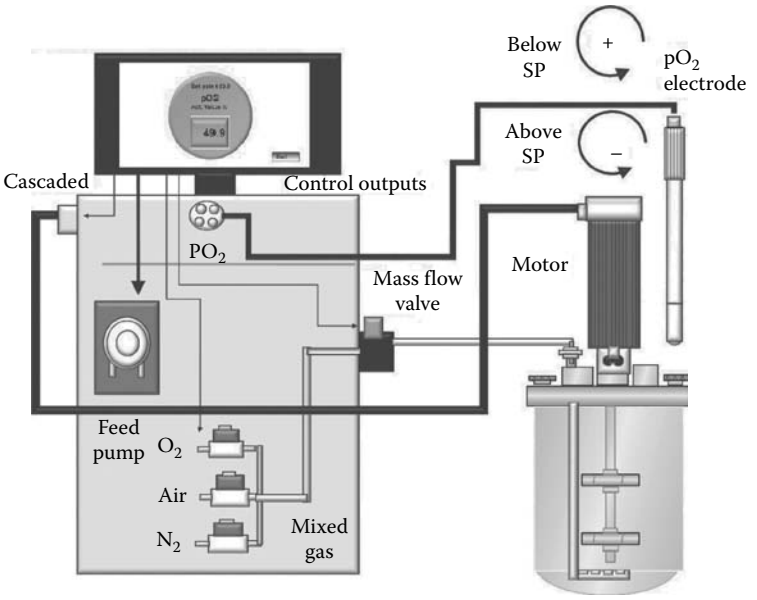

FIGURE 15.8 Dissolved oxygen measurement and control.

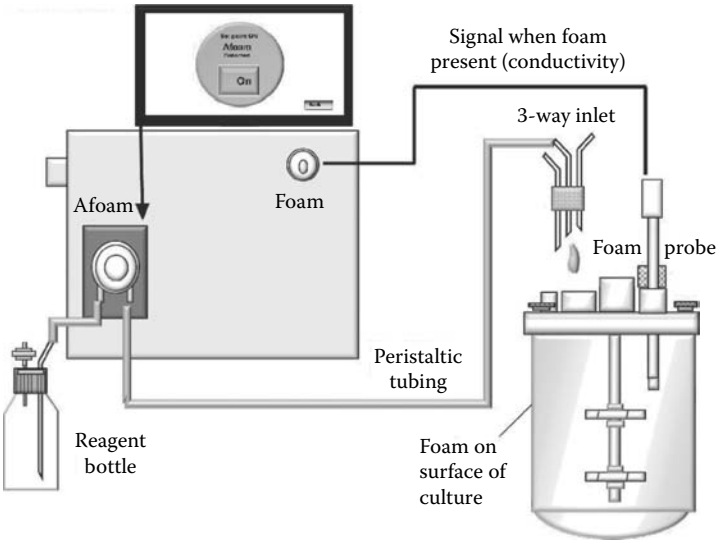

FIGURE 15.9 Foam control system.

15.7.6 Antifoam Control

The formation of foam is detected by a conductance-type probe that is fitted in the vessel headspace. Once foam is detected, the probe gives the controller the signal to dispense a dose of antifoam. A delay timer ensures the antifoam reagent has adequate time to reduce the foam level before another dose of antifoam is added. The sensitivity of foam detection should be adjusted to suit the conditions prevailing in the bioreactor. A sheath of inert material around the probe prevents splashes of foam from giving "false positives" (see Figure 15.9). Normally, the metal top plate is

used to provide the electrical circuit for the probe to operate so a flying lead is provided that fits into a socket somewhere on the top plate.

Antifoam reagents can be mineral oils, vegetable oils, or certain alcohols. Commercial preparations are available for use in pharmaceutical fermentations. The key thing with using oils is that they can form a skin on the surface of the culture and interfere with gas transfer at the liquid/air interface. If foam is allowed to build up unchecked, then it can eventually reach the exit gas filter, thereby blocking it and providing a path for contamination.

15.7.7 Feed Control

The addition of fresh nutrients and mineral salts to a culture vessel can be achieved in one of three ways:

1. *Fed-batch:* Fresh medium is added at a key point in the fermentation (usually when the initial supply of carbon source has been exhausted and continues to the end of the fermentation without withdrawal of culture (except samples). See Figure 15.10.
2. *Perfusion:* Fresh medium is added discontinuously several times across the spectrum of fermentation. The cells are retained and the culture supernatant is drawn off to be replaced with an equivalent quantity of fresh medium. This technique is sometimes used for animal cell culture, especially when the cells have been immobilized.
3. *Continuous:* In this case, the medium removed from the culture is continuously replaced by a fresh nutrient feed at an identical flow rate. In a Chemostat, the medium usually contains a growth-limiting substrate and the rate of growth of the whole culture is subsequently determined by the flow rate with which this limiting nutrient is added. However, in a Turbidostat the nutrient supply is plentiful and the organism grows at its maximum specific growth rate, thus maintaining a constant concentration of biomass throughout fermentation. The spent medium is removed via an overflow weir in the side of the vessel or using a level sensor and dip tube to draw culture from the bulk of the liquid using a peristaltic pump.

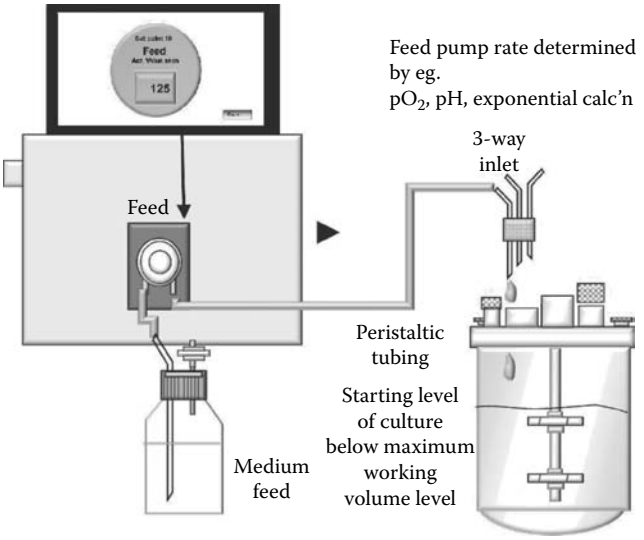

FIGURE 15.10 Feed control system.

15.7.8 Factors Influencing Chemostat Operation

- *Dilution rate:* The ratio of flow rate to volume (rate of change of concentration).
- *Residence time:* Volume/flow rate (i.e., how long a molecule of substrate stays in the vessel).
- *Steady state:* When the number of cells produced balances the number removed. It can typically take several residence times before a culture reaches a steady state.
- *Specific growth rate:* Defined by the Monod equation $\mu = \mu m\ S/(K_s + S)$, where μm is the maximum specific growth rate, S is the concentration of growth-limiting substrate, and K_s is the half saturation coefficient (i.e., growth will increase as substrate concentration increases until μm is reached.

15.7.8.1 Advantages and Disadvantages of Continuous Culture

Continuous culture: A method of allowing culture to be grown in a bioreactor at a specific growth rate. The growth rate is determined by the flow of medium through the vessel (dilution rate).

The advantages of **continuous culture** are

- Cells are in a constant physiological state (steady state).
- It can be used with immobilization for high cell concentration and low feed.
- Most downstream processing works best in a continuous mode.
- Cleaning and shutdown times are much less frequent.
- It is well suited to water treatment and environmental processes.

The disadvantages of continuous culture are

- Not as efficient as fed-batch cultures in the production of secondary metabolites (antibiotics) and recombinant proteins, the production of which is generally triggered at the end of the growth phase.
- Contamination can be detrimental to the process.
- Continuous processes have yet to be licensed by regulatory authorities for the production of pharmaceuticals because no there is no batch-lot traceability.
- Weir systems are more susceptible to contaminations, especially if the culture level rises above the desired level.

15.7.9 Fed-Batch Fermentation

Fed-batch fermentation is most commonly used for industrial production of secondary metabolites and recombinant proteins. Fed-batch fermentation increases biomass and yield of desired product far beyond that obtained in even the best optimized batch or continuous cultures. For example, during growth in batch culture, *E. coli* can attain a biomass concentration in the region of 16–20 OD_{600} units, compared with fed-batch cultures, which can exceed 350 OD_{600} units. Also, in the case of the yeast *P. pastoris*, the organism is initially grown on glycerol for high biomass concentration, and once this is achieved, the organism is challenged with methanol, after starvation, to trigger the induction of the AOX gene and, in turn, recombinant protein production.

The rate of feed can be controlled in several different ways:

- *Time:* A flow rate is set and maintained until a fixed time has elapsed and then it is increased or decreased accordingly.
- *Using the pO_2 value according to the available dissolved oxygen:* When nutrient is supplied too quickly the culture may not be able to metabolize it aerobically and switch to anaerobic pathways. To prevent this, additional oxygen must be added or the feed rate limited to match the dissolved oxygen concentration.

BOX 15.2 EXPONENTIAL FEEDING

Fed-batch fermentation can be controlled according to an equation for exponential feeding, based on the work of Ejiofor et al. (1996) and Lee et al. (1997),

$$F(t) = \mu XV/(S_F - S)Y_{X/S} \times EXP(\mu t)$$

Flow rate at time t (L/h) = (specific growth rate (μ) × vessel working volume at time 0 (V, in L) × cell concentration at time 0 (X) DCW g/L/(feed substrate concentration (S_F) g/L) – (substrate concentration in culture (S) g/L) × biomass yield on substrate ($Y_{x/s}$) g/g × $EXP(\mu t)$

In a typical fed batch, S will be taken to be as close to zero as possible. Choosing a low specific growth rate well below the maximum specific growth rate for the organism (μ_{max}), will allow the culture to grow without accumulations of unwanted products of cell metabolism and within the ability of the bioreactor to supply adequate dissolved oxygen for aerobic growth. Care must be taken that the specific growth rate is not so low that it impedes a steady increase in biomass.

Typical values would be 0.4 g/g for *E. coli* biomass productivity growing on glucose and a specific growth rate of 0.12–0.15/h.

An even simpler version of an exponential feed can be set up using the equation $F(t) = F(o)\ EXP(\mu t)$ where $F(o)$ is the initial feed rate at the start of the batch phase.

- *By pH:* If the microbe produces acid in, for example, an excess of glucose, then the fall in pH can be used as trigger to adjust the supply of feed.
- *Exponential feeding:* This is designed to allow the organism to grow at a chosen, specific growth rate, up to its maximum. See Box 15.2 for an explanation of the methodology behind exponential feeding.

All of these methods can be easily achieved using process control software, which is an essential component of **modern bioreactor** process control.

Modern bioreactor: A system consisting of a few pieces of equipment that provide controlled environmental conditions for the growth of microbes (and/or production of specific metabolites) in liquid culture while preventing entry and growth of contaminating microbes from the outside environment. Note this definition includes single-use systems.

15.8 ADDITIONAL SENSORS

There are several additional parameters that can be measured and, in turn, controlled during the course of fermentation. The most important of these are discussed in the following synopsis.

15.8.1 Redox

This refers to the reduction/oxidation (redox) potential of a system or a chemical, usually expressed relative to a standard hydrogen half-cell with a redox potential of 0.00 V. It follows that a reducing half-cell will have a negative value whereas an oxidizing agent will have a positive one. Oxidation/reduction reactions are generally reversible.

Although the redox value obtained during the course of aerobic fermentation is not generally informative because of the complex nature and multiplicity of biochemical reactions, the opposite is true in anaerobic fermentations because the redox electrode, and, in turn, the value obtained, is very sensitive to oxygen, thus providing a safety indicator for anaerobiosis; a redox value below –200 mV is a good indicator of anaerobic conditions. The redox electrode is very similar to a pH electrode and the conditions for handling and care are almost identical. An electrical zero can usually be set and shorting out the electrode connections should give a reading close to 0 mV. However, pH buffer

4 should never be used with redox electrodes because it will cause the electrode to malfunction and soaking for 24 h in electrolyte may be needed to restore the probe's function.

15.8.2 Airflow

This has already been discussed earlier in connection with dissolved oxygen control. Most bioreactors use a thermal mass flow controller in which airflow is measured by detecting the change in temperature of a heating element before and after the air passes over it. The temperature difference is proportional to flow rate, and this can be processed to give a signal for control. Of course, the flow control systems can measure other gas flows, not just air.

A simpler system uses solenoid valves to introduce each gas into a premixing chamber at manually set flow rates and then controls the final gas flow into the bioreactor with a single mass flow control valve. Anaerobic cultures, requiring no oxygen, can also be catered for (see Box 15.3).

15.8.3 Weight

Load cell: A method for measuring changes in weight in a bioreactor vessel using deformation of a crystal as an indicator of changes in the load. Load cells are used when it would be impractical to use a conventional balance.

This parameter is useful for continuous and/or fed-batch cultures in which the rate of addition of feed must be known and controlled very accurately. It is possible to mount a whole bioreactor on a balance and "tare" out its weight. However, a more precise approach is to use a system with a small **load cell** mounted in

BOX 15.3 ANAEROBIC CULTURE

Culture of anaerobes can be simplified, and the chances of success can be increased by following a few simple guidelines:

- A zero reading using a standard polarographic-dissolved oxygen electrode is not a guarantee of genuinely anaerobic conditions. Use of a redox probe for continuous measurement to ensure that a value of –200 mV is achieved or adding a small quantity of the indicator resazurin to the medium (pale yellow in anaerobic conditions) are the surest methods. Maintenance of a particular redox value is usually achieved by adding fresh medium when the value rises too much.
- Silicone tubing cannot be used for reagent delivery because air can pass through the pores in the tubing and result in oxygen getting into the culture. Gas-tight tubing (e.g., Viton) is necessary, but it cannot be used in the pump heads of peristaltic pumps because any flattening permanently deforms the tube and damages it (it cannot be clamped off for the same reason). MarprBene tubing used in the pump heads is much less permeable to oxygen, and any small trace that does enter via this route can be flushed from the culture if some growth has first been allowed to develop before using the reagent pumps.
- The culture can be kept under a blanket of oxygen-free gas (e.g., ultrapure nitrogen or nitrogen and carbon dioxide) via the headspace or sparger. The culture medium can also have nitrogen bubbled through it before autoclaving. A low flow rate (e.g., ≤ 0.5 VVM) can be used for maintenance of the oxygen-free atmosphere.
- Where a flammable product such as methane is produced as a product of fermentation, care must be taken with safe removal of the exit gas, and it may also be a wise precaution to place the whole unit in an extraction hood and consider specific chemical sensors with alarms for the laboratory.

such a way that only the vessel and its contents are measured. The deformation of the load cell provides an output signal, which then transduced, and in turn transmitted to the controller module in the form of electrical signal. Control is normally by setting a maximum and/or minimum weight in a manner that is analogous to feed pump control.

A commonly used variant of this system is to measure very accurately the amount of reagent (e.g., alkali) added to a bioreactor. In this case, the reagent bottle is placed on an analytical balance, which has a computer output (normally RS232), and the decrease in weight is used as a measure of the amount of reagent added.

15.8.4 Pressure

The use of pressure as a control parameter is more common in larger ISS bioreactors; an increased pressure increases the concentration of dissolved oxygen in the fermentation broth. Although, a small glass vessel can often be operated under conditions of overpressure (e.g., up to 0.5–0.7 bar), it is advisable to seek advice from the manufacturer.

A piezoelectric-electric sensor normally provides an electrical signal, as a consequence of deformation of the crystal by the internal pressure, typically in the range of 0–2 bar. The control element is a **proportional valve**, which restricts the flow of gas out of the bioreactor and thereby creates a back-pressure. A mechanical overpressure valve or burst- disc is an essential safety requirement if overpressure is to be used.

Proportional valve: A valve which can be adjusted electrically or pneumatically from 0 to 100% open or closed. For example, the action of the valve is in proportion to the degree of change required by the controller to maintain a certain level of dissolved oxygen by adjusting the airflow rate.

15.8.5 Online Measurement of Biomass

A direct measurement of the number of organisms in a culture is clearly desirable for the control of feed-rate, oxygenation, and general process optimization. Normally, measurements of total cell numbers, wet weight, dry weight, and viable cell counts are made by taking samples intermittently and carrying out the relevant laboratory analysis. Fluorescence microscopy has also been used to measure the number of viable cells internally with a probe or externally through the vessel glass window. The probe-based system is usually suited to bench-scale vessels, similar in design to the optical density probe described below.

15.8.5.1 Optical Density/Turbidity Systems

The increase in turbidity [optical density (OD)] and the subsequent scattering of light by the microbial populations provide a good mean to measure microbial growth. The OD sensor is directly mounted inside of the vessel and connected to the electronic circuit via fiberoptic cable. A two-point calibration procedure is used and results can be expressed in various units. A range up to 200 g/L dry weight is measurable with a good deal of accuracy. This method is cost-effective and works well for cultures in the logarithmic phase of growth. However, it should be remembered that this method does not distinguish between live or dead cells.

15.8.5.2 Capacitance/Conductance-Based Biomass Monitor

This uses a totally novel approach to determine the numbers of viable cells of all types of organisms (bacteria, yeast, filamentous fungi, and animal cells). A probe in the vessel uses a radiofrequency electrical field to measure the natural capacitance of living cells with an intact plasma membrane, thus building up a charge the intensity that is proportional to the number of viable cells, with each type of cell having its own specific range. The signal is processed and can be expressed as dry weight or concentration in cells per milliliter. During the course of fermentation, an antifouling system is used to maintain the ability of the probe to give accurate readings over long time periods.

This type of instrument makes possible the control of feed pumps by biomass concentration and could form the basis for an automated transfer system for inoculating larger vessels.

15.8.6 Exit Gas Analysis

Measurement of the amounts of different gases leaving a bioreactor vessel can provide valuable information about the metabolic processes taking place under the conditions in which the culture is growing. For example, the ratio of oxygen and carbon dioxide entering and leaving the vessel, or **respiratory quotient** (RQ), can be used to determine whether yeasts are producing biomass or alcohol (see Box 15.4). The RQ can be calculated by most fermentation software packages and can then be used as part of a

Respiratory quotient (RQ): RQ is a mathematically derived value related to the use of oxygen by a microbial culture as compared with the evolution of carbon dioxide. This value can be used to adjust feed rates of sugars to manipulate microbial physiology.

BOX 15.4 CALCULATION OF RQ

When data are obtained from an exit gas analysis, it is generally required that the parameter RQ is calculated to gain insight into the metabolism of the organism under investigation. This is normally done by programming a definition into a computer software package for data logging and control. Here is a generalized outline of the steps needed:

- RQ = CPR (CO_2 production rate)/OUR (oxygen uptake rate)
- CPR = (flow CO_2 out) × [(concentration CO_2 out) – (flow CO_2 in)] × (concentration CO_2 in) g·mol CO_2 per hour
- OUR = (flow O_2 in) × [(concentration O_2 in) – (flow O_2 out)] × (concentration O_2 out) g·mol O_2 per hour
- Concentrations of gases in inlet gas (AIR) O_2 – of 20.95%; CO_2 = 0.03%

The working volume of the bioreactor (*WV*) and the gas flow rate (*FR*) must be known to make the calculation:

VUO_2 (volumetric uptake O_2) = [FR × 0.2095 – (exit O_2/100)/WV]
$VPCO_2$ (volumetric production CO_2) = [(FR × (exit CO_2/100)/WV – 0.0003)/WV]

Typical values for *exit* O_2 could reach approximately 16% and for *exit* CO_2 approximately 5%.

For instance, values of RQ for yeast biomass fermentation would need to be kept near 1 for optimal biomass production.

A worked example of the above definitions:

WV = 1 L, FR = 1 min^{-1} (1 vessel volume of gas per minute, a typical flow rate).
Exit O_2 = 16% and exit CO_2 = 5%
$VUO_2 = 1 \times (0.2095 – 0.16)/1 = 0/0494$
$VPCO_2 = 1 \times (0.05 – 0.0003)/1 = 0.0494$
RQ = 0.497/0.494 = 1.006

To achieve control, a sequence along the lines of the following would have to be set up:

If RQ < 0.95, then FR = FR × 1.05
If RQ > 1.05, then FR = FR × 0.95

control algorithm so that the flow rate of a feed pump can be altered accordingly. The entry gas does not need to be analyzed providing it is air because the amounts of oxygen and carbon dioxide will be those of the atmosphere. The flow rate of the air into the vessel will need to be accurately measured, normally by using a thermal mass flow controller. The exit gas may need to be conditioned (e.g., moisture removed) before going into the analyzer depending on the type of instrument used. Recent interest in biofuels has lead to a requirement for methane, and in some cases hydrogen, to be measured in the exit gas; several commercial systems can meet this requirement.

15.8.6.1 Infrared Carbon Dioxide Analyzer

A hot wire is used to generate a source of infrared radiation that passes through the gas that leaves the bioreactor into the sample chamber. An infrared detector measures the amount of radiation reaching it after some is absorbed by the gas. An optical filter is used to make sure the detector only responds to the gas of interest. A "chopper" or rotating shutter is used to allow the detector to see a reference source at regular intervals. This type of detector allows for continuous measurement with good sensitivity, accuracy, and selectivity. Output signals are normally provided as analogue signals (e.g., 0–10 V) or a string of ASCII characters for printing or transmission to computer software.

15.8.6.2 Paramagnetic Oxygen Analyzer

Oxygen has a particular physical property that this type of analyzer utilizes: it is more susceptible to a magnetic field than other gases. This property is measured using a finely balanced test apparatus suspended in the test chamber of the analyzer. A dumbbell of gas-filled spheres is linked to a support mechanism suspended in a magnetic field created by permanent magnets. If oxygen is present in the test gas, its attraction to the magnetic field will cause the dumbbell to be displaced. The movement is detected using a mirror in the center of the balance system, which displaces a beam of light shone via the mirror onto a photocell. The signal from the photocell will be proportional to the concentration of oxygen present in the sample. A low flow rate is needed for this system to work properly, so inlet gas is typically pumped into the detector cell with most being discarded through bypass pipeline. Once again, suitable analogue and computer outputs are often provided. Infrared detectors and paramagnetic oxygen analyzers need to be calibrated before use.

15.8.6.3 Mass Spectrometer

This represents a step upward in versatility, capability, and cost. A wide range of gases can be analyzed in the gaseous and dissolved form. These include oxygen, carbon dioxide, argon, nitrogen, ammonia, hydrogen, methanol, ethanol, and several other organic volatiles. Isotope ratios (e.g., C^{12}/C^{13}) can also be detected.

This method of analysis is rapid, thus allowing or a multiinlet system to be used, which "shares" the analyzer among several separate vessels within a bank of bioreactors. The physical principle involved is the ionization of gas molecules by an electron source, usually a hot filament, followed by their separation in a magnetic field (the quadropole analyzer uses a combination of RF and DC electrical fields) according to their mass/charge ratio. This separation takes place in a virtual vacuum to minimize collisions before sorting. The magnetic field is tuned so that only the ions of interest will be focused onto the detector system, a Faraday cup; a metal plate which generates a tiny electric current whenever a gas ion strikes it. This signal can be amplified and displayed. By retuning the magnetic field very quickly (milliseconds), different ions can be detected and measured sequentially.

15.9 "SUBSTRATE SENSORS"

Sensors for the detection of substrates usually depend on chemical or enzymic reactions within the fermentation vessel or by sensing the release of volatile components into the exit gas (see Chapter 13 in this edition for extensive coverage of this aspect). Two of the most common examples are given in Sections 15.9.1 and 15.9.2.

15.9.1 Glucose Measurement and Control

The more sophisticated versions incorporate a small dialysis unit in a sterilizable probe to take minute quantities of liquid from the medium for analysis. An enzymic reaction linked to a transducer provides a measurable current that can be amplified to give an output signal. This can provide a measurement of glucose from less than 1 g/L of glucose to over 100 g/L.

15.9.2 Methanol Measurement and Control

In this case, a chemical sensor is used to measure the concentration of methanol vapor in the exit gas stream (the sensors are usually variants of the type used in "breathalyzer" systems). The concentration of methanol in the vapor can be directly related to the concentration in the culture medium. A probe-type alternative uses a carrier gas to remove the alcohol vapor from the culture. A signal transducer and amplifier system provides the output-measured value. This type of sensor is typically used to monitor growth and protein overexpression by the yeast *P. pastoris*.

15.10 BIOREACTOR PREPARATION AND USE

15.10.1 Disassembly of the Vessel

The fermentation is shut down from the control unit and transfer lines plus cable connections removed. Reagents lines are emptied and may be refilled with water. After fermentation, the vessel and reagent tubing should be re-autoclaved, ensuring that inlets and outlets are properly prepared. The culture should be disposed of according to health and safety regulations. The clip/clamps/bolts, which retain the vessel top plate, are undone until the whole assembly springs free. The top plate can now be lifted upward away from the glass vessel, taking care that the air sparger, drive shaft/impellors, and temperature probe completely clear the vessel safely.

15.10.2 Cleaning

The pH and dissolved oxygen electrodes should be removed and stored in suitable reagents according to the manufacturer's instructions. Periodic cleaning and regeneration of the electrodes are also covered by these instructions. Doing this maintenance is very cost-effective. The vessel should be rinsed several times in distilled water to remove any loose culture residues. Cleaning of growths of culture on the vessel walls may require disassembly and light brushing of the glass. At this point, an examination of any chips or cracks in the vessel glass can be carried out and a replacement made if necessary. Vessels must be stored clean and dry. In use, any spillages of reagents or medium should be wiped up immediately with a damp cloth and not be allowed to dry out. Contact between the top plate and liquids with high chloride ion content (e.g., common salt solutions, hydrochloric acid) should be avoided to prevent corrosion. The pump heads and covers must be thoroughly cleaned if a tube breaks and reagent leaks out. Peristaltic tubing should be sterilized using water in the line and not strong acid or base.

15.10.3 Preparations for Autoclaving

The vessel seal should be removed checked for damage and can be dipped in water to aid relocation. On replacing the seal, it must be correctly located so that there is no chance of any part lifting or kinking. At this point, the vessel can be filled with medium to a maximum of 70–80% full (if active aeration is to be used, this space is vital for gas exchange). The minimum medium volume is the amount needed to adequately cover the electrodes. The vessel top plate can now be replaced, and any clamping ring or bolts tightened firmly. The ports for electrodes have O-ring seals, which

should be checked for damage and may be wetted with a little water to aid relocation. Electrodes normally push directly into the port fitting, and the collar is tightened down to compress the O-ring seal. All other fittings such as pipes are fitted in the same way. Ports not in use have "stoppers" fitted, and their O-ring seals should be checked also. The pH electrode should be calibrated in appropriate buffers (i.e., pH 7, then pH 4 or pH 9) for the usual two-point calibration. The pH and dissolved oxygen electrodes should be fitted, taking care not to damage them by careless insertion into the port. Both must be tightly capped to prevent moisture getting into the electrical contacts. For the dissolved oxygen electrode, a cap may have to be improvised from aluminum foil. The Pt-100 temperature sensor must be fitted and capped unless it fits into a pocket and so can be removed totally. If used, the foam probe is fitted so that it is above the liquid level (Figure 15.11). A foam probe can be pulled out of a vessel after autoclaving with little risk of contamination but cannot be pushed down.

Reagent bottles are prepared in a similar way to the bioreactor vessel. A cap or head plate (including a seal) is fitted with a short tube and longer dip tube. A disposable filter is then connected to the short tube with silicone tubing. The shorter pipe must not dip into the liquid, and nothing must block the free passage of air through the filter. The long pipe dips into the liquid as far as possible, usually with a plastic/silicone tubing extension. This pipe should be fitted with a length of silicone tubing that is long enough to reach the peristaltic pump. The tubing is clamped so that no liquid can escape during autoclaving. A similar procedure is used for sampling and/or harvest bottles except that two short pipes are used so neither dips into the collected culture.

The exit gas cooler should be fitted to one of the larger available ports. A short length of silicone tubing should be attached to the top of the air outlet, and a small 0.22- or 0.45-µm filter fitted. The air outlet line must be kept open during autoclaving. A short length of silicone tubing must be fitted to the air sparger inlet pipe with a 0.2-µm disposable filter mounted on top. The tubing between the sparger pipe and the filter must be clamped shut during autoclaving. If a port is to be used for inoculation or piercing with a needle, a silicone membrane must be fitted into the empty port and a clamping collar/cap used to hold it in place.

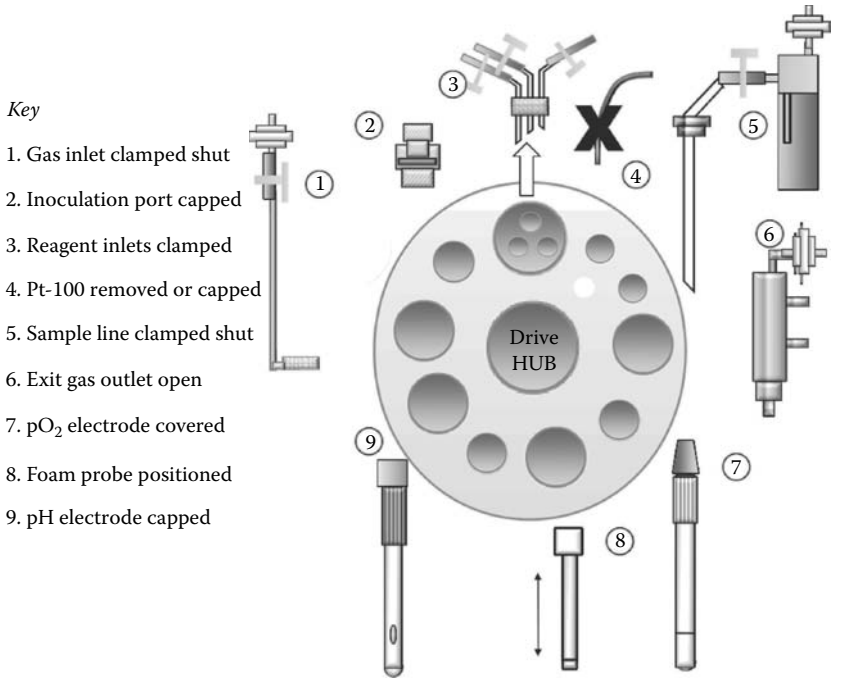

FIGURE 15.11 Vessel top plate prepared for autoclaving.

15.10.4 Autoclaving

The vessel and any reagent/sampling bottles already connected by silicone tubing are assembled together on a steel tray or in an autoclave basket. A final check should be made that at least one route is available for air to enter and leave the vessel(s) and that all lines dipping into liquid are clamped closed. If the vessel has top drive and a mechanical seal, the seal must be lubricated (normally with glycerin).

If the medium cannot be autoclaved, a suitable volume of distilled water should be used (e.g., 10–20 mL/L of working volume to keep the electrodes wet). If a larger volume of, for example, phosphate-buffered saline (PBS), is used, this must be removed via a sample line before the actual medium and inoculum are aseptically transferred. A quantity of liquid is certain to be lost during autoclaving (~10%) so the medium is overdiluted to compensate for this or sterile distilled water is added afterward to restore the volume. Some form of indicator such as autoclave tape should be included to provide a warning if the correct sterilization procedure has not been carried out. Autoclaving at 151°C for a minimum of 30 min up to 1 h is normally considered adequate for vessel sterilization but consider potential damage to the constituent chemicals of the medium. However, some work may require temperatures of 134°C for several hours to ensure sterility. If in doubt, a safety committee should be consulted. Also, the autoclave used must have good pressure equalization during the cooling-down phase of operation to prevent medium being boiled off. The vessel and any accessory bottles must be allowed to cool completely before handling.

15.10.5 Setup after Autoclaving

The air sparger is connected to the rotameter by a piece of silicone tubing from the top of the filter to the air outlet of the rotameter. The air sparger line is unclipped between the metal pipe and the air filter. The exit gas cooler is connected to the water supplydirectly or via the bioreactor base unit. The tubing for water in, water out, and drain is connected to the vessel jacket for a water system, and the water is turned on so that the vessel jacket is filled. Alternatively, any pads or heater cartridges are connected to the base unit or temperature control module; the cold finger is connected to the water supply.

The tubing from the reagent bottles is connected to the multiway inlet (if necessary), and the silicone tubing from the reagent bottles is located in the relevant peristaltic pump. Any aseptic connections must be made first if the reagent bottles were autoclaved separately from the vessel (see Box 15.5). The clamps are removed so liquid can flow freely. A manual switch is often fitted,

BOX 15.5 PREPARATION OF TUBING FOR ASEPTIC CONNECTION

Any silicone tubing to be joined needs the two ends to be prepared as follows:

1. The end of the tubing that remains open is simply covered in aluminum foil held in place with autoclave tape. For added security, the open end can be sealed with a short piece of glass rod flattened at one end to make a “bung”.
2. The other side has a short length of stainless steel pipe pushed into the silicone tubing. The exposed length of pipe is covered with foil which is taped closed.
3. Silicone tubing is connected to any of the inlet pipes intended for use for reagent addition. The tubing must stretch to the peristaltic pump heads when the vessel is in place.
4. The tubing is closed with clamps or any other closure system that will withstand autoclaving (the arterial clamps used in medicine are often used where a connection must be opened and closed many times, e.g., to a sampling device). The tubing that goes to the sampling device from the top plate must be clamped shut during autoclaving.

which allows the pumps to be primed with liquid before use. The drive motor is located onto the top plate (if appropriate), ensuring a good connection is made to the drive shaft. The Pt-100 temperature sensor is connected to the control module, and the pH electrode is connected by removing the shorting cap and screwing in the cable. The dissolved oxygen electrode is connected to the appropriate cable (this requires some care, but the connector should lock firmly when it is correctly positioned by aligning the marks on the connector collar and the probe top). Connections to the foam probe are made, usually one wire into the electrode and one on the vessel top plate to make a circuit. The mains electricity to the instrumentation modules is switched on, allowing some hours (minimum of 2, preferably > 6) for the dissolved oxygen electrode to polarize properly. Setting the temperature control at this stage will ensure the bioreactor is ready to inoculate after calibration of the dissolved oxygen electrode. After polarization, the dissolved oxygen electrode is calibrated for the zero point using nitrogen gas and then the air supply is turned on. The maximum stirrer speed to be used and the maximum airflow required on the rotameter are set. After leaving for approximately 15 min, the 100% level is set. The bioreactor is now ready to inoculate.

15.10.6 Inoculation of a Bioreactor Vessel

This section assumes that all of the set-up procedures listed above have been carried out. The simplest way to inoculate a fermentor is to have a dedicated port fitted with a membrane, which is capped off before autoclaving. The inoculum (which should normally be no more than 5–10% of the total culture volume) is aseptically transferred to a sterile, disposable syringe of a suitable size. The port fitting is removed and held vertically to prevent contamination of the bottom end. The syringe needle is quickly pushed through the membrane, and the inoculum is transferred into the vessel. The vessel may be actively aerated during this procedure to minimize the risk of a contaminant getting into the vessel (safety considerations permitting). The syringe needle is quickly withdrawn and the silicone membrane reseals. The port fitting is now replaced. For added security, a couple of drops of 70% ethanol can be placed on the membrane surface before piercing and ignited to provide a thermal barrier. Alternatively, an "aseptic connection" can be made to an inlet pipe. If the line connected has a "Y" coupling in it, then the same aseptic connection could be used to introduce medium. This technique is useful if a dedicated inoculation port cannot be provided. Figure 15.12 shows the alternative methods.

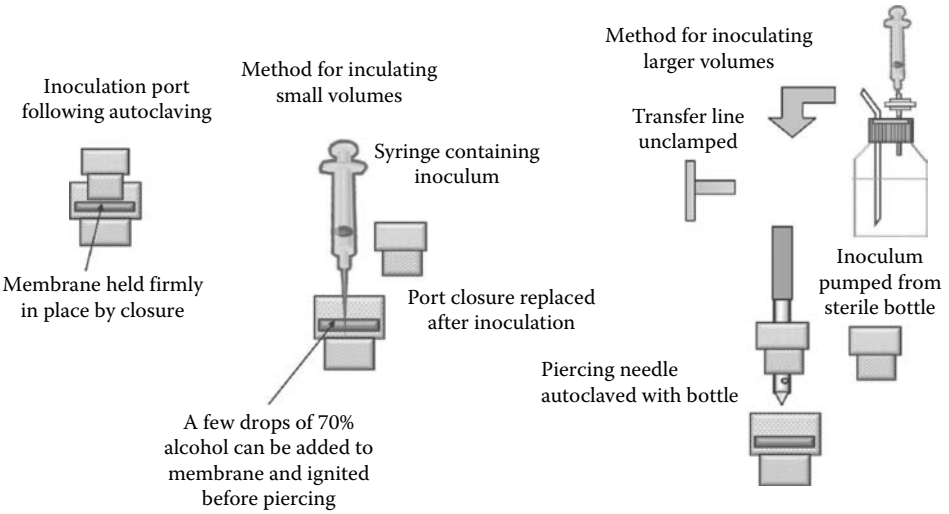

FIGURE 15.12 Inoculation of a bioreactor vessel.

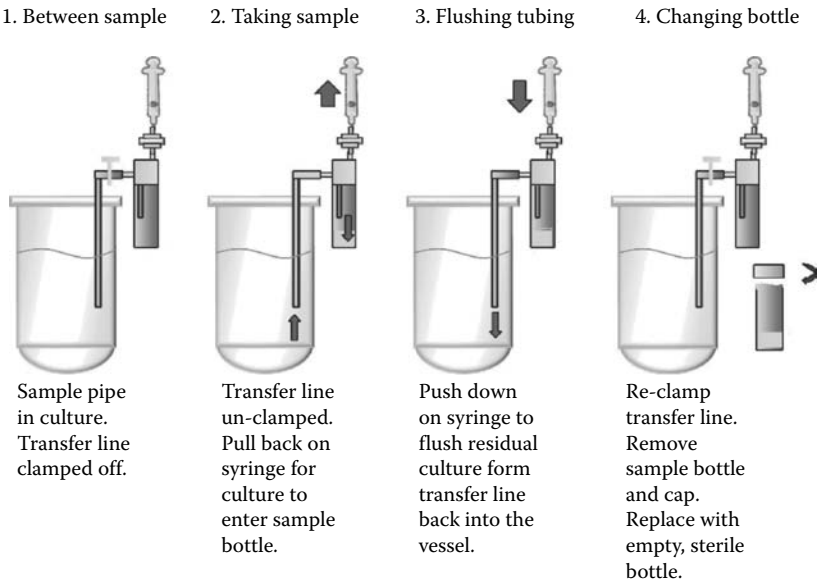

FIGURE 15.13 Sampling.

15.10.7 Sampling from a Bioreactor Vessel

All sampling starts with a sample pipe, which should dip into the bulk of the culture liquid. At its simplest, a sampling device consisting of a bottle connected to two metal needles/pipes permanently fixed through the metal and rubber seals of its cap. One pipe is connected to a 0.22-μm air filter whereas the other, which is linked by silicone tubing (clamped off until a sample is needed), is connected to the sampling pipe. A syringe is fitted to the air filter after autoclaving. The sample device is usually attached to the vessel top plate so that the glass bottle hangs down vertically beneath the cap and a supply of bottles of the same size are autoclaved ready for use. When a sample is to be taken, the clamp on the sample pipe tubing is released and the syringe pulled back to create a partial vacuum in the sample bottle; consequently, the culture will flow into the sample bottle. When the required volume of sample has been taken (never more than 75% of the total bottle volume) the syringe is pushed in to clear the line and the sample tubing is clamped shut again. The sample bottle with the culture is quickly removed and capped with a sterile cap from a new glass bottle, which replaces it under the sampling device (Figure 15.13). It is often preferable simply to discard the first few milliliters of the next sample by using it as a "wash" for the transfer line, putting a fresh bottle under the sampling device to actually take the sample. The use of disposable sterile syringes and one-way valves manufactured for medical applications can now make an inexpensive, reusable, and reliable sampling system for bench-scale bioreactors. Resterilizable sampling systems for ISS vessels provide similar functions in large-scale industrial bioreactors.

15.11 EXAMPLES OF COMMON BIOREACTOR APPLICATIONS

The following examples provide some insight into how to configure, optimize, and refine the use of bioreactors for a range of applications.

15.11.1 Multiple, Parallel Bioreactors for Process Analytics

This category of bioreactors has some distinctive features that make it particularly suited to rapid process development and obtaining experimental results with statistical validity. This is

particularly relevant with the promotion of the Process Analytic Technology (PAT) initiative advocated by the U.S. Food and Drug Administration agency in the United States (FDA 2004). The objective of the initiative is to champion the need to generate more data on biological production processes at an earlier stage of development. The use of small, multiple bioreactors is appropriate for this work.

These systems are usually easier to set up than a conventional bioreactor, provide measurement/control of all of the major process parameters, and can be adapted for the growth of virtually all types of microbes and cells. Key features to consider are

- Size*:* The vessel has similar construction, configuration, and fittings to a conventional bench-scale unit, but they are significantly smaller (typical working volumes of 300–1000 mL) and housed in a base unit capable of accepting four to eight vessels (possibly in groups of two to four).
- *Flexibility*: Multiple peristaltic pumps independently provide reagent and medium feeds to each vessel. Separate heaters/cooling actuators and stirrer systems provide individual control of temperature and stirrer speed. A single DDC control unit provides for different process parameters, profiles, and links to external supervisory software. Several standard probes can be accommodated, including optical density for biomass monitoring or redox for anaerobic applications. The instrumentation must also be flexible and expandable enough to accommodate additional process control elements.
- *Easy handling:* This is certainly the most crucial point. A lot of vessels mean a lot of flexible tubing, a lot of sensors to calibrate, and a lot of items to take to and from the autoclave. An advantage with autoclavable systems is that they can be operated using two complete sets of vessels, so there is minimal downtime for cleaning and preparation. Small-scale ISS systems are an alternative, but these are necessarily large and complex.
- *Validation:* The equipment should be suitable for process validation especially for pilot and production-scale bioreactors.

15.11.1.1 How Do Multiple Bioreactors Fit into the Philosophy of PAT?

Cell culture for production of therapeutic proteins has advanced dramatically in recent years. Bioreactors of several thousand liters can be used, so process optimization is of key importance. A cell culture bioreactor has to take account vessel aspect ratio, internal fittings, and considerable flexibility in gas mixing and flow control. A magnetically coupled drive system provides a means to help minimize the risk of contamination during prolonged culture times. The drive system must not damage the cells or support substrates and allow for good mixing even at speeds well below 100 rpm. For monoclonal antibody and therapeutic protein production, separation systems such as a **spin filter** are usually required, even at this small scale.

Spin filter: This device is normally attached to the drive shaft of an animal cell bioreactor and allows culture liquid to be removed while leaving the cells inside of the bioreactor. For example, it allows for slow-growing cells to produce antibodies over a long period by regular harvesting of culture supernatant and replenishment by a controlled medium feed.

Rapid selection and screening of clones for productivity can be achieved using microtiter plates or shake flasks rather than bioreactors. Statistical studies using specialist Design of Experiment (DoE) software can determine the likely key parameters to be measured and controlled. Temperature, pH, and rate of feed addition are often the most critical.

The desired clones can then be tested in multiple, parallel bioreactor system, thus facilitating sufficient replicates for statistical validity. Excursion testing of key parameters can also be performed at this stage to find the limits of productivity for the process. Additional process optimization and fine tuning can be made in terms of medium composition, control strategies, and downstream processing.

The accumulated data will be presented along with information from production-scale fermentation as part of a submission to obtain approval for a license to manufacture.

15.11.1.2 Advantages of Using Multiple, Parallel Fermentation Systems for PAT

- Allows for the use of replicates for producing statistically valid results.
- Because many conditions may still remain to be tested after computer simulations, time can be saved compared with repeated experiments using a single vessel in series.
- Several different parameter changes can be performed at once for excursion testing (e.g., different temperatures).
- Handling and preparation will be optimized for practical details such as fitting tubing post-sterilization and priming pumps, etc.
- A small-scale system can be accommodated in a research laboratory and the work can be done without the need for special facilities.

Small-scale, live fermentations form a key part the successful implementation of the PAT process in by

- Confirming predicted results from statistical analysis and computer simulations
- Discovering other factors not included in the simulations (e.g., media composition or shear-sensitivity of clones)
- Providing data directly applicable to scale-up
- Use with larger-scale process trials to provide real-time optimization using scale-down techniques
- Allowing refinement of process strategies related to practical aspects of the process such as feeding rates, etc

Irrespective of PAT requirements, testing at this scale can optimize many of the process parameters for applications such as high-density culture (see Section 15.11.2 below).

15.11.2 High-Density Cultures for Biomass and Proteins

15.11.2.1 What Is Special about High-Density Culture?

High-density culture is a strategy that allows maximal product formation (usually a recombinant protein) in the minimum time and/or smallest volume. This has several elements and emphasizes the importance of biological steps along with optimization of the process within the bioreactor. The essential steps are

1. Creation of clones that produce high yields of product and/or biomass. These two criteria may not always be met by the same clone. One strategy is to split the process so that biomass formation is an initial step under one set of conditions, followed by a change to induce product formation. The clones will have been subject to various manipulation and analyses.
2. Multiple gene copies leading to overexpression (increases productivity but no other changes).
3. Deletion mutations so cells produce mainly product (redirecting cell machinery).
4. Use of "helper" genes to improve productivity.
5. Use of fusion proteins (markers, translocators) (e.g., to aid movement of target proteins across the cell membrane).
6. Use of metabolic flux analysis to find out key pathways for nutrient use with defined media.

15.11.2.1.1 Process Optimization

Process optimization in the bioreactor, especially with regard to medium composition and the strategy used. Fed-batch culture is often to be preferred because it allows for rapid production of biomass in one medium in an initial batch phase, followed by induction and product formation, maybe using a different medium composition as a feed. Factors to consider in the optimization process are

- *Excursion testing:* As mentioned above for PAT, excursion testing is also applicable here to find the limits of productivity. Temperature, pH, and feed are usual choices for optimization, if dissolved oxygen is in excess or feed rates are balanced to match available pO_2.
- *Choice of medium:* A defined chemical medium with an additional carbon source is usually preferred because it can enhance growth by supplying essential trace elements in the correct quantities for optimal growth, is easier to remove from the product, and does not promote growth of contaminants.
- *Control of process parameters specifically associated with high-density culture:* These include high temperatures during the logarithmic phase of growth that may require enhanced cooling (use of a chiller, cooling coils, additional cold fingers, etc.) and addition of oxygen to supplement the quantity that can be attained by aeration alone.
- *High-density culture:* This depends on efficient control of key process parameters, especially during the logarithmic phase of growth, and involves the use of cascades of process parameters such as stirrer speed, gas flow, and oxygen supplementation to maximize the availability of dissolved oxygen for cell metabolism (see Box 15.6). An alternative approach is to limit the availability of carbon source to match the quantity of dissolved oxygen available to the culture. This strategy means culture times are increased, but it has a definite advantage at the large scale where oxygen supplementation would be prohibitively expensive. An exponential feeding strategy would allow feed rates to increase synchronously with increasing cell numbers.
- *Monitoringof biomass formation:* This is done using an OD measurement (typically OD_{600}) or indirectly by exit gas analysis to calculate oxygen uptake rates.
- *Choice of inducer:* For example, isopropyl thio-Galactopyranoside (IPGT) for *E. coli* and methanol for *P. pastoris.*
- *Change of physical conditions (starvation, oxygen spike, gas supplementation, temperature rise or fall):* These strategies were used successfully for decades before genetic modification was possible and usually stress the organism so that its metabolism switches on new genes as a survival response to harsh growth conditions.

15.11.2.1.2 Product Removal

This depends on where the desired substance has been produced. If it is in the cell, harvest of the biomass followed by a cell disruption step is usually necessary. If the product has been released into the culture supernatant, then it is possible to remove the product during the fermentation by a filtration or perfusion step. Subsequent downstream processing would optimally involve

- The fewest number of steps means fewest losses
- Concentration of product in the cell or in the culture for harvest (continuous removal or isolation in inclusion bodies or outer membranes)
- Use of markers/fusion proteins to aid purification; for example, an affinity column to isolate the fusion protein or green fluorescent protein (GFP) to show activity of selected genes.

BOX 15.6 HOW OXYGEN TRANSFER RATE (OTR) AFFECTS GROWTH AND HOW TO INFLUENCE IT FOR HIGH DENSITY CULTURES?

The obvious answer to this question is that if oxygen becomes the growth-limiting substance, then growth will be impeded if an adequate supply of dissolved oxygen cannot be provided to the culture; hence the need to optimize or supplement the oxygen levels in the culture when high cell densities are required. If oxygen transfer is limited, this can lead to the need to also limit the addition of substrate to match the capability of the bioreactor to ensure aerobic growth. This does not prevent the culture from attaining a high density, but it does increase the time required for it to do so. However, it may represent a better strategy than oxygen supplementation if scale-up is envisaged for the process because large-scale addition of oxygen would almost certainly be uneconomic.

The reverse argument may also apply to some recombinant strains of *E. coli* during the lag phase of growth. If a gas flow rate and stirring speed are used that are too high, subsequent growth can be severely limited or the culture could even die completely. There is a need for a brief period of growth in an environment richer in carbon dioxide than would be necessary for wild-type strains. High stirrer speeds and gas flow rates can strip out other dissolved gases from the culture liquid. Laboratory bioreactors may not be efficient enough for this problem to become apparent at the small scale until a move to a larger scale bioreactor with more efficient oxygen transfer shows this to be a problem.

Influences on Oxygen Transfer Rate (OTR):

- kLa value (OTR = kLa × solubility of O_2 at a given temperature);
- The design of the sparger, stirrer, and vessel [e.g., aspect ratio, number of impellors (3 is best) and motor power];
- Rate of active aeration in vessel volumes per minute (VVM) (1.5 is optimal and 2 is usually the maximum); and
- Temperature, pressure, and ionic concentration (solubility).

Strategies for improvement:

- Higher airflow rates, but this can lead to foam problems;
- More and larger impellors, but this requires more motor power, which means increased cost at an industrial scale;
- More energy to the stirrer for a higher maximum speed, but this adds more heat into the vessel and cooling is a problem at the industrial scale; and
- Increase vessel pressure to improve solubility of oxygen, but this is unsuitable for glass vessels.

At the laboratory scale, anything is possible, but production scale vessels are far more limited by physics and engineering.

Additional factors influencing high density microbial culture can include

- Adaptation of productive clones to bioreactor conditions (e.g., may be shear sensitive).
- Choice of inorganic supplements in the feed; for example, phosphates and/or reagents and use of ammonia water as the base reagent for *E. coli* high-density fermentations.
- Fed-batch fermentation with growth rate controlled below maximum specific growth rate to help prevent oxygen limitation/substrate excess. Use of exponential feeding with OD measurement can provide for direct control of cell growth.

- Use of indirect feedback control for feed rate (e.g., by operating the bioreactor as a pH stat or on the basis of an "oxygen spike", which requires care because a dying culture will also have a lower oxygen requirement).
- Direct, accurate measurement and tight control of feed concentration in the bulk culture (e.g., if methanol feed reaches a concentration >4–6% in the culture medium, it can kill a culture of *P. pastoris*).

15.11.2.2 Typical Examples

One of the most common microbes for recombinant culture is *E. coli*. This is because the genome is well understood and the addition of new genes using plasmids is relatively easy. The disadvantage is that *E. coli* does not have all of the necessary glycosylation pathways necessary to ensure a particular protein will be folded correctly to produce a biologically active molecule (reviewed by Choi et al 2006).

Some aspects of *E. coli* metabolism limit growth and product formation. In addition, some genetically modified strains differ significantly from wild-type strains in their physical and physiological requirements. Examples include an enhanced sensitivity to shear and the requirement for an initial period of growth in an environment relatively rich in carbon dioxide, requiring a lowering of the flow rate of air supply and decreasing the stirring speed in the first few hours of fermentation to achieve this.

The yeast most commonly used for recombinant work is *P. pastoris*. This also has a well-characterized genome and a range of commercial applications for recombinant protein production. The method of induction for product formation is well documented, and the mechanism of induction is achieved by switching from glucose/glycerol to methanol as a carbon source. One major advantage of *P. pastoris* is the ability of the AOX promoter mechanism to be used for production of a wide range of different recombinant proteins; a suitable protocol has been reported (Minning et al. 2001).

P. pastoris high-density fermentations require methanol measurement, which can be carried out directly or indirectly. If measurement of methanol concentration in the culture is made indirectly (exit gas), the methanol feed has to be introduced via a dip tube under the surface of the culture to avoid false reading as a result of methanol splashing.

15.11.3 Mammalian Cell Culture for Production of Therapeutic Protein

Commercial production of recombinant proteins in mammalian cell culture has been a modern success story, with productivity rising from milligrams per day to better than 1 g/day in only a few years. This has been achieved by careful selection of cell lines suited to growth in bioreactors, intensive process optimization for a small panel of these cell lines (with fed batch being the preferred method), and increase in volume of production vessels from hundreds of liters into the thousands. The use of mammalian cells ensures that glycosylation and other post-translational modifications are fully functional and appropriate for the desired therapeutic proteins.

The CHO (Chinese Hamster Ovary) cell line is one of the most commonly used cell lines for research and production of therapeutic proteins. **Hybridoma cell lines** have similar growth requirements but are used for production of specific proteins such as monoclonal antibodies. A range of culture volumes, vessels, and techniques have been successfully used, some of which are described in the following subsections.

Hybridoma cell line: A cell derived from the artificial fusion of a normal (e.g., an antibody-producing cell line from the spleen) with a transformed (immortal) cell line (e.g., a myeloma). The resulting hybrid is immortal and can produce a specific antibody if the correct spleen cell was selected after challenge of an animal with a specific antigen.

15.11.3.1 Small-Scale Cultures: Less than 1-L Volumes

15.11.3.1.1 Deep-Well Plates

Although the standard 96-well plates can be used, they are not ideal for cell culture. The larger size of the deep well variety allows for better mixing at slow speeds, which are necessary for cell culture work because of cell sensitivity to shearing.

15.11.3.1.2 Shake Flasks

Because growth is typically in suspension, moving to an incubator shaker will provide an easy path to better mixing and gas transfer than would be available in a static cultivation system. It is also a good first step if scale-up to disposable bags or a bioreactor is contemplated. Any small-scale system will usually require an incubation chamber with some or all of the following features:

- *Temperature Control:* The sensitivity of mammalian cells to changes in temperature makes accurate temperature control in the incubation chamber imperative. An external Pt-100 temperature sensor can be used in a test flask to ensure that control is based on liquid temperature.
- *Humidity control:* Humidity of cell culture affects osmolarity, which plays a significant role on growth and productivity of cell lines. Deep well plate cultures can decrease in volume significantly over time because of evaporation and high surface area.
- *CO_2 measurement and control:* This is to be expected for mammalian cell culture with measurement and control of this key parameter. Gas usage is kept to the minimum possible, and the atmosphere is quickly regenerated on closing the incubation chamber after manipulation of culture.
- *Validation of cleaning regimes:* The risk of unwanted microbial contamination is a major issue for cell culture work. Normal methods of cleaning an incubation chamber can be ineffective or can leave chemical residues. A suitable decontamination system would use a process that could be validated with electronic sensors and by using a biological test system. Decontamination systems based on the use of hydrogen peroxide offer this capability for incubators and other equipment.

15.11.3.2 Bag Shaker/Rocker

The use of disposable bags for cell culture production has become popular because of the removal of the need for sterilization and subsequent validation. The bags are placed on a rocking mechanism, and gentle tilting or orbital action are used to promote mixing and gas transfer in the bulk culture. A gas supply system and a manifold are used to transfer blended gas into the bag via a sterile filter; a mobile Pt-100 temperature sensor is placed under a bag to allow for accurate temperature control.

Bags are typically mounSted on a frame on a special tray. Each bag is made from materials that can be fully validated and is fitted with gas inlet and outlets, a medium inlet plus a separate harvest pipe, and a port for sampling. Single-use, disposable culture systems for production tasks have the following advantages and disadvantages.

Advantages

- No cleaning and revalidation are required
- Shorter time to productivity compared with commissioning and installing a conventional bioreactor
- Flexibility in overall capacity, its distribution, and location within a production facility
- Simpler mixing and aeration strategies with large rocker/shaker bags
- Easier to use with lower services costs (e.g., no steam required)

Disadvantages

- Can be expensive in the longer term compared with reusable systems
- Decontamination of culture and disposal of bags not as straightforward as sterilization of conventional systems
- Limitations to the number of inlets, sensors, and mixing devices, which can be fitted
- Only usable for cell cultures to date, whereas conventional bioreactors can often be adapted for different uses

15.11.3.3 Large-Scale Culturing in Bioreactors

Mammalian and insect cell culture can be carried out in STRs with relatively few modifications. The key modifications required are

- Low shear impellors, typically 0.35–0.5 vessel diameters
- A round-bottom vessel (hemispherical or, at least, dished)
- Removal of any baffles
- Special gas blending and possibly a modified sparger with a sinter or small holes for small bubbles
- Use of nonstick coating on the glass of the vessel to prevent cells from sticking
- Use of gasing and stirring regimes specifically intended to reduce foaming (e.g., pulsing of gas rather than a continuous flow)

Beyond these basic modifications, a range of other adaptations can be made according to specific requirements.

15.11.3.3.1 Links to an External Analyzer

Some of the key parameters for cell culture cannot be measured directly in the vessel (e.g., glucose, glutamate, lactate, and ammonia concentrations). Cell-free culture supernatant can be removed via a simple static filter and fed to an autoanalyzer for these chemicals to be measured online but outside of the vessel.

15.11.3.3.2 Conductivity Measurement for CIP

Large *in situ* vessels are often cleaned using CIP; traces of chemicals are then removed by rinsing with water. Because cell cultures are extremely sensitive to chemical contamination, a conductivity probe can be used to check that all traces of ionic materials have been removed before starting.

15.11.3.3.3 Use of a Gas Basket

A gas basket is only really suitable for bench-scale fermentations because a pressure drop in the tubing is problematic in larger systems. The gas basket uses porous silicone tubing to pass a blended gas into the bioreactor vessel without causing foam. The tubing is wrapped around a support frame to make a tightly wrapped coil, which presents a large surface area to the medium. This replaces a more conventional sparger.

15.11.3.3.4 Headspace Gasing

This is the traditional method for cell culture because foaming is much reduced and it accounts for the typical squat aspect ratio of a cell culture vessel (1:1). This provides a large surface area relative to the depth of the culture. Headspace gasing is still commonly used for addition of carbon dioxide for pH control, so leaving the sparger as the outlet for the blended gas is required for control of dissolved oxygen. However, any combination of gas or gases can be directed into the headspace.

15.11.3.3.5 Custom Gas Mixing

The standard "3 + 1" [air/N_2/O_2 for dissolved oxygen control and carbon dioxide (CO_2) for the acid side of pH control] gas mixing unit with mass flow control for the blended gas is applicable to most applications. If a different type of blending is required, mass flow valves can be fitted for each inlet gas and the composition of the blend controlled via a local controller or remote software. Of course, this can be linked to the values for dissolved oxygen and pH. Gasing of cell cultures is often started with a high concentration of nitrogen and only a little air because too much oxygen can be harmful to the cells.

15.11.3.3.6 Immobilization Systems

If particular cell lines do not grow well in suspension, they can be immobilized on discs or beads of a supporting matrix and grow on the surface and inside of these structures. Support discs are often placed in a special holder within the vessel and angled impellors used to direct a flow of medium through this central chamber. The advantage with the use of beads for cell immobilization is that it is scale independent and does not rely on a solution proprietary to a single vessel manufacturer.

15.11.3.3.7 Spin Filter/Perfusion

This is used for immobilized cell cultures and those with cells in suspension. A rotating filter (typically 10–20 μm mesh size) keeps cells from entering and creates a pool of cell-free medium inside of the filter cup that can be removed continuously or occasionally for replenishment with fresh media.

15.11.3.3.8 Secure Sampling

A requirement is to have a sampling device that can be used repeatedly without risk of contamination. Several systems are available that meet this criterion and disposable options use components more usually found in medical applications.

15.11.3.4 What Are the Advantages of Performing Cell Culture in Conventional Bioreactors?

- Scale-up issues can be directly addressed because large-scale cultures (e.g., 20,000 L) will typically be performed using modified STRs.
- The potential to add sensors, inlets, outlets, perfusion systems, and other peripherals is far greater than for disposable systems.
- A large body of application data already exists for many common cell lines going back more than 2 decades.
- Process control capabilities are far better than for disposable systems, which often have limitations in terms of the number and type of control loops possible.
- The hardware is reusable, and this has cost advantages in the long term
- Sterilization of contaminated batches before disposal is easier to deal with in standard bioreactors.

15.11.3.5 What Are the Key Operational Factors for Mammalian Cell Culture in Bioreactors?

- Cell numbers not as high as microbial culture
- Temperature for growth in a narrow range
- Cells are more sensitive to shear and osmotic shock
- CO_2 and oxygen supplementation may be needed
- Cells can grow immobilized on beads/carriers or suspended
- Thick foam destroys cells (i.e., low gas flow rates are required)
- Longer time scale (e.g., 10–14 d)

15.11.3.6 Which Choices Can Improve Productivity in Recombinant Cell Culture?

- Selection of clones that adapt well to bioreactors—not necessarily those which perform well in, for example, shake flasks.
- Careful selection of clones and adapting recombinant techniques to work with a strictly limited number of choices. This can help to reduce time for scale-up and allow some issues to be bypassed by working with well-characterized cell lines.

- Suspension culture is preferred in large-scale systems rather than immobilizing cells because this reduces the number of steps, costs, and the chance of poor results due to lack of attachment, etc.
- Fed-batch culture provides similar benefits in mammalian cell culture as those found in microbial cultures (Altamirano et al. 2004) (i.e., productivity is best if substrate concentration is limited) toxin dilution, and the opportunity to use perfusion techniques for material expressed into the culture supernatant.
- Choice of defined, serum-free growth media on grounds of cost-saving and eliminating steps in downstream processing to remove these substances.
- A low gas flow rate and the use of a conventional ring sparger can limit the damage caused to the cells by the formation of thick foam. Chemicals such as Pluronic (Sigma Chemicals) can help protect cells. Many different gasing strategies are used, including only adding oxygen in pulses when required and gas blends starting mainly with nitrogen.
- Use of real-time analyzers to simultaneously measure glutamate and glucose consumption along with levels of lactate and ammonia production by the culture (the latter can attain toxic levels).

15.11.4 Solid-State, Algal, and Other Bioreactors for Biofuels

Biofuel production and solid-state fermentations (SSFs) have been dealt with extensively in Chapters 9 and 14, respectively.

15.11.4.1 Biofuels

Biofuel technologies for the production of bioethanol, biogas (methanol), biodiesel, and hydrogen have recently attracted significant public interest. Biodiesel is typically produced by chemical treatment of plant oils or algal biomass as feedstock.

15.11.4.1.1 Biogas

Biogas is typically methane generated by anaerobic digestion of manure or sewage waste material. These fermentations can be carried out in any standard bioreactor at the laboratory scale, with options for commercial sensors t measure key gas production. Because gases such as methane and hydrogen are explosive in air at concentrations beginning at approximately 5%, care is needed to ensure a buildup of exhaust gases is not possible. Commercial-scale processes are invariably in digesters, which are much simpler than pharmaceutical bioreactors.

For biogas production, a typical bioreactor configuration would be

- Bacterial system ≥ 0.75 L total volume
- Located in an area with an extraction system for exit gas
- Water-jacketed for rapid temperature change
- Control of temperature, speed, pH, pO_2, foam, and flow plus exit gas analysis for methane
- Pressure sensor for safety and indication of leaks
- Process control software for logging and control
- Monitoring of the local environment for high methane concentration

Most forms of digestion for methane production fall into this category. Because control of dissolved oxygen is not usually required, the status of the fermentation can be measured using redox potential as an alternative. Mixtures of gas can be introduced to keep a reducing atmosphere, and even a limited control of redox is possible by liquid or gas in some circumstances.

15.11.4.1.2 Bioethanol

Bioethanol production is principally a fermentation process with substrates such as sugar and starch crops, lignocellulose materials such as wood chips, and agricultural materials such as straw or grass fiber. Woody feedstocks often require pretreatment with enzymes or physicochemical agents to break down long-chain molecules such as celluloses or lignin to smaller sugars. This pretreatment allows for the maximal yield from the subsequent fermentation process of converting the resulting sugars to ethanol. A typical bioreactor for ethanol production would be configured as follows:

- A bacterial-type system ≥ 0.75 L total volume.
- Water-jacketed for rapid temperature change.
- Control of temperature, speed, pH, pO_2, foam, and flow.
- Substrate feeding (and removal).
- Process control software for logging and control.
- For lignin and other celluloses, high temperature operation may be needed (e.g., up to 80°C).

15.11.4.2 Use of Photosynthetic Organisms for Biofuel Production

Algae have an important role to play because they are not food crops and do not even require land-based cultivation. They can provide a rich source of energy in the form of biomass, oils, and even direct production of hydrogen. Dependent on light for growth, algal cultures require bioreactors with lighting that can be flexibly controlled. Again, the STR is a valuable research tool for small-scale studies, but large-scale commercialization typically involves a lower level of technology and use of natural resources such as sunlight in desert regions. Factors important for photosynthetic culture include

- *Good temperature control:* Because lighting invariably adds heat directly in the vessel or around it, good temperature control is required. A water jacket is a good choice for efficient removal of heat, but it needs modification if it is not to interfere with external lighting.
- *The quantity and quality of light:* A white light will provide the widest range of available wavelengths. Alternatives may provide a spectrum optimized for photosynthesis. Conventional fluorescent tubes may be used or recent developments based on LED lighting can provide a flexible alternative.
- *Control of light intensity:* A stepped or continuously variable control of light intensity is desirable so that the light intensity can match the growth of the culture. Linking light intensity to OD is a good strategy for automated control.
- *Scale-up:* Some form of scale-up strategy may be needed. Glass vessels are clearly a good choice for bench-scale research, but lighting may also be need above, for example, a 10-L working volume. Production-scale processes are often based on relatively simple tanks or long lengths of tubing and so do not require matching vessel geometry or mixing strategy at the laboratory scale.
- *Mixing:* Mixing may be at low speed, and a marine impellor could give better results than flat-bladed impellors in this case.

15.11.4.3 Bioremediation

The construction of a standardized environmental chamber with control of key physical and chemical parameters has been lacking for some time. Environmentally controlled chambers for solid substrates have recently been constructed (see Box 15.7) and should prove invaluable in the following domains:

- Wastewater treatment
- Breakdown of liquid pollutants in soils

BOX 15.7 HOW DO SOLID STATE DRUM BIOREACTORS WORK?

A rotating drum or fixed tray supports a solid substrate that can be held at a fixed temperature, mixed (for systems with a rotating mechanism), and gased. Rotating systems need a mechanical seal that can turn in either direction if maximum flexibility for mixing strategies is envisaged. Speed of rotation is typically slow (e.g., <10 rpm) and may be intermittent. Operating temperature range can be wide, from a few degrees above freezing point for soil remediation trails to almost 100°C for biogas/biofuel applications. For this reason, a chiller, heating thermocirculator, or steam generator may be needed to provide the necessary temperature control. Preheating of the input gas may also be beneficial for good temperature control with a solid substrate.

Measurement of dissolved oxygen and pH is not normally possible for solid substrates because of a lack of moisture and the abrasive nature of many solid substrates. Exit gas analysis is possible to detect conversion of a specific carbon substrate to carbon dioxide, consumption of oxygen, and calculation of variables such as RQ. Bioconversion/remediation is usually expressed in terms of the amount of carbon dioxide evolved in a given time. Where a complex substrate like soil is used, more than one microbe may contribute to the bioremediation.

In some solid state systems, sterilization or steam pretreatment of the substrate is possible *in situ,* and this will generally increase the moisture content. If this is not desirable (e.g., the substrate becomes sticky or forms pellets), the quantity of steam added directly can be limited and a suitable gas flow rate found to remove much of the excess moisture. A sterilizable system extends the range of applications for solid-state bioreactors to the production of enzymes from solid substrates for pharmaceutical use.

- Bioremediation of soils in landfill
- Decontamination/recycling of solid/semi-solid waste products (e.g., slurries, fats, etc.)
- Composting and anaerobic digestion
- Solid-state enzyme production
- Production of enhanced animal feeds

15.12 CURRENT TRENDS AND FUTURE PROSPECTS IN FERMENTOR DESIGN AND APPLICATIONS

Fermentors have come a long way from their earliest days in the 1940s. The objective was to raise productivity in a given space by using submerged culture for penicillin production to replace surface culture. The conventional STR has held a dominant role in the pharmaceutical industry, academic research, the food industry, and many other areas ever since that time. However, STRs have never been the only choice, and specialized reactors for wastewater treatment, enzyme production, and bioremediation have been available in some form for decades. However, recent interest in microbial processes involving more specialized and extreme environments has caused the STR to be adapted in various ways. They include

- Greater temperature range, especially for the culture of thermophiles at temperatures of 80ºC and beyond
- Production of structured tissues in the fermentor, produced in areas contained by a mesh or within three-dimensional scaffolds

- Use of more aggressive chemical environments, necessitating vessels designed without any metal parts that cannot corrode or influence culture conditions
- A rise in the need for strictly anaerobic environments, with the use of inert gas overlays in the vessel and feed bottles, control based on redox, and use of totally nonporous tubing for reagent lines

These examples are in addition to the SSFs, photobioreactors, biofuel, and cell culture systems mentioned above.

One important point is that research-scale work is often performed using laboratory-scale fermentors, but the final production scale will not usually be based on STRs. Taking biofuel as an example, commercial systems use tubing that can be attached to fences in sunny geographical regions for algal culture. In medicine, *in vitro cell* culture systems now use disposable cartridges tagged with patent details that provide the same end result as culture in a fermentor but with a totally different design. A simple biogas digester for domestic use need be no more sophisticated than a simple plastic container and an electrical heating strip. These systems are cost-effective on the large scale or mass market but are poorly monitored and controlled in comparison to fully equipped fermentors.

Regarding instrumentation and control, the trend is toward controlling processes based on microbial metabolism rather than simple feedback control of a few key process parameters such as temperature, pH, and feed rates. Software exists for metabolic monitoring and control, with multifunctional analyzers providing biochemical data such as lactate and glucose concentrations in real time. Existing sensors are also changing with the rise of optical probes for dissolved oxygen and pH. They require less in the way of calibration and maintenance, improving reliability and making validation easier. Another advantage of these sensors is their small size, allowing well-instrumented vessels of just a few milliliters to be used for many of the tasks that would have previously required a full-sized bench fermentor.

This trend combines perfectly with the rise of single-use culture systems that have a clear role in rapid development of validated processes without the need for expensive infrastructure. An interesting hybrid technology is developing, with single-use vessels being combined with conventional STR services and control equipment to provide a "reversible" solution for disposable and reusable applications. To date, these disposable technologies have concentrated on mammalian cell culture, but interest in adapting the technology for bacterial cultures is growing. The fact that so many applications exist, with still new modifications of the STR being made, is validation of its basic concept and inherent flexibility.

SUMMARY

Bioreactors are composed of several different components that can be grouped according to function (i.e., temperature control, pH measurement, etc.). A wide range of peripheral devices can enhance the basic facilities of the bioreactor.

Bioreactor instrumentation is based on DDC systems that offer advantages in terms of the flexibility of control and the ability to store operational protocols.

Many different types of vessels exist and include air lift, fluidized bed, and hollow fiber and specially modified STRs. Special categories of STRs include those for in situ sterilization and containment of pathogenic or genetically manipulated organisms.

Practical guidance has been provided for autoclaving, inoculation, and sampling to ensure safe and reliable operation for any make or type of bioreactor.

Examples have been provided for the use of bioreactors for wide range of common applications in research and industry, including cultivation of microbial cells, algal fermentations, mammalian cell culture, and bacterial and yeast culture at high cell densities.

Current topics regarding new culture methodologies such as process analytics, exponential feeding, solid-state substrates, and the place of single-use systems have been considered.

REFERENCES

Altamirano, C., C. Paredes, A. Illanes, J.J. Cairo, and F. Godia. 2004. Strategies for fed- batch cultivation of t-PA producing CHO cells: Substitution of glucose and glutamine and rational design of culture medium. *J Biotechnol* 110:171–9.

Choi, J.H, K.C. Keum, and S.Y. Lee. 2006. Production of recombinant proteins by high cell density culture of *Escherichia coli. Chem Eng Sci* 61:876–85.

Ejiofor, A.O., Y. Chisti, and M. Moo-Young. 1996. Culture of *Saccharomyces cerevisiae* on hydrolysed waste cassava starch for production of baking-quality yeast. *Enz Microb Technol* 18:519–25.

FDA. 2004. *Guidance for industry: PAT—A Framework for Innovative Pharmaceutical Development, Manufacturing, and Quality Assurance*. U.S. Food and Drug Administration: Washington, DC.

Lee, J., S.Y. Lee, and S. Park. 1997. Fed-batch culture of *Escherichia coli* by exponential feeding of sucrose as a carbon source. *Biotechnol Techniques* 11:59–62.

Minning, S.A. Serrano, P. Ferrer. C. Sola, R.D. Schmid, and F. Valero. 2001. Optimization of the high-level production of *Rhizopus oryzae* lipase in *Pichia pastoris. J Biotechnol* 86:59–70.

This page intentionally left blank

16 Control of Industrial Fermentations: An Industrial Perspective

Craig J.L. Gershater and César Arturo Aceves-Lara

CONTENTS

16.1 REQUIREMENT FOR CONTROL

In the early 1970s, fermentation processes were perceived to be as much art as science. The best indicator for a fermentation progress was the experience operator looking through a site glass and observing the color and texture of the foam layer on top and sometimes by smelling near to the bioreactor. Much progress in control bioprocess has occurred during the past 40 years.

Control is generally defined as the power to direct or influence. In the case of fermentation control, the requirement to control a given biotechnological process is generally dictated by the need to bring about a desired outcome such as maximizing output of product formation. Control is applied to provide a near optimal environment for microorganisms. Microorganisms used in industrial processes have been isolated by virtue of their ability to overproduce certain commercially significant attributes. These attributes can range from the ability to produce carbon dioxide for leavening activity in the case of *Saccharomyces cerevisiae* (baker's yeast) to the production of useful microbial metabolites such as alcohol from yeast or antibiotics from filamentous bacteria.

Whatever the reason for commercial exploitation, the microorganism will have been obtained directly or indirectly from an ecosystem very remote from that of the fermentation laboratory and process plant. The metabolic attribute to be exploited will have evolved as a result of environmental factors unknown to the fermentation scientist, and therefore process optimization must seek to replicate those environmental factors responsible for expression of the desired attribute in the totally "artificial" environment of the industrial bioreactor or fermentor.

16.1.1 Microbial Growth

The principal fermentation control requirement is population growth (see Chapter 3 for more details) of the microorganism of interest. In its natural habitat, the microbe will respond to environmental stimuli such as excess nutrients by synthesizing enzymes and biomass capable of exploiting the resource as effectively as possible. In the fermentor system, the microbe will be inoculated into the fermentation medium "feast" and will thus attempt to colonize this environment through rapid growth.

The role of the fermentation control strategy is to provide—by control of environmental effectors such as temperature, aeration, pH, and dissolved oxygen—the optimum conditions for growth and colonization. The fermentation scientist uses an environment that is capable of being controlled to a limited degree (i.e., the fermentor) to develop a control strategy that will modify inputs to the fermentor system to achieve the desired outputs. This system of modifying inputs to obtain a desired output from a control system is often described as a control loop.

16.1.2 Nature of Control

A fermentation development program seeks to establish what control set points are needed for the control loops in the control system. It is easy to forget that the control system can be human. There are many examples of accurate human control loop systems, including the motor car. In the motor car, the driver observes the speed of the vehicle (the output from the system) by looking at the speedometer (sensor). If the car is traveling too fast, the control system (the driver) reacts by reducing pressure on the accelerator, thus reducing the flow of fuel to the engine (the input to the system). The car slows and the driver observes whether the speed matches the desired outcome (speed limit); if it does, the adjustment to the accelerator will be modified again, and so on. Control of a fermentation system can similarly be by manual intervention of control valves adjusted as a result of changes observed on gauges; however, this chapter will concentrate on the elements of automatic (computer) control.

16.1.3 Control Loop Strategy

The basic element of a control system is the control loop. Figure 16.1 summarizes the various components that make up the control loop. At the center of the control loop is the system requiring control, the fermentor. The system can be affected by several influences, and in this case it is the temperature of the system that is to be controlled. A very simple control loop is shown in which only cooling may be applied to the fermentor principally to remove metabolic heat during incubation. The temperature of the fermentor is measured using a thermometer, and a human operator or a control system can monitor this measurement and make adjustments if the desired temperature (the set point) and the actual temperature are not equal (error in the system). If the temperature of the fermentor is above the set point, the flow of cooling water is turned on (input to the system) and once the temperature equals the set point, the control valve is switched off. In reality, dynamic fermentor systems are never fully stable and constant monitoring and control are required, hence the advantage of automated systems, which maintain constant vigil on the process and adjust inputs to the system as and when required automatically.

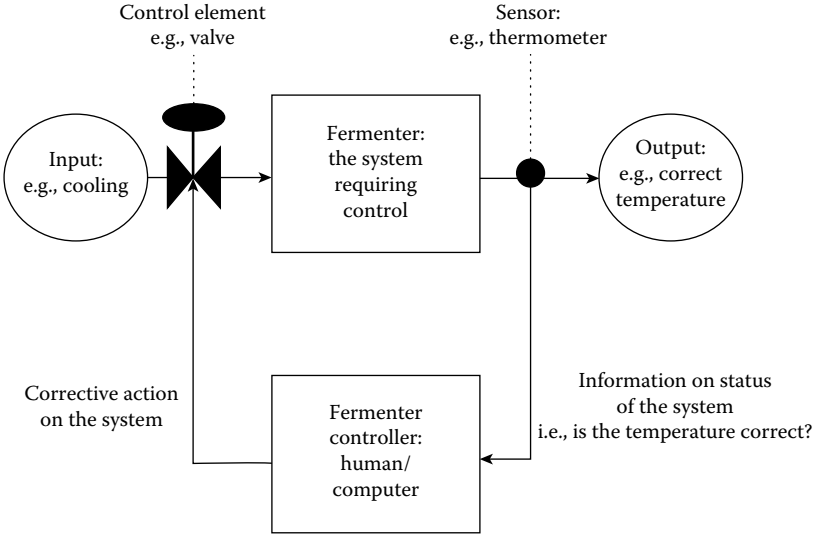

FIGURE 16.1 Simple control loop.

16.2 SENSORS

Development of fermentation processes thus far has been accomplished primarily in large-scale reactors (>10 L) with the aid of relatively few sensors. The problem with monitoring the fermentation system is maintaining the sterile integrity of the fermentor, hence any sensor has to be capable of sterilization *in situ* during steam sterilization or remotely and then aseptically introduced to the fermentor.

16.2.1 Historical Perspective

In the 1940s, the sensors were largely based on manual sampling and offline analysis; control was improved through the 1950s and 1960s by the use of limited electrical signals controlling pneumatic outputs (valves, etc.). In the 1970s, new sensors capable of being sterilized were introduced, including pH and dissolved oxygen probes. In addition, more accurate methods of measuring flow rates (both liquid and gas) became available and other engineering parameters such as motor power to the agitator and enhanced nutrient feed addition systems were developed. In addition, improvements to sensors and other measuring devices mini-computers were introduced to provide simple control and data logging.

Recently, a wide range of new sensors (see Chapter 11 for more details) have emerged for online analysis of fermentation parameters. Recent techniques that have become available include biomass probes, online liquid chromatography systems, near infrared spectroscopy, and so on. For the most part, the reliability and relevance of some of the measurements together with prohibitive cost tend to preclude these sensors from everyday fermentations.

16.2.2 Typical Fermentation Sensors

The control elements (sensors) that should be considered routine for most (aerobic) fermentation systems are

1. *Temperature:* Temperature is measured using a platinum resistance thermometer (PRT probe), where the increase in temperature is proportional to the increase in electrical resistance in the probe. Temperature will be controlled by the addition of cooling water to a jacket or cooling finger of a fermentor; heat will be added by direct heating of the vessel or its contents (electrical heating mantle or "hot finger") or by the injection of hot water or steam to the circulating water in a jacket or heat exchanger.
2. *Airflow rate:* Airflow rate Is measured using a standard pressure drop device such as variable area flow meters or more often a mass flow sensor. Airflow will generally be controlled using a proportional (0 to 100% open) valve upstream of the sterile inlet filter on a fermentor. Airflow is frequently expressed as VVM, or the volume of gas per volume of liquid per minute; fermentor design generally permits up to 2 VVM.
3. *Vessel pressure:* Vessel pressure is measured using diaphragm-protected Bourdon gauges or strain-gauge pressure transducers. Pressure in the vessel is induced during *in situ* steam sterilization and during normal incubation with the introduction of air. Control of vessel pressure is by regulation of the vent gas from a fermentor. Pressure is generally a negatively acting loop in that a fully driven output valve (100% open) results in minimal pressure in the fermentor. The units of pressure are generally bar gauge (i.e., pressure within the reactor above atmospheric).
4. *Vessel agitation rate:* Vessel agitation rate Is measured using proximity detectors to detect the speed of the shaft. Impellors or mixers are controlled by standard motor controllers, and the units are revolutions per minute. Agitation power is sometimes measured using

current transformers measuring the electrical power consumption of the motor; the units of power are Watts. pH is measured using steam-sterilizable combined glass electrodes. pH is controlled by the use of buffers or by the addition of acids or base titrants.

5. *Dissolved oxygen:* Dissolved oxygen is measured using polargraphic-type probes; here galvanic voltages on a membrane-covered oxygen-reducing cathode induce a current (amperometric) proportional to the amount of oxygen diffusing through the membrane. Dissolved oxygen is controlled by altering the status of those control loops affecting dissolved oxygen generation. An increase in dissolved oxygen is induced in fermentation medium by (1) increasing the airflow rate (volumetric increase in oxygen), (2) increasing agitator speed (smaller air bubbles increasing the surface area available for diffusion), and (3) increasing overpressure in the fermentor (generally increasing the residence time for air bubbles). Dissolved oxygen is measured as the partial pressure of oxygen at the electrode surface and hence is expressed as percentage saturation (often referred to as dissolved oxygen tension, DOT). To obtain a mass, a fully saturated solution of oxygen in water is approximately equivalent to 1.2 mM/L.
6. *Foam:* Foam is detected by observation, conductance, or capacitance probes completing an electric circuit when foam is contacted. Foam is controlled by reducing the cause of foaming (i.e., high aeration and/or agitation rates or by the addition of antifoaming agents).

Figure 16.2 shows the main control elements of a fermentor. There are many different cofigurations that may be specified, but the one shown would be capable of providing dta and control options for an aerobic fermentation.

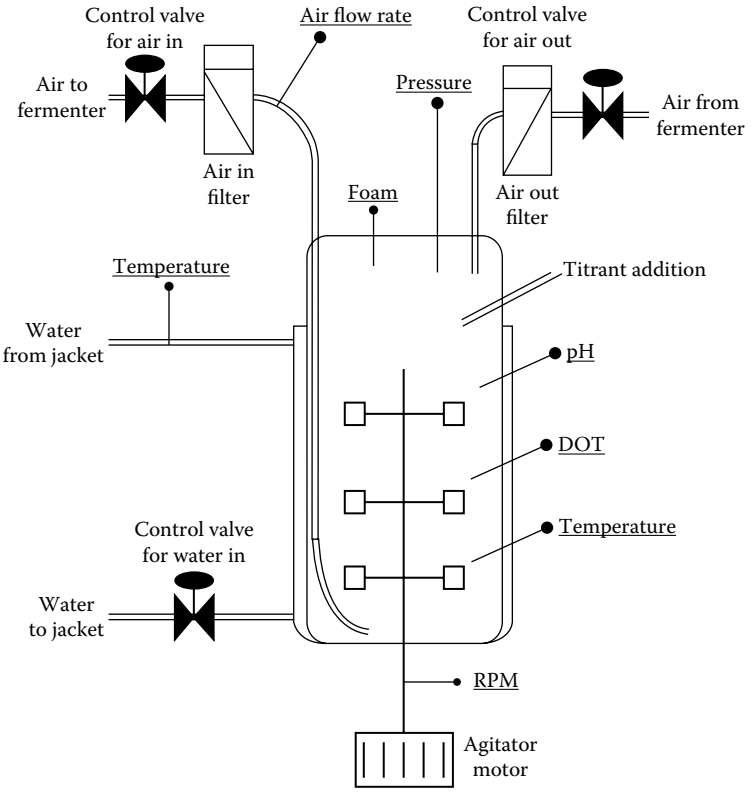

FIGURE 16.2 Basic elements for control of a fermentor.

16.2.3 Control Action

Temperature control would be achieved by the regulated supply of temperature controlled water to the jacket of the fermentor. In the case illustrated, there are two thermometers in the system—one indicating the temperature of the medium/broth and the other indicating the temperature of the return water flow. In this configuration, the two signals may be compared and control options could include linking their function to provide a regulated flow of temperature-controlled water to the jacket via the control valve shown.

Airflow control would be achieved by regulating the linear gas flow rate to the system by adjusting the airflow control valve shown in response to signals coming from the airflow sensor. Pressure control is achieved by regulating the flow of off gas from the fermentor. It is probably beneficial to have the airflow and pressure control functions independent of each other. For the most part these control loops will act to the limit of their engineering configuration, and if a particular set point (i.e., for airflow) cannot be achieved because of excess back-pressure, then this may be noted as a process constraint and the operating protocol adjusted accordingly. Agitator speed is controlled by direct feedback of the revolutions per minute using a suitable tachometer.

pH is generally controlled by the addition of acid or base titrant in response to changes in pH value during the fermentation. One important aspect of the pH loop is the calibration of the probe before and after sterilization. These are achieved before sterilization by the adjustment of slope and intercept values on the pH controller to be used during the fermentation. Subsequent to sterilization it is possible to check the calibration of the pH probe by comparing the pH of a sample of medium withdrawn from the fermentor using a calibrated external pH meter. The function of the pH-control loop will be discussed in more detail later.

Dissolved oxygen control is achieved in several different ways. It is possible to rely totally on increasing agitator speed to shear air bubbles rising through the broth to increase surface area and thus mass transfer of oxygen from the gaseous to liquid phase. However, it is also possible to cascade the control output from the dissolved oxygen controller to agitator speed, airflow, and pressure or any combination of these. In a particularly high-oxygen-demanding fermentation, all three outputs may be specified, and care has to be exercised in the use of independent control loops such as agitator speed that this loop will be the "slave" to the DOT "master" control loop function. The function of the DOT control loop will be discussed in more detail later. Foam is controlled by the addition of antifoam agents via the feed addition system in response to a contact probe detecting rising foam.

16.3 CONTROLLERS

Control instrumentation has developed rapidly in recent years, and the range of options available for fermentation control is extensive (see Chapter 10 for more details). The development of integrated circuits in the last 30 years or so has meant that complex control functions can be devolved to cheaper instruments, or conversely more sophisticated control options have become increasingly available to the fermentation scientist.

16.3.1 Types of Control

Two fundamental types of control may be incorporated into a fermentation system: sequence control and loop control. Sequence control is that part of control that permits automation of the fermentor operation such as sterilization and other valve automation sequences; that is, for the most part providing an ordered array of digital (on/off) signal control. Loop control is generally associated with that part of control dealing with combinations of digital and analogue control signals, and although used in sequence control (particularly automated sterilization sequences), is most often associated with control of incubation. The industrial fermentation scientist will frequently wish to adapt the

control strategy for optimal process performance and to ensure versatility; modified control programs may be specified, although the costs and potential delays associated with this approach are likely to be significant.

Control of fermentation systems can be achieved by the use of discrete single-loop controllers, by programmable logic controllers controlling sequence and loop functions, and by the use of specific software packages to control all aspects of the fermentation. This type of control is sometimes called *distributed digital control* (DDC) and defines boundaries of operation in which whole plant control can be achieved using computer-based systems.

16.3.2 Control Algorithms

Whatever type of controller is selected for fermentation control, effective action will depend on the response of the controller. This response is determined by the nature of the control algorithms programmed into the system. A control algorithm is a mathematical representation of the steps required to achieve effective control, most often programmed as equations in which the controller output is a function of signal deviation away from a set point. As indicated in Figure 16.1, most controllers will function as feedback control systems; that is, the deviation of measured variable compared with the desired set point will determine how large the control effect should be on the fermentor system via the appropriate control algorithm.

16.3.3 PID

The types of control algorithm most frequently encountered are three-term or PID controllers. The PID controller is made up of three elements—P, proportional; I, integral; and D, derivative/differential—the purpose of these functions is to provide a fast-acting response to process deviation and scale the response to the output to achieve smooth control action. The characteristics of PID control are

- Proportional control provides an output, the magnitude of which is proportional to the deviation between the measured variable and the set point.
- Integral control tends to reduce the effect of proportional control alone, helping to bring the measured variable back to the set point faster by minimizing the integral of control error.
- Derivative action also tends to reduce the effect of proportional control alone, this time by estimating the slope of measured variable with time and maximizing the slope of the measured variable compared with the set point.

The effect of PID control on an uncontrolled variable is shown in Figure 16.3. As indicated, the algorithm tends to "drag" the analogue value toward the set point, the speed and effectiveness of this control response are a function of the parameters specified by the PID algorithm, and the process of setting these parameters is termed *tuning the loop*. The method is generally carried out by trial and error with the loop online. There are three parameters associated with PID loop tuning: the proportional band (usually set as a percentage of full-scale deflection of the analogue signal), the integral time, and the derivative time. The method chosen for loop tuning will be recommended in control instrument vendors' instructions, and the sequence is generally as follows:

1. Set the proportional band first with no integral (maximum value) or derivative function (minimum value).
2. When oscillations occur with small process perturbations, decrease the integral time (from its maximum) until oscillations reoccur, and then reset the integral time to minimize oscillations.

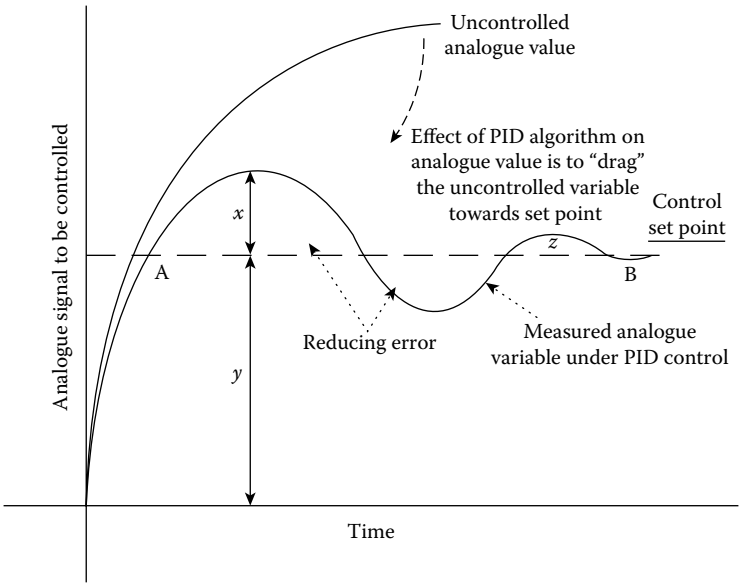

FIGURE 16.3 PID control.

3. Establish whether control is adequate with PID control alone, If not satisfactory following process perturbations, increase the derivative time constant (from its minimum) to minimize oscillations.

PID loop performance can be assessed by measuring the initial overshoot as a ratio of *x:y*. A measure of PID loop effectiveness can be assessed by examining the control error decay ratio of *z:x*. In addition, the "gain" of the controller (i.e., how fast the measured variable attains the set point when full control is applied) is described by point A. Point B describes the "settling time" for the loop (i.e., when the measured variable is within a fixed percentage of the set-point value, e.g., ±5%).

16.4 DESIGN OF A FERMENTATION CONTROL SYSTEM

The first stage in designing a fermentation control system is to clearly establish what the process objectives are for the automation project.

16.4.1 Control System Objectives

Objectives may be typically divided into various categories of control.

1. Control of basic incubation functions only, typically airflow, agitator speed, and temperature;
2. Automation of the control of incubation only relying on manual operation of valves associated with sterilization;
3. Full automation of the fermentor system including all sterilization and auxiliary vessel control;
4. Advanced control options including event-based control; and
5. Advanced computing methods for inferential control.

Whatever type of controller is considered necessary, the process scientist will have to specify the type of control and then make this specification available to the manufacturer of various control

systems. Although the more complex the fermentor system is to be controlled, the more detailed the specification will need to be.

1. Basic control will typically be achieved using single-loop controllers and is frequently associated with autoclavable fermentors. These controllers tend to combine amplification of process signals and control function in one "box"; this functionality may also include a local readout function in engineering units (i.e., values recognizable to the operator). There is a wide range of commercially available single-loop controllers, some of which have been developed with control of fermentation processes in mind. Configuration of the controllers will follow manufacturers' guidelines, but as with all control options, factors such as signal type (current or voltage) and output device will have to be considered before final control specifications can be issued to potential vendors.
2. Incubation control may include other features, including operation of feed delivery systems and control of more complex loops such as dissolved oxygen by multiple outputs that may be specified by the operator. The specification in this case may be more complex and subject to negotiation with the instrument vendor. Sterilization of this type of vessel may be by autoclaving or by *in situ* steam sterilization, but this will be done manually, probably to minimize cost.
3. Full incubation and sterilization control of the fermentor will require a control function for valve sequencing (digital control) and control of analogue parameters for incubation (process variables and control of proportional valves). The requirement for valve sequencing and more complex patterns of analogue control is met by the use of programmable logic controllers (PLCs) or often fermentor manufacturer's own control software running on a personal computer. This type of control is generally required for larger fermentors (>20 L) or when several identical vessels are to be purchased and manual sterilization will be too manpower-intensive. The need for a detailed specification is determined by whether the vendor's own software meets the needs of the fermentation scientist. If it does, then the basic requirements of sterilization and incubation control may be easily identified from the vendor's own specification. However, if pre-existing software does not meet the needs of the scientist, then a much more complex and detailed specification may be required because it is most likely that the software will have to be written specifically for the purpose. It is in the best interests of customer and vendor to agree to the objectives of the bespoke software before the code is written; costs and time scales can very quickly escalate out of control. The benefit of using the vendor's own software is speed of implementation and probably lower costs; the disadvantages are that you get what the vendor thinks you want, not what you might actually need. The opposite is generally the case with PLCs; costs and time scales will be higher, but if you get the specification right, you get exactly what you want and need.
4. Advanced incubation control regimes may be required where complex fermentation patterns are required and changes to set points may be needed online, particularly in response to specified "events." This will be discussed in more detail later. The need for a detailed specification is very high under these circumstances, and clear milestones and checkpoints must be agreed during contract negotiations. It is quite likely that stage payments will be part of a contract. Large fermentor control tasks may be related to complexity of control and numbers of fermentors within a system. If the task involves many fermentors to be controlled, then a system of distributed control will probably be required. The architecture for distributed control is shown in Figure 16.4.

   Figure 16.4 illustrates one possible control option for the control of four fermentors. In this configuration, each fermentor is independent of the next and control is affected by each fermentor being equipped with its own controller (in this case a PLC). This type of distributed control has the advantage that failure of a control system will only affect one

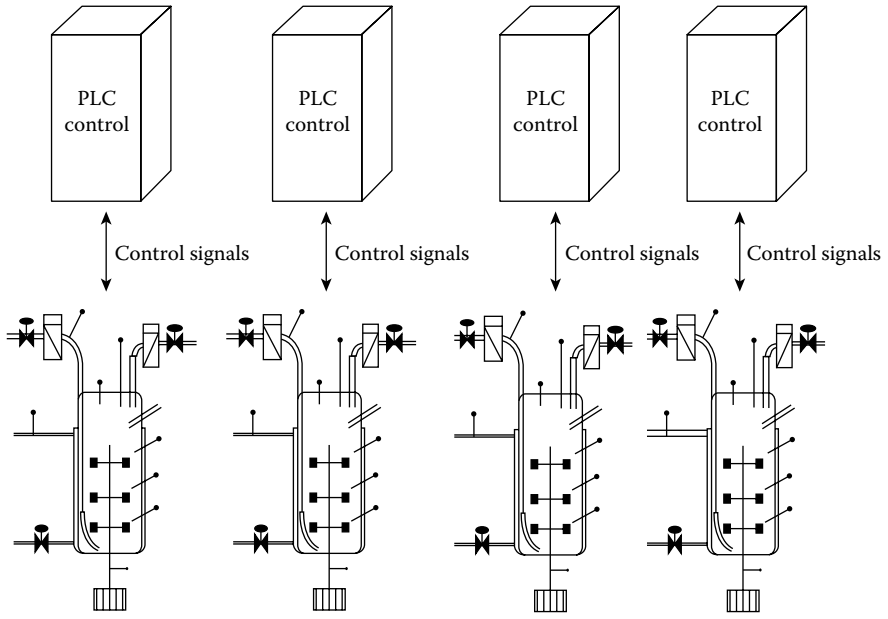

FIGURE 16.4 Distributed fermentor control.

fermentor; the experimental design may be ruined by such an occurrence, but without a distributed system, failure of a single controller will result in failure of the entire run. The disadvantage of distributed control is that the cost may be prohibitive to implement one controller per vessel. In the author's laboratory, a compromise has been reached with vessels larger than 100 L in working volume where a single PLC controls a pair of identical fermentors.

5. Advanced computing methods may be required where analytical systems are inadequate to optimize the fermentation process and cost of goods or value of product warrant investment in "next-generation" computing methods. Inference methods are available that algorithmic sensors can function to estimate for analytes and processes for which no other sensor or probe exists. The sort of computing methods being developed include expert systems, metaheuristic algorithms, artificial neural networks, and model-based systems. These self-learning or decision-making systems rely on process pattern recognition to identify regions of the fermentation process more or less susceptible to perturbations. Once identified remedial action beyond the scope of experienced operators or less sophisticated controllers can be initiated to reduce cost, avoid catastrophes, or simply improve the process. These systems can often only be justified in production environments where the value of the product warrants large investment in time and money to maximize productivity. As these methods become more widely available, the costs of implementation of advanced computing methods will decrease and wider applications will be sought and introduced.

16.4.2 Fermentation Computer Control System Architecture

In defining the overall strategy for computer control of fermentations, system architecture will emerge to indicate how the system will be operated; how data will flow around the system; and how that data can be captured, stored, and interrogated when required. The control system when configured is an information exchange system.

Information about the progress of the fermentation is detected by sensors and transmitted to amplification/signal conditioning units that forward this information to the controller. The controller receives the information; compares it to pre-existing information about how the fermentation should proceed (set points); and then after generating new information in the form of an algorithmic output, transmits information back to the fermentor to a control unit capable of receiving information and translating that signal into a control action. Over and above this control function the operator can observe the flow of information (data), intervene if necessary (new information), and recall past information from a data storage system. Figure 16.5 shows an example of a fermentor control system architecture in which the information exchange is indicated.

In Figure 16.5, there is flow of analogue and digital sensor data from the fermentor vessel to the control cabinet. The input data are marshaled in I/O (input/output) cards, the main function of which is to convert a mixture of signals to a common electrical signal type for the computer to interpret. These signals are passed to the PLC (in this case) where control strategies (set points, etc.) are programmed. In the PLC, the input data are fed into PID algorithms and other control functions, and an output signal is fed back to the fermentor via I/O cards. The control signal returning to the fermentor may have to be transduced to a more usable format for the process plant; this may take the form of pneumatic signals scaled from the frequently used 4–20 mA to the equivalent 0–1 bar pressure. The PLC in Figure 16.5 is connected to the operator terminal, which may be a PC with a video display unit (VDU) or a standalone plant terminal. If located on the process plant floor, then the whole cabinet has to be splash- and dust-proof, often referred to as an IP55 rating.

The PLC is also connected to a data highway onto which other fermentor systems are connected. In Figure 16.5, all of the fermentors are in communication with a supervisory and data acquisition system (SCADA), the function of which is to collect all of the plant data and store it for later retrieval and possible interrogation. It should be understood that the SCADA is not a database; it generally cannot give answers to database-type queries, but using advanced graphics and trending graphs can present the operator with comprehensive information on plant status.

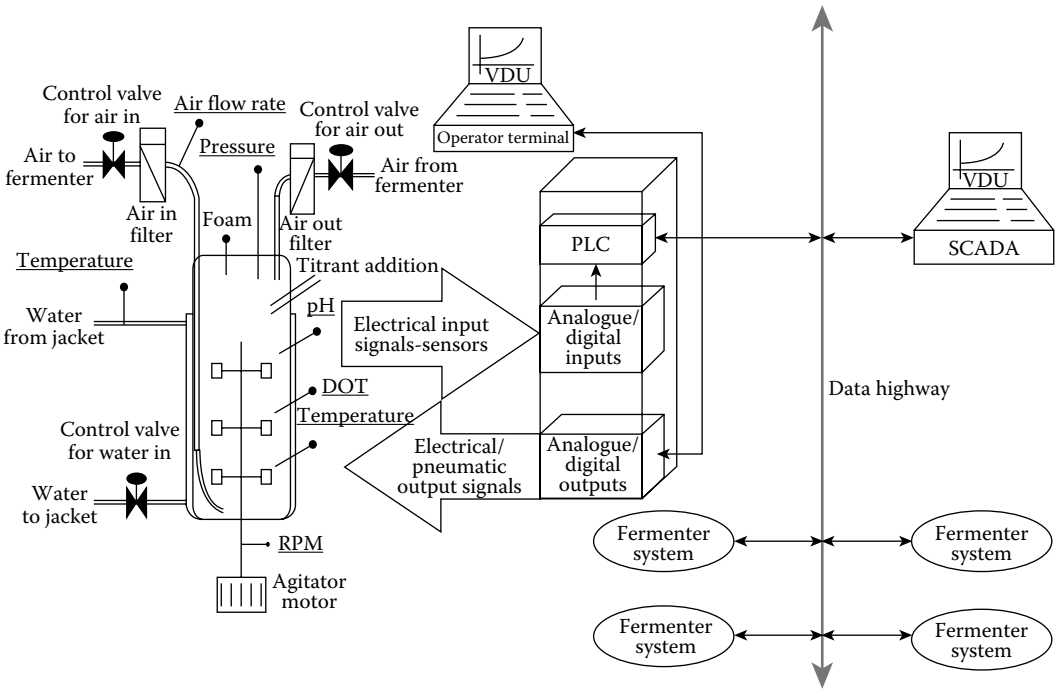

FIGURE 16.5 Fermentor control system architecture indicating information exchange.

16.4.3 Fermentation Plant Safety

One of the overriding functions of a fermentation control system is monitoring and action relevant to safety. A fermentor is a potentially dangerous piece of equipment because it uses live steam (to 135°C), overpressure (to ≥2 bar gauge), acids, bases, and the microorganism and its products. The automated control system can ensure by program interlocks, etc., that the plant is operated with the maximum safety margins on every function, and specifying this is perhaps the most important part of the acquisition of a new control system.

16.5 FERMENTOR CONTROL SPECIFICATION

When planning for a new fermentor control system, the specification for the system is crucial to the success of the project. The specification will be used to judge vendor's response and to subsequently quote and oversee the project to completion. Time and effort spent generating a comprehensive system specification are rewarded many times over during implementation and commissioning.

16.5.1 Specifying Sequence Control

One of the most important tasks when planning to automate a fermentor system, particularly for sterilization and other automated sequences, is to accurately specify what the sequences are to be automated and how this will be achieved. There are fixed unit operations associated with fermentor control and the specification will define these and indicate how this control will be achieved.

16.5.2 Fermentation Unit Operations

Taking batch fermentation as a typical example, the unit operations to be selected might include

- *Blank sterilization:* This is generally used as a prebatching cleansing sequence when all steam and drain valves are opened.
- *Medium batching:* The fermentor is usually in a safe state for opening and preparation. In the author's laboratory, the safe state is defined by "standby." In standby, all valves are shut with the exception of valves venting the vessel interior to atmosphere. During batching, probe calibration and insertion into the vessel must be complete before water is added to the vessel!
- *Medium sterilization:* The sterilization sequence will be partly dictated by the fermentor vessel configuration and geometry. Steam sterilization of the medium can be achieved by direct steam injection or by indirect heating via a heat exchanger or vessel jacket. Whatever the mode of sterilization chosen, it is crucial that the correct valves are operated in the correct sequence, not just for process integrity but also for safety.
- *Medium hold:* It is useful to maintain the fermentation medium in a safe state after sterilization. It is at this time that final adjustments to the fermentor setup can be made (e.g., pH adjustment via a tartan feed system or temperature alteration before inoculation).
- *Fermentor inoculation:* To introduce inoculum into the sterilized fermentor requires opening the vessel in a controlled manner and introducing inoculum using strict aseptic techniques throughout. If introducing the inoculum via peristaltic pumps, then a reduction in vessel pressure will be required.
- *Incubation:* Although not strictly a sequence, there are clearly certain valves that must be opened to permit incubation of the culture to proceed under specified conditions. The principal function of the incubation sequence is to start the clock counting the hours elapsed

since inoculation. During incubation, the full functionality of the control system may be used to program the correct fermentation "trajectory" for the run. This will involve specifying set points for all of the main controllers, including agitator speed, airflow, temperature, and feeds if available, as well as controls responding to more metabolic influences such as pH and dissolved oxygen.

- *Harvest:* It may be necessary to specify a sequence dealing with harvest operations. This could entail prechilling or suitable pH adjustment of the broth to permit easier product recovery operations. Harvest could also include "killing" the vessel; that is, sterilizing the vessel interior (with or without cells) before safe opening and cleaning.
- *Cleaning:* Several options may be available here, including full sterilization or heating in the presence of caustic detergents to fully automated clean-in-place (CIP) systems with complex valve operations of their own.

16.5.3 Vessel States

Fermentation unit operations may be termed *vessel states*, and the transition between them must be strictly regulated in an automated plant; for example, initiating automatic sterilization of the batch during the incubation should be avoided at all costs. State changes can be summarized in a state diagram (Figure 16.6).

Each one of the states in the diagram defines a part of the control program specifying sequences to be executed for effective control of the fermentation system. Navigating around the state diagram defines the safe operation of the vessel under automatic control. Certain transitions are under operator control such as from standby to medium sterilization. Other states are attained automatically as a result of a particular sequence finishing, such as the transition from sterilization of the medium sterilization to broth hold. Within an automated control system there is the opportunity to initiate emergency action that could come about as a result of alarm settings or operator intervention. This is indicated in Figure 16.6, where a state called emergency hold may be attained from anywhere in the program. Such a state can be programmed to do whatever is deemed appropriate for safe containment of the process; in the author's laboratory *emergency hold* constitutes a safe universal shutdown of the fermentation process sealing the vessel but retaining set points for possible restart of incubation.

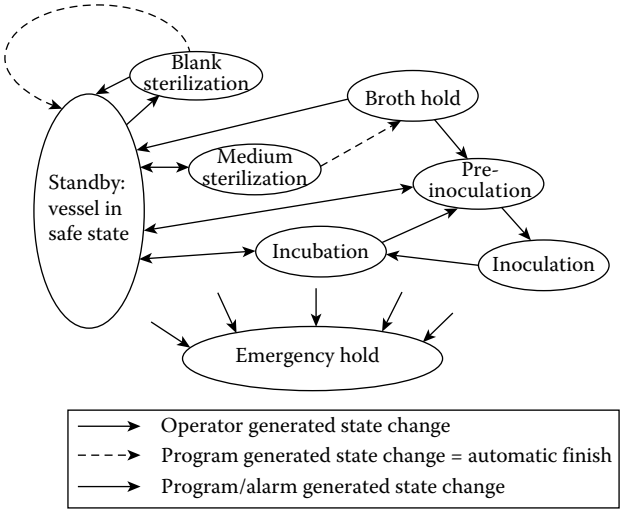

FIGURE 16.6 Control state diagram.

16.5.4 Sequence Logic

Control of multiple valves on an automated fermentor requires the program to control the opening and closing of valves such that the state operation is effectively and safely completed. Each of the vessel states indicated previously and possibly many others have to be programmed taking best human operator practice and engineering constraints into account. Defining the sequence follows a pattern of working that ensures ambiguities are minimized and objectives are clearly stated. Taking one of the states in Figure 16.6, sterilization of the fermentor plus medium, the system developer must start with a complete description of the fermentor and the valves associated with sterilization (which is likely to be most of them). A comprehensive description will come from accurate drawings of the plant; these drawings are often referred to as piping and instrumentation drawings (P&ID, not to be confused with PID for control). The drawing will identify the units of control to be defined in the program. Modern operating systems will tend to function with structured code, and it is possible to consider individual blocks of code controlling individual units of control.

This can be illustrated with reference to Figure 16.7, a typical fermentor configuration (as a notional P&ID) is shown for sterilization, and only those valves that are relevant to this highly simplified representation are shown.

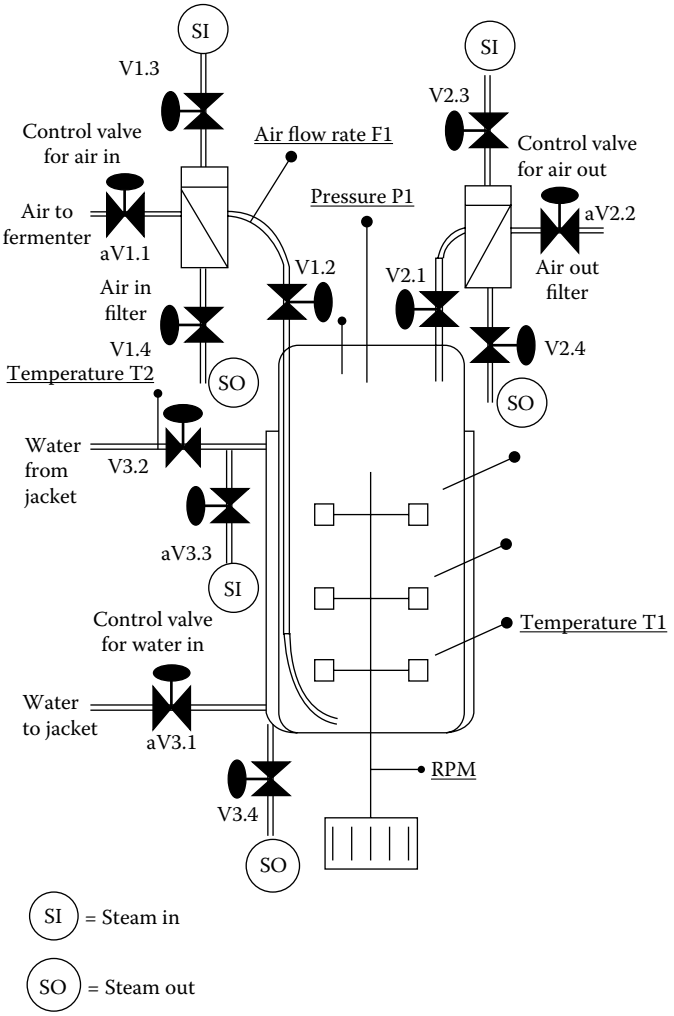

FIGURE 16.7 Control of sterilization example.

The P&ID identifies the key elements for the following groups of valves:

- Air in group V1.X
- Air out group V2.X
- Jacket group V3.X

SEQUENCE LOGIC for sterilization operations:

1. START: all valves closed
2. Drain jacket
3. Heat-up phase
4. Direct steam injection
5. Air filter sterilization
6. Sterilization temperature
7. Air filter pressurization
8. Crash cool
9. Ballast air
10. Broth hold

16.5.5 Flow Charting

P&ID drawings, valve descriptions (Table 16.1), and status charts (Table 16.2) are essential in defining the operation to be automated. However, before code can be written, the operation is translated into a flow chart of valve operation and decision gates that must be followed. The flow of code to accomplish the task will follow the chart (Figure 16.8). The "English" translation of the flow chart is approximately as follows:

- START: All valves are closed and remain closed unless instructed otherwise.
- DRAIN jacket: The jacket drain valves are opened for a specified time (dependent on jacket geometry).
- HEAT: Cycle commences by opening air out valves to allow for the escape of air and by opening steam valves to the jacket.
- FILTER: The sterilization of the air inlet filters must be complete before the medium so that sterile air can be admitted to break the vacuum caused by collapsing steam after sterilization is complete. The commencement of filter sterilization may be dependent on the temperature of the medium in the fermentor.
- DIRECT: To assist in heating the medium to sterilization temperature, steam can be admitted via the air in filter and down the air sparge pipe. The point at which this occurs can be determined by the medium temperature.
- PRESSURIZE: At some point during the sterilization of the medium (0.5 total sterilization time?) the air in filters are pressurized to prevent ingress of contaminants before ballast air.
- CRASH COOL: When the sterilization time is complete, the fermentor and its contents are "crash-cooled" (to minimize time at elevated temperatures) by shutting off the supply of steam and admitting cold water to the heat exchanger system.
- BALLAST AIR: While the temperature of the medium is still above boiling, the vessel is pressurized with sterile air to prevent the vessel pulling a vacuum and thus permitting possible ingress of contamination microorganisms.
- BROTH HOLD: When the temperature of the medium is at some predetermined level (35°C), the vessel is held in a quasi-incubation mode, ready for inoculation and/or other treatment.

TABLE 16.1
Valve Descriptions for Example Fermentor (Figure 16.7)

Air in Group	Air Out Group	Jacket Group
V2.1	Digital air out valve	
aV2.2	Analogue control valve for pressure	
V2.3	Digital steam to air out filter	
V2.4	Digital steam out from air out filter	
aV3.1	Analogue water to jacked valve	
V3.2	Digital water from jacket valve	
aV3.3	Analogue control valve steam to jacket	
V3.4	Digital jacket drain/condensate out valve	
aV1.1	Analogue control valve: air to vessel	
V1.2	Digital air ex: filter block valve	
V1.3	Digital steam to air in filter	
V1.4	Digital steam out from air in filter	
	BOTH: analogue and time i.e., pH > 6.5 AND < 24 h true EITHER or BOTH: i.e., pH > 6.5 true OR time < 24 h OR both true EITHER or true (but not both): either pH > 6.5 true OR time < 24 h true EITHER or NEITHER (but not both): i.e., neither pH > 6.5 OR time < 24 h, OR pH, OR time, but NOT pH AND …time true NEITHER: …neither pH > 6.5 OR time < 24 h true	

In this simple example, many different factors have been taken into account, but the flow chart is far from complete; for example, there is no mechanism in this for operators to enter set points. Again with this example there are only 12 valves; on a 4500-L pilot-scale fermentor used for research and production there may be 70 or more valves organized in many functional groups, hence programming such a system will require many days/weeks of specifying, programming, and testing before the fermentor control system may be commissioned.

16.6 CONTROL OF INCUBATION

Specifying the sequence logic of a fermentor control system is only part of the control task, arguably the most important function of the fermentor control system is to control the incubation of the microorganism of interest. Returning to the case made for the control of fermentations at the start of the chapter, the purpose of the control system is to provide an optimal environment for growth and expression of an attribute associated with that growth. This is very difficult; one can pose the rhetorical question, what is the natural habitat for *Escherichia coli*? The answer given by many might

TABLE 16.2
Valve Status Chart for Sterilization Sequence Logic

	Valve Status									
Valves	**START**	**Drain**	**Heat**	**Filter**	**Direct**	**STER**	**Press**	**Cool**	**Ballast**	**Hold**
Air in										
aV1.1	0	0	0	0	0	0	$a = 1$	$a = 1$	a	a
V1.2	0	0	0	0	1	1	0	0	1	1
V1.3	0	0	0	1	1	1	0	0	0	0
V1.4	0	0	0	1	0	0	$1 \Rightarrow 0$	0	0	0
Air out										
V2.1	0	0	1	1	1	1	1	1	1	1
aV2.2	0	0	$a = 1$	a	a	a	a	a	a	a
V2.3	0	0	0	0	0	1	0	0	0	0
V2.4	0	0	0	0	0	1	0	0	0	0
Jacket										
aV3.1	0	0	0	0	0	0	0	$a = 1$	a	a
V3.2	0	0	0	0	0	0	0	1	1	1
aV3.3	0	0	$a = 1$	a	a	a	a	0	0	0
V3.4	0	1	1	1	1	1	1	0	0	0

be "the intestinal tract of most vertebrate animals," but enteric bacteria can be isolated from many mesophillic environments and evolved probably billions of years before the advent of colons.

Therefore, when faced with the prospect of defining the environmental conditions to maximize microbial productivity, how does the fermentation scientist decide what conditions to apply? In answering this question, a distinction should be made between fermentation development strategies for research and development organizations and manufacturing. Each function imposes different constraints. Within the manufacturing sector fermentation development will be investigating the factors associated with a well-established fermentation process where the objectives of a development fermentor will be to obtain relatively modest increases in productivity (leading to substantial financial savings on large-scale production) or to achieve reduction in "cost of goods." In a research and development environment, the constraints usually come from working with a wide range of culture types, limited/no knowledge of those cultures, limited/no knowledge of the fermentation systems, and with very short development times required.

16.6.1 Specification for Incubation Control

Specifying the control options for a fermentor system must then take into account not only the type of organisms to be grown but also what sort of control options will actually be required. The control options for a typical research and development fermentor system are described in Sections 16.6.1.1–16.6.1.7.

16.6.1.1 Temperature

Control of incubation temperature will be achieved by the use of system of addition of heat and cooling. This control loop is fundamental to fermentor systems. The degree of accuracy of control during incubation will probably be on the order of a set point in the range 20–50°C (±0.1°C). Response times may also be important, and controlled ramp rates of better than 1°C/min may be necessary.

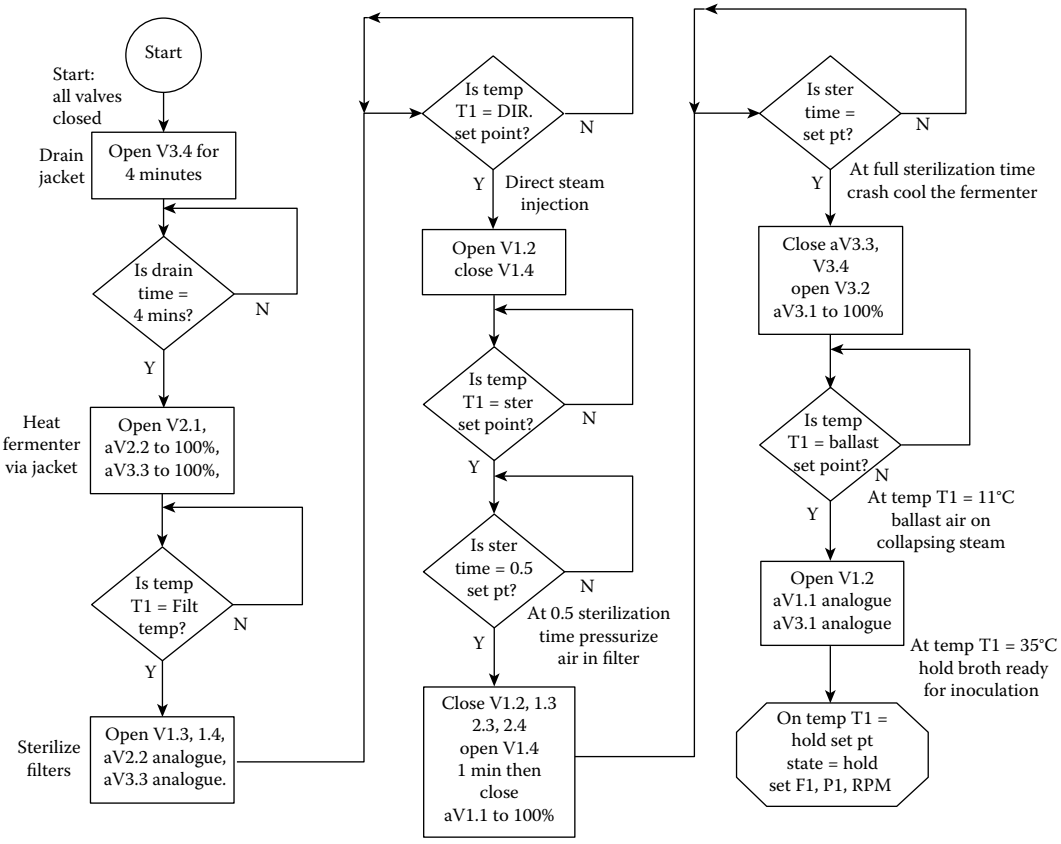

FIGURE 16.8 Example flow chart for sterilization of a fermentor.

16.6.1.2 Aeration

For most industrially significant processes the microorganisms will be aerobic. Supply of air to the fermentor will need to be controlled typically in the range 0–2 VVM. The accuracy of the control system will need to be on the order of ±1% of full-scale deflection (FSD). This is generally a fast-acting loop, and obtaining adequate ramp rates is not a problem.

16.6.1.3 Agitation

The stirrer for a traditional fermentor is used to minimize gradients within the bulk broth, the larger the vessel the greater the potential for gradient (mass transfer) problems. Sufficient motor power has to be available to obtain uniform mixing times to be on the order of 1–2 min or less (determined from the addition of a marker into the bulk liquid and the time taken to homogeneity recorded). These fast mixing times may not be achievable in pilot-scale vessels (3000 L + working volumes) and these system constraints must be identified and resolved, for example, in scaled-down experimental designs (modeling large-scale parameters in small-scale vessels). Agitation ramp rates may be high, and the control system should be capable of ramp rates equivalent to 10% of FSD per minute.

16.6.1.4 Pressure

This control loop only applies to pressure-rated vessels. The control of pressure is required for accurate control of *in situ* steam sterilization as well as for some incubation regimes. The control requirement during incubation may come from maintaining adequate pressure for high oxygen

transfer or to simulate hydrostatic head pressure in large-scale vessels in scale-down experiments in smaller scale vessels. Control of pressure is critically linked to safety, and safeguards within the control system must ensure that the vessel cannot be overpressurized. Pressure can be a very fast-acting loop, and obtaining adequate ramp rates is not a problem. The function of this loop may be in conflict with the aeration loop, and the fermentation scientist has to bear in mind that control of these two loops may be incompatible. For example, a set point for pressure near the safe operating limit of the vessel may be impossible to achieve with extremely low airflow rates (0.1 VVM).

16.6.1.5 Hydrogen Ion Concentrations, the pH

Most industrial fermentations need to be run within a certain range of pH values for maximal productivity. Although media are formulated in such a way that it ensures that a certain level of buffering capacity is "built in," there is often a requirement to control the pH away from this "natural" value. This is achieved most often by the addition of acid or base titrants. Addition of acid or base titrants requires a feed system of some description. Under these circumstances the control of the feed system is subordinated to the pH controller; in other circumstances the feed system may act under the direction of another controller or independently, which will be discussed in more detail below. When tuning a pH control loop it is very difficult to define the "correct" PID settings because the strength of the titrants will vary. Therefore, the "gain" of the controller (i.e., how quickly a response will be achieved) will also vary greatly. This problem of adequate pH control can be addressed by user definable dead bands around the set point where no control action is initiated. The purpose of the dead band is to allow for the natural buffering capacity of the medium to have sufficient time to act so that titrants are not added close to the set point on a detuned loop, which will be the case with variable titrant concentrations.

In Figure 16.9, the response of a pH control loop after acid or base addition is shown. It will be noted that there is a proportional action on the additions of titrant made (i.e., the larger the "error" the more frequent the control action). The closer the measured pH gets to the set point, the longer the delay between each addition of titrant; however, when the dead band threshold is crossed, all titrant addition stops and the natural buffering capacity of the medium results in an approach to

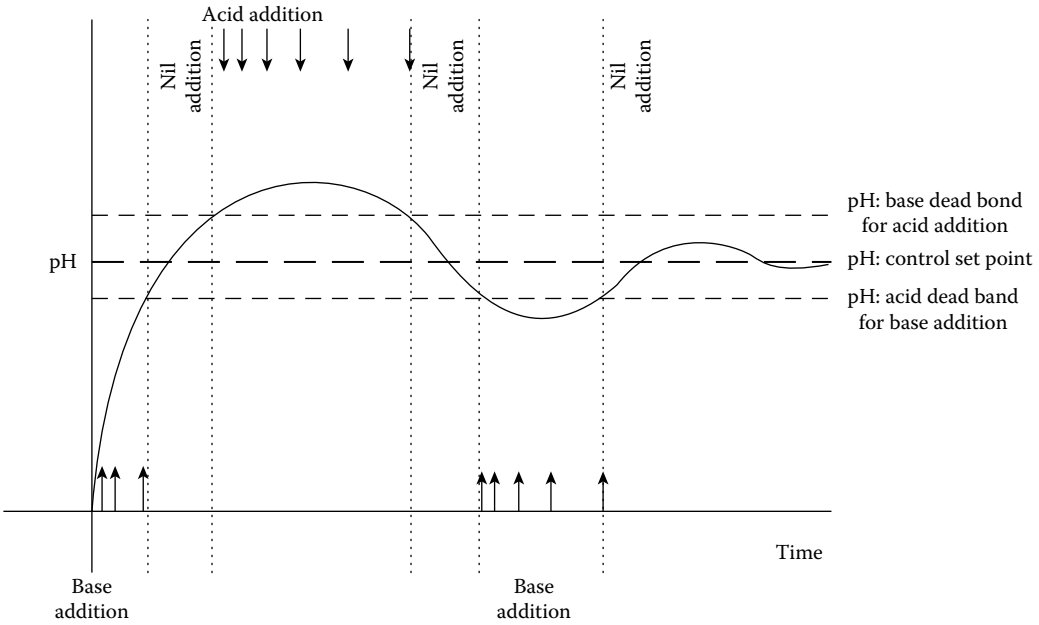

FIGURE 16.9 pH control by titrant addition.

the set point within the dead band limits. The setting of the dead band limits may be asymmetrical about the set point depending on the criticality or tendency of the fermentation to be acid or base tolerant. Mineral acid titrants may be substituted for organic acids or the principal carbohydrate energy source such as glucose. In this case the buffering capacity or delay equates to the metabolic rate for the consumption of the sugar, and protons generated by catabolism will require a delay of some minutes before a noticeable effect on the pH will be detected. This type of control of pH by metabolic action is really a means of permitting the microorganism to autoregulate the supply of carbon.

16.6.1.6 Dissolved Oxygen

The control of dissolved oxygen in aerobic fermentations may be critical to the successful outcome of that fermentation. The requirement for oxygen may be very high during the rapid growth phase of a batch culture, and oxygen limitation may result in inadequate growth and incomplete oxidation of the primary energy source. The control of dissolved oxygen is generally achieved by increasing the "driving force" for the mass transfer of oxygen from the gaseous phase to the liquid phase. The methods or outputs available to the control system to achieve this include increasing the agitator speed, which generally increases the shear on the air bubbles, making them smaller and increasing their surface area available for gaseous exchange.

The second output that may be programmed is to simply increase the airflow rate, which ensures a greater volumetric airflow through the liquid. The last output that may be incorporated into a dissolved oxygen controller is vessel overpressure, which will have the effect of increasing the hydrostatic head pressure and preventing rapid flushing of "precious" air from the fermentor.

All of these outputs can be specified for a dissolved oxygen controller individually or in any combination of all three. The output of the dissolved oxygen controller (master) must be cascaded onto the closed-loop controllers for agitator, airflow, and pressure (slaves) as required. The consequence of this is that the function of the closed-loop controller will be subordinated to that of the dissolved oxygen controller to achieve the desired dissolved oxygen tension in the fermentation broth.

This type of control may be considered a replenishment system in which the microorganisms' metabolism is the oxygen sink and the outputs of the controller replenish the resulting deficiency. In setting up a dissolved oxygen controller it may be necessary to set default set points for each of the closed-loop controllers such that at the start of the fermentation a baseline level of agitator speed, airflow rate, and vessel pressure will permit adequate mass transfer of oxygen for microbial metabolic action to ensue. As the microbe respires, the depletion of dissolved oxygen will occur and the output of the dissolved oxygen controller will increase to compensate. Depending how the DOT control loop is specified, the outputs can be scaled to one or more of the specified closed-loop controllers.

In Figure 16.10, the dissolved oxygen controller (master) is linked to all three closed-loop controllers (slaves). As the DOT falls, the oxygen controller output will rise, and this will cause an increase in agitator speed from a default closed-loop set point to a maximum revolutions per minute specified for the DOT output. In the example, the DOT continues to fall as the output of the controller passes a threshold equivalent to one third of the total output range of the DOT controller. At this point the second specified closed-loop output is subordinated to the DOT controller and takes over from agitator speed, leaving the set point for the first output at its specified maximum. The second output, in this case airflow, increases to try and compensate for the fall in dissolved oxygen, and when this output limit is reached (two-third of the DOT controller output), then the third closed loop (in the example, vessel pressure) takes over, leaving airflow at a maximum value. Eventually the rate of replenishment equals the rate of oxygen depletion, and DOT is controlled in the example with revolutions per minute at its maximum set point, vessel pressure at its minimum, and airflow responding as the principal output of the DOT controller as a PID loop.

In addition to control by oxygen replenishment, it is also possible to initiate dissolved oxygen control by depletion. With the slave outputs set to relatively high output values, medium batched

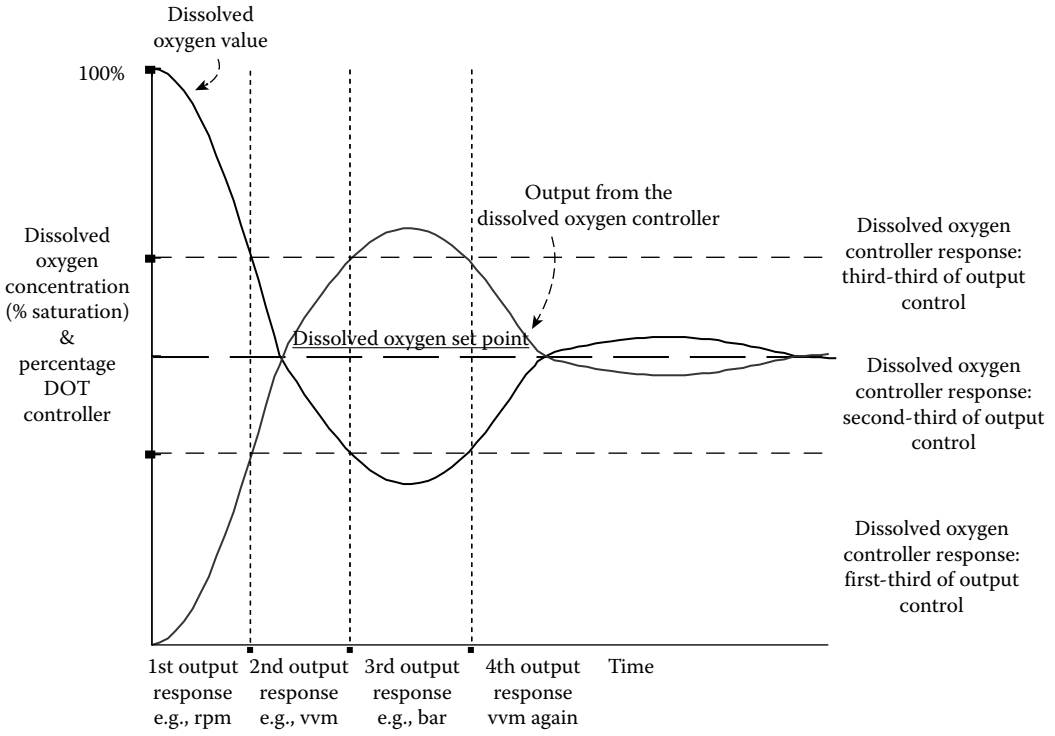

FIGURE 16.10 Dissolved oxygen control by master/slave cascade control.

with little or no energy source present can have the DOT controlled by the regulated feed of, for example, carbohydrate. Under these circumstances the feed system becomes the cascaded slave output and only delivers glucose at a rate equivalent to the metabolic rate of the organism under fixed oxygen mass transfer limitations set by the closed-loop outputs (speed, air, and pressure).

16.6.1.7 Feed Systems and Antifoam

Most fermentor systems will be equipped with a mechanism for introducing various feed solutions under aseptic conditions. The method for achieving this will depend largely on the size and configuration of the fermentor itself. On smaller laboratory-scale vessels, feeds will be controlled by the use of peristaltic pumps working on flexible-walled tubing. On larger vessels such as those found in the pilot plant (>10–20 L), it is possible that purpose designed and constructed addition vessels independently sterilizable will deliver feeds using shot-wise additions of feed solutions.

Whatever the method of addition chosen, it is very likely that feeds will be pulsed in some way and therefore the variables available for control are pulse width (i.e., size of liquid 'shot') and interval between pulses. In the author's laboratory, fixed pulse width or liquid volume shot size and variable intervals provide a satisfactory control option for the addition of feeds. The set-point for a feed controller can be several shots in a specified interval of control or the feed controller can be cascaded onto a master controller such as pH or dissolved oxygen. The output of the feed controller can be linked to the interval such that the larger the output of the controller (further away from the desired number of shots) the shorter the interval and hence the more rapid the feed rate. Calibration of a feed system is difficult and will be affected by tubing age and vessel back-pressure. It is possible to introduce another sensor to take over the control of feed additions (i.e., a balance for the feed reservoir), and this type of control loop for feeds can provide very accurate and nonpulsed control of feed flows, but costs may be high and it is only really applicable to smaller-scale vessels (<20 L).

Antifoam addition is variation of the feed control loop where the sensor is a contact probe detecting rising foam. The control variables here may be time related. To prevent overaddition of antifoam agent (which may destroy dissolved oxygen control by bursting air bubbles) a splash time interval can be specified in which the contact probe would need to be covered for more than a few seconds to initiate antifoam addition. Similarly, if the probe remains covered after antifoam pumps being switched on, then secondary control action can be specified in which the aiflow rate and/or agitation speed may be reduced to minimize the generation of foam. Clearly, if this happens then the dissolved oxygen controller will be affected, but the output of the antifoam controller may be the ultimate master controller of closed loops to prevent loss of broth by foam-out.

16.7 ADVANCED INCUBATION CONTROL

The control options specified above represent the basic control elements for most fermentation development purposes. However, many fermentation development programs will require more than just a system of fixed set-point control, and that is where we can return to some of the observations made at the start of the chapter. To close this chapter, we present a description of an advanced PLC in the author's laboratory that is capable of more advanced fermentation control options.

The wild-type microorganism in its natural habitat (whatever that is), as previously discussed, is subject to transient environments. When a fermentation scientist attempts to grow the microbe and encourages it to express the desired attribute, a fermentation regime will be imposed that will only represent a tiny fraction of all of the influences that the organism will encounter. Given that most fermentations will be run under fixed set-point regimes, the environment that is thus imposed will effectively be a "snapshot" of the full range of conditions that have brought about the expression, through evolutionary pressure, of the desired phenotype. Another option for control is therefore to provide a mechanism in which events beyond the fixed set-point control regime can be specified.

16.7.1 Fermentation Profiles

A typical fermentation control profile is shown below (Figure 16.11). The main features of the profile are captured in Table 16.3. When analyzing the progress of fermentation, it is sometimes useful to identify the key features and in which phase of the growth of the organism they occur. For this

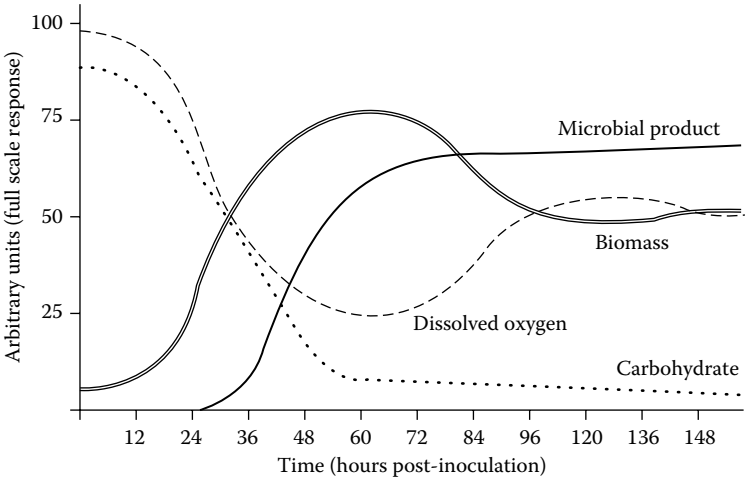

FIGURE 16.11 Typical fermentation profile for a filamentous microorganism producing a secondary metabolite.

TABLE 16.3
Fermentation Profile Data for Key Analytes at Various Growth Phases ("Snapshots")

Analyte	Time (h)	Valve (Arbitrary)	Grow Phase
Biomass	12	10	Lag
	24	25	Acceleration
	36	50	Exponential
	48	70	Deceleration
	60	75	Stationary
	84	60	Decline
	148	50	Harvest
Carbohydrate	0	85	Inoculation
	24	70	Acceleration
	36	35	Exponential
	48	20	Deceleration
	60	10	Stationary
	148	5	Harvest
Dissolved oxygen	0	100%	Inoculation
	24	80%	Acceleration
	36	40%	Exponential
	48	30%	Deceleration
	60	25%	Stationary
Microbial product	24	0	Acceleration
	36	10	Exponential
	48	35	Deceleration
	60	50	Stationary
	72	60	Decline
	148	65	Harvest

purpose it is useful to use standard definitions for the growth phases, although their strict interpretation is obviously open to debate. In the example given, the following features become apparent:

- Harvest time is a long time after product accretion has ceased (this is frequently the case with old processes that have been inherited).
- Carbohydrate uptake is largely linear over the growth phase of the organism and is depleted by 60 h.
- Biomass accretion occurs between 0 and 60 h and then after substrate depletion goes into the decline phase.
- Dissolved oxygen profile is the mirror image of the growth profile.
- Product accretion has its onset at 24 h and is complete by 72 h.
- Harvest time using this protocol can be at 72–84 h.
- Dissolved oxygen is not limiting; therefore, under this fixed set-point regime would higher biomass yield more product (increasing fermentor vessel volumetric productivity)?
- Carbohydrate is depleted by 60 h, a further carbohydrate feed at either this point or when the DOT was less than 40% of saturation may promote a further product accretion phase.
- pH is not shown here, but the level is likely to fall between 12 and 60 h and this may require pH control by titrant addition.

This type of profile is typical of the kind that would be obtained with fixed set-point control for the principal closed-loop controllers (not including DOT control).

16.7.2 Event-Tracking Control

As indicated above, with the carbohydrate feed option it is possible to identify an event in the fermentation that serves to trigger another control action. Hence an event is a specific change in state or time or any combination of changes that can initiate a new event. In the case cited, a carbohydrate feed could be initiated at 60 hours postinoculation (time-based event) or if the dissolved oxygen measurement fell below 40% of saturation (analogue value event). Computer control systems, particularly those specified by the customer, can easily accommodate program decision gates that will test the status of the fermentation and apply another control action on the fermentation if the decision gate criteria are met. To define what the decision gates should be and what values of analyte or combinations of analyte values should be used requires the fermentation scientist to establish set points for control loops that he or she can control and then observe the effect on analytes that do not have online sensors (biomass, carbohydrate, and product in this example).

As soon as the fermentation scientist wishes to use event-based control, then further options may be sought to extend this capability. In the author's laboratory the PLC fermentor control system has been programmed with four types of user-definable events:

1. *Time-based events*: These become true at a specified number of hours postinoculation.
2. *Analogue value events:* These become true when a process value or combination of two process values exceed a threshold limit.
3. *Elapsed time events:* These become true at a defined time after another event has occurred.
4. *Boolean events:* These are logical combinations of any two other events using standard Boolean operators.

The trigger events for the most part can be almost any process signal or event "flag" indicating the status of that event. In addition, system events or alarm levels can be specified (this apart from warning alarms is a very powerful use of alarms signals). The events can be organized in any combination giving virtually limitless fermentation control strategies. The events themselves can initiate new set points, ramp rates (rates of change between set points), or new events. It is possible to "latch" initiating events such that dependent events will remain true even if the initiating event is no longer true.

Figure 16.12 shows three graphs for event-based control. Graph 3 shows the status (true/false) of three fermentation process events. Graph 2 shows set points for two output controllers (these could be any type of controller as discussed previously) to be driven by the specified events (1, 2, and 3). Graph 1 is the fermentation profile against which the new set-point control regime is to be imposed. A summary of the main changes is given below.

- Event 2 becomes true first (e.g., time value = 12 h) and the set point for controller 1 is changed from the default set point (arbitrary value 25) to the event 2 set-point (50) control action initiated at the end of the lag phase.
- The rate of change from one set point to the other can also be specified and in the graph it is comparatively slow—ramp-rate control action over acceleration phase.
- At approximately 40 h event 1 becomes true. The set point of controller 1 changes from event set-point 2 to event set-point 1 (arbitrary value 75) with a faster ramp rate—control action at end of the exponential phase, start of deceleration phase.
- Events 1 and 2 are true at this time. This initiates event 3 also becoming true, the set point for controller 2 changes from arbitrary value 10 to 100 (for example, could be a feed rate)—example feed rate response could be in response to deceleration phase.
- At approximately 50 h, event 1 then no longer is true and set-point controller 1 returns to event set-point 2 level (50). Note that event 3 set point is latched and remains true for the remainder of the batch—start of stationary phase.

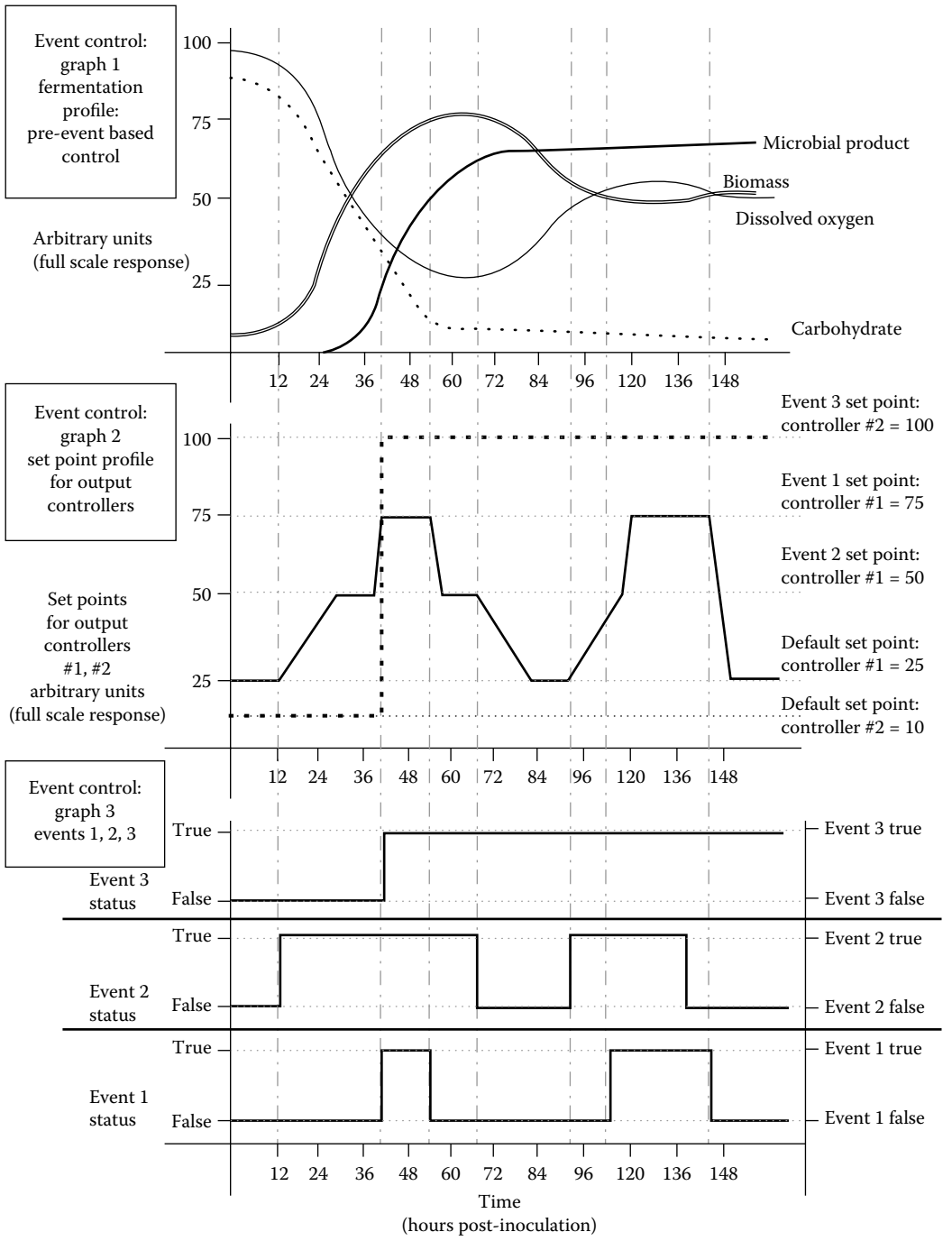

FIGURE 16.12 Example of event-based control for two controllers.

- At approximately 70 h, events 1 and 2 are no longer true and the default set point for controller 1 returns to the default level of 25 (~84 h)—70 h end of product accretion phase.
- At approximately 90 h, event 2 becomes true again, and the event 2 set-point (50) for controller 1 is used. Before the event 2 set point is reached, event 1 becomes true and the event

1 set point (75) is used again (faster ramp rate). Event 1 set point is in use for controller 1 by 120 h—recovery from decline/death phase by 90 h (scavenged substrates?).
- At approximately 140 h, event 2 is no longer true, and a short time later event 1 is no longer true; at this point the controller 1 set point is reduced from 100 to 25 (default set point)—harvest time.

The results of this event-based control will be judged by comparing the fermentation profile (as shown in Figure 16.12: graph 1) with the one generated for the event control regime.

16.7.3 Boolean Control and Rule Generation

It may be seen from the example in Figure 16.12 that complex patterns of control can be imposed on the fermentation and more or less significant changes to the growth environment and expression of phenotype will follow. However, it is difficult for the fermentation scientist to know which fermentation control regime to impose. This lack of knowledge comes from not knowing how the organism will respond to changes in individual control loops but also what the interactions with other control loops will be. To address this, Boolean logic can be used to introduce an element of control by "choice." With Boolean logic it is possible to present options or choices from which the control system can select a preprogrammed path for control. This type of experiment is then generating a new kind of response variable—one based on the control path selected by the metabolism or response of the total fermentations system in which

Fermentation system = stainless steel vessel + valves + sensors + services (air, electricity, etc.) + medium + microorganism + microbial metabolism + expressed phenotype

The five Boolean operators that can be used are AND, OR, XOR, NAND, and NOR. On their own these terms are rather impenetrable. Table 16.4 summarizes what they mean; examples given all represent truth statements affecting just two fermentation events—a pH value and a time value.

If Boolean options or choices are presented to the system, then the path selected by the total system can represent a "rule" by which the response of the microorganism to an imposed environment can be described. To illustrate the principle of control by rules, Figure 16.13 shows a simple XOR rule statement.

The rule defined in Figure 16.13 is remarkably simple and helps to define glucose feed regime by pH and dissolved oxygen control. Having established this rule a fermentation experiment can then test which route is chosen under defined conditions of medium or mass transfer for oxygen, and so

TABLE 16.4
Boolean Truth Table for Fermentation Control

Boolean Operator	Event a (pH > 6.5) Status	Event b (Time < 24 h) Status	Comments (Example Event Combinations)
AND	Yes	Yes	
OR	Yes	No	
	No	Yes	
	Yes	Yes	
XOR	Yes	No	
	No	Yes	
NAND	No	No	
	No	Yes	
	Yes	No	
NOR	No	No	

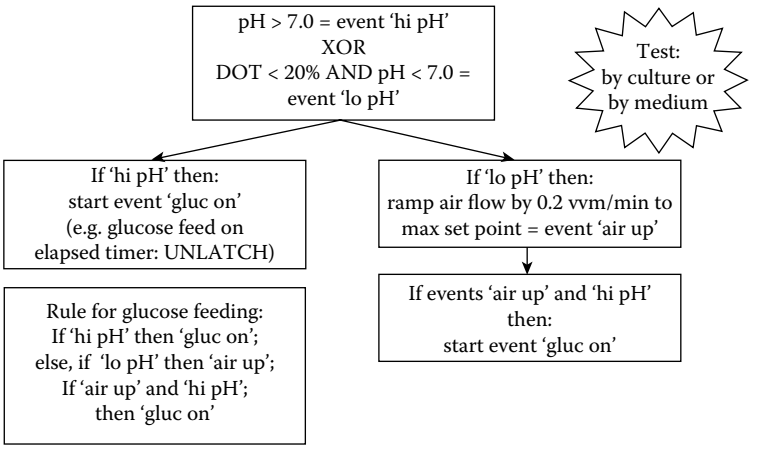

FIGURE 16.13 Example of control by rule: Specifying a rule for glucose addition.

on. Another powerful use for control by rules comes with culture or mutant evaluation in which the chosen route may indicate a propensity toward one pattern of metabolism or another, which may have been induced within a putative mutant culture. Clearly this is just one of many rules that could be introduced, and libraries of rules or elements that make up rules can be constructed to provide an array of control options to explore microbial metabolism under controlled conditions.

16.7.4 Summary of Event and Nonstable Set-Point Control

A summation of the possible interactions for event-based control is shown in Figure 16.14; here control options are defined as possible inputs and outputs to an experimental system in which events become control loops themselves evaluating whether conditions defined by rules are satisfied. This type of control system is an extension of the standard media and control recipes normally prepared and fermentation response data will produce a data set of online, offline, and derived data that generate rules for high productivity.

Returning to some of the opening discussion points in this chapter, the fermentation scientist is being asked to establish the correct conditions for a microorganism to express a desirable attribute or phenotype in a totally artificial environment; event and rule-based control together with transient and variable set-point control (nonstable) may help establish what unique set of factors and their interactions support the expression of a rare and valuable phenotype.

16.8 OTHER ADVANCED FERMENTATION CONTROL OPTIONS

This chapter has focused on a tiny part of control technology available for fermentation systems. The reader should be aware that other control philosophies are in use, and this technology is certain to continue to change and develop. Some of the control philosophies currently in use or in advanced development are described in the following subsections.

16.8.1 Knowledge-Based Systems

Knowledge-based systems (KBSs) can be considered an extension of the sort of control capability described previously in which previously held "expert knowledge" is captured in a control system often referred to as an *expert system*. With this type of control already established, facts and data associated with a process can be held in a database of knowledge against which future decisions can be made. The principal difference with expert systems and the event-based control described here is

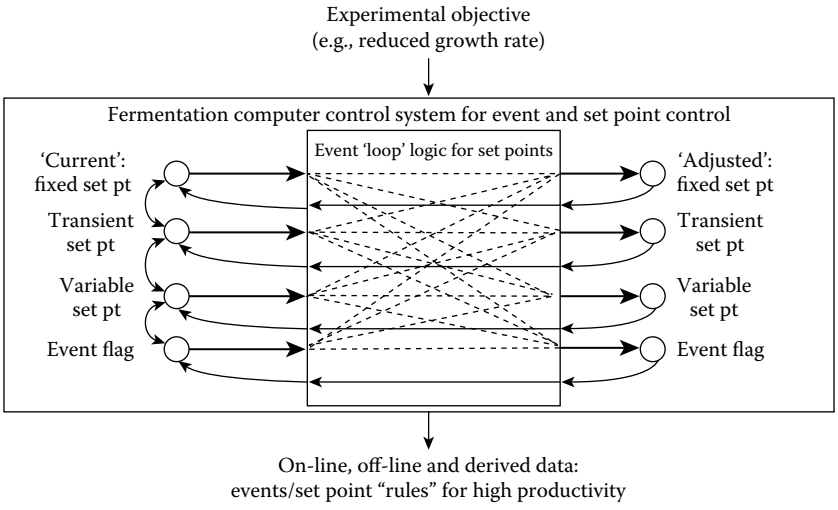

FIGURE 16.14 Control of fermentation by event loops and set-point rules.

that KBSs will only work on existing knowledge and will not necessarily generate new knowledge. The power of expert systems lies in their ability to execute potentially hundreds of rules per second controlling many functions associated with plant operation simultaneously. Early warning patterns can be recognized from this previous knowledge to alert either human or computer control operations of an excursion from normal operating parameters.

16.8.2 Artificial Neural Networks

Much discussion has been made in recent years of "intelligent" computer systems. By intelligent systems we mean systems capable of learning. The mechanism by which this occurs is beyond the scope of this chapter but for the most part is very similar to the control loop principle in which an input to a system is modified by attempting to minimize the error between desired and actual outcome. The use of neural networks in fermentation will come from the ability of these systems to recognize patterns and take actions on unknown data on the basis of those learned patterns. It is possible that the event-based system described here will be augmented by neural net ideas to help with obtaining data or process inferences not available by direct measurement. Artificial neural networks (ANNs) do not in themselves assist in providing data on the exact nature of process input interactions because the training and optimization of an ANN is a pure black box model of the process.

16.8.3 Metaheuristic Algorithms

Optimization based on natural systems, such as genetic algorithms (GAs), ants colony optimization (ACO) algorithms, and particle swarm optimization (PSO), dates from the beginning of the 1990s. These algorithms are important when the objective function has several optima and one is interested in a global minimum. Evolutionary algorithms, also of stochastic nature, can be used for nonlinear optimization and may indeed find global optima.

16.8.3.1 GAs

In this case, control philosophy has been influenced by modern biological genetics. Again it is not possible to describe completely how these systems work here, but a brief description will be given. GA are algorithms that operate on a finite set of points, called a *population*. The different

populations are interpreted as generations. They are derived on the principles of natural selection and incorporate operators for fitness assignment, selection of points for recombination, recombination of points, and mutation of a point.

GAs are capable of searching vast areas of experimental space and by a process of natural selection of rules or algorithms that come closest to minimizing some process cost function tend to optimize on a process goal. This type of system may assist in rule induction by eliminating rules not fit for the process environment.

16.8.3.2 PSO

The PSO is a new search method based on the simulation of animal social behavior. This method has been applied in several studies to solve constrained and nonconstrained optimization problems (e.g., Broth nutrient optimization). The PSO algorithm work as follows: A position and velocity vector in the search space are associated with each individual from a population, with a dimension equal to the total parameters, resulting in a swarm size equal to the particle number. The particle position vector behaves under the restriction of three conditions (actual particle position vector, better previously assigned particle position vector, and better previously assigned swarm position vector) that allow delimiting a geographically searching space according to a linear vectorial combination, bringing out the particle to assume a new particle position vector. Starting at the swarm lower limit, each particle pathway is calculated in iterative way, obtaining new particle position vector.

16.8.4 Modeling

For many years, there has been a disparity between what modeling could apparently offer (see Chapter 7 for more details) and the acceptance and use of modeling by the process community for everyday control and optimization problems. This may now be changing with the advent of advanced user-friendly software to assist in forming and testing model predictions. There are many kinds of models that may be constructed in attempting to describe a complex system the key to approximation is simple models (i.e., relating carbon dioxide evolution to biomass or growth estimations). These types of relationships can be defined relatively easily by curve-fitting raw data and then predicting based on alteration of parameters defined in function generated from curve fits. When several functions describing microbial growth and productivity have been created, then they can be combined in a mathematical relationship potentially useful in predicting fermentation outcomes. Biological models are usually divided into two categories: nonstructured and structured models. Nonstructured models do not consider the biological structure and the state of the cells. They are usually represented with empirical equations. On the other hand, structured models taken into account the cell physiology. Most of the models used in bioprocess are nonstructured, but an increasing of structured models are appearing recently.

Optimization, monitoring, and control can be applied combining successful models to online measurements. Then thousands of fermentations can be correctly run in software before committing to expensive stainless steel vessels.

16.9 RECENT TRENDS IN FERMENTATION CONTROL

Advances in several fields have allowed for new possibilities in the areas of measurement and control. New sensor technologies such as the use of fluorescence and the microsensor arrays allowed for shrinking of sensor systems for use in a wide range of applications (e.g., in microtiter plates).

16.9.1 New Sensor Technology

The ability to measure yield of product directly online has long been a fondly held objective of fermentation technologists and researchers alike. Use of new sensors (see Chapter 11 for more

details) with simple optical fiber connections that fit in the fermentor vessels and detect changing amounts of fluorescence in a dye make this possible. Light of a specific wavelength is used to excite the fluorescence, which can then be measured fluorimetrically.

Linking the expression of the desired protein with a fluorescent detection system can provide direct, online measurements related to yield. A simple analogue output signal from the detector system allows for integration of the new data with process control software. This, in turn, can modify other measured parameters to maximize production.

This system can also be used as a new way to detect standard parameters (e.g., pH, dissolved oxygen, and dissolved carbon dioxide concentration). The fluorescent detection systems can be incorporated in the sensor probes or separately as tiny "patches." These can be placed in simple disposables such as microtiter plate wells or added to incubation flasks. This enables rapid screening based on small volumes with some indication of the prevailing environmental conditions in the culture. These data can influence judgments about which isolates to use for a particular process and generate data of potential use in scale-up.

Another factor aiding real-time measurement of novel process parameters is the development of simple microfiltration systems to allow for separation of cells from the supernatant culture medium that can then be taken to an external analyzer. In this case, the separation system is key, rather than the analytical processes. However, the common feature is the acquisition of data in real time to inform control profiles designed to optimize yield and/or extend productivity in terms of metabolites or biomass.

Finally, many sensors are becoming much smaller, leading to microsensors arrays. These microdevices are particularly useful for bioprocess to capture information on transient changes related to stress production situations. They are based on methods that allow nanovolume handling of nucleic acids, proteins, or other cellular materials. These nanovolumes are analyzed using miniature electronic devices.

16.9.2 Software Sensors

The impossibility of measurement online of the reactant and product concentrations (e.g., biomass) stop the optimization and control applications. An interesting alternative is the use of software sensors currently named "state observers." Software sensors use the available online information and a model to predict the state variables online.

There are two classes of software sensors used commonly in bioprocess. The first ones are based on a perfect knowledge of a model structure (e.g., Luenberger and Kalman). These software sensors have as advantage a short convergences time but their weakness is in the parameters uncertainty. The second classes are the asymptotic observers. Asymptotic observers are based only on the mass and energy balance, which is the main advantage. On the other hand, asymptotic observers have long time of convergences.

Generally, software sensors are quite accurate for some parts of the process (e.g., growth stage). Unfortunately, they are often less accurate during certain product synthesis portions of the process because not all cellular metabolisms are well understood. Then, it is necessary to develop more robust models that take into account these variations.

16.9.3 Expansion of the Capability of DDC Instrumentation

Virtually all commercial fermentors now use control instrumentation (see Chapter 14 for more details) based on DDC. A few manufacturers have developed systems with all control functions directly handled by the computer. This has some advantages or additional of new capabilities and library routines if a standard process control software package is used. Also, modern computers have more than adequate processing power to cope with real-time process control. The downside of

this approach is, of course, the potential for a computer failure leaving the fermentor with no control whatsoever.

A "halfway" position is to allow external software to interact directly with supervisory process control software. Calculation of some control characteristics is made externally, and the result Is passed to the fermentor software as, for example, a revised set point for one or more parameters. Windows™-based operating systems allow for just this process through Object Linking and Embedding (OLE). For example, a short script in Visual Basic™ could link supervisory software with an Excel™ spreadsheet making calculations and generating set points in real time based on fermentation data.

This introduces another layer in the control process but has the advantage of one or more independent microprocessors providing control at the fermentor.

An increasing trend regarding usability is the use of color touch screens, even for bench-scale fermentors. They typically use a graphical user interface and incorporate some of the features previously only found in PC-based software, such as trend graphing. Alternative approaches involve enhancements to navigation between menus and the use of tabs for rapid access to options. Often, the more advanced functions of the controller, such as configuration of PID loops, are now placed in restricted sections where the casual user cannot accidentally make fundamental changes.

16.9.4 Use of Common Communication Protocols

A general trend in fermentation control is to add more peripheral items such as balances, pumps, and additional gases almost irrespective of the scale of the process.Several manufacturers of components such as mass flow control valves and peristaltic pumps are offering them for use with the Modbus serial protocol. This allows for great flexibility in adding these items to a fermentor as the physical connection and firmware changes are very easy to implement. The Modbus protocol is a genuine common standard allowing for the potential range of equipment that can be added to a standard fermentor to be greatly increased.

The trend for interactivity is also shown at a higher level of process control. Fermentor instrumentation and supervisory software can be linked to other devices or programs using the OLE for Process Control (OPC) protocol. This requires each device has a driver written in its firmware or software and this allows two-way communication with any other enabled systems. Client and server systems are catered for within the specifications of the OPC standards.

The potential use for this system in industrial process control of fermentation is to realize another long-held desire—linking of upstream and downstream processes together with the actual incubation phase in the fermentor for optimization which is truly process-wide and fully integrated. Of course, Microsoft Office™ applications are OPC enabled so; for example, a controller could transfer data directly to an Excel spreadsheet via OPC.

16.9.5 Use of Databases for Storage Bioprocess Data

Actually computer progress enable to storage large volumes of bioprocess data. These data bioprocess can be visualized with historian utilities. Furthermore, data can be studied with mathematical tools, as principal component analysis (PCA), partial least-squares regression (PLS), statistical analysis, etc. These mathematical tools can be used for several purposes, including to find abnormal operational conditions of a bioprocess, to establish a set point, and to optimize a bioprocess operating condition.

Unfortunately, there are two bottlenecks that stop the correct use of databases. First, the current commercial software with mathematical tools is not very much In use in the bioprocess industry. Secondly, there is a need for tools to facilitate data set preparation.

SUMMARY

This chapter has attempted to elucidate the complexity of fermentation systems and the difficult task facing the fermentation scientist who has to elucidate the key features of a fermentation to significantly enhance microbial productivity with a minimum expenditure of resources.

Fermentation development has traditionally used a heuristic approach to refine empirical knowledge.

The requirement for empiricism is still very much present, but modern fermentation control systems and techniques should allow for a more systematic approach to fermentation optimization (see Chapters 6 and 14 for more details).

It is likely that modern computing techniques such as event tracking and rule-based controls will augment the application of microbial physiology to solving problems of applied microbiology.

Microbial physiology knowledge itself in turn may benefit from advanced control ideas by increasing understanding how a microorganism can successfully respond to its environment.

FURTHER READINGS

Alford, J.S. (2006). Bioprocess Control: Advances and Challenges. *Comp. Chem. Eng*., 30 (10–12), 1464–1475.

Alford, J.S. (2009). Principles of Bioprocess Control. *CEPR*, 105 (11), 44–51.

Bailey, J.E., D.F. Ollis (1986). *Instrumentation and Control, in Biochemical Engineering Fundamentals*, 2nd edn, Maidenhead: McGraw-Hill, 658–722.

Beluhan, D., D. Gosak, N. Pavlovic, M. Vampola (1995). Biomass estimation and optimal control of the fermentation process, *Comp. Chem. Eng*., 19(Suppl.), 387–392.

Blackmore, R. S., J. S. Blome, J. O. Neway (1996). A complete computer monitoring and control system using commercially available, configurable software for laboratory and pilot plant *Escherichia coli* fermentations, *J. Ind. Microbiol*., 16, 383–389.

Chen, W., C. Graham, R.B. Ciccarelli (1997). Automated fed-batch fermentation with feed-back controls based on dissolved oxygen (DO) and pH for production of DNA vaccines, *J. Ind. Microbiol. Biotechnol*., 18, 43–48.

Diaz, C., P. Dieu, C. Feuillerat, P. Lelong, M. Salome (1995). Adaptive control of dissolved oxygen concentration in a laboratory-scale bioreactor, *J. Biotechnol*., 43, 21–32.

Dochain, D. (2003). State and Parameter Estimation in Chemical and Biochemical Processes: A Tutorial. *J. of Process Control*, 13 (8), 801–818.

Gregory, M. E., P. J. Keay, P. Dean, M. Bulmer, N.F. Thornhill. (1994). A visual programming environment for bioprocess control, *J. Biotechnol*., 33, 233–241.

Kong, D.Y., R. Gentz, J.L. Zhang (1998), Development of a versatile computer integrated control system for bioprocess controls, *Cytotechnology*, 26, 227–236.

Kurtanjek, Z. (1994). Modelling and control by artificial neural networks in biotechnology, *Comp. Chem. Eng*., 18(Suppl.), 627–631.

Omstead, D.R. (ed.) (1990). Computer *Control of Fermentation Processes*, Boca Raton, USA, CRC Press.

Onken, U., P. Weiland (1985). Control and optimisation, in Rehm, H.-J. and Reed, G. (eds.) *Biotechnology*, Vol. 2, Weinheim: VCR Verlag, 787–806.

Romeu, F.J. (1995). Development of biotechnology control systems, *ISA Trans*., 34, 3–19.

Sys, J., A. Prell, I. Havlik (1993). Application of the distributed control system in fermentation experiments, *Folia Microbiol*., 38, 235–241.

Wang, H.Y. (1986) Bioinstrumentation and computer control of fermentation processes, in Demain, A.L. and Solomon, N.A. (eds.) *Manual of Industrial Microbiology and Biotechnology*, Washington DC: ASM, 308–320.

17 Monitoring and Control Strategies for Ethanol Production in *Saccharomyces Cerevisiae*

Gilles Roux, Zetao Li, and Boutaib Dahhou

CONTENTS

17.1 INTRODUCTION

Fermentation processes are dynamic (i.e., nonlinear and nonstationary) in nature, thus leading to many difficulties in modeling. In addition, the lack of specific sensors makes certain variables inaccessible by online estimation. Measuring the state variables (the smallest possible subset of system variables that can represent the entire state of a dynamical system) is difficult, especially online, and its reliability is uncertain. The difficulties encountered by the control engineer, when studying this type of process, result from the fact that the process model is based on nonlinear algebraic relations and differential equations. These difficulties make the biotechnological process an excellent field

for application of advanced automatic control tools (Dahhou et al. 1991a). All available information on the process [e.g., environmental variables (temperature, pH, stirring, etc.)] and control loop signals must be exploited to ensure that the process is operating reliably under the given conditions. For fermentation processes, supervision becomes an issue of primary importance for increasing the reliability, availability, and safety of these systems. Unfortunately, the lack of process knowledge, the absence of reliable sensors, and the unpredictable behavior of microorganisms make this task very difficult, sometimes impossible, for the human operator. Several schemes of supervision applied to various domains (chemical process, petroleum process, wastewater treatment process, etc.) have been proposed (Antsaklis and Passino 1993; Aguilar-Martin 1996; Dojat et al. 1998). However, all of these can be described in general by the scheme shown in the Figure 17.1.

According to Kotch (1993), two main tasks are to be considered in a supervision system: process monitoring and supervisory control. The process monitoring part uses data collection and signal processing to decide if the process is in an abnormal state and if a corrective action must be taken. Such intervention, along with diagnosis, is regarded as a supervisory control task.

Within this framework, the development of an integrated methodology for control of the fermentation processes requires approaching modeling, adaptive techniques, and supervision for process control. In this section, the integrated methodology of the process control is formulated by adding a supervisory block (see Diagram 17.1). This block is dedicated to the acquisition of data (measurements, alarms, back to working condition) and process control parameters. In other words, this block collects and exploits all information resulting from the modeling, estimation, observation, control loop, environment, and the expert knowledge of the processes.

17.2 MODEL SYSTEM

A commercial strain of *Saccharomyces cerevisiae* UG5 was used growing on mineral salts glucose medium. The composition of the growth medium is listed in Table 17.1. The carbon source was glucose monohydrate (cerelose). The bioreactor was filled with tap water and the medium steam sterilized at 120°C for 20 min in the bioreactor. After cooling, the vitamin solution was added aseptically by filtration. The organism was cultivated in 2-, 20-, and 2-dm^3 bioreactors for batch, fed-batch,

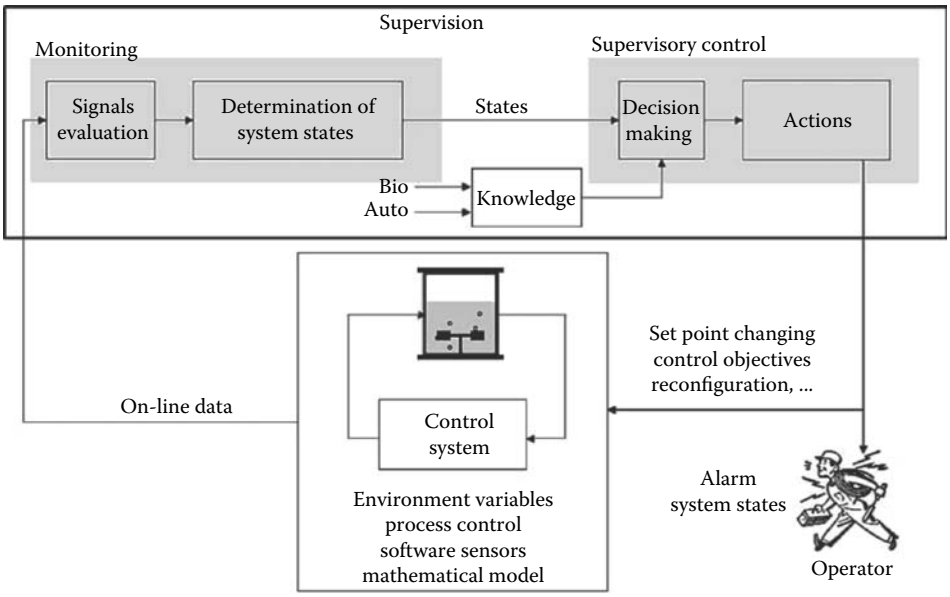

FIGURE 17.1 Supervision scheme.

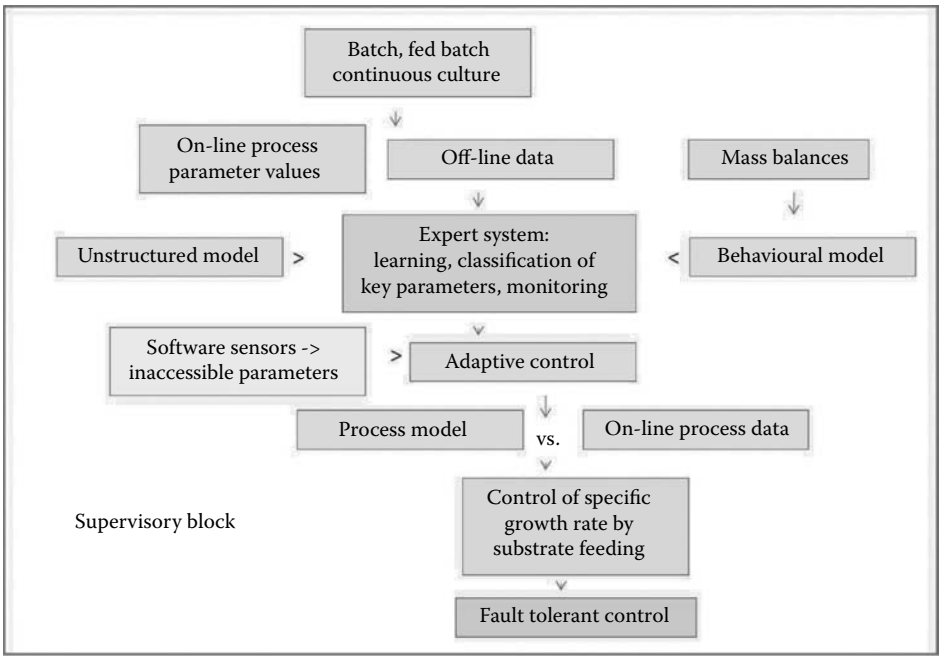

DIAGRAM 17.1 Integrated process control methodology.

TABLE 17.1
Composition of Growth Medium

KH_2PO_4	3 g.dm^{-3}
$(NH_4)_2SO_4$	3 g.dm^{-3}
Sodium glutamate	1 g.dm^{-3}
$Na_2HPO_4.12H_2O$	3 g.dm^{-3}
$CaCl_2.12H_2O$	0.25 g.dm^{-3}
$MgSO_4.7H_2O$	0.25 g.dm^{-3}
$ZnSO_4.7H_2O$	5 mg.dm^{-3}
$(NH_4)_2FeSO_4.6H_2O$	1.5 mg.dm^{-3}

and continuous fermentations, respectively. The bioreactors were equipped with instrumentation to control pH, temperature, and stirrer speed. Aqueous ammonia was used for pH adjustment.

For fed-batch and continuous modes, fresh medium was supplied to the reactor when and as required. The input flow rate of nutrient was controlled by means of a peristaltic pump and calculated from the glucose concentration measurement. For continuous mode, a level sensor was used to maintain the bioreactor at constant volume. The environmental variables (e.g., temperature, pH, and stirrer speed) were regulated at the specified set points with hardware controllers. Typical operating conditions and parameters of the experimental process are summarized in Table 17.2.

17.2.1 Offline Measurements

Samples were taken during the fermentation for the offline determination of substrate, ethanol, and biomass. Glucose concentration was measured with an industrial enzymatic analyzer YSI 27A (Yellow Springs Instrument, Co, OH), which consisted of an immobilized glucose oxidase membrane with an oxygen sensor. Ethanol concentration was determined by gas chromatography using

TABLE 17.2
Operating Conditions of the Variable Reactor Types Used

	Batch	Fed-batch	Continuous
Temperature (°C)	30	30	30
pH	3.8	3.8	3.8
Working Volume (dm^3)	1.5	6–16	1.5
Stirrer Speed ($rev.min^{-1}$)	200	300	200
Aeration ($dm^3.h^{-1}$)	3	32	3
Flow rate ($dm^3.h^{-1}$)	–	0–2	0.01–0.36
Input Subtrate ($g.dm^{-3}$)	–	160	20–300

isopropanol as an internal standard. Biomass concentration was estimated from dry weight and turbidity measurements at 620 min.

17.2.2 Online Measurements

Online glucose concentration was determined using the YSI enzymatic analyzer (Queinnec et al. 1992). The working scale for glucose measurement could be set manually and is capable of measuring between 20 and 300 $g{\cdot}dm^3$ of glucose with an accuracy of approximately 95%. A programmable logic controller (PLC) was used to manage the procedure for rinsing of the enzyme membrane, rinsing the syringe delivery mechanism, injection of the sample and control of the glucose measurement.

17.3 MODELING

The unstructured model (the most widely used unstructured models to describe cell growth are the Monod kinetic model) is based on the observation of the macroscopic kinetics within the reactor. We consider that the biomass activity can be sufficiently specified using only a single variable. Generally, the microbial concentration in the medium and changes in the biomass composition are completely ignored. These models are generally based on original Monod equation (Monod 1942) or a similar equation, including the various enzymatic reactions. The constants appearing in these mathematical equations are empirical and often determined by optimization based on experimental data. Other equations describing consumption of the substrate and the biosynthesis of products are necessary to write the model.

In our case, the process behavior is described by a model developed by using a fuzzy classification method (Piera et al. 1989). A fuzzy classification method is an algorithm (based on fuzzy logic) that operates in homogeneous classes of combinations of a set of abstract objects or signals. This type of model does not require any mathematical knowledge of the process and builds a representation of the process in the form of physiological states. The physiological states of a biological process can be defined as being a defined interval in which the principal physiological variables remain constant. This model does not try to describe the evolution of the process variables but rather to determine the current situation on the basis of these variables. The goal of this methodology is to design a process model in which supervision and diagnosis can be exercised effectively.

17.3.1 Unstructured Models

17.3.1.1 Methodology

We used our own software, which was developed under MATLAB® (Bâati et al. 2004). To solve the system of nonlinear algebraic equations representing the culture, the Gauss–Newton method (which is a method used to solve nonlinear least-squares problems) with a mixed quadratic and

cubic line search procedure was applied. For numerical integration, Runge–Kutta algorithms are a family of implicit and explicit iterative methods for the approximation of solutions of ordinary differential equations. Several algorithms with different orders, according to the difficulty of the modeling equations, were used (which check for integrity and thus prevent frequent numerical problems). The optimization runs were carried out using a multitasking Pentium computer.

A learning process in this case meaning a heuristic search strategy that allows selection of the most appropriate model from a range of models stored in a database. A heuristic search is a method that might not always find the best solution but it guarantees to find a good solution in reasonable time. A fermentation process, which is nonlinear, can be modeled by the following dynamic equations:

$$\begin{aligned} \dot{X}(t) &= \Omega(X(t), u(t), \eta(t)) \\ Y(t) &= HX(t) \end{aligned} \tag{17.1}$$

where $X(t)$ is the state vector (set of concentrations), generally including biomass, substrate, and product concentration); $Y(t)$ is the observation vector (set of measured concentrations), which can be measured; $u(t)$ is the input vector (set of control variables), which can be used to take into account the effect of environmental variables; and $\eta(t)$ is the kinetic vector (set of kinetic parameters), which contains the main biological parameters of the fermentation reaction. The Tvector $\eta(t)$ is composed of complex functions of the state variables and of several biological constants and its expression is varied for different fermentation processes. Therefore, the primary task of modeling is to identify which model of $\eta(t)$ is suited to the specifics of a process and then to determine the corresponding biological constants. A set Ξ of models of $\eta(t)$ is stored in the database: $\Xi = \{f_1(\theta_1, X(t), f_1(\theta_1, X(t)), \ldots\}$ where, θ_i is the unknown parameter vector (set of unknown kinetic parameters). Minimization of the criteria between the output of the model $Y^m(t)$ $Y^m(t)$ and the output of the process $Y(t)$ allows the best match parameter vector θ_i^* for i selection of the model of $\eta(t)$ to be obtained:

$$J_i = \min_{\theta_i \to \theta_i^*} \int_0^{t_F} (Y^m(t) - Y(t))^T Q (Y^m(t) - Y(t)) \tag{17.2}$$

A parameter adjustment rule facilitates this task, and an optimization algorithm can be used. The basic idea of parameter adjustment is to start with some estimate of the correct weight settings, modify the weight in the algorithm on the basis of accumulated experiences, and promote the features that appear to be good predictors by increasing their weights and by decreasing bad ones.

The minimization of the criterion $J = \min_{k \to k^*} \{J_k\}$ allows suitable model k^* and the corresponding parameter vector θ^* for the real fermentation process to be obtained [i.e., $\eta(t) = f_{k^*}(\theta^*, X(t))$]. A heuristic search strategy from the database containing the different models of $\eta(t)$ allows the "model match" task to be realized from any k to k^*.

Fermentation processes are characterized by biological degradation of substrate $S(t)$ (glucose) by a population of microorganisms $C(t)$ (biomass) into metabolites, such as alcohol $P(t)$ (ethanol). The physical model of the process is usually described by a set of nonlinear differential equations derived from the material mass-balances and involves modeling of the growth rate. These equations are

$$\begin{cases} \dfrac{dC(t)}{dt} = \mu(t)C(t) - D(t)C(t) \\ \dfrac{dS(t)}{dt} = -\dfrac{1}{Y_{c/s}}\mu(t)C(t) + D(t)S_{in}(t) - D(t)S(t) \\ \dfrac{dP(t)}{dt} = -\dfrac{Y_{p/s}}{Y_{c/s}}\mu(t)C(t) - D(t)P(t) \end{cases} \tag{17.3}$$

In a batch fermentation in which all nutrients are initially introduced into the bioreactor the dilution rate, $D(t) = 0$.

In fed-batch fermentation, fresh nutrient in the culture medium is added as and when required. Here, the dilution rate $D(t)$ is given by

$$\begin{cases} D(t) = \dfrac{F(t)}{V(t)} \\ \dfrac{dV(t)}{dt} = F(t) \end{cases} \tag{17.4}$$

The specific growth rate $\mu(t)$ is a function of the process state and several biological parameters θ ($\theta \in R^n$). These parameters are time dependent and moreover, they depend on the environmental conditions, which are then held fixed.

The usual approach in bioprocess modeling is to adopt particular analytical structures for specific growth rate and calibrate the kinetic coefficients from experimental data. However, this modeling is often hazardous because the reproducibility of experiments is often uncertain because the same environmental conditions may be difficult to obtain and so prevent changes in the internal state of the organism.

Many analytical laws have been suggested in the literature for specific growth rate modeling that take into consideration the limitation and/or inhibition of the growth by certain process variables.

17.3.1.2 Model Validation

The aim was to seek a model of the specific speed of growth which is able to take into account the specifics of alcoholic fermentation, while remaining mathematically simple. This model will be used in the design of estimation, control, fault-detection and isolation algorithms for the automatic control of the fermentation process. The selected model is

$$\mu(t) = \mu(\theta, S) = \mu_m \frac{S(t)}{K_s + S(t)} \tag{17.5}$$

The specific growth rate is of the Monod type. The influence of the substrate concentration on the growth is defined by a time limitation of an absence of substrate. Specific rates of degradation and production are coupled with the growth by yield coefficients. Using this choice, a simple model in which the parameters are easy to determine is provided. Experimental data were used to calculate the numerical values of the parameters μ_m, K_s, and the yield coefficients $Y_{c/s}$ and $Y_{P/s}$. The results obtained are given in Table 17.3.

The determination of the model is carried out by looking for the best minimization of the criterion needed (Equation 17.2) by using experimental data available for fermentation in discontinuous mode. The discontinuous mode is much richer in kinetic information than the continuous one, which provides only stationary states. The results obtained by applying the selected model in an experiment are presented in Figure 17.2. This figure represents the comparison of the measured values and those given by the model. These results show that the selected model correctly simulates the

TABLE 17.3
The Process Model Parameterst

μ_m	$0.38 h^{-1}$
K_s	$5\ g.dm^{-3}.h^{-1}$
$Y_{c/s}$	0.07
$Y_{p/s}$	0.16

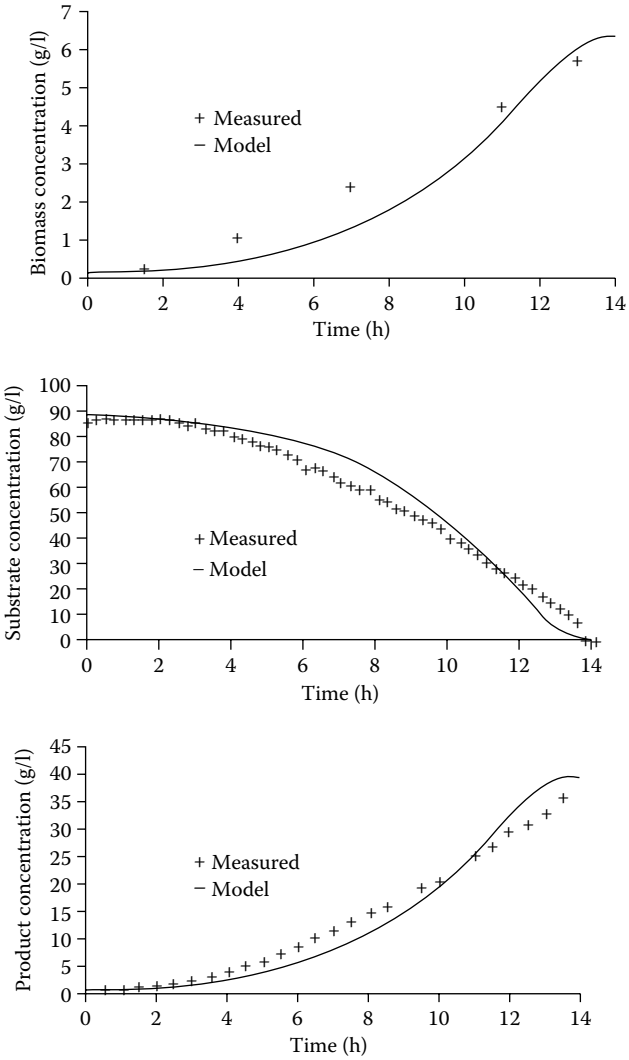

FIGURE 17.2 Model validation.

process as defined by the experimental data. The validation of the model parameters was carried out by using other experiments. This model [cf. Equations 17.3 and 17.5] will be used in others sections for the development of estimation, control and fault detection, and isolation algorithms.

17.3.2 Behavioral Models

17.3.2.1 Methodology

The complexity of this task requires a combination of classification techniques and expert knowledge. The process states, their causal relations, and the transition conditions are identified using classification. However, expert knowledge is necessary to validate the results in agreement with the nature of the process. It is possible, starting from expert knowledge, to give validation to the supervisory model. Suggested methodology uses classification under the supervision of the expert system to obtain a process model. This is based on the iterative application of fuzzy techniques. The objective of the method is to identify a set of significant states for the expert system. It can be summarized by the stages shown in Figure 17.3 (Waissman-Vilanova et al. 1999; Waissman-Vilanova 2000).

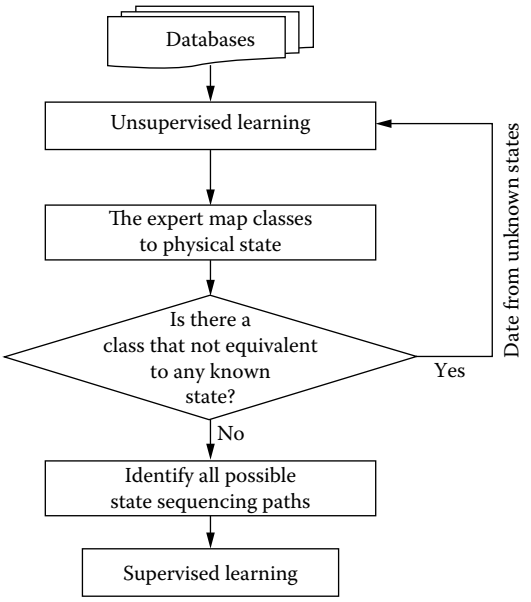

FIGURE 17.3 Methodology application.

At the beginning, given a set of measured data, no knowledge on the process states is available (i.e., all data correspond to the same general state). Unsupervised learning of data is applied and a set of classes is obtained. The expert must then map the set of classes to a set of physiological states. Three situations are possible:

1. One class is equivalent to a physiological state.
2. A set of classes is equivalent to a physiological state.
3. Any class is equivalent to any known state.

If a class exists of this final type, a new unsupervised learning process is applied, considering just the data assigned to that class. This procedure is called *data refinement*. When all data are classified in known states, all possible sequencing paths of the state are identified. This is accomplished by looking on every possible temporal correlation observed on all data available.

17.3.2.2 Application

The database considered here is constructed by real data extracted from batch-mode biotechnological process. Several signals are available by online measurement. Among them, the expert system chooses a subset of four signals that contain the most relevant information to determinate the physiological state in the process, including

- Percentage of dissolved oxygen pO_2
- pH
- Percentage of rO_2 in output gas
- Percentage of rCO_2 in output gas

For the methodology applied to the application, four data set records are considered. Three data sets are considered for learning and one data set for testing the results obtained by the methodology. All of the physiological states are determined by the expert system with the help of offline measurement

analysis (i.e., intra- and extracellular analysis). Figure 17.4 presents the different steps for extracting a process behavioral model. In step I, with unsupervised learning of all of the data available, we obtain a set of three classes, and two physiological states (2 and 4) are identified (consumption of acid and oxidative metabolism under ethanol). Class A does not present a physiological state but a set of several states. To refine the data in class A, unsupervised learning is used (step II). Amongst the six extracted classes, the expert system identified two states. State 1 (fermentation) is identified by union of three classes and state 2 (acid consumption) by union of two classes. In step III, the set of data in B is used. By means of unsupervised learning, states 3 (diauxic) and 2 are recognized. The direct observation of all state sequencing leads to building an automatic control structure representing the process model (Nakkabi et al. 2002) as shown in Figure 17.5. The transitions conditions are presented in Table 17.4.

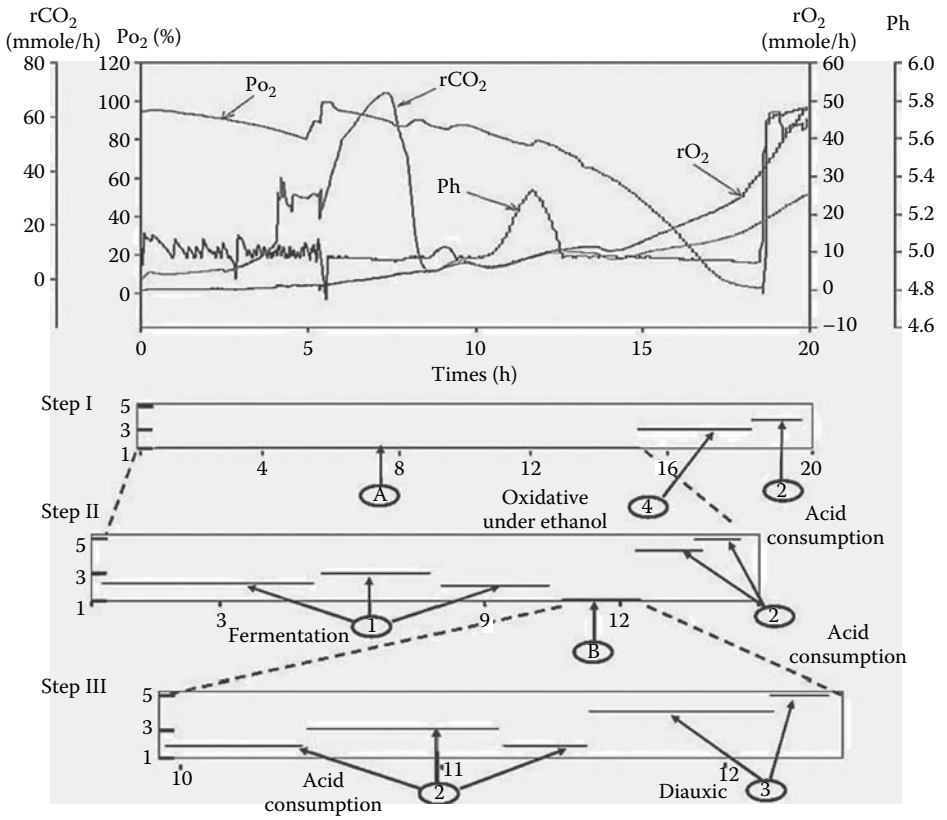

FIGURE 17.4 Behavioral model: construction steps.

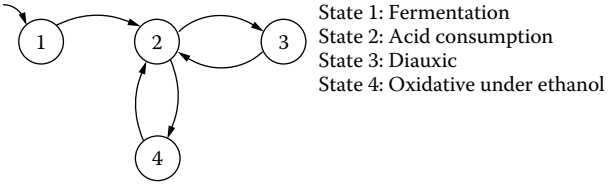

FIGURE 17.5 Behavioral model: automaton.

TABLE 17.4
Behavioral Model: Transitions

Transitions	Conditions
Transition 1 to 2	$-1.037*pH + 0.118* PO_2 - 0.008* rO_2 > 0$
Transition 2 to 3	$1.082*pH - 0.104* PO_2 + 0.04* rO_2 + 0.001* rCO_2 > 0$
Transition 3 to 2	$-0.88*pH + 0.018* PO_2 + 0.001* rO_2 - 0.05* rCO_2 > 0$
Transition 2 to 4	$1.33*pH - 0.21* PO_2 + 0.06* rO_2 + 0.067* rCO_2 > 0$
Transition 4 to 2	$60.13*pH + 17.59*PO_2 - 0.027*rO_2 - 0.027*rCO_2 > 0$

17.4 ADAPTIVE TECHNIQUES

The achievement of a good control and an effective monitoring of fermentation processes require the availability of real-time information regarding the physiological states of the process. However, the bioprocesses' dynamics are still badly understood, and many methodological problems of modeling are yet to be solved. In the laboratory, certain variables can be evaluated using offline analysis. In most cases, they require too long a time to be of direct use in real-time control of biological reactions. Moreover, commercial bioprocesses instrumentation suffers from a crucial lack of reliable and inexpensive direct sensors.

The nonstationary character of these processes encourages the use of methods such as adaptive control (linear or nonlinear), making it possible to represent the nonlinearity of the model and take into account the variations of their parameters. It is the nature of these processes that leads to the development of algorithms that exploit the inherent nonlinear structure of their models.

17.4.1 Estimation and Software Sensors

In the context of this problem, the techniques of adaptive filtering and estimation, commonly called *software sensors,* seem to be an inevitable alternative (Ben Youssef 1996; Ben Youssef et al. 1996; Nejjari et al. 1999a, b). The objective is to recreate the unavailable variables by using online measurements, offline experimental data, and the physicochemical model of the process.

The nonlinear and nonstationary characters of these processes, bringing into play the living microorganisms, constitute a considerable limitation of the performance obtained by the estimation procedure based on a linear approach. Given the strongly nonlinear character of these processes, we chose the use of nonlinear, adaptive techniques based on the structure of the model for this type of process. The model used for developing estimation methods and software sensor algorithms is that obtained from experimental data, as explained in Section 17.3. As mentioned earlier, the two principal problems that appear in the control of the fermentation processes are the inaccessibility of certain biological variables and the critical temporal variability of the kinetic parameters. The motivation is to know how to use measurements and the model's equations to minimize the errors introduced by measurement noise. For that, we use the techniques of filtering, which take into account the measurements available (substrate concentration) and the information resulting from unstructured models. Thus, we make a joint estimate of states and parameters. The diagram of the developed algorithm is represented by Figure 17.6.

The software sensor proposed uses the available data to rebuild the state variables and/or the estimated kinetic parameters. The estimator (an algorithm for calculating an estimate of a given quantity by using the observed data) described in Zeng et al. (1993b) was applied to three types of fermentation (batch, fed-batch, and continuous modes). Figure 17.7 shows the estimated biomass concentration, the estimated product concentration, and the estimated specific growth rate obtained by the adaptive estimation algorithm. The estimation results are satisfactory compared with the offline analysis (symbols) of biomass and product concentrations.

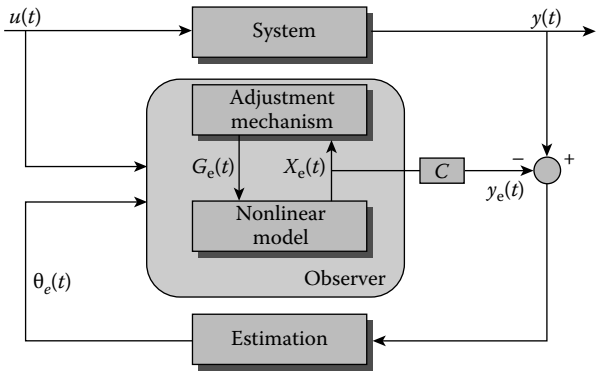

FIGURE 17.6 Adaptive estimation scheme.

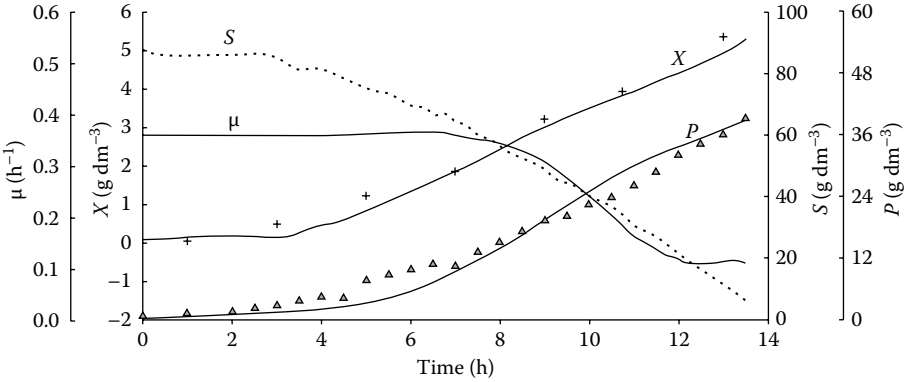

FIGURE 17.7 Estimation: batch mode.

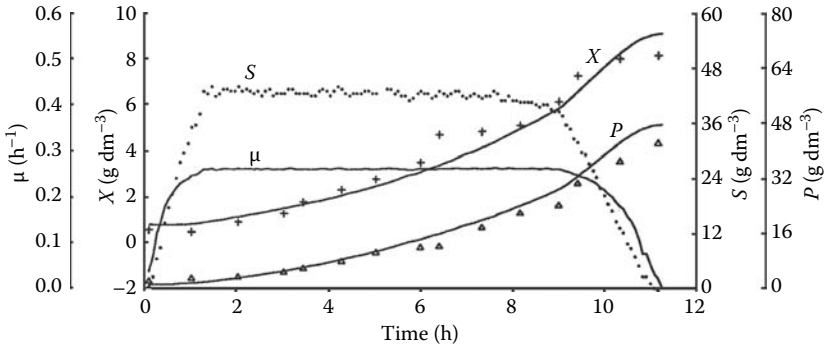

FIGURE 17.8 Estimation: fed-batch mode.

Controlled fed-batch fermentation is shown in Figure 17.8. The substrate feed flow rate controlled to regulate the substrate concentration in the reactor at 44 g/dm^3. The input substrate concentration $S_{in}(t)$ was set at 160 g/dm^3. The estimation results of biomass concentration, product concentration, and specific growth rate are given in Figure 17.8. Good agreement was found between the online estimations and measurements obtained by offline analysis (symbols).

The results obtained from a controlled continuous fermentation process are given in Figure 17.9. In this application, the substrate concentration $S(t)$. and the biomass concentration $C(t)$. were

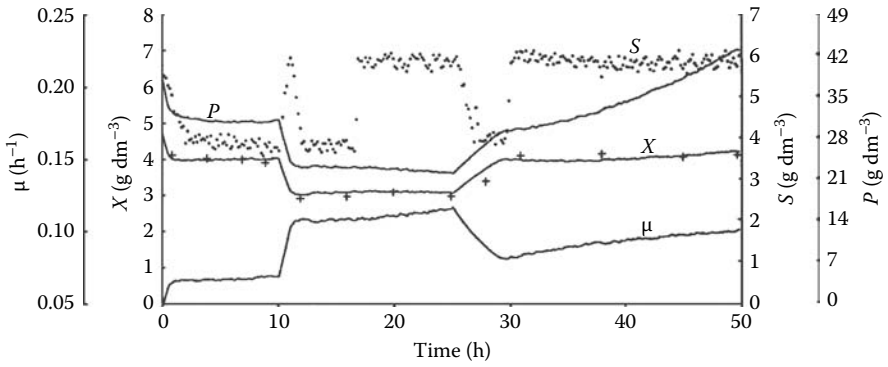

FIGURE 17.9 Estimation: continuous mode.

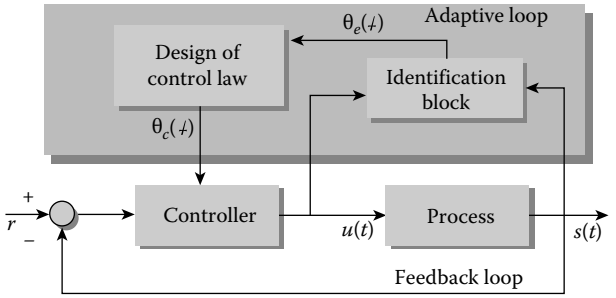

FIGURE 17.10 Adaptive control scheme.

controlled by manipulating the dilution rate $D(t)$ and the input substrate concentration $S_{in}(t)$. The evolution of estimated biomass concentration, product concentration, and specific growth rate are illustrated in Figure 17.9. These estimated results are again satisfactory, as shown by the offline biomass analysis (symbols).

17.4.2 Control

This section presents results obtained from the linear approach in which we used the nonlinear model of the fermentation process operating in continuous mode (see Section 17.3) to determine the synthesis parameters of the linear controller.

We used the approach of the indirect adaptive control scheme (Dahhou et al. 1991a, b, c); the system parameters are estimated directly, as shown in Figure 17.10. These estimates are used for the readjustment of the regulatory parameters. In this type of algorithm, the plant parameters are estimated online and used to calculate the controller parameters. These parameters are considered by the controller as if they were true parameters. This approach is founded on the certainty equivalence principle [The problem can be separated into two stages (1) obtain the values of the estimated parameter, and (2) at time t, solve the controller optimization problem using the estimates parameters in place of the true parameters].

We have chosen to present the experimental results obtained from the control of alcoholic fermentation in continuous mode. The principal objective is the regulation and the tracking of the substrate concentration inside of the bioreactor as the dilution rate changes (Dahhou et al. 1993). The control objective is the minimization of a specific quadratic criterion (M'Saad et al. 1990). The control law is coupled with a robust estimator. Input and output data are first filtered and normalized, which reduces the effects of unmodeled dynamics and noise. The parameter adaptation algorithm takes the form of standard recursive least-squares with forgetting factor, data normalization factor,

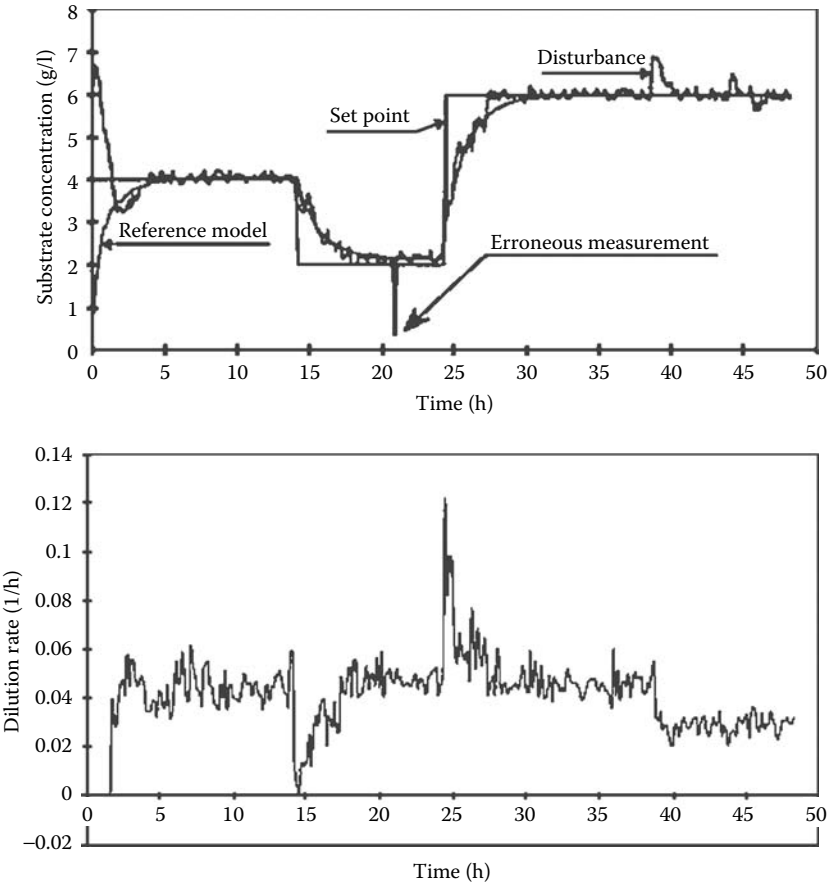

FIGURE 17.11 Evolution of substrate concentration and dilution rate.

and adaptation freezing associated with the definition of an available information signal (M'Saad et al. 1989). The forgetting factor approach enables the recursive algorithm to reduce the effect of the older error data by multiplying the error data by a discounting factor. The adaptation freezing allows for stopping the estimation algorithm in the absence of persistent excitation. The results obtained are represented by the graphs in Figure 17.11. The substrate concentration profile follows the requested model reference output. The inlet substrate concentration change generates a perturbation on the output, which has been rejected after 2 h. The second graph of Figure 17.11 shows the corresponding manipulated input profile, which does not saturate. The estimated model is represented by parameters, the evolutions of which are given by the graphs in Figure 17.12. We note that the freezing parameter is sometimes activated (zones 1, 2, and 3) and this depends on the available information signal. At this time, we believe that the activation of the freezing parameter is justified according to the measurement of the information signal (i.e., a required condition of persistent excitation is not satisfied, but we can suppose that the system dynamic is changing also). For us, the fact that this condition is not checked can cause a drift of the parameters and thus it can have a risk of instability. The freezing of the parameters was a means to mitigate this problem. However, this drift of the parameters can be justified by a change of system dynamics. This change can be due to the nature of the process (e.g., by the aging of the microorganisms and contamination). In these circumstances, freezing the parameters can be a serious error of appreciation and comprehension. This reasoning leads us along to think that consideration should be given to the possibility that the process can be subjected to operational faults of operation that result in abnormal situations.

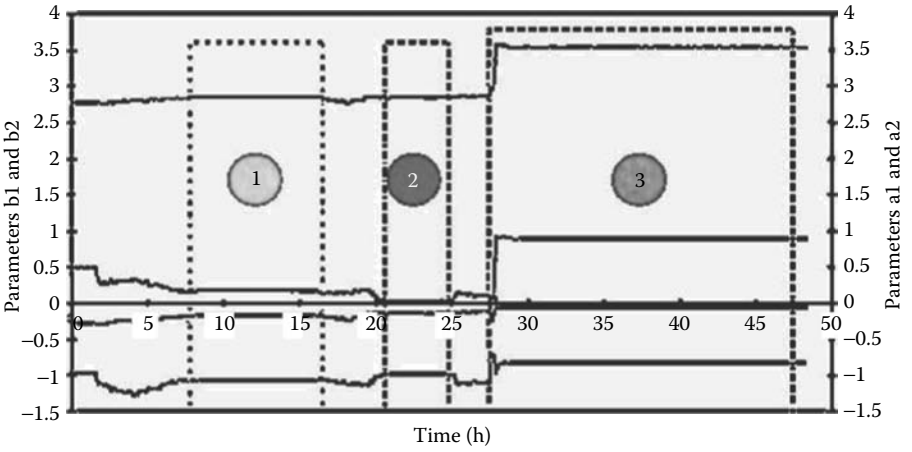

FIGURE 17.12 Estimation of system parameter.

17.5 SUPERVISION FOR PROCESS CONTROL

Modeling, estimation, filtering, and control aspects mentioned previously constitute a lower layer level of control that does n ot account for all of the information resulting from the process. We adopted a strategy that consists of adding a layer of higher level supervisory block in which all of this information can be exploited.

If a hierarchical order is established, the feedback loop and the adaptation loop will provide the lower level. We considered the layer immediately above the adaptive loop, which is the supervision layer. In this level, the evolution of the signals coming from the adaptation and feedback loops are used to recognize specific situations and to act on the parameters of the different algorithms of control and estimation. The general idea of the supervision is the evaluation of the significant signals of the system to test its performances on the basis of certain predefined criteria, which can be inherent to the controller or within the process. The violation of these criteria starts a second task for the supervisor: it must act on the system in a way not envisaged by the controller to improve its performances or to help the operator to make a decision at the time when an indication of some dysfunction appears. These anomalies can be related to the biological reaction or ascribed to the operation of the hardware (actuators, sensors, etc.). Figure 17.13 illustrates an example of such a supervision block.

17.5.1 Classification

We used the model derived in the modeling section for supervisory purposes (Nakkabi et al. 2002). This model is validated by experiment to confirm the expected optimal production. Thereafter, we use this model like a reference in the supervisory system for real-time monitoring of an alcoholic fermentation process. The results of the first experiment of the supervised process are presented in Figure 17.14.

Table 17.5 presents the different functions concerning the acknowledged four physiological states. Note that the difference between $t + 1$ and t corresponds to one acquisition. By using the automatic control obtained in Figure 17.15 and Table 17.5, it is possible to know the state of the system and its tendency. Actually, the membership's function (for a fuzzy set, this is a generalization of the indicator function in classical sets) of state 1 (fermentation), during the instant *t,* is the highest followed by the one of state 2 (consumption of acid). This order indicates that the processes are in functional state 1 with tendency to switch to state 2; this transition is authorized by the global model

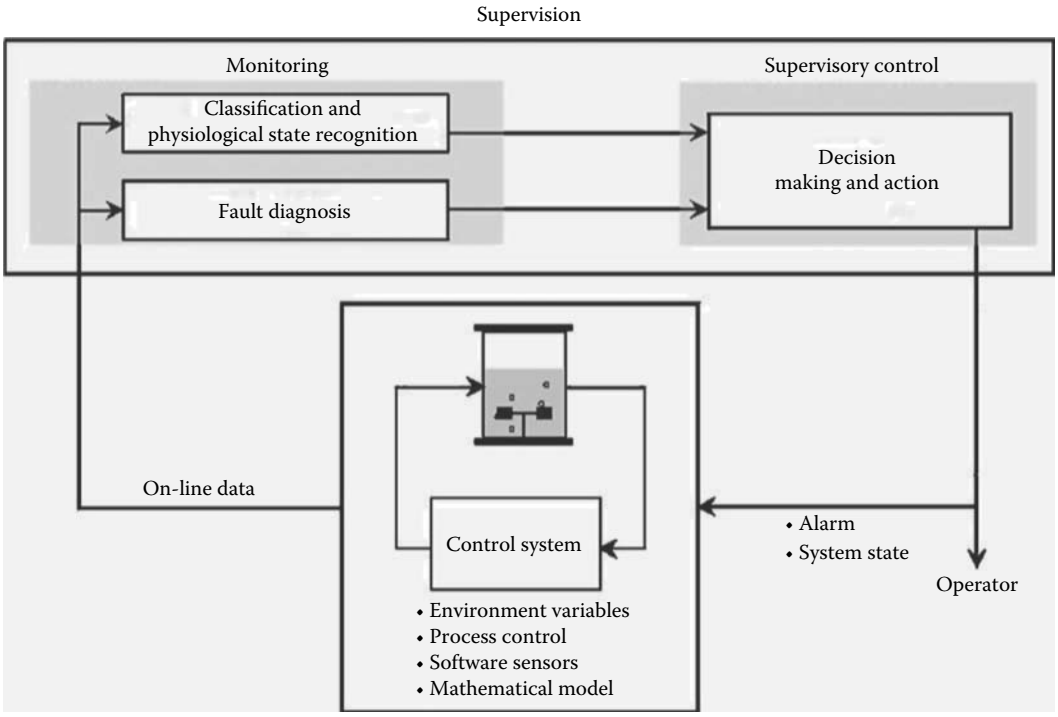

FIGURE 17.13 Physiological states and fault detection.

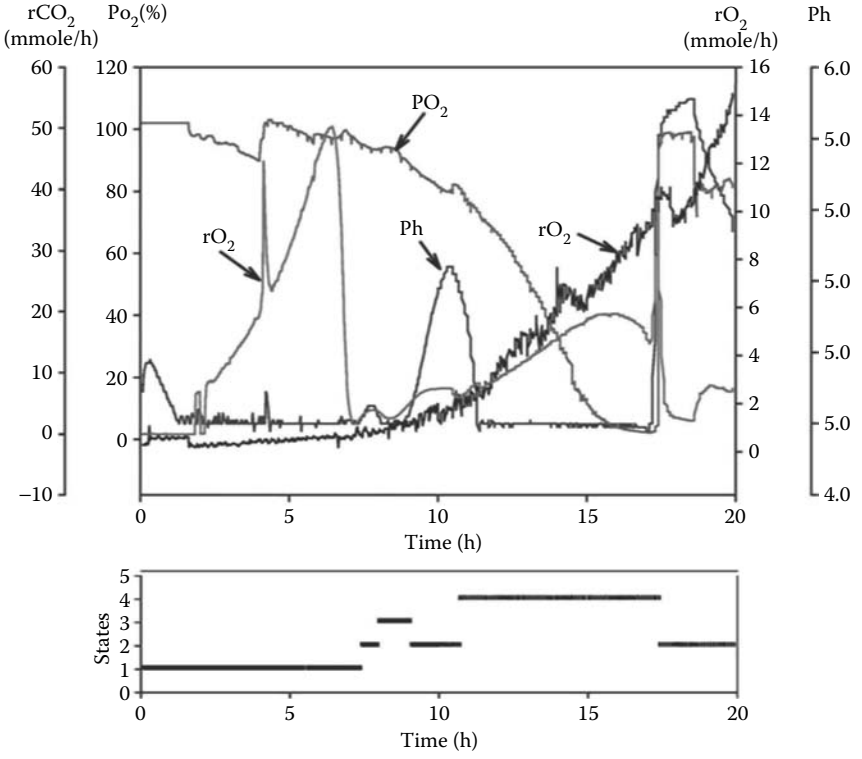

FIGURE 17.14 Good learning.

TABLE 17.5
Membership's Function for Good Learning

	Time			
States	***t***	***t* + 1**	***t* + 2**	***t* + 3**
Fermentation	0.29	0.35	0.32	0.24
Acid consumption	0.26	0.32	0.31	0.29
Diauxic	0.22	0.11	0.15	0.28
Oxidative under ethanol	0.23	0.22	0.22	0.19
	normal	normal	normal	normal
	Situation			

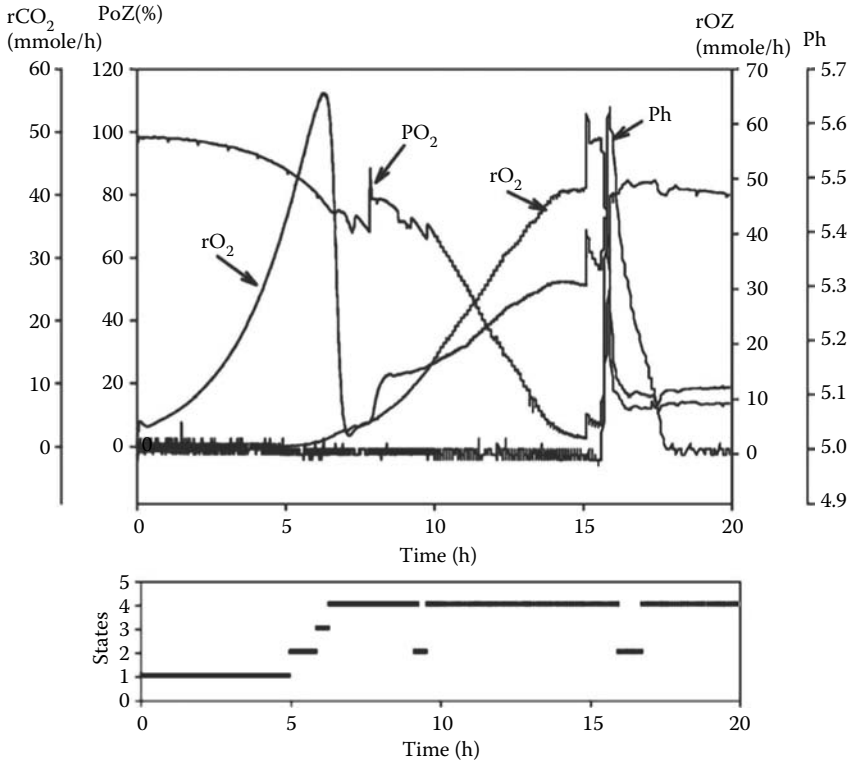

FIGURE 17.15 Bad learning.

of the process (Figure 17.15); therefore, the situation is considered as normal. The same analysis keeps its validity for the instants $t + 1$ and $t + 2$. At $t + 3$ the membership's function is the greatest; the system is, then in state 2 with an inclination to shift to state 3. The situation is always considered normal because this transition is authorized by the process model (Figure 17.15). Furthermore, the supervision system did not detect any unusual physiological behavior compared with the reference model, suggesting that the system is operationally satisfactory.

Table 17.6 shows the different membership function. At the instant *t,* the process is at state 3 (diauxic state), which represents the highest value of the membership function. The membership function of state 2 (consumption of acid), comes after, indicating the process tendency. The situation is considered as normal because the transition is allowed by the process model. At the instant

TABLE 17.6
Membership's Function for Bad Learning

	Time			
States	t	$t+1$	$t+2$	$t+3$
Fermentation	0.01	0.03	0.01	0.01
Acid consumption	0.32	0.12	0.12	0.21
Diauxic	0.41	0.46	0.46	0.37
Oxidative under ethanol	0.26	0.41	0.41	0.41
	normal	alarm	alarm	abnormal
	Situation			

$t + 1$, the process remains at state 3 but changes its tendency to state 4 (oxidative under ethanol state). According to the process model (Figure 17.15), this transition is not authorized. In this case, an alarm is set off. This analysis remains true for the instant $t + 2$ At the instant $t + 3$, the tendency of the process is confirmed and the system switches from state 3 to state 4. The situation is abnormal, pointing to an abnormality in the process. Then, the supervision system can readily detect a different physiological behavior from those usual ones; this is explained by the fact that the phase of diauxic is shorter. Indeed, one notices in the figure that there is no intermediate consumption of acid (there is no increase in pH) between the ethanol consumption and the glucose consumption. This may indicate a better capacity for oxidation.

17.5.2 Fault Detection and Isolation

Fault detection and isolation (FDI) is one of the most important tasks assigned to intelligent supervisory control systems. A fault is understood as any kind of dysfunction in the actual dynamic system that leads to an unacceptable anomaly in the overall system performance. Such malfunctions may occur in the sensors, in the actuators, or in the components of the process (Kabbaj 2004).

In this section, we are interested with faults in process dynamics. In model-based fault detection methods, a fault is considered as a variation of one or several parameters compared with a reference value. The problem is then to detect these parameters' variations, to distinguish between those resulting from faults and those resulting from normal behavior, and to decide if these variations are indeed significant compared with uncertainties in the model and the noise in the measured data. It is well known that the FDI procedure is explicitly divided into two stages: residual generation and residual evaluation. The principle is to use the measurements of output and input signals and the process mathematical model to generate residuals; we used these residuals as indicators of dysfunction. These residuals are defined as the difference between the estimated and real values of the various outputs. After evaluation, the fault is detected and isolated. In the model-based methods, the residuals can be generated using observers, parameter estimation, and parity relations.

We develop here a method based on adaptive observers for FDI (Zhang 2000) in an alcoholic fermentation process (Kabbaj et al. 2001). The faults are modeled as changes in the system parameters $\theta = [\theta_1, \theta_2, ..., \theta_n]^T$. The fault-free operating mode is characterized by the nominal vector θ^0, which is supposed to be known. The residuals are generated using a state observer on the basis of nominal parameters θ^0 , and a set of adaptive observers as shown by Figure 17.16. Each adaptive observer estimates only one parameter of the supervised system, in addition to the state variables. The residuals $\gamma_0, \gamma_1, \ldots \gamma_n$ are defined as being the prediction error of each observer.

Faults in the process system (no fault in actuators or sensors) will be considered. As is well known biotechnology, the growth rate is one of most important parameters to describe the evolution of the microbial population. The variation of this parameter is sensitive to the operating conditions

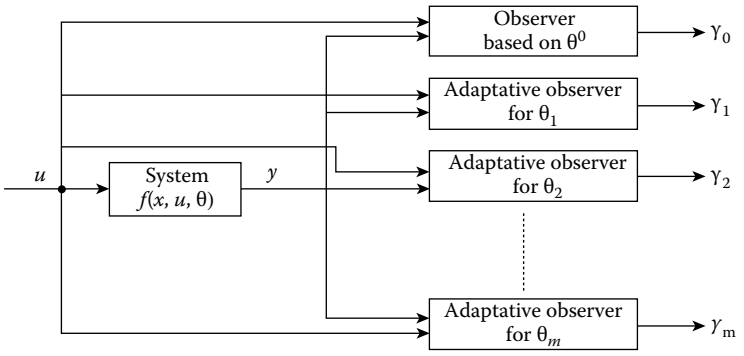

FIGURE 17.16 Bank of observers.

(pH, temperature, agitation, oxygen, etc.). The modeling of these various influences within a single mathematical expression is very complex. To supervise the variables of the environment, we can rather supervise the structural parameters of the growth rate (Equation 17.5). Faults are so modeled as changes in the system parameters $\theta = [\mu_m K_s]$ (the maximum growth rate and the saturation constant). The fault-free operating mode is characterized by the nominal vector $\theta^0 = [\mu_m^0\ K_s^0]$, which is supposed to be known.

17.5.2.1 Adaptive Observers for FDI

As explained earlier, the scheme consists in developing two adaptive observers denoted *observer*^{j} ($j = 1, 2$) and a state observer, based on nominal parameters θ^0, called *observer*^{0}. Each adaptive observer estimates only one parameter of the supervised system in addition to the state variables. We have opted for an estimator using the nonlinearity of the process and the approach of the model reference to reconstitute the state variables and the parameters of the model (Zeng et al. 1993a). Instead of estimating the growth rate like a time-varying parameter, we instead estimate the structural parameters. This makes the estimation algorithm better adapted to the fault detection approach used.

Let $\hat{S}^0(t)$, $\hat{S}^1(t)$, and $\hat{S}^2(t)$ be the estimated outputs given by the *observer*^{0}, *observer*^{1}, and *observer*^{2}, respectively. The residuals may be defined as being the corresponding estimation errors

$$\begin{aligned} \gamma_0 &= \hat{S}^0(t) - S(t) \\ \gamma_1 &= \hat{S}^1(t) - S(t) \\ \gamma_2 &= \hat{S}^2(t) - S(t) \end{aligned} \tag{17.6}$$

The residual γ_1 is associated with the maximum growth rate $\theta_1 \equiv \mu_m$ and the residual γ_2 with the saturation constant $\theta_2 \equiv K_s$.

17.5.2.2 Residual Behaviors

In the fault-free operating mode, all of the residuals γ_0, γ_1, and γ_2 are practically zero, and as such any departures from zero will be detected as a fault. If the fault corresponds to a change in a single parameter, all of the residuals except one will persistently differ from zero. If, after a transient, γ_j ($j = 1,2$) converges back to zero, the fault corresponds to a change in θ_j. Figures 17.17 and 17.18 showthe residuals' behavior when the parameter μ_m changes from 0.38 to 0.40 h^{-1} and K_5 from 5 to 4.7 g/L, respectively.

Microbiologically speaking, any changes in growth conditions in the bioreactor (e.g., temperature, pH, or aeration) will have an adverse effect on substrate consumption rate (K_s) which, in turn, diminishes growth rate (μ).

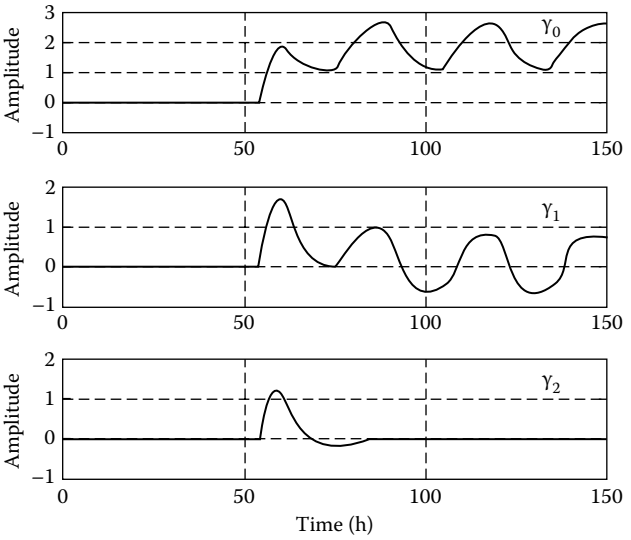

FIGURE 17.17 Residuals evaluation with fault in μ_m (without noise).

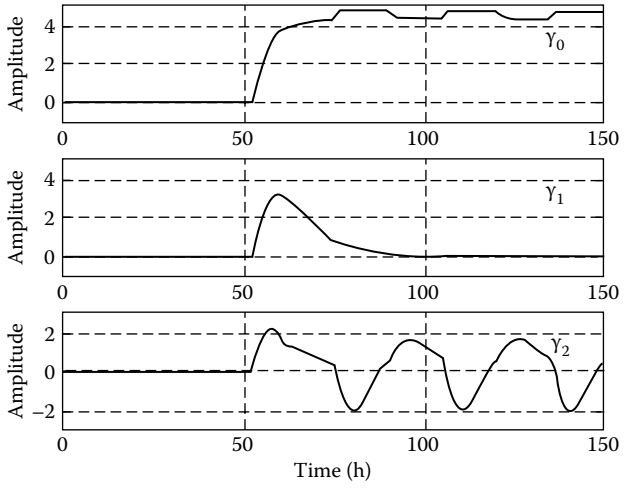

FIGURE 17.18 Residuals evaluation with fault in K_S (without noise).

This method of detection and isolation of faults on the basis of the adaptive observers gives satisfactory results without the presence of noise. However, following Kabbaj et al. (2002), we noted that it very is difficult to detect and isolate faults in the presence of noise. To mitigate this problem, we propose a new methodology that combines analytical and knowledge for FDI. This combines the knowledge about process and the information hidden in data to extract a behavioral model in the form of a decision tree. This model is then used for an automatic residual evaluation. This approach proves to be remarkably robust. Thus, faults of the type described are detected and isolated even in presence of measurement noise (Nakkabi et al. 2003).

The generated residuals are used in classification to recognize the process state (state 1: no faults, state 2: faults in μ_m, or state 3: faults in K_S). In addition, we propose these residuals (γ_1 and γ_2) using some composite residuals defined by

$$\begin{aligned} s_1 &= \gamma_0 - \gamma_1 \\ s_2 &= \gamma_0 - \gamma_2 \end{aligned} \tag{17.7}$$

These kinds of residuals are very significant and helpful in the classification procedure because they are robust to measurement noise. The goal is to diagnose the kind of fault by evaluating the given residuals. Therefore, two behavior models ($M1, M2$) are implemented. Each of them is designed to be sensitive to one fault, as shown in Figure 17.19. These models are generated as explained in Figure 17.3 (Section 17.3.2.1). The models' output ($f1, f2$) denotes the presence or not of fault. For each fault the training data are collected in the presence of measurement Gaussian noise with zero mean and variance equal to 0.5. The effect of this noise on residuals is very important compared with faults. Thus, residual evaluation is delicate. The validation has been done on multiple data with different noise of variance 0.2, 0.3, 0.5, and 1. The results obtained with variance equal to 1 are presented.

As can be seen from Figure 17.20, residuals are generated as growth rate (μ_m) changes from 0.38 to 0.40 h^{-1}. As dictated by the design, a fault is detected should any residuals (e.g., γ_1) depart from a zero value. Unfortunately, this behavior is not clearly observed in the residuals γ_1 and γ_2 plotted in Figure 17.20 because of a high level of noise in the measurements. In this case the composite residuals can be used, but just for fault detection. The residual evaluation using behavioral models

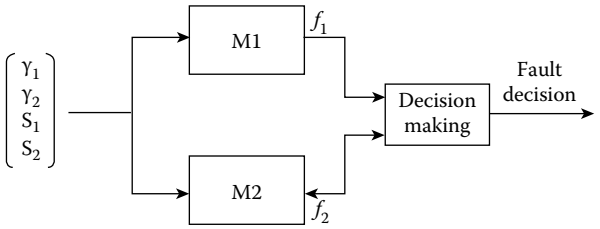

FIGURE 17.19 Decision making using behavioral models.

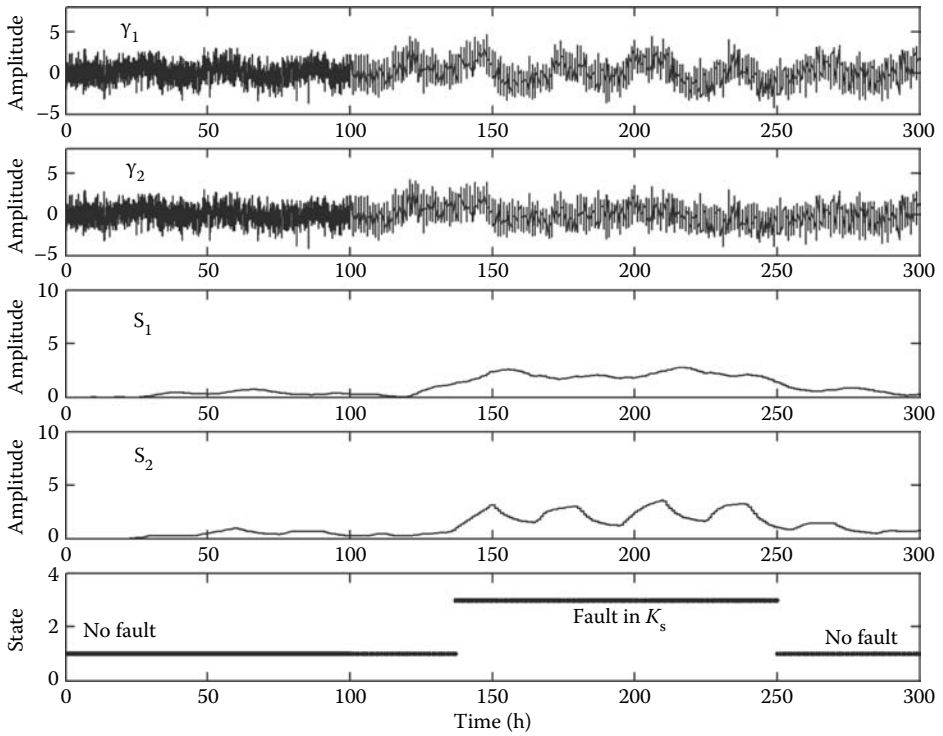

FIGURE 17.20 Residuals valuation with fault in μ_m (with noise).

allows us to detect and isolate faults as shown in the bottom of Figure 17.20 by the transient from state 1 (no fault) to state 2 (fault in μ_m).

The fault is now simulated by changing the parameter K_s from 5 to 4.7 g/L at $t = 130\ h$ and from 4.7 to 5 g/L at $t = 250$ h. The corresponding residuals are illustrated in Figure 17.21. Similarly, the behavioral models based on residual evaluation show clearly the transient from state 1 (no fault) to state 3 (fault in K_s) at $t = 130$ h and from state 3 to state 1 at $t = 250$ h.

17.5.2.3 Principle of Fault-Tolerant Control

The control law is of the form $u = K(x,\varphi)$, where the controller parameter vector is $\varphi \in R^q$. Using this controller, the closed-loop system is $\dot{x} = f(x,\theta,\varphi)$ and $y = Cx$. The choice of the controller parameter vector φ is called *controller configuration*. One assumes that this choice is related with a cost function $J(\theta,\varphi)$. Let $p_1(\theta,\varphi)$, $p_2(\theta,\varphi)$ … $p_i(\theta,\varphi)$, and $p_m(\theta,\varphi)$ are m parameters depending of the closed-loop system with respective to the constraint condition. These m parameters can take values of eigenvalues (these are a special set of scalars associated with a linear system of equations that are sometimes also known as characteristic roots, characteristic values or proper values; these values describe the dynamic of the process) of the closed-loop system or other values following the application context. Then the objective of controller parameter configuration is that the closed-loop system satisfies

$$\min \quad J(\theta,\varphi) \tag{17.8}$$

$$p_i(\theta,\varphi) \in \Omega_i, \ \forall i = 1,\ldots,m \tag{17.9}$$

Equation 17.8 can be analytic or nonanalytic. Equation 17.9 represents the constraint condition of the controller parameters choice. Ω_i represents a certain domain in the complex plane. For example, if p_i is an eigenvalue, then Ω_i can be chosen as the left-half s plane. The constraint condition (Equation 17.9) implies a set of crucial indexes that should be satisfied. The closed-loop system is called a system with good stability if Equation 17.9 is satisfied.

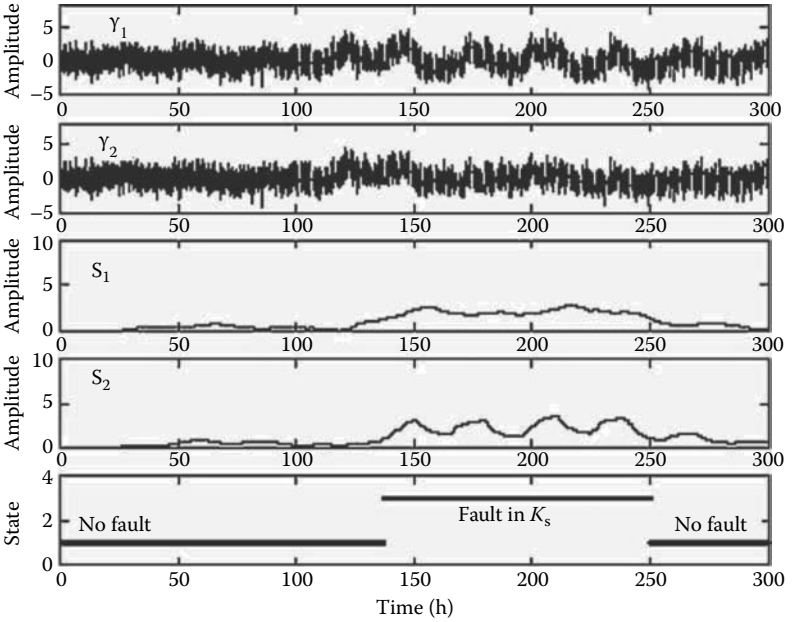

FIGURE 17.21 Residuals evaluation with fault in K_S (with noise).

After the occurrence of the fault, we accommodate the fault by controller reconfiguration. We change the controller parameter vector according to the system information. We use fault detection, isolation, and identification procedures to get this information. Then, in different periods the controller parameter vector is chosen as follows:

1. *Before the fault occurrence:* The system parameter vector is known and equal to θ^0. Δ is only the point θ^0. The controller parameter vector should be optimized in the domain $\Psi_M(\theta^0)$. The optimum controller parameter vector in this case as φ^0. $\Psi_M(\theta^0)$ contains all possible maximum available domain $\Psi_M(\Delta^i)$, where Δ^i is any domain containing the point θ^0. The optimum result in this case is the best one of the results corresponding to all possible $\Psi_M(\Delta^i)$.
2. *After the fault occurrence and before the fault detection:* The system parameter vector in this case is θ^f, and the corresponding maximum available domain is $\Psi_M(\theta^f)$. Because we do not know the fault occurrence, the controller parameter vector φ^0 is still used, which may be not in the domain $\Psi_M(\theta^f)$. So, Equation 17.9 may be not satisfied, therefore the system may be unstable.
3. *After the fault is detected but it is not isolated:* We have known the fault occurrence; we will change the controller parameter vector to accommodate the fault. Because the fault has not been isolated, we do not know the location of the system faulty parameter vector, so we considered that θ may be any point in its maximum possible domain Δ^M. The maximum available domain corresponds to Δ^M is $\Psi_M(\Delta^M)$. Because Δ^M contains all possible Δ, $\Psi_M(\Delta^M)$ will be subset of any $\Psi_M(\Delta)$; that is to say $\Psi_M(\Delta^M)$ is the smallest of all possible maximum available domains $\Psi_M(\Delta)$. If the condition in Equation 17.9 is satisfied by the open-loop system, then $\Psi_M(\Delta^M) \neq \phi$ because it at least has an element φ^{off}, where φ^{off} is the controller parameter vector value, which places the system in a closed-loop state. The controller parameter vector should be optimized in the domain $\Psi_M(\Delta^M)$, which is only a small subset of $\Psi_M(\theta^f)$, but not in the whole domain $\Psi_M(\theta^f)$ because we do not know $\Psi_M(\theta^f)$ in this case. We note that the optimum controller parameter vector in this case is φ^d. The result in this case is worse than the one optimized using $\Psi_M(\theta^f)$, but it is the best choice in this case. The condition in Equation 17.9 is satisfied because $\Psi_M(\Delta^M)$ is a subset of $\Psi_M(\theta^f)$.
4. *After the fault is isolated and is identified:* We assume that the estimation of the system parameter vector is $\tilde{\theta}^f$. Because we know that the best optimum result is based on $\Psi_M(\theta^f)$, we want to get the estimated value of θ^f as quickly as possible. Usually a precise estimation cannot be obtained immediately; therefore, we assume that in the early period (when the fault is identified) the estimation is given with the error limits. In other words, the estimation is not a point but a possible domain defined by a line segment. Because the fault has been isolated, this domain will be in a parallel of the coordinate axes that passes the point θ^0. We note this line segment as the domain Δ^{ii}, then Δ^{ii} will be a subset of Δ^M and it contains the point θ^f. Along with the operation of the fault identification, the domain Δ^{ii} will become smaller and smaller, and at the end it converges to the point θ^f. Accordingly, the correspondent maximum available domain $\Psi_M(\Delta^{ii})$ is a subset of $\Psi_M(\theta^f)$ and it contains the domain $\Psi_M(\Delta^M)$. The controller parameter vector should be optimized in $\Psi_M(\Delta^{ii})$. We note the optimum controller parameter vector in this case as φ^{ii}. The result in this case will be worse than the one optimized in $\Psi_M(\theta^f)$ but better than the ones optimized in $\Psi_M(\Delta^M)$. Along with the operation of the fault identification, $\Psi_M(\Delta^{ii})$ will become bigger and bigger and converges to $\Psi_M(\theta^f)$. So, the optimum result will become increasingly better and better and converge to the one that best corresponds to $\Psi_M(\theta^f)$.

The objective of the control is to make the specific growth rate $\mu(t)$ of the system in Equation 17.3 follow the rate $\mu_r(t)$ of a given reference model. This is done by manipulating the dilution rate $D(t)$. The reference model is chosen as (Li and Dahhou 2006)

$$\begin{cases} \dfrac{dC_r(t)}{dt} = \mu_r(t)C_r(t) - r(t)C_r(t) \\ \dfrac{dC_r(t)}{dt} = \dfrac{1}{Y_{c/s}}\mu_r(t)C_r(t) + r(t)S_{in}(t) - r(t)S_r(t) \\ \dfrac{dP_r(t)}{dt} = \dfrac{Y_{p/s}}{Y_{c/s}}\mu_r(t)C_r(t) - r(t)P_r(t) \end{cases} \tag{17.10}$$

It has a same structure as the process system model. In the reference model in Equation 17.10, $r(t)$ is input of the reference model and $\mu_r(t)$ is the same structure of $\mu(t)$.

The control variable is chosen as (Li and Dahhou 2006)

$$D(t) = T(t)r(t) - L(t)\hat{\mu}(t) \tag{17.11}$$

with

$$\begin{aligned} T(t) &= \frac{a_r(t)}{\hat{a}(t)} \\ L(t) &= \frac{a_r(t)}{\hat{a}(t)} - 1 \end{aligned} \tag{17.12}$$

and

$$\hat{\mu}(t) = \hat{\mu}_m \frac{S(t)}{\hat{K}_s + S(t)} \tag{17.13}$$

The terms $\hat{a}(t)$ and $a_r(t)$ are given by (Zeng et al. 1993b)

$$\hat{a}(t) = \frac{1}{Y_{p/s}}\hat{\mu}(t)\left(1 - \frac{\hat{\mu}(t)}{\mu_m}\right)\frac{C(t)}{S(t)} \tag{17.14}$$

$$a_r(t) = \frac{1}{Y_{p/s}}\mu_r(t)\left(1 - \frac{\mu_r(t)}{\mu_{mr}}\right)\frac{C_r(t)}{S_r(t)} \tag{17.15}$$

The constraint condition of Equation 17.9 of the controller parameter choice is chosen as

- Ensuring that the eigenvalue of the closed-loop system is in the left-half s plane or, in other words, the closed-loop system is stable;
- Ensuring the gain k_c can be limited in the area between the two values k_c^0 and k_c^1:

$$k_c(t) = \frac{T(t)}{\delta(t)L(t) + 1} \tag{17.16}$$

When the fault is associated with a parameter μ_m, we know that $K_s = K_s^0$. For the parameter μ_m, we know from its estimation $\hat{\mu}_m$ and the corresponding bounds $\mu_m^b \le \mu_m \le \mu_m^a$ that we can get

$$\delta(t) = \frac{\hat{\mu}_m}{\mu_m} \tag{17.17}$$

According to the limits it will be

$$\delta^{\min}(t) = \frac{\hat{\mu}_m}{\mu_m^a} \text{ and } \delta^{\max}(t) = \frac{\hat{\mu}_m}{\mu_m^b} \tag{17.18}$$

When the fault is associated with a parameter K_s, we know that $\mu_m = \mu_m^0$. For the parameter K_s, we know from its estimation $\hat{K}_s$, and the corresponding limits $K_s^b \le K_s \le K_s^a$, we can get

$$\delta(t) = \frac{K_s + S(t)}{\hat{K}_s + S(t)} \tag{17.19}$$

According to the limits it will be

$$\delta^{\min}(t) = \frac{K_s^b + S(t)}{\hat{K}_s + S(t)} \text{ and } \delta^{\max}(t) = \frac{K_s^a + S(t)}{\hat{K}_s + S(t)} \tag{17.20}$$

For different faults, using Equation 17.14 or Equation 17.16, we can calculate the controller parameters $L(t)$ and $T(t)$.

To show the validity of the method, simulation experiments have been done on the alcoholic fermentation process. The nominal value of the system parameter vector is $[\mu_m, K_s] = [0.38, 5.0]$. The parameter vector value of the reference model is $[\mu_{mr}, K_{sr}] = [0.30, 5.0]$. The fault takes place at $t = 100$ h. The faulty parameter vector is $[\mu_m, K_s] = [0.38, 2.0]$.

1. *Non-FTC control:* To make the comparison, in the first we give two results of non-FTC control. One is fixed parameter control and another is adaptive control. In the non-FTC control situation, the result of controller parameter calculation is not modified.
   - *Fixed parameter control:* In the controller parameter calculation, the process parameter vector $[\mu_m, K_s]$ is substituted by its nominal value $[\mu_m^0, K_s^0]$. Figure 17.22 presents the control result. It shows that after the fault occurrence at $t_f = 100h$ the control effect becomes very bad. There is a large follow error between $\mu(t)$ and $\mu_r(t)$. Figure 17.23 shows the system gain $k_c(t)$. It shows that after the fault occurrence the gain $k_c(t)$ has great variation and its deviation from 1 is large. This is caused by the parameter vector difference between θ^f of the postfault system and θ^0, which is used to calculate the controller parameters and the variable $\mu(t)$.
   - *Adaptive control:* In the controller parameter calculation, the process parameter vector $[\mu_m, K_s]$ is substituted by its estimation value $[\hat{\mu}_m, \hat{K}_s]$. This estimation is provided by

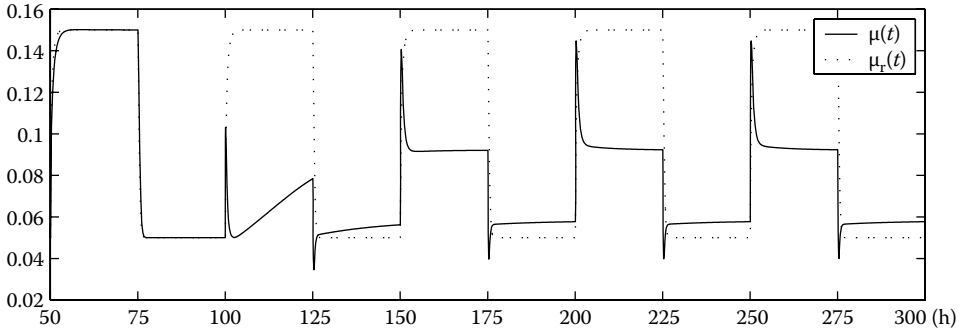

FIGURE 17.22 The control result (fixed parameter control).

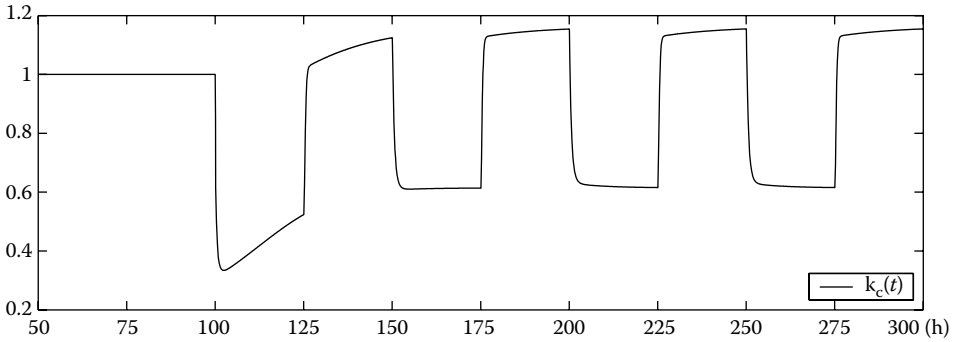

FIGURE 17.23 The system gain (fixed parameter control).

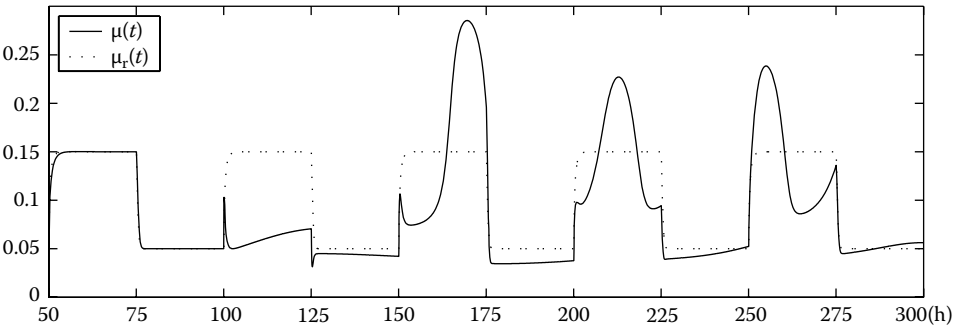

FIGURE 17.24 The control result (adaptive control).

a parameter-state joint estimate procedure. For details of the parameter-state joint estimate, the reader is refereed to Zeng et al. (1993b). Figure 17.24 shows the control result. It shows that after the fault occurrence the control effect is very bad. Figure 17.25 shows that the system gain $k_c(t)$ shows great variation and the deviation from 1 is large.

2. *FTC control:* In the FTC control manner, k_c^0 is chosen as 0.85.
   - *FTC control with fault isolation and identification but without constraint to the controller parameter L(t):* In the controller parameter calculation, the process parameter vector $[\mu_m, K_s]$ is substituted by its estimation value $[\hat{\mu}_m, \hat{K}_s]$. This estimation is provided by the intervals that are based on the fault isolation and identification method. Figure 17.26 shows the control result. It shows that the control effect is much better than the ones of Figures 17.22 and 17.24. However, in the beginning period after the fault occurrence there is also an evident control error. Figure 17.27 shows the gain $k_c(t)$. It shows that $k_c(t)$ has not been limited by the condition $k_c(t) \geq 0.85$.
   - *FTC control with fault isolation, identification, and with constraint to the controller parameter L(t):* In the first we calculate the controller parameters by the same way as in the previous case (without constraint), then the calculated result is modified according to the fault-tolerant control procedure (Li and Dahhou 2006). Figure 17.28 presents the control result. It shows that the effect is much better than the ones of preceding examples. In the begin period after the fault occurrence, the control error is much smaller than the one of Figure 17.26. Figure 17.29 presents the gain $k_c(t)$. It shows that, in the beginning period after the fault occurrence, the deviation of $k_c(t)$ from 1 is much smaller than the case of Figure 17.27, and it accords with the condition $k_c(t) \geq 0.85$. And in the following time, $k_c(t)$ always equals 1, and the control arrives at its optimum.

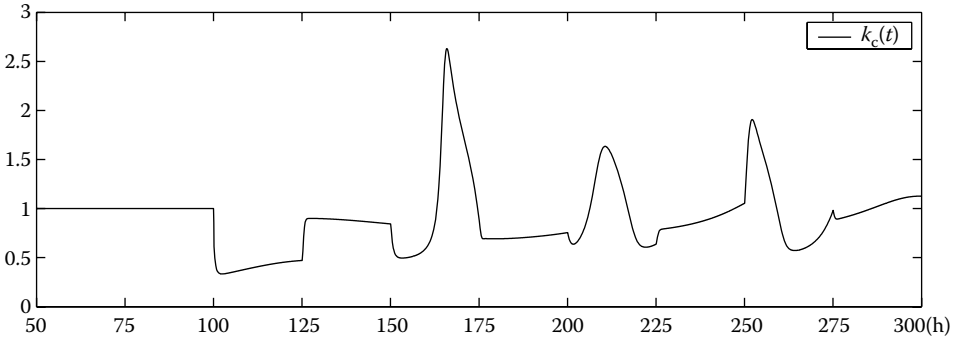

FIGURE 17.25 The system gain (adaptive control).

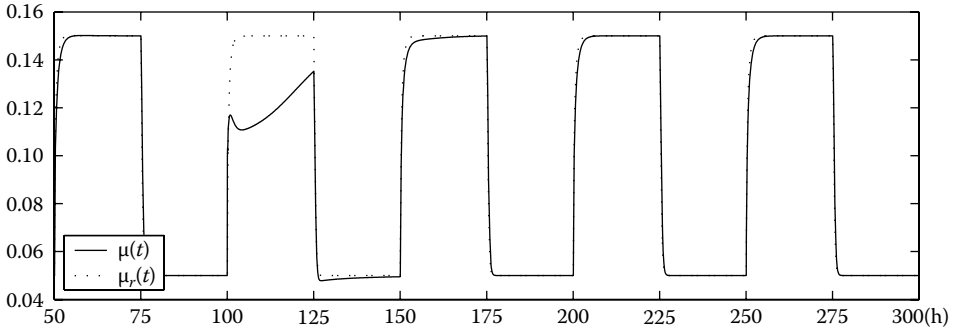

FIGURE 17.26 The control result (without constraint of the controller parameter $L(t)$).

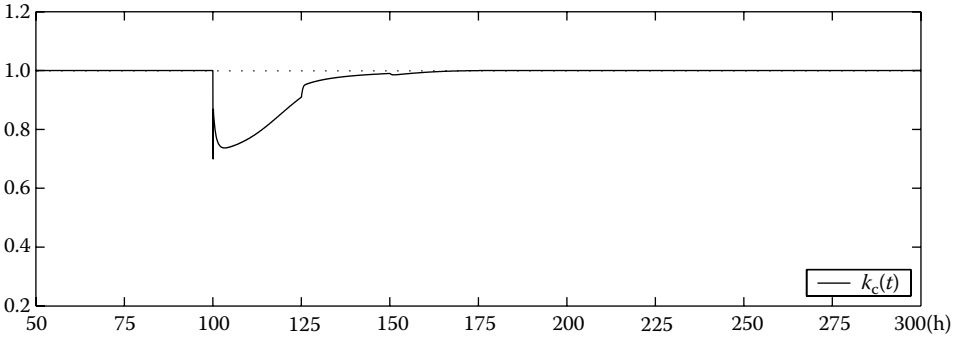

FIGURE 17.27 The system gain (without constraint of the controller parameter $L(t)$).

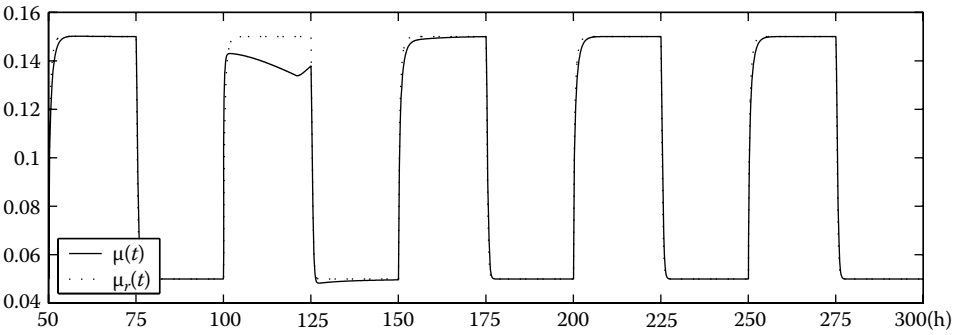

FIGURE 17.28 The control result (with constraint of the controller parameter $L(t)$).

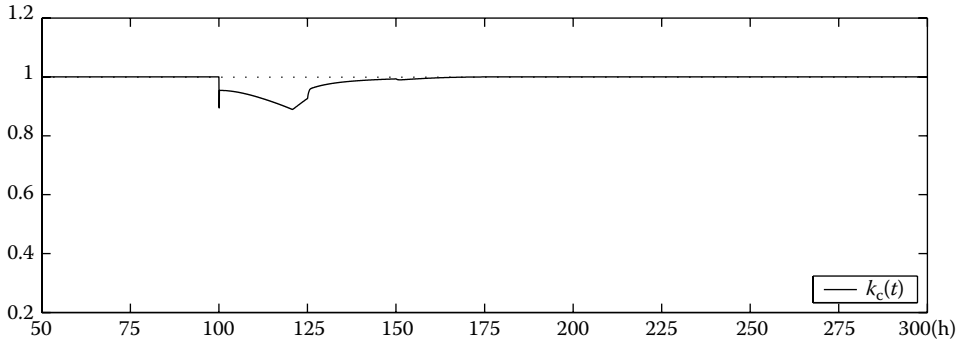

FIGURE 17.29 The system gain (with constraint of the controller parameter $L(t)$).

17.6 CONCLUSIONS

In this chapter, we tried to highlight the stages to be followed and the difficulties engineers can meet to ensure good control of the biotechnological processes and, in particular, the alcoholic fermentation processes. We developed two approaches of modeling according to the objective considered: one is quantitative and the other is qualitative. The models obtained from mass balance considerations are called *nonstructured models* and those obtained from the methods of classification are called *behavioral models*. The nonstructured models were used for the development of the algorithms of the software sensors, controls, and fault detection and isolation. The behavioral models were used for the determination of physiological states and the fault detection and isolation problem. These behavioral models use the environmental variables such as temperature, pH, and stirrer speed, as well as the expert system's knowledge of the processes to determine the physiological states.

The validation of the nonstructured model obtained was carried out to determine the best minimization of a mathematical criterion by using experimental data available for fermentation in discontinuous mode. We preferred this mode because it is richer in kinetic information than the continuous mode, which provides only stationary states.

The classification method was applied to the alcoholic fermentation process. It was supposed that the behavior during batch processing influences the phenomena observed during the continuous phase. Therefore, a good knowledge of the physiological states during the batch phase is of prime importance for the biologist. In agreement with the expert system describing the process, a total of four signals were selected, which, according to its knowledge, contain the most relevant information to determine the physiological states.

Considering the lack of reliable and inexpensive sensors in the field of biotechnological processes, we were motivated by the development of software sensors. We used the nonstructured model for the development of these types of algorithms. The experimental results showed that from the measurement of the substrate concentration, one can estimate the biomass and product concentrations with the help of an adaptive observer that jointly estimates the state and the parameters. This algorithm was validated based on three types of experiments (batch, fed-batch, and continuous modes) and gave satisfactory results.

Experimental results obtained from the control of alcoholic fermentation in continuous mode are presented. The objective was the regulation and the tracking of the substrate concentration inside of the bioreactor while acting on dilution rate. The results obtained are also satisfactory. We obtained these results by the application of an indirect adaptive control scheme using an estimator with freezing parameter when the condition of persistent excitation is not satisfied. This situation can be caused by a change of the system dynamics, and thus we concluded that it was necessary to develop

a supervisory system to supervise the control algorithms and to detect and isolate the faults coming from process dynamics at the same time.

In the supervision system, the two approaches of modeling are used for the determination of physiological states and for faults detection and isolation. For the determination of physiological states, the classification method based on fuzzy techniques was used. This method enabled us to construct a behavioral model that was used in a supervision system as a reference model for online monitoring task. The nonstructured model obtained was used for development of FDI algorithms. The method used is based on adaptive observers. This method gives satisfactory results in noise-free conditions, but it proves limited in the presence of noise. To solve this problem, a combined analytical and knowledge-based method was proposed for FDI.

The FTC method proposed in this work has two specifics:

1. It uses the idea of active FTC and of passive FTC. Therefore, in the early period after the fault occurrence, when the information of the system fault is insufficient, the crucial performance of the system can also be maintained. Along with increasing the amount of information, the control effect of the FTC system becomes progressively more perfect. The realization of this objective benefits from a reconfigurable controller, the design of which is based on the available controller parameter space analysis.
2. The use of interval-based fault isolation and identification approach. This interval-based isolation and identification approach is very quick. This is the more important factor to make the FTC system produce a beneficial effect. This interval-based isolation and identification approach provides superior/inferior limits of the faulty parameter, thus making the design of the above reconfigurable controller possible. This FTC method has been used in the simulation of a fermentation microbial-specific growth rate process; the results show the good performance of the method.

SUMMARY

The development of an integrated process control methodology requires the design of a supervisory block containing all available information and procedures.

This supervisory block recognizes specific indicators/parameters and acts, if necessary, on the process or by informing the operator.

Two approaches to modeling were implemented: the behavioral model and the nonstructured model. Whereas the former is based on the use of a fuzzy classification technique, the latter is based on mass balance considerations. The behavioral model is obtained by using the online measurement of environmental variables (temperature, pH, stirrer speed, etc.) and describes the physiological states of the process. The nonstructural model is obtained from mass balance considerations and is used for the development of software sensors, control scheme, and FDI algorithms.

The whole of the results obtained and the algorithms developed using these modeling approaches are used in a supervisory block to ensure an effective monitoring of the process.

The application of this methodology to fermentation processes gave satisfactory results.

REFERENCES

Aguilar-Martin, J. 1996. Knowledge-based real time supervision. *Tempus-Modify* Workshop. Budapest, Hungary.

Antsaklis, P.J., and K.M. Passino, eds. 1993. *An Introduction to Intelligent and Autonomous Control*. Norwell, MA: Kluwer Academic Publishers.

Bâati, L., G. Roux, B. Dahhou, and J.L. Uribelarrea. 2004. Unstructured modeling growth of Lactobacilius acidophilus as a function of the temperature. *Math Comput Simul* 65:137–45.

Ben-Youssef, C. 1996. Filtrage, estimation et commande adaptative d'un procédé de traitement des eaux usées. Ph.D. thesis. Institut National Polytechnique de Toulouse.

Ben-Youssef, C., B. Dahhou, F.Y. Zeng, and J.L. Rols. 1996. Estimation and filtering of nonlinear systems: Application to a wastewater treatment process. *Int J Syst Sci* 27:497–505.

Dahhou B., G. Chamilothoris, and G. Roux. 1991a. Adaptive predictive control of a continuous fermentation process. *Int J Adapt Cont Signal Process* 5:351–62.

Dahhou, B., G. Roux, and A. Cheruy. 1993. Linear and nonlinear adaptive control of alcoholic fermentation process. *Int J Adapt Cont Signal Process* 7:213–33.

Dahhou, B., G. Roux, and I. Queinnec. 1991b. Adaptive control of a continuous fermentation process. Presented at the Symposium on Modeling and Control of Technological Systems, Lille, France, pp. 738–43.

Dahhou, B., G. Roux, I. Queinnec, and J.B. Pourciel. 1991c. Adaptive pole placement control of a continuous fermentation process. *Int J Syst Sci* 22:2625–38.

Dojat, M., N. Ramaux, amd D. Fontaine. 1998. Scenario recognition for temporal reasoning in medical domains. *Artif Intell Med* 14:139–55.

Kabbaj, N. 2004. Développement d'algorithmes de détection et d'isolation de défauts pour la supervision des bioprocédés. Ph.D. thesis. Université de Perpignan.

Kabbaj, N., A. Doncescu, B. Dahhou, and G. Roux. 2002. Wavelet based residual evaluation for fault detection and isolation. Presented at the 17th IEEE International Symposium on Intelligent Control, Vancouver, British Columbia, Canada.

Kabbaj, N., M. Polit, B. Dahhou, and G. Roux. 2001. Adaptive observers based fault detection and isolation for an alcoholic fermentation process. Presented the 8th IEEE International Conference on Emerging Technologies and Factory Automation. Antibes-Juan les Pins, France.

Kotch, G.-G. 1993. Modular reasoning. A new approach towards intelligent control. Ph.D. thesis. Swiss Federal Institute of Technology. Zurich, Suisse.

Li, Z., and B. Dahhou. 2006. An observers based fault isolation approach for nonlinear dynamic systems. Presented at the Second IEEE-EURASIP International Symposium on Control, Communications and Signal Processing 2006. (ISCCSP'06), Marrakech, Morocco.

Monod, J. 1942. *Recherche sur la Croissance des Cultures Bactériennes*. Edition Hermes: Paris.

M'Saad, M., I.-D. Landau, and M. Duque. 1989. Example applications of the partial state reference model adaptive control design technique. *Int J Adapt Cont Signal Process* 3:155–65.

M'Saad, M., I.-D. Landau, and M. Samaan. 1990. Further evaluation of the partial state reference model adaptive control design. *Int J Adapt Cont Signal Process* 4:133–46.

Nakkabi, Y., N. Kabbaj, B. Dahhou, G. Roux, and J. Aguilar. 2003. A combined analytical and knowledge based method for fault detection and isolation. Presented at the 9th IEEE International Conference on Emerging Technologies and Factory Automation. Vol. 2, pp. 161–6, Lisbon, Portugal.

Nakkabi,Y., A. Doncescu, G. Roux, M. Polit, and V. Guillou. 2002. Application of data mining in biotechnological process. Presented at the Second IEEE International Conference on Systems, Man, and Cybernetics, Hammamet, Tunisia.

Nejjari, F., B. Dahhou, A. Benhammou, and G. Roux. 1999a. Nonlinear multivariable adaptive control of an activated sludge wastewater treatment process. *Int J Adapt Cont Signal Process* 13:347–65.

Nejjari, F., G. Roux, B. Dahhou, and A. Benhammou. 1999b. Estimation and optimal control design of a biological and wastewater treatment process. *Int J Math Comp Simul* 48:269–80.

Piera, N., P. Desroches, and J. Aguilar-Martin. 1989. Lamda: An incremental conceptual clustering system. Report 89420. LAAS/CNRS.

Queinnec, I., C. Destruhaut, J.-B. Pourciel, and G. Goma. 1992. An effective automated glucose sensor for fermentation monitoring and control. *World J Microbiol Biotechnol* 8:7–13.

Waissman-Vilanova, J. 2000. Construction d'un modèle compartemental pour la supervision de procédés: Application à une station de traitement des eaux. Ph.D. thesis. Institut National Polytechnique de Toulouse.

Waissman-Vilanova, J., R. Sarrate-Estruch, B. Dahhou, and J. Aguilar-Martin. 1999. Building an automaton for condition monitoring in a biotechnological process. Presented at the *5th* European Control Conference, Karlsruhe, Alemagne.

Zeng, F.Y., B. Dahhou, and M.T. Nihtila. 1993a. Adaptive control of nonlinear fermentation process via MRAC technique. *J Appl Math Model* 17:58–69.

Zeng, F.Y., B. Dahhou, M.T. Nihtila, and G. Goma. 1993b. Microbial specific growth rate control via MRAC method. *Int J Syst Sci* 24:1973–85.

Zhang, Q. 2000. A new residual generation and evaluation method for detection and isolation of faults in nonlinear systems. *Int J Adapt Control Signal Process* 14:759–73.

This page intentionally left blank

Appendix: Suppliers List

This suppliers list is not exhaustive and no recommendation is implied by inclusion.

Instrumentation, sensors, and software, etc.

http://www.aber-instruments.co.uk/	biomass monitor
http://www.adc-service.co.uk/page5.html	gas analyzers
http://www.broadleyjames.com/	pH and pO_2 electrodes, instrumentation
http://www.buglab.com/	external optical density sensor
http://www.foxylogic.com/	control software
http://www.cerexinc.com/	optical density monitor with sample chamber
http://www.wireworkswest.com/fermworks/	fermentation software for process plants
http://www.finesse.com/	sensors, controllers, software
http://www.fluorometrix.com/products/cellphase/	external pO_2 analyzer
http://www.flownamics.com/	sample probes and analyzers
http://www.gelifesciences.com	single-use systems
http://www.hamiltoncomp.com	pO_2 sensors
http://invitrogen.com	media
http://www.ksr-kuebler.com/website/index.php	level sensors for larger fermentors
http://www.red-y.com/en/	mass flow measurement and control
http://uk.mt.com/home	Mettler Toledo—sensors, balances, etc.
http://www.magellaninstruments.com/	perfusion/filtration system
http://www.millipore.com	filters, tangential flow filtration, single use
http://www.novabiomedical.com	analytical devices e.g., ammonia, lactate, etc.
http://www.processmeasurement.uk.com/	Monitek optical density systems
http://www.ptiinstruments.com/products	methanol sensor
http://www.oceanoptics.com/homepage.asp	optical sensors for pH, pO_2, etc.
http://www.pall.com/	filters, microfiltration, etc.
http://www.hitec-zang.com/html/biotech.htm	RQ monitoring
http://ravenbiotech.com/	methanol sensing and control
http://www.russellph.com/foam2.htm	antifoam sensor
http://www.schleicher-schuell.com	tangential flow filtration
http://www.watson-marlow.com/	peristaltic pumps
http://www.ysi.com/lifesciences.htm	glucose, carbon dioxide sensors, etc.

Fermentation equipment

http://www.abec.com/design.htm
http://www.applikon.com/
http://www.bioxplore.net/home-en.html
http://www.sartorius.com
http://www.sartorius-stedim.com (single-use systems)
http://www.belach.se/kent_series.html
http://www.biolafitte.com/Fermentors.htm (Pierre Guerin)
http://www.broadleyjames.com/
http://www.bioengineering.ch/
http://www.biotroninc.com/eng (BioG range)
http://www.dasgip.de/

http://www.electrolab.co.uk/
http://www.infors-ht.com/
http://www.bemarubishi.co.jp/
http://www.newmbr.ch/
http://www.nbsc.com/Main.asp (New Brunswick Scientific)
http://www.novaferm.se/
http://www.wavebiotech.com/products/

This page intentionally left blank

BIOLOGICAL SCIENCES & LIFE SCIENCES

Fermentation Microbiology and Biotechnology

Third Edition

Fermentation Microbiology and Biotechnology, Third Edition explores and illustrates the diverse array of metabolic pathways employed for the production of primary and secondary metabolites as well as biopharmaceuticals. This updated and expanded edition addresses the whole spectrum of fermentation biotechnology, from fermentation kinetics and dynamics to protein and co-factor engineering.

The third edition builds upon the fine pedigree of its earlier predecessors and extends the spectrum of the book to reflect the multidisciplinary and buoyant nature of this subject area. To that end, the book contains four new chapters:

- Functional Genomics
- Solid-State Fermentations
- Applications of Metabolomics to Microbial Cell Factories
- Current Trends in Culturing Complex Plant Tissues for the Production of Metabolites and Elite Genotypes

Organized and written in a concise manner, the book's accessibility is enhanced by the inclusion of definition boxes in the margins explaining any new concept or specific term. The text also contains a significant number of case studies that illustrate current trends and their applications in the field.

With contributions from a global group of eminent academics and industry experts, this book is certain to pave the way for new innovations in the exploitation of microorganisms for the benefit of mankind.

K12604

CRC Press
Taylor & Francis Group
an informa business
www.crcpress.com

6000 Broken Sound Parkway, NW
Suite 300, Boca Raton, FL 33487
711 Third Avenue
New York, NY 10017
2 Park Square, Milton Park
Abingdon, Oxon OX14 4RN, UK

ISBN: 978-1-4398-5579-9
90000
9 781439 855799